AD-A140 578 A TREATISE ON ACOUSTIC RADIATION(U) NAVAL RESEARCH LAB 1/7
WASHINGTON DC S HANISH 1981

UNCLASSIFIED F/G 20/1 NL

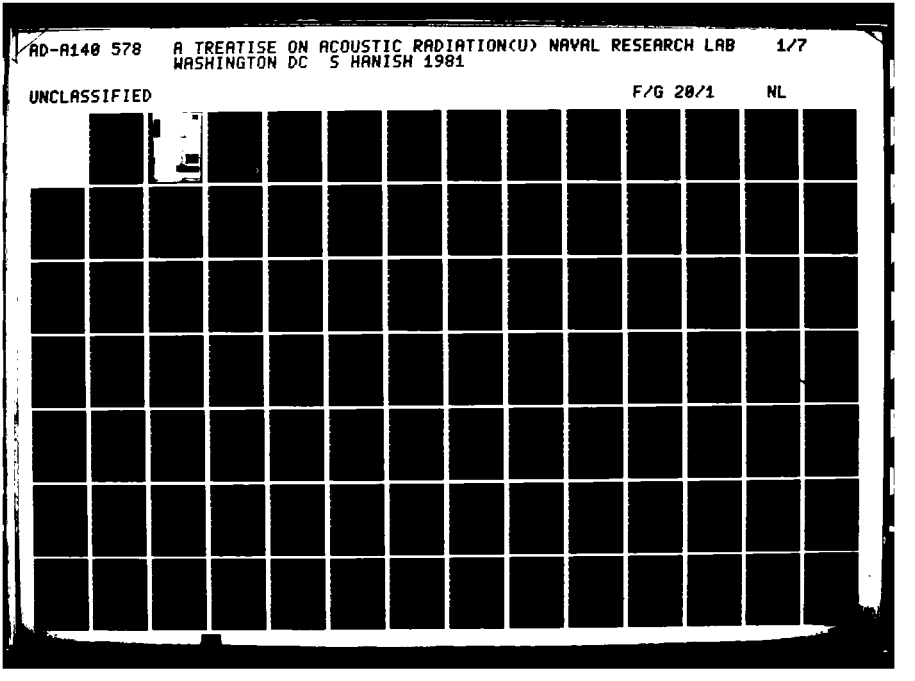

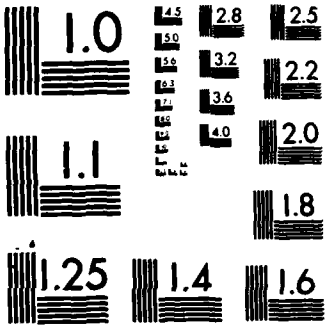

MICROCOPY RESOLUTION TEST CHART
NATIONAL BUREAU OF STANDARDS-1963-A

AD-A140 578

A Treatise on Acoustic Radiation

DTIC
APR 27 84

84 04 10 074

NAVAL RESEARCH LABORATORY
Washington, D.C.

Approved for public release; distribution unlimited.

A Treatise on Acoustic Radiation

S. HANISH, Ph.D.

Senior Scientist and Consultant
Naval Research Laboratory
Washington, D.C.

DTIC COPY INSPECTED 2

Accession For
NTIS GRA&I [X]
DTIC TAB [ ]
Unannounced [ ]
Justification
By
Distribution/
Availability Codes
Dist | Avail and/or Special
A-1

1981

NAVAL RESEARCH LABORATORY
Washington, D.C.

DTIC ELECTE APR 2 7 1984 D A

This document has been approved for public release and sale; its distribution is unlimited.

To my wife

In science, as in life, we humbly follow the Creator who said: וַיֹּאמֶר אֱלֹהִים יְהִי אוֹר

Genesis 1:3

PREFACE

The theory of acoustic radiation, well known from classical times, has been greatly expanded in recent years through the efforts of many physicists in many countries. The present monograph is intended to gather together in a single volume both the chief results of the classical period and the leading contributions of modern authors.

Sam Hanish
Washington, D.C.
October 1, 1981

ACKNOWLEDGMENT

The author acknowledges with gratitude the financial support and encouragement in the production of this book of Mr. Charles Walker, U.S. Naval Ship Systems Command, Dr. Joel Sinsky, U.S. Naval Electrons Command and Office of Naval Technology, and Dr. Robert Pohanka of the U.S. Office of Naval Research.

CONTENTS

1.1	LINEAR ACOUSTIC EQUATIONS VALID TO FIRST ORDER APPLICABLE TO FLUIDS AT REST	1
1.2	EQUATIONS OF ACOUSTIC INTENSITY VALID TO SECOND ORDER	3
1.3	ACOUSTIC POWER	4
1.4	DIRECTIVITY OF RADIATED POWER	6
1.5	THE COMPLEX RADIATION PATTERN FUNCTION	6
1.6	VECTOR SPECIFIC ACOUSTIC ADMITTANCE	7
1.7	ACOUSTIC SOURCES AND THEIR ASSOCIATED ACOUSTIC FIELD	8
1.8	SOUND GENERATED BY VOLUME DISTRIBUTED SOURCES	11
1.9	EIGENFUNCTION SOLUTIONS OF THE DIFFERENTIAL EQUATION OF THE SCALAR VELOCITY POTENTIAL FIELD	17
1.9a	RADIATION OF SOUND FROM AN INFINITELY LONG CYLINDER OF CIRCULAR CROSS SECTION	18
1.9b	RADIATION OF SOUND FROM A CYLINDER OF ELLIPTICAL CROSS–SECTION	19
1.9c	RADIATION OF SOUND FROM A SPHERE	24
1.9d	RADIATION OF SOUND FROM A PROLATE SPHEROID	26
1.9e	RADIATION OF SOUND FROM AN OBLATE SPHEROID	30
1.10	THE NUMERICAL CALCULATION OF VELOCITY POTENTIAL ON A RADIATING SURFACE	32
1.11	REACTIVE POWER	36
1.12	KIRCHOFF APPROXIMATION IN DIFFRACTION THEORY	38
1.13	DEFINITION OF FRAUNHOFER REGION, FRESNEL REGION. NEAR FIELD REGION IN THE SCALAR FIELD OF ACOUSTIC WAVES	39
2.1	THEORY OF THE SPHERICAL RADIATOR	47
2.2	ACOUSTIC INTENSITY AND ACOUSTIC POWER OF SPHERICAL RADIATORS	52
2.3	RADIATIVE CAPACITY OF THE *N*'TH ORDER SPHERICAL RADIATOR	55
2.4	INCREMENT OF MASS AND ACCESSION OF INERTIA FOR SPHERICAL RADIATORS	58
2.5	NEAR FIELD AND FAR FIELD OF SPHERICAL RADIATORS	60
2.6	ACOUSTIC POWER FROM POINT SOURCES, ONE SPHERICAL CAP, TWO SPHERICAL CAPS OF OPPOSITE VELOCITY AT THE POLES OF A SPHERICAL RADIATOR	62

2.7	ACOUSTIC RADIATION FROM A ZONAL RADIATOR ON A SPHERICAL BAFFLE	64
2.8	EMPIRICAL ANALYSIS OF 3-DIMENSIONAL STEADY STATE FIELDS BY THE METHOD OF PACHNER	66
2.9	LOW FREQUENCY RADIATION OF MULTIPOLES IN THE FORM OF SPHERICAL BUBBLES	71
2.9a	MECHANICAL RESONANCE OF BUBBLES AS MONOPLE RADIATORS	71
2.9b	VIBRATION AND RESONANCE OF A SPHERICAL BUBBLE WITH NON-UNIFORM RADIAL MOTION	73
2.9c	RADIATION FIELD OF SPHERICAL BUBBLE WITH HARMONIC RADIAL MOTION WHICH IS A FUNCTION OF POLAR ANGLE θ BUT NOT OF AZIMUTHAL ANGLE ϕ	75
2.9d	RADIATION FIELD OF A SPHERICAL BUBBLE WITH HARMONIC RADIAL MOTION WHICH IS AN ARBITRARY FUNCTION OF SPHERICAL ANGLES θ, ϕ	76
3.1	THE CALCULATION OF ACOUSTIC RADIATION BASED ON GREEN'S FUNCTIONS	79
3.2	PHYSICAL MEANING OF THE GREEN'S FUNCTION	79
3.3	GREEN'S FUNCTIONS BASED ON 1ST ORDER ACOUSTIC FIELD EQUATIONS	80
3.4	1-D GREEN'S FUNCTIONS OF THE STURM-LIOUVILLE EQUATION; AND 2-D, 3-D GREEN'S FUNCTIONS	86
3.5	CHARACTERISTIC GREEN'S FUNCTIONS $G(\xi, \xi';\lambda)$	94
3.6	ACOUSTIC RADIATION INTO WAVEGUIDES I	95
3.7	ACOUSTIC RADIATION INTO WAVEGUIDES II	103
3.7a	RADIATION OF A HARMONIC POINT SOURCE INTO A WEDGE WAVEGUIDE	103
3.7b	RADIATION FIELD OF A POINT SOURCE IN A CIRCULAR WAVEGUIDE	104
3.7c	RADIATION FIELD OF A POINT SOURCE IN A RECTANGULAR SEMI-INFINITE OPEN WAVEGUIDE OR IN A RECTANGULAR BOUNDED WAVEGUIDE	105
3.7d	RADIATION FIELD FROM A HARMONIC POINT SOURCE ABOVE A PLANE	107
3.7e	RADIATION FIELD OF A HARMONIC POINT SOURCE IN A PARALLEL PLATE WAVEGUIDE	108
3.7f	ALTERNATE ("BIORTHOGONAL") FORM OF RADIAL DEPENDENCE OF FIELDS IN CYLINDRICAL COORDINATES	110
3.7g	RADIATION OF A HARMONIC POINT SOURCE IN FREE SPACE	111

3.7h RADIATION OF A HARMONIC POINT-SOURCE IN SEMI-INFINITE QUARTER SPACE 112

3.7i GENERAL RULE FOR INTERCONVERTING 3-D AND 2-D GREEN'S FUNCTIONS 113

3.8 RADIATION IN THE PRESENCE OF SCATTERING BAFFLES 113

3.8a RADIATION OF A HARMONIC POINT SOURCE ADJACENT TO A CIRCULAR CYLINDRICAL BAFFLE 114

3.8b RADIATION FIELD OF A LINE SOURCE ADJACENT TO AND PARALLEL WITH A CIRCULAR CYLINDRICAL BAFFLE 116

3.8c RADIATION FIELD OF A POINT SOURCE ADJACENT TO AN ELLIPTIC CYLINDER 118

3.8d RADIATION FIELDS OF POINTS SOURCES AND LINE SOURCES ADJACENT TO A STRIP 123

3.8e RADIATION FIELD OF A POINT SOURCE ADJACENT TO A SPHERE 123

3.8f RADIATION FIELD OF A HARMONIC POINT SOURCE ADJACENT TO A PROLATE SPHEROID 126

3.8g RADIATION FIELD OF A HARMONIC POINT SOURCE ADJACENT TO AN OBLATE SPHEROID 128

3.8h RADIATION FIELD OF A HARMONIC POINT SOURCE ADJACENT TO A WEDGE WITH AN INFINITELY LONG EDGE 130

3.8i RADIATION FIELD OF A LINE SOURCE ADJACENT TO, AND PARALLEL WITH, A WEDGE 131

3.8j RADIATION FIELD OF A HARMONIC POINT SOURCE ADJACENT TO A HALF PLANE 133

3.8k RADIATION FIELD OF A HARMONIC LINE SOURCE, ADJACENT TO, AND PARALLEL WITH, THE EDGE OF A HALF-PLANE 134

3.8l RADIATION FIELD OF A HARMONIC POINT SOURCE ADJACENT TO A CONE 135

3.8m RADIATION FIELDS OF HARMONIC MULTIPOLES ABOVE A PLANE 136

IIIA.1 EVALUATION OF RADIATION INTEGRALS 140

IIIA.2 SELECTION OF CONTOURS OF INTEGRATION IN THE ξ-PLANE FOR APPROXIMATE EVALUATION OF RADIATION INTEGRALS 141

IIIA.3 MODAL THEORY OF WAVEGUIDES FOR DISCRETE MODES 143

IIIA.4 MODAL THEORY OF WAVEGUIDES WHICH SHOW CONTINUOUS-SPECTRUM MODES 148

IIIA.5 BRANCH POINTS AND BRANCH CUTS IN RADIATION INTEGRALS 148

IIIA.6 GENERALIZED EXAMPLE OF THE EVALUATION OF A RADIATION INTEGRAL 153

IIIA.7 CANONICAL INTEGRALS WHICH ARE USEFUL IN THE CALCULATION OF RADIATION INTEGRALS 155

IIIA.8 ASYMPTOTIC EVALUATION OF MULTIPLE INTEGRALS 159

IIIB.1 METHOD OF OBTAINING NEW GREEN'S FUNCTIONS—EXAMPLE OF THE GREEN'S FUNCTION FOR AN AXIAL (MAGNETIC) DIPOLE WITHIN A CORNER REFLECTOR 160

4.1 THEORY OF ACOUSTIC RADIATION BASED ON PLANE WAVE EXPANSIONS 167

4.2a RADIATION FIELD OF A RECTANGULAR FLEXURAL PLATE WITH FIXED VELOCITY DISTRIBUTION IN A INFINITELY LONG LOSSLESS DUCT 169

4.2b RADIATION FIELD OF A RECTANGULAR PLATE FIXED VELOCITY DISTRIBUTION IN AN INFINITE PLANE RIGID BAFFLE 171

4.2c RADIATION FIELD OF FORCE-DRIVEN RECTANGULAR PLATE IN AN INFINITE RIGID BAFFLE 171

4.3 KING-BOUWKAMP RADIATION INTEGRAL FOR CIRCULAR RADIATION IN BAFFLES 177

4.4 WEYL'S EXPANSION AND 3-D GREEN'S FUNCTIONS 179

4.5 THE RADIATION SOUND IN THE LIMIT OF HIGH FREQUENCIES-THE GEOMETRIC CASE 181

4.6 THE RADIATION OF SOUND IN THE LIMIT OF HIGH FREQUENCIES—THE GEOMETRIC CASE PLUS TERMS OF HIGHER ORDER 185

4.7 THEORY OF RADIATION FROM COMPOSITE SOURCES 187

4.7a RADIATION FIELD AND FIELD INTENSITY OF A LINEAR ARRAY OF EXTENDED SOURCES 190

5.1 ACOUSTIC RADIATION FROM SOURCE-BAFFLE COMPOSITES WHICH ARE VERY LARGE OR VERY SMALL RELATIVE TO THE RADIATED WAVELENGTH 193

5.2 MULTIPOLE DESCRIPTION ON SOUND SOURCES 194

5.3 GREEN'S FUNCTIONS AND ACOUSTIC MULTIPOLE FIELDS 195

5.4 ACOUSTIC MULTIPOLE DESCRIPTION OF VOLUME DISTRIBUTED SOURCES 199

5.5 ACOUSTIC MULTIPOLE DESCRIPTION FOR SURFACE DISTRIBUTED SOURCES 205

5.6 NUMERICAL CALCULATION OF ACOUSTIC RADIATION BY SMALL SOURCES LOCATED IN LARGE BAFFLE 209

5.6a RADIATION OF SOUND BY A SMALL CIRCULAR PISTON IN A SPHERICAL BAFFLE OF LARGE ka 210

5.6b RADIATION FROM AN INFINITE STRIP IN A CYLINDER OF LARGE DIAMETER 215

5.6c RADIATION FROM A RECTANGULAR PISTON SET IN AN INFINITE CYLINDER OF LARGE DIAMETER 221

5.7 MULTIPOLE EXPANSIONS AND PLANE WAVE REPRESENTATIONS 224

6.1 INSTANTANEOUS AND HARMONIC ACOUSTIC INTENSITY AND POWER 229

6.2 RADIATED INTENSITY AND POWER OF A POINT SOURCE (MONOPOLE, DIPOLE, QUADRUPOLE) 231

6.3 ACOUSTIC RADIATION IMPEDANCE 233

6.4 RADIATION OF STEADY STATE ACOUSTIC POWER FROM A LARGE FLEXURAL PLATE WITH FIXED VELOCITY DISTRIBUTION IN AN INFINITE RIGID BAFFLE 234

6.5 MECHANICAL RADIATION IMPEDANCE OF A VIBRATING CIRCULAR MEMBRANE IN AN INFINITE RIGID BAFFLE 239

6.6 CALCULATION OF RADIATION IMPEDANCE FROM DIRECTIVITY OF RADIATED SOUND 240

6.6a. CALCULATION OF REAL POWER RADIATED BY TWO IDENTICAL SPHERICAL SOURCES 244

6.6b. CALCULATION OF THE ACOUSTIC POWER RADIATED BY A PAIR OF UNIFORM-VELOCITY DISKS IN AN INFINITE RIGID BAFFLE 246

6.7 RADIATION FIELD, POWER AND IMPEDANCE OF A COMPOSITE SOURCE ON A SEPARABLE SURFACE HARMONICALLY EXCITED 248

6.7a. RADIATION FIELD, ACOUSTIC POWER AND MECHANICAL IMPEDANCE OF AN ARRAY OF VIBRATING RINGS ON AN INFINITE RIGID CYLINDRICAL BAFFLE 251

6.7b. RADIATION FIELD, ACOUSTIC POWER AND MECHANICAL RADIATION IMPEDANCE OF A PLANE PERIODIC ARRAY OF RECTANGULAR RADIATORS 255

6.7c. RADIATED ACOUSTIC POWER AND ACOUSTIC FIELD OF A RECTANGULAR WAVEGUIDE WITH A PERFORATED WALL 260

6.8 PRINCIPAL DIRECTION, ANGULAR DEVIATION RATIO, RADIATION FACTOR, GAIN FACTOR 265

6.8a. PRESSURE GAIN FACTOR OF ARRAYS OF DIRECTIONAL SOURCES 266

6.8b. SUMMARY OF FORMULAS DESCRIBING ANGULAR DEVIATION RATIO AND PRESSURE GAIN FACTOR OF ARRAYS OF POINT SOURCES 267
6.9 RADIATION RESISTANCE OF VIBRATING ELASTIC PANELS IN TERMS OF MODAL CORRELATION FUNCTIONS 276
6.10 RADIATION RESISTANCE OF RIBBED PANELS 280
6.11 REAL POWER AND REACTIVE POWER CALCULATED ON THE BASIS OF RETARDED AND ADVANCED GREEN'S FUNCTIONS 289
7.1 POISSON'S SOLUTION OF THE INITIAL VALUE PROBLEM OF VOLUME DISTRIBUTED SOURCES 293
7.1a TRANSIENT RADIATION FROM ACOUSTICALLY SMALL VOLUME SOURCES 295
7.1b TRANSIENT RADIATION OF ACOUSTIC MULTIPOLES 297
7.2 GENERAL FORMULAS FOR THE CALCULATION OF TRANSIENT RADIATION FROM SOURCES ON A SURFACE 301
7.2a TRANSIENT RADIATION IN ABSTRACT FORMULATION 306
7.2b TRANSIENT RADIATION OF A MONOPOLE IN FREE SPACE 307
7.3a TRANSIENT RADIATION OF A RIGID PISTON IN AN INFINITE RIGID BAFFLE 311
7.3b INDICIAL IMPEDANCE OF A RIGID PISTON IN A RIGID INFINITE BAFFLE 314
7.3c TRANSIENT RADIATION FIELD OF A VIBRATING PLATE EDLGE CLAMPED IN A RIGID WALL 315
7.3d TRANSIENT RADIATION FROM A PISTON MEMBRANE 317
7.3e EXAMPLES OF TRANSIENT RADIATION FROM A PISTON MEMBRANE 320
7.4 TRANSIENT RADIATION FROM SPHERES 324
7.4a THE POLYNOMIAL B_n (jkr_0) AND ITS LAPLACE INVERSIONS 324
7.4b TRANSIENT RADIATION FROM SPHERES EXCITED BY ARBITRARY TIME SIGNALS 327
7.4c TRANSIENT RADIATION FROM A SPHERICAL SOURCE OF ORDER $n = 0$ FOR AN IMPULSE EXCITATION 330
7.4d TRANSIENT EXCITATION OF SPHERES BY A SINUSOIDALLY MODULATED STEP FUNCTION 330
7.4e TRANSIENT RADIATION FROM A SPHERICAL SOURCE OF ORDER $n = 0$ FOR A STEP-SINUSOID EXCITATION 331
7.4f TAIL END OF TRANSIENT RADIATION FROM A SPHERICAL SOURCE OF ORDER $n = 0$ 333

7.4g TRANSIENT RADIATION FROM A SPHERICAL SOURCE OF ORDER $n = 0$ 334

7.4h CHARACTERISTIC WAVES OF EXTERIOR SPACE 336

7.4i RATIO $R^{(k)}$ OF INITIAL VELOCITY POTENTIAL AMPLITUDE OF TRANSIENT WAVES TO THE VELOCITY POTENTIAL AMPLITUDE OF STEADY STATE WAVES IN THE FAR FIELD 337

7.5 THE TIME-DEPENDENT GREEN'S FUNCTION OF A RIGID CYLINDER 338

7.6 THE TRANSIENT FIELD FROM AN INFINITE LINE SOURCE OF UNIFORM STRENGTH 342

7.7 A GEOMETRIC ACOUSTICS INTERPRETATION OF THE TIME-DEPENDENT GREEN'S FUNCTION OF A LINE SOURCE IN THE PRESENCE OF AN INFINITE RIGID CYLINDER 345

7.8 ACOUSTIC RADIATION OF SPHERES EXPRESSED AS PARTICULAR INTEGRALS OF THE DIFFERENTIAL EQUATIONS EXPRESSING BOUNDARY COUNDITIONS 346

7.9 SOUND GENERATED IN LIQUIDS BY SPLASHES 348

7.9a SOUND GENERATED BY THE IMPACT OF A HIGH VELOCITY RIGID SPHERE ON A LIQUID 349

7.9b PRESSURE LEVEL, PULSE SHAPE AND ENERGY SPECTRA OF ACOUSTIC RADIATION IN WATER GENERATED BY VERTICAL IMPACT OF SINGLE DROPS, AND RAIN 352

7.9c SOUND RADIATED UNDERWATER BY IMPACT OF RAIN ON THE WATER SURFACE 356

7.10 RADIATION OF SOUND FROM A POINT FORCE IN MOTION 357

8.1 PARAMETRIC EQUATIONS AND DISPLACEMENTS OF A RADIATING ELASTIC SHELL 359

8.2 EQUATIONS OF MOTION OF A SHELL DRIVEN IN FORCED VIBRATION BY SURFACE LOADS 360

8.3 TEMPORAL IMPULSE RESONSE OF A HOMOGENEOUS ISOTROPIC SHELL 362

8.4 THEORY OF RANDOM DISPLACEMENT DUE TO RANDOM FORCES ACTING ON A SHELL 365

8.5 THEORY OF RANDOM RADIATION 367

8.6 RESPONSE OF FINITE SUPPORTED PLATES TO CONVECTING TURBULENT PRESSURE FIELDS 370

8.7 DIRECT RADIATION OF SOUND FROM COMPLAINT SURFACES EXCITED BY HYDRODYNAMIC PRESSURES CAUSED BY FLOW TURBULENCE. (Case of large plane surfaces with no edge effects.) 383

9.1	SOUND RADIATION BY A SEMIINFINITE PLATE	395
9.2	SOUND RADIATION FROM AN INFINITE PLATE REINFORCED WITH A FINITE SET OF BEAMS AND DRIVEN BY A POINT FORCE	397
9.3	SOUND RADIATION BY AN INFINITE PERIODIC SLOTTED ARRAY	403
9.4	RADIATION IMPEDANCE OF A CYLINDER OF FINITE HEIGHT	408
9.5	RADIATION FIELD AND RADIATION RESISTANCE OF A FINITE CYLINDRICAL SHELL IN A RIGID BAFFLE	412
9.6	RADIATION FIELD OF RECTANGULAR PISTONS VIBRATING HARMONICALLY IN AN INFINITE RIGID BAFFLE	422
9.7	RADIATION OF SOUND BY FLUID FLOW OVER CONTOURED OBJECTS	426
9.7a	RADIATION CAUSED BY LINEAR FLOW OVER A RIGID OBJECT	426
9.7b	RADIATION CAUSED BY ROTATIONAL FLOW OVER RIGID OBJECTS	427
9.7c	RADIATION FROM MOVING SOUND SOURCES	430
9.8	RADIATION OF SOUND INTO A LAYERED HALF-SPACE	431
9A.1	INTRODUCTION	433
9A.2	*LIST OF CONVENTIONAL RADIATIONS OF SOUND* AND THEIR MODELS	433
10.1	THERMOOPTICAL SOURCES	437
10.2	SOLUTION OF EQ. 10.1.6 WHEN β IS CONSTANT	438
10.3	SOUND GENERATION BY THERMAL SOURCES	443
10.4	RADIATION OF SOUND CAUSED BY TEMPERATURE OSCILLATIONS ON A PLANE SURFACE	443
10.5	SOUND RADIATED BY A COLLAPSING BUBBLE CONTAINING SUPERHEATED VAPOR	445
10.5a	GROWTH RATES OF SUPERHEATED BUBBLES	445
10.5b	SIMPLIFIED THEORY OF THE GROWTH AND COLLAPSES OF BUBBLES	449
10.5c	ACOUSTIC RADIATION FROM A COLLAPSING BUBBLE	451
10.6	RADIATION OF SOUND FROM CAVITATING VOLUMES	453
10.7	CAVITATION NOISE AS A TRAIN OF SOUND PULSES GENERTED AT RANDOM TIMES	457
11.1a	EXPERIMENTAL CURVES OF SHOCK WAVE FORMATION AND PROPAGATION	461
11.1b	BUBBLE OSCILLATIONS	464
11.1c	PRESSURE PULSES AFTER DETONATION	465

11.1d ENERGY OF DETONATION AND ITS DISSIPATION 466

11.1e RAYLEIGH-WILLIS CURVES FOR RELATING COLLAPSE TIME OF A BUBBLE TO A BUBBLE ENERGY IN THE BUBBLE CAUSED BY A CHEMICAL EXPLOSION 467

11.2 THEORETICAL MODEL OF PULSE PRESSURE RADIATION 474

11.2a NEED FOR APPROXIMATIONS 474

11.2b HYDRODYNAMIC AND THERMODYNAMIC PROPERTIES OF WATER AT THE SHOCK FRONT 474

11.2c THERMODYNAMIC PROPERTIES OF THE GAS SPHERE 478

11.2d THERMOYNAMIC PROPERTIES OF THE GASEOUS PRODUCTS 481

11.2e SAMPLE CALCULATIONS OF THERMODYNAMIC PROPERTIES OF GAS PRODUCTS 483

11.3 KIRKWOOD-BETHE THEORY OF SHOCK WAVE FORMATION 487

11.3a CALCULATION OF THE DISSIPATION PARAMETER X AND THE TIME SPREAD FACTOR γ_t 491

11.3b CONTINUATION OF SAMPLE CALCULATION 494

11.4 SECONDARY PRESSURE PULSES 498

11.4a FORMULATION OF THE THEORY OF SECONDARY PRESSURE PULSES 498

11.4b SEVERAL PERIODS OF PULSATION 502

11.4c SIMILARITY 503

11.4d EMPIRICAL MODEL OF THE PRESSURE-TIME CURVE 504

1.4e EXPERIMENTAL MEASUREMENTS PROCEDURE 506

12.1 INTRODUCTION 511

12.2 CONSTRUCTION OF FINITE ELEMENTS OF AN ELASTIC CONTINUUM 511

12.2a DEGREES OF FREEDOM OF A FINITE ELEMENT 512

12.2b LOCAL NODES AND GLOBAL NODES 512

12.2c KINETIC AND POTENTIAL ENERGIES OF A FINITE ELEMENT IN DISCRETE FORM 515

12.2d GENERALIZED FORCES ON A FINITE ELEMENT 516

12.2e EQUATIONS OF MOTION IN DISCRETE FORM 517

12.3 SOLUTION OF THE DISCRETE MODEL IN SPACE-TIME 518

12.4 INTERPOLATION FORMULAS 520

12.4a GENERALIZATION OF INTERPOLATION FUNCTIONS 522

12.5 ELEMENT-STIFFNESS MATRIX 523

12.5a ELEMENT-MASS MATRIX 524
12.5b DAMPING MATRIX 525
13.1 INTRODUCTION, FINITE ELEMENT RADIATION 527
13.1a SYMBOLIC REPRESENTATION OF INTERACTING SYSTEMS 527
13.2 FLUID-SOLID INTERACTION OF RADIATING SURFACES 528
13.2a CONTINUUM EQUATIONS OF PLATE-FLUID INTERACTION 530
13.2b THE DISCRETIZED ACOUSTIC FIELD 531
13.2c THE DISCRETIZATION OF THE ELASTIC SYSTEM (DYNAMIC BENDING OF PLATES) 533
13.2d THE COUPLED SET OF DISCRETIZED EQUATIONS OF A VIBRATING PLATE IN A FLUID 534
13.3 HELMHOLTZ INTEGRAL REPRESENTATION OF THE ACOUSTIC INTERACTION PRESSURE 536
13.4 THE FLUID-SOLID AS ONE (COMPOSITE) CONTINUUM 538
13.4a TERMINATION OF THE SOLID-FLUID COMPOSITE 539
13.5 TRANSIENT RADIATION FROM A VIBRATING FLUID-SOLID INTERFACE 540
13.6 EXAMPLES OF CALCULATION OF RADIATION BY *FINITE ELEMENTS* 540
14.1 INTRODUCTION, FINITE AMPLITUDE RADIATION 545
14.1a ZONE OF INTERACTION IN VARIOUS MODELS 546
14.1b PARAMETERS NEEDED FOR CALCULATING PARAMETRIC ACOUSTIC ARRAYS 546
14.2 PREDICTION MODELS OF PARAMETRIC ARRAYS 551
14.3 PARAMETRIC PROJECTORS WITH TRANSIENT PRIMARIES 564
14.3a BANDWIDTH OF PARAMETRIC TRANSMITTERS 565
14.3b LIMIT ON THE PERFORMANCE OF PARAMETRIC PROJECTOR BY ACOUSTIC SATURATION 565
14.3c DIFFRACTION EFFECTS IN PARAMETRIC ARRAYS 570

CHAPTER I
FUNDAMENTALS

1.1. LINEAR ACOUSTIC EQUATIONS VALID TO FIRST ORDER APPLICABLE TO FLUIDS AT REST [1]

Sound energy in a compressible non-viscous fluid distributes itself spatially and temporally as a scalar material field. By such a field is meant one whose dynamic and thermodynamic description can be made by an idealized *continuous function* of space and time (that is 4-space), viewed macroscopically. The field variable appropriate to the transmission of sound in such a fluid is the *velocity potential* Φ (units: meter^2/sec). We may theoretically calculate Φ in space and time coordinates using the following thermodynamic and dynamic considerations. At thermodynamic equilibrium the state of the fluid is fixed at every point by the equilibrium values of vector velocity V_0, scalar pressure P_0, scalar density ρ_0, absolute temperature T_0, and entropy S_0. When a sound disturbance traverses the fluid at speed c these field quantities change to V, P, ϱ, T, and S respectively, the incremental changes giving rise to excess (that is, acoustic) quantities: the excess particle velocity $\vec{u}$, the excess pressure p, the excess density δ, the excess temperature θ, and the excess entropy σ. These acoustic quantities are generally nonlinear functions of one another, and of the equilibrium field quantities. This nonlinearity arises in part from the fact that the fluid acceleration $d\vec{u}/dt$ in its Eulerian description is a function of *both* space coordinates and time, namely, $d\vec{u}/dt = \partial\vec{u}/\partial t + (\vec{u}\cdot\vec{\nabla})\vec{u}$. In the radiation problems considered here we assume $|\vec{u}|$ and $\vec{\nabla}\vec{u}$ to be small quantities of first order so that $(\vec{u}\cdot\vec{\nabla})\vec{u}$ is a quantity of second order, which is negligible relative to $\partial\vec{u}/\partial t$. If we assume in addition that $|\vec{u}|$ is small compared to the wave velocity c it will turn out that the acoustic field quantities will appear to the first order only in the equation of momentum, heat transfer, and thermodynamic state. These first order equations are the linear approximations of classical acoustics. A typical example of linearization, much used in the theory of radiation of sound in a compressible medium, is physically associated with the generation of a time-variation of mass density $\varrho(\vec{r}_0, t_0)$ or entropy $S(\vec{r}_0, t_0)$ at a point in space, which is measurable as a time-varying acoustic pressure $p(\vec{r}_0, t_0)$. Between quantity p and quantities ϱ, S there is a *constitutive relation* which must be specified in any theoretical model of the radiation process. A simple useful model states that the total pressure p_T in a small volume of fluid of static pressure P_0 is linearly related to the time variation of mass density $\Delta\varrho$ and entropy ΔS in that volume:

$$p_T = P_0 + \left(\frac{\partial p_T}{\partial \varrho}\right)_s \Delta\varrho + \left(\frac{\partial p_T}{\partial S}\right)_\rho \Delta S + \ldots = P_0 + p + \ldots .$$

An even more useful model, valid when amplitudes of measured pressure are small, and the time variation is rapid, states that the ΔS contribution can be negleated:

$$p(\vec{r}_0, t_0) = C^2(\vec{r}_0, t_0)\,\delta(\vec{r}_0, t_0);\; C^2 \equiv \left(\frac{\partial p_T}{\partial \varrho}\right)_s ;\; \delta \equiv \Delta\varrho$$

Here $C(\vec{r}_0, t_0)$ is the adiabatic speed of (sound) propagation of changes in mass density. Similar considerations in the near equilibrium transfer of momentum and of heat lead to other linear formulas, a collection of which is presented below:

$$p = c^2\delta \tag{1.1.1}$$

$$u = -\frac{1}{\varrho}\int \text{grad}\, p dt \tag{1.1.2}$$

$$\theta = (\gamma - 1)\ \frac{Tp}{\varrho c^2} \tag{1.1.3}$$

$$u = -\nabla\Phi \tag{1.1.4}$$

$$p = \varrho\ \frac{\partial\Phi}{\partial t} \tag{1.1.5}$$

$$\varrho\ \frac{\partial u}{\partial t} = -\text{grad}\, p. \tag{1.1.6}$$

Here, γ is the ratio of specific heat at constant pressure to that of constant volume. Additional linerizations from the law of conservation of mass in any closed system lead (in the absence of viscosity) to the simple wave equations in Φ, or p:

$$\nabla^2\Phi - \partial^2\Phi/c^2\partial t^2 = 0 \tag{1.1.7}$$

$$\nabla^2 p - \partial^2 p/c^2\partial t^2 = 0 \tag{1.1.8}$$

These are Eulerian equations associated with the Lagrange density $\mathfrak{L}$ (units: $Nm\ m^{-3}$) of the scalar field. One may form the Lagrange $\mathfrak{L}$-function by subtracting the potential energy density $\mathcal{V}$ from the kinetic energy density $\mathcal{T}$ which, in terms of Φ, leads to

$$\mathcal{T} = \tfrac{1}{2}\varrho|\nabla\Phi|^2 \tag{1.1.9a}$$

$$\mathcal{V} = \tfrac{1}{2}\varrho\left(\frac{\partial\Phi}{\partial t}\right)^2 \tag{1.1.9b}$$

$$\mathfrak{L} = \mathcal{T} - \mathcal{V}\,. \tag{1.1.9c}$$

In general $\mathfrak{L}$ is a function of the 3-space coordinates $x_1 = x$, $x_2 = y$, $x_3 = z$, and the 'time coordinate', $x_4 = ict$, together with the derivatives of Φ with respect to x_i. The introduction of $\mathfrak{L}$ assists us in the formation of the associated stress-energy tensor $\mathcal{W}$ whose sixteen components describe the energy density distribution in the corresponding material field. We may write $\mathcal{U}$ as a 4×4 matrix with components ($i, j = 1, 2, 3, 4$) which in turn, when written in terms of $\mathfrak{L}$, have the form:

$$Wij = \mathfrak{L}\ \delta_{ij} - \left(\frac{\partial\Phi}{\partial x_i}\right)[\partial\mathfrak{L}/\partial(\partial\Phi/\partial x_j)] \tag{1.1.10}$$

where δij is the Kronecker delta. Of the sixteen components in the 4×4 matrix the four in the fourth column (W_{i4}) describe the space-time components of field energy density. One of these, the W_{44} component, is the time-invariant energy density $\mathcal{H}$ of the material field. For linear acoustic systems (that is, for systems in which $p = c^2\delta$), $\mathcal{H}$ has the form,

$$\mathcal{H} = \tfrac{1}{2}\ \ \varrho\ |u|^2 + \tfrac{1}{2}\,(p^2/\ \varrho\ c^2)\quad \text{(units; } Nm\ m^{-3}\text{)}. \tag{1.1.11}$$

The other three components $W_{i4}(i = 1, 2, 3)$ of the fourth column are the time-space energy densities (that is, the *sound intensities*). These are the components proportional to I_i, i.e. to the three-vector $\underline{I}$ which gives the direction and magnitude of the flow of energy due to the sound disturbance. In symbols,

$$W_{i4} = -\frac{\partial \Phi}{\partial (ict)} \left(\varrho \frac{\partial \Phi}{\partial x_i} \right), \quad \text{(units: } Nm\, m^{-3}\text{)} \tag{1.1.12a}$$

$$ic\, W_{i4} = pu_i = I_i, \quad (N\, m/(m^2 s) \tag{1.1.12b}$$

in which p, u_i are complex functions of space and time. The remaining W_{ij} are the nine components of fluid stresses in a 3×3 stress matrix which in any particular case can be rotated to a set of principal axes, one being in general the direction of the travelling wave.

1.2 EQUATIONS OF ACOUSTIC INTENSITY VALID TO SECOND ORDER [2]

The acoustic intensity component I_i given by Eq. 1.1. (12b) is a linear approximation to a more general non-linear formula. To illustrate its derivation let E be the internal energy per unit of mass of the fluid system. For quasi static changes in entropy and specific volume the First Law of Thermodynamics requires that

$$dE = TdS - pdV = TdS + p(d\varrho / \varrho^2). \tag{1.2.1}$$

Since the propagation of sound is essentially adiabatic, $dS = 0$, and $\partial E/\partial \varrho = p/\varrho^2$. Now the entity ϱE is the internal energy density (units: Nmm^{-3}). Upon the passage of the sound wave through a unit volume of medium the change in density leads to a change in E of magnitude

$$\partial(\varrho E)/\partial \varrho = \varrho \frac{\partial E}{\partial \varrho} + E = \frac{p}{\varrho} + E = H \tag{1.2.2}$$

The symbol H is the *enthalpy* of the fluid (units: $Nm\, kg^{-1}$) and is a function of mass density. We note that

$$\partial H/\partial \varrho = \frac{\partial E}{\partial \varrho} - (p/\varrho^2) + \frac{(\partial p/\partial \varrho)_s}{\varrho} = \frac{C^2}{\varrho} \tag{1.2.3}$$

We assume that for very small particle displacements $\varrho = \varrho_0 + \delta$ and $E = E_0 + E'$. To find a relation between those quantities and 1.2.3 we form the following Taylor series expansion of ϱE at the thermodynamic coordinates ϱ_0, U_0, valid to quantities of second order in ϱ,

$$\varrho E = \varrho_0 E_0 + (\varrho - \varrho_0)[\partial(\quad\quad] \quad + \frac{1}{2}(\varrho - \varrho_0)^2 [\partial(\varrho E)/\partial \varrho^2]_{\quad} \tag{1.2.4a}$$

$$= \varrho_0 E_0 + H_0 \delta + (c \quad) + \ldots . \tag{1.2.4b}$$

Now the sound field contains an additional kinetic energy density due to the particle velocity u of magnitude $1/2(\varrho |u|^2) = 1/2\ ((\varrho_0 + \delta)|u|^2)$. Since the quantity $\delta |u|^2$ is of third order we reject it and add the remainder to 1.2.4b to form the *total acoustic* energy density to second order in δ and $|u|$. The first term $\varrho_0 E_0$ in this total energy is the internal energy of a unit volume of fluid in the

absence of sound disturbances. We shall omit it. The second term $H_0\delta$ when integrated over a finite volume vanishes since the total mass of fluid does not change during the traversal of sound. Thus the total acoustic energy density $\mathfrak{W}$ in the sound field to quantities of second order is

$$\mathfrak{W} = \frac{1}{2}\ \varrho_0|u|^2 + (c^2\delta^2/2\ \varrho_0), \left(\frac{Nm}{m^3}\right) \tag{1.2.5}$$

This quantity is time invariant. In order to find the time-varying (= flux) energy densities we shall equate the time rate of change of total energy in volume V to the flux of energy out of V through the vector surface area A. The total energy per unit volume is $\varrho|u|^2/2 + \varrho\ E$. The *change* in energy per unit mass due to traversal of sound is$(|u|^2/2) + H$. If this quantity is multiplied by the result is the time rate of change of energy per unit mass through unit area in the direction of u. Hence the energy flux balance leads to the equation

$$\frac{\partial}{\partial t}\int_V \left(\frac{\varrho|u|^2}{2} + \varrho E\right) dV = -\int_V \varrho u\left(\frac{|u|^2}{2}\right) + H)\cdot dA \tag{1.2.6}$$

Now $\varrho u(|u|^2/2)$ is a quantity of *third* order, which is negligible for linearized sound waves. The mean flux (areal) density is thus ϱuH. For small changes in coordinates, $H = H_0 + H'$, and since $dH = TdS + dp/\varrho$, we may form a Taylor series at H_0 to the first order in p by noting that for adiabatic changes $H = H_0 + p/\varrho + \ldots$. Therefore $\varrho uH = \varrho uH_0 + up$. On the average (in time) the integration of ϱuH_0 over area A vanishes. Hence the energy flux E through all areas A_k is given by

$$\dot{E} = \int_A pu\cdot dA = \sum_k pu_k A_k, (k = 1, 2, 3 \ldots), \quad \text{(units: } Nms^{-1}) \tag{1.2.7}$$

The quantity pu is the symbol I_i which appeared in Eq. 1.1, (12b) and is an areal flux of energy. In contrast the quantity $\varrho\vec{u}$ is a momentum flux density $j(Nsm^{-3})$. For small changes in density $\varrho = \varrho_0 + \delta$, and so, to quantities of second order

$$j = \varrho_0 u + \delta u \tag{1.2.8}$$

If the acoustic system is linear we may write $p = c^2\delta$ (Eq. (1)) so that the momentum flux density is

$$j = \varrho_0 u + \frac{I}{c^2} \tag{1.2.9}$$

1.3. ACOUSTIC POWER

The symbol $\dot{E}$ in 1.2.7 is the acoustic power flowing through areas A_k. In its calculation we must allow u and p to be arbitrary functions of space and time. When the time variation is sinusoidal at radian frequency ω we may represent it by the real part of the complex number $e^{-i\omega t}$. Adopting complex notation we define the pressure p to be the real part of a complex pressure P, and the particle velocity u_k to be the real part of a complex velocity V_k. The relation between these quantities is given by

$$p = (Pe^{-i\omega t} + P^* e^{i\omega t})/2 \tag{1.3.1a}$$

$$u_k = (V_k e^{-i\omega t} + V_k^* e^{i\omega t})/2 \tag{1.3.1b}$$

in which the asterisk * denotes complex conjugate. The real and imaginary components of P, V_k may have useful meaning. We shall write them as $P^{(1)}$, $P^{(2)}$, $V_k^{(1)}$, $V_k^{(2)}$ respectively. In terms of these *sinusoidal* components the total acoustic sinusoidal power generated by an area A_k which is normal to velocity V_k is,

$$\dot{E} = W_i + W_q \tag{1.3.2a}$$

$$W_i = (\tfrac{1}{2}) \int_{A_k} [(P^{(1)} V_k^{(1)} + P^{(2)} V_k^{(2)}) + (P^{(1)} V_k^{(1)} - P^{(2)} V_k^{(2)}) \quad \cos 2\omega t]\, dA_k \tag{1.3.2b}$$

$$W_q = (\tfrac{1}{2}) \int_{A_k} (P^{(1)} V_k^{(2)} + P^{(2)} V_k^{(1)}) \sin 2\omega t\, dA_k \tag{1.3.2c}$$

The symbol W_i is the real time-varying acoustic power whose mean value $<W_i>$ over a cycle of radian frequency ω is $\int_{A_k} (P^{(1)} V_k^{(1)} + P^{(2)} V_k^{(2)}) dA_k$. The latter quantity may be expressed in terms of P, V_k to yield the widely used formulas for time-average sinusoidal intensity J_k and power $<W_i>$.

$$J_k = \tfrac{1}{2} \operatorname{Re}\{P V_k^*\} \tag{1.3.3a}$$

$$<W_i> = \tfrac{1}{2} \operatorname{Re} \int_{A_k} P V_k^*\, dA_k \tag{1.3.3b}$$

where Re means real part. The symbol W_q is the imaginary time-varying acoustic power. Its mean value (in time) is zero. It is sometimes convenient to calculate *sinusoidal* acoustic power in terms of absolute amplitudes of pressure and particle velocity, $|P|$, $|V_k|$. To do this let $P = |P| e^{-i\psi}$, $V_k = |V_k| e^{-i\phi}$, and use 1.3.2a to give

$$W_i = \tfrac{1}{2} \int_{A_k} |P|\,|V_k| \cos(\psi - \phi)[1 + \cos 2(\psi + \omega t)]\, dA_k \tag{1.3.4a}$$

$$W_q = \tfrac{1}{2} \int_{A_k} |P|\,|V_k| \sin(\psi - \phi) \sin 2(\psi + \omega t)\, dA_k . \tag{1.3.4b}$$

The time average real power is seen to be

$$<W_i> = \tfrac{1}{2} \int_{A_k} |P|\,|V_k| \cos(\psi - \phi)\, dA \tag{1.3.4c}$$

In analogy with comparable electrical parameters 1.3.4C is sometimes called the *vector real power* while the quantity $1/2 \int_{A_k} |P|\,|V_k| \sin(\psi - \phi)\, dA_k$ is called the instantaneous vector reactive power. We note that total sinusoidal vector power W may be found from the formula

$$W = \tfrac{1}{2} \sum_k \int_A P V_k^*\, dA_k \tag{1.3.4d}$$

A more general formula for sinusoidal power which is useful in analysis is based on the velocity potential Φ. From Eq. 1.1.12 it is seen that,

$$W \propto \operatorname{Im} \int_A \frac{\partial \Phi}{\partial t} \frac{\partial \Phi}{\partial n}\, dA$$

in which $\partial\Phi/\partial n$ is the normal derivative.

1.4. DIRECTIVITY OF RADIATED POWER

In a steady state field the intensity of acoustic energy flux (that is, real acoustic power per unit area) at a differential area where the pressure is p; and the particle velocity $\mathbf{V}$, is given by 1/2 Re$\{pV^*\}$, Sect. 1.3. Since the real power propagates out to infinity where the differential area over a spherical surface is $r_\infty^2 \sin\theta\, d\phi$, and where the pressure and particle velocity are related through the equation $p_\infty = \varrho c\, \mathbf{V}$, we see that the differential of real acoustic power is given by

$$dP = \frac{1}{2}\ \frac{p_\infty p_\infty^*}{\varrho c}\ r_\infty^2 \sin\theta d\theta d\phi. \tag{1.4.1}$$

Here the lower case symbol $p_\infty = p_0(\theta, \phi)\ \exp i(\omega t - kr + \pi/2)$. In the general case therefore the acoustic power has directivity in the spherical angles θ, ϕ. To investigate this directivity it is convenient to fix one variable (say ϕ) and plot $dP/d\theta$ vs. θ for the range of the variable. This plot defines the directivity of radiated power in the (variable) angle concerned. We thus have the following defining relations for the two variables θ, ϕ:

$$\theta \text{ directivity: } \frac{1}{2}\ \frac{p_\infty(\theta, \phi_0) p_\infty^*(\theta, \phi_0)}{\varrho c}\ r_\infty^2\ \sin\theta \quad \text{vs } \theta \tag{1.4.2}$$

This is sometimes called the θ-characteristic of the radiated power.

$$\phi \text{ directivity: } \frac{1}{2}\ p_\infty(\theta_0, \phi)\ p_\infty^*(\theta_0, \phi)\ r_\infty^2\ \sin\theta_0 \text{ vs } \phi \tag{1.4.3}$$

This is sometimes called the ϕ characteristic of the radiated power.

These formulas are useful in determining the proper location of a radiator for the most effective directional radiation of acoustic power into the far field ($r \to \infty$).

1.5. THE COMPLEX RADIATION PATTERN FUNCTION

The mean (real) power $\langle W_i \rangle$ radiated by an area A over a cycle of pressure varying sinusoidally with time ($= e^{-i\omega t}$) is given by Eq. 1.3. (3). This may be rewritten in the form

$$\langle W_i \rangle = \frac{1}{4} \int_A (PV_n^* + P^* V_n)\, dA. \tag{1.5.1}$$

Here V_n is normal to A. By use of Eqs. 1.1. (4) and (5) we may write $\langle W_i \rangle$ as

$$\langle W_i \rangle = \frac{i\ \varrho\, ck}{4} \int_A \left(\Phi\ \frac{\partial \Phi^*}{\partial n} - \Phi^*\ \frac{\partial \Phi}{\partial n} \right) dA. \tag{1.5.2}$$

We now assume an origin of coordinates on or near a radiating source and let r_0, r, R, be the distances from this origin to the source point, from the source point to the observation point and from the origin to the observation point respectively. For outgoing waves diverging to infinity the asymptotic form of the velocity potential in terms of the spherical coordinates (R, θ, φ) is,

$$\text{(a)}\quad \Phi_{R\to\infty} \to K(\theta, \phi)e^{ikR}/R, \qquad \text{(b)}\quad K(\theta, \phi) = K_1 + K_2. \tag{1.5.3}$$

The dimensions of K are (meter^3/sec). Now for $R \to \infty$, $\partial\Phi/\partial n = \partial\Phi/\partial R = ik\Phi - \Phi/R \sim ik\Phi$. Therefore the mean real power can be written,

$$\langle W_i \rangle = \frac{\varrho ck^2}{2} \int_A \Phi\Phi^* \, dA. \tag{1.5.4}$$

This is readily seen from the above formulas to take on the form

$$\langle W_i \rangle = \frac{\varrho ck^2}{2} \int_0^{2\pi} d\phi \int_0^{\pi/2} |K(\theta, \phi)|^2 \sin\theta d\theta \tag{1.5.5}$$

The integration over real angles θ thus gives real power radiated to infinity. The same formula may be used to obtain reactive power. An idea, first developed by Bouwkamp [3], consists in extending the integration over the variable θ_{in} Eq. 1.5.5 to all complex angles, and then taking the imaginary part of the result to form the *reactive power.* In Bouwkamp's notation the total complex peak amplitude of power w, whose imaginary part is the peak *amplitude* of reactive power, is given by the formula

$$w = \varrho_0 ck^2 \int_0^{2\pi} d\phi \int_0^{\pi/2 + i\infty} |K(\theta, \phi)|^2 \sin\theta d\theta. \tag{1.5.6}$$

Here,

$$w = w_1 + iw_2$$

The reason for the choice of the limit $+ i\infty$ rather than $- i\infty$ is developed in Chap. VI. Since this amplitude fluctuates in time $\exp(-i\omega t)$ the root-mean-square average power is 1/2 of the peak. The rms real power is Eq. 1.5.5. The rms reactive power is,

$$w_2 = \text{Im} \left\{ \frac{\varrho_0 ck^2}{2} \int_0^{2\pi} d\phi \int_0^{\pi/2 + i\infty} |K(\theta, \phi)|^2 \sin\theta d\theta \right\} \tag{1.5.7}$$

An application of this formula to the case of radiation from a membrane in an infinite rigid plane is described in Sect. 6.5.

1.6. VECTOR SPECIFIC ACOUSTIC ADMITTANCE

For sinusoidal varying field quantities with time given by the real part of $e^{-i\omega t}$ the ratio of vector particle velocity $\boldsymbol{u}$ to scalar pressure p is defined to be the *vector acoustic admittance* $\boldsymbol{Y}$. From Eqs. 1.1 (4), 1.1 (5) we find this admittance to be

$$\vec{Y} = \frac{-\nabla\Phi}{\varrho\partial\Phi/\partial t} = \frac{\nabla\Phi}{i\omega\varrho\Phi} \quad \text{(units: } m^3 N^{-1} s^{-1}\text{)}. \tag{1.6.1}$$

In the practical generation of sound by an area A_k it is the normal component of velocity u_k $(= -\partial\Phi/\partial n)$ that generates the acoustic power that reaches the far field. Computation of admittance is therefore usually confined to the normal component Y_k, which is seen to be

$$Y_n = (\partial\Phi/\partial n)/i\omega\varrho\Phi. \tag{1.6.2}$$

The convention used here is that the normal n to a vibrating surface points away from the medium facing the surface. The reciprocal Y_n^{-1} is called the normal specific acoustic impedance Z_n. When there are two areas i, j, the ith area generating sinusoidal acoustic pressure and the jth area receiving acoustic pressure, the interaction force F upon the jth area due to the ith area is written $(F_i)_j$. Corresponding to this force is a normal interaction acoustic impedance Z_{ij} defined by the formula

$$Z_{ij} \equiv \frac{(F_i)_j}{V_i}\ , \ V_i \equiv \text{reference velocity, independent of coordinate.} \tag{1.6.3}$$

Now the vector acoustic power received by jth area is $(1/2)(F_i)_j\,(V_j)$, which in conjunction with Eq. 1.3. (4d) shows that the interaction impedance may be calculated from

$$Z_{ij} \equiv \frac{1}{(V_i V_j^*)_{Av}} \int_{A_j} P_i V_j^* dA_j,\ V_j = \text{ vel. normal to } A_j. \tag{1.6.4}$$

Note that the interaction impedance between two radiating areas is in general a function of their normal velocities. In particular cases (and sometimes for pure convenience) V_j^* is assumed independent of coordinate (i.e., a constant). Then the approximation is made that

$$Z_{ij} = \frac{1}{V_i} \int_{A_j} P_i dA_j. \tag{1.6.5}$$

Radiation impedance is discussed in greater detail in Chap. VI.

When Y_n and Z_n are available they may be used to calculate the radiated intensity of the field. From the definition of the velocity potential and from 1.3.3b it is seen that,

$$I_n = \tfrac{1}{2}\,\omega^2\varrho^2\,\mathrm{Re}\{\Phi\, Y_n \Phi^*\} \tag{1.6.6}$$

or

$$I_n = \tfrac{1}{2}\,\mathrm{Re}\{\vec{\nabla}\Phi\, Z_n \cdot (\vec{\nabla}\Phi)^*\}. \tag{1.6.7}$$

1.7. ACOUSTIC SOURCES AND THEIR ASSOCIATED ACOUSTIC FIELD

An acoustic field exhibits time-varying energy per unit volume at an observation point r, t. The instantaneous acoustic power per unit area $I(r, t)$ of this volume is defined in Sect. 1.2 as the product of the pressure $p(r, t)$ and the particle velocity $\vec{u}(r, t)$.

$$\vec{I}(r, t) = p(\vec{r}, t)\,\vec{u}(\vec{r}, t) \tag{1.7.1}$$

Since the measured pressure is a scalar quantity it is very convenient to describe the acoustic field by a scalar velocity potential $\psi(r, t)$ which is defined by the pair of field relations,

$$\text{(a)}\quad p(\vec{r}, t) = \varrho_0(\vec{r}, t)\ \frac{\partial\psi}{\partial t}\ (\vec{r}, t). \quad \text{(b)}\quad \vec{u}(\vec{r}, t) = -\vec{\nabla}\psi(\vec{r}, t) \tag{1.7.2}$$

(see Sect. 1.1) in which ϱ_0 is the local equilibrium mass density. A source of acoustic pressure is therefore also a source of acoustic velocity potential. Let $q(\vec{r}_0, t)$ (units: $m^3S^{-1}m^{-3}$) be such a source at point $\vec{r}_0$, t_0. The potential field at this point may be modeled, with lesser or greater complexity depending on the number of terms used the pressure-density relation of Sect. 1.1. A simple model, based on 1.1.1, is:

$$-\nabla^2\psi(\vec{r}_0, t) + \frac{1}{c^2}\frac{\partial^2\psi}{\partial t^2}(\vec{r}_0, t) = 4\pi q(\vec{r}_0, t) \tag{1.7.3}$$

It states that if the source output q increases with time there is an increase in the concentration of velocity potential ($= -\nabla^2\psi$) at the observation point, which, because of wave formation, simultaneously increase the potential propagating away ($= c^{-2}\partial^2\psi/\partial t^2$). The factor 4π, inserted by some authors, and omitted by others, has its origin in electrostatic theory. In this theory the electrostatic potential due to a unit charge at $\vec{x}'$ is $1/r$, $r = |\vec{x} - \vec{x}'|$, and the scalar potential at $\vec{x}$ due to a charge $q(x')$ is the volume integral,

$$\Phi(\vec{x}) = \int_{\text{vol}} \frac{q(\vec{x}')}{|\vec{x}' - \vec{x}'|}\, d\vec{x}'$$

The Laplacian of $\Phi(\vec{x})$ in the $\vec{x}$ coordinates is then,

$$\nabla^2\Phi(\vec{x}) = \int_{\text{vol}} q(\vec{x}')\,\nabla^2\left(\frac{1}{|\vec{x} - \vec{x}'|}\right)d\vec{x}' = \int_{\text{vol}} q(\vec{x})\,(-4\pi\delta(\vec{x} - \vec{x}')\, d\vec{x}'$$

$$= -4\pi q(\vec{x})$$

This result is used by some authors to justify the use of 4π in the field 1.7.3 to describe sources. When there are no local sources at point r, t, 1.7.3 states that the tendency to concentrate potential there is balanced by dispersal of potential at the same point.

In addition to generating sound at source points acoustic sources can also be thought of as generating sound at distant observation points over a propagation path. The transfer function which connects the source field to observation field is the Green's function $G(r, t|r_0, t_0)$ of four variables. It is the field caused by a space-time impulse or delta function, and satisfies the linear small amplitude equation analogous to 1.7.3:

$$\left(\nabla_0^2 - \frac{1}{c^2}\frac{\partial^2}{\partial t_0^2}\right) G(\vec{r}, t|\vec{r}_0, t_0) = -4\pi\delta(\vec{r} - \vec{r}_0)\delta(t - t_0) \tag{1.7.4}$$

The units assigned to G are $m^{-1}s^{-1}$ as compared to the units of ψ which are m^2s^{-1}. The reason for this difference is that G is defined on the basis of per unit time per unit volume so that G transforms into ψ after an integration over volume and over time. Eq. 1.7.4 is an equation governing the propagation of a scalar (acoustic pressure) field. The propagation of a vector (particle velocity) field G is represented in terms of an operator L whose properties are such that,

$$L(\nabla_0, t_0)\,\vec{G}(\vec{r}, t|\vec{r}_0, t_0) = -\hat{a}\,4\pi\delta(\vec{r} - \vec{r}_0)\delta(t - t_0)$$

in which $\hat{a}$ is a unit magnitude vector.

Similarly the propagation of dyadic fields $\vec{\vec{G}}$ (say fields of mechanical stress in elastic solids) is governed by

$$L(\nabla_0, t_0)\,\vec{\vec{G}}(\vec{r}, t|\vec{r}_0, t_0) = -\hat{a}_i\hat{a}_j\,4\pi\delta(\vec{r}-\vec{r}_0)\,\delta(t-t_0)$$

In confined spaces the field may be represented as a collection of modes. Thus G in general is a matrix whose elements are scalars, vectors, and dyadics.

Radiation theory seeks to couple ψ(at a point $\vec{r}_0$, t_0) and G (between two points $\vec{r}$, $\vec{r}_0$ and t, t_0). This coupling is performed in two steps: in the first step 1.7.3 is multiplied by G, 1.7.4 by ψ, and the two equations are subtracted. In a second step two vectors $G\,\vec{\nabla}_0\,\psi$ and $\psi\,\vec{\nabla}\,G$ are formed and Green's theorem is then used to relate them to the following terms in the subtracted equation:

$$\int_v (G\,\nabla_0^2\,\psi - \psi\,\nabla_0^2 G)\,dV = \int (G\vec{\nabla}\,\psi - \psi\,\vec{\nabla}\,G)\cdot d\vec{S} \tag{1.7.5}$$

$$\frac{1}{c^2}\int\left(\psi\frac{\partial^2 G}{\partial t_0^2} - G\frac{\partial^2\psi}{\partial t_0^2}\right)dt_0 = \frac{1}{c^2}\left[\psi\frac{\partial G}{\partial t_0} - G\frac{\partial\psi}{\partial t_0}\right]_0^t \tag{1.7.6}$$

The positive direction of the normal to the elementary area $d\vec{S}$ is *away* from volume V. When the subtracted equation is integrated over volume and time, and 1.7.5, 1.7.6 are applied, an integral formulation of the velocity potential is obtained:

$$\begin{aligned}4\pi\psi(r, t) &= 4\pi\int_0^t dt_0\int_{\text{vol}} G(r, t|r_0, t_0)\,q(r_0, t_0)\,dV(r_0)\\ &+\int_0^t dt_0\int (G\,\vec{\nabla}_0\,\psi(r_0, t_0) - \psi(r_0, t_0)\vec{\nabla}_0 G)\cdot d\vec{S}(r_0)\\ &-\frac{1}{c^2}\int dV_0(r_0)\left[\frac{\partial G}{\partial t_0}\Big|_{t_0=0}\psi_0(r_0) - G\Big|_{t=0}\frac{\partial\psi_0}{\partial t}(r_0)\right]\end{aligned} \tag{1.7.7}$$

[4]. This is called here the *integral equation of the scalar velocity potential field.* The terms on the right had side have the following meaning: the first is the potential field created by the true sources q; the second is the field ψ_f due to reflection, scattering and diffraction of the first term, generated as if the surface S were rigid, plus a field ψ_v generated by surface motion v; the third is the field due to initial velocity potential $\psi_0(r_0)$ and its initial time-derivative $\partial\psi_0(r_0)/\partial t$. In general only q, ψ_0, $\partial\psi_0/\partial t$ may be specified. The surface-originated field (= second term), sometimes called the field of fictitious source, is therefore unknown. This makes 1.7.7 an integral equation.

When the volume V is free of reflecting surfaces 1.7.7 reduces to,

$$\psi(\vec{r}, t) = \int_0^t\int_v dt_0\,G(\vec{r}, t|\vec{r}_0, \vec{t}_0)\,q(\vec{r}_0, t_0)\,dV(\vec{r}_0) \tag{1.7.8}$$

By rearrangement, 1.7.7 can be cast in a form which reveals physically significant components. In the particular (but inportant) case in which G is constructed so that $\partial G/\partial n_0 = 0$, and in which the field is in steady state (time given by $\exp(-i\omega t)$), it can be written in the form,

$$\text{total field:}\qquad \psi(\vec{r}, t) = e^{-i\omega t}\{\psi_0(\vec{r}) + \psi_f(\vec{r}) + \psi_v(\vec{r})\}$$

$$\text{field of true sources:}\qquad \psi_0(\vec{r}) = \int G(\vec{r}|\vec{r}_0)\,q(\vec{r}_0)\,dV(\vec{r}_0)$$

$$\text{diffracted field:} \quad \psi_f(\vec{r}) = \frac{1}{4\pi} \int G(\vec{r}|\vec{r}_0) \frac{\partial \psi_0}{\partial n}(\vec{r})\, d\vec{r}_0 \tag{1.7.9}$$

$$\text{surface velocity field:} \quad \psi \ (\vec{r}) = \frac{1}{4\pi} \int G(\vec{r}|\vec{r}_0) \quad v_n(\vec{r}_0)\, d\vec{r}_0$$

[5].

Sources q have several physical causes of which only the most significant are used in applications. We consider these next.

1.8. SOUND GENERATED BY VOLUME DISTRIBUTED SOURCES

The physical agents that cause potential to be generated in a small volume of medium centered at a point r_0 are conveniently classifiable into two types:

(1) agents inducing time-varying changes in mass density.
(2) agents inducing time-varying net mechanical stresses.

These can be described with the help of Fig. 1.8.1. Here the field of velocity potential (that is, of sound) is contained in volume V which is bounded by surfaces S', S''. The volume source q is distributed over volume V_0 bounded by surface S_0. In V_0 the agents labelled (1) are summarized as follows:

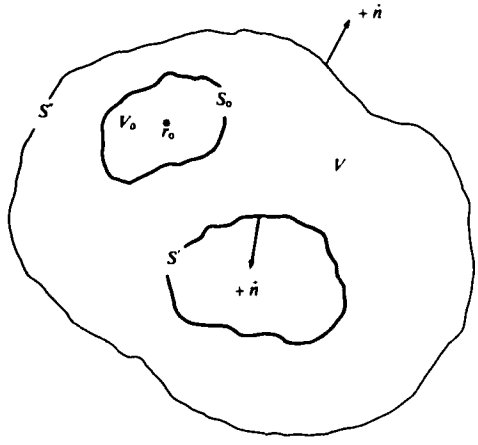

Fig. 1.8.1. Geometrical relations of volume sources.

(a) at point r_0 some device, or phenomenon, causes a flow of medium $Q(r_0, t_0)$ (units: $m^3 s^{-1} m^{-3}$) into or out of fixed volume V_0. Since this flow is a point phenomenon it is uniform in all directions, thereby making the generated potential omnidirectional

(b) at point r_0 some device causes a flow of heat $\epsilon(r_0, t_0)$ per unit volume (units: $Nms^{-1}m^{-3}$) For a medium of specific heat per unit volume C_p $\left(\text{units: } \frac{Nm}{m^3 °K}\right)$ this is equivalent to a time-varying flux of temperature ϵ/c_p (units: $°KS^{-1}$). If the same medium has an adiabatic compressibility $\gamma\kappa$ (units: m^2N^{-1}) where γ is the ratio of specific heat at constant pressure to specific heat at constant volume, the change in volume per unit volume due to a change in temperature is $\alpha\gamma K$, in which α is the change in pressure per unit temperature at constant volume, $\alpha = (\partial P/\partial T)_V$. Thus the source of potential at r_0 due to heat flow is $\epsilon\alpha\gamma\kappa/c_p$ (m^3s^{-1}/m^3). In calculating the measured acoustic pressure due to this potential by means of 1.7.2 one must consider the compressibility here to be a function of total pressure, $\kappa = \kappa(P(t))$. Because ϵ is a function of time as well, the time-derivative of this potential contains several terms, some negligible. This point is discussed in reference [6].

The agents labelled (2) are summarized as follows:

(a) across the small volume centered at r_0 some physical agency (gravitation, electromagnetism, etc.) induces a space-time varying body force $\vec{F}(r_0, t_0)$ per unit volume. For a medium of mass density ϱ the mass in the small volume undergoes an acceleration $\vec{F}/\varrho$ (units: ms^{-2}), whose net magnitude across V_0 is $\nabla\cdot(\vec{F}/\varrho)$. The velocity potential corresponding to this acceleration is,

$$\int_{-\infty}^{t} \nabla\cdot\left(\frac{\vec{F}(r_0, t_0)}{\varrho}\right) dt_0 \qquad \text{(units: } s^{-1}\text{)} \tag{1.8.1}$$

Since the vector divergence is an operation involving two mathematical points it yields a result dependent on angle. Hence this potential field directional.

(b) across the small volume centered at r_0 some physical agency (e.g. turbulence) induces a time varying body stress $\mathfrak{T}$ (units: Nm^{-2}) per unit volume. Since $\mathfrak{T}$ is specified by two directions and a magnitude, the mass in V_0 undergoes a net acceleration $\vec{\nabla}\cdot\mathfrak{T}/\varrho\cdot\vec{\nabla}$. The velocity potential corresponding to this acceleration is,

$$\int_{-\infty}^{t}(\vec{\nabla}\cdot\mathfrak{T}(r_0, t_0)/\varrho\cdot\vec{\nabla})\,dt_0 \qquad \text{(units: } s^{-1}\text{)} \tag{1.8.2}$$

This source of potential is clearly directional.

ASSIGNMENT OF SIGNS TO SOURCES OF VELOCITY POTENTIAL

The various sources described above have differing physical origin: one would then expect differing signs. The sources Q are associated with the first order equation of continuity

$$\frac{1}{P_0}\frac{\partial p}{\partial t} + \nabla\cdot\vec{V} = Q$$

while the sources attributable to force $\vec{F}$ are associated with the dynamic equation of motion

$$\varrho_0\frac{\partial\vec{V}}{\partial t} + \vec{\nabla}p = \vec{F}$$

This is explained in Sect. A.6. There it is seen that the formation of 1.7.3, requires the subtraction of the time-derivative of the equation of continuity from the divergence of the equation of motion. This mathematical manipulation makes the components of sources q to have differing signs:

$$q = Q + \frac{\varepsilon\alpha\gamma\kappa}{C_p} - \left[\int_{-\infty}^{t}\nabla\cdot\left[\frac{\vec{F}}{\varrho}(r_0, t_0) - \mathfrak{T}\frac{(r_0, t_0)}{\varrho}\cdot\vec{\nabla}\right]dt_0\right] \tag{1.8.3}$$

The opposite signs of forces in the brackets arises from this: $\vec{F}$ accelerates the mass in V_0 in the same direction as the acceleration, while $\mathfrak{T}\cdot\vec{\nabla}$, as it increases, accelerates this mass in opposite direction.

Sources q in 1.8.3 are the most important in the theory of radiation, but they do not include all possible sources. Of the latter the viscous sources have here been neglected.

VELOCITY POTENTIAL GENERATED BY VIBRATING SURFACES

When there are no volume distributed sources in a region where the surfaces S', or S'', or both, are vibrating, the potential field $\psi(r, t)$ in V, Fig. 1.8.1, is directly related to the fields $\psi(r_0, t_0)$, and $\partial\psi(r_0', t_0)/\partial t_0$, on the surface, as required by 1.7.7:

$$\psi(r, t) = \frac{1}{4\pi}\int_0^t dt_0\int_S[G\vec{\nabla}_0\psi(r_0, t_0) - \psi(r_0, t_0)\vec{\nabla}_0 G]\cdot dS(r_0) \tag{1.8.4}$$

in which the initial conditions have been suppressed. It is important to note that this equation is valid

only when $\vec{r}$ is not on surface S. For the case where $\vec{r}$ is allowed to approach $\vec{r}_0$ on S, the surface integral of $\nabla^2(1/\varrho)$ is -2π, so that

$$\nabla^2\left(\frac{1}{|\vec{\varrho}-\vec{\varrho}'|}\right) = -2\pi\,\delta(\vec{\varrho}-\vec{\varrho}')$$

$$" \qquad = 0 \quad \vec{\varrho} \neq \dot{\varrho}$$

Thus the 4π in 1.8.4 is replaced by 2π. The agency causing potential field $\psi(r_0, t_0)$ is the force on the medium delivered by the vibrating surface. Since the particle velocity anywhere in the medium is $\mathrm{v} = -\vec{\nabla}\psi$, and since the positive normal in Fig. 1.8.1 points away from V, the normal component of particle velocity of fluid adjacent to the surface is equal to the normal velocity v_n of the surface:

$$\partial\psi/\partial n = \mathrm{v}_z \qquad (\text{units: } m\,s^{-1}) \tag{1.8.5}$$

Here v_z is positive when pointing into the medium. For normal gradients only, 1.8.4 simplifies to:

$$\psi(r, t) = \frac{1}{4\pi}\int_0^t dt_0 \int_S \left[G(r, t|r_0, t_0)\,\mathrm{v}_n(r_0, t_0) - \psi(r_0, t_0)\,\frac{\partial G}{\partial n}(r, t|r_0, t_0)\right] dS. \tag{1.8.6}$$

The surface S includes S' and S''. In usual radiation problems, v_z is finite only over a small portion of S', and S'' acts as a reflector. When S'' is effectively at infinity there is no reflection: thus, one requires ψ to be such that,

$$\lim_{R_1\to\infty} \int_{S''} \left[G(r, t|r_0, t_0)\,\frac{\partial\psi}{\partial n}(r_0, t_0) - \psi(r_0, t_0)\,\frac{\partial G(r, t|r_0, t_0)}{\partial n}\,dS'' = 0\right] \tag{1.8.7}$$

in which $R_1 = |\underline{r} - \underline{r}_0|$. In this limit the radiation field is spherical,

$$\lim_{R_1\to\infty} 4\pi R_1^2\left[\frac{\partial\psi}{\partial R_1}(R_1, t_0) - \psi(R_1, t_0)\,\frac{\partial G}{\partial n/G}\right] = 0. \tag{1.8.8}$$

If G falls off as R_1^{-1}, and ψ falls off as R^{-1} (or faster), the limit will be satisfied. This is actually the case of an unbounded medium for which

$$G = \exp(ikR_1)/R_1 \tag{1.8.9}$$

For this special case Eq. 1.8.8 then becomes the *radiation condition* at infinity.

ANALYTIC SOLUTIONS OF EQ. 1.8.6

Eq. 1.8.6 is an integral equation relating $\psi(r, t)$ in V and $\psi(r_0, t_0)$ on S. Its solution in the general case requires application of numerical methods. These methods are discussed in Sect. 1.10. In particular cases, which occur frequently, an analytic solution can be obtained by restricting the ratio A/λ (radiating area to wavelength) to be either very large, or very small. First, when the radiated wavelength is small enough to make $|A/\lambda| \gg 1$, and when every portion of the radiating area is moving in phase, the mechanical resistance of the medium (defined as the ratio of $(\varrho\partial\psi/\partial t)/-\nabla\psi$ averages over area to the product of mass density and sound speed, ρ_c. Thus, over the radiating surface where the instantaneous velocity is v_z, a local velocity potential ψ is assumed to obey the relations,

$$p = \varrho \frac{\partial \psi}{\partial t} = \varrho c \ \ v_z, \text{ or } \frac{\partial \psi}{c \partial t} = v_z \tag{1.8.10}$$

Several simple formulas are obtained using this relation by assuming $\psi(r, t) = \psi(r) \exp(-i\omega t)$, and by further assuming that the medium is unbounded. Then 1.8.9 and 1.8.10 may be substituted into the ψ term of 1.8.6, yielding:

$$\psi \frac{\partial G}{\partial n} = \frac{v_n}{-ik} \left[-\frac{1}{R} + ik \right] \frac{\partial R}{\partial n} \left(\frac{\exp ikR}{R} \right), \quad k = \frac{\omega}{c} \tag{1.8.11}$$

At infinity $|1/R| \ll |k|$. Furthermore, Fig. 1.8.2 shows that when $R \to \infty$, $\partial R/\partial n$ decreases as R increases so that $\partial R/\partial n = -\cos \gamma$, provided the normal $\vec{n}$ points into volume V. Since in deriving 1.8.6 $\vec{n}$ is taken to point away from V, this means:

$$\frac{\partial R}{\partial n} = \cos \gamma \tag{1.8.12}$$

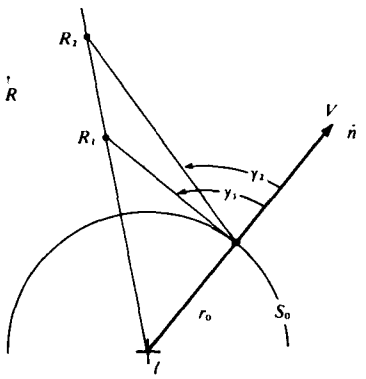

Fig. 1.8.2. The angle γ diminishes as R increases provided R "sees" r_0.

The velocity potential in the far field ($R \gg r_0 > \lambda$) then becomes,

$$\psi(\vec{R}) = \frac{1}{4\pi} \int \frac{\exp ik|R - r_0|}{|R - r_0|} \times v_n \ [1 + \cos \gamma] \, dS(r_0) \tag{1.8.13}$$

The factor 1 + cos γ is analogous to Kirchoff's correction to Fresnel diffraction theory. In a second case, an opposite extreme occurs when the radiated wavelength λ is very large so that $|A/\lambda| \ll 1$. In the far field both the R^{-1} and ik terms in 1.8.11 are negligible. Eq. 1.8.6 then reduces in the steady state to,

$$\psi(\vec{R}) = \frac{1}{4\pi} \int \frac{e^{ik|\vec{R} - \vec{r}_0|}}{|\vec{R} - \vec{r}_0|} \ v_n(r_0) \, dS(r_0) \tag{1.8.14}$$

A third case consists of a steady state solution of 1.8.6 when G is the free-space Green's function and the normal derivative to the vibrating surface is $\partial/\partial z$. Then,

$$\psi(\vec{r}|\omega) = \frac{1}{4\pi} \int_S \left[\frac{e^{ikR}}{R} \left(-\frac{\partial \psi}{\partial z} \right) - \psi \left\{ \frac{e^{ikR}}{-R^2} + \frac{ike^{ikR}}{R} \right\} \frac{\partial R}{\partial z} \right] dS$$

Again $\partial R/\partial z = \cos \gamma$ and $-\partial \psi/\partial z = v_z$. In the far field the term in R^{-2} is negligible. Also,

$$-ik\psi = \frac{p}{\varrho c}$$

Thus,

$$\psi(\vec{r}, \omega) = \frac{e^{-i\omega t}}{4\pi} \int_S \left\{ \left(v_z(\vec{r}_0) + \frac{p(\vec{r}_0)}{\varrho c} \cos \gamma \right) \right\} \frac{e^{ik|\vec{r} - \vec{r}_0|}}{|\vec{r} - \vec{r}_0|} \, dS(\vec{r}_0), \tag{1.8.15}$$

This is an integral equation in the velocity potential ψ or acoustic pressure $p = \varrho \partial \psi / \partial t = -ik\varrho\omega\psi_0$.

In these three cases the approach to solution of the integral equation 1.8.6 has been the modification of the $\psi \nabla G$ term so as to obtain a simple integral. The medium was taken to be unbounded (i.e. S'' in Fig. 1.8.1 is removed to infinity). A fourth analytic solution is made available by bounding the medium with a boundary on which the normal derivative of G vanishes. A simple procedure is to define a function $F(r|r_0)$ which satisfies Helmholtz's equation for steady waves, $(\nabla^2 + k^2) F = 0$, and which obeys the relations,

$$G(r|r_0) = g(r|r_0) + F(r|r_0)$$

$$\frac{\partial g}{\partial n_0} = - \frac{\partial F}{\partial n_0} \tag{1.8.16}$$

An oft-used example is the introduction of an infinite rigid plane boundary, effectively dividing the medium in two. Then 1.8.16 becomes,

$$G(R|R_0) = \frac{\exp ik|R_u - R_0|}{|R_u - R_0|} + \frac{\exp ik|R_l - R_0|}{|R_l - R_0|} \tag{1.8.17}$$

Where R_u, R_l are location vectors of points in the upper and lower half-spaces respectively. Upon forming $\partial G/\partial n_0$ it is seen from the definition of normal derivative n_0 that the second term is the negative of the first, so that the derivative vanishes on the plane. When a vibrating surface S is placed in the plane, and radiation in one half-space is considered the velocity potential is given by 1.8.6 to be,

$$\psi(\vec{R}) = \frac{1}{2\pi} \int_{s'} \frac{\exp ik|\vec{R} - \vec{R}_0|}{|\vec{R} - \vec{R}_0|} \, v_n(\vec{R}_0) \, dS(R_0) \tag{1.8.18}$$

This is Rayleigh's formula for radiation from a rigid plane in the steady state. When the vibration is transient the potential becomes,

$$\psi(\vec{R}, t) = \frac{1}{2\pi} \int_0^{'} dt_0 \int dS(\vec{R}_0) \, v_n(\vec{R}_0, t_0) \quad \frac{\delta[|\vec{R} - \vec{R}_0|/c - (t - t_0)]}{|\vec{R} - \vec{R}_0|} \tag{1.8.19}$$

The possibility of generating analytic solutions of the integral equation 1.8.6 by constructing a G such that $\partial G/\partial n$ vanishes on the boundary surface is greatly enhanced when the surface has special geometric forms. These forms can be thought of as 3-dimensional waves which initially conform to the shape of the vibrating surface and the propagate out to infinity without change of shape. Examples are plane waves, spherical waves, cylindrical waves, etc. They are called separable wave solutions of the Helmholtz steady state wave equation, $(\nabla^2 + k^2) \psi = 0$. There are 11 such separable coordinate systems. For them it is always possible to construct a Green's function such that $\partial G/\partial n_0$ vanishes on S. Thus the integral equation 1.8.6 is always analytically solvable (at least formally) if the radiation has a waveform in steady state agreeing with, or conforming to, one of these separable systems. The appropriate field equation is then

$$\psi(\vec{R}) = \frac{1}{4\pi} \int_s G(\vec{R}|\vec{R}_0) \, v_n(\vec{R}_0) \, dS(\vec{R}_0) \tag{1.8.20}$$

$$\frac{\partial G(\vec{R}|\vec{R}_0)}{\partial n} = 0, \text{ on } S$$

BOUNDARY CONDITIONS

In Fig. 1.8.1 the surface S' can be thought of as dividing two regions of acoustic fields: ψ_i inside S' and ψ_0 outside. When S' is the simple division surface the particle velocity must be continuous across it,

$$-\frac{\partial \psi_1}{\partial n} = -\frac{\partial \psi_2}{\partial n} \tag{1.8.21}$$

When however the radiating surface has a local specific acoustic admittance y_s, defined here as the ratio $-\nabla\psi/\psi$ (units: m^{-1}), then the difference of potentials across the surface is,

$$\psi_2 - \psi_1 = \frac{v_z}{y_S} \tag{1.8.22}$$

$$y_S = g_S + ib_S \tag{1.8.23}$$

The symbol g is the specific acoustic conductivity and b is the specific acoustic susceptance. Multiplication of y_S by area gives the acoustic admittance,

$$y_A = y_S S \qquad \text{(units: } m\text{)}$$

$$y_A = g_A + ib_A \tag{1.8.24}$$

The symbol g_A is the acoustic conductivity and b_A is the acoustic susceptance. A frequently quoted example of y_A is that of a small hole of diameter d much smaller than a wavelength. It is nearly a pure conductivity of value $g_A = d$, [7] Rayleigh "The Theory of Sound", Vol. 2, Sect. 306. Dove Publications, 1945.

An alternate statement of boundary condition arises from the dynamical relation that the negative gradient of pressure at the surface must equal the mass acceleration of the fluid at the surface. Choosing the normal n to be positive away from the medium and the normal component of fluid velocity v_z to be positive into the medium one writes the boundary condition as,

$$-\frac{\partial p}{\partial n} = \varrho_0 \frac{\partial v_n}{\partial t} = -\varrho_0 \frac{\partial v_z}{\partial t}$$

Because $p = \varrho_0 \dfrac{\partial \psi}{\partial t}$, it is seen that,

$$\frac{\partial \psi}{\partial n} = v_z$$

$\nabla\psi \cdot \nabla n = \partial/\partial n = \partial/\partial z$. Hence, the general boundary condition at the surface is,

$$-\frac{\partial \psi}{\partial z} = v_z \tag{1.8.25}$$

1.9. EIGENFUNCTION SOLUTIONS OF THE DIFFERENTIAL EQUATION OF THE SCALAR VELOCITY POTENTIAL FIELD

The calculation of the radiated acoustic field is often accomplished by solving the differential equation 1.7.3 for points in volume V, Fig. 1.8.1, subject to the boundary condition 1.8.5 on surface S'' (as it is removed to infinity) and the continuity condition 1.8.7 on surface S'. If the field $\psi(r, t) = \psi(r)e^{-i\omega t}$ the solution of the differential equation $(\nabla^2 + k^2)\,\psi(r, t) = 0$ is directly obtainable in separated form $\psi(r) = \Psi(\xi_1)\,\Psi(\xi_2)\,\Psi(\xi_3)$, provided the coordinate system ξ_i, $i = 1, 2, 3$ is separable, that is, it is one of 11 known systems [8]. Each $\Psi(\xi_i)$ is governed by an ordinary differential equation of the form,

$$\frac{d}{d\xi}\left[p(\xi)\,\frac{d\Psi}{d\xi}\right] + [q(\xi) + \lambda r(\xi)]\Psi = 0 \tag{1.9.1}$$

in which λ is a separation constant and $r(\xi)$ is a weight function. The solution Ψ depends on λ, that is, $\Psi = \Psi(\xi; \lambda)$, while λ itself depends on the boundary conditions,

$$p(\xi)\,\frac{d\Psi(\xi)}{d\xi} + \alpha_{a,b}\,\Psi(\xi) = 0, \quad \xi = \xi_a, \xi_b \tag{1.9.2}$$

Here, α_a is a constant corresponding to one terminus ξ_a of the range ξ, and α_b is a second constant at terminus ξ_b. Since the solution Ψ is bounded in ξ, one can expect solutions Ψ_m of 1.9.1 only for discrete λ_m, $m = 1, 2, \cdots$. **For real p, q, r all the eigenvalues λ_m are real, and the eigenfunctions (or modes) ψ_m from an orthgonal set, meaning that any field variable $f(\xi)$ can be represented as a sum of eigenfunctions,**

$$f(\xi) = \sum_m f_m \Psi_m(\xi), \quad f_m = \frac{\int r(\xi)\, f(\xi)\, \Psi_m(\xi)\, d\xi}{N_m}. \tag{1.9.3}$$

$$N_m = \int r(\xi)\,[\Psi_m(\xi)]^2\, d\xi.$$

in which the range of integration is over the range of ξ between its boundaries. When the range of ξ is infinite the eigenvalues λ and the eigenfunction $\Psi(\xi; \lambda)$ form continua. The solutions then for the field of velocity potential are:

$$\psi(r, \omega) = e^{-i\omega t}\int_{-\infty}^{\infty} f(\lambda_1)\,\Psi(\xi_1; \lambda_1)\,\Psi(\xi_2; k^2, \lambda_1)\, d\lambda_1, \text{ 2-dimensions}$$

$$\psi(r, \omega) = e^{-i\omega t}\int_{-\infty}^{\infty}\int_{-\infty}^{\infty} f(\lambda_1, \lambda_2)\,\Psi(\xi_1; \lambda_1)\,\Psi(\xi_2; \lambda_2)\,\Psi(\xi_3; k^2, \lambda_1, \lambda_2)\, d\lambda_1\, d\lambda_2 \quad \text{3-dimensions} \tag{1.9.4}$$

$$\vec{r} = \vec{r}(\xi_1, \xi_2, \xi_3), \quad \lambda_3 = \lambda_3(k^2; \lambda_1, \lambda_2)$$

[9]. Here, $f(\lambda_1)$, $f(\lambda_1, \lambda_2)$ are analogous to constants in expansion in Fourier series. In applications to calculation of radiation of sound both model solutions, 1.9.3 and continuum solutions 1.9.4 are used, sometimes in the same problem. These formulas, when applied to cylindrical, spherical, spheroidal geometrics, provide the following radiation models.

1.9a. RADIATION OF SOUND FROM AN INFINITELY LONG CYLINDER OF CIRCULAR CROSS SECTION

In cylindrical coordinates r, ϕ, z, Fig. 1.9.1, the Helmholtz equation for steady waves has the factored solution,

$$\psi(r, \phi, z, t) = e^{-i\omega t} R(r)\, \Psi(\phi)\, Z(z) \tag{1.9.5a}$$

in which

$$\frac{1}{r}\ \frac{d}{dr}\left(r\,\frac{dR}{dr}\right) = -\left(k_r^2 - \frac{m^2}{r^2}\right) R = \nabla_r^2 \tag{1.9.5b}$$

$$\frac{d^2\Psi}{d\phi^2} = -m^2\Psi = \nabla_\phi^2 \tag{1.9.5c}$$

$$\frac{d^2Z}{dZ^2} = -k_z^2 Z = \nabla_z^2 \tag{1.9.5d}$$

where ∇_r^2, ∇_ϕ^2, ∇_z^2 are connected to the Laplacian operator ∇^2 by

$$\nabla^2 = \nabla_r^2 + \nabla_\phi^2 + \nabla_z^2 \tag{1.9.5e}$$

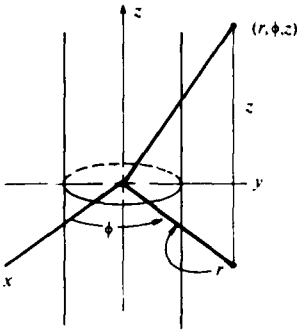

Fig. 1.9.1. Cylindrical Coordinates

Substitution of 1.9.5 into

$$(\nabla^2 + k^2)\psi = 0 \tag{1.9.6}$$

places a restriction on possible value of k_r, k_z (but none on m):

$$k^2 = k_r^2 + k_z^2 \tag{1.9.7}$$

The problem of radiation of velocity potential from an infinitely long circular cylinder can be solved in this coordinate system. First, since $\Psi(\phi)$ is periodic in 2π one takes m to be an integer, and the associated eigenfunctions to be $\cos m\phi$ and $\sin m\phi$. These form a system of modes. Second the solution of 1.9.5b in outgoing waves is the Hankel function of the first kind $H_m^{(1)}(k,r)$. This solution though subscripted m is a continuum in $k_z = \sqrt{\lambda}$. Third, the solution of 1.9.5d is $Z(k_z, \omega)$, as yet unspecified. This is a continuum both in k_z and in ω. Assembling all factored solutions yields the potential field everywhere,

$$\psi(r, \phi, k_z, \omega) = e^{-i\omega t} \sum_m \left[C_m \cos m\phi + D_m \sin m\phi\right] Z(k_z, \omega)\, H_m^{(1)}\left(r\sqrt{k^2 - k_z^2}\right) \tag{1.9.8}$$

Here C_m, D_m are constants which are to be determined from boundary conditions on the radial component of surface velocity $V(\phi, z, t)$. The latter, because $\Psi(\phi)$ and $Z(z)$ are separated, has the form,

$$V(\phi, z, t) = \Psi(\phi)\, Z(z, t) \tag{1.9.9}$$

so that the specification for $Z(k_z, \omega)$ is,

$$Z(k_z, \omega) = \int_{-\infty}^{\infty}\int Z(z, t) e^{-ik_z z + i\omega t}\, dz dt$$

In these terms,

$$V(\phi, k_z, \omega) = \sum_m \left[A_m \cos m\phi + B_m \sin m\phi\right] Z(k_z, \omega) e^{-i\omega t} \tag{1.9.10}$$

Here, A_m, B_m are Fourier coefficients:

$$A_m = \frac{\int_0^{2\pi} V(\phi) \cos m\phi \, d\phi}{\int_0^{2\pi} \cos^2 m\phi \, d\phi} \; ; B_m = \frac{\int_0^{2\pi} V(\phi) \sin m\phi \, d\phi}{\int_0^{2\pi} \sin^2 m\phi \, d\phi}$$

This is again a representation which contains both modal and continuum factors. On the surface of the cylinder $r = R_0$ this velocity is related to the velocity potential field 1.9.8 through the boundary condition 1.8.25:

$$- \frac{\partial \psi}{\partial r} \Big|_{r=R_0} = V \tag{1.9.11}$$

Substitution of 1.9.8 and 1.9.10 into 1.9.11 leads to:

$$C_m = - \frac{A_m}{\sqrt{k^2 - k_z^2}\, H_m^{(1)'}(R_0\sqrt{k^2 - k_z^2})} \; ; \quad D_m = - \frac{B_m}{\sqrt{k^2 - k_z^2}\, H_m^{(1)'}(R_0\sqrt{k^2 - k_z^2})} \tag{1.9.12}$$

$$H_m^{(1)}(q) = dH_m^{(1)}(q)/dq$$

With this result, and using 1.9.4 one arrives at the potential field everywhere in volume V (for the unbounded domain) by integration of 1.9.8 over k_z and ω:

$$\psi(r, t) = \frac{-1}{(2\pi)^2} \int_{-\infty}^{\infty} d\omega \int_{-\infty}^{\infty} dk_z \sum_m \left(A_m \cos m\phi + B_m \sin m\phi\right) Z(k_z, \omega)$$

$$\times \frac{H_m^{(1)}(r\sqrt{k^2 - k_z^2})\, e^{-i\omega t}}{\sqrt{k^2 - k_z^2}\, H_m^{(1)'}(R_0\sqrt{k^2 - k_z^2})} \tag{1.9.13}$$

Since the integral contains singularities on the real axis one must take k_z to be a complex variable and evaluate the integral by contour integration in the complex plane. This is explained in Appendix I at the end of this chapter. The radiated sound field generated by the velocity distribution $V(\phi, z, t)$ (specified arbitrarily by 1.9.10); and the particle velocity $\vec{u}$ everywhere, are readily obtain from 1.9.13:

$$p(r, \phi, z, t) = \varrho \frac{\partial \psi(r, \phi, z, t)}{\partial t} \; ; \vec{u}(r, \phi, z, t) = - \nabla \psi(r, \phi, z, t) \tag{1.9.14}$$

1.9b. RADIATION OF SOUND FROM A CYLINDER OF ELLIPTICAL CROSS—SECTION

An infinitely long cylinder of elliptical cross-section is a good geometrical model for the study of radiation from a vibrating strip in an infinite medium. The coordinate description of the cross-section is shown in Fig. 1.9.2. Here the coordinate transformation from rectangular coordinates x, y to orthogonal curvilinear coordinates μ, ϕ is conveniently expressed in complex form,

$$\mu + i\vartheta = w = \cosh^{-1}\left(\frac{2z}{a}\right) \tag{1.9.15}$$

$$Z = x + iy$$

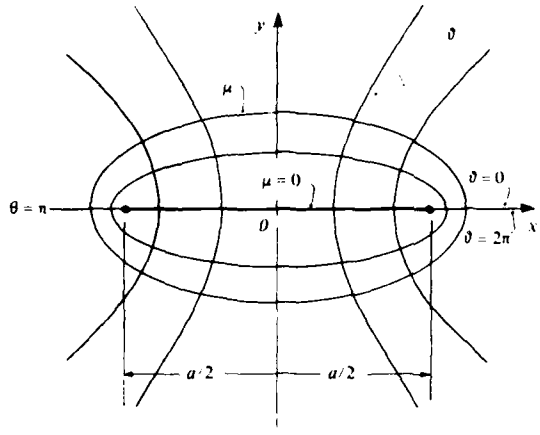

Fig. 1.9.2. Elliptic coordinates.

in which $x = \pm a/2$ are the locations of the foci of the ellipse, μ = const. form a family of confocal ellipses, and ϑ = const. form a family of confocal hyperbolas. In real terms,

$$x = \frac{a}{2} \cosh\mu \cos\vartheta; \; y = \frac{a}{2} \sinh\mu \sin\vartheta \tag{1.9.16}$$

The scale factors h_μ, h_ϑ needed to give μ, ϑ the dimensions of length are defined by,

$$h_\mu^2 = \left(\frac{\partial x}{\partial \mu}\right)^2 + \left(\frac{\partial y}{\partial \mu}\right)^2;$$

$$h_\vartheta^2 = \left(\frac{\partial x}{\partial \vartheta}\right)^2 + \left(\frac{\partial y}{\partial \vartheta}\right)^2$$

so that,

$$h_\mu = h_\vartheta = \frac{a}{2} \sqrt{\sinh^2\mu + \sin^2\theta} = \frac{a}{2} \sqrt{\cosh^2\mu - \cos^2\theta} \tag{1.9.17}$$

In these elliptic coordinates the Helmholtz equation for steady state velocity potential reduces to,

$$\nabla\cdot\nabla\psi + k^2\psi = 0$$

or

$$(\nabla_\theta^2 + \nabla_\mu^2 + k^2 h_\vartheta^2)\,\psi = 0, \quad \psi = \psi(\mu, \vartheta) \tag{1.9.18}$$

in which the gradient operation (needed later) in directions $\vec{a}_\mu$, $\vec{a}_\vartheta$ is:

$$\vec{\nabla}\psi = \frac{2}{a h_\vartheta} \left[\vec{a}_\mu \frac{\partial \psi}{\partial \mu} + \vec{a}_\vartheta \frac{\partial \psi}{\partial \vartheta}\right] \tag{1.9.19}$$

Since the Helmholtz equation is factorable in elliptic coordinates, it separates into two ordinary differential equations [9],

$$\frac{d^2\Theta}{d\vartheta^2} = -(b - h^2\cos^2\vartheta)\,\Theta = \nabla_\vartheta^2 \tag{1.9.20}$$

$$\frac{d^2M}{d\mu^2} = (b - h^2\cosh^2\mu)\,M = \nabla_\mu^2 \tag{1.9.21}$$

$$\psi = M(\mu)\,\Theta\,(\vartheta)$$

in which b is a separation constant. Substitution of 1.9.20 and 1.9.21 into 1.9.18 places a restriction on h. It must be taken as $ka/2$, which is a measure of the 'acoustic size' of the elliptical cross-section. Fig. 1.9.2 shows that the separated solution Θ can be periodic in π or in 2π, along an ellipse μ = const.

This double periodicity is possible only if b forms a family of discrete numbers (that is, eigenvalues), making Θ_m a complete set of eigenfunctions. The double periodicity is due to the fact that the degenerate ellipse $\mu = 0$ lies in the x-axis and thus becomes a unique *line* in the cross-section of the strip. This is in contrast to cylinders of circular cross-section for which the only degeneracy is the zero-radius *circle* at the origin in the xy plane.

There are four types of eigenfunction solutions (called angular Mathien functions) of 1.9.20 which arise because Θ can be either an even or an odd function of ϑ, and can be periodic over the π or 2π ranges noted above. These types are designated by standard symbols S_e, S_o indicating even or odd, and subscripted by $2m$ or $2m + 1$, indicating range of periodicity. A simpler set of symbols, convenient for this discussion, is listed in the following table. In it there also appears a list of symmetriesof $\Theta(\vartheta)$ about $\vartheta = \text{const.}$

Table 1.9.1. Symbols of Angle Mathieu Functions

Standard symbol	this text	periodicity angle	symmetry of Θ about $\vartheta = \text{const.}$
$Se_{2m}(h, \cos\vartheta)$	$T(2m, h, \vartheta)$	π	symmetrical about $\vartheta = \pi/2$ and $3\pi/2$
$Se_{2m+1}(h, \cos\vartheta)$	$U(2m + 1, h, \vartheta)$	2π	symmetrical about $\vartheta = \pi$
$So_{2m}(h, \cos\vartheta)$	$V(2m, h, \vartheta)$	π	antisymmetrical about $\vartheta = \pi/2$ and $3\pi/2$
$So_{2m+1}(h, \cos\vartheta)$	$W(2m + 1, h, \vartheta)$	2π	antisymmetrical about $\vartheta = \pi$

The integer subscripts $2m$, $2m + 1$ designates the order of the Mathieu function. These angle functions can be pictured roughly as single cycle or double cycle sines or cosines in the range $0 \leqslant \vartheta \leqslant 2\pi$:

T: has the symmetry of a single cycle cosine.
U: has the symmetry of a double cycle cosine.
V: has the symmetry of a single cycle sine curve.
W: has the symmetry of a double cycle sine curve.

Although pictured as sinusoidal T, U, V, W are, in general, complicated functions of angle ϑ, which, because they are periodic can be expanded in Fourier series:

$$
\begin{aligned}
T &= \sum_{m=0}^{\infty} B_T(2m, h, 2m)\cos 2m\vartheta, & \sum_m B_T &= 1 \\
U &= \sum_{m=0}^{\infty} B_U(2m + 1, h, 2n + 1)\cos(2n + 1)\vartheta, & \sum_m B_U &= 1 \qquad (1.9.22) \\
V &= \sum_{m=0}^{\infty} B_V(2m, h, 2m)\sin 2m\vartheta, & \sum_m B_V &= 1 \\
W &= \sum_{m=0}^{\infty} B_W(2m + 1, h, 2m + 1)\sin(2n + 1)\vartheta, & \sum_m B_W &= 1
\end{aligned}
$$

The integers $2n$, or $2n + 1$, designate the order of the sine or cosine function in this expansion.

All T, U, V, W are orthogonal in the range $0 \leq \vartheta \leq 2\pi$. Their normalizations are:

$$(1) \int_0^{2\pi} T^2 d\vartheta = M_T(2m, h); \quad (2) \int_0^{2\pi} U^2 d\vartheta = M_U(2m + 1, h) \quad (3) \int_0^{2\pi} V^2 d\vartheta = M_V(2m, h)$$

$$(4) \int_0^{2\pi} W^2 d\vartheta = M_W(2m + 1, h) \tag{1.9.23}$$

Since T, U, V, W can be calculated by numerical procedures it has proven useful to tabulate the expansion coefficients B [10]. In such tables it is usual to find B normalized in a manner to make $T = 1$ for $\vartheta = 0$ for all h. During the calculation of B the allowed values of the separation constants (i.e. the eigenvalues) are also calculated.

The solutions of 1.9.21 are radial Mathieu functions, $R_1(2m, h, \mu)$ and $R_2(2m, h, \mu)$. They can be represented by expansions in Bessel functions J_n and Neuman functions N_n using the same expansion coefficients B_T from 1.9.22:

$$R_1(2m, h, \mu) = \sqrt{\frac{\pi}{2}} \sum_{m=0}^{\infty} (-1)^{n-m} B_T(2m, h, 2n) J_{2n}(h \cosh \mu) \tag{1.9.24}$$

$$R_2(2m, h, \mu) = \sqrt{\frac{\pi}{2}} \sum_{m=0}^{\infty} (-1)^{n-m} B_T(2m, h, 2n) N_{2n}(h \cosh \mu) \tag{1.9.25}$$

$$R_2(2m, h, \mu) = \frac{1}{B_T(2m, h, \vartheta)} \sqrt{\frac{\pi}{2}} \sum_{m=0}^{\infty} (-1)^{n-m} \quad B_T(2m, h, 2n) N_m\left(\frac{h}{2} e^{\mu}\right) J_n\left(\frac{h}{2} e^{-\mu}\right)$$

Here again $2m$ designates the order of the Mathieu function and n designates the order of the sine or cosine expansion term. The Wronskian of these solutions, often used in the calculation of radiation from strips, is specifically made unity by proper choice of B:

$$\Delta(R_1, R_2) = R_1 R_2' - R_2 R_1' = 1 \tag{1.9.26}$$

In the problem of modeling the radiation of acoustic velocity potential from an infinitely long strip, width a, vibrating in an unbounded medium, the strip is taken to be a degenerate ellipse, $\mu = 0$, whose normal component of surface velocity ϑ_n is distributed in the manner shown in Fig. 1.9.3. For $y > 0$, ϑ_n points out of the ellipse; for $y < 0$ it points into the ellipse. Thus,

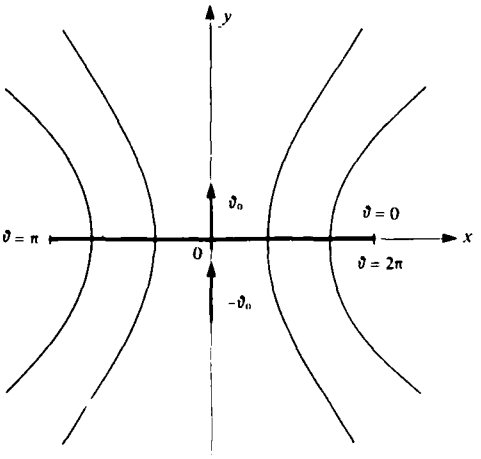

Fig. 1.9.3. Model of a vibrating strip.

$$\begin{aligned} \vartheta_n &= \vartheta_0 e^{-i\omega t} \quad 0 < \vartheta < \pi \\ \vartheta_n &= -\vartheta_0 e^{-i\omega t} \quad \pi < \vartheta < 2\pi \end{aligned} \tag{1.9.27}$$

To begin the analysis it is first required to find the relation between specified ϑ_n and unknown velocity potential ψ. At the boundary the requirement posed by 1.8.25 is:

$$\nabla_\mu \psi \big|_{\mu=0} = \frac{1}{h\mu} \frac{\partial \psi}{\partial \mu} \Big|_{\mu=0} = -\vartheta_n$$

From 1.9.17, $h_\mu = h_\vartheta = a/2 \sin \vartheta$, so that

$$\frac{\partial \psi}{\partial \mu}\Big|_{\mu=0} = -\frac{a}{2}\sin\vartheta v_0 \tag{1.9.28}$$

This means gradient ψ is negative for $y > 0$ and positive for $y < 0$. Since ϑ_n is antisymmetric about $\vartheta = \pi$, and periodic in period 2π, 1.9.28 can be expanded in angle eigenfunctions W (see Table 1.9.1):

$$\frac{\partial \psi}{\partial \mu}\Big|_{\mu=0} = -\frac{a}{2} v_0 \sin\vartheta = \sum_m A_m W(2m+1, h, \vartheta)$$

Multiplying both sides by W, integrating ϑ from 0 to 2π, and using the orthogonal properties of W, 1.9.23, lead to:

$$-\frac{a}{2} v_0 \sum_{m=0}^{\infty} B_w(2m+1, h, 2m+1) \int_0^{2\pi} \sin[(2n+1)\vartheta] \sin\vartheta d\vartheta = A_m M_w(2m+1, h)$$

Only $n = 0$ is finite. Hence,

$$\frac{\partial \psi}{\partial \mu}\Big|_{\mu=0} = -\frac{a\pi}{2} v_n \sum_{m=0}^{\infty} B_w(2m+1, h, 1) \frac{W(2m+1, h, \vartheta)}{M_w(2m+1, h)} \tag{1.9.29}$$

This represents the normal derivative of the velocity potential on the surface of the vibrating strip caused by the assigned surface velocity. The potential ψ everywhere else must conform to this required condition. Since ψ obeys Helmholtz's equation it too can be represented as a sum of partial elliptic waves of the form $W(2m+1, h, 2m+1) R^{(1)}(2m+1, h, \mu)$, where $R^{(1)} = R_1 + iR_2$ is the radial function for outgoing waves (time being given by $\exp(-i\omega t)$). Thus,

$$\psi(\mu, \vartheta) = \sum_{m=0}^{\infty} C_w(2m+1, h, 1) \frac{W(2m+1, h, \vartheta)}{M_w(2m+1, h)} R^{(1)}(2m+1, h, \mu)$$

Forming the derivative $\partial\psi/\partial\mu|_{\mu=0}$ and comparing with 1.9.29 shows that

$$C_w = -\frac{a\pi}{2}\vartheta_n \frac{B_w}{(R^{(1)'})_{\mu=0}}, \quad R^{(1)'} \equiv \frac{d}{dx} R^{(1)}(x)$$

The velocity potential everywhere caused by ϑ_n is then expressible in elliptic coordinates:

$$\psi(\mu, \vartheta) = -\frac{a}{2}\pi v_n e^{-i\omega t} \sum_{m=0}^{\infty} B_w(2m+1, h, 1) \frac{W(2m+1, h, \vartheta)}{M_w(2m+1, h)} \frac{R^{(1)}(2m+1, h, \mu)}{\frac{dR^{(1)}}{d\mu}(2m+1, h, 0)} \tag{1.9.30}$$

Here B_w, W, $R^{(1)}$, M_w, $R^{(1)'}$ are tabulated quantities. Again the radiated, acoustic pressure and particle velocity are obtained from 1.9.30 by use of 1.9.14.

Eq. 1.9.30 is a modal sum of eigenfunctions W. The modes are physically introduced by the periodicity of the potential field in angle ϑ. Since the distribution of radial velocity ϑ_n is here specified independent of z the radiation from the vibrating strip is 2-dimensional. Thus the continuum solution 1.9.13 of the radiating circular cylinder does not have an analogue in this case of a vibrating strip excited by velocity distribution 1.9.27.

1.9c. RADIATION OF SOUND FROM A SPHERE

In spherical coordinates r, ϑ, ϕ, Fig. 1.9.4, $x = r \sin\vartheta \cos\phi$, $y = r \sin\vartheta \sin\phi$, $z = r\cos\vartheta$, and the gradient operation is

$$\vec{\nabla}\psi = \vec{a}_r \frac{\partial\psi}{\partial r} + \frac{\vec{a}_\vartheta \cdot \partial\psi}{r\partial\vartheta} + \vec{a}_\phi \frac{\cdot\partial\psi}{r\sin\vartheta\partial\phi} \tag{1.9.31}$$

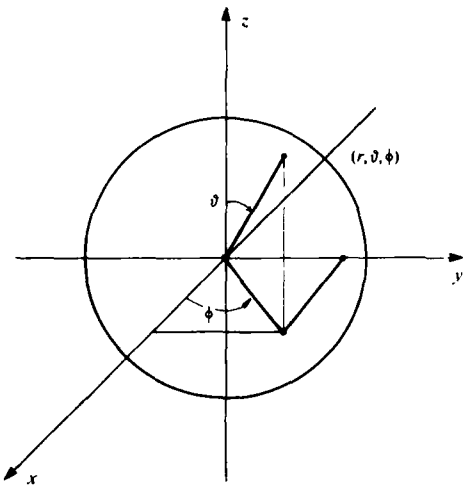

Fig. 1.9.4. Spherical radiator.

The Helmholtz equation in these coordinates has the factored solution:

$$\psi(r, \vartheta, \phi, t) = e^{-i\omega t} R(r)\ \Theta\ (\vartheta)\Phi(\phi) \tag{1.9.32a}$$

in which

$$\frac{1}{r^2}\frac{d}{dr}\left(r^2 \frac{\partial R}{\partial r}\right) = -\left[k^2 - \frac{n(n-1)}{r^2}\right] R = \nabla_r^2 \tag{1.9.32b}$$

$$\frac{1}{r^2\sin\vartheta}\frac{d}{d\vartheta}\left[\sin\vartheta \frac{d\Theta}{d\vartheta}\right] = -\left[\frac{n(n+1)}{r^2} - \frac{m^2}{r^2\sin^2\vartheta}\right]\Theta = \nabla_\vartheta^2 \tag{1.9.32c}$$

$$\frac{1}{r^2\sin\vartheta}\frac{d^2\Phi}{d\phi^2} = \frac{-m^2}{r^2\sin\vartheta}\Phi = \nabla_\phi^2 \tag{1.9.32d}$$

Since Θ is periodic in π the separation constant n is an integer. Similarly Φ is periodic in 2π, which sets the requirement that m also be an integer. If Θ, ϕ are solutions in the real domain m and n are positive; if they are complex solutions, m and n must extend from $-\infty$ to $+\infty$.

The real solutions $\Theta\Phi$ constitute the angular functions for spherical coordinates: $\Theta = P_n^m(\cos\vartheta)$, $\Phi = \cos m\phi$ or $\sin m\phi$, and the combination are spherical harmonics Y_e, Y_o, defined by:

$$Y_e(\vartheta, \phi; m, n) = \cos(m\phi)\, P_n^m(\cos\vartheta)$$

$$Y_o(\vartheta, \phi; m, n) = \sin(m\phi)\, P_n^m(\cos\vartheta) \tag{1.9.33}$$

in which $P_n^m(\vartheta)$ is the associated Legendre function.

The complex solutions are

$$X_n^m(\vartheta, \phi) = e^{im\phi} P_n^m(\cos\vartheta) \tag{1.9.34}$$

Since m, n are discrete, the solutions Y(or X) form a mutually orthogonal set of eigenfunctions over a sphere of unit radius, whose normalization constant is,

$$N(m, n) = \int_S Y^2 dS = \frac{4\pi(n+m)!}{\varepsilon_m(n-m)!\,(2n+1)},\quad \varepsilon_0 = 2,\ \varepsilon_{m\neq 0} = 1 \tag{1.9.35}$$

The real radial solutions R_1, R_2 are found by setting $R = J(r)/\sqrt{r}$ to be the half-order Bessel functions,

$$R_1 = j_n(kr) \equiv \sqrt{\frac{\pi}{2k}}\ \frac{J_{n+1/2}(kr)}{\sqrt{r}}\ ;\ R_2 = n_n(kr) = \sqrt{\frac{\pi}{2k}}\ \frac{N_{n+1/2}(kr)}{\sqrt{2r}} \tag{1.9.36}$$

The complex radial solution (for time given by exp $-i\omega t$) is:

$$R_3 = h_n(kr) = R_1 + iR_2 \tag{1.9.37}$$

Assembling all factors 1.9.32 through 1.9.34 in 1.9.31 leads to the general time-harmonic radiated velocity potential,

$$\psi(r, \vartheta, \phi) = e^{-i\omega t} \sum_{m=0}^{\infty} \sum_{n=0}^{\infty} (A_{mn} \cos m\phi + B_{mn} \sin m\phi)\, P_n^m(\cos \vartheta) \begin{Bmatrix} j_n(kr) \\ n_n(kr) \\ h_n(kr) \end{Bmatrix} \tag{1.9.38}$$

Here, A_{mn}, B_{mn} are expansion constants.

For radiation inside a sphere one chooses j_n in this equation: ψ then describes standing waves inside the sphere. For radiation into a volume made up of the space between spherical shells one chooses a linear combination of j_n and n_n to describe the standing waves. For radiation outside the sphere into an infinite medium one chooses h_n to describe outgoing waves.

We consider now the exterior problem of the radiation of sound from a sphere on whose surface there is an arbitrary distribution of radial velocity, $v_n = v_0(\vartheta, \phi)$. v_n being a smooth function of ϑ, ϕ it can be expanded in eigenfunctions 1.9.32c, d by use of the orthogonality property 1.9.35:

$$v_0(\vartheta, \phi) = \sum_{n=0}^{\infty} \sum_{m=0}^{\infty} \frac{\varepsilon_m}{4\pi} (2n + 1) \frac{(n - m)!}{(n + m)!} \int_0^{2\pi} d\alpha \int_0^{\pi} d\beta \sin \beta\, \vartheta_0(\alpha, \beta) \tag{1.9.39}$$

$$\times [Y_e(\vartheta, \phi; m, n)\, Y_e(\alpha, \beta; m, n) + Y_0(\vartheta, \phi; m, n)\, Y_0(\alpha, \beta; m, n)].$$

When $V_0(\vartheta, \phi)$ is specified the velocity potential everywhere in the field must satisfy a boundary condition at the surface $r = R_0$. Using the radial component $\nabla_r \psi$ of the gradient 1.9.31, the condition posed by 1.8.25 is;

$$-\frac{\partial \psi}{\partial r}\Big|_{r=R_0} = v_0(\vartheta, \phi), \tag{1.9.40}$$

Taking the radial derivative of 1.9.38, substituting 1.9.39 in 1.9.40, and comparing term by term lead to the general formula for the radiated velocity potential:

$$\psi(r, \vartheta, \phi, t) = -\frac{e^{-i\omega t}}{k} \sum_{n=0}^{\infty} \sum_{m=0}^{\infty} \frac{1}{N(m, n)} \frac{h_n(kr)}{h_m'(kR_0)} \int_0^{2\pi} d\alpha \int_0^{\pi} d\beta \sin \beta\, v_0(\alpha, \beta) \tag{1.9.41}$$

$$\times [Y_e(\vartheta, \phi; m, n)\, Y_e(\alpha, \beta; m, n) + Y_0(\vartheta, \phi; m, n)\, Y_0(\alpha, \beta; m, n)].$$

This solution is completely modal, there is no continuum of eigenvalues.

From it the radial component of intensity of sound anywhere in the field is easily derived:

$$I_r = p(r, \vartheta, \phi, t)\, u_r(r, \vartheta, \phi, t)$$

$$I_r = i\omega \varrho_0 \psi(r, \vartheta, \phi, t) \frac{\partial \psi}{\partial r}(r, \vartheta, \phi, t)$$

Thus the acoustic power Π radiated to infinity is,

$$\Pi = \lim_{r\to\infty} \int_0^{2\pi} d\phi \int_0^{\pi} d\vartheta \left[i\omega\varrho_0 \frac{\partial \psi}{\partial r} \right] r^2 \sin\vartheta d\vartheta. \tag{1.9.42}$$

Radiated power for explicit forms of ψ(or ultimately surface velocity v_n) are developed in Chap. VI.

1.9d. RADIATION OF SOUND FROM A PROLATE SPHEROID

A prolate spheroid is the 3-D figure of an ellipse rotated about its major axis, Fig. 1.9.5. Here the foci are at $\pm a/2$ and a field point $\vec{r}(x, y, z)$ is expressed in radial μ and angles ϑ, ϕ by means of the coordinate transformations:

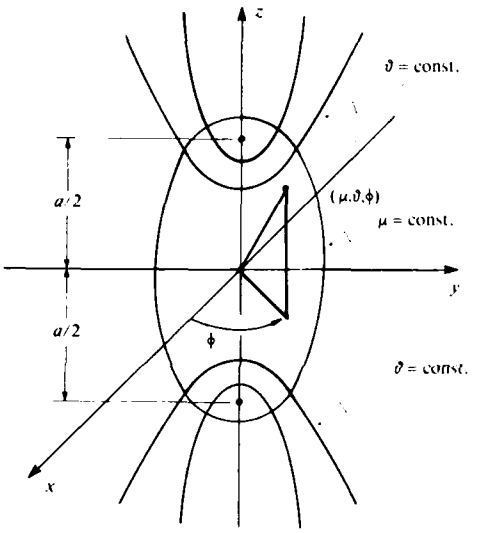

Fig. 1.9.5. Prolate spheroidal radiator.

$$\begin{matrix} x \\ y \end{matrix} = \frac{a}{2} \sinh\mu \sin\vartheta \begin{matrix} \cos\phi \\ \sin\phi \end{matrix}; z = \frac{a}{2} \cosh\mu \cos\vartheta \tag{1.9.43a}$$

For convenience in writing the following shorthand notation is often used,

$$\cosh\mu = \xi; \cos\vartheta = \eta; z = \frac{a}{2} \xi\eta \tag{1.9.43b}$$

An element of volume in this coordinate system is

$$d\mathcal{V} = dxdydz = h_\mu h_\vartheta h_\phi d_\mu d\vartheta d\phi \tag{1.9.44}$$

in which the scale factors h_i are given by,

$$h_\mu = h_\vartheta = \frac{a}{2} \sqrt{\cosh^2\mu - \cos^2\vartheta} \tag{1.9.45a}$$

$$h_\phi = \frac{a}{2} \sinh\mu \sin\vartheta. \tag{1.9.45b}$$

The gradient operation, needed for radiation problems, is

$$\nabla \equiv \vec{a}_\mu \frac{\partial}{h_\mu \partial_\mu} + \vec{a}_\vartheta \frac{\partial}{h_\vartheta \partial\vartheta} + \vec{a}_\phi \frac{\partial}{h_\phi \partial\phi}$$

where the $\vec{a}$'s are unit vectors.

Helmholtz's equation in velocity potential ψ is sparable in this elliptical system of coordinates.

$$\psi = S(\eta) R(\xi) \Phi(\phi) e^{-i\omega t} \tag{1.9.46}$$

In terms of separation constants A, m the trio of separated (ordinary differential) equations become,

$$(1) \quad \frac{d}{d\eta} \left[(1-\eta^2) \frac{dS}{d\eta} \right] = - \left[A - h^2\eta^2 - \frac{m^2}{1-\eta^2} \right] S \tag{1.9.47a}$$

$$(2)\quad \frac{d}{d\xi}\left[(\xi^2-1)\frac{dR}{d\xi}\right]=\left[A-h^2\xi^2+\frac{m^2}{\xi^2-1}\right]R \tag{1.9.47b}$$

$$(3)\quad \frac{d^2\Phi(\phi)}{h_\phi\partial\phi^2}=-\frac{m^2\Phi}{h_\phi} \tag{1.9.47c}$$

Here,

$$h=\frac{ka}{2};\ k=\frac{\omega}{c}=\frac{2\pi}{\lambda}$$

Coordinate ranges are,

$$-1\leqslant\eta\leqslant+1;\qquad 1\leqslant\xi<\infty;\qquad 0<\phi<2\pi.$$

Since ϕ is periodic in 2π the constant m is zero or a positive integer, and the eigenfunctions $\Phi(\phi)$ are $\cos m\phi$, $\sin m\phi$.

For the condition m integer the equation for $S(\eta)$ 1.9.47a yields finite solutions $S(\eta; m, l)$ only for discrete values of $A(h; m, l)$. To find them one forms the expansion,

$$\text{even solution: } S(h,\eta; m, l)=\sum_{n=0}^{\infty} d(h; m, l; 2n)\,P_{2n}^{m}(\eta),\ l=m, m+2, m+4, \text{etc.} \tag{1.9.48a}$$

$$\text{odd solution: } S(h,\eta; m, l)=\sum_{n=0}^{\infty} d(h; m, l; 2n+1)\,P_{2n+1}^{m}(\eta),\ l=m+1, m+3, \text{etc.} \tag{1.9.48b}$$

When these solutions are inserted in 1.9.47a two sets of recursion formulas in the d-constants are obtained. They are solved simultaneously for d and A by use of the theory of continued fractions. Unique values are obtained by normalizing according to the rule,

$$\sum_{n}{}' \frac{(n+2m)!}{n!}\,d(h; m, l; n)=\frac{(l+m)!}{(l-m)!} \tag{1.9.48c}$$

in which the prime sign means summation is n even if $l-m$ is even, or n odd, if $l-m$ is odd. All functions S_{ml} are orthogonal to each other in the interval $\eta=\pm 1$. Their normalization constant is,

$$M(h; m, l)=\int_0^{\pi}[S(h,\cos\vartheta;\mu,\lambda]^2\sin\vartheta d\vartheta=\int_{-1}^{m,l} S_{me}^2(h,\eta)\,d\eta$$

$$=\sum_{n}{}'[d(h; m, l; n)]^2\left(\frac{2}{2n+2m+1}\right)\frac{(n+2m)!}{n!} \tag{1.9.48d}$$

In actual applications to radiation problem the numerical evaluation of $S_{ml}(h,\eta)$ and $M(h; ml)$ is greatly facilitated by published tables of d's, P_n^m, A's and M itself [11].

The radial solutions $R(\xi)$ exhibit a behaviour similar to $S(\eta)$ except over a different range of variable ξ. When m is an integer the differential equation 1.9.47b yields a finite solution only for discrete values of $A(h; m, l)$ which are the same as for the angular solutions S. Thus, when the d-constants of 1.9.48a and 1.9.48b are known one can immediately calculate two solutions $R^{(1)}$, $R^{(2)}$ by expansions in spherical Bessel functions 1.9.36:

$$R^{(1)}(h\xi;\, m,\, l) = \frac{(l-m)!}{(l+m)!}\left(\frac{\xi^2-1}{\xi^2}\right)^{m/2} \sum_n{}' i^{n+m-l}\, d(h;\, m,\, l;\, n)\, \frac{(n+2m)!}{n!}\, j_{n+m}(h\xi) \tag{1.9.49a}$$

$$R^{(2)}(h\xi;\, m,\, l) = \frac{(l-m)!}{(l+m)!}\left(\frac{\xi^2-1}{\xi^2}\right)^{m/2} \sum_n{}' i^{n+m-l}\, d(h;\, m,\, l;\, n)\, \frac{(n+2m)!}{n!}\, m_{n+m}(h\xi) \tag{1.9.49b}$$

The complex radial solution, analogous to Hankel functions, is defined for time representation exp $-i\omega t$,

$$R^{(3)} = R^{(1)} + iR^{(2)} \tag{1.9.49c}$$

The Wronskian for R is often needed in problem of radiation from spheroids,

$$\Delta(R^{(1)}, R^{(2)}) = R^{(1)}R^{(2)\prime} - R_2R_1^{(1)} = \frac{1}{h(\xi^2-1)} \tag{1.9.49d}$$

These radial functions are also tabulated [12]. Assembling all factors 1.9.48 through 1.9.49 leads to the general time-harmonic radiated velocity potential for the prolate spheroid,

$$\psi(r,\, t) = e^{-i\omega t} \sum_m \sum_l (A_{ml} \cos m\phi + B_{ml} \sin m\phi)\, S(\eta;\, m,\, l) \begin{matrix} R^{(1)} \\ R^{(2)} \\ R^{(3)} \end{matrix} (h\xi;\, m,\, l) \tag{1.9.50}$$

in which A_{ml}, B_{ml} are expansion constants in the Fourier series for coordinate ϕ. The symbols η, ξ are defined by 1.9.43b. For radiation inside the spheroid one uses $R^{(1)}$ to describe standing waves; for radiation inside a "spheroidal annulus", one uses a linear combination of $R^{(1)}$ and $R^{(2)}$. For radiation external to the spheroid, one uses $R^{(3)}$ to describe outgoing waves in harmonic time exp($-i\omega t$).

We consider next radiation into an infinite medium of sound from a short cylinder modelled as a zone on a prolate spheroid, Fig. 1.9.6. The spheroid is specified by $\mu = \mu_0$ with foci at $\pm a/2$. Its semi-major axis is $a/2 \cosh \mu_0$, and semi-minor axis is $a/2 \sinh \mu_0$. On this surface let there be a ring extending from $-\eta_0 (= -\cos \vartheta_0)$ to $+\eta (= \cos \vartheta_0)$, and assume the component of velocity normal to the surface μ_0 = const. is,

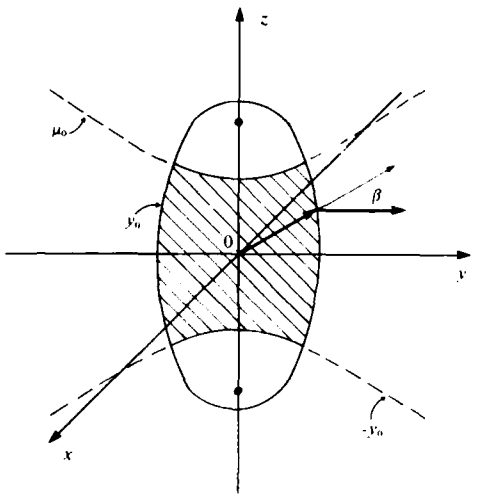

Fig. 1.9.6 Model of a short-cylinder radiator.

$$\begin{aligned} v_n &= V_0|\cos\beta| \qquad -\eta_0 \leqslant \eta \leqslant \eta_0 \\ v_n &= 0 \qquad\qquad \text{elsewhere} \end{aligned} \tag{1.9.51a}$$

in which β is the angle between the normal to the surface and the xy plane. It is defined by,

$$\cos\beta = \frac{1}{h_\mu}\frac{\partial r}{\partial \mu} \tag{1.9.51b}$$

Since $r = (x^2 + y^2)^{1/2} = a/2 \sinh \mu \sin \vartheta$, this is,

$$\cos\beta = \frac{\cosh \mu_0 \sin \vartheta}{\sqrt{\cosh^2 \mu_0 - \cos^2 \vartheta}}$$

Now the boundary condition 1.8.25 for radiation of velocity potential ψ is:

$$-\frac{1}{h_\mu}\frac{\partial \psi}{\partial \mu}\Big|_{\mu=\mu_0} = v_n \tag{1.9.52}$$

Since v_n in 1.9.50a is independent of ϕ we set $m = 0$ in 1.9.50, and reduce 1.9.52 to,

$$-\sum_l A_{0l}\ \frac{S(h, \cos\vartheta; 0, l)}{\frac{a}{2}\sqrt{\cosh^2\mu_0 - \cos^2\vartheta}}\ \frac{dR^{(3)}(h, \cosh\mu; 0, l)}{d\mu}\Big|_{\mu=\mu_0} = \frac{V_0 \cosh\mu_0 \sin\vartheta}{\sqrt{\cosh^2\mu_0 - \cos^2\vartheta}} \tag{1.9.53}$$

The factor $\sqrt{\cosh^2\mu_0 - \cos^2\vartheta}$ is independent of l and can be cancelled. By use of orthogonality of angular functions S , 1.9.48d, the constant A_{0l} is directly found by multiplying both sides of this equation by $S \sin\vartheta$ and integrating over the range $0 \leqslant \vartheta \leqslant 2\pi$. The radiated velocity potential, 1.9.50 for the short cylinder then becomes,

$$\psi(\vec{r}, t) = -V_0\ \frac{a}{2}\ \cosh\mu_0\ e^{-i\omega t}\ \sum_l\ \frac{\int_{\vartheta_0}^{\vartheta_0} S(h, \cos\vartheta; 0, l)\sin^2\vartheta d\vartheta}{M(h; 0, l)\ \frac{dR^{(3)}}{d\mu}(h, \cosh\mu; 0\ l)\big|_{\mu=\mu_0}} \tag{1.9.53a}$$

$$\times S(h, \cos\vartheta; 0, l)\, R^{(3)}(h, \cosh\mu; 0, l)$$

The acoustic pressure radiated and its associated particle velocities are obtainable from ψ by use of 1.7.2. In the far field

$$R^{(3)}(h, \cosh\mu; 0, l) \to (i)^{l-1}\ \frac{e^{ikr}}{kr}$$

Hence the farfield pressure is

$$p(r, \theta|\omega) = (i)^l\ V_0\ \frac{a}{2}\quad \varrho c \cosh\mu_0\ \frac{\sum_{l\,\text{even}}\ \int_{\vartheta_0}^{+\vartheta_0} S(h, \cos\vartheta; 0, l)\sin^2\vartheta d\vartheta}{M(h; 0, l)\ \frac{dR^{(3)}}{d\mu}(h, \cosh\mu; 0, l)\big|_{\mu=\mu_0}}$$

$$\times\ S(h, \cos\vartheta; 0, l)\ \frac{e^{ikr}}{r} \tag{1.9.53b}$$

The vector particle velocity anywhere is

$$\vec{u} = -\vec{\nabla}\psi = V_0 \cosh\mu_0 e^{i\omega t}\ \frac{\sum_{l\,\text{even}}\ \int_{\vartheta_0}^{+\vartheta_0} S(h, \cos\vartheta; 0, l)\sin^2\vartheta d\vartheta}{M(h; 0, l)\left[\frac{dR^{(3)}}{d\mu}(h, \cosh\mu; 0, l)\right]_{\mu=\mu_0}}$$

$$\times\left\{\frac{1}{\sqrt{\cosh^2\mu - \cos^2\theta}}\quad \left[\vec{a}_\mu\ \frac{dR^{(3)}}{d\mu}(h, \cosh\mu; 0, l) + \vec{a}_\theta\ \frac{dS}{d\theta}(h, \cos\theta; l)\right]\right\} \tag{1.9.53c}$$

1.9e. RADIATION OF SOUND FROM AN OBLATE SPHEROID

An oblate sphereoid is the figure of a 3-D ellipsoid rotated about the minor axis, Fig. 1.9.7. It is specified by the ellipsoidal surface ν = const. and hyperboloidal surface ϑ = const. Any field point x, y, z transforms to coordinates ν, θ, ϕ:

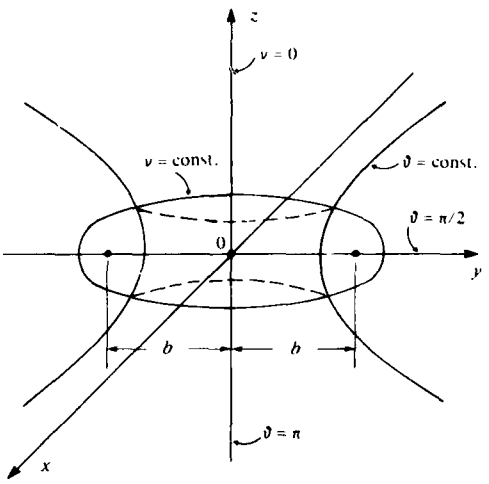

Fig. 1.9.7. Oblate spheroid radiator.

$$\begin{matrix} x \\ y \end{matrix} = b \cosh \nu \sin \vartheta \begin{matrix} \cos \phi \\ \sin \phi \end{matrix}; \quad z = b \sinh \nu \cos \vartheta \tag{1.9.54a}$$

in which b is the semi-major axis. The volume element is,

$$dxdydz = h_\nu h_\vartheta h_\phi \, d\nu d\vartheta d\phi$$

$$\begin{aligned} h_\nu &= h_\vartheta = b\sqrt{\sinh^2 \nu + \cos^2 \vartheta} \\ h_\phi &= b \cosh \nu \sin \vartheta \end{aligned} \tag{1.9.54b}$$

The gradient operator ∇ needed for calculation of radiation is

$$\nabla = \vec{a}_\nu \frac{\partial}{h_\nu \partial \nu} + \vec{a}_\vartheta \frac{\partial}{h_\vartheta \partial \theta} + \vec{a}_\mu \frac{\partial}{h_\phi \partial \phi}$$

On comparing 1.9.54a with 1.9.43a it is seen that if the replacement is made,

$$\mu \to \nu - i\pi/2$$

$$\frac{a}{2} \to ib; \; h = \frac{ka}{2} = ikb \tag{1.9.54c}$$

then

$$\begin{aligned} \frac{a}{2} \sinh \mu &= ib \sinh(\nu - i\pi/2) = b \cosh \nu \\ \cosh \mu &= \cosh(\nu - i\pi/2) = -\sinh \nu \end{aligned} \tag{1.9.54d}$$

that is, 1.9.54a is obtained. All radiation formulas for the oblate case are then obtainable from those of the prolate case by transformation 1.9.54c. The time-harmonic radiated velocity potential is then directly derived from 1.9.50,

$$\psi(r, t) = e^{-i\omega t} \sum_m \sum_l (A_{ml} \cos m\phi + B_{ml} \sin m\phi) \; S(ikb, \cos \vartheta; m, l) \begin{matrix} R^{(1)} \\ R^{(2)} \\ R^{(3)} \end{matrix} (ikb, -i \sinh \nu) \tag{1.9.55}$$

The choice of $R^{(1)}$, $R^{(2)}$, $R^{(3)}$ follows the same rules as in the prolate case.

We consider next the radiation of sound from a free disk into an infinite medium. The disk is modelled as an oblate ellipse $\nu = 0$. The ideal velocity distribution is

$$v_n = v_0 e^{-i\omega t} \quad 0 \leq \vartheta \leq \pi/2 \tag{1.9.56}$$

$$v_n = -v_0 e^{-i\omega t} \quad \frac{\pi}{2} \leq \vartheta \leq \pi$$

Since v_n is here specified to be independent of ϕ we set $m = 0$ in 1.9.55. Also, since the radiation is in the form of outgoing waves to infinity we choose $R^{(3)}$ as the appropriate radial function (for time specified as exp $-i\omega t$):

$$\psi(r, t) = e^{-i\omega t} \sum_l A_l S(ikb, \cos\vartheta; 0, l) R^{(3)}(ikb, -i \sinh \nu) \tag{1.9.57}$$

The boundary condition on the surface of the disk relates this velocity potential to the specified v_n as required by 1.8.25:

$$-\frac{1}{h_\nu} \frac{\partial \psi}{\partial \nu}\Big|_{\nu=0} = v_n \tag{1.9.58}$$

Using 1.9.54b for calculating h_ν one forms $\partial\psi/\partial\nu$ at $\nu = 0$ and equates the result to 1.9.56,

$$-\frac{1}{b \cos\vartheta} \sum_l A_l S(ikb, \cos\vartheta; 0, l) \frac{dR^{(3)}(ikb, -i \sinh \nu)}{d\nu}\Big|_{\nu=0} = v_n$$

To determine A_l we transfer $b \cos\vartheta$ to the right hand side, multiply both sides by $S \sin\vartheta$ and integrate over $0 \leq \vartheta \leq \pi$. Since the angular function S is orthogonal in this range we obtain from 1.9.48d,

$$A_l = -b \frac{\int_{-1}^{+1} v_n S(ikb, \eta; 0, l)\, \eta d\eta}{M(ikb; 0, l) \frac{dR^{(3)}}{d\nu}(ikb, -i \sinh \nu)\big|_{\nu=0}} \tag{1.9.59}$$

$$\eta = \cos\vartheta$$

Now, the angular functions S can be expanded in series of Legendre functions, 1.9.48,

$$S(ikb, \eta; 0, l) = \sum_{m=0}^{\infty} \begin{pmatrix} d(ikb; 0, l; & 2m \\ & 2m+1 \end{pmatrix} \begin{matrix} P_{2m}(\eta): & \text{odd} \\ P_{2m+1}(\eta): & \text{even} \end{matrix}$$

To perform the integration in 1.9.59 one notes that both v_n and η switch signs from + to - at $\vartheta = \pi/2$. Thus, v_n can be taken out of the integration as v_n. Also, since $\eta = P_1(\eta)$ one finds by use of the orthogonality of the Legendre functions in the range $-1 \leq \eta \leq +1$ that,

$$\int_{-1}^{+1} P_{2n}(\eta) P_1(\eta)\, d\eta = 0 \qquad \text{for all } \nu$$

$$\int_{-1}^{+1} P_{2n+1}(\eta) P_1(\eta)\, dy = \tfrac{2}{3} \quad \text{for } n = 0$$

$$P_1(\eta)\, dy = 0 \quad \text{for } n \neq 0$$

The radiated velocity potential is then,

$$\psi(r,\ t) = -\ \frac{2}{3}\ bv_0 e^{-i\omega t} \sum_{l=1,3,5\ldots} \frac{d(ikb;\ 0,\ l;\ 1)}{M(ikb;\ 0,\ l)} \frac{R^{(3)}\ (ikb,\ -i\ \sinh\ \nu)}{\dfrac{dR^{(3)}}{d\nu}\ (ikb,\ -i \sinh \nu)\Big|_{\nu=0}}$$

$$\cdot S(ikb,\ \cos\vartheta;\ 0,\ l) \tag{1.9.60}$$

The radiated acoustic pressure and associated particle velocity are obtainable by use of 1.7.2. Numerical calculation of these results in materially aided by published tables of oblate spheroidal functions [11, 12].

RADIATION OF SOUND FROM OTHER CLASSICAL FIGURES

The Helmholtz wave equation is separable in these other systems:

(1) parabolic cylinder coordinates
(2) conical coordinates
(3) rotational parabolic coordinates
(4) paraboloidal coordinates
(5) ellipsoidal coordinates.

These are sketched in Fig. 1.9.8. The method of calculating radiation from these figures closely follows the procedures used in the above detailed cases of spheres, cylinders and spheroids. However the numerical calculation is currently hampered by lack of published tables of the special functions that appear in the radiation formulas.

1.10 THE NUMERICAL CALCULATION OF VELOCITY POTENTIAL ON A RADIATING SURFACE

In the theory of acoustic radiation it is often necessary to determine the reaction of the medium on the sound-generating surface. This requires one to find the velocity potential on the vibrating surface itself. It was noted in the discussions of Section 1.8 that when the observation point is on the surface the factor 4π must be replaced by 2π. Thus, in the steady state, the field on S, when there are no volume sources and when the medium is unbounded, is governed by the surface Helmholtz integral formulation of the form [15],

$$-2\pi\psi(\vec{r}) + P\int_S \psi(\vec{r}_0)\ \frac{\partial G}{\partial M_0}\ (\vec{r}|\vec{r}_0)\ dS(\vec{r}_0) = \int_S G(\vec{r}|\vec{r}_0)\ v_n(\vec{r}_0)\ dS(\vec{r}_0),\ \vec{r}\ \text{on}\ S$$

$$G(\vec{r}|\vec{r}_0) = \frac{e^{ik|\vec{r}-\vec{r}_0|}}{|\vec{r}-\vec{r}_0|} \tag{1.10.1}$$

The appearance of the negative sign in the first term and the symbol $\dot{P}$ (principal part) in the second term are discussed below. When the observation point is *inside* the (closed) radiating surface, $\psi(\vec{r})$ vanishes. Eq. 1.10.1 then becomes the interior Helmholtz integral formulation.

The numerical calculation of 1.10.1 for the case of $\vec{r}$ on S or r inside S can be carried out approximately by partitioning the surface S into N cells of finite size, and converting the integral equation into a system of algebraic equations in N unknown $\psi(\vec{x}_i)$, $i = 1, 2, \ldots N$.

An alternative formulation which is suitable for numerical calculation is to interpret source q in 1.7.3 as a source strength per unit area ($m^3/s \times 1/m^2 = ms^{-1}$). Then in the absence of reflecting surfaces, the steady state velocity potential anywhere is,

$$\psi(\vec{r}, t) = e^{-i\omega t} \int \frac{e^{ik|\vec{r}-\vec{r}_0|}}{|\vec{r}-\vec{r}_0|} q(\vec{r}_0)\, dS(\vec{r}_0) \tag{1.10.2}$$

The boundary condition on the surface is 1.7.2b, in which $\vec{u}$ and $-\nabla\psi$ point in the same direction, and the ∇ operation is on the $\vec{r}$ coordinates. Here, because of the selection of the sign of positive $\vec{n}$ and positive v_n (which appear as $[\text{grad}_0 \Phi_0]_n$ and v^- in Fig. 1.11.1),

$$\frac{\partial \psi}{\partial n}\Big|_{\vec{r}\to\vec{r}_0} = v_n \tag{1.10.3}$$

The positive normal points away from the medium, Fig. 1.8.1, while positive v_n points into the medium. Since 1.10.2 is an integration over $\vec{r}_0$, and since $\exp ik|\vec{r}-\vec{r}_0|$ is not singular when $\vec{r}\to\vec{r}_0$, one can write

$$v_n = \frac{\partial \psi(\vec{r})}{\partial n}\Big|_{\vec{r}\to\vec{r}_0} = \left[\frac{\partial}{\partial n}\int \frac{e^{ik|\vec{r}-\vec{r}_0|}}{|\vec{r}-\vec{r}_0|}\bar{q}(\vec{r}_0)\, dS(\vec{r}_0)\right]_{\vec{r}\to\vec{r}_0} \tag{1.10.4}$$

As $\vec{r}\to\vec{r}_0$ the integer becomes a mathematical "distribution,"

$$\frac{\partial}{\partial n}\frac{e^{ik|\vec{r}-\vec{r}_0|}}{|\vec{r}-\vec{r}_0|} = -2\pi\,\delta(\vec{r}-\vec{r}_0)\, e^{ik|\vec{r}-\vec{r}_0|} + P\,\frac{\partial}{\partial n}\frac{e^{ik|\vec{r}-\vec{r}_0|}}{|\vec{r}-\vec{r}_0|} \tag{1.10.5}$$

The negative sign in the delta term is due to the choice of the normal as positive when it points away from the medium [16]. The symbol P is the "principal part," meaning the singularity $\vec{r} = \vec{r}_0$ is to be excluded in any subsequent integration. Thus,

$$v_n(\vec{r}) = -2\pi q(\vec{r}) + P\int \frac{\partial}{\partial n}\left[\frac{e^{ik|\vec{r}-\vec{r}_0|}}{|\vec{r}-\vec{r}_0|}\right] q(\vec{r}_0)\, dS(\vec{r}_0),\ \vec{r}\ \text{on}\ S \tag{1.10.6}$$

The integration is performed by first taking $\vec{r}\neq\vec{r}_0$ (that is, $\vec{r}$ is not on the surface) and then taking the limit of the answer as $\vec{r}\to\vec{r}_0$.

Eq. 1.10.1 and 1.10.6 can be put in the following similar forms:

$$(1)\quad \frac{\mathcal{H}}{2\pi}(k;\vec{r},\vec{r}_0)\,|\psi(\vec{r}_0)| - \lambda^{-1}\psi(\vec{r}) = \lambda^{-1}\frac{\mathcal{V}}{2\pi}(k;\vec{r},\vec{r}_0)\,|v_n(\vec{r}_0)| \tag{1.10.7a}$$

$$(2)\quad \frac{\mathcal{H}}{2\pi}(k;\vec{r},\vec{r}_0)\,|q(\vec{r}_0)| - \lambda^{-1} q(\vec{r}) = \lambda^{-1}\frac{v_n}{2\pi}(\vec{r}) \tag{1.10.7b}$$

where, $\lambda^{-1} = +1$; $k = k(\lambda)$ and, where $\mathcal{H}$, $\mathcal{V}$ are operators,

$$\mathcal{H}\{\ \} \equiv P\int \frac{\partial}{\partial n}\frac{e^{ik|\vec{r}-\vec{r}_0|}}{|\vec{r}-\vec{r}_0|}\{\ \}\, dS(\vec{r}) \tag{1.10.7c}$$

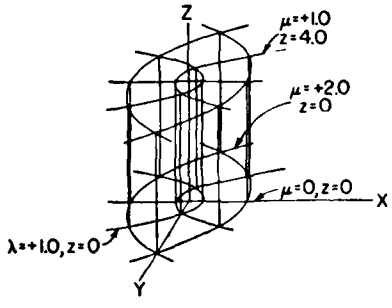

Parabolic cylinder coordinates .

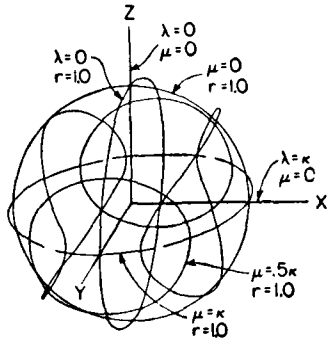

Conical coordinates.

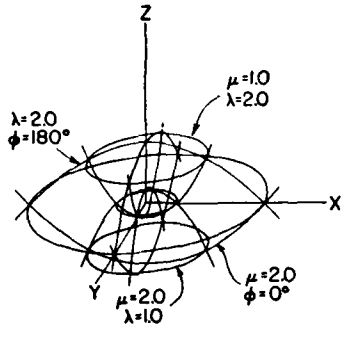

Parabolic coordinates.

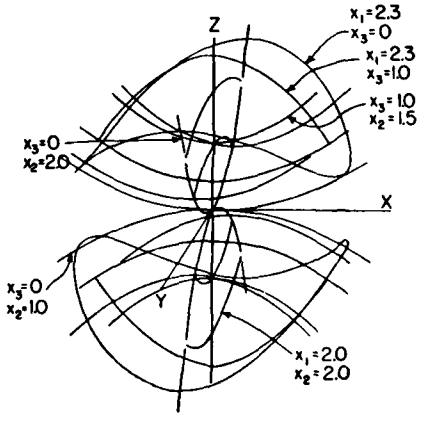

Parabolidal coordinates.

Fig. 1.9.8 Four coordinate systems in which the Helmholtz wave equation is separable [14].

$$\mathcal{V}\{\quad\} \equiv P\int \frac{e^{ik|\vec{r}-\vec{r}_0|}}{|\vec{r}-\vec{r}_0|}\{\quad\}\,dS(\vec{r}) \tag{1.10.7d}$$

Eqs. 1.10.7 may be solved by eigenfunction expansion. The eigenfunctions ψ_m of the operator $\mathcal{H}$ are solutions of,

$$\begin{aligned} &\mathcal{H}\,\psi_m(\vec{r}_0) = k_m(\lambda)\psi_m(\vec{r}), \\ &\int \psi_m\psi_n\,dS = N_m,\ n = m \\ &\int \psi_m\psi_n\,dS = 0,\quad n \neq m \end{aligned} \tag{1.10.8}$$

Thus by expansion in ψ_m 1.10.7a becomes,

$$\sum_m A_m \frac{\mathcal{H}(k/\lambda);\vec{r},\vec{r}_0)\{\psi_m(\vec{r}_0)\}}{2\pi} - \sum_m \lambda^{-1}A_m\psi_m(\vec{r}) = \lambda^{-1}\frac{\mathcal{V}(k;\vec{r},\vec{r}_0)\{\nu_m(\vec{r}_0)\}}{2\pi}$$

Multiplying through by ψ_n^*, integrating over area, and using the orthogonality 1.10.8 leads to,

$$\psi(\vec{r}) = \sum_m \frac{\psi_m(\vec{r})\int \lambda^{-1}\dfrac{\mathcal{V}(k;\vec{r},\vec{r}_0)\{\nu_n(r_0)\}}{2\pi}\psi_m^*(\vec{r}_0)\,dS}{N_m(k_m-\lambda^{-1})} \tag{1.10.9}$$

From this it is seen that 1.10.7a has a solution for every k_m (r) unless $k_m = \lambda^{-1}$. When $k_m = \lambda^{-1}$, 1.10.7a still has a solution if,

$$\lambda^{-1}\int \frac{\mathcal{V}(k;\vec{r},\vec{r}_0)}{2\pi}\,\nu_n(\vec{r}_0)\,\psi_m^*(\vec{r}_0)\,dS(\vec{r}_0) = 0. \tag{1.10.10}$$

The general solution of 1.10.6 is the sum of this particular solution 1.10.9 plus the complementary solution ψ_m. This means that when $k_m = \lambda^{-1}$ and when 1.10.10 holds the solution is not unique because any multiple of ψ_m is also a solution.

A similar reasoning shows that a solution $q(\vec{r})$ which satisfies 1.10.6 for all k_m except $k_m = \lambda^{-1}$, and is a solution at $k_m = \lambda^{-1}$ if ψ_m is such that,

$$\lambda^{-1}\int \frac{\nu_n}{2\pi}(\vec{r}_0)\,\psi_m^*(\vec{r}_0)\,dS(\vec{r}_0) = 0 \tag{1.10.11}$$

is not unique, and therefore that the representation 1.10.2 breaks down at a sequence of values of $k = k_m$.

The interior Helmholtz formulation obtained from 1.10.1 by setting the term $2\pi\,\psi(\vec{r})$ to zero can be solved directly by numerical means and yields a unique solution. It does however have computational difficulties [17].

In view of the theoretical problems and practical computation problem associated with solving 1.10.1 and 1.10.6, a new approach was made [17a, b]. In it, a field $\psi(\vec{r}), \vec{r}$ on S, was obtained which satisfied both 1.10.1, including the term $2\pi\,\psi(\vec{r})$, and simultaneously with this term excluded. In computation this means partitioning the surface S into N cells, constructing and $N \times N$ matrix of simultaneous equations for observation point $\vec{r}$ on S as required by 1.10.1 when $2\pi\,\psi(\vec{r})$ is included, then adding one or several additional equations to this matrix by choosing $\vec{r}$ to be interior so that the term $2\pi\,\psi(\vec{r})$ vanishes. The resultant non-square matrix $M \times N$ is thus over-determined, and is solvable by a least-squares orthonormalizing procedure [18]. Solution gives $\psi(\vec{r})$ for all points $\vec{r}$ on S for all wavenumbers k, including k_m. The velocity potential so found is substituted into 1.7.7 in the

steady state, and the field $\psi(\vec{r}, t)$ everywhere is obtained by simple integration of $\psi(\vec{r})$ over the surface in the absence of volume sources.

When this technique was applied to simple shapes for which closed form solutions are known the agreement improved steadily with increased number of auxiliary equations contributed by the interior solution. This conclusion was borne out also by physical experiments with odd shaped arrays [17a].

This technique is aptly suited to the calculation of radiation sound from arbitrarily shaped radiators. A bibliography of this problem is given at the end of this chapter.

1.11 REACTIVE POWER

The use of the Helmholtz Equation for the steady state as given by 1.7.7 requires a careful definition of the positive direction to be assigned to the vectors representing acoustic quantities. Considering a surface with a distribution of monopole sources only (i.e., $\nabla_0 G_K = 0$), we write the field at r as

$$\psi(r) = \frac{1}{4\pi} \int_{S_0} G_k(r|r_0)\, \mathrm{grad}_0\, \Phi(r_0) \cdot dS_0 \tag{1.11.1}$$

Let the surface S consist of two concentric spheres, of which one has an indefinitely large radius. We desire to find the field in the space between the spherical surfaces, assuming that the outer surface extends to infinity. For time given by $\exp(-i\psi t)$ we *select* $G_K = \exp(ikr)/r$, because we desire to build up the field at r by means of outgoing spherical waves. Now for a monopole radiator on S we desire the source strength to be positive, that is, for a velocity v we desire,

$$\mathrm{grad}_0\, \Phi(r_0) \cdot dS_0 = v\, dS = \text{positive number} \tag{1.11.2}$$

However in deriving 1.11.1 by means of Green's theorem we took the gradient operator to have a positive direction when pointing away from the volume between the spherical surface, i.e., from the inner spherical surface to the origin. Fig. 1.11.1 shows the conventions. Here $-[\mathrm{grad}_0\, \Phi_0]_m = V_+$ or $[\mathrm{grad}_0\, \Phi_0]_m = V_-$; and ∂/∂_z is directed as shown. From 1.1.4 we require the positive v to be given by $v_- = -\partial\Phi/\partial z$. Hence we must write

$$v_- = \mathrm{grad}_0\, \Phi(r_0) \cdot dS_0 = -(\partial\Phi/\partial z)\, dS. \tag{1.11.3}$$

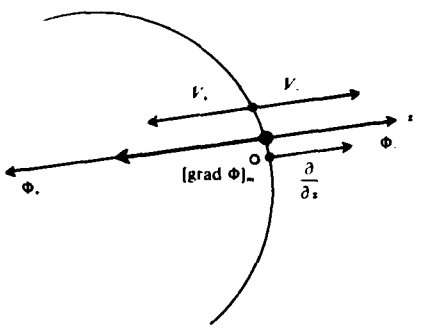

Fig. 1.11.1. Assignment of signs to velocities and gradients.

and so, 1.11.1 reduces to

$$\psi(r) = -\frac{1}{4\pi} \int_s \frac{\partial\Phi}{\partial z} \frac{e^{ikr}}{r}\, dS \tag{1.11.4}$$

For a piston in an infinite rigid baffle the righthand side of this equation must be multiplied by a factor of 2,

$$\psi(r) = -\frac{1}{2\pi} \int_s \frac{\partial\Phi}{\partial z} \frac{e^{ikr}}{r}$$

$$dS = \frac{1}{2\pi} \int_s \frac{V e^{ikr}}{r}\, dS \tag{1.11.5}$$

Now Rayleigh's formula 1.8.18 for the field in an infinite baffle has the form,

$$\phi(r) = -\frac{1}{2\pi}\int \frac{\partial \Phi}{\partial n}\ \frac{e^{-ikr}}{r}\ dS \tag{1.11.6a}$$

Here, time is taken to be the real part of $\exp(j\psi t)$ and the direction of positive n is from the source point (in the piston) toward the field point. Since Rayleigh takes $v = \partial\phi/\partial n$, he writes

$$\phi(r) = -\frac{1}{2\pi}\int_S v\ \frac{e^{-ikr}}{r}\ dS \tag{1.11.6b}$$

Hence the velocity potential used by Rayleigh is the negative of the velocity potential used by modern authors, $\phi(r) = -\Phi(r)$, with the result that the signs of 1.1.4 and 1.11.5 are reversed in Rayleigh's work. To assist the reader in these matters of signs we summarize the differences in operator conventions between the older acoustic literature as represented by Rayleigh, and the modern acoustic literature as represented by ref. [19].

	Rayleigh [20]	[Ref. 4 Chap. 7]
time	$\exp(j\psi t)$	$\exp(-i\psi t)$
pressure	$-\varrho\partial\phi/\partial t$	$\varrho\partial\Phi/\partial t$
velocity	$\nabla\phi$	$-\nabla\Phi$
positive grad. on S	points into domain where field is evaluated	points away from domain where field is evaluated

In addition to the selection of signs noted above we must determine the sign to be attached to the imaginary component ($=Q$) of the "vector power" given by 1.3.4d. This depends on the choice of representation of time as the real part of $\exp(j\psi t)$ or $\exp(-i\psi t)$, and on the choice between PV_k^* and P^*V_k to represent the complex acoustic intensity. To have a consistent notation we have adopted $\exp(-i\psi t)$ as the most convenient representation. This adoption has the following advantages [21]:

(1) the symbol $\exp(ikx)$ then represents the phase of a plane wave traveling in the *positive x* direction;

(2) the wave number k, if complex ($= k_1 + ik_2$), lies in the *first quadrant* of the complex k plane. As a consequence the evaluation of radiation integrals by contour integration may be undertaken with confidence because of the vast literature available, as exemplified by [4].

In contrast the choice $\exp(j\psi t)$ leads to the symbol $\exp(-jkx)$ for the positive-traveling plane wave, and the wavenumber k, if complex, lies in the *fourth* quadrant of the complex k plane. This choice requires contours of integration which are mirror-images of those that are valid for $\exp-i\psi t$. The evaluation of radiation integrals may also be accomplished with this choice. However, the literature of examples is much less representative.

When oscillating sinusoidally in time the normal particle velocity (as well as the acoustic pressure) may be represented as a *phasor*, that is, a radial vector rotating counterclockwise with velocity ωt. The two phasors, pressure $Pe^{i\phi}$ and particle velocity $Ve^{i\psi}$ have in general an angular separation ($= \psi - \phi$). If the particle velocity in the complex phasor plane has a component in time quadrature with the phasor of pressure, and if this component *leads* the pressure by $\pi/2$ radians (in the positive counterclockwise direction) then the reactive power calculated by 1.3.4d for time given by $\exp(-i\omega t)$ will be defined to be *positive*. If the component lags the pressure then Q will be given a negative sign.

We summarize here in a table the most important consequences of the various choices of complex representation for acoustic quantities found in the literature of acoustics. In the first column of this table the acoustic quantity to be described is listed. In the second and third columns the consequence of selecting $\exp(j\omega t)$ or $\exp(-i\omega t)$ are given.

Acoustic Quantity	$\exp(j\omega t)$	$\exp(-i\omega t)$	
Complex pressure 1.1.5	$j\omega\varrho\Phi$	$-i\omega\varrho\Phi$	1.11.(7)
Complex particle velocity 1.1.4	$-\nabla\Phi$	$-\nabla\Phi$	(8)
(Rayleigh's choice of Complex vel. potential ($\phi = -\Phi$).	$-j\omega\varrho\phi$ (Pressure)		(9)
	$\nabla\phi$ (Velocity)		(10)
$I_m(1/2 \int PV^* dA)$	$-Q_{AV}$(= Reactive Power)	$+Q_{AV.}$	(11)
$I_m(1/2 \int P^* V dA)$	$+Q_{AV.}$	$-Q_{AV.}$	(12)
Mass Reactance	$j\omega M$	$-i\omega M$	(13)
Stiffness Reactance	$K/j\omega$	$-K/i\omega$	(14)
Plane Wave Traveling in positive x direction	e^{-jkx}	e^{ikx}	(15)
Complex k	4th Quadrant of k-plane	1st Quadrant of k-plane	(16)
$\mathrm{Re}(1/2 \int PV^* dA)$	$+ W_i$(= real power)	$+ W_i$	(17)
$\mathrm{Re}(1/2 \int P^* V dA)$	$+ W_i$	$+ W_i$	(18)

1.12. KIRCHOFF APPROXIMATION IN DIFFRACTION THEORY

Consider a circular aperture in a plane rigid baffle and define a positive Z-direction extending to the left of the plane. A plane wave front perpendicular to Z and travelling to the right falls upon the baffle. The velocity potential Φ_i and normal gradient for this wave is

$$\Phi_i = B_i e^{-ikz}, \text{(1a)}; \qquad (\partial\Phi_i/\partial z)_{z=0} = -ikB_i \qquad \begin{matrix}(1.12.1a)\\(1.12.1b)\end{matrix}$$

When the wave emerges from the aperture it generates a diffracted sound field to the right of the baffle. If the normal ($= n$) is defined to be positive when drawn from the plane of the baffle *into* the diffracted region, the diffracted field Φ_d is given by Rayleigh's formula

$$\Phi_d = \frac{1}{2\pi}\int_A \left(\frac{\partial\Phi_d}{\partial n}\right)\frac{e^{ikr}}{r}\,dA \qquad (1.12.2)$$

Now the normal particle velocity in the aperture in the plane of the baffle is a *complex number*, the presence of whose real part renders the calculation of the *diffracted field* very laborious. Kirchoff made the approximation that this real part *over most of the aperture* is small enough relative to the imaginary part to be neglected. In symbols, for time represented by $e^{-i\omega t}$,

$$\frac{\partial \Phi_d}{\partial n} \approx \frac{\partial \Phi_i}{\partial n} = -ikB_i, \text{(3a)}; \qquad \text{Re}\left\{\frac{\partial \Phi_d}{\partial n}\right\} \approx 0 \qquad (1.12.3b)$$

Hence

$$\Phi_d \approx \frac{-ikB_i}{2\pi} \int_A \frac{e^{ikr}}{r}\, dA \qquad (1.12.4)$$

To test this assumption we assume a circular aperture of radius a and calculate the complex number

$$R_1 + iI_1 = \frac{1}{2\pi} \frac{\partial}{\partial n} \int_A \frac{e^{ikr}}{r}\, dA \qquad (1.12.5)$$

for various ka. Now the Kirchoff approximation requires the real part R_1 to be zero, and a plot of the imaginary part versus radial distance a to be the straight line $I_1 = 1$. Actual calculations of Eq.(5) for small ka ($ka < 4$) show that $I_1 \neq 1$, and $R_1 \neq 0$, that is, the approximation is poor. As ka increases the plots of I_1 vs a tend to oscillate about the line $I_1 = 1$, and the plot of R_1 vs a tends to approach zero. However, as $a \to a$ both I_1 and R_1 become indefinitely large. It is more appropriate then to estimate the validity of the approximation by finding *average* values of R_1 and I_1 over the aperture by integration. For $ka = 1, 5$ these averages are

$$\langle R_1 + iI_1 \rangle_{AV.} = -1.2k - i\,0.84k, \qquad ka = 1$$

$$= -0.16k - i\,0.99k, \quad ka = 5$$

The general trend therefore appears to be that Kirchoff's approximation may be used to calculate the field near the aperture when ka is sufficiently large (i.e. $ka > 5$). If the same approximation is used for calculating the far field the resultant plot of pressure versus polar angle gives good agreement with exact theory up to the angle of the first null. At those angles where Kirchoff's approximation leads to amplitude nulls exact theory yields shallow minima, the maximum difference between the two calculations being approximately 10%. Phase plots of far field pressure versus polar angle calculated on the basis of the approximation show considerable error of phase near the nulls. The approximation points to a sudden jump of π radians of phase shift at the nulls, whereas exact theory shows a gradual variation of phase through the angle of the null position, with phase shifts much less than π radians.

In sum: *if the mean radius of the aperture is 1λ or greater the Kirchoff approximation gives an average particle velocity over the aperture which is in phase with the pressure, (i.e., which is purely imaginary). Similarly, if the radius is 1λ* or greater the diffraction pattern calculated on the Kirchoff assumptions agree well with exact theory, at least up to the first null [22].

1.13. DEFINITION OF FRAUNHOFER REGION, FRESNEL REGION. NEAR FIELD REGION IN THE SCALAR FIELD OF ACOUSTIC WAVES

Let there be a vibrating disc, diameter D, in the xy plane at the origin of a Cartesian system xyz. In the plane of the disc we select an arbitrary point Q whose polar coordinates ϱ, β are called the

aperture coordinates at chosen point. At point Q there is a normal component of harmonic velocity $f(\varrho, \beta)$ at wavelength λ which generates a sound field at an external point P whose *field coordinates* are R, θ, ϕ. The distance from source point Q to field point P is r.

Now the field at P due to a unit source at Q is $2e^{ikr}/r$, which is the Green's function for the semi infinite space above the rigid plane $z = 0$. If all the sources in the disc are summed, the total field at P can be calculated by the modern version of Rayleigh's formula,

$$\psi(P) = -\frac{1}{2\pi}\int_s \frac{\partial \psi}{\partial n}\,\frac{e^{ikr}}{r}\,dS \tag{1.13.1}$$

Here, the coordinate time is given by the real part of $e^{i\omega t}$ and the normal to the plane $z = 0$ points in the direction of positive z. Since the calculation of this formula for arbitrary r is tedious, it is conventional to approximate r by suitable formulas designed to simplify the integration. To understand these formulas we sketch below in the (vector) relations between the aperture coordinates (ϱ, β) and the field coordinates (R, θ, ϕ).

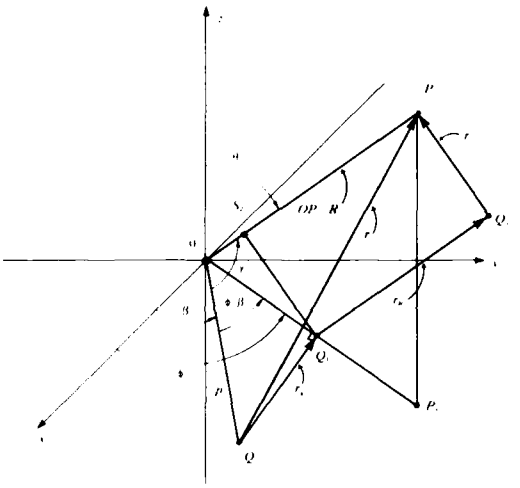

Fig. 1.13.1. Geometric construction used to define near field regions of a radiating surface.

In this figure plane OPP_1 is perpendicular to the xy plane. The vector $\boldsymbol{r}$ is seen to be the sum of the three orthogonal components in the directions of the unit spherical coordinate vectors. These components are labelled r_R, r_θ, and r_ϕ respectively, and have the form

$$\begin{aligned} r_R &= Q_1Q_2 = R - \varrho \sin\theta \cos(\phi - \beta) \\ r_\theta &= Q_2P = -\varrho \cos\theta \cos(\phi - \beta) \\ r_\phi &= QQ_1 = \varrho \sin(\phi - \beta) \end{aligned} \tag{1.13.2}$$

The formulas given by 1.13.2 have been derived by writing the vectors ϱ, R in Cartesian coordinates, i.e.,

$$\boldsymbol{\varrho} = \boldsymbol{i}\varrho\cos\beta + \boldsymbol{j}\varrho\sin\beta$$

$$\boldsymbol{R} = \boldsymbol{i}R\sin\theta\cos\phi + \boldsymbol{j}R\sin\theta\sin\phi + \boldsymbol{k}R\cos\theta$$

and then finding the components of $\boldsymbol{r}$ which are 1) perpendicular to the plane OPP_1, 2) perpendicular to OP and lying in the plane OPP_1 and 3) parallel to OP and lying in the plane OPP_1.

We note that the angle γ between $\boldsymbol{R}$ and $\boldsymbol{\varrho}$ is given by

$$\boldsymbol{R}\cdot\boldsymbol{\varrho} = R\varrho\cos\gamma = R\varrho\sin\theta\cos(\phi - \beta)$$

and that

$$\begin{aligned} r &= \sqrt{r_R^2 + r_\theta^2 + r_\phi^2} = \sqrt{R^2 + \varrho^2 - 2\varrho R\cos\gamma} \\ &= r_R\sqrt{1 + X} = R\sqrt{1 + X'} \end{aligned} \tag{1.13.3}$$

in which

$$X = \left(\frac{r_\theta}{r_R}\right)^2 + \left(\frac{r_\phi}{r_R}\right)^2, X' = \left(\frac{\varrho}{R}\right)^2 - \frac{2\varrho}{R}\cos\gamma \tag{1.13.4}$$

To approximate r we may assume in the first instance that $X^2 < 1$ (or $X'^2 < 1$). In particular if the field point is on the z-axis (where $\cos\gamma = 0$) and the source point is on the edge of the disc, the requirement that $X^2 < 1$ leads to the assumption that R is at least equal to $D/2$. With such stipulations we expand the square root $\sqrt{1 + X}$ in powers of X, that is,

$$\sqrt{1+X} = 1 + \frac{X}{2} - \frac{X^2}{8} + \frac{X^3}{16} - \frac{5X^4}{132} + , [X^2 < 1] \tag{1.13.5}$$

The result is

$$r = r_R\left[1 + \frac{1}{2}\left[\left(\frac{r_\theta}{r_R}\right)^2 + \left(\frac{r_\psi}{r_R}\right)^2\right] - \frac{1}{8}\left[\left(\frac{r_\theta}{r_R}\right)^2 + \left(\frac{r_\phi}{r_R}\right)^2\right]^2 + \ldots \tag{1.13.6}$$

If r_θ/r_R and r_ϕ/r_R are so small that the second term on the right in this formula may be neglected, we obtain the Fraunhofer approximation of *phase* which is that in the *phase factor* e^{ikr} we may write

$$r \approx r_R = R - \varrho\sin\theta\cos(\phi - \beta) \tag{1.13.7}$$

For the amplitude factor ($= 1/r$) we use $r = R$. 1.13.7 states that in the "Fraunhofer approximation" the phase of the elementary wave originating at Q and observed at P is given by kh_R, where r_R is the radial component (in spherical coordinates) of the vector QP. This formula is applicable only at distances R (or greater) such that the phase error introduced by the first neglected term on the right-hand side of 1.13.6 is less than $2\pi/q$, where q is a selected factor. We thus arrive at the condition that the distance R must be such that

$$\frac{k}{2}\frac{r_\theta^2 + r_\psi^2}{r_R} < \frac{\partial\pi}{q} \tag{1.13.8}$$

By means of 1.13.2 we can rewrite this as

$$\frac{1}{2\lambda}\frac{\varrho^2[\cos^2\theta\cos^2(\phi - \beta) + \sin^2(\phi - \beta)]}{R - \varrho\sin\theta\cos(\phi - \beta)} < \frac{1}{q}.$$

Let the coordinates of the observation point be $(0, 0, R)$, i.e., let P be on the axis, then for the far field we require that

$$R > \frac{q\varrho^2}{2\lambda}. \tag{1.13.9a}$$

For a maximum $\varrho = D/2$, where D is the diameter of the disc, we then have,

$$R > \frac{qD^2}{8\lambda}. \tag{1.13.9b}$$

A widely used value of maximum phase error associated with radiation from the edge of the disc is $q = 8$ [23]. With this value, the application of the Fraunhofer formula (= Eq. (7)) is valid for distances R such that

$$R > \frac{D^2}{\lambda} \tag{1.13.9c}$$

For distances less than this we may add to the factors determining the phase of an elementary wave originating at Q the term neglected above; that is, the second term on the right-hand side of Eq. (6). In the region $R < D^2/\lambda$ we therefore assume that a suitable value for r in the phase e^{ikr} is

$$r \approx R - \sin\theta\cos(\phi - \beta) + \frac{\varrho^2}{2}\,\frac{[1 - \sin^2\theta\cos^2(\phi - \beta)]}{(R - \varrho\sin\theta\cos(\phi - \beta))}\,. \tag{1.13.10}$$

For the amplitude factor $1/r$ we again assume that $r \approx R$. With these choices there is a residual phase error in the field at point P due to the third and higher terms in Eq. (6). We now select a factor s and a distance R^* such that the phase error due to the third term in Eq. (6) is less than $2\pi/s$. The distance R^* is then determined by the requirement that

$$\frac{k}{8}\left\{\frac{r_\theta^2 + r_\phi^2}{r_R^3}\right\} < \frac{2\pi}{s} \tag{1.13.11a}$$

or

$$\frac{s}{\lambda 8}\left\{\frac{\varrho^4[1 - \sin^2\theta\cos^2(\phi - \beta)]^2}{[R^* - \varrho\sin\theta\cos(\phi - \beta)]^3}\right\} < 1. \tag{1.13.11b}$$

If we observe the field at point (O, O, R^*), this inequality then appears as

$$R^{*3} > \frac{s}{8\lambda}\,\varrho^4. \tag{1.13.12a}$$

For a maximum $\varrho = D/2$ we have

$$R^* > \left(\frac{s}{8}\right)^{1/3}\frac{D}{2}\left(\frac{D}{2\lambda}\right)^{1/3}, \qquad \text{(circular aperture)} \tag{1.13.12b}$$

Selecting $s = 8$ once again (that is, allowing the maximum phase error due to a point on the edge of the disc to be $2\pi/8$ radians) we find that for a circular aperture the region in which Eq. (10) is valid is

$$R^* > \frac{D}{2}\left(\frac{D}{2\lambda}\right)^{1/3} \qquad \text{(circular aperture).} \tag{1.13.13}$$

We now combine Eqs. (9c) and (13) and define a region of radial distance r_f greater than R^* but less than R, in which Eq (10) is a satisfactory representation of r in the phase e^{ikr} within the allowable phase errors noted above. This is the *Fresnel region* for a circular aperture and is defined by the inequality

$$\frac{D}{2}\left(\frac{D}{2\lambda}\right)^{1/3} < r_f < \frac{D^2}{\lambda}\,, \qquad \text{(14a)}; \qquad r_f > \frac{D}{2}\,. \tag{1.13.14b}$$

The region of radial distance r_n less than R^* is called the *near field*, and is given by the formula

$$0 \leq r_n < \left(\frac{s}{8}\right)^{1/3}\left(\frac{D}{2}\right)\left(\frac{D}{2\lambda}\right)^{1/3}, \qquad \text{(circular aperture).} \tag{1.13.15}$$

In the "near field" no approximations in phase or amplitude of e^{ikr}/r are made.

The regions defined above are applicable to apertures of circular shape. For a square aperture (side = D) **Polk [23]** found that for a $\lambda/8$ phase error at the edge the distance limits (= r_f) of the Fresnel region are given by

$$\frac{(2)^{1/3}}{2} D\left(\frac{D}{\lambda}\right)^{1/3} < r_f < \frac{D^2}{\lambda}, \qquad \begin{matrix}\text{Fresnel Region} \\ \text{(square aperture)}\end{matrix} \tag{1.13.16}$$

REFERENCES

1. P. M. Morse, K. U. Ingard "Linear Acoustic Theory", Encyclopedia of Physics, Vol. XI/1, Acoustics 1, Springer, Berlin 1961, pp. 2-14.
2. L. Landau, E. Lifshitz, "Fluid Mechanics", Addison-Wesley, Reading, Mass., 1959, Chap. 8.
3. C. J. Bouwkamp, Phillips Res. Reports, Vol. I, p. 252 (1946).
4. P. M. Morse, H. Feshbach, "Methods of Theoretical Physics", McGraw-Hill, 1953, p. 837.
5. L. L. Foldy, H. Primakoff, JASA. *17, 109-120 (1945).*
6. P. M. Morse, K. V. Ingard, "Theoretical Acoustics", McGraw-Hill (1968), p. 324.
7. Ref. [4], Chapter. 5.
8. Ref. [4], p. 459.
9. Ref. [4], p. 1407.
10. "Handbook of Mathematical Functions", U.S. Dept. of Commerce, Nat. Bur. of Stds., Applied Math., Series 55, p. 748.
11. C. Flammer, "Spheroidal Wave Functions", Stanford V. Press, Stanford, Ca. 1957.
12. S. Hanish et al., "Tables of Spheroidal Wave Functions", Naval Research Laboratory Reports 7088-7093, Naval Res. Lab., Washington, D.C. 1970.
13. Ref. [4], p. 1512.
14. Ref. [4], p. 656.
15. V. D. Kupradze, "Fundamental Problems in the Mathematical Theory of Diffraction", trans. C. D. Benster (NBS Rept., No. 2008, Oct. 1952).
16. W. D. MacMillan, "The Theory of the Potential", McGraw-Hill, 1930, p. 120.
17. a. H. A. Schenck, JASA *44*, 41-58, 1968.
    b. L. G. Copley, "Two Approaches to the Helmholtz Integral for Slender Axi symmetic Sound Radiators", Cambridge Acoustical Assoc. Inc. Final Report U-186-131, Part I. June 1964.
18. J. Todd, Ed. "Survey of Numerical Analyses", McGraw-Hill, New York, 1962.
19. Ref. [4], Chap. 7.
20. Lord Rayleigh, "Theory of Sound", Dover Publications, New York, 1945, Vol. 2, p. 107.
21. C.J. Bouwkamp, Phillips Res. Rept. 1, 1946, p. 252.
22. R. D. Spence, "Kirchoff Approximation", JASA.
23. C. Polk, "Optical Fresnel-Zone Gain of a Rectangular Aperture", IRE Trans. on Antennas and Prop, Vol. *AP-4*, 65-69, (1956).

BIBLIOGRAPHY ON RADIATION OF SOUND FROM ARBITRARY SHAPED BODIES.

1. G. M. L. Gladwell, "A Variational Formulation of Acousto-Structural Vibration Problems," J. Sound Vib. **4**, 172-186 (1966).

2. G. M. L. Gladwell and V. Mason, "Variational Finite Element Calculation of the Acoustic Response of A Rectangular Panel," J. Sound Vib. **14**, 115-135 (1971).

3. J. L. Butler, "Solution of Acoustical-Radiation Problems by Boundary Collocation," J. Acoust. Soc. Am. **48**, 325-336 (1970).

4. R. R. Smith, J.T. Hunt, and D. Barach, "Finite Element Analysis of Acoustically Radiating Structures with Applications to Sonar Transducers," J. Acoust. Soc. Am. **54**, 1277-1288 (1973).

5. L. G. Copley, "Fundamental Results Concerning Integral Representations in Acoustic Radiation," J. Acoust. Soc. Am. **44**, 22-32 (1968).

6. L. H. Chen and D. G. Schweikert, "Sound Radiation from An Arbitrary Body," J. Acoust. Soc. Am. **35**, 1626-1632

7. J. L. Hess, "Solution of the Helmholtz Equation for Steady Acoustic Waves," Douglas Aircraft Div. Rept. No. 31655 (10 April 1964).

8. G. B. Brundit, "A Solution to the Problem of Scalar Scattering from a Smooth, Bounded Obstacle Using integral Equations," Q. J. Mech. Apply. Math. **18**, 473-489 (1965).

9. G. Chertock, "Sound Radiation from Vibrating Surfaces," J. Acoust. Soc. Am. **36**, 1305-1313 (1964).

CHAPTER II
THREE-DIMENSIONAL HARMONIC RADIATION

2.1 THEORY OF THE SPHERICAL RADIATOR [1], [2], [3].

The *N*'th Order Spherical Radiator

By a spherical harmonic radiator of order n we shall mean a spherical surface, radius r_0, which has a normal component of surface velocity given by $v_n(\theta, \phi)\, e^{j(\omega t + \Omega_n)}$, the factor v_n being a surface spherical harmonic, $U_n(\theta, \phi)$, of order n. In symbols,

$$v_n = U_n(\theta, \phi) \tag{2.1.1}$$

$$U_n(\theta, \phi) = \sum_{m=0}^{n} (u_{mn} \cos m\phi + u'_{mn} \sin m\phi)\, P_n^m(\cos \theta) \tag{2.1.2}$$

Here, u_{mn}, u'_{mn} are real, explicitly specified numbers whose units are those of velocity (ms^{-1}). The symbols P_n^m (cos θ) are associated Legendre functions of the first type [4]. Now an n'th order spherical radiator generates a velocity potential $\Phi_n(r, \theta, \phi, t)$ at the field point r which, in the absence of boundaries, satisfies the Helmholtz equation $(\nabla^2 + k^2)\Phi_n = 0$ for outgoing waves dissipating at infinity. In particular, this equation separates in spherical coordinates into a product of three factors, $Y_n(\theta, \phi)\, h_n^{(2)}(kr) e^{j\omega t}$, which together define the *spherical wave function* at the frequency ω (see 1.9.33, 1.9.34). The superscript 2 in $h_n^{(2)}$ means that time is given by $e^{j\omega t}$ instead of $e^{-j\omega t}$. The radial function, $h_n^{(2)}(kr)$ will be discussed later in detail. Since the pressure (p) and normal particle velocity (u_n) are related by the formula $-jk\varrho c u_n$ = grad p, as given by Eq. 1.1.6, the field pressure $p_n(r, \theta, \phi, t)$ is seen to be

$$p_n(r, \theta, \phi, t) = -j\varrho c\, U_n(\theta, \phi)\, \frac{h_n^{(2)}(kr)}{\left[\dfrac{dh_n^{(2)}(z)}{dz}\right]_{z=kr_0}}\, e^{j(\omega t + \Omega_n)} \tag{2.1.3}$$

A collection of q radiators of different orders $n + 1, n + 2, \ldots q$ will produce a field pressure which is the superposition of the pressures due to individual radiators; that is,

$$p = \sum_{r=1}^{q} p_{n+r}, \; n \text{ fixed.} \tag{2.1.4}$$

Each spherical radiator of order n contributes a spatial distribution of pressure at any radius in accordance with the spherical harmonic $U_n(\theta, \phi)$, weighted by the value of the radial function $h_n^{(2)}(kr)$ at that radius. The difference between near-field and far-field pressures therefore are due to the influence of the radial functions, $h_n^{(2)}(kr)$ only. In the literature of classical times [5], the radial functions and their derivatives appeared as products of finite polynomials, $f_n(jkr)$, $F_n(jkr)$, (the Stokes function and the Rayleigh function respectively), and the factor e^{jkr}/jkr. Written in full these polynomials were defined by the formulas,

$$f_n(jkr) = \frac{1}{n!} \sum_{s=0}^{m} \binom{m}{s} \frac{(n+s)!}{2^s (jkr)^s} \tag{2.1.5}$$

$$F_n(jkr) = \frac{1}{n!} \sum_{s=0}^{m} \binom{m}{s} \frac{(n+s)!}{2^s (jkr)^s} (1 + s + jkr). \tag{2.1.6}$$

Symbols $\binom{n}{s}$ are binomial coefficients defined by,

$$\binom{n}{s} = \frac{n!}{s!(n-s)!}$$

The relation between F_n and the spherical Bessel functions $h_n^{(2)}$ defined by Morse [6] may be written in terms of a pair of useful entities A_n, B_n. In this notation the radial function factor of the spherical wave function and its derivative have the forms,

$$h_n^{(2)}(kr) = A_n(jkr)\, e^{-jkr}\, e^{j(n/2+1)\pi} \tag{2.1.7}$$

$$\left[\frac{dh_n^{(2)}(z)}{dz}\right]_{z=kr_0} = B_n(jkr_0)\, e^{-jkr_0}\, e^{j(n+1/2)\pi} \tag{2.1.8}$$

$$\frac{h_n^{(2)}(z)}{\left[\frac{dh_n^{(2)}(z)}{dz}\right]_{z=z_0}} = j\,\frac{A_m(jz)}{B_m(jz_0)}\, e^{-j(z-z_0)}. \tag{2.1.9}$$

$$z = kr,\ z_0 = kr_0$$

The symbols $A_n(x)$, $B_n(x)$ represent polynomials in the variable $(1/x)$. These polynomials were introduced by Brillouin [7] who defined them by the formulas,

$$A_n(x) = \frac{f_n(x)}{x} = \sum_{p=0}^{n} a_n^p (x)^{-(p+1)} \tag{2.1.10a}$$

$$B_n(x) = \frac{F_n(x)}{x^2} = \sum_{p=0}^{n+1} b_n^p (x)^{-(p+1)} \tag{2.1.10b}$$

$$B_n(x) = A_n(x) - \frac{dA_n(x)}{dx} \tag{2.1.10c}$$

$$a_n^0 = b_n^0 = 1,\ b_n^p = p a_n^{p-1} + a_n^p$$

$$a_n^p = \frac{[(2n+1)^2 - 1]\,[(2n+1)^2 - 3^2] \ldots [(2n+1)^2 - (2p-1)^2]}{p!\, 8p}. \tag{2.1.11}$$

Both A_n and B_n are complex. Ref. [8] therefore defines the radial functions in terms of amplitudes $D_n(z)$, $D_n'(z)$ and phases $\delta_n(z)$, $\delta_n'(z)$, such that,

$$h_n(z) = -iD_n e^{j\delta_n} \rightarrow jD_n e^{-j\delta_n} \tag{2.1.12a}$$

From 2.1.7, it is seen that,

$$D_n = A_n(jkr);\ \delta_n = kr - \pi\left(\frac{n+1}{2}\right) \tag{2.1.12b}$$

Also,

$$h_n'(z) = iD_n' e^{-j\delta_n'} \rightarrow -jD_n' e^{-j\delta_n'} \tag{2.1.13a}$$

From 2.1.8, the amplitudes and phases reduce to,

$$D_n' = B_n(jkr);\ \delta_n' = kr - \pi\left(\frac{m}{2} + 1\right) \tag{2.1.13b}$$

as everywhere, $+j = -i$.

An alternative notation of the radial function is that of Stenzel [9] who defines two quantities $S_n(kr)$ and $C_n(kr)$ such that

$$f_n(jz) = e^{jz}\,[S_n(z) + jC_n(z)] \tag{2.1.14}$$

$$F_n(jz) = e^{jz}\,[U_n(z) + jV_n(z)] \tag{2.1.15}$$

$$\left.\begin{aligned} S_n(z) &= \sqrt{\frac{\pi z}{2}}\, J_{n+1/2}(z) \\ C_n(z)\ (= -1)^n &\sqrt{\frac{\pi z}{2}}\, J_{-n-1/2}(z) \end{aligned}\right\} \tag{2.1.16a}$$

(Note: the symbol j of this chapter equals i of Stenzel [9].)

We thus see that in the notation of Stenzel

$$\frac{A_n(jkr)}{B_n(jkr_0)} = j\,\frac{4\pi C_0^2}{2\lambda r}\left[\frac{S_n(kr) + jC_n(kr)}{U_n(kr_0) + jV_n(kr_0)}\right] e^{jk(r-r_0)} \tag{2.1.16b}$$

The variation of $h_n^{(2)}(kr)$ with distance r from the origin may be determined from the series described by 2.1.10a, 2.1.10b. We have,

$$A_n \rightarrow \frac{1}{jkr},\ kr \rightarrow \infty \tag{2.1.17a}$$

$$A_n \rightarrow \frac{\bar{n}}{(jkr)^{n+1}}(1 + jkr),\quad \begin{aligned} &kr \rightarrow 0 \\ &\bar{n} = 1.3.5 \ldots (2n-1) \end{aligned} \tag{2.1.17b}$$

also,

$$B_n \rightarrow 1/jkr,\quad kr \rightarrow \infty. \tag{2.1.17c}$$

In the near field therefore of a collection of nth order spherical radiators 2.1.4, the magnitude of pressure is dominated by terms in $(kr)^{-(n+1)}$, and by the source velocities U_n. Further discussions of the near field are found in Sect. 2.5.

If the normal component of surface velocity of a spherical radiator is a specified arbitrary function $v(\theta_0, \phi_0)$ we may once again use Eq. 2.1.2 this time however, u_{mn} and u'_{mn} are to be determined from the set of equations,

$$\left.\begin{matrix} u_{mn} \\ u'_{mn} \end{matrix}\right\} = \frac{(2n+1)}{4\pi}\,\varepsilon_m\,\frac{(n-m)!}{(n+m)!}\int_A v(\theta_0, \phi_0)\left\{\begin{matrix} \cos m\phi_0 \\ \sin m\phi_0 \end{matrix}\right\} P_n^m(\cos\theta_0)\,dA \tag{2.1.18a}$$

$$\varepsilon_0 = 1,\ \varepsilon_{m\neq 0} = 2 \tag{2.1.18b}$$

The velocity potential Φ at any point in the field due to this distribution of normal velocity on the unit surface $r = r_0 = 1$ then becomes,

$$\Phi(r, \theta, \phi, t) = e^{j\omega t} \sum_{n=0}^{\infty} \sum_{m=0}^{n} \frac{2n+1}{4\pi} \frac{(n-m)!}{(n+m)!} \frac{P_n^m(\cos\theta)\, h_m^{(2)}(kr)}{-k \left[\dfrac{dh_n^{(2)}(z)}{dz} \right]_{z=kr_0}}$$

$$\times \int_0^{2\pi} d\phi_0 \int_0^{\pi} V(\theta_0, \phi_0) \cos m(\phi - \phi_0)\, P_n^m(\cos\theta_0) \sin\theta_0\, d\theta_0 d\phi_0 \tag{2.1.18c}$$

We have implied in 2.1.18 that $v(\theta_0, \phi_0)$ is real, that is all points on the spherical surface move in phase. However, in the most general case we must allow $v(\theta_0, \phi_0)$ to be complex, that is, the phase of the surface velocity at point $(\theta_0, \phi_0 r_0)$ is allowed to differ from the phase given by the time ($= \exp(j\omega t)$). For convenience in this case we write the spherical wave function in complex form by introducing a complex surface spherical harmonic, $Y_n^m(\theta, \phi)$. Thus the mn'th spherical wave function at field point (θ, ϕ, r) is written

$$Y_n^m(\theta, \phi)\, h_n^{(2)}(kr)\, e^{j\omega t} \tag{2.1.19a}$$

where

$$Y_n^m(\theta, \phi) \equiv e^{-jm\phi} P_n^m(\cos\theta). \tag{2.1.19b}$$

These functions form an orthogonal series in the space of the spherical coordinates θ, ϕ. We can therefore expand the velocity potential in an infinite series of these complex functions, and write the **amplitude of Φ in a series of complex spherical harmonics with amplitude coefficient U_{mn},**

$$\Phi = \sum_{n=0}^{\infty} \sum_{m=-n}^{+n} U_{mn}\, Y_n^m\, h_n^{(2)} \tag{2.1.20}$$

$$\left[\frac{\partial \Phi}{\partial r} \right]_{r=r_0} = -v(\theta, \phi) = k \sum_{n=0}^{\infty} \sum_{m=-n}^{+n} U_{mn}\, Y_n^m \left[h_n^{(2)\prime}(z) \right]_{z=kr_0} \tag{2.1.21}$$

By multiplying both sides of this equation with the conjugate surface spherical harmonic Y_n^{m*}, and by using the normalization formula

$$N_n^{|m|} = \int\int_{\text{sphere}} Y_n^m\, Y_n^{m*}\, dS = \frac{4\pi(n + |m|)!}{(2n+1)(n-|m|)!} \tag{2.1.22}$$

where the integration is performed over a sphere of unit radius, we find the expansion constants U_{mn} to be

$$U_{mn} = \frac{\int_0^{\pi} du \int_0^{2\pi} dv\, V(u, v)(e^{-jmv})^*\, P_n^{|m|}(\cos u) \sin u}{-k[h_n^{(2)\prime}(z)]_{z=kr_0} N_n^{|m|}\, C}. \tag{2.1.23a}$$

Here

$$C = 1,\ m \geq 0;\quad C = (-1)^m \frac{(n-|m|)!}{(n+|m|)!},\ m < 0;\quad P_n^{-m} = CP_n^{|m|} \tag{2.1.23b}$$

The velocity potential generated by a sphere of radius r_0 whose surface is vibrating with a normal component of velocity given by $V(\theta, \phi)e^{j\omega t}$ has therefore the form

$$\Phi(r, \theta, \phi, t) = \sum_{n=0}^{\infty} \sum_{m=-n}^{+n} \frac{A_n(jkr)\, e^{j[\omega t - k(r-r_0)]}}{(jk)\, B_n(jkr_0)\, N_n^{|m|}\, C} \times \int_0^{\pi} du \int_0^{2\pi} dv\, V(u, v)\, e^{-jm(\phi - v)}\, P_n^{|m|}(\cos u)\, P_n^m(\cos\theta) \sin u \tag{2.1.24a}$$

or the form,

$$\Phi(r, \theta, \phi, t) = \sum_{n=0}^{\infty} \sum_{m=n}^{n} \frac{A_n(jkr)\, e^{j[\omega t - k(r-r_0)]}\, \varepsilon_m}{(jk)\, B_n(jkr_0)\, N_n^m} \times \int_0^{\pi} \sin u du \int_0^{2\pi} dv\, V(u, v)\, P_n^m(\cos u)\, P_n^m(\cos\theta)\, [\cos m(\phi - v)] \tag{2.1.24b}$$

in which ε_m is the Neuman factor defined in 2.1.18b.

From the velocity potential given by these equations we may derive the complex acoustic pressure p and the complex particle velocities u, v, w, at any point (r, θ, ϕ) in the field. For convenience we define a constant X such that

$$X \equiv \frac{e^{j\omega t}}{N_n^{|m|}\, C} \int_0^{\pi} du \int_0^{\pi} dv V(u, v)\, e^{jmv}\, P_n^{|m|}(\cos u) \sin u$$

so that

$$\Phi(r, \theta, \phi, t) = \sum_{n=0}^{\infty} \sum_{m=-n}^{+n} X\, \frac{A_n(jkr)\, e^{-jk(r-r_0)} e^{-jm\phi}}{jk\, B_n(jkr_0)}\, P_n^m(\cos\theta) \tag{2.1.24c}$$

From Eq. 1.1.5 and 1.1.6 we find that

$$p = \varrho c \sum_{n=0}^{\infty} \sum_{m=-n}^{+n} X\, \frac{A_n(jkr)\, e^{-jk(r-r_0)} e^{-jm\phi}}{B_n(jkr_0)}\, P_n^m(\cos\theta) \tag{2.1.25}$$

$$u = \sum_{n=0}^{\infty} \sum_{m=-n}^{n} X\, \frac{B_n(jkr)\, e^{-jk(r-r_0)} e^{-jm\phi}}{B_n(jkr_0)}\, P_n^m(\cos\theta) \tag{2.1.26}$$

$$v = -\sum_{n=0}^{\infty} \sum_{m=-n}^{+n} X\, \frac{A_n(jkr)}{(jkr)\, B_n(jkr_0)}\, e^{-jk(r-r_0)} e^{-jm\phi}\, \frac{dP_n^m(\cos\theta)}{d\theta} \tag{2.1.27}$$

$$w = -\sum_{n=0}^{\infty} \sum_{m=-n}^{+n} X\, \frac{mA_n(jkr)}{(kr \sin\theta)\, B_n(jkr_0)}\, e^{-jk(r-r_0)} e^{-jm\phi}\, \frac{\partial P_n^m(\cos\theta)}{\partial\phi} \tag{2.1.28}$$

In these formulas the integer m takes on negative values. It is often convenient to restrict m to positive values ($m \geq 0$). We may then use 2.1.24b and define even (subscript e) and odd (subscript 0) constants W_i such that,

$$\begin{Bmatrix} W_{e_{(mn)}} \\ W_{0_{(mn)}} \end{Bmatrix} = \frac{e^{j\omega t}\, \varepsilon_m}{N_n^m} \int_0^{\pi} \sin u du \int_0^{2\pi} dv V(u, v)\, P_n^m(\cos u) \begin{Bmatrix} \cos mv \\ \sin mv \end{Bmatrix}, \tag{2.1.29}$$

$$m = 0, 1, 2, \ldots . n$$

so that

$$\Phi(r, \theta, \phi, t) = \sum_{n=0}^{\infty} \sum_{m=0}^{n} (W_{e_{(mn)}} \cos m\phi + W_{0_{(mn)}} \sin m\phi)\, \frac{A_n(jkr)}{jk\, B_n(jkr_0)}\, P_n^m(\cos\theta) \tag{2.1.30}$$

A further simplification of this involved notation has been introduced by Reschevkin [10] who made W_e, W_0 non-dimensional by dividing each by the quantity $W_{e(00)}$ obtained from (29) by setting $m = 0$, and then defined a *spherical harmonic of order n*, $(\overline{P}_n(\theta, \phi))$, by the formula

$$\overline{P}_n(\theta, \phi) = \sum_{m=0}^{n} \left(\frac{We_{(mn)}}{We_{(00)}} \cos m\phi + \frac{Wo_{(mn)}}{We_{(00)}} \sin m\phi \right) P_n^m(\cos\theta) \tag{2.1.31}$$

The velocity potential of spherical radiator in this notation then is written

$$\Phi(r, \theta, \phi, t) = \sum_{n=0}^{\infty} We_{(00)} \overline{P}_n(\theta, \phi) \frac{A_n(jkr)}{jk\, B_m(jkr_0)} e^{-jk(r-r_0)} \tag{2.1.32}$$

From 1.1.4 and 1.1.5 we find again that the amplitudes of pressure and particle velocity are

$$p = \varrho c \sum_{n=0}^{\infty} We_{(00)} \overline{P}_n(\theta, \phi) \frac{A_n(jkr)}{B_n(jkr_0)} e^{-jk(r-r_0)} \tag{2.1.33}$$

$$u = \sum_{n=0}^{\infty} We_{(00)} \overline{P}_n(\theta, \phi) \frac{B_n(jkr)}{B_n(jkr_0)} e^{-jk(r-r_0)} \tag{2.1.34}$$

$$v = \sum_{n=0}^{\infty} We_{(00)} \frac{A_n(jkr)}{(kr)\, B_n(jkr_0)} \frac{\partial \overline{P}_n(\theta, \phi)}{\partial \theta} e^{-jk(r-r_0)} e^{j\pi/2} \tag{2.1.35}$$

$$w = \sum_{n=0}^{\infty} We_{(00)} \frac{A_n(jkr)}{(kr \sin\theta)\, B_n(jkr_0)} \frac{\partial \overline{P}(\theta, \phi)}{\partial \theta} e^{-jk(r-r_0)} e^{j\pi/2} \tag{2.1.36}$$

2.2 ACOUSTIC INTENSITY AND ACOUSTIC POWER OF SPHERICAL RADIATORS

The formulas for pressure and particle velocity listed in the previous section may be used directly to obtain the acoustic intensities I_q in directions q by use of 1.3.3a, that is, by the formula

$$I_q = \tfrac{1}{2} \operatorname{Re}\{p\, q_r^*\}$$

Here q_r represents the component of particle velocity normal to the vector area over which the acoustic intensity is being calculated. The particle velocity vector q at any point (r, θ, ϕ) may be written in terms of the unit orthogonal vectors $\boldsymbol{a}_r$, $\boldsymbol{a}_\theta$, $\boldsymbol{a}_\phi$, in the form

$$\hat{\boldsymbol{q}} = u\boldsymbol{a}_r + v\boldsymbol{a}_\theta + w\boldsymbol{a}_\phi$$

This motion of the medium is conceived to be generated by a given normal component of surface velocity $V(\theta, \phi)$ which may be complex. In general we set

$$V(\theta, \phi) = V^{(1)}(\theta, \phi) + i\, V^{(2)}(\theta, \phi)$$

Referring to 2.1.29 of the previous section we now append the superscripts (1) or (2) to the constants $W_{e_{(mn)}}$, $W_{0_{(mn)}}$, to distinguish the contribution of the real and imaginary part of the given surface velocity. In addition we write the *total* acoustical quantities at a point in the field as the sum of these contributions, that is, we write

$$p(r, \theta, \phi, t) = p^{(1)} + ip^{(2)} \tag{2.2.1}$$

$$u(r, \theta, \phi, t) = u^{(1)} + iu^{(2)} \tag{2.2.2}$$

$$v(r, \theta, \phi, t) = v^{(1)} + iv^{(2)} \tag{2.2.3}$$

$$w(r, \theta, \phi, t) = w^{(1)} + iw^{(2)} \tag{2.2.4}$$

Note here that $p^{(i)}$, $u^{(i)}, v^{(i)}$, $w^{(i)}$ themselves are complex numbers. From these equations we can now construct the formulas for intensity as follows,

$$I_r = \tfrac{1}{2}\,\mathrm{Re}\{(p^{(1)} + ip^{(2)})(u^{(1)} + iu^{(2)*})\} \tag{2.2.5}$$

$$I_\theta = \tfrac{1}{2}\,\mathrm{Re}\{(p^{(1)} + ip^{(2)})(v^{(1)} + iv^{(2)*})\} \tag{2.2.6}$$

$$I_\phi = \tfrac{1}{2}\,\mathrm{Re}\{(p^{(1)} + ip^{(2)})(w^{(1)} + iw^{(2)*})\} \tag{2.2.7}$$

The products contained within the braces of the above formulas reduce to double sums. To elucidate their meaning we assume that $V(\theta, \phi)$ is real, that is, all the quantities with superscript (2) are assumed to vanish. Then we may write the intensities in the $\boldsymbol{a}_r$, $\boldsymbol{a}_\theta$, $\boldsymbol{a}_\phi$ directions as follows,

$$I_r = \tfrac{1}{2}\,\varrho c\,\mathrm{Re}\left\{\sum_{s=0}^{\infty}\sum_{t=0}^{\infty} We_{0s}\,We_{ot}^{*}\,\overline{P}_s\overline{P}_t\,\frac{A_s(jkr)\,B_t^{*}(jkr)}{B_s(jkr_0)\,B_t^{*}(jkr_0)}\right\} \tag{2.2.8}$$

$$I_\theta = \tfrac{1}{2}\,\varrho c\,\mathrm{Re}\left\{\sum_{s=0}^{\infty}\sum_{t=0}^{\infty}\frac{We_{0s}\,We_{ot}^{*}}{(jkr)}\,\overline{P}_s\left[\frac{\partial\overline{P}_t}{\partial\theta}\right]\frac{A_s(jkr)\,A_t^{*}(jkr)}{B_s(jkr_0)\,B_t^{*}(jkr_0)}\right\} \tag{2.2.9}$$

$$I_\phi = \tfrac{1}{2}\,\varrho c\,\mathrm{Re}\left\{\sum_{s=0}^{\infty}\sum_{t=0}^{\infty}\frac{We_{0s}\,We_{ot}^{*}}{jkr\sin\theta}\,\overline{P}_s\left[\frac{\partial P_t}{\partial\phi}\right]\frac{A_s(jkr)\,A_t^{*}(jkr)}{B_s(jkr_0)\,B_t^{*}(jkr_0)}\right\}, \tag{2.2.10}$$

Now if $V(\theta, \phi)$ corresponds to a *single* spherical harmonic of order l then each of the double sums in the above equations reduces to one term, namely, the term arising from $s = l$, $t = l$. This is a result of the application of the orthogonality properties of the associated Legendre polynomials in 2.1.22, which states that

$$\int Y_n^m\,Y_p^{q*}\,dS = 0 \qquad \text{if } m \neq q,\ n = p$$

$$\int Y_n^m\,Y_p^{q*}\,dS = N_n^{|m|} \text{ if } m = q,\ n = p$$

When $s = t = l$ an examination of 2.1.(33), (34), (35) and (36) shows that p is in time quadrature ($= \exp(j\pi/2)$ factor) with v and w over a complete cycle of sinusoidal time. Since there is no change in phase between $\overline{P}$ and $\partial\overline{P}/\partial\theta$, and between $\overline{P}$ and $\partial\overline{P}/\partial\phi$, we see that $I_\theta = I_\phi = 0$. In contrast, p and u are not in time quadrature, i.e. $I_r \neq 0$. From this comes the general rule [11] that a *spherical radiator of order n acting along generates a flow of energy in the radial direction only.* When, however, $V(\theta, \phi)$ is an arbitrary function of the coordinates then all terms in the double sum are present in 2.2(8), (9), (10). Cross-products of factors (such as $(A_s)(A_t^*)$ for example) are no longer real numbers. Then I_θ, I_ϕ do not vanish, and energy flow tangential to any spherical surface will be present.

The average power Π_n in the n th order spherical radiator radiated out to infinity over a complete cycle of time is an important acoustical parameter. We may obtain this quantity by integrating the acoustic intensity I_r over the surface of a sphere whose origin coincides with the origin of the spherical radiator. From 2.2.8 above we see that both A_s and B_t are complex functions of r. However, from Eqs. 2.1.17a and 2.1.17c it is noted that both A_s and B_t approach $1/jkr$ as $kr \to \infty$. For simplicity then we shall integrate I_r over a spherical surface of indefinitely large radius. Thus, the average power is

$$\Pi_n = \iint_{\text{sphere}} I_r \, dS, \; kr \to \infty$$

$$= \int_0^{2\pi} r^2 d\phi \int_0^{\pi} \sin\theta d\theta \tfrac{1}{2}\varrho c \, \text{Re} \left\{ \sum_{s=0}^{\infty} \sum_{t=0}^{\infty} We_{(os)} \, We_{(ot)} \right.$$

$$\left. \times \frac{\overline{P}_s \overline{P}_t^*}{k^2 r^2 \, |B(jkr_0)|^2} \right\} \tag{2.2.11a}$$

Noting that unless $s = t = n$ the integrals vanish, and noting further that

$$\int_0^{2\pi} \begin{matrix} \cos^2 m\phi \\ \sin^2 m\phi \end{matrix} \int_0^{\pi} \sin\theta d\theta \, [P_n^m(\cos\theta)]^2 = \frac{4\pi(n+m)!}{(2n+1)(n-m)!\,\varepsilon_m} \tag{2.2.11b}$$

we see that 2.2.11 reduces to

$$\Pi_n = \frac{4\pi\varrho c}{2k^2 \, |B_n(jkr_0)|^2} \sum_{m=0}^{n} \frac{(n+m)![We_{mn}^2 + W_{0(mn)}^2]}{(n-m)!(2n+1)\,\varepsilon_m} \tag{2.2.12}$$

In order to compare the average power among various orders ($= n$) of spherical radiator we need a reference amplitude for the constants W_e, W_0. We shall adopt the scheme of rendering $(W_{e(mn)}^2 + W_{0(mn)}^2)$ a maximum for any mn. From 2.1. 34 at $r = r_0$, we note that for $V(\theta, \phi)$ *real*

$$u = \sum_{m=0}^{\infty} We_{0n} \, \overline{P}_n \tag{2.2.13a}$$

$$u = \sum_{n=0}^{\infty} \sum_{m=0}^{n} \mathrm{U}_{mn} \tag{2.2.13b}$$

in which,

$$\mathrm{U}_{mn} = \sqrt{W_{e(mn)}^2 + W_{0(mn)}^2} \; \cos m(\phi - \psi) \, P_n^m(\cos\theta) \tag{2.2.13c}$$

$$\cos m\psi = W_{e(mn)} / \sqrt{W_{e(mn)}^2 + W_{0(mn)}^2} \tag{2.2.13d}$$

Now at some point (ϕ_0, θ_0) on the surface $r = r_0$ the amplitude U_{mn} is a maximum. By adjusting the reference meridian on the sphere so that $\phi_0 = \psi$, we may write,

$$|We_{(mn)}^2 + W_{0(mn)}^2| = \frac{|U_{mn}|_{\max}^2}{[P_n^m(\cos\theta_0)]^2} \tag{2.2.13e}$$

Hence in terms of this reference maximum velocity amplitude we can reformulate 2.2.12 above to read,

$$\Pi_{mn} = \tfrac{1}{2} R_{mn} |U_{mn}|^2_{\max} \tag{2.2.14a}$$

in which the symbol R_{mn} is defined to be the radiation resistance in the mn th order, with the form

$$R_{mn} = \frac{\varrho c S}{(k^2 r_0^2)\,|B_n(jkr_0)|^2} \left[\frac{(n+m)!}{\varepsilon_m (n-m)!\,(2n+1)[P_n^m(\cos\theta)]^2_{\max}} \right] \tag{2.2.14b}$$

Where (as before) $\varepsilon_0 = 1$, $\varepsilon_{m\neq 0} = 2$
and $S = 4\pi r_0^2$

As an example let $m = n = 2$. Then $[P_n^m(\cos\theta)]_{\max} = 3$, see ref. [12].
Hence,

$$R_{22} = \frac{4}{15}\, \varrho c S [k^6 r_0^6/(k^6 r_0^6 - 2k^4 r_0^4 + 9k^2 r_0^2 + 81)] \tag{2.2.15a}$$

Similarly, when $m = n = 0$, $(P_n^m)_{\max} = 1$, $\varepsilon_0 = 1$. From ref. [13] we note that $|B_0(jkr)|^2 = (1 + k^2 r_0^2)/k^4 r_0^4$. Thus

$$R_{00} = \varrho c S\,(k^2 r_0^2/(1 + k^2 r_0^2)) \tag{2.2.15b}$$

For comparison among various orders of spherical radiators we may write the radiation resistance in the following nondimensional form,

$$\frac{R_{mn}}{x \varrho c S} = \frac{1}{k^2 r_0^2\,|B_m(jkr_0)|^2}, \tag{2.2.16a}$$

$$x = \frac{(n+m)!}{(n-m)!\,\varepsilon_m (2n+1)[p_n^m(\cos\theta)]^2_{\max}}. \tag{2.2.16b}$$

For $kr_0 \to \infty$ the right-hand side of 2.2.16a approaches unity for all n and the radiation resistance then equals $x\,\varrho c S$ with x given by 2.2.16b.

2.3. RADIATIVE CAPACITY OF THE *N*'TH ORDER SPHERICAL RADIATOR

The time-invariant energy density ($= \mathcal{H}$) of linear acoustic fields is the sum of the kinetic energy density $\mathcal{T}$ and the potential energy density $\mathcal{U}$, where in terms of the maximum amplitude field quantities of pressure and particle velocity,

$$\mathcal{H} = \mathcal{T} + \mathcal{U}, \text{ (a)}; \quad \mathcal{U} = \tfrac{1}{2} p^2/\varrho c^2, \text{ (b)}; \quad \mathcal{T} = \tfrac{1}{2}\varrho\{|u|^2 + |v|^2 + |w|^2\} \text{ (c) (units: } Nm/m^3) \tag{2.3.1}$$

The factor $\frac{1}{2}$ appears in these equations during integration of the momenta ($= pq/c$, or $= \varrho u$) which are linear functions of pressure or particle velocity. For a spherical radiator of order n one finds from 2.1.33 to 2.1.36 that the time averaged sinusoidal energy densities are,

$$\mathcal{U}_n = \frac{\varrho}{2\cdot 2} |W_{com}|^2 |\bar{P}_n|^2 \frac{|A_n(jkr)|^2}{|B_n(jkr_0)|^2} \quad \text{(a)}$$

$$\mathcal{J}_n = \frac{\varrho}{2\cdot 2} |W_{com}|^2 \left\{ \bar{P}_n^2(\theta,\phi) \frac{|B_n(jkr)|^2}{|B_n(jkr_0)|^2} \right\} \quad (2.3.2)$$

$$+ \left|\frac{\partial \bar{P}_n}{\partial \theta}\right|^2 \frac{|A_n(jkr)|^2}{|B_n(jkr_0)|^2} \frac{1}{k^2r^2} + \left|\frac{\partial \bar{P}}{\partial \phi}\right|^2 \frac{|A_n(jkr)|^2}{|B_n(jkr_0)|^2 k^2r^2 \sin^2\theta} \quad \text{(b)}$$

(The additional factor of $\frac{1}{2}$ appears in these equations because p^2 and $|u|^2$ etc. are products of peak amplitude which are averaged in *time* over a cycle.) Now $A_n(jkr)$ is a polynomial in the variable $(1/jkr)$. Let the sum of the energy densities of $\mathcal{U}_n$, $\mathcal{J}_n$ that vary as $1/r^2$ be designated by a single prime superscript ($= \mathcal{U}_n'$, $\mathcal{J}_n'$) and the sum of those that vary as $1/r^4$, $1/r^6$ etc. be designated by a double primed superscript ($= \mathcal{U}_n''$, $\mathcal{J}_n''$). In a physical sense the double primed energy densities represent stagnant energy oscillating with frequency 2ω at a particular locality in the sound field. The single primed energy densities represent travelling energy diverging to infinity. To find the total stagnant energy E_n'' in the unbounded space surrounding the n th order radiator we integrate $\mathcal{U}_n'' + \mathcal{J}_n''$ over all space. The quantity E_n'' is important because it designates the amount of stagnant sound energy averaged over a cycle of time that the radiator must supply to the sound field to insure the radiation of real energy ($= \Pi_n\, 2\pi/\omega$) over the same cycle out to infinity. Brillouin [7] has proposed that the ratio of total stagnant to radiated energy (namely the ratio $\omega E_n''/2\pi\,\Pi_n$) be used to serve as a measure of the *radiative capacity* RC of the n'th order radiator. In symbols we may define the radiative capacity by the formula

$$(RC)_n \equiv \frac{\omega \int_V (\mathcal{U}_n'' + \mathcal{J}_n'')\, dV}{2\pi\,\Pi_n} \quad (2.3.3)$$

As an example of the calculation of $(RC)_n$ let $m = 0$, $n = 2$. Then

$$\mathcal{U}_2' = \frac{\varrho}{4} |W_{e02}|^2 P_2^2(\theta) \left[\frac{(1/k^2r^2)}{\left(\frac{1}{k^2r_0^2} - \frac{2}{k^4r_0^4} + \frac{9}{k^6r_0^6} + \frac{81}{k^8r_0^8} \right)} \right] \quad \text{(a)}$$

$$\mathcal{U}_2'' = \left(\frac{\varrho}{4} \right) |W_{e02}|^2 P_2^2(\theta) \left[\frac{(3/k^4r^4) + (9/k^6r^6)}{\frac{1}{k^2r_0^2} - \frac{2}{k^4r_0^4} + \frac{9}{k^6r_0^6} + \frac{81}{k^8r_0^8}} \right] \quad \text{(b)} \quad (2.3.4)$$

$$\mathcal{J}_2' = \mathcal{U}_2' \quad \text{(c)}$$

$$\mathcal{J}_2'' = (\varrho/4) |We_{(02)}|^2 P_2^2(\cos\theta) \left[\frac{-(2/k^4r^4) + (9/k^6r^6) + (81/k^8r^8)}{(1/k^2r_0^2)-(2/k^4r_0^4) + (9/k^6r_0^6) + (81/k^8r_0^8)} \right]$$

$$+ \left[\frac{dP_2}{d\theta} (\cos\theta) \right]^2 \left[\frac{(1/k^4r^4) + (3/k^6r^6) + (9/k^8r^8)}{(1/k^2r_0^2)-(2/k^4r_0^4) + (9/k^6r_0^6) + (81/k^8r_0^8)} \right] \quad \text{(d)}$$

Now the maximum value of P_2 $(\cos\theta)$ is 1.0. Hence, using Eq. 2.2.13e we see that,

$$|W_{e02}|^2_{max} = |U_{02}|^2_{max} \quad (2.3.5)$$

Furthermore we note that

$$\int_0^\pi P_m^2(\cos\theta) \sin\theta d\theta = \frac{2}{2m+1}, \quad \int_0^\pi \left(\frac{dP_m(\cos\theta)}{d\theta} \right)^2 \sin\theta d\theta = \frac{2n(n+1)}{2n+1}$$

Substituting these results into the volume integration of $\mathcal{U}_2'' + \mathcal{T}_2''$ over all space we arrive at the equation

$$E_{02}'' = \int_V (\mathcal{U}_2'' + \mathcal{T}_2'')\, dV$$

$$= \int_0^{2\pi} \int_0^{\pi} \int_{r_0}^{\infty} (\mathcal{U}_2' + \mathcal{T}_2')\, r^2\, dr d\phi \sin\theta d\theta$$

$$= \frac{\varrho}{4} |U_{02}|^2_{max} \frac{4\pi}{5k^3} \frac{(7/kr_0) + (12/k^3r_0^3) + (27/k^5r_0^5)}{(1/k^2r_0^2) - (2/k^4r_0^4) + (9/k^6r_0^6) + (81/k^8r_0^8)} \tag{2.3.6a}$$

To calculate the energy radiated out to infinity in one cycle we use 2. .2 14a and .14b. These equations lead to the formula,

$$\frac{\omega \Pi_2}{2\pi} = \frac{4\pi}{5k^3} \frac{\pi\varrho |U_{02}|^2_{max}}{[(1/k^2r_0^2) - (2/k^4r_0^4) + (9/k^6r_0^6) + (81/k^8r_0^8)]} \tag{2.3.6b}$$

The radiative capacity thus reduces to

$$(RC)_2 = \frac{1}{4\pi} \left[\frac{7}{kr_0} + \frac{12}{k^3r_0^3} + \frac{27}{k^5r_0^5} \right] \tag{2.3.7}$$

Similar calculations for spherically radiators (i.e., for $m = 0$) of orders $n = 0$, $n = 1$ lead to the radiative capacities

$$(RC)_0 = \frac{1}{4\pi\, kr_0}, \text{(a)}; \qquad (RC)_{01} = \frac{1}{4\pi} \left(\frac{3}{kr_0} + \frac{2}{k^3r_0^3} \right), \quad \text{(b)} \tag{2.3.8}$$

To illustrate the concept of stagnant energy we append here a table of radiative capacities originally computed by Brillouin [7] for symmetrical spherical radiators $n = 0$, $n = 1$, $n = 2$, in the range $0.01 \leqslant kr_0 \leqslant 10$.

	RC (Radiative Capacity)		
kr_0	$n = 0$	$n = 1$	$n = 2$
0.01	7.96	159,174	$21{,}487 \times 10^6$
0.02	3.98	19,906	$671{,}554 \times 10^3$
0.05	1.592	1,278	$6{,}883 \times 10^3$
0.1	0.796	161.5	215.82×10^3
0.2	0.398	21.087	6.837
0.5	0.1592	1.751	77.508
1.0	0.0796	0.398	3.661
2.0	0.0398	0.1393	0.465
5.0	0.01592	0.0490	0.1197
10.0	0.00796	0.0240	0.0567

From this table we can estimate the great importance of the stagnant energy in the radiation of low frequency (= long wavelength) sound. Not only does the stagnant energy for a given order n required to be deposited in the acoustic field increase rapidly as the acoustic dimensions (= kr_0) decrease, but for any given acoustic dimension the stagnant energy increases very rapidly with increasing order (= n) of spherical radiator. For example, if we are required to radiate 10^6 watts out to infinity from a spherical radiator whose acoustic size is $kr_0 = 1$, we will be required to deposit in the sound field 79600, 398000, 3661000 watts respectively for spherical radiators of order 0 (= pulsating sphere), order 1 (= oscillating sphere), and order 2.

2.4 INCREMENT OF MASS AND ACCESSION OF INERTIA FOR SPHERICAL RADIATORS [14]

The sinusoidal displacement of the medium in the near field of a sound source may generate acoustic pressure in time quadrature with the local particle velocity. This pressure originates at field points where the medium undergoes bulk acceleration, giving rise to the phenomenon of accession of inertia. Let $M_{(mn)}$ represenet this accession of inertia in the mn'th mode (that is, a pressure field defined by the mn'th spherical harmonic). We define $M_{(mn)}$ by means of the average kinetic energy, $T_{(mn)Av}$, in the mn'th mode:

$$M_{(mn)} = \frac{2T_{(mn)AV}}{|U_{mn}|^2_{eff.}} \tag{2.4.1}$$

in which $|U_{mn}|^2_{eff}$ is the square of the absolute value of the root-mean-square radial velocity over the spherical surface. To find $T_{(mn)Av.}$ we recall [15] that in a dynamic system oscillating sinusoidally in time where there are passive elements that may store energy in potential form (= V) or in kinetic form (= T) the average (in time) reactive energy (= Q_{Av}) at radian frequency ω is given by the formula

$$Q_{Av} = 2\omega (V_{Av} - T_{Av}) \tag{2.4.2}$$

In linear acoustic radiation problems the pressure reaction of the fluid medium in time quadrature with particle velocity is inertial only ($V_{Av} = 0$). Hence

$$Q_{Av} = -2\omega T_{Av} \qquad \text{(for fluids)} \tag{2.4.3}$$

Now we may find this reactive power by taking the imaginary part of 1.3.4d,

$$Q = \pm \tfrac{1}{2} \ \text{Im} \int_S p\, u^* dS \tag{2.4.4}$$

The choice of sign depends on the choice of complex representation of time. If we select $\exp(-i\omega t)$ then from the discussion in Sect. 1.1.1. we must choose the plus sign. In the present Chapter we take $\exp(j\omega t)$ so that in light of that discussion we must use the negative sign. Combining 2.4.3 and 2.4.4 with proper choice of sign we obtain,

$$T_{AV} = \frac{1}{4\omega} \ \text{Im} \int_S pu^* \, dS \tag{2.4.5}$$

Formulas for p and u have already been derived in 2.1.33 and .34. Using them in this equation we see that

$$T_{AV} = \frac{\varrho r_0^2}{2k} \operatorname{Im}\left\{ \sum_{s=0}^{\infty} \sum_{t=0}^{\infty} \frac{We_{(0s)} We_{(0t)}}{2} \frac{A_s(jkr_0)}{B_s(jkr_0)} \times \int_0^{2\pi} d\phi \int_0^{\pi} \overline{P}_s \overline{P}_t \sin\theta d\theta \right\} \tag{2.4.6}$$

The evaluation of the double integral in the above equation may be performed by use of 2.2.11b. If we employ the orthogonal properties of the associated Legendre polynomials we conclude that all terms in s and t of this equation vanish except the diagonal ones, i.e., terms having $s = t = n$. Hence, 2.4.6 reduces to,

$$T_{AV} = \frac{\varrho r_0^2}{2k} \operatorname{Im}\left\{ \sum_{n=0}^{\infty} \frac{A_m(jkr_0)}{B_m(jkr_0)} \sum_{m=0}^{s} \frac{|We_{mn}^2 + Wo_{(mn)}^2| 4\pi(n+m)!}{2(2n+1)(n-m)!\,\varepsilon_m} \right\} \tag{2.4.7}$$

Now the constants that appear in the summation on m may be rewritten by use of Eq. 2.2.13e, from which we note that

$$\frac{|We_{(mn)}^2 + Wo_{mn}^2|}{2} = \frac{|\mathbf{U}_{mn}|_{\text{eff}}^2}{[P_n^m(\cos\theta)]_{\max}^2}$$

Substituting this into 2.4.7, and using the result to define T_{mn} by the relation

$$T_{Av} = \sum_{m=0}^{\infty} \sum_{m=0}^{n} T_{mn} \tag{2.4.8}$$

we return to 2.4.1 and finally obtain an explicit expression for the accession of inertia M_{mn}. For convenience we replace $\operatorname{Im}\{T\}$ by $\operatorname{Re}\{T/j\}$.

$$M_{mn} = \frac{\varrho r_0^3}{[P_n^m(\cos\theta)]_{\max}^2} \operatorname{Re}\left\{ \frac{A_m(jkr_0)}{(jkr_0)\,B_m(jkr_0)} \frac{4\pi(n+m)!}{(2n+1)(n-m)!\,\varepsilon_m} \right\} \tag{2.4.9}$$

To apply this formula we require explicit expressions for A_n, B_n. These may be obtained directly from 2.1.10a and 2.1.10b. To find $[P_n^m(\text{case})]_{\max}$ we may consult ref. [4] or ref. [16]. Utilizing these sources we construct below a short table of formulas for the accession of inertia in the first few modes, $n = 0, 1, 2$; $m = 0, 1, 2$.

Accession of Inertia			
m \ n	0	1	2
0	$\frac{3M}{1 + k^2r_0^2}$	$M\left(\frac{2 + k^2r_0^2}{4 + k^4r_0^4}\right)$	$\frac{3}{5} M \frac{k^4r_0^4 + 6k^2r_0^2 + 27}{k^6r_0^6 - 2k^4r_0^4 + 9k^2r_0^2 + 81}$
1		M_{01}	$(4/3)\,M_{02}$
2			$(4/3)\,M_{02}$

Here $M = (4/3)\pi r_0^3 \varrho$, that is, M is the mass of fluid represented by the volume of the static sphere. All the formulas in this table are functions of kr_0, that is, functions of frequency. As the frequency approaches zero ($kr_0 \to 0$) there remains a residual inertial mass which is designated in the literature as the *increment of mass* for a body vibrating in an incompressible fluid. A detailed discussion of this quantity may be found in [17]. We note however that the *accession of inertia* is an acoustic quantity (i.e. a quantity dependent on the compressibility of the medium) and this differs markedly from the quantity of *incremental mass*, which is hydrodynamic in nature. The two quantities merge into one only when the wavelength of propagation of acoustic waves becomes indefinitely large.

2.5 NEAR FIELD AND FAR FIELD OF SPHERICAL RADIATORS

To study the near field pressure and particle velocity of spherical radiators we need formulas for the spherical radial functions and their derivatives that show the relative importance of radial distance in determining the amplitude and phase of field, that is, formulas in ascending powers of r. A typical example may be obtained by rearranging $h_n^{(2)}(kr)$ given by Eq. 2.1.7 to read

$$h_n^{(2)}(kr) = \frac{(2n)!\, je^{-jkr}}{2^n n!\,(kr)^{n+1}} \sum_{p=0}^{n} (jkr)^p \binom{n}{n-p} \frac{(2n-p)!}{(2p)!}\, 2^p \tag{2.5.1}$$

This formula may be inserted directly into the equation for the velocity potential 2.1.24a and all field variables derived in the usual way. Instead of $h_n^{(2)}(kr)$ it is sometimes more revealing to write $A_n(x)$, $B_n(x)$ directly in ascending powers of χ $(= jkr)$. Referring back to Eqs. 2.1.10a, 10b, we can rearrange terms so that we obtain the following formulas,

$$A_n(x) = \frac{a_n^n}{\chi^{n+1}} \left[1 + \frac{a_n^{n-1}}{a_n^n}\chi + \frac{a_n^{n-2}}{a_n^n}\chi^2 + \ldots + \frac{a_n^0}{a_n^n}\chi^n\right] \tag{2.5.2}$$

$$B_n(x) = \frac{b_n^{n+1}}{\chi^{n+2}} \left[1 + \frac{b_n^n}{b_n^{n+1}}\chi + \frac{b^{n-1}}{b_n^{n+1}}\chi^2 + \ldots + \frac{b_n^0}{b_n^{n+1}}\chi^{n+1}\right] \tag{2.5.3}$$

The ratios a_n^{n-1}/a_n^n, b_n^n/b_n^{n+1} etc. can be calculated directly by use of 2.1.11. For the polynomial A_n let r, q be integer superscripts on the constant A_n^m, and let $l = r - q$. Then

$$\frac{a_n^q}{a_n^r} = \frac{(8^l) \prod_{p=1}^{l} (q+p)}{\prod_{p=1}^{l} [(2n+1)^2 - (2(r-p)+1)^2]} \tag{2.5.4}$$

As an example of the use of this formula let $n = 3$. Then

$$A_3 = \frac{15}{(jkr)^4} \left[1 + jkr - \frac{2}{5}k^2r^2 - j\frac{k^3r^3}{15}\right] \tag{2.5.5}$$

Here we have set $A_n^n = 1.3.5 \ldots (2n-1) = \bar{n}$.
For the polynomial B_n let s, t be integer superscripts on the constant A_n^m, and let $l = t - s$. Then

$$\frac{b_n^s}{b_n^t} = \frac{(n(n+1)+s(s+1))(8^t)\prod_{p=1}^{t}(s-1+p)}{2s\left[\frac{(n(n+1)+t(t+1))}{2t}\right]\prod_{p=1}^{t}[(2n+1)^2-(2(t-1-p)+1)^2]} \tag{2.5.6}$$

As an example we find for $n = 3$

$$B_3(jkr) = \frac{60}{(jkr)^5}\left[1 + jkr - \frac{9}{20}k^2r^2 - j\frac{7}{20}k^3r^3 + \frac{1}{60}k^4r^4\right] \tag{2.5.7}$$

Here we have set $b_n^{n+1} = \bar{n}\,(n+1)$. Now by application of 2.1.33, 34, 35, 36 we can determine the near field pressure and particle velocity for spherical radiators. These are

$$p = \varrho c \sum_{n=0}^{\infty} \frac{We_{(0m)}\overline{P}_n(\theta)\,\bar{n}}{B_n(jkr_0)(jkr)^{n+1}}(1 + jkr + \ldots)e^{-jk(r-r_0)} \qquad \text{(a)}$$

$$u = \sum_{n=0}^{\infty} \frac{We_{(0n)}\overline{P}_n(\theta)\bar{n}(n+1)e^{-jk(r-r_0)}}{B_n(jkr_0)\,(jkr)^{n+2}}\left(1 + jkr + \frac{b_n^{n-1}}{b_n^{n+1}}(jkr)^2 + \ldots\right) \qquad \text{(b)}$$

$$v = -\sum_{n=0}^{\infty} We_{(0n)}\frac{\bar{n}}{(jkr)^{n+2}}\frac{\partial\overline{P}_n(\theta)e^{-jk(r-r_0)}}{\partial\theta\,B_n(jkr_0)}(1 + jkr + \ldots) \qquad \text{(c)} \tag{2.5.8}$$

$$w = -\sum_{n=0}^{\infty} We_{(0n)}\frac{\bar{n}}{(jkr)^{n+2}}\frac{\partial\overline{P}_n(\phi)e^{-jk(r-r_0)}}{\partial\phi\,B_n(jkr_0)}(1 + jkr + \ldots) \qquad \text{(d)}$$

We note that as $kr \to 0$ the velocity components v and w are in phase quadrature with the pressure. However the radial particle velocity component u has a in-phase term to the order of $(jkr)^{-(n+1)}$. Hence for the n'th order spherical radiator the ratio of the pressure to the in-phase particle velocity of the radial component of velocity is

$$\frac{p}{[u]_{\text{in-phase}}} \to \frac{\varrho c}{(n+1)}, \qquad kr \to 0 \tag{2.5.9}$$

that is, the normal specific acoustic resistance of the n'th order radiator diminishes as $1/(n+1)$ for $kr \to 0$. Furthermore, as $kr \to 0$ the near field velocity potential (and therefore the near field pressure) is dominated by the term $(1/kr)^{n+1}$ which may be considerably larger than the magnitude of the real pressure wave travelling out to infinity.

The radiation field at great distances from the spherical radiator source may also be studied by allowing $kr \to \infty$ so that the polynomials $A_n(jkr) \to 1/jkr$. From 2.1.31, and 2.1.33 we see that the pressure in the far field is given by

$$p \to \frac{\varrho c}{jkr} e^{-jk(r-r_0)} \left\{ \frac{We_{00}}{B_0(jkr_0)} + \frac{We_{01} P_1(\cos\theta)}{B_1(jkr_0)} + \frac{We_{02} P_2(\cos\theta)}{B_2(jkr_0)} + \ldots \right.$$

$$+ \frac{[We_{(11)} \cos\phi + Wo_{(11)} \sin\phi] P_1^1(\cos\theta)}{B_1(jkr_0)} + \frac{[We_{(12)} \cos\phi + Wo_{(12)} \sin\phi] P_2^1(\cos\theta)}{B_2(jkr_0)}$$

$$\left. + \frac{[We_{(22)} \cos 2\phi + Wo_{(22)} \sin\phi] P_2^2(\cos\theta)}{B_2(jkr_0)} + \ldots \right\} \qquad (2.5.10)$$

The absolute value of the *angular* distribution of pressure at some fixed radius (for the condition $r \to \infty$) may be found for the points (r, θ_0, ϕ_0) etc. by finding the real ($= Re$) and imaginary ($= \mathrm{Im}$) components of this equation and writing

$$|p(\theta, \phi)| \sim \sqrt{(\mathrm{Re}\, p(\theta, \phi)^2 + (\mathrm{Im}\, p(\theta, \phi))^2} \qquad (2.5.11)$$

We note that the angular distribution of radial sound intensity in the far field (given by 2.2.8 is different from the distribution of pressure written in 2.5.11 above. The radial intensity is proportional to the cross products of spherical harmonics $\overline{P}$, $\overline{P}$, while the pressure is proportional to a single spherical harmonic $\overline{P}_n$.

2.6 ACOUSTIC POWER FROM POINT SOURCES, ONE SPHERICAL CAP, TWO SPHERICAL CAPS OF OPPOSITE VELOCITY AT THE POLES OF A SPHERICAL RADIATOR

The real power Π_0 radiated to infinity from a *point source*, (that is, from a source of order $n = 0$ and kr_0 very small) is found from 2.2.14a and 2.2.15b to be,

$$\Pi_{00} = \frac{\varrho \omega^2 Q_s^2}{8\pi c}, \qquad (kr_0 \to 0) \qquad \text{(a)} \qquad (2.6.1)$$

in which

$$Q_s = 4\pi r_0^2 |U_{00}|_{\max} \qquad \text{(b)}$$

We desire now to compare this power with the power radiated from a spherical cap at the pole of an otherwise acoustically rigid sphere (radius r_0), assuming the cap to subtend a very small angle $\theta = \alpha$ where α is $\frac{1}{2}$ the angle of the subtending cone from the center of the sphere to the cap. For circular symmetry (i.e. for $m = 0$) we assume that the radial velocity $v(\theta)$ over the cap is constant ($= v_0$) from the center of the cap to its edge, and is zero over the remainder of the sphere. Substituting this velocity distribution into Eq. 2.1.18 and then allowing the subtended angle to become very small we find the n th spherical harmonic velocity coefficient to be

$$u_{0n} = \left(\frac{2n+1}{4\pi}\right)\int_0^{2\pi} d\phi \int_0^{\alpha} v_0 P_n(\cos\theta)\sin\theta d\theta \qquad \text{(a)} \qquad (2.6.2)$$

$$\rightarrow \frac{2n+1}{4\pi r_0^2} Q,\ kr_0 \rightarrow 0 \qquad \text{(b)}$$

in which $Q = |V_0|\,\pi(r_0\alpha)^2$. The average power Π_+ radiated out to infinity over one cycle from a polar cap of this type is found from Eq. 2.1.14b to be

$$\Pi_+ = \sum_{n=0}^{\infty} \frac{\varrho c(2n+1)Q^2}{8\pi k^2 r_0^4 |B_n(jkr_0)|^2} \qquad (2.6.3)$$

If a second cap with similar angular dimensions ($= \alpha$) is located at the opposite pole of the same sphere (i.e., at $\theta = \pi$), with a velocity distribution of identical type as above, excepting that the constant velocity is $-v_0$ rather than $+v_0$, the *sum* of the velocities of the two caps (one with plus velocity, the other with minus velocity) when substituted into Eq. 2.1.1.(18) yield velocity expansion coefficients with the form

$$u_{0n} = \frac{2n+1}{4\pi r_0^2}(2Q),\ (n \text{ odd}) \qquad \text{(a)}$$

$$= 0, \qquad (n \text{ even}) \qquad \text{(b)} \qquad (2.6.4)$$

We now substitute these coefficients into 2.1.14b and find that the average real power $\Pi(+-)$ from two small caps with velocities $\pm v_0$ at the poles of an otherwise rigid sphere of radius r_0 is

$$\Pi_{(+-)} = \sum_{n=1,3,5\ldots}^{\infty} \frac{\varrho c(2n+1)Q^2}{2\pi k^2 r_0^4 |B_n(jkr_0)|^2} \qquad (2.6.5)$$

This may be called the real power from a "spherical dipole". We now follow Reschevkin [18] and compare the real power from one cap of this spherical dipole with that of a point source in an infinite rigid baffle, that is, we shall compare the relative effectiveness of a finite baffle to an infinite baffle in raising the acoustic radiation resistance of a simple source. Considering the simple source first we note that an infinite rigid baffle placed in a medium doubles the resistance of the medium to source velocity. Hence a source with fixed power input when placed in an infinite rigid baffle will have its source strength reduced by a factor of $1/\sqrt{2}$. If the source strength of the source in the baffle is raised to the source strength originally generated in the unbounded medium then the power must be quadrupled for all space (or doubled for only half space). Hence the real power from a point source in an infinite rigid baffle radiated into half space at the *original* source strength Q is

$$\Pi_{00} = \frac{\varrho\omega^2 Q^2}{4\pi c}$$

We now divide $\frac{1}{2}$ of 2.6.5 above by this half-space power to form the comparison ratio β. This ratio then reduces to

$$\beta = \frac{1}{k^4 r_0^4} \sum_{n=1,3,5\ldots}^{\infty} \frac{(2n+1)}{|B_n(jkr_0)|^2} \tag{2.6.6}$$

A plot of β vs kr_0 (see ref. [18]) shows that when $kr_0 = 1$, $\beta \approx 0.6$ and that a further large increase in kr_0 does not radically increase β. Now to a first approximation the cap is located in a finite baffle (= a hemisphere) whose actual dimension is $\frac{1}{2}$ the circumference of the sphere ($= \pi r_0$). Let us select a frequency such that $kr_0 = 1$, or $\pi r_0 = \lambda/2$. In making this selection we wish to settle upon $\beta \approx 0.6$ as an appropriate goal for the raised value of resistance due to the use of a finite baffle. If we select this baffle to be a rigid disc of diameter $2R$, and set the following condition,

diameter of rigid finite baffle = $\frac{1}{2}$ circumference of rigid sphere,

we obtain, $$2R = \lambda/2 \qquad (\text{for } kr_0 = 1)$$

or

$$R = \lambda/4 \tag{2.6.7}$$

This means that in the first approximation the addition of a rigid baffle of diameter $\lambda/2$ to a dipole will raise its radiation resistance to 6/10 of the resistance of a point source in an infinite rigid baffle. A further increase in the size of the finite baffle does not proportionately increase the resistance, that is, the net gain of further increase is small unless the baffle size is made very large.

2.7 ACOUSTIC RADIATION FROM A ZONAL RADIATOR ON A SPHERICAL BAFFLE [19]

By a zonal radiator we shall mean a radiating surface of revolution described on a baffle of revolution having the same axis, that is, a coaxial radiating band on a spherical, cylindrical or spheroidal baffle. We shall consider here a hard spherical baffle (radius r_0) on which there is a radiating zone lying between the angles θ_0 and $\pi - \theta_0$, i.e., symmetrical about the equator where θ is the polar angle of a spherical coordinate system at the center of the sphere. To study the radiation properties of such a zone we select a distribution of normal velocity over the spherical baffle of the following form in the constant v_0,

$$\left.\begin{aligned} v(\theta, t) &= v_0 e^{j\omega t}, \qquad \theta_0 \leqslant \theta \leqslant \pi - \theta_0 \\ &= 0, \qquad \text{elsewhere} \end{aligned}\right\} \tag{2.7.1}$$

Now, according to 2.1.29 the expansion of this velocity distribution in spherical harmonics leads to the expansion constants

$$We_{on} = \frac{e^{j\omega t}\, 2\pi(2n+1)\, v_0}{4\pi} \int_{\theta_0}^{\pi - \theta_0} P_n(\cos\theta) \sin\theta d\theta \tag{2.7.2a}$$

If subscript n is an odd integer the function $P_n(\cos\theta)$ is an odd function and the integration over the symmetrical limits causes the integral to vanish. If n is even then [20]

$$(2n + 1)\int_{\theta_0}^{\pi-\theta_0} P_n(\cos\theta)\sin\theta d\theta = [P_{n+1}(\cos\theta) - P_{n-1}(\cos\theta)]_{\theta_0}^{\pi-\theta_0} \qquad (2.7.2b)$$

Two cases arise here. If n is zero then the right-hand side reduces to

$$[P_1(\cos\theta) - 1]_{\theta_0}^{\pi-\theta_0} = 2\cos\theta_0 \qquad (a)$$

Here we have used the well-known formula [21]

$$P_n^m(-x) = (-1)^{n-m} P_n^m(x) \qquad (b) \qquad (2.7.3)$$

If n is 2, 4, 6 .... etc. then the right-hand side of 2.6.2b reduces to

$$2[P_{n+1}(\cos\theta_0) - P_{n-1}(\cos\theta_0)] \qquad (c)$$

The expansion coefficients $We_{(on)}$ are thus completely determined, i.e.,

$$We_{(00)} = v_0 e^{j\omega t}\cos\theta_0 \qquad (a)$$

$$We_{(on)} = v_0 e^{j\omega t}[P_{n+1}(\cos\theta_0) - P_{n-1}(\cos\theta_0)],\ n = 2, 4, \ldots \qquad (b) \qquad (2.7.4)$$

We may now find the pressure at any field point by substituting these constants into Eq. 2.1.33. This pressure is,

$$p = \varrho c v_0 e^{j\omega t} e^{-jk(r-r_0)}\left\{\frac{A_0(jkr)}{B_0(jkr_0)}\cos\theta_0 + \sum_{n\ 2,4,6\ldots}^{\infty} \frac{A_n(jkr)}{B_n(jkr_0)} P_n(\cos\theta)[P_{n+1}(\cos\theta_0) - P_{n-1}(\cos\theta)]\right\} \qquad (2.7.5)$$

Now the mechanical (radiation) impedance of the medium to the motion of the zonal radiator ($= Z_R$) is defined as the ratio of the mechanical force F of the reacting medium on the zone divided by the average normal component of surface velocity. We may determine F by integrating the acoustic pressure over the surface of the zone. Thus,

$$Z_R = \frac{F}{v_0} = \frac{\int\int_{zone}(r_0, \theta, \phi)\, dS}{v_0} \qquad (2.7.6)$$

To perform the integration of the acoustic pressure over the area ($= 4\pi r_0^2 \cos\theta_0$) of the zone we again employ 2.6.2b to 2.6.3c and obtain,

$$\frac{Z_R}{4\pi r_0^2 \varrho c \cos\theta_0} = \left\{ \frac{A_0(jkr_0)}{B_0(jkr_0)} \cos\theta_0 + \sum_{n=2,4,6\ldots}^{\infty} \frac{A_n(jkr_0)[P_{n+1}(\cos\theta_0) - P_{n-1}(\cos\theta_0)]^2}{B_n(jkr_0)(2n+1)\cos\theta_0} \right\} \tag{2.7.7}$$

This is the radiation impedence density of a symmetrical zonal radiator on a hard spherical baffle. Similarly, the angular distribution of radial acoustic intensity per unit polar angle ($= dP/d\theta$) which contributes to the radiated power in the far field may be obtained from 1.4.2, 2.2.8, 2.7.2a, 2.7.2b, and by allowing $A_n \to 1/jkr$ and $B_n \to 1/jkr$. Thus

$$\frac{dP}{d\theta} = \frac{\varrho c v_0^2}{2k^2} \left\{ \frac{\cos^2\theta_0}{|B_n(jkr_0)|^2} + \sum_{n=2,4,6\ldots}^{\infty} \frac{[P_{n+1}(\cos\theta_0) - P_{n-1}(\cos\theta_0)]^2 P_n^2(\cos\theta)}{|B_n(jkr_0)|^2} \right\} \sin\theta \tag{2.7.8}$$

Note that all other cross-product components predicted by 2.2.8 do not ultimately contribute to the integrated radiated (real) power and hence have been omitted from the above equation. This is so because of the orthogonal properties of the associated Legendre functions, i.e.

$$\int_0^{\pi} P_n P_m \sin\theta d\theta = \frac{2}{(2n+1)}, \quad n = m$$
$$= 0 \qquad\qquad n \neq m$$

Hence only the diagonal products of the matrix of products pp^* survive the integration of the radial intensity over the area of a sphere. The result leads to 2.7.8. By plotting $(dP/d\theta)$ vs. θ we may also obtain the θ-characteristic of directive power as defined by 1.4.2. This plot of power is in general very different from a plot of pressure constructed by using 2.7.5.

2.8 EMPIRICAL ANALYSIS OF 3-DIMENSIONAL STEADY STATE FIELDS BY THE METHOD OF PACHNER [22]

We consider a radiating surface of any shape at the origin of a spherical coordinate system r, θ, ϕ, and surround the radiator with a spherical surface of radius R_0 where R_0 is as small as possible. In the region $R_0 < r < \infty$ the radiated field velocity potential ($= \Phi$) in the steady state may be developed into a series of complex spherical wave functions as follows,

$$\Phi(r, \theta, \phi, t) = \sum_{n=0}^{\infty} \sum_{m=-n}^{n} (\mathfrak{Q}_{mn}^{(1)} + j\,\mathfrak{Q}_{mn}^{(2)})$$
$$\times e^{-jm\phi} P_n^m(\cos\theta)\, h_n^{(2)}(kr)\, e^{j\omega t} \tag{2.8.1}$$

A refined analysis by Bouwkamp [23] has shown that when r is less than R_0 the real part of 2.8.1 is not a solution of the homogeneous (Helmholtz) wave equation. Hence 2.8.1 is not applicable *inside*

the smallest circumscribing spherical surface surrounding the radiator.

For convenience in writing we recast 2.8.1, in terms of the following newly defined entities:

$$\text{rotation matrix} = \begin{bmatrix} \cos m\phi,\ \sin m\phi \\ -j \sin m\phi,\ j \cos m\phi \end{bmatrix} \quad \text{(a)} \qquad (2.8.2)$$

$$\text{column matrix} = \begin{bmatrix} \alpha(r,\ t) \\ \beta(r,\ t) \end{bmatrix} \quad \text{(b)}$$

$$\alpha(r,\ t) = j_n(kr)\, u(t) + n_n(kr)\, v(t) + n_n(kr)\, w(t) - j_n(kr)\, x(t) \qquad \text{(c)}$$

$$\beta(r,\ t) = -n_n(kr)\, u(t) + j_n(kr)\, v(t) + j_n(kr)\, w(t) + n_n(kr)\, x(t) \qquad \text{(d)}$$

$$u(t) = \mathcal{E}_{mn}^{(1)} \cos \omega t \qquad \text{(e)}$$

$$v(t) = \mathcal{E}_{mn}^{(1)} \sin \omega t \qquad \text{(f)}$$

$$w(t) = \mathcal{E}_{mn}^{(2)} \cos \omega t \qquad \text{(g)}$$

$$x(t) = \mathcal{E}_{mn}^{(2)} \sin \omega t \qquad \text{(h)}$$

Thus, 2.8.1 reduces to

$$\Phi(r,\ \theta,\ \phi,\ t) = \sum_{n=0}^{\infty} \sum_{m=-n}^{+n} \begin{bmatrix} \cos m\phi,\ \sin m\phi \\ -j \sin m\phi,\ j \cos m\phi \end{bmatrix} \begin{bmatrix} \alpha \\ \beta \end{bmatrix} P_n^m(\cos \theta) \qquad (2.8.3)$$

We assume now that at some fixed radius $r = R_1$, and instantaneous time $t = t_1$ we are able to measure the instantaneous velocity potential (i.e., acoustic pressure) over the entire surface $r = R_1$. Let $\Psi(\theta, \phi, R_1, t_1)$ be this *empirically* determined potential which, for the moment, will be considered a continuous function of its variables. We can expand this empirical function into an infinite series of surface spherical harmonics which are independent of the *variable* time. In terms of the expansion constants $E_{mn}^{(1)} + j\, E_{mn}^{(2)}$ we have,

$$\Psi(\theta,\ \phi,\ R_1,\ t_1) = \sum_{m=0}^{\infty} \sum_{m=-n}^{n} \begin{bmatrix} \cos m\phi,\ \sin m\phi \\ -j \sin m\phi,\ j \cos m\phi \end{bmatrix} \qquad (2.8.4)$$

$$\times \begin{bmatrix} E_{mn}^{(1)} \\ E_{mn}^{(2)} \end{bmatrix} P_n^m(\cos \theta),$$

The constants $E_{mn}^{(1)}$, $E_{mn}^{(2)}$ are *computable* complex numbers that can be found by applying the orthogonal properties of spherical harmonics according to the classical method. For a discussion of this method and for explicit formulas of computation see [39] and Sect. 2.1.1. We now compare Eq. (4) with Eq. (3) and see that

$$E_{mn}^{(1)} = \alpha(R_1, t_1) \qquad \text{(a)}$$

$$E_{mn}^{(2)} = \beta(R_1, t_1) \qquad \text{(b)} \tag{2.8.5}$$

These are a pair of simultaneous equations in the unknown amplitudes $E_{mn}^{(1)}$, $E_{mn}^{(2)}$ and the *unknown time*, t_1, in terms of the empirically found entities $E_{mn}^{(1)}$ and $E_{mn}^{(2)}$. Since there are three unknowns and two equations we find additional equations by making a subsidiary measurement over the *same* surface (i.e., $r = R_1$) at a time $t = t_2$, and obtain the empirical velocity potential $\Psi(\theta, \phi, R_1, t_2)$. Treating this empirical quantity as a function of coordinates we can compute the expansion constants $G_{mn}^{(1)}$, $G_{mn}^{(2)}$ by the classical method used above to obtain $E_{mn}^{(1)}$, $E_{mn}^{(2)}$ and write

$$\Psi(\theta, \phi, R_1, t_2) = \sum_{m=0}^{\infty} \sum_{m=-n}^{+n} \begin{bmatrix} \cos m\phi, \sin m\phi \\ -j \sin m\phi, j \cos m\phi \end{bmatrix} \times \begin{bmatrix} G_{mn}^{(1)} \\ G_{mn}^{(2)} \end{bmatrix} P_n^m(\cos\theta), \tag{2.8.6}$$

Comparing Eq. (6) with Eq. (3) we thus find that

$$G_{mn}^{(1)} = \alpha(R_1, t_2) \qquad \text{(a)}$$
$$G_{mn}^{(2)} = \beta(R_1, t_2) \qquad \text{(b)} \tag{2.8.7}$$

Here, as before, $G_{mn}^{(1)}$, $G_{mn}^{(2)}$ are known complex numbers in terms of which $\mathcal{E}_{mn}^{(1)}$, $\mathcal{E}_{mn}^{(2)}$, t_2 are to be determined. Combining 2.8.7 with 2.8.5 we arrive at a sufficient number of simultaneous equations to determine the expansion constants $\mathcal{E}_{mn}$ which are to be ultimately used to calculate the field of 2.8.3 at any radius $r > R_0$.

The use of two complex expansion constants $\mathcal{E}_{mn}$ in 2.8.1 covers the general case where the source points on the radiating surface move with non-uniform phase. In many applications the motion of the radiating surface is uniform In these cases we have

$$G_{mn}^{(2)} = E_{mn}^{(2)} = 0, w(t) = x(t) = 0 \qquad \text{(a)}$$

$$E_{mn}^{(1)} = \alpha(R_1, t_1) \qquad \text{(b)}$$

$$G_{mn}^{(1)} = \alpha(R_1, t_2) \qquad \text{(c)} \tag{2.8.8}$$

2.8.8.b, c are two simultaneous equations in the unknown quantities $\mathcal{E}_{mn}^{(1)}$, t_1 and t_2. To reduce the number of unknowns Pachner [22] made the selection

$$\omega t_2 = \omega t_1 - \pi/2 \tag{2.8.9}$$

Using this we see that

$$E_{mn}^{(1)} = jn\,(kR_1)\;\; \mathcal{E}_{mn}^{(1)} \cos \omega t_1 \;+\; n_n\,(kR_1)\; \mathcal{E}_{mn}^{(1)} \sin \omega t_1 \quad \mathcal{E} \text{ (a)}$$

$$G_{mn}^{(1)} = jn\,(kR_1)\;\; \mathcal{E}_{mn}^{(1)} \sin \omega t_1 - n_n\,(kR_1)\;\; \mathcal{E}_{mn}^{(1)} \cos \omega t_1 \qquad \text{(b)} \tag{2.8.10}$$

In these equations E_{mn}, G_{mn}, and $\mathcal{E}_{mn}$ are complex. However when $m = 0$, these numbers are real. Solving these equations simultaneously for the case $m = 0$ we obtain

$$\tan \omega t_1 = \frac{G_{0m}^{(1)}\, j_n(kR_1) \;+\; E_{0m}^{(1)}\, n_n(kR_1)}{E_{0m}^{(1)}\, j_n(kR_1) - G_{0m}^{(1)}\, n_n(kR_1)} \tag{2.8.11}$$

It is to be noted that this equation must be true for all values of n. Hence the ratio given by the right hand side must be independent of n. Substituting 2.8.11 back into 2.8.10a we obtain the real and imaginary parts of $\mathcal{E}_{mn}^{(1)}$. Now, referring back to 2.1.29 we let

$$\mathcal{E}_{mn}^{(1)} = We_{(mn)} + j\, Wo_{(mn)}, \tag{2.8.12}$$

Using the definition of $\overline{P}_n\,(\theta)$ given by 2.1.31 we cast the sum on m into the simpler form,

$$\sum_{m=-n}^{n} \mathcal{E}_{mn}^{(1)}\, e^{-jm\phi}\, P_n^m\,(\cos\theta) = We_{0n}\, \overline{P}_n(\theta), \tag{2.8.13}$$

Hence 2.8.1 for the case of uniform phase may be written

$$\Phi(r, \theta, \phi, t) = \sum_{n=0}^{\infty} We_{on} \overline{P}_n\,(\theta)\, h_n^{(2)}(kr)\, e^{j\omega t}, \tag{2.8.14a}$$

The real part of the equation is easily seen to be

$$\mathrm{Re}\{\Phi\} = \sum_{n=0}^{\infty} We_{0n}\, \overline{P}_n(\theta)\, [j_n\,(kr) \cos \omega t$$

$$+\; n_n\,(kr) \sin \omega t], \tag{2.8.14b}$$

We desire now to find the directivity function Φ eff of the radiator. This is defined as the square root of the time average value of the real part of the velocity potential squared over a period $2\pi/\omega$. Performing this averaging process we find

$$\Phi(r, \theta, \phi)_{\mathrm{eff}} = \frac{1}{\sqrt{2}} \left\{ \left(\sum_{n=0}^{\infty} We_{0n} \overline{P}_n(\theta)\, j_n(kr) \right)^2 \right.$$

$$\left. + \left(\sum_{n=0}^{\infty} We_{0n} \overline{P}_n(\theta)\, n_n(kr) \right)^2 \right\}^{1/2} \tag{2.8.15}$$

The directivity function finds immediate use in far field measurements where it is referred to as the "pattern function." In the far field the asymptotic value of $h_n^{(2)}(kr)$ is

$$h_n^{(2)}(kr) \underset{r\to\infty}{\to} \frac{e^{-jkr}}{kr}(-j)^{-n-1} = \frac{e^{-jkr}}{kr} e^{j\left\{\frac{\pi}{2}\right\}(n+1)} \tag{2.8.16}$$

Hence, in the far field, the real part of the velocity potential may be approximated to within a constant by the formula

$$\mathrm{Re}\{\Phi\} \underset{r\to\infty}{\to} \frac{1}{kr} \sum_{n=0}^{\infty} We_{0n} \overline{P}_n(\theta)\left[\cos\frac{\pi}{2}(n+1)\cos(\omega t - kr) + \sin\frac{\pi}{2}(n+1)\sin(\omega t - kr)\right] \tag{2.8.17}$$

On a time average basis therefore the far field pressure pattern may be approximated to within a constant by the formula

$$\Phi(\theta, \phi) \sim \left\{\left(\sum_{n=0}^{\infty} We_{0n}\overline{P}_n(\theta)\cos\frac{\pi}{2}(n+1)\right)^2 + \left(\sum_{n=0}^{\infty} We_{0n}\overline{P}_n(\theta)\sin\frac{\pi}{2}(n+1)\right)^2\right\}^{1/2} \tag{2.8.18}$$

In a numerical example Pachner applied the above method to obtain an empirical description of the sound field of a rigid piston in a rigid wall. He selected a circular piston radiator already calculated by Backhaus [24] who derived the following formula for the sound field at any distance R, ($R >$ piston radius a),

$$\Phi = \sum_{n=0}^{\infty} a_{0,2n} P_{2n}(\cos\theta)\left[j_n(kR)\cos\omega t + n_n(kR)\sin\omega t\right] \tag{2.8.19}$$

We note that this formula may be derived from (2.8.14b) above for the case $m = 0$. To obtain $a_{0,2n}$ we refer to Backhaus's formulas [25] from which, setting $m = 0$ and $ka = 8$ one obtains the following set of coefficients,

$$\begin{aligned} a_{00} &= 0.1432 & a_{02} &= -0.4636 \\ a_{04} &= 1.6461 & a_{06} &= 1.2466 \\ a_{08} &= 0.4126 & a_{0,10} &= -0.0771 \end{aligned} \tag{2.8.20}$$

Now to check his procedure Pachner assumed that the values of Φ calculated by 2.8.19, 2.8.20 at distance $kR = 10$ are a set of *measured instantaneous values* at time $\omega t_1 = 0$, $\omega t_2 = -\pi/2$. Pachner then employed the method detailed above to find 2.8.14b. In our terms this reduces to substituting the instaneous values of Φ into 2.1.18a and performing a numerical integration to find u_{0n} ($= We_{0n}$). The final result leads to the following coefficients,

$$\begin{aligned} a_{00} &= 0.142 & a_{02} &= -0.473 \end{aligned}$$

$$a_{04} = 1.66 \qquad a_{06} = -1.16$$

$$a_{08} = 0.437 \qquad a_{0,10} = -0.102 \qquad (2.8.21)$$

On comparing 2.8.21 with 2.8.20 we see that the numerical procedure of Pachner is quite adequate. This is even more apparent when the far field is calculated by means of 2.8.18 using alternately 2.8.20 and 2.8.21 for the coefficients We_{0m}. A table of the *normalized* far field directivity function as calculated by 2.8.20 and 2.8.21 for various angles θ is shown below.

	Φ_{ell}, using 2.8.20	Φ_{ell}, using 2.8.21
0°	1.000	1.000
10°14′	0.769	0.768
23°22′	0.172	0.174
36°14′	0.121	0.105
48°32′	0.092	0.093
60°00′	0.008	0.018
70°15′	0.038	0.032
78°51′	0.054	0.057
85°18′	0.058	0.063
89°05′	0.059	0.065

Pachner estimates that for the case $m = 0$ the precision of his numerical method is mainly contingent on the refinements used in the numerical integrations for obtaining We_{0m}. For $m \neq 0$ the precision falls with increasing m.

2.9 LOW FREQUENCY RADIATION OF MULTIPOLES IN THE FORM OF SPHERICAL BUBBLES

The radiation of spherical bubbles of gas in free space closely approximates the radiation of multipoles when the radius of the bubble is small relative to the wavelength of the radiation. Since a gaseous bubble has elasticity and since its motion generates inertia forces in the medium, its dynamical response has features of *resonance*. This is discussed first.

2.9a MECHANICAL RESONANCE OF BUBBLES AS MONOPLE RADIATORS

Let the bubble be excited by a harmonic acoustic pressure field, $p = |p| \exp(-i\omega t)$. Assume (1) that the radius of the bubble is small relative to the wavelength of sound of the incident acoustic pressure (2) that the frequency of the applied forces is not greater than the lowest order resonant frequency of the bubble (3) that the polytropic gas law $pV^{\kappa} = \text{const.}$ is valid.

Starting with assumption (3) it is seen that an incremental gas pressure δp causes an incremental change in radius δR over the area A of the bubble:

$$\delta p = -\frac{\gamma p_0}{V_0}\, dV = -\frac{\gamma p_0 A_0}{V_0}\, \delta R \tag{2.9.1}$$

Here subscript zero represents equilibrium values. The force δp accelerates an annular mass of fluid medium of amount $m = Al\varrho_0$, where l is the thickness of the mass (as yet unspecified). The dynamic equation of motion is then,

$$Al\varrho \frac{d^2}{dt^2}(\delta R) = -\frac{\gamma p_0 A}{V}\, \gamma R$$

or

$$\delta\ddot{R} + \frac{3\gamma p_0}{\varrho_0 l R_0}\, \gamma R = 0, \qquad A = 4\pi R^2, \qquad V = \tfrac{4}{3}\pi R^3 \tag{2.9.2}$$

If δR is small enough the bubble will oscillate with a resonant frequency Ω

$$\Omega^2 = \frac{3\gamma p_0}{\varrho_0 l R_0} \tag{2.9.3}$$

To find l we resort to the theory of radiation of sound of a pulsating sphere. The mechanical impedance presented by the medium to the motion of a sphere of radius R_0 pulsating in harmonic time $\exp(-i\omega t)$ at low frequency is:

$$Z \cong -i\omega(4\pi R_0^2)\, R_0\varrho_0 + \varrho_0 c(4\pi R_0^2)(kR_0)^2,\ k = \frac{2\pi}{\lambda} = \omega/c \tag{2.9.4}$$

[26]. The first term represents mass reactance $-i\omega M$ where M is 3 × the mass of fluid in the volume of the bubble,

$$M = 3 \times \tfrac{4}{3}\pi R_0^3 = (4\pi R_0^2)\, R_0\varrho_0 = AR_0\varrho_0 \tag{2.9.5}$$

From this one concludes that the equivalent thickness l of annular fluid accelerated is equal to the radius R_0 of the equilibrium sphere. Hence the resonant frequency in the lowest (monopole) mode is

$$\Omega^2 = \frac{3\gamma p_0}{\varrho_0 R_0^2}, \text{ or } f_{\text{Res}} = \frac{1}{2\pi R_0}\sqrt{\frac{3\gamma p_0}{\varrho_0}} \tag{2.9.6}$$

When the bubble radius is small, say 10^{-4} cm, the gas compression and expansion come isothermal ($\lambda = 1$), and the surface tension σ(units: $Nm/m^2 = Nm^{-1}$) exerts a significant pressure of amount $2\sigma/R_0$ on the gas [27]. Thus a small increase δR in radius results in a pressure decrease δp,

$$\delta p = -\frac{2\sigma}{R_0}\left(\frac{\delta R}{R_0}\right) \tag{2.9.7}$$

A sum of 2.9.7 and 2.9.1 gives the total pressure change associated with a change in radius,

$$\delta p = -\frac{3\gamma p_0}{R_0} q\delta R \qquad g = 1 + \frac{2\sigma}{3p_0 R_0} \tag{2.9.8}$$

Surface tension therefore modifies the resonant frequency, and 2.9.6 becomes,

$$f_{res} = \frac{1}{2\pi R_0}\sqrt{\frac{3p_0}{\varrho_0} g} \quad R_0 < 3\times 10^{-3}\, cm \tag{2.9.10}$$

2.9b VIBRATION AND RESONANCE OF A SPHERICAL BUBBLE WITH NON-UNIFORM RADIAL MOTION

Let the radial displacement ζ of the bubble be a function of the polar angle θ and azimuthal angle ϕ. It can then be expanded in surface spherical harmonic, $Y_n(\theta, \phi)$, orthogonal in the interval $0 \leqslant \phi \leqslant 2\pi$:

$$\zeta(\theta, \phi) = \sum_n Y_n(\theta, \phi) \tag{2.9.11a}$$

$$Y_n(\theta, \phi) = A_{0n} Y_{0n}^{(e)}(\mu) + \sum_{m=1}^{n} [A_{mn} Y_{mn}^{(e)}(\mu, \phi) + B_{mn} Y_{mn}^{(0)}(\theta, \phi)] \tag{2.9.11b}$$

$$(1)\ Y_{0n}^{(e)}(\mu) = P_n(\mu), (2)\ Y_{mn}^{(e)} = \cos m\phi\, P_n^m(\mu), (3)\ Y_{mn}^{(0)} = \sin m\phi\, P_n^m(\mu), \tag{2.9.11c}$$

$$\mu = \cos\theta \tag{2.9.11d}$$

Here the superscripts e, 0 mean even, odd respectively. The form $Y_{0n}^{(e)}(\mu) = 0$ divides the spherical surface into zones of latitude; the forms $\cos m\phi$, $\sin m\phi$ divide the surface into sectors of longitude. $P_n^m(\mu)$ are the associated Legendre functions of order n and degree m.

The constants A_{mn}, B_{mn} can be found, when the displacement is specified, by use of orthogonality of the Y_n:

$$A_{mn} = \frac{1}{N_{mn}^{(e)}} = \int_0^{2\pi} d\varphi \int_0^{\pi} \zeta(\theta, \phi)\, Y_{mn}^{(e)} \sin\theta d\theta$$

$$N_{mn}^{(e)} = \int_0^{2\pi} d\phi \int_0^{\pi} [Y_{mn}^{(e)}(\mu, \phi)]^2 \sin\theta d\theta = \frac{4\pi}{\varepsilon_n(2n+1)} \frac{(n+m)!}{(n-m)!} \tag{2.9.12}$$

$$\varepsilon_0 = 1, \varepsilon_n = 2, n = 1, 2, 3 \ldots$$

These mathematical forms facilitate the calculation of the resonant frequency of bubbles in non-uniform radial motion.

Let the radial displacement be zonal (that is, in parallel belts) over the surface of the sphere and harmonic in time:

$$\zeta(r, \theta, t) = \zeta_n(r, \theta, t) = A_{0m}(r)\, Y_{0m}^{(e)}(\mu) \cos(\omega t + \alpha) \tag{2.9.14}$$

Assume the stiffness of the bubble is controlled by surface tension σ so that the difference between the internal pressure $p^{(i)}$ and the external pressure $p^{(0)}$ is.

$$p^{(i)} - p^{(0)} = \sigma \left(\frac{1}{R_1} + \frac{1}{R_2} \right) \tag{2.9.15}$$

where R_1, R_2 are the principal radii of curvature of the curved surface of the bubble. Now the radial velocity of the surface is,

$$\frac{d\zeta}{dt}\Big|_{r=R_0} = - A_{on}((R_0)\, \omega\, Y_{0n}^{(e)} \sin(\omega t + \alpha) \tag{2.9.16}$$

It is required to find $A_{0n}(R_0)$ such that the velocity potential $\psi_n^{(1)}$ of the radial motion of the gas inside the bubble and the potential $\psi_n^{(0)}$ outside the bubble yield the same velocity at the surface. In accord with 2.9.16 let,

$$\psi_n = B_{0m}(r)\, \omega\, Y_{0m}^{(e)} \sin(\omega t + \alpha) \tag{2.9.17}$$

Then, at the surface

$$- \frac{d\psi_m}{dr} = \frac{d\zeta}{dt} \tag{2.9.18}$$

or

$$\frac{dB_{0n}(r)}{dr}\Big|_{r=R_0} = A_{0n}(R_0) \tag{2.9.19}$$

Choosing the radial derivative to be positive outward from the surface one can meet the requirement by combining, 2.9.16 through 2.9.19 and employing a continuation of radial coordinate of a compatible type. **One solution obtained by critical inspection, is**

$$\psi_n^{(1)} = \frac{r^n A_{0n}}{n R_0^{n-1}}\, \omega\, Y_{0n}^{(e)} \sin(\omega t + \alpha) \tag{2.9.20}$$

$$\psi_n^{(0)} = - \frac{R_0^{n+2}}{(n+1) r^{n+1}}\, A_{0n}\, \omega\, Y_{0n}^{(e)} \sin(\omega t + \alpha) \tag{2.9.21}$$

The incremental (acoustic) pressures at $r = R_0$ are obtained by $p_n^{(i)} = \varrho^{(i)}\, \partial\psi^{(i)}/\partial t$, $p_n^{(0)} = \varrho^{(0)}\, \partial\psi^{(0)}/\partial t$. Thus the left hand side of 2.9.15 can readily be calculated. To find the right hand side one applies the geometric theory of surfaces [28] in conjunction with 2.9.14. This leads to the form,

$$\frac{1}{R_1} + \frac{1}{R_2} = \frac{2}{R_0} + \frac{(n-1)(n+2)}{R_0^2} A_{0n} Y_{0n}^{(e)} \cos(\omega t + \alpha) \tag{2.9.22}$$

Because 2.9.15 deals with incremental quantities the term $2/R_0$ will be neglected. Substituting 2.9.22, 2.9.21, 2.9.20 into 2.9.15 one obtains an expression for the resonant frequency of a bubble radiating in a zonal spherical mode of degree n:

$$f_{res} = \frac{1}{2\pi} \left\{ n(n+1)(n-1)(n+2) \frac{\sigma}{R_0^3} \frac{1}{[(n+1)\varrho^{(i)} + n\varrho^{(0)}]} \right\}^{1/2} \tag{2.9.23}$$

For a spherical bubble of air surrounded by a liquid it is seen that $\varrho^{(i)}$ is negligible compared to $\varrho_{(0)} = \varrho_0$. Hence,

$$f_{res} = \frac{1}{2\pi} \left\{ (n+1)(n-1)(n+2) \frac{\sigma}{\varrho_0 R_0^3} \right\}^{1/2} \tag{2.9.24}$$

It is noted that a zonal radiator of degree $n = 1$, described by $P_1(\mu) = \cos\theta$, is not a free mode of vibration.

2.9c RADIATION FIELD OF A SPHERICAL BUBBLE WITH HARMONIC RADIAL MOTION WHICH IS A FUNCTION OF POLAR ANGLE θ BUT NOT OF AZIMUTHAL ANGLE ϕ

In a zonal radiator of degree n the normal component of surface velocity is given by 2.9.16 and the surface acoustic pressure by $p_n(R_0) = -i\omega\varrho\,\psi_n^{(0)}$, where $\psi_n^{(0)}$ is 2.9.21. It is convenient to represent them as functions of complex time:

$$v_n(R_0) = \mathrm{Re}\{-i\omega A_{0n} Y_{0n}^{(e)}(\mu) \exp[-i(\omega t + \alpha)]\}, \tag{2.9.25}$$

$$p_n(R_0) = \mathrm{Re}\left\{ - \frac{\omega^2 R_0 A_{0n} \varrho_0}{n+1} Y_{0n}^{(e)}(\mu) \exp[-i(\omega t + \alpha)] \right\} \tag{2.9.26}$$

in which $\mu = \cos\vartheta$ and α is an unspecified phase. Now the acoustic radiation itself of a bubble whose radial motion is an arbitrary function of θ can be represented as a sum of products of zonal harmonics and spherical Bessel functions,

$$p(r|\omega) = \sum_n C_{0n} h_n(r) Y_{0n}^{(e)}(\mu) \exp[-i(\omega t + \alpha)] \tag{2.9.27}$$

For each n one can equate 2.9.27 for $r = R_0$ to 2.9.26. This gives,

$$C_{0n} = - \frac{\omega^2 R_0 A_{0n} \varrho_0}{(n+1) h_n(R_0)} \qquad (\text{units: } Nm^{-1}) \tag{2.9.28}$$

Thus, the radiated pressure field everywhere in free space is,

$$p(r|\omega) = -\sum_{n=0}^{\infty} \frac{\omega^2 R_0 A_0 \varrho_0}{(n+1)h_n(R_0)} h_n(r)\, Y_{0n}^{(e)}(\mu) \exp[-i(\omega t + \alpha)] \tag{2.9.29}$$

The case $n = 0$ is that of a monopole because $Y_{00}^{(e)}(\mu) = 1$. Let Q_ω be its volume velocity. Then, by 2.9.25,

$$Q_\omega = 4\pi R_0^2 v_n = -4\pi R_0^2\, i\omega A_{00} \tag{2.9.30}$$

or

$$A_{00} = \frac{iQ_\omega}{4\pi R_0^2 \omega} \tag{2.9.31}$$

Because $h_0(r) = (\exp ikr)/r$, it is seen that the radiation field of a monopole spherical bubble is

$$p_0(r|\omega) = -\frac{i\omega\varrho_0 Q_\omega}{4\pi} \frac{e^{i(kr-\omega t)}}{r} \exp(-ikR_0) \tag{2.9.32}$$

When the acoustic size kR_0 of the radiator is very small and $r \gg R_0$ the factor $\exp(-ikR_0)$ can be neglected relative to $\exp(ikr)$. The radiator is then a point source.

2.9d RADIATION FIELD OF A SPHERICAL BUBBLE WITH HARMONIC RADIAL MOTION WHICH IS AN ARBITRARY FUNCTION OF SPHERICAL ANGLES θ, ϕ.

Let the normal component of surface velocity of the bubble be a known function $v = V(\theta, \phi)e^{-i\omega t}$. Because one wishes to relate it to the radiated field it is first expanded in surface spherical harmonics, defined in 2.9.11c:

$$V(\theta, \phi) = \sum_{m,n} [A_{mn} Y_{mn}^{(e)}(\mu, \phi) + B_{mn} Y_{mn}^{(0)}(\mu, \phi)] \tag{2.9.33a}$$

$$\begin{Bmatrix} A_{mn} \\ B_{mn} \end{Bmatrix} = \left(\frac{2n+}{4\pi} \right) \varepsilon_n \frac{(n-m)!}{(n+m)!} \int_0^{2\pi} d\phi \int_0^{\pi} V(\theta, \phi) \begin{Bmatrix} Y_{mn}^{(e)}(\mu, \phi) \\ Y_{mn}^{(0)}(\mu, \phi) \end{Bmatrix} \sin\theta d\theta \tag{2.9.33b}$$

$$\varepsilon_0 = 1;\ \varepsilon_n = 2,\ n \neq 0;\ B_{00} = 0$$

Substituting 2.9.33b back into 2.9.33a and collecting terms one obtains:

$$v = V(\theta, \phi)e^{-i\omega t} = \sum_{m,n} P_n^m(\mu)\, L_{mn}(\phi) e^{-i\omega t} \tag{2.9.33c}$$

$$L_{mn}(\phi) = \int_0^{2\pi} d\phi_0 \int_0^{\pi} V(\theta_0, \phi_0) \cos m(\phi - \phi_0) P_n^m(\cos\theta_0) \sin\theta_0 d\theta_0 \qquad (2.9.33d)$$

$$\times \left(\frac{2n+1}{4\pi} \right) \varepsilon_n \frac{(n-m)!}{(n+m)!} \qquad \text{(units: } ms^{-1}\text{)}$$

Now for outgoing spherical waves the velocity potential ψ must contain the spherical Bessel function $h_n(kr)$.

$$\psi(r, \theta, \phi | \omega) = \sum_{m,n} [C_{mn} Y_{mn}^{(e)}(\mu, \phi) + D_{mn} Y_{mn}^{(0)}(\mu, \phi)] h_n(kr) e^{-i\omega t} \qquad (2.9.34a)$$

$$h_n(z) = -i(-1)^n \left(\frac{d}{zdz} \right)^n \left(e^{iz}/z \right) \qquad (2.9.34b)$$

The constants C_{mn}, D_{mn} are determined from the boundary conditions. At the surface $r = R_0$,

$$\frac{\partial \psi}{\partial r}\Big|_{r=R_0} = -V(\theta, \phi) e^{-i\omega t} = \sum_{m,n} [C_{mn} Y_{mn}^{(e)}(\mu, \phi) + D_{mn} Y_{mn}^{(0)}(\mu, \phi)] \left[\frac{kdh_n(z)}{dz} \right] e^{-i\omega t}$$

Comparison with 2.9.33c shows that,

$$C_{mn} = -\frac{A_{mn}}{kh'(kR_0)}; \qquad D_{mn} = -\frac{B_{mn}}{kh'(kR_0)}$$

Substitution of this result back into 2.9.34 give the velocity potential everywhere,

$$\psi(r, \theta, \phi | \omega) = -\sum_{m,n} P_n^m(\mu) L_{mn}(\phi) \frac{h_n(kr)}{kh_n'(kR_0)} e^{-i\omega t} \qquad \text{(units: } m^2 s^{-1}\text{)} \qquad (2.9.35)$$

$$h_n'(z) = \frac{dh_n(z)}{dz}$$

Again, the case $n = 0$ corresponds to that of a monopole, with $V(\theta, \phi) = V_0$. Because $h_0(z) = -ie^{iz}/z$, and $h_0'(z) = -h_1(z) = \left(\frac{z+i}{z^2} \right) e^{iz}$, it is seen that the monopole velocity potential is,

$$\psi_0(r | \omega) = iVR_0^2 \frac{\exp(ikr)}{r} \frac{\exp(-ikR_0)}{(i + kR_0)} e^{-i\omega t} \qquad (2.9.36)$$

If, in addition $|kR_0| \ll 1$, the radiated field reduces to that of a point source with source strength $Q_0 = 4\pi R_0^2 V_0$.

REFERENCES

1. Lord Rayleigh, "Theory of Sound", Dover Publications, New York, 1945, Chap. XVII.
2. H. Stenzel and O. Brosze, "Leitfaden zur Berchnung von Schallvorgängen", Springer Verlag, Berlin 1958, p. 111 ff.
3. S. N. Rschevkin, "The Theory of Sound", MacMillan Co., New York, 1963, Chap. VIII.
4. E. W. Hobson, "Theory of Spherical and Ellipsoidal Harmonics", Cambridge, New York, 1931.
5. Ref. (1), pp. 237-238.
6. P. M. Morse, "Vibration and Sound", McGraw Hill Book Co., New York, 1948, p. 316.
7. J. Brillouin, "Rayonnement Transitoire Des Sources Sonores et Problems Connexes", Comptes Rendues Cahiers D'Acoustique, No. 13, (1950).
8. P. M. Morse and H. Feshbach, "Methods of Theoretical Physics", Vols. I, II, p. 1477, McGraw Hill Book Co., New York (1953), p. 1477.
9. Ref. [2], p. 113.
10. Ref. [3], p. 284.
11. Ref. [3], p. 318.
12. Ref. [8], p. 1325.
13. Ref. [1], Vol. II, p. 238.
14. Ref. [3], p. 327.
15. E. Guillemin, "Introduction to Circuit Theory", J. Wiley and Sons, New York, 1953, p. 518.
16. W. Magnus, F. Oberhettinger, "Formulas and Theorems for the Functions of Mathematical Physics", Chelsea Pub. Co., New York, 1954, p. 54.
17. H. Lamb, "Hydrodynamics", 6 Ed. Dover Publications, New York, 1945, p. 122.
18. Ref. [3], p. 336.
19. T. Nimura, Y. Watanabe, "Sound Radiation from the Zonal Radiators", *Tohoku Univ. Sci.* Reports, Series B Electrical Communications 5-6, 1953-1955, p. 176.
20. E. Jahnke, F. Emde, W. Losch, "Tables of Higher Functions", 6th Ed. McGraw Hill Book Co., New York, 1960, p. 110 ff.
21. A. Erdelyi et al., "Higher Transcendental Functions", McGraw Hill, New York, 1953, Vol. 1, p. 145.
22. J. Pachner, "On The Dependence of Directivity Patterns on the Distance from the Emitter", JASA, *86,* p. 92, Jan. 1956.
23. C. J. Bouwkamp, "A Contribution to the Theory of Acoustic Radiation", Phillips Res. Reports 1, p. 251 (1945).
24. H. Backhaus, "Das Schallfeld der kreisformigen Kolbenmembran", Ann. der Physik V Folge 1930, p. 1.
25. Ref. (24), p. 17.
26. P. M. Morse, K. U. Ingard, "Theoretical Acoustics", McGraw-Hill (1969) p. 315.
27. L. D. Landau, E. M. Lifshitz, "Fluid Mechanics", p. 231, Pergamon Press, 1959.
28. H. Lamb, "Hydrodynamics", 6th Ed., Dover Pub., New York, p. 473.

CHAPTER III
THE CALCULATION OF ACOUSTIC RADIATION FIELDS BY USE OF GREEN'S FUNCTIONS

3.1 THE CALCULATION OF ACOUSTIC RADIATION BASED ON GREEN'S FUNCTIONS

In Chap. I the calculation of acoustic radiation was done by solving differential equation 1.2.3, subject to the boundary condition 1.8.25 and the condition at infinity 1.8.7. The solution took the form of a sum of eigenfunctions in discrete modal form 1.9.3 or continuum form 1.9.4. In this section we use the alternative method of calculating the acoustic field by solving the integral equation 1.7.7. Since this method requires an appropriate Green's function for the space involved we consider the properties of Green's functions.

3.2 PHYSICAL MEANING OF THE GREEN'S FUNCTION

Green's functions are intimately related to the physics of point sources. In the integral equation 1.7.7, we assume the source distribution q is a simple source (or "point source") in steady state:

$$q = \frac{Q}{4\pi}\,\delta(\vec{r}-\vec{r}_0)e^{-i\omega t} \qquad \text{(units: } s^{-1}\text{)} \tag{3.2.1}$$

in which Q has the units of m^3s^{-1}. We place this source in an unbounded medium so that the surface integral in 1.7.7 vanishes. Then the velocity potential everywhere is,

$$\psi(\vec{r}, t) = e^{-i\omega t}\int dV_0\,\frac{e^{ik|\vec{r}-\vec{r}_0|}}{|\vec{r}-\vec{r}_0|}\,\frac{Q}{4\pi}\,\delta(\vec{r}-\vec{r}_0) \tag{3.2.2}$$

When $|\vec{r}_0|$ is very large, we make the double approximation that,

in phase $e^{ik|\vec{r}-\vec{r}_0|}$: $\quad |\vec{r}-\vec{r}_0| \cong r - x_0\,\frac{x}{r} - y_0\,\frac{y}{r}$

in amplitude $\frac{1}{|r-r_0|}$: $|\vec{r}-\vec{r}_0| \cong r$

where $\quad r = \sqrt{x^2+y^2+z^2}$

(see Sect. 1.12) in which x_0, y_0 are the rectangular components of the distribution, and x, y, z are the rectangular coordinates of the field (or observation point). Eq. 3.2.2 then reduces to,

$$\psi(\vec{r}, t) = \frac{Qe^{-i\omega t}}{4\pi r}\,e^{ikr} \qquad \text{(units: } m^2s^{-1}\text{)} \tag{3.2.3}$$

The quantity $\exp(ikr)/r$ is the far field approximation of the Green's function in unbounded space. It is the field at $\vec{r}$ due to the point source at $\vec{r}_0$ of *magnitude* 4π. The inclusion of 4π in this definition of the point source is discussed in Sect. 1.7. Several authorities in acoustic theory define Green's functions as fields due to delta function sources of *unit magnitude*. The quantity 4π then disappears from 3.2.1 but reappears in 3.2.2 as part of the definition of G. Since the two conventions are currently in use they are summarized here:

Source	Green's Function
$\frac{Q}{4\pi}\,\delta(\vec{r}-\vec{r}_0)$	$\frac{e^{ik\lvert\vec{r}-\vec{r}_0\rvert}}{\lvert\vec{r}-\vec{r}_0\rvert}$
$Q\delta(\vec{r}-\vec{r}_0)$	$\frac{e^{ik\lvert\vec{r}-\vec{r}_0\rvert}}{4\pi\lvert\vec{r}-\vec{r}_0\rvert}$

(3.2.4)

Now, in place of volume distributions of sources, which we set here to zero, we consider the surfaces $S(S', S'')$, Fig. 1.8.1, to have a distribution of normal component of velocity $v_n(r_0^s)$. The field anywhere in volume V according to 1.7.7 and boundary conditions 1.10.3 is,

$$\psi = \frac{1}{4\pi}\int [G(\vec{r}|\vec{r}_0^s)\, v_n(r_0^s) - \psi(\vec{r}_0^s)\,\frac{\partial G}{\partial n_0}\,(\vec{r}|\vec{r}_0^s)]\, dS(\vec{r}_0^s) \tag{3.2.5}$$

Here (as everywhere except when otherwise stated) the positive normal points away from the medium and positive v_n points into the medium. Since the medium is bounded we can no longer use 3.2.4 for G. However we may be able to construct a G such that $\partial G/\partial n_0$ vanishes on surfaces S. In that case, the field is determined solely by the first term,

$$\psi = \frac{1}{4\pi}\int_S G(\vec{r}|\vec{r}_0^s)\, v_n(r_0^s)\, dS(r_0^s), \qquad \frac{\partial G}{\partial n_0} = 0 \tag{3.2.6}$$

Comparison of this result with 3.2.2 shows that when velocity distributions determine the field, the point source is specified in terms of volume velocity Q and free field G, while surface sources are specified in terms of normal component of velocity v_n and non-free field G. This distinction appeared in 1.10.1 and 1.10.6 where the physical difference between fields due to surface and volume velocities is emphasized.

3.3 GREEN'S FUNCTIONS BASED ON 1ST ORDER ACOUSTIC FIELD EQUATIONS

The Green's functions defined by 1.7.4 determine the velocity potential ψ through 1.7.7. The acoustic field however can also be defined in terms of acoustic pressure p and particle velocity $\vec{v}$. It is useful to relate Green's functions for ψ to the determination of p and $\vec{v}$.

At a point $\vec{r}$, t we imagine a small fixed volume ΔV. The Euler field equation of continuity of mass through it is,

$$\frac{\partial \varrho_T}{\partial t} = \varrho_T \mathcal{Q} - \nabla\cdot(\varrho_T \vec{V}_T) \tag{3.3.1}$$

ϱ_T: total mass density (Ns^2m^{-4})

$\mathcal{Q}$: scalar volume velocity ($m^3s^{-1}m^{-3} = s^{-1}$)

$\vec{V}_T$: total particle velocity (ms^{-1})

Here $\mathcal{Q}$ is positive when the volume flow is inward toward $\vec{r}$. In the presence of acoustic fields ϱ, $\vec{v}$, p, and equilibrium ϱ_0, V_0, P_0,

$$\begin{aligned} &\text{(a)} \quad \varrho_T = \varrho_0 + \varrho \qquad\qquad \text{(c)} \quad P_T = P_0 + p \\ &\text{(b)} \quad \vec{V}_T = \vec{V}_0 + \vec{V} \end{aligned} \tag{3.3.2}$$

When

$$\varrho \ll \varrho_0, |\vec{V}| \ll |\vec{V}_0|$$

we can approximate the acoustic pressure by

$$p = \varrho c^2, c^2 = P_0/\varrho_0 \tag{3.3.3}$$

By retaining only first order terms 3.3.1 reduces to,

$$\frac{\partial p}{c^2 \partial t} \cong \varrho_0 \mathcal{Q} - \varrho_0(\nabla\cdot\vec{V}) \qquad \text{(units: } Nsm^{-4}\text{)} \tag{3.3.4}$$

This equation states that a time-increment of mass $\varrho_0 \mathcal{Q}$ flowing into ΔV at $\vec{r}$ causes an increase in acoustic pressure with time. Also, a positive value of divergence of velocity out of the area enclosing ΔV is accompanied by diminution of acoustic pressure with time.

For the same fixed volume ΔV we write the Euler dynamic field equation for the acceleration of mass due to applied volume forces F_T:

$$\frac{\partial \varrho_T \vec{V}_T}{\partial t} = \vec{F}_T(\vec{r}, t) - \nabla p_T(\vec{r}, t) \qquad \text{(units: } Nm^{-3}\text{)} \tag{3.3.5}$$

Here F_T is positive when it points away from r. When the excitation force is acoustic we set $\vec{F}_T = \vec{f}$ and $\varrho_T V_T = (\varrho_0 + \varrho)(V_0 + V) \cong \varrho_0 V$. Thus, to 1st order in the acoustic approximation 3.3.5 becomes:

$$\varrho_0 \frac{\partial \vec{V}}{\partial t}(r, t) \cong \vec{f}(\vec{r}, t) - \nabla p(\vec{r}, t) \tag{3.3.6}$$

This equation states that a positive force acting on the mass in ΔV centered at $\vec{r}$ causes a positive increase in particle velocity at $\vec{r}$ in the same direction. Also, a positive gradient of acoustic pressure in any direction is accompanied by a decrease of particle velocity with time in the same direction.

Let us now take $\mathcal{Q}$, f as causes ("generators") of the acoustic field:

$$\frac{1}{P_0}\frac{\partial p}{\partial t} + \vec{\nabla}\cdot\vec{V} = \mathcal{Q} \qquad (\text{units: } s^{-1}) \tag{3.3.7}$$

$$\varrho_0 \frac{\partial \vec{V}}{\partial t} + \vec{\nabla} p = \vec{f} \qquad (\text{units: } N\,m^{-1}) \tag{3.3.8}$$

Our objective is to define a set of operators $\mathcal{G}$ which will allow us to calculate pressure and particle velocity in the following way:

$$p(\vec{r}, t) = \mathcal{G}_{p\mathcal{Q}}\,\mathcal{Q} + \vec{\mathcal{G}}_{pf}\cdot\vec{f} \tag{3.3.9}$$

$$\vec{v}(\vec{r}, t) = \vec{\mathcal{G}}_{v\mathcal{Q}}\,\mathcal{Q} + \vec{\vec{\mathcal{G}}}_{vf}\cdot\vec{f} \tag{3.3.10}$$

The symbolic operators $\mathcal{G}$ are defined as,

$$\begin{aligned}
\mathcal{G}_{ij} X &\equiv \int\int_{V_0} G_{ij}(\vec{r}, t|\vec{r}_0, t_0)\, X(\vec{r}_0, t_0)\, dV_0 dt_0 \\
\vec{\mathcal{G}}_{ij}\cdot\vec{X} &\equiv \int\int_{V_0} \vec{G}_{ij}(\vec{r}, t|\vec{r}_0, t_0)\cdot\vec{X}(\vec{r}_0, t_0)\, dV_0 dt_0 \\
\vec{\vec{\mathcal{G}}}_{ij}\cdot\vec{X} &\equiv \int\int \vec{\vec{G}}_{ij}(\vec{r}, t|\vec{r}_0, t_0)\cdot\vec{X}(r_0, t_0)\, dV_0 dt_0.
\end{aligned} \tag{3.3.11}$$

Substitution of 3.3.9, 3.3.10 into 3.3.7, and splitting of terms in $\mathcal{Q}$ from terms in $\vec{f}$ lead to,

$$\frac{1}{P_0}\frac{\partial}{\partial t}\left(\mathcal{G}_{p\mathcal{Q}}\,\mathcal{Q}\right) + \nabla\cdot\left(\vec{\mathcal{G}}_{v\mathcal{Q}}\,\mathcal{Q}\right) = \tag{3.3.12}$$

$$\frac{1}{P_0}\frac{\partial}{\partial t}\left(\vec{\mathcal{G}}_{pf}\cdot\vec{f}\right) + \nabla\cdot\left(\vec{\vec{\mathcal{G}}}_{vf}\cdot\vec{f}\right) = 0 \tag{3.3.13}$$

We now make $\mathcal{Q}$ a delta source in space and time:

$$\mathcal{Q} = \delta(\vec{r} - \vec{r}_0)\,\delta(t - t_0) \tag{3.3.14}$$

Upon performing the integrations called for in 3.3.11, one arrives at,

$$\frac{1}{P_0}\frac{\partial}{\partial t} G_{p\mathcal{Q}} + \nabla\cdot\vec{G}_{v\mathcal{Q}} = \delta(\vec{r} - \vec{r}_0)\,\delta(t - t_0) \tag{3.3.15}$$

A similar operation may be performed on 3.3.13. But since this equation is homogeneous one can dispense with volume integration and arrive immediately at

$$\frac{1}{P_0}\ \frac{\partial}{\partial t}\vec{G}_{pf} + \vec{\nabla}_0\vec{\vec{G}}_{vf} = 0 \tag{3.3.16}$$

The second equation, 3.3.8, is treated in the same way through 3.3.9, 3.3.11, resulting in the pair:

$$\varrho_0 \frac{\partial}{\partial t}\vec{G}_{v\mathcal{Q}}\ \mathcal{Q} + \nabla\ G_{p\mathcal{Q}}\ \mathcal{Q} = 0 \tag{3.3.17}$$

$$\varrho_0 \frac{\partial}{\partial t}\ G_{\vec{v}f} \cdot \vec{f} + \nabla(\ G_{pf} \cdot \vec{f}) = \vec{f} \tag{3.3.18}$$

3.3.17 is homogeneous and thus reduces to

$$\varrho_0\ \frac{\partial}{\partial t}\ \vec{G}_{v\mathcal{Q}} + \nabla G_{p\mathcal{Q}} = 0 \tag{3.3.19}$$

In 3.3.18 we set

$$\vec{f} = \delta(\vec{r} - \vec{r}_0)\ \delta(t - t_0) = \delta(\vec{r} - \vec{r}')\ \delta(t - t')\ \vec{\vec{1}}\ \delta(r' - \vec{r}_0)\ \delta(t' - t_0)$$

in which $\vec{\vec{1}}$ is a unit dyadic, and arrive at

$$\varrho_0\ \frac{\partial}{\partial t}\vec{\vec{G}}_{vf} + \vec{\nabla}\ \vec{G}_{pf} = \vec{\vec{1}}\ \delta(r' - \vec{r}_0)\ \delta(t' - t_0) \tag{3.3.20}$$

The collection 3.3.15, 3.3.16, 3.3.19 and 3.3.20 are defining equations for the Green's functions G_p , G_{pf}, G_v , G_{vf}.

The question now arises, what is the relation of these Green's functions to the conventional Green's function for the unbounded domain where governing equation is 1.7.4? To find this relation we eliminate $\vec{G}_v$ from 3.3.15 and 3.3.19 and obtain

$$\left(\nabla^2 - \frac{\varrho_0}{P_0}\ \frac{\partial^2}{\partial t^2}\right)G_{p\mathcal{Q}} = -\varrho_0\ \frac{\partial}{\partial t}\ \delta(r - r_0)\ \delta(t - t_0)$$

Comparison with 1.7.4 shows that

$$G_{p\mathcal{Q}} = \frac{\varrho_0}{4\pi}\ \frac{\partial}{\partial t}\ g \tag{3.3.21}$$

$$g = \frac{e^{ikR}}{R},\ R = |\vec{r} - \vec{r}_0|$$

Thus, if there are no body forces (i.e. $\vec{f} \equiv 0$) then the radiated acoustic pressure due to source $\mathcal{Q}$ in 3.3.9 is

$$p = -\int dt_0 \int_{V_0} \frac{\varrho_0}{4\pi} \frac{\partial g}{\partial t}(\vec{r}, t|\vec{r}_0, t_0)\ \mathcal{Q}\ (\vec{r}_0, t_0)\, dV_0 \tag{3.3.22}$$

The negative sign is inserted because Green's functions are defined for negative sources only (see 1.7.4). If we observe that

$$\frac{\partial g}{\partial t}\mathcal{Q} = \frac{\partial}{\partial t}(g\mathcal{Q}) - g\frac{\partial \mathcal{Q}}{\partial t}$$

and noting that $\mathcal{Q}$ is not a function of t, it is seen that

$$p = \frac{\varrho_0}{4\pi}\frac{\partial}{\partial t}\int dt_0 \int_{V_0} g(r, t|r_0, t_0)\ \mathcal{Q}\ (\vec{r}_0, t_0)\, dV_0 \tag{3.3.23}$$

Similarly from 3.3.19 it is deduced that

$$\vec{G}_{\vec{r}\mathcal{Q}} = -\frac{\nabla g}{4\pi} \tag{3.3.24}$$

Again, since the Green's functions are defined for negative sources one has

$$p = -\int dt_0 \int_{V_0} \vec{G}_{\vec{r}\mathcal{Q}} \cdot \vec{f}\, dV_0$$

or

$$p = \int dt_0 \int_{V_0} \vec{f}(\vec{r}_0, t_0) \cdot \frac{\vec{\nabla} g}{4\pi}\, dV_0(\vec{r}_0) \tag{3.3.25}$$

Since $$\vec{f} \cdot \vec{\nabla} g = \nabla \cdot (\vec{f} g) - (\nabla \cdot \vec{f}) g$$

then an integration by parts shows that if V_0 is made large enough,

$$\int_{V_0} \nabla \cdot (\vec{f} g)\, dV_0(r_0) = 0$$

because $\vec{f}$ is zero outside the source region. Thus an alternative form of 3.3.25 is

$$p(\vec{r}, t) = -\int dt_0 \int_{V_0} [\vec{\nabla}_0 \cdot \vec{f}(\vec{r}_0, t_0)]\, g(\vec{r}, t|\vec{r}_0, t_0)\, dV_0 \tag{3.3.26}$$

The symbol $\vec{f}$ stands for both body forces and stress forces. From 1.8.3,

AD-A140 578 A TREATISE ON ACOUSTIC RADIATION(U) NAVAL RESEARCH LAB 2/7
WASHINGTON DC S HANISH 1981

UNCLASSIFIED F/G 20/1 NL

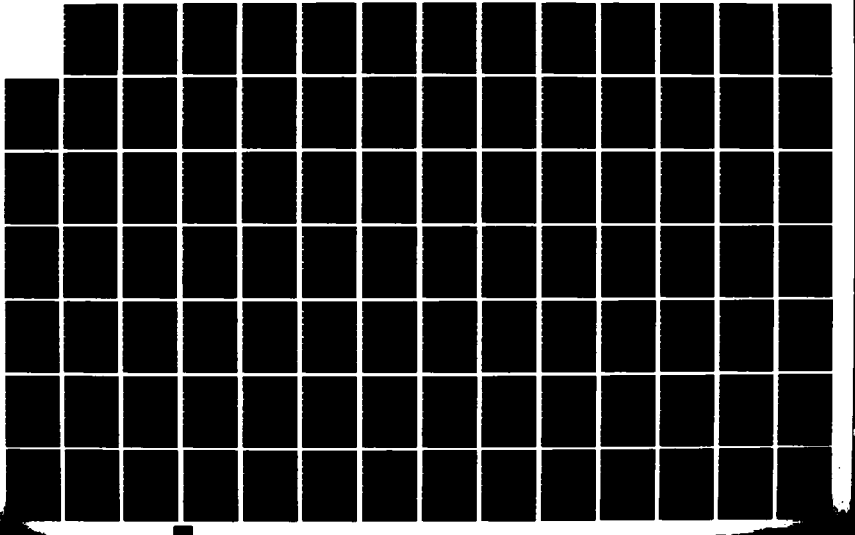

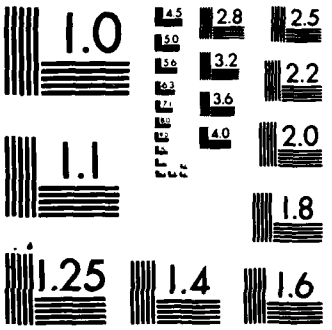

MICROCOPY RESOLUTION TEST CHART
NATIONAL BUREAU OF STANDARDS-1963-A

$$\vec{f} = \vec{F} - \vec{\vec{\mathfrak{T}}} \cdot \vec{\nabla}$$

so that one can expand 3.3.26 to read,

$$p(\vec{r}, t) = -\int dt_0 \int_{V_0} \vec{\nabla} \cdot \vec{F}(\vec{r}_0, t_0)\, g(\vec{r}, t | \vec{r}_0, t_0)\, dV_0$$

$$+ \int dt_0 \int_{V_0} (\vec{\nabla}_0 \cdot \mathfrak{T} \cdot \vec{\nabla})\, g(\vec{r}, t | \vec{r}_0, t_0)\, dV_0 \qquad (3.3.27)$$

Now the components of $\nabla \cdot \mathfrak{T} \cdot \nabla$ in rectangular coordinates are:

$$\vec{\nabla} \cdot \vec{\vec{\mathfrak{T}}} \cdot \vec{\nabla} \equiv \left(\hat{i} \frac{\partial}{\partial x} + \hat{j} \frac{\partial}{\partial y} + \hat{k} \frac{\partial}{\partial z} \right) \cdot \left\{ \hat{i} \left(\frac{\partial T_{xx}}{\partial x} + \frac{\partial T_{yx}}{\partial y} + \frac{\partial T_{zx}}{\partial z} \right) \right.$$

$$+ \hat{j} \left(\frac{\partial T_{yx}}{\partial x} + \frac{\partial T_{yy}}{\partial y} + \frac{\partial T_{yz}}{\partial z} \right)$$

$$\left. + \hat{k} \left(\frac{\partial T_{zx}}{\partial x} + \frac{\partial T_{zy}}{\partial y} + \frac{\partial T_{zz}}{\partial z} \right) \right\}$$

$$= \frac{\partial^2 T_{xx}}{\partial x^2} + \frac{\partial^2 T_{xy}}{\partial x \partial_y} + \ldots$$

Upon two successive integration by parts,

$$\int_{V_0} g(\nabla \cdot \mathfrak{T} \cdot \nabla)\, dV_0 = g(\nabla \cdot \mathfrak{T})\Big|_{V_1}^{V_2} - \int \nabla g \cdot \mathfrak{T} \cdot \nabla$$

$$- \int \nabla g \cdot \mathfrak{T} \cdot \nabla = -\nabla g \cdot \mathfrak{T}\Big|_{V_1}^{V_2} + \int \nabla g \nabla : \mathfrak{T}$$

Since both $\nabla \cdot \mathfrak{T}$ and $\mathfrak{T}$ are zero outside of the source volume both first terms of integration vanish and the alternative of 3.3.27, corresponding to 3.3.25 becomes,

$$p(\vec{r}, t) = \int dt_0 \int_{V_0} \vec{F} \cdot \nabla_0 g\, dV_0 + \int dt_0 \int_{V_0} \nabla_0 g \nabla_0 : \mathfrak{T}\, dV_0 \qquad (3.3.28)$$

The meaning of the second term is elucidated by expansion in rectangular coordinates:

$$\nabla g \nabla : \mathfrak{T} = \left(\hat{i} \frac{\partial}{\partial x} + \hat{j} \frac{\partial}{\partial y} + \hat{k} \frac{\partial}{\partial z} \right) g \quad \left(\hat{i} \frac{\partial}{\partial x} + \hat{j} \frac{\partial}{\partial y} + \hat{k} \frac{\partial}{\partial z} \right) : (\hat{i}\hat{i} T_{xx} + \hat{i}\hat{j} T_{xy} + \ldots)$$

$$\nabla g \nabla : \mathfrak{T} = \left(\hat{i}\hat{i} \frac{\partial^2 g}{\partial x^2} + \hat{i}\hat{j} \frac{\partial^2 g}{\partial x \partial y} + \ldots \right) : \quad (\hat{i}\hat{i} T_{xx} + \hat{i}\hat{j} T_{xy} + \ldots$$

$$\nabla g \nabla : \mathfrak{T} = \left(\frac{\partial^2 g}{\partial x^2} \right) T_{xx} + \left(\frac{\partial^2 g}{\partial x \partial y} \right) T_{xy} + \ldots$$

3.3.28 and 3.3.23 give the acoustic pressure radiated by sources 1.8.3 provided the medium is unbounded, that is there are no reflecting surfaces. When sources radiate into confined spaces the Green's functions must be changed to include the reflected fields as well as the direct fields, 1.7.7. In the following sections we treat of radiation into confined spaces.

3.4 1-D GREEN'S FUNCTIONS OF THE STURM-LIOUVILLE EQUATION; AND 2-D, 3-D GREEN'S FUNCTIONS

In Sect. 1.9 the solution of the Sturm-Liouville equation 1.9.1 subject to boundary conditions 1.9.2 was obtained in modal form 1.9.3 or continuum form 1.9.4. Any reasonable field variable $F(\xi)$ could then be represented as a sum of eigenfunctions (or modes):

$$\text{(a)} \quad F(\xi) = \sum_m F_m \psi_m(\xi) \qquad \text{(b)} \quad F_m = N_m^{-1} \int r(y)\, F(\xi)\, \psi_m(\xi)\, d\xi \tag{3.4.1}$$

In particular a point source with spatial dependence $F(\xi) = \delta(\xi - \xi_0)$, is represented by

$$\delta(\xi - \xi_0) = r(\xi_0) \sum_m \psi_m(\xi)\, \psi_m^*(\xi_0) \qquad \xi_1 < \xi < \xi_2, \tag{3.4.2}$$

in which $r(\xi_0)$ is the weight function:

Here we have suppressed the normalization N_m^{-1} by rescaling each ψ_m with $N_m^{-1/2}$ so that ψ_m becomes orthonormal. The modes ψ_m are the eigenfunctions of the operator $H(\xi)$, defined by the relation.

$$H(\xi)\, \psi_m(\xi) = -\lambda_m\, r(\xi)\, \psi_m(\xi) \tag{3.4.3}$$

$$H(\xi) \equiv \frac{d}{d\xi} \left[p(\xi) \frac{d}{d\xi} \right] + q(\xi)$$

Now let the field Ψ in 1.9.1 be generated by a point source. It then is the Green's function $g(\xi, \xi_0; \lambda)$

$$[H(\xi) + \lambda r(\xi)]\, g(\xi, \xi_0; \lambda) = -4\pi\delta(\xi - \xi_0) \tag{3.4.4}$$

This can be solved by expansion of both g and the delta function in modes:

$$\sum_m [H(\xi) + \lambda(r(\xi))]\, g_m(\xi_0, \lambda)\, \psi_m(\xi) = -4\pi r(\xi_0) \sum_m \psi_m(\xi)\, \psi_m^*(\xi_0)$$

Applying 3.4.3 to each mode and equating left and right terms for each m lead to,

$$g_m(\xi_0, \lambda) = -\frac{4\pi\, \psi_m^*(\xi_0)}{\lambda - \lambda_m}$$

[1]. Thus,

$$\text{(a)} \qquad g(\xi, \xi_0; \lambda) = -4\pi \sum_m \frac{\psi_m(\xi)\, \psi_m^*(\xi_0)}{\lambda - \lambda_m} \tag{3.4.5}$$

When applied to the Helmholtz equation in a homogeneous isotropic medium of an enclosure one sets $\lambda = k^2$, $\lambda_m = k_m^2$, and ξ is made a vector:

$$\text{(b)} \qquad G_k(\vec{r}\,|\,\vec{r}_0) = -4\pi \sum \frac{\psi_m(\vec{r})\, \psi_m^*(r_0)}{k^2 - k_m^2}$$

In a theoretical application of this result it will be advantageous to consider λ to be a complex variable $\lambda = \mathrm{Re}\,\lambda + i\ \mathrm{Im}\lambda$, and use 3.4.5 to obtain a representation of delta function 3.4.2 as a contour integral in the complex λ plane. Thus, if counterclockwise contour C is selected so as to enclose all the singularities of g, then

$$\frac{1}{2\pi i} \oint_C g(\xi, \xi_0; \lambda)\, d\lambda = -4\pi \sum_m \psi_m(\xi)\, \psi_m^*(\xi_0)\, \frac{1}{2\pi i} \oint_C \frac{d\lambda}{\lambda - \lambda_m}$$

By Cauchy's theory of residues, for each m one has,

$$\frac{1}{2\pi i} \oint_C \frac{d\lambda}{\lambda - \lambda_m} = 1$$

Hence, using 3.4.2,

$$-\frac{1}{2\pi i} \oint_C g(\xi, \xi_0; \lambda)\, d\lambda = 4\pi\, \frac{\delta(\xi - \xi_0)}{r(\xi_0)}\,. \tag{3.4.6}$$

[2].
This is the desired representation. In it the weight function $r(\xi_0)$ appears explicitly. It is useful to absorb it into the definition of ψ_m so that 3.4.2 becomes

$$\delta(\xi - \xi_0) = \sum_m \psi_m(\xi)\, \psi_m(\xi_0) \tag{3.4.7}$$

This representation will find considerable use in further development of the properties of 2-D and 3-D Green's functions which we consider next.

Acoustic fields with complex space-time dependence can be represented as sums of fields with simpler space-time dependence. The most useful representations are listed below:

(a) plane waves in $\vec{k}$, ω space: $\vec{\Psi}(\vec{r}, t) = \int \vec{\Psi}(\vec{k}, \omega) e^{i(\vec{k}\cdot\vec{r} - \omega t)}\, \frac{d\vec{k}\, d\omega}{(2\pi)^4}$

(b) modes in $\vec{k}$ - space "guided" (that is, oscillatory) in time:

$$\vec{\Psi}(\vec{r}, t) = \int \sum_m a_m(\vec{k}, t)\vec{\Psi}_m(\vec{k})\, e^{i\vec{k}\cdot\vec{r}} \frac{d\vec{k}}{(2\pi)^3} \tag{3.4.8}$$

(c) modes in transverse $\vec{k}_t - \omega$ space guided along the axial (z) direction:

$$\vec{\Psi}(\vec{\varrho}, t; z) = \int \sum_m a_m(\vec{k}_t, \omega; z)\vec{\Psi}_m(\vec{k}_t, \omega) \times e^{i(\vec{k}_t\cdot\vec{\varrho} - \omega t)} \frac{d\vec{k}_t d\omega}{(2\pi)^3}$$

[3].

Since we shall be concerned in this section with radiation into confined spaces (waveguides) we shall consider the representation 3.4.8C in greater detail. This equation is interpreted in the context of Fig. 3.4.1 which shows free space $A(x,y,z)$ and waveguide space $B(x,y,z)$. In A the transverse field is taken as unbounded. It can be represented as a sum of expanding plane waves,

$$\vec{\Psi}(\vec{k}_t, \vec{\varrho}; \omega, t) = \vec{\Psi}(k_t, \omega)\, e^{i(\vec{k}_t\cdot\vec{\varrho} - \omega t)} \tag{3.4.9}$$

in which $\vec{\Psi}$ is the acoustic wavefield vector, whose components are pressure and particle velocity,

$$\vec{\Psi} = \begin{pmatrix} p(k_t, \omega) \\ V(k_t, \omega) \end{pmatrix} \tag{3.4.10}$$

If the axial field is also unbounded it can be represented as continuum complex sinusoids $\exp(ik_z z)$ in which k_z is the propagation constant in the z-direction. The total field is therefore representable as a sum of elementary waves,

$$\vec{\Psi}(\vec{\varrho}, t; z) = \int \vec{\Psi}(k_t, \omega)\, e^{i(\vec{k}_t\cdot\vec{\varrho} - \omega t)}\, e^{ik_z z} \frac{d\vec{k}_t d\omega}{(2\pi)^3} \tag{3.4.11}$$

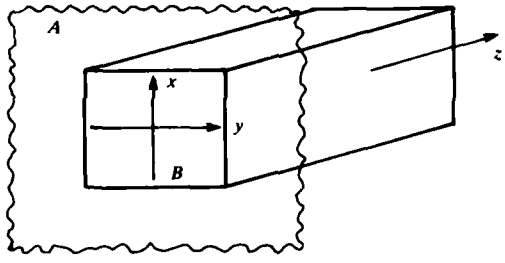

Fig. 3.4.1. Geometry of z-guided acoustic wave fields.

Because the axial field is coupled to the transverse field the axial wavenumber k_z is a function of the transverse wavenumber and frequency $k_z = k_z(k_t, \omega)$. The question arises: for every k_t, ω how many discrete k_α, $\alpha = 1, 2 \ldots$ satisfy the source-free field equations,

$$\mathfrak{L}\vec{\Psi}(\vec{\varrho}, t; z) = \mathfrak{L}\begin{pmatrix} p \\ V \end{pmatrix} = 0 \tag{3.4.12}$$

in which $\mathfrak{L}$, is defined by 3.3.7 and 3.3.8 for the conditions $\mathfrak{Q}$, $\vec{f}$ are zero, and the z-dependence is exp $ik_z z$? Writing $\vec{\nabla} = \vec{\nabla}_t + \partial/\partial z\, \vec{z}_0$, $\vec{v} = \vec{v}_t + v_z \vec{z}_0$, it is seen that for $\nabla_t = ik_t$, $\partial/\partial t = i\omega$, 3.4.12 becomes

$$-i \begin{Bmatrix} \dfrac{\omega}{P_0} & (-\vec{k}_t - k_a\vec{z}_0)\cdot \\ (-\vec{k}_t - k_a\vec{z}_0)\cdot & \omega\varrho_0 \end{Bmatrix} \begin{pmatrix} p \\ \vec{V} \end{pmatrix} = 0 \tag{3.4.13}$$

This is satisfied for k_a such that det $\mathfrak{L} = 0$, namely,

$$k_a = \pm\sqrt{(\omega^2/c^2) - k_t^2} \tag{3.4.14}$$

Thus only for these two values of k_a is $\Psi(\vec{r},t;z)$ other than zero. These correspond to waves $\Psi_a = \begin{pmatrix} p_a \\ \vec{v}_a \end{pmatrix}$ traveling in direction $z > 0$ for which the + sign is valid, and waves traveling in the direction $z < 0$ for which the − sign is valid. To find Ψ_a we first eliminate $\vec{v}$ from 3.3.7 and 3.3.8 and obtain (for $\mathfrak{Q}$, f both zero)

$$\nabla_p^2 - \frac{1}{c^2}\frac{\partial_p^2}{\partial t^2} = 0 \tag{3.4.15}$$

$$c^2 = P_0/\varrho_0$$

In $\vec{k}_t$, ω space, for $p_a = p_a(k_t, \omega)$, this equation gives a relation for p_a,

$$\left[k_a^2 - \left(\frac{\omega^2}{c^2} - k_t^2\right)\right] p_a = 0 \tag{3.4.16}$$

Since the quantity in parenthesis vanishes we can take p_a to be any constant other than zero. For convenience let $p_a = 1$. In a similar way for the case $\vec{f} = 0$ if 3.3.8,

$$\vec{\nabla}_t p + \varrho_0 \frac{\partial \vec{V}}{\partial t} = -ikp\vec{z}_0$$

is transformed into $\vec{k}_t - \omega$ space, it reduces to a pair of equations, one intransverse space,

$$i\vec{k}_t p - i\omega\varrho_0 \vec{V}_t = 0, \text{ or } \vec{V}_t = \frac{\vec{k}_t p}{\varrho_0\omega};$$

and one in z-space,

$$-i\omega\varrho_0 v_z\vec{z}_0 = -ik_a p\vec{z}_0, \text{ or } v_z = \frac{k_a p}{\varrho_0\omega}.$$

Thus, for the choice $p = 1$,

$$V_a = \frac{\vec{k}_t + k_a\vec{z}_0}{\varrho_0\omega}$$

and the appropriate $\vec{\Psi}_\alpha$ is,

$$\vec{\Psi}_\alpha = \begin{pmatrix} 1 \\ \dfrac{\vec{k}_t + k_\alpha \vec{z}_0}{\varrho_0} \end{pmatrix}, \alpha = \pm 1 \tag{3.4.17}$$

$\vec{\Psi}_\alpha$ is an eigenfunction in the form of a column matrix. To determine its normalization we note that 3.4.13 can be written as a characteristic equation,

$$H_\alpha \vec{\Psi}_\alpha = \lambda_\alpha \vec{\Psi}_\alpha$$

$$\lambda_\alpha = k_\alpha \begin{pmatrix} 0 & \vec{z}_0 \\ \vec{z}_0 & 0 \end{pmatrix} = k_\alpha \Gamma$$

The normalization is then:

$$N = \left(\vec{I}_\alpha, \begin{pmatrix} 0 & \vec{z}_0 \\ \vec{z}_0 & 0 \end{pmatrix}^+ \vec{\Psi}_\alpha^+ \right) = \frac{2k_\alpha}{\varrho_0 \omega}, \alpha = +1, -1 \tag{3.4.18}$$

in which the entity (,) is the inner (or dot) product described below, and $d\Psi_\alpha^+$ is the adjoint field. The adjoint field, by definition, satisfies field equations in which the operators $\partial/\partial t$ and $\vec{\nabla}$ are transformed to $-\partial/\partial t$, $-\vec{\nabla}$ respectively.

The eigenfunctions Ψ_α constitute a complete set in α-space. Any function in $\vec{k}_t, \omega$ space can be expanded in it. In particular the Green's function for z-guided waves, whose form is,

$$G(\vec{r}, t | \vec{r}', t') = \int G(\vec{k}_t, \omega; z, z') e^{i\vec{k}_t \cdot (\vec{\varrho} - \vec{\varrho}')} e^{-i\omega(t-t')} d\vec{k}_t d\omega \tag{3.4.19}$$

may be so expanded as follows:

$$\vec{G} = \sum_\alpha a(\vec{k}_t, \omega; z, z') \Psi_\alpha(\vec{k}_t, \omega)$$

Taking the inner product of both sides with $\Gamma^+ \vec{\Psi}_\beta^+$, and using the orthogonal property 3.4.18 lead to an explicit form for expansion coefficient A. Then,

$$G(\vec{k}_t, \omega; z, z') = \sum_m \frac{\vec{I}_\alpha(\vec{k}_t, \omega)}{N_\alpha} (G, \Gamma^+ \vec{\psi}_\alpha^+) \tag{3.4.20}$$

In this context the sum has only two terms, $\alpha = \pm 1$. In each term the inner product, which in this case is simply the dot product of the adjoint field represented by a column vector $\Gamma^+ \Psi_\alpha^+$ with a second column $\vec{G}$, may be written as ψ_+^α with a second column vector $\vec{G}$, may be written as $\Psi_\alpha^+ G_\alpha$ where G_α is the scaler 1-dimensional Green's function in z. Here, the dot (or scalar) product of two vector functions $f(x) = \{f_0(x), f_1(x)\}$ and $g = \{g_0(x), g_1(x)\}$ is defined as

$$(f, g) = \int_\Gamma [k^2 f_0(x)\, g_0^*(x) + f_1(x)\, g_1^*(x)]\, d\sigma_\Gamma = (f_0, g_0)_{L_2(\Gamma)} + (f_1, g_1)_{L_2(\Gamma)}$$

It is governed by a 1st order differential equation derivable in the following way: by definition an operator $\mathfrak{L}$ has an associated Green's function G if $\mathfrak{L}\, G = 1$. In the case of a linear acoustic field, the appropriate operator is obtain from the left hand sides of 3.3.7 and 3.3.8, which for z-guided waves becomes,

$$\mathfrak{L} \rightarrow \begin{pmatrix} \dfrac{1}{P_0}\dfrac{\partial}{\partial t} & \vec{\nabla}_t + \dfrac{\partial}{\partial z}\vec{z}_0 \\ \vec{\nabla}_t + \dfrac{\partial}{\partial z}\vec{z}_0 & \varrho_0 \dfrac{\partial}{\partial t} \end{pmatrix} \tag{3.4.21}$$

Thus $G(\vec{\varrho}, z, t|\vec{\varrho}', z', t')$ is governed by the 3-D relation,

$$\mathfrak{L}\, G = \vec{\vec{1}}\,\delta(\vec{\varrho} - \vec{\varrho}')\,\delta(z - z')\,\delta(t - t') \tag{3.4.22}$$

When the expansion of G in $\vec{k}_t - \omega$ space 3.4.19 in substituted into 3.4.22 it is immediately seen that the equation governing the 1-D Green's function, here identifiable as G_a is,

$$\left[\frac{d}{dz} - ik_a(\vec{k}_t, \omega)\right] G_a(\vec{k}_t, \omega; z, z') = \delta(z - z') \tag{3.4.23}$$

Since G_a is a physical wave field it must vanish at great distances from the source which generates it,

$$\lim G_a \rightarrow 0 \text{ as } |z - z'| \rightarrow \infty \tag{3.4.24}$$

This can occur only if $\operatorname{Im} k_a \neq 0$. Now $\delta(z - z')$ is a unit source which generates waves in the positive and negative z-directions simultaneously. It thus describes a discontinuity in wave field which must be shared by G. This is seen by first allowing z to be greater than z'. Then, symbolically, $\delta(z - z')$ vanishes and the solution of 3.4.24 together with 3.4.14 is,

$$G_{+1} \propto e^{+i(z-z')\sqrt{\left[\frac{\omega}{c}\right]^2 - k_t^2}} = e^{ik_{+1}(z-z')},\ z > z' \tag{3.4.25}$$

$$\operatorname{Im} k_{+1} > 0$$

Similarly, when $z < z'$ the waves travel in the negative direction and for time given by $\exp -i\omega t$ G must have the form

$$G \propto e^{-i(z-z')\sqrt{\left[\frac{\omega}{c}\right]^2 - k_t^2}} = e^{ik_{-1}(z-z')},\ z < z' \tag{3.4.26}$$

$$\operatorname{Im} k_{-1} < 0$$

Thus the z-derivative across the source at z' undergoes a discontinuity of unit magnitude and negative sign. This discontinuity is a characteristic property of Green's functions in general.

By combining 3.4.19, 3.4.20, 3.4.25, 3.4.26 the dyadic representation of the Green's function for z-guided waves is,

$$G(\vec{r}, t|\vec{r}', t') = |G_{ij}| = \begin{pmatrix} G_{11} & G_{12} \\ G_{21} & G_{22} \end{pmatrix} = \int \sum_{a} \frac{\vec{\Psi}_a(\vec{k}_t, \omega)\, \vec{\Psi}_a^*(k_t, \omega)}{N_a(\vec{k}_t, \omega)} e^{i[\vec{k}_t \cdot \vec{\varrho}' - \omega(t-t')]} \times e^{ik_a(z-z')} \frac{d\vec{k}_t d\omega}{(2\pi)^3} \tag{3.4.27}$$

in which the subscriptive $i\,j$ refers (schematically) to the components of Ψ_a:

$$(I_a)_{ij} = \begin{pmatrix} i \\ j \end{pmatrix};\ \text{(a)}\quad \vec{\Psi}_{a1}\vec{\Psi}_{a1} = (\vec{1})\ (\vec{1})$$

$$\text{(b)}\quad \vec{\Psi}_{a1}\vec{\Psi}_{a2} = (\vec{1}) \left(\frac{\vec{k}_t + k_{+1}\vec{z}_0}{\varrho_0 \omega} \right) \tag{3.4.28}$$

$$\text{(c)}\quad \vec{\Psi}_{a2}\vec{\Psi}_{a1} = \left(\frac{\vec{k}_t + k_{+1}\vec{z}_0}{\varrho_0 \omega} \right) (\vec{1})$$

$$\text{(d)}\quad \vec{\Psi}_{a2}\vec{\Psi}_{a2} = (\vec{k}_t + k_{-1}\vec{z}_0)\,(\vec{k}_t + k_{-1}\vec{z}_0)$$

Since 3.4.18 gives the value of N_a, the explicit formula for the Green's function G_{p2} in the form of z-guided waves defined by 3.3.21 in a transverse unbounded, homogeneous stationary medium is,

$$G_{p2}(\vec{r}, t|\vec{r}', t') = \int \frac{1}{\left(\frac{2\sqrt{\frac{\omega^2}{c^2} - k_t^2}}{\varrho_0 \omega} \right)} e^{i\vec{k}_t \cdot [\vec{\varrho} - \vec{\varrho}'] - i\omega(t-t')}\, e^{\pm i(z-z')\sqrt{\left|\frac{\omega}{c}\right|^2 - k_t^2}} \frac{d\vec{k}_t d\omega}{(2\pi)^3} \tag{3.4.29}$$

in which the + sign is valid for $a > z'$, and the - sign for $z < z'$.

This completes the formulation of 3-D Green's functions in $\vec{\varrho}$, z space for the case where the transverse field (in $\vec{\varrho}$) is unbounded. We now turn to the case where the transverse field is bounded.

In B, Fig. 3.4.1 a bounded field, say a 2-D point source, can be expanded (formally) in 2-D eigenfunction $\Phi(\vec{\varrho})$, here taken to form a complete set:

$$\delta(\vec{\varrho} - \vec{\varrho}') = \sum_i \vec{\Phi}_i(\vec{\varrho})\, \vec{\Phi}_i^*(\vec{\varrho}') \tag{3.4.30}$$

In many applications $\Phi(\vec{\varrho})$ is separable into products of 1-D eigenfunctions $\Phi(u)\,\Phi(v)$ which are also assumed to form complete sets in curvelinear coordinates u, v:

$$\text{(a)}\quad \delta(u - u') = h_u \sum_i \Phi_i(u)\,\Phi_i^*(u'), \qquad \text{(b)}\quad \delta(v - v') = h_v \sum \Phi_i(v)\,\Phi_i^*(v') \tag{3.4.31}$$

The symbols h_u, h_v are scale factors for curvelinear coordinates u, v, defined by an element of area $dS = h_u u\, h_v v$. It was shown in 3.4.6 that each such series can be represented as the result of a contour integration of a 1-D Green's function in the complex λ-plane:

$$\sum_p \Phi_p(u)\,\Phi_p^*(u') = \frac{\delta(u-u')}{h_u} = -\frac{1}{2\pi i}\int_{c_u} g_u(u, u';\lambda_u)\,d\lambda_u$$

$$\sum_q \Phi_q(v)\,\Phi_q^*(v') = \frac{\delta(v-v')}{h_v} = -\frac{1}{2\pi i}\int_{c_v} g_v(v, v';\lambda_v)\,d\lambda v \qquad (3.4.32)$$

$$\sum_s \Phi_s(z)\,\Phi_s^*(z') = \frac{\delta(z-z')}{h_z} = -\frac{1}{2\pi i}\int_{c_z} g_z(z, z';\lambda_z)\,d\lambda_z$$

The contour C_u encloses only the singularities of g_u, and the contour C_v only those of g_v. In the transverse-axial system discussed here the 3-D Green's function is simply the product of the 2-D function and the Green's function $g_z(z, z';\lambda_z)$ for the axial component. Since the axial field is coupled to the transverse field one has in general $\lambda_z = \lambda_z(\lambda_u, \lambda_v)$. Thus the 3-D Green's function is representable as a sequence of contour integrations:

$$G(\vec{r}|\vec{r}') = \left(\frac{1}{-2\pi i}\right)^2 \int_{c_u}\int_{c_v} g_u(u, u';\lambda_u)\,g_v(v, v';\lambda_v)\,g_z(z, z';\lambda_z)\,d\lambda_u\,d\lambda_v. \qquad (3.4.33)$$

in which C_u, C_v have already been defined.

Assume next that in waveguide propagation in the z-coordinate the waveguide is bounded between z_1, z_2. Then λ_z takes on discrete values, λ_{zi}, in which the subscript i means the ith eigenvalue correspond to the ith transverse mode $\Phi_i(\vec{Q})$. The 3-D Green's function is

$$G(\vec{r}|\vec{r}') = \sum_i \Phi_i(\vec{Q})\,\Phi_i^*(\vec{Q}')\; g_z(z, z';\lambda_{zi}) \qquad (3.4.34)$$

This case is sketched in Fig. 3.4.2. A second case is a field consisting of transverse waves in plane vz guided along the u-direction. One can evaluate this case by deforming the contour C_u away from the singularities of g_u in the λ_u plane into contour C_u' which encloses the singularities of g_z in the same plane. Then,

$$\int_{C_u} g_z(z, z';\lambda_z)\,d\lambda_u = \sum_j \Phi_j(z)\,\Phi_j^*(z)$$

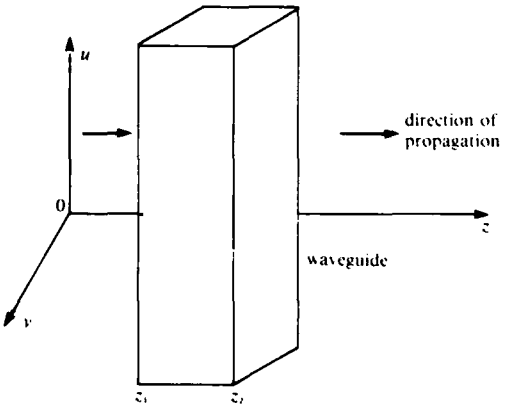

Fig. 3.4.2. Finite length waveguide.

Thus the 3-D Green's function 3.4.33 is evaluated to be,

$$G(\vec{r}|\vec{r}') = \sum_i \Phi_i(v)\,\Phi_i^*(v') \sum_j \Phi_j(z)\,\Phi_j^*(z')\; g_u(u, u'; \lambda_{uij}) \tag{3.4.35}$$

in which λ_{uij} is the discrete eigenvalue corresponding to the ij transverse mode (in plane vz) and $g_u(u, u'; \lambda_{uij})$ is the 1-D Green's function in the u-coordinate. In a similar way transverse waves in the uz plane guided along v can form a basis for representing a 3-D Green's function. This case is handled by deforming the contour C_v in the λ_v plane away from the singularities of g_v into contour C_v' enclosing the singularities of g_v in the same plane. The result is 3.4.35 again, this time with v, v' replaced by u, u' respectively, and λ_{uij} replaced by λ_{vij}.

3.5 CHARACTERISTIC GREEN'S FUNCTIONS $g(\xi, \xi'; \lambda)$ [4]

In the derivation of 3.4.5, 3.4.6 it was shown that the completeness relation of 1-D eigenfunctions $\Phi(\xi)$ is,

$$\delta(\xi - \xi') = \sum_i \Phi_i(\xi)\,\Phi_i^*(\xi') \tag{3.5.1}$$

in which index i is the index of eigenvalues associated with $\Phi(\xi)$. When the space of $\Phi(\xi)$ is bounded, index i is discrete; but when it is unbounded index i is continuous, and the sum 3.5.1 is replaced by an integral. For the case of discrete eigenvalues the property of orthogonality over interval Δ of ξ is

$$\int_\Delta \Phi_i(\xi)\,\Phi_j(\xi)\,d\xi = \delta_{ij} = \begin{matrix} 1 & i = j \\ 0 & i \neq j \end{matrix} \tag{3.5.2}$$

while for the case of continuous eigenvalues η orthogonality is expressed as an integral,

$$\int \Phi(\xi; \eta)\,\Phi(\xi, \eta)\,d\xi' = \delta(\eta - \eta') \tag{3.5.2}$$

Now 3.4.6 expresses a relation between the delta function 3.5.1 and the 1-D characteristic Green's function $g(\xi, \xi'; \lambda)$. The construction of g is therefore important, particularly in view of 3.4.33. To find g we consider two solutions $\psi_{1,2}(\xi)$ of the Sturm-Liouville equation 1.9.1: $\psi_1(\xi)$ valid for waves traveling in the negative ξ direction, and the second $\psi_2(\xi)$ traveling in the positive ξ direction. These solution satisfy boundary conditions 1.9.2. The characteristic g, being of function over *all*, is therefore a function of both solutions,

$$g(\xi, \xi'; \lambda) = A\psi_1(\xi_<)\,\psi_2(\xi_>) = A\psi_1(\xi)\,\psi_2(\xi'),\ \xi < \xi'$$

$$g(\xi, \xi'; \lambda) = A\psi_1(\xi_<)\,\psi_2(\xi_>) = A\psi_1(\xi')\,\psi_2(\xi),\ \xi > \xi' \tag{3.5.3}$$

in which subscript symbols $<$ and $>$ express the two forms on the right-hand-side. The constant A must be determined so as to satisfy the jump condition for Green's functions,

$$A\left\{p(\xi')\left[\psi_1(\xi)\frac{d}{d\xi}\psi_2 - \frac{d}{d\xi}\psi_1(\xi)\,\psi_2\xi\right]\right\}_{\xi=\xi} = -1$$

from which

$$A = \left(\frac{-1}{pW(\psi_1, \psi_2)}\right)_{\xi=\xi} \tag{3.5.4}$$

where $W(\psi_1, \psi_2)$ is the Wronskian of solutions ψ_1, ψ_2. Thus, in general, the 1-D characteristic Green's function is:

$$g(\xi, \xi'; \lambda) = \frac{\psi_1(\xi_<)\,\psi_2(\xi_>)}{[-pW(\psi_1, \psi_2)]_{\xi=\xi}} \tag{3.5.5}$$

It is understood that $\psi(\xi)$ means $\psi(\xi, \lambda)$. This form repeated three times makes up the integrand of 3.4.33.

3.6 ACOUSTIC RADIATION INTO WAVEGUIDES I

In Sect. 3.4 the calculation of acoustic fields by use of Green's functions was seen to lead in a natural way to a representation of delta sources as contour integrals, 3.4.32. We now take up the problem of calculating the radiation of such sources into waveguides. This problem can be approached by first defining *angular, radial* and *axial* transmission. Characteristic functions play an important role in the theory of open and closed waveguides. In *angular transmission*, Fig. 3.6.1, a (line) source at ϱ', ϕ', creates a field which is described by the characteristic Green's function g_ϕ, governed by the equation,

$$\left(\frac{d^2}{d\phi^2} + \lambda\right) g_\phi(\phi, \phi'; \lambda) = -\delta(\phi - \phi') \tag{3.6.1}$$

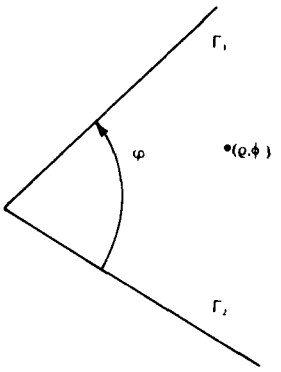

Fig. 3.6.1. Angular transmission in a wedge waveguide.

For walls with reflection coefficients Γ_1, Γ_2 respectively,

$$g_\phi(\phi, \phi'; \lambda) = \frac{(e^{-i\mu\phi_<} + \Gamma_1 e^{+i\mu\phi_<})(e^{-i\mu(\varphi-\phi_>)} + \Gamma_2 e^{i\mu(\varphi-\phi_>)})}{-2i\mu(e^{-i\mu\varphi} - \Gamma_1\Gamma_2 e^{+i\mu\varphi})} \tag{3.6.2}$$

where $\mu = \sqrt{\lambda}$

If the walls are pressure release we take $\Gamma_1 = \Gamma_2 = -1$ and find,

$$g_\phi(\phi, \phi'; \lambda) = \frac{\sin\mu\phi_<\,\sin\mu(\varphi - \phi_>)}{\mu\,\sin\mu\varphi} \tag{3.6.3}$$

If the walls are rigid, take $\Gamma_1 = \Gamma_2 = 1$; then

$$g_\phi(\phi, \phi'; \lambda) = \frac{\cos \mu\phi_< \cos \mu(\varphi - \phi_>)}{-\mu \sin \mu\varphi} \tag{3.6.4}$$

If φ is 2π there are no walls. Then

$$g_\phi(\phi, \phi'; \lambda) = -\frac{\cos \mu[\pi - |\phi - \phi'|]}{2\mu \sin \mu\pi} \tag{3.6.5}$$

[5].

In *radial transmission* Fig. 3.6.2 the parameters in the Sturm-Liouville equation 1.9.1 have the form, $p(\xi) \to \varrho$, $q(\xi) \to \tau\varrho$, $\lambda r(\xi) \to -\lambda/\varrho$. The characteristic Green's function then satisfies the equation,

$$\left(\frac{d}{d\varrho}\,\varrho\,\frac{d}{d\varrho} + \tau\varrho - \lambda/\varrho\right) g_\varrho(\varrho, \varrho'; \tau, \lambda) = -\delta(\varrho - \varrho') \tag{3.6.6}$$

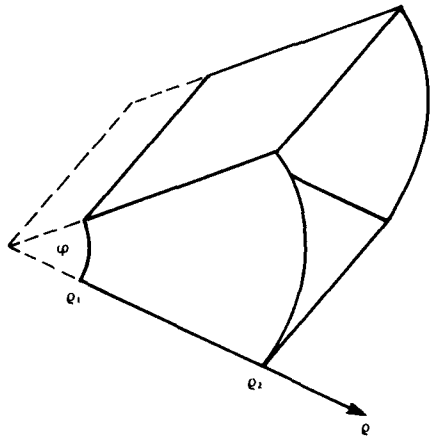

Fig. 3.6.2. Radial transmission in a wedge waveguide.

When the waveguide is unbounded in the radial domain one has $0 < \frac{\varrho}{\varrho_1} < \infty$, and

$$g_\varrho(\varrho, \varrho'; \tau, \lambda) = \frac{\pi i}{2} J_\nu(\sqrt{\tau}\varrho_<) H_\nu^{(1)}(\sqrt{\tau}\varrho_>), \nu = \sqrt{\lambda} \tag{3.6.7}$$

in which J_ν, H_ν are Bessel and Hankel functions respectively. Here, for convergence at $\varrho \to \infty$ it is required that Im $\sqrt{\tau} > 0$ provided time is given by exp$-i\omega t$.

In *axial transmission* the characteristic Green's function is $g_z(z, z'; \lambda)$. A discussion of its form is given in Section 3.4.

SOURCE DESCRIPTION

Acoustic radiation into a waveguide is eminently describable by the theory of mode functions. Let there be first a point source $4\pi\,\delta(\vec{r} - \vec{r}_0)$, with harmonic time-dependence exp$(-i\omega t)$ located at $\vec{r}_0$ inside the waveguide, or on its walls. The linear small amplitude field $G(\vec{r}, \vec{r}_0)$ at $\vec{r}$ then satisfies 1.7.4 in the steady state

$$(\nabla^2 + k^2)\, G(\vec{r}|\vec{r}_0) = -4\pi\delta(\vec{r} - \vec{r}_0),\ \vec{r} = (\xi_1, \xi_2, \xi_3) \tag{3.6.8}$$

(Helmholtz's equation). A natural representation of $\vec{r}$ in this waveguide is vector with two components, transverse $\vec{\varrho} = (\xi_1, \xi_2)$ and axial $z = \xi_3$. In this coordinate system the Laplace operator also

has transverse and axial components, $\nabla^2 = \nabla_t^2 + \partial^2/\partial z^2$. Such decomposition allows the field to be expressed as a product of a transverse field $\Phi(\vec{\varrho}, \omega)$ and an axial field $Z(z, \omega)$. The transverse field at any cross section $z' =$ Const., created by a point source at $\vec{\varrho}'$, z' is governed by the equations:

$$(\nabla_t^2 + k_t^2)\,\Phi(\vec{\varrho}, \omega) = -4\pi\delta(\vec{\varrho} - \vec{\varrho}') \quad k_t^2 = k^2 - k_z^2 \tag{3.6.9}$$

At the walls of the waveguide the field satisfies boundary conditions of the form

$$\alpha\Phi + \beta\,\frac{\partial\Phi}{\partial n} = 0 \tag{3.6.10}$$

in which α, β are constants, or general functions of frequency, and $\partial/\partial n$ is the normal derivative. Upon choosing *particular* values ot α, β one may reduce 3.6.9 to homogeneous form (no delta sources present), and obtain solutions in terms of orthogonal modes $\Phi_i(\vec{\varrho}, \omega)$ $i = 1, 2 \ldots$, which satify both 3.6.9 and 3.6.10. Orthogonality is defined by the integral,

$$\int_\Delta w(\vec{\varrho})\,\Phi_i(\vec{\varrho})\,\Phi_j(\vec{\varrho})\,d\vec{\varrho} = \delta_{ij} \tag{3.6.11}$$

The symbol $w(\varrho)$ is a weighting function, generally the scale factor h of curvilinear coordinates (see 3.4.31) and the symbol Δ represents the interval of orthogonality, in this case the separation distance of the walls. The set of $\Phi_i(\vec{\varrho})$ is infinite in number and is complete, meaning that it can be used to represent the 2-D point source in 3.6.8. By using 3.6.11 it is easily seen that,

$$\delta(\vec{\varrho} - \vec{\varrho}') = w(\varrho') \sum_i \Phi_i(\vec{\varrho})\,\Phi_i^*(\vec{\varrho}') \tag{3.6.12}$$

In numerical work one can assign the units of $\sqrt{W(\varrho')}\ \Phi_i(\vec{\varrho})$ to be meter^{-1}.

With 3.6.8 through 3.6.12 in mind we turn to various simple-shaped waveguides and list the appropriate description of 2-D sources in the plane $z =$ const. In each case we consider two types of boundary conditions at the walls. In the first we set $\alpha = 0$ in 3.6.10: this condition states that $\partial\phi/\partial_n = 0$, which, because Φ represents acoustic velocity potential, means the wall is rigid. The characteristic functions (eigenfunctions) are given the special symbol $\psi_i(\vec{\varrho})$. In the second we set $\beta = 0$: then Φ (acoustic pressure in the steady state) vanishes, meaning the wall is "pressure release". The characteristic functions are then $\Phi_i(\vec{\varrho})$. The cases are:

A. SOURCE DESCRIPTION IN RECTANGULAR COORDINATES

1. finite rectangular cross-section, side a (x coordinate), side b (y coordinate)

pressure release wall:

$$\delta(\vec{\varrho} - \vec{\varrho}') = \begin{cases} \displaystyle\sum_i \Phi_i(\vec{\varrho})\,\Phi_i(\vec{\varrho}'), & 0 < \overset{x}{x'} < a,\ 0 < \overset{y}{y'} < b, \\ \displaystyle\frac{4}{ab} \sum_{m=1}^{\infty} \sum_{n=1}^{\infty} \sin\frac{m\pi x}{a} \sin\frac{n\pi y}{b} \sin\frac{m\pi x'}{a} \sin\frac{n\pi y'}{b}, \end{cases} \tag{3.6.13}$$

rigid wall:

$$\delta(\vec{Q}-\vec{Q}') = \begin{cases} \sum_i \psi_i(\vec{Q})\psi_i(\vec{Q}'), & 0<\overset{x}{x'}<a,\ 0<\overset{y}{y'}<b, \\ \dfrac{1}{ab}\sum_{m=0}^{\infty}\sum_{n=0}^{\infty}\varepsilon_m\varepsilon_n \cos\dfrac{m\pi x}{a}\cos\dfrac{n\pi y}{b}\cos\dfrac{m\pi x'}{a}\cos\dfrac{n\pi y'}{b}, \end{cases} \tag{3.6.14}$$

$$\varepsilon_0 = 1, \quad \varepsilon_m = 2, \quad m \geq 1, \quad m = 0, 1, 2 \ldots$$

II. semi-infinite rectangular cross-section, side a $\to \infty$ (x coordinate), side b(y coordinate)

pressure release wall:

$$\delta(\vec{Q}-\vec{Q}') = \begin{cases} \sum_i \Phi_i(\vec{Q})\Phi_i(\vec{Q}'), & 0<\overset{x}{x'}<\infty,\ 0<\overset{y}{y'}<b, \\ \dfrac{4}{\pi b}\displaystyle\int_0^{\infty} d\xi \sum_{n=1}^{\infty} \sin\xi x \sin\frac{n\pi y}{b} \sin\xi x' \sin\frac{n\pi y'}{b}, \end{cases} \tag{3.6.15}$$

rigid wall:

$$\delta(\vec{Q}-\vec{Q}') = \begin{cases} \sum_i \psi_i(\vec{Q})\psi_i(\vec{Q}'), & 0<\overset{x}{x'}<\infty,\ 0<\overset{y}{y'}<b, \\ \dfrac{2}{\pi b}\displaystyle\int_0^{\infty} d\xi \sum_{n=0}^{\infty} \varepsilon_n \cos\xi x \cos\frac{n\pi y}{b} \cos\xi x' \cos\frac{n\pi y'}{b}, \end{cases} \tag{3.6.16}$$

III. quarter-space rectangular cross-section, side a $\to \infty$ (x coordinate), side b $\to \infty$ (y coordinate)

pressure release wall:

$$\delta(\vec{Q}-\vec{Q}') = \begin{cases} \sum_i \Phi_i(\vec{Q})\Phi_i(\vec{Q}'), & 0<\overset{x}{x'}<\infty,\ 0<\overset{y}{y'}<\infty, \\ \dfrac{4}{\pi^2}\displaystyle\int_0^{\infty} d\xi \int_0^{\infty} d\eta \sin\xi x \sin\eta y \sin\xi x' \sin\eta y', \end{cases} \tag{3.6.17}$$

rigid wall:

$$\delta(\vec{Q}-\vec{Q}') = \begin{cases} \sum_i \psi_i(\vec{Q})\psi_i(\vec{Q}'), & 0<\overset{x}{x'}<\infty,\ 0<\overset{y}{y'}<\infty, \\ \dfrac{4}{\pi^2}\displaystyle\int_0^{\infty} d\xi \int_0^{\infty} d\eta \cos\xi x \cos\eta y \cos\xi x' \cos\eta y', \end{cases} \tag{3.6.18}$$

IV. half-space rectangular cross-section, $x \to \infty$, $y \to \pm\infty$

pressure release at $x = 0$:

$$\delta(\vec{Q}-\vec{Q}') = \begin{cases} \sum_i \Phi_i(\vec{Q})\Phi_i^*(\vec{Q}'), & 0>\overset{x}{x'}<\infty,\ -\infty<\overset{y}{y'}<\infty, \\ \dfrac{1}{\pi^2}\displaystyle\int_0^{\infty} d\xi \int_{-\infty}^{\infty} d\eta \sin\xi x\, e^{-j\eta y} \sin\xi x'\, e^{+j\eta y}, \end{cases} \tag{3.6.19}$$

rigid wall at $x = 0$:

$$\delta(\vec{\varrho} - \vec{\varrho}') = \begin{cases} \sum_i \psi_i(\vec{\varrho})\,\psi_i^*(\vec{\varrho}') & 0 < \substack{x \\ x'} < \infty,\ -\infty < \substack{y \\ y'} < \infty, \\ \dfrac{1}{\pi^2} \displaystyle\int_0^\infty d\xi \int_{-\infty}^\infty d\eta \cos \xi x\, e^{-j\eta y} \cos \xi x'\, e^{+j\eta y'}, \end{cases} \tag{3.6.20}$$

V. parallel plate, thickness a (x direction), $y \to \pm\infty$ (y direction)

pressure-release walls at $x = 0$, $x = a$:

$$\delta(\vec{\varrho} - \vec{\varrho}') = \begin{cases} \sum_i \Phi_i(\vec{\varrho})\,\Phi_i^*(\vec{\varrho}'), & 0 < \substack{x \\ x'} < a,\ -\infty < \substack{y \\ y'} < \infty, \\ \dfrac{1}{\pi a} \displaystyle\sum_{m=1}^{\infty} \int_{-\infty}^{\infty} d\eta \sin \frac{m\pi x}{a}\, e^{-j\eta y} \sin \frac{m\pi x'}{a}\, e^{j\eta y'}, \end{cases} \tag{3.6.21}$$

rigid walls at $x = 0$, $x = a$:

$$\delta(\vec{\varrho} - \vec{\varrho}') = \begin{array}{l} \displaystyle\sum_i \psi_i(\vec{\varrho})\,\psi_i^*(\vec{\varrho}'), \quad 0 < \substack{x \\ x'} < a,\ -\infty < \substack{y \\ y'} < \infty, \\ \dfrac{1}{2\pi a} \displaystyle\sum_{m=0}^{\infty} \int_{-\infty}^{\infty} d\eta\, \varepsilon_m \cos \frac{m\pi x}{a}\, e^{-j\eta y} \cos \frac{m\pi x'}{a}\, e^{j\eta y'}, \\ \varepsilon_0 = 1, \quad \varepsilon_m = 2, \quad m \geq 1, \quad m = 0, 1, 2 \ldots \end{array} \tag{3.6.22}$$

VI free space.

A free space "waveguide" can be thought of as a waveguide with walls in the xy plane at very great distances from the waveguide axis, and with the waves traveling in the z direction. Since Φ_i, ψ_i are the same one has:

$$\delta(\vec{\varrho} - \vec{\varrho}') = \sum_i \Phi_i(\vec{\varrho})\,\Phi_i^*(\vec{\varrho}') = \sum_i \psi_i(\vec{\varrho})\,\psi_i^*(\vec{\varrho}'), \qquad -\infty < \substack{x \\ x'} < \infty, \quad -\infty < \substack{y \\ y'} < \infty,$$

$$= \frac{1}{4\pi^2} \int_{-\infty}^{\infty} d\xi \int_{-\infty}^{\infty} d\eta\, e^{-j(\xi x + \eta y)}\, e^{+j(\xi x' + \eta y')}, \tag{3.6.23}$$

$$\Phi_i(\vec{\varrho}) = \psi_i(\vec{\varrho}) = \frac{1}{2\pi}\, e^{-j(\xi x + \eta y)}, \quad -\infty < \xi < \infty, -\infty < \eta < \infty;\ k_n^2 = \xi^2 + \eta^2.$$

B. SOURCE DESCRIPTION IN CYLINDRICAL COORDINATES

In polar coordinates ϱ, ϕ an annulus inner radius a, outer radius b, may be complete, $0 \leq \phi \leq 2\pi$, or incomplete, $0 < \phi < \varphi$. The incomplete (sector) case is different from the complete (annulus) case. These are treated in turn.

I. sector

pressure release at $\phi = 0$ and $\phi = \varphi$:

$$\delta(\phi - \phi') = \sum_q \Phi_q(\phi)\,\Phi_q(\phi') = \frac{2}{\varphi} \sum_{m=1}^{\infty} \sin\frac{m\pi\phi}{\varphi} \sin\frac{m\pi\phi'}{\varphi}, \quad 0 < \begin{matrix}\phi \\ \phi'\end{matrix} < \varphi, \tag{3.6.24}$$

$$\Phi_q(\phi) = \sqrt{\frac{2}{\varphi}} \sin q\phi, \quad q = \frac{m\pi}{\varphi}, \quad m = 1, 2, \ldots .$$

rigid walls at $\phi = 0$, $\phi = \varphi$:

$$\delta(\phi - \phi') = \sum_q \psi_q(\phi)\,\psi_q(\phi') = \frac{1}{\varphi} \sum_{m=0}^{\infty} \varepsilon_m \cos\frac{m\pi\phi}{\varphi} \cos\frac{m\pi\phi'}{\varphi}, \quad 0 < \begin{matrix}\phi \\ \phi'\end{matrix} < \varphi, \tag{3.6.25}$$

$$\psi_q(\phi) = \sqrt{\frac{\varepsilon_m}{\varphi}} \cos q\phi, \quad q = \frac{m\pi}{\varphi}, \quad m = 0, 1, 2, \ldots, \quad \varepsilon_m = \begin{cases} 1, & m = 0, \\ 2, & m \geq 1. \end{cases}$$

II. annulus

In this case there are no walls in the ϕ-domain. Since the field is periodic in 2π the form of the modal functions are unrestricted except for this requirement of periodicity. An angular source therefore has the alternate forms:

$$\delta(\phi - \phi') = \begin{cases} \dfrac{1}{2\pi} \displaystyle\sum_{m=0}^{\infty} \varepsilon_m \cos m\phi \cos m\phi' + \frac{1}{\pi} \sum_{m=1}^{\infty} \sin m\phi \sin m\phi', \\ \dfrac{1}{2\pi} \displaystyle\sum_{m=0}^{\infty} \varepsilon_m \cos m(\phi - \phi'), \\ \dfrac{1}{2\pi} \displaystyle\sum_{m=-\infty}^{\infty} e^{-jm(\phi - \phi')}, \quad 0 \leq \phi \leq 2\pi. \end{cases} \tag{3.6.26}$$

III. finite angular sector, sides $\varrho = b$, included angle φ.

Here the 2-D delta source is the product of two 1-D deltas: $\delta(\vec{\varrho} - \vec{\varrho}') = \delta(\varrho - \varrho')\delta(\phi - \phi')/\varrho'$. The radial modal function is proportional to the Bessel function J_q. The 2-D cases are:

pressure release walls: for $0 \leq \phi \leq \varphi$, $0 \leq \varrho \leq b$,

$$\delta(\varrho - \varrho') = \sum_i \Phi_i(\varrho)\,\Phi_i(\varrho')$$

$$= \frac{4}{\varphi b^2} \sum_{m=1}^{\infty} \sum_{n=1}^{\infty} \frac{\sin q\phi J_q(p\varrho) \sin q\phi' J_q(p\varrho')}{J_{q+1}^2(pb)}, \quad q = \frac{m\pi}{\varphi}, \; p = \frac{x_{nq}}{b} \tag{3.6.27}$$

The roots x_{nq} are defined by $J_q(x_{nq}) = 0$, $n = 1, 2, 3 \ldots$ q fixed.

rigid walls:

$$\delta(\vec{\varrho} - \vec{\varrho}') = \sum_i \psi_i(\vec{\varrho})\, \psi_i(\varrho'), \quad 0 \leqslant \begin{matrix}\vec{\varrho} \\ \vec{\varrho}'\end{matrix} \leqslant b, \quad 0 \leqslant \begin{matrix}\phi \\ \phi'\end{matrix} \leqslant \varphi,$$

$$= \frac{2}{\varphi} \sum_{m=0}^{\infty} \sum_{n=1}^{\infty} \varepsilon_m \frac{p^2}{[(pb)^2 - q^2] J_q^2(pb)} \cos q\phi J_q(p\varrho) \cos q\phi' J_q(p\varrho'), \quad (3.6.28)$$

$$q = \frac{m\pi}{\varphi}, p = \frac{x'_{nq}}{b},$$

The roots x'_{nq} are defined by $J'_q(x'_{nq}) = 0$, $n = 1, 2 \ldots$ $\varepsilon_0 = 1$, $\varepsilon_m = 2$, $m \geqslant 1$

The 1-D cases are:

pressure release at $\varrho = b$:

$$\frac{\delta(\varrho - \varrho')}{\varrho'} = \sum_l \Phi_l(\varrho)\, \Phi_l^*(\varrho') = \frac{2}{b^2} \sum_{n=1}^{\infty} \frac{J_q(l\varrho)\, J_q(l\varrho')}{J_{q+1}^2(lb)} \qquad 0 < \varrho < b$$

$$l = \frac{x_{nq}}{b}\ ; J_q(x_{nq}) = 0,\ n = 1, 2, 3 \ldots q \text{ fixed.}$$

$$\Phi_l(\varrho) = \frac{\sqrt{2}}{b} \frac{-1}{J_{q+1}(x_{nq})} J_q(l\varrho) \quad (3.6.29)$$

(in conjunction with $\delta(\phi - \phi')$ the symbol $q = m\pi/\varphi$)

rigid wall at $\varrho = b$:

$$\psi_l(\varrho) = l\sqrt{\frac{2}{(lb)^2 - q^2}} \frac{J_q(l\varrho)}{J_q(lb)} \quad (3.6.30)$$

$$l = \frac{x'_{nq}}{b};\ J'_q(x'_{nq}) = 0,\ n = 1, 2, 3. \ldots$$

IV. open angular sector, included angle φ

pressure release walls:

$$\delta(\vec{\varrho} - \vec{\varrho}') = \sum_i \Phi_i(\vec{\varrho})\, \Phi_i(\vec{\varrho}'), 0 < \begin{matrix}\vec{\varrho} \\ \vec{\varrho}'\end{matrix} < \infty, 0 < \begin{matrix}\phi \\ \phi'\end{matrix} < \varphi,$$

$$= \frac{2}{\varphi} \sum_{m=1}^{\infty} \int_0^{\infty} \xi \sin q\phi\, J_q(\xi\varrho) \sin q\phi'\, J_q(\xi\varrho')\, d\xi, \quad (3.6.31)$$

$$\Phi_i(\vec{\varrho}) = \sqrt{\frac{2\xi}{\varphi}} \sin q\phi \, J_q(\xi\varrho), q = \frac{m\pi}{\varphi}, \quad m = 1, 2, \ldots, 0 < \xi < \infty;$$
$$k_{ti}'^2 = \xi^2.$$

rigid walls:

$$\delta(\varrho - \varrho') = \sum_i \psi_i(\varrho)\, \psi_i(\varrho'), 0 < \frac{\phi}{\phi'} < \varphi, 0 < \frac{\varrho}{\varrho'} < \infty,$$
$$= \frac{1}{\varphi} \sum_{m=0}^{\infty} \int_0^{\infty} \xi\varepsilon_m \cos q\phi \, J_q(\xi\varrho) \cos q\phi' \, J_q(\xi\varrho') \, d\xi, \tag{3.6.32}$$
$$\psi_i(\varrho) = \sqrt{\frac{\varepsilon_m \xi}{\varphi}} \cos q\phi \, J_q(\xi\varrho), q = \frac{m\pi}{\varphi}, \quad m = 0, 1, 2, \ldots, 0 < \xi < \infty;$$
$$k_{ti}''^2 = \xi^2, \varepsilon_m = \begin{cases} 1, m = 0, \\ 2, m \geq 1. \end{cases}$$

V. Circular waveguide

pressure release walls:

$$\delta(\vec{\varrho} - \vec{\varrho}') = \begin{cases} \sum_i \Phi_i(\varrho)\, \Phi_i^*(\varrho'), \quad 0 \leq \frac{\phi}{\phi'} \leq 2\pi, 0 \leq \frac{\varrho}{\varrho'} \leq \infty, \\ \frac{1}{\pi b^2} \sum_{m=-\infty}^{\infty} \sum_{n=1}^{\infty} \frac{e^{-jm\phi} J_m(p\varrho)\, e^{jm\phi'} J_m(p\varrho')}{J_{m+1}^2(pb)}, \end{cases} \tag{3.6.33}$$
$$p = \frac{x_{nm}}{b}; J_m(x_{nm}) = 0, n = 1, 2, \ldots$$
$$\Phi_i(\varrho) = \frac{1}{b\sqrt{\pi}\, J_{m+1}(pb)} e^{-jm\phi} J_m(p\varrho), m = 0, \pm 1, \pm 2, \ldots,$$
$$n = 1, 2, \ldots; k_{ti}'^2 = \left(\frac{x_{nm}}{b}\right)^2.$$

rigid walls:

$$\delta(\vec{\varrho} - \vec{\varrho}') = \sum_i \psi_i(\vec{\varrho})\ \psi_i^*(\vec{\varrho}')$$
$$= \frac{1}{\pi} \sum_{m=-\infty}^{\infty} \sum_{n=1}^{\infty} \frac{p^2}{[(pb)^2 - m^2]\, J_m^2(pb)} e^{-jm\phi} J_m(p\varrho)\, e^{jm\phi'} J_m(p\varrho'), \tag{3.6.34}$$
$$p = \frac{x'_{nm}}{b}; J'_m(x'_{nm}) = 0, n = 1, 2, \ldots$$
$$\psi_i(\vec{\varrho}) = \frac{p}{\sqrt{\pi[(pb)^2 - m^2]}\ J_m(pb)} e^{jm\phi} J_m(p\varrho), m = 0, \pm 1, \pm 2, \ldots,$$
$$n = 1, 2, \ldots; k_{ti}'^2 = \left(\frac{x'_{nm}}{b}\right)^2.$$

In 3.6.33 and 3.6.34 the symbol p is the radial wavenumber.

3.7 ACOUSTIC RADIATION INTO WAVEGUIDES II

The representation of point sources and line sources in expansions of modal functions Φ_i or ψ_i characteristic of the waveguide permits one to readily construct the Green's functions for the Helmholtz wave equation needed for the calculation of the radiation field. In the classical theory of modes the 3-D Green's function in Helmholtz separable orthogonal curvilinear coordinates ξ_1, ξ_2, ξ_3 for *each selection of separation constants* $k(k_1, k_2, k_3)$ is,

$$G_k(\vec{r}|\vec{r}') = -\left(\frac{4\pi h_1}{h_2 h_3}\right) \sum_q \frac{w(\xi_2', \xi_3')}{N_q} W_q(\xi_2, \xi_3) \bar{W}_q(\xi_2', \xi_3') \frac{y_{1q}(\xi_{1<}) y_{2q}(\xi_{1>})}{\Delta} \tag{3.7.1}$$

[6]. Here, h_i are scale factors, w is the orthogonality weight factor, N_q is the normalization, W_q are the eigenfunctions; y_1, y_2 are the two independent solutions in the ξ_1 coordinate, and Δ is their Wronskian. The overbar on $\bar{W}_q$ indicates the adjoint (see 3.4.18). Thus $W_q/\sqrt{N_q}$ corresponds to Φ_i or ψ_i listed above. It is therefore seen that the completeness relations in which $\delta(x - x')$ is expanded in eigenfunctions serves to specify them. In general W_q, y_{1q}, y_{2q} are functions of separation constants k_i.

The selection of which of the physical coordinates represents the direction of propagation of the wavequide characterizes the transmission. For example, in cylindrical coordinates ϱ, ϕ, z, if ϱ is taken to be ξ_1 the transmission is *radial*; if ϕ is taken to be ξ_1 the transmission is *angular*. In rectangular coordinates x, y, z the transmission is *transverse* if $\varrho = \sqrt{x^2 + y^2} = \xi_1$ and is *axial* if $z = \xi_1$. Examples are treated in the next section.

3.7a RADIATION OF A HARMONIC POINT SOURCE INTO A WEDGE WAVEGUIDE

An open (sector) cylinder $-\infty < z < +\infty$ Fig. 3.6.1 whose cross-section is a wedge (angle φ) is excited by a harmonic point source at $\vec{r}' = (\varrho', \phi', z')$. The 2-D Green's function is taken in radial transmission form, that is, the eigenfunctions are functions of angle ϕ, while the radial function is a 1-D Green's function in ϱ:

$$G_k(\vec{\varrho}|\vec{\varrho}') = \sum_\mu \Phi_\mu(\phi) \Phi_\mu(\phi') g_\varrho(\varrho, \varrho'; \mu, \tau) \tag{3.7.2}$$

The form of g_ϱ is given by 3.5.2. In three dimensions, for each separation constant ζ belonging to the z-coordinate,

$$G_\zeta(\vec{r}|\vec{r}') = e^{i\zeta(z-z')} \sum_\mu \Phi_\mu(\phi) \Phi_\mu(\phi') g_\varrho(\varrho, \varrho'; \mu, \tau) \tag{3.7.3}$$

Now the acoustic field propagates in both the radial and axial directions. There are therefore two propagation constants, k_ϱ, k_z. These must be coupled because their corresponding fields both obey Helmholtz's equation in three dimensions. The coupling is: $k_\varrho^2 + k_z^2 = \left(\frac{\omega}{c}\right)^2$. When the field is bounded in both the ϱ and z coordinate, or in either, only discrete values of k_ϱ and k_z are permitted: $(k_\varrho)_{mn}^2 + (k_z)_{mn}^2 = \left(\frac{\omega}{c}\right)^2$. When the field is unbounded in *both* the ϱ and z coordinates the wavenumbers form a continuum. In the discrete case the field is found by summing over all modal numbers mn. In the continuum case the field is found by integration over k_ϱ or k_z.

The wedge waveguide is an example of a continuous set of wavenumbers. Substitution of plane wave solutions into Helmholtz's equation leads to the coupling statement that $\tau = k^2 - \zeta^2$. The functions $\Phi_\mu(\phi)$ are specified by the nature of the walls: for pressure release walls one uses 3.6.24, while for rigid walls one uses 3.6.25. The complete 3-D Green's function is finally found by integration $\int(\ )\, d\zeta/2\pi$ of 3.7.3 if the eigenfunctions are the normalized forms given in this chapter. [7]. Two forms are:

pressure release walls:

$$G(\vec{r}|\vec{r}';k) = \frac{i}{2\varphi}\int_{-\infty}^{\infty} d\zeta \sum_{m=1}^{\infty} J_\mu(\sqrt{k^2-\zeta^2}\ \varrho_<)\, H_\mu^{(1)}(\sqrt{k^2-\zeta^2}\ \varrho_>)\, e^{i\zeta(z-z')} \times \sin\mu\phi \sin\mu\phi' \tag{3.7.4}$$

rigid walls:

$$G(\vec{r}|\vec{r}';k) = \frac{i}{4\varphi}\int_{-\infty}^{\infty} d\zeta \sum_{m=0}^{\infty} \varepsilon_m J_\mu(\sqrt{k^2-\zeta^2}\ \varrho_<)\, H_\mu^{(1)}(\sqrt{k^2-\zeta^2}\ \varrho_>)\, e^{i\zeta(z-z')} \times \cos\mu\phi \cos\mu\phi' \tag{3.7.5}$$

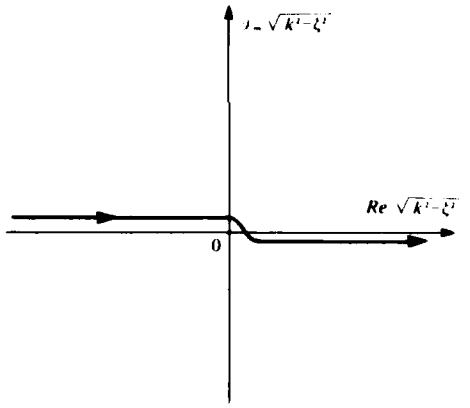

Fig. 3.7.1. Path of integration of 3.7.4 and 3.7.5.

$$\varepsilon_0 = 1,\ \varepsilon_m = 2,\ m \geq 1;\ \mu = m\pi/\varphi$$

For definition of subscripts $<$, $>$ see 3.5.3.

Since the integrand is complex and contains branch singularities the path of integration must be specified, Fig. 3.7.1. Here $\vartheta_m\sqrt{k^2-\zeta^2} \geq 0$. Discussion of integration paths is taken up in Appendix 3.1.

The physical acoustic velocity potential radiated by a point source $q = Q\delta(\vec{r}-\vec{r}')$ where Q is the source strength (m^3/s) is given by 1.7.8,

$$\psi = \int G(\vec{r}|r';k)\, Q\delta(r')\, dV(\vec{r}')\, e^{-i\omega t} \tag{3.7.6}$$

3.7b RADIATION FIELD OF A POINT SOURCE IN A CIRCULAR WAVEGUIDE

A circular cylinder $-\infty < \varrho < +\infty$ is excited by a point source at $\vec{r}'(\varrho', \phi', z')$. There are standing waves in the ϱ-coordinate and propagation in the z-coordinate. The 3-D Green's function is therefore a product of eigenfunctions in the ϱ-coordinate and a 1-D Green's functions in the z-coordinate:

$$G(\vec{r}|\vec{r}') = \sum_i \Phi_i(k_\varrho;\vec{\varrho})\,\overline{\Phi}_i(k_\varrho;\vec{\varrho}')\, g_i(z, z';k_i) \tag{3.7.7}$$

For a circular waveguide the eigenfunctions in the ϕ-coordinate are required to satisfy only periodicity, 3.6.26. The eigenfunctions in the ϱ-coordinate are given by 3.6.29 or 3.6.30; alternatively, 3.6.33, 3.6.34. The 1-D Green's function in the *unbounded* z coordinate is,

$$g_z = \frac{i \exp ikz|z - z'|}{2k_z} \tag{3.7.8}$$

Because k_ϱ is discrete, they are indexed by subscripts mn,

$$(\chi)^2_{mn} + (k_z)^2 = (\omega/c)^2, \chi = k_\varrho \tag{3.7.9}$$

In modal description the transverse field shows a lattice of circular nodes in the ϱ-coordinate and radial nodes in the ϕ coordinate. Hence the use of two modal numbers mn. The radiated field is therefore found by double summation over all modes. Two useful cases are obtained from boundary conditions 3.6.10. These are:

pressure release wall at $\varrho = b$:

$$G(\vec{r}|\vec{r}') = \sum_{n=1}^{\infty} \frac{1}{2\pi} \sum_{m=-\infty}^{\infty} e^{im(\phi-\phi')} \frac{2}{b^2} \frac{J_m(\chi_{mn}\varrho)\, J_m(\chi_{mn}\varrho')}{J^2_{m+1}(\chi_{mn}b)} \frac{i \exp i\sqrt{(\omega/c)^2 - \chi^2_{mn}}\ |z - z'|}{2\sqrt{(\omega/c)^2 - \chi^2_{mn}}}$$

$$J_m(\chi_{mn}b) = 0,\ n = 1, 2, 3, \ldots \text{ for } m \text{ fixed.} \tag{3.7.10}$$

rigid wall at $\varrho = b$:

$$G(\vec{r}|\vec{r}') = \sum_{n=1}^{\infty} \frac{1}{2\pi} \sum_{m=-\infty}^{\infty} e^{im(\phi-\phi')} 2\left[\frac{\chi^2_{mn}}{\chi^2_{mn}b^2 - m^2}\right] \frac{J_m(\chi'_{mn}\varrho)\, J_m(\chi'_{mn}\varrho')}{J^2_m(\chi_{mn}b)} \tag{3.7.11}$$

$$\times \frac{i \exp i\sqrt{(\omega^2/c^2) - \chi^2_{mn}}\ |z - z'|}{2\sqrt{(\omega/c)^2 - \chi^2_{mn}}}$$

$$J'_m(\chi'_{mn}b) = 0,\ n = 1, 2, 3 \ldots \text{ for } m \text{ fixed}$$

$$J'_m(u) \equiv \frac{dJ_m(u)}{du}\ .$$

3.7c RADIATION FIELD OF A POINT SOURCE IN A RECTANGULAR SEMI-INFINITE OPEN WAVEGUIDE OR IN A RECTANGULAR BOUNDED WAVEGUIDE

A waveguide $-\infty < z < \infty$ whose cross-section is a semi-infinite rectangle, $0 \leqslant y \leqslant b\ 0 \leqslant x < \infty$, is excited by a point source at $\vec{r}'(x', y', z')$. There is a standing wave in the y-coordinate. Thus the 3-D Green's function is constructed of a product of eigenfunctions in the xy plane and a 1-D Green's function in the z-coordinates

$$G(\vec{r}|\vec{r}') = \sum_i \Phi_i(k_x, k_y; \vec{\varrho})\, \Phi_i(k_x, k_y; \vec{\varrho}')\, g_z(z, z'; k_z),\ \vec{\varrho} = (x, y) \tag{3.7.12}$$

The wavenumbers in the z and x-coordinates are continuous while those in the y direction are discrete. The coupling statement is thus,

$$k^2 = \xi^2 + k_y^2 + \zeta^2, \quad \xi = k_x; \zeta = k_y \tag{3.7.13}$$

The eigenfunctions in the transverse plane are obtained from 3.6.15 or 3.6.16, and g_z for the *unbounded* z-domain is obtained from 3.7.8. Because ξ, ζ are continuous the radiation field is obtained by both summation and integration. From 3.6.10 two cases can be immediately obtained:

pressure release at $x = 0$, $y = 0$, $y = b$:

$$G(\vec{r}|\vec{r}') = \int_0^\infty d\xi \sum_{n=1}^{\infty} \frac{4}{\pi b} \sin \xi x \sin \frac{n\pi y}{b} \sin \xi x' \sin \frac{n\pi y'}{b} \frac{i \exp i\sqrt{k^2 - \xi^2 - (n\pi/b)^2}\ |z - z'|}{2\sqrt{k^2 - \xi^2 - (n\pi/b)^2}} \tag{3.7.14}$$

When the cross-section of the waveguide is bounded both in y and x, $0 \leqslant x \leqslant a$,

$$G(\vec{r}|\vec{r}') = \sum_{m=1}^{\infty} \sum_{n=1}^{\infty} \frac{4}{ab} \sin \frac{m\pi x}{a} \sin \frac{n\pi y}{b} \sin \frac{m\pi x'}{a} \sin \frac{n\pi y'}{b}$$

$$\times \frac{i \exp i\sqrt{k^2 - (m\pi/a)^2 - (n\pi/b)^2}\ |z - z'|}{2\sqrt{k^2 - (m\pi/a)^2 - (n\pi/b)^2}} \tag{3.7.15}$$

rigid wall at $x = 0$, $y = 0$, $y = b$:

$$G(\vec{r}|\vec{r}') = \int_0^\infty d\xi \sum_{n=0}^{\infty} \frac{2}{\pi b} \varepsilon_n \cos \xi x \cos \frac{n\pi y}{b} \cos \xi x' \cos \frac{n\pi y'}{b} \frac{i \exp i\sqrt{k^2 - \xi^2 - (n\pi/b)^2}\ |z - z|}{2\sqrt{k^2 - \xi^2 - (n\pi/b)^2}}$$

$$\varepsilon_0 = 1, \varepsilon_n = 2, n \geqslant 1 \tag{3.7.16}$$

When the cross-section of the waveguide is bounded both in y and x, $0 \leqslant x \leqslant a$,

$$G(\vec{r}|\vec{r}') = \sum_{m=0}^{\infty} \sum_{n=0}^{\infty} \frac{1}{ab} \varepsilon_m \varepsilon_n \cos \frac{m\pi x}{a} \cos \frac{n\pi y}{b} \cos \frac{m\pi x'}{a} \cos \frac{n\pi y'}{b}$$

$$\times \frac{i \exp i\sqrt{k^2 - (m\pi/a)^2 - (n\pi/b)^2}\ |z - z'|}{2\sqrt{k^2 - (m\pi/a)^2 - (n\pi/b)^2}} \tag{3.7.17}$$

3.7d RADIATION FIELD FROM A HARMONIC POINT SOURCE ABOVE A PLANE.

The theory of acoustic fields in waveguides can be applied to solve this problem. A *free* plane in two dimensions is specified by cylindrical coordinates $0 < \varrho < \infty$; $0 < \phi < 2\pi$. Because of periodicity 2π of ϕ, the field can be described in modes,

$$\Phi_i(\vec{\varrho}) = \sqrt{\frac{\xi}{2\pi}}\, e^{im\phi} J_m(\xi\varrho),\ m = 0, \pm 1, \pm 2, \ldots, \tag{3.7.18}$$

Thus the 3-D Green's function is a product of modes in the ϱ, ϕ plane and a 1-D Green's function in the z-coordinate.

$$G(\vec{r}|\vec{r}') = \sum_i \Phi_i(\vec{\varrho}; \xi)\, \Phi_i(\vec{\varrho}'; \xi)\, g_z(z, z'; k_z) \tag{3.7.19}$$

Now g_z can be constructed of various independent solutions and their Wronskians,

$$\left\{\begin{matrix}\exp ik_z z_> \\ \times \exp -ik_z z_<\end{matrix}\right\}, \left\{\begin{matrix}\exp ik_z z_> \\ \times \cos k_z z_<\end{matrix}\right\}, \left\{\begin{matrix}\exp ik_z z_> \\ \times \sin k_z z_<\end{matrix}\right\};\ W = u_1 u_2' - u_1' u_2 \tag{3.7.20}$$

in which the subscript symbols $<, >$ indicate two choices: if $z > z'$, use $\exp ik_z(z - z')$; if $0 \leqslant z < z'$, use $\exp ik_z(z' - z)$. Because the plane is a boundary of the z domain one must specify a boundary condition. Two simple conditions lead to the forms:

$$\text{pressure release boundary:}\quad g_z = \exp ik_z z_> \sin k_z z_< / k_z \tag{3.7.21}$$

$$\text{rigid boundary:}\quad g_z = \exp ik_z z_> \cos k_z z_< / (-ik_z) \tag{3.7.22}$$

Thus bounded z-domains have different Wronskians from unbounded domains. The Wronskians in 3.7.21 and 3.7.22 are defined as

$$W\left\{\exp ik_z z, \begin{matrix}\sin k_z z \\ \cos k_z z\end{matrix}\right\}$$

This choice agrees with [8]. Since the radial and axial fields are coupled the coupling statement is,

$$k^2 = \xi^2 + k_z^2 \tag{3.7.23}$$

The corresponding 3-D Green's functions can immediately be obtained from these equations by integration over ξ:

pressure release boundary at $z = 0$:

$$G(\vec{r}|\vec{r}') = \int_0^\infty d\xi \sum_{m=-\infty}^{\infty} \sqrt{\frac{\xi}{2\pi}}\, e^{im\phi} J_m(\xi\varrho) \sqrt{\frac{\xi}{2\pi}}\, e^{-im\phi} J_m(\xi\varrho') \tag{3.7.24}$$

$$\times \frac{1}{\sqrt{k^2 - \xi^2}} \exp i\sqrt{k^2 - \xi^2}\; z_> \sin k_z z_<$$

The summation on ϕ can be made for m positive only:

$$\frac{1}{2\pi} \sum_{m=-\infty}^{\infty} e^{im(\phi-\phi')} = \frac{1}{2\pi} \sum_{m=0}^{\infty} \varepsilon_m \cos m(\phi - \phi')$$

$$\varepsilon_0 = 1,\ \varepsilon_m = 2,\ m \geqslant 1$$

rigid boundary at $z = 0$:

$$G(\vec{r}|\vec{r}') = \int_0^\infty d\xi \sum_{m=-\infty}^{\infty} \sqrt{\frac{\xi}{2\pi}}\, e^{im\phi} J_m(\xi\varrho) \sqrt{\frac{\xi}{2\pi}}\, e^{im\phi} J_m(\xi\varrho') \tag{3.7.25}$$

$$\times \frac{i}{\sqrt{k^2 - \xi^2}} \exp i\sqrt{k^2 - \xi^2}\; z_> \cos\sqrt{k^2 - \xi^2}\; z_<$$

3.7e RADIATION FIELD OF A HARMONIC POINT SOURCE IN A PARALLEL PLATE WAVEGUIDE

A 2-D parallel plate waveguide, $0 \leqslant x \leqslant a$, $-\infty < y < \infty$ is excited by a harmonic point source at x', y'. There are standing waves in the x-direction and progressive waves in the $\pm y$ direction. The eigenfunctions for pressure-release walls at $x = 0$, $x = a$ are given by 3.6.21, and for rigid walls by 3.6.22. The 3-D Green's function for each set of wavenumbers is obtained from 3.7.1:

$$G(\vec{r}|\vec{r}') = \sum_i \Phi_i(x, y; k_x, k_y)\, \overline{\Phi}_i(x', y'; k_x, k_y)\, g_i(z, z'; k_i) \tag{3.7.26}$$

Because the fields in all three directions are coupled the coupling statement is,

$$k_z = \sqrt{k^2 - \left(\frac{m\pi}{a}\right)^2 - \eta^2}$$

If the z-domain is unbounded the 1-D Green's function is given by 3.7.8; if bounded, by 3.7.21, 3.7.22. We consider the bounded cases first.

pressure release at $x = 0$, $x = a$ and $z = 0$:

$$G(\vec{r}|\vec{r}') = \int_0^\infty d\eta \sum_{m=0}^{\infty} \frac{1}{\sqrt{\pi a}} \sin \frac{m\pi x}{a} e^{i\eta y} \frac{1}{\sqrt{\pi a}} \sin \frac{m\pi x'}{a} e^{-i\eta y}$$

$$\times \frac{\exp i\sqrt{k^2 - \left(\frac{m\pi}{a}\right)^2 - \eta^2}\ z_< \sin \sqrt{k^2 - \left(\frac{m\pi}{a}\right)^2 - \eta^2}\ z_>}{(-)\sqrt{k^2 - \left(\frac{m\pi}{a}\right)^2 - \eta^2}} \tag{3.7.28}$$

rigid boundary at $x = 0$, $x = a$ and $z = 0$:

$$G(\vec{r}|\vec{r}') = \int_0^\infty d\eta \sum_{m=0}^{\infty} \sqrt{\frac{\varepsilon_m}{2\pi a}} \cos \frac{m\pi x}{a} e^{i\eta y} \sqrt{\frac{\varepsilon_m}{2\pi a}} \cos \frac{m\pi x'}{a} e^{-i\eta y}$$

$$\times \frac{i \exp i\sqrt{k^2 - \left(\frac{m\pi}{a}\right)^2 - \eta^2}\ z_< \cos \sqrt{k^2 - \left(\frac{m\pi}{a}\right)^2 - \eta^2}\ z_>}{\sqrt{k^2 - \left(\frac{m\pi}{a}\right)^2 - \eta^2}} \tag{3.7.29}$$

When the field is unbounded in the z coordinate, the two cases are:

pressure release at $x = 0$, $x = a$:

$$G(\vec{r}|\vec{r}') = \int_0^\infty d\eta \sum_{m=0}^{\infty} \frac{1}{\sqrt{\pi a}} e^{i\eta y} \sin \frac{m\pi x}{a} \frac{1}{\sqrt{\pi a}} e^{-i\eta y} \sin \frac{m\pi x'}{a}$$

$$\times \frac{i \exp i\sqrt{k^2 - \left(\frac{m\pi}{a}\right)^2 - \eta^2}\ |z - z'|}{2\sqrt{k^2 - \left(\frac{m\pi}{a}\right)^2 - \eta^2}} \tag{3.7.30}$$

rigid boundary at $x = 0$, $x = a$:

$$G(\vec{r}|\vec{r}') = \int_0^\infty d\eta \sum_{m=0}^{\infty} \sqrt{\frac{\varepsilon_m}{2\pi a}} e^{i\eta y} \cos \frac{m\pi x}{a} \sqrt{\frac{\varepsilon_m}{2\pi a}} e^{-i\eta y} \cos \frac{m\pi x'}{a}$$

$$\times \frac{i \exp i\sqrt{k^2 - \left(\frac{m\pi}{a}\right)^2 - \eta^2}\ |z - z'|}{2\sqrt{k^2 - \left(\frac{m\pi}{a}\right)^2 - \eta^2}} \tag{3.7.31}$$

3.7f ALTERNATE ("BIORTHOGONAL") FORM OF RADIAL DEPENDENCE OF FIELDS IN CYLINDRICAL COORDINATES

In dealing with cylindrical coordinates an alternate form of the integrand has proven advantageous. We describe this form next. In 3.7.24, 3.7.25 the integral has the form,

$$I = \int_0^\infty d\xi\, \xi\, J_m(\xi\varrho)\, J_m(\xi\varrho')\, \{\quad\} \tag{3.7.32}$$

The evaluation of this integral is often facilited by extending the range of integration to $-\infty < \xi > \infty$, and then continuing ξ into the complex-ξ plane. Because,

$$J_m(\xi\varrho) = \tfrac{1}{2}\,[H_m^{(1)}(\xi\varrho) + H_m^{(2)}(\xi\varrho)] \tag{3.7.33}$$

and because

$$\int_0^\infty d\xi\, \xi\, H_m^{(2)}(\xi\varrho)\, J_m(\xi\varrho') = \int_{-\infty}^{0} d\xi\, \xi\, H_m^{(1)}(\xi\varrho)\, J_m(\xi\varrho')$$

one can rewrite 3.7.32 in two alternative forms by interchanging ϱ, ϱ':

$$I = \tfrac{1}{2}\int_{-\infty}^{\infty} d\xi\, \xi\, H_m^{(1)}(\xi\varrho)\, J_m(\xi\varrho')\, \{\quad\} = \tfrac{1}{2}\int_{-\infty}^{\infty} d\xi\, \xi\, H_m^{(1)}(\xi\varrho')\, J_m(\xi\varrho)\, \{\quad\} \tag{3.7.34}$$

In the complex-ξ plane $H_m^{(1)}$ is multiple-valued on the negative real axis. One must therefore make a branch cut there, and deform the contour of integration C_1 to pass *above* the negative real axis, and above $\xi = 0$. The contour is completed by a great semicircle in the upper-half of the ξ plane. The contribution of this semi-circle to the value of I depends on the asymptotic form,

$$|H^{(1)}(\xi\varrho)\, J_m(\xi\varrho')| \sim \frac{1}{\pi\sqrt{\varrho\varrho'\,|\xi|}}\, \exp[-(\mathrm{Im}\ \xi)\,(\varrho - \varrho')] \tag{3.7.35}$$

When $\varrho > \varrho'$ the contribution of the first integral in 3.7.34 vanishes. Because ϱ and ϱ' are interchangeable in 3.7.35 the contribution of the second integral vanishes on the great semi-circle when $\varrho < \varrho'$. The two regimes ($\varrho \lessgtr \varrho'$) are put in one formula by use of "greater than" (>) and "less than" (<) signs in the arguments of the Bessel and Hankel functions,

$$I = \tfrac{1}{2} - \int_{-\infty(C_1)}^{\infty} d\xi\, \xi\, J_m(\xi\varrho_<)\, H_m^{(1)}(\xi\varrho_>)\, \{\quad\} \tag{3.7.36}$$

The symbol $-\infty\,(C_1)$ means contour integration in the complex-ξ plane as discussed above.

The product of Bessel and Hankel transforms in 3.7.36 is called "biorthogonal" in this context, in contrast to the product of two Bessel functions in 3.7.32 which is called "Hermitian".

3.7g RADIATION OF A HARMONIC POINT SOURCE IN FREE SPACE

The 3-D Green's function of a harmonic point source in cylindrical coordinates ϱ, ϕ, z is 3.7.19. In free space the 2-D acoustic field in the plane $z = 0$ is unbounded in the ϱ-coordinate, and periodic in the ϕ coordinate. The modal description follows from 3.7.36 and 3.7.18:

$$\Phi_i(\varrho, \phi; \xi) = \frac{1}{\sqrt{2\pi}} e^{im\phi} \sqrt{\frac{\xi}{2}} J_m(\xi\varrho) \tag{3.7.37}$$

$$\bar{\Phi}_i(\varrho, \phi; \xi) = \frac{1}{\sqrt{2\pi}} e^{-im\phi} \sqrt{\frac{\xi}{2}} H_m^{(1)}(\xi\varrho) \tag{3.7.38}$$

Here, as before, $\bar{\Phi}_i$ is the adjoint modal function, or simple conjugate for time-harmonic excitation. Again, the 1-D Green's function g_z for the case z-unbounded is 3.7.8. Using the coupling statement 3.7.23 one then obtains,

$$G(\vec{r}|\vec{r}'; k) = \int_{-\infty(C_1)}^{\infty} d\xi \sum_{m=-\infty}^{\infty} \frac{1}{\sqrt{2\pi}} e^{im\phi} \sqrt{\frac{\xi}{2}} J_m(\xi\varrho_<) \frac{1}{\sqrt{2\pi}} e^{-im\phi'} \sqrt{\frac{\xi}{2}} H_m^{(1)}(\xi\varrho_>)$$

$$\times \frac{i}{2} \frac{\exp i\sqrt{k^2 - \xi^2}\,|z - z'|}{\sqrt{k^2 - \xi^2}} \tag{3.7.39}$$

The notation $|z - z'|$ could equally well have been written $(z_< - z_>)$. If the point source is placed at the origin the acoustic field becomes independent of coordinate ϕ. This means one must set $m = 0$ as well as ϱ', z'. Then,

$$G(\vec{r}|\vec{0}) = \frac{i}{8\pi} \int_{-\infty(C_1)}^{\infty} \xi \frac{H_0^{(1)}(\xi\varrho) \exp i\sqrt{k^2 - \xi^2}}{\sqrt{k^2 - \xi^2}} |z|\, d\xi \tag{3.7.40}$$

In lieu of integrating over ξ one may choose to integrate over $k_z = \sqrt{k^2 - \xi^2}$. Because

$$\frac{\xi d\xi}{\sqrt{k^2 - \xi^2}} = -dk_z \tag{3.7.41}$$

it appears that 3.7.40 is easily transformable to k_z dependence. However, by deforming the contour C_1 so that ξ runs from $+ i\infty$ to the left of the branch cut of the integrand of 3.7.40, then around branch point k, then to $+ i\infty$ to the right of the branch cut, it will be seen that as ξ varies from $-\infty(C_1)$ to $+\infty$, k_z varies from $+\infty$ to $-\infty$. The minus is cancelled and 3.7.40 is replaced by an integral over the real k_z domain:

$$G(\vec{r}|0) = \int_{-\infty}^{\infty} \frac{iH_0^{(1)}}{4} (\sqrt{k^2 - k_z^2}\,\varrho)\, e^{ik_z z} \frac{dk_z}{2\pi}, \quad z' = 0 \tag{3.7.42}$$

The radiation of a harmonic point source in free space can also be expressed in rectangular coordinates. The 3-D Green's function is,

$$G(\vec{r}|\vec{r}'; k_x, k_y) = \sum_i \Phi_i(x, y; k_x, k_y)\,\bar{\Phi}_i(x', y'; k_x, k_y)\,g_z(z, z'; k_z)$$

The modes Φ_i are obtained from 3.6.23 and g_3 is obtained from 3.7.8. The coupling statement is,

$$k^2 = \xi^2 + \eta^2 + k_z^2, \quad \xi = k_x, \eta = k_y$$

Thus,

$$G(\vec{r}|\vec{r}'; k) = \int_{-\infty}^{\infty} d\xi \int_{-\infty}^{\infty} d\eta \;\; \frac{1}{2\pi}\; e^{i(\xi x + \eta y)} \;\; \frac{1}{2\pi}\; e^{-i(\xi x + \eta y')} \; \frac{i \exp i\sqrt{k^2 - \xi^2 - \eta^2}\;|z - z'|}{2\sqrt{k^2 - \xi^2 - \eta^2}} \tag{3.7.43}$$

All formulas 3.7.39, 3.7.40, 3.4.42, 3.7.43 have the same closed form solution,

$$G(\vec{r}|\vec{r}'; k) = \frac{e^{ikR}}{4\pi R}, R = |\vec{r} - \vec{r}'|$$

3.7h RADIATION OF A HARMONIC POINT-SOURCE IN SEMI-INFINITE QUARTER SPACE

A semi-infinite quarter space, $0 \leqslant x < \infty$, $0 \leqslant y < \infty$, $0 \leqslant z < \infty$ is excited by a point source at x', y', z'. Because the 2-D acoustic field in plane $z = 0$ is bounded by the walls $x = 0$, $y = 0$, it can be described as a sum of modes: 3.6.17 for pressure-release walls, or 3.6.18 for rigid walls. Also, because the field is bounded in the z-coordinate the 1-D Green's function g_z in 3.7.19 is given by 3.7.21 for a pressure-release boundary, or by 3.7.22 for a rigid boundary. In the region z(or z') > 0 the radial field is coupled to the axial field. The coupling of the wavenumbers takes the form,

$$k_z^2 = k^2 - \xi^2 - \eta^2, \xi = k_x, \eta = k_y$$

Because k_x, k_y are continuous the 3-D field 3.7.19 is obtained by a double integration. From boundary conditions 3.6.10 two cases are immediately formulated,

pressure release at wall $x = 0$, wall $y = 0$, and wall $z = 0$:

$$G(\vec{r}|\vec{r}'; k) = \int_0^{\infty} d\xi \int_0^{\infty} d\eta \;\; \frac{2}{\pi}\; \sin \xi x \sin \eta y \;\; \frac{2}{\pi}\; \sin \xi x' \sin \eta y'$$

$$\times \; \frac{\exp i\sqrt{k^2 - \xi^2 - \eta^2}\; z_<\; \sin \sqrt{k^2 - \xi^2 - \eta^2}\; z_>}{-\sqrt{k^2 - \xi^2 - \eta^2}} \tag{3.7.44}$$

rigid wall at wall $x = 0$, wall $y = 0$ and wall $z = 0$:

$$G(\vec{r}|\vec{r}';\, k) = \int_0^\infty d\xi \int_0^\infty d\eta \;\; \frac{2}{\pi} \;\; \cos \xi x \cos \eta y \;\; \frac{2}{\pi} \;\; \cos \xi x_s' \cos \eta y'$$

$$\times \;\; \frac{\exp i\sqrt{k^2 - \xi^2 - \eta^2}' \;\; z_< \cos \sqrt{k^2 - \xi^2 - \eta^2}' \;\; z_>}{-i\sqrt{k^2 - \xi^2 - \eta^2}} \qquad (3.7.45)$$

When the quarter space is infinite g. in 3.7.19 takes on the form 3.7.8.

3.7i GENERAL RULE FOR INTERCONVERTING 3-D AND 2-D GREEN'S FUNCTIONS

The examples cited in 3.7a through 3.7h allow one to construct a general rule for relating 2-D and 3-D Green's functions. Eq. 3.7.42 is a Fourier transform with respect to z of the 2-D Green's function $\frac{i}{4} H_0^{(1)}(k\varrho)\sqrt{x^2 - k_z^2}\,\varrho)$. The conversion is easily generalized in two rules:

Rule #1: A 2-D Green's function $G(\varrho, \phi;\, k_t)$ or $G(x, y;\, k_x, k_y)$ can be converted into a 3-D Green's function by inverse Fourier transformation with respect to the axial coordinate, provided the transverse wavenumbers (k_t or k_x, k_y) are made to couple with the axial wavenumber,

$$G(\vec{r}|\vec{r}';\, k) = \int_{-\infty}^{\infty} e^{ik_z(z-z')}\, G(\varrho, \phi|\varrho', \phi';\, \sqrt{k^2 - k_z^2}\;)\;\frac{dk_z}{2\pi} \qquad (3.7.46)$$

or

$$G(\vec{r}|\vec{r}';\, k) = \int_{-\infty}^{\infty}\int_{-\infty}^{\infty} e^{i\sqrt{k^2 - k_x^2 - k_y^2}\;\;(z-z')} G(x, y|x', y';\, \sqrt{k^2 - k_x^2 - k_y^2}\;)\;\frac{dk_x dk_y}{(2\pi)^2} \qquad (3.7.47)$$

Rule #2: A 3-D Green's function $G(\vec{r}|\vec{r}';\, k)$ can be converted into a 2-D Green's function by direct Fourier transformation with respect to the axial coordinate z',

$$G(\varrho, \phi|\varrho', \phi';\, k,\, k_z) = \int_{-\infty}^{\infty} e^{ik_z(z'-z)}\, G(\vec{r}|\vec{r}';\, k)\, dz' \qquad (3.7.48)$$

or

$$G(x,\, y|x',\, y';\, k,\, k_x,\, k_y) = \int_{-\infty}^{\infty} \int e^{i\sqrt{k^2 - k_x^2 - k_y^2}\;\;(z'-z)} G(\vec{r}|\vec{r}';\, k)\, dz' \qquad (3.7.49)$$

Each of these integrals is evaluated in the real domain in which Fourier transformation requires a factor of $1/2\pi$ when the inverse transformation (that is, integration over wavenumber) is being made. This differs from formulas, like 3.7.39, in which integration over wavenumber is a contour integral and not a Fourier transformation. The factor $1/2\pi$ does not explicitly appear in this case.

3.8 RADIATION IN THE PRESENCE OF SCATTERING BAFFLES

Radiation theory describes the acoustic field generated by acoustic sources in bounded or unbounded space. Section 3.7 treated the case of internal radiation in the guise of a harmonic point

source in waveguides. In this Section we consider the acoustic field radiated by a harmonic source exterior (but adjacent) to a scattering baffle. Only baffles having simple shapes will be discussed in detail.

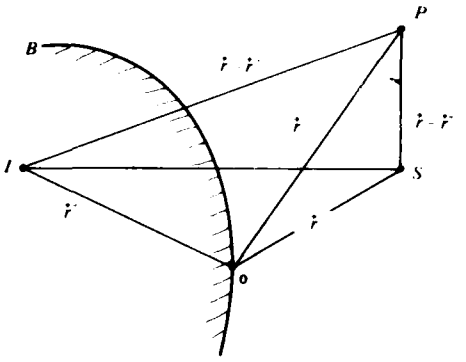

Fig. 3.8.1. Point source adjacent to a baffle.

Fig. 3.8.1 shows the general physical problem. A harmonic point source at S radiates an acoustic field to a point P exterior to the convex baffle B. The effect of the baffle on the radiated field is accounted for by placing an *image* I of the source S inside the baffle. The radiation field at P is then the sum of the freefield $G_0(\vec{r}|\vec{r}')$ from S and the image field $F(\vec{r}|\vec{r}'')$ from I.

$$G(\vec{r}|\vec{r}') = G_0(\vec{r}|\vec{r}') + F(\vec{r}|r''). \tag{3.8.1}$$

While G_0 is discontinuous when the observation point P coincides with S, the field F is always continuous because P cannot be inside B. Thus F obeys the source-free Helmholtz equation,

$$(\nabla^2 + k^2)F = 0 \tag{3.8.2}$$

From the infinity of solutions of this equation one must be selected which also satisfies the boundary condition on B:

$$\alpha G + \beta \vec{\nabla}_n G = 0, \text{ on } B \tag{3.8.3}$$

in which $\vec{\nabla}_n$ is the normal gradient (∂/∂_n) and α, β are general functions of space and (harmonic) time.

Eq. 3.8.1 has a different interpretation: it is the incident field p^i at $\vec{r}$ described by G_0 plus the field p^s $(= F)$ scattered by the baffle,

$$G(\vec{r}|\vec{r}') = p^i(\vec{r}|\vec{r}') + p^s(\vec{r}|\vec{r}') \tag{3.8.4}$$

It is thus seen that the theory which describes the scattering by a convex baffle of the field radiated by a harmonic point source also describes the radiation problem of this section. This rule will be used to help formulate several important problems in external radiation.

3.8a RADIATION OF A HARMONIC POINT SOURCE ADJACENT TO A CIRCULAR CYLINDRICAL BAFFLE

The 3-D Green's function in cylindrical coordinates ϱ, ϕ, z of a point source in free space is expressed by 3.7.39 as a contour integral over the radial wavenumber ξ. By transforming variables 3.7.41 the integration domain becomes k_r which is a real variable:

$$G(\vec{r}|\vec{r}';k) = \int_{-\infty}^{\infty} dk_z \sum_{m=-\infty}^{\infty} \frac{1}{2\pi} e^{im(\phi-\phi')} \frac{1}{2} J_m(\varrho_< \sqrt{k^2-k_z^2}) H_m^{(1)}(\varrho_> \sqrt{k^2-k_z^2}) \frac{i}{2} e^{ik_z(z-z')} \tag{3.8.5}$$

When time is specified as exp $-i\omega t$ the Bessel function J_m represents standing (converging plus diverging) waves, while the Hankel function $H_m^{(1)}$ represents diverging waves. This means an observer at a distance from a point source sees part of the field receding from him and part of it approaching him.

In contrast to this situation described by the product $J_m\, H_m^{(1)}$ the field scattered by the cylindrical baffle always appears diverging to this observer, at least insofar as it is "visible" to him. Thus the radial dependence of the scattered field has the form $H_m^{(1)}(\xi\varrho_<)\, H_m^{(1)}(\xi\varrho_>)$. When the free field and the scattered field are superimposed the radial dependence becomes,

$$[J_m(\xi\varrho_<) + B_m H_m^{(1)}(\xi\varrho_<)]\, H_m^{(1)}(\xi\varrho_>), \quad \xi = \sqrt{k^2-k_z^2} \tag{3.8.6}$$

in which B_m is a factor which is to be adjusted to match boundary conditions on surface $\varrho = a$. Two simply matched boundary conditions are pressure-release surface and rigid surface. The 3-D Green's function in these cases are:

pressure release surface at $\varrho = a$:

$$G(\vec{r}|\vec{r}';k) = e^{-i\omega t} \int_{-\infty}^{\infty} dk_z \sum_{m=-\infty}^{\infty} \frac{1}{2\pi} e^{im(\phi-\phi')} \frac{1}{2} \left[J_m(\varrho_< \sqrt{k^2-k_z^2}) - \frac{J_m(a\sqrt{k^2-k_z^2})}{H_m^{(1)}(a\sqrt{k^2-k_z^2})} \right.$$
$$\left. \times H_m^{(1)}(\varrho_< \sqrt{k^2-k_z^2}) \right] H_m^{(1)}(\varrho_> \sqrt{k^2-k_z^2}) \frac{i}{2} e^{ik_z(z-z')} \tag{3.8.7}$$

rigid surface at $\varrho = a$:

$$G(\vec{r}|\vec{r}';k) = e^{-i\omega t} \int_{-\infty}^{\infty} dk_z \sum_{m=-\infty}^{\infty} \frac{1}{2\pi} e^{im(\phi-\phi')} \frac{1}{2} \left[J_m(\varrho_< \sqrt{k^2-k_z^2}) - \frac{J_m'(a\sqrt{k^2-k_z^2})}{H_m^{(1)\prime}(a\sqrt{k^2-k_z^2})} \right.$$
$$\left. \times H_m^{(1)}(\varrho_< \sqrt{k^2-k_z^2}) \right] H_m^{(1)}(\varrho_> \sqrt{k^2-k_z^2}) \frac{i}{2} e^{ik_z(z-z')}$$
$$J_m'(x) = \frac{\partial}{\partial x} J_m(x) \tag{3.8.8}$$

In applications one can often simplify the above formulas and their derivatives by use of the Wronskian identities.

$$W\{J_m(z), H_m^{(1)}(z)\} = J_m(z)\, H_m^{(1)\prime}(z) - J_m'(z)\, H_m^{(1)}(z)$$
$$= \frac{2i}{\pi z}, \quad z = a\sqrt{k^2-k_z^2} \tag{3.8.9}$$

$$W\{H_m^{(1)}(z), H_m^{(2)}(z)\} = -\frac{4i}{\pi z} \tag{3.8.10}$$

In radiation problems the source point is often on the baffle. When the baffle surface is pressure-release the normal derivative of the Green's function is proportional to the normal component of surface velocity. Taking the derivative of 3.8.7 with respect to $\varrho_<$ and using 3.8.9 it is seen that the part of the integrand in brackets becomes,

$$\frac{-2i}{\pi a H_m^{(1)}(a\sqrt{k^2 - k_z^2})}$$

Hence for the source on the baffle at $\varrho' = a$,

$$\frac{\partial G(\vec{r}|\vec{r}'; k)}{\partial \varrho_<}\bigg|_{\varrho_< = a} = e^{-i\omega t}\int_{-\infty}^{\infty} dk_z \sum_{m=-\infty}^{\infty} \frac{1}{2\pi} e^{im(\phi-\phi')} \frac{1}{2}\left[\frac{-2i}{\pi a}\right] \frac{H_m^{(1)}(\varrho_>\sqrt{k^2 - k_z^2})}{H_m^{(1)}(a\sqrt{k^2 - k_z^2})}$$

$$\times \frac{i}{2} e^{ik_z(z-z')} \tag{3.8.11}$$

Similarly, when the baffle surface is rigid, and the source point is on it at $\varrho' = a$,

$$G(\vec{r}|\vec{r}'; k)\bigg|_{\varrho_< = a} = e^{-i\omega t}\int_{-\infty}^{\infty} dk_z \sum_{m=-\infty}^{\infty} \frac{1}{2\pi} e^{im(\phi-\phi')} \frac{1}{2}\left[\frac{2i}{\pi a\sqrt{k^2 - k_z^2}}\right] \frac{H_m^{(1)}(\varrho_>\sqrt{k^2 - k_z^2})}{H_m^{(1)}(a\sqrt{k^2 - k_z^2})}$$

$$\times \frac{i}{2} e^{ik_z(z-z')} \tag{3.8.12}$$

3.8b RADIATION FIELD OF A LINE SOURCE ADJACENT TO AND PARALLEL WITH A CIRCULAR CYLINDRICAL BAFFLE

A line source (ϱ', $\phi' = 0$, z') parallel to the axis (z) of a circular cylindrical baffle ($\varrho = a$) is specified by the source velocity potential density,

$$\hat{\Phi}(\vec{r}) = \Phi\delta(\vec{\varrho} - \vec{\varrho}')\, e^{-i\omega t}\vec{z}_0 \qquad \text{(units: } m^2 s^{-1} m^{-2}\text{)} \tag{3.8.13}$$

Here Ψ is the line source strength and $\vec{z}_0$ is a unit vector in the z-direction. The 2-D Green's function, associated with this source when $|\Psi| = 1$, and the medium is unbounded, is:

$$G(\vec{\varrho}|\vec{\varrho}') = \frac{i}{4} H_0^{(1)}(k|\vec{\varrho} - \vec{\varrho}'|), \qquad k = \omega/c \tag{3.8.14}$$

$$G(\vec{\varrho}|\vec{\varrho}') = \frac{i}{4} \sum_{m=-\infty}^{\infty} \cos[m(\phi - \phi')]\, J_m(k\varrho_<)\, H_m(k\varrho_>), \quad \text{(units: none)} \tag{3.8.15}$$

[9].

The baffle itself, which can have any local surface acoustic impedance $Z(ka)$, introduces a scattered field $F(\vec{r})$, 3.8.1. Two cases of ideal impedance are:

baffle is pressure release at $\varrho = a$***:***

$$G(\vec{\varrho}\,|\,\vec{\varrho}') = \frac{i}{4} \sum_{m=-\infty}^{\infty} \cos[m(\phi - \phi')] \left[J_m(k\varrho_<) - \frac{J_m(ka)}{H_m^{(1)}(ka)} H_m^{(1)}(k\varrho_<) \right] H_m^{(1)}(k\varrho_>) \tag{3.8.16}$$

When the line source is on the surface $\varrho = a$ the field everywhere vanishes. The normal derivative of the field is however finite everywhere. By use of 3.8.9 one arrives at:

$$\frac{\partial G(\vec{\varrho}\,|\,\vec{\varrho}')}{\partial \varrho_<}\bigg|_{\varrho_< = a} = \frac{i}{4} \sum_{m=-\infty}^{\infty} \cos[m(\phi - \phi')] \left[\frac{-2i}{\pi ka} \right] \frac{H_m^{(1)}(k\varrho_>)}{H_m^{(1)}(ka)} \tag{3.8.17}$$

in which $\varrho_<$ is any radius $\varrho \geq a$. The farfield of 3.8.16 is obtained by use of the asymptotic form of the Hankel function,

$$\lim_{k\varrho \to \infty} H_m^{(1)}(k\varrho) \sim \sqrt{\frac{2}{\pi k\varrho}} \exp\left[i\left(k\varrho - \frac{\pi}{4} \right) \right] (-i)^m \tag{3.8.18}$$

and by noting that

$$\sum_{m=-\infty}^{\infty} i^{-m} \cos[m(\phi - \phi')] J_m(k\varrho) = e^{-ik\varrho\cos(\phi - \phi')} \tag{3.8.19}$$

it is,

$$G(\vec{\varrho}\,|\,\vec{\varrho}') \sim \frac{i}{4} \left[e^{-ik\varrho\cos(\phi - \phi')} - \sum_{m=-\infty}^{\infty} \cos m(\phi - \phi') (-i)^m \frac{J_m(ka)}{H_m^{(1)}(ka)} H_m^{(1)}(k\varrho') \right]$$
$$\times \sqrt{\frac{2}{\pi k\varrho}} \exp\left[i\left(k\varrho - \frac{\pi}{4} \right) \right] \tag{3.8.20}$$

The first term in the brackets is the free field farfield planewave due to the line source; the second term is the scattered field.

baffle is rigid at $\varrho = a$***:***

$$G(\vec{\varrho}\,|\,\vec{\varrho}') = \frac{i}{4} \sum_{m=-\infty}^{\infty} \cos m(\phi - \phi') \left[J_m(k\varrho_<) - \frac{J_m'(ka)}{H_m^{(1)\prime}(ka)} H_m^{(1)}(k\varrho_<) \right] H_m^{(1)}(k\varrho_>) \tag{3.8.21}$$

On the surface $\varrho_< = a$, the field is simplified

$$G(\vec{\varrho}\,|\,a) = \frac{i}{4} \sum_{m=-\infty}^{\infty} \cos m(\phi - \phi') \left[\frac{2i}{\pi ka} \right] \frac{H_m^{(1)}(k\varrho_>)}{H_m^{(1)\prime}(ka)} \tag{3.8.22}$$

The farfield of 3.8.21 is again obtained by 3.8.18 and 3.8.19:

$$G(\vec{\varrho}\,|\,\vec{r}') = \frac{i}{4}\left[\exp(-ik\varrho'\cos(\phi-\phi') - \sum_{m=-\infty}^{\infty}\cos m(\phi-\phi')(-i)^m \frac{J'_m(ka)}{H_m^{(1)'}(ka)} H_m^{(1)}(k\varrho')\right]$$

$$\times \sqrt{\frac{2}{\pi k\varrho}}\exp[i(k\varrho - \pi/4)]. \qquad (3.8.23)$$

In all choices of baffle impedance if the field is caused by a distribution $\Psi(\vec{\varrho}')$ (units: s^{-1})of line sources over a surface $S(\varrho')$, the radiated velocity potential is,

$$\psi(\vec{\varrho}) = \int_s G(\vec{\varrho}\,|\,\vec{\varrho}')\,\Phi(\vec{\varrho}')\,dS(\varrho') \qquad \text{(units: } m^2s^{-1}) \qquad (3.8.24)$$

3.8c RADIATION FIELD OF A POINT SOURCE ADJACENT TO AN ELLIPTIC CYLINDER

An elliptic cylinder Fig. 3.8.2 in elliptic coordinates u, v, z, is related to the rectangular coordinate x, y, z by the transformation:

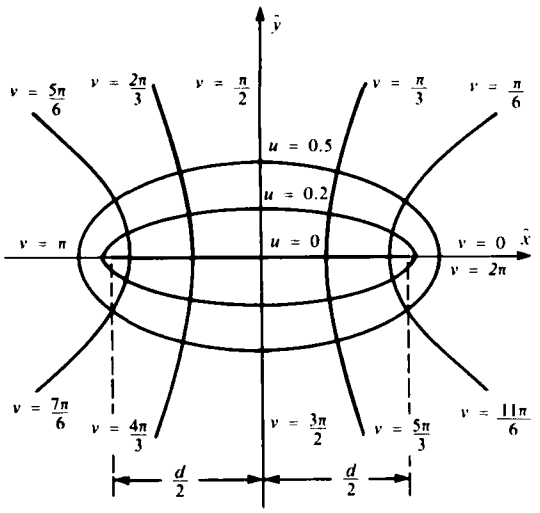

Fig. 3.8.2. Geometry of an elliptic cylinder.

$$x = \frac{d}{2}\xi\eta;\ y = \frac{d}{2}\sqrt{1-\xi^2}\sqrt{1-\eta^2};\ z = z$$

$$\xi = \cosh u;\ \eta = \cos v \qquad (3.8.25)$$

$$0 \leqslant u < \infty;\ 0 \leqslant v \leqslant 2\pi;\ -\infty < z < \infty$$

The surfaces ξ = const. are confocal ellipses; d is the interfocal distance; ξ^- is the eccentricity; the surfaces η = const. are confocal hyperbolic cylinders of two sheets at interfocal distance d.

The separation of Helmholtz's equation $(\nabla^2 + k^2)\psi(\vec{r}) = 0$ in elliptic cylinder coordinates leads to a description of the fields in terms of radial and angular functions,

even radial (Mathieu) functions: $Re_m^{(1),\,(2),\,(3)}(c, \xi)$
odd radial (Mathieu) functions: $Ro_m^{(1),\,(2),\,(3)}(c, \xi)$
even (odd) angular Mathieu functions $Se_m(c, \eta)$, $So_m(c, \eta)$,

in which $c = kd/2$, and $\mathrm{Re}_m^{(1)} + i\mathrm{Re}_m^{(2)}$. A brief description of Mathieu functions is given in Sect. 1.9b and reference [10]. Now the 2-D Green's function in elliptic coordinates is:

$$G(\vec{\varrho}\,|\,\vec{\varrho}\,';\, k_z) = \frac{i}{4}\, H_0^{(1)}(k_z \varrho), \qquad \varrho = |\vec{\varrho} - \vec{\varrho}\,'|$$

$$G(\vec{\varrho}\,|\,\vec{\varrho}\,';\, k_z) = \frac{i}{4}\left\{ 4 \sum_{m=0}^{\infty}{}^{\sim} Re_m^{(1)}(c, \xi_<)\, Re_m^{(3)}(c, \xi_>)\, Se_m(c, \eta')\, Se_m(c, \eta) \times \frac{1}{\Omega_m^{(e)}} \right. \tag{3.8.26}$$

$$\left. + 4 \sum_{m=0}^{\infty} Ro_m^{(1)}(c, \xi_<)\, Ro_m^{(3)}(c, \xi_>)\, So_m(c, \eta')\, So_m(c, \eta) \times \frac{1}{\Omega_m^{(0)}} \right\}$$

[11]. Here $\Omega_m^{(e)}$, $\Omega_m^{(0)}$ are the normalization of even and odd angle functions discussed in Sect. 1.9b, Eq. 1.9.23 etc. The conversion to a 3-D Green's function follows the rule given in 3.7.46. When the baffle is taken into account the 3-D Green's function must be modified because of the scattering term, 3.8.1. Two useful cases are:

pressure release at surface $\xi = \xi_1$: Source point is at (ξ_0, η_0, z_0), observation point is at $(\xi_>, \xi_<; \eta; z)$.

$$G(\xi, \eta, z\,|\,\xi_0, \eta_0, z_0;\, k) = i \int_{-\infty}^{\infty} \frac{dk_z}{2\pi}\, e^{ik_z(z-z_0)} \times \sum_{m=0}^{\infty} \left\{ \frac{1}{\Omega_m^{(e)}}\, Re_m^{(3)}(\gamma, \xi_>) \right.$$

$$\times \left[Re_m^{(1)}(\gamma, \xi_<) - \frac{Re_m^{(1)}(\gamma, \xi_1)}{Re_m^{(3)}(\gamma, \xi_1)}\, Re_m^{(3)}(\gamma, \xi_<) \right] Se_m(\gamma, \eta_0)\, Se_m(\gamma, \eta) +$$

$$\left. \times \frac{1}{\Omega_m^{(0)}}\, Ro_m^{(3)}(\gamma, \xi_>) \left[Ro_m^{(1)}(\gamma, \xi_<) - \frac{Ro_m^{(1)}(\gamma, \xi_1)}{Ro_m^{(3)}(\gamma, \xi_1)}\, Ro_m^{(3)}(\gamma, \xi_<) \right] So_m(\gamma, \eta_0)\, So_m(\gamma, \eta) \right\},$$

in which

$$\gamma = \frac{d}{2} \sqrt{k^2 - k_z^2} \tag{3.8.27}$$

When the point source is on the baffle the velocity potential field is everywhere zero. The normal derivative with respect to u_1 on the surface $\xi = \xi_1$ is, however, finite everywhere. Since the Wronskian of the Mathieu radial function is

$$R^{(1)}(c, \xi)\, R^{(3)\prime}(c, \xi) - R^{(1)\prime}(c, \xi)\, R^{(3)}(c, \xi) = i \tag{3.8.28}$$

in which the derivatives are taken with respect to u [12] it follows that for source point(ξ_0, η_0, z_0) and observation point $(\xi_1; \eta, z)$,

$$\left. \frac{\partial G(\vec{r}\,|\,\vec{r}_0;\, k)}{\partial u_<} \right|_{u_< = u_1} = - \int_{-\infty}^{\infty} \frac{dk_z}{2\pi}\, e^{ik_z(z-z_0)}$$

$$\times \sum_{m=0}^{\infty} \left\{ \frac{1}{\Omega_m^{(e)}}\, \frac{Re_m^{(3)}(\gamma, \xi_0)}{Re_m^{(3)}(\gamma, \xi_1)}\, Se_m(\gamma, \eta_0)\, Se_m(\gamma, \eta) + \right. \tag{3.8.29}$$

$$\left. + \frac{1}{\Omega_m^{(0)}}\, \frac{Ro_m^{(3)}(\gamma, \xi_0)}{Ro_m^{(3)}(\gamma, \xi_1)}\, So_m(\gamma, \eta_0)\, So_m(\gamma, \eta) \right\}.$$

In the farfield, for source point at (ξ_0, η_0, o) and observation point at (r, θ, η), r being the radial distance from the origin of coordinates to the observation point, and θ the polar angle measured from the z-axis, the field is:

$$G(r, \theta, \eta | \xi_0, \eta_0, 0; k) = \frac{1}{\sqrt{2\pi}} \frac{e^{ikr}}{kr} \sum_{m=0}^{\infty} (-i)^m \left\{ \frac{1}{\overline{\Omega}_m^{(e)}} \left[Re_m^{(1)}(c \sin\theta, \xi_0) - \right.\right.$$

$$\left. - \frac{Re_m^{(1)}(c \sin\theta, \xi_1)}{Re_m^{(3)}(c \sin\theta, \xi_1)} Re_m^{(3)}(c \sin\theta, \xi_0) \right] Se_m(c \sin\theta, \eta_1)\, Se_m(c \sin\theta, \eta) +$$

$$+ \frac{1}{\overline{\Omega}_m^{(0)}} \left[Ro_m^{(1)}(c \sin\theta, \xi_0) - \frac{Ro_m^{(1)}(c \sin\theta, \xi_1)}{Ro_m^{(3)}(c \sin\theta, \xi_1)} Ro_m^{(3)}(c \sin\theta, \xi_0) \right] \quad (3.8.30)$$

$$\left. \times So_m(c \sin\theta, \eta_0)\, So_m(c \sin\theta, \eta) \right\},$$

where
$$\overline{\Omega}_m^{(e),(0)} = \left| \Omega_m^{(e),(0)} \right|_{\gamma = c \sin\theta} \quad (3.8.31)$$

In the derivation of this formula one uses

$$\lim_{\xi \to \infty} Re_m^{(3)}(\gamma, \xi) \sim \frac{(-i)^m e^{-i\pi/4} e^{i\gamma\xi}}{\sqrt{\gamma\xi}} \quad (3.8.32)$$

This formula is valid when γ is replaced by $c(= kd/2)$.

baffle is rigid at $\xi = \xi_1$: Source point is at (ξ_0, η_0, z_0); observation point is at $(\xi_<, \xi_>; \eta; z)$:

$$G(\xi, \eta, z | \xi_0, \eta_0, z_0) = i \int_{-\infty}^{\infty} \frac{dk_z}{2\pi} e^{ik_z(z - z_0)} \times \sum_{m=0}^{\infty} \left\{ \frac{1}{\Omega_m^{(e)}} Re_m^{(3)}(\gamma, \xi_>) \right. \quad (3.8.33)$$

$$\times \left[Re_m^{(1)}(\gamma, \xi_<) - \frac{Re_m^{(1)\prime}(\gamma, \xi_1)}{Re_m^{(3)\prime}(\gamma, \xi_1)} Re_m^{(3)}(\gamma, \xi_<) \right] Se_m(\gamma, \eta_0)\, Se_m(\gamma, \eta) +$$

$$\left. + \frac{1}{\Omega_m^{(0)}} Ro_m^{(3)}(\gamma, \xi_>) \left[Ro_m^{(1)}(\gamma, \xi_<) - \frac{Ro_m^{(1)\prime}(\gamma, \xi_1)}{Ro_m^{(3)\prime}(\gamma, \xi_1)} Ro_m^{(3)}(\gamma, \xi_<) \right] So_m(\gamma, \eta_0)\, So_m(\gamma, \eta) \right\},$$

The subscripts of $\xi_<, \xi_>$ are defined in 3.5.3. When the observation point (ξ_1, η, z) is on the baffle but the source point (ξ_0, η_0, z_0) is off the baffle the calculation of the field is simplified by use 3.8.28,

$$G(\xi_1, \eta, z | \xi_0, \eta_0, z_0; k) = - \int_{-\infty}^{\infty} \frac{dk_z}{2\pi} e^{ik(z - z_0)}$$

$$\times \sum_{m=0}^{\infty} \left\{ \frac{1}{\Omega_m^{(e)}} \frac{Re_m^{(3)}(\gamma, \xi_0)}{(\partial/\partial u_1) Re_m^{(3)}(\gamma, \xi_1)} Se_m(\gamma, \eta_0)\, Se_m(\gamma, \eta) + \right. \quad (3.8.34)$$

$$\left. + \frac{1}{\Omega_m^{(e)}} \frac{Ro_m^{(3)}(\gamma, \xi_0)}{(\partial/\partial u_1) Ro_m^{(3)}(\gamma, \xi_1)} So_m(\gamma, \eta_0)\, So_m(\gamma, \eta) \right\}.$$

The farfield of 3.8.32 generated by a source point at $(\xi_0, \eta_0, 0)$ can be written in terms of spherical coordinates r, θ as measured from the origin of coordinates:

$$G(r, \theta, \eta | \xi_0, \eta_0, 0) = \frac{1}{\sqrt{2\pi}} \times \frac{e^{ikr}}{kr} \sum_{m=0}^{\infty} (-i)^m \left\{ \frac{1}{\overline{\Omega}_m^{(e)}} \left[Re_m^{(1)}(c \sin\theta, \xi_0) - \right.\right.$$

$$\left. - \frac{Re_m^{(1)\prime}(c \sin\theta, \xi_1)}{Re_m^{(3)\prime}(c \sin\theta, \xi_1)} Re_m^{(3)}(c \sin\theta, \xi_0) \right] Se_m(c \sin\theta, \eta_0)\, Se_m(c \sin\theta, \eta) +$$

$$+ \frac{1}{\overline{\Omega}_m^{(0)}} \left[Ro_m^{(1)}(c \sin\theta, \xi_0) - \frac{Ro_m^{(1)\prime}(c \sin\theta, \xi_1)}{Ro_m^{(3)\prime}(c \sin\theta, \xi_1)} Ro_m^{(3)}(c \sin\theta, \xi_0) \right]$$

$$\left. \times So_m(c \sin\theta, \eta_0)\, So_m(c \sin\theta, \eta) \right\}, \qquad (3.8.35)$$

Here, $\overline{\Omega}_m^{(e),(0)}$ is defined by 3.8.31.

When the source point is on the rigid baffle $\xi = \xi_1$ the field generated anywhere is,

$$G(\xi, \eta, z | \xi_1, \eta_0, z_0) = -\int_{-\infty}^{\infty} \frac{dk_z}{2\pi} e^{ik_z(z-z_0)}$$

$$\times \sum_{m=0}^{\infty} \left\{ \frac{1}{\Omega_m^{(e)}} \frac{Re_m^{(3)}(\gamma, \xi)}{(\partial/\partial u_1) Re_m^{(3)}(\gamma, \xi_1)} Se_m(\gamma, \eta_0)\, Se_m(\gamma, \eta) + \right. \qquad (3.8.36)$$

$$\left. + \frac{1}{\Omega_m^{(0)}} \frac{Ro_m^{(3)}(\gamma, \xi)}{(\partial/\partial u_1) Ro_m^{(3)}(\gamma, \xi_1)} So_m(\gamma, \eta_0)\, So_m(\gamma, \eta) \right\},$$

in which γ is given by 3.8.27. Placing the source on the baffle at $z_0 = 0$ allows one to find the farfield of 3.8.36 in a direct way:

$$G(r, \theta, \eta; \xi_1, \eta_0, 0) = \frac{i}{\sqrt{2\pi}} \times \frac{e^{ikr}}{kr} \sum_{m=0}^{\infty} (-i)^m \left\{ \frac{Se_m(c \sin\theta, \eta_0)\, Se_m(c \sin\theta, \eta_1)}{\overline{\Omega}_M^{(e)} (\partial/\partial u_1) Re_m(c \sin\theta, \xi_1)} + \right.$$

$$\left. + \frac{So_m(c \sin\theta, \eta_0)\, So_m(c \sin\theta, \eta)}{\overline{\Omega}_M^{(0)} (\partial/\partial u_1) Ro_m^{(3)}(c \sin\theta, \xi_1)} \right\}. \qquad (3.8.37)$$

$\overline{\Omega}_m^{(e),(0)}$ is defined in 3.8.31.

RADIATION FIELD OF A LINE SOURCE ADJACENT TO, AND PARALLEL WITH, AN ELLIPTIC CYLINDER

This line source, of radiation velocity potential given by,

$$\hat{\Phi}(\vec{r}_0) = \Phi \delta(\vec{\varrho} - \vec{\varrho}_0)\, e^{-i\omega t}\, \vec{z}_0 \qquad \text{(units: } m^2 s^{-1} m^{-2})$$

is associated with a Green's function for free space,

$$G(\vec{\varrho}\,|\,\vec{\varrho}_0;\, k_t) = \frac{i}{4}\, H_0^{(1)}(k_t|\vec{\varrho} - \vec{\varrho}_0|)$$

The expansion of $H_0^{(1)}(k, \varrho)$ in elliptic coordinates is given in 3.8.26. The radiated velocity potential field of a continuum of line sources on a surface $S(\varrho)$ coaxial with the z-axis, is,

$$\psi = \int_S G(\vec{\varrho}\,|\,\vec{\varrho}_0;\, k_t)\, \Psi(\vec{\varrho}_0)\, dS(\vec{\varrho}_0)$$

The 2-D fields for the cases of a pressure-release baffle and rigid baffle are listed here for two choices of source points and observation points.

pressure release at surface $\xi = \xi$

(1) line source at (ξ_0, η_0); observation point at (ξ, η).

$$G(\xi, \eta\,|\,\xi_0, y_0;\, k_t) = \frac{i}{4}\, \Bigg\{ 4 \sum_{m=0}^{\infty} \Bigg\{ \frac{1}{\Omega_m^{(e)}} \left[Re_m^{(1)}(c, \xi_<) - \frac{Re_m^{(1)}(c, \xi_1)}{Re_m^{(3)}(c, \xi_1)}\, Re_m^{(3)}(c, \xi_<) \right]$$

$$\times\, Re_m^{(3)}(c, \xi_>)\, Se_m(c, \eta_0)\, Se_m(c, \eta) +$$

$$+ \frac{1}{\Omega_m^{(0)}} \left[Ro_m^{(1)}(c, \xi_<) - \frac{Ro_m^{(1)}(c, \xi_1)}{Ro_m^{(3)}(c, \xi_1)}\, Ro_m^{(3)}(c, \xi_<) \right]$$

$$\times\, Ro_m^{(3)}(c, \xi_>)\, So_m(c, \eta_0)\, So_m(c, \eta) \Bigg\} \Bigg\}. \qquad (3.8.38)$$

The subscripts in $\xi_<, \xi_>$ are defined in 3.5.3.

(2) line source at (ξ_0, η_0); observation point in the farfield at (ξ, η). The asymptotic points obtained by use of 3.8.32 and 3.8.26,

$$\lim_{\xi \to \infty} G(\xi, \eta\,|\,\xi_0, \eta_0;\, k_t) \to \frac{i}{4}\, \Bigg\{ \sum_{m=0}^{\infty} \frac{4(-i)^m\, e^{i(c\xi - m\cdot\frac{\pi}{4}}}{\sqrt{c\xi}}$$

$$\times \Bigg\{ \frac{1}{\Omega_m^{(e)}} \left[Re_m^{(1)}(c, \xi_0) - \frac{Re_m^{(1)}(c, \xi_1)}{Re_m^{(3)}(c, \xi_1)}\, Re_m^{(1)}(c, \xi_0) \right]$$

$$\times\, Se_m(c, \eta_0)\, Se_m(c, \eta) +$$

$$+ \frac{1}{\Omega_m^{(0)}} \left[Ro_m^{(1)}(c, \xi_0) - \frac{Ro_m^{(1)}(c, \xi_1)}{Ro_m^{(3)}(c, \xi_1)}\, Ro_m^{(3)}(c, \xi_0) \right] So_m(c, \eta_0)\, So_m(c, \eta) \Bigg\} \Bigg\}. \qquad (3.8.39)$$

baffle is rigid at $\xi = \xi_1$

(1) line source at (ξ_0, η_0); observation point at (ξ, η):

$$G(\xi, \eta | \xi_0, \eta_0; k_1) = \frac{i}{4} \times 4 \sum_{m=0}^{\infty} \left\{ \frac{1}{\Omega_m^{(e)}} \left[Re_m^{(1)}(c, \xi_<) - \frac{Re_m^{(1)\prime}(c, \xi_1)}{Re_m^{(3)\prime}(c, \xi_1)} Re_m^{(3)}(c, \xi_<) \right] \right.$$
$$\times Re_m^{(3)}(c, \xi_>) \, Se_m(c, \eta_0) \, Se_m(c, \eta) +$$
$$+ \frac{1}{\Omega_m^{(0)}} \left[Ro_m^{(1)}(c, \xi_<) - \frac{Ro_m^{(1)\prime}(c, \xi_1)}{Ro_m^{(3)\prime}(c, \xi_1)} Ro_m^{(3)}(c, \xi_<) \right]$$
$$\left. \times Ro_m^{(3)}(c, \xi_>) \, So_m(c, \eta_0) \, So_m(c, \eta) \right\}. \tag{3.8.40}$$

(2) line source at (ξ_0, η_0); observation point in the farfield at (ξ, η):

$$\lim_{\xi \to \infty} G(\xi, \eta | \xi_0, \eta_0; k_1) \to \frac{i}{4} \left\{ \sum_{m=0}^{\infty} \frac{4(-i)^m \, e^{ic\xi - im\frac{\pi}{2}}}{\sqrt{c\xi}} \right.$$
$$\times \left\{ \frac{1}{\Omega_m^{(e)}} \left[Re_m^{(1)}(c, \xi_0) - \frac{Re_m^{(1)\prime}(c, \xi_1)}{Re_m^{(3)\prime}(c, \xi_1)} Re_m^{(3)}(c, \xi_0) \right] \right.$$
$$\times Se_m(c, \eta_0) \, Se_m(c, \eta) +$$
$$\left. + \frac{1}{\Omega_m^{(0)}} \left[Ro_m^{(1)}(c, \xi_0) - \frac{Ro_m^{(1)\prime}(c, \xi_1)}{Ro_m^{(3)\prime}(c, \xi_1)} Ro_m^{(3)}(c, \xi_0) \right] So_m(c, \eta_0) \, So_m(c, \eta) \right\}. \tag{3.8.41}$$

3.8d RADIATION FIELDS OF POINT SOURCES AND LINE SOURCES ADJACENT TO A STRIP

In Fig. 3.8.2 the surface $u = 0$ defines a strip. All formulas derived in 3.8.25 through 3.8.39 are applicable to strip if ξ_1 (wherever it occurs) is replaced by 1.

3.8e RADIATION FIELD OF A POINT SOURCE ADJACENT TO A SPHERE

In Fig. 3.8.3 a point source S at (r_0, θ_0, ϕ_0) is placed adjacent to a sphere, radius a, centered at the origin of coordinates x, y, z. The surface of the sphere may have differing local (or point) acoustic impedance. Several cases of acoustic radiation may readily be formulated.

First, in free space, the radiated field is,

$$G(r, \theta, \phi | r_0, \theta_0, \phi_0; k) = e^{ikR}/4\pi R$$

$$G(r, \theta, \phi | r_0, \theta_0, \phi_0; k) = \frac{ik}{4\pi} \sum_{n=0}^{\infty} (2n + 1) \sum_{m=0}^{\infty} \varepsilon_m \frac{(n - m)!}{(n + m)!} \cos[m(\phi - \phi_0)] P_n^m(\cos \theta_0)$$

$$\times P_n^m(\cos \theta) j_n(kr_<) h_n(kr_>). \tag{3.8.42}$$

[13].

Here, $k = \omega/c$; $R = |\vec{r} - \vec{r}_0|$; $\varepsilon_0 = 1$, $\varepsilon_m = 2$ for $m \geqslant 1$; $P_n^m(\cos \theta)$ is the associated Legendre polynomial; j_n, h_n are spherical Bessel and spherical Hankel functions respectively.

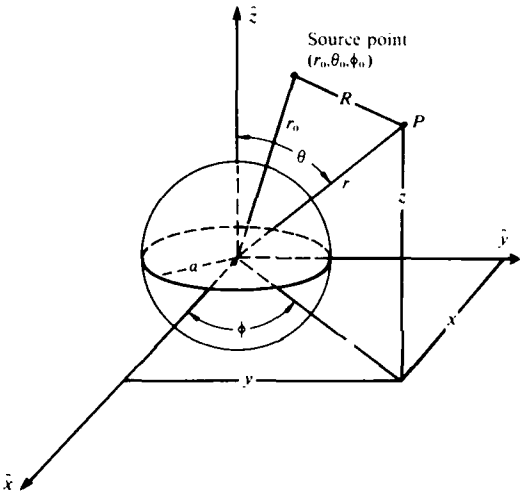

Fig. 3.8.3. Spherical geometry.

When the point source is adjacent to the sphere this field must be modified. We consider two types of spherical surface impedance

surface r = a is pressure-released:

$$G(r, \theta, \phi | r_0, \theta_0, \phi_0; k) = \frac{k}{4\pi} \times$$

$$i \sum_{n=0}^{\infty} \sum_{l=1}^{n} (2n + 1)[j_n(kr_<) - a_n h_n^{(1)}(kr_<)] h_n^{(1)}(kr_>)$$

$$\times \left\{ P_n(\cos \theta_0) P_n(\cos \theta) + 2 \frac{(n - l)!}{(n + l)!} \right.$$

$$\left. \cdot P_n^l(\cos \theta_0) P_n^l(\cos \theta) \cos[l(\phi - \phi_0)] \right\}. \tag{3.8.43a}$$

in which

$$a_n = \frac{j_n(ka)}{h_n^{(1)}(ka)}$$

The factor 2 in the braces arises from $\varepsilon_l = 2$ for $l \geqslant 1$.

When S is on the surface the field everywhere vanishes. However the radial derivative (with respect to $r_<$) is finite. For a source at $r_0 = a$, $\theta_0 = 0$, $\phi_0 = 0$, the terms in l disappear. Because $P_n(1) = 1$ it follows that the derivative field is,

$$\left. \frac{\partial G)r, \theta, \phi | r_0, 0, 0)}{\partial r_<} \right|_{r_< = a} = \frac{ki}{4\pi} \left[- \frac{ik}{(ka)^2} \right] \sum_{n=0}^{\infty} (2n + 1) P_n(\cos \theta) \frac{h_n^{(1)}(kr_0)}{h_n^{(1)}(ka)}. \tag{3.8.43b}$$

This formula is derived by use of the Wronskian identity,

$$W\{j_n(z), h_n^{(1)}(z)\} = j_n h_n' - j_n' h_n = i/(z)^2 \tag{3.8.44}$$

$$j_n' = \frac{dj_n(z)}{dz}\,; \quad \frac{dj_n(kr)}{dr} = kj_n'$$

The farfield for a source at $(r_0, 0, 0)$ is obtained from 3.8.42 by use the asymptotic form,

$$h_n^{(1)}(z) = -i\,\frac{e^{iz}}{z}\,(-i)^n \tag{3.8.45}$$

It is:

$$\lim_{r\to\infty} G(r, \theta | r_0, 0, 0) = \frac{ki}{4\pi} \sum_{n=0}^{\infty} (2n + 1)\,[j_n(kr_0) - a_n h_n^{(1)}(kr_0)]\,(-i)\,\frac{e^{ikr}}{kr}\,(-i)^n$$

$$\times P_n(\cos\theta) \tag{3.8.46}$$

surface $r = a$ is rigid: For a source at r_0, θ_0, ϕ_0 the field is,

$$G(r, \theta, \phi | r_0, \theta_0, \phi_0; k) = \frac{k}{4\pi}\, i \sum_{n=0}^{\infty} \sum_{l=1}^{n} (2n + 1)[j_n(kr_<) - a_n' h_n^{(1)}(kr_<)]h_n^{(1)}(kr_>)$$

$$\times \left\{ P_n(\cos\theta_0)\, P_n(\cos\theta) + 2\,\frac{(n - l)!}{(n + l)!}\, P_n^l(\cos\theta_0)\, P_n^l(\cos\theta)\cos[l(\phi - \phi_0)] \right\}. \tag{3.8.47}$$

$$a_n' = j_n'(z)/h_n^{(1)'}(z)$$

When the point source is situated on the sphere at location $(a, 0, 0)$ the field is obtained by setting $r_< = a$, using 3.8.44, and neglecting all terms in l:

$$G(r, \theta | a, 0, 0) = \frac{ki}{4\pi} \sum_{n=0}^{\infty} (2n + 1) \left[\frac{i}{(ka)^2} \right] \frac{h_n^{(1)}(kr)}{h_n^{(1)'}(ka)} \tag{3.8.48}$$

In the farfield, for a source at $(r_0, 0, 0)$, the field is constructed from 3.8.47, 3.8.49 and from the symmetry in coordinate ϕ which requires all terms in l to vanish:

$$\lim_{r\to\infty} G(r, \theta | r_0, 0, 0; k) = \frac{ki}{4\pi} \sum_{n=0}^{\infty} (2n + 1)[j_n(kr_0) - a_n' h_n^{(1)}(kr_0)] \left[-i\,\frac{e^{ikr}}{kr}\,(-i)^n \right] P_n(\cos\theta) \tag{3.8.50}$$

3.8f RADIATION FIELD OF A HARMONIC POINT SOURCE ADJACENT TO A PROLATE SPHEROID

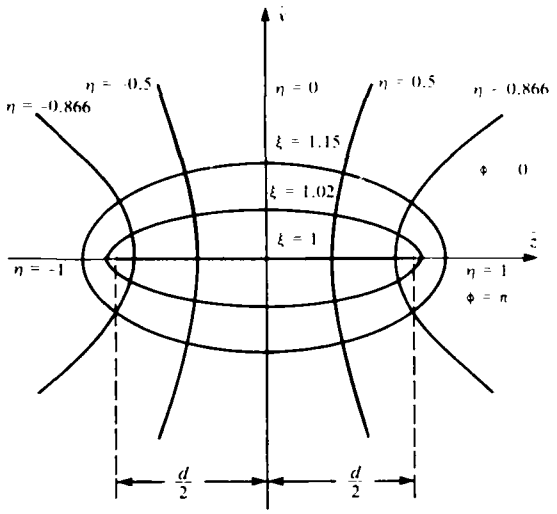

Fig. 3.8.4 Prolate spheroidal geometry.

Prolate spheroidal geometry is shown in Fig. 3.8.4. The axis of rotational symmetry is $\hat{z}$. A brief review of this geometry has been made in Sect. 1.9. A point source at $\vec{r}_0 = (\xi_0, \eta_0, \phi_0)$ generates a field in free space given by

$$G(\vec{r}|\vec{r}_0; k) = \frac{e^{ikR}}{4\pi R}$$

$$R = |\vec{r} - \vec{r}_0|$$

which can be expressed in spheroidal coordinates by

$$G(\xi, \eta, \phi|\xi_0, \eta_0, \phi_0; k) = \frac{ik}{2\pi} \sum_{m=0}^{\infty} \sum_{n=0}^{\infty} \cdot \varepsilon_m \cos m(\phi - \phi_0) \frac{S_{mn}(c, \eta_0) S_{mn}(c, \eta)}{N_{mn}(c)} \times R_{mn}^{(1)}(c, \xi_<) R_{mn}^{(3)}(c, \xi_>) \quad (3.8.51)$$

Here, $S_{mn}(c, \eta)$ is the prolate angular spheroidal wave function; $R_{mn}^{(j)}(c, \xi)$ is the prolate radial spheroidal wave function of kind $j = 1, 2, 3$, $k = \omega/c$; $N_{mn}(c)$ is the normalization of the angular functions; $c = kd/2$; ε_m is the Neumann factor, $\varepsilon_0 = 1$, $\varepsilon_m = 2$ for $m \geq 1$; and the subscripting in $\xi_<$, $\xi_>$ is defined in 3.5.3. A full discussion (but with different notation) of these wave functions can be found in [14]. In the presence of a prolate spheroid this field may be modified. Two cases can be directly formulated:

Surface ξ = const. is pressure release: The field at $\vec{r} = (\xi, \eta, \phi)$ due to a source at $\vec{r}_0 = (\xi_0, \eta_0, \phi_0)$ is,

$$G(\xi, \theta, \phi|\xi_0, \theta_0, \phi_0; k) = \frac{k}{2\pi} i \sum_{m=0}^{\infty} \sum_{n=m}^{\infty} \frac{\varepsilon_m}{N_{mn}} \times \left[R_{mn}^{(1)}(c, \xi_<) - \frac{R_{mn}^{(1)}(c, \xi_1)}{R_{mn}^{(3)}(c, \xi_1)} R_{mn}^{(3)}(c, \xi_<)\right] R_{mn}^{(3)}(c, \xi_>) \times S_{mn}(c, \eta_0) S_{mn}(c, \eta) \cos m(\phi - \phi_0). \quad (3.8.52)$$

The normal derivative of the field on the surface $\xi = \xi_1$ due to a point source at $\vec{r}_0 = (\xi_0, \eta_0, \phi_0)$ is obtained from 3.8.52 by use of the Wronskian

$$W\{R_{mn}^{(1)}(c,\xi),\, R_{mn}^{(3)}(c,\xi)\} = \frac{i}{c(\xi^2-1)} = R_{mn}^{(1)}R_{mn}^{(3)\prime} - R_{mn}^{(1)\prime}R_{mn}^{(3)}$$

$$R_{mn}'(c,\xi) \equiv \frac{d}{d\xi}\, R_{mn}^{(1)} \tag{3.8.53}$$

$$\frac{\partial G}{\partial \xi}\,(\xi_1,\theta,\phi\,|\,\xi_0,\eta_0,\phi_0;k) = \frac{ki}{2\pi} \times \sum_{m=0}^{\infty}\sum_{n=m}^{\infty} \frac{\varepsilon_m}{N_{mn}(c)} \times \left[\frac{-i}{c(\xi_1^2-1)}\right] \frac{R_{mn}^{(3)}(c,\xi_0)}{R_{mn}^{(3)}(c,\xi_1)}$$

$$\times S_{mn}(c,\eta)\, S_{mn}(c,\eta_0)\cos m(\phi-\phi_0) \tag{3.8.54}$$

The farfield due to a point source at $\vec{r}_0 = (\xi_0, \eta_0, \phi_0)$ is obtained by noting that,

$$R_{mn}^{(3)}(c,\xi) \to (-i)\,(-i)^{-n}\,\frac{e^{ic\xi}}{c\xi} \tag{3.8.55}$$

Thus,

$$\lim_{c\xi\to\infty} G(\xi,\eta,\phi\,|\,\xi_0,\eta_0,\phi_0;k) = \frac{ki}{2\pi}\,(-i)\,\frac{e^{ic\xi}}{c\xi} \sum_{m=0}^{\infty}\sum_{n=m}^{\infty} \varepsilon_m \frac{(-i)^n}{N_{mn}} \left[R_{mn}^{(1)}(c,\xi_0) - \frac{R_{mn}^{(1)}(c,\xi_1)}{R_{mn}^{(3)}(c,\xi_1)}\, R_{mn}^{(3)}(c,\xi_0)\right]$$

$$\times S_{mn}(c,\eta_0)\, S_{mn}(c,\eta)\cos m(\phi-\phi_0). \tag{3.8.56}$$

surface $\xi = \xi_1$ is rigid: The field at $\vec{r} = (\xi,\eta,\phi)$ due to a point source at $\vec{r}_0 = (\xi_0,\theta_0,P_0)$ is,

$$G(\xi,\eta,\phi\,|\,\xi_0,\eta_0,\phi_0;k) = \frac{ki}{2\pi} \times \sum_{m=0}^{\infty}\sum_{n=m}^{\infty} \frac{\varepsilon_m}{N_{mn}}$$

$$\times \left[R_{mn}^{(1)}(c,\xi_<) - \frac{R_{mn}^{(1)\prime}(c,\xi_1)}{R_{mn}^{(3)\prime}(c,\xi_1)}\, R_{mn}^{(3)}(c,\xi_<)\right]$$

$$\times R_{mn}^{(3)}(c,\xi_>)\, S_{mn}(c,\eta_0)\, S_{mn}(c,\eta)\cos m(\phi-\phi_0). \tag{3.8.57}$$

in which,

$$R_{mn}^{(3)\prime}(c,\xi) = \frac{d}{d\xi}\, R_{mn}^{(3)}(c,\xi)$$

On the surface $\xi = \xi_1 = \text{const.}$ we set $\xi_< = \xi_1$ and $\xi_> = \xi_0$. By use of 3.8.53 the surface field due to the source at (ξ_0,η_0,ϕ_0) is,

$$G(\xi_1, \eta, \phi | \xi_0, \eta_0, \phi_0; k) = \frac{ki}{2\pi} \sum_{m=0}^{\infty} \hat{\sum_{n=m}} \frac{\varepsilon_m}{N_{mn}(c)} \left[\frac{i}{c(\xi_1^2 - 1)} \right] \frac{R_{mn}^{(3)}(c, \xi_0)}{R_{mn}^{(1)'}(c, \xi_1)} R_{mn}^{(1)}(c, \xi_<)$$

$$\times S_{mn}(c, \eta_0) S_{mn}(c, \eta) \cos m(\phi - \phi_0). \tag{3.8.58}$$

The farfield of a point source at (ξ_0, η_0, ϕ_0) adjacent to the surface $\xi = \xi_1$ is obtained by use of 3.8.54 and 3.8.57:

$$\lim_{c\xi \to \infty} G(\xi, \eta, \phi | \xi_0, \eta_0, \phi_0; k) = \frac{ki}{2\pi} \sum_{m=0}^{\infty} \sum_{n=m}^{\infty} \frac{\varepsilon_m}{N_{mn}(c)} \left[R_{mn}^{(1)}(c, \xi_0) - \frac{R_{mn}^{(1)'}(c, \xi_1)}{R_{mn}^{(3)'}(c, \xi_1)} \right.$$

$$\left. \cdot R_{mn}^{(3)}(c, \xi_0) \right] (-i)(-i)^n \frac{e^{ic\xi}}{c\xi} \times S_{mn}(c, \eta_0) S_{mn}(c, \eta) \cos m(\phi - \phi_0). \tag{3.8.59}$$

3.8g RADIATION FIELD OF A HARMONIC POINT SOURCE ADJACENT TO AN OBLATE SPHEROID

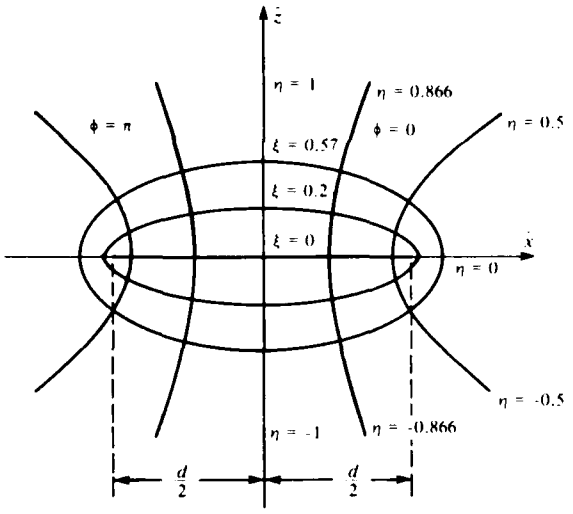

Fig. 3.8.5. Oblate spheroidal geometry.

Oblate spheroidal geometry is shown in Fig. 3.8.5. The axis of rotational symmetry is $\hat{z}$. This geometry was reviewed in Sect. 1.9e in connection with the radiation of sound from oblate spheroids. There it was shown that all formulas for the oblate case are obtainable from the prolate case by the transformation,

$$c \to -ic; \xi \to i\xi \tag{3.8.60}$$

$$N_{mn}(c) \to \tilde{N}_{mn}(-ic)$$

In particular, the free field of a point source at (ξ_0, η_0, ϕ_0) is,

$$G(\xi, \eta, \phi | \xi_0, \eta_0, \phi_0; k) = ik \sum_{m=0}^{\infty} \sum_{n=m}^{\infty} \varepsilon_m \cos m(\phi - \phi_0)$$

$$\times \frac{S_{mn}(-ic, \eta_0) S_{mn}(-ic, \eta)}{\tilde{N}_{mn}(-ic)}$$

$$\times R_{mn}^{(1)}(-ic, i\xi_<) R_{mn}^{(3)}(-ic, i\xi_>) \tag{3.8.61}$$

The same source adjacent to an oblate spheroid radiates an acoustic field whose mathematical description depends on the spheroid's (local) acoustic impedance. Two useful cases are:

surface ξ = const. is pressure release: The field at (ξ, η, ϕ) due to a point source at (ξ_0, η_0, ϕ_0) is given by,

$$G(\xi, \eta, \phi | \xi_0, \eta_0, \phi_0; k) = \frac{ki}{2\pi} \times \sum_{m=0}^{\infty} \sum_{n=m}^{\infty} \frac{\varepsilon_m}{N_{mn}}$$

$$\times \left[R_{mn}^{(1)}(-ic, i\xi_<) - \frac{R_{mn}^{(1)}(-ic, i\xi_1)}{R_{mn}^{(3)}(-ic, i\xi_1)} R_{mn}^{(3)}(-ic, i\xi_<) \right] R_{mn}^{(3)}(-\mathrm{ic}, \mathrm{i}\xi_>)$$

$$\times S_{mn}(-ic, \eta_0) S_{mn}(-ic, \eta) \cos m(\phi - \phi_0). \tag{3.8.62}$$

The normal derivative with respect to ξ of the field on the surface $\xi = \xi_1$ due to a point source at $\vec{r} = (\xi_0, \eta_0, \phi_0)$ is obtained from 3.8.62 by use of the Wronskian determinant,

$$W\{R_{mn}^{(1)}(-ic, i\xi), R_{mn}^{(3)}(-ic, i\xi)\} = \frac{i}{(-ic)[(i\xi)^2 - 1]} = \frac{1}{c[\xi^2 + 1]} \tag{3.8.63}$$

In the present case the Wronskian is negative. Thus, on surface $\xi = \xi_1$,

$$\frac{\partial G}{\partial \xi} (\xi_1, \eta, \phi | \xi_0, \eta_0, \phi_0; k) = \frac{ki}{2\pi} \times \sum_{m=0}^{\infty} \sum_{n=m}^{\infty} \frac{\varepsilon_m}{N_{mn}} \frac{1}{R_{mn}^{(3)}(-ic, i\xi_1)} \left[\frac{-1}{c(\xi^2 + 1)} \right]$$

$$\times R_{mn}^{(3)}(-ic, i\xi_0) S_{mn}(-ic, \eta_0) S_{mn}(-ic, \eta) \cos m(\phi - \phi_0). \tag{3.8.64}$$

The farfield of a point source at (ξ_0, η_0, ϕ_0) is obtained from 3.8.62 by use of the asymptotic form.

$$R_{mn}^{(3)}(-ic, i\xi) \to (-i)(-i)^n \frac{e^{i(-ic)(i\xi)}}{(-ic)(i\xi)} \tag{3.8.65}$$

Thus,

$$\lim_{c\xi \to \infty} G(\xi, \eta, \phi | \xi_0, \eta_0, \phi_0; k) = \frac{ki}{2\pi} (-i) \frac{e^{ic\xi}}{c\xi} \sum_{m=0}^{\infty} \sum_{n=m}^{\infty} \varepsilon_m \frac{(-i)^n}{N_{mn}}$$

$$\left[R_{mn}^{(1)}(-ic, i\xi_0) - \frac{R_{mn}^{(1)}(-ic, i\xi_1)}{R_{mn}^{(3)}(-ic, i\xi_1)} R_{mn}^{(3)}(-ic, i\xi_0) \right]$$

$$\times S_{mn}(-ic, \eta_0) S_{mn}(-ic, \eta) \cos m(\phi - \phi_0). \tag{3.8.66}$$

surface at $\xi = \xi_1$ is rigid: The field at (ξ, η, ϕ) due to a point source at (ξ_0, η_0, ϕ_0) is,

$$G(\xi, \eta, \phi | \xi_0, \eta_0, \phi_0; k) = \frac{ki}{2\pi} \times \sum_{m=0}^{\infty} \sum_{n=m}^{\infty} \frac{\varepsilon_m}{\tilde{N}_{mn}}$$

$$\times \left[R_{mn}^{(1)}(-ic, i\xi_<) - \frac{R_{mn}^{(1)\prime}(-ic, i\xi_1)}{R_{mn}^{(3)\prime}(-ic, i\xi_1)} R_{mn}^{(2)}(-ic, i\xi_<) \right]$$

$$\times R_{mn}^{(3)}(-ic, i\xi_>) S_{mn}(-ic, \eta_0) S_{mn}(-ic, \eta) \cos m(\phi - \phi_0). \tag{3.8.67}$$

When the observation point is on the surface $\xi_< = \xi_1$ and the source point is at (ξ_0, η_0, ϕ_0), the field is obtained by use of the Wronskian 3.8.63. In this case the Wronskian is positive.

$$G(\xi_1, \eta, \phi | \xi_0, \eta_0, \phi_0; k) = \frac{ki}{2\pi} \times \sum_{m=0}^{\infty} \sum_{n=m}^{\infty} \frac{\varepsilon_m}{\tilde{N}_{mn}} \frac{1}{R_{mn}^{(3)\prime}(-ic, i\xi_1)} R_{mn}^{(3)}(-ic, i\xi_0) \left[\frac{1}{c[\xi^2 + 1]} \right]$$

$$\times S_{mn}(-ic, \eta_0) S_{mn}(-ic, \eta) \cos m(\phi - \phi_0). \tag{3.8.68}$$

When the observation point is in the farfield and the source point is at (ξ_0, η_0, ϕ_0) the field is obtained by use of 3.8.65,

$$\lim_{c\xi \to \infty} G(\xi, \eta, \phi | \xi_0, \eta_0, \phi_0; k) = \frac{ki}{2\pi} (-i) \frac{e^{ikc\xi}}{c\xi} \sum_{m=0}^{\infty} \sum_{n=m}^{\infty} \varepsilon_m \frac{(-i)^n}{\tilde{N}_{mn}}$$

$$\left[R_{mn}^{(1)}(-ic, i\xi_0) - \frac{R_{mn}^{(1)\prime}(-ic, i\xi_1)}{R_{mn}^{(3)\prime}(-ic, i\xi_1)} R_{mn}^{(3)}(-ic, i\xi_0) \right]$$

$$\times S_{mn}(-ic, \eta_0) S_{mn}(-ic, \eta) \cos m(\phi - \phi_0). \tag{3.8.69}$$

3.8h RADIATION FIELD OF A HARMONIC POINT SOURCE ADJACENT TO A WEDGE WITH AN INFINITELY LONG EDGE

Fig. 3.8.6 shows the geometry of the wedge excited by point source radiation. Here the closed angle of the wedge is 2Ω. The open angle of the wedge is defined by a parameter ν such that,

$$\nu\pi = 2\pi - 2\Omega \tag{3.8.70}$$

Thus $\nu = 1$ for $\Omega = \pi/2$, and 2 for $\Omega = 0$. For a point source at (P_0, ϕ_0, z_0) the wedge is illuminated with a field

$$g(R; k) = \frac{e^{ikR}}{4\pi R} \tag{3.8.71}$$

This 3-D Green's function is given by 3.8.5. Upon diffraction the total field at p, ϕ, z may be calculated for two cases:

wedge surface is pressure release at $\phi = \Omega$:

$$G(\varrho, \phi, z | \varrho_0, \phi_0, z_0; k) = \frac{i}{4\pi\nu} \times$$

$$\sum_{n=0}^{\infty} \varepsilon_n \sin \frac{n(\phi - \Omega)}{\nu} \sin \frac{n(\phi_0 - \Omega)}{\nu}$$

$$\int_{-\infty}^{\infty} e^{it(z-z_0)} J_\tau(\varrho_< \sqrt{(k^2 - t^2)}) H_\tau^{(1)}(\varrho_> \sqrt{(k^2 - t^2)}) dt, \tag{3.8.72}$$

or, alternatively,

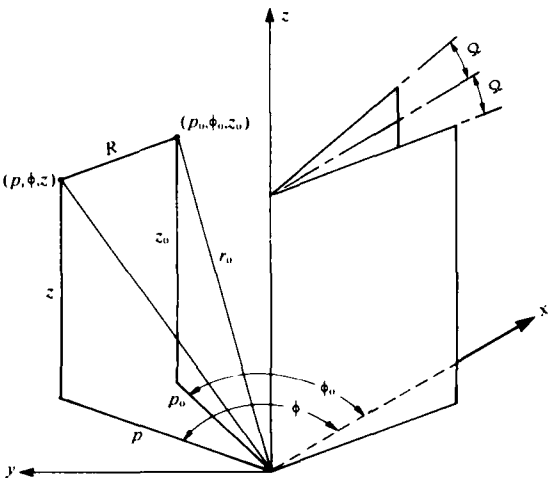

Fig. 3.8.6 Geometry of a wedge for point source radiation.

$$G(\varrho, \phi, z | \varrho_0, \phi_0, z_0; k) = \frac{ki}{2\pi\nu} \sum_{n=0}^{\infty} \varepsilon_n \sin \frac{n(\phi - \Omega)}{\nu} \sin \frac{n(\phi_0 - \Omega)}{\nu}$$

$$\sum_{s=0}^{\infty} \frac{(-\frac{1}{2} k\varrho\varrho_0)^{2s+\tau}}{s!\Gamma(s + \tau + 1)} \frac{h_{2s+\tau}^{(1)}(k\sqrt{\{\varrho^2 + \varrho_0^2 + (z - z_0)^2\}})}{(\sqrt{\{\varrho^2 + \varrho_0^2 + (z - z_0)^2\}})^{2s+\tau}} \tag{3.8.73}$$

[15]. Here $h^{(1)}{}_{2s+\tau}$ is a spherical bessel function of (generally) fractional order and $\tau = n/\nu$.

wedge surface $\phi = \Omega$ *is rigid:*

The radiated field in this case is obtained from 3.8.72, or 3.8.73 by the replacement,

$$\sin \frac{n(\phi - \Omega)}{\nu} \sin \frac{n(\phi_0 - \Omega)}{\nu} \rightarrow \cos \frac{n(\phi - \Omega)}{\nu} \cos \frac{n(\phi_0 - \Omega)}{\nu} \tag{3.8.74}$$

3.8i RADIATION FIELD OF A LINE SOURCE ADJACENT TO, AND PARALLEL WITH, A WEDGE

A line source, parallel with the z-axis of cylindrical coordinates, passes through point ϱ_0, ϕ_0 in the xy plane. In the absence of the wedge it radiates a field,

$$G(\vec{\varrho} | \vec{\varrho}_0; k_t) = \frac{i}{4} H_0^{(1)}(k_t \varrho), \varrho = |\vec{\varrho} - \vec{\varrho}_0|, \vec{\varrho} = (x, y)$$

$$= \frac{i}{4} \sum_{m=-\infty}^{\infty} \cos m(\phi - \phi_0) J_m(k_t \varrho_<) H_m(k_t \varrho_>) \tag{3.8.75}$$

When the wedge is present the radiated field is modified by diffraction. The effect of the wedge depends on the impedance of its walls. Two types of radiation field can be formulated directly. They are [16],

wedge-walls at $|\phi| = |\Omega|$ are pressure release:

The radiated field of the baffled line source is,

$$G(\vec{\varrho}\,|\,\vec{\varrho}_0;\, k_\tau) = \frac{i}{2\pi\nu} \sum_{n=0}^{\infty} \varepsilon_n \sin \frac{n(\phi-\Omega)}{\nu} \sin \frac{n(\phi_0-\Omega)}{\nu} J_\tau(k\varrho_<) H_\tau^{(1)}(k\varrho_>),\ \tau = \frac{n}{\nu}$$

$$= \frac{i}{2\pi\nu} \sum_{n=0}^{\infty} \varepsilon_n \sin \frac{n(\phi-\Omega)}{\nu} \sin \frac{n(\phi_0-\Omega)}{\nu} \sum_{s=0}^{\infty}$$

$$\cdot \frac{(\frac{1}{2}k\varrho\varrho_0)^{2s+\tau}}{s!\Gamma(s+\tau+1)} \frac{H_{2s+\tau}^{(1)}(k\sqrt{(\varrho^2+\varrho_0^2)})}{[\sqrt{(\varrho^2+\varrho_0^2)}]^{2s+\tau}} \tag{3.8.76}$$

wedge-walls at $|\phi| = |\Omega|$ are rigid:

The radiated field of the baffled line source in this case is,

$$G(\vec{\varrho}\,|\,\vec{\varrho}_0;\, k_\tau) = \frac{i}{2\pi\nu} \sum_{n=0}^{\infty} \varepsilon_n \cos \frac{n(\phi-\Omega)}{\nu} \cos \frac{n(\phi_0-\Omega)}{\nu} \times J_\tau(k\varrho_<) H_\tau^{(1)}(k\varrho_>),\ \tau = \frac{n}{\nu}$$

$$= \frac{i}{2\pi\nu} \sum_{n=0}^{\infty} \varepsilon_n \cos \frac{n(\phi-\Omega)}{\nu} \cos \frac{n(\phi_0-\Omega)}{\nu}$$

$$\cdot \sum_{s=0}^{\infty} \frac{(\frac{1}{2}k\varrho\varrho_0)^{2s+\tau}}{s!\Gamma(s+\tau+1)} \frac{H_{2s+\tau}^{(1)}(k\sqrt{(\varrho^2+\varrho_0^2)})}{[\sqrt{(\varrho^2+\varrho_0^2)}]^{2s+\tau}} \tag{3.8.77}$$

Expansions of $J_\tau(k\varrho_<)H_\tau^{(1)}(k\varrho_>)$ in Series

Eqs. 3.8.76, 3.8.77, as well as 3.8.72, 3.8.73, illustrate useful expansions of products of Bessel and Hankel functions of fractional order. They are repeated here for future reference:

$$J_\tau(k\varrho_<) H_\tau^{(1)}(k\varrho_>) = \sum_{s=0}^{\infty} \frac{(\frac{1}{2}k\varrho\varrho_0)^{2s+\tau}}{\Gamma(s+\tau+1)} \frac{H_{2s+\tau}^{(1)}(k\sqrt{(\varrho^2+\varrho_0^2)})}{[\sqrt{\varrho^2+\varrho_0^2}]^{2s+\tau}} \tag{3.8.78}$$

[17] [18].

Also,

$$\frac{i}{2k} \int_{-\infty}^{\infty} e^{ik_z(z-z_0)} J_\tau(\varrho_<\sqrt{k^2-k_z^2}) H_\tau^{(1)}(\varrho_>\sqrt{k^2-k_z^2})\, dk_z$$

$$= i \sum_{s=0}^{\infty} \frac{(\frac{1}{2}k\varrho\varrho_0)^{2s+\tau}}{s!\Gamma(s+\tau+1)} \frac{h_{2s+\tau}^{(1)}(k\sqrt{\varrho^2+\varrho_0^2+(z-z_0)^2})}{[\sqrt{\varrho^2+\varrho_0^2+(z-z_0)^2}]^{2s+\tau}}$$

$$= ie^{-2i\tau\pi} \sum_{s=0}^{\infty} \frac{\Gamma(s+\tau+1)}{S!} (2s+2\tau+1)\, j_{s+\tau}(kr_<)\, h_{s+\tau}^{(1)}(kr_>)$$

$$\times P_{S+\tau}^{\tau}(\cos\theta)\, P_{S+\tau}^{\tau}(\cos\theta_0) \tag{3.8.79}$$

[19]. Here Γ is the gamma function with integer argument.

3.8j RADIATION FIELD OF A HARMONIC POINT SOURCE ADJACENT TO A HALF PLANE

Fig. 3.8.7 shows the geometry associated with the radiation field of a point source located at (ϱ_0, ϕ_0, Z_0) in the presence of a half-plane, $0 \leqslant x < \infty$, $-\infty < z < \infty$. Here, $\vec{\varrho}_0 = (x, y)$ is a vector in the x, y plane while ϕ_0 is the angle it makes with the x-axis. In the absence of the baffle the radiation field is

$$g(\vec{r}|\vec{r}_0|k) = e^{ikR}/4\pi R$$

which is given in cylindrical coordinates by 3.8.5. In the presence of the half-plane the radiation field becomes modified. Two cases can be easily formulated. They are,

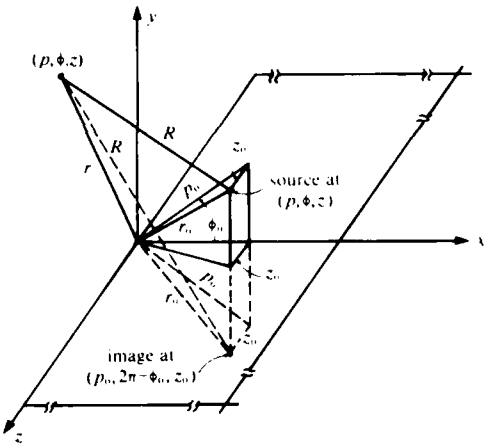

Fig. 3.8.7 Geometry of a point source adjacent to a half plane.

(a) *half-plane is pressure released on both sides*: The radiated field is

$$G(\varrho, \phi, z|\varrho_0, \phi_0, z_0; k) = \frac{i}{8\pi} \sum_{n=0}^{\infty} \varepsilon_n \sin(\tfrac{1}{2}n\phi) \sin(\tfrac{1}{2}n\phi) \cdot \int_{-\infty}^{\infty} dt\, e^{it(z-z_0)} J_\nu[\varrho_< \sqrt{(k^2 - t^2)}\,] H_\nu^{(1)}[\varrho_> \sqrt{(k^2 - t^2)}\,] \tag{3.8.80}$$

in which $\nu = n/2$.

Alternatively, this may be written in the forms,

$$G(\varrho, \phi, z|\varrho_0, \phi_0, z_0; k) = \frac{ki}{4\pi} \sum_{n=0}^{\infty} \varepsilon_n \sin(\tfrac{1}{2}n\phi) \sin(\tfrac{1}{2}n\phi_0) \sum_{s=0}^{\infty} \frac{(\frac{1}{2}k\varrho\varrho_0)^{2s+\nu}}{s!\Gamma(s+\nu+1)} \frac{h_{2s+\nu}^{(1)}(k\sqrt{\{\varrho^2 + \varrho_0^2 + (z-z_0)^2\}})}{(\sqrt{\{\varrho^2 + \varrho_0^2 + (z-z_0)^2\}})^{2s+\nu}} \tag{3.8.81}$$

$$G(\varrho, \phi, z|\varrho_0, \phi_0, z_0; k) = \frac{k}{4\pi} \sum_{n=0}^{\infty} \varepsilon_n \sin(\tfrac{1}{2}n\phi) \sin(\tfrac{1}{2}n\phi_0) \times ie^{-2i\nu\pi} \sum_{s=0}^{\infty} \frac{\Gamma(s+2\nu+1)}{s!} (2s+2\nu+1) j_{s+\nu}(kr_<) h_{s+\nu}^{(1)}(kr_>) P_{s+\nu}^{-\nu}(\cos\theta) P_{s+\nu}^{-\nu}(\cos\theta_0). \tag{3.8.82}$$

[20].

(b) *half plane is rigid on both sides*:

The radiated field is given by the alternative forms 3.8.80, 3.8.81, 3.8.82 excepting that the following change is made:

$$\varepsilon_n \sin\left(\frac{n\phi}{2}\right)\sin\left(\frac{n\phi_0}{2}\right) \to \varepsilon_n \cos\left(\frac{n\phi}{2}\right)\cos\left(\frac{n\phi_0}{2}\right). \tag{3.8.83}$$

3.8k RADIATION FIELD OF A HARMONIC LINE SOURCE ADJACENT TO, AND PARALLEL WITH, THE EDGE OF A HALF-PLANE

In the absence of the half-plane a line source parallel to the z-axis and passing through a point ϱ_0, ϕ_0 in the xy plane radiates a field given by the Hankel function,

$$G(\varrho, \phi, |\varrho_0, \phi_0; k_t) = \frac{i}{4} H_0^{(1)}(kR), R = |\vec{\varrho} - \vec{\varrho}_0|, \varrho = (x, y)$$

When the half-plane is present the radiated field is modified in a manner which depends on the local surface impedance of the plane. Two cases of ideal impedance are:

(a) *the half-plane surface is pressure-released on both sides*:

The radiated field is given by,

$$G(\varrho, \phi|\varrho_0, \phi_0; k_t) = \frac{i}{4} \sum_{n=0}^{\infty} \varepsilon_n \sin\left(\frac{n\phi}{2}\right)\sin\left(\frac{n\phi_0}{2}\right) J_\nu(k_t\varrho_<) H_\nu^{(1)}(k_t\varrho_>) \tag{3.8.84}$$

$$\varepsilon_0 = 1, \varepsilon_n = 2, n \geqslant 1; \nu = n/2$$

The subscripts $<, >$ are explained in 3.5.3. An alternative form is found by use of 3.8.78,

$$G(\varrho, \phi|\varrho_0, \phi_0; k_t) = \frac{i}{4} \sum_{n=0}^{\infty} \varepsilon_n \sin\left(\frac{n\phi}{2}\right)\sin\left(\frac{n\phi_0}{2}\right)$$

$$\sum_{s=0}^{\infty} \frac{\frac{1}{2}(k_t\varrho\varrho_0)^{2s+\nu}}{s!\Gamma(s+\nu+1)} \frac{H_{2s+\nu}^{(1)}(k_t\sqrt{\varrho^2+\varrho_0^2})}{(\sqrt{\varrho^2+\varrho_0^2})^{2s+\nu}} \tag{3.8.85}$$

[21].

(b) *the half plane is rigid on both sides:*

The radiated field is given by 3.8.84 or 3.8.85 excepting that the change 3.8.83 is made.

3.8I RADIATION FIELD OF A HARMONIC POINT SOURCE ADJACENT TO A CONE

Fig. 3.8.8 shows the geometry of a point source at spherical coordinates (r_0, θ_0, ϕ_0) radiating a field to (r, θ, ϕ) in the presence of a cone defined by $\theta = \theta_1$, $\pi/2 \leqslant \theta_1 \leqslant \pi$, or by the interior semi-vertex angle $\delta = \pi - \theta_1$.

In the absence of the cone the field radiated by the point source is proportional to the Green's function for free space,

$$g(\vec{r}|\vec{r}_0; k) = \frac{e^{ikR}}{4\pi R}, \quad R = |\vec{r} - \vec{r}_0|$$

When the cone is introduced the field undergoes a modification dependent on the surface local impedance of the cone. Two cases of ideal impedance are:

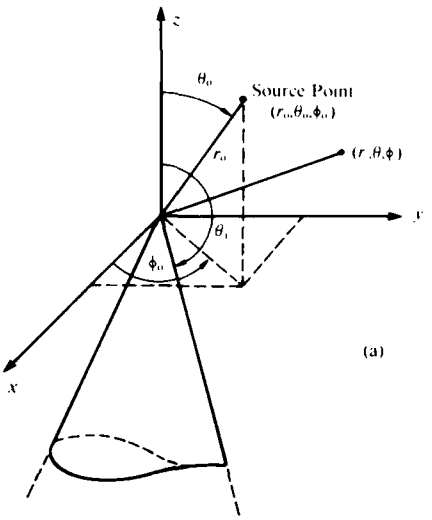

Fig. 3.8.8. Geometry of a point source adjacent to a cone.

(a) *cone surface is pressure released*: The radiated field is given by the modified Green's function,

$$G(r, \theta, \phi|r_0, \theta_0, \phi_0; k) = \frac{k}{4\pi} \times \frac{2i}{\sin\theta_1} \sum_{m=0}^{\infty} \varepsilon_m \cos m(\phi - \phi_0) \sum_{p>0} (2p + 1) j_p(kr_<) h_p^{(1)}(kr_>)$$
$$\times \frac{P_p^m(\cos\theta) P_p^m(\cos\theta_0)}{(\partial/\partial\theta_1) P_p^m(\cos\theta_1) (\partial/\partial p) P_p^m(\cos\theta_1)}, \tag{3.8.86}$$

The summation in p is not over integers, but over the positive roots of an equation in fixed $\theta = \theta_1$:

$$P_p^m(\cos\theta_1) = 0, \; m \text{ integer} \tag{3.8.87}$$

Also, by definition,

$$\frac{\partial}{\partial p} P_p^m(\cos\theta_1) \equiv \left[\frac{\partial}{\partial \nu} P_\nu^m(\cos\theta_1) \right]_{\nu=p} \tag{3.8.88}$$

[22]

(b) *cone surface is rigid*:

$$G(r, \theta, \phi|r_0, \theta_0, \phi_0; k) = \frac{k}{4\pi} \times \frac{-2i}{\sin\theta_1} \sum_{m=0}^{\infty} \varepsilon_m \cos m(\phi - \phi_0) \sum_{q>0} (2q + 1) j_q(kr_<) h_q^{(1)}(kr_>)$$
$$\times \frac{P_q^m(\cos\theta) P_q^m(\cos\theta_0)}{P_q^m(\cos\theta_1) (\partial^2/\partial q \partial\theta_1) P_q^m(\cos\theta_1)}, \tag{3.8.89}$$

By definition,

$$\left(\frac{\partial^2}{\partial q \partial \theta_1} \right) P_q^m(\cos\theta_1) = \left[\left(\frac{\partial^2}{\partial \nu \partial \theta_1} \right) P_\nu^m(\cos\theta_1) \right]_{\nu=q}$$

The summation in q is over all non-negative values of q such that,

$$\left(\frac{\partial}{\partial \theta_1} \right) P_q^{-m}(\cos\theta_1) = 0, \tag{3.8.90}$$

[23].
In 3.8.87, the case m is an integer is treated by the relation,

$$P_\nu^m(\cos\theta_1) = (-1)^m \frac{\Gamma(\nu + m + 1)}{\Gamma(\nu - m + 1)} P_\nu^{-m}(\cos\theta_1) \tag{3.8.91}$$

It follows that the zeros of $P_\nu^{-m}(\cos\theta_1)$ are the same as the zeros of $P_\nu^m(\cos\theta_1)$ along with the $2m$ zeros $\nu = -m, -m+1 \ldots m-1$ of the gamma functions. Furthermore when ν is not an integer the solutions $P_\nu^m(\cos\theta)$ and $P_\nu^m(-\cos\theta)$ are independent. Their Wronskian is,

$$\begin{aligned} &P_\nu^m(\cos\theta) \frac{d}{d\theta_1} P_\nu^m(-\cos\theta_1) - P_\nu^m(-\cos\theta_1) \frac{d}{d\theta_1} P_\nu^m(\cos\theta_1) \\ &= \frac{2}{\pi} \frac{\sin(\nu - m)\pi}{\sin\theta_1} \frac{\Gamma(\nu + m + 1)}{\Gamma(\nu - m + 1)} \end{aligned} \tag{3.8.92}$$

From this relation one may obtain expressions for derivatives needed in 3.8.90.

3.8m RADIATION FIELDS OF HARMONIC MULTIPOLES ABOVE A PLANE

Eqs. 3.7.24 and 3.7.25 give the radiation fields of a monopole source above a pressure release plane, and a rigid plane, respectively, expressed in cylindrical coordinates. When the surface impedance of the plane is neither pressure-release nor rigid the Green's function can still be found by use of a surface reflection coefficient Γ. To simplify the formulation let the point source be located at $\varrho_0 = 0$, $\phi_0 = 0$, $z = z_0$. Then, in 3.7.39, $m = 0$, $J_0(0) = 1$, and the free field becomes,

$$\begin{aligned} G(\varrho, \phi, z|0, 0, z_0; k) &= \frac{i}{8\pi} \int_{-\infty(C_1)}^{\infty} d\xi\, \xi\, H_0^{(1)}(\xi\varrho) \frac{\exp i\sqrt{k^2 - \xi^2}\,|z - z_0|}{\sqrt{k^2 - \xi^2}} \\ &= \frac{e^{ikR}}{4\pi R} \end{aligned} \tag{3.8.93}$$

where

$$R = \sqrt{\varrho^2 + (z - z_0)^2}$$

and C_1 is a contour of integration on the complex ξ-plane. In the presence of an infinite plane with finite specific impedance $z(\omega)$ the monopole Green's function becomes,

$$G(\varrho, \phi, z|0, 0, z_0; k) = \frac{i}{8\pi} \int_{\infty(C_1)}^{\infty} d\xi\, \xi \frac{H_0^{(1)}(\xi\varrho)}{\sqrt{k^2 - \xi^2}} \left[e^{i\sqrt{k^2 - \xi^2}\,|z - z_0|} + \Gamma(\sqrt{k^2 - \xi^2})\, e^{-i\sqrt{k^2 - \xi^2}\,(z + z_0)} \right] \tag{3.8.94}$$

Now,

$$\Gamma = \frac{\sqrt{k^2 - \xi^2} - k \dfrac{\varrho_m c}{z(\omega)}}{\sqrt{k^2 - \xi^2} + k \dfrac{\varrho_m c}{z(\omega)}} \tag{3.8.95}$$

in which ϱ_m is the mass density of the material of the plane, and c is its sound speed. Fig. 3.8.9 shows the relation of k, ξ, $k_z (= \sqrt{k^2 - \xi^2})$. In terms of angle θ, 3.8.95 becomes,

$$\Gamma = \frac{z(\omega)\cos\theta - \varrho c}{z(\omega)\cos\theta + \varrho c} \tag{3.8.96}$$

[24]. The two cases of ideal impedance ("soft", "hard") are easily derived: when the plane is pressure-release (= soft) $z(\omega) = 0$ and $\Gamma = -1$. Use of transformation 3.7.41 then leads directly into 3.7.24. Similarly, when the plane is rigid, $z(\omega) \to \infty$, $\Gamma = +1$, and transformation 3.7.41 leads to 3.7.25.

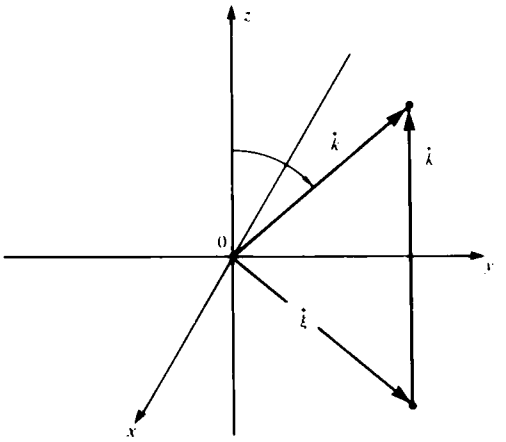

Fig. 3.8.9. The wavevector $\vec{k}$ and its components.

The same physical problem can be expressed in spherical coordinates. Let the origin be at $\vec{r} = (r, \theta, \varphi) = (0, 0, 0)$. A monopole placed at the origin radiates a free field proportional to the Green's function: $(i\,k/4\pi)\, h_0^{(1)}(kr)$ where $h_0^{(1)}(kr)$ is the spherical Hankel function [25]. This free field is modified when there is an impedance plane at $-z_0$. The image of the monopole in this plane is located at $(r_0 = 2z_0, \theta_0 = \pi, \phi_0 = 0)$. If it were radiating in free space its free field would be proportional to the Green's function 3.8.42, selected for the case $m = 0$, and $r < r_0 = 2z_0$:

$$G(r, \theta | 2z_0, \pi, 0) = \frac{ik}{4\pi} \sum_{n=0}^{\infty} (2n + 1)\, P_n(\pi)\, P_n(\cos\theta)\, j_n(kr)\, h_n(2kz_0) \tag{3.8.97}$$

The total field of monopole plus image would therefore be,

$$G(r, \theta | r_0 = z_0, 0, 0) = \frac{ik}{4\pi} \left[h_0^{(1)}(k_z) + \Gamma(k_z) \sum_{n=0}^{\infty} (2n + 1)(-1)^n P_n(\cos\theta)\, j_n(kr)\, h_n(2kz_0) \right] \tag{3.8.98}$$

where $P_n(\pi) = (-1)^n$.

The radiation field of harmonic dipoles and quadrupoles above a plane can be found by use of 3.3.28. In the case of a dipole of (vector) source strength $\vec{D}$ (units: $m^4 s^{-1}$) the velocity potential at field point $\vec{r}$ due to a dipole at $\vec{r}_0$ is:

$$\psi(\vec{r}) = \vec{D} \cdot (\vec{\nabla}_0 G(\vec{r} | r_0; k)), \tag{3.8.99}$$

$$\vec{\nabla}_0 = \hat{i} \frac{\partial}{\partial x_0} + \hat{j} \frac{\partial}{\partial y_0} + \hat{k} \frac{\partial}{\partial z_0} \tag{3.8.100}$$

in which the vector operation leads to a sum of 3 scalars. Similarly, in the case of a quadrupole of (tensor) source strength $\vec{\vec{Q}}$ (units: m^5s^{-1}) the velocity potential at field point $\vec{r}$ is,

$$\psi(\vec{r}) = \vec{\vec{Q}} : (\vec{\nabla}_0 G(\vec{r}|\vec{r}_0; k)\vec{\nabla}_0) \tag{3.8.101}$$

in which the tensor operation leads to a sum of 9 scalars, as explained in the discussion of 3.3.28.

Eq. 3.8.99 gives the radiated field for any orientation of a dipole. Let the dipole be at ($r_0 = z_0$, 0, 0), and let its vector source strength have components (D_x, D_y, D_z). Now, although the dipole is at the origin of coordinates, its derivative do not vanish. It is seen that since $\vec{R} = \vec{r} - \vec{r}_0$, the gradient with respect to $\vec{r}_0$ is the negative of the gradient with respect to R. Thus in the first term of 3.8.98 $\nabla_0 G = -\nabla G$. In the second term one changes $\partial/\partial y_0$, $\partial/\partial y_0$ into $-\partial/\partial x$, $-\partial/\partial x$; however, since the image source is at $z = -2z_0$, it is seen that $\partial/\partial z_0 = \partial/\partial z$ because of the negative sign. Upon carrying through the gradient operation it is found that the velocity potential of a dipole in the presence of a plane surface is,

$$\begin{aligned}\psi(\vec{r}) &= D_x[A Y_{11}^{(c)} + \Gamma B(Y_{1,n-1}^{(e)} j_{n-1} + Y_{1,n+1} j_{n+1})] \\ &+ D_y[A Y_{11}^{(0)} + \Gamma B(Y_{1,n-1}^{(0)} j_{n-1} + Y_{1,n+1}^{(0)} j_{n+1})] \\ &+ D_z\{A Y_{01}^{(c)} + \Gamma B[n Y_{0,n-1} j_{n-1} - (n+1) Y_{0,n-1} j_{n-1}]\} \\ A &= \frac{1 - ikr}{4\pi r^2} e^{ikr};\ B = \frac{ik^2}{4\pi} \sum_{n=0}^{\infty} (-1)^n h_n(2kz_0)\{\quad\}\end{aligned} \tag{3.8.102}$$

[26]. Here, $Y_{mn}^{(c),(0)}$ are spherical harmonics defined as,

$$Y_{mn}^{(c)} = \cos(m\phi) P_n^m(\cos\theta),\ n = 0, 1, 2 \ldots;\ m = 0, 1, 2 \ldots m-1, n$$

$$Y_{mn}^{(0)} = \sin(m\phi) P_n^m(\cos\theta)$$

$$Y_{0n}^{(c)} = P_n(\cos\theta)$$

From the definition of the spherical Hankel function

$$h_1(kr) = -\frac{e^{ikr}}{kr}\left(1 + \frac{i}{kr}\right)$$

it is seen that for a free field ($\Gamma = 0$) the dipole velocity potential is,

$$\psi_D(r, \omega) = \frac{ik^2}{4\pi} e^{i(\omega t - kr)}[D_x Y_{11}^{(c)} + D_y Y_{11}^{(0)} + D_z Y_{01}^{(c)}] e^{i\omega t} \quad \text{(units: } m^2s^{-1}\text{)} \tag{3.8.103}$$

By comparison the velocity potential of a monopole of source strength S_0 (units: m^3s^{-1} is,

$$\psi_M(r, \omega) = \frac{ik}{4\pi} h_0(kr) S_\omega e^{-i\omega t} \qquad \text{(units: } m^2 s^{-1}) \tag{3.8.104}$$

in which

$$h_0(kr) \equiv \frac{e^{ikr}}{ikr}$$

The associated Green's functions are found from 3.8.102, 3.8.103 by omitting the source strengths:

$$g_D = [(g_D)_x, (g_D)_y, (g_D)_z] = \frac{ik^2}{4\pi} h_1(kr) [Y_{11}^{(c)}, Y_{11}^{(0)}, Y_{01}^{(c)}] \tag{3.8.105}$$

$$g_m = \frac{ik}{4\pi} h_0(kr)$$

Eq. 3 8.102 shows that when the source point and observation point are on the half plane ($z_0 = 0$) all terms in B vanish except $n = 1$ because $j_0(0) = 1, j_n(0) = 0, n \neq 1$. The velocity potential for a vertical dipole ($D_x = 0, D_y = 0, D_z$) therefore becomes,

$$\psi(0) = \frac{ik^2}{4\pi} h_1(0) \cos 0^0 - \Gamma \frac{ik^2}{4\pi} h_1(0) \cdot 1 \tag{3.8.106}$$

For a rigid half plane, $\Gamma = +1$, hence $\psi_D(0) = 0$, [27].

APPENDIX TO CHAPTER III

III A.1 EVALUATION OF RADIATION INTEGRALS

Radiation integrals in cylindrical coordinates take on various forms. A typical one is,

$$\vartheta(\varrho,z) = \int_{-\infty}^{\infty} H_n^{(1)}(\xi\varrho)\, e^{\sqrt{k^2-\xi^2}\,|z|}\, f(\xi,\varrho,z)\, d\xi \qquad \text{IIIA.1.1a}$$

An example is the radiation field of a monopole above a plane, 3.8.94, in which,

$$f(\xi,\varrho,z) = \frac{i}{8\pi}\,\xi\left\{\frac{1}{\sqrt{k^2-\xi^2}} + \left[\frac{\sqrt{k^2-\xi^2} - k\,\dfrac{\varrho_m c}{z(\omega)}}{\sqrt{k^2-\xi^2} - k\,\dfrac{\varrho_m c}{z(\omega)}}\right]\frac{\exp(-i\sqrt{k^2-\xi^2}\,(z+|z|))}{\sqrt{k^2-\xi^2}}\right\} \qquad \text{IIIA.1.1b}$$

The various symbols are defined in the text accompanying 3.8.94 and 3.8.95. In particular the entity in square brackets is the reflection coefficient Γ. Such integrals generally cannot be evaluated in closed form. It is customary to approximate them by asymptotic methods. These are described next. Since the integration III A1.1a is to be done in the complex ξ-plane it is necessary to (1) determine the singularities of the integrand (2) define a contour of integration which allows a rapid evaluation of the integral to within an acceptable approximation. As for singularities: first, it is known that the Hankel function $H_n^{(1)}$ ($= J_n + iN_n$) has an isolated singularity at the origin because there the Neuman function N_n approaches negative infinity. In addition the Hankel function is double-valued along the negative real axis, which thus constitutes a branch cut. Second, the function $f(\xi,z)$ given by III A 1.1b, has a pair of branch points at $\xi = \pm k$, because of the factor $\sqrt{k^2-\xi^2}$. Third, the reflection coefficient has poles at $\xi = \pm a$ at which its denominator vanishes. These singularities contribute to the value of the integral in the manner shown below.

To define a contour of integration which allows a rapid evaluation of the integral an observer at field point $\vec{r}$ interprets III A.1.1a as a sum of plane waves issuing from a monopole source point $\vec{r}_0$ and reflected in the plane,

$$\vartheta \propto \sum_n \exp i\vec{K}_n\cdot\vec{r} = \sum_n \exp(ikz\cos w_m + ik\varrho\sin w_n)$$

Here the continuous variable ξ in $\sqrt{k^2-\xi^2}$ $(= k\sqrt{1-(\xi/k)^2} = k\cos w)$ is, for purposes of illustration, temporarily made discrete for each angle w_n of the direction of the nth wave. All those waves in direction K_n which are close to the unique ray governed by Snell's law which connects source and receiver are nearly in phase, hence contribute strongly to the field at $\vec{r}$. These waves are defined by the poles of $f(\xi, z)$ in III A.1.1b. All those waves in directions very different from this ray are mostly out-of-phase, hence cancel each other and contribute little to the field. The objective then is to chose a contour which sums up as economically as posssible the in-phase components and reject the out-of-phase components. Even when the monopole is in a free field there is a unique ray satisfying the condition of a Fermat path, around which in-phase waves yield the field, and far from which they cancel.

Besides these direct rays (or waves) and reflected rays there are other rays which are incident on a plane between two media at the critical angle. They propagate along the boundary and shed energy back into the medium of incidence. Their contribution to the field at $\vec{r}$ is the *lateral wave*. It is calculated by integration around the branch cut generated by $\sqrt{k^2-\xi^2}$.

IIIA. 2 SELECTION OF CONTOURS OF INTEGRATION IN THE ξ-PLANE FOR APPROXIMATE EVALUATION OF RADIATION INTEGRALS

In the radiation integral IIIA.1.1a let $\xi\varrho$ become very large. For this condition let the complex variable ξ be represented by $x + iy$, and let all the exponential factors (including those of $H_n^{(1)}(\xi\varrho)$ and $f(\xi, \varrho, z)$) be represented by $\exp \Omega[u(x, y) + iv(x, y)]$. The integral then becomes asymptotically,

$$\vartheta(\varrho, z) \cong \int_C f(x + iy) \exp\{\Omega[u(x, y) + iv(x, y)]\}\, d(x + iy) \qquad \text{IIIA.2.1}$$

The symbol Ω is a large, positive real parameter, and C is a contour of integration in the ξ-plane selected to permit an approximate evaluation of the integral.

The choice of C depends on these considerations: C is to pass through those values of x, y for which $\exp[\Omega u(x, y)]$ is largest and then through values of x, y such that this exponential falls in value as rapidly as possible to the end points of integration. In addition, in the same range of x, y where the exponential is largest it is desired to suppress rapid oscillations in phase given by $\exp[i\Omega\, v(x, y)]$. These requirements can be satisfied together. First, a (saddle) point $\xi_s\ (x_s, y_s)$ is found which maximizes $\exp[\Omega\, u(x, y)]$. It is that point at which,

$$\frac{\partial u}{\partial x} = \frac{\partial u}{\partial y} = \frac{\partial v}{\partial x} = \frac{\partial v}{\partial y} = 0$$

Second, to force $\exp[\Omega\, u(x, y)]$ to fall away as rapidly as possible from ξ_s, the path C is chosen such that the *change of slope* of u is maximized along an elementary length l of the contour. This is done by projecting a 3-D plot of $u(x, y)$ versus points (x, y) onto the ξ-plane in the form of level lines, then constructing a contour C on this same plane to pass through ξ_s and at the same time so oriented near ξ_s that

$$\frac{\partial^2 u}{\partial \alpha \partial s} = \frac{\partial}{\partial \alpha}\left[\frac{\partial u}{\partial x}\cos\alpha + \frac{\partial u}{\partial y}\sin\alpha\right] = -\frac{\partial u}{\partial x}\sin\alpha + \frac{\partial u}{\partial y}\cos\alpha = 0 \qquad \text{IIIA.2.2.}$$

in which α is the angle which the line element l makes with the x-axis. Since $\partial u/\partial x = \partial v/\partial y$, $\partial u/\partial y = -\partial v/\partial x$, and $\sin\alpha = dy/dl$, $\cos\alpha = dx/dl$, it is seen that IIIA.2.2 is equivalent to the condition that

$$-\frac{\partial v}{\partial l} = 0, \text{ or } v = \text{const.}$$

This means that if the contour C passes through ξ_s and follows a path along which the phase is stationary then the change in slope will be maximized. However, because point ξ_s cannot be either a maximum of $\exp[\Omega\, u(x,y)]$, or a minimum, but must be a *minimax* (or saddle point) [28] there will be two such paths along which the change in slope is maximized. This is discussed below. Along the physically correct path IIIA.2.1 is approximated by removing the oscillatory phase out of the integral sign:

$$\vartheta(\varrho, z) \cong \exp[i\Omega v(\xi_s)] \int_{SDP} f(x, y)\, e^{\Omega u(x,y)}\, d(x + iy) \qquad \text{IIIA.2.4}$$

in which SDP means "steepest descent path."

The selection of SDP near ξ_s gives the most advantageous path along which to evaluate IIIA.2.1 near ξ_s. Along the rest of the contour C one may continue with SDP, or swing over to another convenient path whatever, as long as $\exp[\Omega\, u(x, y)]$ is continuously decreasing as the end points of C are approached.

The two paths in the ξ-plane along which the change in slope of $\exp[\Omega\, u(x, y)]$ is maximized are distinguished by whether the change causes the value of the exponential to increase or decrease. It is often convenient to block out regions surrounding ξ_s in the ξ-plane where the 3-D surface $\exp[\Omega\, u(x, y)]$ is decreasing ("valleys"), or increasing ("mountains"). To do this one makes a Taylor series expansion of the function $q(\xi) = u(x, y) + iv(x, y)$ in small quantities $\xi - \xi_s$:

$$q(\xi) = q(\xi_s) + \frac{q''(\xi_s)(\xi - \xi_s)^2}{2!} + \ldots \qquad \text{IIIA.2.5}$$

in which, by definition, $q'(\xi_s) = 0$, and the primes indicate orders of derivatives. Because q is a complex number one can write,

$$\begin{aligned} \exp[\Omega u(x, y)] &\approx \exp\left|\tfrac{1}{2}\Omega q''(\xi_s)(\xi - \xi_s)^2\right| \cos 2\varphi \\ \exp[i\Omega v(x, y)] &\approx \exp i\left|\tfrac{1}{2}\Omega q''(\xi_s)(\xi - \xi_s)^2\right| \sin 2\varphi \qquad \text{IIIA.2.6} \\ \varphi &= \arg(\xi - \xi_s) + \tfrac{1}{2}\arg q''(\xi_s) \end{aligned}$$

in which the constant term $q(\xi_s)$ is omitted, and *the factor 2 in 2φ is due to the squaring operation.* The required regions are found by assigning lines φ = const. emanating from ξ_s to separate valleys from mountains. These are:

(a) *lines $\varphi = 0$, $\varphi = \pi$*

Here $\cos 2\varphi \approx 1$. Thus $\exp[\Omega\, u(x, y)]$ is positive and increases most rapidly ($\cos 2\varphi$ is largest) with change in ξ away from ξ_s. These lines are therefore paths of steepest ascent (mountain paths).

(b) *lines $\varphi = \pi/2$, $\varphi = -\pi/2$*

Here $\cos 2\varphi \approx -1$. Thus $\exp[\Omega\, u(x, y)]$ is negative and decreases most rapidly with change in ξ away from ξ_s. These lines are therefore paths of steepest descent (valley paths).

(c) *lines $\varphi = \pm \pi/4$, $\varphi = \pm 3\pi/4$*

Here $\cos 2\varphi = 0$. Thus $\exp[\Omega\, u(x, y)] = \text{const.} = 1$. The phase $\exp[i\Omega\, v(x, y)]$ varies most rapidly because $|\sin 2\varphi| = 1$ along these lines with change in ξ away from ξ_s. They are paths of constant level (foot-of-the-mountain paths).

In the nomenclature of saddle points the condition $q'(\xi_s) = 0$ defines a saddle point of order 1. Similarly the two conditions $q'(\xi_s) = 0$, $q''(\xi_s) = 0$ defines a saddle point of order 2. In the case of a second order saddle point IIIA.2.6 changes to,

$$\exp\{\Omega[u(x, y) + iv(x, y)]\} \approx \exp\left|\frac{1}{3!}\, q'''(\xi_s)(\xi - \xi_s)^3\right| (\cos 3\varphi + i \sin 3\varphi)$$

$$\varphi = \arg(\xi - \xi_s) + \frac{1}{3}\arg q'''(\xi_s)$$

A similar set of lines φ = const. can be selected to distinguish mountains from valleys.

The topography of a first order saddle point is shown in Fig. IIIA.2.1 and that of a second order saddle point in Fig. IIIA.2.2,

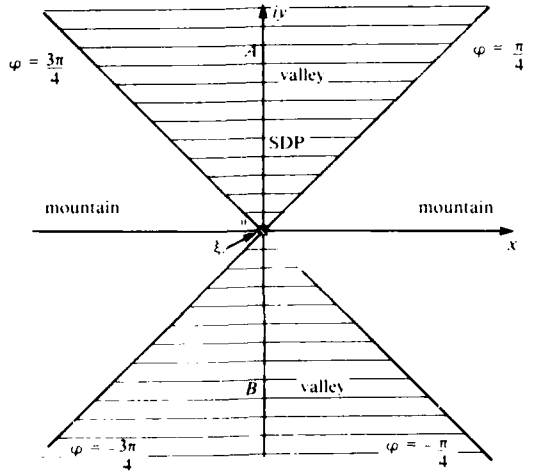

Fig. IIIA.2.1. Topography of a first order saddle point. AB is an SDP.

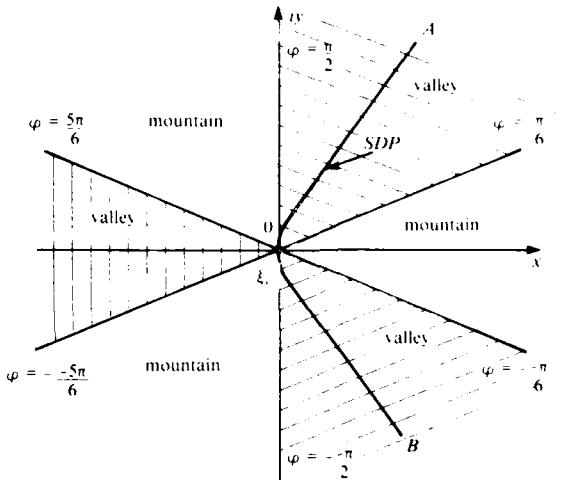

Fig. IIIA.2.2. Topography of a second order saddle point. AB is an SDP.

The mountain-valley topography of an m'th order saddle point can be sketched in a similar fashion to show $m + 1$ mountains and $m + 1$ valleys.

In application the condition $q'(\xi_s) = 0$ may yield two or more saddle point solutions. They can be sketched along the same lines. For example the topography in the ξ-plane of two isolated first-order saddle points is shown in Fig. IIIA.2.3. Each point has two valleys and two mountains; but these must be shared as shown.

IIIA.3 MODAL THEORY OF WAVEGUIDES FOR DISCRETE MODES

In performing the integration of IIIA.1.1 for the case of a source in a bounded medium (or waveguide) it is required to find the poles of the integrand. These correspond to discrete modes of propagation of the radiated field inside the waveguide. A simple waveguide which illustrates this modal theory is a two dimensional structure of plane parallel rigid plates spaced d units apart. The field inside this waveguide is taken in the first instance to be plane waves travelling at angles $\pm \alpha$ with the axial (z-axis) direction. Because the plates are rigid mirror-image waves, representing reflections, are also present. Fig. III.A.3.1 shows a pair of plane propagating waves labelled 1, 2, accompanied by a selected pair of image waves, $R1$, $R2$. Actually, all waves shown are parts of infinite (spatially) periodic trains. This means that labels 1, 2 indicate positions occupied by successive wavefronts of given phase.

The basic requirement for the existence of a mode of propagation is that reflected wavefront $R1$ arrive at position 2 with a phase indentical to the direct wave occupying that position. This requirement is satisfied if the length AB normal to both $R1$ and 2 is an integral number of wavelengths λ:

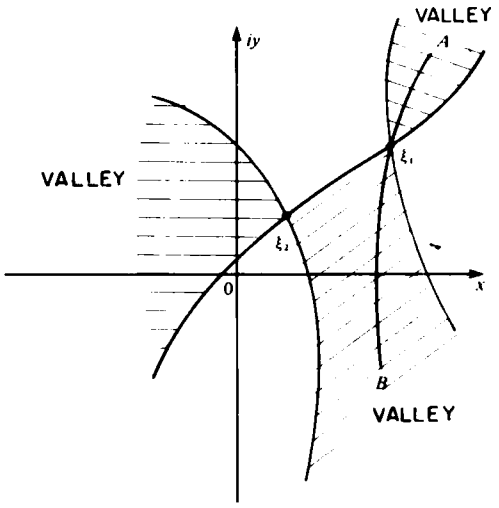

Fig. IIIA.2.3. Topography of two first order saddle points.

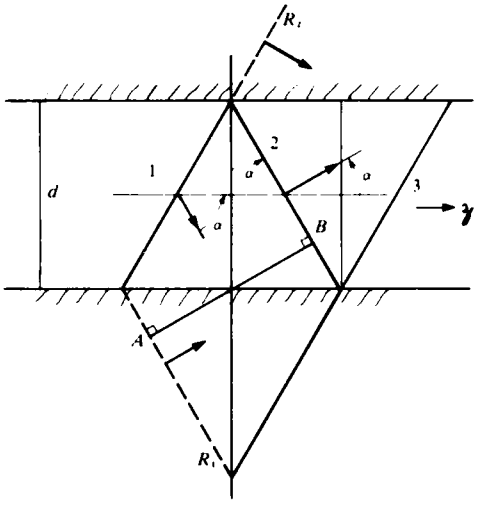

Fig. IIIA.3.1. Plane waves in a parallel plate waveguide.

$$AB = m\lambda, m = 1, 2, 3. \ldots \qquad \text{IIIA.3.1}$$

From geometrical construction this means,

$$2d \sin \alpha = m\lambda \qquad \text{IIIA.3.2}$$

Thus, for fixed λ, m and d, the angle α is fixed: no waves at other directions in the waveguide contribute to this mode:

Eq. IIIA.3.2 has an alternative form which features frequency $f = c/\lambda$ in place of λ, c being the speed of sound,

$$f = \frac{mc}{2d \sin \alpha} \qquad \text{IIIA.3.3}$$

From IIIA.3.2 and IIIA.3.3. one can deduce the following rules:

(1) A specific real mode m can propagate at *any* frequency above a minimum f_{min} determined by $\sin \alpha = 1$,

$$f_{min} = \frac{mc}{2d} \qquad \text{IIIA.3.4}$$

At this minimum (or cut-off) frequency the wavefronts 1, 2 are parallel to the walls of the waveguide.

(2) A mode m can exist at frequencies below f_{min}, but only at imaginary angles $i\beta$:

$$f = \frac{mc}{2d \sin(\pi/2 + i\beta)} = \frac{mc}{2d \cosh \beta} \qquad \text{IIIA.3.5}$$

Mode m in this case is nonpropagating (that is, *evanescent*).

(3) At a fixed frequency, and for a specific waveguide, the number m_{max} of real discrete modes is finite,

$$m_{max} = \frac{2fd}{c}, \sin\alpha = 1 \qquad \text{IIIA.3.6}$$

and the number of discrete evanescent modes is infinite,

$$m = \frac{2fd}{c} \cosh\beta \qquad \text{IIIA.3.7}$$

An alternative way of deriving model transmission in waveguides is to apply the theory of images. Suppose there is a source in a plane parallel waveguide made of acoustically hard walls. Because there are *two* walls there will then be an infinite series of images of this source all located in a line perpendicular to the waveguide passing through the real source. This line of images simulates a (transmission) diffraction grating. If the source is midway between the walls of the waveguide the grating becomes periodic with images separated by distance 2D. Since all the images transmit fields at a single wavelength λ they will interfere destructively with such other (that is, be out of phase) in directions specified by arbitrary angles θ measured relative to the axial direction of the waveguide. However, at particular angles θ_m of transmission all of the image fields are in phase. These are the angles of constructive interference given by,

$$\sin\theta_m = \frac{m\lambda}{2d} \qquad (m = 0, \pm 1, \pm 2 \ldots). \qquad \text{III.A.3.8}$$

The symbol m is the *order of (constructive) interference.* The sum of image fields travelling at angles $\pm\theta_m$ defines the m'th *normal mode.* Since θ_m depends on wavelength λ it is seen that the m'th mode can propagate in the waveguide at any frequency which satisfies the condition III.A.3.8. Thus, it is appropriate to talk of mode m at different frequencies f. As the wavelength changes from λ to λ' the whole set of m modes travel at new angles θ'_m. If a frequency is such that $m\lambda/2d$ is greater than unity then the mode m cannot propagate. This is the condition of cut-off.

When the real source is effectively a point of radiation the maximum (given by III.A.3.8) are all nearly equal amplitude. However, when the real source is spatially finite and comparable to a wavelength in size then it radiates directionally. This means it has its own diffraction pattern which modifies the interference pattern of the periodic grating. The modal amplitudes then have different amplitudes at their reflective angles of travel.

Each mode in a parallel plate waveguide is a superposition of two waves $\exp ik_z z[\exp + ik_m x + \exp - ik_m x]$ in which $k_m = (k^2 - k_z^2)^{1/2}$ (Chap. III). The coordinate X has the range $0 \leqslant x \leqslant d$. Now

$$k_m = k \sin\theta_m = \frac{km\lambda}{2d} = \frac{m\pi}{d}. \qquad \text{III.A.3.9}$$

Hence the analytic form of the travelling modes is,

$$\cos\left(\frac{m\pi x}{d}\right)\exp ik_{z(m)}\left[z - c_m t\right] m = 0, \pm 1, \pm 2, \ldots, \qquad \text{III.A.3.10}$$

The set of an infinite number of modes in coordinate x constitutes an orthogonal basis for the expansion of an arbitrary field in coordinate x. The speed of travel of the *m'th* mode at a specified frequency w (that is, its phase velocity) in a parallel plate waveguide with hard walls is,

$$C_m = \frac{\omega}{k_z} = C_o\sqrt{1-\frac{k_m^2}{k^2}} = \frac{C_o}{\sqrt{1-\frac{\omega_{\theta m}^2}{\omega^2}}}, \omega_{om} = \frac{m\pi C_o}{d} \qquad \text{III.A.3.11}$$

When the radiation signal is a short pulse a time-varying wavefront will be generated containing a wideband of frequencies. Because of the diffraction grating property of the waveguide the source of this signal will excite a field consisting of discrete modes. The number of modes will be determined by the spatial fourier decomposition of the spatially extended source acting an an aperture excitation across the transverse section of the waveguide where it is located. Of the number of excited modes only those that satisfy III.A.3.8 will propagate. Because the radiated sound contains many frequencies the speed of travel of a specified mode will vary with frequency as required by III.A.3.11. The angle θ_m will also vary with each frequency.

Suppose now that a model number m is fixed. It is immediately seen from III.A.3.8 that over a small subband of frequencies there will be a number N of adjacent angles θ_m at which this mode will travel. Thus the field associated with the subband will be given by the sum,

$$\psi_m(x,z,t,N) = \sum_{n=1}^{N} A_n \cos\left(\frac{m\pi x}{d}\right) \cos\left[k_{z(m)}^n z - k_{z(m)}^{(n)} C_{(m)}^{(n)} t\right] \qquad \text{III.A.3.12}$$

Here, the spread of wavenumbers $k_{z(m)}^{(n)}$ and speeds $C_m^{(n)}$ *is* assumed *small* relative to the average wavenumber $\bar{k}_{z(m)}$ and average speed C_m. In order for these *adjacent* N waves to interfere constructively, and therefore build up the field at time t, it is required that their *phases* be nearly the same. This means the time phase ϕ in III.A.3.12 must be stationary over the band of frequencies. Hence;

$$\frac{d\phi}{dk_{z(m)}} = 0 \quad or \quad z - \frac{d}{dk_{z(m)}}[k_{z(m)}\, C_m] \;\; t = 0.$$

This sets the requirement that the group of waves travel at the group velocity,

$$C_{g(m)} = \frac{d}{dk_{z(m)}}\left[k_{z(m)} C_m\right] = \frac{d\omega}{dk_{z(m)}}. \qquad \text{III.A.3.13}$$

Thus over a narrow subband of frequencies the m'th mode, *if present*, will propagate with the group velocity $C_{g(m)}$. For a parallel plate waveguide one may deduce from the relation $k_z^2 = k^2 - k_m^2$ that

$$C_{g(m)} = Co\sqrt{1 - \frac{\omega_{om}^2}{\omega^2}}. \qquad \text{III.A.3.14}$$

This formula indicates that when the m *th* mode of a transient signal is present in the waveguide an observer at a distant point will first observe this mode being carried by high frequencies with the speed of sound C_o. As time increases the m th mode will be carried by the low frequencies and pass the observer at a speed less than C_o by the amount shown by the formula. Finally, after a sufficient time the mth mode will vanish completely.

The variation of phase and group velocity with frequency depends on the physical nature of the waveguide. The ocean is often considered to be a waveguide. In particular, a shallow ocean, has been modeled as a liquid layer of thickness d with mass density ρ, and sound speed C, over a liquid substratum with density ρ_2 and sound speed C_2. For such a model the phase and group velocity curves have been calculated from the formula for the field of discrete modes by the method of stationary phase [28b]. These are plotted versus (normalized) frequency f for the first three modes m Fig. III.A.3.1, reproduced below from Fig. 4-10 of Ref. [28b]. When this waveguide is excited by a pulse an observer at a distant point can predict the following: the field will be a superposition of modes. Each mode will exhibit its own time history. For example, the first mode, if present, will be carried by the low frequencies at early time. This is predicted by the left portion of the $\frac{U_1}{\alpha_1}$ curve ($\alpha_1 = c_1$) where the speed of propagation is the highest. The angle of arrival will be high in the range $0 < \theta_m < 90°$. As time increases it will be carried by the high frequencies. This is predicted by the right portion of the $\frac{U_1}{\alpha_1}$ curve. The angle of arrival will be low in the range of $o < \phi_m < 90°$. Finally at a late time it will be carried at a frequency $f_a d/c_1, \approx 0.46$. As predicted by the central portion of the $\frac{U_1}{\alpha_1}$ curve. Because the group velocity is nearly stationary near f_A this group of waves carrying the first mode will interfere constructively to give a large, amplitude response. This response is called the Airy phase occurring at f_A .

A similar time history will occur for modes 2,3 etc. Actually at any specific time an observer will see a superposition of modes in which individual modes may or may not be resolvable. The sum of all modes will then constitute the transient signal passing his point of observation. The time history of the transient will be altered as the distance of observation increases. This is due to the fact that individual modes travel at different speeds over different frequency bands. The initial shape of the transient signal at the source is then said to be *dispersed* (in time and space) by the agency of waveguide propagation. Such dispersion is called *geometric* to distinguish it from *intrinsic* dispersion caused by the molecular structure of the medium.

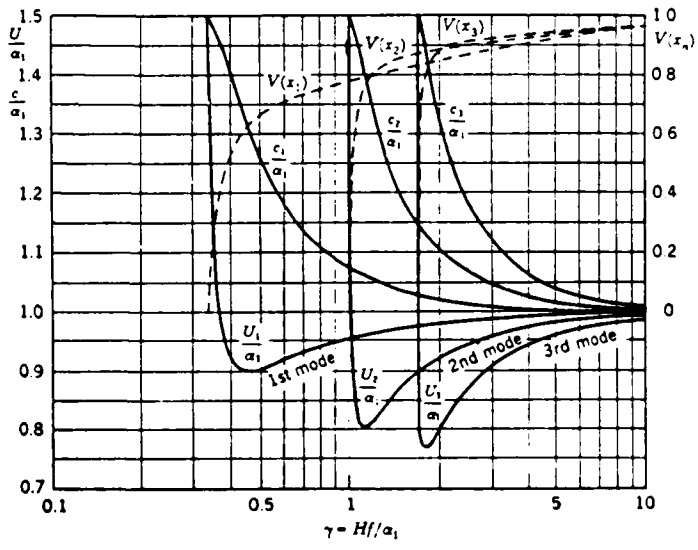

Fig. IIIA.3.2. Liquid layer over liquid substratum. Phase- (c/α_1) and group- (U/α_1) velocity curves and excitation amplitudes for $\rho_2/\rho_1 = 2.0$, $\alpha_2/\alpha_1 = 1.5$ in the first three modes. (*After Pekeris.*)

IIIA.4 MODAL THEORY OF WAVEGUIDES WHICH SHOW CONTINUOUS-SPECTRUM MODES

In the previous section, because the walls of the waveguide are rigid and all reflections total, the modes are all discrete. A different set of modes occurs when the walls allow energy to escape. Fig. IIIA.4.1 shows a parallel plane waveguide in which the upper plane is a free surface, below which is the waveguide itself between $z = 0$ and $z = h$ filled with a medium characterized by density ϱ, and speed of sound C_1; and terminating in a second medium ϱ_2, C_2, which extends from $z > h$ to infinity. The wavefield in the guide is taken to be a pair of plane waves labelled 1, 2 whose propagation directions make angles $\pm\ \alpha$, respectively with the horizontal direction. These are accompanied by refracted waves F_1, F_2 whose angles of propagation are $\pm\ \alpha_2$ determined by Snell's law of refraction:

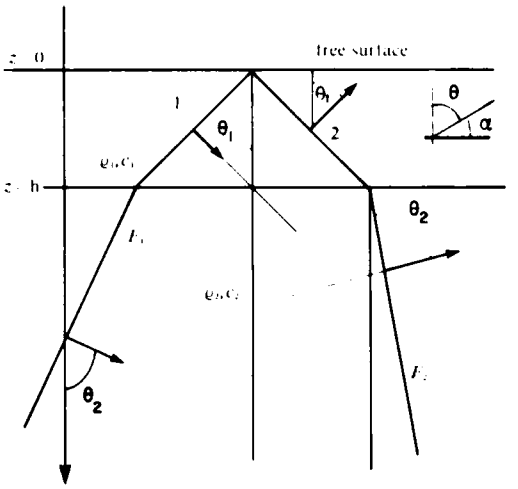

Fig. IIIA.4.1. A waveguide which leaks energy into a semi-infinite medium.

$$\cos \alpha_2 = \frac{c_2}{c_1} \cos \alpha_1 \qquad \text{IIIA.4.1}$$

In applications to the ocean it is customary to take $C_2 > C_1$.

Now the maximum real angle α_{1C} that α_1 can be occurs when $\cos\alpha_2 = 1$, or $\alpha_2 = 0$:

$$\cos \alpha_{1_c} = \frac{c_1}{c_2} \qquad \text{IIIA.4.2}$$

It is the critical angle. At all angles $\alpha_{1C} < \alpha_1 \leqslant 0$ the angle α_2 is purely imaginary and there is no real refracted wave. Since reflection from the plane $z = h$ is total, without change of phase, the plane is effectively rigid and all modes are discrete. When $\alpha_1 = \alpha_{1C}$, $\cos \alpha_2 = 1$ so that $\alpha_2 = 0$. Then, a refracted wave appears at angle $\alpha_2 = \pi/2$ accompanied by envanescent waves. This refracted wave is real for all $\alpha_{1C} < \alpha_1 < \pi/2$. In this range the modes are no longer discrete (see discussion below). When α_1 is extended into imaginary angles by setting $\alpha_1 = \pi/2 - i\beta$ it is seen that $\cos(\pi/2 - i\beta) = i \sinh \beta$, which is purely imaginary. The refracted angle then has both a real part $\pi/2$ and an imaginary part $-i\beta_2$, and the acoustic field in medium 2 clings to the plane $z = h$ because it is evanescent.

In the range $\alpha_{1C} < \alpha_1 < \pi/2$ where all refracted waves in medium 2 are real the z-dependent eigenfunction which satifies both the condition of a free surface at $z = 0$ and the wave equation for all values of $z > 0$ is $\sin \gamma z$ in which γ is a continuum of wavenumbers. This continuum forms the continuous part of the spectrum of wavenumbers of the waveguide along the abscissa of real angles in the complex wavenumber plane, in addition to the discrete spectrum which appears in the range $0 < \alpha_1 < \alpha_{1C}$. Along the ordinate of imaginary angles $\pi/2 - i\beta, 0 < \beta < \infty$ it is also possible to have both discrete and continuous parts of the wavenumber spectrum.

IIIA.5 BRANCH POINTS AND BRANCH CUTS IN RADIATION INTEGRALS

The previous section IIIA.4 has dealt with possible forms of the modal structure of the wavenumber spectrum as it appears in the complex ξ-plane of a typical radiation integral IIIA.1.1. Besides the modal structure belonging to the wavenumber ξ itself there are singularities in the ξ-plane

associated with the $k_z = \sqrt{k^2 - \xi^2}$ wavenumber. These singularities are branch points at $k = \pm \xi$, and branch cuts (or branch lines) which extend from the branch points out of infinity. They are discussed next.

In radiation integrals of the type IIIA.1.1 the factor $\exp i\sqrt{k^2 - \xi^2}\ z$ ($= \exp i k_z z$), represents travelling waves in the z direction. As such it must possess the property that wavenumber k_z be real over the range $-k < \xi < k$, that is

$$\sqrt{k^2 - \xi^2} > 0 \qquad -k < \xi < k \qquad \text{IIIA.5.1}$$

In addition, when $|k_z z|$ approaches infinity (meaning that ξ becomes indefinitely large) it is required that the wavefield vanish. Such a requirement can be satisfied if $\exp i\ [\text{Re}\ k_z + i\ \text{Im}\ k_z]\ z$ is finite when z approaches infinity. This in turn implies that,

$$\Im m \sqrt{k^2 - \xi^2} > 0 \text{ for all } \xi \qquad \text{IIIA.5.2}$$

These basic requirements can be interpreted in terms of the geometry of k_z on the ξ-plane. There it is seen that for any value of ξ there are two possible values of k_z. In terms of magnitude $|k_z|$ and phase θ, where $\alpha < \theta < \alpha + 2\pi$, it is seen that when $\theta = \alpha$ (an arbitrary angle) the function k_z has two values, $+ |k_z|$ if θ approaches α, and $- |k_z|$ if θ approaches $\alpha + 2\pi$. Thus along the line $\theta = \alpha$ the function k_z is not analytic. If the line $\theta = \alpha$ is cut out of the complete ξ-plane the rest of the plane represents one branch of k_z defined by the branch cut $\theta = \alpha$. Since α can be *any* line originating at $+ k$(or $- k$) and running out to infinity along a straight or curved path it is seen that a branch of k_z can be defined in an infinite number of ways by choice of angle α. When a choice is made, and a branch defined, a second branch is obtained by crossing the cut and allowing the angle θ to take on values $\alpha + 2\pi < \theta < \alpha + 4\pi$. The angular sweep $\alpha < \theta < \alpha + 2\pi$ defines the first sheet of the Riemann surface of k_z, and $\alpha + 2\pi < \theta < \alpha + 4\pi$ defines the second sheet. Since the value of a radiation integral is undefined on the branch cut a contour of integration required by IIIA.1.1 must pass around the cut and not cross it.

The geometry of branch cuts on the complex ξ-plane associated with k_z is shown in Fig. IIIA.5.1. Here the branch points are at $\xi = \pm k$, and the branch cuts are arbitrarily selected to run as shown. For a field point at ξ one can define two angles α, β by the formula,

$$\sqrt{k^2 - \xi^2} = \sqrt{k - \xi}\ \sqrt{k + \xi} = |\sqrt{k^2 - \xi^2}|\ \exp\left[\frac{\alpha + \beta}{2}\right]. \qquad \text{IIIA.5.3}$$

These angles are positive counter clockwise from the horizontal with the convention that α, β are both zero when vectors $\vec{OK}, -\vec{OK}$ point toward the origin. All points in this figure excepting those on the branch-cut, are analytic. It therefore constitutes the "top" sheet of a 2-sheeted Riemann surface. As such it is required in the following that $\alpha + \beta$ should not exceed 2π. On Fig. IIIA.5.1 one can identify regions where Re k_z and Im k_z take on special values. To find these one notes that,

$$\text{Re}\ k_z = |k_z| \cos\left[\frac{\alpha\ \beta}{2}\right]$$

$$Im\ k_z = |k_z| \sin\left[\frac{\alpha + \beta}{2}\right] \qquad \text{IIIA.5.4}$$

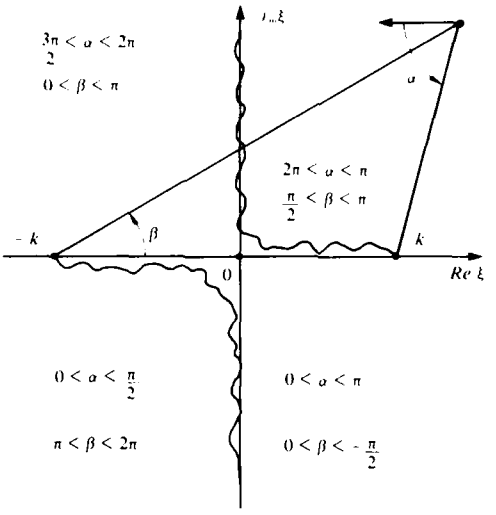

Fig. IIIA.5.1. Definition of the k_z angles α, β in the complex ξ-plane.

In the first quadrant it is seen that when $\alpha = \pi$, $\beta = 0$; when $\alpha = 3\pi/2$, $\beta = \pi/2$; and when $\alpha = 2\pi$, $\beta = 0$. Thus, $\pi < \alpha + \beta < 2\pi$, and so,

$$\frac{\pi}{2} < \frac{\alpha + \beta}{2} < \pi.$$

Therefore Re $k_z < 0$ and Im $k_z > 0$ in the first quadrant. In the second quadrant, several possibilities occur: when ξ lies between $-k$ and 0, it is seen that $\alpha \to 2\pi$ and $\beta \to 0$; on the other hand when ξ lies beyond $-k$ it is seen that $\alpha = 2\pi, \beta = \pi$. Thus $2\pi < \alpha + \beta < 3\pi$. Because of the rule that $\alpha + \beta \leqslant 2\pi$, one subtracts 2π units from each side, so that

$$0 < \frac{\alpha + \beta}{2} < \frac{\pi}{2}$$

Therefore Re $k_z > 0$ and Im $k_z > 0$ in the second quadrant. In the third quadrant for a point ξ between $-k$ and 0, $\alpha \to 0$ as $\beta \to 2\pi$; while for a point beyond-k, $\alpha \to 0$ as $\beta \to \pi$. Hence $\pi < \alpha + \beta < 2\pi$, and

$$\frac{\pi}{2} < \frac{\alpha + \beta}{2} < \pi$$

Therefore Re $k_z < 0$ and Im $k_z > 0$ in the third quadrant. In the fourth quadrant for a point ξ lying between 0 and $+k$, $\alpha \to 0$ as $\beta \to 2\pi$; while for a point beyond $+k$, $\alpha \to \pi$ as $\beta \to 2\pi$. Thus $2\pi < \alpha + \beta < 3\pi$. Again subtracting 2π from each side it is seen that,

$$0 < \frac{\alpha + \beta}{2} < \frac{\pi}{2}$$

Thus Re $k_z > 0$ and Im $k_z > 0$ in the fourth quadrant.

From this discussion the entire "top sheet" of the complex ξ-plane as defined by the cuts in Fig. IIIA.5.1 exhibits Im $k_z > 0$. This construction of cuts is important in field problems for which time is chosen to be represented by $\exp(-i\omega t)$ because then a plane wave component propagating in the positive z - direction is described as $\exp i(k_z z - \omega t) = \exp i((\mathrm{Re}\, k_z + i\ \mathrm{Im}\, k_z) - \omega t)$ which becomes finite (= bounded) as $|k_z| z \to \infty$ since Im $k_z > 0$. Contours of integration may be plotted on Fig. IIIA.5.1 from $-\infty$ to $+\infty$ in any complex direction and the value of the associated integral will be finite as long as the poles and branch cuts of the integral are not crossed.

The complex ξ-plane, as described above, helps to define the nature of k_z by means of comparing (by taking differences) the magnitude of the radial propagation constant $|\xi|$ with the propagation constant $k\,(=\frac{\omega}{c})$ of harmonic waves in homogeneous unbounded space. It is often equally useful to consider the acoustic radiation from a source as a collection of plane waves traveling in all real (and imaginary) directions. This is accomplished by representing ξ as a function of a complex polar angle w. Fig. IIIA.5.2 defines k_z, ξ in the cylindrical coordinate system r, ϕ, z ($\phi = 0$):

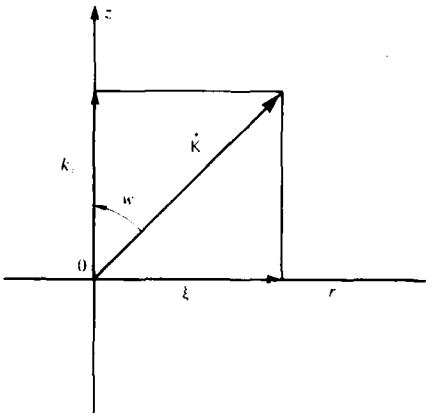

Fig. IIIA.5.2. Definition of complex polar angle w.

$$k_z = k\cos w;\ \xi = k\sin w \qquad \text{IIIA.5.5}$$

$$k = |\vec{K}|;\ w = w_r + iw_i \qquad \text{IIIA.5.6}$$

Thus the real and imaginary parts of ξ are,

$$\mathrm{Re}\,\xi = k\sin w_r \cosh w_i$$

$$\mathrm{Im}\,\xi = k\cos w_r \sinh w_i \qquad \text{IIIA.5.7}$$

In this transformation to angle it is seen that k_z no longer describes a branch singularity on the complex w-plane. The mapping relations between the ξ-plane and the w-plane are shown in Fig. IIIA.5.3.

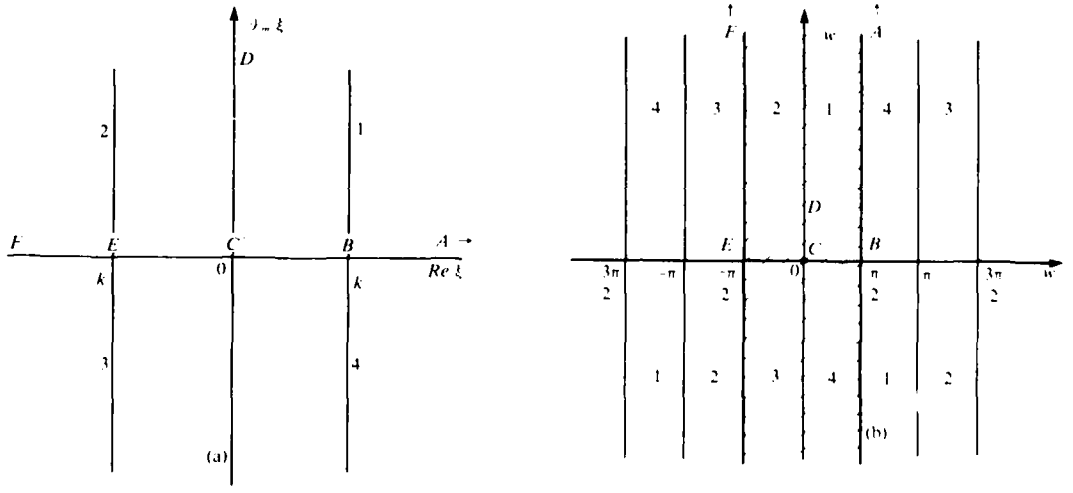

Fig. IIIA.5.3. Mapping relations between ξ-plane and w-plane where $\xi = k \sin w$.

These pair of sketches show:

(1) the line Re $\xi \geq k$ (namely $B'A'$) maps into line $w_r = \pi/2$ (namely AB), and the line Re $\xi \leq -k$ (i.e. $E'F'$) maps into line $w_r = -\pi/2$ (i.e. EF).

(2) the line segment $B'C'E'$ of the ξ-plane where $-k <$ Re $\xi < +k$, maps uniquely into the line segment BCE of the w-plane where $-\pi/2 <$ Re $w < +\pi/2$.

(3) the upper ξ-plane maps into regions 1, 2 of the w-plane, and the lower ξ-plane maps into the regions regions 3, 4 of the w-plane. Thus the entire ξ-plane maps into the shaded regions of Fig. IIIA.5.3b. However since sin w, is periodic the mapping from the ξ-plane to the w-plane is periodic. This means the entire ξ-plane may be mapped uniquely into any one of an infinite number of segments π units wide on the w-plane. But the quadrants of the ξ-plane occupy different positions in a given segment of the w-plane depending on which period is involved. Fig. IIIA.5.3b shows the sequence of quadrants labelled 1, 2, 3, 4.

The mapping $k_z = k \cos w$ simplifies evaluation of radiation integrals in which k_z ($= \sqrt{k^2 - \xi^2}$) appears. It is required however, according to IIIA.5.2 that Im $k_z > 0$. To find the regions in the w-plane where this condition is met one assumes that k may itself be complex ($k = k_r + i k_i$), so that,

$$\text{Re}\, k_z = k_r \cos w_r \cosh w_i + k_i \sin w_r \sinh w_i \qquad \text{IIIA.5.8}$$

$$\text{Im}\, k_z = k_r \cos w_r \cosh w_i - k_r \sin w_r \sinh w_i$$

Because, in general, $k_i \ll k_r$, assume first that $k_i = 0$. It is then seen that in the region $0 < w_r < \pi$, $0 < w_i < -\infty$, the condition Im $k_z > 0$ is satisfied. Similarly in the region $-\pi < w_r < 0$, $0 < w_i < +\infty$, the condition is also satisfied. Fig. IIIA.5.4a shows a complete (shaded) region in the w-plane in which a contour-type radiation integral can be evaluated. Because of the periodicity in the mapping, similar regions can be found in the w-plane. Next one can let k_i be finite but small. The shaded region $-\pi < w_r < 0$ is then off set slightly to the right by an amount,

$$\Delta = \tan^{-1} \frac{k_i}{k_r}$$

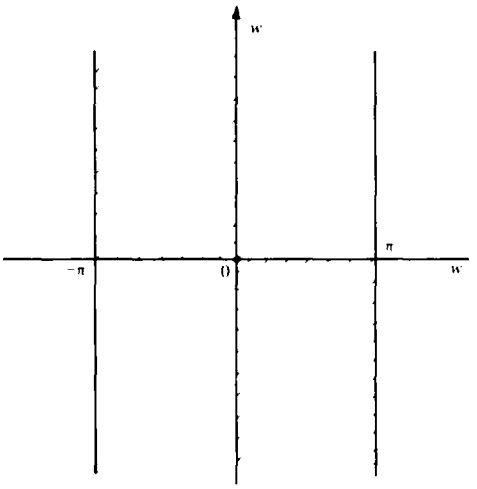

Fig. IIIA.5.4a. Shaded regions in the complex w-plane in which Im $k_z > 0$ and $k_i = 0$.

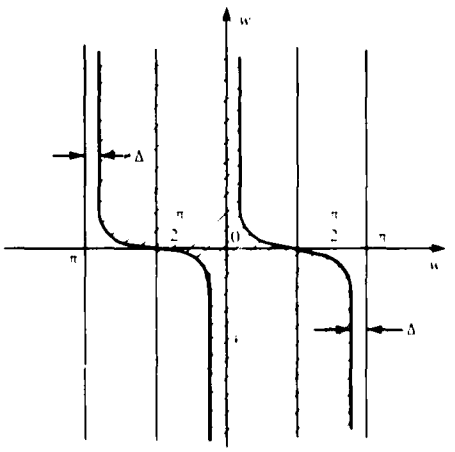

Fig. IIIA.5.4b. Shaded regions in which Im $k_z > 0$ and $k_i > 0$.

At the same time the shaded region $0 < w_r < \pi$ is offset slightly to the left by a same amount. Fig. IIIA.5.4b, shows these offsets.

IIIA.6 GENERALIZED EXAMPLE OF THE EVALUATION OF A RADIATION INTEGRAL

In radiation integral IIIA.1.1 the singularities of the integrand are listed as follows:

(1) the Hankel function $H_n(= J_n + i N_n)$ has a multiple pole of order z^{-n}, $n > 0$, and a logarithmic singularity of order $\ln(z/2)$, $n = 0$, and a branch cut along $\mathrm{Re}\xi < 0$ at the origin [29].

(2) the function $f(\xi)$ has two branch points at $\pm k_1$ because of $\sqrt{k^2 - \xi^2}$.

(3) the function of $f(\xi)$ may have additional branch points because of reflecting boundaries. Assume there are two of them at $\pm k_v$.

(4) the function $f(\xi)$ may have simple poles representing modes in waveguides, and simple poles representing evanescent waves (surface waves, "leaky waves") at waveguide interfaces. Assume there is a simple pole at $\xi = + a_p$.

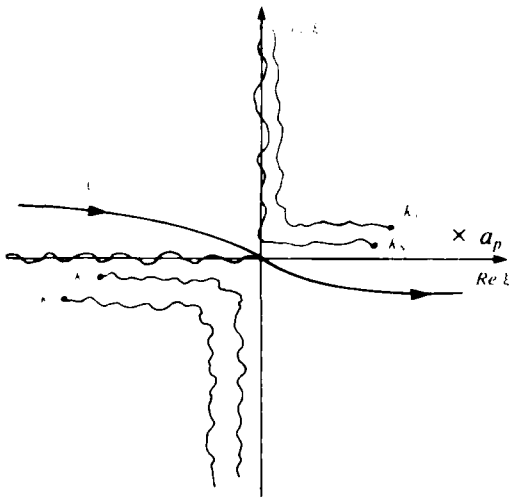

Fig. IIIA.6.1. Integration contour of AI.1.1 together with associated singularities.

Because the integral cannot be evaluated in closed form one may choose the saddle point method to obtain a good approximation. The first step is to note that the time representation is exp $-i\omega t$. This sets the requirement that $\mathrm{Im}\, k_z > 0$ at all points of the ξ-plane except those on the branch cuts. The choice of branch cuts in Fig. IIIA.5.1 satisfies the requirement that $\mathrm{Im}\, k_z > 0$. Fig. IIIA.6.1 shows the contour of integration of IIIA.1.1 in the ξ-plane with all singularities and branch cuts. As noted in the preceding section a transformation to polar angle w,

$$\xi = k \sin w$$

eliminates $\pm k_1$ from the list of branch points. Fig. III.A.6.2 shows the result of transforming Fig. IIIA.6.1 to the w-plane. The branch points $\pm k_v$ are transformed to $\pm W_v$, the pole at a_p is transformed into w_p, and the contour C is transformed into contour $\overline{P}$.

The next step in the approximate evaluation of IIIA.1.1 is to deform the path $\overline{P}$ into a new path P which corresponds to the path of steepest descent through the saddle point. This is determined in the following way. Let a radiating point of spherical waves be at cylindrical coordinates ϱ, z and an observation point of the radiated field be at ϱ_1, z_1. When the medium is homogeneous and free of boundaries, there is one ray at angle α with the z-axis which intercepts the observation point. When the medium is inhomogenous and bounded there may be several such rays at several angles α_r which intercept the observation point. For each one in the domain of real angles $k_{z_r} = k \cos \alpha_r$. The angle α defines the saddle point of integration. Associated with angle α is a group of plane waves traveling in nearly the same direction with nearly the same phase. The aim of approximate integration along a deformed path is to add up the contributions of this group of wavenumbers (in variable ξ) as the path traverses the point $w_r = \cos \alpha$, and effectively ignore the noncontributors along the remainder of the

path. The significance of this procedure may be understood when it is realized that the value of the integral along path $\overline{P}$ in Fig. IIIA.6.2 is generally a very poor approximation to the true value. In terms of the "mountain-valley" symbolism of Section IIIA.1 the path $\overline{P}$ traces a track from $-\infty$ to $+\infty$ far from the saddle point thus undergoing frequent cancellation because of the oscillations of the integrand. In contrast the path of steepest descent through the saddle-point gives nearly the correct value of the radiation at the observation point if it is "far enough" away from the radiator. The qualifier "far-enough" arises because the integral IIIA.1.1 must first be cast in the form IIIA.2.1. This is done by assuming the distance from the source to the receiver is large relative to the size of the source. In effect the Hankel function in IIIA.1.1 is replaced by its asymptotic value for large argument $\xi\varrho$,

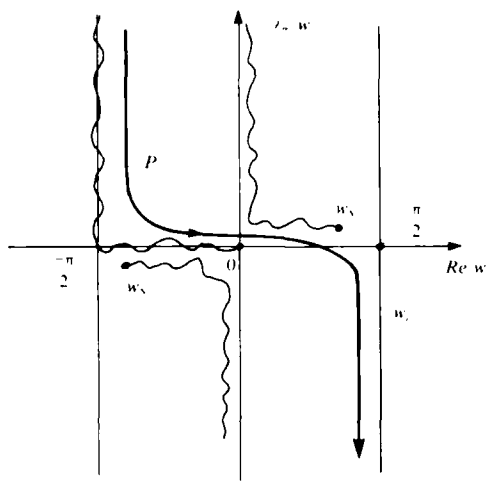

Fig. IIIA.6.2. Integration contour of IIIA.1.1 on the w-plane together with associated singularities.

$$H_\nu^{(1)}(\xi\varrho) \sim \sqrt{\frac{2}{\pi\xi\varrho}}\, e^{i(\xi\varrho - \nu\pi/2 - \pi/4)} \qquad -\pi < \arg \xi\varrho < 2\pi \qquad \text{IIIA.6.1}$$

In terms of angles,

$$\varrho = L \sin \alpha$$

$$z = L \cos \alpha$$

$$\xi = k \sin w$$

$$k_z = k \cos w$$

Since

$$\lim_{\xi\varrho\to\infty} e^{ik\varrho}\, e^{ikz} \to \exp ikL(\cos w \cos \alpha + \sin w \sin \alpha)$$

$$\lim_{\xi\varrho\to\infty} e^{ik\varrho}\, e^{ikz} \to = \exp ikL \cos(w - \alpha)$$

the integral IIIA.1.1 takes the form

$$I = \int f(w)\, e^{\Omega q(w)}\, dw$$

in which

$$\Omega = kL;\ q(w) = \cos(w - \alpha);\ f(w) = f(k \sin w) \cos w \qquad \text{IIIA.6.2}$$

Because kL is taken to be very large it is seen from Section IIIA.1 that the saddle point is determined from the root $\bar{\alpha}$ which satisfies the relation,

$$\frac{d[kL\cos(w-\bar{\alpha})]}{dw}=0 \qquad \text{IIIA.6.3}$$

When the saddle point at angle $\bar{\alpha}$ is found the path P is then deformed to achieve steepest descent. The method of performing the deformation is described in Sect. IIIA.1. The result is shown in Fig. IIIA.6.3. The deformed path *ABCDEFG* is the path of steepest descent. Of this path the part *ABCEFG* is on the first sheet of the Riemann surface defined by the branch cuts. The dotted line *CD* shows that part of the path which is on the second sheet. It is not included in the value of the integral. The contribution of each part of the contour has physical significance: the field due to the path through F in the neighborhood of the saddle point cos $\bar{\alpha}$ is the geometric, or "ray-optic" field. This is the field which obeys Snell's laws. The field contributed by the contour *DC* around the branch cut is the field of *lateral waves* which arises from those rays of the source which strike the boundaries at critical angles of refraction, and run along the boundary while shedding energy back to the observation point. The field contributed by path G around the simple pole shown is that of surface waves radiating evanescent modes [30].

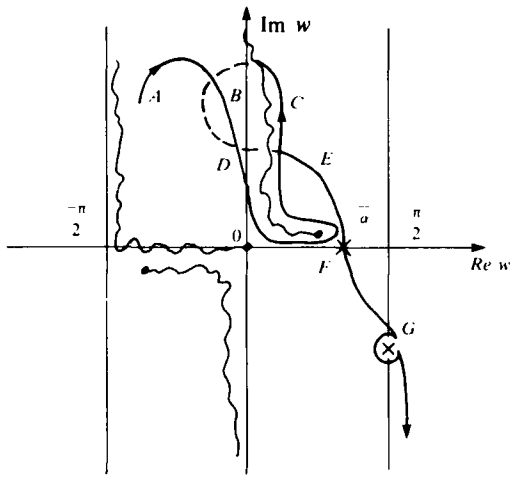

Fig. IIIA.6.3. Path of steepest descent in the evaluation of the radiation integral AI.1.1.

If the integration along contour P is broken into a sum of the integral through saddle point F and the contributions of all singularities and branch cuts it is often useful to formulate the saddle-point integral in terms of a comparison or "canonical" integrals which are easily calculated from available tables of numerical values. Several such canonical integrals are described next.

IIIA.7 CANONICAL INTEGRALS WHICH ARE USEFUL IN THE CALCULATION OF RADIATION INTEGRALS

In IIIA.5.5 the complex variable w can be replaced by a new variable s such that $s = 0$ when $dg(w)/dw = q'(w) = 0$ and such that $q(w)$ is approximated as a polynomial $Q(s)$ in the vicinity of the saddle point,

$$I(\Omega)=\int F(s)\exp[\Omega Q(s)]\,ds$$

$$F(s)=f(w)\ \frac{dw}{ds}\ ;\ \frac{dw}{ds}=\frac{dQ(s)/ds}{dq(w)/dn}=\frac{Q'(s)}{q'(w)} \qquad \text{IIIA.7.1}$$

Several forms of $F(s)$ and $Q(s)$ lead to useful comparison integrals.

I. Let $Q(s)$ describe a single isolated saddle point at $w = w_s$ and assume that the equation $q'(w) = 0$ has an n'th order zero at w_s. Then a simple *choice* of $Q(s)$ is,

$$Q(s) = q(w_s) - s^{n+1} \qquad \text{IIIA.7.2}$$

Because the value of the integral will depend on the contour in the immediate vicinity of the saddle point one expands $F(s)$ in a Taylor series about $s = 0$,

$$F(s) = F(0) + F'(0)s + \frac{F''(0)s^2}{2!} + \ldots \qquad \text{IIIA.7.3}$$

The path of steepest descent from the saddle point $s = 0$ is the one for which $\text{Im}\, Q(s) = 0$. This is the real axis in the s-plane. Assume only one term $F(0)$ is sufficient to give the asymptotic field and assume $n = 1$. Then $F(0)$ must be evaluated at $s = 0$, that is at $(dw/ds)_{s=0}$. From IIIA.7.1,

$$\left(\frac{dw}{ds}\right)_{s=0} = \left(\frac{-2s}{q'(w)}\right)_{s=0}$$

This form is indeterminate. By L'Hospital's Rule,

$$\left(\frac{dw}{ds}\right)_{s=0} = \lim_{s\to 0}\left[\frac{\frac{d}{ds}(-2s)}{\frac{d}{ds}\,[q'(w)]}\right] = \frac{-2}{q''(w_s)\left(\frac{dw}{ds}\right)_{s=0}}$$

or

$$\left(\frac{dw}{ds}\right)_{s=0} = \sqrt{\frac{-2}{q''(w_s)}}$$

Substituting this result into IIIA.7.1 and noting that $F(0) = f(w_s)$, one obtains

$$I(\Omega) \cong f(w_s)\sqrt{\frac{-2}{q''(w_s)}}\,\exp[\Omega q(w_s)]\int_{-\infty}^{\infty} e^{-\Omega s^2}\,ds$$

in which

$$\int_{-\infty}^{\infty} e^{-\Omega s^2}\,ds = \frac{\Gamma(\frac{1}{2})}{\Omega^{1/2}} = \sqrt{\frac{\pi}{\Omega}}$$

and $\Gamma(z)$ is the Gamma function. Finally, for this case of a single isolated saddle point with one term of IIIA.7.3,

$$I(\Omega) \cong f(w_s)\sqrt{\frac{-2\pi}{\Omega q''(w_s)}}\,\exp[\Omega q(w_s)],\ \Omega \to \infty \qquad \text{IIIA.7.4}$$

A complete expansion in which all terms of IIIA.7.3 appear is found from the integral,

$$\int_{-\infty}^{\infty} s^n e^{-\Omega s^2}\, ds = \frac{\Gamma\left(\frac{1+m}{2}\right)}{\Omega^{(1+m/2)}}, \; n \text{ even}$$

$$\int_{-\infty}^{\infty} s^n e^{-\Omega s^2}\, ds = 0 \qquad , \; n \text{ odd}$$

Setting $n > 1$ one finds

$$I(\Omega) \cong \frac{\exp[\Omega q(w_s)]}{\sqrt{\Omega}} \sum_{n=0}^{\infty} \frac{\frac{d^n F(0)}{ds^n}}{(2n)!} \frac{\Gamma(n+\frac{1}{2})}{\Omega^n} \qquad \text{IIIA.7.5}$$

(2) As a second case let $Q(s)$ again describe a single isolated saddle point and assume $f(w)$ has a simple pole at $w = w_0$ near w_s. In the s-plane let $w = w_0$ be mapped into $s = s_0$. Then,

$$F(s) = \frac{F_0}{s - s_0} + E(s); \; Q(s) = q(w_s) - s^2$$

Here F_0 is a constant and $E(s)$ is regular at $s = 0$ and $s = s_0$. Again the path of steepest descent is that for which $\text{Im}\; Q(s) = 0$, namely the real s axis. However because the contour of integration passes through the singularity $s = s_0$ it must be deformed into a small semi-circle labelled contour C to by-pass it. Thus,

$$I(\Omega) \cong E(0) \int_{-\infty}^{\infty} \exp[\Omega Q(s)]\, ds + F_0 \int_c \frac{\exp[\Omega Q(s)]}{s - s_0}\, ds \qquad \text{IIIA.7.6}$$

The value of the first integral is $E(0)(\pi/\Omega)^{1/2}$, where $E(0) = (\sqrt{-2/q''(w_s)} + F_0/s_0)\, e^{\Omega q(w_s)}$. One notes immediately that F_0 is the residue of $F(s)$ at $s = s_0$, and that $s_0 = \sqrt{q(w_s) - q(w_0)}$ .The value of the second integral depends on the sign of $\text{Im}\; s_0$. Now,

$$\lim_{\varepsilon \to 0} \frac{1}{s - s_0 \mp i\varepsilon} = \mathcal{P} \frac{1}{s - s_0} \pm \pi i\, \delta(s - s_0)$$

in which P means the Cauchy principal part. When $\text{Im}\; s_0 = 0$ the second integral in IIIA.7.6 becomes the sum $I_p + I_i$, defined as follows:

$$I_p = \mathcal{P} F_0 \int_c \exp[\Omega q(w_s)] \frac{\exp[-\Omega s^2]}{s - s_0}\, ds$$

$$I_p = 2iF_0 \sqrt{\pi} \exp[-\Omega s_0^2]\, R(-is_0\sqrt{\Omega}) \exp[\Omega q(w_s)]$$

$$R(z) = \int_z^{\infty} e^{-x^2}\, dx, \qquad \text{IIIA.7.7}$$

$$I_i = -F_0 \int_c \pi i\, \delta(s - s_0) \exp[\Omega Q(s)]\, ds$$

or

$$I_i = -\pi i F_0 \exp[-\Omega s_0^2] \exp[\Omega q(w_s)]$$

Thus, when $\text{Im } s_0 = 0$, the value of the integral IIIA.7.6 is,

$$I(\Omega) \cong \exp[\Omega q(w_s)] \{2i\sqrt{\pi} F_0 \exp[-\Omega s_0^2] R(-is_0\sqrt{\Omega}) - \pi i F_0 \exp[-\Omega, s_0^2] + \sqrt{\pi/\Omega}\, E(0)\}. \qquad \text{IIIA.7.8}$$

When however $\text{Im } s_0 \neq 0$ then I_s vanishes because the pole s_0 is no longer on the real s-axis. Then,

$$I(\Omega) \cong \exp[\Omega q(w_s)] \{\pm 2iF_0\sqrt{\pi}\exp[-\Omega s_0^2] R(\mp is_0\sqrt{\Omega}) + \sqrt{\pi/\Omega}\, E(0)\} \qquad \text{IIIA.7.9}$$

in which the choice of sign depends on the choice $\text{Im } s_0 \gtrless 0$ is $\Omega \to \infty$. Thus the case of a simple pole near an isolated saddle point has led to the canonical integral IIIA.7.7, which is an error function, or alternative, a Fresnel integral.

(3) As a third case let $f(w)$ have an algebraic branch-point singularity $W = w_b$ (which maps into $s = s_b$) near a single isolated saddle point $w = w_s$. This condition may be represented by choosing

$$F(s) = F_0(s)(s - s_b)^\alpha, \; 0 < \alpha < 1; \; Q(s) = q(w_s) - s^{n+1}$$

These representations lead to the requirement of evaluating integrals of the form

$$I(\Omega) = \int_{-\infty}^{\infty} s^n (s - s_b)^\alpha e^{-\Omega s^{n+1}}\, ds, \; m = 0, 1, 2, \ldots$$

By suitable transformation it may be shown [31] that the corresponding canonical integral is the parabolic cylinder function. In a typical application $f(w)$ may have the form,

$$f(w) = a + b\sqrt{w - w_b}\,, \text{ near } w_b.$$

Then the integration around the branch cut leads asymptotically to the form

$$I(\Omega) \cong \frac{2\sqrt{\pi}}{[\Omega |q'(w_s)|]^{1/2}} [\sqrt{w - w_b}\, f(w)]_{w_s} \exp\{\Omega q(w_b) - i\tfrac{3}{2} \arg[-q'(w_b)]\} \qquad \text{IIIA.7.10}$$

[32].

(4) As a fourth case let $f(w)$ be regular but allow the presence of two closely spaced saddle points. This condition may be represented by choosing,

$$Q(s) = a_0 + \sigma s - \frac{s^3}{3}$$

The saddle points are then at $s = \pm\sqrt{\sigma}$. If σ is finite then it is permissible to treat each saddle point

separately in the evaluation of the integral IIIA.7.1. When however $|\sigma|$ is arbitrarily small the evaluation of the integral,

$$I(\Omega) \cong F(0) \int \exp\left[\Omega\left(a_0 + \sigma s - \frac{s^3}{3}\right)\right] ds,\ \Omega \to \infty$$

can be expressed in terms of Airy functions [33]. This reference also treats other choices of $F(s)$ and $Q(s)$.

IIIA.8 ASYMPTOTIC EVALUATION OF MULTIPLE INTEGRALS

Frequently radiation integrals appear in the form

$$I(\Omega) = \int_{-\infty}^{\infty} \int\int f(\vec{K}) \exp[i\Omega q(\vec{K})]\, d\vec{K} \qquad \text{IIIA.8.1}$$

$$\vec{K} = (K_x, K_y, K_z)$$

Here $q(\vec{K})$ is a real function. Let $q(\vec{K}_s)$ be a stationary point, defined by

$$\frac{\partial q(\vec{K})}{\partial K_x} = \frac{\partial q(\vec{K})}{\partial K_y} = \frac{\partial q(\vec{K})}{\partial K_z} = 0 \text{ when } \vec{K} = \vec{K}_s$$

To evaluate IIIA.8.1, form a 3×3 matrix of elements,

$$\frac{\partial^2 q}{\partial K_i\, \partial K_j} \quad i = x, y, z; j = x, y, z$$

Let d_i, $i = 1, 2, \ldots n$ be the eigenvalues of this matrix and define a function τ

$$\tau = \sum_{i=1}^{n} \operatorname{sgn} d_i$$

in which

$$\operatorname{sgn} d_i = -1 \text{ if } d_i < 0$$

$$\operatorname{sgn} d_i = +1 \text{ if } d_i > 0$$

Then the asymptotic (meaning $\Omega \to \infty$) approximation of $I(\Omega)$ is,

$$I(\Omega) \sim \frac{f(\vec{K}_s)\ \exp[i\Omega q(\vec{K}_s)]\ \left(\frac{2\pi}{\Omega}\right)^{n/2} \exp[i\pi/4\tau]}{\left|\det\left(\frac{\partial^2 q}{\partial K_{s_i}\, \partial K_{s_j}}\right)\right|^{1/2}} \qquad \text{IIIA.8.2}$$

APPENDIX IIIB

IIIB.1 METHOD OF OBTAINING NEW GREEN'S FUNCTIONS - EXAMPLE OF THE GREEN'S FUNCTION FOR AN AXIAL (MAGNETIC) DIPOLE WITHIN A CORNER REFLECTOR

We consider a corner reflector made up of two (infinite) plane sheets of metal in the form of a V. In cylindrical coordinates (r, ϕ, z) we define the angular disposition of the sheets as $\phi = 0$ and $\phi = \psi$. Inside this angle, at the source point $Q(r_0, \phi_0, z_0)$ close to the junction of the sheets, we place a vertical magnetic dipole of source strength Kdz_0 (oriented in the z direction). The observation point $P(r, \phi, z)$ is any point inside the angle of the sheets. It is a well known result of the theory of electromagnetics that the magnetic field at P can be described by the z-component Π_z^* of the Hertz vector Π^* and that Π_z^* satisfies the *scalar* inhomogeneous wave equation (= Helmholtz equation) in the steady state,

$$(\nabla^2 + k^2)\ \Pi_z^* = \frac{kdz_0}{-i\omega\mu}\ \delta(r - r_0) \tag{1}$$

Here, k is the propagation constant for the medium, μ is the magnetic permeability of the medium and $\delta(r - r_0)$ is the Dirac delta function. Note that time is given by the real part of $e^{i\omega t}$. At the surface of the *metal* sheets the boundary condition is

$$\frac{\partial \Pi_z^*}{\partial \phi} = 0, (\phi \text{ or } \phi_0 = 0, \phi \text{ or } \phi_0 = \psi). \tag{2}$$

Eqs. (1) and (2) constitute a boundary value problem that can be solved by separating variables and using Fourier series and Fourier integrals. We first expand Π_z^* in an orthonormal set of angle functions $(\varepsilon_m/\psi)^{1/2} \cos m\pi\phi/\psi$ in both the ϕ and ϕ_0 coordinates. To satisfy Eq. (2) we thus write

$$\Pi_z^* = \sum_{m=0} \frac{\varepsilon_m}{\psi}\ \Pi_m^*(r, z|r_0, z_0) \cos \frac{m\pi}{\psi}\phi \cos \frac{m\pi}{\psi}\phi_0 \tag{3}$$

in which $\varepsilon_0 = 1$, $\varepsilon_m = 2$ $(m \neq 0)$. We see that $\partial\Pi_z^*/\partial\phi$ will be zero when either ϕ or ϕ_0 is equal to zero or to ψ. Since the domain of z is infinite we can form the Fourier integral

$$\Pi_m^*(r, z|r_0, z_0) = \frac{1}{2\pi} \int_{-\infty}^{+\infty} \overline{\Pi}_m(r|r_0)\, e^{-ih(z-z_0)}\, dh \tag{4}$$

Hence,

$$\Pi_z^* = \frac{1}{2\pi} \int_{-\infty}^{+\infty} e^{-ih(z-z_0)}\, dh \sum_{m=0}^{\infty} \frac{\varepsilon_m}{\psi}\ \overline{\Pi}_m(r|r_0) \cos \frac{m\pi\phi}{\psi} \cos \frac{m\pi\phi_0}{\psi} \tag{5}$$

Now in cylindrical coordinates we can write the delta function in the form

$$\delta(r - r_0) = \delta(r - r_0)\ \frac{\delta(\phi - \phi_0)}{r}\ \delta(z - z_0) \tag{6}$$

The r.h.s. can formally be expanded in Fourier Series and Integral as follows:

$$\delta(\phi - \phi_0) = \sum_{m=0}^{\infty} \sqrt{\frac{\epsilon_m}{\psi}} \cos\ \frac{m\pi\phi}{\psi}\ \sqrt{\frac{\epsilon_m}{\psi}} \cos\ \frac{m\pi\phi_0}{\psi} \tag{7a}$$

$$\delta(z - z_0) = \frac{1}{2\pi} \int_{-\infty}^{+\infty} e^{-ih(z-z_0)}\, dh \tag{7b}$$

We now substitute Eq. (5) into Eq. (1). Noting that,

$$\nabla^2 \equiv \frac{1}{r}\ \frac{\partial}{\partial r}\left(r\ \frac{\partial}{\partial r}\right) + \frac{1}{r^2}\ \frac{\partial^2}{\partial \varphi^2} + \frac{\partial^2}{\partial z^2}$$
$$= \nabla_r^2 + \nabla_\phi^2 + \nabla_z^2$$

we can easily verify that,

$$\nabla_z^2\ \Pi_z^{\cdot} = -h^2\ \Pi_z^{\cdot} \tag{8a}$$

$$\nabla_\phi^2\ \Pi_z^{\cdot} = -\frac{1}{r^2}\left(\frac{m\pi}{\psi}\right)^2 \Pi_z^{\cdot} \tag{8b}$$

Using Eqs. (6) to (8b) we can reduce Eq. (1) to the form

$$\frac{1}{r}\left[\frac{\partial}{\partial r}\left(r\ \frac{\partial}{\partial r}\right) + (k^2 - h^2)\, r - \frac{1}{r}\left(\frac{m\pi}{\psi}\right)^2\right] \bar{\Pi}_m(r|r_0)$$
$$= \frac{kdz_0}{-i\omega\mu}\ \frac{\delta(r - r_0)}{r} \tag{9}$$

When written out in this form the solution $\bar{\Pi}_m(r/r_0)$ is clearly seen to be the Green's function of the wedge shaped (infinite) medium arising from a source point at r_0. Two solutions of the homogeneous equation corresponding to Eq. (9) are

$$J_\nu(\nu r),\ H_\nu(\nu r)$$

where

$$\nu = \frac{m\pi}{\psi},\ \nu = \sqrt{k^2 - h^2}$$

The Wronskian determinant Δ of these solutions is 3.8.9 (with $+i \rightarrow -i$).

$$\Delta = \frac{-2i}{\pi r \nu}$$

To find the particular solution of the inhomogeneous Eq. (9) we use the general technique [34] that

$$\prod_m (r|r_0) = H_\nu^{(2)}(\nu r) \int^r \frac{kdz_0}{-i\omega\mu} \frac{\delta(r - r_0)\, J_\nu(\nu r)\, \nu dr}{r(\nu\Delta)}$$

$$+ J_\nu(\nu r) \int_r \frac{kdz_0}{-i\omega\mu} \frac{\delta(r - r_0)}{r(\nu\Delta)} H_\nu^{(2)}(\nu r)\, \nu dr \tag{10}$$

In Eq. (10) we first select $r < r_0$. Then because $\delta(r - r_0)$ has a value only at $r = r_0$ we see that the first integral drops out and $\bar{\Pi}_m(r/r_0)$ equals the second integral with $r = r_0$. Similarly for $r > r_0$ the second integral will vanish and $\bar{\Pi}_m(r/r_0)$ will be equal to the first integral with $r = r_0$. Combining all terms we find that,

$$\dot{\prod_z} = \frac{kdz_0}{-4\omega\mu} \sum_{m=0}^{\infty} \frac{\varepsilon_m}{\psi} \cos \nu\phi \cos \nu\phi_0$$

$$\times \int_{-\infty}^{+\infty} J_\nu(\nu r_0)\, H_\nu^{(2)}(\nu r)\, e^{-ih(z-z_0)}\, dh,\ r > r_0 \tag{11}$$

For $r < r_0$ we interchange r with r_0, and r_0 with r in the integrand of this equation. The path of integration in Eq. (11) is shown in Fig. III B.1. When $\nu r \gg 1$ we may solve the integral by asymptotic methods. First the Hankel function is represented by the form

$$H_\nu^{(2)}(\nu r) \sim \sqrt{\frac{2}{\pi\nu r}}\, e^{-i\nu r}$$

$$\times e^{i(\nu\pi/2 + \pi/4)} \tag{12}$$

When Eq. (12) is substituted into Eq. (11) the resultant integral is in a form that can be evaluated by the method of steepest descents if the path of integration is *transformed to a complex plane.* This may be done by the transformation

$$h = k \cos\alpha,\ (\alpha = \alpha_1 + i\alpha_2)$$

The integral then transforms to

$$-e^{i(\nu\pi/2 + \pi/4)} \int_{\pi - i\infty}^{i\infty} J_\nu(kr_0 \sin\alpha) \sqrt{\frac{2}{\pi kr \sin\alpha}}\, e^{ik[r\sin\alpha + z\cos\alpha]}\, k \sin\alpha d\alpha$$

A sketch of the path is shown in Fig. IIIB.2.

For field points at great distances from the origin we define the spherical coordinates R, θ by the formulas

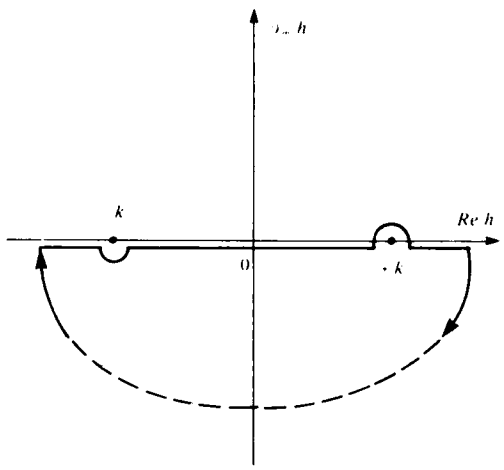

Fig. IIIB.1 Contour of Integration in h-plane

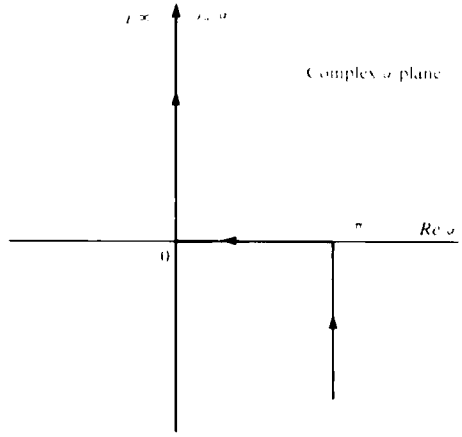

Fig. IIIB.2 Contour of Integration in α-plane

$$z = R\cos\theta, r = R\sin\theta$$

The integral then reduces to the form

$$-\sqrt{\frac{2}{\pi R\sin\theta}}\; e^{ikz\cos\theta}\, e^{i(\pi/2+\pi/4)} \times \int_{\pi}^{i\infty} J_0(kr_0\sin\alpha)\,(k\sin\alpha)^{1/2}\, e^{-ikR[\cos(\theta-\alpha)]}\, d\alpha$$

We now change the path of integration to that of "steepest descent". Assuming kR to be large the latter path may be obtained by a transformation

$$\cos(\theta-\alpha) = 1 - ix^2 \ (x \text{ real})$$

The saddle point occurs at $d\cos(\theta-\alpha)/d\alpha = 0$, i.e., the saddle point is located at $\theta = \alpha$.

Since $\alpha = \theta - \arccos(1 - ix^2)$ it is easily found that

$$d\alpha = \frac{-\sqrt{2i}}{\sqrt{1 - ix^2/2}}\, dx$$

The integral then becomes

$$\frac{2i}{\sqrt{\pi R\sin\theta}}\, e^{ikz\cos\theta}\, e^{i\pi/2}\, e^{-ikR} \times \int_{\cdot}^{\cdot} \frac{J_0(kr_0\sin\alpha)\,(k\sin\alpha)^{1/2}\, e^{-ikR}}{\sqrt{1 - ix^2/2}}\, dx$$

According to the method of steepest descent significant contributions to this integral occur only near the saddle point. Hence we set $\alpha = \theta$ and expand the denominator in powers of x^2 such that

$$\frac{1}{\sqrt{1 - ix/2^2}} = 1 + \frac{ix^2}{4} + \ldots..$$

Recalling that

$$\int_{-\infty}^{+\infty} e^{-x^2/kR}\, dx = \sqrt{\frac{\pi}{kR}}$$

we find the asymptotic solution of the integral to be

$$2ie^{i\nu\pi/2}\, \frac{e^{-ikR}}{R}\, J_\nu(kr_0 \sin\theta)\, e^{ikz_0\cos\theta} \tag{13}$$

Using this result in Eq. (11) we find the asymptotic (= far field) form of the z-component of the magnetic Hertz vector to be

$$\Pi_m^* \sim \frac{e^{-ikR}}{R} \left(\frac{kdz_0}{2i\omega\mu\psi} \right) e^{ikz_0\cos\theta}$$

$$\times \sum_{m=0}^{\infty} \varepsilon_m \cos\nu\phi \cos\nu\phi_0\, e^{i\nu\pi/2} J_\nu(kr_0 \sin\theta) \tag{14}$$

At this point it is desirable to express the dipole strength of the source as -4π units. The Π_m^* will become a *Green's function* $G(R, \theta, \phi; r_0, z_0, \phi_0)$ for the wedge. Writing

$$\frac{Kdz_0}{-i\omega\mu} = -4\pi \tag{15}$$

One finds that the Green's function for the wedge is

$$G \rightarrow \frac{e^{-ikR}}{R} \left(\frac{2\pi}{\psi} \right) e^{ikz_0\cos\theta} \sum_{m=0}^{\infty} \varepsilon_m \cos\nu\phi \cos\nu\phi_0$$

$$\times e^{i\nu\pi/2} J_\nu(kr_0 \sin\theta) \tag{16}$$

in which $\nu = m\pi/\psi$.

The form of Eq. (16) now contains no electromagnetic parameters. It is a purely geometric construction which gives the far field of a point source in a corner reflector. It can thus be directly applied to finding the radiation field of an acoustic surface located in a corner reflector by linear superposition of the field from all points on the source surface.

REFERENCES

1. N. Marcuvitz, L. Felsen, "Radiation and Scattering of Waves", Prentice Hall Inc., Englewood Cliffs, N.J., Eq. 3.3.10.
2. Ref. [1], Eqs. 3.3.10, 3.3.11.
3. Ref. [1], Chap. 1.
4. Ref. [1], p. 244, 250.
5. Ref. [1], p. 309.
6. P.M. Morse, H. Feshbach, "Methods of Theoretical Physics" Vol. I., p. 892.
7. Ref. [1], p. 664.
8. P.M. Morse, K.V. Ingard, "Theoretical Acoustics", McGraw Hill, 1968, p. 371.
9. P.M. Morse, H. Feshbach, "Methods of Theoretical Physics", Vol. II., p. 1372.
10. M. Abramowitz, I. Stegun, "Handbook of Mathematical Functions" U.S. Dept. of Commerce AM5.55, p. 722.
11. Ref. [9], p. 1421.
12. Ref. [9], p. 640.
13. Ref. [9], p. 1466.
14. Ref. [9], p. 1502.
15. J.J. Bowman et al, "Electromagnetic and acoustic scattering" p. 271, where VS_n must be multiplied by $K/4\pi$.
16. Ref. [15], p. 264.
17. Ref. [15], p. 265, Vol. 9, No. 2, p. 168.
18. A.A. Tuzhilin, Sov-Phys. Acous.
19. Ref. [15], p. 270.
20. Ref. [15], p. 331.
21. Ref. [15], p. 329.
22. Ref. [15], p. 639.
23. Ref. [15], p. 651.
24. Ref. [8], p. 370.
25. Ref. [9], p. 1465.
26. Ref. [8], p. 374.
27. Ref. [8], p. 373-374.
28. Ref. [9], p. 439.
29. Ref. [9], p. 627.
30. Ref. [1], p. 465.
31. Ref. [1], p. 419.
32. Ref. [1], p. 431.
33. Ref. [1], p. 374, 410.
34. Ref. [6], Vol. I.

CHAPTER IV
THE CALCULATION OF ACOUSTIC RADIATION BY USE OF FOURIER EXPANSIONS

INTRODUCTION

Chapter III considered the theory of acoustic radiation from point sources, multipoles, and line sources. The basic tool for calculating radiation fields was the Green's function, whose form depended on the coordinate system used, and on the boundaries of the radiation space. In this chapter the source of radiation is an extended surface. The calculation of its radiation will be based on the theory of plane wave expansions, which will be shown to be a Fourier transformation, and therefore possesses the power of Fourier analysis. Both the theory of Green's functions and of Fourier transformation are interrelated, and one can be used as well as the other. However the radiation problems treated in this chapter are advantageously solved by Fourier methods.

4.1 THEORY OF ACOUSTIC RADIATION BASED ON PLANE WAVE EXPANSIONS

Let $\psi(\vec{r}, t)$ be a field of acoustic velocity potential. The time-dependence of ψ can be resolved into an infinite number of angular frequencies ω. Similarly its space-dependence can be resolved into an infinite number of spatial frequencies, or wavenumbers, k. In terms of k, ω the potential field can be expanded into an infinite number of plane waves traveling in all conceivable directions, both real and imaginary. (For a discussion of imaginary directions, see Appendix IIIA.) In rectangular coordinates this expansion becomes,

$$\psi(x, y, z, t) = \int_{-\infty}^{\infty} \iiint \Psi(k_x, k_y, k_z|\omega) \exp i[k_x x + k_y y + k_z z - \omega t] \frac{dk_x dk_y dk_z d\omega}{(2\pi)^4} \tag{4.1.1}$$

This form of Fourier integral inserts the factors of 2π in $\vec{k} - \omega$ space and omits them in real space. The field will be assumed small-amplitude and will therefore satisfy Helmholtz's equation, $(\nabla^2 + k^2)\psi = 0$, $k = \omega/c$, c is the speed of sound in the medium. For a homogeneous isotropic medium k will be a constant, and the solution of this equation in plane waves will require that,

$$k^2 = k_x^2 + k_y^2 + k_z^2 \tag{4.1.2}$$

This relation will appear repeatedly in later formulations. $\Psi(k_x, k_y, k_z|\omega)$ itself can be obtained from 4.1.1 by inverse Fourier transformation,

$$\Psi(k_x, k_y, k_z|\omega) = \int_{-\infty}^{\infty} \iiint \psi(x, y, z, t) \exp -i[k_x x + k_y y + k_z z - \omega t]\, dx dy\, dz dt \tag{4.1.3}$$

Thus with each temporal frequency there is associated an infinite number of spatial wavenumbers.

The acoustic field is also a field of particle velocity, $\vec{v} = (v_x, v_y, v_z) \exp -i\omega t$. Each component v_i can, in a similar way, be expanded in plane waves.

$$v_i(x, y, z, t) = \int_{-\infty}^{\infty}\int\int\int V_i(k_x, k_y, k_z|\omega) \exp i[k_x x + k_y y + k_z z - \omega t] \frac{dk_x dk_y dk_z d\omega}{(2\pi)^4} \tag{4.1.4}$$

$$V_i(k_x, k_y, k_z|\omega) = \int_{-\infty}^{\infty}\int\int\int v_i(x, y, z, t) \exp -i[k_x x + k_y y + k_z z - \omega t]\, dx dy dz dt \tag{4.1.5}$$

$$i = x, y, z$$

For small amplitude fields, the velocity potential and the velocity are everywhere related by the equation,

$$-\nabla\psi = \vec{v} \tag{4.1.6}$$

or

$$-\left[\hat{i}\frac{\partial}{\partial x} + \hat{j}\frac{\partial}{\partial y} + \hat{k}\frac{\partial}{\partial z}\right]\psi(x, y, z, t) = \hat{i}v_x + \hat{j}v_y + \hat{k}v_z$$

In particular, the z-component of this vector relation is,

$$v_z(x, y, z, t) = -\int_{-\infty}^{\infty}\int\int\int ik_z\Psi(k_x, k_y, k_z|\omega) \exp i[k_x x + k_y y + k_z z - \omega t] \frac{dk_x dk_y dk_z d\omega}{(2\pi)^4} \tag{4.1.7}$$

Thus, at a radiating surface $z = 0$, since the plane waves in the expansion have all wavefronts normal to the surface, 4.1.4 and 4.1.7 provide two equivalent forms,

$$v_z(x, y, 0, t) = \int_{-\infty}^{\infty}\int\int\int V_z(k_x, k_y, 0|\omega) \exp i[k_x x + k_y - \omega t] \frac{dk_x dk_y d\omega}{(2\pi)^3}$$

$$v_z(x, y, 0, t) = -\int_{-\infty}^{\infty}\int\int\int ik_z\Psi(k_x, k_y, 0|\omega) \exp i[k_x x + k_y y - \omega t] \frac{dk_x dk_y d\omega}{(2\pi)^3}$$

The units of $V_z(k_x, k_y, 0|\omega)$ are $m^3 s^{-1}$.

From this it is concluded that on the radiating surface,

$$\Psi(k_x, k_y, 0|\omega) = \frac{V_z(k_x, k_y, 0)}{k_z} \tag{4.1.8}$$

Because the acoustic field is continuous from the radiation surface outward, the velocity potential that satisfies the boundary condition on the surface must have the form,

$$\psi(x, y, z, t) = \int_{-\infty}^{\infty}\int\int \frac{iV_z(k_x, k_y)}{\sqrt{k^2 - k_x^2 - k_y^2}} \exp i[k_x x + k_y y + k_z z - \omega t] \frac{dk_x dk_y d\omega}{(2\pi)^3} \tag{4.1.9}$$

Here $V_z(k_x, k_y)$ is the Fourier transform of the normal component of surface velocity.

A similar derivation may be made in cylindrical coordinates ϱ, ϕ, z. In the plane $z = 0$ the normal component of velocity, expressed as a plane wave expansion with time omitted is,

$$v_z(x, y) = \int_{-\infty}^{\infty}\int V(k_x, k_y) \exp i[k_x x + k_y y] \frac{dk_x dk_y}{(2\pi)^2} \tag{4.1.10}$$

Introduction of polar coordinates $\varrho, \phi, k_r, \alpha$ by the formulas,

$$\vec{\varrho} = \varrho[\hat{i}\cos\phi + \hat{j}\sin\phi]; \vec{k}_r = k_r[\hat{i}\cos\alpha + \hat{j}\sin\alpha] = \hat{i}k_x + \hat{j}k_y \tag{4.1.11}$$

leads to the form,

$$v_z(\varrho, \phi) = \int\int V(k_r, \alpha) \exp i[k_r\varrho\cos(\phi - \alpha)] \frac{k_r dk_r d\alpha}{(2\pi)^2} \tag{4.1.12}$$

in which k_r is seen to be the Jacobian determinant of the polar coordinate transformation in $\vec{k}_r$. On the same surface $z = 0$ the velocity potential has an identical form,

$$\psi(\varrho, \phi, 0) = \int\int \Psi(k_r, \alpha, 0) \exp i[k_r\varrho\cos(\phi - \alpha)] \frac{k_r dk_r d\alpha}{(2\pi)^2} \tag{4.1.13}$$

Using boundary condition 4.1.6, and continuing the potential into the medium one obtains,

$$\psi(\varrho, \phi, z) = \int\int \frac{iV(k_r, \alpha)}{kz} \exp i[k_r\varrho\cos(\phi - \alpha)]\, e^{ik_z z} \frac{k_r dk_r d\alpha}{(2\pi)^2} \tag{4.1.14}$$

Now,

$$\exp i[k_r\varrho\cos(\phi - \alpha)] = \sum_{m=-\infty}^{\infty} i^m J_m(k_r\varrho)\, e^{im(\phi - \alpha)} \tag{4.1.15}$$

[1]. Since the limits of integration in rectangular coordinates x, y are both $-\infty$ to $+\infty$, the transformation 4.1.11 changes them to 0 to ∞ in coordinate k_r and 0 to 2π in coordinates ϕ, α. The velocity potential everywhere then becomes,

$$\psi(\varrho, \phi, z, t) = \sum_{m=-\infty}^{\infty} \int \frac{d\omega}{2\pi} \int_0^{\infty} \frac{k_r dk_r}{2\pi} \int_0^{2\pi} \frac{d\alpha}{2\pi} \frac{i^{m+1} V(k_r, \alpha|\omega)}{\sqrt{k^2 - k_r^2}} J_m(k_r\varrho)\, e^{im(\phi - \alpha)} e^{iz\sqrt{k^2 - k_r^2}} e^{i\omega t} \tag{4.1.16}$$

4.2a RADIATION FIELD OF A RECTANGULAR FLEXURAL PLATE WITH FIXED VELOCITY DISTRIBUTION IN AN INFINITELY LONG LOSSLESS DUCT

Eq. 3.7.17 gives the radiation field of a point source in a rectangular duct, $0 \leq x \leq a$, $0 \leq y \leq b$, with rigid walls. In this section a determination is made of the radiation field of a flexural rectangular

plate, $0 \leqslant x \leqslant a$, $0 \leqslant y \leqslant b$, with fixed velocity distribution $v_z(x, y, t)$ in the same duct. Because both the cross-sectional dimensions of the duct and the plate are finite it will be advantageous to use the theory of modes. In a later section the plate alone will be finite. The determination of the radiation field will then be made by using both modal theory, and expansion in plane waves.

Let $\Psi_m(x)$, $\Psi_n(y)$, $m = 0, 1, 2 \ldots$, $n = 0, 2, \ldots$ be a set of orthonormal functions in the (bounded) region of the plate. For convenience define $\varphi_{mn}(x, y) = \Psi_m(x)\ \Psi_n(y)$. Let $v_z(x, y, 0, t)$ be the normal component of particle velocity at plane $z = 0$, $-\infty < z < \infty$. If the time fluctuation is harmonic, and the variation in x, y arbitrary, v_z can be expanded in spatial plate modes at each frequency ω,

$$v_z(x, y, 0, t) = \sum_{m,n} V_{mn}\varphi_{mn}(x, y)\, e^{-i\omega t} \tag{4.2.1}$$

Here v_z is a fixed distribution in x, y, independent of the reaction of the medium on the flexural motion of the plate and V_{mn} (units: ms^{-1}) are the expansion constants. In the medium itself the acoustic velocity potential can also be expressed as an expansion of normalized characteristic functions of the *duct*, $\gamma_{pq}(x, y, z) = \Gamma_p(x)\,\Gamma_q(y) \exp i\,\zeta_{pq}\, z$, different, in general, from φ_{mn},

$$\psi(x, y, z, t) = \sum_{p,q} \Psi_{pq}\,\gamma_{pq}(x, y, z)\, e^{-i\omega t} \tag{4.2.2}$$

Here Ψ_{pq} (units: m^2s^{-1}) are the expansion constants, and

$$\zeta_{mn} = \sqrt{k^2 - (k_x)^2_{mn} - (k_y)^2_{mn}}\ \ldots.$$

At the plate surface $z = 0$, 4.2.1 and 4.2.2 are related through the boundary conditions 4.1.6,

$$\sum_{p,q}\ \Psi_{pq}\, i\zeta_{pq}\gamma_{pq} = -\ \sum_{m,n}\ V_{mn}\,\varphi_{mn},\ z = 0. \tag{4.2.3}$$

Since the functions γ_{pq} are orthogonal over the area of the plate, and are normalized, it is immediately seen that the expansion constants are given by

$$\Psi_{pq} = \frac{i}{\zeta_{pq}}\ \sum_{m,n}\ V_{mn} \int \varphi_{mn}(x, y)\,\gamma_{pq}(x, y, 0)\, dS(x, y) \tag{4.2.4}$$

This equation states that in each mode pq the velocity potential receives contributions from *all* velocity modes mn of the plate. This means the boundary condition has effectively coupled all duct modes to *each* plate mode. To emphasize this important result 4.2.4 is rewritten in the form,

$$\Psi_{pq} = \sum_{m,n}\ I_{pqmn}\, V_{mn}, \quad I_{pqmn} = \frac{i}{\zeta_{pq}} \int_{\ } \gamma_{pq}\varphi_{mn}\, dS \tag{4.2.5}$$

In addition, it is noted that the potential field repeats itself periodically along the length direction (z) of the duct. Since the duct is assumed lossless and infinitely long, there is no diminution of average acoustic intensity as the field propagates.

4.2b RADIATION FIELD OF A RECTANGULAR PLATE WITH FIXED VELOCITY DISTRIBUTION IN AN INFINITE PLANE RIGID BAFFLE

Let the plate dimensions be $2L_x$, $2L_y$. The plane wave expansion of the potential field is given by 4.1.9, in which,

$$V_z(k_x, k_y|\omega) = \int_{-L_x}^{L_x}\int_{-L_y}^{L_y} v_z(x, y)\, e^{-i(k_x x + k_y y)}\, dxdy \text{ (units: } m^4 s^{-1}) \tag{4.2.6}$$

v_z itself is expressed by 4.2.1 as a sum of plate modes. Applying 4.2.6 in modal form to 4.1.9 one arrives at the potential field expressed in *both* plane wave and modal form,

$$\psi(x, y, z, t) = \int_{-\infty}^{\infty} \frac{d\omega}{2\pi} \sum_{m,n} \int_{-\infty}^{\infty}\int \frac{dk_x}{2\pi}\frac{dk_y}{2\pi} \left[\int_{-L_x}^{L_x}\int_{-L_y}^{L_y} V_{mn}(\omega)\, \varphi_{mn}(x, y)\, e^{-i(k_x x + k_y y)}\, dxdy\right] \times \frac{ie^{i(k_x x + k_y y + k_z z - \omega t)}}{\sqrt{k^2 - k_x^2 - k_y^2}} \tag{4.2.7}$$

In words: each plate mode $V_{mn}\,\varphi_{mn}$ in spatial coordinates x, y is Fourier transformed into a plate mode expressed in spatial wavenumbers k_x, k_y. The result is multiplied by $(k^2 - k_x^2 - k_y^2)^{-1/2}$, and is then inverse Fourier transformed back into real space. After integration over all frequencies ω one finally finds the acoustic velocity potential everywhere, $0 \leqslant z < \infty$. The radiated pressure field is constructed from ψ by use of 1.9.14.

4.2c RADIATION FIELD OF A FORCE-DRIVEN RECTANGULAR PLATE IN AN INFINITE RIGID BAFFLE

A. CALCULATION OF AMPLITUDES

A rectangular homogeneous, isotropic plate, thickness h, is located in an x, y, z system of coordinates that span the range $0 \leqslant x \leqslant a$, $0 \leqslant y \leqslant b$, with the origin at one corner. Upon excitation by time-varying forces in a compressible medium it undergoes a forced vibration, which is damped by internal friction and external acoustic radiation. In contrast to the case of a plate vibrating with fixed velocity distribution, only the force ($q(x, y, t)$) here is fixed, the velocity distribution dw/dt being variable.

In a first approximation, the plate is considered lossless and *thin*, meaning that the normal component of displacement (w) of its neutral plane is a good approximation to the same component at its surface. At low enough frequency, where rotary inertia and shear deformation are unimportant, the equation of motion of the plate is assumed to take the form,

$$\left(\frac{D}{\varrho h}\nabla^4 + \frac{\partial^2}{\partial t^2}\right) w(x, y, t) = \frac{q(x, y, t)}{\varrho h} \tag{4.2.8}$$

The units of each term are those of acceleration (ms^{-2}). In particular,

$$D = \frac{Eh^3}{12(1-\nu^2)} \qquad \text{(units: } Nm\text{)}$$

ϱ = mass density $\qquad (Ns^2m^{-4})$

$$\nabla^4 = \left(\frac{\partial^2}{\partial x^2} + \frac{\partial^2}{\partial y^2} \right)^2 \qquad (m^{-4})$$

q = forcing function $\qquad (Nm^{-2})$

The solution of 4.2.8 in modes is obtained by first setting $q \equiv 0$, and choosing time to be harmonic,

$$w(x, y, t) = W(x, y)\, e^{-i\omega t}$$

Then,

$$\nabla^4 W = \frac{\omega^2}{(D/\varrho h)} W \qquad \text{(units: } m^{-3}\text{)} \tag{4.2.9}$$

Thus the operator ∇^4 satisfies an eigenvalue problem with its eigenvalue $\Lambda^4 = \omega^2/(D/\varrho h)$ (units: m^{-4}). If the plate is infinite in extent the eigenvalues form a continuum: if finite, they form a discrete set, with $\omega \rightarrow \omega_{mn}$. A useful case is a simply supported plate; then,

$$W(x, y) = \sum_{m,n} A_{mn}\, W_{mn}(x, y) \tag{4.2.10}$$

$$W_{mn}(x, y) = \sin \frac{m\pi x}{a} \sin \frac{m\pi y}{b} \tag{4.2.11}$$

$$\omega_{mn} = \sqrt{\frac{D}{\varrho h}} \left[\left(\frac{m\pi}{a} \right)^2 + \left(\frac{n\pi}{b} \right)^2 \right] \tag{4.2.12}$$

in which ω_{mn} are the natural frequencies of free vibration. The eigenvalue of the operator ∇^4 is

$$\Lambda_{mn} = \left[\frac{\omega_{mn}^2}{D/\varrho h} \right]^{1/4} = \sqrt{\left(\frac{m\pi}{a} \right)^2 + \left(\frac{n\pi}{b} \right)^2} \qquad \text{(units: } m^{-1}\text{)} \tag{4.2.13}$$

It is called the wavenumber corresponding to m, n and is written in the alternative forms:

$$\Lambda_{mn} = k_{mn} = \frac{2\pi}{\lambda_{mn}} \tag{4.2.14}$$

Since k_{mn} is a spatial quantity it identifies a mode mn which can be forced at *any* frequency ω. It is the magnitude of a wavenumber vector,

$$\vec{k}_{mn} = \hat{i}k_m + \hat{j}k_n$$

$$k_m = \frac{2\pi}{\lambda_m} = \frac{m\pi}{a}\ ; k_n = \frac{2\pi}{\lambda_n} = \frac{n\pi}{b} \tag{4.2.15}$$

In the theory of free vibration of plates, as well as acoustic radiation from plates, the wavenumber k_{mn}, associated with the free modes of vibration of the plate, must be compared to the wavenumber k_p, associated with the propagation of flexural waves in the plate. The form of k_p is obtained by multiplying both sides of 4.2.9 with ω^2; then,

$$\nabla^4 W - \frac{\omega^4}{c_b^4} W = 0$$

$$c_b(\omega) = 4\sqrt{\frac{\omega^2 D}{\varrho h}} \qquad (\text{units: } ms^{-1}) \tag{4.2.16}$$

$$k_p(\omega) = \frac{\omega}{c_b} = \frac{\omega^{1/2}}{\left(\frac{D}{\varrho h}\right)^{1/4}} \qquad (\text{units: } m^{-1}) \tag{4.2.17}$$

It is seen that c_b (and k_p) are proportional to a positive power of frequency, meaning that high frequency waves in a plate travel faster than low frequency waves.

When the plate is forced into vibration by a harmonic force $q(x, y, t) = Q(x, y) \exp(-i\omega t)$, 4.2.8 reduces to the form,

$$(\nabla^4 - k_p^4)\, W(x, y) = \frac{Q(x, y)}{D}, \qquad (\text{units: } m^{-1}) \tag{4.2.18}$$

Now $Q(x, y)$ is a sum of applied forces $Q^{(A)}$ independent of plate displacement and reaction forces Q_R generated by the acoustic impedance of the medium. In the case where Q_R is negligible 4.2.18 can be solved by expanding both W and $Q^{(A)}$ in modes W_{mn} of free vibration of the plate. Because displacement modes are uncoupled to force modes the expansions can use the same subscripting,

$$W(x, y) = \sum_{m,n} A_{mn} W_{mn}(x, y);\ Q^{(A)}(x, y) = \sum_{m,n} Q_{mn}^{(A)} W_{mn}(x, y) \tag{4.2.19}$$

$$A_{mn} = \frac{\int\int W(x, y)\, W_{mn}(x, y)\, dxdy}{\int\int [W_{mn}(x, y)]^2\, dxdy}$$

$$Q_{mn}^{(A)} = \frac{\int\int Q^{(A)}(x, y)\, W_{mn}(x, y)\, dxdy}{\int\int [W_{mn}(x, y)]^2\, dxdy}$$

Each W_{mn} obey the eigenvalue equation 4.2.9,

$$\nabla^4 W_{mn} = k_{mn}^4 W_{mn} \tag{4.2.20}$$

Application of this relation to 4.2.18 shows that,

$$A_{mn} = \frac{Q_{mn}^{(A)}}{D[k_{mn}^4 - k_p^4]} \tag{4.2.21}$$

in which, because the modes W_{mn} are (by definition) orthogonal over the area of the plate,

$$Q_{mn}^{(A)} = \frac{\int_0^a \int_0^b Q^{(A)}(x, y)\, W_{mn}(x, y)\, dxdy}{\int_0^a \int_0^b [W_{mn}(x, y)]^2\, dxdy} \qquad \text{(units: } Nm^{-2}\text{)} \tag{4.2.22}$$

The displacement in steady state forced vibration of the plate caused by applied forces which are independent of displacement is then,

$$w(x, y, t) = e^{-i\omega t} \sum_{m,n} \frac{Q_{mn}^{(A)}}{D[k_{mn}^4 - k_p^4]} W_{mn}(x, y) \tag{4.2.23}$$

The condition $k_{mn} = k_p$ under drive amplitude Q_{mn} forces the displacement w to become indefinitely large. It is the condition of *mechanical resonance* which occurs at values m, n such that,

$$\omega_{mn} = \sqrt{\frac{D}{\varrho h}} \left[\left(\frac{m\pi}{a} \right)^2 + \left(\frac{n\pi}{b} \right)^2 \right] \qquad \text{(units: } s^{-1}\text{)} \tag{4.2.24}$$

In practical vibration of plates $|w|$ at resonance is limited by internal friction.

The result 4.2.23 is no longer valid when the driving force $q(x, y, t)$ includes both reaction forces $Q_R = p(x, y, t)$ and applied forces $Q^{(A)}(x, y, t)$. Then,

$$q(x, y, t) = Q^{(A)}(x, y, t) - p(x, y, t). \tag{4.2.25}$$

The minus sign appears here to express *reaction* of the medium in contrast to *action* of the driving force. The inclusion of $p(x, y, t)$ radically changes plate dynamics. If an attempt is made to solve 4.2.8 when 4.2.25 is the forcing function a difficulty arises. Because p depends on displacement, and displacement depends on $Q^{(A)}$, it is seen that the modes which describe $p(x, y, t)$ are no longer decoupled from the modes which describe $Q^{(A)}$. Thus, if one writes the modes of p in the form,

$$p(x, y, 0, t) = \sum_{m,n} P_{mn}(x, y, 0 | \omega)\, e^{-i\omega t} \tag{4.2.26}$$

each P_{mn} is coupled to *all* displacement modes W_{pq} through a coupling parameter Z,

$$P_{mn}(x, y | \omega) = \sum_{p,q} -i\omega Z_{mnpq}(\omega)\, A_{pq}\, W_{pq}(x, y) \tag{4.2.27}$$

The factor $-i\omega A_{pq} W_{pq}(x, y)$ is a modal velocity, and $Z_{mnpq}(w)$ is a modal specific acoustic impedance (units: Nsm^{-5}). Applying this result to 4.2.18, 4.2.19, 4.2.20 one obtains for the mn'th mode,

$$(k_{mn}^4 - k_p^4)\, A_{mn} - \sum_{p,q} i\omega \frac{Z_{mnpq}(\omega)}{D} A_{pq} \frac{W_{pq}}{W_{mn}} = \frac{Q_{mn}^{(A)}(x, y)}{D}, \tag{4.2.28}$$

$n, m = 0, 1, 2. \ldots$

The totality of all modes mn forms a matrix equation is unknown displacement amplitudes A_{mn} and known force amplitudes $Q_{mn}^{(A)}$. When Z_{mnpq} is known, A_{mn} is obtained by matrix inversion. The calculation of Z_{mnpq} is a difficult task. An outline procedure for obtaining it in particular cases is sketched here.

B. CALCULATION OF MODE COUPLING FACTORS OF A SIMPLY SUPPORTED PLATE RADIATING SOUND FROM A RIGID BAFFLE

Let the center of a plate, $-L_x \leqslant \chi \leqslant L_x$, $-L_y \leqslant y \leqslant L_y$, be the origin of coordinates. The pq'th mode of displacement anywhere in the plate is,

$$w_{pq} = A_{pq} W_{pq} = A_{pq} \cos k_p x \cos k_q y \tag{4.2.29}$$

$$k_p = \frac{p\pi}{2L_x}\ ; k_q = \frac{q\pi}{2L_y}\ ; p, q = 1, 3, 5, \ldots$$

In view of 4.2.7 where a Fourier transform in k_x, k_y is performed it will be useful to take the finite cosine transform of w_{pq}. With a slight change in notation, one has,

$$w_{pq}(k_p, k_q, \gamma_x, \gamma_y) = \int_{-L_x}^{L_x}\int_{-L_y}^{L_y} A_{pq} \cos k_p x \cos k_q y \cos \gamma_x x \cos \gamma_y y \, dxdy \tag{4.2.30}$$

Eq. 4.2.7 in steady state then leads to the form,

$$\psi_{pq}(k_p, k_q) = \int_{-\infty}^{\infty}\int \frac{d\gamma_x d\gamma_y}{(2\pi)^2} \frac{i(-i\omega)\, w_{pq}(k_p, k_q, \gamma_x, \gamma_y)}{k_z} e^{i(k_x x + k_y y + k_z z - \omega t)} \tag{4.2.31}$$

Now the mn'th modal force on the surface of the plate ($z = 0$) is,

$$F_{mn}(k_m, k_y) = \int_{-L_x}^{L_x}\int_{-L_y}^{L_y} p(x, y, 0) \cos k_m x \cos k_n y \, dxdy \tag{4.2.32}$$

$$p(x, y, z, t) = \varrho \frac{\partial \psi}{\partial t} = -i\omega\varrho\, \psi(x, y, z, t) \tag{4.2.33}$$

Substitution of 4.2.31 into the modal form of 4.2.33 at $z = 0$ and 4.2.32, gives F_{mn}. However, because of 4.2.30 it is seen that,

$$\int_{-L_x}^{L_x}\int_{-L_y}^{L_y} e^{i(k_x x + k_y y)} \cos k_m x \cos k_n y \, dxdy = \frac{w_{mn}(k_m, k_n, \gamma_x, \gamma_y)}{A_{mn}}$$

Thus,

$$F_{mn}(k_m, k_n) = \frac{-i\omega\varrho}{A_{mn}} \sum_{p,q} \int_{-\infty}^{\infty}\int \frac{d\gamma_x d\gamma_y}{(2\pi)^2} \frac{i(-i\omega)\, w_{pq}(k_p, k_q, \gamma_x, \gamma_y)\, w_{mn}(k_m, k_n, \gamma_x, \gamma_y)}{k_z} \tag{4.2.34}$$

In terms of amplitude of surface velocity $-\omega A_{pq}$, the modal force is,

$$F_{mn} = \sum_{p,q} -i\omega H_{mnpq} W_{pq}$$

where,

$$H_{mnpq} = \rho\omega \int_{-\infty}^{\infty}\int \frac{d\gamma_x d\gamma_y}{(2\pi)^2 k z} \int\int \cos k_p x \cos k_q y \cos \gamma_x x \cos \gamma_y y \, dxdy \qquad (4.2.35)$$
$$\times \int\int \cos k_m x \cos k_n y \cos \gamma_x x \cos \gamma_y y \, dxdy$$

Here, H_{mnpq} is a coupling mechanical impedance (units: $Ns\ m^{-1}$). It is converted to the required coupling specific acoustic impedance by multiplication with $(ab)^{-1}$:

$$Z_{mnpq} = \frac{H_{mnpq}}{ab} \qquad (4.2.36)$$

C. CALCULATION OF THE RADIATION FIELD OF THE PLATE IN THE FORM OF A MODAL SUM

The amplitudes A_{mn}, obtained from 4.2.28, 4.2.35, 4.2.36, allow one to calculate the normal component of plate surface velocity in the steady state by means of 4.2.19,

$$V_z(\gamma_x, \gamma_y | \omega) = -i\omega \sum_{m,n} A_{mn} W_{mn}(\gamma_x, \gamma_y | \omega) \qquad (4.2.37)$$

where

$$W_{mn}(\gamma_x, \gamma_y | \omega) = \int\int\int W_{mn}(x, y)\, e^{-i\gamma_x x - i\gamma_y y} e^{+i\omega t} \, dxdydt$$

The radiated velocity potential field is then obtained by substitution of 4.2.37 into 4.1.9:

$$\psi(x, y, z, t) = \int_{-\infty}^{\infty}\int\int \frac{i(-i\omega) \sum_{m,n} A_{mn} W_{mn}(\gamma_x, \gamma_y | \omega)}{\gamma_z} \exp i[\gamma_x x + \gamma_y y + \gamma_z z - i\omega t] \frac{d\gamma_x d\gamma_y d\omega}{(2\pi)^3}$$

in which

$$\gamma_z = \sqrt{k^2 - \gamma_x^2 - \gamma_y^2} \qquad (4.2.38)$$

The radiated pressure field is then found from 4.2.33.

D. CALCULATION OF THE RADIATION FIELD OF THE PLATE BY MEANS OF GREEN'S FUNCTIONS

Because the baffle here is assumed rigid one may apply Rayleigh's formula 1.8.18 to find the acoustic velocity potential in the steady state at point R' on the plate due to a velocity $V_z = -i\omega\, w(R_0)$ at point R_0 on the plate:

$$\psi(R'|\omega) = \frac{1}{2\pi}\int_s \frac{\exp[ikr]}{r}(-i\omega)\, w(\vec{R}_0)\, dS(\vec{R}_0) \quad r = |\vec{R}' - \vec{R}_0| \tag{4.2.39}$$

To use this formula one requires an explicit form $w(\vec{R}_0)$. It is found from the equation of plate motion. By use of 4.2.18, 4.2.33, 4.2.39, the dynamic equation governing the displacement of a plate which experiences a reaction from the medium is,

$$(\nabla^4 - k_p^4)\, w(x, y|\omega) = \frac{Q^{(A)}(x', y')}{D} + \frac{\varrho\omega^2}{2\pi D}\oint w(x_0, y_0)\frac{e^{ikr}}{r}\, dS(x_0, y_0)$$

$$\vec{R}_0 = \hat{i}x_0 + \hat{j}y_0;\ \vec{R}' = \hat{i}x' + \hat{j}y';\ r = |\vec{R}' - \vec{R}_0| \tag{4.2.40}$$

This is an integral-differential equation in the unknown displacement $w(x, y|\omega)$. It can be converted into a more useful form if one can find the 2-D Green's function $G(\vec{r}|\vec{r}_0|\omega)$ which satisfies the following equation with its associated boundary conditions:

$$(\nabla^4 - k_p^4)\, G(x, y|x', y'|\omega) = -\delta(x - x')\,\delta(y - y')\, e^{-i\omega t} \tag{4.2.41}$$

$$\partial G/\partial n = 0\text{: on the surface of the plate}$$

in which the units of G are m^2. The negative sign on the right hand side indicates a *concentration* of G at x', y'. The converted result is,

$$w(x, y|\omega) = e^{-i\omega t}\left\{\oint \frac{Q^{(A)}(x', y')}{D}\, G(x, y|x', y'|\omega)\, dS(x', y')\right.$$

$$+\oint \frac{\varrho\omega^2}{2\pi D}\, G(x, y|x', y'|\omega)\, dS(x', y')\oint \omega(x_0, y_0) \tag{4.2.42}$$

$$\left.\times \frac{\exp ik\sqrt{(x' - x_0)^2 + (y' - y_0)^2}}{\sqrt{(x' - x_0)^2 + (y' - y_0)^2}}\, dS(x_0, y_0)\right)$$

This is now an integral equation in unknown w because w appears on both sides of the equation. In the general case an approximate solution may be attempted by partitioning the surface into N cells $\Delta S(i)$, $i = 1, 2 \ldots N$ and converting 4.2.42 into a system of algebraic equations in unknown $w(j)$, $j = 1, 2 \ldots N$:

$$w(j) - \sum_{i=1}^{N} \frac{\varrho\omega^2}{2\pi D}\, G(ji)\, \Delta S(i) \sum_{l=1}^{N} q(il)\, w(l)\, \Delta S(l) = \sum_{i=1}^{N} \frac{G(ji)}{D}\, Q^{(A)}(i)\, \Delta S(i) \tag{4.2.43}$$

in which i, j, l identify the coordinates (x', y'), (x, y), (x_0, y_0) respectively.

Once the displacements $w(x, y|\omega)$, or $w(j)$, are found from 4.2.43 they can be used directly in 4.2.39 to obtain the radiated velocity potential. The potential ir turn, determines the radiated pressure field in accordance with 4.2.33.

4.3 KING-BOUWKAMP RADIATION INTEGRAL FOR CIRCULAR RADIATION IN BAFFLES

The calculation of radiation fields by Fourier methods is applicable to radiators in other coordinate systems. An important case is that if circular pistons whose geometry is described by cylindrical coordinates. A planar radiator of circular shape, radius a, is centered at the origin of a

rectangular coordinate system x, y, z. An elementary area dS of this radiator radiates sound to a field point $\vec{r} = (r'', \varphi'', z)$, Fig. 4.3.1. By superposition of all such areas the total field at the point can be determined.

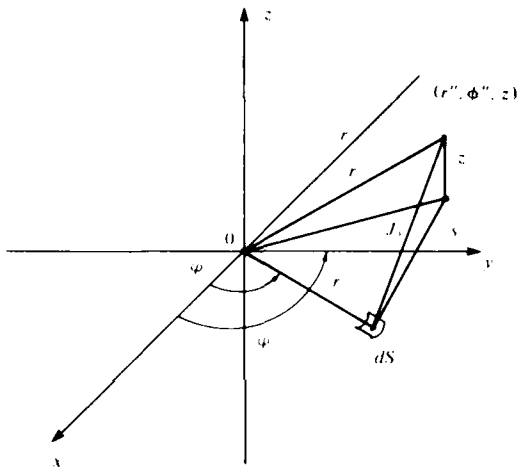

Fig. 4.3.1. Geometry of radiation from a plane area dS.

The superposition is given by Rayleigh's formula, 4.2.39. To use it one requires $\exp ikr/r$ in the coordinates of Fig. 4.3.1. Using the Fourier-Bessel transform pair,

$$\text{(a) } f(s) = \int_0^\infty g(\xi)\, J_0(\xi s)\, \xi d\xi$$

$$\text{(b) } g(\xi) = \int_0^\infty f(s)\, J_0(\xi s)\, s ds \tag{4.3.1}$$

and choosing $f(s) = e^{iks}/s$, one sees from a table of integrals [2] that 4.3.1a becomes,

$$\frac{e^{iks}}{s} = \int_0^\infty \frac{J_0(\xi s)\xi d\xi}{\sqrt{\xi^2 - k^2}} \tag{4.3.2}$$

For $z > 0$,

$$\frac{e^{ikq}}{q} = \int_0^\infty \frac{J_0(\xi s)e^{-\sqrt{\xi^2 - k^2}\, z}}{\sqrt{\xi^2 - k^2}}\, \xi d\xi \tag{4.3.3}$$

in which $q^2 = s^2 + z^2$. This is a measure of the spherical field radiated by dS to point (r'', φ'', z). Substitution of 4.3.3 into 4.2.39 leads to a formula for the radiated velocity potential,

$$\psi(\vec{R}) = \frac{e^{-i\omega t}}{2\pi} \oint_S (-i\omega)\, w(\vec{R}_0) \int_0^\infty \frac{J_0(\xi s)\, e^{-\nu z}}{\nu}\, \xi d\xi dS(\vec{R}_0), z \geq 0 \tag{4.3.4}$$

$$\vec{R} = (r'', \phi'', z);\ \vec{R}_0 = (r', \phi');\ \nu = \sqrt{\xi^2 - k^2}$$

Now in cylindrical coordinates $w(R_0)$ is necessarily periodic in 2π, and can be represented by a Fourier series,

$$w(\vec{R}_0) = \sum_{m=0}^{\infty} [w'_m(r') \cos m\varphi' + w'_{m,n}(r') \sin m\varphi'], \qquad \text{(units: } m\text{)} \tag{4.3.5}$$

It will be useful to consider the symmetrical ($\cos m\varphi'$) term first. The integral to be evaluated then has the form,

$$\int_0^a \int_0^{2\pi} w'_m(r') \cos m\varphi' \, J_0(\xi s) \, r' dr' d\varphi'$$

From Fig. 4.3.1

$$s = [r'^2 + r''^2 - 2r'r'' \cos(\varphi'' - \varphi')]^{1/2}$$

Because of the addition theorem in the theory of Bessel functions [3],

$$J_0(\xi s) = \sum_{m=0}^{\infty} \varepsilon_m J_m(\xi r'') \, J_m(\xi r') \cos m(\varphi'' - \varphi')$$

$$\varepsilon_m = 1, \varepsilon_m = 2, m \neq 0,$$

The integral over φ' is,

$$\int_0^{2\pi} \cos m(\varphi'' - \varphi') \cos m\varphi' d\varphi' = \cos m\varphi'' \int_0^{2\pi} \cos^2 m\varphi' d\varphi' = \cos m\varphi'' \; \frac{2\pi}{\varepsilon_m}$$

4.3.4 therefore reduces to the following equation in the velocity potential,

$$\text{(a)} \quad \psi(r'', \varphi'', z|\omega) = e^{-ikz} \sum_{m=0}^{\infty} (-i\omega) \cos m\varphi'' \int_0^{\infty} J_m(\xi r'') f'_m(\xi) \frac{e^{-\nu z}}{\nu} \xi d\xi, \tag{4.3.6}$$

where

$$\text{(b)} \quad f'_m(\xi) = \int_0^a J_m(\xi r') \, w'_m(r') \, r' dr'$$

Eq. 4.3.6a is the *King-Bouwkamp* radiation integral.

When the nonsymmetrical term in 4.3.5 is considered, the integral over φ' is,

$$\int_0^{2\pi} \cos m(\varphi'' - \varphi') \sin m\varphi' d\varphi' = \sin m\varphi'' \int_0^{2\pi} \sin^2 m\varphi' d\varphi' = \pi \sin m\varphi''$$

The velocity potential in this case becomes

$$\psi(r'', \varphi'', z|\omega) = \frac{e^{-ikz}}{2} \sum_{m=0}^{\infty} \varepsilon_m (-i\omega) \sin m\varphi'' \int_0^{\infty} J_m(\xi r'') f''_m(\xi) \frac{e^{-\nu z}}{\nu} \xi d\xi \tag{4.3.7}$$

$$f''_m(\xi) = \int_0^a J_m(\xi r') \, w''(r') \, r' dr' \ldots,$$

A superposition of 4.3.6.a and 4.3.7 gives the general case of a circular piston in a rigid baffle.

4.4 WEYL'S EXPANSION AND 3-D GREEN'S FUNCTIONS

The description of radiation fields by plane wave expansions in spherical coordinates provide a powerful tool for solving many radiation problems. Such expansions are associated with the freefield Green's function, which describes a field at x, y, z due to a source at x_0, y_0, z_0, ...

$$\frac{e^{ikR}}{R} = \frac{ik}{2\pi}\int e^{ik[(x-x_0)\cos\alpha+(y-y_0)\cos\beta+(z-z_0)\cos\gamma}\,d\Omega(\alpha,\beta,\gamma) \qquad (4.4.1)$$

$$R = \sqrt{(x-x_0)^2+(y-y)^2+(z-z_0)^2}$$

(Weyl's expansion), in which $d\Omega$ is an elementary solid angle, and $\cos\alpha$, $\cos\beta$, $\cos\gamma$ are direction cosines. In spherical coordinates θ, ϕ,

$$\cos\alpha = \sin\theta\cos\phi;\ \cos\beta = \sin\theta\sin\phi;\ \cos\gamma = \cos\theta;\ d\Omega = \sin\theta d\theta d\phi$$

Now the angle θ is the polar angle measured from the z-axis of an x, y, z coordinate system. In real space it ranges from 0 to π. However, because of symmetry of the field the range can be taken as 0 to $\pi/2$. In this range each plane wave [$\exp(ik\cos\theta - i\omega t)$] is oscillatory and thus represent the outward traveling field. However, Eq. 4.4.1 must also have a local, non-traveling field to represent the nearfield, or inertial field, of the source. The angle θ must therefore take on imaginary values, namely $\cos\theta \rightarrow \cos[\pi/2 \pm i\delta] = \mp i\sinh\delta$. The choice of negative sign which gives $-i\delta$, hence $+i\sinh\delta$, is here appropriate because $\exp ik(z-z_0)\cos[\pi/2 - i\delta] = \exp(-k\sinh\delta)$, and thus represents decaying waves when $z > z_0$. Eq. 4.4.1 therefore reduces to,

$$\frac{e^{ikR}}{R} = \frac{ik}{2\pi}\int_0^{\pi/2-i\infty} d\theta \int_0^{2\pi} d\phi\, e^{ik[(x-x_0)\sin\theta\cos\phi+(y-y_0)\sin\theta\sin\phi+(z-z_0)\cos\theta]} \times \sin\theta d\theta d\phi \qquad (4.4.2)$$

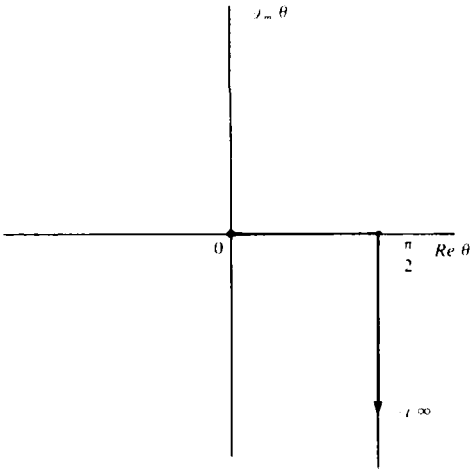

Fig. 4.4.1. Path of integration of Weyl's expansion.

The integration path starting at $\theta = 0$ in the complex θ-plane is shown in Fig. 4.4.1. The integration over ϕ may be carried out by noting that,

$$(x-x_0)\sin\theta\cos\phi + (y-y_0)\sin\theta\sin\phi$$

$$= \sin\theta\, r\cos(\varphi - \zeta)$$

$$r = \sqrt{(x-x_0)^2+(y-y_0)^2};$$

$$\zeta = \tan^{-1}\left(\frac{x-x_0}{y-y_0}\right)$$

$$\int_0^{2\pi} e^{ik[r\sin\theta\cos(\phi-\zeta)]}\,d\phi = 2\pi J_0(r\sin\theta)$$

The 3-D Green's function, with $(4\pi)^{-1}$ included, is then

$$g(R) = \frac{e^{ikR}}{4\pi R} = \frac{ik}{4\pi}\int_C J_0(r\sin\theta)\, e^{ik(z-z_0)\cos\theta}\sin\theta d\theta \qquad (4.4.3)$$

where contour C extends from $\theta = 0$ to $\theta = \pi/2$, then from $\theta = \pi - i0$ to $\theta = \pi/2 - i\infty$.

From its construction it is seen that Weyl's expansion can be used to describe a steady state field of plane planes traveling in all θ-directions, initially generated by a point source, with waves in real angles θ going to the farfield, and waves in imaginary angles θ remaining in the nearfield.

4.5 THE RADIATION OF SOUND IN THE LIMIT OF HIGH FREQUENCIES-THE GEOMETRIC CASE

The radiation of sound at high frequencies from a radiator of arbitrary shape may be calculated by a method of approximation with very good precision. A case of particular importance is the 2-dimensional radiation from a vibrating cylinder of convex cross-section analyzed by Lax and Feshbach [4].

Consider first a plane defined by the polar coordinates r, ϕ. A general plane wave whose propagation vector $\boldsymbol{k}$ lies in this plane and makes an angle u with the direction $\phi = 0$ contributes a complex pressure p at point $P(r, \phi)$. The phase of this wave relative to $e^{i\omega t}$ is given by the formula

$$e^{i\boldsymbol{k}\cdot\boldsymbol{r}} = e^{ikr\cos(\phi - u)}$$

Fig. 4.5.1 shows this elementary plane wave and its associated angles. Now let there be a vibrating cylindrical surface of infinite axial length whose trace in the plane defined above is described analytically by the function $a(\varphi)$. Each element of surface (i.e., each elementary section of the trace) generates a wave which can be decomposed into elementary plane waves of the type described above. A sum of these elementary plane waves gives the pressure at any external field point. At the surface of the cylinder there is a prescribed pressure distribution $p(a(\varphi))$ to which the pressure at P must reduce as distance r approaches surface $a(\varphi)$. To insure this reduction one first multiplies each elementary plane wave traveling in direction u by a complex expansion constant $g(u)$ exp $[-ikb(u)]$ and adds the contributions to the pressure at P from plane waves in all direction, *including complex ones.* One thus obtain the contour integral,

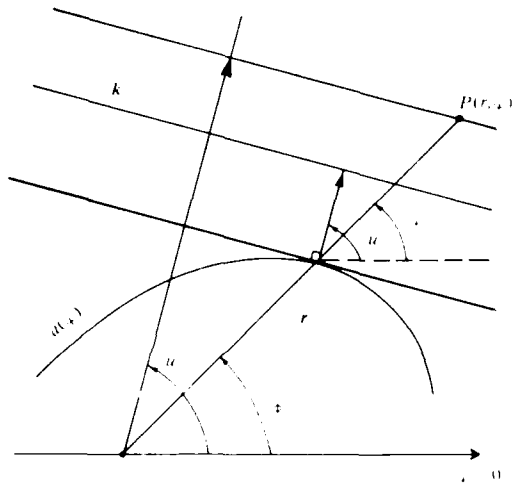

Fig. 4.5.1. Plane wave components radiated by a surface $a(\varphi)$.

$$p(r, \varphi) = \int_{-\pi/2+i\infty}^{\pi/2-i\infty} e^{ikr\cos(\varphi - u)} g(u)\, e^{ikb(u)}\, du \qquad (4.5.1)$$

The rationale in the choice of limits on polar angle u is this: the surface $a(\varphi)$ being convex, only points that lie in the range $-\pi/2 < \varphi < \pi/2$ can possibly see the field point P, if the waves are assumed to be unable to go around the "dark side" of surface $a(\varphi)$. Here the limits on complex u have been chosen so as to insure convergence of the integral when time is given by $e^{i\omega t}$ [5].

For a discussion of the meaning of the term "complex direction" the reader is referred to Sect. 4.4. The complex expansion constants must be so selected that on the radiating surface $r = a(\varphi)$ the complex pressure is prescribed to be given by $p = (\varphi)$. Hence

$$p(a(\varphi)) = \int_{-\pi/2+i\infty}^{\pi/2-i\infty} e^{ik\zeta(u)} g(u)\, du \qquad (4.5.2a)$$

$$\zeta(u) = b(u) - a(\varphi)\cos(\varphi - u) \qquad (4.5.2b)$$

AD-A140 578 A TREATISE ON ACOUSTIC RADIATION(U) NAVAL RESEARCH LAB 3/7
WASHINGTON DC S HANISH 1981

UNCLASSIFIED F/G 20/1 NL

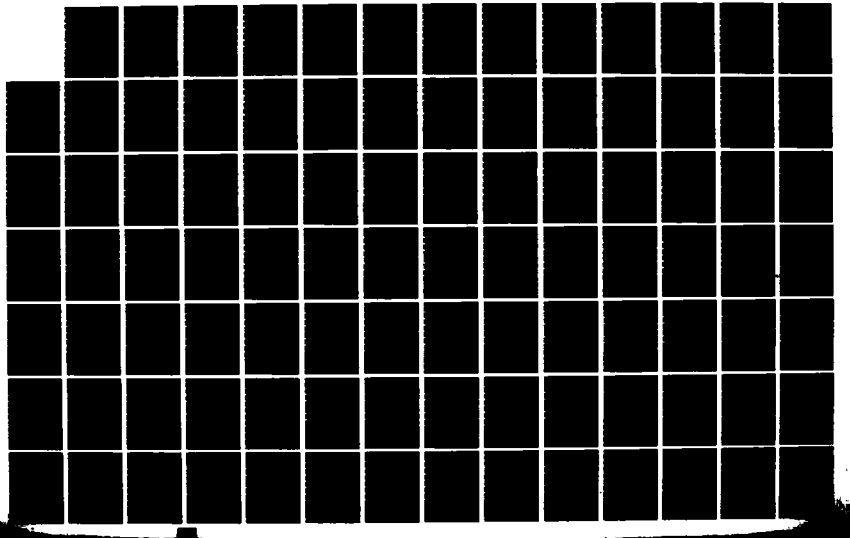

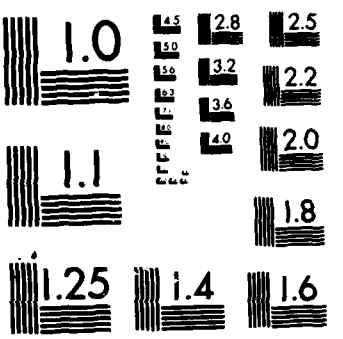

MICROCOPY RESOLUTION TEST CHART
NATIONAL BUREAU OF STANDARDS-1963-A

This is a Fredholm integral equation of the first type in the unknown amplitudes $g(u)$ and unknown phases $b(u)$. A solution of it which is asymptotically correct in the limit of high frequencies (i.e. large $ka(\varphi)$) can be obtained (see Appendix IIIA), by means of the saddle point method. Consider a point $a(\varphi)$ and erect at it a normal whose direction is U_0, see Fig. 4.5.2.

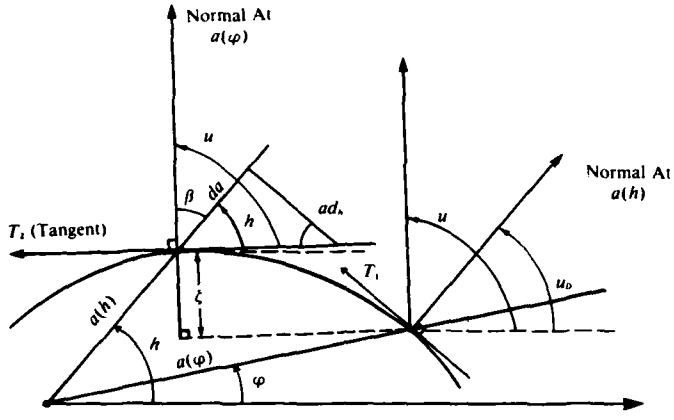

Fig. 4.5.2. Geometry of normals and tangents needed for saddle-point method of solving integral equation 4.5.2a.

At this point expand the phase function ζ of 4.5.2b in a Taylor series of powers in the variable direction $(u - u_0)$,

$$\zeta(u, \varphi) = \sum_{n=0}^{\infty} \frac{\zeta^{(n)}(u, \varphi)\,(u - u_0)^n}{n!} \tag{4.5.3a}$$

$$\zeta^{(n)} = \frac{\partial^n \zeta}{\partial u^n}\Bigg]_{u=u_0}, \quad \zeta^{(0)} = \zeta(u_0) \tag{4.5.3b}$$

From 4.5.3b it is seen that the first term ($= \zeta^{\circ}$) in this Taylor series is independent of direction u. It has the form,

$$\zeta^{(0)} = b(u_0) - a(\varphi)\cos(\varphi - u_0)$$

The phase $e^{-ik\,\zeta^{(0)}}$ can be factored out from 4.5.2a and placed outside the integral sign. This quantity corresponds to the phase of $p(\varphi)$ at the surface point $a(\varphi_0)$. Since it is arbitrarily prescribed one may for convenience select $b(u_0)$ such that $\zeta^{(0)} = 0$. This is permissible in radiation problems. In symbols, $b(u_0)$ is chosen such that,

$$b(u_0) = a(\varphi)\cos(\varphi - u_0) \tag{4.5.4a}$$

From this it may be inferred that in general there is an angle h (measured from the line $\varphi = 0$) such that

$$b(u) = a(h)\cos(h - u) \tag{4.5.4b}$$

Substituting this into 4.5.2b one finds that

$$\zeta(u) = a(h)\cos(h - u) - a(\varphi)\cos(\varphi - u) \tag{4.5.4c}$$

To this stage in the analysis no stipulation has been made concerning the frequency of radiation. Assume this frequency is very high. This corresponds in the mathematical sense to the assumption that the phase angle $\exp(-ikb(u))$ at point $a(\varphi)$ on the radiating surface changes very rapidly with direction u in all directions (complex directions included) except in the neighborhood of the normal $u = u_0$. In an acoustical sense all the elementary plane waves composing the high frequency radiation emanating from $a(\varphi)$ interfere with each other destructively in all directions except the normal direction. The phase function $\zeta(u)$ is therefore stationary at $u = u_0$,

$$\frac{\partial \zeta}{\partial u} = 0 \Bigg]_{u=u_0} \tag{4.5.5}$$

Since

$$\frac{\partial \zeta}{\partial \varphi} = \frac{\partial \zeta}{\partial u}\,\frac{\partial u}{\partial \varphi}$$

this implies that,

$$\frac{\partial \zeta}{\partial \varphi} = 0 \Bigg]_{u=u_0} \tag{4.5.6}$$

Using 4.5.4c to perform this last operation one obtains,

$$\frac{\partial \zeta}{\partial \varphi} = [a(\varphi)\sin(\varphi - u) - a'(\varphi)\cos(\varphi - u)]_{u=u_0} = 0 \tag{4.5.7}$$

or

$$u_0 = \varphi - \tan^{-1}\left(\frac{a'(\varphi)}{a(\varphi)}\right)$$

At point $a(\varphi)$ the normal direction is given by angle u_0. However at $a(\varphi)$ there are plane waves emanating in arbitrary directions ($= u$). If the radiating body is convex there will always be another point $a(h)$ on the surface whose normal points in these directions u. The equation of this normal may be obtained from 4.5.7,

$$u = h - \tan^{-1}\left(\frac{a'(h)}{a(h)}\right) \tag{4.5.8}$$

Fig. 4.5.2 shows the relation between u, u_0, h, ϕ, $a(\phi)$, $a(h)$ and other parameters.

The entity $\zeta\,(u, \varphi)$ is the path difference between radiation from $a(\varphi)$ and $a(h)$ in the direction u. From 4.5.8 it is seen that,

$$\frac{du}{dh} = 1 - \frac{d}{dh}\left(\tan^{-1}\frac{a'(h)}{a(h)}\right) \tag{4.5.9a}$$

$$= \frac{(a'^2 + a^2)^{1/2}}{\varrho(h)}$$

where $\varrho(h)$ is the radius of curvature of the trace at point $a(h)$ with the form

$$\varrho(h) = \frac{(a'^2 + a^2)^{3/2}}{a^2 + 2a'^2 - aa''}$$

also from Fig. 4.5.2 it is seen that ζ when considered as a vector, is collinear with the tangent at $a(h)$ and $d^2\zeta/du^2$ is collinear with the curvature at $a(h)$. Now from 4.5.5

$$\left.\frac{\partial^2\zeta}{\partial u^2}\right]_{u=u_0} = \text{constant} \tag{4.5.9c}$$

This constant (considered as a vector) points in the direction of the curvature at $a(h)$ *in the limiting condition when* $h \to \varphi$ (i.e. when $u = u_0$). Hence one may take the constant as the radius of curvature ($= \varrho(\varphi)$) at $a(\varphi)$. Recalling 4.5.4a one can write,

$$\left.\frac{\partial^n\zeta}{\partial u^n}\right]_{u=u_0} = \frac{d^n b(u_0)}{du^n} - b(u_0)\cos\frac{n\pi}{2} - \frac{db(u_0)}{du}\sin\frac{n\pi}{2} \tag{4.5.10}$$

The first non-vanishing derivative is $n = 2$.

$$\frac{\partial^2\zeta}{\partial u^2} = \varrho(\varphi) = \frac{d^2 b(u)}{du^2} + b(u_0)$$

To a first approximation then, the path difference between rays at $a(h)$, $a(\varphi)$ is

$$\zeta \cong \frac{1}{2}\,\varrho(\varphi)\,(u - u_0)^2 \tag{4.5.11}$$

Now consider the point $a(\varphi)$ and note in Fig. 4.5.2 that at very high frequencies the contributions of all plane waves radiating in all directions u in 4.5.2a tend to cancel except the contributions due to angles near $u = u_0$. As a first approximation then take $g(u)$ to be very nearly $g(u_0)$ over the *effective* range of integration (= range with a confined spread over $u = u_0$). Hence,

$$p(a(\varphi)) \cong g(u_0)\int_C e^{-ik\varrho(\varphi)(u-u_0)^2}\,du \tag{4.5.12}$$

Here the contour C in the complex u-plane has the same limits as 4.5.2a but is deformed near the saddle point $u = u_0$ in such a manner that it crosses the real axis once at the real angle u_0 (see Appendix IIIA for details on contour integration.) Since the integrand is an even function of u one can divide the integral in two equal parts, transform u to $\bar{u} \pm u_0$ and integrate twice over $d\bar{u}$ along a real straight line u from 0 to ∞. By use of a table of definite integrals, ref. [6], the following form is finally obtained,

$$g(u_0) = (\varphi)\left[\frac{ik\varrho(\varphi)}{2\pi}\right]^{1/2} \tag{4.5.13}$$

This equation states that in the high frequency limit the amplitude of the elementary plane wave radiated from point $a(\varphi)$ in the normal direction $u = u_0$ is proportional to the prescribed pressure amplitude $\varrho(\varphi)$ multiplied by the curvature factor $\varrho(\varphi)^{1/2}$. Returning now to 4.5.1 assume that the field point is very far from the radiating surface (i.e. r is very large), and consider first that $\varphi = 0$, and $g(u) \times \exp(-ikb(u))$ is unity. From ref. [7],

$$\int_c e^{ikr\cos u}\, du = \pi H_0^{(1)}(kr) \tag{4.5.14a}$$

and

$$\lim_{r\to\infty} H_0^{(1)}(kr) = \sqrt{\frac{2}{\pi kr}}\, e^{ikr}\, e^{-i\pi/4} \tag{4.5.14b}$$

It is expected then that at very large r the pressure given by 4.5.1 will vary with distance r according to the right-hand side of 14b. Now select a far-field point in a direction u_0 and find on the cylinder a point whose normal is in this same u_0-direction. In accordance with 4.5.13 the direction-contingent amplitudes of the elementary plane waves that contribute most to the far field pressure are very nearly all equal to $g(u_0)$, and their direction-contingent phases are very nearly all equal to $\exp(-ikb(u_0))$ where the function $b(u)$ is given by 4.5.4b and u_0 is given by 4.5.7. Applying the method of steepest descents once more to 4.5.1 we see that $\varphi = u_0$ is the saddle point. Using 4.5.14b one finds the pressure at far field point $P(r, u_0)$ by summing only the *contributing elementary plane waves.* This pressure is

$$\begin{aligned} p(r, u_0) &\underset{r\to\infty}{\to} \pi \sqrt{\frac{2}{\pi kr}}\, e^{ikr}\, e^{-i\pi/4}\, p(\varphi)\, i^{1/2} \left(\frac{k}{2\pi}\right)^{1/2} \varrho(\varphi)^{1/2}\, e^{-ikb(u_0)} \\ &\to \left(\frac{\varrho(\varphi)}{r}\right)^{1/2} (\varphi) \exp(ik[r - b(u_0)])R \end{aligned} \tag{4.5.15}$$

Here φ is the angle in Fig. 4.5.2 such that the normal at $a(\varphi)$ points in the u_0 direction. The factor R is introduced here in the form $R = 1$ because one has assumed $g(u_0)$ to be given by 4.5.13. In general, $g(u_0)$ is a complicated function of powers of $\varrho(\varphi)½$ of which the first term only (= the geometric acoustics case) is shown in 4.5.13. An explicit formula for R in the more general case is derived in ref. [4] and discussed in the next Section.

Eq. 4.5.15 is the formula for the far field pressure generated by a prescribed distribution of pressure (= $p(\varphi)$) over the surface $a(\varphi)$. Instead of pressure one may prescribe the normal velocity, $v_n(\varphi)$, over the surface. A course of reasoning similar to that followed above leads to the final result that the pressure at point $P(r, u_0)$ in the far field is given by

$$p(r, u_0) \underset{r\to\infty}{\to} \left[\frac{\varrho(\varphi)}{r}\right]^{1/2} \varrho c v_n(\varphi) \exp(ik[r - b(u_0)])R' \tag{4.5.16}$$

In the first approximation (= the geometric acoustics case) $R' = 1$. A more elaborate formula for R' (= physical acoustics case) in powers of $\varrho(\varphi)½$ is derived in ref. [4], and discussed in the next Section.

4.6 THE RADIATION OF SOUND IN THE LIMIT OF HIGH FREQUENCIES-THE GEOMETRIC CASE PLUS TERMS OF HIGHER ORDER

In Sect. 4.5 a first approximation to $g(u)$ was taken to be $g(u_0)$. In the next order of approximation consider that the variable angle u to be given by $u = u_0 + w(z)$ where $z = u - u_0$ and

$$w(z) = z + \alpha z^2 + \beta z^3 + \ldots \tag{4.6.1}$$

To find α, β, etc compare 4.5.3a and 4.5.11 with 4.6.1. By a direct manipulation of symbols it is seen that

$$\text{(a)} \quad \alpha = -\frac{\zeta^{(3)}}{6\varrho(\varphi)} \qquad \text{(b)} \quad \beta = \frac{5}{2}\alpha^2 - \frac{\zeta^{(4)}}{24\varrho(\varphi)} \tag{4.6.2}$$

in which

$$\zeta^{(i)} \equiv \frac{d^{(i)}\zeta}{d\phi^{(i)}}$$

and

$$\zeta^{(2)} = \varrho(\varphi);\ \zeta^{(3)} = \frac{d\varrho(\phi)}{du_0};\ \zeta^{(4)} = -\varrho(\varphi) + \frac{d\varrho(\varphi)}{du_0} \tag{4.6.3}$$

Using these formulas ref [4] continued the analysis beyond the geometric approximations discussed in Sect. 4.5. It was then found that for the cases of given surface pressure $p(a(\varphi))$, and given surface velocity $v_n(a(\varphi))$, the improved approximations are,

$$g(u_0) = \left[\frac{ik\varrho(\varphi)}{2\pi}\right]^{1/2} S(\varphi)\,\mathcal{R} \tag{4.6.4}$$

and

$$g(u_0) = \left[\frac{ik\varrho(\varphi)}{2\pi}\right]^{1/2} \varrho c v_n(\varphi) R' \tag{4.6.5}$$

where

$$R = 1 - \frac{1}{ik\varrho(\varphi)}\left[3\beta + 3\alpha\,\frac{1}{\varrho(\varphi)^{1/2}S(\varphi)}\,\frac{d}{du_0}\,(\varrho(\varphi)^{1/2}S(\varphi)) - \frac{1}{2}\,\frac{1}{\varrho(\varphi)^{1/2}S(\varphi)}\,\frac{d^2}{du_0^2}\,(\varrho(\varphi)^{1/2}S(\varphi))\right] \tag{4.6.5}$$

$$R' = 1 - \frac{1}{ik\varrho(\varphi)}\left[3\beta - \frac{1}{2} + 3\alpha\,\frac{1}{\varrho(\varphi)^{1/2}v_n}\,\frac{d}{du_0}\,(\varrho(\varphi)^{1/2}v_n) - \frac{1}{2}\,\frac{1}{\varrho(\varphi)^{1/2}v_n}\,\frac{d^2}{du_0^2}\,(\varrho(\varphi)^{1/2}v_n)\right] \tag{4.6.6}$$

Substitutions of these into 4.5.15 and 4.5.16 yield finally formulas for the far field pressure which contain explicitly not only the case of "geometric optics" (i.e., case where $R = R' = 1$) but also contain additional terms of higher order in inverse powers of $k\varrho(\varphi)$.

The mechanical reaction of the medium (= radiation impedance $Z(\varphi)$) to a surface prescribed pressure (= $\varrho(\varphi)$ or normal velocity (= $v_n(\varphi)$) may be found by forming the ratio of $v_n(\varphi)$ to $p(\varphi)$. The ratio takes on the following form,

$$\frac{1}{Z(\varphi)} = Y(\varphi) = \frac{v_n(\varphi)}{S(\varphi)}$$

$$= \frac{1}{\varrho c}\left\{1 - \frac{1}{2ik\varrho(\varphi)} + \frac{1}{2(k\varrho(\varphi))^2}\left[\left(15\alpha + 6\beta - \frac{1}{4}\right)\right.\right. \tag{4.6.7}$$

$$\left.\left. + \frac{12\alpha\dfrac{dg}{du_0}}{g(u_0)} + \frac{2\dfrac{d^2g}{du_0^2}}{g(u_0)}\right]\right\}$$

In this equation we may use $\varrho\,½\varrho(\varphi)$ for $g(u)$ when the surface pressure is prescribed and $\varrho\,½\,v_n$ when the surface (normal) velocity is prescribed.

DISCUSSION

From this Section and Sect. 4.5 one may conclude that at high frequencies and great distances the acoustic field pressure generated by a radiating cylindrical surface in the angular direction u_0 is determined chiefly by the prescribed surface pressure ($= \varrho(\varphi_0)$) or prescribed surface velocity ($= v_n(\varphi_0)$) and the radius of curvature $\varrho(\varphi_0)$ at a surface point $a(\varphi_0)$ whose normal is in the angular u_0 direction. Thus the far field pressure in a given direction arises principally from *one* point on the radiating surface. Each element of the surface radiates normal to itself so that the radiating surface may be regarded as a source of numerous "rays" pointing out perpendicularly from the surface, each ray having in the "geometrical optics" case an infinitesimally narrow width. Such narrow beams generate wave fronts in the far field which have the same angular distribution of pressure or particle velocity that were originally prescribed over the radiating surface. This reproduction of fine detail is predicted by 4.5.15 and 4.5.16. When $k\varrho(\varphi)$ is large but not infinite, the "rays" transform to diffraction patterns with finite main beams. The "width" of one beam (i.e. the angular width where the pressure is $1/\sqrt{2}$ of the peak pressure) is approximately $2\pi/k\varrho(\varphi)$. Radiation from elementary areas is no longer perpendicular to the surface and the field at distant points is no longer due to one point on the surface, but to several neighboring points. Hence reproduction in the far field of the fine detail of pressure or velocity distribution over the generating surface is now only approximate with attendant blurring.

Finally it is noted that the radiation admittance of a surface for $ka(\varphi)$ large is, in the limit of high frequency, equal to $1/\varrho c$ ($=$ a real number). For this result, see 4.6.7. When a first correction is made for the case where $1/k\varrho(\varphi)$ is not negligible compared with unity one finds that the correction term, to first order in $K\varrho(\varphi)$, is $-1/2\ ik\varrho(\varphi)$, and imaginary number. The first correction thus introduces a reactive admittance.

4.7 THEORY OF RADIATION FROM COMPOSITE SOURCES

Acoustic radiators are often collections (or arrays) of identical sources. A theory of such composites is most easily constructed if the sources are all located in an infinite rigid baffle.

Let $V_z(\vec{R}_0)$ be the distribution of the normal ($= z$) component of surface velocity of a composite radiator in an infinite rigid baffle. Then by Rayleigh's formula 1.8.18 the velocity potential of the radiated field is,

$$\psi(\vec{R}) = \frac{1}{2\pi}\oint\frac{e^{ik|\vec{R}-\vec{R}_0|}}{|\vec{R}-\vec{R}_0|}V_z(\vec{R}_0)\,dS(\vec{R}_0) \tag{4.7.1}$$

The evaluation of this integral for arbitrary choice of field point $\vec{R}$ and velocity distribution V_s is very difficult. A powerful simplification is obtained by use of the *farfield approximation*. Fig. 4.7.1 shows the parameters in this approximation. Here, α, β, γ are direction angles of vector R.

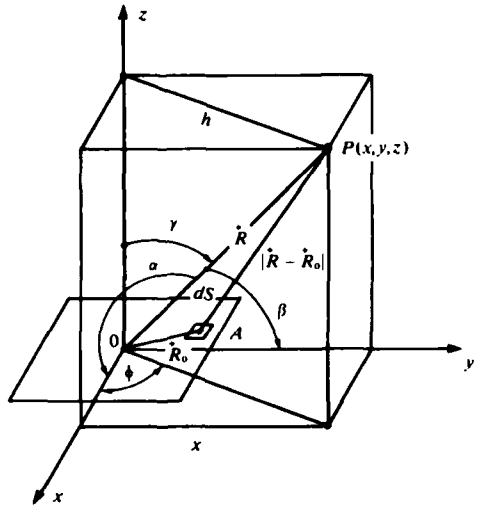

Fig. 4.7.1. Parameters in farfield approximation.

First, for $\vec{R}$ anywhere:

$$|\vec{R} - \vec{R}_0| = \sqrt{(x - x_0)^2 + (y - y_0)^2 + z^2}$$

or

$$|\vec{R} - \vec{R}_0| = \sqrt{R^2 - 2xx_0 - 2yy_0 + R_0^2}$$

$$R^2 = |\vec{R}|^2;\ R_0^2 = |\vec{R}_0|^2;\ \vec{R}_0 = \hat{i}x_0 + \hat{j}y_0$$

Assume $\vec{R}$ is in the farfield of the radiating area $dS(R_0)$; by this is meant the conditions,

$$(1)\ R^2 \gg R_0^2;\ (2)\ \frac{2xx_0}{R^2} \ll 1;\ (3)\ \frac{2yy_0}{R^2} \ll 1$$

Then,

$$|\vec{R} - \vec{R}_0| \cong R\sqrt{1 - \frac{2xx_0}{R^2} - \frac{2yy_0}{R^2}}$$

or

$$|\vec{R} - \vec{R}_0| \cong R\left(1 - \frac{xx_0}{R^2} - \frac{yy_0}{R^2}\right)$$

Because the magnitude R is so large relative to magnitude R_0 both $\vec{R}$ and $\vec{R}_0$ point very nearly in the same direction, that is, are very nearly parallel. The approximation is then made that the direction cosines ($\cos\alpha$, $\cos\beta$, $\cos\gamma$) of AP are the same as those of $0P$. Thus,

$$(1)\ \cos\alpha = \frac{x}{R} \qquad (2)\ \cos\beta = \frac{y}{R} \qquad (3)\ \sin\gamma = \frac{h}{R}$$

However,

$$h\cos\phi = x;\ h\sin\phi = y$$

so that,

$$\sin\gamma = \frac{h}{R} = \frac{x}{(\cos\phi)R} = \frac{\cos\alpha}{\cos\phi}$$

From this relation it is concluded that the following formulas from spherical geometry hold:

$$\cos\alpha = \sin\gamma\cos\phi;\ \cos\beta = \sin\gamma\sin\phi$$

The distance AP in this farfield approximation becomes,

$$|\vec{R} - \vec{R}_0| \cong R - x_0 \cos\alpha - y_0 \cos\beta$$

$$\cong R - x_0 \sin\gamma \cos\phi - y_0 \sin\gamma \sin\phi$$

Eq. 4.7.1 is therefore itself reduced to the farfield approximation,

$$\psi = \frac{1}{2\pi} \frac{e^{ikR}}{R} \oint V_s(x_0, y_0)\, e^{-ik(x_0 \sin\gamma\cos\phi + y_0 \sin\gamma\sin\phi)}\, dx_0 dy_0 \tag{4.7.2}$$

A convenient procedure at this point is to normalize this equation by choosing $\gamma = 0$ and defining a reference source strength,

$$Q_{ref} = \oint V_s(\vec{R}_0)\, dS(\vec{R}_0) \tag{4.7.3}$$

Thus, in terms of the directionality factor $F(\gamma, \phi)$,

$$\psi = \frac{1}{2\pi} Q_{ref} \frac{e^{ikR}}{R} F(\gamma, \phi)$$

where,

$$F(\gamma, \phi) = \frac{1}{Q_{ref}} \oint V_s(\vec{R}_0) \exp -ik(x_0 \sin\gamma \cos\phi + y_0 \sin\gamma \sin\phi)\, dS(\vec{R}_0) \tag{4.7.4}$$

In the farfield the intensity vector is purely radial,

$$I_r = \frac{1}{2} p v_r^* = \frac{1}{2} \left[-i\omega\varrho\, \psi \left(-\frac{\partial \psi}{\partial r} \right)^* \right]$$

Because, in this approximation;

$$-\frac{\partial \psi}{\partial r} = -ik\psi$$

it is seen that

$$I_r = \frac{1}{2} k w \varrho\, |\psi|^2 = \frac{k^2 \varrho c}{2} \times \frac{1}{4\pi^2} Q_{ref}^2 |F(\gamma, \phi)|^2 \tag{4.7.5}$$

in which Q_{ref} is a peak value. This can further be simplified by defining a reference intensity I_{ref} associated with a point source with source strength Q_{ref} radiating into halfspace from an infinite rigid baffle:

$$I_{ref} = I_{ref}(\text{half-space}) = 4I(\text{full space}) = \frac{4}{2} \times \frac{\varrho c}{4r^2} \left(\frac{2\pi}{\lambda} \right)^2 \left(\frac{1}{2\pi} \right)^2 Q_{ref}^2$$

or

$$I_{ref} = \frac{k^2 \varrho c}{8\pi^2} Q_{ref}^2 \tag{4.7.6}$$

Substitution of 4.7.6 into 4.7.5 leads directly to the intensity at a farfield point $\vec{R} = (R, \gamma, \phi)$ due to a composite source in an infinite rigid baffle:

$$I(R, \gamma, \phi) = I_{ref}(R)\, |F(\gamma, \phi)|^2 \tag{4.7.7}$$

This formula states that the radiation of a composite source generates a farfield intensity equal to the product of the intensity due to a point source in an infinite rigid baffle having a source strength equal to the volume velocity of the composite source, and the square of the directionality factor $F(\gamma, \phi)$.

Several examples of this rule are taken up in this treatise. In the next subsection we consider one example of a linear array.

4.7a RADIATION FIELD AND FIELD INTENSITY OF A LINEAR ARRAY OF EXTENDED SOURCES

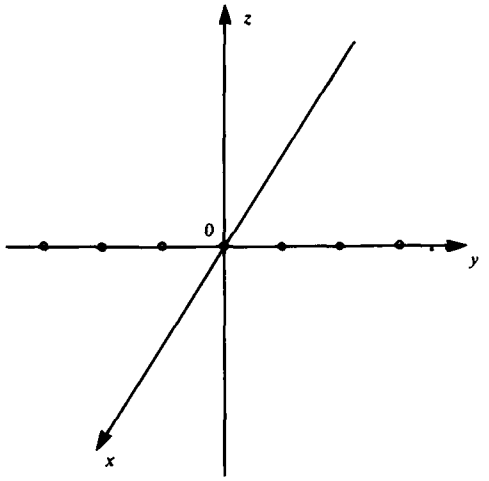

Fig. A.7.2. A linear array of $2N + 1$ sources.

An array of $2N + 1$ identical extended sources are equally and symmetrically spaced at intervals d along the y-axis of an x, y, z coordinate system, Fig. 4.7.2. Because the radiation field is rotationally symmetric about the y-axis the analysis will be restricted to the yz plane, where $\phi = 90°$. In 4.7.4 one replaces y_0 by $y_0 + nd$, $-N \leqslant n \leqslant N$, and obtains an F-factor for the n'th element in the array,

$$F(\gamma, \phi) = e^{-iknd\sin\gamma} F(\gamma)$$

$$F(\gamma) = \frac{1}{Q_{\text{ref}}} \oint V(\vec{R}_0)\, e^{-iky_0\sin\gamma}\, dS(\vec{R}_0) \qquad (4.7.8)$$

The velocity potential of the total array is a sum of the potentials of the individual elements,

$$\psi(R, \gamma) = \frac{1}{2\pi}\, Q_{\text{ref}}\, \frac{e^{ikR}}{R}\, F(\gamma) \sum_{n=-N}^{N} e^{-iknd\sin\gamma} \qquad (4.7.9)$$

Setting $\exp[-iknd \sin\gamma] = \alpha^n$, and noting that,

$$\alpha^n \sum_{-N}^{N} \alpha^n = \sum_{n=0}^{2N} \alpha^n;\quad \sum_{-N}^{N} \alpha^n = \frac{1}{\alpha^N} \sum_{n=0}^{2N} \alpha^n = \frac{1}{\alpha^N} \left[\frac{\alpha^{2N+1} - 1}{\alpha - 1}\right]$$

and

$$\sum_{-N}^{N} \alpha^n = \frac{\alpha^{N+1/2} - \alpha^{-(N+1/2)}}{\alpha^{1/2} - \alpha^{-1/2}} \qquad (4.7.10)$$

it is seen that the sum in 4.7.9 becomes,

$$\sum_{n=-N}^{N} \alpha^n = \frac{\sin[(N + \tfrac{1}{2})kd \sin\gamma]}{\sin(\tfrac{1}{2}kd \sin\gamma)}$$

Thus,

$$\psi(R, \gamma) = \frac{1}{2\pi}\, Q_{ref}\, \frac{e^{ikR}}{R}\, (2N + 1)\, F(\gamma)\, D(kd/2 \sin\gamma) \qquad (4.7.11)$$

where

$$D = \frac{1}{2N + 1} \frac{\sin[(2N + 1)\, kd/2 \sin\gamma]}{\sin(kd/2 \sin\gamma)} \tag{4.7.12}$$

Now $F(\gamma)$ is the directivity of a single extended source, and D is the directivity of $2N + 1$ point sources. The directivity of the composite is $F(\gamma)\, D\, (kd/2 \sin\gamma)$. This result that the directivity of a composite radiator of $2N + 1$ identical elements is the product of the directivity of one of the elements and the directivity of $2N + 1$ point sources, is the *product rule*. It is valid in all of linear acoustics.

The same conclusion is reached when the number of sources is an even number N. In this case it is convenient to place the origin of the coordinate system at the outermost leftside source. Then,

$$\sum_{n=0}^{N-1} e^{-inkd\sin\gamma} = \sum_{n=0}^{N-1} \alpha^n = \frac{\alpha^n - 1}{\alpha - 1} = \frac{\sin[Nkd/2 \sin\gamma]}{\sin(kd/2 \sin\gamma)}\, e^{-i(N-1)kd/2\sin\gamma} \tag{4.7.13}$$

The velocity potential of the compound source in the farfield approximation is obtained from 4.7.9:

$$\psi(R, \gamma) = \frac{1}{2\pi}\, Q_{\text{ref}}\, \frac{e^{ikR}}{R}\, NF(\gamma)\, E\left(\frac{kd}{2} \sin\gamma\right) \tag{4.7.14}$$

$$E = \exp[-i(N - 1)\, \frac{kd}{2}\, \sin\gamma]\, \frac{\sin[Nkd/2 \sin\gamma]}{N \sin(kd/2 \sin\gamma)} \tag{4.7.15}$$

Eqs. 4.7.14 and 4.7.15 hold for both N even and N odd. The product rule is again verified.

A calculation of farfield radiated intensity from an array of N(even or odd) sources may be carried out by 4.7.5 in conjunction with 4.7.14 and 4.7.15:

$$I_r(\gamma) = \frac{k^2 \varrho c}{2}\, \frac{1}{4\pi^2}\, Q_{\text{ref}}^2 N^2 |F(\gamma)|^2 \left[\frac{\sin[Nkd/2 \sin\gamma]}{N \sin(kd/2 \sin\gamma)}\right] \tag{4.7.16}$$

REFERENCES

1. P.M. Morse, H. Fesbach, loc. at. p. 1371.
2. I.S. Gradihteyn/I.M. Ryzhik "Table of Integrals Series and Products" p. 707.
3. G.N. Watson "Theory of Bessel Functions", p. 128, Cambridge U. Press.
4. M. Lax, H. Feshbach, "On the Radiation Problem at High Frequencies", Jour. Acous. Soc. Am., Vol. 19, July 1947, p. 683.
5. J.A. Stratton, "Electromagnetic Theory", McGraw-Hill Book Co., Inc., New York, 1941, p. 367.
6. Ref. [2] p. 307.
7. A. Sommerfeld, "Partial Differential Equations in Physics", Academic Press, New York, 1949, p. 89.

CHAPTER V

MULTIPOLE ANALYSIS AND RADIATION FROM SURFACES OF LARGE RADIUS OF CURVATURE

5.1. ACOUSTIC RADIATION FROM SOURCE-BAFFLE COMPOSITES WHICH ARE VERY LARGE OR VERY SMALL RELATIVE TO THE RADIATED WAVELENGTH

In Chapter II of this treatise the steady state acoustic radiation to infinity from closed surfaces in the separable coordinate systems of the Helmholtz equation was studied by the application of the integral equation of linear acoustics 1.7.7. This is a branch of the Sturm-Liouville boundary value problem with solutions in the form of Green's functions. Careful formulation of Eq. 1.7.7 in the steady state for surface distributed sources shows that both the unknown field (viz. velocity potential) and its normal derivative over the surface in question are required to obtain the field at any external point. By appropriate construction of the Green's function it is possible to reduce these requirements and obtain the field by integration over monopole-type surface sources (= normal derivatives of the unknown field on the surface) alone, or by integration over dipole-type surface sources (= unknown field on the surface) alone (see Sect. 1.8). In either case the applied Green's functions (or their derivatives) in the steady state are known to be singular at discrete temporal or spatial frequencies, as may be seen from their eigenfunction expansions 3, 4, 5. These are the resonant frequencies of the vibrating volume of fluid internal to the enclosing surface distribution of sources. At these frequencies then the integral equations which determine the field diverge and the method of Green's functions fails. One exception does however exist. In the event that the distribution of sources (monopole or dipole) over the surface is analytic, and is orthogonal (over the range of the surface at the resonant frequency) to the eigenfunctions in the Green's function expansion then the integral of this distribution multiplied by this Green's function vanishes, and the infinite term in the series given by 3, 4, 5 is dropped from consideration [1]. The field is then finite even though the fluid volume is resonant.

Within the above noted limitations the method of integral equations and Green's functions outlined in Chapter III is successful in linear acoustics, at least to the extent of obtaining formal solutions of boundary value problems of sources, baffles and scalar waves. When the source-baffle composite is very small or very large compared to the wavelength of radiation then other methods, far more suitable to the numerical evaluation of its near and far field, are available in the more general theory. These comprise the method of acoustic multipole fields and the method of Sommerfeld-Watson transformation, both of which are reviewed in detail in this chapter. All methods however depend upon a knowledge of an appropriate Green's function for the spatial boundaries of the problem. A review of the procedure for obtaining new Green's function is presented in the Appendix IIIB.

This case is drawn from the field of electromagnetics has proved to be a fertile source of Green's functions for use in acoustics. Research in Electromagnetic radiation and scattering [2]. Although the electromagnetic field is vectorial while the acoustic field is scalar, there are two electromagnetic boundary conditions whose mathematical descriptions are exactly analogous to typical acoustic problems. For example, let E_t represent the tangential component of electric field strength and ϕ the scalar acoustic potential. The statement then that on a perfectly

conducting surface $E_t = 0$, is analogous to the statement that on a pressure-release surface $\phi = 0$. Similarly letting H_t represent the tangential component of magnetic field strength then the statement that on a perfectly conducting surface $(\partial H_t/\partial n)_s = 0$, is exactly analogous to the statement that on a rigid surface $(\partial\phi/\partial n)_s = 0$.

The case in question in Appendix IIIB determines the Green's function of an axial magnetic dipole in a metallic corner reflector. It is exactly analogous to the problem of an acoustic point source in a rigid corner reflector. Although the case is described in detail it is readily seen to be a particular instance of a general formula for obtaining Green's functions. A full discussion of the general approach is found in ref. [3].

5.2. MULTIPOLE DESCRIPTION OF SOUND SOURCES

The concept of the multipole description of a field quantity has special prominence in the theory of electrostatics. The field of a localized distribution of charge for example may be expanded in spherical harmonics involving inverse powers of distance, each term of which describes (under appropriate restrictions) a species of multipole, such as monopole, dipole, etc. A convenient review of the method is found in ref. [4]. Extensions of the multipole concept to the description of radiation, scattering, hydrodynamics, etc. may be found in standard treatises on these subjects. In the analysis of the generation of acoustic fields the elementary notions of monopole, dipole and quadrupole source description are often used (see Chap. I). We can summarize these sources as follows. An acoustic simple source in the steady state generating sound at frequency f in a fluid medium of characteristic impedance ρc is defined as a *point* which is injecting mass into the fluid at a sinusoidal time varying rate dQ/dt (units: m^3/sec). The time average intensity radiated ($= I$) is given by

$$I = \frac{\varrho S^2 f^2}{8cr^2} = \frac{\varrho c S^2 k^2}{32\,\pi^2 r^2} \tag{5.2.1}$$

in which S is the source strength (or peak amplitude of dQ/dt) and $k = 2\pi/\lambda = \omega/c = 2\pi\ \ f/c$. A dipole source is defined as the juxtaposition of two simple sources an infinitesimal distance apart and pulsating π radians out of phase. The *far field* intensity of a dipole source is given by

$$I = \frac{\pi^2 \varrho c\, S^2\, (\cos^2\theta)\, f^4}{2c^4 r^2} = \frac{\varrho c\, S^2\, (\cos^2\theta)\, k^4}{32\,\pi^2 r^2} \tag{5.2.2}$$

From its nature it is seen that an acoustic dipole source injects no net mass into the propagating fluid over the time of a sinusoidal cycle. It excites sound by the to-and-fro oscillation of mass along a particular direction, and can thus be symbolized as a vector arrow, the head of which is plus and the tail minus. An acoustic quadrupole source is the juxtaposition of two dipoles an infinitesimal distance apart. If the alignment of the force vectors is $-\ +\ +\ -$ the quadrupole is longitudinal and its far field intensity will be proportional to $f^6\,(\cos^4\theta)/r^2$. If the alignment is $\pm\ \mp$ the quadrupole is lateral and its far field intensity will be proportional to $f^6\,(\sin^2 2\theta)/r^2$. These force vectors are loosely analogous to stress vectors, and hence a system of fluctuating stresses on an elementary volume of fluid (or solid) may be equivalent to a sound source of acoustic multipole nature.

Fundamental sources which generate sound in the transient state may be similarly described. For a simple transient source the sound pressure $p(r,t)$ at a field point r is given by

$$p(r,t) = \frac{1}{4\pi r}\,\frac{dQ}{dt}\,(t - \frac{r}{c}) \tag{5.2.3}$$

Similarly for an acoustic dipole transient source in which the force vector arrow has Cartesian components $F_1(t)$, $F_2(t)$, $F_3(t)$ the pressure at field point $r = \sqrt{x_1^2 + x_2^2 + x_3^2}$ is

$$p(r,t) = -\frac{\partial}{\partial x_1}\frac{F_1(t-\frac{r}{c})}{4\pi r} - \frac{\partial}{\partial x_2}\frac{F_2(t-\frac{r}{c})}{4\pi r} - \frac{\partial}{\partial x_3}\frac{F_3(t-\frac{r}{c})}{4\pi r}$$

$$= \frac{1}{4\pi r^2}\sum_{i=1}^{3} x_i\left[\frac{1}{c}F_i'(t-\frac{r}{c}) + \frac{1}{r}F_i(t-\frac{r}{c})\right] \tag{5.2.4}$$

where the prime indicates derivative with respect to argument.

The treatment of higher order multipoles may be pursued by extending the above scheme. However the current use of multipoles beyond the quadrupole-type to describe complex sound generating sources is not common.

5.3. GREEN'S FUNCTIONS AND ACOUSTIC MULTIPOLE FIELDS

Let $\Phi_2(\vec{r})$ represent the potential field of a distribution of acoustic dipoles $q(\vec{r_0})$. For the steady state Φ satisfies the Helmholtz equation,

$$(\nabla_0^2 + k^2)\,\phi_2(\vec{r_0}) = -q(\vec{r_0}) \tag{5.3.1}$$

Now since each elementary dipole field is the resultant of two simple point sources of equal strength A but opposite polarity, one can define a density distribution of simple sources $A(\vec{r_0})$ and write [5],

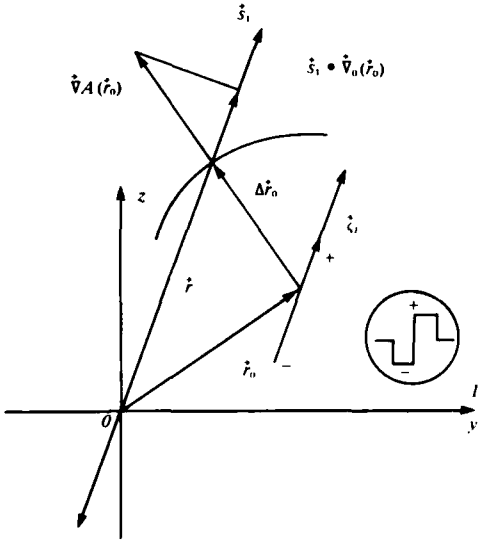

Fig. 5.3.1. Geometry of dipole at $\vec{r_0}$

$$q(\vec{r_0}) = \lim_{\Delta r_1 \to 0} \frac{A(\vec{r_0} + \Delta\vec{r_0}) - A(\vec{r_0})}{|\Delta\vec{r_0}|} \tag{5.3.2}$$

The geometry of the dipole pole at $\vec{r_0}$ is shown in Fig. 5.3.1. The meaning of 5.3.2 can be understood from it in the following way: as the observation point $\vec{r}$ approaches $\vec{r_0}$ from the dipole direction $\vec{s_1}$ it sees a field shown in circle 1. This field is the derivative of a space-impulse $\delta(\vec{r} - \vec{r_0})$. However if the observation approaches $\vec{r_0}$, along $\Delta\vec{r_0}$, the component field in the direction $\vec{s_1}$ is the *directional derivative* of the space impulse.

Thus the limit the right-hand side of this equation is the directional derivative of the delta function in the direction $\vec{s_1}$ (the axis of the dipole) multiplied by the amplitude Q of the dipole source.

Hence

$$q(\vec{r}_0) = Q\left[\frac{\partial \delta(\vec{r} - \vec{r}_0)}{\partial s_1}\right]_{s_1} \tag{5.3.3}$$

The differential operator $\partial s_1 = \partial/\partial s_1$ affects only the $\vec{r}_0$ coordinates.

Recalling now that the Green's function $G(\vec{r} \mid \vec{r}_0)$ is a solution of the inhomogeneous Helmholtz equation with a delta function source $(\nabla_0^2 + k^2) G(\vec{r} \mid \vec{r}_0) = -\delta(\vec{r} - \vec{r}_0)$ we use Eqs. (1) and (3) above and write

$$\begin{aligned} \partial_s [\{\nabla_0^2 + k^2\} QG(\vec{r} \mid \vec{r}_0)] &= -Q\, \partial_s [\delta(\vec{r} - \vec{r}_0)] \\ &= (\nabla_0^2 + k^2)\, \Phi_2(\vec{r}, \vec{r}_0) \end{aligned} \tag{5.3.4}$$

Noting that the operator $\nabla_0^2 + k^2$ is linear we interchange the order of the derivative operators on the left-hand side of this equation and conclude that the field of the dipole sources is given by

$$\Phi_2(\vec{r}, \vec{r}_0) = Q\, \partial_{s_1} \{G(\vec{r} \mid \vec{r}_0)\} \tag{5.3.5}$$

The directional derivative relative to the dipole axis s_1 has the form

$$\frac{\partial}{\partial s_1} \equiv \vec{s}_1 \cdot \vec{\nabla}_0 \tag{5.3.6}$$

where ∇ is the gradient operator in the source coordinates. Eq. (5) can be generalized to any number of directions s_1, s_2, etc. Thus

$$\Phi_{(2^n)}(\vec{r}) = Q_n (\partial_{s_1}\, \partial_{s_2} \ldots\, \partial_{s_n})\, G(\vec{r} \mid \vec{r}_0) \tag{5.3.7}$$

Here the total differential operator in parenthesis is obtained by cross multiplication of individual operators in n directions. The factor Q_n is the amplitude of the multipole and Φ_{2^n} is the field of a multipole of order 2^n.

To illustrate the use of 5.3.7 we first let $n = 0$ and select $G(\vec{r} \mid \vec{r}_0)$ for infinite space. Then

$$\Phi_0(r) = \frac{Q_0}{-4\pi} \frac{e^{ik|\vec{r} - \vec{r}_0|}}{|\vec{r} - \vec{r}_0|} = \frac{Q}{-4\pi} \frac{e^{ikR}}{R} \tag{5.3.8}$$

in which $R = |\vec{r} - \vec{r}_0|$.

When $n = 1$ the field of the dipole relative to the axis of the dipole is

$$\Phi_2(\vec{r}, t) = Q_2 \vec{s}_1 \cdot \vec{\nabla}_0 G(\vec{r} \mid \vec{r}_0) e^{-i\omega t}$$
$$= \frac{Q_2}{-4\pi} e^{ikR} \left[\frac{\cos\theta}{R^2} - \frac{ik\cos\theta}{R} \right] e^{-i\omega t} \qquad (5.3.9)$$

Thus the field of a dipole has a near field with a predominent term varying as $1/R^2$ and a far-field term varying as $1/R$. The angle dependence of both near field and far field remains constant, i. e., cos θ. In the near field (where $kR \ll 1$) the radial particle velocity $v_R = -\frac{\partial \Phi}{\partial R}$ varies as (2 cos θ/R^3) $e^{-i\omega t}$ and the tangential particle velocity $v_\theta = -\frac{1}{R}\frac{\partial \Phi}{\partial \theta}$ varies as (sin θ/R^3) $e^{-i\omega t}$. Hence the particle velocity streamlines in the neighborhood of the dipole are described by the formula $dR/Rd\theta = 2\cos\theta/\sin\theta$, or $R = \text{const} \times \sin^2\theta$. The field pressure ($\rho\partial\Phi_2/\partial t$) and particle velocities ($= -\nabla\Phi_2$) are given by

$$p = \frac{Q_2}{4\pi} i\omega\varrho e^{ikR} \cos\theta \left[\frac{1}{R^2} - \frac{ik}{R} \right] e^{-i\omega t} \qquad (5.3.10a)$$

$$v_R = -\frac{Q_2}{4\pi} \left\{ e^{ikR} \cos\theta \left[-\frac{2}{R^3} + \frac{ik}{R^2} \right] \right. \qquad (5.3.10b)$$
$$\left. + e^{ikR} \cos\theta\, ik \left[\frac{1}{R^2} - \frac{ik}{R} \right] \right\} e^{-i\omega t}$$

$$v_\theta = -\frac{Q_2}{4\pi} \frac{e^{ikR}}{R} \sin\theta \left[\frac{1}{R^2} - \frac{ik}{R} \right] \qquad (5.3.10c)$$

These formulas enable one to obtain the acoustic intensity radiated by a dipole.

DISCUSSION ON DIPOLE SOUND INTENSITY IN THE STEADY STATE

The radial flow of sound intensity in the steady state is given by,

$$\mathcal{P}_r (I_D)_r = \mathcal{R}_e \frac{1}{2} \{ p v_R^* \}$$
$$= \mathcal{I}_m \frac{1}{2} \{ p v_R^* \}$$

in which p, v_R are peak magnitudes.

Thus,

$$\mathcal{P}_r (I_D)_r = \frac{1}{2} \frac{Q_2^2 \varrho c}{(4\pi R)^2} \frac{k^4 \cos^2\theta}{R^2} \qquad (5.3.11)$$

$$\mathfrak{I}_m (I_D)_r = \frac{-1}{2} \frac{Q_2^2 k^4}{(4\pi R)^2} \varrho c \cos^2\theta \left[\frac{1}{kR} + \frac{2}{k^3 R^3} \right] \tag{5.3.12}$$

Similarly the two components of sound intensity for tangential flow I_θ are

$$\begin{aligned} \mathfrak{R}_e (I_D)_\theta &= 0 \\ \mathfrak{I}_m (I_D)_\theta &= \frac{k^3 Q_2^2}{(4\pi)^2 r^3} \cos\theta \sin\theta \left[1 + \frac{1}{k^2 r^2} \right] \end{aligned} \tag{5.3.13}$$

Integration of the sound energy over a unit sphere shows that the *net* tangential flow of energy vanishes over any complete spherical surface. In addition the only acoustic intensity component surviving as $R \to \infty$ is whose angle dependence is $\cos^2\theta$.

DISCUSSION

Eq. 5.3.7 indicates that the n'th directional derivative of a Green's function describes the 2 n'th multipole of the field corresponding to the Green's function. An important application of this mathematical result is in the analysis of a dipole and a quadrupole field inside an enclosure.

The Green's function of an enclosure is given by a I-D Sturm-Liouville Green's function, 3.4.5b

$$G_k (\hat{r} \mid \hat{r}_0) = -4\pi \sum_m^\infty \frac{\Phi_m^* (\hat{r}_0) \Phi_m (\hat{r})}{k^2 - k_m^2} \tag{5.3.14}$$

in which the Φ_n, are normalized eigenfunctions of the Helmholtz equation in the geometry of the enclosure, and the k_n are the corresponding eigenvalues. According 5.3.7 therefore one may find the dipole field in an enclosure by writing

$$\Phi_2 (\hat{r}) = Q_2 \sum_m^\infty \frac{\{s \cdot \nabla_0 \Phi_m^* (\hat{r}_0)\} \Phi_m (\hat{r})}{k_m^2 - k^2} \tag{5.3.15}$$

If the dipole axis $\hat{s}$ (arrow with head "plus" and tail "minus") is in the direction of the z axis, then $\hat{s} \cdot \nabla_0$ signifies $\partial / \partial_{z_0} = \cos\theta \, \partial / \partial r$. In general, for unit directions $\hat{s}_1$, $\hat{s}_2$ etc. the compound directional derivative required by 5.3.7 is given by

$$\begin{aligned} \partial_{s_1} \partial_{s_2} \ldots \partial_{s_n} &= \prod_1^n \left[(\hat{i}\alpha_n + \hat{j}\beta_n + \hat{k}\gamma_n) \right. \\ &\left. \cdot \left(\hat{i} \frac{\partial}{\partial x_n'} + \hat{j} \frac{\partial}{\partial y_n'} + \hat{k} \frac{\partial}{\partial z_n'} \right) \right] \\ &\quad " = A_1 A_2 \ldots A_n \end{aligned} \tag{5.3.16}$$

where

$$A_i = \alpha_i \frac{\partial}{\partial x_i} + \beta_i \frac{\partial}{\partial y_i} + \alpha_i \frac{\partial}{\partial z_i}$$

Here α_i, β_i, γ_i are the direction cosines of the *i'th* axis of a multipole of order 2^n and the differential operators refer to the source coordinates $\vec{r}_0$ only. The symbol $\prod$ signifies the operation of taking a product. To find the field of a quadrupole in an enclosure we let $n = 2$ and obtain for the differential directional operators

$$\partial_{s_1}\partial_{s_2} = \alpha_2\left(\alpha_1\frac{\partial^2}{\partial x_1\,\partial x_2} + \beta_1\frac{\partial^2}{\partial y_1\,\partial x_2} + \gamma_1\frac{\partial^2}{\partial z_1\,x_2}\right)$$

$$+ \beta_2\left(\alpha_1\frac{\partial^2}{\partial x_1\,\partial y_2} + \beta_1\frac{\partial^2}{\partial y_1\,\partial y_2} + \gamma_1\frac{\partial^2}{\partial z_1\,\partial y_2}\right) \tag{5.3.17}$$

$$+ \gamma_2\left(\alpha_1\frac{\partial^2}{\partial x_1\,\partial z_2} + \beta_1\frac{\partial^2}{\partial y_1\,\partial z_2} + \gamma_1\frac{\partial^2}{\partial z_1\,\partial z_2}\right)$$

This is then applied to the Green's function G_k given by 5.3.14. In a typical example we may construct the field of a quadrupole in a spherical enclosure as follows,

$$\Phi_4(\hat{r}) = Q_4\left\{\alpha_1\frac{\partial}{\partial r^1} + \beta_1\frac{\partial}{r^1\,\partial\theta^1} + \gamma_1\frac{\partial}{r^1\sin\theta^1\,\partial\phi^1}\right\}$$

$$\times\left\{\alpha_2\frac{\partial}{\partial r^1} + \beta_2\frac{\partial}{r^1\,\partial\theta^1} + \gamma_2\frac{\partial}{r^1\sin\theta\,\partial\phi^1}\right\}$$

$$\times\sum_m^{\infty}\frac{\Phi_m(\hat{r}_0)\,\Phi_m(\hat{r})}{k_m^2 - k^2}$$

The symbols r^1, θ^1, ϕ^1 are the coordinates of the quadrupole considered as a source of sound.

5.4. ACOUSTIC MULTIPOLE DESCRIPTION OF VOLUME DISTRIBUTED SOURCES

Acoustic sources may be classified according to their spatial distributions of pressure in the far field. To describe this classification we begin with the integral equation of linear acoustics 1.7.7 for the potential field $\psi(\vec{r})$ in the steady state,which has the form,

$$\iint\left[\psi(\hat{r}_0)\frac{\partial}{\partial n_0}g(\hat{r}\mid\hat{r}_0) - g(\hat{r}\mid\hat{r}_0)\frac{\partial}{\partial n_0}\psi(\hat{r}_0)\right]dS_0$$

$$+ \iiint g(\hat{r}\mid\hat{r}_0)\,q(\hat{r}_0)\,dV_0 = \psi(\hat{r}) \tag{5.4.1}$$

The normal $\partial/\partial n_0$ points away from the medium.

In this section we will consider only volume distributed sources ($= q(\hat{r}_0)$) and defer surface sources to a later discussion. Let the medium be infinite so that the Green's function $g(\hat{r}/\hat{r}_0)$ corresponds to a spherical wave. Expanding this wave in normalized complex spherical harmonics $Y_m(\phi, \theta)$ one obtains [6],

$$g(\hat{r} \mid \hat{r}_0) = -\frac{e^{ikR}}{4\pi R} = -ik \sum Y^*_{ml}(\phi_0, \theta_0)\, Y_{ml}(\theta, \phi)$$

$$\times j_l(kr_0)\, h_l(kr) \tag{5.4.2}$$

$$R = |\hat{r} - \hat{r}_0|,\ r = |\hat{r}|,\ r_0 = |\hat{r}_0|$$

in which Y^* represents the complex conjugate harmonic. Combining 5.4.1, 5.4.2 gives,

$$\psi(\hat{r}) = -ik \sum_{m,l} Y_{ml}(\theta, \phi)\, h^{(1)}_l(kr) \int Y^*_{ml}(\theta_0, \phi_0)\, j_l(kr_0)\, q(\hat{r}_0)\, dV_0 \tag{5.4.3}$$

In the far field the limiting form of the spherical Hankel function is,

$$\lim_{kr \to \infty} h_l(kr) \to \frac{e^{ikr}}{kr} i^{-l-1} \tag{5.4.4}$$

The field $\Psi(r)$ at large values of kr may thus be written,

$$\text{(a)}\ \Psi(\hat{r}) \sim \frac{e^{ikr}}{r} \sum_{m,l} A_{ml}\, Y_{ml}(\theta, \phi)$$

in which (5.4.5)

$$\text{(b)}\ A_{ml} = -i^{-l} \int_{V_0} Y^*_{ml}(\theta_0, \phi_0)\, j_l(kr_0)\, q(r_0)\, dV_0$$

Eq. 5.4.5a is a general description of the far field for an arbitrary distribution of acoustic sources $q(r_0)$. We now limit the size of r_0 to distances much smaller than a wavelength, that is, we desire kr_0 to be very small ($\ll 1$). Noting that

$$\lim_{kr_0 \to 0} j_l(kr_0) \to \frac{(kr_0)^l}{1.3.5 \ldots (2l+1)} \tag{5.4.6}$$

we modify 5.4.5b to read,

$$A_{ml} \sim \frac{-i^{-l} k^l}{1.3.5 \ldots (2l+1)} \int_{V_0} \{ q(r_0)\, r_0^l \}\, Y^*_{ml}(\theta_0, \phi_0)\, dV_0 \tag{5.4.7}$$

Eq. 5.4.7 in conjunction with 5.4.5a provides the basis for the classification of sources in terms of ***multipoles.*** We consider first a source consisting of a time varying injection of mass $q\,(r_0) = -\partial Q/\partial t$, which for steady state becomes $i\omega Q$. The first few coefficients A_{ml} then have the forms

$$\text{(a)}\quad A_{00} = -i\omega \int Q(r_0)\frac{1}{\sqrt{4\pi}}\,dV_0$$

$$\text{(b)}\quad A_{01} = \frac{\omega k}{3} \int Q(r_0)\,r_0\sqrt{\frac{3}{4\pi}}\cos\theta_0\,dV_0$$

$$\text{(c)}\quad A_{11} = \frac{\omega k}{3} \int Q(r_0)\,r_0\sqrt{\frac{3}{8\pi}}\sin\theta_0\,e^{-i\phi_0}\,dV_0 \qquad (5.4.8)$$

$$\text{(d)}\quad A_{02} = \frac{i\omega k^2}{5} \int Q(r_0)\,r_0^2\sqrt{\frac{5}{4\pi}}\left(\frac{3}{2}\cos^2\theta_0 - \frac{1}{2}\right)dV_0$$

$$\text{(e)}\quad A_{12} = \frac{-i\omega k^2}{5} \int Q(r_0)\,r_0^2\sqrt{\frac{15}{8\pi}}\sin\theta_0\cos\theta_0\,e^{-i\phi_0}$$

$$\text{(f)}\quad A_{22} = \frac{i\omega k^2}{5} \int Q(r_0)\,r_0^2\frac{1}{4}\sqrt{\frac{15}{8\pi}}\sin^2\theta_0\,e^{-2i\phi_0}\,dV_0$$

Restricting ourselves to field contributions which are independent of coordinate ϕ (i.e. restricting m to zero) we can write the separate contributions $l = 0, 1, 2 \ldots$ to the field in the forms,

$$\text{(a)}\quad \Psi_{00} \sim \frac{e^{i(kr-\omega t)}}{r}\left(\frac{-i\omega}{\sqrt{4\pi}}\right)\int Q(r_0)\frac{1}{\sqrt{4\pi}}\,dV_0$$

$$\text{(b)}\quad \Psi_{01} \sim \frac{e^{i(kr-\omega t)}}{r}\sqrt{\frac{3}{4\pi}}\cos\theta\,\frac{\omega k}{3}\int Q(r_0)\,r_0\sqrt{\frac{3}{4\pi}}\cos\theta_0\,dV_0 \qquad (5.4.9)$$

$$\text{(c)}\quad \Psi_{02} \sim \frac{i\omega e^{i(kr-\omega t)}}{r}\sqrt{\frac{5}{4\pi}}\left(\frac{3}{2}\cos^2\theta - \frac{1}{2}\right)\frac{k^2}{5}$$

$$\times \int Q_0(r_0)\,r_0^2\sqrt{\frac{5}{4\pi}}\left(\frac{3}{2}\cos^2\theta_0 - \frac{1}{2}\right)dV_0$$

DISCUSSION

The far field Ψ_{oo} is independent of direction. It is called the *monopole field* and is usually the predominant component at low frequencies. The field Ψ_{oi} depends on cos θ and is called the *dipole* field of the source term $i\omega Q$. Its amplitude differs from zero only if the integrand of 5.4. (9b) is non-symmetrical. Eq. 5.4.9c is an example of a higher order multipole that may be generated by the source. Visualizing the source distribution Q as a collection of point sources we state that if the first *moment* of all these points relative to the origin is not zero there is a dipole field; if the second moment is not zero there is a quadrupole field, etc.

We consider next the source $q = (\partial F_i/\partial X_i)(i\omega\rho)^{-1}$ which corresponds to an oscillating body force on the volume of fluid. Using 5.4.1 above we can find the field at r by writing

$$\psi(r) = \iiint g(\hat{r} \mid \hat{r}_0) \left[\frac{\partial F_i}{i\omega\varrho\,\partial x_i}\right] dV_0 \tag{5.4.10}$$

Now if $\hat{\mathfrak{F}}$ is the vector force whose components are $F_i/i\omega\varrho$

$$\nabla\cdot(g\,\hat{\mathfrak{F}}) = \nabla g\cdot\hat{\mathfrak{F}} + g\nabla\cdot\hat{\mathfrak{F}} \tag{5.4.11}$$

Hence,

$$\psi(r) = \int_{V_0}\nabla\cdot(g\,\hat{\mathfrak{F}})\,dV_0 - \int \nabla g\cdot\hat{\mathfrak{F}}\,dV_0 \tag{5.4.12}$$

The first term on the right may be converted to a surface integral,

$$\int_{V_0}\nabla\cdot(g\,\hat{\mathfrak{F}})\,dV_0 = \int_{s_0} g\,\hat{\mathfrak{F}}_n\,dS_0$$

If $\hat{\mathfrak{F}}_n(r_0)$ is finite in spatial extension we can always find a surface of integration of large enough size that F_n is zero.

Hence in the far field ($r \gg r_0$)

$$\psi(r) = -\int_{V_0}\nabla g\cdot\hat{\mathfrak{F}}\,dV_0 \tag{5.4.13}$$

Now,

$$\nabla g = -\nabla\frac{e^{ikR}}{4\pi R} = \frac{e^{ikr}}{4\pi}\left[\frac{\hat{R}}{R^3} - \frac{ik\hat{R}}{R^2}\right] \tag{5.4.14}$$

For R very large we make the approximation

$$R \to r - \hat{r}_0 \cdot \hat{a}_r \tag{5.4.15a}$$

Neglecting the term in R^{-3} we reduce 5.4.14 to the form

$$\nabla g \approx \frac{-ik}{4\pi} \frac{e^{ikr}}{r} e^{-ik(\hat{r}_0 \cdot \hat{a}_r)} \hat{a}_r \tag{5.4.15b}$$

Expanding the exponential involving r_0 in a Taylor series about $r_0 \cdot \hat{a}_r = 0$ we have

$$e^{-ik(\hat{r}_0 \cdot \hat{a}_r)} \approx 1 - ik(\hat{r}_0 \cdot \hat{a}_r) - \frac{k^2}{2} \hat{r}_0 \hat{r}_0 \cdot \hat{a}_r \cdot \hat{a}_r \tag{5.4.15c}$$

Hence 5.4.13 may be reduced to

$$\psi(r) = \frac{ik}{4\pi} \frac{e^{ikr}}{r} \hat{a}_r \cdot \left\{ \int \hat{\mathcal{F}} \, dV_0 - \int ik(\hat{\mathcal{F}} \hat{r}_0 \cdot \hat{a}_r) \, dV_0 \right.$$
$$\left. - \frac{k^2}{2} \int (\hat{\mathcal{F}} \hat{r}_0 \hat{r}_0 \cdot \hat{a}_r \cdot \hat{a}_r) \, dV_0 + \ldots \right\} \tag{5.4.16}$$

DISCUSSION

All terms on the right in 5.4.16 show dependence on direction of observation. Hence an oscillating body force exhibits no monopole radiation (at least for the limit $kr_0 \to 0$). The first term depends on one direction, namely the angle between $\hat{\mathcal{F}}$ and the line of observation ($= \hat{a}_r$). It is the dipole term. The second term depends on this same angle plus the additional angle between the radius vector from the origin to the force $\hat{\mathcal{F}}$ and the line of observation (see Fig. 5.4.1). It is the *quadrupole* term.

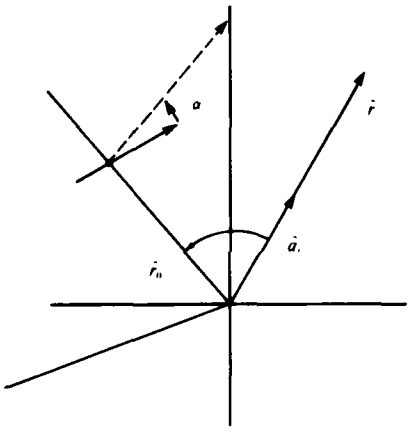

Fig. 5.4.1. Geometrical relations of force distribution.

The third term depends on the square of this latter angle. It is the *octopole* term.

Quadrupole radiation can also arise from the source term involving fluid stresses T_{ij}. We set

$$q = \frac{1}{i\omega\varrho} \frac{\partial T_{ij}}{\partial x_i \, \partial x_j}$$

and write the field at r as,

$$\psi(r) = \iiint g(\hat{r} \mid \hat{r}_0) \frac{1}{i\omega\varrho} \frac{\partial T_{ij}}{\partial x_i \, \partial x_j} dV_0 \tag{5.4.17}$$

We integrate by parts twice,

$$\int_{V_0} g \frac{\partial^2 T_{ij}}{\partial x_i \, \partial x_j} dV = \int \frac{\partial}{\partial x_i} \left\{ g \frac{\partial T_{ij}}{\partial x_j} \right\} dV_0$$

$$- \int \frac{\partial T_{ij}}{\partial x_j} \frac{\partial g}{\partial x_i} dV_0$$

$$\int \frac{\partial g}{\partial x_i} \frac{\partial T_{ij}}{\partial x_j} dV_0 = \int \frac{\partial}{\partial x_j} \left(\frac{\partial g}{\partial x_i} T_{ij} \right) dV_0$$

$$- \int \frac{\partial^2 g}{\partial x_i \, \partial x_j} T_{ij} \, dV_0$$

All volume integrals of divergences vanish because the distribution of T_{ij} is finite and the integral over a large enough surface (= Gauss theorem) vanishes. Thus

$$\psi(r) = - \int \frac{\partial^2 g}{\partial x_i \, \partial x_j} \frac{T_{ij}}{i\omega\varrho} dV_0 \tag{5.4.18}$$

The quantity $\partial^2 g / \partial x_i \, \partial_{xj}$ is a dyadic in the r_0 coordinates the components of which can be obtained by introducing the approximation 5.4.15a and then differentiating 5.4.15c twice. This gives

$$\nabla\nabla g \approx - \frac{e^{ikr}}{4\pi r} \left\{ - \frac{k^2}{2} \hat{a}_r \hat{a}_r + \ldots \right\} \tag{5.4.19}$$

Hence,

$$\psi(r) \approx - \frac{k^2}{i\omega\varrho} \frac{e^{ikr}}{8\pi r} \int_{V_0} \hat{a}_r \cdot T_{ij} \cdot \hat{a}_r \, dV_0 \tag{5.4.20}$$

Since this field is a function of two directions it is evidently a quadrupole field.

5.5. ACOUSTIC MULTIPOLE DESCRIPTION FOR SURFACE DISTRIBUTED SOURCES

In Sect. 5.4 the theory of multipole description of *volume* distributed sources was developed. In this section a similar theory is constructed of *surface* distributed sources.

Consider a surface S containing source points $\hat{\xi}$ (ξ_i). Let $\hat{\eta}$ represent the location vector of a fixed point on the surface. In the medium external to the surface is a field point $\hat{x}$. Define r, R by the formulas,

$$r = \left[\sum_j (x_j - \xi_j)^2\right]^{\frac{1}{2}}, \quad R = \left[\sum_j (x_j - \eta_j)^2\right]^{\frac{1}{2}} \tag{5.5.1}$$

The Green's function for the *infinite domain* between field x and source point $\hat{\xi}$ is given by

$$G(\hat{x} \mid \hat{\xi} \mid \omega) = e^{ikr}/r \tag{5.5.2}$$

We desire to study the field at $\hat{x}$ as a superposition of fields due to each term of a power series decomposition of G. To this end form a Taylor series of G about the point in the variable ξ_i. Symbolically

$$G = \frac{e^{ikR}}{R} + \sum_{\nu=1}^{\infty} \frac{1}{\nu!} d^{\nu} T(\xi_i, \eta_i) \tag{5.5.3}$$

in which

$$d^{\nu} T(\xi_i, \eta_i) = \left[(-\xi_1 - \eta_1)\frac{\partial}{\partial \xi_1} + (\xi_2 - \eta_2)\frac{\partial}{\partial \xi_2} + (\xi_3 - \eta_3)\frac{\partial}{\partial \xi_3}\right]^{\nu} \frac{e^{ikr}}{r}\Big|_{\hat{\xi} = \hat{\eta}} \tag{5.5.4}$$

It will be useful to define the direction cosines of $\hat{R}$ by the relation

$$\hat{R} = R[\hat{i}\cos\theta_1 + \hat{j}\cos\theta_2 + \hat{k}\cos\theta_3] \tag{5.5.5}$$

$$\cos\theta_i = \frac{x_i - \eta_i}{R} \tag{5.5.6}$$

Now, from 5.5.1 it is seen that,

$$\frac{\partial r}{\partial \xi_j} = -\frac{\partial r}{\partial x_j} \tag{5.5.7}$$

Transforming the operation $\partial / \partial \xi_j$ to $- \partial / \partial x_j$ one may define the quantity G^* by the relation,

$$G^* = \frac{e^{ikr}}{r} = \sum_{\nu=0}^{\infty} \frac{(-1)^\nu}{\nu!} \partial^\nu T^*(\xi_i, \eta_i) \tag{5.5.8}$$

$$\partial^\nu T^*(\xi_i, \eta_i) = \left[(\xi_1 - \eta_1) \frac{\partial}{\partial x_1} + (\xi_2 - \eta_2) \frac{\partial}{\partial x_2} + (\xi_3 - \eta_3) \frac{\partial}{\partial x_3} \right]^\nu \frac{e^{ikr}}{r} \Big|_{\xi = \eta} \tag{5.5.9}$$

To find the field at $\hat{x}$ fields of all sources on S are summed using 1.7.7 in the steady state.

For the infinite medium the field $\psi(r)$ is

$$- \frac{1}{4\pi} \int \left(\frac{\partial \psi}{\partial n^*} \right) \frac{e^{ikr}}{r} dS + \frac{1}{4\pi} \int (\psi)_{\xi_i} \frac{\partial}{\partial n^*} \left(\frac{e^{ikr}}{r} \right) dS = \psi(r) \tag{5.5.10}$$

Here n^* is the normal vector *pointing away* from the volume of space where the field point is located. We note that

$$\frac{\partial}{\partial n^*} = \nabla \cdot n^* = n_1^* \frac{\partial}{\partial \xi_1} + n_2^* \frac{\partial}{\partial \xi_2} + n_3^* \frac{\partial}{\partial \xi_3} \tag{5.5.11}$$

Also, we define another derivative

$$\frac{\partial}{\partial n^\dagger} = n_1^* \frac{\partial}{\partial x_1} + n_2^* \frac{\partial}{\partial x_2} + n_3^* \frac{\partial}{\partial x_3} \tag{5.5.12}$$

Now substitute 5.5.8, 5.5.9 directly into the first term on the left hand side of 5.5.10. However, in the second term use $\partial / \partial n^+$ in lieu of $\partial / \partial n^*$. Noting that

$$\sum_{\nu=0}^{\infty} \frac{(-1)^{\nu+1}}{\nu!} = \sum_{\nu=1}^{\infty} \frac{(-1)^\nu}{(\nu-1)!} \tag{5.5.13}$$

and using 5.5.7 write 5.5.10 in the new form

$$- \frac{1}{4\pi} \int \left(\frac{\partial \psi}{\partial n^*} \right)_{\xi_i} \sum_{\nu=0}^{\infty} \frac{(-1)^\nu}{\nu!} d^\nu T^*(\xi_i, \eta_i) \, dS$$

$$+ \frac{1}{4\pi} \int (\psi)_{\xi_i} \frac{\partial}{\partial n^\dagger} + \sum_{\nu=1}^{\infty} (-1)^\nu d^{\nu-1} T^*(\xi_i, \eta_i) \, dS = \psi(r) \tag{5.5.14}$$

This can still further be reduced by noting that for $\nu = 0$

$$d^0 T^* = e^{ikR}/R$$

Hence,

$$4\pi\psi(r) = -\frac{e^{ikR}}{R}\int\left(\frac{\partial\psi}{\partial n^*}\right)dS +$$

$$+\sum_{\nu=1}^{\infty}\frac{(-1)^{\nu-1}}{(\nu-1)!}\int\left\{\left(\frac{\partial\psi}{\partial n^*}\right)_{\xi_i}\frac{d^2 T^*(\xi_i,\eta_i)}{\nu}\right.$$

$$\left.-\psi\frac{\partial}{\partial n^\dagger}d^{\nu-1}T^*(\xi_i,\eta_i)\right\}dS \qquad (5.5.15)$$

Expansion of the first few terms leads to,

$$4\pi\psi(r) = \frac{-e^{ikR}}{R}\int\left(\frac{\partial\psi}{\partial n^*}\right)_{\xi_i}dS$$

$$+\int\left\{\left(\frac{\partial\psi}{\partial n^*}\right)_{\xi_i}\left[(\xi_i-\eta_1)\frac{\partial}{\partial x_1}+(\xi_2-\eta_2)\frac{\partial}{\partial x_2}+(\xi_3-\eta_3)\frac{\partial}{\partial x_3}\right]\frac{e^{ikr}}{r}\Big|_{\hat\xi=\hat r}\right.$$

$$\left.-(\psi)_{\xi_i}\left(n_1^*\frac{\partial}{\partial x_1}+n_2^*\frac{\partial}{\partial x_2}+n_3^*\frac{\partial}{\partial x_3}\right)\frac{e^{ikr}}{r}\Big|_{\hat\xi=\hat\eta}\right\}dS$$

$$-\int\left\{\left(\frac{\partial\psi}{\partial n^*}\right)_{\xi_i}\left(\frac{1}{2}\right)\left[(\xi_1-\eta_1)^2\frac{\partial^2}{\partial x_1^2}+(\xi_2-\eta_2)^2\frac{\partial^2}{\partial x_2^2}+(\xi_3-\eta_3)^2\frac{\partial^2}{\partial x_3^2}\right.\right.$$

$$+2(\xi_1-\eta_1)(\xi_2-\eta_2)\frac{\partial^2}{\partial x_1\,\partial x_2}+2(\xi_1-\eta_1)(\xi_3-\eta_3)\frac{\partial^2}{\partial x_1\,\partial x_3}$$

$$\left.+2(\xi_2-\eta_2)(\xi_3-\eta_3)\frac{\partial^2}{\partial x_2\,\partial x_3}\right]\frac{e^{ikr}}{r}\Big|_{\hat\xi=\hat r}$$

$$-(\psi)_{\xi_i}\left(n_1^*\frac{\partial}{\partial x_1}+n_2^*\frac{\partial}{\partial x_2}+n_3^*\frac{\partial}{\partial x_3}\right)$$

$$\left.\times\left[(\xi_1-\eta_1)\frac{\partial}{\partial x_i}+(\xi_2-\eta_2)\frac{\partial}{\partial x_2}+(\xi_3-\eta_3)\frac{\partial}{\partial x_3}\right]\frac{e^{ikr}}{r}\Big|_{\hat\xi=\hat\eta}\right\}dS$$

Now

$$\frac{\partial}{\partial x_1}\frac{e^{ikr}}{r} = \left[-\frac{e^{ikr}}{r^2}+\frac{ike^{ikr}}{r}\right]\frac{\partial r}{\partial x_1} \qquad (5.5.16)$$

In the far field,

$$r \to R, \quad \frac{\partial r}{\partial x_1} \to \cos\theta_1 \tag{5.5.17}$$

Neglecting terms in $1/r^2$ it is seen that,

$$\frac{\partial}{\partial x_1}\left(\frac{e^{ikr}}{r}\right) \approx \frac{ike^{ikR}}{R}\cos\theta_1 \tag{5.5.18}$$

As a general rule, in the far field

$$\frac{\partial^{\epsilon+f+g}}{\partial x_1^{\epsilon}\,\partial x_2^{f}\,\partial x_3^{g}}\left(\frac{e^{ikr}}{r}\right) \approx (ik)^{\epsilon+f+g}\cos\theta_1^{\epsilon}\cos\theta_2^{f}\cos\theta_3^{g}\,\frac{e^{ikR}}{R} \tag{5.5.19}$$

Now, restricting ourselves to the *far field* we represent the field from a source of "equivalent diameter" a by the formula

$$\begin{aligned} 4\pi\,\psi(R)\,\chi\,\frac{e^{ikR}}{R}\Big[& -K_0 \\ & + ika\sum_j K_{1j}\cos\theta_j \\ & + (ika)^2\sum_{j,k} K_{2jk}\cos\theta_j\cos\theta_k \\ & + \ldots\Big] \end{aligned} \tag{5.5.20}$$

in which the K symbols (dimensions: m^3/sec) have the form

$$\begin{aligned} K_0 &= \int \frac{\partial\psi}{\partial n}\,dS \\ K_{1j} &= \int \left[\frac{(\xi_j-\eta_j)}{a}\,\frac{\partial\psi}{\partial n} - n_j\,\frac{\psi}{a}\right] dA \\ K_{2jk} &= \int \left[\frac{(\xi_k-\eta_k)}{2a}\left(\frac{\partial\psi}{\partial n}\right) - \frac{n_k\,\psi}{a}\right]\left(\frac{\xi_j-\eta_j}{a}\right) dA \\ K_{3jkl} &= \int \left[\frac{(\xi_l-\eta_l)}{6a}\,\frac{\partial\psi}{\partial n} - \frac{\eta_1\,\psi}{a}\right]\frac{(\xi_j-\eta_j)}{a}\,\frac{(\xi_k-\eta_k)}{a}\,dA \end{aligned} \tag{5.5.21}$$

These equations apply to the far field only, and describe the far field from an *arbitrary source.* In the near field conditions are much more complicated.

DISCUSSION:

The symbol K_0 is clearly a scalar quantity. All the subsequent K symbols in 5.5.21 contain factors in $(\xi_j - \eta_j)/a$ which represent angles (see the analogous formula given by 5.5.6, above). Hence they are components of a tensor of rank given by the first digit of the subscript. Each term in 5.5.20 thus represents the field generated by individual multipoles into which the surface distributed source has been decomposed. In particular we have

the monopole field $\quad -K_0$

the dipole field $\quad ika \sum_j K_{1j} \cos\theta_j$

the quadrupole field $\quad (ika)^2 \sum_{j,k} K_{2jk} \cos\theta_j \cos\theta_k$

etc.

Except for K_0 all the K symbols are not unique because their numerical value depends on the choice of reference point η. However it can be shown that for a particular source the first non-vanishing K symbol in 5.5.20 is independent of the choice of η. Eq. 5.5.20 is convergent for all values of ka. When $ka < 1$ the rate of convergence is fast and the lower order multipoles determine the field. When ka is large the number of multipoles required for a given accuracy may tend to a very great number and the higher order multipoles may determine the field. The numerical calculation of the K symbols using 5.5.21 is difficult. However when ka is small one can expand ψ in an ascending power series in ka with coefficients of expansion which are determinable by solving *potential* (rather than wave) type of problems. Thus for small ka the K symbols may be calculated by methods of potential theory.

5.6. NUMERICAL CALCULATION OF ACOUSTIC RADIATION BY SMALL SOURCES LOCATED IN LARGE BAFFLE

The radiation of a scalar field by a multipole has been described in the previous sections for spatial domain which are essentially free field (i.e., the baffle effect is small). When the multipole is placed on or near a curved baffle of large acoustic size the radiation issuing from it is strongly modified. The analysis of such radiation may be accomplished using the methods outlined in Chapters I, II, III. These standard procedures however lead to solutions in terms of harmonic series which converge with such extreme slowness as to require thousands of terms. Attempts by mathematicians to improve convergence finally proved successful in the work of Sommerfeld [7] and Watson [8]. Both of these authors attacked the problem of finding the radiation field of an electromagnetic dipole located near the surface of the earth. To improve convergence they formed a new series (= Sommerfeld-Watson series) obtained by contour integration in the complex plane and substituted it in place of the customary harmonic series. A few terms of the new series readily yielded the numerical solution of their problem. Their method is quite general and applications of it to the problem of acoustic radiation are presented in the following sections.

5.6a. RADIATION OF SOUND BY A SMALL CIRCULAR PISTON IN A SPHERICAL BAFFLE OF LARGE *ka*

On the surface of an acoustically hard sphere (radius a) is set a circular piston radius $a\theta_0$ vibrating with a velocity $Ve^{-i\omega t}$ and generating sound waves in a surrounding fluid medium of characteristic impedance ρc. The ratio of radius $a\theta_0$ to the wavelength of sound ($= \lambda$) is much smaller than unity. Under these conditions the radiation field p at any polar point r, θ (piston center as origin) is given by an infinite series of spherical eigenfunctions $P_n(\cos\theta)h_n(1)(kr)$ which are products of the Legendre polynomials P_n and the spherical bessel functions h_n. The well-known formula formula [9] for this series is

$$\frac{p(r,\theta)}{(i/4)\varrho cVe^{-i\omega t}\theta_0^2} = \sum_{n=0}^{\infty} \frac{(2n+1)P_n(\cos\theta)h_n^{(1)}(kr)}{\left[\frac{dh_n^{(1)}(Z)}{dZ}\right]_{Z=ka}} \tag{5.6.1}$$

Here n is a positive integer and hence $P_n(\cos\theta)$ is continuous for all values of $0 < \theta < \pi$. For the acoustic field on the surface $r = a$ the series on the right converges well in the range of small ka (< 10) and converges poorly when ka is large, requiring at least $n \approx 2ka$ terms. In the latter region convergence can be improved by use of the Sommerfeld-Watson transformation.

The first step in this transformation is to consider the right side of 5.6.1 to be the residues of a contour integral $\int_c d\nu A(\nu)$ in the complex $n\ (= \nu)$ plane whose integrand $A(\nu)$ contains (in part) the general form shown with n changed to ν. The factor $P_\nu(\cos\theta)$ then becomes, for ν not integer, a hypergeometric function F, defined by

$$P_\nu(\cos\theta) = F\left(-\nu, \nu+1; 1; \frac{1-\cos\theta}{2}\right) \tag{5.6.2}$$

Hypergeometric functions of non-integral order are singular when the fourth (and last) parameter in the parenthesis of 5.6.2 is unity. In the physical problem in question we require this singular point to coincide with the piston center at $\theta = 0$. Hence the appropriate form of the complex eigenfunction when n is replaced by ν is $P_\nu(-\cos\theta)h_\nu(kr)$ which is singular at $\theta = 0$ and regular at $\theta = \pi$. Noting that

$$P_n(\cos\theta) = (-1)^n P_n(-\cos\theta) \tag{5.6.3}$$

it is seen that the residue series to be transformed has the more appropriate form

$$\sum (2n+1)(-1)^n P_n(-\cos\theta)h_n(kr)/h_n'(ka)$$

The sequence $(-1)^n$ is recognized as the residue contribution of the poles of $1/\sin \nu\pi$ if the contour of integration in the complex ν – plane encloses the entire positive real axis on which the poles are located. Selection of a *clockwise* direction of integration and including a divisor of $2\pi i$ show that the desired integral takes on the form,

$$U = -\int_C \frac{2\nu+1}{2i \sin \nu\pi} P_\nu(-\cos\theta) \frac{h\nu\,(kr)}{h_\nu^1\,(ka)}\, d\nu \tag{5.6.4}$$

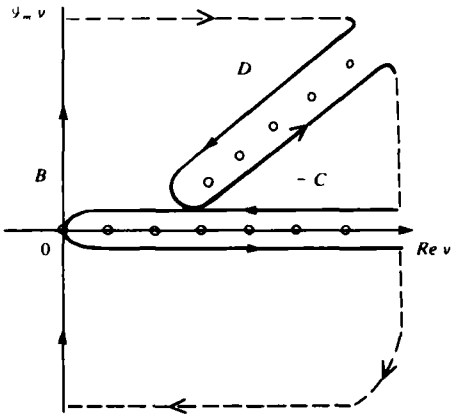

Fig. 5.6.1. Contour of integration in the complex-ν plane.

The residue series of 5.6.1 is contained in the integral 5.6.4 if C is closed at $\nu \to +\infty$. The second step in the Sommerfeld-Watson transformation is to open the contour C (which does not change the value of U) and make it part of a larger contour with the objective of finding an alternate residue series that converges more rapidly for large ka than 5.6.1. The new contour, shown in Fig. 5.6.1 consists of the original contour C reversed to counterclockwise direction (hence designated $-C$), plus the contour B running along the imaginary axis, plus a contour D surrounding (but not closed about) all the poles of $h_\nu'\,(ka) = 0$, which are located in the first quadrant. Since the new contour encloses no poles the total line integral along its path must vanish. Hence,

$$\int_B + \int_D = \int_C \tag{5.6.5}$$

provided the contributions of all dotted contours at infinity can be shown to vanish, which is done by reference [7]. Now if the integrand of 5.6.4 were an *odd* function of the subscripts then the integration along the imaginary axis ($= \int B$) would also vanish. This condition on the subscripts can be achieved by change of variable $\nu \to s - 1/2$. The integral of 5.6.4 then has the new form,

$$\int \frac{sds}{i \cos s\pi} \frac{P_{s-1/2}(-\cos\theta)\, h_{s-1/2}(kr)}{h'_{s-1/2}\,(ka)} \tag{5.6.6}$$

Writing the hypergeometric function as

$$P_{s-\frac{1}{2}}(-\cos\theta) = F\left(\frac{1}{2}-s, \frac{1}{2}+s; 1; \frac{1}{2}+\frac{1}{2}\cos\theta\right) \tag{5.6.7}$$

it is easily demonstrated that changing s to $-s$ does not alter the value of F, *i. e.*, F is an even function of s. The ratios of spherical bessel functions are also even in view of the fact that they are essentially cylindrical Hankel functions $H_p(x)$ of half order and that $H_{-p}(x) = e^{ip\pi} H_p(x)$. The remaining factor $s/\cos s\pi$ is clearly odd hence the integrand is an odd function of s and the integral of 5.6.6 along B vanishes. To evaluate the integral along D we close the contour at infinity and sum the residues at the roots ν_m of $h'_\nu - 1/2\,(ka) = 0$, replacing s by the dummy variable ν for convenience of literature reference. Using 5.6.5 and the above conclusions concerning the contour integration we arrive at the result that the U of 5.6.4 is representable by the new series

$$U = -2\pi \sum_{\nu_m} \frac{\nu P_{\nu-\frac{1}{2}}(-\cos\theta)\, h_{\nu-\frac{1}{2}}(kr)}{\cos\nu\pi \left[\dfrac{\partial h'_{\nu-\frac{1}{2}}(ka)}{\partial\nu}\right]_{\nu=\nu_m}} \tag{5.6.8}$$

The roots ν_m are located in the first quadrant of the ν plane and are complex numbers which monotonically increase in both imaginary and real parts as ka increases. For large ka Sommerfeld [10] has shown that

$$\nu_m \approx ka\left\{1 + \frac{1}{2}(4m+1)^{\frac{2}{3}}\left(\frac{3\pi}{4ka}\right)^{\frac{2}{3}} e^{\frac{i\pi}{3}}\right\} \tag{5.6.9}$$

In this range of ka the hypergeometric function can be approximated [11] by writing

$$P_{\nu-\frac{1}{2}}(-\cos\theta) \approx \frac{e^{-i\nu(\pi-\theta)+i\pi/4}}{\sqrt{2\pi(\nu-\frac{1}{2})\sin\theta}} \tag{5.6.10}$$

Similarly for large $|\nu_m|$ one can write

$$\cos\nu_m\pi \approx e^{-i\nu_m\pi/2}$$

Asymptotic forms for the ratio $h_\nu/(\partial h\nu/\partial\nu)$ are also given by Sommerfeld who finds that

$$\lim_{ka\to\infty} \frac{h\nu}{\frac{\partial}{\partial\nu}[h_\nu + ka\, h'_\nu]} \approx \frac{h\nu}{ka\,\frac{\partial}{\partial\nu}[h'_\nu]} \to \frac{1}{ka\,\alpha^2}$$

in which

$$\alpha^2 = 2\left(1 - \frac{\nu}{ka}\right)$$

Noting from the formulas for ν_m in 5.6.9 that

$$R_e\{\nu_m\} = ka + 0.443\,(4m+1)^{\frac{2}{3}}\,(ka)^{\frac{1}{3}} \tag{5.6.11a}$$

$$\vartheta_m\{\nu_m\} = \sqrt{3}\,(0.443)\,(4m+1)^{\frac{2}{3}}\,(ka)^{\frac{1}{3}} \tag{5.6.11b}$$

it is easily computed that for large ka

$$\frac{h\nu}{\frac{d}{d\nu}(h'_\nu)} = \frac{1}{a^2} = \frac{(ka)^{\frac{2}{3}}\,e^{\frac{i\pi 2}{3}}}{1.772\,(4m+1)^{2/3}} \tag{5.6.11c}$$

Collecting all numerical coefficients in the large ka approximation to 5.6.8 and allowing $|\nu_m| \approx ka$ it is seen that the ka dependence of the surface pressure is $(ka)^{7/6}$ with an associated magnitude multiplier of $\sqrt{8\pi}/1.772$. The phase of $p(a, \theta)$ on the surface independent of θ may be found by transferring the term $i/4$ to the right-hand side of 5.6.1 and summing all contributions of constant exponentials. This is exp $[2\pi i/3 + i\pi/4 + i\pi/2]$ which is exp $(17\pi i/12)$ or exp $(-7\pi i/12)$. The phase of $p(a, \theta)$ which is dependent on angle θ is found directly from 5.6.11a, 5.6.11b). Dividing by the factor 4(transferred with $i/4$) it is concluded that

$$p(\theta) = \frac{0.707\,\varrho c\,V\theta_0^2\,(ka)^{\frac{7}{6}}}{(\sin\theta)^{\frac{1}{2}}} \sum_m \frac{e^{-0.767\,(4m+1)^{\frac{2}{3}}\,(ka)^{\frac{1}{3}}}}{(4m+1)^{\frac{2}{3}}}\,e^{i\phi_m} \tag{5.6.12}$$

where

$$\phi_m = \frac{-7\pi}{12} + ka\left[1 + 0.443\,(4m+1)^{\frac{2}{3}}\,(ka)^{-\frac{2}{3}}\right]\theta - \omega t \tag{5.6.13}$$

This formula derived by Junger [12], shows the surface pressure for large ka to be a superposition of damped oscillatory waves radiating from the source at $\theta = 0$ and traversing the sphere in a positive θ direction directly into the "shadow region". The rate of damping increases strongly with the order m of the root ν_m and with the magnitude of ka. For large ka only a few terms in the series of 12 are needed to insure convergence. From 13 it is seen that curves of constant phase travel through space in accordance with relation $d\phi m/dt = 0$. Writing

$$\frac{d}{dt} = \frac{\partial}{\partial a\theta}\left(\frac{\partial a\theta}{\partial t}\right) = \frac{\partial}{\partial a\theta}\,c_t \tag{5.6.14}$$

in which c_t is the trace velocity of the wave regarded as a moving point on a meridian circle it is found directly that

$$c_t = \frac{ck}{\left(\frac{\partial \phi_m}{\partial a\theta}\right)} = \frac{c}{1 + \frac{0.443\,(4m+1)^{\frac{2}{3}}}{(ka)^{\frac{2}{3}}}} \tag{5.6.15}$$

Thus for a sphere of large ka the trace velocity of the diffracted waves is always less than the free space sound velocity $C = \omega/k$.

DISCUSSION

The presence of $(\sin\theta)^{-1/2}$ in 5.6.11a indicates infinite (*i. e.*, non-physical) amplitudes at $\theta = 0$ and $\theta = \pi$. The infinity at $\theta = \pi$ may be removed by use of less restrictive ka approximations. The infinity at $\theta = 0$ is an essential feature of the method since it indicates the presence of a source (= singular point in the field). Close to this singular point and in the range $0 < \theta < 90°$ the convergence of 5.6.11a is poor. In contrast 5.6.11a converges well in the region $90° < \theta < 180°$ for small circular piston radiators. In regions of poor convergence Junger [12] suggests using the Kirchoff approximation (= geometric acoustics approximation) which ignores the curvature of the sphere. In this approximation the trace velocity is that of free space (= C) rather than the lesser magnitude C_t. Adoption of this approximation thus leads to an error in phase of the computed wave, particularly increasing as θ increases. In the range $0 < \theta < 90°$ the wave travels a longer path on a sphere than on the projected plane so that the amplitude loss of the wave is greater in the actual case (a sphere) than in the approximation case (by geometric acoustics). However in the range $90° < \theta < 180°$ the wave travelling over the sphere comes to a focus at 180°, indicating a rising pressure as the point $\theta = \pi$ is approached. This of course is not predicted by the Kirchoff approximation. The approximation that baffle curvature may be neglected in computing the acoustic radiation on and near small pistons in large ka baffles is confirmed by Greenspon and Sherman [13] who found that for separation of pistons on a cylinder as far as 1.5λ the mutual impedance is independent of piston location (i. e., circumferential or axial). It is noted finally that the reduction in amplitude of pressure in the "shadow region" is exponential rather than spherical, and that the rate of decay with θ increases with the order m of the travelling wave (called "creeping wave"). Computation of field pressures by Junger [12] using the Watson transformation shows values closely approximating those of (checkable) harmonic series even for distances as near as 1λ from the source, provided the baffle size is large.

The previous analysis leading to 5.6.12 gives the pressure at angle θ arising from the generated wave traveling in the positive θ direction. There is an additional pressure at angle θ due to the wave traveling in the negative θ direction. This may be accounted for by replacing 5.6.10 with the new *symmetrical* form,

$$P_{\nu-\frac{1}{2}}(-\cos\theta) \approx \frac{e^{-i\nu\pi + i\pi/4}}{\left[2\pi\left(\nu - \frac{1}{2}\right)\right]^{\frac{1}{2}}} \left\{ \frac{e^{i\nu\theta}}{(\sin\theta)^{\frac{1}{2}}} + \frac{e^{i\nu(2\pi-\theta)}}{\sin(2\pi-\theta)^{\frac{1}{2}}} \right\} \tag{5.6.16}$$

The remaining analysis proceeds along the course already given. In the added term the factor $[\sin(2\pi - \theta)]^{1/2} = i(\sin\theta)^{1/2}$, showing that there is a $\pi/2$ phase shift as the negative wave passes through the point $\theta = \pi$ which is a focal point of creeping waves.

5.6b. RADIATION FROM AN INFINITE STRIP IN A CYLINDER OF LARGE DIAMETER

On a infinite cylinder of large diameter is located an infinite vibrating strip of angular size $-\theta_0 < \theta < +\theta_0$. The normal velocity over the strip is $Ve^{-i\omega t}$ and is zero elsewhere. The pressure field at point (r, θ) in the medium outside the cylinder where the sonic velocity is c can be expressed as a sum of cylindrical multipoles with coefficients A_n,

$$p = \sum_n A_n \cos(n\theta) H_n^{(1)}(kr) \tag{5.6.17}$$

The surface velocity magnitude $|v|$ can be expanded in a Fourier cosine series

$$|v| = \frac{V}{\pi}\theta_0 \sum_{n=0}^{\infty} \in_n \left(\frac{\sin n\theta_0}{n\theta_0}\right)\cos(n\theta)$$
$$\in_o = 1, \in_{n\neq 0} = 2 \tag{5.6.18}$$

Since the normal surface velocity is related to the gradient of pressure by

$$v = \frac{1}{ik\varrho c}\frac{\partial p}{\partial r}$$

it is then seen that the surface pressure $p(\theta)$ may be obtained by combining 5.6.17 and 5.6.18 for $r = a$. The result is,

$$p(\theta) = \frac{i\varrho c\, Ve^{-i\omega t}}{\pi}\theta_0 \sum_{n=0}^{\infty} \in_n \frac{H_n^{(1)}(ka)}{H_n^{(1)\prime}(ka)} \frac{\sin(n\theta_0)}{(n\theta_0)} \cos n\theta \tag{5.6.19}$$

This is called the "wave harmonic" or cylindrical multipole series for frequency ω.

As indicated in Sect. 5.6a harmonic series which are applicable to radiation and scattering problems converge poorly when ka is large (i. e., $ka > 10$). To improve convergence in this range of ka the harmonic series is converted by a Sommerfeld-Watson transformation to residue series of a contour integral for which often one or two terms are sufficient to yield the desired answer. The application of such a transformation to cylindrical radio wave radiation was completed by Sensiper (14).

The first step in the transformation is to represent 5.6.19 in the form of a contour integral in the *complex* n ($= \nu$) plane. The range of n is initially increased to cover $-\infty$ to $+\infty$ by noting that since

$$H_n^{(1)}(z) = e^{-in\pi} H_{-n}^{(1)}(z)$$

one may write

$$\frac{H_n^{(1)}(ka)}{H_n^{(1)\prime}(ka)}\cos n\theta = \frac{e^{-in\pi}H_{-n}^{(1)}e^{-in\theta}}{2e^{-in\pi}H_{-n}^{(1)\prime}} + \frac{e^{in\theta}H_n^{(1)}}{2H_n^{(1)\prime}}$$

so that 5.6.19 takes on the new form,

$$p(\theta) = \frac{i\varrho cV\theta_0}{\pi}\sum_{n=-\infty}^{+\infty}\frac{H_n^{(1)}(ka)}{H_n^{(1)\prime}(ka)}e^{in\theta} \tag{5.6.20}$$

for the case $\sin n\,\theta_0 \approx n\theta_0$.

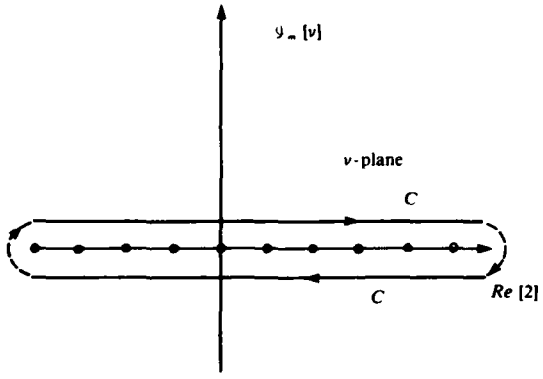

Fig. 5.6.2 Contour of integration of integral I.

Now 5.6.20 can be considered a sum of residues of a contour integral I in the complex ν plane. The appropriate form of I is given by

$$I = \int_c \frac{A(\nu)}{\sin \nu\pi}\,d\nu$$

in which the contour c encloses the real axis in a *clockwise* contour (Fig. 5.6.2) and $A(\nu)$ has no singularities within C.

Applying the theory of residues one obtains,

$$\begin{aligned} I &= -2\pi i \sum \left.\frac{A(\nu)}{\frac{d}{d\nu}(\sin \nu\pi)}\right|_{\nu=n} \\ &= -2i\sum_{n=-\infty}^{+\infty} e^{in\pi}A(n) \end{aligned} \tag{5.6.21}$$

Comparing 5.6.20 and 5.6.21 it is seen that

$$p(\theta) = \frac{i\varrho cV\theta_0}{\pi}\left(\frac{1}{-2i}\right)\int_c \frac{H_\nu^{(1)}(ka)}{H_\nu^{(1)\prime}(ka)}\frac{e^{i\nu\theta}e^{-i\nu\pi}}{\sin \nu\pi}\,d\nu \tag{5.6.22}$$

The contour C is next reversed to a counterclockwise circuit ($= -C$), opened at $+\infty$ and $-\infty$ and then made part of two larger contours as shown in Fig. 5.6.8. The new branches C_0 make loops

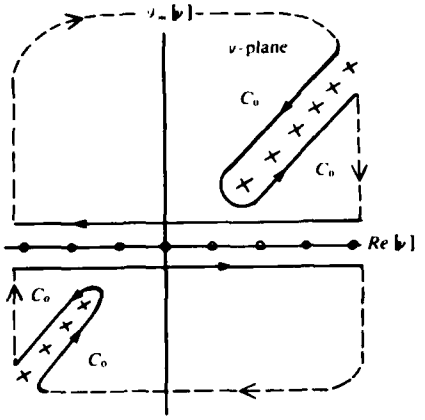

Fig. 5.6.3. Modification of the contour of Fig. 5.6.2.

around the poles of $A(\nu)$ in the first and third quadrants. The poles of $A(\nu)$ are the zeros ν_m, $m = 0, 1, 2 \ldots$ which satisfy the relation $H_{\nu m}(1)'(ka) = 0$. If ν_m is a zero then $-\nu_m$ is also a zero as may be seen from the Hankel function formula of the simple connection between H_ν and $H_{-\nu}$. The closures at infinity can be shown [15] to add nothing to the value of the line integral. Since the new contours enclose no poles the integrals along their course vanish. Hence, for each contour

$$\int_{C_0} = \int_C$$

Eq. 5.6.22 thus transforms to,

$$p(\theta) = \frac{i\varrho c V \theta_0}{\pi}(-\pi) \sum_{m=0}^{\infty} \left\{ \frac{H_{\nu m}^{(1)}(ka)\, e^{i\nu_m(\theta-\pi)}}{\left[\frac{\partial H_\nu^{(1)\prime}(ka)}{\partial \nu}\right]_{\nu=\nu_m} \sin \nu_m \pi} \right.$$

$$\left. + \frac{H_{-\nu_m}^{(1)}(ka)}{\left[\frac{\partial H_\nu^{(1)\prime}(ka)}{\partial \nu}\right]_{\nu=-\nu_m}} \frac{e^{-i\nu_m(\theta-\pi)}}{-\sin \nu_m \pi} \right\} \tag{5.6.23}$$

Recalling that

$$H_\nu^{(1)}(z) = \frac{ie^{-i\nu\pi/2}}{\sin \nu\pi}\left\{e^{-i\nu\pi/2} J_\nu'(z) - e^{i\nu\pi/2} J_{-\nu}'(z)\right\}$$

and that $H_\nu(1)'(ka) = 0$ at $\nu = \nu_m$, it is seen that of the three terms in the derivative $(\partial H_\nu / \partial \nu)$ taken at $\nu = \nu_m$ only one term survives, so that

$$\left.\frac{\partial H_\nu^{(1)\prime}(ka)}{\partial \nu}\right|_{\nu=\nu_m} = \frac{ie^{-i\nu_m\pi/2}}{\sin \nu_m \pi}$$

$$\times \left\{\frac{\partial}{\partial \nu}\left[e^{-i\nu\pi/2} J_{\nu_m}'(ka) - e^{-i\nu\pi/2} J_{-\nu_m}'(ka)\right]\right\}$$

Now the procedure of replacing ν_m by $-\nu_m$ changes the value of the bracketed quantity by a negative sign. Using once again the relation

$$H_{\nu_m}^{(1)}(k\varrho) = e^{-i\nu\pi} H_{-\nu_m}^{(1)}(k\varrho)$$

it is seen that the two terms in 5.6.23 can be combined to give the result that,

$$p(\theta) = \frac{i\varrho c V \theta_0}{\pi} e^{-i\omega t} \left\{ (-2\pi) \sum_{m=0}^{\infty} \times \right.$$

$$\left. \frac{-H_\nu^{(1)}(ka)}{\left[\dfrac{\partial H_\nu^{(1)\prime}(ka)}{\partial \nu}\right]_{\nu=\nu_m}} \frac{\cos \nu_m (\theta - \pi)}{\sin \nu_m \pi} \right. \tag{5.6.24}$$

The series in 5.6.24 is over positive roots ν_m only and is thus suitable for computation. However the waves emanating from the vibrating strip travel in both the positive and negative θ direction. To show the presence of these negative waves the last factor in 5.6.24 may be written in the form,

$$\frac{\cos \nu_m (\pi - \theta)}{\sin \nu_m \pi} = \left. \frac{e^{-i\nu(\pi-\theta)}}{2 \sin \nu\pi} \right|_{\nu=\nu_m}$$

$$\left. - \frac{e^{i\nu(\pi-\theta)}}{2 \sin \nu\pi} \right|_{\nu=-\nu_m} \tag{5.6.25a}$$

The factor $(1/\sin \nu\pi)$ may be expanded in two ways:

$$\frac{1}{\sin \nu\pi} = -2i \sum_{q=0}^{\infty} e^{i\nu\pi(1+2q)} \tag{5.6.25b}$$

$$= 2i \sum_{q=0}^{\infty} e^{-i\nu\pi(1+2q)} \tag{5.6.25c}$$

Inserting 5.6.25b in the first term of 5.6.25a and 5.6.25c in the second term one obtains the result that

$$\left. \frac{\cos \nu(\pi - \theta)}{\sin \nu\pi} \right|_{\nu=\nu_m} = -i \sum_{q=0}^{\infty} \left\{ \left. e^{-i\nu(\theta+2\pi q)} \right|_{\nu=-\nu_m} \right.$$

$$\left. + e^{i\nu(\theta+2\pi q)} \right|_{\nu=\nu_m} \tag{5.6.25d}$$

Thus, for each value of m there are two waves, one circumnavigating the cylinder in the positive direction q times, and one in the negative direction q times. Since $\nu_m = \nu_1 + i\nu_2$ these creeping waves decay exponentially in amplitude as $|\theta|$ increases. The rate of decay increases with the order m of the root. For large ka the series given by 5.6.24 converges rapidly since the first root ν_0 is of the order of ka. One term is often sufficient to give a very accurate value of the pressure at angle θ.

For finite width strips we reinsert $\sin n\theta_0/n\theta_0 = j_0(\nu\theta_0)$ inside the summation sign of 5.6.24. Writing $\nu = \nu_1 + i\nu_2$ it is seen that

$$j_0(\nu\theta_0) = |j_0(\nu\theta)|e^{i\alpha} \tag{5.6.26a}$$

where

$$|j_0(\nu\theta_0)|^2 = \frac{\sin^2\nu_1\theta_0\cos h^2\nu_2\theta_0 + \cos^2\nu_1\theta_0\sin h^2\nu_2\theta}{\nu_1^2 + \nu_2^2} \tag{5.6.26b}$$

and

$$\alpha = \tan^{-1}\left\{\frac{\tan h\,\nu_2\theta_0}{\tan\nu_1\theta_0}\right\} - \tan^{-1}\frac{\nu_2}{\nu_1} \tag{5.6.26c}$$

To find explicit forms of 5.6.24 it is necessary to express the ratio of Hankel functions as complex numbers having magnitude and phase. Following Sensiper [14] one can write for the condition ka large that

$$\frac{\nu_m}{ka} = 1 - \frac{\delta_m^2}{2} + \cdots$$

and

$$\frac{d\nu_m}{d(ka)} = 1 - \frac{1}{6}\delta_m^2 - \cdots$$

where

$$\delta_m \cong \left(\frac{3\nu_m}{ka}\right)^{\frac{1}{3}} e^{-i\pi/3}$$

and r_m is the solution of $J_{2/3}(r) - J_{-2/3}(r) = 0$.

By using the differential equation for cylinder functions Sensiper shows that

$$\frac{H_{\nu_m}(ka)}{\left[\frac{\partial H_\nu'(ka)}{\partial\nu}\right]_{\nu=\nu_m}} = \frac{d\nu_m|d(ka)}{1 - \left(\frac{\nu_m}{ka}\right)^2}$$

Hence, retaining terms in δ^2 only one arrives at

$$\frac{H_{\nu_m}(ka)}{\left[\frac{\partial H'_\nu(ka)}{\partial \nu}\right]_{\nu=\nu_m}} \approx \frac{(ka)^{\frac{2}{3}} e^{2i\pi/3}}{(3r_m)^{2/3}} \tag{5.6.27}$$

Junger [12] designates $(3r_m)^{2/3}$ by the symbols $4C_m$ for the purpose of facilitating use of published values of roots ν_m by Franz [16]. The first few numerical values of C_m are

$$C_0 = 0.4043,\ C_1 = 1.2920,\ C_2 = 1.9130,\ C_3 = 2.4461$$

For calculation we may set $q = 0$ in 5.6.25d because of the rapid attenuation of the creeping waves. Considering only the positive values $\nu = \nu_m$ because of symmetry in polar angle one substitutes 5.6.25d, 5.6.26a, 5.6.26b, 5.6.27 into 5.6.24 obtain

$$(a)\, p(\theta) = \varrho c V \theta_0 (ka)^{\frac{2}{3}} \sum_{m=0}^{\infty} \frac{|j_0(\nu_m \theta_0)|}{2C_m} e^{-\vartheta_m [\nu_m] \theta i \phi} e^m \tag{5.6.28}$$

where

$$(b)\, \phi_m = -\frac{1}{3}\pi + \alpha_m + Re\{\nu_m\}\theta - \omega t$$

This equation was derived by Junger [12].

The constant $-1/3\,\pi$ arises because of a residual negative sign. In the region of the image strip (i. e., at and near $\theta = \pi$) there is interference between the waves circumnavigating in positive θ and in negative θ. To account for the latter one adds to additional terms by allowing the polar angle to be $2\pi - \theta$ instead of θ. Usually one such added term is sufficient. Outside the interference region (i. e., width of the image strip) such additional terms are not needed.

Convergence of the series in 5.6.28 will clearly be poor in the small region over the radiating strip. For this region Junger suggests using the following formula for a strip set in an infinite plane baffle

$$p(\theta) = \frac{1}{2}\varrho c V \{G[ka(\theta + \theta_0) \pm G\, ka(\theta - \theta_0)\} \tag{5.6.29}$$

in which

$$G = \int_0^x H_0(x)\,dx = \chi H_0(x) + \frac{\pi}{2} x$$

$$\times [H_1(x)\bar{H}_0(x) - \bar{H}_1(x) H_0(x)]$$

where $\bar{H}_n$ is the Struve function.

The plus sign refers to values of θ in the cone $-\theta_0 < \theta < +\theta_0$, and the minus sign refers to values of θ outside this cone. Thus by use of 5.6.28, 5.6.29 one may calculate the complete pressure field over the entire surface of the cylinder, including the region directly on and adjacent to the strip at $\theta = 0°$, and at the antipodal image strip at $\theta = 180°$. The formulas recorded in this section however are best suited to cylinders of large acoustic size, say $ka > 20$, although good approximations are obtained by them in the range $ka \sim 3$.

5.6c. RADIATION FROM A RECTANGULAR PISTON SET IN AN INFINITE CYLINDER OF LARGE DIAMETER

On a rigid cylinder radius a of infinite length is set a rectangular piston of axial length $2z_0$ and circumferential width $2a\theta_0$. The piston moves with a velocity $Ve^{-i\omega t}$ and radiates sound into an infinite medium of characteristic impedance ϱc. The acoustic size ka of the cylinder is assumed to be very large relative to the wavelength $\lambda = 2\pi c/\omega$ of radiation while the piston itself is assumed to be small relative to this λ. The acoustic field $p(r, \theta, z)$ may be constructed of standing waves in the θ-direction and travelling waves in the radial r-direction and the axial z-direction. In the θ-direction the field is periodic, while in the z-direction the field is non-periodic. Introducing the Fourier integral for the field in the non-periodic direction we can describe the acoustic pressure at any point r, θ, z as

$$p(r, \theta, z) = \frac{1}{2\pi} \int_{-\infty}^{+\infty} dk_z \int_{-\infty}^{+\infty} p(r, \theta, k_z)\, e^{ik_z(z - z')}\, dz' \tag{5.6.30}$$

where $p(r, \theta, k_z)$ is the periodic field in the θ-direction and is given by

$$\begin{aligned} &(a)\ p(r, \theta, k_z) = \sum_{n=0}^{\infty} \epsilon_n A_n \cos n\theta\, H_n^{(1)}(k_r r) \\ &(b)\ k_r = \sqrt{k^2 - k_z^2} \end{aligned} \tag{5.6.31}$$

When $r = a$ and $z = 0$ it is required that the normal particle velocity u_r over the piston be $V_r e^{i\omega t}$. Now

$$\begin{aligned} u_r &= \frac{1}{ik\varrho c} \frac{\partial p}{\partial r}(r, \theta, k_z)\bigg|_{r=a} \\ &= \sum_{n=0}^{\infty} \frac{\epsilon_n k_r A_n \cos n\theta}{ik\varrho c} \left[\frac{dH_n(x)}{dx}\right]_{x = k_r a} \\ \epsilon_0 &= 1, \quad \epsilon_{n\neq 0} = 2 \end{aligned} \tag{5.6.32}$$

Expanding the known value of $|u_r|$ in the Fourier series,

$$\begin{aligned} (a)\ |u_r|_{\substack{r=a \\ z=0}} &= \frac{V\theta_0}{\pi} \sum_{n=0}^{\infty} \in_n j_n (n\,\theta_0) \cos n\theta \\ (b)\ j_0 (x) &= \sin x/x \end{aligned} \tag{5.6.33}$$

5.6.32 and 5.6.33a are equated to find the value of expansion constants A_n. This result reduces 5.6.31a to the form

$$p (r, \theta, k_z) = \sum_{n=0}^{\infty} \frac{\in_n V\theta_0\, ik\varrho c\, j_0 (n\theta_0)}{\pi\, k_r\, H_n' (k_r a)} \cos n\theta\, H_n^{(1)} (k_r r) \tag{5.6.34}$$

Since this is independent of z' we may next evaluate

$$\int_{-\infty}^{+\infty} e^{-ik_z z'}\, dz' = 2\, z_0 \left(\frac{\sin k_z Z_0}{k_z z_0} \right)$$

The final form of 5.6.30 as restricted to the surface pressure is thus

$$\begin{aligned} p (a, \theta, z) = {} & \frac{i\rho c V (ka\ \theta_0)(z_0/a) e^{-i\omega t}}{\pi^2} \sum_{n=0}^{\infty} \in_n j_0 (n\,\theta_0) \cos n\theta \\ & \times \int_{-\infty}^{+\infty} \frac{j_0 (k_z z_0)\, e^{ik_z z}}{\sqrt{k^2 - k_z^2}} \frac{H_n^{(1)} [(k^2 - k_z^2)^{1/2} a]}{H_n^{(1)\prime} [(k^2 - k_z^2)^{1/2} a]}\, dk_z \end{aligned} \tag{5.6.35}$$

As indicated in Sec. 5.6a the convergence of this "harmonic" series is also poor when ka is large and so, by a suitable Sommerfeld-Watson transformation, a new series may be evolved which converges more rapidly in the desired range. Following the procedure of Sect. 5.6.28 and noting in particular that 5.6.27 becomes transformed to

$$\frac{\mathrm{H}_{\nu_m} (k, a)}{\left[\dfrac{\partial H_\nu' (k, a)}{\partial \nu} \right]_{\nu = \nu_m}} \approx \frac{(k^2 - k_z^2)^{\frac{1}{3}}\, a^{\frac{2}{3}}\, e^{2i\pi/3}}{(3r_m)^{2/3}} \tag{5.6.36}$$

it is easily deduced that the appropriate Sommerfeld-Watson series is the same as given by 5.6.28 with the argument of the Hankel functions changed from ka to $a\sqrt{k^2 - k_z^2}$ Thus

$$(a)\, p(a, \theta, z) = \varrho c V \theta_0 (ka)(z_0/a) a^{\frac{2}{3}} e^{-i\{\omega t + \pi/3\}}$$

$$\times \frac{1}{\pi} \sum_{n=0}^{\infty} \frac{|j_0(\nu_m \theta_0)|\, I_m(z, \theta)}{2c_m} e^{ia_m} \tag{5.6.37}$$

in which

$$(b)\, I_m(z, \theta) = \int_{-\infty}^{+\infty} \frac{j_0(k_z z_0)}{(k^2 - k_z^2)^{1/6}} e^{-\vartheta_m[\nu_m(x)\theta]}\, e^{i[k_z z + R_e\{\nu_m(x)\theta\}]}\, dk_z$$

and

$$(c)\, x = a\sqrt{k^2 - k_z^2}$$

The numerical values of a_m are found in ref. [12]. In this reference the author has evaluated the integral $I_m(z, \theta)$ by the method of stationary phase which is applicable when ka is large. Designating the helix angle ν to be $\tan^{-1}(a\theta/z)$ he finds that the acoustic pressure at any point of the surface excepting near the piston ($\theta = 0$) and near its image ($\theta = 180°$) to be given by

$$p(\gamma, \theta) = \frac{\varrho c\, V\, \theta_0 (ka \sin\gamma)^{\frac{1}{6}} \tan\gamma \sin(kz_0 \cos\gamma)}{(2\pi\theta)^{1/2}}$$

$$\times \sum_{m=0}^{\infty} \frac{|j_0(\nu_m \theta_0)|}{c_m} e^{-a_m (ka \sin\gamma)^{1/3}\theta + i\phi_m(\gamma, \theta)} \tag{5.6.38}$$

where

$$\varphi_m(\gamma, \theta) = -7\pi/12 + a_m + ka\theta/\sin\nu + c_m (\mathrm{kasin}\,\nu)^{1/3}\theta - \omega t$$

The constants a_m, c_m are used to define the exact roots ν_m of $H_\nu'(x) = 0$. These together with constants b_m and d_m, appear in

$$I_m\ [\nu_m(x)] = a_m X^{1/2} + b_m X^{-1/3}$$

$$Re\ [\nu_m(x)] = X + c_m X^{1/3} - d_m X^{-1/3}$$

Numerical values of these constants may be found in ref. [12].

Pressure calculations generated by a small piston on a large cylinder using 5.6.38 in simplified form have been made by [12] using sums of three terms $m = 0, 1, 2$ on a desk calculator. Comparison was then made with the numerical results on an identical problem solved by the wave harmonic series method in a work by Greenspon and Sherman [13]. The piston size in question was $2a\theta_0 \times 2z_0$, $\theta_0 = 2.5°$, $kz_0 = \pi/2$, located on a circular cylindrical baffle $ka = 36$. Typical comparisons of normalized pressure amplitude $|p(\theta, z = 0)|/\rho cV$ are given below for angular spacing θ_f of the field point on the baffle greater than 3°.

Comparison of Methods		
θ_f (degrees)	Harmonic Series	Sommerfeld-Watson Ser.
3.23	0.4109	0.410
9.68	0.1478	0.150
20.98	0.0538	0.0545

The agreement is good. Comparisons of phase angle calculated by the two methods also agree to within a few degrees. Pressure distribution adjacent to and directly over the piston must be calculated by other means, e. g., the Kirchhoff formulas for a piston in an infinite baffle. The numerical advantage of the Watson procedure, evident here, must however be weighed against the serious difficulty of finding the roots ν_m which, though relatively simple in the above case, may prove extremely tedious for other geometries and other surface impedance conditions.

5.7 MULTIPOLE EXPANSIONS AND PLANE WAVE REPRESENTATIONS

A volume source of velocity potential, $q(r_0)\exp(-i\omega t)$ (units. s^{-1}), which vanishes outside a radius $|r| = R$, radiates a monochromatic field $\psi(r)$ in infinite free space:

$$\psi(r) = \int_{|r_0|\leq R} q(r_0)\,\frac{e^{ik|r-r_0|}}{4\pi|r - r_0|}\,d^3r_0 \tag{5.7.1}$$

(see Eq. (1.7.8). Using Weyl's expansion one substitutes 4.4.1 and interchanges the order of integration to get,

$$\psi(r) = \frac{ik}{2\pi}\int_{-\pi}^{\pi} d\beta \int_{C^{\pm}} d\alpha \sin\alpha\; q(K)e^{iK\cdot r} \tag{5.7.2}$$

where

$$\tilde{q}(K) = \int q(r_0)e^{-iK\cdot r_0}d^3r_0 \tag{5.7.3}$$

and

$$s = \hat{i}\sin\alpha\cos\beta + \hat{j}\sin\alpha\sin\beta + \hat{k}\cos\alpha\,,\quad K = ks \tag{5.7.4}$$

Here $C^{\pm}$ are contours of integration shown in Fig. 5.7.1. Contour C^{-} is used when $z > R$ and contour C^{-} when $z < R$. Eq. 5.7.2 defines the *angular spectrum of plane waves.* Eq. 5.7.3 appears to be a Fourier transform in the conjugate variables K and r_0. As such, K must be real. But $q(r_0)$ is finite and continuous hence $\tilde{g}(K)$ itself is the boundary value (taken on the real K_x, K_y, K_z axis) of an entire analytic function in 3-D complex K space [17]. Thus K in 5.7.2 takes on real and complex values along contours $C^{\pm}$, that is, variable $\alpha = \mathrm{Re}\alpha + i\mathrm{Im}\alpha$ in the unit vector s. To generate a multiple expansion of the acoustic wavefield one next expands the spectral amplitudes $\tilde{q}(K)$ into a series of spherical harmonics $Y(\alpha, \beta)$,

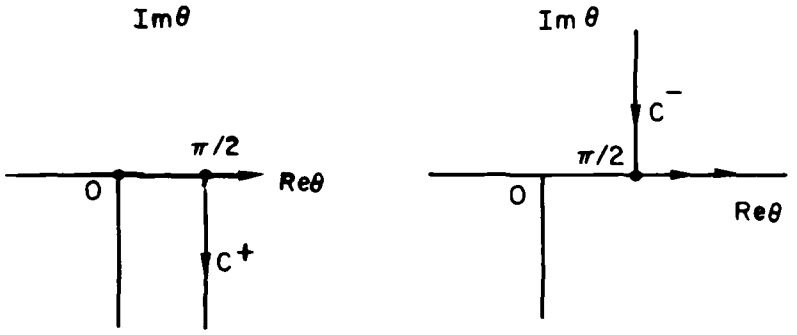

Fig. 5.7.1. Definition of contours of integration C^+ and C^-

$$\tilde{q}(K) = \sum_{l=0}^{\infty} \sum_{m=-l}^{l} (-i)^l a_{ml}\, Y_{ml}(\alpha, \beta) \tag{5.7.5}$$

where the coefficients a_{ml} (called *multipole moments*) have the form,

$$a_{ml} = i^l \int_{-\pi}^{\pi} d\beta \int_0^{\pi} d\alpha \sin\alpha\, \tilde{q}(K)\, Y_{ml}^*(\alpha, \beta) \tag{5.7.6}$$

Here only *real* values of α are used. Once the set a_{ml} is found Eq. 5.7.5 can be shown to be valid also for complex values of α all along the contours $C^{\pm}$.

Substitutions of 5.7.3 into 5.7.6 and rearrangement of terms lead to a formula of a_{ml} in terms of the volume source $q(r_0)$,

$$a_{ml} = 4\pi \int_{r_0 \leq R} q(r_0) \Lambda_{ml}^*(r_0)\, d^3 r_0 \tag{5.7.7}$$

where

$$\Lambda_{ml}^*(r_0) \equiv (i)^l \frac{1}{4\pi} \int_{-\pi}^{\pi} d\beta \int_0^{\pi} d\alpha \sin\alpha\, Y_{ml}(\alpha, \beta) e^{-iks\cdot r} \tag{5.7.8}$$

Assuming all the a_{ml} are found one can substitute 5.7.5 into 5.7.2, interchange the order of integration and summation, and arrive at a formula for the velocity potential field at field point r:

$$\psi(r) = k \sum_{l=0}^{\infty} \sum_{l=-m}^{n} a_{ml} \Pi_{ml}(r) \tag{5.7.9}$$

$$\Pi_{ml}(r) = (-i)^l \frac{i}{2\pi} \int_{-\pi}^{\pi} d\beta \int_{C^{\pm 1}} d\alpha \sin\alpha\, Y_{ml}(\alpha, \beta) e^{iks\cdot r} \tag{5.7.10}$$

By performing the integration it can be shown [18] that,

$$\Pi_{ml}(r) = h_l^{(1)}(kr)\, Y_{ml}(\theta, \phi) \tag{5.7.11}$$

in which r, θ, ϕ are the spherical polar coordinates of vector r and $h_l^{(1)}$ is the spherical Hankel function of the first kind. Formula 5.7.9 is the multipole expansion of $\psi(r)$ in terms of the multipole moments a_{ml} which depend on the volume source through 5.7.7 and 5.7.8.

In the farfield, in direction $u = r/|r|$, the approximation $|r - r_0| \sim r - r_0$, u is substituted into 5.7.1, and 5.7.3 is used to give,

$$\psi(ru) \sim \tilde{q}(K)_{K=ku} \frac{e^{ihr}}{r} \tag{5.7.12}$$

It is seen that $\tilde{q}(K)$ is the radiation pattern of the farfield radiated by the source $q(r_0)$ and $\tilde{q}(Ku)$ is the complex amplitude of a *simple* plane wave propagating in direction u. Thus along contours $C^{\pm}$ the only unit vectors that contribute to the farfield are those that are *real*, that is, only that portion of the contours which lie along the real axis of α. The contributions of the unit vectors along the complex part of $C^{\pm}$ yield *evanescent waves* which die out before reaching the farfield. The contributions of all real plane waves traveling in directions other than u cancel each other by destructive phase interference [19].

In terms of multipole moments a_{ml} given by 5.7.7, the farfield may be expressed as a summation of spherical harmonics:

$$\psi(ku) \sim \frac{e^{ik_k}}{r} \sum_{l=0}^{\infty} \sum_{m=-l}^{+l} (-i)^l a_{ml}\, Y_{ml}(\theta, \phi) \quad (kr \to \infty). \tag{5.7.13}$$

When the source $q(r_0)$ is localized in an area σ_R the vector r_0 is two-dimensional (2D). The transform $\tilde{q}(K)$ becomes 2-D also and appears as $\tilde{q}(K^T)$ thus the *farfield directorate function* becomes the 2-D (or transverse) transform of the "aperture" distribution across the surface. The magnitude of K^T is seen by 5.7.4 to be,

$$|K^T| = k = \omega/c \tag{5.7.14}$$

If $\tilde{q}(K^T)$ vanishes for all components of K^T which satisfy 5.7.14 then the source density $q(r_0)$ generates only evanescent (nonradiating) waves. This means that a (possibly) complicated nearfield can exist without any real radiation getting into the farfield [20]. It is then seen that all the multipole moments a_{ml} associated with the source $q(r_0)$ also vanish.

A further observation is of considerable importance in the theory of radiation. In Fig. 5.7.1 the part of the contours $C^{\pm}$ which goes from $\alpha = \pi/2$ to $\pm\infty$ can be quite arbitrarily modified without disturbing the part along the real axis. Thus a measured farfield can be associated with one of any number of nonradiating modes in the nearfield. Indeed one can specify a *desired* evanescent wavefield arbitrarily, independent of the radiation into the farfield [20].

REFERENCES

1. P. M. Morse, H. Feshback, "Methods of Theoretical Physics", Vol. I, p. 822.
2. E. Meyer, "Neuere Analogien zwischen akustischen und elektromagnetischen Schwingungen und Wellenfeldern", The 4th International Congress on Acoustics, Congress Report II 1962 p. 139.
3. Ref. [1], p. 828ff.
4. J. D. Jackson "Classical Electrodynamics" J. Wiley and Sons, New York 1963.
5. M. Yaldiz, O. K. Mawardi, JASA *32,* p. 1685 (1960).
6. Ref. [1], p. 1466.
7. A. Sommerfeld "Partial Differential Equations" Academic Press, New York 1949, Chap. 6.
8. G. N. Watson, Proc. Roy. Soc. London *A 95,* 83-89, 546-563 (1919).
9. P. M. Morse "Vibration and Sound" McGraw Hill Book Co., 2nd Ed. p. 321-326.
10. Ref. [7], p. 287.
11. Ref. [7], p. 283.

12. M. C. Junger "Surface Pressures Generated by Pistons on Large Spherical and Cylindrical Baffles" JASA *41,* 1336-1346, (1967).

13. J. E. Greenspon, C. H. Sherman "Mutual Radiation Impedance and Near Field Pressure for Pistons on A Cylinder" JASA *36,* 149-153 (1964).

14. S. Sensiper "Cylindrical Radio Waves" IRE Trans. Antenna Prop. AP.-5, 56-70 (1957).

15. J. R. Wait "Electromagnetic Radiation from Cylindrical Structures" Pergamon Press, New York, 1959.

16. W. Franz "Zeitshrift Naturforsch" *99,* 705-716 (1954).

17. E.T. Copson, "Theory of Functions of a Complex Variable," Oxford Press, 1935 Sect. 5.5.

18. A.J. Devaney and E. Wolf, J. Math. Phys. **15**, p. 234 (1972).

19. M. Lax, H. Feshbach J. Acous. Soc. Am. **19**, p. 583 (1974).

20. A.J. Devaney and E. Wolf, Physical Review D **8**, 8 (1973).

CHAPTER VI

ACOUSTIC POWER AND RADIATION IMPEDANCE OF ACOUSTIC RADIATORS

6.1. INSTANTANEOUS AND HARMONIC ACOUSTIC INTENSITY AND POWER

The real instantaneous intensity of an acoustic field at a point $(\vec{r}, t)$ is the product of a real vector particle velocity and a real scalar acoustic pressure,

$$\vec{I}(\vec{r}, t) = p(\vec{r}, t)\,\vec{u}(\vec{r}, t) \tag{6.1.1}$$

In linear acoustics both p and u are derivable from a scalar velocity potential ψ (see Chap. I),

$$p = \varrho \frac{\partial \psi}{\partial t}(\vec{r}, t);\ \vec{u} = -\vec{\nabla}\psi(\vec{r}, t)$$

The negative sign has the meaning that if the potential is increasing in a particular direction the particle velocity is increasing in the opposite direction. In terms of velocity potential the instantaneous intensity is,

$$I = -\varrho \frac{\partial \psi}{\partial t}\vec{\nabla}\psi \qquad \text{(Units: } Nm^{-1}s^{-1}\text{)} \tag{6.1.2}$$

In general the intensity over an area S varies from point to point. Thus the instantaneous acoustic power propagating through the area is,

$$\vec{W} = -\oint \varrho \frac{\partial \psi}{\partial t}(\vec{r}, t)\,\vec{\nabla}\psi(\vec{r}, t)\,dS(\vec{r}) \tag{6.1.3}$$

When the time variation in the acoustic field is harmonic ($exp\ -i\omega t$) the acoustic field is expressed in complex amplitudes P, U:

$$p = \frac{Pe^{-i\omega t} + P^* e^{+i\omega t}}{2} = Re\,P\cos\omega t + I_m P \sin\omega t$$

$$u_j = \frac{U_j e^{-i(\omega t + \theta)} + U_j^* e^{+i(\omega + \theta)}}{2} = Re\,U_j \cos(\omega t + \theta) + I_m U_j \cos(\omega t + \theta) \tag{6.1.4}$$

in which u_j is a component of particle velocity in the vector $\vec{u}$. In 6.1.4 both p and u are real quantities expressed as complex variables.

Here θ is an arbitrary phase angle. Substitution of 6.1.4 into 6.1.1 yields the harmonic intensity,

$$I = \frac{1}{4}\left[P^* U_j e^{-i\theta} + P U_j^* e^{+i\theta} + P U e^{-2i(\omega t + \theta)} + P^* U^* e^{2i(\omega t + \theta)}\right]$$

When averaged over time of many cycles the last two terms vanish. The average (or root mean square) intensity is then,

$$I_{AV} = \frac{1}{4}\{2\cos\theta\, Re\,[PU_j^*] + 2\sin\theta \quad I_m\,[PU^*]\} \tag{6.1.5a}$$

In the usual case $\theta = 0$; then,

$$I_{AV} = \frac{1}{2} Re\,\{PU_j^*\} \tag{6.1.5b}$$

Similarly, when ψ is a sinusoid with complex amplitude Φ,

$$\psi = \frac{\Psi e^{-i\omega t} + \Psi^* e^{+i\omega t}}{2} = Re\,\Psi \cos\omega t + \vartheta_m \Psi \sin\omega t$$

it is seen that Ψ plays the role of p, and $\nabla\Psi$ the role of u. Hence, for $\theta = 0$, and for component u_j,

$$I_{AV} = \frac{1}{2} Re\,\{pu_j^*\} = \frac{1}{2} Re\,\{-i\omega\varrho\,[Re\,\Phi + i\ I_m\,\Phi]\,[Re\,U_j - i\ I_m\,U_j]$$

In particular cases one can take the phase of U_j to be a reference phase, and set it to zero. Then,

$$I_{AV}(\vec{r}|\,\omega) = \frac{1}{2}\omega\varrho\, U_j(\vec{r}|\,\omega)\ I_m\,\Psi(\vec{r}|\,\omega) \tag{6.1.6}$$

Clearly 6.1.6 takes its origin in 6.1.4 where p, u are real quantities. An alternative case occurs when velocity potential is inherently a complex number,

$$\begin{aligned}\psi(\vec{r}|\,\omega) = A(\vec{r})\, e^{-i\omega t} &= Re\,A(\vec{r})\cos\omega t + I_m\,A(\vec{r})\sin\omega t \\ &+ i\,[\ I_m\,A(r)\cos\omega t - Re\,A(r)\sin\omega t]\end{aligned} \tag{6.1.7}$$

Then the time-averaged intensity at $\vec{r}$ from 6.1.2 and 6.1.5b is,

$$\vec{I}_{AV}(\vec{r}) = \frac{1}{2}\varrho\, Re\{-i\omega A(\vec{r})[-\vec{\nabla}A(\vec{r})]^*\} \tag{6.1.8}$$

The time-averaged acoustic power W is obtained from 6.1.5, or 6.1.8 by integration of intensity over area,

$$W = \oint I_{AV}(\vec{r})\, dS(\vec{r}) \tag{6.1.9}$$

6.2 RADIATED INTENSITY AND POWER OF A POINT SOURCE (MONOPOLE, DIPOLE, QUADRUPOLE)

A simple (point) source, of effective radius a much less than a wavelength, generates sound in a medium by a time-varying injection of mass, $Q_\omega e^{-i\omega t}$ (units: $m^3 s^{-1}$). Because the field of velocity potential is governed by the linear equation of propagation $(\nabla^2 + k^2)\psi = 0$, $k = 2\pi/\lambda$, one immediately finds that,

$$\psi = A(\vec{r})e^{-i\omega t};\ A(\vec{r}) = A_0 e^{ikr}/r;\ A_0 = \frac{Q_\omega}{4\pi} \tag{6.2.1}$$

Substitution of 6.2.1 into 6.1.8 leads to the radiated intensity,

$$I_{AV}(r|w) = \frac{1}{2}\varrho\omega\, Re\left\{i\frac{Q_\omega}{4\pi}\frac{e^{ikr}}{r}\left[\frac{Q_\omega^*}{4\pi}\frac{e^{ikr}}{r}\left(-ik-\frac{1}{r}\right)\right]\right\}$$

$$'' \quad = \frac{1}{2}\frac{\varrho c\,|Q_\omega|^2 k^2}{16\pi^2 r^2} \tag{6.2.2}$$

In this formula $|Q_\omega|$ is a peak amplitude.

At a spherical surface $r = a$ the time-averaged acoustic power radiated is found from 6.1.9,

$$W_{AV} = \frac{1}{2}\frac{\varrho c|Q_\omega|^2 k^2}{4\pi} \tag{6.2.3}$$

When the mass-injection is transient $Q(t)$, the associated radial particle velocity of the sound field is $u(t) = Q(t)/4\pi a^2$. From the wave equation $(\nabla^2 - c^{-2}\partial/\partial t^2)p = 0$ the field of pressure in spherical coordinates has the form $p = P(r-ct)/r$. The pressure p is governed by Newton law, $-\partial p/\partial r = \varrho\partial u/\partial t$, so that,

$$\frac{1}{r}\frac{\partial P(r-ct)}{\partial r} - \frac{P(r-ct)}{r^2} = -\varrho(4\pi a^2)^{-1}\frac{\partial Q(t)}{\partial t} \tag{6.2.4}$$

Choosing $P(r-ct) = exp\,(ikr - ict)$, and allowing $ikP/a \ll P/a^2$ because $a \ll \lambda$ for a point source, one again is led to 6.2.2 and 6.2.3.

For a dipole point source of strength $\vec{D}$ ($= Q\vec{d}$, $\vec{d}$ being the vector distance between the + source and the − source), the (particle) velocity potential is,

$$\psi = \vec{D}\cdot\vec{\nabla}_0 g(\vec{r}|\vec{r}_0|\omega)\,e^{-i\omega t} \tag{6.2.5a}$$

In general $\vec{D}$ is arbitrarily oriented relative to the x, y, z coordinate system. It has three components D_x, D_y, D_z. The contribution of one component, say D_z, to the field at (R, θ_R, ϕ) measured relative to $\vec{r}_0$ is:

$$\psi_z(R, \theta_R|\omega) = -\frac{ikD_z}{4\pi}\frac{e^{ikR}}{R}\left[1 + \frac{i}{kR}\right]\cos\theta_R\, e^{-i\omega t}$$
$$R = |\vec{r} - \vec{r}_0| \tag{6.2.5b}$$

D_x, D_y also contribute to the field at (R, θ_R, ϕ).

The intensity of radiated sound at (R, θ_R, ϕ) contributed by D_z is obtainable from 6.1.8:

$$I_z = \frac{1}{2}Re\{p\,u_z^*\}.\ \text{Hence,}$$

$$I_z(R, \theta_R|\omega) = \frac{1}{2}Re\left\{\left[-\frac{k^2 D_z\,\varrho c}{4\pi R}\cos\theta_R\left(1 + \frac{i}{kR}\right)\right]\right.$$
$$\left.\times\left[-\frac{k^2 D_z}{4\pi R}\cos\theta_R\left(1 - \frac{2i}{kR} - \frac{2}{k^2R^2}\right)\right]\right\}$$
$$= \frac{1}{2}Re\left\{\frac{k^4 D_z^2}{(4\pi\ R)^2}\cos^2\theta_R\left[1 - \frac{i}{kR} - \frac{2i}{k^3R^3}\right]\right\} = \frac{1}{2}\left(\frac{k^2|D_z|}{4\pi R}\right)^2\cos^2\theta_R \tag{6.2.6}$$

in which θ_R is the spherical angle of the vector $\vec{R}$. In this formula, $|D|$ is a peak amplitude.

For a quadrupole point source, of tensor strength $\vec{\vec{Q}}$ (units: $m^5 s^{-1}$) the velocity potential at $\vec{r} = (r, \theta, \phi)$ is,

$$\psi(\vec{r}|\omega) = (\vec{\vec{Q}} : \vec{\nabla}_0 g(\vec{r}|\vec{r}_0|\omega)\vec{\nabla}_0)\,e^{-i\omega t} \tag{6.2.7}$$

In general $\vec{\mathcal{Q}}$ has 9 components, of which only six are independent because of symmetry. There are three components of intensity: in spherical coordinate, I_r, I_θ, I_ϕ; in rectangular coordinates, I_x, I_y, I_z. One, several, or all six components of ψ may contribute to one component of intensity at a field point. For example, using 6.1.8, the contribution of the $\mathcal{Q}_{xx}$ component to I_x is

$$I_x = \frac{1}{2} Re\{pu_x^*\} = \frac{1}{2} Re\left\{ -i\omega\varrho \quad \mathcal{Q}_{xx} \frac{\partial^2 g}{\partial x^2} \left[-\frac{\partial}{\partial x} \quad \mathcal{Q}_{xx} \frac{\partial^2 g}{\partial x^2} \right]^* \right\} \tag{6.2.8}$$

$$g = \frac{e^{ikR}}{4\pi R}; \quad R = |\vec{r}-\vec{r}_0|$$

The contributions of all other components to I_x are additive.

6.3. ACOUSTIC RADIATION IMPEDANCE.

A surface radiating acoustic waves experiences a force of the medium acting back upon it. The force is of two types: a spring-like force associated with the compressibility of the medium; and a mass-like force associated with the acceleration of the fluid. Because of the matching of pressure and particle velocity between medium and radiating surface at the boundary, this reaction of the medium is formulated in several ways. First there is the specific acoustic impedance (units: Ns/m^3) which is the ratio of acoustic pressure to particle velocity. Such a ratio is local on the plate. By integration over a portion of the plate, or the whole plate, one obtains a second measure of medium reaction, the mechanic impedance (units: Ns/m), which is the ratio of force to particle velocity. A third measure of reaction of the medium is acoustic impedance (units: Nsm^{-5}) which is the ratio of acoustic pressure to volume velocity.

The calculation of impedance can be carried out in two alternate, but equivalent ways: in the first way the acoustic pressure on the surface is obtained by methods of chapters 1-5. By integration over surface area the total force F of the medium upon the surface is calculated. Finally, a reference velocity $Vref$ is calculated as a function of ka at some arbitrary point of the surface and the ratio $Z = F/V\text{ref}$ formed. $V\text{ref}$ is the complex particle velocity at that point and is calculated from the gradient of pressure at the surface point, In the second way the radiated power W is obtained by methods of this chapter. The three impedances are then defined in terms of this (steady state) power:

$$-\nabla p|_{\text{surface}} = V_{\text{ref}}.$$

While the pressure on the surface may be calculated from a specified normal component of surface velocity the form of the particle velocity in the medium must account for in-phase and out-of-phase components (which is the nearfield effect). Hence the specified normal component of surface velocity and normal component of particle velocity are different physical quantities. The former is an elastic plate entity while the later is an acoustic entity.

$$Z(\omega) = \frac{2W}{|Vref|^2} \qquad \text{(units: Nsm}^{-1}\text{)} \tag{6.3.1}$$

$$z(\omega) = \frac{2W}{S|Vref|^2} \qquad \text{(units: Nsm}^{-1}\text{)} \tag{6.3.2}$$

$$\mathcal{Z}(\omega) = \frac{2W}{S^2|Vref|^2} \qquad \text{(units: Nsm}^{-5}\text{)} \tag{6.3.3}$$

$$\text{Vref} = \frac{\oint V(\dot{r}_0)\, dS(\dot{r}_0)}{S} \qquad \text{(units: } ms^{-1}\text{)} \tag{6.3.4}$$

In the following sections several cases of the calculation of acoustic power and impedance are discussed in detail.

6.4. RADIATION OF STEADY STATE ACOUSTIC POWER FROM A LARGE FLEXURAL PLATE WITH FIXED VELOCITY DISTRIBUTION IN AN INFINITE RIGID BAFFLE.

In the steady state the surface of a vibrating flexural plate upon which there is a complex distribution of normal velocity $v_z(x, y, |\omega)$ and complex pressure $p(x, y|\omega)$ will radiate acoustic power according to 6.1.9:

$$W = \frac{1}{2} Re \oint \{p v_z^*\}\, dS \tag{6.4.1}$$

in which p and v_z^*, express peak amplitudes. For a rectangular plate $2L_x$ wide, $2L_y$ long in an infinite rigid baffle, the radiated power is calculated by use of the velocity potential 4.1.9:

$$W = \frac{1}{2} Re \int_{-L_x}^{L_x} \int_{-L_y}^{L_y} \left[\int_{-\infty}^{\infty}\int (-i\omega\varrho)\, i \frac{V_z(k_x, k_y)}{\sqrt{k^2 - k_x^2 - k_y^2}} \exp i(k_x x + k_y y) \frac{dk_x\, dk_y}{(2\pi)^2} \right] \tag{6.4.2}$$

$$\times \left[- \int_{-\infty}^{\infty}\int (-i)(-i) \frac{k_z}{k_z} V_z^*(k_x', k_y') \exp - i(k_x' x + k_y' y) \frac{dk_x'\, dk_y'}{(2\pi)^2} \right] dx\, dy$$

Now,

$$\lim_{L_x, L_y \to \infty} \int_{-L_x}^{L_x} \int_{-L_y}^{L_y} e^{i(k_x - k_x')x}\, e^{i(k_y - k_y')y} \frac{dx\, dy}{(2\pi)^2} = \delta(k_x' - k_x')\, \delta(k_y - k_y') \tag{6.4.3}$$

Thus, if $2L_x$ and $2L_y$ are "large enough,"

$$\lim_{L_x, L_y \to \infty} \int_{-\infty}^{\infty}\int V_z^*(k_x', k_y'|\omega)' \frac{2L_x \sin[L_x(k_x - k_x')]}{2\pi L_x (k_x - k_x')} \frac{2L_y \sin[L_y(k_y - k_y')]}{2\pi L_y (k_y - k_y')} dk_x' dk_y'$$

$$= V_z^*(k_x, k_y|\omega) \tag{6.4.4}$$

The acoustic power radiated by the flexural plate then becomes,

$$W(k, \omega) = \frac{1}{2} Re \left\{ \omega\varrho \int_{-\infty}^{\infty}\int \frac{|V_z(k_x, k_y|\omega)|^2}{\sqrt{k^2 - k_x^2 - k_y^2}} \frac{dk_x\, dk_y}{(2\pi)^2} \right\} \tag{6.4.5}$$

Here; the units of $V_z(k_x, k_y|\omega)$ are $m^3 s^{-1}$.

In 6.4.5 the radiated power is real when the integrand is real, that is, when

$$k_p^2 < k^2 \; ; \; k_p^2 = k_x^2 + k_y^2 \tag{6.4.6}$$

Alternatively, the condition is $(k_x/k)^2 + (k_y/k)^2 < 1$. Since $k_x = 2\pi/\lambda_x$, $k_y = 2\pi/\lambda_y$, where λ_x, λ_y are wavelengths in the x, y directions respectively, in the plate, and $k = 2\pi/\lambda$, where λ is the wavelength in the medium the condition of radiation of real power may also be expressed as,

$$\left(\frac{\lambda}{\lambda_x}\right)^2 + \left(\frac{\lambda}{\lambda_y}\right)^2 < 1 \tag{6.4.7}$$

When the left hand side is greater than unity the power radiated out to infinity is *imaginary*. It is reactive power associated with a pressure field which decays exponentially in the near field of the radiating source. Each wavenumber k_x, k_y, k is a function of frequency ω. The particular frequency ω_c at which

$$\frac{k_p^2(\omega_c)}{k^2(\omega_c)} = 1 \tag{6.4.8}$$

is the *coincidence,* or critical, frequency. It is the lowest frequency in forced drive at which a flexing plate can radiate real power. The function $k_p(\omega)$ exhibits *dispersion* of progressive flexural waves in the plate. Dispersion relations depend on dynamics of plate vibration. Two useful special cases of dispersion are discussed below,

Case I. Power radiated by a force driven flexural plate that is elastically thin and lossless.

A large, thin, undented elastic plate, of bending stiffness $D = Eh^3/12\,(1-\sigma^2)$ (units: Nm), where E is Young's modulus (units: Nm^{-2}), h is the plate thickness (units: m), σ is Poisson's ratio (units: *none*), supports progressive flexural waves. Their phase speed C_p depends on frequency,

$$C_p = \omega^{1/2}\left[\frac{D}{\varrho_m h}\right]^{1/4} \qquad \text{(units: } ms^{-1}\text{)} \tag{6.4.9}$$

$$\varrho_m = \frac{mass}{volume} \qquad \left(\text{units: } \frac{NS^2}{m^4}\right)$$

[1]. The wavenumber corresponding to this speed is,

$$k_p = \frac{\omega}{C_p} = \omega^{1/2}\left[\frac{\varrho_m h}{D}\right]^{1/4} \qquad \text{(units: } m^{-1}\text{)} \tag{6.4.10}$$

By definition, the wavelength of the corresponding flexural wave is $\lambda_p = 2\pi\, k_p^{-1}$, or

$$\left(\frac{2\pi}{f}\right)^{1/2}\left(\frac{D}{\rho_m h}\right)^{1/4} \qquad \text{(units: } m\text{)} \tag{6.4.11}$$

Similarly, the wavelength in the medium is $\lambda = c/f$. Thus the requirement 6.4.6 for radiation of real power can be expressed by the relation,

$$\frac{\lambda}{\lambda_p} = \sin\theta, \; 0 \leqslant \theta \leqslant \pi/2 \tag{6.4.12}$$

$$\sin\theta = \frac{C}{(2\pi f)^{1/2}\left(\frac{D}{\rho_m h}\right)^{1/4}} \tag{6.4.13}$$

This θ is the physical angle, measured from the normal to the plate, at which plane waves in the medium are radiated from progressive plate waves whose phase advances across the plate in a straight line (called "straight-crested" waves). Fig. 6.4.1a shows the geometrical configuration in terms λ, λ_p, and also in terms of $-k$, k_p. As the frequency diminishes $\sin\theta$ increases. At the lowest frequency (= critical frequency) for radiation of real power $\theta = \pi/2$ (i.e. $\lambda = \lambda_p$); the acoustic wave travels parallel to the plate at a temporal frequency,

$$f_c = \frac{C^2}{2\pi}\sqrt{\frac{\rho_m h}{D}} \qquad \text{(units: } s^{-1}\text{)} \tag{6.4.14}$$

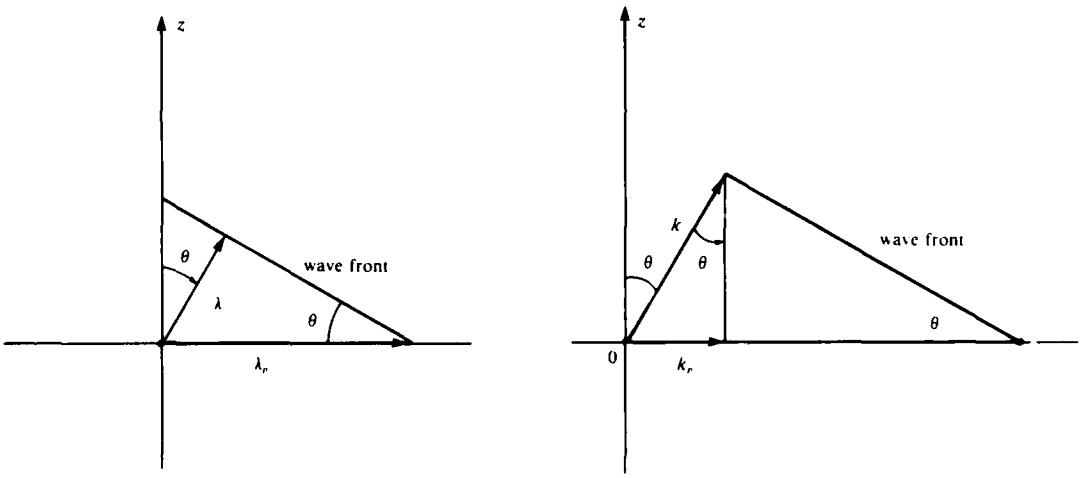

Fig. 6.4.1a. $\sin\theta = \lambda/\lambda_p$ Fig. 6.4.1b. $\sin\theta = k_p/k$

Fig. 6.4.1. Plane waves radiated from a plate

As the drive frequency f rises above f_c the acoustic wavelength decreases as f^{-1} while the bending wavelength decreases as $f^{-1/2}$. Thus λ/λ_p, and hence θ, grows smaller as the frequency rises. At very high frequency $\lambda/\lambda_p \to 0$, hence $\theta \to 0$, and the radiated plane waves leave the plate nearly in the direction of the $z-$axis. The acoustic pressure radiated can then be calculated from 6.4.5 on the assumption that $k_p^2 \ll k^2$. First, one notes by Rayleigh's theorem that,

$$\int_{-\infty}^{\infty}\int |V_z(k_x, k_y|\omega)|^2 \frac{dk_x}{2\pi}\frac{dk_y}{2\pi} = \int_{-\infty}^{\infty}\int |V_z(x, y|\omega)|^2 d_x d_y \tag{6.4.15}$$

The right hand side of this equation can serve to define an average squared velocity by division with area S:

$$|V_z|^2_{AV} = \int_{-\infty}^{\infty}\int |V_z(x, y|\omega)|^2 \, d_x \, d_y / S \tag{6.4.16}$$

Thus the acoustic power radiated at high frequencies becomes,

$$W(\omega) = \frac{1}{2} \varrho c \, S \, |V_z|^2_{AV} \tag{6.4.17}$$

in which $|V_z|$ is the peak amplitude of the normal component of surface velocity averaged over the plate. It is often useful to try to include the effect of the wavenumber ratio in the same high-frequency range. One can then approximate 6.4.5:

$$W(\omega) \cong \frac{1}{2} \frac{\varrho c \, S \, |V_z|^2}{\sqrt{1 - k_p^2/k^2}}, \qquad f \gg f_c \tag{6.4.18}$$

Case II. Power radiated by a force-driven plate that is elastically thin and lossy

When the vibrating plate is damped the phase speed of the plate bending waves is complex,

$$C_p^4 = \frac{\omega^2 D}{\varrho_m h}(1 - i\eta) \tag{6.4.19}$$

that is, $C^p \propto (1 - i\eta)^{1/4}$, where η is a damping parameter. In usual elastic plates $\eta < 1$; the phase speed is then approximated as $C_p \propto 1 - i\eta/4$, and because $k_p = \omega/c_p$ the important damping quantity becomes,

$$\left[1 - \left(\frac{k_p}{k}\right)^2 \left(1 + \frac{i\eta}{4}\right)^2\right]^{1/2} = \left[1 - \left(\frac{k_p}{k}\right)^2 - \frac{i\eta}{2}\left(\frac{k_p}{k}\right)^2 + \frac{\eta}{16}\left(\frac{k_p}{k}\right)^2\right]^{1/2}$$

At frequencies much less than the critical frequency the effects of damping are important. In this range $(k_p/k)^2 \gg 1$; neglecting the term in η^2 because it is small the above quantity is approximately,

$$\sqrt{-\left(\frac{k_p}{k}\right)^2 \left(1 + i\frac{\eta}{2}\right)} \to \frac{k_p}{k}\left(\frac{\eta}{4} - i\right)$$

The reciprocal of this is

$$\frac{\left(\frac{k}{k_p}\right)\left(\frac{\eta}{4}+i\right)}{\frac{\eta^2}{16}+1}$$

Since one is interested only in the real part of this entity one arrives at the approximation that,

$$Re\left[1-\left(\frac{k_p}{k}\right)^2\left(1+\frac{i\eta}{4}\right)^2\right]^{-1/2} \cong \frac{\eta}{4}\,\frac{k}{k_p},\ \frac{k}{k_p} \ll 1 \tag{6.4.20}$$

In this wavelength region k_p is very large and proportional to $f^{1/2}$. Thus k/k_p changes slowly with f and can be assumed constant, that is, 6.4.20 can be placed outside of the integral sign in 6.4.5 as long as $k/k_p < 1$. Eq. 6.4.5, thus modified, can be evaluated approximately by use of 6.4.15 through 6.4.18. However, in addition to this damping which accompanies near field (= evanescent) wave fields, there is a damping that accompanies the propagation of waves traveling over the plate into the far field. A simple model of this type of damping consists in making the propagation constant complex, $k_p\,(1 + i\eta/4)$ and giving each traveling wave on the plate a phase of amount

$$exp\, ik_p r_0\left(1+\frac{i\eta}{4}\right) = exp\left(-\eta r_0 \frac{k_p}{4}\right) exp\, ikr,\ \vec{r}_0 = \hat{i}\, x_0 + \hat{j}\, y_0$$

Thus the power absorbed in the near-and farfield, attributable to damping, is proportional to $(exp - \eta r_0 k_p/4)^2 = exp\,(-\eta k_p r_0/2)$. The power absorbed by the vibrator at very low frequencies is therefore

$$W(r_0|\omega) = \frac{1}{2}\varrho c S\,|V_z|^2_{AV}\, e^{-\eta k_p r_0/2}\left(\frac{\eta k}{4k_p}\right)$$
$$\left(\frac{k_p}{k}\right)^2 \gg 1;\ \eta^2 \ll 1;\ f \ll f_c \tag{6.4.21}$$

An important physical fact described by this formula is that the plate radiates sound at drive frequencies well below the critical frequency provided the plate is damped. The same damped plate naturally radiates at drive frequencies well above the critical frequency. But this radiation diminishes as the progressive wave spreads across the plate from the center of force input. Thus the real radiated acoustic power density (that is, power per unit plate area) depends on where the unit radiating area of the plate is located, which means, in this case, the location r_0:

$$\frac{W(r_0|\omega)}{S} = \frac{1}{2}\varrho c\,|V_z|^2\, e^{-\frac{1}{2}\eta k_p r_0} \qquad \left(\text{units: } Nms^{-1}m^{-2}\right. \tag{6.4.22}$$

6.5. MECHANICAL RADIATION IMPEDANCE OF A VIBRATING CIRCULAR MEMBRANE IN AN INFINITE RIGID BAFFLE.

A circular membrane, radius a, is assumed to have a displacement $w(\vec{R}_0)$ given by 4.3.5. At the steady state frequency ω this displacement becomes a sinusoidal acceleration $w(\vec{R}_0)$, and thus causes sound to be radiated. The velocity potential of this sound field is given by 4.3.6a. The acoustic power radiated is obtained from it by 6.1.3 expressed in steady state:

$$W = \frac{1}{2}\{\oint p v_z^* ds\} \tag{6.5.1}$$

in which p, v_z are peak amplitudes. Making the substitutions called for, one obtains,

$$W = \frac{1}{2}\int_0^a \int_0^{2\pi} r'' dr'' d\phi'' (-i\omega\varrho) \sum_{m=0}^{\infty} (-i\omega)\cos m\phi'' \int_0^{\infty} J_m(\xi r'')$$

$$\times \frac{f_m'(\xi)\, e^{-\sqrt{\xi^2-k^2}\, z}}{\sqrt{\xi^2-k^2}}\, \xi d\xi \left[(-i\omega)\, w_m(r'', \phi'')\cos m\phi''\right]^* \tag{6.5.2}$$

By interchanging the order of integration of r'' and ξ it is seen from 4.3.6b that

$$\text{(a)}\ [f_m''(\xi)]^* = \int_0^a J_m(\xi r'')\,[W_m(r'', \phi'')]^*\, r''\, dr'' \qquad \text{(units: } m^3\text{)}$$

also,

$$\text{(b)}\ \int_0^{2\pi} \cos m\phi''\,(\cos m\phi'')^*\, d\phi'' = \frac{2\pi}{\epsilon_m} \tag{6.5.3}$$

$$\epsilon_0 = 1;\ \epsilon_m = 2,\ m \neq 0$$

Because r'' and r' must be the same in order to calculate the power radiated by each elementary area on the vibrating membrane, 6.5.2 at $z = 0$ reduces to the form,

$$W = \frac{1}{2} i\omega^3 \varrho \sum_{m=0}^{\infty} \frac{2\pi}{\epsilon_m} \int_0^{\infty} \frac{|f_m(\xi)|^2\, \xi d\xi}{\sqrt{\xi^2-k^2}} \tag{6.5.4}$$

in which $fm(\xi)$ is the same as both $f_m''(\xi)$, 6.5.3a, and $f_m'(\xi)$, 4.3.6b.

In 6.5.4 $|f_m(\xi)|^2$ is a real number and $\sqrt{\xi^2-k^2}$ is purely imaginary when $0 \leqslant \xi < k$. Thus the power radiated is purely real in this range, and purely imaginary when $\xi > k$. For each Fourier component therefore,

$$Re\, W_m = \frac{\pi \omega^3 \varrho}{\in_m} \int_0^k \frac{|f_m(\xi)|^2 \xi\, d\xi}{\sqrt{k^2 - \xi^2}} \tag{6.5.5}$$

$$\vartheta_m W_m = \frac{\pi \omega^3 \varrho}{\in_m} \int_k^\infty \frac{|f_m(\xi)|^2 \xi\, d\xi}{\sqrt{\xi^2 - k^2}} \tag{6.5.6}$$

Where, as before, $f_m(\xi)$ is based on peak amplitudes of displacement. Equations 6.5.5 and 6.5.6, enable us to find the mechanical radiation impedance by use of the relation 6.3.1. Application of 6.3.1 requires a selection of *Vref*. In this case it is convenient to choose the displacement at the center of the membrane given by the *m'th* Fourier component, $\omega_m'(0)$, 4.3.5, and write,

$$[Vref]_m = -i\omega\, w_m'(0) \tag{6.5.7}$$

The *m'th* (Fourier) mechanical radiation impedance is defined as,

$$Z_m = \frac{W_m}{|Vref|_m^2} = R_m - i X_m \tag{6.5.8}$$

The appearance of a negative sign before the reactive component X_m is due to the choice of time representation is $exp\,(-i\omega t)$, and the fact that X_m is an inertial impedance, ωM, where M is the effective mass. From 6.5.5, 6.5.6 it is seen then that the components of Z_m are given by,

$$R_m = \frac{\pi \omega^3 \varrho}{\in_m} \frac{1}{|Vref|^2} \int_0^k \frac{|f_m(\xi)|^2 \xi\, d\xi}{\sqrt{k^2 - \xi^2}} \qquad \left(\text{units: } \frac{Ns}{m}\right) \tag{6.5.9}$$

$$X_m = \omega M_m = \frac{\pi \omega^3 \varrho}{\in_m} \frac{1}{|Vref|^2} \int_k^\infty \frac{|f_m(\xi)|^2 \xi\, d\xi}{\sqrt{\xi^2 - k^2}}, \qquad \left(\text{units: } \frac{Ns}{m}\right) \tag{6.5.10}$$

Eq. 6.5.10 also serves to define the effective mass of the medium in the *m'th* Fourier component of surface displacement.

6.6. CALCULATION OF RADIATION IMPEDANCE FROM DIRECTIVITY OF RADIATED SOUND.

The analysis of acoustic power and impedance of a circular membrane in an infinite rigid baffle given by 6.5.1 through 6.5.10 can be modified to show how acoustic impedance can be obtained from a knowledge of the directivity of the radiated sound.

In Fig. 4.3.1 the direction of radiation $\vec{q}$ from an elementary area dS is specified by the wavenumber $k\ \hat{a}_q$ in which $\hat{a}_q$ is a unit vector which makes an angle θ with the x, y (or r, ϕ) plane. Thus the component of the wavenumber in the direction $\vec{s}$ is $k \cos\theta$. This is identified with ξ of 6.5.5:

$$\begin{aligned} Re\, W_m &= \frac{\pi \omega^3 \varrho}{\in_m} \int_{\frac{\pi}{2}}^{0} \frac{|f_m (k \cos\theta)|^2}{k \sin\theta}\ k \cos\theta\, (-k \sin\theta\, d\theta) \\ &= \frac{\pi \omega^3 k}{\in_m} \int_0^{\pi/2} |f_m (k \cos\theta)|^2 \cos\theta\, d\theta \end{aligned} \tag{6.6.1}$$

In 6.5.6, the quantity $\sqrt{\xi^2 - k^2}$ is always real and can grow indefinitely large. It is convenient then to let $\xi = k \cosh\theta$:

$$\begin{aligned} \Im_m W_m &= \frac{\pi \omega^3 \varrho}{\in_m} \int_0^{\infty} \frac{|f_m (\mathrm{f}_m (k \cosh\theta)|^2\, k \cosh\theta\, (k \sinh\theta d\theta)}{k \sinh\theta} \\ ,, &= \frac{\pi \omega^3 \varrho\, k}{\in_m} \int_0^{\infty} |f_m (k \cosh\theta)|^2 \cosh\theta d\theta \end{aligned} \tag{6.6.2}$$

It is useful to attempt to write 6.6.2 in terms of trigonometric instead of hyperbolic functions. Thus let $\theta = iu$, then $\cos\theta d\theta = i \cos u du$, and 6.6.2 becomes,

$$I_m W_m = \frac{\pi \omega^3 k \varrho}{\in_m} i \int_0^{-i\infty} |f_m (k \cos u)|^2 \cos u\, du \tag{6.6.3}$$

Since the integration in 6.6.1 is over the range $\theta = 0$ to $\pi/2$, one can translate u by a change of variable $u = \pi/2 - \zeta$ so that 6.6.3 begins integration over the variable ζ at $\pi/2$.

$$I_m W_m = \frac{\pi \omega^3 k \varrho\, i}{\in_m} \int_{\pi/2}^{\pi/2 + i\infty} |f_m (k \sin\zeta)|^2 \sin\zeta\, (-d\zeta) \tag{6.6.4}$$

Replacing $2\pi/\in_m$ by C.3.7b, it is seen that

$$I_m W_m = -\frac{1}{2} \omega^3 k \varrho\, i \int_0^{2\pi} \int_{\pi/2}^{\pi/2 + i\infty} |\cos m\phi\, f_m (k \cos\zeta)|^2 \sin\zeta d\zeta d\phi \tag{6.6.5}$$

Because the total power of the *m'th* Fourier component is,

$$W_m = Re\, W_m + i\ I_m W_m$$

One can combine 6.6.1 and 6.6.5,

$$W_m = \frac{1}{2}\,\omega^3 \varrho k \int_0^{2\pi} d\phi \int_0^{\pi/2 + i\infty} |K_m(\zeta, \phi)|^2 \sin\zeta d\zeta \tag{6.6.6}$$

where

$$|K_m(\zeta, \phi)|^2 = |\cos m\phi f_m(k\cos\zeta)|^2 \qquad \text{(units: } m^6\text{)} \tag{6.6.7}$$

The path of integration of variable ζ is shown in Fig. 6.6.1.

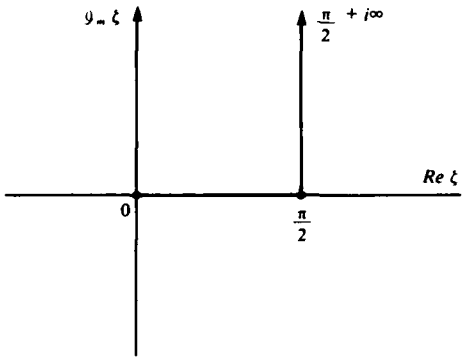

Fig. 6.6.1. Path of integration of ζ in 6.6.6

Now from the definition of the far field the velocity potential 4.3.6a has the asymptotic value for each Fourier component,

$$\psi_m(R, \zeta, \phi) \to -i\omega K_m(\zeta, \theta)\frac{e^{ikR}}{R} \tag{6.6.8}$$

in which R is the radial distance from the origin to the field point. The potential of an omni-directional source above the plane of the vibrating membrane is

$$\psi_0(R, 0, 0) \to -i\omega K_0(0, 0)\frac{e^{ikR}}{R} \tag{6.6.9}$$

From the theory of the monopole point source 6.2.1 it is seen that

$$K_0(0, 0) = \frac{Q_\omega}{4\pi(-i\omega)} \times 2 \tag{6.6.10}$$

in which the factor 2 is inserted because of radiation into half space, and $Q_\omega = V_{AV} S$, where V_{AV} is the peak amplitude averaged over the area S of the membrane.

The directivity of radiation D is defined then as the ratio,

$$D \equiv \frac{\sum_m \psi_m}{\psi_0} = \frac{\sum_{m=0}^{\infty} K_m(\zeta, \phi)}{K_0(0, 0)} \tag{6.6.11}$$

Now,

$$D \cdot D^* = |D|^2 = \frac{|\sum_{m=0}^{\infty} K_m(\zeta, \phi)|^2}{|K_0(00)|^2} \tag{6.6.12}$$

Because the partial potentials are orthogonal over the intervals $0 \leqslant \phi \leqslant 2\pi$, the cross products $K_m K_n$ generate no power in the integral 6.6.6. Thus,

$$|\sum_{m=0}^{\infty} K_m(\zeta, \phi)|^2 = \sum_{m=0}^{\infty} |K_m(\zeta, \phi)|^2 \tag{6.6.13}$$

The total *rms* power W radiated into half space is therefore the sum of the m partial powers. From 6.6.6, 6.6.10, 6.6.11 and 6.6.12 it is seen that,

$$\begin{aligned} W &= \frac{1}{2}\omega^3 \varrho k \int_0^{2\pi} d\phi \int_0^{\pi/2+i\infty} \frac{|Q_w|^2}{4\pi^2\omega^2} |D(\zeta, \phi)|^2 \sin\zeta d\zeta \\ &= \frac{1}{4\pi} k^2 \varrho c |V_{AV}|^2 S^2 \int_0^{2\pi} \frac{d\phi}{2\pi} \int_0^{\pi/2+i\infty} |D(\zeta, \phi)|^2 \sin\zeta d\zeta \end{aligned} \tag{6.6.14}$$

This is an important formula which states that the radiation from the membrane in an infinite rigid baffle can be calculated as the radiation from a monopole point source $W_{monopole}$ of *peak* source strength $Q_{\cdot} = V_{AV} S$ radiating into half-space multiplied by a directivity factor f_D:

$$\begin{aligned} W &= W_{monopole} \times f_D \\ W_{monopole} &= \frac{1}{4\pi} k^2 \varrho c |V_{AV}|^2 S^2 \\ f_D &= \frac{1}{2\pi} \int_0^{2\pi} d\phi \int_0^{\pi/2+i\infty} |D(\zeta, \phi)|^2 \sin\zeta d\zeta \end{aligned} \tag{6.6.15}$$

The radiation impedance of this membrane can be obtained directly from 6.3.1:

$$Z(\omega) = \frac{2 k^2 \varrho c \left|\frac{V_{AV}}{Vref}\right|^2 S^2 \int_0^{2\pi} \frac{d\phi}{2\pi} \int_0^{\pi/2+i\infty} |D(\zeta, \phi)|^2 \sin\zeta d\zeta}{4\pi} \tag{6.6.16}$$

in which Vref is the peak amplitude of acoustic complex particle velocity (having inphase and out-of-phase components) at the reference point.

Eq. 6.6.14 can be generalized for any type of acoustic radiator by referring the power to full space instead of half-space. Thus, in general, a radiator which generates a directivity pattern $D(\zeta, \phi)$ in the far field radiates a total *rms* power into *all* space given by,

$$W = \frac{k^2\rho c|V_{AV}|^2 S^2}{2 \cdot 2(4\pi)(2\pi)} \int_0^{2\pi} d\phi \int_0^{\pi+i\infty} |D(\zeta,\phi)|^2 \sin\zeta d\zeta \qquad (6.6.17a)$$

in which V_{AV} is the average over S of the *peak* amplitude of surface velocity. The first factor 2 in the denominator is inserted because the radiation resistance of the medium is halved when the infinite rigid baffle is removed, meaning that for fixed volume velocity the radiated power is halved. The second factor 2 is inserted because the radiation space has been doubled.

As a check on 6.6.17a let the radiation be a point source. Then $|D(\zeta,\phi)|^2 = 1$ and, for real angles ζ only,

$$W_{rms} = \frac{k^2\rho c|Q_\omega(1)|^{2}_{peak}}{2 \cdot 2 \cdot 4\pi \cdot 2\pi} 2\pi \cdot 2$$

$$W_{rms} = \frac{k^2\rho c|Q_\omega(1)|^{2}_{peak}}{8\pi} = \frac{k^2\rho c|Q_\omega(1)|^{2}_{rms}}{4\pi}$$

in which

$$|Q_\omega(1)|^2_{peak} = |V_{AV}\, S|^2_{peak}.$$

This result agrees with the classical theory of radiation from a monopole point source of source strength Q_ω (units: m^3/s).

In the far field the evanescent waves associated with complex values of ζ vanish. For a surface normal velocity v_ω the radiated power becomes

$$W_{rms} = \frac{k^2\rho c}{32\pi^2} \int_0^{2\pi} d\phi \int_0^{\pi} 1 f_\omega(\delta,\phi)|^2 \sin\delta d\theta \quad \left[\text{units: } \frac{Nm}{s}\right] \qquad 6.6.17b$$

$$f_\omega(\theta,\phi) = \int\int_{-\infty}^{\infty} v_\omega(r_0) e^{-i\mathbf{K}\cdot\mathbf{r}_0} d^2\mathbf{r}_0 \quad \left[\text{units: } \frac{m^3}{s}\right] \qquad 6.6.17c$$

in which $f_\omega(\theta,\phi)$ replaces $V_{AV}SD(\zeta,\phi)$. The far field intensity in a particular direction is

$$I = \frac{k^2\rho c}{32\pi^2 r^2} |f_\omega(\theta,\phi)|^2 \quad \left[\text{units: } \frac{Nm}{m^2 s}\right. \qquad 6.6.17d$$

In these equations v_ω is peak amplitude.

Two cases of 6.6.17 are treated below.

6.6a. CALCULATION OF REAL POWER RADIATED BY TWO IDENTICAL SPHERICAL SOURCES.

Let each spherical source have a volume velocity Q_ω (units: $m^3\ s^{-1}$). Then in 6.6.17a, $V_{AV}S = 2Q_\omega(1)$

$$A = \frac{k^2\rho c 4|Q_{\omega}(1)|^2}{32\pi^2} = \frac{k^2\rho c|Q_{\omega}(1)|^2}{8\pi^2}$$

in which $|Q_{\omega}(1)|$ is a peak value. Now the *rms* intensity $I(2)$ radiated by two coincident point sources is,

$$I(2) = \frac{k^2\rho c|Q_{\omega}(2)|^2_{peak}}{32\pi^2 r^2} = \frac{k^2\rho c|Q_{\omega}(1)|^2_{peak}}{8\pi^2 r^2}$$

Thus,

$$A = \frac{k^2\rho c}{8\pi^2} \times \frac{8\pi^2 r^2}{k^2\rho c} I_{rms}(2) = r^2 I_{rms}(2)$$

Because the field is rotationally symmetric $D(\xi, \phi) = D(\xi)$. Integration over ϕ yields 2π. The real power of two sources is then,

$$Re\, W(2) = r^2\, I_{rms}(2) \times 2\pi \times \int_0^{\pi} |D(\xi)|^2 \sin\xi d\xi$$

In terms of the intensity $I(1)$ of one source, $I(2) = 4\,I(1)$. Extending the integration in ξ over all space, one has the real power of two sources,

$$Re\, W(2) = 8\pi r^2 I_{rms}(1) \int_0^{\pi} |D(\xi)|^2 \sin\xi d\xi \tag{6.6.18}$$

Now the directivity $D(\xi)$ of two equal sources is equal to the directivity of one source $D_1(\xi)$ multiplied by the directivity of two point sources $D_2(\xi)$. For a rotationally symmetric point source, $D_1(\xi) = P_n(\cos\xi)$, in which P_n is an *n'th* order Legendre polynomial, and $D_2(\xi) = \cos(a\cos\xi)$, $a = kd/2$, where d is the separation distance between the sources. Thus from 6.6.18 the real power radiated by two identical spherical sources is:

$$Re\, W(2) = 8\pi r^2 I(1) \int_0^{\pi} P_n^2(\cos\xi)\cos^2(a\cos\xi)\sin\xi d\xi \tag{6.6.19}$$

Assume first that the sources are coincident ($a = 0$). Then,

$$\int_0^{\pi} P_n^2(\cos\xi)\sin\xi d\xi = \frac{2}{2n+1}$$

and so,

$$Re\, W(2) = \frac{4\,[4\pi r^2\, I(1)]}{2n+1},\ n = 0, 1, 2 \ldots \tag{6.6.20}$$

For the case $n = 0$, corresponding to a breathing sphere, the power of two sources given by 6.6.20 is four times the power of one source. For $n \neq 0$, the power of one source is

$$Re\, W(1) = \frac{4\pi r^2 I(1)}{2n+1} \tag{6.6.21}$$

When $d \neq 0$, the ratio of the real power of one source in a group of two sources is obtained from 6.6.19 and 6.6.21:

$$\frac{Re\ W(2)}{2\ Re\ W(1)} = \frac{4\pi r^2 I(1) \int_0^{\pi} P_n^2(\cos\zeta) \cos^2(a\cos\zeta) \sin\zeta d\zeta}{\left(\frac{4\pi r^2 I(1)}{2n+1}\right)} \tag{6.6.22}$$

Since

$$\cos^2(a\cos\zeta) = \frac{1}{2}(1 + \cos 2a\cos\zeta)$$

it is seen that 6.6.22 becomes,

$$\frac{Re\ W(2)}{2\ Re\ W(1)} = (2n+1)\left\{\frac{1}{2}\cdot\frac{2}{2n+1} + \frac{1}{2}\int_{-1}^{+1} P_n^2(y)\cos 2ay\, dy\right\} \tag{6.6.23}$$

Two values of n are frequently important. They are,

a. $n = 0$. Then, $P_0(y) = 1$, and

$$\frac{Re\ W(2)}{2\ Re\ W(1)} = 1 + \frac{\sin kd}{kd} \tag{6.6.24}$$

b. $n = 1$. Then $P_1(y) = y$, and

$$\frac{Re\ W(2)}{2\ Re\ W(1)} = 1 + 3\frac{\sin kd}{kd} + \frac{6\cos kd}{(kd)^2} - \frac{6\sin kd}{(kd)^3} \tag{6.6.25}$$

Since the ratio of real powers is the same as the ratio of radiation resistances 6.6.24 and 6.6.25 show how the radiation resistance of a pair of identical spherical radiators vary with their separation distance d. The terms in d can then be interpreted as expressions of *mutual* resistance.

6.6b. CALCULATION OF THE ACOUSTIC POWER RADIATED BY A PAIR OF UNIFORM-VELOCITY DISKS IN AN INFINITE RIGID BAFFLE.

Two disks, each radius a, are symmetrically placed relative to the origin in the xy plane and separated by a distance d. The total *rms* acoustic power generated by a uniform velocity V_0 over the surface of the disks and radiated into half-space is given by 6.6.14, in which,

$$V_{AV} S = 2(\pi a^2) V_0$$

The directivity function of *both* disks combined is known to be the product,

$$D(\zeta, \phi) = \frac{2J_1(ka\sin\zeta)}{ka\sin\zeta} \cos\left(\frac{\pi d}{\lambda}\sin\zeta\sin\varphi\right)$$

[2]. Here, the field point in spherical coordinates is $\vec{r} = (r, \zeta, \phi)$ where ζ is the polar angle measured from the z-axis, ϕ is the azemuth angle measured from the x-axis and r is the radial distance from the origin. Using the trigonometric relation $\cos^2 \alpha = (1 + \cos 2\alpha)/2$ one obtains from 6.6.14 the power $W(2)$ of two sources,

$$W(2) = \frac{(ka)^2 \varrho c (\pi a^2)}{2\pi} V_0^2 \int_0^{2\pi} d\phi \int_0^{\pi/2+i\infty} \frac{4 J_1^2 (ka \sin \zeta)}{(ka \sin \zeta)^2} \left[\frac{1 + \cos (kd \sin \zeta \sin \phi)}{2}\right] \times \sin \zeta d\zeta \tag{6.6.26}$$

in which V_0 is a peak velocity amplitude. The radiation impedance 6.3.1 of one disk in the pair is

$$Z(1) = \frac{Z(2)}{2} = \frac{1}{2} \frac{2W}{|Vref|^2} \tag{6.6.27}$$

Because the reference velocity $Vref$ is assumed to be (here) the same as the uniform velocity V_0, one can reduce 6.6.27 to a sum of two terms,

$$Z(1) = Z_{11}(ka) + Z_{12}(ka, kd)$$

in which Z_{11} is the self radiation impedance (units: Nsm^{-1}) and Z_{12} is the mutual radiation impedance. The form of Z_{11} is,

$$Z_{11}(ka) = R_{11} - iX_{11} = \frac{(ka)^2 \varrho c (\pi a^2)}{\pi} \int_0^{2\pi} d\phi \int_0^{\pi/2+i\infty} \frac{J_1^2 (ka \sin \zeta)}{(ka \sin \zeta)^2} \sin \zeta d\zeta \tag{6.6.28}$$

The integrals have closed forms:

$$R_{11} = \pi a^2 \varrho c \left[1 - \frac{J_1 (2\,ka)}{ka}\right] = \pi a^2 \varrho c \left[2 \int_0^{\pi/2} \frac{J_1^2 (ka \sin \zeta)}{(ka \sin \zeta)^2} \sin \zeta d\zeta\right] \tag{6.6.29}$$

$$X_{11} = \pi a^2 \varrho c \frac{\mathbf{H}_1 (2ka)}{ka} = \pi a^2 \varrho c \left[2 \int_{\pi/2+i0}^{\pi/2+i\infty} \frac{J_1^2 (ka \sin \zeta)}{(ka \sin \zeta)^2} \sin \zeta d\zeta\right] \tag{6.6.30}$$

$\mathbf{H}_1 (2\,ka)$ is the Struve function, a tabulated quantity [3].

Eq. 6.6.26 also provides a means of calculating the mutual impedance.

$$Z_{12} = \pi a^2 \varrho c \frac{(ka)^2}{\pi} \int_0^{2\pi} d\phi \int_0^{\pi/2+i\infty} \frac{J_1^2 (ka \sin \zeta)}{(ka \sin \zeta)^2} \cos (kd \sin \zeta \sin \phi) \sin \zeta d\zeta \tag{6.6.31}$$

The integral here also has a closed form solution.

$$Z_{12} = \pi\, a^2\, \varrho c\, 2 \sum_{m=0}^{\infty} \sum_{n=0}^{\infty} \frac{\Gamma (m + n + 1/2)}{\sqrt{\pi}\, m!\, n!} \left(\frac{a}{d}\right)^{m+n} J_{m+1} (ka)\, J_{n+1} (ka)\, h_{m+n}^{(1)} (kd) \tag{6.6.32}$$

in which $h_{m+n}^{(1)} (kd)$ is the spherical Hankel function for out-going waves and Γ is the gamma function.

6.7. RADIATION FIELD, POWER AND IMPEDANCE OF A COMPOSITE SOURCE ON A SEPARABLE SURFACE HARMONICALLY EXCITED.

An $M \times N$ array of extended sources is located on a surface $S(\xi, \eta)$ whose normal is ζ. Assume (1) that the radiation field ψ from the elements in the steady state is governed by the Helmholtz equation (2) that the Helmholtz equation in the velocity potential ψ is separable in coordinates ξ, η, ζ (3) that this condition of separability generates a complete set of characteristic functions which are orthogonal over the surface of the baffle.

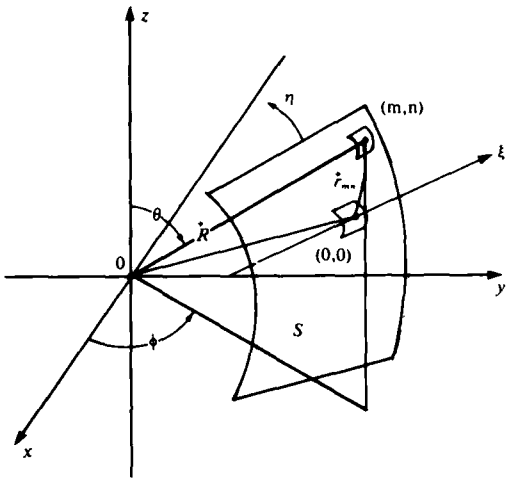

Fig. 6.7.1. Geometric parameters of composite sources in a baffle.

Fig. 6.7.1 shows a baffle surface $S(\xi, \eta)$ in a rectangular x, y, z coordinate system. Two elements of the $M \times N$ array are shown: one element labelled (00) is at the center of symmetry of the array. Its center is the origin of the ξ, η coordinates on the surface S. A second element labelled (mn) is the $mn'th$ element in the array. Its center is at distance $\vec{r}_{mn}$ from the origin in the (00) element. The spherical coordinates of any point in the baffle are R, θ, ϕ.

The construction of the radiation field is based on the three assumptions noted above. Let the velocity distribution of the $mn'th$ element on the surface S have the fixed form $V_{mn}(\xi, \eta | \omega)$. By means of assumption (3) it can be expanded in a set of orthogonal functions $X_\alpha(\xi)$, $X_\beta(\eta)$:

$$V_{mn}(\xi, \eta | \omega) = e^{-i\omega t} \sum_{\alpha, \beta} V_\alpha(m) X_\alpha(\xi) V_\beta(n) X_\beta(\eta) \tag{6.7.1}$$

$$V_\alpha(m) = \frac{\int_C V_{mn}(\xi, \eta) X_\alpha^*(\xi) \, d(A_\xi \xi)}{N_\alpha}; \quad V_\beta(n) = \frac{\int_{C'} V_{mn}(\xi, \eta) X_\beta^*(\eta) \, d(A_\eta \eta)}{N_\beta} \tag{6.7.2}$$

Here, α, β are characteristic numbers. They are discrete when the range of integration C (or C') is finite; and continuous when C (or C') is infinite. C (or C') itself is the interval of orthogonality, and A_ξ, A_η are the scale factors of the curvilinear coordinate ξ, η respectively. N_α, N_β are the normalization constants,

$$N\alpha = \int [X_\alpha(\xi)]^2 \, d(A_\xi \xi); \; N_\beta = \int [X_\beta(\eta)]^2 \, d(A_\eta \eta) \tag{6.7.3}$$

Because of coupling to the fluid thus velocity V_{mn} generates a potential field $\phi_{mn}(\xi, \eta, \zeta)$. By assumption (2) noted above, ϕ_{mn} can also be expanded in the same set of orthogonal functions,

$$\psi_{mn}(\xi, \eta, \zeta) = e^{-i\omega t} \sum_{\alpha, \beta} \Psi_{\alpha\beta}^{(mn)} R_{\alpha\beta}(\zeta) X_\alpha(\xi) X_\beta(\eta) \tag{6.7.4}$$

in which $R_{\alpha\beta}(\zeta)$ is the radial separation function and $\psi_{\alpha\beta}^{(mn)}$ is an expansion constant. At the surface $\zeta = \zeta_0$ the boundary condition is the continuity of the normal component of surface velocity;

$$V_{mn}(\xi, \eta) = \frac{\partial \psi}{\partial n}(\xi, \eta, \zeta)\Big|_{\zeta = \zeta_0} \tag{6.7.5}$$

Customarily, a minus sign should appear on the right hand side of 6.7.5 (see discussion in Sect. 1.11). However, the positive normal is defined here as pointing *away* from the medium (that is, into the surface S). Substituting 6.7.4 into 6.7.5, and comparing with 6.7.1 shows that,

$$\psi_{\alpha\beta}^{(mn)} = \frac{V_\alpha(m)\ V_\beta(n)}{\left.\dfrac{d\,R_{\alpha\beta}(\zeta)}{d\,(A_\zeta\,\zeta)}\right|_{\zeta=\zeta_0}} \tag{6.7.6}$$

Thus the velocity potential everywhere generated by the *mn'th* element is,

$$\psi_{mn}(\xi,\eta,\zeta) = e^{-i\omega t}\sum_{\alpha,\beta}\frac{V_\alpha(m)\ V_\beta(n)}{\left.\dfrac{d\,R_{\alpha\beta}(\zeta)}{d\,(A_\zeta\,\zeta)}\right|_{\zeta=\zeta_0}} R_{\alpha\beta}(\zeta)\,X_\alpha(\xi)\,X_\beta(\eta) \tag{6.7.7}$$

By linear superposition, the total field is the simple sum of all elementary fields,

$$\psi(\xi,\eta,\zeta) = e^{-i\omega t}\sum_{m=1}^{m}\ \sum_{n=1}^{n}\ \psi_{mn}(\xi,\eta,\zeta) \tag{6.7.8}$$

The acoustic power W_{mn} (units: Nms^{-1}) radiated by the *mn'th* element will be determined by integrating the product of the normal component of velocity $V_{mn}(\xi, y)$ and the pressure $p(\xi, \eta)$ due to *all* the elements of the $M \times N$ array including itself over its surface. Here, V_{mn} is arbitrarily fixed, but, in general, it must be determined by solving the differential equations of motion of the vibrating surface subject to internal driving forces and external reaction of the medium. Thus, the time-averaged sinusoidal power radiated is:

$$W_{mn} = \frac{1}{2}\int\int dS_{mn}(\xi,\eta)\,p(\xi,\eta)\,V_{mn}^{*}(\xi,\eta) \tag{6.7.9}$$

The factor ½ appears here bcause p and V_{mn} are peak magnitudes. From W_{mn} one may obtain the mechanical radiation impedance $Z_{mn}(\omega)$. This is defined by 6.3.1 in terms of a reference velocity *Vref*, 6.3.4:

$$Z_{mn}(\omega) = \frac{2\,W_{mn}}{|Vref|^2} \qquad \text{(units: } Ns\,m^{-1}\text{)} \tag{6.7.10}$$

$$'' = \frac{1}{|Vref|^2}\int\int dS_{mn}(\xi,\eta)\,p(\xi,\eta)\,V_{mn}^{*}(\xi,\eta) \tag{6.7.11}$$

Substitution of 6.7.7 and 6.7.8 into 6.7.11 leads to the form,

$$Z_{mn}(\omega) = \frac{1}{|Vref|^2} \int\int dS_{mn}(\xi,\eta) \sum_{j=1}^{J} \sum_{k=1}^{K} (-i\omega\varrho) \sum_{\alpha} \sum_{\beta} \frac{V_\alpha(j)\, V_\beta(k)}{\left.\frac{dR_{\alpha\beta}}{d(A_\zeta \zeta)}\right|_{\zeta=\zeta}} R_{\alpha\beta}(\zeta_\alpha) X_\alpha(\xi) X_\beta(\eta) \times V^*_{mn}(\xi,\eta) \tag{6.7.12}$$

For purposes of clarity the radiating elements are relabelled (jk) to distinguish them from the particular element $j = m$, $k = n$ on which the impedance is being calculated. In this context, $J = M$, $K = N$. When the double sum over j, k is reduced to one term $j = m$, $k = n$, one obtains the *self mechanical impedance* of the mn'th element. When this term in the sum is excluded, one obtains the *mutual mechanical impedance* of the *mn'th* element.

The limits of integration in 6.7.12 depends on the geometrical parameters of the elements in the array. Several cases are listed here:

Case I. The radiating elements are (curvilinear) rectangles ℓ units long, w units wide in an infinite rectangular lattice, their centers spaced uniformly at d units apart. Then,

$$\int\int dS_{mn}(\xi,\eta) \to \int_{md-\frac{\ell}{2}}^{md+\ell/2} d\xi \int_{nd-\frac{w}{2}}^{nd+w/2} d\eta \tag{6.7.13}$$

Case II. The radiating elements are circular, radius a, their centers spaced uniformly d units apart in an infinite rectangular lattice. Then,

$$\int\int dS_{mn}(\xi,\eta) \to \int_0^{2\pi} d\phi \int_{r_{mn}}^{r_{mn}+a} r dr \tag{6.7.14}$$

$$r_{mn} = d\sqrt{m^2+n^2}$$

Case III. The radiating elements are periodic in one dimension (that is, a matrix consisting of one row or one column). Then one sets m (or n) to zero in 6.7.13, or 6.7.14. A special case is that of radiating rings on a cylindrical baffle of radius a:

$$\int\int dS_{on}(\xi,\eta) \to \int_{-\pi}^{\pi} a d\phi \int_{nd-\frac{w}{2}}^{nd+w/2} d\eta \tag{6.7.15}$$

Eq. 6.7.12 is the mechanical impedance of one element in the array. Often it is necessary to calculate the total impedance of the array. This is a simple sum,

$$Z(\omega) = \sum_{m=1}^{M} \sum_{n=1}^{N} Z_{mn}(\omega) \tag{6.7.16}$$

6.7a. RADIATION FIELD, ACOUSTIC POWER AND MECHANICAL IMPEDANCE OF AN ARRAY OF VIBRATING RINGS ON AN INFINITE RIGID CYLINDRICAL BAFFLE. [4]

An array of $2N + 1$ ring radiators, each height h, radius a, is arranged periodically with period d on an infinite rigid cylinder. Fig. 6.7.2 shows the geometric parameter of this array. Let the radial velocity of the $n'th$ radiating ring be fixed,

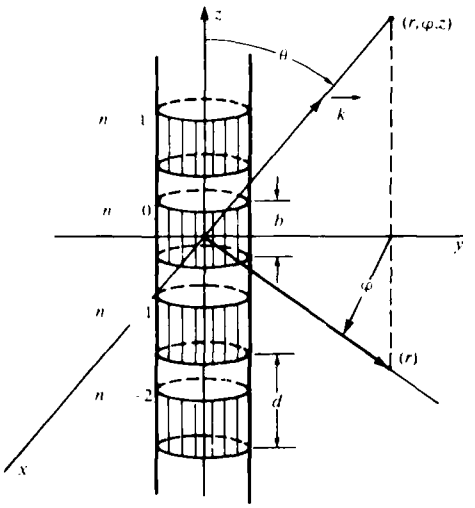

Fig. 6.7.2. Geometrical parameter of an array of $2N + 1$ rings.

$$V_n(a, \phi, z) = v_n f(\phi) F(z), \quad \begin{cases} |z - nd| < \frac{h}{2} \\ \text{otherwise} \end{cases}$$
$$'' \qquad = 0 \qquad (6.7.17)$$

Here v_n is chosen to include a phase angle to account for an arbitrarily selected steering in direction of the polar angle θ_0,

$$v_n = V \exp(i\vec{k}_0 \cdot \vec{r}_n)$$
$$'' = V \exp(ind\gamma_0)$$
$$\gamma_0 = k \cos\theta_0 ; k = \frac{\omega}{c} \qquad (6.7.18)$$

The array shown in Fig. 6.7.2 is symmetrical relative to the xy plane.

To find the radiated field, acoustic power and mechanical impedance of this array one employs the developments in 6.7.1 through 6.7.16. First, the characteristic functions X_α, X_β in cylindrical coordinates r, ϕ, z which satisfy Helmholtz's equation in the steady state are of the type,

$$\begin{matrix} \cos m\phi \ exp\ i\gamma z \\ \sin m\phi \end{matrix} \qquad (6.7.19)$$

Since the coordinate ϕ is periodic in 2π the characteristic number m is an integer, $m = 0, 1, 2, \ldots \infty$. However, for a single ring on an infinite cylindrical baffle the wavenumber γ is continuous. Thus, setting $\alpha = m$, $\beta = \gamma$ in 6.7.1, and choosing $\cos m\phi \ exp\ i\gamma z$ of the two choices in 6.7.19, one has,

$$V_m = \frac{\int_{\pi}^{\pi} f(\phi) \cos m\phi d\phi}{\pi \in_m} \qquad \text{(units: none)} \qquad (6.7.20)$$

$$V_\gamma = \int_{-\infty}^{\infty} F(z) \exp(-i\gamma z)\, dz \qquad \text{(units: } m\text{)} \qquad (6.7.21)$$

$$\in_0 = 2; \quad \in_m = 1, \quad m \neq 0.$$

The minus sign in $exp\,(-i\gamma z)$ is the conjugate function required by 6.7.2. The convention also is adopted that the direct Fourier transform does not employ a $\frac{1}{2}\pi$ factor. Now $F(z)$ is periodic. Thus 6.7.21 is the transform of a periodic function,

$$V_\gamma = \int_{-\infty}^{\infty} F(z)\, exp\,(-i\gamma z)\, dz = \sum_{n=-N}^{N} exp\,(-ind\gamma)\, \mathcal{F}(\gamma) \tag{6.7.22}$$

and

$$\mathcal{F}(\gamma) = \int_{-h/2}^{h/2} F(z)\, exp\,(-i\gamma z)\, dz \qquad \text{(units: } m\text{)} \tag{6.7.23}$$

Second, for cylindrical waves the radial function $R_{\alpha\beta}$ in 6.7.4 is a Hankel function of the first kind (that is, outgoing waves for time $exp\ -i\omega t$),

$$\begin{aligned} R_{m\gamma} &= H_m^{(1)}\left(r\sqrt{k^2-\gamma^2}\right) \\ \frac{dR_{m\gamma}}{dn} &= \sqrt{k^2-\gamma^2}\ \frac{d\,H_m^{(1)}(x)}{dx} = \sqrt{k^2-\gamma^2}\ H_m^{(1)\prime} \end{aligned} \tag{6.7.24}$$

Substitution of 6.7.20 through 6.7.24 into 6.7.7 and 6.7.8 leads to a formula for the field of the velocity potential at any point on or outside of the array due to the *n'th* ring:

$$\psi_n(r,\phi,z) = V \sum_{m=0}^{\infty} V_m \cos m\phi \int_{-\infty}^{\infty} e^{ind(\gamma-\gamma_m)} \frac{\mathcal{F}(\gamma)\, H_m^{(1)}\left(r\sqrt{k^2-\gamma^2}\right) e^{i\gamma z}}{\sqrt{k^2-\gamma^2}\, H_m^{(1)\prime}\left(a\sqrt{k^2-\gamma^2}\right)} \frac{d\gamma}{2\pi} \tag{6.7.25}$$

The factor $1/2\pi$ is inserted because of the previously noted convention on Fourier transforms. Now the acoustic power radiated by the n' ring due to the velocity potential contributed by the *n'th* ring is equal to the integration of the product of the acoustic $p_n(r, \rho, z)$ contributed by the *n'th* ring and the velocity of the n' ring over the area of the n' ring: a

$$\begin{aligned} W(n'|n) = \frac{-i\omega\rho v}{2} \int_{-\pi}^{\pi} a\,d\phi \int_{nd-h/2}^{nd+h/2} dz \sum_{m=0}^{\infty} V_m \cos m\phi \int_{-\infty}^{\infty} e^{-ind(\gamma-\gamma_m)}\, \mathcal{F}(\gamma)\, e^{i\gamma z} \\ \times \frac{H_m^{(1)}\left(r\sqrt{k^2-\gamma^2}\right)}{\sqrt{k^2-\gamma^2}\, H_m^{(1)\prime}\left(a\sqrt{k^2-\gamma^2}\right)} \frac{d\gamma}{2\pi} \times \left[V^* e^{-ind\gamma_m} f^*(\phi)\, F^*(z)\right] \end{aligned} \tag{6.7.26}$$

Because,

$$\begin{aligned} \int_{nd-h/2}^{nd+h/2} dz\, e^{i\gamma z} F^*(z) &= e^{ind\gamma}\, \mathcal{F}^*(\gamma) \\ \int_{-\pi}^{\pi} d\phi \cos m\phi f(\phi) &= V_m^* \pi \in_m \end{aligned} \tag{6.7.27}$$

and adding the contributions of all n rings, it is seen that the power radiated by the n' ring is,

$$W_n' = -\frac{i\omega\varrho\,|V|^2}{4}\,a\sum_{m=0}^{\infty}\epsilon_m|V_m|^2\int_{-\infty}^{\infty}|\mathfrak{F}(\gamma)|^2\frac{H_m^{(1)}(r\sqrt{k^2-\gamma^2})}{\sqrt{k^2-\gamma^2}\,H_m^{(1)'}(a\sqrt{k^2-\gamma^2})}$$
$$\times\sum_{n=-N}^{N}exp\,[-i(n-n')(\gamma-\gamma_0)\,d]\,d\gamma \qquad (6.7.28)$$

Here, the additional factor of 2 appearing in 6.7.26 and 6.7.28 is inserted because V is taken to be a peak value.

The mechanical radiation impedance is obtained from 6.3.1 in conjunction with 6.7.28. Assuming $|V|^2 = |Vref|^2$ one finds the *self-impedance* (where $n = n'$) to be,

$$(Z_n')_{self} = \frac{-i\omega\varrho a}{2}\sum_{m=0}^{\infty}\epsilon_m|V_m|^2\int_{-\infty}^{\infty}|\mathfrak{F}(\gamma)|^2\frac{H_m^{(1)}(a\sqrt{k^2-\gamma^2})}{\sqrt{k^2-\gamma^2}\,H_m^{(1)'}(a\sqrt{k^2-\gamma^2})}\,d\gamma \qquad (6.7.29)$$

The mutual inpedance is twice 6.7.28 divided by $|V|^2$ for the condition $n \neq n'$.

It is often desired to know the total mechanical radiation impedance of $2N+1$ rings. This is found by summing W_n' over all n'. Because it is easily verified that,

$$\sum_{n=-N}^{N}\sum_{n=-N}^{N}e^{-i(n-n')(\gamma-\gamma_0)d} = \Big|\sum_{n=-N}^{N}e^{-in(\gamma-\gamma_0)d}\Big|^2$$

the total impedance reduces to,

$$Z_{TOT} = \frac{-i\omega}{2}\,a\sum_{m=0}^{\infty}\epsilon_m|V_m|^2\int_{-\infty}^{\infty}|\mathfrak{F}(\gamma)|^2\frac{H_m^{(1)}(a\sqrt{k^2-\gamma^2})}{\sqrt{k^2-\gamma^2}\,H_m^{(1)'}(a\sqrt{k^2-\gamma^2})}$$
$$\times\Big|\sum_{n=-N}^{N}e^{in(\gamma-\gamma_0)d}\Big|^2 \qquad (6.7.30)$$

When the number of rings becomes infinite a great simplification occurs because then a specific choice of n' is immaterial one can set $n' = 0$. Then, in 6.7.28 it is required to find the sum,

$$T = \sum_{n=-\infty}^{\infty}e^{-2\pi ins},\quad s = \frac{(\gamma-\gamma_0)\,d}{2\pi} \qquad (6.7.31)$$

This sum may be found by use of Poisson's Sum Formula. First, the Fourier Transform of each term in 6.7.31 is determined. It is equivalent to taking the transform of unity:

$$\mathfrak{F}\{exp(-2\pi ins)\cdot 1\} = \delta(s-n) = \delta\left[\frac{(\gamma-\gamma_0)\,d}{2\pi} - n\right]$$

$$,, \qquad = \delta\left[\frac{d}{2\pi}\left(\gamma-\gamma_0-\frac{2\pi n}{d}\right)\right]$$

$$,, \qquad = \frac{2\pi}{d}\,\delta\left[\gamma-\gamma_0-\frac{2\pi n}{d}\right]$$

Next, in accordance with the Sum Formula, the sum of all terms 6.7.31 in real space is equal to the sum of all terms in Fourier transform space,

$$\sum_{n=-\infty}^{\infty} e^{-in(\gamma-\gamma_0)d} = \frac{2\pi}{d}\sum_{n=-\infty}^{\infty}\delta(\gamma-\gamma_n) \qquad (6.7.32)$$

$$\gamma_n = \gamma_0 + \frac{2\pi n}{d}$$

The acoustic power radiated by the *n'th* element is then found by substituting 6.7.32 into 6.7.28 under the condition $n' = 0$:

$$W_n = \frac{-i\omega\varrho\,|V|^2\,a}{4}\sum_{m=0}^{\infty}\epsilon_m|V_m|^2\left(\frac{2\pi}{d}\right)\sum_{n=-\infty}^{\infty}|\mathfrak{F}(\gamma_n)|^2\frac{H_m^{(1)}(a\beta_n)}{\beta_n H_m^{(1)\prime}(a\beta_n)} \qquad (6.7.33)$$

$$\beta_n = \sqrt{k^2-\gamma_n^2}\;;\;\gamma_n = \gamma_0 + \frac{2\pi n}{d}$$

This formula enables us to apply 6.3.1 to obtain the mechanical radiation impedance of the *n'th* element in an infinite array of ring elements. Often, this impedance is normalized with respect to $\varrho c\,A$, where $A = 2\pi ah$. It is then useful to define a normalized impedance $\mathfrak{z}_\infty$ such that,

$$(Z_n)_\infty = [\varrho c\,2\pi ah]\,\mathfrak{z}_\infty$$

where,

$$\mathfrak{z}_\infty \equiv \frac{ka}{2}\,\frac{1}{dh}\sum_{m=0}^{\infty}\epsilon_m|V_m|^2\sum_{n=-\infty}^{\infty}|\mathfrak{F}(\gamma_n)|^2\frac{[-i\,H_m^{(1)}(a\beta_n)]}{a\beta_n H_m^{(1)\prime}(a\beta_n)} \qquad (6.7.34)$$

When the number N of rings in an array is no longer infinite, but large enough, one can approximate the total radiation impedance of the composite as if the array were infinite:

$$Z_{TOT} \approx N(Z_n)_\infty \qquad (6.7.35)$$

6.7b. RADIATION FIELD, ACOUSTIC POWER AND MECHANICAL RADIATION IMPEDANCE OF A PLANE PERIODIC ARRAY OF RECTANGULAR RADIATORS. [5]

Let an indefinite number of identical radiating elements be arranged with centers at the points of a rectangular lattice in a infinite rigid baffle, and let them all be identically oriented in space at angle μ. Fig. 6.7.3 shows the location of the centers of the lattice. A center (mn) is located ma units in the x direction and nb units in the y direction. Because the lattice is skewed the center (1,2) is shifted 2ℓ units to the right, and occupies the center $(1', 2')$. The distance ℓ by definition is given by the relation:

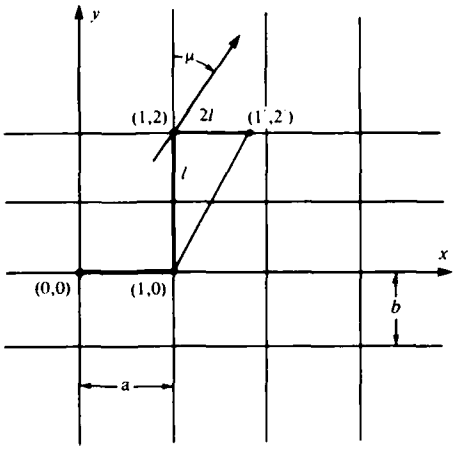

Fig. 6.7.3. Location of array centers in a skewed lattice.

$$\tan\mu = \frac{n\ell}{nb} = \frac{\ell}{b} \tag{6.7.36}$$

Thus the x component of a skewed center (m, n) is,

$$ma + n\ell$$

Two elementary areas, one in element (m, n) and the other in element (0,0) are located by distances R_x, R_y in the non-skewed lattice of Fig. 6.7.4. An arbitrary point in the $m, n'th$ element is written (x'_m, y'_n).

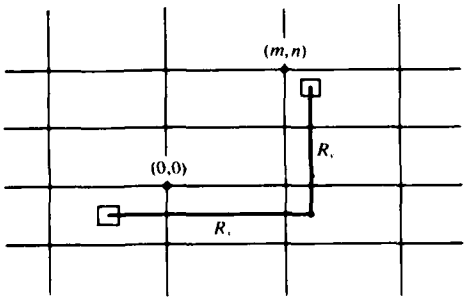

Fig. 6.7.4. Location of elementary areas in a non-skewed lattice.

Assume each radiator is given a fixed distribution of normal surface velocity and is steered in angle γ. Thus, on surface m, n:

$$V_{mn} = V\, w(x'_m, y'_n) \exp(-i\gamma_m) \tag{6.7.37}$$

Here V is a peak reference velocity (units: ms^{-1}) w is a dimensionless distribution, and γ_{mn} is the phase shading parameter. The velocity potential anywhere in the half-space, on, or above, the baffle, radiated by the $m, n'th$ radiator is given by Rayleigh's formula 1.8.18,

$$\psi_{mn}(x, y, z) = \frac{1}{2\pi} V \exp(-i\gamma_{mn}) \int\int w(x'_m, y'_n) \frac{e^{ik \cdot R}}{R} dS(x'_m, y'_n) \tag{6.7.38}$$

in which,

$$\vec{R} = R[\hat{i}\sin\theta\cos\phi + \hat{j}\sin\theta\sin\phi + \hat{k}\cos\theta] = \hat{i}R_x + \hat{j}R_y + \hat{k}R_z$$

$$\vec{k} = k[\hat{i}\sin\Theta\cos\Phi + \hat{j}\sin\Theta\sin\Phi + \hat{k}\cos\Theta]$$

$$R = [(x-x_m')^2 + (y-y_n')^2 + z^2]^{1/2} \tag{6.7.39}$$

In this formula the vector $\vec{R}$ originates in the elementary area of the *mn'th* radiator and points in the direction of the field point (x, y, z). To calculate the radiated field, acoustic power and impedance of one elementary radiator we choose the (0,0) radiator, and locate the field point at arbitrary (x_m, y_n, z). A first step in the analyses is to examine $exp\,(ikR)/R$. A plane wave expansion in spherical coordinates is given by Wegl's formula, 4.4.1. In it we choose $z = z_0 = 0$, so that,

$$\left.\frac{exp\,(ikR)}{R}\right|_{z=z_0=0} = \frac{ik}{2\pi}\int_0^{\pi/2-i\infty} d\theta \int_0^{2\pi} d\phi\, exp\,i\,(k\,R_x\sin\theta\cos\phi + kR_y\sin\theta\sin\phi) \times \sin\theta d\theta \tag{6.7.40}$$

Here, as before, the plane waves in the range $0 \leqslant \theta \leqslant \pi/2$ represent progressive (outward traveling) waves, while the waves in the range $0 \leqslant i\theta \leqslant -\infty$ represent evanescent (or inhomogeneous) waves. The distances R_x, R_y are calculated according to the conventions of Figs. 6.7.3 and 6.7.4,

$$R_x = ma + n\ell + x_m' - x_0'$$
$$R_y = nb + y_m' - y_0' \tag{6.7.41}$$

The steering parameter γ_{mn} can also be written in spherical coordinates θ_0, ϕ_0, of the steered direction:

$$\gamma_{mn} = k\,(ma + n\ell)\sin\theta_0\cos\phi_0 + k\,(nb)\sin\theta_0\sin\phi_0 \tag{6.7.42}$$

However, from Fig. 6.7.3,

$$\ell\sin\theta_0\cos\phi_0 + b\sin\theta_0\sin\phi_0 = \sqrt{\ell^2 + b^2}\sin(\phi_0 + \mu)$$
$$tan\,\mu = \frac{\ell}{b} \tag{6.7.43}$$

Hence,

$$exp\,(-i\gamma_{mn}) = exp\,(-ik\,m\,a\sin\theta_0\cos\phi_0)\,exp\,[-i\sqrt{\ell^2 + b^2}\sin\theta_0\sin(\phi_0 + \mu)] \tag{6.7.44}$$

Returning to 6.7.41 one notes that R_x contains $ma + n\ell$, and R_y contains nb, both of which are independent of integration over the primed coordinates in 6.7.38. Because m, n can be negative as well as positive, the phase factors in 6.7.38 that can be taken out of the integral sign can be written for each mn in the convenient form:

$$\varphi = e^{2\pi ims}\, e^{2\pi int} \tag{6.7.45}$$

where,

$$s = \frac{1}{2\pi} k\, a\, (\sin\theta \cos\phi - \sin\theta_0 \cos\phi_0) \tag{6.7.46}$$

$$t = \frac{1}{2\pi} k \sqrt{\ell^2 + b^2}\, [\sin\theta \sin(\phi + \mu) - \sin\theta_0 \sin(\phi_0 + \mu)] \tag{6.7.47}$$

The velocity potential ψ anywhere due to *all* the radiators in the array is obtained by summing 6.7.38 over all m, n. Because V_{mn} is the same for each radiator, only one integration is needed over one radiator. The additive effect of all the other radiators is found from the sum,

$$\Phi = \sum_{m=-\infty}^{\infty} e^{2\pi ims} \sum_{n=-\infty}^{\infty} e^{2\pi int} \tag{6.7.48}$$

which is outside the integral sign. A similar situation was found in the calculation of the radiation field of rings on a cylindrical baffle, 6.7.22, 6.7.23. They both conform to the general rule that the radiation field of composite arrays is the product of the field from one element in the array multiplied by the field of an array of point sources fixed at the same lattice points.

Now by Poisson's Sum Formula, analogous to 6.7.32, one may write 6.7.48 in the form,

$$\Phi = \sum_{m=-\infty}^{\infty} \sum_{n=-\infty}^{\infty} \delta(m' - s)\, \delta(n' - t) \tag{6.7.49}$$

where m', n' are the Fourier pairs of m, n respectively. Since they are integers over the same $\pm\infty$ range as mn the prime may be dropped.

Substituting 6.7.49, 6.7.46, 6.7.47, 6.7.40 into 6.7.38, and summing over all mn, one finds the velocity potential at point (x_0', y_0, z) on surface $S_{0,0}$ due to all the array to be,

$$\psi(x_0', y_0') = e^{-i\omega t} \sum_{m=-\infty}^{\infty} \sum_{n=-\infty}^{\infty} \frac{1}{2\pi} V \iint w(x_m', y_n') \frac{ik}{2\pi} \int_0^{\pi} \int_{-\infty}^{\infty} \sin\theta d\theta \int_0^{2\pi} d\phi\, \delta(m - s)\, \delta(n - t) \tag{6.7.50}$$

$$exp\,[-ik\,(x_m' - x_n')\sin\theta\cos\phi]\; exp\,[-ik\,(y_m' - y_0')\sin\theta\sin\phi]\; dS\,(x_m', y_n']$$

This formula enables us to determine the acoustic power radiated by the central element of the infinite array.

$$W_{0,0} = \frac{1}{2} \int\int p(x_0', y_0')\, V_{0,0}^{*}\, dS(x_0', y_0') \tag{6.7.51}$$

Since this element is not steered one sets $\theta_0 = 0 = \phi_0$. Noting that $p = -i\omega\psi$, and substituting 6.7.50 and 6.7.37 into 6.7.51 one finds that the required integral over x_0', y_0' is independent of that required over x_m', y_n'; but identical with it excepting it is its conjugate. The result of this repeated integration over area $S_{0,0}$ and S_{mn} is the absolute square of the integral over the central element area alone. It is also proportional to the directivity factor of the central element,

$$|D(\theta, \phi)|^2 = \frac{|\int\int w(x_0, y_0)\, exp\,[-ik\,(x_0 \sin\theta\cos\phi + y_0 \sin\theta \sin\phi]\, dS_{0,0}|^2}{S_{eff}^2} \tag{6.7.52}$$

in which S_{eff} is the effective (or weighted) area of one element, defined by,

$$S_{eff} = \int\int w(x_0, y_0)\, d\, S_{0,0} \tag{6.7.53}$$

Thus the acoustic power radiated by the central element of an infinite planar array of elements is given by,

$$W_{0,0} = \frac{1}{2} \sum_{m=-\infty}^{\infty} \sum_{n=-\infty}^{\infty} -i\omega\varrho \frac{VV^*}{2\pi} \frac{(ik)}{2\pi} \int_0^{\pi/2 - i\infty} \sin\theta d\theta \int_0^{2\pi} d\phi\, S_{eff}^2 |D(\theta, \phi)|^2$$

$$\times\, \delta\left(m - \frac{a}{\lambda} \sin\theta\cos\phi\right)\, \delta\left[n - \sqrt{\frac{l^2 + b^2}{\lambda}} \sin\theta \sin(\theta + \mu)\right] \tag{6.7.54}$$

in which we have used the fact that $k = 2\pi/\lambda$. Eq. 6.7.54 is analogous to 6.6.17 because it expresses radiated power in terms of an integration over directivity.

To evaluate 6.7.54 a change of variables is made:

$$\begin{aligned} u &= \sin\theta\cos\phi\,;\; v = \sin\theta\sin(\phi + \mu) \\ \sin\theta &= \left[u^2 + \left(\sqrt{\frac{l^2 + b^2}{b}}\, v - \frac{l}{b} u\right)^2\right]^{1/2} \\ tan\,\phi &= \frac{v}{u} \frac{1}{\cos\phi} - tan\,\mu \end{aligned} \tag{6.7.55}$$

The limits of integration for both u and v become $-\infty$ to $+\infty$. Because

$$\delta\left(m - \frac{a}{\lambda}\sin\theta\cos\phi\right) = \frac{\lambda}{a}\,\delta(u_m - u);\; u_m = \frac{m\lambda}{a} \tag{6.7.56}$$

$$\delta\left[n - \frac{\sqrt{l^2+b^2}}{\lambda}\sin\theta\sin(\phi+\mu)\right] = \frac{\lambda}{\sqrt{l^2+b^2}}\,\delta(v_n - v);\; v_n = \frac{n\lambda}{\sqrt{l^2+b^2}} \tag{6.7.57}$$

and because the Jacobian is $\cos\theta\sin\theta$ so that $du\,dv = \cos\theta\sin\theta\,d\theta d\phi$ the integral over θ and ϕ is directly performed so that 6.7.54 reduces to,

$$W_{0,0} = \frac{1}{2}\sum_{m=-\infty}^{\infty}\sum_{n=-\infty}^{\infty}(-i\omega\varrho)\frac{|V|^2}{2\pi}\frac{(ik)}{2\pi}\frac{|D(u_m, v_n)|^2 S_{eff}^2}{\left[1-\left(v_n\frac{\sqrt{l^2+b^2}}{b} - u_m\frac{l}{b}\right)^2 - u_m^2\right]^{1/2}} \tag{6.7.58}$$

$$\times\frac{2\pi}{ka}\times\frac{2\pi}{k\sqrt{l^2+b^2}}$$

The mechanical radiation impedance of the central radiator is obtained from 6.3.1,

$$\begin{aligned} Z_{0,0}(\omega) &= \frac{2W_{0,0}}{|V|^2} \\ &= \frac{\varrho c S_{eff}^2}{a\sqrt{l^2+b^2}}\sum_{m=-\infty}^{\infty}\sum_{n=-\infty}^{\infty}\frac{|D(u_m, v_n)|^2}{\left[1-\left(v_n\frac{\sqrt{l^2+b^2}}{b} - u_m\frac{l}{b}\right)^2 - u_m^2\right]^{1/2}} \end{aligned} \tag{6.7.59}$$

The real part of the radiation impedance 6.7.59 is built up with those values of u_m, v_n such that the denominator is real. All the remaining u_m, v_n contribute to the reactive impedance. The mutual impedance between the *mn'th* element in the array and the central element is found by using the *mn'th* term alone. The self-impedance is found by using only the term $m = 0$, $n = 0$.

Because the array has an infinite number of elements the radiation impedance of the *mn'th* element is the same excepting for steering. To account for steering one replaces 6.7.56 and 6.7.57 by the following new values:

$$u_m = \frac{m\lambda}{a} + \bar{u}, \qquad \bar{u} = \sin\theta_0\cos\phi_0 \tag{6.7.60}$$

$$v_n = \frac{n\lambda}{\sqrt{l^2+b^2}} + \bar{v}, \qquad \bar{v} = \sin\theta_0\sin(\phi_0+\psi) \tag{6.7.61}$$

In arrays of a finite number of elements all the above formulas are calculated with m, n finite.

The radiation pattern of an infinite lattice of radiators in a plane appears as an infinite number of lobes, all of the same size as the central lobe. The lobe structure is due to mutual constructive and destructive interference. Eq. 6.7.50 indicates that lobes occur in directions given by angles θ, ϕ such that,

$$s = m, \text{ or } \frac{a}{\lambda}(\sin\theta\cos\phi - \sin\theta_0\cos\phi_0) = m, \quad m = 0, \pm 1, \pm 2, \ldots$$

$$t = n, \text{ or } \frac{\sqrt{l^2 + b^2}}{\lambda}[\sin\theta\sin(\phi + \mu) - \sin\theta_0\sin(\phi_0 + \mu)] = n, \quad n = 0, \pm 1, \pm 2, \ldots \tag{6.7.62}$$

The above development applies to radiating elements of any shape. An array often occurring in practice consists of circular pistons, radius d_e, located in a equi-spaced rectangular lattice, $a = b = d$, in which the skew $l = 0$, and steered in elevation θ_0, but not steered in azimuth ($\phi_0 = 0$). The radiation impedance of the central single radiating disc is obtained by 6.7.59:

$$Z_{0,0} = \frac{\varrho c S_{eff}^2}{d^2} \sum_{n=-\infty}^{\infty} \sum_{m=-\infty}^{\infty} \frac{\left(\dfrac{2J_1(kd_e\sqrt{u_m^2 + v_n^2})}{kd_e\sqrt{u_m^2 + v_n^2}}\right)^2}{\sqrt{1 - u_m^2 - v_n^2}} \tag{6.7.63}$$

$$u_m = \frac{m\lambda}{d} + \sin\theta_0; \quad v_n = \frac{n\lambda}{d}; \quad d \geq 2d_e$$

It is emphasized that this is a formula for an array consisting of an infinite number of elements.

6.7c. RADIATED ACOUSTIC POWER AND ACOUSTIC FIELD OF A RECTANGULAR WAVEGUIDE WITH A PERFORATED WALL. [6]

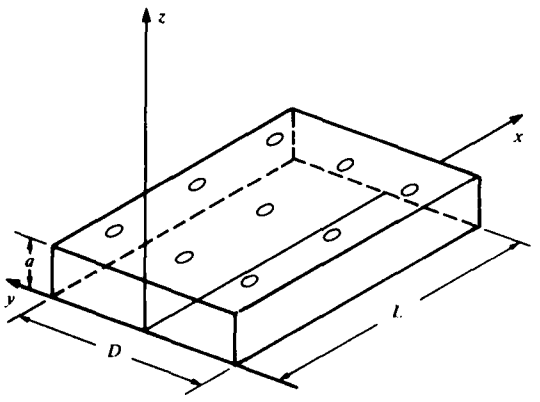

Fig. 6.7.5. Waveguide with a perforated wall.

A segment of a rigid wall waveguide, length L, width D, height a, has one wall perforated with holes of diameter d much less than a wavelength λ, spaced sufficiently apart so as to be moninteracting. Fig. 6.7.5 shows the waveguide and its associated coordinate system.

To restrict the number of modes inside the waveguide to be considered assume the acoustic size γa of the cross-section is so small as to admit only the plane wave mode at frequency ω. The field in the waveguide is then described by the velocity potential ψ_1,

$$\psi_1 = A, \exp i\xi x \cos\gamma z \tag{6.7.64}$$

$$\xi^2 + \gamma^2 = k^2 \tag{6.7.65}$$

Here ξ, γ are the x and z components of the propagation vector $\vec{K}$,

$$\vec{K} = \hat{\imath}\,\xi + \hat{k}\,\gamma \tag{6.7.66}$$

and $k\ (=\omega/c)$ is the propagation constant of the medium. The field outside the waveguide can be quite complex. A simple case occurs when the perforated wall radiates a single two-dimensional plane wave, potential ψ_2, given by,

$$\psi_2 = A_2 \exp i\vec{K}\cdot\vec{r} = A_2 \exp i(\xi x + \gamma z) \tag{6.7.67}$$

The constants A_1, A_2 are determined by specifying that at $x = 0$ the particle velocity is known to be uniform across the cross-sectional area, and to have the peak value V_1. Thus,

$$\psi_1 = \frac{V_1}{-i\xi} \exp i\xi x \cos\gamma z,\ 0 \leqslant z < a \tag{6.7.68}$$

At each perforation it is assumed that the z-component of particle velocity is continuous across the wall,

$$\frac{\partial \psi_1}{\partial z} = \frac{\partial \psi_2}{\partial z},\ z = a \tag{6.7.69}$$

Using 6.7.68 and 6.7.67, and allowing $\sin\gamma a \cong \gamma a$, $\exp i\gamma a \approx 1$, it is seen that,

$$\psi_2 = \frac{\gamma a\, V_1}{-\xi} \exp i(\xi x + \gamma z),\ \ z \geqslant a \tag{6.7.70}$$

In addition to boundary condition 6.7.69 there is the requirement of balance of forces at the interface $z = a$. For a *specific* acoustic admittance y_s at the interface, 1.8.22 states that,

$$\psi_2 - \psi_1 = \frac{v_z}{y_s} = \frac{v_z S}{y_A} \tag{6.7.71}$$

in which y_A is the (generally complex) acoustic admittance of the perforation. Now v_z is continuous through the perforation. Thus we can use 6.7.68,

$$v_z = -\left.\frac{\partial \psi_1}{\partial z}\right|_{z=a} = \left.\frac{-V_1\gamma}{-i\xi}(-\sin\gamma z)\exp i\xi x\right|_{z=a} = \frac{-V_1\gamma}{i\xi}\sin\gamma a \exp i\xi x$$

Furthermore the field ψ_2 is of order γa which makes it negligible in 6.7.71,

$$-\psi_1 \cong \frac{v_z S}{y_A}$$

or,

$$\frac{V_1}{-i\xi} \exp i\xi x \cos \gamma a \cong \frac{-v_1 \gamma S}{i\xi} \frac{\sin \gamma a}{y_A} \exp i\xi z$$

This reduces to a dispersion relation which fixes the value of γ,

$$\cos \gamma a \cong \frac{\gamma a S}{y_A a} \sin \gamma a \tag{6.7.72}$$

A simple solution, consistent with all assumptions, is to take $\gamma a \ll 1$, and write,

$$1 \cong \frac{(\gamma a)^2 S}{y_A a}$$

or

$$\gamma = \frac{h}{a}, \; h = \left(\frac{y_A a}{S}\right)^{1/2} \tag{6.7.73}$$

This unique value of γ allows one to obtain the unique value of ξ from 6.7.65,

$$\xi = \sqrt{k^2 - \gamma^2} = \sqrt{k^2 - \frac{h^2}{a^2}} \cong k\left[1 - \frac{h^2}{2(ka)^2}\right] \tag{6.7.74}$$

These values of γ and ξ explicitly fix the normal component of particle velocity and acoustic pressure on the surface $z = a$, and thus allow one to calculate the radiation everywhere by evaluation of an integral. However, 6.7.74 is a real number. As such it does not account for the loss of acoustic energy as the wave propagates down the waveguide. A simple mathematical model of this loss is to define an attenuation factor α such that the diminution of acoustic pressure follows the law $exp(-\alpha x)$. Assuming that the magnitude $(\gamma/k)^2 \ll 1$ one can write $|\xi| \cong k$. Thus the acoustic pressure on the surface $z = a$ is,

$$\begin{aligned} p(x, a|\omega) &= -i\omega\varrho \frac{\gamma a V_1}{-k} \exp i(\xi x + \gamma a) \exp(-\alpha x) \\ &= i\varrho c V_1 (\gamma a) e^{-\alpha x} \exp i(\xi x + \gamma a) \end{aligned} \tag{6.7.75}$$

Similarly, the normal component of particle velocity at the surface $z = a$ is,

$$v_z = -\left.\frac{\partial \psi_2}{\partial z}\right|_{z=a} = -\frac{(\gamma a)\, V_1}{-k}\, i\gamma \exp i(\xi x + \gamma a)\, e^{-\alpha x}$$

$$= i\frac{(\gamma a)^2\, V_1}{ka}\, e^{-\alpha x} \exp i(\xi x + \gamma a) \tag{6.7.76}$$

The acoustic intensity at the surface is,

$$I_0(x, a|\omega) = \frac{1}{2} Re\{p v_z^*\}_{z=a}$$

$$= \frac{1}{2} \varrho c\, V_1^2 \frac{(\gamma a)^3}{ka}\, e^{-2\alpha x} \tag{6.7.77}$$

The acoustic intensity inside the waveguide at any cross-sectional area is that of a plane wave with particle velocity V_1 at $x = 0$:

$$I_x(x) = \frac{1}{2} \varrho c\, V_1^2 e^{-2\alpha x} \tag{6.7.78}$$

The change of intensity for an incremental distance Δx is,

$$\frac{\Delta I_x(x)}{\Delta x} = \frac{1}{2} \varrho c\, V_1^2 (-2\alpha) e^{-2\alpha x}$$

A balance of the real acoustic power radiated from the surface $z = a$ across an area $D\Delta x$ and the power reduction inside the waveguide in this same length Δx is given by,

$$I_0 D\Delta x = -\left(\frac{\Delta I_x}{\Delta x}\right) a D\Delta x$$

or

$$\frac{1}{2} \varrho c\, V_1^2 \frac{(\gamma a)^3}{ka} e^{-2\alpha x} = -\frac{1}{2} \varrho c\, V_1^2 (-2\alpha) e^{-2\alpha x} a$$

The attenuation is then,

$$\alpha = \frac{(\gamma a)^3}{2a\,(ka)} \tag{6.7.79}$$

Now the acoustic pressure field everywhere is obtainable

$$p(\vec{r}\,|\omega) = -i\omega\varrho\psi$$

$$,, = \frac{-i\omega\varrho}{4\pi} e^{-i\omega t} \int_S \left[v_z(\vec{r}_0) + \frac{p(\vec{r}_0)}{\varrho c} \cos\gamma \right] \frac{e^{ik|\vec{r}-\vec{r}_0|}}{|\vec{r}-\vec{r}_0|} dS(\vec{r}_0) \qquad (6.7.80)$$

It is to be noted that the factor 4π rather that 2π because this segment of the radiating waveguide is assumed to approximate a point source when observed in the far field. In terms of spherical polar angle θ and azimuth angle ϕ the far field approximation is:

$$|\vec{r}-\vec{r}_0| = r - x\sin\theta\cos\phi - y\sin\theta\sin\phi$$

$$\cos\gamma \cong \cos\theta$$

Using the approximation one substitutes 6.7.75 and 6.7.76 into 6.7.80 to obtain,

$$p(r,\theta,\phi\,|\omega) = \frac{-i\omega\varrho e^{-i\omega t}}{4\pi} \frac{i V_1 (\gamma a)^2}{ka} \exp i\gamma a \left[1 + \frac{k}{\gamma}\cos\theta\right] \frac{e^{ikr}}{r} \int_s e^{-\alpha x} e^{ik\xi x} \qquad (6.7.81)$$

$$\times e^{-ik[x\sin\theta\cos\phi - y\sin\theta\sin\phi]}\, dxdy.$$

To simplify the evaluation of the integral the attenuation over x can be averaged separately,

$$\frac{1}{L}\int_0^L e^{-\alpha x}\, dx = \frac{1}{\alpha L}[1 - e^{-\alpha L}]$$

Choose L such that $\alpha L = 1$, that is L is the distance such that the travelling wave in the waveguide decays to e^{-1} of its initial value at $x = 0$. Thus the attenuation magnitude is approximately $1 - e^{-1}$ or approximately 0.6. Because the x and y factors in the integrand are separate one finds,

$$\int_{-D/2}^{D/2} e^{-ik\epsilon y} dy = D \frac{\sin\left[\frac{KD}{2}\in\right]}{\frac{kD}{2}\in}, \quad \in = \sin\theta\sin\phi$$

$$\int_0^L e^{-ik\zeta x} dx = L e^{i(\xi - k\zeta)\frac{L}{2}} \frac{\sin\left[(\xi - k\zeta)\frac{L}{2}\right]}{(\xi - k\zeta)\frac{L}{2}}, \quad \zeta = \sin\theta\cos\phi$$

In the horizontal plane $\theta = \pi/2$. The pressure in the far field is then,

$$\text{(a)}\quad p(r, \pi/2, \phi\,|\,\omega) = \frac{\omega\varrho e^{-i\omega t}}{4\pi}\,\frac{V_1(\gamma a)^2}{ka}\,(\exp i\gamma a)\,\frac{e^{ikr}}{r}\left[\exp i(\xi - k\cos\phi)\frac{L}{2}\right] f_H LD$$

in which (6.7.82)

$$\text{(b)}\quad f_H = \frac{\sin\left[\dfrac{kD}{2}\sin\phi\right]}{\dfrac{kD}{2}\sin\phi} \times \frac{\sin\left[\dfrac{kL}{2}\left(\dfrac{\xi}{k} - \cos\phi\right)\right]}{\dfrac{kL}{2}\left(\dfrac{\xi}{k} - \cos\phi\right)}$$

In the vertical plane, $\phi = 0$. The pressure in the far field is then,

$$\text{(a)}\quad p(r, \theta, 0\,|\,\omega) = \frac{\omega\varrho e^{-i\omega t}}{4\pi}\,\frac{V_1(\gamma a)^2}{ka}\,(\exp i\gamma a)\,\frac{e^{ikr}}{r}\left[\exp i(\xi - k)\frac{L}{2}\right] f_V LD$$

(6.7.83)

$$\text{(b)}\quad f_V = \frac{\sin\left[(\xi - k\sin\theta)\dfrac{L}{2}\right]}{(\xi - k\sin\theta)\dfrac{L}{2}}\left[1 + \frac{k}{\gamma}\cos\theta\right]$$

In 6.7.82 and 6.7.83 the wavenumbers γ, ξ are specific entities given explicitly by 6.7.73 and 6.7.74. Both 6.7.82b and 6.7.83b illustrate the product theorem, see Sect. 4.7a.

6.8. PRINCIPAL DIRECTION, ANGULAR DEVIATION RATIO, RADIATION FACTOR, GAIN FACTOR [7]

A symmetrical directional sound source designed for underwater signalling will have, for unshaded operation, a *principal direction,* in the far field in which the acoustic pressures generated by all elements of radiating surface arrive with the same phase. The ratio of the acoustic pressure p in any direction (given by the spherical angles θ, σ) to the pressure p_0 in the principal direction is defined to be the *angular deviation ratio* $\mathfrak{D}(\theta, \phi)$. Since the acoustic power flowing through a spherical area (radius R) in the far field is proportional to the square of the pressure amplitude the effect of directionality on power may be calculated by finding the coefficient ($\mathcal{J}$) of the square of the average angular deviation ratio over the total far field spherical area, i.e.

$$\mathcal{J} = \frac{\int_S \mathfrak{D}^2 dS}{4\pi R^2} \tag{6.8.1}$$

This average defines the *radiation factor,* that is, a factor by which the real acoustic power due to an omnidirectional radiator of pressure p_0 is reduced when replaced by a directional source with the same pressure p_0 in the principal direction only. When comparing powers the quantity $\mathcal{J}$ [illegible] shows by how much the pressure in the principal direction of a directional radiator is increased over

the pressure of an omnidirectional radiator of the same power. This quantity is called the pressure gain factor V:

$$V = \mathcal{G}^{1/2} \tag{6.8.2}$$

6.8a. PRESSURE GAIN FACTOR OF ARRAYS OF DIRECTIONAL SOURCES

In the far field of an array of n point sources the acoustic pressures at a field point in a specified direction due to any two sources will have phase angles of arrival which will differ by an amount $\Delta = kb$, b being the path difference between the sources. Selecting an arbitrary reference point we describe the phase angle of arrival from the μ th source relative to this reference as $\Delta\mu$. Hence for plane waves the phase of the μ th source relative to the reference is exp $(j\Delta\mu)$. Let there be a special direction (different from the principal direction) in which the radiation from all sources is artificially adjusted to be in phase in the far field. This is the shaded direction in which the natural phase angle from the μ'th source relative to the reference point is $\Delta_\mu' = kb'$. The phase shading in the shaded direction is accomplished by making $\Delta_\mu + \Delta_\mu' = 0$, or to each point source we give a phase angle $-kb'$ where b' is the path difference between the radiation in the shaded direction and the reference point. The phase in any other direction is therefore exp $[j(\Delta_\mu + \Delta_\mu')]$. We now replace the n point sources by n directional sources such that the pressure from the μ th source at point (θ, ϕ) is given by $p_\mu R(\theta, \phi)$. Considering the sound field of all the directional sources together, one can form the resultant pressure in the far field at angle θ, ϕ when all the sources are shaded to be in phase in the shaded direction to be,

$$p(\theta, \phi) = \sum_{\mu=1}^{n} p_\mu \mathcal{R}_\mu(\theta, \phi)\, e^{j(\Delta_\mu + \Delta_\mu')} \tag{6.8.3}$$

In the shaded direction $\Delta_\mu + \Delta_\mu' = 0$ and $\mathcal{R}_\mu(\theta, \phi) = 1$, hence the angular deviation ratio $\mathcal{R}_A$ of the array of n sources becomes,

$$\mathcal{R}_A = \left| \frac{\sum_{\mu=1}^{n} p_\mu \mathcal{R}_\mu(\theta, \phi)\, e^{j(\Delta_\mu + \Delta_\mu')}}{\sum_{\mu=1}^{n} p_\mu} \right| \tag{6.8.4}$$

If all the sources have identical angular deviation ratios and principal pressures then,

$$\mathcal{R}_A = \frac{\mathcal{R}(\theta, \phi)}{n} \left| \sum_{\mu=1}^{n} e^{j(\Delta_\mu + \Delta_\mu')} \right| \tag{6.8.5}$$

We desire now the gain factor for an array of n point sources. Setting $\mathcal{R}(\theta, \phi) = 1$ we see that,

$$\mathcal{R}_A^2 = \frac{1}{n^2} \left| \sum_{\nu=1}^{n} \sum_{\mu=1}^{n} \cos(\Delta_\mu - \Delta_\nu - \Delta_\mu' + \Delta_\nu') \right| \tag{6.8.6}$$

To perform the integration $\int_s \mathfrak{R}^2\, dS$ let the line joining the two sources, μ and ν, be the axis of the sphere over which the surface integration is to be performed. The result of the integration is a pressure gain factor for n sources:

$$V = \sqrt{\frac{n^2}{\sum_{\mu,\nu=1}^{n} \frac{\sin ka_{\mu\nu}}{ka_{\mu\nu}} \cos(\Delta'_\mu - \Delta'_\nu)}} \tag{6.8.7}$$

in which $a_{\mu\nu}$ is the distance between the sources μ, ν. This in generalized form is Rayleigh's formula [ ]. In a special case let $a_{\mu\nu} = s\lambda/2$, $s = 1, 2, 3 \ldots$. Then, for the condition of no shading the double sum in the formula is equal to n, the number of sources in the array, and so the pressure gain factor reduces to $V = n^{1/2}$. *Hence for arrays of n point sources separated by integer multiples of half-wavelengths the sound pressure on the principal axis in the sound field is $n^{1/2}$ times the sound pressure due to one source. By symmetry the radiation impedance is the same for all sources in this special array.*

6.8b. SUMMARY OF FORMULAS DESCRIBING ANGULAR DEVIATION RATIO AND PRESSURE GAIN FACTOR OF ARRAYS OF POINT SOURCES.

The Straight Line Array — An array of n equidistant point sources on the x-axis (separation distance between points = a) (Fig. 6.8.1) generates a far field pattern which depends on one parameter, the angle γ between the x-axis and the vector to the field point P. If the sources are shaded so that the far field pressures from all the sources are in phase at the angle γ' then the far field shading, the angular deviation ratio, and the pressure gain factor at any other angle γ are given by,

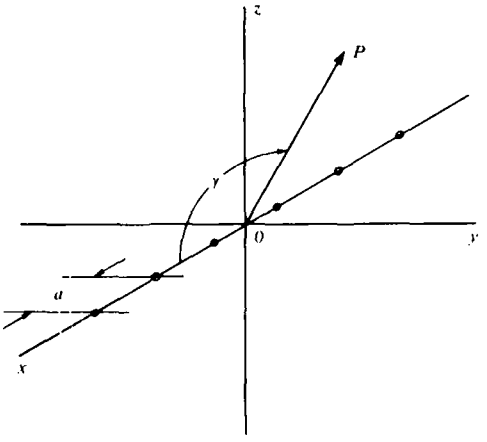

Fig. 6.8.1. Geometry of a line array of point sources.

$$\text{(a)}\quad k(b - b') = ka(\cos\gamma - \cos\gamma')$$

$$\text{(b)}\quad \mathfrak{R}(\gamma, \gamma') = \left| \frac{\sin n\,\mathrm{X}}{n \sin \mathrm{X}} \right|$$

$$\text{(c)}\quad \mathrm{X} = \frac{\pi a}{\lambda}(\cos\gamma - \cos\gamma') \tag{6.8.8}$$

$$\text{(d)}\quad V = \sqrt{\frac{n^2}{n + 2\sum_{\mu=1}^{n} (n - \mu) \frac{\sin \mu ka}{\mu ka} \cos \mu\, ka \cos\gamma'}}$$

The requirement (often found in practice) to have vanishing side-lobes imposes conditions on the entity na/λ. For $\gamma' = 90°$, namely for the state of no shading, the condition of no side lobes is by making $na/\lambda \ll 1$. For $\gamma' = 0°$, we must set $(2na/\lambda) \ll 1$.

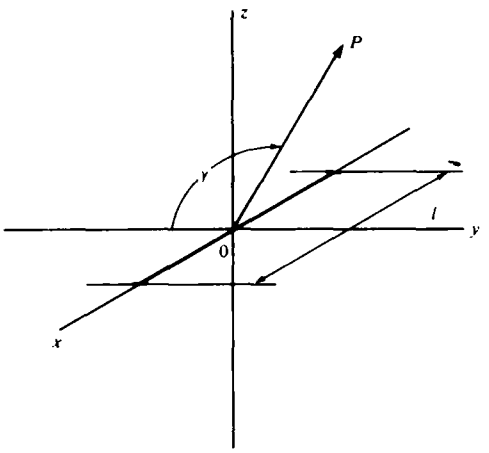

Fig. 6.8.2. Geometry of a line array.

The total length of the line is $\ell = (n-1)a$. If the number of point sources in length ℓ is increased indefinitely with a corresponding diminution of a to zero then $na \to \ell$, the array becomes a continuous line, Fig. 6.8.2. The angular deviation ratio and pressure gain factor in turn become,

$$\text{(a)} \quad \mathfrak{R}(\gamma, \gamma') = \left| \frac{\sin \Upsilon}{\Upsilon} \right|$$

$$\text{(b)} \quad \Upsilon = \frac{\pi \ell}{\lambda} [\cos\gamma - \cos\gamma'] \qquad (6.8.9)$$

$$\text{(c)} \quad V = \sqrt{\frac{2k\ell}{\frac{\cos k\ell f - 1}{\frac{1}{2} k\ell f} + \frac{\cos k\ell g - 1}{\frac{1}{2} k\ell g} + 2\,Si(k\ell f) + 2\,Si(k\ell g)}}$$

$$\text{(d)} \quad f = 1 - \cos\gamma', \quad g = 1 + \cos\gamma', \quad Si = \text{sine integral} = \int \frac{\sin x}{x}\, dx$$

The Circular Array — Let n be an even number of point sources on a circle in the xy plane and select origin of coordinates at center of the circle. These n sources can be thought of as m $(= n/2)$ linear arrays each containing two point sources, spaced like spokes on a wheel at equal angle separation on a circle of diameter d Fig. 6.8.3. The angular deviation ratio of each of these m arrays is $\mathfrak{R} = \cos x$, $x = \pi a/\lambda\,[\cos\gamma - \cos\gamma']$. We label these arrays $\mu = 0, 1, 2, \ldots m-1$, the array $\mu = 0$ lying along the x-axis. Let the positive z-axis be determined by the right-hand rule (= clockwise rotation of the x-axis into the y-axis). If the field point vector is projected on the xy plane and the clockwise angle from the x-axis (i. e. from $\mu = 0$) to the projection be designated as α, then the angle α_μ between the projection and the μ-th two point array will be $\alpha + \mu\pi/m$. Let γ be the angle between the field point vector and the x-axis and β the angle between the field point-vector and its

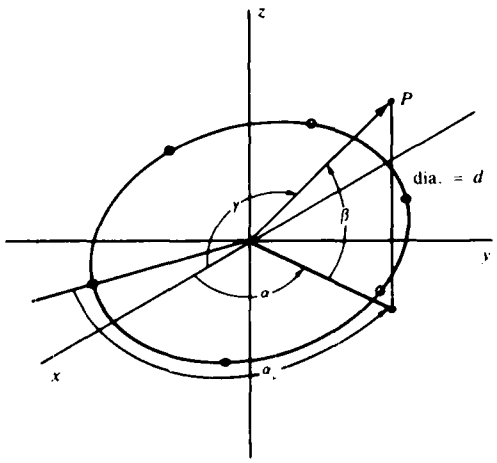

Fig. 6.8.3. Geometry of a circular array of point sources.

projection in the xy plane. We see from these definitions that $\cos\gamma = \cos\beta\cos\alpha_\mu$. Designating the shaded direction by the angles β', α' we may obtain the angular deviation ratio at angles β, α by summing m two-point source arrays, and by substituting in 6.8.2 obtain the pressure gain factor. These are,

$$\text{(a)}\quad \mathfrak{R} = \frac{1}{m}\left|\sum_{\mu=0}^{m-1}\cos\left\{\frac{\pi d}{\lambda}\left[\cos\beta\cos\left(\alpha+\mu\frac{\pi}{m}\right)-\cos\beta'\cos\left(\alpha'+\mu\frac{\pi}{m}\right)\right]\right\}\right| \tag{6.8.10}$$

$$\text{(b)}\quad V = \sqrt{\frac{n^2}{\sum_{\mu,\nu=1}^{m}\dfrac{\sin\left(kd\sin\dfrac{\mu-\nu}{n}\pi\right)}{kd\sin\dfrac{\mu-\nu}{n}\pi}\cos\left[kd\cos\beta'\sin\left(\alpha'+\dfrac{\mu+\nu}{n}\pi\right)\sin\dfrac{\mu-\nu}{n}\pi\right]}}$$

When it is required that the side lobes vanish we must set $(2\pi d/\lambda) \ll 2.4$ if $\beta' = 0$, and $(\pi d/\lambda) \ll 2.4$ if $\beta' = 90°$. The value of $\mathfrak{R}$ in depends upon $\alpha, \beta, \alpha', \beta'$. To simplify calculation one may obtain a "latitude section" by setting $\beta = b'$, and a "vertical section" by setting $\alpha = \alpha'$. Using the series developments,

$$\cos(x\sin\omega) = J_0(x) + 2\sum_{p=1}^{\infty} J_{2p}(x)\cos 2p\omega$$

$$\cos(x\cos\omega) = J_0(x) + 2\sum_{p=1}^{\infty}(-1)^p J_{2p}(x)\cos 2p\omega$$

the angular deviation ratio at α for the condition $\beta = \beta'$ is,

$$\mathfrak{R}_{\beta=\beta'} = \left|J_0(V) + 2\sum_{q=1}^{\infty} J_{2qm}(V)\cos 2qm\frac{\alpha+\alpha'}{2}\right|,\quad V = \frac{2\pi d}{\lambda}\cos\beta'\sin\frac{\alpha-\alpha'}{2} \tag{6.8.11}$$

and the angular deviation ratio at β for the condition $\alpha = \alpha'$ is,

$$\mathfrak{R}_{\alpha=\alpha'} = \left|J_0(W) + 2\sum_{q=1}^{\infty}(-1)^{qn} J_{2qn}(W)\cos 2qn\alpha'\right|,\quad W = \frac{\pi d}{\lambda}(\cos\beta - \cos\beta') \tag{6.8.12}$$

The Circular Line — When every point on the circular array is a point source the new configuration is a radiating circular line Fig. 6.8.4. If an arbitrary plane is passed through the origin perpendicular to the field point vector (through the origin) the circular line (radius R) will be intersected at two reference points corresponding to the selected field point. Let A,B,C be the direction cosines of the field vector. Any point on the circular line will contribute a ray to the field point with a path difference of b with respect to the reference points where $b = R(A\cos\alpha + B\sin\alpha)$.

Let the shaded direction of the circular line be given by α', β', and fix a plane through the origin perpendicular to the field point vector in the shaded direction. An element on the circular line will contribute a ray with path difference b' with respect to the new reference points. Thus the angular deviation ratio due to all circular line elements $ds = Rd\alpha$ becomes,

$$\mathcal{R} = \left(\frac{1}{2\pi R}\right)\int_0^{2\pi} e^{jk(b-b')}\,ds \tag{6.8.13}$$

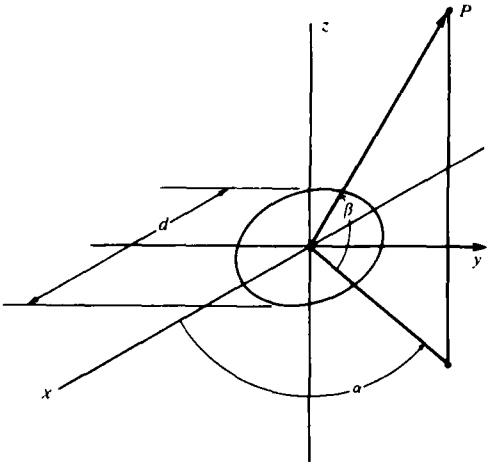

Fig. 6.8.4. Geometry of a circular line array.

Recalling that $J_n(z) = (j^{-n}/\pi)\left(\int_0^{\pi} e^{jz\cos t}\cos n\,t\,dt\right)$ and that $A = \cos\alpha\cos\beta$, $B = \sin\alpha\cos\beta$, the formulas for the angular deviation ratio and the gain factor may be reduced to,

$$\text{(a)}\quad \mathcal{R} = J_0\left[\frac{\pi d}{\lambda}(F_1 + F_2)^{1/2}\right],$$

$$d = 2\mathcal{R},$$

$$F_1 = (\cos\alpha\cos\beta - \cos\alpha'\cos\beta')^2,$$

$$F_2 = (\sin\alpha\cos\beta - \sin\alpha'\cos\beta')^2, \tag{6.8.14}$$

$$\text{(b)}\quad V_{\alpha'=0} = \sqrt{\frac{kd}{2\sum_{r=0}^{\infty}\epsilon_r J_r^2\left(\frac{kd}{2}\cos\beta'\right)\sum_{p=0}^{\infty}J_{2r+2p+1}(kd)}}, \qquad \epsilon_0 = 1,\ \epsilon_r = 2,\ r \neq 0$$

$$\text{(c)}\quad V_{\beta'=90^\circ} = \sqrt{\frac{kd}{2\sum_{p=0}^{\infty}J_{2p+1}(kd)}}$$

$$\text{(d)}\quad \mathcal{R}_{\beta=\beta'} = \left|J_0\left(\frac{2\pi d}{\lambda}\cos\beta'\sin\frac{\alpha-\alpha'}{2}\right)\right|,$$

$$\text{(e)}\quad \mathcal{R}_{\alpha=\alpha'} = \left|J_0\left(\frac{2\pi d}{\lambda}[\cos\beta - \cos\beta']\right)\right|.$$

We note that for $\ell = d$, $d \gg \lambda$, the pressure gain factor of the radiating circular line is larger than the gain factor of the radiating straight line by about $\sqrt{\pi}$.

The Spherical Array — In Fig. 6.8.5 we divide the polar angle π of a spherical source of diameter D into $s + 1$ equal parts and define s circles of latitude with designations $p = 1, 2, \ldots s$. The diameter d_p of the p th circle of latitude is $d_p = D \sin (p\pi/s + 1)$. If each circle defined in this way is a radiating circular line its angular deviation ratio for a "latitude section" (i. e. $\beta = B'$) from 6.8.14d is,

$$\mathfrak{R}_p = \left| J_0 \left(\frac{2\pi D}{\lambda} \cos\beta' \sin \frac{\alpha - \alpha'}{2} \sin \frac{p\pi}{s+1} \right) \right| \tag{6.8.15}$$

Now the magnitude of the pressure from the p th circle is proportional to its diameter, hence proportional to sin $(p\pi/s + 1)$. Since, in the compensation direction $R_p = 1$ it is seen that the angular deviation ratio in a latitude section of a sum of s coaxial rings for the condition $\beta' = 0$ is,

$$\mathfrak{R}_{\beta = \beta' = 0} = \frac{\sum_{p=1}^{s} \mathfrak{R}_p \sin \left(\frac{p\pi}{s+1} \right)}{\sum_{p=1}^{s} \sin \left(\frac{p\pi}{s+1} \right)} \tag{6.8.16}$$

Recalling that $\sum_{p=1}^{s} \sin \left(\frac{p\pi}{s+1} \right) = \text{cotangent} \left(\frac{\pi}{2(s+1)} \right)$ it is seen that for a latitude section the angular deviation ratio is,

$$\beta = \beta' = 0 = tg \frac{\pi}{2(s+1)} \left| \sum_{p=1}^{s} J_0 \left(\frac{2\pi D}{\lambda} \sin \frac{\alpha - \alpha'}{2} \sin \frac{p\pi}{s+1} \right) \sin \frac{p\pi}{s+1} \right| \tag{6.8.17}$$

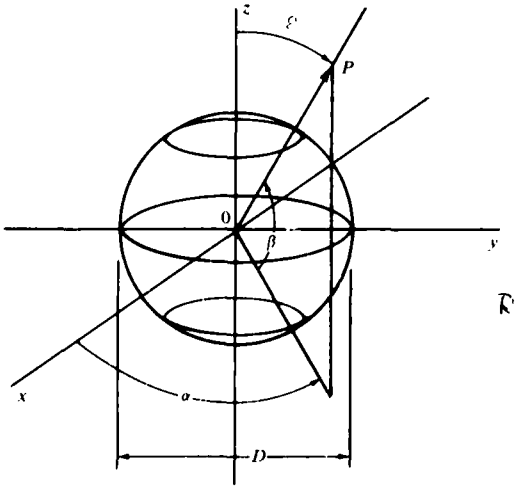

Fig. 6.8.5. Geometry of a spherical array.

For a vertical section (i. e. $\alpha = \alpha'$) we may similarly add the pressures due to s circles of latitude to find $\mathfrak{R}$. However there is an additional phase difference at a field point in a vertical section due to the varying location of the p th ring along the vertical axis. This appears as a factor x in the following formula for the vertical section,

$$\mathfrak{R}_{\alpha = \alpha'} = tg \frac{\pi}{2(s+1)} \left| \sum_{p=1}^{s} J_0(y) \sin \left(\frac{p\pi}{s+1} \right) \cos x \right| \tag{6.8.18}$$

$$x = (\pi D/\lambda) \cos (p\pi/s + 1) (\sin\beta - \beta')$$

$$y = (\pi D/\lambda) (\cos\beta - \cos\beta') \sin (p\pi/s + 1)$$

The Radiating Spherical Surface — We now assume that the sphere is completely covered with point sources and is shaded in the direction of the z-axis. We expect a rotationally symmetric pattern so that the polar angle ε (Fig. 6.8.5) between the z-axis and the field point vector is the only variable. The angular deviation ratio for a spherical radiating surface shaded in the z-direction and the pressure gain factor may be derived to be,

$$\text{(a)} \quad \mathfrak{R} = \frac{\sin\left(\frac{2\pi D}{\lambda}\sin\frac{\varepsilon}{2}\right)}{\frac{2\pi D}{\lambda}\sin\frac{\in}{2}}$$

$$\text{(b)} \quad V = \sqrt{\frac{k^2 D^2}{C + \ell n\, 2kD - Ci\,(2kD)}} \tag{6.8.19}$$

in which $C = 0.577$ is Euler's constant. For no side lobes we require that $(2D/\lambda) \ll 1$.

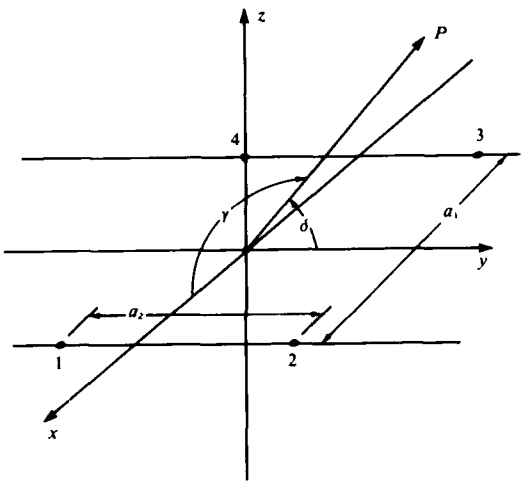

Fig. 6.8.6 Array of four source points.

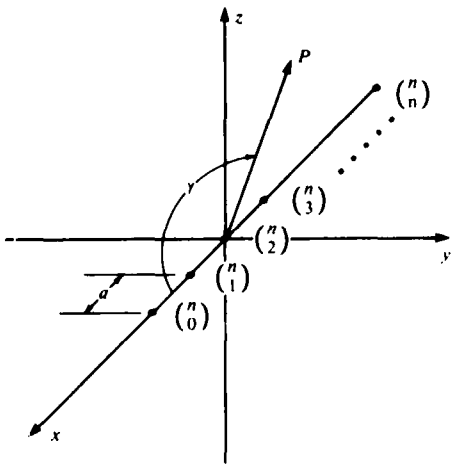

Fig. 6.8.7. Array of $n + 1$ sources on a line with biomeal shading.

Combination of Arrays — In an array A of point sources having the angular deviation ratio $\mathfrak{R}_A$ we may replace each source by a secondary array B having a ratio $\mathfrak{R}_B$. If the intensities and directivities of all the secondary sources are equal then the angular deviation ratio of the combination array is the *product* $\mathfrak{R}_A\,\mathfrak{R}_B$. This is called the Product Theorem (see Sect. 6.6).

We dispose the primary and secondary arrays in the xy plane, and seek to find the angular deviation ratios of combinations commonly used in array practice. Each combination is accompanied by a sketch.

Case I. Fig. 6.8.6. Four Source Points

$$\mathfrak{R} = \cos\left(\frac{\pi a_1}{\lambda}\cos\gamma\right)\cos\left(\frac{\pi a_2}{\lambda}\cos\delta\right) \tag{6.8.20}$$

Case II. Fig. 6.8.7. $n + 1$ points (distance a between them) on a line, each point m ($m = 0, 1, 2 \ldots n$) with intensity given by the binomial coefficient $\binom{n}{m}$ in sequence.

$$\mathfrak{R}_{n+1} = \left|\cos^n\left(\frac{\pi a}{\lambda}\cos\gamma\right)\right| \tag{6.8.21}$$

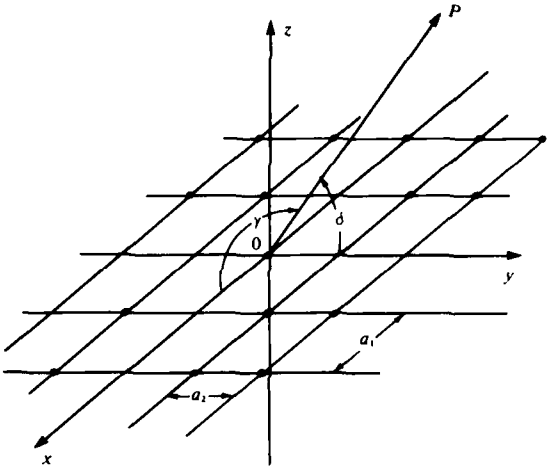

Fig. 6.8.8 Rectangular array of point sources.

Case III. Fig. 6.8.8. $n \times n$ array of points in xy plane, separation a_1 in x-direction and a_2 in y-direction,

$$\mathfrak{R} = \left| \frac{\sin\left(\frac{n\pi a_1}{\lambda}\cos\gamma\right)\sin\left(\frac{n\pi a_2}{\lambda}\cos\delta\right)}{n\sin\left(\frac{\pi a_1}{\lambda}n\cos\gamma\right)\, n\sin\left(\frac{\pi a_2}{\lambda}\cos\delta\right)} \right| \tag{6.8.22}$$

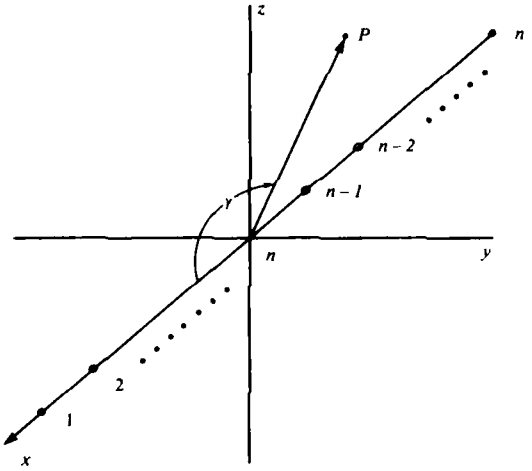

Fig. 6.8.9. Linear array of n array each having n elements.

Case IV. Fig. 6.8.9. The n linear array, each element of which is also an n linear array disposed in same direction. The linear intensity distribution is

1, 2, 3, ... n ... 3, 2, 1. for which

$$\mathfrak{R} = \left(\frac{\sin nx}{n\sin x}\right)^2, x = \frac{\pi a}{\lambda}\cos\gamma \tag{6.8.23}$$

Case V. m linear basic components each of which is an $n + 1$ binomial array.

$$\mathfrak{R} = \left(\frac{\sin mx}{m\sin x}\right)\cos^n x \tag{6.8.24}$$

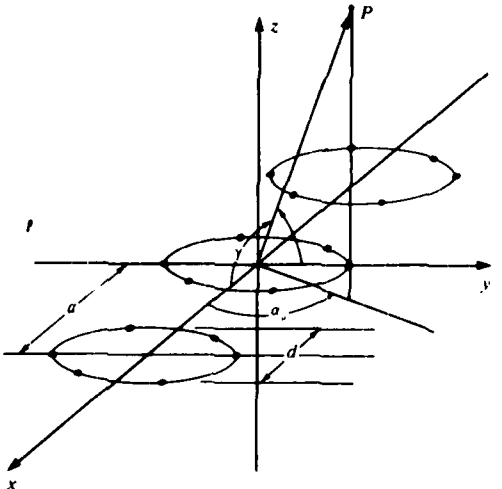

Fig. 6.8.10. Linear Array of circular arrays of point sources.

Case VI. Fig. 6.8.10. p (= even number) point sources in a circle of diameter d (thought of as $m = p/2$ two-source arrays), and n such circles arrays in linear array on x-axis,

$$\mathfrak{R} = \left| \frac{\sin\left(\frac{n\pi a}{\lambda}\cos\gamma\right)}{n\sin\left(\frac{\pi a}{\lambda}\cos\gamma\right)} \frac{1}{m} \sum_{\mu=0}^{m-1} \cos\left(\frac{\pi d}{\lambda}\cos\gamma_\mu\right) \right| \tag{6.8.25}$$

$$\alpha_\mu = \alpha + \mu\pi/m$$

$$\cos\gamma_\mu = \cos\alpha_\mu\cos\beta$$

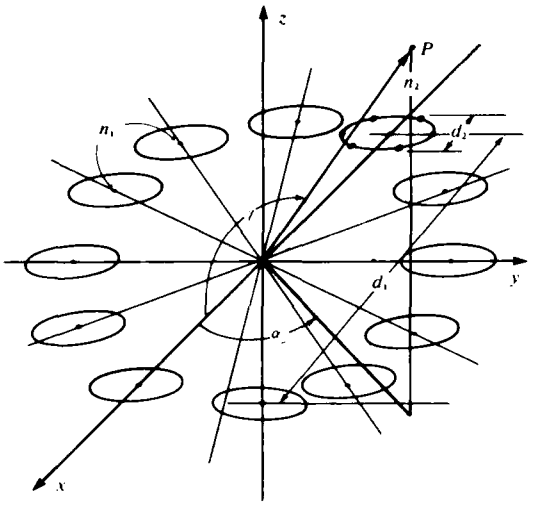

Fig. 6.8.11. Ring of Circular Rings.

Case VII. Fig. 6.8.11. n_1 (= even number) point sources on a circular ring, each point source being itself a circular ring of n_2(= even number) point sources.

$$\mathfrak{R} = \frac{1}{m_1}\left| \sum_{\mu=0}^{m_1-1} \cos\left(\frac{\pi d_1}{\lambda}\cos\gamma_\mu\right) \frac{1}{m_2} \sum_{\mu=0}^{m_2-1} \right.$$

$$\left. \cos\left(\frac{\pi d_2}{\lambda}\cos\gamma_\mu^0\right) \right| m_1 = \frac{n_1}{2},\ m_2 = \frac{n_2}{2}. \quad (6.8.26)$$

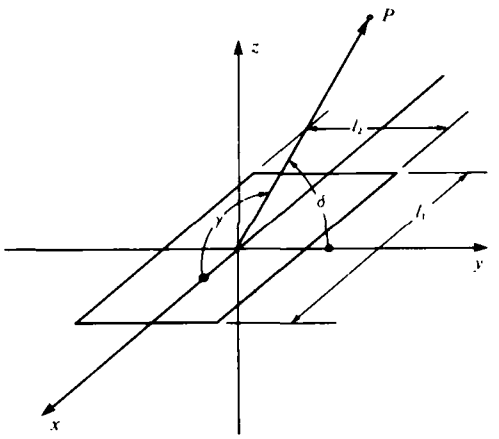

Fig. 6.8.12. Rectangular piston.

Case VIII. Fig. 6.8.12. Rectangular piston diaphragm, sides l_1, l_2

$$\mathfrak{R} = \left| \frac{\sin X}{X} \frac{\sin Y}{Y} \right| \quad (6.8.27)$$

$$X = (\pi l_1/\lambda)\cos\gamma$$

$$Y = (\pi \frac{l_2}{\lambda})\cos\delta$$

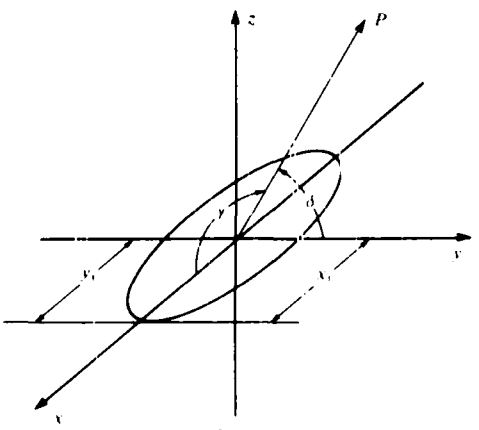

Fig. 6.8.13. Elliptical positon

Case IX. Fig. 6.8.13. Elliptical Piston

$$\mathfrak{R} = \left| \frac{2J_1\left(\frac{2\pi}{\lambda}\sqrt{x_1^2\cos^2\gamma + y_1^2\cos^2\delta}\right)}{\frac{2\pi}{\lambda}\sqrt{x_1^2\cos^2\gamma^0 + y_1^2\cos^2\delta}} \right|$$

(6.8.28)

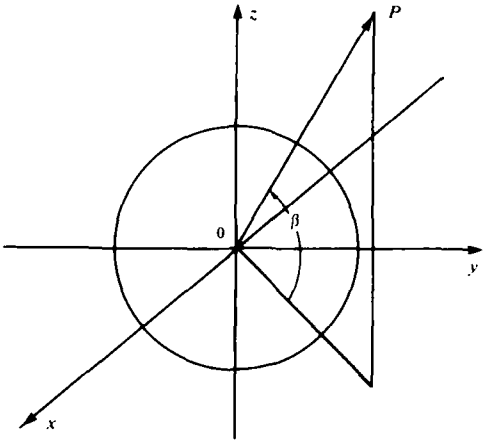

Fig. 6.8.14. Circular piston

Case X. Fig. 6.8.14. Circular Piston

$$\mathfrak{R} = \left| \frac{2J_1\left(\frac{\pi d}{\lambda}\cos\beta\right)}{\left(\frac{\pi d}{\lambda}\cos\beta\right)} \right| \tag{6.8.29}$$

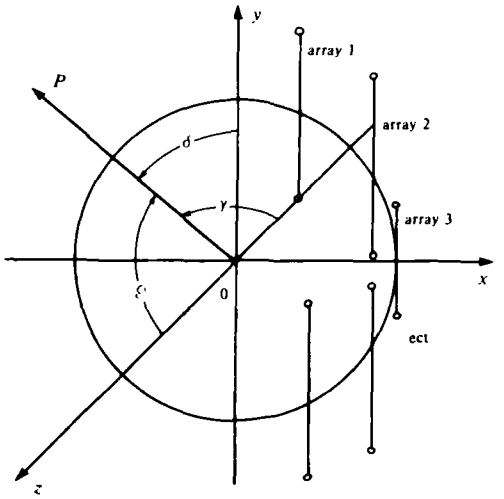

Fig. 6.8.15. Circular array of source arrays.

Case XI. Fig. 6.8.15. Circular Array of 2 source arrays (both in y plane).

$$\mathfrak{R} = \left| \frac{\sin\frac{2\pi a}{\lambda}\cos\delta}{2\sin\frac{\pi a}{\lambda}\cos\delta} \right| \frac{1}{m} \times \left| \sum_{\mu=0}^{m-1} \cos\frac{\pi d}{x}\cos\varepsilon_\mu \right| \tag{6.8.30}$$

General Rule 1: *Let a be the separation distance of the sources on a 2-source array, d be the diameter of a circular radiating line, ℓ be the length of a radiating straight line, D be the diameter of a spherical surface, and d be the diameter of a circular piston surface radiator. Then if ℓ = d = a = D the half angle at the main lobe 3 db points are in the ratios as* $\sqrt{2}$: $\sqrt{4}$: $\sqrt{6}$: $\sqrt{6}$: $\sqrt{8}$ *for the two-source, circular ring, straight line, spherical surface, circular piston respectively.*

General Rule 2: *If the beam width of a radiator is to be independent of steering angle in a plane, the shaded circular array is useful; in space, the shaded spherical array is useful.*

6.9 RADIATION RESISTANCE OF VIBRATING ELASTIC PANELS IN TERMS OF MODAL CORRELATION FUNCTIONS.

An elastic panel supported at its edges in an arbitrary way is driven by a force $F(\mathbf{x}_s)e^{-i\omega t}$ so that it radiates from one surface $S(\mathbf{x}) = S(x,y)$ into the contiguous medium. At the same time it is subject to an acoustic pressure on this surface arising from the reaction of the medium and from the radiation of possible distant sources $Q(\mathbf{r})e^{-i\omega t}$, $\mathbf{r} = \mathbf{x}_0 - \mathbf{x}_{s_0}$. Under these excitations the displacement field $w(\mathbf{x}_s)e^{-i\omega t}$ normal to the plate surface and the field of velocity potential $\phi(\mathbf{x}_s)e^{-i\omega t}$ on the surface can be described by a set of coupled inhomogeneous differential equations:

$$\mathscr{L}_{F,w}\{w(\mathbf{x}_s)\} + \mathscr{L}_{F,\phi}\{\phi(\mathbf{x}_s)\} = F(\mathbf{x}_s) \quad \text{(units: } N\text{)} \tag{6.9.1}$$

$$\mathscr{L}_{\Phi,\phi}\{\phi(\mathbf{x}_s)\} + \mathscr{L}_{\Phi,w}\{w(\mathbf{x}_s)\} = Q(\mathbf{x}_s) \quad \text{(units: } s^{-1}\text{)} \tag{6.9.2}$$

Here $\mathscr{L}_{F,w}$, etc. represent integral-differential operators which have simple interpretations: $\mathscr{L}_{F,w}\{w\}$ is the force required to drive the panel at point $\mathbf{x}_s$ on the plate and $\mathscr{L}_{F,\phi}\{\phi\}$ is the force of reaction of the medium. The other operators have similar definitions.

We make now several assumptions. (1) the panel notion can be described as a sum of (spatial) modes, that is,

$$w(\mathbf{x}_s,\omega) = \sum_m w_m(\omega)\ W_m(\mathbf{x}_s) \tag{6.9.3}$$

in which $W_m(x)$ are orthonormal functions over the area of the panel,

$$\int W_m(\mathbf{x})\ W_m(\mathbf{x})d\mathbf{x} = \delta_{mn} = \begin{cases} 1, & m = n \\ 0, & n \neq n \end{cases} \tag{6.9.4}$$

(2) the operator $L_{F,w}$ can be approximated as a sum of mass ($\mathscr{M}$), damping ($\mathscr{D}$) and stiffness ($\mathscr{K}$) operators. (3) in the steady state $\mathscr{M}$, $\mathscr{D}$ and $\mathscr{K}$ are scaler operators. (4) the operator $\mathscr{K}$ obeys the relation $\mathscr{K}\{w\} = -Kw$. With these four assumptions in mind we substitute 6.9.3 into 6.9.1, then multiply through by $W_n(x)$ and integrate over area. The use of 6.9.4 then leads to the dynamic equation of motion in the mth mode,

$$(a) \quad Z'_m\, w_m(\omega) + \int \mathscr{L}_{F,\phi}\{\phi(\mathbf{x}_s)\} W_m(\mathbf{x}_s)d\mathbf{x}_s = F_m(\omega)$$

$$(b) \quad \begin{cases} M_m\delta(m,n) \\ D_m\delta(m,n) \\ K_m\delta(m,n) \end{cases} = \begin{cases} \int W_m(\mathbf{x}_s)\mathscr{M}\ W_n(\mathbf{x}_s)d\mathbf{x}_s \\ \int W_m(\mathbf{x}_s)\mathscr{D}\ W_n(\mathbf{x}_s)d\mathbf{x}_s \\ \int W_m(\mathbf{x}_s)\mathscr{K}\ W_n(\mathbf{x}_s)d\mathbf{x}_s \end{cases} \tag{6.9.5}$$

$$(c) \quad F_m(\omega) = \int F(\mathbf{x}_s,\omega)\ W_m(\mathbf{x}_s)d\mathbf{x}_s$$

$$(d) \quad Z'_m = -M_m\omega^2 - i\omega D_m - K_m$$

The acoustic field also may be simplified by an analysis based on several assumptions. These are: (1) a modal description may be assigned to the velocity potential on the surface,

$$\phi(x_s,\omega) = \sum_r \phi_r(\omega)\,\Phi_r(\mathbf{x}_s) \tag{6.9.6}$$

Here $\Phi_r(\mathbf{x}_s)$ are orthonomal modal functions over the area of the panel,

$$\int \Phi_r(\mathbf{x}_s)\,\Phi_s(\mathbf{x}_s)\,d\,\mathbf{x}_s = \delta_{rs} \tag{6.9.7}$$

and $\phi_r(\omega)$ are modal amplitudes. (2) each displacement mode $W_m(\mathbf{x}_s)$ is coupled to *all* the acoustic potential modes $\Phi_r(\mathbf{x}_s)$. (3) the displacement modes are *not* orthogonal to the velocity potential modes,

$$\int \Phi_r(x)\;W_m(x)\;d\mathbf{x} \neq \delta_{mr} \tag{6.9.8}$$

(4) the operator $L_{\Phi,\phi}$ is a sum of mass $\mathcal{M}^{(A)}$, damping $\mathcal{D}^{(A)}$ and stiffness $\mathcal{K}^{(A)}$ operators. Based on these assumptions we can write the coupling term in 6.9.5 to be,

$$(a) \qquad \int \mathcal{L}_{t,\phi}\,\{\phi(\mathbf{x}_s)\}\;W_m(\mathbf{x}_s)\,d\mathbf{x}_s = \sum_r L_{mr}\,\phi_r(\omega)$$

$$(b) \qquad L_{mr} = \int W_m(\mathbf{x}_{s(1)}\mathcal{L}_{t,\phi}\,\Phi_r(\mathbf{x}_{s(1)})\;d\mathbf{x}_{s(1)}.$$

The acoustic field, represented by $\phi(\mathbf{x}_s)$ in 6.9.2, is thus reducible to a sum of modes whose amplitude $\phi_r(\mathbf{x}_s)$ obey the dynamic equation,

$$(a) \qquad (-M_r^{(A)}\omega^2 - i\omega D_r^{(A)} - K_r^{(A)})\phi_r(\omega) + \sum_m L_{rm}^{(A)}\,W_m(\omega) = Q_r(\omega)$$

$$(b) \qquad \begin{cases} \delta_{rs}\,M_r^{(A)} \\ \delta_{rs}\,D_r^{(A)} \\ \delta_{rs}\,K_r^{(A)} \end{cases} = \begin{cases} \Phi_r(\mathbf{x})\,\mathcal{M}^{(A)}\Phi_s(\mathbf{x})\;d\mathbf{x} \\ \int \Phi_r(\mathbf{x})\,\mathcal{D}^{(A)}\Phi_s(\mathbf{x})\;d\mathbf{x} \\ \Phi_r(\mathbf{x})\,\mathcal{K}^{(A)}\Phi_s(\mathbf{x})\;d\mathbf{x} \end{cases} \tag{6.9.10}$$

$$(c) \qquad Q_r(\omega) = \int Q(x_s,\omega)\,\Phi_r(\mathbf{x}_s)\;d\mathbf{x}_s$$

$$(d) \qquad L_{rm} = \int \Phi_r(\mathbf{x}_{s(2)})\,\mathcal{L}_{\Phi,w}\;W_m\;(\mathbf{x}_{s(2)}$$

$$(e) \qquad Z_r^{(A)'} = -\,M_r(A)\omega^2 - i\omega D_r^{(A)} - K_r(A)$$

To calculate $M_r^{(A)}$, $K_r^{(A)}$ one assumes the characteristic impedance of the medium is $\rho_a c_a$, and the propagation wavenumber is $k_a = \omega/c_a$. Since our goal is to find the radiation resistance R_{RAD} which describes the real power transfer from the mth displacement mode to the nth velocity potential mode we separate out one term in the sum term in 6.9.10a and solve for $\phi_r(\omega)$:

$$(a) \qquad \phi_r(\omega) = \frac{Q_r'(\omega) - L_{rm}^{(A)}w_m(\omega)}{Z_r^{(A)'}} \tag{6.9.11}$$

$$(b) \qquad Q_r'(\omega) = Q_r(\omega) - \sum_{n\neq m}' L_{rn}^{(A)}w_n(\omega).$$

Let us assume there are no sources in the field, $Q_r(\omega) = 0$, and further assume that amplitude $\phi_r(\omega)$ is determined approximately by $w_m(\omega)$ alone. This means that $Q_r'(\omega) = 0$, and the amplitudes $\phi_r(\omega)$ become,

$$\phi_r(\omega) = -\frac{L_{rm}^{(A)}\, w_m(\omega)}{Z_r^{(A)'}}. \tag{6.9.12}$$

Use of 6.9.5a, 6.9.9a and 6.9.12, then leads to a much reduced expression for the modal force $F_m(\omega)$:

$$-\left[Z_m' - \frac{L_{mr}\, L_{rm}^{(A)}}{Z_r^{(A)'}}\right] w_m(\omega) = F_m(\omega). \tag{6.9.13}$$

Multiplying the left-hand side by $-i\omega/-i\omega$, and redefining symbols, one has

$$(Z_m + Z_{(rm)\mathrm{RAD}})\, \dot{w}_m(\omega) = F_m(\omega) \tag{6.9.14}$$

$Z_m = \dfrac{Z_m'}{-i\omega}$ = mechanical impedance of the mth displacement mode in units of Ns/m.

$Z_{(rm)\mathrm{RAD}} = \dfrac{L_{mr}\, L_{rm}^{(A)}}{i\omega\, Z_r^{(A)'}}$ = radiation impedance of the mth displacement mode coupled to the rth velocity potential mode in units of Ns/m.

The real part of $Z_{(rm)\mathrm{RAD}}$ is the desired radiation resistance,

$$R_{(rm)\mathrm{RAD}} = \mathrm{Re}\left\{\begin{array}{l}\dfrac{1}{i\omega\, Z_r^{(A)'}} \int W_m(\mathbf{x}_{s(1)})\, \mathscr{L}_{F,\phi} \Phi_r(\mathbf{x}_{s(1)}\, d\mathbf{x}_{s(1)} \\ \times \int \Phi_r(\mathbf{x}_{s(2)})\, \mathscr{L}_{\Phi,w}\, W_m(\mathbf{x}_{s(2)})\, d\mathbf{x}_{s(2)}\end{array}\right\} \tag{6.9.15}$$

In the cases of interest to acoustic radiation theory the operators $\mathscr{L}_{F,\phi}$ and $\mathscr{L}_{\Phi,w}$ are simple constants, or functions independent of spatial coordinates. They can therefore be removed from the integral sign,

$$(a)\ R_{(rm)\mathrm{RAD}} = \mathrm{Re}\left\{A_m(\omega) \int W_m(\mathbf{x}_{s(1)}\, \Phi_r(\mathbf{x}_{s(1)}) d\mathbf{x}_{s(1)} \int \Phi_r(\mathbf{x}_{s(2)})\, W_m(\mathbf{x}_{s(2)}) d\mathbf{x}_{s(2)}\right\}$$

$$(b)\ A = \frac{1}{i\omega\, Z_r^{(A)'}}\, \mathscr{L}_{F,\phi}\, \mathscr{L}_{\Phi,w}. \tag{6.9.16}$$

An important application of this formula is to elastic panels excited by random forces and reaction pressures which generate a large number of modes both in the panel itself and in the acoustic medium. Because these modes occur at random frequencies and in random numbers the field of displacement and velocity potential is called "reverberant" [8]. The radiation resistance of the panel is then calculated from an ensemble average over all the modes in the panel and in the medium,

$$R_{\mathrm{RAD}} = \mathrm{Re}\left\{< A_m(\omega) >_{(m)} < \int W_m(\mathbf{x}_{s(1)}) \Phi_r(\mathbf{x}_{s(1)}) d\mathbf{x}_{s(1)} \int \Phi_r(\mathbf{x}_{s(2)})\, W_m(\mathbf{x}_{s(2)}) d\mathbf{x}_{s(2)} >_{(m)}\right\} \tag{6.9.17}$$

AD-A140 578 A TREATISE ON ACOUSTIC RADIATION(U) NAVAL RESEARCH LAB 4/7
WASHINGTON DC S HANISH 1981

UNCLASSIFIED F/G 20/1 NL

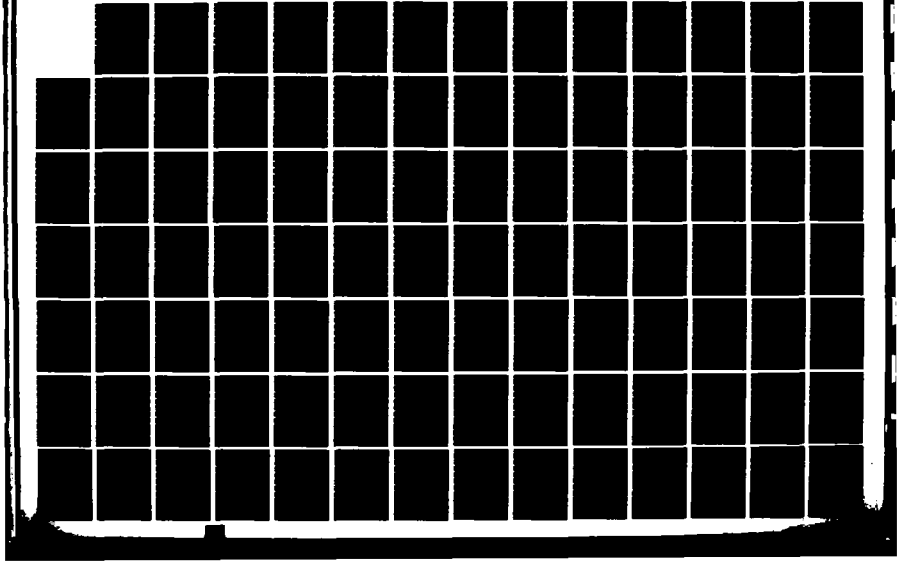

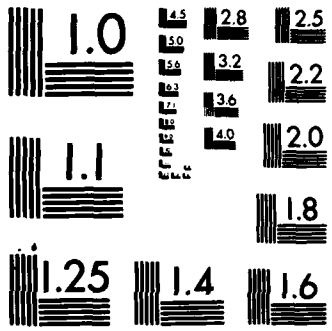

MICROCOPY RESOLUTION TEST CHART
NATIONAL BUREAU OF STANDARDS-1963-A

Since the integation process is essentially a summation, and since the statistical average of a product of two sums of terms is the sum of the averages of individual products of these terms, it is seen that,

$$R_{\mathrm{RAD}} = \mathrm{Re}\{<A_m>_m \Big[\int\int <W_m(\mathbf{x}_1)\, W_m(\mathbf{x}_2)><\Phi_r(\mathbf{x}_1)\, \Phi_r(\mathbf{x}_2)>\, d\mathbf{x}_1 d\mathbf{x}_2 + \int\int <W_m(\mathbf{x}_1)\Phi_r(\mathbf{x}_2)><W_m(\mathbf{x}_2)\Phi_r(x_1)>\, d\mathbf{x}_1 d\mathbf{x}_2 + \int\int <W_m(\mathbf{x}_1)\Phi_r(\mathbf{x}_1)><W_m(\mathbf{x}_2)\Phi_r(x_2)>\, d\mathbf{x}_1 d\mathbf{x}_2 \tag{6.9.18}$$

where, to simplify the notation $\mathbf{x}_s$ means $\mathbf{x}_{s(1)}$, etc. We now make the physical asumption that the reverberant displacment field is uncorrelated with the reverberant acoustic of velocity potential, so that the last intregrals in 6.9.18 vanish. Hence,

$$R_{\mathrm{RAD}} = \mathrm{Re}\left\{<A_m>_m \int\int R_w(\mathbf{x}_{s(1)},\, \mathbf{x}_{s(2)})\; R_\Phi\,(\mathbf{x}_{s(1)},\mathbf{x}_{s(2)})\, d\mathbf{x}_{s(1)} d\mathbf{x}_{s(2)}\right\} \tag{6.9.19}$$

$R_W(\mathbf{x}_1,\, \mathbf{x}_2) = <W_m(\mathbf{x}_1)\, W_m(\mathbf{x}_2)>_{(m)} =$ cross correlation of the reverberant displacement field. (units: non-dimensional)

$R_\Phi(\mathbf{x}_1,x_2) = <\Phi_r(\mathbf{x}_1)\Phi_r(\mathbf{x}_2)>_{(r)} =$ cross correlation of the reverbant acoustic) velocity potential field. units: non-dimensional)

where A_m is given by 6.9.16b. Eq. 6.9.19 states that the radiation resistance of a reverberant panel is proportional to the double surface integral of the product of the cross correlations (between spatial points) of the displacement field and the acoustic field both averaged over ensembles of randomly occurring modes. This same conclusion is found in Lyon and Maidanik [8] who evaluated $<A_m>_m$ on the basis that the power flow between modes may be modeled as a power flow between randomly excited harmonic oscillators. Their expression 6.9.19 is,

$$R_{\mathrm{RAD}}(\omega) = \frac{1}{2\pi \epsilon_s \epsilon_R} \rho_a c_a k_a^2 \int\int d\mathbf{x}_{s(1)} d\mathbf{x}_{s(2)}\, R_W(\mathbf{x}_{s(1)},\, \mathbf{x}_{s(2)}) R_\Phi(\mathbf{x}_{s(1)},\, \mathbf{x}_{s(2)}) \tag{6.9.20}$$

(units: Ns/m).

The symbols ϵ_s, ϵ_r are constants whose magnitudes depend on frequency range. At "higher frequencies" $\epsilon_R = 1/8$, $\epsilon_S = 1/4$ for the case of a two-dimensional structure [8]. It is important to note that while 6.9.19 and 6.9.20 have been derived by statistical averaging over many modes they are equally applicable to the case of forced drive in single modes.

When the panel vibraiton is either single mode or reverberant at the (forced) harmonic frequency ω it radiates a real acoustic power in the amount,

$$P(\omega) = <v_p^2>\; R_{\mathrm{RAD}}\,(\omega) \tag{6.9.21}$$

Here the mean-square normal component of velocity is defined in terms of the total energy E_T in the panel and the mass M_P of the panel,

$$<v_p^2> = \frac{E_T}{M_P} \tag{6.9.22}$$

In actual calculation of 6.9.20 the cross correlation fields R_w, R_Φ are *assumed* functions of spatial coordinates x,y of the surface. For example when a panel whose length in the x–direction is l, and in the y–direction h, is simply supported in an infinite regid baffle one *assumes*,

$$R_w(\mathbf{x}_1, \mathbf{x}_2) = \prod_{i=1}^{2} \sin\left(x_i + \frac{l}{2}\right) k_{px} \sin\left(y_i + \frac{h}{2}\right) k_{py}\, U\left[\left(\frac{l}{2}\right)^2 - x_i^2\right] U\left[\left(\frac{h}{2}\right)^2 - y_i^2\right] \quad (6.9.23)$$

[9], in which $U(a-b)$ has ony two values, O when $a < b$ and 1 when $a > b$. Similarly, for the acoustic field in the medium one assumes,

$$R_\Phi(\mathbf{x}_1, \mathbf{x}_2) = \frac{\sin k_a|\mathbf{x}_1 - \mathbf{x}_2|}{k_a|\mathbf{x}_1 - \mathbf{x}_2|} \quad (6.9.24)$$

These two cross correlation functons allow many cases of panel radiation to be treated (see Section 4.2).

6.10 RADIATION RESISTANCE OF RIBBED PANELS

Introduction:

Elastic surfaces set into vibration by spatial and temporal forces develop displacement patterns which are broadly classified *as free or forced.* When the disburbing force is essentially an impulse which terminates at time $t = 0$ a displacement vibration pattern appears whose form depends solely on the initial forced displacement and forced velocity. The vibration is then *free.* When however the forcing function continues indefinitely in time a vibration pattern appears whose form depends continuously on the spatial and temporal character of the driving force. The vibration is then *forced.* In the following exposition the statement that the elastic panel is vibrating in a mode means that a displacement vibration pattern of a natural mode is in existence no matter what the reason. A *modal pattern* can exist at any drive frequency when properly forced by the spatial character of the forcing function. A *reasonant modal pattern* exists only at the frequency of free virbration of the mode. It can be either forced by the drive at proper frequency or be free at the conclusion of the impulse. Any band of drive frequencies may correspond to one, two, several, or many resonant modes. The density of resonant modes increases with frequency. Estimates drawn from the theory of room acoustics show that a reverberant panel, volume V, has a mean number ΔN of resonant peaks within ω and $\omega + \Delta\omega$ given by $\Delta N \simeq \dfrac{V\omega^2}{2\pi^3 C^3}\Delta\omega$. This estimate may prove useful in applications.

Equations of motion of the panel; radiated power and pressure fields

The forced harmonic vibration of a finite-size thin rectangular plate loaded by a forcing function $Q(x,y)$ is described by 4.2.18,

$$(\nabla_T^4 - k_p^4) W = \frac{Q}{D};\ k_p(\omega) = \frac{\omega}{C_b} = \text{flexural wave number}$$

Here k_p is the temporal Fourier transform variable. Multiplying both sides by $-i\omega$ and defining $\dot{Q}(x,y) = -i\omega Q(x,y)$ (units: $Ns^{-1}m^{-2}$) lead to,

$$(\nabla_T^2 + k_p^2)(\nabla_T^2 - k_p^2)\dot{W}(x,y,\omega) = \dot{Q}(x,y,\omega)/D. \quad (6.10.1)$$

Let $\dot{W}(\mathbf{K}_T,\omega)$, $\dot{Q}(\mathbf{K}_T,\omega)$ be the spatial Fourier transforms of $\dot{W},\dot{Q}$ respectively, and let the transform of $\nabla_T^2\dot{W} = -k_T^2\dot{W}(\mathbf{K}_T,\omega)$, where $k_T^2 = |\mathbf{K}_T|^2$. Then the spatial transform of 6.10.1 is,

$$(k_T^2 - k_p^2)(k_T^2 + k_p^2)\dot{W}(\mathbf{K}_T,\omega) = \frac{\dot{Q}(\mathbf{K}_T,\omega)}{D} \quad (6.10.2)$$

The three-dimensional Fourier transform of the acoustic pressure in the medium in terms of the two-dimensional amplitude spectrum is,

$$p(x,y.z) = \int p(\mathbf{K}_T,\omega)\ e^{i\mathbf{K}_T\cdot\mathbf{r}_0} e^{ik_z z}\ \frac{d\mathbf{K}_T}{(2\pi)^2} \tag{6.10.3}$$

(see Sec. 3.7i). Here the total propagation wavenumber in the medium is the vector,

$$\mathbf{k} = \mathbf{K}_T + \hat{k}k_z,\ K_T = \hat{i}\mathbf{K}_x + \hat{j}\mathbf{K}_y.$$

Because the medium and the plate are coupled through radiation one requires at any frequency ω that

$$k_0^2 = \left(\frac{\omega}{C_0}\right)^2 = |\mathbf{K}|^2 = \mathbf{K}_T^2 + k_z^2$$

At the surface of the radiating panel, the boundary condition is Newton's force-acceleration law:

$$-\frac{\partial p(x,y,z)}{\partial z}\bigg|_{z=0} = \rho_0 \frac{\partial \dot{W}}{\partial t} = -i\omega\rho_0 \dot{W}. \tag{6.10.4}$$

Upon Fourier transformation, this becomes.

$$p(\mathbf{K}_T,\omega) = \frac{\omega\rho_0}{k_z}\ \dot{W}(\mathbf{K}_T,\omega). \tag{6.10.5}$$

The acoustic power $P(\omega)$ radiated from the surface is given by 1.7.1. In the steady state,

$$P(\omega) = \frac{1}{2}\ \mathrm{Re}\left\{\int p(x,y,0|\omega)\ \dot{W}^*(x,y|\omega)\ dS(x,y)\right\}.$$

Replacing $p, \dot{W}$ by their Fourier transforms one has,

$$P(\omega) = \frac{1}{2}\ \mathrm{Re}\left\{\int_{-\infty}^{\infty}\int\left[\int\int p(\mathbf{K}_T,\omega)e^{i\mathbf{K}_T\cdot\mathbf{r}_0}\ \dot{W}^*(R_T,\omega)e^{-i\mathbf{K}'_T\cdot\mathbf{r}_0}\frac{d\mathbf{K}'_T}{(2\pi)^2}\ \frac{d\mathbf{K}_T}{(2\pi)^2}\right.\right.$$

$$\left.\left.\times\ dS(\mathbf{r}_0).\right.\right.$$

Here it is assumed that the plate is embedded in an infinite rigid baffle so that the range of integration in area S can be extended to infinity. Noting that

$$\int_{-\infty}^{\infty}\int e^{i(\mathbf{K}_r-\mathbf{K}'_T)\cdot\mathbf{r}_0}\ dS(r_0) = \delta(K_T-K'_T)(2\pi)^2$$

it is seen from 6.10.5 that:

$$P(\omega) = \frac{1}{2}\ \mathrm{Re}\left\{\int \frac{\omega\rho_0}{k_z}\ |\dot{W}(\mathbf{K}_T,\omega)|^2\ \frac{d\mathbf{K}_T}{(2\pi)^2}\right\} \tag{6.10.6}$$

in which

$$k_z = (k_0^2 - k_T^2)^{1/2},\ k_0 = \frac{\omega}{C_0}.$$

Equation 6.10.6 shows that the radiated power can be obtained from a knowledge of the amplitude spectrum $\dot{W}(\mathbf{K}_T,\omega)$ of the normal component of surface velocity. Its form arises from the use of the boundary condition 6.10.5. Despite its simple-looking appearance the actual calculation of $\dot{W}(\mathbf{K}_T,\omega)$ must depend on the driving forces 6.10.2, and hence may be quite complicated.

In contrast to 6.10.6 a different formulation for calculating the radiation from plates is derived in Sec. 8.5. There the real power radiated from a plate into half-space bounded by a rigid baffle is found to be,

$$(a) \quad P(\omega) = \frac{<\dot{W}^2>_{peak}}{2} R_{rad}(\omega) \tag{6.10.7}$$

$$(b) \quad R_{rad}(\omega) = \frac{k^2 \rho_0 c_0 S^2}{4\pi^2} \int_0^{2\pi} d\phi \int_0^{\pi/2} |D\ (\zeta,\phi)|^2 \sin\zeta\, d\zeta \quad \left[\text{units: } \frac{Ns}{m}\right].$$

Ultimately this formula is obtained from 6.6.17a which describes radiation into full space ($0 \leqslant \zeta \leqslant \pi,\ 0 \leqslant \phi \leqslant 2\pi$) of a surface that develops a far-field radiation pattern $D(\zeta,\phi)$. In half-space ($0 \leqslant \zeta \leqslant \pi/2,\ 0 \leqslant \phi \leqslant 2\pi$) 6.6.17a reduces to 6.6.14 which is the same as 6.10.7. The calculation of the mean-square velocity $<\dot{W}^2>_{peak}$ can be approached via a summation of modal velocities, 8.5.2.

Because of the complex nature of plate radiation caused by excitation of abitrary form it is useful to consider first forced vibration of the plate at any frequency ω in a single mode (call it the *mn'th* mode). A single modal vibration may be *modeled* as a two-dimensional array of rectangular piston radiators each vibrating at frequency ω and phse θ_i. The symbol i serves to label the elementary piston in question. For simplicity, phase θ_i is recorded as + or— depending on whether the phase at the center of the equivalent plate cell is positive or negative. The acoustic power radiated by all the cells can be written from a knowledge of the mutual acoustic impedance R_{ij}:

$$(a) \quad P_{mn}(\omega) = \frac{1}{2}\sum_{ij} Q_i Q_j\ R_{ij}^{(A)} \quad (\text{units: } Nms^{-1})$$

$$(b) \quad Q_i = (<\dot{W}^2>)_i^{1/2}\ S_i \quad (\text{units: } m^3) \tag{6.10.8}$$

$$(c) \quad R_{ij}^{(A)} = \frac{k^2 \rho c}{4\pi^2} \int_0^{2\pi} d\phi \int_0^{\pi/2} |D_{ij}|^2 \sin\zeta\, d\zeta \quad (\text{units: } Nsm^{-5})$$

Here $|D_{ij}|^2$ is the square of the radiation pattern of any *two* pistons (*i'th* any *j'th*) as recorded in the farfield, and $R_{ij}^{(A)}$ is the *acoustic* resistance (units: Nsm^{-5}). According to the conventional labelling of modes a mode designated *mn* implies an array of *m* cells (or pistons) in the *x*-direction and *n* cells in the *y*-direction [10]. Fig. 6.10.1 shows a piston model of a simply supported plate, $l \times h$ in size, excited by forced drive in the 3,6 mode at frequency $f = \omega/2\pi$. In this model λ_{px}, λ_{py} are the plate wavelengths in the *x*-direction and *y*-direction respectively and λ_a is the wavelength of the acoustic field in the medium ($\lambda_a = 2\pi/k_0$). The radiation proper-

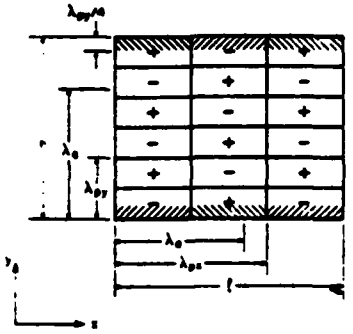

Fig. 6.10.1 A simply supported plate force-driven in the 3, 6 mode (after [11])

ties of this structure depend on the relative magnitudes of h, λ_a, λ_{py} etc. Assume that at frequency $f = c_0/\lambda_a$

$$(a) \quad h >> \frac{\lambda_a}{2} >> \frac{\lambda_{py}}{2}, \lambda_{px} >> \lambda_a$$

$$(b) \quad k_p/k_a > 1, \; k_{py}/k_a > 1, \; k_{px}/k_a < 1 \tag{6.10.9}$$

In this frequency range the phase cells can be modeled as point monopoles at the cell centers. Because $h >> \lambda_a/2$ and $\lambda_{px} >> \lambda_a$ the monopoles are decoupled [11]. Thus there is successive cancellation of volume velocity in the manner shown in Fig. 6.10.2. However, from 6.10.9b the specification in the y-direction is $\lambda/\lambda_{py} > 1$, while in the x-direction it is $\lambda_a/\lambda_{px} < 1$. This means that the radiation from the strip $(\lambda_{py}/4)l$ in the x-direction is much more efficient than the radiation from the strip $(\lambda_{px}/4)h$ in the y-direction. The reason is that a strip in the x-direction is radiating above coincidence, while a strip in the y-direction is radiating below coincidence. (Coincidence in this plate is described below.) Neglect of the latter leads to the concept of "x-strip modes." By exchanging subscript x for subscript y one can also develop the concept of "y-strip modes." Fig. 6.10.3 shows a k_T-space picture of the radiation modes of the plate shown in Fig. 6.10.1. By definition this is a plot of k_{py} vs k_{px} with the parameter being frequency divided by wave speed (c_p, plate; c_0 medium). The quarter-circle $k_p =$ constant indicates the relation,

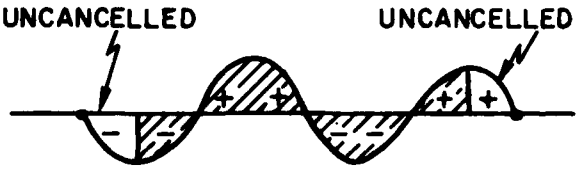

Fig. 6.10.2 Successive cancellation of volume velocity (shaded areas) leaving two uncancelled segments.

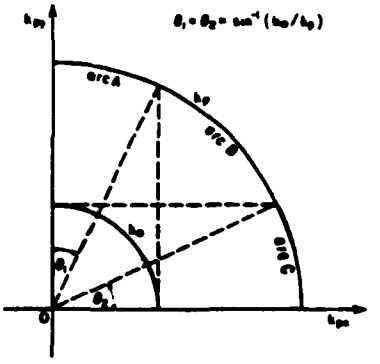

Fig. 6.10.3 k-space when $k_a \frac{1}{2} >> 1$ and $k_a \frac{h}{2} >> 1$ (after [11])

$$k_T^2 = k_{px}^2 + k_{py}^2 = k_p^2 = \text{const.}$$

Similarly, the quarter-circle k_a = const. indicates

$$k_a^2 = k_{px}^2 + k_{py}^2 = (\text{coincidence wave number})^2.$$

On this plot one defines coincidence by defining regions:

above coincidence: $k_p < k_a \quad (c_p \geqslant c_0)$
coincidence: $k_p = k_a \quad (c_p = c_0)$
below coincidence: $k_p > k_a \quad (c_p \leqslant c_0)$

The radiation resistance of a plate is a maximum when the frequency is above coincidence. By definition the x-strip modes lie on arc A while the y-strip modes lie on arc C.

A different radiation field is developed by a plate shown in Fig. 6.10.4. In this case one specifies:

$$(a)\ k_a \frac{l}{2} > 1,\ k_a \frac{h}{2} > 1$$
$$(b)\ \frac{k_p}{k_a} >> 1;\ \frac{k_{px}}{k_a} >> 1;\ \frac{k_{py}}{k_a} >> 1 \qquad (6.10.10)$$

Since $k = 2\pi/\lambda = \omega/c$, it is seen that at fixed frequency Eq. 6.10.10b reduces to,

$$(c)\ \frac{\lambda_a}{\lambda_p},\ \frac{\lambda_a}{\lambda_{px}},\ \frac{\lambda_a}{\lambda_{py}} >> 1$$

and

$$(d)\ \frac{c_o}{c_p},\ \frac{c_o}{c_{px}},\ \frac{c_o}{c_{py}} >> 1$$

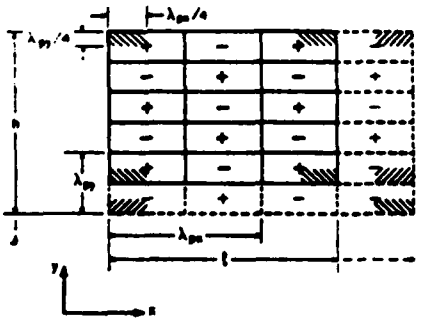

Fig. 6.10.4 A simply supported plate price-driven in the 3, 5 mode (full lines) or 4, 6 mode (dashed lines) (after [11]).

These conditions signify that radiation in both x and y directions are well below coincidence which makes them poor radiators. Successive cancellation of volume velocity leaves a residue of four corner monopoles of area approximately

$$\left[\frac{\lambda_{px}}{4}\right]\left[\frac{\lambda_{py}}{4}\right]$$

Because of conditions 6.10.10a these monopoles are *decoupled* from each other, and each contributes 1/4 of the total power radiated by the plate. At the frequency in question the plate is said to radiate in "piston modes." Such modes are located on arc *B* of Fig. 6.10.3.

Instead of 6.10.10a (= an acoustically large plate) one can specify.

$$k_a \frac{l}{2} << 1,\ k_a \frac{h}{2} << 1 \tag{6.10.11}$$

These conditions signify the plate is acoustically small. The piston monopoles are then strongly coupled so that the total power radiated depends on their relative phases. A convenient way to account for phase is to count the number of pistons in the rows and colums of the array matrix. An array is then specified as: (a) odd-odd (b) even-odd (c) even-even. The radiated power for these choices becomes:

(a) odd-odd. All four corner monopoles are in phase. The mutual resistance increases the radiation resistance of each element by a factor of four. Hence the radiated power is 16 times that of the uncoupled case.

(b) even-odd. Fig. 6.10.4 shows the 3,6 mode to consist of two dipoles in phase. Since the resistance of each dipole is doubled the total resistance is four times the resistance of one dipole. Hence the total output is four times the power of one dipole.

(c) even-even. Fig. 6.10.4 shows the 4,6 mode to be essentially a single quadrupole radiator because the phases are - + - +.

These states of radiation are shown in Fig. 6.10.5. Because $k_a << \pi/l$ and $k_a << \pi/h$, and $k_p >> k_a$, there are no strip modes at the frequency given in $k_p(=\omega/c_T$. This means no modes are to be found in arc *A* or arc *C*. All the modes are piston modes on arc *B*.

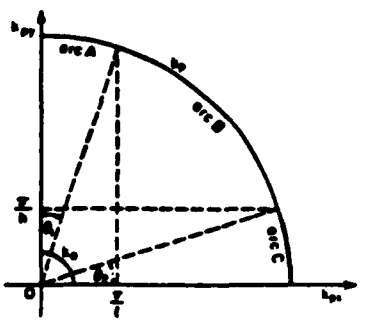

Fig. 6.10.5 *k*-space of a simply supported plate when $\frac{k_a l}{2}, \frac{k_a h}{2} << 1$ (after [11])

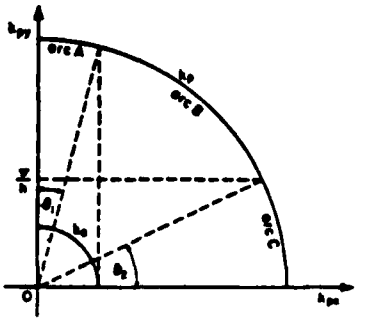

Fig. 6.10.6 *k*-space of a simply supported plate when $\frac{k_a l}{2} >> 1, \frac{k_a h}{2} >> 1$ (after [11]).

A plate which is acoustically large in the x-direction but acoustically small in the y-direction is specified by,

$$\frac{k_a l}{l} >> 1, \quad \frac{k_a h}{2} << 1$$

In the frequency range to there $k_{px} < k_a$ the radiation corresponds to that of x-strip which are coupled. The strips are in-phase if the mode in the y-direction is odd, but are out of-phase of the y mode is even. In the latter case the strips form an x-strip "dipole." Fig. 6.10.6 shows the mode describing this strip radiation to be located along arc A. When $k_{px} >> k_a$ only monopole (= piston radiation) is to be found at the frequency $\omega = k_p c_p$, $k_p >> k_a$. However these monopole are coupled in the y-direction because of the large wavelengths implied by the condition $\frac{k_a h}{2} << 1$. Again when the mode is odd in the y-direction the monopoles are in phase, while if it is even the radiation corresponds to that of a dipole. These piston modes occupy the arc B of Fig. 6.10.6. At the frequency $\omega = k_p c_p, k_p >> k_a$ no modes occupy arc C. This means there are no y-strip modes.

In actual calculation of real power radiated from a panel one is required to first calculate its radiation resistance. A convenient formula for doing this appears in Eq. 6.9.19, or (more explicity) 6.9.20 which is a form derived by Lyon and Maidanik [12]. The latter is repeated here for convenience,

$$R_{\text{RAD}} = \frac{16}{\pi} \rho_a c a_a k_a^2 \int\int d\mathbf{x}_1 \, d\mathbf{x}_2 \, R_w(\mathbf{x}_1, \mathbf{x}_2) \, R_\Phi(\mathbf{x}_1 \mathbf{x}_2) \tag{6.10.12}$$

in which $\mathbf{x}_1, \mathbf{x}_2$ are points on the surface of the plate. To use these formulas one requires explicit expressions for the cross correlation $R_w(\mathbf{x}_1, \mathbf{x}_2)$ of modal displacements, and the cross-correlation $R_\Phi(\mathbf{x}_1, \mathbf{x}_2)$ of the modal acoustic field. In a simple but useful case the panel is assumed to be simply supported in an infinite rigid baffle. Then R_w is given by 6.9.23 and R_Φ by 6.9.24. Upon performing the integration called for by 6.10.12 with these choices of correlations it will be found that explicit formulas for radiation resistance of a simply supported panel force-driven in a single-mode are obtainable only in approximation. A list of them drawn from Maidanik [11] is presented here.

List of Radiation Resistances of a Simply Supported Panel Force-Driven in Single Modes

Case I. $k_p/k_a < 1$ (above coincidence)

$$R_{RAD} \approx \frac{\rho_a c_a A_p}{\left[1 - \left[\frac{k_p}{k_a}\right]^2\right]^{1/2}} \tag{6.10.13}$$

Case II. $k_p \approx k_a$ (near or at coincidence)

$$R_{\text{RAD}} \approx \frac{\rho_a c a_a A_p}{3\sqrt{\pi}} \left[\left[\left(\frac{k_p}{k_{px}}\right) k_p l\right]^{1/2} + \left[\left(\frac{k_p}{k_{py}}\right) k_p h\right]^{1/2}\right] \tag{6.10.14}$$

Case III. $k_p/k_a > 1$ (below coincidence)

(1) $\frac{k_{px}}{k_a} < 1; \frac{k_{py}}{k_a} > 1$ (x-strip modes)

$$R_{\mathrm{RAD}}^{x} = \left[\frac{\rho_a c_a A_p \left(\frac{k_a}{k_{py}}\right)^2}{k_a h}\right]\left\{\frac{1 + \left\{\frac{k_p^2 - k_a^2}{k_{py}^2}\right\}}{[(k_p^2 - k_a^2)/k_{py}^2]^{3/2}}\right\} \tag{6.10.15}$$

(2) $\frac{k_{py}}{k_a} < 1; \frac{k_{px}}{k_a} > 1$ (y-strip modes)

$$R_{\mathrm{RAD}}^{y} = \frac{\rho_a c_a A_p \left(\frac{k_a}{k_{px}}\right)^2}{k_a l}\left\{\frac{1 + \left\{\frac{k_p^2 - k_a^2}{k_{px}^2}\right\}}{[(k_p^2 - k_a^2)/k_{px}^2]^{3/2}}\right\} \tag{6.10.16}$$

Case IV. $\frac{k_p}{k_a}, \frac{k_{px}}{k_a}, \frac{k_{py}}{k_a} >> 1$; and $\frac{k_a l}{2}, \frac{k_a h}{2} > 1$ (well below coincidence)

$$R_{\mathrm{RAD}} = \frac{\left(\frac{8\rho_a c_a}{\pi}\right)k_a^2}{(k_{px}\ k_{py})^2} \tag{6.10.17}$$

Case V. $\frac{k_a l}{2}, \frac{k_a h}{2} << 1$

(1) odd-odd modes

$$R_{\mathrm{RAD}}^{00} = \frac{\left(\frac{32\rho_a c_a}{\pi}\right)k_a^2}{(k_{px}\ k_{py})^2}\left\{1 + O\left[\left(\frac{k_a l}{2}\right)^2 + \left(\frac{k_a h}{2}\right)^2\right]\right\} \tag{6.10.18}$$

(2) even (x-direction) — odd (y direction) modes

$$R_{\mathrm{RAD}}^{e0} \approx \left(\frac{32\rho_a c_a}{3\pi}\right)\frac{k_a^2}{(k_{px}\ k_{py})^2}\left(\frac{k_a l}{2}\right)^2\left[1 + O\left(\frac{k_a h}{2}\right)^2\right] \tag{6.10.19}$$

(3) even (y-direciton)—odd (x-direction) modes. To find R_{RAD}^{0e} replace l by h in 4.2.62

(4) even-even modes.

$$R_{\mathrm{RAD}}^{ee} \approx \frac{32\rho_a c_a}{15\pi}\frac{k_a^2}{(k_{px}\ k_{py})^2}\left(\frac{k_a l}{2}\right)^2\left(\frac{k_a h}{2}\right)^2 \tag{6.10.20}$$

Case VI. $\frac{k_a h}{2} << 1$; $\frac{k_a l}{2} > 1$ (long narrow panels)

(1) odd modes in y-direction:

$$R^0_{RAD} \approx \begin{cases} \dfrac{4\rho_a c_a\, k_a l}{(k_{py})^2}, & \dfrac{k_{px}}{k_a} < 1 \\ \dfrac{16\,\rho_a c_a}{\pi}\,\dfrac{k_a^2}{(k_{py}\,k_{px})^2}, & \dfrac{k_{px}}{k_a} > 1 \end{cases} \tag{6.10.21}$$

(2) even modes in y-direction:

$$R^e_{RAD} \approx \begin{cases} \dfrac{4\rho_a c_a\, k_a l}{3k_{py}^2}\left[\dfrac{k_a h}{2}\right]^2, & \dfrac{k_{px}}{k_a} < 1 \\ \dfrac{16\,\rho_a c_a}{3\pi\, k_{px}^2 k_{py}^2}\left[\dfrac{k_a h}{2}\right]^2, & \dfrac{k_{px}}{k_a} >> 1 \end{cases} \tag{6.10.22}$$

In addition to single mode excitation the vibrating band in many practical situation must be treated as possessing a reverberant field of displacement. These radiate as x-strip modes (arc A in Fig. 6.10.5), y-strip modes (arc C), and piston modes (arc B). The acoustic power radiated is a sum of powers from these modes [11]

$$P_a = \sum_A \langle v_p^2 \rangle_A\, R^x_{RAD}\,(A) + \sum_B \langle v_p^2 \rangle_B\, R_{RAD}\,(B) + \sum_C \langle v_p^2 \rangle\, R^y_{RAD}\,(C) \tag{6.10.23}$$

For frequencies above coinsidence (where $k_j/k_a < 1$) the radiation resistance is independent of modal wavenumbers. Eq. 6.10.13 therefore applies to A, B, C modes indiscriminantly. For frequencies below coincidence we may assume that the modal density distributed along arc k_p at *forced drive* within a given narrow frequency aband is large enough to allow replacement of the summation signs in 6.10.23 by integral signs. Assuming $k_a l/2\; k_a h/2 > 1$ it is found [11] that,

$$R_{RAD} = \rho_a c_a\, A_p \left[\left(\frac{\lambda_a \lambda_p}{A_p}\right) g_1\left(\frac{f}{f_p}\right) + \frac{P_f \lambda_p}{A_p}\, g_2\left(\frac{f}{f_p}\right)\right],\ f < f_p. \tag{6.10.24}$$

$$R_{RAD} = \rho_a c_a\, A_p \left[\left(\frac{l}{l_p}\right)^{1/2} + \left(\frac{h}{l_r}\right)^{1/2}\right],\ f = f_p \tag{6.10.25}$$

where

$$g_1(\alpha) = \begin{cases} \dfrac{4}{\pi^4}\,\dfrac{(1-2\alpha^2)}{\alpha(1-\alpha^2)^{1/2}}, & f < \dfrac{1}{2} f_p, \\ 0, & f > \dfrac{1}{f_p}, \end{cases} \tag{6.10.26}$$

$$g_2(\alpha) = \frac{1}{(?-} - \frac{\left\{(1-\alpha^2)\ln\left[\dfrac{(1+\alpha)}{(1-\alpha)}\right] + 2\alpha\right\}}{(1-\alpha^2)^{3/2}} \tag{6.10.27}$$

$$P_r = 2(l + h) \tag{6.10.28}$$

Simlarly, for the cae $\frac{k_a l}{2}$, $\frac{k_a h}{2} << 1$ (acoustically small panels), one may assume,

(1) that the odd-even, even-even, and even-odd modes can be neglected compared to the "odd-odd" modes.

(2) that all modes have an equal probablity of occurrence.

(3) that $k_p l$, $k_p h >> \pi$.

Under these assumptions the radiation resistance to be used in the calculation of radiated acoustic power to given by,

$$R_{\text{RAD}} = \rho_a c_a A_p \left[\frac{r}{\pi^4}\right] P_r \frac{\lambda_p}{A_p} \cdot \left[\frac{f}{f_p}\right]^{1/2} \tag{6.10.29}$$

In all of these formulas $\lambda_p = 2\pi/k_p$, and A_p is the area of the panel.

6.11 REAL POWER AND REACTIVE POWER CALCULATED ON THE BASIS OF RETARDED AND ADVANCED GREEN'S FUNCTIONS

A different method of calculating radiation describes in this section is best illustrated by an example. Consider an infinite plane $z = 0$ on which the normal (surface) velocity $v_n(R_0,t_0)$ vanishes everywhere except over a small surface S. The velocity potential field everywhere in the half space $z \geqslant 0$ is given by 1.8.19:

$$\psi(\vec{R},t) = \frac{1}{2\pi} \int_0^t dt_0 \int dS(\vec{R}_0)\, v_n(\vec{R}_0,t_0)\, G_{\text{ret}}(\vec{R},\vec{R}_0|t,t_0) \tag{6.11.1a}$$

$$G_{\text{ret}} = \frac{\delta[t - t_0 - R/C]}{R};\ R = |\vec{R} - \vec{R}_0| \tag{6.11.1b}$$

Suppose now that to the retarded wave potential G_{ret} one adds the advanced wave potential G_{adv} to obtain a quantity $\bar{G}$, and subtracts G_{adv} to obtain a quantity H:

$$\begin{aligned} \bar{G} &= \frac{1}{2}\{G_{\text{ret}} + G_{\text{adv}}\} \\ H &= \frac{1}{2}\{G_{\text{ret}} - G_{\text{adv}}\} \\ G_{\text{ret}} &= \bar{G} + H \end{aligned} \tag{6.11.2}$$

In a physical sense $\bar{G}$ represents a sum of positive and negative and negative travelling waves due to a point source, while H represents a solution of the homogeneous (no source) wave equation. Now assume the sign of time t is changed,

$$G_{\text{ret}}(-t) = \frac{\delta\{-[t^* + R/c]\}}{R} = \frac{\delta[t^* + R/c]}{R}$$

$$G_{\text{adv}}(-t) = \frac{\delta\{-[t^* + R/c]\}}{R} = \frac{\delta[t^* - R/c]}{R}$$

$$t^* = t + t_0$$

It is seen that both G_{ret} and G_{adv} exchange roles. Substitution on 6.9.2 leads to,

$$\bar{G}(-t) = \frac{1}{2}\left\{\frac{\delta(t^* - R/c)}{R} + \frac{\delta(t^* + R/c)}{R}\right\} \tag{6.11.3a}$$

$$H(-t) = -\frac{1}{2}\left\{\frac{\delta(t^* - R/c)}{R} - \frac{\delta(t^* + R/c)}{R}\right\} \tag{6.11.3b}$$

The total power (reactive plus real) developed by the source velocity is given by interpation of

$$W(t) = \int I(\vec{R}_0,t)\,dS(\vec{R}_0) = \int \rho \frac{\partial \psi}{\partial t} v_n \delta S = \int \rho \left\{\frac{\partial \psi_G}{\partial t} + \frac{\partial \psi_H}{\partial t}\right\} v_n\, dS \tag{6.11.4}$$

where,

$$v_n = -\frac{\partial \psi}{\partial n}$$

The normal to the surface ($=n$) here points away from the medium. Applying 6.9.3 one sees that the power in 6.9.4 contributed by $\bar{G}$ changes sign when t becomes $-t$ because $\frac{\partial}{\partial(-t)} = -\frac{\partial}{\partial t}$. This power must therefore be nondissipative (that is it must be reactive). In contrast, the power contributed by H does not change sign when t becomes $-t$. It is real (or dissipative) power.

The concept of the advanced potential (that is, advanced Green's function) may therefore be used to distinguish real from imaginary power of a radiating source [13].

REFERENCES

1. E. Skudrzyk "Foundations of Acoustics." Vol. I.
2. Ref. [1], p.
3. Tables of Struve functions.
4. "Radiation Impedance and Gain of a One-Dimensional Array of Rings On An Infinite Rigid Cylinder" I. I. Belyakov and M.D. Smaryshev, Sov. Phy.-Acous. *18,* No. 2. Oct-Dec. 1972.
5. "Determination of the Gain and Single-Element Radiation Impedance of a Large Plane Periodic Array", M.D. Smaryshev, Sov. Phy.-Acous. *14,* No. 2. p. 218-223 Oct.-Dec. 1968.
6. V. M. Batenchuk et al. "Sound radiation from a plane waveguide with one perforated wall" Sov. Phy.-Acous. Vol. 26 (2) March-April 1980, p. 92-95.
7. K. Feik "Gerichteter Schall" Hochfreq und Electroakustik *64,* 35-62 (1955).
8. R.H. Lyon and G. Maidanik, JASA 34, 623 (1962); J. Schwinger, Phys. Rev. *75,* 1912-1925 (1949).
9. G. Maidanik, JASA 34, 809 (1962).

10. A.W. Leissa "Vibration of Plates" NASA SP-160, Sup. of Documents, U.S. Gov't Printing Office, Wash., D.C. 20402 (page 45).

11. G. Maidanik "Response of Ribbed Panels" JASA **34**, 809-826 (1962).

12. R.H. Lyon and G. Maidanik, JASA **34**, 623 (1962).

13. J. Schwinger, Phys. Rev. **75**, (1912-1925) (1949).

CHAPTER VII
THEORY OF TRANSIENT RADIATION

7.1 POISSON'S SOLUTION OF THE INITIAL VALUE PROBLEM OF VOLUME DISTRIBUTED SOURCES [1], [2], [3]

The transient solution for the velocity potential field Φ in the presence of space distributed sources and finite valued initial conditions is given by Eq. 1.7.7. The third term of this equation is the solution of the initial value problem,

$$\Phi(r, t) = -\frac{1}{c^2}\int_{v_0} dV_0 \left[\left(\frac{\partial G}{\partial t_0}\right)_{t_0=0}\Phi_0(r_0) - G_{t_0=0}\frac{\partial \Phi}{\partial t_0}(r_0)\right] \tag{7.1.1}$$

Here $\Phi_0(r_0)$, $\partial\Phi_0(r_0)/\partial\, t_0$ are the values over a *volume* of space of the velocity potential and derivative potential respectively at time $t_0 = 0$. G is the Green's function for the space in question. For simplicity we select infinite space where the Green's function in three dimensions may be written in the form

$$G = g\frac{(R, \tau)}{4\pi} = \frac{\delta_0\left(\frac{|r - r_0|}{c} - (t - t_0)\right)}{4\pi|r - r_0|} \tag{7.1.2}$$

in which δ_0 is the delta function symbol. To simplify geometrical constructions further the origin of coordinates is located at the observation point r, Fig. 7.1.1;

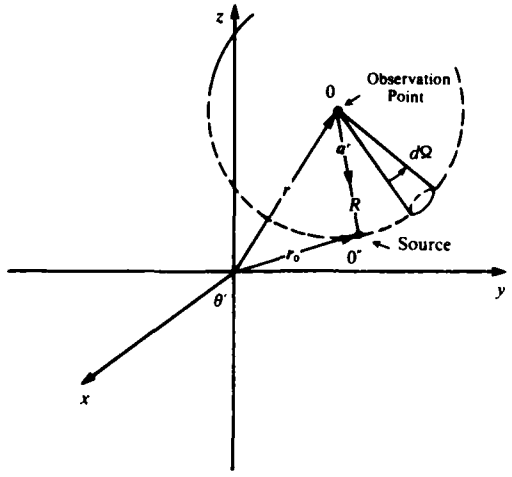

Fig. 7.1.1. Geometry associated with Poisson's solution of the Initial Value Problem.

The volume of source space ($= V_0$) where the initial values of Φ, $\partial\,\Phi/\partial\,t$ are prescribed is now given by the element of volume,

$$dV_0 = R^2 dR d\Omega \tag{7.1.3}$$

$$d\Omega = \sin\theta_0 d\theta_0 d\phi_0$$

$$R = |r - r_0|^*$$

in which,

$$r_0 = r + Ra_r$$

$$a_r = (\sin\theta_0 \cos\phi_0,\ \sin\theta_0 \sin\phi_0,\ \cos\theta_0).$$

In this source space we combine 7.1.1 and 7.1.2, and write the field at r_0 to be,

$$\Phi(r_\infty, t) = \frac{1}{4\pi} \int d\Omega \left[\int \frac{d|r_0|}{c} \frac{|r_0|}{c} \left(\frac{\partial \Phi_0}{\partial t_0} (r_0) \right) \delta_0\left(\frac{|r_0|}{c} - t \right) \right.$$

$$\left. - \int \frac{d|r_0|}{c} \frac{|r_0|}{c} \Phi_0(r_0), \frac{\partial}{\partial t_0} \delta_0\left(\frac{|r_0|}{c} - (t - t_0) \right) \right]_{t_0=0} \tag{7.1.4}$$

This equation involving the delta function and its time derivative may be directly integrated by making use of the following two properties of these special functions [4]:

$$\int_{-\infty}^{+\infty} f(\xi)\, \delta_0(\xi - x)\, d\xi = f(x) \tag{7.1.5a}$$

$$\int_{-\infty}^{+\infty} f(\xi) \frac{d\delta}{d\xi} (\xi - x) d\xi = -\frac{d}{dx} f(x) \tag{7.1.5b}$$

Assuming a set of distribution functions Φ, $\partial\,\Phi/\partial\,t$ which vanish at infinity we apply these formulas to 7.1.4 for the distance $|r_0| = ct$ (as required) and obtain the result,

$$\Phi(r_\infty, t) = t \int \frac{d\Omega}{4\pi} \frac{\partial \Phi_0}{\partial t} (0 + cta_r) + \frac{\partial}{\partial t} t \int \frac{d\Omega}{4\pi} \Phi_0(0 + cta_r) \tag{7.1.6a}$$

When the observation point r differs from zero 7.1.6a is generalized to the form,

$$\Phi(r, t) = t \int_\Omega \frac{d\Omega}{4\pi} \frac{\partial \Phi_0}{\partial t} (r + cta_r)$$

$$+ \frac{\partial}{\partial t} t \int_\Omega \frac{d\Omega}{4\pi} \Phi_0(r + cta_r) \tag{7.1.6b}$$

This is Poisson's solution (formulated in 1819) in three dimensions of the initial value problem of wave propagation.

Discussion: Eq. 7.1.6b may be thought of in the following way. At source time $t_0 = 0$ there is distributed throughout space an acoustic pressure (= first term) and a velocity potential) = second term). This distribution is a function of coordinates r_0, θ, ϕ. As time increases a wave of pressure and

velocity potential propagates throughout space, and arrives at the observation point. To find the field at the observation at any time $t(t > 0)$ 7.1.6b states that we must *average* the *initial* pressure and velocity potential over a sphere (centered at the observation point) whose radius is just ct, using the (mathematical) distribution of the initial field prescribed by the problem. In brief the field at the center of the sphere where the observer is located is determined by an average field over the sphere whose radius is the "time of flight" $(= ct)$.

Eq. 7.1.6b is a solution of the initial value problem in 3-dimensions. For additional solutions in 2, 1 dimensions the reader is referred to [6]. Instead of initial distributions in volume space we have another problem in transient radiation which arises from the distribution of impulsive sources over the *surface* boundaries of a domain. This problem, whose formal solution is given by the second term of 1.7.7 will be discussed in detail in the following sections.

7.1.a Transient Radiation from Acoustically Small Volume Sources

The velocity potential everywhere generated by a volume distributed source $q(\mathbf{r}_0, t_0)$ in free space is given by 1.7.7. In the absence of radiation from extraneous surfaces and from imposed initial conditions, this potential is obtained from the free space Green's function:

$$\psi(\mathbf{r},t) = \int dt_0 \int_{\text{vol}} \frac{\delta\left[\frac{|r - r_0|}{c} - (t - t_0)\right]}{4\pi |r - r_0|} q(r_0, t_0)\, dV(r_0) \tag{7.1.7}$$

Assume $q(\mathbf{r}_0, t)$ is the monopole source Q (see Eq. 1.8.3). Then since QdV has the units of $m^3 s^{-1}$ it is interpretable as the differential volume velocity $d\dot{V}(r_0, t_0)$. From the properties of the delta function an integration over t_0 and r_0 readily yields the formula,

$$\psi(r, t) = \frac{\dot{V}\left(t - \frac{r}{c}\right)}{4\pi r} \quad \text{(units: } m^2 s^{-1}\text{)}. \tag{7.1.8}$$

Because of the approximation $|r - r_0| \sim r$, 7.18 is valid only when $|r|$ is very much larger than the characteristic wavelength being radiated. In deriving this expression it has been assumed that the direction of the positive normal to the volume's surface is away from the medium. The acoustic pressure radiated to a point at distance r is then

$$p = \rho_0 \frac{\partial \psi}{\partial t} = \rho_0 \frac{\partial \dot{V}(t^*)}{\partial t^*} \frac{\partial t^*}{\partial t} = \frac{\rho_0 \ddot{V}\left(t - \frac{r}{c}\right)}{4\pi r}. \tag{7.1.9}$$

$$t^* = t - \frac{r}{c}.$$

If the positive normal to the volume's surface is written as n_+ then from the discussion in Sect. 1.11 it is seen that the surface velocity into the medium is,

$$v_+ = -\frac{\partial \psi}{\partial n_+}. \tag{7.1.10}$$

The corresponding radial (surface) velocity written as v is found from 7.1.8 using the conventions of Fig. 1.11.1;

$$v(r, t) = -\frac{\partial \psi}{\partial r} = -\frac{\partial \psi}{\partial t^*} \frac{\partial t^*}{\partial r} = \frac{\ddot{V}\left(t - \frac{r}{c}\right)}{4\pi r c} \tag{7.1.11}$$

Eqs. 7.1.10 and 7.1.11 show that the acoustic field generated at distances $r >> \lambda$ is proportional to the temporal history of the volume *acceleration* at the source point calculated at *retarded* time, that is, time t delayed by amount r/c.

The instantaneous power radiated to this far field is the integral

$$W(t) = \int \frac{p^2(\mathbf{r}, t)}{\rho_0 C} \, dS(\mathbf{r}) = \int \rho c \, v^2(\mathbf{r}, t) \, dS(\mathbf{r}) \tag{7.1.12}$$

where S is a closed surface surrounding the source. At distance r one has $dS = r^2 \sin\theta v\theta v\phi$. Since $\ddot{V}$ is omnidirectional the instantaneous power becomes.

$$W(t) = \frac{\rho_0 \ddot{V}^2(t)}{4\pi c} \quad \text{(units: } Nm\ s^{-1}\text{)}. \tag{7.1.13}$$

The mean value of power radiated is obtained by averaging the square of the volume acceleration in time T,

$$\bar{\ddot{V}} = \frac{1}{T} \int \ddot{V}^2(t) \, dt \tag{7.1.14}$$

so that,

$$W_{AV} = \frac{\rho_0 \bar{\ddot{V}}^2}{4\pi c}. \tag{7.1.15}$$

We next consider the source $q(\mathbf{r}_0, t_0)$ to be caused by a force $\mathbf{F}(r_0, t_0)$ per unit volume, from 1.8.3,

$$q(\mathbf{r}_0, t_0) = -\int_{-\infty}^{t_0} \frac{\nabla \cdot \mathbf{F}(r_0 \tau)}{\rho_0} \, d\tau \quad \text{(units: } s^{-1}\text{)}.$$

Assuming the time interval $\Delta\tau$ of integration is short enough so that the integrand becomes the divergence of an inpulse $\mathbf{F}^*$ we write,

$$q(\mathbf{r}_0, t_0) = \frac{-\nabla^* \cdot \mathbf{F}^*(r_0, t_0)}{\rho_0} \tag{7.1.16}$$

$$\mathbf{F}^* \approx F \Delta\tau \hat{\mathbf{e}} \quad \text{(units: } Nsm^{-3}\text{)} \tag{7.1.17}$$

in which $\hat{\mathbf{e}}$ is a unit vector. With this definition of source q the field of velocity potential is again determined by 7.1.7,

$$\psi = \int dt_0 \int_{\text{vol}} \frac{\delta\left[\frac{|\mathbf{r} - \mathbf{r}_0|}{c} - (t - t_0)\right]}{4\pi |\mathbf{r} - \mathbf{r}_0|} \left[\frac{-\nabla \cdot \mathbf{F}^*(\mathbf{r}_0, t_0)}{\rho_0}\right] dV(\mathbf{r}_0). \tag{7.1.18}$$

At distances $r >> \lambda$,

$$\psi = \frac{-1}{4\pi r \rho_0} \int_{\text{vol}} \nabla \cdot \mathbf{F}^*\left(\mathbf{r}_0, t - \frac{r}{c}\right) dV(\mathbf{r}_0). \tag{7.1.19}$$

Since the component of the gradient that is applicable in this case of spherical waves is the radial component we can write,

$$\nabla \cdot \mathbf{F}^* = \frac{\partial F}{\partial n_+} \Delta\tau \, \hat{\mathbf{e}} \cdot \hat{\mathbf{n}}_+ = \frac{\partial F}{\partial r} \Delta\tau \, \hat{\mathbf{e}} \cdot \hat{\mathbf{r}} = -\frac{\dot{F}\Delta\tau}{c} \hat{\mathbf{e}} \cdot \hat{\mathbf{r}}$$

so that

$$\psi(r,t) = \frac{1}{4\pi r\rho_0}\int_{vol}\frac{\dot{F}\Delta\tau}{c}\,\hat{\mathbf{e}}\cdot\hat{\mathbf{r}}\,d\dot{V}(r_0) \tag{7.1.20}$$

or

$$\psi(r,t) = \frac{1}{4\pi r\rho_0 c}\mathscr{F}(t-\tfrac{r}{c})\cdot\hat{\mathbf{r}} \tag{7.1.21}$$

where

$$\mathscr{F}(t-\tfrac{r}{c}) = \int \dot{F}(\mathbf{r}_0,\ t-\tfrac{r}{c})\,\Delta\tau\,\hat{\mathbf{e}}\,dV(\mathbf{r}_0), \quad \text{(units: } N\text{)}.$$

Using the conventions of Fig. 1.11.1 the radial velocity v is seen to be,

$$\mathbf{v} = \frac{-\partial\psi}{\partial r} = \frac{1}{4\pi r\rho_0 c^2}(\mathscr{F}\cdot\hat{\mathbf{r}})\,\hat{\mathbf{r}} \tag{7.1.22}$$

in which

$$\mathscr{F}(t^*) = \frac{\partial^2\mathscr{F}}{\partial t^{*2}},\ t^* = t - R/c, \quad \text{(units: } Ns^{-1}\text{)}. \tag{7.1.23}$$

The mean value (time averaged) power is again given by an integral over a sphere of radius r,

$$W_{AV} = \int \rho c\,(\mathbf{v}\cdot\mathbf{v})\,dS(r)$$

$$W_{AV} = \int\int \frac{\rho_0 c}{(4\pi r\rho_0 c^2)^2}\,(\mathscr{F}\cdot\hat{\mathbf{r}})^{\bar{2}}\,r^2\sin\theta\,d\theta\,d\phi.$$

If we align the *axes* of $\boldsymbol{F}$ and $\hat{\mathbf{r}}$ such that

$$(\mathscr{F}\cdot\hat{r})^2 = \ddot{F}^2\cos^2 0$$

then,

$$W_{AV} = \frac{1}{16\pi^2\rho_0 c^3}\,\frac{2}{3}\,\ddot{\bar{F}}^2(2\pi) \quad \text{(units: } Nms^{-1}\text{)}. \tag{7.1.24}$$

In the steady state (at frequency ω),

$$W_{AV} = \frac{\rho_0\omega^4}{12\pi c^3}\left[\frac{F}{\rho_0}\right]^2 \tag{7.1.25}$$

Here, $\mathscr{F}$ (units: Ns) is the force impulse over the volume V ($F = FV\Delta\tau$), and the ratio F/ρ_0 is the magnitude of dipole source strength (units: m^4s^1). This ratio is the same as the symbol $|D_\omega|$ of Ref. [3a], and $|A|$ of Ref. [3b].

7.1b TRANSIENT RADIATION OF ACOUSTIC MULTIPOLES

According to 1.7.7 the velocity potential at $\mathbf{r}$, t due to a volume source $q(\mathbf{r}_0,t)$ in an unbounded medium is,

$$\psi(\mathbf{r}, t) = \int_0^t dt_0 \int_v \frac{\delta\left[\frac{R}{c} - (t - t_0)\right]}{4\pi R} q(\mathbf{r}_0, t_0)\, dV(\mathbf{r}_0) \quad \text{(unit: s}^2\text{)}$$

$$R = |\mathbf{r} - \mathbf{r}_0|. \tag{7.1.26}$$

Let $q(\mathbf{r}_0, t_0)$ be considered a set of acoustic multipoles defined by 1.8.3. We seek first the contribution of the dipole (or force) term. The radiated acoustic pressure due to this term is,

$$p_D(R, t) = \rho \int_0^t dt_0 \int_V \left[\frac{\partial/\partial t'}{\partial t} \int_{-\infty}^{t_0} \frac{\nabla \cdot \mathbf{F}(\mathbf{r}_0, t')}{\rho}\, dt'\right] \frac{\delta\left[R_c - (t - t_0)\right]}{4\pi R}\, dV(\mathbf{r}_0)$$

$$= \int_0^t dt_0 \int_V \frac{\delta\left[\frac{R}{c} - (t - t_0)\right]}{4\pi R} \nabla \cdot \mathbf{F}(\mathbf{r}_0, t_0)\, dV(\mathbf{r}_0). \tag{7.1.27}$$

To evaluate 7.1.27 one first integrate by parts:

$$\int G \nabla \cdot F\, dV = \int - F \cdot \text{grad}\, G\, dV + \int_0^\infty \nabla \cdot (G\mathbf{F})\, dV(r_0). \tag{7.1.28}$$

Since $\mathbf{F}$ vanishes outside the (point) source region the second term on the rhs is seen by use of Gauss's divergence theorems to vanish. In the first term on the rhs, we note that

$$\mathbf{F} \cdot \text{grad}\, G = \text{grad}\left[\frac{\delta\left[\frac{R}{c} - (t - t_0)\right]}{4\pi R}\right]$$

$$\mathbf{F} \cdot \text{grad}\, G = \frac{1}{4\pi R} \sum_{i=1}^{3} \delta'\left[\frac{R}{c} - (t - t_0)\right]\left[\frac{1}{c}\right]\left[\frac{-X_{i0}}{R}\right] F_i(\mathbf{r}_0, t_0) \tag{7.1.29}$$

$$+ \frac{1}{4\pi} \sum_{i=1}^{3} \delta\left[\frac{R}{c} - (t - t_0)\right] \frac{1}{R^2}\left[\frac{-X_{i0}}{R}\right] F_i(\mathbf{r}_0, t_0)$$

in which $\delta'(t)$ is the derivative with respectable.

Integration over t_0 (as called for in 7.1.27) together with use of 7.1.5 then give,

$$p_D(R, t) = \frac{-1}{4\pi R} \sum \frac{-X_{i0}}{R}\left[\frac{-1}{c}\int_V F'_i(\mathbf{r}_0, t - R/c)\, dV(\mathbf{r}_0) - \frac{1}{R}\int_V F(\mathbf{r}_0, t - R/c)\, dV(\mathbf{r}_0)\right]. \tag{7.1.30}$$

Since a multipole is essentially a point function we can assume it to be located at the origin:

$$\mathbf{F}(\mathbf{r}_0, t_0) = \delta(\mathbf{r}_0)\mathbf{f}(t_0) \quad \text{(units of } f\text{: N)}. \tag{7.1.31}$$

Taking account of the minus sign of the dipole term in 1.8.3 one arrives at a formula for the radiated field of a transient dipole:

$$p_D(\mathbf{r}, t) = \frac{1}{4\pi r} \sum_{i=1}^{3} \left[\frac{X_{i0}}{r}\right]\left[\frac{1}{c} f_i^{\bullet}(t - R/c) + \frac{1}{r} f_i(t - R/c)\right]. \tag{7.1.32a}$$

Here $|X_{i0}/r|$ are the direction cosines ($= \cos\theta_i$). This expression agrees with 5.2.4. An alternate form is obtained by defining a transient increment of source strength ΔD_i operation over a brief time interval Δt,

$$\Delta D_i(t - r/c) \equiv \frac{\Delta f_i\left[t - \frac{r}{c}\right]\Delta t}{\rho} \quad \text{(units: m 4 /s)}. \tag{7.1.32b}$$

For short enough time,

$$\frac{\Delta D_i}{\Delta t} \to \frac{\partial D_i}{\partial t}.$$

Hence 7.1.13 takes on the form

$$p_D(\mathbf{r}, t) = \frac{\rho}{4\pi} \sum_{i=1}^{3} \left[\frac{x_{i0}}{r}\right]\left[\frac{1}{rc} \frac{\partial^2 D_i(\tau)}{\partial \tau^2} + \frac{1}{r^2} \frac{\partial D_i(\tau)}{\partial \tau}\right]_{\tau = t - r/c}. \tag{7.1.32c}$$

The contribution of the quadrupole term of 1.8.3 to the radiated pressure is

$$p_q(R, t) = \rho \int_0^{t'} dt_0 \int_V \left[\frac{\partial}{\partial t'} \int_{-\infty}^{t_0} \nabla \cdot \frac{\tau(\mathbf{r}_0, t')}{\rho} \cdot \nabla_0 dt'\right] \frac{\delta\left[\frac{R}{c} - (t - t_0)\right]}{4\pi 4} dV(\mathbf{r}_0)$$

$$p_q(R, t) = \int_0^{t'} dt_0 \int_V G \nabla_0 \cdot \overline{\tau}(r_0, t_0) \cdot \nabla_0 dV(\mathbf{r}_0) \tag{7.1.33}$$

in which

$$G(\mathbf{r}, t/r_0, t_0) = \frac{\delta\left[\frac{R}{c} - (t - t_0)\right]}{4\pi R}.$$

After integrating twice by parts using the reasoning of 7.1.28, 7.1.29, and 5.4.18 on reduces 7.1.33 to,

$$p_q(R, t) = \int_0^{t'} dt_0 \int_V \overline{\tau}(\mathbf{r}_0, t_0) : \nabla_0 G(\mathbf{r}, t/r_0, t_0) \nabla_0 dV(\mathbf{r}_0) \tag{7.1.34}$$

in which the double dot indicates an operation of double divergence. Assuming now that the quadrupole being a point source is located at the origin one can write,

$$\bar{\tau}(\mathbf{r}_0, t) = \delta(\mathbf{r}_0)\mathbf{t}(t_0) \quad \text{(units of t: Nm)} \tag{7.1.35}$$

in which the quantity $\mathbf{t}(t_0) = \{t_{ij}\}$, $i = x, z = j$ is a dyadic with 9 components. The quantity $\nabla_0 G \nabla_0$ is also a dyadic with 9 components,

$$\nabla_0 G \nabla_0 = \left\{ \frac{\partial^2}{\partial X_{i0} \partial X_{j0}} \frac{\delta\left[\frac{R}{c} - (t - t_0)\right]}{4\pi R} \right\}, \quad i = 1, 2, 3, = j.$$

Thus 7.1.34 is a sum of a term $p_{i0}(R, t)$. To exemplify the method of calculating any one of them we choose a particular component, say the longitudinal component xx. Now,

$$\frac{\partial^2}{\partial X_{10}^2} G = \frac{1}{4\pi}\left[\frac{X_{10}^2}{C^2R^3}\delta''(\tau) \frac{-3X_{10}^2}{R^4C}\delta'(\tau) + 3\frac{X_{10}^2}{R^5}\delta(\tau)\right] \tag{7.1.36}$$

$$\tau = \frac{R}{c} - (t - t_0).$$

Thus by use of 7.1.5,

$$P_{xx}(R, t) = \frac{x_{10}^2}{4\pi}\int_0^t dt_0 \int_V \left[\frac{S''(\tau)}{C^2R^3} - \frac{3\delta'(\tau)}{R^4C} + \frac{3\delta(\tau)}{R^5}\right] t_{xx}(t_0)\delta(r_0)\, dV(r_0)$$

$$P_{xx}(R, t) = \frac{X_{10}^2}{4\pi r^2}\left\{\frac{t_{xx}''(t - R/c)}{C^2 r} + \frac{3t_{xx}'(t - r/c)}{cr^2} + \frac{3t_{xx}(t - r/c)}{r^3}\right\}. \tag{7.1.37}$$

Thus the radiation of a transient longitudinal (x-direction) quadrupole. The quantity t_{xx} may be interpreted as an impulse source strength Q_{xx} (over time Δt) by use of the definition,

$$\Delta Q_{xx} = \left[\frac{t_{xx}(t - r/c)}{\rho}\right]\Delta t \quad \text{(units: m}^5\text{/s)}. \tag{7.1.38}$$

In spherical coordinates r, θ, ϕ,

$$\frac{X_{10}}{r} = \frac{r \sin\theta \cos\phi}{r} = \sin\theta \cos\phi.$$

Hence in terms of impulsive source strenghts (7.1.38) the radiated pressure is,

$$p_{xx}(\mathbf{r}, t) = \frac{\rho}{4\pi}\sin^2\theta \cos^2\phi \left\{\frac{\partial^3 Q_{xx}(\tau)}{\partial\tau^3(C^2 r)} + \frac{3\partial^2 Q_{xx}(\tau)}{\partial C^2(Cr^2)} + \frac{3\partial Q_{xx}(-C)}{\partial\tau(r^3)}\right\} \tag{7.1.39a}$$

in which we have taken Δt so small that

$$\frac{\Delta Q_{xy}}{\Delta t} = \frac{\partial Q_{xy}}{\partial t}.$$

The structure of an xz guadrupole is obtained in similar fashion:

$$p_{xz}(\mathbf{r}, t) = \frac{\delta}{4\pi} \cos\theta \sin\theta \cos\phi \times \left\{ \frac{1}{C^2 r} \frac{\partial^3 Q_{xz}(\tau)}{\partial \tau^3} + \frac{3}{Cr^2} \frac{\partial^2 Q_{xz}(\tau)}{\partial \tau^2} + \frac{3}{r^3} \frac{\partial Q_{xz}(\tau)}{\partial \tau} \right\} \tag{7.1.39b}$$

in which

$$\tau = t - r/c$$

$$\Delta Q_{xz} \equiv \frac{t_{xz}(\tau)}{\rho} \Delta t.$$

As before. the prime signs indicate derivatives with respect to argument.

The remaining terms of 1.8.3 may be similarly treated. We define monopole source strength Q as,

$$Q(\mathbf{r}_0, t_0) = \delta(\mathbf{r}_0) Q(t_0), \text{ (units of } Q\text{: m}^3/\text{s}). \tag{7.1.40}$$

Substituting this into 7.1.26, then using the relation $p = \rho \partial\psi/\partial t$, one arrives at the radiation formula for the acoustic field of a transient monopole source:

$$p_Q(r, t) = \frac{\rho}{4\pi_{r_\epsilon}} \frac{\partial}{\partial \tau} Q(\tau), \quad \tau = t - r/c. \tag{7.1.41}$$

In the same way the radiation due to transient heat flow is obtained by defining (units: Nm/s)

$$\epsilon(\mathbf{r}_0, t_0) = \delta(\mathbf{r}_0)\epsilon(t_0), \text{ (units of } \epsilon\text{: Nm/s)}. \tag{7.1.42}$$

Thus the radiated pressure is,

$$p_\epsilon(r, t) = \frac{\rho}{4\pi r} \frac{\partial}{\partial \tau} \left[\frac{\alpha\gamma\kappa}{C_p} \epsilon(\tau) \right] \tag{7.1.43}$$

$$\tau = t - r/c.$$

7.2 GENERAL FORMULAS FOR THE CALCULATION OF TRANSIENT RADIATION FROM SOURCES ON A SURFACE

Let $\psi(r, t)$ represent a time-varying (non-sinusoidal) velocity potential associated with a small amplitude acoustic field. We assume this field to be caused by a distribution of acoustic sources over a closed surface S_0. At time $t < t_0$ let the acoustic field be non-existent over all space,

$$\psi(t) = \partial\psi/\partial t = 0, t < t_0 \tag{7.2.1}$$

When $t = t_0 = 0$ the sources on S_0 are suddenly excited to produce a field $\psi(r, t)$ on S_0 and in all space external to S_0. At the instant of excitation we allow 7.2.1 to still prevail. Subsequently (when $t^* > t_0 = 0$) the field $\psi(r, t)$ no longer identically vanishes over all space. Under these conditions the field at r and at time t^* may be determined from the second term of Eq. 1.7.7, in which G is replaced by $g/-4\pi$ to emphasize certain aspects of the radiated field,

$$\psi(r, t^*) = \int_0^{t^*} dt_0 \int_{S_0} dS_0 \cdot \left(\frac{g}{-4\pi} \operatorname{grad}_0 \psi - \psi \operatorname{grad}_0 \frac{g}{-4\pi} \right) \tag{7.2.2}$$

Here $-g/4\pi$ is the time varying nonsinusoidal Green's function for the scalar wave equation and the type of boundary surface in question. By this is meant that Green's function g satisfies the following differential equation,

$$\text{(a)} \quad \nabla_0^2 \frac{g}{-4\pi} - \frac{1}{c^2} \frac{\partial^2 g}{\partial t^2} \left(\frac{1}{-4\pi} \right) = \delta(r - r_0)\, \delta(t - t_0)$$

In the steady state,

$$\text{(b)} \quad g = \frac{\exp ikR}{R}; \tag{7.2.3}$$

in the transient state

$$\text{(c)} \quad g = \frac{\delta\left[\frac{r - r_0}{c} - (t - t_0)\right]}{|r - r_0|}$$

According to the symbol conventions used in this treatise we locate sources in space-time at r_0, t_0, and observation points in space-time at r, t. Now both g and ψ may be considered as sums of spectral components, thus possessing the Fourier transforms G, Ψ respectively,

$$\text{(a)} \quad g(r, t | r_0, t_0) = \frac{1}{2\pi} \int_{-\infty}^{+\infty} G(r | r_0 | \mathrm{K})\, e^{-iKc(t - t_0)}\, dKc$$

$$\text{(b)} \quad \psi(r, t_0) = \frac{1}{2\pi} \int_{-\infty}^{+\infty} \Psi(r, \omega)\, e^{-i\omega t_0}\, d\omega \tag{7.2.4}$$

The advantage of this representation is that $G(r|r_0|\mathrm{K})$ is the field at r due to a "monochromatic wave" (= *single* spectral component) at r_0. By considering single spectral wave components only the complex problems associated with finding general time-varying solutions to the wave equation is much simplified. We may therefore directly substitute 7.2.4a, 7.2.4b, into 7.2.2 and attempt a solution of the resulting integral equation. This is, in general, a very difficult mathematical problem if the distribution of sources and the acoustic nature of the surface are arbitrary. Analytic procedures lead to intractable equations and numerical methods must be used. In many important applications however the sound generating surfaces (= baffles) may be so constructed that 7.2.2 becomes further simplified by the elimination of the first or the second term on the right-hand side. Thus we may make the surface surrounding the sources ideally acoustically hard, or ideally acoustically soft. In symbols, we may select surfaces in such a way that in the steady state, at all surface points where there are no sources,

$$\text{(a)}\quad \text{hard surface:}\quad \frac{\partial G(rr_0K)}{\partial n} = 0,\ r \text{ on } S_0, \tag{7.2.5}$$

or

$$\text{(b) soft surface: } G(r\,r_0\,K) = 0, \qquad r \text{ on } S_0,$$

For the hard surfaces 7.2.5a, 7.2.4a, 7.2.4b and 7.2.2 are first combined. Then, writing the operator $dS_0\,\text{grad}_0 = dA_0\,\partial/\partial\,n_0$, where the normal n_0 points into the *interior* of the surface, one obtains,

$$\psi(r,\,t) = \frac{1}{4\pi^2}\int_0^{t^+} dt_0 \int_A dA_0 \int_{-\infty}^{+\infty}\int_{-\infty}^{+\infty} \frac{G}{-4\pi}\,(r|r_0|\mathrm{K})\,\frac{\partial}{\partial n_0}\,\Psi(r_0,\,\omega)\,e^{-i\mathrm{K}ct}$$

$$\times\, e^{i(\mathrm{K}c-\omega)t_0}\,d\omega d\mathrm{K}c. \tag{7.2.6}$$

[6]

It is noted that all the mathematical operators on the right-hand side operate on the source coordinates (r_0, t_0), and in particular that the Fourier transformation of ψ is on the t_0 coordinates. Now,

$$\int_0^{t^+} dt_0\, e^{i(\mathrm{K}c-\omega)t_0}\, e^{-i\mathrm{K}ct} = \frac{-i}{\mathrm{K}c-\omega}\,\{e^{-i\omega t^+} - e^{-i\mathrm{K}ct}\} \tag{7.2.7}$$

in which, for $t>0$, one sets $\exp(-i\mathrm{K}ct)\exp(i\mathrm{K}ct^+) = 1$. With this choice, 7.2.6 may then be written as a sum of two terms,

$$\psi(r,\,t) = \psi_{ss}(r,\,t) + \psi_{tr}(r,\,t) \tag{7.2.8a}$$

where

$$\psi_{ss}(r,\,t) = \frac{-i}{4\pi^2}\int_{-\infty}^{+\infty} e^{-i\omega t}\,d\omega\left[\int_{-\infty}^{+\infty}\frac{d\mathrm{K}c}{\mathrm{K}c-\omega}\int_{A_0}\frac{G(r|r_0|\mathrm{K})}{-4\pi}\,\frac{\partial}{\partial n_0}\,\Psi(r_0,\,\omega)\,dA_0\right] \tag{7.2.8b}$$

$$\psi_{tr}(r,\,t) = \frac{-i}{4\pi^2}\int_{-\infty}^{+\infty} e^{-i\mathrm{K}ct}\,d\mathrm{K}c\left[\int_{-\infty}^{+\infty}\frac{d\omega}{\omega-\mathrm{K}c}\int_{A_0}\frac{G(r|r_0|\mathrm{K})}{-4\pi}\,\frac{\partial}{\partial n_0}\,\Psi(r_0,\,\omega)\,dA_0\right] \tag{7.2.8c}$$

Here, as before $G(r|r_0|\mathrm{K})$ is the Fourier transform of $g(r|r_0|t)$.

In 7.2.8b the entity inside the brackets on the right-hand side is the Fourier transform of that part of the field which is expressible in terms of the ω coordinate spectral components. Eq. 7.2.8b thus represents the field arising from the time fluctuation of the surface velocities. The corresponding entity in the brackets of 7.2.8c is the Fourier transform of that part of the field which is expressible in terms of the $\mathrm{K}c$ coordinate spectral components. Eq. 7.2.8c thus represents the field arising from the time fluctuation of the time-dependent Green's function.

In 7.2.8b, 7.2.8c the path of integration in the complex K-plane passes through the simple poles of G and the isolated pole $\mathrm{K}c = \omega$ along the real K-axis. To evaluate these integrals we must close the contour "at infinity" by contour integration in the K-plane using Jordan's Lemma. This procedure is

described in Appendix 7A. It is applied here to evaluation of 7.2.8b and 7.2.8c. Since we desire solutions which are convergent for both the temporal condition $t \to \infty$, and the spatial condition $r \to \infty$, we must appropriately shape the contour in each case. To do this we make K complex by assigning a small damping constant, i.e.,

$$K = K_1 \pm iK_2 \tag{7.2.9}$$

The choice of sign depends on the following considerations. Select the time coordinate to be given by $e^{-i\omega t}$. Since spatially divergent waves which die out at infinity are required we chose G in such a way that

$$G(r|r_0|K) \to \frac{e^{iKcr/c}}{r}, \; r \to \infty \tag{7.2.10}$$

Combining this with the factor e^{-iKct} in 7.2.8c and using 7.2.7 we find that the *total* exponential factor in 7.2.8c will (for large r and large t) eventually become

$$\exp[iK_1CT] \exp[i(\pm iK_2)CT] \tag{7.2.11}$$

in which $T = r/c - t$ is the retarded time. Two cases are possible

$$\text{Case I} : T > 0, \text{ i.e. } r/c > t$$

$$\text{Case II}: T < 0, \text{ i.e. } r/c < t$$

Case I: When $t < r/c$ the principle of causality requires that both ψ_{ss} and ψ_{rr} vanish. For convergence in time we select the plus sign in 7.2.11, i.e., the pole $\omega = Kc$ lies above the axis of reals. Now if the *Im* $K > 0$ the Green's function is analytic, that is, G has no poles in the upper half of the K-plane. (This is the analytic statement of causality). Hence when $t < r/c$ we run the contour of integration above the pole $\omega = Kc$ parallel to the axis of reals from $-\infty$ to $+\infty$ and close the contour in the upper half plane. Since the closed contour embraces no poles the result of the contour integration is that both ψ_{ss} and ψ_{rr} vanish, as required.

Case II: when $t > r/c$ we select the minus sign in 7.2.11.

The contour line of integration in the complex K-plane now runs slightly below the axis of reals from $-\infty$ to $+\infty$. The choice of contour closure between the upper and lower half-plane is determined once again by convergence requirements. We consider 7.2.8b first. Assume the singularities of $G(r|r_0|K)$ to be simple poles in the lower half plane so that $G(r|r_0|K)$ can be written in the form $R(r|r_0|K_p)/(K - K_p)$. It is then seen that a closure of the contour in the lower half plane would leave residues of singularities of the type $K_pc = \omega, K_p = (K_p)_1 \pm i(K_p)_2$ in the evaluated integral. Upon inversion from ω to t there would appear the factors e^{iK_pct}, which, in view of our choice minus sign in 7.2.9 would make the field $\psi_{ss}(r, t)$ divergent as $t \to \infty$. We must therefore close the contour of 7.2.8b in the upper half plane. Since there is only one enclosed pole ($Kc = \omega$), one obtains the convergent solution,

$$\psi_{ss}(r, t) = \frac{1}{2\pi} \int_{-\infty}^{+\infty} e^{-i\omega t} d\omega \int_{A_0} \frac{G(r_0|r_0|\omega)}{-4\pi} \frac{\partial}{\partial n} \Psi(r_0, \omega) \, dA_0 \tag{7.2.12}$$

Next we consider 7.2.8c. If we close the contour in the upper half plane the single enclosed pole $\omega = Kc$ would make 7.2.8c equal to 7.2.8b but with opposite sign. The sum of the two fields, $\psi_{ss} + \psi_{tr}$, would then vanish. This is inadmissible. We must therefore close the contour of 7.2.8c in the lower half plane, which leads to the result that will be the sum of residues of singularities of G in the lower half plane,

$$\psi_{tr}(r, t) = -\frac{1}{2\pi} \sum_{p} e^{-iK_p ct} \int_{-\infty}^{+\infty} \frac{d\omega}{\omega - K_p c}$$

$$\times \int_A R(r|r|K) \frac{\partial}{\partial n_0} \Psi(r_0, \omega)\, dA_0 \tag{7.2.13}$$

In view of the choice of the minus sign (see 7.2.11) it follows that,

$$\psi_{tr} \to 0, \; t \to \infty \tag{7.2.14}$$

The field ψ_{tr} has therefore the nature of a *transient* field. In contrast ψ_{ss} does not vanish as $t \to \infty$.

Both 7.2.8b, 7.2.8c may be written in a different and more illuminating form by expanding the Green's function G in a series of products of orthonormal functions $\Phi_n(r)$ as shown in 3.4.5b,

$$\frac{G(r|r_0|K)}{4\pi} = \sum_{n} \frac{\Phi_n^*(r_0)\, \Phi_n(r)}{K_n^2 - K^2} \tag{7.2.15}$$

(units of $\Phi_n = (\text{meter})^{-3/2}$)

If we perform the integration over the variable K in the K plane by contour integration, running the contour *above* the axis of reals from $-\infty$ to $+\infty$, and then closing the contour at infinity in the *lower* half plane, we obtain for 7.2.8c the following formula,

$$\psi_{tr}(r, t) = \frac{ic^2}{2\pi} \sum_{n=0}^{\infty} \frac{\sin K_n ct}{K_n c} \int_{-\infty}^{+\infty} \frac{d\omega}{\omega - K_n c}$$

$$\times \int_A \Phi_n^*(r_0)\, \Phi_n(r) \frac{\partial}{\partial n_0} \Psi(r_0, \omega)\, dA \tag{7.2.16}$$

Here, as before, $t > r/c$. In this sum all the poles K_n lie in the right half of the K plane. For convergence as $t \to \infty$ we require the imaginary parts of K_n to be negative. Eq. 7.2.16 is useful for *interior domains*, i.e., domains in which resonant frequencies exist. For exterior domains (= infinite space) we may more easily use the following. In 7.2.2 place a distribution of delta sources. Then,

$$\psi(r, t) = \frac{1}{4\pi} \int_0^{t^+} \int dS_0 \cdot \left\{ \frac{\delta_0[t_0 - (t - R/c)]}{R} \vec{\nabla}_0 \psi_S \right.$$

$$\left. - \psi_S \vec{\nabla}_0 \left[\frac{\delta[t_0 - (t - R/c)]}{R} \right] \right\} \tag{7.2.17}$$

Integration over t_0 yields,

$$\psi(r, t) = \frac{1}{4\pi} \int dS_0 \cdot \left[\frac{\nabla_0 \psi(r_0, t_0)}{R} + \frac{R}{R^3} \psi(r_0, t_0) \right.$$
$$\left. \frac{-R}{CR^2} \frac{\partial}{\partial t} \psi(r_0, t) \right] \tag{7.2.18}$$
$$R = \vec{r} - r.$$

This formula embodies the Kirchoff-version of Huygens' principle which is that the wavefront at r, and at time t, may be determined by adding together all the equivalent sources in a previously existing wavefront calculated at the earlier time $t - R/c$.

The general formulas derived in this section are difficult to apply. In the following sections we will consider particular cases which have proved tractable.

7.2a TRANSIENT RADIATION IN ABSTRACT FORMULATION

The transient radiation generated by a surface forced to vibrate by transient forces is given by 1.7.7 in terms of Green's functions. Alternatively the wave equation 1.7.3 is solved, subject to initial as well as boundary, conditions. When the vibrating surface conforms to a separable surface in one of the eleven coordinate systems of the Helmholtz equation [6a] this alternative solution is advantageous for analysis and calculation. The procedure is outlined here.

Let ξ, η, ζ be a system of separable coordinates, $X_\alpha^{(1)}(\xi)$, $X_\beta^{(2)}(\eta)$ be orthogonal characteristic functions which describe surfaces in these coordinates, and let $X_{\alpha\beta}^{(3)}(\zeta)$ be the function which shows the normal-to-the-surface (radial) dependence of the solution to the wave equation. The velocity potential everywhere in the steady state is obtained by superposition of these characteristic functions,

$$\psi(\vec{r}, \omega) = \sum_{\alpha\beta} A_{\alpha\beta}(\omega) X_\alpha^{(1)}(\xi) X_\beta^{(2)}(\eta) X_{\alpha\beta}^{(3)}(\zeta) e^{-i\omega t} \tag{7.2.17}$$

The physical cause of this potential is a normal component of velocity on a selected surface. Although this velocity is itself caused by applied forces it is useful to calculate the radiation field by assuming a fixed velocity distribution. Assume then that the normal velocity at surface $\zeta = \zeta_0$ has the form,

$$v(\zeta_0, t) = V f_1(\xi) f_2(\eta) f(t) \tag{7.2.18}$$

in which f_1, f_2, f are non-dimensional descriptors of the spatial and temporal variation of velocity and v is the magnitude of velocity. Upon Fourier transformation of 7.2.18 with respect to time the boundary condition in the steady state becomes,

$$-\nabla_n \psi(\xi, \eta, \zeta_0, \omega) = v(\zeta_0, \omega)$$

or

$$\sum_{\alpha\beta} A_{\alpha\beta}(\omega)\ X_{\alpha}^{(1)}(\xi)\ X_{\beta}^{(2)}(\eta)\left(\frac{\partial X_{\alpha\beta}^{(3)}(\zeta)}{\partial h_{\zeta}\zeta}\right)_{\zeta=\zeta_{\alpha}} = -Vf_1(\xi)f_2(\eta)f(\omega) \tag{7.2.19}$$

The symbols h_{ζ} (as well as h_{ξ}, h_{η} used below) are scale factors of the separable coordinate system. Also,

$$f(\omega) = \int_{-\infty}^{\infty} f(t)\, e^{+i\omega t}\, dt \qquad \text{(units: } s\text{)}$$

Each coefficient $A_{\alpha\beta}$ can be isolated by orthogonality,

$$A_{\alpha\beta}(\omega) = \frac{-Vf(\omega)\int\int f_1(\xi)f_2(\eta)\ X_{\alpha}^{(1)}(\xi)\ X_{\beta}^{(2)}(\eta)\, d(h_{\xi}\xi)\, d(h_{\eta}\eta)}{N_{\alpha}^{(1)}\, N_{\beta}^{(2)}\left(\frac{\partial X_{\alpha\beta}^{(3)}(\zeta)}{\partial h_{\zeta}\zeta}\right)_{\zeta=\zeta_{\alpha}}} \tag{7.2.20}$$

Again, $N_{\alpha}^{(1)}$, $N_{\beta}^{(2)}$ are normalizations. Substitution of 7.2.20 into 7.2.17 and execution of an inverse Fourier transformation with respect to time lead to an expression for the transient velocity potential everywhere:

$$\psi(\vec{r},\ t) = \frac{-V}{2\pi}\sum_{\alpha,\beta}\int_{-\infty}^{\infty}\frac{f(\omega)\, d\omega e^{-i\omega t}}{N_{\alpha}^{(1)}N_{\beta}^{(2)}}\ \frac{1}{\left(\frac{\partial X_{\alpha\beta}^{(3)}(\zeta)}{\partial h_{\zeta}\zeta}\right)_{\zeta=\zeta_{\alpha}}}$$

$$\int\int f_1(\xi)f_2(\eta)\ X_{\alpha}^{(1)}(\xi)\, X_{\beta}^{(2)}(\eta)\, d(h_{\xi}\xi)\, d(h_{\eta}\eta) \tag{7.2.21}$$

The factor $1/\pi$ is inserted in the inverse Fourier transformation and omitted in the direct transformation.

This formula will now be applied to several examples.

7.2b TRANSIENT RADIATION OF A MONOPOLE IN FREE SPACE

In monopole radiation there is no variation of the velocity potential field with spherical angles θ, ϕ. Hence for a monopole of spherical radius $r = \mathrm{R}$, and a specified velocity

$$v(\mathrm{R}\ \omega) = Vf(\omega) \tag{7.2.22}$$

the expansion constant $A_{\alpha\beta}$ in 7.2.20 reduces to

$$A_{\alpha\beta}(\omega) = \frac{-Vf(\omega)}{\left(\frac{\partial X^{(3)}(r)}{\partial r}\right)_{r=R}} \tag{7.2.23}$$

Eq. 3.2.3 indicates that,

$$X^{(3)}(r) = \frac{e^{ikr}}{r} \tag{7.2.24}$$

Thus, the velocity potential everywhere $r \geq R$ is,

$$\psi(r, R) = \frac{VR^2 f(\omega)\, e^{ik(r-R)} e^{-i\omega t}}{(1 - ikR)r} \tag{7.2.25}$$

Accordingly, the transient pressure field due to 7.2.20 is given $p = -i\omega\varrho\psi$, where ψ is 7.2.17 and 7.2.21:

$$p(r, t) = \int_{-\infty}^{\infty} \frac{(-i\omega\varrho)VR^2 f(\omega) e^{i\omega/c(r-R)}}{r(1 - i\omega/cR)}\, e^{-i\omega t}\, \frac{d\omega}{2\pi} \tag{7.2.26}$$

In this formula the radius R is kept constant during the integration. For an expanding monopole R = R (t). If the radial velocity ω R (t) is much less than the speed of sound c the error of keeping R (t) constant during the integration is small. In this case it is a good approximation to integrate 7.2.26 for R = const., then substitute the indefinite integral,

$$R(t) = \int v f(t)\, dt \tag{7.2.27}$$

in the result.

Several cases have been treated [6b].

Case I. Radial velocity is a rectangular pulse.

In this case,

$$v(t) = \begin{cases} V = V_0 & 0 < t < T_0 \\ 0 & \text{otherwise} \end{cases}$$

Then,

$$f(\omega) = \frac{1}{-i\omega}\, [1 - \exp(i\omega T_0)] \qquad \text{(units: } s\text{)}$$

Upon integration of 7.2.26 one obtains,

$$p(r, t) = \begin{cases} 0 & t < \dfrac{r-R}{c} \\ \varrho c V_0\, \dfrac{R}{r}\, \exp\left\{-\dfrac{c}{R}\left[t - \dfrac{r-R}{c}\right]\right\}, & t\,\dfrac{r-R}{c} < t < \dfrac{c}{r-R} + T_0 \\ \varrho c V_0\, \dfrac{R}{r}\left[\exp\left\{-\dfrac{c}{R}\left[t - \dfrac{r-R}{c}\right]\right\}\right. & \\ \left. - \exp\left\{-\dfrac{c}{R}\left[t - \left(\dfrac{r-R}{c} + T_0\right)\right]\right\}\right], & t > \dfrac{r-R}{c} + T_0 \end{cases} \tag{7.2.28}$$

Using the approximation that 7.2.27 is constant during integration, then substituting it into 7.2.28, one finds a convenient formula for the transient pressure field in terms of time variable t as a replacement for R (t):

$$R(t) = \int V_0 dt = V_0 t \qquad 0 < t < T_0 \tag{7.2.29}$$

$$R(t) = R_0 \qquad t > T_0$$

Thus,

$$p(r, t) = \cdot \begin{cases} 0 & t < \dfrac{r}{c} \\ \varrho c \dfrac{V_0^2}{r} t \exp\left\{ \dfrac{r}{V_0} \left(\dfrac{1}{t} - \dfrac{c + V_0}{r} \right) \right. & \dfrac{r}{c} < t < T_0 \\ \varrho c V_0 \dfrac{R_0}{r} \left[\exp\left\{ - \dfrac{c}{R_0} \left[t - \dfrac{r - R_0}{c} \right] \right\} \right., & \\ \left. - \exp\left\{ - \dfrac{c}{R_0} \left[t - \left(\dfrac{r - R_0}{c} + T_0 \right) \right] \right\} \right], & t > T_0 \end{cases} \tag{7.2.30}$$

Fig. 7.2.1 show the transient response as a function of the choice of T_0 relative to R /c. The labels indicate,

a_1: a rectangular pulse

b_1: $T_0 \gg R/c$

c_1: $T_0 \approx R/c$

d_1: $T_0 \ll R/c$

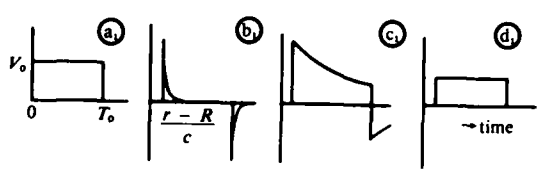

Fig. 7.2.1. Transient response of a monopole excited by a rectangular pulse as a function of the magnitude T_0 (after [6b]).

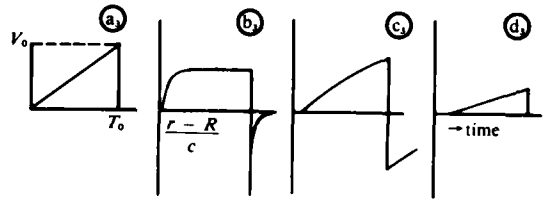

Fig. 7.2.2. Transient reponse of a monopole radiator excited by a saw-tooth pulse as a function of T_0 (after [6b]).

Case II. Radial velocity is a linear ramp saw tooth

In this case,

$$v(t) = \begin{cases} at, & 0 < t < T_0 \\ 0 & \text{otherwise} \end{cases}$$

Then,
$$a = \frac{V_0}{T_0}$$

$$f(\omega) = \frac{1}{T_0}\left[\frac{\exp(i\omega T_0)}{(-i\omega)^2} + \frac{T_0\exp(i\omega T_0)}{(-i\omega)} - \frac{1}{(-i\omega)^2}\right]$$

When this is substituted in 7.2.26 and integrated, the pressure field everywhere becomes,

$$p(r,t) = \begin{cases} 0 & t < \dfrac{r-R}{c} \\ \dfrac{a\varrho R^2}{r}\left[1-\exp\left\{-\dfrac{c}{R}\left[t-\dfrac{r-R}{c}\right]\right\}\right], & \dfrac{r-R}{c} < t < \dfrac{r-R}{c} + T_0 \\ \dfrac{a\varrho R^2}{r}\left[\exp\left\{-\dfrac{c}{R}\left[t-\left(\dfrac{r-R}{c}+T_0\right)\right]\right\}\right. & \\ \left.-\exp\left\{-\dfrac{c}{R}\left[t-\dfrac{r-R}{c}\right]\right\}\right]- & \\ -\dfrac{T_0 a\varrho cR}{r}\exp\left\{-\dfrac{c}{R}\left[t-\left(\dfrac{r-R}{c}+T_0\right)\right]\right\}, & t > \dfrac{r-R}{c} + T_0 \end{cases} \tag{7.2.31}$$

Again one can find $R(t)$ from 7.2.27,

$$\begin{aligned} R(t) &= \int at\,dt = \frac{at^2}{2}, & t < T_0 \\ R(t) &= R_0 & t > T_0 \end{aligned} \tag{7.2.32}$$

By assuming $R(t)$ is nearly constant during integration of 7.2.26, then substituting it into 7.2.31, one obtains:

$$p(r,t) = \begin{cases} 0 & t < \dfrac{r}{c} \\ \dfrac{a^3\varrho}{4r}\,t^4\left[1-\exp\left\{\left(\dfrac{2r}{at^2}-\dfrac{2c}{at}-1\right)\right\}\right] & \dfrac{r}{c} < t < T_0 \\ \dfrac{a\varrho R_0^2}{r}\left[-\exp\left\{-\dfrac{c}{R_0}\left[t-\dfrac{r-R_0}{c}\right]\right\}\right. & \\ \left.+\exp\left\{-\dfrac{c}{R_0}\left[t-\left(\dfrac{r-R_0}{c}+T_0\right)\right]\right\}\right]- & \\ -\dfrac{T_0 a\varrho cR_0}{r}\exp\left\{-\dfrac{c}{R_0}\left[t-\left(\dfrac{r-R_0}{c}+T_0\right)\right]\right\} & t > T_0 \end{cases} \tag{7.2.33}$$

in which, as before, $a = V_0/T_0$.

Fig. 7.2.2 shows details of the transient response as a function of the choice of T_0 relative to R /c.

a_3: a saw-tooth pulse
b_3: $T_0 \gg$ R /c
c_3: $T_0 \approx$ R /c
d_3: $T_0 \ll$ R /c

Two other cases of importance are:

$$\text{quadratic pulse:} \quad v(t) = \begin{cases} \dfrac{V_0}{T_0^2}\, t^2 & 0 < t < T_0 \\ 0 & \text{otherwise} \end{cases}$$

$$\text{triangular pulse:} \quad v(t) = \frac{V_0}{T}\, t \qquad 0 < t < T_0/2$$

$$- \frac{V_0}{T}\, t + 2V_0 \qquad T_0/2 < t < T_0$$

These are discussed by Probst, [6b].

7.3a TRANSIENT RADIATION OF A RIGID PISTON IN AN INFINITE RIGID BAFFLE

The theory of the harmonic generation of sound by a rigid piston in an infinite rigid baffle, completely investigated in classical times may be extended to include the generation of transient signals. The appropriate coordinate system here is that of cylindrical coordinates r, ϕ, Z. Let r_0, ϕ_0, Z_0 be the *source coordinates* of a vector $\vec{r}_0$ and let dS_0 be an element of piston area of a piston of radius b. Now if n_0 is the normal pointing *away* from a volume V_0 in which the sound field is under study then for a piston executing harmonic motion of frequency $\omega = kc$ in an infinite rigid baffle the velocity potential at the tip of vector $\vec{r}$ whose coordinates are r, ϕ, Z, is given by

$$\Phi_\delta(r, \phi, z, t) = \frac{-e^{j\omega t}}{2\pi} \iint_{S_0} \frac{e^{-jkR}}{R} \frac{\partial \Phi}{\partial n_0}\, dS_0 \tag{7.3.1}$$

in which $R = |\vec{r} - \vec{r}_0|$. Let $v(\vec{r}_0)$ be the normal component of piston velocity whose positive direction points into the volume V_0. Then, from the boundary condition 1.8.25,

$$v(r_0, \phi_0, z_0) = - \frac{\partial \Phi_\delta}{\partial n_0} \tag{7.3.2}$$

To evaluate 7.3.1 subject to boundary condition 7.3.2 we expand the spherical function e^{-jkR}/R into an infinite series of integrals in cylindrical coordinates [7]

$$\frac{e^{-jkR}}{R} = -j \sum_m (2 - \delta_{om}) \cos[m(\phi - \phi_0)]$$
$$\times \int_0^\infty \frac{J_m(ur)\, J_m(ur_0)}{\sqrt{k^2 - u^2}}\, e^{\sqrt{k^2 - u^2}\,|z - z_0|}\, u\, du \tag{7.3.3}$$

Substitution of 7.3.3 into 7.3.1 followed by an integration over the area of the piston yields the complete harmonic solution of the integral 7.3.1. To, find the transient solution due to the excitation $V(r_0, \phi_0)\, \delta_0(t)$ we make the formal transformation $j\omega \rightarrow s$ in 7.3.1, 7.3.2, 7.3.3. The transformed function $\Phi_\delta(s)$ then represents the Laplace transform of the velocity potential at the field point (r, ϕ, z) due to a velocity distribution $v(r_0, \phi_0,)$ over the piston area, excited in time as a Dirac impulse function at $t = 0$. In effect the transformation $j\omega \rightarrow s$ causes the time variable in the real domain to change from $e^{+j\omega t}$ to $\delta_0(t)$. Since we are interested in more general time functions we next allow the velocity to change from $v(r_0, \phi_0)\, \delta_0(t)$ to $v(r_0, \phi_0, t)$ and form the Laplace transformation $L\{v\}$ of this latter velocity. The transient solution due to $v(r_0, \phi_0, t)$ is then found by multiplying the Laplace transform $\Phi(r, \phi, z, s)$ by $L\{v\}$ and then performing the inverse transformation to recover the time domain. For convenience we change variables in 7.6.3 by letting $uc = \zeta$, (units of ζ: $\sec^{-1}$). Then, for a disc of radius b, we have

$$\text{(a)} \qquad \Phi(r, \phi, z, s) = \Phi_\delta(r, \phi, z, s)\ \mathcal{L}\{v\}$$

Now,

$$j[k^2 - u^2]^{1/2} = j\left[-\frac{s^2}{c^2} - \frac{\zeta^2}{c^2}\right]^{1/2} = \frac{1}{c}\sqrt{s^2 + \zeta^2}$$

because $\sqrt{-1} = -j$. Thus

$$\text{(b)} \qquad \Phi(r, \phi, z, s) = \frac{1}{2\pi}\int_0^{2\pi} d\phi_0 \int_0^b \mathcal{L}\{v\} \sum_m (2 - \delta_{om})$$

$$\times \cos[m(\phi - \phi_0)] \int_0^\infty \frac{J_m(\zeta r/c)\, J_m(\zeta r_0/c)\, e^{-|z - z_0|/c\sqrt{s^2+\zeta^2}}}{c\sqrt{s^2 + \zeta^2}}\, \zeta d\zeta\, r_0 dr_0 \tag{7.3.4}$$

We shall perform the inverse transformation of 7.3.4, by first taking $L^{-1}\{\Phi_s\}$. From [8],

$$\mathcal{L}^{-1}\left\{\frac{e^{-|z - z_0|/c\sqrt{s^2+\zeta^2}}}{\sqrt{s^2 + \zeta^2}}\right\} = U\left(t - \frac{|z - z_0|}{c}\right) J_0\left(\sqrt{t^2 - |z - z_0|^2/c^2}\right) \tag{7.3.5}$$

where,

$$U(x) = 0, \qquad x < 0$$

$$U(x) = 1, \qquad x \geq 0.$$

$\Phi(r, \phi, z, t)$ is then obtained by forming the convolution of 7.3.5 with $L^{-1}\{v\}$. The result is,

$$\Phi(r, \phi, z, t) = \int_{-\infty}^{t} U\left(\tau - \frac{|z - z_0|}{c}\right) c d\tau \int_0^{2\pi} d\phi_0 \int_0^b \sum_m (2 - \delta_{om})$$

$$\times \cos[m(\phi - \phi_0)]\, v(r_0, \phi_0, t - \tau) \int_0^\infty J_0(u\sqrt{c^2\tau^2 - |z - z_0|^2}\,)\, J_0(ur)\, J_m(ur_0)$$

$$\times u du r_0 dr_0 \tag{7.3.6}$$

[9]

This formula represents the complete transient sound field in the semi-infinite space $Z \geqslant 0$ due to a transient excitation of a piston of the form $v(r_0, \phi_0, t)$. For further investigation we reduce the complexity of 7.3.6 by letting $v = V\,U(t)$, selecting V to be constant over the piston area. Then $m = 0$, and,

$$\int_0^{2\pi} d\phi_0 \int_0^{b} J_0(ur_0)\, r_0 dr_0 = \frac{2\pi b}{u}\, J_1(ub) \tag{7.3.7}$$

For a rigid piston therefore,

$$\Phi(r, \phi, z, t) = cVb \int_{-\infty}^{t} d\tau\, U\left(\tau - \frac{|z - z_0|}{c}\right) \tag{7.3.8}$$

$$\times \int_0^{\infty} J_0(u\sqrt{c^2\tau^2 - |z - z_0|^2})\, J_1(ub)\, J_0(ur)\, du$$

The transient pressure field is $\varrho\,\partial\Phi/\partial t$. Since $\int_{-\infty}^{t} = \int_0^t$ in 7.3.8, the pressure can be written as follows:

$$p(r, \phi, z, t) = \varrho cVb\, U\left(t - \frac{|z - z_0|}{c}\right)$$

$$\times \int_0^{\infty} J_0(u_0\sqrt{c^2t^2 - |z - z_0|^2})\, J_1(ub)\, J_0(ur)\, du. \tag{7.3.9}$$

To perform the integration when $Z_0 = 0$ we consult [10] and obtain the formula,

$$p(r, \phi, z, t) = \varrho cV\, U\left(t - \frac{z}{c}\right) \frac{A}{\pi} \tag{7.3.10a}$$

in which

$$A = 0, \quad b < |r - (c^2t^2 - z^2)^{1/2}| \tag{7.3.10b}$$

$$A = \cos^{-1}\left[\frac{r^2 + (c^2t^2 - z^2) - b^2}{2r\sqrt{c^2t^2 - z^2}}\right], \quad |r - (c^2t^2 - z^2)^{1/2}| < b < |r + (c^2t^2 - z^2)^{1/2}| \tag{7.3.10c}$$

$$A = \pi, \quad b > |r + \sqrt{c^2t^2 - z^2}\,| \tag{7.3.10d}$$

[9].

Eq. 7.3.10 represents the transient pressure at a field point in the half space $z \geqslant 0$. To understand its significance we refer to Fig. 7.3.1 in which a piston (radius b) is shown in the xy plane at the origin of coordinates. In this figure the field point P (located at the tip of the z-coordinate) forms the apex of a "kinematic cone" whose base traces out a circle in the xy plane. For $Ct = z$, the cone is the line $z\,a_z$. When $ct > z$, the radius of the base of the cone ($= \sqrt{c^2t^2 - z^2}$) increases with time. The point of the base circle ($= A$) nearest the origin is $r - \sqrt{c^2t^2 - z^2}$, and the point ($= B$) farthest from the origin is $r + \sqrt{c^2t^2 - z^2}$. For time $t (t \geqslant z/c)$ in which the contour of the base is outside of and does not intersect the contour of the piston the field at P is non-existent. This is the condition before the initiation of the transient field at P. Also when the base of the cone has grown so large as to completely enclose the contour of the piston the transient field at P vanishes. This condition marks the close of the transient state. Both of these states at P, namely the states before the onset and after the

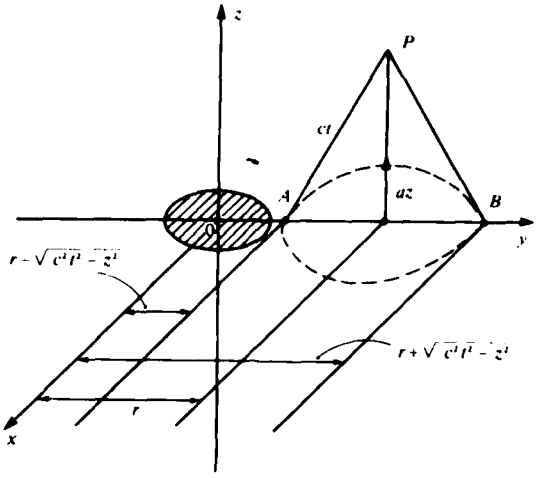

Fig. 7.3.1. Geometric relations in the transient radiation from a circular piston in a rigid baffle.

cessation of the transient are given by 10b. During the time of the existence of the transient two additional states are possible. In one, the piston contour encloses point A. This is the condition given by 10c. In the other the piston contour encloses points A and B. This is the condition given by 10d. Both of these states are possible, contingent on the location of P and the magnitude of the radius b of the piston.

7.3b INDICIAL IMPEDANCE OF A RIGID PISTON IN A RIGID INFINITE BAFFLE

In the previous section we may find the reaction force $f(t) \cup (t)$ of the medium on the piston by letting $z = z_0 = 0$ and integrating the pressure over the surface of the piston. The indicial impedance $z(t)$ of the medium to the motion of the piston is defined as the ratio $f(t)/V$. It is found by integrating 7.3.9 over the area of the piston with use of 7.3.7, then dividing by the uniform velocity V,

$$Z(t) = \varrho c 2\pi b^2 \int_0^\infty J_1^2(ub)\, J_0(uct)\ \frac{du}{u} \tag{7.3.11}$$

To evaluate the integral it is simplest for form $d\,Z(t)/dt$ first,

$$\frac{dZ(t)}{dt} = -\varrho c 2\pi b^2 c \int_0^\infty J_1^2(ub)\, J_1(uct)\, du \tag{7.3.12}$$

From [11],

$$\dot{Z}(t) = -\varrho c^3 \sqrt{\frac{4b^2}{c^2} - t^2}\ ,\quad \frac{2b}{c} \geqslant t \tag{7.3.13}$$

We may integrate 7.3.13 with respect to t provided we know $Z(0)$. From 7.3.11 above we find

$$Z(0) = \varrho c \pi b^2 \left[\frac{1}{2} \int_0^\infty \frac{J_1^2(ub)\, du}{u} \right]$$

$$Z(0) = \varrho c \pi b^2 \tag{7.3.14}$$

Hence the indicial impedance is found by integration to be,

$$Z(t) = \varrho c \pi b^2 - \varrho c^3 \left[\frac{t\sqrt{4b^2/c^2 - t^2}}{2} + \frac{2b^2}{c^2} \sin^{-1} \frac{t}{(2b/c)} \right], \quad (2b/c) \geq t \quad (7.3.15)$$

Discussion:

The indicial impedance of medium to a piston excited by a step function of displacement is a function of time. At $t = 0$, for a piston of area S, the impedance is ϱcS, that is, the impedance of a plane wave. When $t = 2b/c$, where b/c is the ratio of the radius of the piston to the velocity of sound the indicial impedance vanishes. Between these two values of t the indicial impedance diminishes monotonically from ϱcS to zero.

7.3c TRANSIENT RADIATION FIELD OF A VIBRATING PLATE EDGE CLAMPED IN A RIGID WALL

The transient radiation field of a circular flexible plate radius a vibrating in an infinite wall and radiating sound into a fluid medium may be determined by the use of expansion in normal functions. Let r, φ_0 be the cylindrical coordinates of the plate, and let (R, φ, Z, t) be the velocity potential at a field point due to a transient *displacement* $u(r_0, \varphi_0, t)$ at the surface of the plate. We consider now that the displacement in turn is the time response of the flexible plate to a forcing function $f(r_0, \varphi_0, t)$. The equation of motion describing the transient vibration of the radiation damped plate is given by,

$$\alpha^2 \nabla^4 u + 2\beta \frac{\partial u}{\partial t} + \frac{\partial^2 u}{\partial t^2} = \gamma f(r_0, \varphi_0 t) \quad (7.3.16)$$

where

$$\alpha^2 = \frac{h^2 E}{12\mu(1 - \sigma)}, \beta = \frac{K}{2\mu h}, \gamma = \frac{1}{\mu h}, \nabla^2 = \text{Laplacian Operator}$$

h = plate thickness, σ = Poisson's ratio, μ = density of the plate, k = internal damping factor of plate.

The differential operator $(\nabla^4 + \partial^2/\partial t^2)$ in association with the boundary conditions of an edge-damped plate generates the eigenfunctions $\psi_{mn}(r) \sin m\varphi$, $\psi_{mn}(r) \cos m\varphi$ where,

$$\psi_{mn}(r) = j^m J_m(jz_{mn}) J_m\left(z_{mn} \frac{r}{r_0}\right) - j^m J_n(z_{mn}) J_m\left(j_{mn} \left(\frac{r}{r_0}\right)\right) \quad (7.3.17a)$$

(Note: $j = \sqrt{-1}$, $J_{mn}(z) = J_{mn}(kr)$, $k = \omega/c$) and z_{mn} is the nth root of the equation

$$J_m(jz) J'_m(z) - J_m(z) J'_m(jz) = 0 \quad (7.3.17b)$$

These eigenfunctions ψ_{mn} from a complete orthogonal set of function whose *norms* A_{mn} are given by

$$A_{on} = 2\pi J_0^2(z_{on}) J_0^2(jz_{on})$$

$$A_{mn} = \pi J_m^2(z_{mn}) j^{2m} J_m^2(jz_{mn}) \quad (7.3.17c)$$

We can now expand the arbitrary function $\gamma f(r_0, \varphi_0, t)$ in an infinite series of these eigenfunctions, each term of which is multiplied by an 'expansion constant' $g_{mn}(t)$,

$$\gamma f(r_0, \varphi_0, t) = \sum_{m=0}^{\infty} \sum_{n=0}^{\infty} [g^*_{mn}(t) \cos m\varphi + g^{**}_{mn}(t) \sin m\varphi] \psi_{mn}(r) \tag{7.3.18a}$$

where

$$g^*_{mn}(t) = \frac{1}{a^2 A_{mn}} \int_0^a \int_0^{2\pi} \gamma f(r_0, \varphi_0, t) \psi_{mn}(r_0) \cos m\varphi \, r_0 dr_0 \, d\varphi_0 \tag{7.3.18b}$$

$$g^{**}_{mn}(t) = \frac{1}{a^2 A_{mn}} \int_0^a \int_0^{2\pi} \gamma f(r_0, \varphi_0, t) \psi_{mn}(r_0) \cos m\varphi \, r_0 dr_0 \, d\varphi_0 \tag{7.3.18c}$$

Similarly we assume that the displacement $u(r_0, \varphi_0, t)$ can be expanded in an infinite series of the *same* eigenfunctions with expansion 'constants' of the form $\Theta^*_{mn}(t)$, $\Theta^{**}_{mn}(t)$,

$$u(r_0, \varphi_0, t) = \sum_{m,n} [\theta^*_{mn}(t) \cos m\varphi + \theta^{**}_{mn}(t) \sin m\varphi] \nu_{mn}(r) \tag{7.3.19}$$

If now in 7.3.16 we replace the right hand side by 7.3.18a and then substitute 7.3.19 into the left hand side we can abstract two ordinary differential equations in the variable t by comparing coefficients in $\psi_{mn}(r) \sin m\varphi$ or $\psi_{mn}(\mathbf{r}) \cos m\phi$ from the two sides of the transformed equation. We thus obtain identical equations in $\Theta^*_{mn}(t)$, $\Theta^{**}_{mn}(t)$, of which only one is presented below:

$$\text{(a)} \qquad \frac{d^2\theta^*_{mn}(t)}{dt^2} + 2b \frac{d\theta^*_{mn}(t)}{dt} + \omega^{*2}_{mn} \theta^*_{mn}(t) = g^*_{mn}(t) \tag{7.3.20}$$

where

$$\text{(b)} \qquad \omega^2_{mn} = (z_{mn}/a)^2 h^2 E / 12\mu(1 - \sigma^2)$$

ω^2_{mn} = circular frequencies of free, undamped vibrations of the plate

The solution of 7.3.20a is most easily carried out by transform theory. Let $\theta^*_{mn}(s)$ be the Laplace transform of $\theta^*_{mn}(t)$, $\theta^*_{mn}(s) = \mathcal{L}\{\theta^*_{mn}(t)\}$, and $G_{mn}(s) = \theta\{g^*_{mn}\}$. Then, by standard procedures of the operational calculus we find

$$\Theta_{mn}(s) = \frac{G_{mn}(s)}{s^2 + 2bs + \omega^2_{mn}} + \frac{\Theta_{mn}(0)[s + 2b] - \Theta^1_{mn}(0)}{s^2 + 2bs + \omega^2_{mn}} \tag{7.3.21}$$

Here, $\Theta(0)$ and $\Theta'(0)$ are initial conditions. If we write $s^2 + 2bs + \omega^2_{mn}$ as $(s + b)^2 + \Omega^2_{mn}$, where $\Omega^2_{mn} = (\omega^2_{mn} - b^2)$, we can find the inverse of 7.3.21 in the form,

$$\theta^*_{mn}(t) = \Theta^*_{mn}(0) e^{-bt} \cos \Omega_{mn} t + \frac{b\Theta^*_{mn}(0) - \Theta^{*1}_{mn}(0)}{\Omega_{mn}} e^{-bt} \sin \Omega_{mn} t + \frac{1}{\Omega_{mn}} \int_{-\infty}^{t} g^*_{mn}(\tau) e^{-b(t-\tau)} \sin \Omega_{mn}(t - \tau) \, d\tau \tag{7.3.22}$$

A similar equation can be written for $\theta^{**}_{mn}(t)$. Examination of 7.3.22 shows that it contains two transient terms (that is, terms in e^{-ht}) generated by the initial conditions $\theta_{mn}(0)$ and $\theta'_{mn}(0)$, and one steady state term given by the superposition integral. Eq. 7.3.22 enables us to compute the displacement due to a pressure $\gamma f(r_0, \varphi_0, t)$ acting on the surface of the flexible plate. The resultant normal component of velocity $V(r_0, \varphi_0, t)$ may be written as $\partial u/\partial t$. Since V is a general function of time, not necessarily harmonic, we may find the velocity potential Φ at any point in the semi-infinite space by a formula of Rayleigh [12],

$$\Phi_{\text{Rayleigh}}(r, \varphi, z, t) = -\frac{1}{2\pi} \iint_S V\left((r_0, \varphi_0, t - \frac{r}{a} \right) \frac{dS}{r} \tag{7.3.23}$$

in which $r = |r - r_0|$ and

$$V\left(r_0, \varphi_0, t - \frac{r}{a} \right) = \sum_{m,n} \left[\frac{\partial \theta^{*}_{mn}(t - r/a)}{\partial t} \cos m\varphi_0 + \frac{\partial \theta^{**}_{mn}(t - r/a)}{\partial t} \sin m\varphi_0 \right] \tag{7.3.24}$$

We note that in the derivation of 7.3.23 we assumed that the velocity distribution V is independent of the reaction of the medium, that is, V is a 'forcing velocity' whose spatial and time dependence are independent of the loading due to the medium.

7.3d TRANSIENT RADIATION FROM A PISTON MEMBRANE

The solution 7.3.23 of Sect. 7.3c is left in general form. In the following discussion a more detailed analysis is made of a piston membrane whose dynamical motion is governed by simpler equations.

In 1941 Schoch [13] developed a very useful formula for calculating the steady state radiation field generated by a piston "membrane" in an infinite rigid baffle. Assume the membrane has a convex contour of arbitrary shape and is located in the $x\,y$ plane of a Cartesian coordinate system. A field point P is defined by the cylindrical coordinates (ϱ, ϕ, z), the origin of which is at the $x\,y$ projection of P at point $(\varrho, \phi, 0)$. The radiation field at P due to a normal membrane velocity v_{n1} is given by Rayleigh's formula for the velocity potential, ψ, as modified by [14],

$$\psi_{KM} = \frac{1}{2\pi} \int_A \frac{v_n e^{-ikr}}{r} dA \tag{7.3.25}$$

Here r is the distance from an elementary area ($= dA$) of the vibrating membrane to the field point P, and time is given by the real part of $e^{j\omega t}$. Let v_n be constant over the area. Now,

$$r = \sqrt{z^2 + \varrho^2} \tag{7.3.26}$$

$$dA = \varrho d\varrho d\phi = r dr d\phi$$

By designating distances and angles originating at, or terminating on, the contour by subscripts "1", "2" 7.3.25 may be written

$$\psi(P, k) = \frac{v_n}{2\pi} \int_{\phi_1}^{\phi_2} d\phi \int_{\varrho_1}^{\varrho_2} \frac{e^{-jkr}}{r} \varrho d\varrho d\phi \tag{7.3.27}$$

The meaning of $\varrho_1, \varrho_2, \phi_1, \phi_2$ is shown in Fig. 7.3.2:

The pressure $p = \varrho\ \partial\psi/\partial\ t = jk\varrho c\psi$. Substitution of 7.3.26 into 7.3.27 followed by a simple reduction lead to the following formula for the pressure p,

$$p(P,k) = \frac{v_n \varrho c}{-2\pi} \int_{\phi_1}^{\phi_2} [e^{-jkr_2} - e^{-jkr_1}]\, d\phi \tag{7.3.28}$$

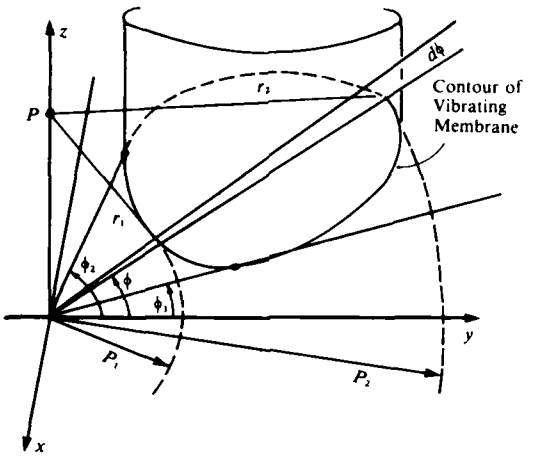

Fig. 7.3.2. Geometrical relations associated with transient radiation from a membrane.

Here, the xy projection of the field point P is located outside the contour.

When the xy projection of P falls inside the contour of the membrane the angular range of ϕ changes to $0 \leqslant \phi \leqslant 2\pi$, and the range of ϱ changes to $0 \leqslant \varrho \leqslant \varrho_1$. If the variable of integration in this case is changed from ϱ to r then by 7.3.26 the limits on r are $z \leqslant r \leqslant r_1$. The integration of 7.3.27 then leads to,

$$p(P, k) = v_n \varrho c\, e^{-jkz} - v_n\ \frac{\varrho c}{2\pi} \int_0^{2\pi} e^{-jkr_1}\, d\phi \tag{7.3.29}$$

Eqs. 7.3.28 and 7.3.29 are the steady state fields at any field P due to a monochromatic wave, frequency $\omega = kc$, originating at the vibrating membrane. We consider next the transient case which may be handled by methods of Sect. 7.2. Assuming that the normal velocity is an impulsive function of time ($= V(t)$) we desire to find the transient radiation field ($= \psi(r, t)$) at any point P. A direct way of calculating this is by means of the Fourier transform. First,

$$V(\omega) = \int_{-\infty}^{+\infty} e^{-j\omega t}\, V(t)\, dt \tag{7.3.30}$$

Also, by definition of the Green's function $G(= 1/2\pi\ e^{-jkr}/r)$,

$$p(P, k) = \int_{\text{vol.}} dr_0\, G(r \mid r_0 \mid k) \tag{7.3.31}$$

Thus, using 7.2.12 we obtain

$$p(P, t) = \frac{1}{2\pi} \int_{-\infty}^{+\infty} p(P, \omega)\, V(\omega)\, e^{+j\omega t}\, d\omega \tag{7.3.32}$$

The choice of the transformation kernel $e^{+j\omega t}$ (instead of $e^{-i\omega t}$) rests upon the desire to have the transient field be represented as a sum of plane waves travelling in all directions of the $\omega(= kc)$ plane.

Now for a wide variety of functions $V(t)$ the classical Fourier transform given by 7.3.30, may not exist. In this case it is appropriate to use the Laplace transform. For simplicity we limit $V(t)$ by stating that $V(t) = 0$ when $t < 0$. Then, making the transformation $j\omega \to s$ we rewrite 7.3.30,

$$V(s) = \int_0^{\infty} e^{-st}\, V(t)\, dt \tag{7.3.33}$$

Similarly, 7.3.32 becomes,

$$p(P, t) = \frac{1}{2\pi j} \int_{\sigma-j\infty}^{\sigma+j\infty} p(P, s)\, V(s)\, e^{st}\, ds \tag{7.3.34}$$

Here, to insure convergence we have shifted the path of integration from the imaginary axis required by 7.3.32 to a parallel line σ units to the right. This is necessary in order that for $t < 0$ there exist no poles of the integrand of 7.3.34 in the contour that is closed at infinity in the right half plane. (See a discussion of contour integration in Appendix VIIA.) The formulas for the pressure are already available from 7.3.28 and 7.3.29. We thus have the two cases:

Case I. The point of observation is outside the cylinder erected on the contour of the membrane (Fig. 7.3.2)

Using 7.3.28 we have,

$$p(P,t) = \frac{1}{-4\pi^2} \varrho c \int_{\sigma-j\infty}^{\sigma+j\infty} \int_{\phi_1}^{\phi_2} (e^{-r_2 s/c} - e^{-r_1 s/c})\, d\phi\, e^{st}\, ds \tag{7.3.35}$$

Let $s = \mu + i\omega$, then according to Jordan's Lemma (see Appendix VIIA) the integral above can be closed by a great arc in the *left* half plane if $(t - r/c) > 0$, and in the right-hand plane (i.e., to the right of $\mu = \sigma$) if $(t - r/c) < 0$. Assuming then that $t \geqslant r/c$ one finds by use of the standard "shift formula" in the theory of the Laplace transform in conjunction with the theory of residues that,

$$p(P, t) = \frac{\varrho c}{-2\pi} \left[\int_{\phi_1}^{\phi_1^*} V\left(t - \frac{r_2}{c}\right) d\phi - \int_{\phi_1}^{\phi_1^*} V\left(t - \frac{r_1}{c}\right) d\phi \right] \tag{7.3.36}$$

The symbol ϕ^* will be explained below.

Case II. The point of observation is inside the cylinder erected on the contour of the membrane.

Repeating the analysis applied in the first case to 7.3.29 it is concluded that,

$$p(P, t) = U\left(t - \frac{z}{c}\right) \varrho c\, V\left(t - \frac{z}{c}\right) - \frac{\varrho c}{2\pi} \int_0^{\phi^*} V\left(t - \frac{r_1}{c}\right) d\phi \tag{7.3.37}$$

Here,

$$U(x) = 1, \qquad x \geqslant 0$$

$$U(x) = 0, \qquad x < 0$$

is the unit step function.

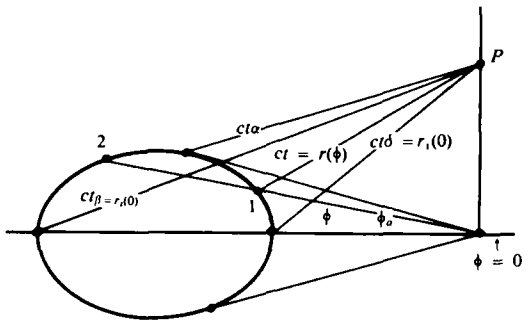

Fig. 7.3.3. Geometrical relations in transient radiation of a membrane for which $V(t) = U(t)$.

The symbol ϕ^* is used in 7.3.36, 7.3.37 to indicate that the limits of integration are functions of time. If $\varrho(\phi)$ is the equation for the contour of the membrane then from 7.3.36,

$$r(\phi) = \sqrt{z^2 + \varrho(\phi)^2}$$

By substituting this formula for r into 7.3.36, 7.3.37 we may perform the integration in the space coordinates as required. In the integrated result the transient field at P is the instantaneous field contributed from the contour at each angle ϕ^*. The appropriate time of arrival from each angle ϕ^* is then,

$$ct = r(\phi^*) \tag{7.3.38}$$

If therefore 7.3.36, 7.3.37 are integrated between variable limits ϕ^*, and if 7.3.38 is then solved explicitly for ϕ^* then the final result will be the field pressure at point P explicitly derived as a function of time (= the transient field). Whenever $ct > r(\phi^*)$ the transient contribution to the pressure at P from the contour at ϕ^* is ended.

Eqs. 7.3.36 and 7.3.37 give the transient radition field in terms of a given normal component of membrane velocity which is a function of time only, $V(t)$. Examples are discussed in the next section.

7.3e EXAMPLES OF TRANSIENT RADIATION FROM A PISTON MEMBRANE [14]

As a simple example of the application of 7.3.36 assume the piston membrane to have an impulsive velocity whose amplitude distribution in time is given by,

$$V(t) = V_0 \qquad t > 0 \tag{7.3.39}$$

$$= 0, \qquad t < 0$$

For convenience in understanding the transient process allow the membrane contour to have one axis of symmetry, and locate the *xy* projection of the field point on this axis of symmetry, outside the membrane contour (= Case I of Sect. 7.3d). Define the angle ϕ_o as the angle to the tangent from the projected point to the contour, Fig. 7.3.3. When the velocity 7.3.39 is substituted into 7.3.36, the transient pressure field becomes,

$$p(P, t) = \frac{\varrho c(2)}{2\pi} V_0 \int_{\phi_\alpha^*}^{\phi_\beta^*} d\phi^* + \frac{\varrho c(2)}{2\pi} \int_0^{\phi_\beta^*} d\phi^* \tag{7.3.40}$$

The factor of 2 in this equation arises from the symmetry of the membrane. Integration of 7.3.40 shows that the pressure may be written in the form,

$$p(P, t) = \frac{\varrho c}{\pi} V_0 \phi_1^*(t), ct_\delta < ct < ct_\alpha \tag{7.3.41a}$$

and

$$p(P, t) = \frac{\varrho c}{\pi} V_0 \phi_2^*(t), ct_\alpha < ct < ct_\beta \tag{7.3.41b}$$

An understanding of these formulas may be improved by noting that the time differences of radiation from specific points on the contour to the same observation point P are very small. Thus one can consider the distance from a point on the contour to the field point P to be expandable in a Taylor series about the point $\phi = \phi^* = 0$ associated with the distance $r_1(0) = ct_\delta$,

$$ct = r(\phi^*) = r_1(0) + \frac{dr_1(0)}{d\phi^*} \phi_1^* + \frac{1}{2!} \frac{d^2 r_1(0)}{d\phi^{*2}} \phi_1^{*2} + \ldots \tag{7.3.42}$$

Symmetry of the membrane and choice of field point lead to the condition that

$$\frac{dr_1(0)}{d\phi^*} = 0. \tag{7.3.43}$$

If time is counted from the initial arrival at P of the sound disturbance from ct_δ, then the path difference occuring during the passage of the transient is,

$$c\Delta t_\delta = ct - ct_\delta = \frac{1}{2!} \frac{d^2 r_1(0)}{d\phi^{*2}} \phi_1^{*2} + \ldots \tag{7.3.44}$$

The variable angle ϕ^* may thus be written in terms of the distance $c \Delta t_\delta$ as follows,

$$\phi_1^* = \sqrt{\frac{2c\Delta t_\delta}{r_1''(0)}} \tag{7.3.45}$$

Hence, 7.3.41a, 7.3.41b may be reduced to the approximations,

$$\begin{aligned}
&\text{(a)} \quad p(P, t) = 0, ct < ct_\delta \\
&\text{(b)} \quad p(P, t) = \frac{\varrho c}{\pi} \sqrt{\frac{2c\Delta t_\delta}{r_1''(0)}}, ct_\delta < ct < ct_\alpha \\
&\text{(c)} \quad p(P, t) = \frac{\varrho c}{\pi} \sqrt{\frac{2c\Delta t_\beta}{r_1''(0)}}, ct_\alpha < ct < ct_\beta \\
&\text{(d)} \quad p(P, t) = 0, ct > ct_\beta
\end{aligned} \tag{7.3.46}$$

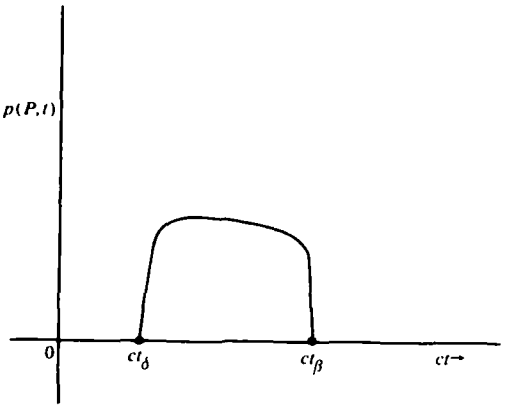

Fig. 7.3.4. Schematic plot of Eq. 7.3.46.

We note that a plot of the transient pressure Eq. 7.3.46 at P vs. ct (Fig. 7.3.4) *has a discontinuous 1st derivative at* $ct = ct_\delta$, $ct = ct_\beta$. These discontinuities are the result of the choice of velocity 7.3.39, in which the onset of the excitation is discontinuous.

As a second example we let the piston motion have the form,

$$V(t) = V_0 e^{j\omega t}, \quad t > 0 \tag{7.3.47}$$

$$= 0, \qquad t < 0$$

For a symmetrical piston under the conditions of Case I, Sect. 7.3d, the field is given by 7.3.36 in the form,

$$\text{(a)} \quad p(P, t) = \frac{\varrho c}{\pi} V_0 \int_0^{\phi^*} e^{j\omega[t - r_1(\phi^*)/c]}\, d\phi^*, \; ct_\delta < ct < ct_a \tag{7.3.48}$$

$$\text{(b)} \quad p(P, t) = -\frac{\varrho c}{\pi} V_0 \int_{\phi^*}^{0} e^{j\omega[t - r_1(\phi^*)/c]}\, d\phi^*, \; ct_a < ct < ct_\beta$$

We consider 7.3.48a first. If the field point is sufficiently distant from the membrane contour the phase of the integral changes rapidly, or slowly, depending on the portion of the membrane being traced out, and depending on the acoustic length $kL (= 2\pi L/\lambda)$ of the contour. If kL is large enough so that many cycles of phase occur during the tracing, the following conclusions will be valid. In the neighborhood of the symmetry axis, $\phi^* = 0$, the phase of the integrand changes slowly. Hence the contribution from this neighborhood to the integral is at a maximum. At all other points on the contour the phase of the integrand varies rapidly as the integration proceeds. The contributions from these points therefore tends to vanish. We thus may consider 7.3.42 as an appropriate representation of $r_1(\phi^*)$. The first term in this equation is independent of ϕ^*, and therefore represents a constant. For convenience this constant is set to unity. The second term contributes nothing because $r_1'(0)$ vanishes. The contribution of the third term has the form,

$$p(P, t) = e^{j\omega t} \frac{\varrho c}{\pi} V_0 \int_0^{\phi^*} \frac{e^{-jkr_1''(0)}}{2} \phi_1^{*2}\, d\phi^*, \; ct_\delta < ct < ct_a \tag{7.3.49}$$

To integrate 7.3.49 use 7.3.40 as an aid in defining a new transformed variable τ given by,

$$\tau^2 = \frac{kr_1''(0)\phi_1^{*2}}{\pi} = \frac{4c\Delta t_\delta}{\lambda} \tag{7.3.50}$$

Eq. 7.3.49 then reduces to,

$$\text{(a)} \quad p(P, t) = e^{j\omega t} \frac{\varrho c V_0}{\sqrt{k\pi r_1''(0)}} \int_0^w e^{-j\pi/2\tau} \, d\tau \tag{7.3.51}$$

in which

$$\text{(b)} \quad w = \sqrt{\frac{4c\Delta t_\delta}{\lambda}}$$

The integral in 7.3.51a is recognized as the complex form of the Fresnel integrals, $C(w)$, $S(w)$ as defined in ref. [1]. Thus,

$$p(P, t) = \frac{e^{j\omega\Delta t_\delta} \varrho c}{\sqrt{\pi k r_1''(0)}} \quad [C_1(w) - jS(w)], \tag{7.3.52}$$

$$0 < \Delta t_\delta < \Delta t_a$$

in which

Here we begin counting time at the instant of first arrival, hence t has been replaced by Δt_δ. 7.3.52 may be rewritten in the form,

$$\text{(a)} \quad p(P, t) = \frac{\varrho c N}{\sqrt{2\pi k r_1''(0)}} \quad e^{j[\omega\Delta t_\delta - \xi(w)]}, \; ct_\delta < ct < ct_a,$$

in which

$$\text{(b)} \quad N = \sqrt{2}\sqrt{C^2(w) + S^2(w)}$$

$$\text{(c)} \quad \xi(w) = \tan^{-1} \frac{S(w)}{C(w)} \tag{7.3.53}$$

The solution given by 7.3.53a is a *transient* solution only. In applying the asymptotic method (= saddle point method) we are stating that when $c\,\Delta\,t \to c\,\Delta\,t_a$ the field at P approaches (in magnitude and angle) a field that can be represented on a Cornu Spiral by the vector from the origin to one eye of the spiral. This asymptotic field is given by,

$$p \sim C(\infty) + jS(\infty) \to \frac{j+1}{2} = \frac{1}{\sqrt{2}} \quad e^{j\pi/4} \tag{7.3.54}$$

When $c\,\Delta\,t = c\,\Delta\,t_\beta$, that is, when $r(\phi^*) = r_2(\phi^*)$ as shown in Fig. 7.3.3 the transient fields must cease. Now the integration required by 7.3.48b between the limits of ct_a and ct, where $ct < ct_\beta$, yields a field (except for a constant) given by the quantities,

$$\text{(a)} \quad p \sim \left(\sqrt{C^2(x) + S^2(x)}\right) e^{j\xi(x)} \qquad \text{(b)} \quad x = \sqrt{\frac{4c\Delta t_\beta}{\lambda}} \tag{7.3.55}$$

The requirement that the transient process vanish when $c\,\Delta\,t = c\,\Delta\,t_\beta$ means that the difference between 7.3.54 and 7.3.55a must vanish. This leads to the following formula of the field at P,

$$p(P,\,t) = \frac{\varrho c e^{j\omega\Delta t_\beta}}{\sqrt{\pi k r_2''(0)}} \left\{ \frac{e^{j\pi/4}}{\sqrt{2}} - \sqrt{C^2(x) + S^2(x)}\; e^{j\xi(x)} \right\}$$

$$= \frac{\varrho c e^{j\omega\Delta t_\beta}}{\sqrt{2\pi k r_2''(0)}} \left\{ \left(\frac{1}{\sqrt{2}} - N\cos\xi \right) + j\left(\frac{1}{\sqrt{2}} - N\sin\xi(x) \right) \right\} \tag{7.3.56}$$

which is valid when

$$c\Delta t_\beta > c\Delta t > c\Delta t_\alpha = 0 \tag{7.3.57}$$

Note that in 7.3.56 the onset of the tail end of the transient process begins at $\Delta\,t_\alpha = 0$, and that the termination is reached when $c\,\Delta\,t = c\,\Delta\,t_\beta$,

Discussion:

Eqs. 7.3.52 and 7.3.56 represent the transient radiation from a membrane of arbitrary (but convex) contour, with one axis of symmetry, which is exited by the transient velocity given by 7.3.47. This solution has been obtained by the asymptotic method of assuming that $r(\phi^*)$ can be given by 7.3.42 in which we retain terms only to the second order in ϕ^*. Hence, ϕ^* must be "small", which means that the point of observation (= point P) must be far from the source, or alternatively, that $c\,\Delta\,t/\lambda$ must be large (i.e., $\lambda \to 0$). A general solution which is valid for *all* field points, at *all* wavelengths for *all* possible contours (not necessarily symmetrical) is clearly a very troublesome entity to obtain.

7.4 TRANSIENT RADIATION FROM SPHERES [26]

Transient radiation from vibrating spherical surfaces may be analyzed by considering first the steady state time-harmonic radiation and then making a Laplace or Fourier inversion from frequency domain to time domain. Let there be a sphere of radius r_0 vibrating with a complex harmonic normal component of surface velocity $V(\theta,\,\phi)\,e^{j\omega t}$ and radiating sound into a non-viscous fluid of unlimited extent. The velocity potential for such a radiator is given by 2.1.18c in which the radial dependence of potential field is written in the form of the ratio $[A_n(z)/B_n(z_0)]\,e^{-(z-z_0)}$, $z = jkr$, $z_0 = jkr_0$. From this ratio it is seen that the nature of the transient radiation will be determined by the poles introduced by the polynomial $B_n(jkr_0)$, and the time delay introduced by the exponential $\exp[-(z - z_0)]$.

7.4a THE POLYNOMIAL $B_n\,(jkr_0)$ AND ITS LAPLACE INVERSIONS

The polynomial $B_n(x)$, $x = jkr_0$, is of degree $n + 2$ in the variable x^{-1} (see 2.1.10b). A more convient form is the product $x^{n+2}\,B_n(x) = F(x)$, which is a polynomial of degree $n + 1$ in the variable x. In symbols,

$$F_n(x) = x^{n+2}\,B_n(x) = b_n^{(n+1)} + b_n^{(n)}\,x + \ldots + b_n^{(1)}x^n + b_n^{(0)}x^{n+1} \tag{7.4.1}$$

Now let $\beta_n^{(1)},\,\beta_n^{(2)}$ .... be the complex roots of $B_n(x) = 0$. Since x is never identically zero we have,

$$\text{(a)}\quad F_n(x) = (x - \beta_n^{(1)})\,(x - \beta_n^{(2)})\ldots(x - \beta_n^{(n+1)}) \tag{7.4.2}$$

Let $f_n(x)$ be $F_n(x)^{-1}$. We desire to form a *partial fraction* expansion of $f_n^n(x)$ and use the theorem that if z_q are the simple roots of $F(z)$, that is if,

$$\text{(b)} \quad f(z) = \frac{1}{\prod_{q=1}^{t+1} (z - \alpha Z_q)}$$

then there are coefficients $C^{(k)}$ such that

$$\text{(c)} \quad f(z) = \sum_{q=1}^{t+1} \frac{C^{(q)}}{\alpha'(z - \alpha z_q)}$$

Here $C^{(k)}$ may be formed by substituting the k'th root of $B_n(x) = 0$ in place of x, and, omitting the factor $(\beta_n^{(k)} - \beta_n^{(k)})$, by writing

$$\text{(d)} \quad C_{n+1}^{(k)} = (\beta_n^{(k)} - \beta_1^{(1)})(\beta_n^{(k)} - \beta_n^{(2)}) \ldots (\beta_n^{(k)} - \beta_n^{(k-1)})(\beta_n^{(k)} - \beta_n{}^{(k+1)}) \ldots (\beta_n^{(k)} - \beta_n^{(n+1)})$$

$$\text{(e)} \quad C_1^{(1)} = 1$$

Calculation of $C_{N+1}^{(k)}$ will be aided by noting from 7.4.2 that when n is odd there will be $n + 1$ complex roots of the forms,

$$\left.\begin{aligned} \beta_n^{(2q-1)} &= -\delta_n^{(q)} + j\omega_n^{(q)} \\ \beta_n^{(2)} &= -\delta_n^{(q)} - j\omega_n^{(q)} \end{aligned}\right\}, q = 1, 2, \ldots \frac{n+1}{2}$$

When n is even there will be n conjugate complex roots ($q = 1, 2, \ldots {}^{n-1}/2$) of the same form, together with one real root. The sum of products $C^{(k)} X^{(k)}$, where $X^{(k)}$ is the kth root, yield certain important classic identities. For a total of $n + 1$ roots these identities are

$$\text{(a)} \quad \sum_{k=1}^{n+1} \begin{aligned} C^{(k)}[x^{(k)}]^p &= 0 && p = 0, 1, \ldots n-1 \\ C^{(k)}[x^{(k)}]^p &= 1 && p = n \\ C^{(k)}[x^{(k)}]^p &= -b_n^{(1)} && p = n+1 \\ C^{(k)}[x^{(k)}]^p &= (b_n^{(1)})^2 - b_n^{(2)} && p = n+2 \end{aligned} \qquad (7.4.3)$$

$$\text{(b)} \quad \sum_{k=1}^{n+1} (C^{(k)} x^{(k)} p/x - x^{(k)}) = xp/F(x), \qquad p = 0, 1, \ldots n$$

in which the coefficients given by 2.1.11.

We return again to Eq. 2.1.18c and write it in a convenient form which will be useful in the display of frequency dependence of its parts:

$$\text{(a)} \quad \Phi(r, \theta, \phi, t) = \sum_{n=0}^{\infty} \Psi_n(r, t)\ \mathcal{P}(\theta, \phi)$$

where

$$\text{(b)} \quad \Psi_n(r, t) = ce^{j\omega t} e^{-j\omega(r - r_0)/c} \frac{A_n(j\omega r_0/c)}{B_n(j\omega r_0/c)} \qquad \text{(units: } ms^{-1}\text{)} \qquad (7.4.4)$$

$$\text{(c)} \quad \mathcal{P}_n(\theta, \phi) = \sum_{m=-n}^{+n} D_{mn} e^{-jm\phi} P_n^m(\cos\theta) \qquad \text{(units: } m\text{)}$$

$$\text{(d)} \qquad D_{mn} = \frac{2n+1}{4\pi}\,\varepsilon_m\,\frac{(n-m)!}{(n+m)!}\,P_n^m(\cos\theta)\times$$

$$\int_0^{2\pi} d\phi \int_0^{\pi} D(\theta_0, \phi_0)\cos m(\phi-\phi_0)\,P_n^m(\cos\theta_0)\sin\theta_0\,d\theta_0 d\phi_0$$

in which $D(\theta_0, \phi_0)$ is the displacement of the surface. Here D_{mn} are the relevant parts of 2.1.18c not otherwise included in Ψ_n. If the formal transformation $j\omega \rightarrow s$ is made in 7.4.4b and the factor $e^{j\omega t}$ is suppressed the result will be $\Psi_n(r, s)$ which is the Laplace transformation of $\Psi_n(r, t)$ with all initial conditions zero. The transformed velocity potential $\Phi(r, \theta, \phi, s)$ also satisfies Helmholtz's equation and represents the velocity potential at the field point r, θ, ϕ due to a velocity distribution $V(\theta, \phi)$ over the sphere *applied as a Dirac impulse function at time $t = 0$, the time variable having been transformed from $e^{j\omega t}$ to $\delta(t)$.* After transformation then, with use of 2.1.9, 2.1.10, we have

$$\text{(a)} \qquad \frac{A_n\left(\frac{sr}{c}\right)}{B_n\left(\frac{sr_0}{c}\right)} = s\,\frac{r_0}{r}\,\frac{\sum_{p=0}^{n} a_n^p\left(\frac{c}{r}\right)^p s^{n-p}}{\prod_{k=1}^{n+1}\left(s-\frac{c}{r_0}\,\beta_n^{(k)}\right)} \tag{7.4.5}$$

$$\text{(b)} \qquad a_n^p = \frac{(n+p)!}{p!(n-p)!2^p}$$

To simplify the symbols let $g(s)$, and $G(r, s)$ be defined such that

$$g_n(s) = \left[\prod_{k=1}^{n+1}\left(s-\frac{c}{r_0}\,\beta_n^{(k)}\right)\right]^{-1} \qquad \text{(units: } s^{n+1}\text{)} \tag{7.4.6}$$

$$G_n(r, s) = \sum_{p=0}^{n} a_n^p\left(\frac{c}{r}\right)^p s^{n-p}\,g_n(s) \qquad \text{(units: } s\text{)} \tag{7.4.7}$$

Substitution of these equations into 7.4.4b leads to,

$$\Phi_n(r, s) = \frac{cr_0}{r}\,e^{-s(r-r_0)/c}\,G_n(r, s) \qquad \text{(units: } m\text{)} \tag{7.4.8}$$

and

$$\Phi(r, \theta, \phi, s) = \sum_{n=0}^{n} \Psi_n(r, s)\,\mathcal{P}_n(\theta, \phi) \qquad \text{(units: } m^2\text{)} \tag{7.4.9}$$

Eq. 7.4.9 is the transformed velocity potential when the excitation in time is an impulse function $\delta(t)$. If the excitation in time is $X(t)$ (units: s^{-1}) with Laplace transform $X(s)$ the transformed function 7.4.8 is modified to read,

$$\text{(a)} \qquad \Psi_n(r, s) = \frac{cr_0}{r}\,e^{-s(r-r_0)/c}\,H_n(r, s)$$

where

$$\text{(b)} \qquad H_n(r, s) = X(s)\,G_n(r, s), \text{(units: } s\text{)} \tag{7.4.10}$$

Then by the convolution theorem in the theory of the Laplace transformation,

$$H_n(r, t) = X(t)^* G_n(r, t) \tag{7.4.11}$$

where the asterisk symbol describes the convolution operation;

$$\alpha(x)^* \beta(x) = \int_{-\infty}^{x} \alpha(\xi)\, \beta(x - \xi)\, d\xi$$

Assuming that the velocity excitation is zero for $t < 0$ we form the Laplace inverse of 7.4.10a to find

$$\text{(a)} \quad \Psi_n(r, t) = \frac{cr_0}{r} H_n(r, \tau) \tag{7.4.12}$$

$$\text{(b)} \quad \tau = t - \left(\frac{r - r_0}{c} \right)$$

and so,

$$\Phi(r, \theta, \phi, \tau) = \frac{cr_0}{r} \sum_{n=0}^{\infty} H_n(r, \tau)\ \mathcal{P}_n(\theta, \phi) \tag{7.4.13}$$

This is the transient velocity potential of a spherical radiator. [16]

7.4b TRANSIENT RADIATION FROM SPHERES EXCITED BY ARBITRARY TIME SIGNALS

Let the arbitrary time signal be $X(t)$. To calculate 7.4.13 we must return to the functions $g(s)$, $G(r, s)$ given by 7.4.6, 7.4.7 respectively. Using the results of Sect. 7.4a, particularly Eq. 7.4.3 we convert 7.4.6 from a product fraction to a sum of partial fractions,

$$g_n(s) = \left(\frac{r_0}{c} \right)^n \sum_{k=1}^{n+1} \frac{C^{(k)}}{\left(s - \frac{c}{r_0} \beta_n^{(k)} \right)} \tag{7.4.14}$$

The inverse $g(t)$ is readily found to be,

$$g_n(t) = \left(\frac{r_0}{c} \right)^n \sum_{k=1}^{n+1} C^{(k)}\, e^{c/r_0 \beta^{(k)} t} \tag{7.4.15}$$

Now the pth derivative of $g(t)$ is

$$g_n^p(t) = \left(\frac{r_0}{c} \right)^{n-p} \sum_{k=1}^{n+1} C^{(k)} (\beta^{(k)})^p\, e^{c/r_0 \beta^{(k)} t} \tag{7.4.16}$$

Applying 7.4.3 we see that the first $n - 1$ derivatives of $g_n(t)$ are zero at time $t = 0$. When $p = n$, $g_n^{(n)}(0) = 1$. Now from the theory of the Laplace transformation the product $s^{n-p} g_n(s)$ is the $(n - p)$th derivative of $g(t)$, provided the $(n - 1)$ derivatives are all zero. This rule allows us to find the inverse of $G_n(r, s)$ of 7.4.7. We thus infer that,

$$G_n(r, t) = U(t) \sum_{p=0}^{n} a_n^p \left(\frac{r_0}{r} \right)^p \sum_{k=1}^{n+1} C_{n+1}^{(k)} (\beta^k)^{n-p}\, e^{c/r_0 \beta^{(k)} t} \text{(units: none)} \tag{7.4.17}$$

where $U(t)$ is the unit step function,

$$U(x) = 0, \quad x < 0$$
$$(x) = 1, \quad x \geq 0$$

When $t = 0$ we see from 7.4.3a that $G_n(r, 0)$ is zero unless $p = 0$. If $p = 0$, then

$$G_n(r, 0) = U(0) \tag{7.4.18}$$

that is, $G_n(r, 0)$ is a unit step function at the origin of time. A useful way of writing 7.4.17 is found by inverting the order of summations, employing the definitions of a_n^p given by 7.4.5b and the definition of $A_n(x)$ given by 2.1.10a, and then writing,

$$G_n(r, t) = U(t)\left(\frac{r}{r_0}\right)\sum_{k=1}^{n+1} C^{(k)}(\beta_n^{(k)})^{n+1} e^{(c/r_0)\beta_n^{(k)}(r-ct)} A_n\left(\frac{r}{r_0}\beta_n^{(k)}\right) \tag{7.4.19}$$

The analysis of transient radiation from spheres is now complete. To find the transient velocity potential we first calculate $H_n(r, t)$ by 7.4.11 and calculate $\Phi(r, t)$ by 7.4.13. Several cases will now be considered.

Case I. $X(t) = \delta_0(t)$

In this case, the sphere is excited by a time signal in the form of a Dirac impulse (units: s^{-1}). The function $H_n(r, t)$ by 7.4.11 is,

$$H_n(r, t) = \int_0^t \mathcal{S}_0(t - \xi)\, G_n(r, \xi)\, d\xi$$

$$H_n(r, t) = G_n(r, t)$$

and $\mathcal{S}_0$ is the impulse (delta) function. Hence, the velocity potential is given by

$$\Phi(r, \theta, \phi, \tau) = \frac{cr_0}{r}\sum_{n=0}^{\infty} G_n(r, \tau)\, \mathcal{P}_n(r, \theta)$$

where $G_n(r, t)$ is found by means of 7.4.19. To study the progress of the pressure wave and the particle velocity wave it will be convenient to consider one member of this series Φ_n at a time, with n arbitrary. The nth partial pressure wave, p_n, is given by $p\,\partial\Phi_n/\partial t = \varrho\partial\Phi_n/\partial\tau$. We recall now that if

$$\text{(a)} \qquad w(t) = U(t)\, W(t)$$

then

$$\text{(b)} \qquad \frac{dw}{dt} = U(t)\,\frac{dW}{dt} + \delta(t)\, W(0) \tag{7.4.20}$$

Applying this equation we find p_n for an impulse excitation to be

$$p_n(r, \theta, \phi, \tau) = \varrho c\, \mathcal{P}_n(\theta, \phi)\left\{U(\tau)\,\frac{c}{r_0}\sum_{k=1}^{n+1} C^{(k)}(\beta_n^{(k)})^{n+2} A_n\left(\frac{r}{r_0}\beta_n^{(k)}\right) e^{c/r_0\beta_n^{(k)}\tau}\right.$$

$$\left. + \delta(\tau)\sum_{k=1}^{n+1} C^{(k)}(\beta^{(k)})^{n+1} A_n\left(\frac{r}{r_0}\beta_n^{(k)}\right)\right\} \tag{7.4.21}$$

Note that $\delta(\tau) = 0$ unless $\tau = 0$. If A_n is expanded according to 2.1.9 and the identities of 7.4.3a are used it is seen that in the second term of 7.4.21 all terms in the series are zero except one, so that the second term is $\delta(\tau)\, r_0/r$. The nth order pressure response to a Dirac delta function excitation consists therefore of an outward travelling wave front at which there is a discontinuity of pressure of two types: a Dirac impulse of magnitude (r_0/r), and a step function initiating $n + 1$ complex exponentials. To find the exact form at the wave front let $\tau = 0$ and consider the first series in 7.4.21 which may be written

$$\sum_{k=1}^{n+1} C^{(k)} \left[a_n^0 \frac{r_0}{r} (\beta^{(k)})^{n+1} + a_n^1 \left(\frac{r_0}{r} \right)^2 (\beta^{(k)})^n + a_n^2 \left(\frac{r_0}{r} \right)^3 (\beta^{(k)})^{n-1} + \ldots \right] \tag{7.4.22}$$

Using 7.4.3a we see that

$$\sum_{k=1}^{n+1} C^{(k)} (\beta^k)^{n+1} = -b_n^{(1)}, \quad \sum_{k=1}^{n+1} C^{(k)} (\beta^k)^n = 1. \tag{7.4.23}$$

All remaining terms in the series, 7.4.22, are zero. Since $b_n^{(1)} = [n(n+1) + 2]/2$, and $a_n^{(1)} = [(2n+1)^2 - 1]/8$, by aid of 7.4.23 we reduce 7.4.21 to the following *formula for the pressure at the wavefront due to a spherical radiator of order n excited by a Dirac impulse,*

$$p_{n\,\tau=0} = \varrho c \, \mathcal{P}_n(\theta, \phi) \frac{r_0}{r} \left\{ \delta(0) - U(0) \frac{c}{r_0} \left[1 + \frac{n^2 + n}{2} \left(1 - \frac{r_0}{r} \right) \right] \right\} \tag{7.4.24}$$

At the wavefront (i.e. $\tau = 0$) therefore there are two discontinuities whose ratio of amplitudes is,

$$\frac{c}{r_0} \left[1 + \frac{n^2 + n}{2} \left(1 - \frac{r_0}{r} \right) \right] \frac{U}{\delta} \tag{7.4.25}$$

When $r = r_0$, i.e. at the surface of the sphere, the ratio is

$$\left(\frac{c}{r_0} \right) \frac{U}{\delta}$$

The radial component of particle velocity U_n in the nth mode may be found from $U_n = -\partial \Phi_n / \partial r$. Recalling that $\tau = t - (r - r_0)/c$, and that $\partial/\partial r = -\partial/c\partial t$, we see by aid of that the radial particle velocity for impulse excitation is

$$u_n = \mathcal{P}_n(\theta, \phi) \left\{ \delta(\tau) \frac{r_0}{r} + U(\tau) \frac{c}{r_0} \left[\sum_{k=1}^{n+1} C^{(k)} (\beta_n^{(k)})^{n+2} B_n \left(\frac{r}{r_0} \beta_n^{(k)} \right) e^{c/r_0 \beta_n^{(k)} \tau} \right] \right\} \tag{7.4.26}$$

When $\tau = 0$ (i.e. at the wavefront) the series in the square brackets above can be expanded by use of 2.1.10. One obtains for this series

$$\sum_{k=1}^{n+1} C^{(k)} (\beta^{(k)})^{n+2} \left[\frac{b_n^0}{\left(\frac{r}{r_0} \right) \beta_n^{(k)}} + \frac{b_n^1}{\left(\frac{r}{r_0} \right)^2 (\beta_n^{(k)})^2} + \ldots \frac{b_n^{n+1}}{\left(\frac{r}{r_0} \right)^{n+2} (\beta^{(k)})^{n+2}} \right] \tag{7.4.27}$$

By aid of 7.4.3a it is easily seen that this series reduces to $-(r_0/r) b_n^{(1)} (1 - r_0/r)$. Hence at the wavefront,

$$u_{n\,\tau=0} = \mathcal{P}_n(\theta, \phi) \frac{r_0}{r} \left\{ \delta(0) - U(0) \frac{c}{r_0} \left[\frac{n(n+1) + 2}{2} \right] \left(1 - \frac{r_0}{r} \right) \right\} \tag{7.4.28}$$

Examination of the pressure and particle velocity at the wavefront in the n the mode shows that as $r \to \infty$ the ratio $p_n/U_n = \varrho\, c$, as it should be for plane waves. *The general formulas 7.4.21 and 7.4.26 show that in a physical sense for a Dirac impulse excitation both acoustic pressure and radial particle velocity for $r > r_0$ are characterized in time τ ($t = t - r - r_0/c$) by a Dirac impulse $\delta(\tau)$ followed by a negative step function* $-\cup_{(\tau)}$, followed in turn by decaying oscillations (i.e. terms in $\exp((c/r_0)\beta_n^{(k)}\tau)$. Accompanying these are transverse particle velocities which by 7.4.11, 7.4.13, 7.4.19 are seen to have the same type of discontinuity as that of the velocity potential, that is, a step function. However, amplitudes of transverse velocities diminish as $1/r^2$, and hence their influence at $r \to \infty$ is negligible.

7.4c TRANSIENT RADIATION FROM A SPHERICAL SOURCE OF ORDER $n = 0$ FOR AN IMPULSE EXCITATION

When the time excitation of a spherical radiator of order n is a Dirac-type impulse, $\delta(t)$ (units: S^{-1}), the resulting pressure and radial particle velocity are given by 7.4.21 and 7.4.26 respectively. For $n = 0$ we set $\mathcal{P}_0 = D_0$ and find from 7.4.21,

$$p_0(r, \theta, \phi, \tau) = \varrho c D_0\left(\frac{r_0}{r}\right)\left\{\delta_0(\tau) - U(\tau)\ \frac{c}{r_0}\ e^{-c/r_0\tau}\right\} \tag{7.4.29}$$

Similarly, from 7.4.26 the radial particle velocity is

$$u_0 = D_0\ \frac{r_0}{r}\ \left\{\delta(\tau) - U(\tau)\ \frac{c}{r_0}\ \left(1 - \frac{r_0}{r}\right) e^{-c\tau/r_0}\right\} \tag{7.4.30}$$

Discussion:

At the wavefront (i.e. at $\tau = 0$) the pressure consists of a positive Dirac-type impulse of magnitude $\varrho c\ D_0(r_0/r)\ \delta(0)$ dropping almost instantaneously to a negative pressure of magnitude $\varrho c\ D_0(c/r)\ U(0)$. After the wavefront has passed a particular radius r the pressure at r is negative and approaching a constant with time τ in accordance with the exponential $\varrho c D_0(c/r)\exp(-c\tau/r_0)$. The radial particle velocity, in contrast, follows a different history. When the wavefront is at the surface ($\tau = 0$, $r = r_0$) the particle velocity is a pure impulse of magnitude $D_0\ \delta\ (0)$. As the transient disturbance moves away from the sphere the wavefront consists of the same positive impulse as before followed almost instantaneously by a negative pressure which builds up in magnitude with distance r as $D_0(c/r)\ (1 - r_0/r)$. As $r \to \infty$ the particle velocity becomes proportional to the pressure by a factor ϱc, i.e. the disturbance in the far field has the character of a *transient plane wave.*

7.4d TRANSIENT EXCITATION OF SPHERES BY A SINUSOIDALLY MODULATED STEP FUNCTION

Let the time-varying signal be a sinusoid modulated by a step function. In symbols, $X(t) = U(t)\ \omega\cos\omega t$. From 7.4.11, 7.4.19 and 2.1.9, we have

$$H_n(r, t) = \int_0^t \omega\cos\omega\gamma\ U(t - \gamma)\ \sum_{p=0}^{n} a_n^p\left(\frac{r_0}{r}\right)^p \tag{7.4.31}$$

$$\times\ \sum_{k=1}^{n+1} C^{(k)}(\beta_n^{(k)})^{n-p}\, e^{c/r_0\beta_n^{(k)}(t-\gamma)}\, d\gamma, \qquad \text{(units: none)}$$

By aid of standard tables of integration,

$$H_n(r,\ t) = U(t)\ \sum_{p=0}^{n} a_n^p \left(\frac{r_0}{r}\right)^p \left(\frac{\omega r_0}{c}\right)^2 \sum_{k=1}^{n+1} \frac{C^{(k)}(\beta_n^k)^{n-p}}{\left(\frac{\omega r_0}{c}\right)^2 + (\beta_n^{(k)})^2}$$

$$\times \left\{ \sin \omega t - \frac{c}{\omega r_0}\ \beta_n^{(k)}(\cos \omega t - e^{c\beta_n^{(k)} t/r_0} \right\} \tag{7.4.32}$$

The velocity potential for this excitation is found by 7.4.13. Since we are interested in the transient response only we reject the terms in $\sin\omega t$ and $\cos\omega t$, and find the transient potential for the nth order due to excitation $U(t)\ \omega\cos\omega t$ to be,

$$\Phi_n(r,\ \theta,\ \phi,\ \tau) = \omega r_0\ \mathcal{P}_n(\theta,\ \phi)\ U(\tau)\ \sum_{k=1}^{n+1} \frac{A_n\left(\frac{r}{r_0}\ \beta_n^{(k)}\right) C^{(k)}(\beta_n^k)^{n+2}\, e^{c\beta_n^{(k)}\tau/r_0}}{\left(\frac{\omega r_0}{c}\right)^2 + (\beta_n^{(k)})^2} \tag{7.4.33}$$

Both 7.4.32 and 7.4.33 will be considered in greater detail.

7.4e TRANSIENT RADIATION FROM A SPHERICAL SOURCE OF ORDER $n = 0$ FOR A STEP-SINUSOID EXCITATION

We consider next a spherical radiator of order zero with step-sinusoid excitation 7.4.4(d), $P_0 = D_{00} = V_0 = 1$ (units: m/s). To find $G(r,\ t)$ we examine 7.4.17 and note that $C_1^{(1)} = 1$ (see Sect. 7.4a) and $\beta_0^{(1)} = -1$ satisfies $F_0(x) = 0$ in 7.4.2. Hence

$$G_0(r,\ t) = U(t)\ e^{-ct/r_0} \tag{7.4.34}$$

For excitation we select $X(t) = U(t)\ \omega\ \cos\omega t$, and using 7.4.11 we find

$$\text{(a)} \qquad H_0(r,\ t) = \omega \cos \omega t^*\ U(t)\ e^{-ct/r_0}$$

or

$$\text{(b)} \qquad H_0(r,\ t) = U(t)\ \{M(\cos \omega t - e^{-ct/r_0}) + N \sin \omega t\},$$

where

$$\text{(c)} \qquad M = k\mathbf{r}_0/(1 + (k_{r_0})^2), \qquad N = kr_0 M \tag{7.4.35}$$

From 7.4.13 the velocity potential for order $n = 0$ at time $\tau - (r - r_0/c)$ is

$$\text{(a)} \qquad \Phi_0 = \left(\frac{cr_0}{r}\right) D_{00} H_0(r,\ \tau)$$

or

$$\text{(b)} \qquad \Phi_0 = \frac{cr_0}{r}\ D_{00}\ U(\tau)\ \{M(\cos \omega\tau - e^{-c/r_0\tau}) + N \sin \omega\tau\} \tag{7.4.36}$$

Noting that when $\tau = 0$, $\delta(\tau)$ multiplied by the term in the brackets, vanishes, we find the pressure in the zero order to be

$$\text{(a)} \qquad p = \varrho \partial \Phi_0 / \partial \tau = \varrho c \ \frac{r_0}{r} \ D_{00} \, \partial H_0 / \partial \tau$$

or

$$\text{(b)} \qquad p = D_{00}(\tau) \varrho c^2 \ \frac{kr_0}{r} \ M\{(kr_0 \cos \omega t - \sin \omega t) + \ \frac{e^{-c/r_0 \tau}}{kr_0} \tag{7.4.37}$$

From 7.4.36 we may also derive the radial particle velocity $U = - \partial \Phi_0 / \partial \, r$,

$$\text{(a)} \qquad u = \frac{r_0 D_{00}}{r} \left\{ \frac{dH_0(r, \tau)}{d\tau} + \frac{c}{r} \ H_0(r, \tau) \right\}$$

or

$$\text{(b)} \qquad u = D_{00}(\tau) \, M \left\{ \ \frac{cr_0}{r^2} \ (\cos \omega t - e^{-c/r_0 \tau} + kr_0 \sin \omega \tau) \right. \tag{7.4.38}$$

$$\left. + (\omega r_0 / r) \left(- \sin \omega \tau + kr_0 \cos \omega \tau - \ \frac{1}{kr_0} \ e^{-c/r_0 \tau} \right) \right\}$$

At the wavefront (i.e. at $\tau = 0$) the ratio $p/u = \varrho c$, a constant, independent of r. When the pressure and particle velocity are available we can find the radial flux of energy, F, which is formed by the product pu (dimensions: $(N - m/m^2)$/sec). The flux is seen from 7.4.37a and 7.4.38a to be a sum, $F = F' + F''$, where F', F'' are the fluxes of radial dependence in $1/r^2$ and $1/r^3$ respectively. One finds,

$$\text{(a)} \qquad ' = \varrho c \left(\ \frac{r_0}{r} \ \right)^2 D_{00}^2 \left[\ \frac{\partial H_0(r, \tau)}{\partial \tau} \ \right]^2 \tag{7.4.39}$$

$$\text{(b)} \qquad '' = \varrho c^2 \ \frac{r_0^2}{r^3} \ D_{00}^2 \, H_0(r, \tau) \frac{\partial H_0(r, \tau)}{\partial \tau}$$

In the far field where $t \to \infty$ (i.e. in the steady state),

$$\left(\ \frac{\partial H_0}{\partial \tau} \ \right)^2 \to M^2 \omega^2 \, [\sin^2 \omega \tau + k^2 r_0^2 \cos \omega \tau] - 2M^2 k r_0 \omega^2 \sin \omega \tau \cos \omega \tau \tag{7.4.40}$$

Over a complete cycle $T = 2\pi/\omega$ the average value of this quantity is $M^2 \, \omega^2 \, (1 + k^2 \, r_0^2)/2$. Hence the average radial flux F_{Av}' of energy dissipating out to infinity in the steady state is

$$\mathcal{F}_{\text{AV}}' = \ \frac{\varrho c}{2} \ \left(\ \frac{r_0}{r} \ \right)^2 \ \frac{D_{00}^2 \omega^2}{1 + (1/k^2 r_0^2)} \tag{7.4.41}$$

The second component of energy, 7.4.39b is *not* dissipated out to infinity but rather is deposited in the total volume of space where it *oscillates* in place. Now in time $d\tau$ the total energy deposited in a volume $4\pi r^2 \, dr$ is $(d/dr) \, (4\pi r^2 \, F'') dr d\tau$. Hence the total energy E'' deposited by the source in all space, but not dissipating out to infinity, is

$$\mathsf{E}'' = 4\pi \varrho c^2 r_0^2 \, D_{00}^2 \int_r^\infty (-1) \ \frac{dr}{r^2} \ \int_0^\infty H_0(r, \tau) \, \frac{\partial H_0(r, \tau)}{\partial \tau} \, d\tau$$

The integrand $H_0 \dfrac{\partial H_0}{\partial t}$ vanishes as $\tau \to \infty$, that is, in the steady state. Rejecting all steady state terms in this integrand because their average is zero in any one period we see that the integral over τ yields $M^2/2$. Hence *the total transient energy E_t'' deposited in all space, not dissipating to infinity, but finally oscillating in place about the source is*

$$E_t'' = 2\pi\varrho c^2 r_0 D_{00}^2 \frac{k^2 r_0^2}{(1 + k^2 r_0^2)^2} \tag{7.4.42}$$

We desire to find the median value of the quantity over a *single period*, recognizing the fact that it has been built up of an infinite number of periods. To this end we note that by integrating 7.4.40 over a cycle that the peak amplitude of steady state energy is reduced to average energy by the multiplication factor $(1 + k^2 r_0^2)/2$. We shall assume without proof that the same factor can be applied to 7.4.42. We therefore find that the *average transient energy* $(E_t'')_{AV}$ deposited in the field per period for a spherical radiator of order $n = 0$ and radius r_0 is,

$$(E_t'')_{AV} = \pi\varrho c^2 r_0 D_{00}^2 \frac{k^2 r_0^2}{1 + k^2 r_0^2} \tag{7.4.43}$$

In contrast the average energy E_{00} radiated out to infinity per period in the steady state for $n = 0$ is found by multiplying Π_{00} 2.2.14a by one period $T = 2\pi/\omega$.

$$E_{00} = \frac{R_{00} |U_{00}|^2_{max}}{2} \times \frac{2\pi}{\omega}$$

$$E_{00} = \frac{\varrho c 4\pi^2 r_0^2}{\omega} \left(\frac{k^2 r_0^2}{1 + k^2 r_0^2} \right) |U_{00}|^2_{max} \tag{7.4.44}$$

We arbitrarily set $|U_{00}|^2_{max} = D_{00}^2 \omega^2$ and form the ratio of 7.4.43 and 7.4.44, to obtain

$$\frac{(E_t'')_{AV}}{E_{00}} = \frac{c}{4\pi r_0 \omega} \tag{7.4.45}$$

On comparing this 7.4.45 with 2.3.8b we note that they are identical. We are therefore lead to the following conclusion: *at the initiation of radiation the transient radiation flux F'' which comprises all radiation varying as $1/r^n$, $n \geqslant 3$ deposits in the space surrounding the source all of the stagnant energy which in the steady state is found oscillating in place.*

7.4f TAIL END OF TRANSIENT RADIATION FROM A SPHERICAL SOURCE OF ORDER $n = 0$

If the excitation on a spherical source of order zero vibrating sinusoidally is suddenly reduced to zero a tail end of transient radiation will be generated. In order to construct an analytic representation of this transient we assume an excitation of the form,

$$X(t) = (1 - U(t))\, \omega \cos \omega t \tag{7.4.46}$$

With this choice the results of the previous excitation are immediately applicable. First we note from 7.4.35b that,

$$H_0 \underset{t\to\infty}{(r, t)} \to M \cos \omega t + N \sin \omega t$$

We require then in our solution that this part of the field cease with the application of the excitation of 7.4.46. The transient term in 7.4.35b must remain. Hence our soulution is of the form

$$\Phi = \frac{cr_0}{r} D_{00} \{[1 - U(\tau)] (M \cos \omega\tau + N \sin \omega\tau) - U(\tau) M e^{-c\tau/r_0}\} \tag{7.4.47}$$

The pressure p and radial particle velocity u are easily derived from this last formula. For $\tau > 0$ the flux of energy F is found from the product pu to be

$$\mathcal{F} = \varrho c \left(1 - \frac{r_0}{r}\right) \left[\frac{r_0}{r} \frac{\omega D_{00}}{1 + k^2 r_0^2} e^{-c/r_0\tau}\right]^2 \tag{7.4.48}$$

whose units are Nm/sm^2.

When the motion of the source ceases the instantaneous flux of energy at the surface $r = r_0$ vanishes. If the point of observation rides with the wave (that is, if τ is constant) it is seen that the total energy E_0'' flowing through a sphere of radius r ($E_0'' = 4\pi r^2 F$) varies with r as $(1 - r_0/r)$. As the tail end of the radiation proceeds out from the source the total flux grows according to this law so that finally a quantity of power $E''(\tau)$ equal to $4\pi r^2 F$ as $r \to \infty$ is carried away to infinity. Neglecting the term in $1/r^3$ in 7.4.48 above we find,

$$E''(t) = \frac{4\pi\varrho c\, r_0^2\, \omega^2\, D_{00}^2\, e^{-2c\tau/r_0}}{(1 + k^2 r_0^2)^2} \tag{7.4.49}$$

If this is integrated over all time τ the total energy E_r'' gathered up from all space and carried off to infinity is seen to be

$$E_r'' = 2\pi\varrho c^2 r_0 D_{00}^2 \frac{k^2 r_0^2}{(1 + k^2 r_0^2)^2} \tag{7.4.50}$$

Eq. 7.4.50 is identical with 7.4.42, that is, the energy deposited in the field at the onset of the transient is equal to the energy gathered up and carried off to infinity at the conclusion of the same sinusoidal signal, as it should be.

7.4g TRANSIENT RADIATION FROM A SPHERICAL SOURCE OF ORDER $n = 1$

We consider now a spherical source of order $n = 1$ excited by a spherically symmetrical signal (that is, $e^{jm\varphi} = 1$). Here $\mathcal{P}_1 = D_{01} \cos\theta$ and the roots of $F_0(x) = 0$ in 7.4.2a above are $-1 \pm j$. By 7.4.2d and 7.4.2e above, and Eq. 2.1.10,

$$C_1^{(1)} = \frac{1}{\beta_1^{(1)} - \beta_1^2} = \frac{1}{2j}, \quad C_1^{(2)} = \frac{1}{\beta_1^{(2)} - \beta_1^{(1)}} = -\frac{1}{2j}$$

$$A_1(x) = \frac{1}{x} + \frac{1}{x^2}$$

Substituting these quantities in 7.4.19 above we find

$$G_1(r, t) = U(t) \left\{\cos \frac{c}{r_0} t + \left(\frac{r_0}{r} - 1\right) \sin \frac{c}{r_0} t\right\} e^{-ct/r_0} \tag{7.4.51}$$

Let the time excitation be a "unit" Dirac impulse $\delta(t)$ (units: $\sec^{-1}$). From 7.4.11,

$$H_1(r, t) = G_1(r, t)$$

Hence, according to 7.4.13 the velocity potential Φ_1 is

$$\Phi_1 = \frac{cr_0}{r} D_{01} \cos\theta\, U(\tau) \left\{ \cos \frac{c}{r_0}\tau + \left(\frac{r_0}{r} - 1 \right) \sin \frac{c}{r_0}\tau \right\} e^{-c\tau/r_0} \tag{7.4.52}$$

The pressure p and radial particle velocity u are,

$$p = \varrho c \left(\frac{r_0}{r} \right) \cos\theta\, D_{01} \left\{ \delta(\tau) - U(\tau) \left(\frac{c}{r_0} \right) e^{-c\tau/r_0} \left[\left(2 - \frac{r_0}{r} \right) \cos \frac{c}{r_0}\tau + \frac{r_0}{r} \sin \frac{c}{r_0}\tau \right] \right\} \tag{7.4.53}$$

$$u = \left(\frac{r_0}{r} \right) \cos\theta\, D_{01} \left\{ \delta(\tau) - \left(\frac{r_0}{r} \right) U(\tau) e^{-c\tau/r_0} \left(1 - \frac{r_0}{r} \right) \left[\cos \frac{c\tau}{r_0} + \frac{r_0}{r} \sin \frac{c\tau}{r_0} \right] \right\} \tag{7.4.54}$$

A more general type of excitation is the step-sinusoid, in which $X(t) = U(t)\, \omega \cos\omega t$. From 7.4.32 it is seen that for $z_0 = kr_0$,

$$\begin{aligned} H_1(r, t) = \frac{U(t)}{4 + z_0^2} \Bigg\{ & \sin\omega t \left[z_0^3(z_0^2 - 2) + \frac{2r_0}{r} z_0^2 \right] \\ & + \cos\omega t \left[2z_0^3 + \frac{r_0}{r} z_0(2 - z_0^2) \right] \\ & + e^{-ct/r_0} \sin \frac{c}{r_0} t \left[4z_0 - \frac{r_0}{r} z_0(2 + z_0^2) \right] \\ & + e^{-c/r_0 t} \cos \frac{c}{r_0} t \left[-2z_0^3 + \frac{r_0}{r} z_0(z_0^2 - 2) \right] \Bigg\} \end{aligned} \tag{7.4.55}$$

We desire to obtain the ratio of the steady state pressure amplitude P to the transient pressure amplitude T as $r \to \infty$. Now both amplitudes are proportional to $\partial H_1(r, t)/\partial t$. To obtain P we perform this derivative and let $r \to \infty$, and $t \to \infty$ simultaneously. Then,

$$\underset{r\to\infty}{P} \sim \omega z_0^3(z_0^3 - 2) \cos\omega t - 2\omega z_0^3 \sin\omega t \tag{7.4.56}$$

To obtain T we perform the derivative, let $r \to \infty$, and reject all steady state terms. This yields,

$$\begin{aligned} \underset{r\to\infty}{T} \sim & \left(4z_0 \frac{c}{r_0} + 2 \frac{c}{r_0} z_0^3 \right) \cos \frac{c}{r_0} \tau e^{-c\tau/r_0} \\ & + \left(2z_0^3 \frac{c}{r_0} - 4z_0 \frac{c}{r_0} \right) \sin \frac{c}{r_0} \tau e^{-c\tau/r_0} \end{aligned} \tag{7.4.57}$$

The amplitude of P is $\omega z_0^3 (z_0^4 + 4)^{1/2}$ while the amplitude of T for $\tau \to 0$ is $2\sqrt{2}\,(c/r_0)\, z_0 (z_0 + 4)^{1/2}$. The ratio (T/P) where T is calculated for the condition $\tau \to 0$ is therefore

$$(T/P)_{r\to\infty} = \frac{2\sqrt{2}}{z_0^2} = \frac{1}{\sqrt{2}} \left(\frac{\lambda}{\pi r_0} \right)^2, n = 1. \tag{7.4.58}$$

The following table of (r_0/λ) vs T/P for a spherical radiator of order $n = 1$ is based upon this equation:

(r_0/λ)	10	5	2	1	0.5	0.2	0.1	0.05	0.02	0.01
$(T/P)_{r\to\infty}$	0.000715	0.00286	0.0179	0.0715	0.286	1.79	7.15	28.6	179	715

7.4h CHARACTERISTIC WAVES OF EXTERIOR SPACE

An important discovery is contained in 7.4.21 and 7.4.26 namely the existence of decaying waves (i.e. terms in $\exp(c/r_0)\,\beta_n^{(k)}\,\tau$) in exterior space due to transient excitation of a spherical source. Since it is possible by a proper choice of excitation to produce one of these waves at a time in the space exterior to the surface $r = r_0$ it is concluded that each wave is independent, and therefore each wave is characteristic of the exterior space, being in this way analogous to the characteristic waves of closed space. These transient oscillations however have no feature of resonance since they diverge away from the source and never return.

Every characteristic wave corresponds to two conjugate roots, $-\delta_n^{(k)} \pm \omega_n^{(k)}$, of the polynomial $B_n(x)$ in the equation $B_n(x) = 0$ (see Sect. 7.4a). The oscillation due to these roots is that of a decaying exponential,

$$e^{-c\delta_n^{(k)}\tau/r_0} \cos\left(\frac{c}{r_0}\,\omega_n^{(k)}\,\tau + \phi\right)$$

In a period $T = (2\pi/\omega)\,(r_0/c)$ of oscillation the ratio D of amplitudes of successive peaks is

$$\frac{1}{\exp\left(\dfrac{-2\pi\delta_n^{(k)}}{\omega_n^{(k)}}\right)}$$

Now for any n we may plot all the kth roots on a complex plane, real part $\delta(k)$ and imaginary part $\omega^{(k)}$. On such a plane the argument $\Omega_n^{(k)}$ of the complex root $\beta^{(k)}$ is $tan^{-1}\,\omega^{(k)}/\delta^{(k)}$. In examining all the roots it is seen that there will be at least *one* pair of complex conjugate roots with minimum (negative) damping, that is, with minimum real part. For $n \leqslant 3$ this argument is exactly,

$$[\Omega_n^k]_{\min,\delta} = \frac{n+2}{n+1}\,\frac{\pi}{2} \tag{7.4.59}$$

For $n > 3$ it is probable that this formula still holds. Assuming that it holds we can calculate the *extinction ratio D due to that root in each value of n which has the minimum damping*. A table of the first eight orders follows,

Order n	1	2	3	4	5	6	7	8
Extinction Ratio D due to root with min. damping	0.0019	0.027	0.75	0.130	0.186	0.239	0.287	0.331

This table shows that characteristic waves corresponding to n small are rapidly extinguished while for n large the decay is small and the characteristic waves become very prominent. Now practical sound sources in baffles (for example, a kettledrum) and all sources whose moving parts are displaced in patterns which are not spherical harmonics of single order n, generate sound fields consisting of a superposition of simple sound sources of order 1, 2 .... n. These sources in the transient state emit characteristic waves of elevated order which have low decay rates, and which thus persist with noticeable effect.

7.4i RATIO $R^{(k)}$ OF INITIAL VELOCITY POTENTIAL AMPLITUDE OF TRANSIENT WAVES TO THE VELOCITY POTENTIAL AMPLITUDE OF STEADY STATE WAVES IN THE FAR FIELD

The polynomials $A_n(jkr)$ reduce for all n to the value $1/jkr$ as $r \to \infty$. The amplutude Φ_{ss} of velocity potential in the far field for a particular order n is therefore by Eq. 2.1.33,

$$(\Phi_n)_{ss} = \frac{2u_{0n}\,\overline{P}_n C^2}{\epsilon_n |B_n(jkr_0)|\,\omega^2 r} \tag{7.4.60}$$

The amplitude $(\Phi_k)_t$ of *one* (i.e. the kth) transient wave in the nth order transient velocity potential may be extracted from 7.4.33 and is seen to be,

$$\frac{(\Phi_k)_t = \omega r_0^2\ \mathcal{P}_n |C^{(k)}(\beta_n^k)^{n+1}|}{r\left|\left(\frac{\omega r_0}{c}\right)^2 + (\beta_n^{(k)})^2\right|} \tag{7.4.61}$$

We now form the ratio of 7.4.61 to 7.4.60 and omitting all factors not involving r, r_0, we obtain

$$R^{(k)} \sim \left| \frac{B_n(jkr_0)}{1 + \left(\frac{\lambda\beta^{(k)}}{2\pi r_0}\right)^2} \right| \tag{7.4.62}$$

When $2\pi r_0/\lambda$ is $\ll 1$, and at the same time $\beta^{(k)}$ is such that $\lambda\beta^{(k)}/2\pi r_0$ is $\gg 1$, then from 7.4.1 $B_n(x) \to b_n^{(n+1)}/X^{n+2}$, and from ratio $R^{(k)}$ above we obtain in the limit

$$\underset{r_0 \to 0}{R^{(k)}} \to \frac{b_n^{(n+1)}}{|(\beta_n^{(k)})^2|(kr_0)^n} \tag{7.4.63}$$

Similarly for r_0 very large, $|B_n\,(kjr_0)| \to 1/kr_0$. The ratio $R^{(k)}$ therefore becomes

$$\underset{r_0 \to \infty}{R^{(k)}} \to \frac{1}{kr_0} \tag{7.4.64}$$

If we desire the ratio $R_p^{(k)}$ of far field transient pressure to far field steady state pressure we are required to form the time derivatives of the velocity potential. There then appears a factor $(c/r_0)\beta_n^{(k)}$ multiplying the kth transient pressure amplitude in the order n and a factor ω multiplying the steady state pressure amplitude in the same order n. Thus an additional factor $\beta_n^{(k)}/kr_0$ must multiply 7.4.63, 7.4.64 and we obtain the following ratios of (initial) pressure amplitudes

$$\text{(a)} \quad R_p^{(k)} \underset{r_0 \to 0}{\to} \frac{b_n^{(n+1)}}{|\beta_n^k|(kr_0)^{n+1}}, \qquad \text{(b)} \quad K_p^{(k)} \underset{r_0 \to \infty}{\to} \frac{\beta_n^{(k)}}{(kr_0)^2}. \tag{7.4.65}$$

The ratios of radial particle velocity $R_u^{(k)}$ have the same form since pressure and particle velocity are proportional in the far field.

Discussion:

The energy carried away by a transient wave to the far field is proportional both to the product of the amplitudes of pressure and radial particle velocity and to the duration of the transient. This duration makes the energy proportional to kr_0 since the transient oscillation of kth wave has the exponential $(c/r_0)\ \beta_n^{(k)}\ t$. We consider the important case of a source whose radius r_0 is small, and calculate the transient energy carried away to infinity by aid of the ratios of 7.4.65. From these ratios we see that when $r_0 \to 0$ the energy is proportional to $1/(kr_0)^{2n+2}$, and from the duration the same energy is proportional to kr_0. *Hence the transient energy carried away to infinity in the nth order is proportional to* $1/(kr_0)^{2n+1}$, *if* r_0 is small.

The inferences that may be drawn from 7.4.63, 7.4.64 and 7.4.65 have important consequences. *We see first that if the dimensions of a sound source are small relative to a wavelength of radiation the initial amplitude of transient waves for each discontinuity in motion (discontinuity either in amplitude or frequency) may be very much greater than the steady state amplitudes from the same source. Hence the transient amplitudes may be the only waves observed in the far field.* Secondly, if the moving face of a source is surrounded by a stationary baffle the combination source plus baffle constitutes a *complex* source representable by a superposition of n simple sources. As the dimensions of the baffle relative to the dimensions of the moving face increase the energy generated in the nth mode shifts toward higher values of n and the transient amplitudes increase, as shown by Eqs. 7.4.65. If we therefore make the moving face of a source-baffle combination not too small relative to the baffle, the combination becomes equivalent to a low order of simple source, and thus effectively suppresses the transient amplitudes. We then form the following rule: *when the dimensions of a sound source are small relative to a wavelength the effect of a baffle is not only to promote the radiation of longer wavelengths in the steady state, but also to reduce the transient amplitudes in the transient state, provided the source dimensions are not too small relative to the baffle dimensions, that is, provided the source-baffle combination is effectively a low order of spherical radiator.*

7.5 THE TIME-DEPENDENT GREEN'S FUNCTION OF A RIGID CYLINDER

We consider a radiating surface on a rigid cylindrical baffle in the form of a circular cylinder (radius a) of infinite extent whose generator is parallel to the z-axis of Cartesian coordinates. In order to find the transient radiated field we require the Green's function G for the cylinder. This is the solution of 1.7.3 in two dimensions. Let there be a point source at x_0, y_0 (polar coordinates r_0, ϕ_0). Then G will be the solution to the following differential equation,

$$\nabla^2 G - \frac{1}{C^2} \frac{\partial^2 G}{\partial t^2} = -2\pi\ \delta_0(x - x_0)\ \delta_0(y - y_0)\ \delta_0(t - t_0) \tag{7.5.1}$$

Introducing polar coordinates r, θ by the transformation

$$x = r\cos\theta, y = r\sin\theta \tag{7.5.2}$$

we require that on the surface $r = a$

$$\left(\frac{\partial G}{\partial r} \right)_{r=a} = 0 \tag{7.5.3}$$

For convenience we set $y_0 = 0$, $t_0 = 0$ and transform 7.5.1 from Cartesian to polar coordinates. In physical space $-\pi < \theta < \pi$ but in function space $-\infty < \theta < +\infty$. We see then that G is a periodic function of θ with period 2π and is defined not only over real space but in the space of a Riemann surface with sheets at $(2m-1)\pi < \theta < (2m+1)\pi$. Accordingly when we apply 7.5.2 to 7.5.1 we require a periodic extension in the coordinate θ of the delta function. Noting that the Jacobian of transformation is r we rewrite 7.5.1 in the form,

$$\nabla^2 G - \frac{1}{C^2} \frac{\partial^2 G}{\partial t^2} = -\frac{2\pi}{r} \delta_0(r - r_0) \delta_0(t) \sum_{m=-\infty}^{\infty} \delta_0(\theta + 2m\pi) \tag{7.5.4}$$

Coordinate transformation has thus introduced an infinity of fictitious sources which contribute diffracted waves to the real field. Now 7.5.4 is linear and function G will be the superposition of individual solutions F for all choices of integer m,

$$G(r, \theta, t | r_0, 0, 0) = \sum_{m=-\infty}^{\infty} F(r, \theta + 2m\pi, t | r_0, 0, 0) \tag{7.5.5}$$

To find functions F we first take the Laplace transform of both sides of 7.5.4. Since causality requires $G = 0$, $\partial G/\partial t = 0$ at time $t = 0$ we obtain the following equation in the transform G,

$$\nabla^2 G - \frac{s^2}{C^2} \bar{G} = -\frac{2\pi}{r} \delta_0(r - r_0) \sum_{m=-\infty}^{+\infty} \delta_0(\theta + 2m\pi) \tag{7.5.6}$$

In terms of 7.5.5 each transformed solution $\bar{F}_m$ in coordinates r, θ satisfies the relation

$$\frac{\partial^2 \bar{F}_m}{\partial r^2} + \frac{1}{r} \frac{\partial \bar{F}_m}{\partial r} - \frac{s^2}{C^2} \bar{F}_m + \frac{1}{r^2} \frac{\partial^2 \bar{F}_m}{\partial \theta^2} = -\frac{2\pi}{r} \delta_0(r - r_0) \delta_0(\theta + 2m\pi) \tag{7.5.7}$$

We may solve the corresponding homogeneous equation by separation of variables. Let $\bar{F}_m = \phi(r) \chi_m(\theta)$. Then separation leads to

$$\frac{r^2 \left\{ \phi'' + \frac{1}{r} \phi' - \frac{s^2}{C^2} \phi \right\}}{\phi} = -\frac{\chi''}{\chi} = -\mu^2 \tag{7.5.8}$$

where μ^2 is a constant (independent of r, θ). It is thus seen that $\phi(r)$ must satisfy the differential relation

$$\phi'' + \frac{1}{r} \phi' + \left(\frac{\mu^2}{r^2} - \frac{s^2}{C^2} \right) \phi = 0 \tag{7.5.9}$$

For an acoustically hard surface the function ϕ must also satisfy the same boundary requirements as G, i.e.,

$$\frac{d\phi}{dr} = \phi' = 0 \text{ at } r = a \tag{7.5.10}$$

At infinity we require further that the total sound field vanish, that is, $\phi \to 0$ as $r \to \infty$. Evidently the solutions of 7.5.9 depend on the parameter μ. Let $\phi(r, \lambda)$ and $\phi(r, \nu)$ be two such solutions obtained by setting $\mu = \lambda$ in the first case and $\mu = \nu$ in the second case. Multiplying 7.5.9 expressed in $\phi(r, \lambda)$ by $\phi(r, \nu)$, and expressed in $\phi(r, \nu)$ by $\phi(r, \lambda)$, then subtracting the two differential equations we obtain

$$\frac{d}{dr}\{r[\phi'(r, \lambda)\,\phi(r, \nu) - \phi(r, \lambda)\,\phi'(r, \nu)]\} + \frac{\lambda^2 - \nu^2}{r}\,\phi(r, \lambda)\,\phi(r, \nu) = 0 \tag{7.5.11}$$

Integrating both sides between $r = a$ and $r = \infty$, and recalling that $\phi \to 0$ as $r \to \infty$ we then obtain

$$\int_a^\infty \phi(r, \lambda)\,\phi(r, \nu)\,\frac{dr}{r} = \frac{a[\phi'(a, \lambda)\,\phi(a, \nu) - \phi(a, \lambda)\,\phi'(a, \nu)]}{\lambda^2 - \nu^2} \tag{7.5.12}$$

If $\lambda \neq \nu$ the r.h.s. of this equation vanishes in view of 7.5.10. Hence the functions $\phi(r, \lambda)$, $\phi(r, \nu)$ are orthogonal in the range $a \leqslant r < \infty$ provided $\lambda = \nu$. Let λ approach ν in magnitude. Then to a first approximation the r.h.s. of 7.5.12 may be written,

$$\left(\frac{a}{\lambda + \nu}\right)\phi(a, \nu)\left\{\frac{\phi'(a, \lambda) - \phi'(a, \nu)}{\lambda - \nu}\right\} \tag{7.5.13}$$

In the limit $\lambda = \nu$ we can thus write 7.5.13 in the form

$$\int_a^\infty [\phi(r, \lambda)]^2\,\frac{dr}{r} = \frac{a}{2\lambda}\,\phi(a, \lambda)\,\frac{\partial \phi'(a, \lambda)}{\partial \lambda} \tag{7.5.14}$$

Returning now to 7.5.9 we write it in the form

$$\phi'' + \frac{1}{r}\,\phi' + \left[\left(\frac{is}{c}\right)^2 - \left(\frac{i\mu}{r}\right)^2\right]\phi = 0 \tag{7.5.15}$$

This is recognized as the standard differential equation for modified Bessel functions of order $i\mu$ and argument sr/c [17]. There are two solutions $I_{i\mu}$, $K_{i\mu}$. As $r \to \infty$ the solution $I_{i\mu} \to \infty$ while the solution $K_{i\mu} \to 0$. We reject solution I. To satisfy 7.5.10 we require that

$$\left[\frac{\partial Ki\mu(sr/c)}{\partial r}\right]_{r=a} = 0 \tag{7.5.16}$$

This formula will hold only for special (non-integer) values of μ designated $\mu_j (j = 1, 2, \ldots)$. The eigenfunctions of 7.5.15 are therefore of the form $\phi \sim K_{i\mu_j}(sr/c)$. In view of 7.5.14 we see further that we can make these eigenfunctions *orthonormal* by writing $\lambda = \mu_j$ and adopting the (subscripted) form $\phi_j(r)$ where

$$\phi_j(r) = \left\{ \frac{c}{sa} \quad \frac{2\mu_j}{Ki\mu_j\left(\frac{sa}{c}\right)\left[\frac{\partial}{\partial\mu} K'i\mu\left(\frac{sa}{c}\right)\right]_{\mu=\mu_j}} \right\}^{1/2} Ki\mu_j\left(\frac{sr}{c}\right) \tag{7.5.17}$$

This is the solution to the homogeneous part of 7.5.7. For the inhomogeneous part we expand $\delta(r - r_0)$ in an infinite series of these orthonormal eigenfunctions in the coordinate r_0,

$$\delta(r - r_0) = \sum_{j=1}^{\infty} A_j \phi_j(r_0) \tag{7.5.18}$$

where

$$A_j = \int_a^{\infty} \delta(r - r_0)\, \phi_j(r_0)\, \frac{dr_0}{r_0} = \frac{\phi_j(r)}{r} \tag{7.5.19}$$

If in 7.5.7 we replace $\delta(r - r_0)$ by 7.5.18 and 7.5.19 and if we write the individual (transformed) solutions of 7.5.7 by F_{mj} where,

$$\bar{F}_{mj} = \frac{\phi_j(r_0)\phi_j(r)}{r}\, \chi_j(\theta) \tag{7.5.20}$$

then the separated equations 7.5.8 are still valid provided ϕ is written,

$$\phi = \frac{\phi_j(r_0)\phi_j(r)}{r}$$

Hence the inhomogenity in r is accounted for by converting $\bar{F}_m$ to $\bar{F}_{mj}$. Returning to 7.5.8 we see that the separated equation for coordinate θ can be written in the form

$$\chi_j'' - \mu_j\chi = -2\pi\delta(\theta + 2m\pi) \tag{7.5.21}$$

The two independent solutions of the homogeneous equation are $\exp(\pm\, \mu j\theta)$. To obtain the inhomogeneous solution we perform a subsidiary integration [18]. Thus,

$$\chi_j = -2\pi e^{-\mu_j\theta} \int_{\theta_{\not\in}} \frac{\delta_0(\theta + 2m\pi)\, e^{\mu_j\theta}}{\Delta}\, d\theta + (-2\pi)\, e^{\mu_j\theta} \int_{\theta_{\not\in}} \frac{\delta(\theta + 2m\pi)\, e^{-\mu_j\theta}}{\Delta} d\theta \tag{7.5.22}$$

Here Δ is the Wronskian determinant ($= 2\mu_j$) of the two independent solutions. If the limit $\theta_{\not\in}$ is less than zero the first integral vanishes while if $\theta_{\not\in}$ is greater than zero the second integral vanishes. We desire χ_j to vanish as $\theta \to \infty$. Hence, since the range of θ is $-\infty$ to $+\infty$ and we desire χ_j to vanish as $\theta \to \infty$ we *select* $\theta_{\not\in}$ to be *greater* than zero and write a particular solution of 7.5.21 to be,

$$\chi_j = \frac{(-2\pi)\, e^{-\mu_j|\theta+2m\pi|}}{2\mu_j} \tag{7.5.23}$$

Assembling all factors we write the transformed Green's function of 7.5.5 in the form,

$$\bar{G} = \sum_{m=-\infty}^{\infty} \sum_{j=1}^{\infty} (-2\pi)\, \frac{c}{sa} \quad \frac{Ki\mu_j\left(\frac{sr_0}{c}\right) Ki\mu_j\left(\frac{sr}{c}\right)}{Ki\mu_j\left(\frac{sa}{c}\right)\left[\frac{\partial}{\partial\mu} Ki\mu\left(\frac{sa}{c}\right)\right]_{\mu=\mu_j}} e^{-\mu_j|\theta+2m\pi|} \tag{7.5.24}$$

This is the transient Green's function for a rigid circular cylinder expressed in transform space.

7.6 THE TRANSIENT FIELD FROM AN INFINITE LINE SOURCE OF UNIFORM STRENGTH

Let there be a source point r_0 and a field point $\vec{Q}$ at a distance $\vec{r}$ in a Cartesian coordinate system. Through the point $\vec{r}_o$ we pass a line source of infinite length and uniform strength parallel to the Z-axis. In the xy plane the projection of r_0 and r are designated by $\vec{\varrho}_0$ and $\vec{\varrho}$, and we define P to be $|\vec{\varrho} - \vec{\varrho}_0|$. The entity $|z_0 - z|$ is called ζ. Fig. 7.6.1 shows all the parameters. If R is the distance between the field point and a source point on the line then the impulsive field contributed by the source point is given by 7.2.3c. The total field $g(Q, t)$ generated by the entire line is then given by superposition,

$$g(Q, t) = -\frac{1}{4\pi} \int_{-\infty}^{+\infty} \frac{\delta\left[\frac{R}{c} - (t - t_0)\right]}{R} dz_0 \qquad (7.6.1)$$

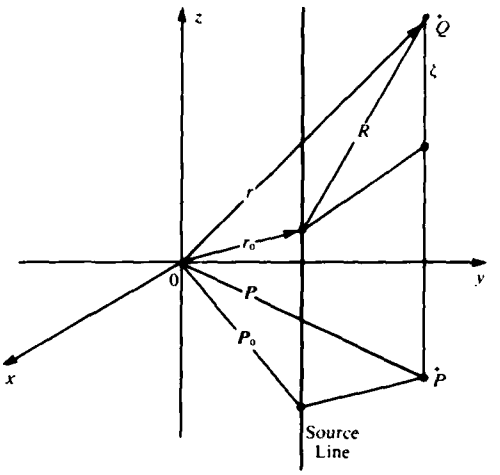

Fig. 7.6.1. Geometric relations of a line source.

in which,

$$\text{(a)} \quad R^2 = \zeta^2 + P^2 \qquad \text{(b)} \quad \zeta = z_0 - z, \qquad \text{(c)} \quad P = \sqrt{(x - x_0)^2 + (y - y_0)^2} \qquad (7.6.2)$$

We net let $\vec{Q}$ lie in the xy plane at point $\vec{P}$ and set $\tau = t - t_0$.

Noting that

$$dz_0 = d\zeta = RdR/\zeta = RdR/\sqrt{R^2 - P^2}$$

we rewrite 7.6.1 for the field point $\vec{P}$ in the form,

$$g(P, \tau) = -\frac{c}{4\pi} \int_{-\infty}^{+\infty} \frac{\delta\left[\frac{R}{c} - \tau\right] \frac{dR}{c}}{\sqrt{R^2 - P^2}} \qquad (7.6.3)$$

Now $g(P, \tau)$ is a real function of P, τ, for all points $r \neq r_0$. Hence $\sqrt{R^2 - P^2} > 0$. By definition the delta function differs from zero only when $R = c\tau$, at which point it has the character of an *even* function. Thus the integral limits of 7.6.3 can be changed to $0 \leqslant R < \infty$, at the same time attaching a multiplying factor of 2. Evaluation of 7.6.3 thus leads to the result,

$$g(P, \tau) = -\frac{2c}{4\pi} \frac{1}{\sqrt{c^2\tau^2 - P^2}}, \quad P < c\tau \qquad (7.6.4)$$

$$= 0, \qquad P > c\tau \qquad \text{(units: } s^{-1}\text{)}$$

If there is a distribution $f_P(\vec{p}_\infty\ t_0)$ of these z-directed line sources over area $A(\vec{\varrho}_0)$ the total field in the plane of distribution (that is, the total 2-dimensional field) is,

$$\Phi(R,\ t) = \int_0^{t} t_0 \int_{A(\vec{\varrho}_0)} dA(\vec{\varrho}_0) \left(- \frac{2c}{4\pi} \frac{1}{\sqrt{c^2\tau^2 - P^2}} \right) f_P(\varrho_0,\ t_0),\ P < c\tau$$

$$\Phi(R,\ t) = 0,\ P > c\tau \tag{7.6.5}$$

Returning to 7.6.4 we note that an impulsive line source generates in a plane a field which is finite at *all* points $P < c\tau$. This is due to late arrival of propagation from distant points on the line to the plane of observation. Thus the 2-dimensional transient field of an impulsive line source differs from the 3-dimensional transient field of an impulsive point source: in the latter the field is found only at the spherical wave front $a_s = c\tau$ while in the former it is found *everywhere* inside the cylindrical wave front $a_c = c\tau$*. However, for spherical sources of *extended* surface (= non point source) the transient field due to field excitation will contain a "tail", as is shown in Sect. 7.4.h. A further discussion of this point is found in C. Barnes, D.V. Anderson "The Sound Field from a Pulsating Sphere", JASA, Vol. 24, 229: 1952.

The geometrical quantities associated with 7.6.4 are shown in Fig. 7.6.2.

The impulsive planar field at the tip of ϱ due to a perpendicular line source that pierces the xy plane at the tip of ϱ_0 is given by 7.6.2. We note the $a = c\tau$ describes an expanding cylindrical surface centered at $\vec{\varrho}_0$ as discussed above. After the wave front passes P the field at P does not vanish. It diminishes as $(c^2\tau^2 - P^2)^{-1/2}$ which (mathematically) never reduces to zero.

We now consider a *uniform* distribution of impulsive in a plane of indefinite extent, say the yz plane, Fig. 7.6.3. Clearly the field will depend solely on the quantity $\xi = x - x_0$, and will be independent of the quantity $\eta = y - y_0$. Since $P^2 = \xi^2 + \eta^2$ we can find the one-dimensional Green's function $g(\xi,\ t)$ in the unbounded domain for this case by integrating 7.6.4 over the range of η from $\sqrt{c^2\tau^2 - \xi^2}$ to $-\sqrt{c^2\tau^2 - \xi^2}$. Fig. 7.6.3 shows the range in question,

Now

$$g(\xi,\ \tau) = - \frac{2c}{4\pi} \int_{-\sqrt{c^2\tau^2-\xi^2}}^{+\sqrt{c^2\tau^2-\xi^2}} \frac{1}{\sqrt{c^2\tau^2 - \xi^2 - \eta 2}}\ d\eta$$

$$= \left(- \frac{2c}{4\pi} \right) \pi \qquad \xi < c\tau \tag{7.6.6}$$

$$= 0 \qquad \xi > c\tau$$

(units: ms^{-1})

In words: this equation states that a one-dimensional transient wave generated by an impulsive distribution of point sources centered at the plane $x_0 =$ const. passing points $x = x_0 \pm \xi$ will leave a field of constant value $2c\pi/(-4\pi)$ spread over the range $x_0 \pm \xi$. When the source distribution extends over successive planes the *total* transient field may be found by integrating 7.6.6 over the appropriate range of $x_0,\ t_0$.

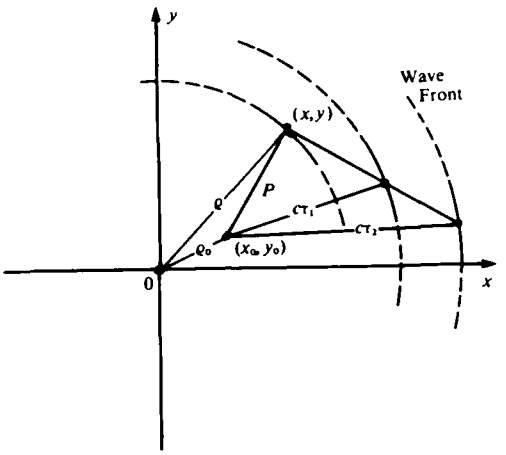

Fig. 7.6.2. Geometric parameters associated with Eq. 7.6.4.

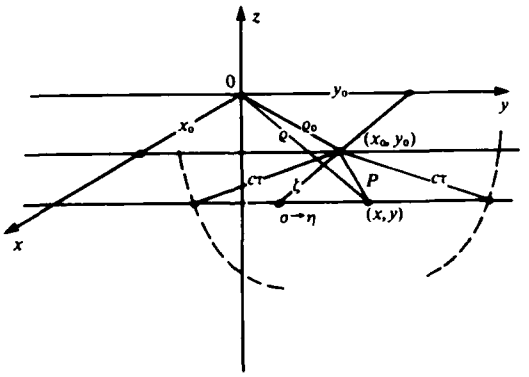

Fig. 7.6.3. Parameters used in the derivation of a 1-*D* Green's function.

7.7. A GEOMETRIC ACOUSTICS INTERPRETATION OF THE TIME-DEPENDENT GREEN'S FUNCTION OF A LINE SOURCE IN THE PRESENCE OF AN INFINITE RIGID CYLINDER

The results of Sect. 7.6 can be used to give a geometric acoustics interpretation to the time-dependent Green's function for a rigid cylinder in the form of Eq. 7.5.5. First in the absence of the rigid cylinder scatterer a pulse front advancing from the source at point $(r_0, 0)$ reaches the field point r at a distance $ct = R$ in time t where $R = (r^2 + r_0^2 - 2rr_0\cos\theta)^{1/2}$. The sound field $g(R, t)$ at r is given by,

$$g(R, t) = \frac{-c}{2\pi} \frac{1}{\sqrt{c^2t^2 - R^2}} \tag{7.7.1}$$

When the cylinder is present we construct the *ray* diagram illustrated in Fig. 7.7.1. Here, as before the line source S is at point $(r_0, 0)$ while the field point P is at point (r, θ). The rays SAA' and SBB' define the shadow boundaries. It is evident from the figure that the Fermat path between S and P is $SA\,QP$. Using this path we define an angle δ such that,

$$\delta = |\theta| - \cos^{-1}\left(\frac{a}{r_0}\right) - \cos^{-1}\left(\frac{a}{r}\right) \tag{7.7.2}$$

The symbol $|\theta|$ is used to allow for paths in the direction such as $SBQ'P'$. In the shadow region $\delta \geqslant 0$ while in the illuminated region δ is negative. The time τ required for the wave front to reach P is easily seen to be

$$\tau = \frac{1}{c}\left\{\sqrt{r_0^2 - a^2} + \sqrt{r^2 - a^2} + a\delta\right\} \tag{7.7.3}$$

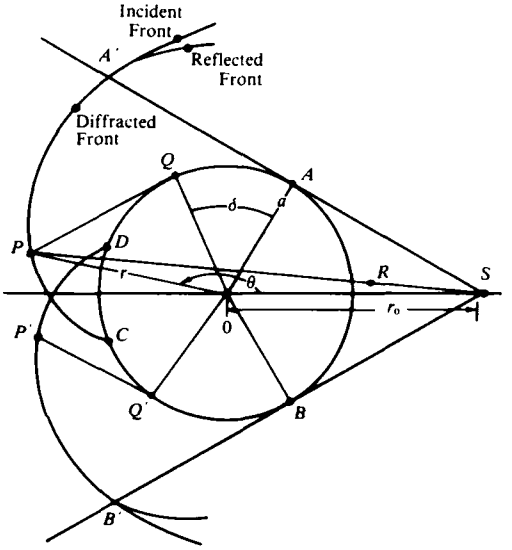

Fig. 7.7.1. Parameters used in the geometric interpretation of the transient Green's function.

The three wave fronts (incident, reflected, diffracted) in Fig. 7.7.1 are thus drawn for the instant $t = \tau$. At velocity c the incident wave front travels from A to A' while the diffracted wave front *on the cylinder* advances from A to C. If the cylinder surface is not rigid the velocity of the wave front on the cylinder will be less than c. Now the sound field at point P in the shadow zone will be given by the sum of functions F in 7.5.5. When $m = 0$ the contribution to the field at P is $F(r, \theta, \tau/r_0, 0, 0)$ in which τ is given by 7.7.3. When $m = +1$ the contribution to P is $F(r, \theta + 2\pi, \tau + [2\pi a/c]|r_0, 0, 0)$, that is, the contribution is delayed by $2\pi a/c$ seconds. For $m > 1$ the time of arrivals are $t = \tau + 2m\pi a/c$. When $m = -1$ the function F must be taken at angle $\theta - 2\pi$. However from 7.5.24 we see that only the absolute value of $\theta \pm 2m\pi$ appears in the formula for the field. Hence we can write,

$$F(r, \theta - 2\pi, t|r_0, 0, 0) = F(r, 2\pi - \theta, t|r_0, 0, 0) \tag{7.7.4}$$

The time taken for the contribution to be made to P by $m = -1$ travelling in the negative direction is the same as the time taken by a contribution $m = 0$ at angle $2\pi - \theta$ travelling in the positive direction. From 7.7.2 and 7.7.3 this time $(= \tau')$ is given by,

Thus the potential field everywhere is obtained by a convolution of the (given) boundary velocity and the transient "system" response called for by the boundary condition 7.8.1.

Consider next a rigid sphere, radius R_0, set in motion by an impulsive force $\mathbf{f}$ which generates a dipole moment in the medium, of dipole strength $|\mathbf{f}|$ (units: $m^4 s^{-1}$). The velocity potential everywhere has then the form,

$$\psi(\mathbf{r}, t^*) = -\text{div}\left[\frac{1}{r}\,\mathbf{f}(t^*)\right].$$

Since $\mathbf{f}$ arbitrarily oriented relative to a spherical coordinate system the fluid velocity at vector point $\mathbf{r}$ is

$$\mathbf{v} = -\nabla\psi = \frac{3(\mathbf{f}\cdot\hat{\mathbf{r}})\hat{\mathbf{r}} - \mathbf{f}}{r^3} + \frac{3(\dot{\mathbf{f}}\cdot\hat{\mathbf{r}})\hat{\mathbf{r}} - \dot{f}}{cr^2} + \frac{(\ddot{\mathbf{f}}\cdot\hat{\mathbf{r}})\hat{\mathbf{r}}}{c^2 r} \tag{7.8.6}$$

where $\hat{\mathbf{r}}$ is a unit vector in the direction $\mathbf{r}$ [10]. The fluid velocity $\mathbf{u}(t)$ in the direction of $\mathbf{f}$ has a component in the direction of $\hat{r}$ given by $v_r = \mathbf{u}\cdot\hat{r}$. At the boundary $r = R_0$, one sets

$$\mathbf{v}\cdot\mathbf{r} = \mathbf{u}\cdot\hat{\mathbf{r}}. \tag{7.8.7}$$

The boundary condition is thus represented by the form,

$$\ddot{\mathbf{f}}(t^*) + \frac{2c}{R_0}\,\dot{f}(t^*) + \frac{2c^2}{R_0^2}\,\mathbf{f}(t^*) = Rc^2\mathbf{u}(t^*). \tag{7.8.8}$$

This ordinary differential equation may be solved by use of the theory of Laplace transforms. Assuming zero initial conditions and using transform pair 1.301 of Ref. [11], one arrives at an expression for the vector dipole strength [12],

$$\mathbf{f}(t^*) = cR_0^2 e^{-\frac{c}{R_0}t^*}\int_a^{t^*}\mathbf{u}(\tau)e^{\frac{c}{R_0}\tau}\sin\left[\frac{c}{R_0}\,(t-\tau)\right]d\tau. \tag{7.8.9}$$

Here the lower limit a is customarily taken to be the origin of time. However, to insure that $\mathbf{f}(t^*)$ eventually vanishes in the distant past one can set $a = \infty$.

Equation 7.8.9 may be used to find the potential field and acoustic radiation of a rigid sphere set into steady motion $\mathbf{u}_0$ from a condition of rest at time $t = 0$. For this case,

$$\begin{aligned}
\mathbf{f}(t) &= cR_0^2\, e^{-\frac{c}{R_0}t}\mathbf{u}_0\int_0^t e^{\frac{c}{R_0}\tau}\sin\frac{c}{R_0}\,(t-\tau)\,d\tau \\
\mathbf{f}(t) &= \frac{1}{2}\,R_0^3\, e^{-\frac{c}{R_0}t}\mathbf{u}_0\left[1 - e^{-\frac{c}{R_0}t}\left(\sin\frac{c}{R_0}\,t + \cos\frac{c}{R_0}t\right)\right] \\
\dot{\mathbf{f}}(t) &= cR_0^2\,\mathbf{u}_0\, e^{-\frac{c}{R_0}t}\sin\frac{c}{R_0}t \\
\ddot{\mathbf{f}}(t) &= -c^2R_0\,\mathbf{u}_0\, e^{-\frac{c}{R_0}t}\left[\sin\frac{c}{R_0}\,t - \cos\frac{c}{R_0}t\right] \\
\ddot{\mathbf{f}}(t) &= -c^2R_0\,\mathbf{u}_0\, e^{-\frac{c}{R_0}t}\sqrt{2}\sin\left(\frac{c}{R_0}t - \pi/4\right).
\end{aligned} \tag{7.8.10}$$

Thus the potential field everywhere is obtained by a convolution of the (given) boundary velocity and the transient "system" response called for by the boundary condition 7.8.1.

Consider next a rigid sphere, radius R_0, set in motion by an impulsive force $\mathbf{f}$ which generates a dipole moment in the medium, of dipole strength $|\mathbf{f}|$ (units: $m^4 s^{-1}$). The velocity potential everywhere has then the form,

$$\psi(\mathbf{r},t^*) = -\text{div}\left[\frac{1}{r}\,\mathbf{f}(t^*)\right].$$

Since $\mathbf{f}$ arbitrarily oriented relative to a spherical coordinate system the fluid velocity at vector point $\mathbf{r}$ is

$$\mathbf{v} = -\nabla\psi = \frac{3(\mathbf{f}\cdot\hat{\mathbf{r}})\hat{\mathbf{r}} - \mathbf{f}}{r^3} + \frac{3(\dot{\mathbf{f}}\cdot\hat{\mathbf{r}})\hat{\mathbf{r}} - \dot{f}}{cr^2} + \frac{(\ddot{\mathbf{f}}\cdot\hat{\mathbf{r}})\hat{\mathbf{r}}}{c^2 r} \tag{7.8.6}$$

where $\hat{\mathbf{r}}$ is a unit vector in the direction $\mathbf{r}$ [10]. The fluid velocity $\mathbf{u}(t)$ in the direction of $\mathbf{f}$ has a component in the direction of $\hat{r}$ given by $v_r = \mathbf{u}\cdot\hat{r}$. At the boundary $r = R_0$, one sets

$$\mathbf{v}\cdot\mathbf{r} = \mathbf{u}\cdot\hat{\mathbf{r}}. \tag{7.8.7}$$

The boundary condition is thus represented by the form,

$$\ddot{\mathbf{f}}(t^*) + \frac{2c}{R_0}\,\dot{f}(t^*) + \frac{2c^2}{R_0^2}\,\mathbf{f}(t^*) = Rc^2\mathbf{u}(t^*). \tag{7.8.8}$$

This ordinary differential equation may be solved by use of the theory of Laplace transforms. Assuming zero initial conditions and using transform pair 1.301 of Ref. [11], one arrives at an expression for the vector dipole strength [12],

$$\mathbf{f}(t^*) = cR_0^2 e^{-\frac{c}{R_0}t^*}\int_a^{t^*}\mathbf{u}(\tau)e^{\frac{c}{R_0}\tau}\sin\left[\frac{c}{R_0}\,(t-\tau)\right]d\tau. \tag{7.8.9}$$

Here the lower limit a is customarily taken to be the origin of time. However, to insure that $\mathbf{f}(t^*)$ eventually vanishes in the distant past one can set $a = \infty$.

Equation 7.8.9 may be used to find the potential field and acoustic radiation of a rigid sphere set into steady motion $\mathbf{u}_0$ from a condition of rest at time $t = 0$. For this case,

$$\begin{aligned}
\mathbf{f}(t) &= cR_0^2\, e^{-\frac{c}{R_0}t}\mathbf{u}_0\int_0^t e^{\frac{c}{R_0}\tau}\sin\frac{c}{R_0}\,(t-\tau)\,d\tau \\
\mathbf{f}(t) &= \frac{1}{2}\,R_0^3\, e^{-\frac{c}{R_0}t}\mathbf{u}_0\left[1 - e^{-\frac{c}{R_0}t}\left(\sin\frac{c}{R_0}\,t + \cos\frac{c}{R_0}t\right)\right] \\
\dot{\mathbf{f}}(t) &= cR_0^2\,\mathbf{u}_0\, e^{-\frac{c}{R_0}t}\sin\frac{c}{R_0}t \\
\ddot{\mathbf{f}}(t) &= -c^2R_0\,\mathbf{u}_0\, e^{-\frac{c}{R_0}t}\left[\sin\frac{c}{R_0}\,t - \cos\frac{c}{R_0}t\right] \\
\ddot{\mathbf{f}}(t) &= -c^2R_0\,\mathbf{u}_0\, e^{-\frac{c}{R_0}t}\sqrt{2}\sin\left(\frac{c}{R_0}t - \pi/4\right).
\end{aligned} \tag{7.8.10}$$

These five formulas allow one to find the fluid velocity everywhere by use of 7.8.6. When, however, the field point is at very great distance r, only the last term in 7.8.6 is significant. Thus, far from the sphere, at retarded time t^*,

$$\mathbf{v}(\mathbf{r},\ t^*) = -\hat{\mathbf{r}}(\mathbf{u}_0 \cdot \hat{\mathbf{r}})\ \sqrt{2}\ \frac{R_0}{r}\ \exp\left(-\frac{c}{R_0}t^*\right)\ \sin\left(\frac{c}{R_0}t^* - \pi/4\right). \tag{7.8.11}$$

This formula is remarkable. It states that a sudden uniform velocity motion of a sphere from rest in a compressible medium results in a distant fluid velocity in the form of a *decaying sinusoid* whose initial amplitude is the component of the initial uniform velocity in the direction of observation modified by spherical divergence.

The total instantaneous acoustic power radiated from the transient motion of the sphere is obtained by integration over a sphere of radius r:

$$W(t^*) = \int \rho c \mathbf{v}^2\ dS(r)$$

Since the coordinate axes can be aligned arbitrarily one can take $\mathbf{u}_0 = \hat{r} = |u_0| \cos\theta$. Hence,

$$W(t^*) = \rho c\ 2\ R_0^2 \int_0^{2\pi}\int_0^{\pi} \exp\left(-2\frac{c}{R_0}t^*\right)\ \sin^2\left(\frac{c}{R_0}t^* - \pi/4\right)\ \cos^2\theta\ \frac{r^2}{r^2}\ \sin\theta\, d\theta\, d\phi$$

$$W(t^*) = \frac{8\pi}{3}\ u_0^2\ \rho c R_0^2\ \exp\left(-\frac{2c}{R_0}t^*\right)\ \sin^2\left(\frac{c}{R_0}t^* - \pi/4\right). \tag{7.8.12}$$

By changing variables, $ct^*/R_0 = x$, and using the formula,

$$\int_0^{\infty} e^{-2x} \sin^2 x dx = \frac{1}{8}$$

it is seen that the total energy radiated over all time is,

$$W = \frac{\pi}{3}\ u_0^2 \rho R_0^3. \tag{7.8.13}$$

This is 1/2 of the kinetic energy ($1/2\ Mu_0^2$) of the mass M of medium in the volume of the sphere accelerated from rest to uniform velocity u_0.

7.9 SOUND GENERATED IN LIQUIDS BY SPLASHES

The sound made by entry of objects form a gaseous medium (air) into a liquid medium (water) is attributable to several mechanisms: in the gas the mechanisms are (1) transient passage through the interface (2) vibrations of the penetrating object (3) the ejection of spray from the initial splash and from secondary splashes (4) the resonant vibration of cavities in the liquid formed by the objects (5) the breaking of bubbles on the free surface. In the liquid the mechanisms are (1) transient passage through the interface (2) vibrations of the penetrating object (3) oscillations of gas bubbles and cavities (4) secondary splashes.

In the following discussion these various mechanisms are codified into 3 types called phases of sound separation: (a) flow establishment phase (b) object vibration phase (c) cavity and bubble phase.

If the objects entering the liquid have arbitrary shape the mathematical description of the radiated sound is complex. It is therefore useful to consider only simple-shaped objects such as spheres, circular pistons, etc.

7.9a SOUND GENERATED BY THE IMPACT OF A HIGH VELOCITY RIGID SPHERE ON A LIQUID

Flow establishment phase

Let a rigid sphere radius a, moving vertically, strike the horizontal free surface of a liquid (density ρ and sound speed c) with velocity V_0. Assume first the impact velocity is supersonic. The initial flow in the liquid is for a very short duration (also supersonic) approximately equal to (1/2) (a/c) (V_0/c). Such a flow generates acoustic radiation composed mostly of very high frequency (short wavelength) components directed radially, as from a hemisphere. It can be thought of as a simple source, Eq. (7.1.22), and modelled as a piston of radius a impacting the liquid and radiating sound into halfspace with source strength $\mathcal{Q}(t) = \pi a^2 V(t - r/c)$.

A first estimate of the radiation in obtainable from (7.2.2) by replacing some speed C with supersonic velocity V_0, then because of the very short time duration of impact at $t = 0$, expanding the exponential to two terms:

$$p(r, t) \simeq \rho V_0^2 \frac{a}{r}\left[1 - \left(t - \frac{r}{c}\right)\frac{V}{a}\right], \qquad \begin{cases} t \geqslant \dfrac{r}{c} \\ V_0 \geqslant c \end{cases}. \tag{7.9.1}$$

The c in r/c is retained because at distance r one assumes the initial supersonic flow has become sonic. This formula is valid for time (1/2) (aV_0/c^2). After this time the flow is thought to be subsonic.

In the regime of subsonic hydrodynamic flow the slug of water pushed into the liquid by the entering object constitutes a source of sound whose characteristics wavelength is such that within one such wavelength of the free surface the source is strongly coupled to the surface and is thus accompanied in its travel by its image (or out-of-phase reflection). The source and its image thus constitute a moving acoustic dipole. An estimation of the vertical dipole strength $D(\tau)$ (units: m^4s^{-1}) of this source is quite complicated: one procedure for making this estimate is to construct a fictitious "pseudobody" made up of the (time-varying) submerged portion of the real object as it penetrates the surface, and its image (by reflection) in the free surface [1]. This pseudobody at any instant is treated as if fully submerged. To estimate its instantaneous dipole strength it is fixed in space momentarily. One then replaces it by a set of simple sources and their images. Each pair of simple sources consists of volume velocities VdA_1, VdA_2 where dA_1, dA_2 are the horizontal components of incremental area on the real and image bodies respectively. The distance between each simple source at dA_1 and its image at dA_2 is $l(z)$. The dipole strength is then

$$D(t) = \int_0^{L(t)} l(z)\, V[dA_1(z) + dA_2(z)] \text{ (units:m}^4\text{/s)} \tag{7.9.2}$$

in which L is the length of the real submerged object and $z = z(t)$. This approximation is valid for far field radiation, but is not useful in describing the pressure on the surface of the object as it enters the liquid. A second procedure in estimating dipole strength is to neglect the contribution of the images and consider radiation into half space from the real body. Then

$$D(t) \sim 2 \int_0^z (z - s) \left[\frac{dz}{dt}\right] \left[\frac{dA}{ds}\right] ds \tag{7.9.3}$$

[14] in which $z = z(t)$ and $A = A(s)$ is the horizontal cross-sectional area of the body as a function of vertical distance s from the nose of the body. For a rigid sphere, radius a, one has $A = \pi\ (2as - s^2)$. Hence its instantaneous dipole source strength is,

$$D(t) \sim 2\pi z^2 \left[\frac{dz}{dt}\right] (3a - z)/3 \tag{7.9.4}$$

$$z = z(t).$$

If the pseudobody is blunt one must multiply $D(t)$ by b, the bluntness factor, which is the ratio of the average distance from nose to tail *around* the body to the distance from nose to tail *through* the body. For long slender bodies $b \simeq 1$; for spherical bodies $b \simeq 3/2$.

When the sphere impacts the free surface at angles other than vertical the radiation of sound in the liquid is of thequadrupole type. A discussion of the quadrupole source strength (defined in 7.1.19) for the case is given by Ref. [14].

Object Vibration Phase

When a high velocity uncompressible sphere strikes the free surface of a liquid the sphere is set into vibration. The lowest mode of free vibration is *spheroidal* in which the sphere is distorted into an ellipsoid of revolution, becoming alternately prolate and oblate in shape. The frequency of this vibration is the value of ω given by,

$$\frac{\kappa a}{\pi} = 0.848,\ k = \frac{\omega}{c_s},\ c_s = \sqrt{\frac{\mu}{\rho}}. \tag{7.9.5}$$

[15]. When the direction of entry of the sphere is vertical and the flow phase is subsonic the sound generated is predominantly dipole in nature. The dipole source strength can then be *estimated* by first calculating the (normal) surface velocity $v(s)$ due to spheroidal motion at frequency ω in 7.9.5 and then adding $v(s)$ to dz/dt in 7.9.3. This procedure requires an explicit knowledge of the forces generated by impact and the kinematics of the entry of the object into the liquid.

Cavity and Bubble Phase

The entry of a high velocity object moving from air into the free surface of a liquid generally creates a cavity and entrains air bubbles. Under the action of unbalanced forces the entrained bubbles vibrate or collapse completely. The theory of the radiation of sound from

collapsing bubbles in freespace is presented in Secs. 10.5b and 10.5c of this treatise. The effect of the liquid surface in modifying (unbounded domain) acoustic radiation from oscillation or collapsing bubbles into the liquid is described in Sec. 11.1e. When the bubbles are physically located within a wavelength (of the characteristic frequency of bubble oscillation) of the free surface their radiation is dipole in nature. To predict this radiation one notes that essentially, if the monopole radiation of a bubble oscillating at frequency f in a free field is calculated by use of Sec. 11.2, the effect of proximity to the free surface is obtained by multiplying this radiation by the factor $kd \cos\theta$, where $k(=\omega/c = 2\pi f/c)$ is the wavenumber of the medium of acoustic propagation, d is the dipole separation distance (small relative to wavelength $\lambda = c/f$) and θ is the polar angle measured from the normal to the free surface. This procedure provides a good farfield approximation.

The cavity formed by the penetrating object undergoes transient distortion and thus itself radiates sound. A useful approximation in predicting this radiation (in the liquid) is to model it as cavitation noise. The theory of cavitation noise is treated in Secs. 10.6 and 10.7 of this treatise.

7.9b PRESSURE LEVEL, PULSE SHAPE AND ENERGY SPECTRA OF ACOUSTIC RADIATION IN WATER GENERATED BY VERTICAL IMPACT OF SINGLE DROPS, AND RAIN

A spherical water droplet, radius a, impacting a free water surface with (normal) velocity V generates a sound pressure pulse in the water. The shape of this pulse is generally reproducible and has the appearance shown in Fig. 7.9.1. The similarity of this figure to pressure pulses due to explosive sound may be observed by referring to Chapter XI of this treatise. In particular similar formulation of the sound energy E radiated into the water is found from the general radiation,

$$E = \int dA(\mathbf{r}) \int_{-\infty}^{\infty} dt \, \frac{p^2}{\rho c}(\mathbf{r}, t) \tag{7.9.6.}$$

in which $p(\mathbf{r}, t)$ is the sound pressure at radius $|\mathbf{r}|$ and time t. In the calculation of E a usual procedure is to filter $p(\mathbf{r}, t)$ through a sequence of broadband filters to obtain the time-varying pressure signature $p_\Delta(r, t)$ in each band. If the geometric mean frequency of a band is designated f the pressure $p_\Delta(\mathbf{r}, t)$ can be considered as that due to a "steady state" dipole. From 5.4.8 and 5.3.10a it is seen that when near field is included, the steady state dipole intensity is given by,

$$\frac{p_f^2}{\rho c} = \frac{Q_2^2}{(4\pi)^2} \frac{k^4 \cos^2\theta}{R^2} \rho c \left[\frac{c^2}{4\pi f^2 R^2} + 1\right] \quad \left[\text{units: } \frac{\text{Nm}}{\text{sm}^2}\right] \tag{7.9.7}$$

in which Q_2 is the dipole source strength in units of m^4/s. Now when p_f is *measured* as a time-varying pressure in (say) half-octave bands the source strength Q_2 is a time-varying quantity. The measured pressure can be normalized with respect to θ, f and ρc, to make it independent of nearfield and angle, and then integrated only over the time coordinates to give the time-averaged energy per unit area. Final multiplication by the area of a hemisphere $(2\pi R^2)$ gives the energy $E_{1/2}$ in (say) a half-octave band at near frequency f,

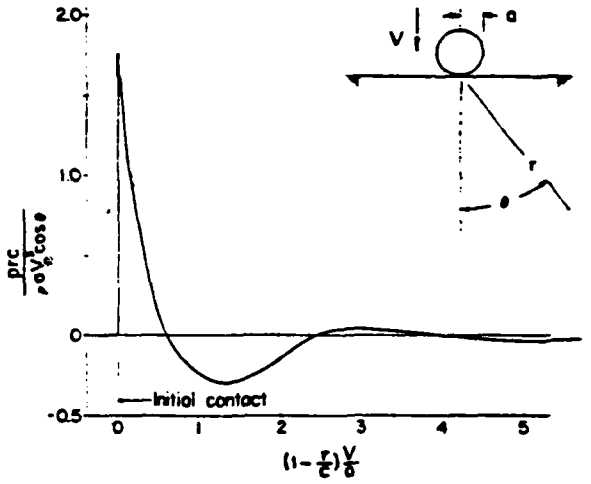

Fig. 7.9.1. The typical shape of the sound pressure pulse radiated into the water by the vertical impact of a water droplet after [1].

$$E_{1/2} = \frac{2\pi R^2}{3\rho c \cos^2\theta \left[1 + \left[\frac{c}{Q\pi fR}\right]^2\right]} \int_{-\infty}^{\infty} p_{1/2}^2(R, t)\, dt, \quad \text{(units: Nm)}. \tag{7.9.8}$$

The factor 3 is inserted because the dipole amplitude (A_{01}) (see Eq. 5.4.8) is normalized to be inversely proportional to $\sqrt{3}$, hence the dipole energy is inversely proportional to the numeric 3. In an experiment of water droplets, inpacting a water surface the half-octave energy spectra of 0.14 cm, 0.24 cm, 0.29 cm and 0.35 cm droplets striking the free surface at impact velocities 200 to 700 cm/sec were obtained. The results [14] are reproduced from here as Fig. 7.9.2. In this figure it is seen that the maximum underwater acoustic noise energy radiated by a single water droplet (0.35 cm) impacting the surface at 700 cm/sec as measured in a half-octave band at the geometric mean frequency of (approximately) 4 kc is nearly 3×10^{-3} erg. The data of Eq. (7.9.2) can be condensed into the dimensionless plot, Fig. 7.9.3. In this figure T is the kinetic energy of the droplet at impact and M is the mach number (V_0/c_0) of the droplet or impact.

Figures 7.9.2 and 7.9.3 give measured energy of impact noise of single water droplets. The noise due to the bubble component of the underwater sound energy from a splash of a water droplet has also been measured [1]. The results are reproduced here as Fig. 7.9.4. This figure shows that the formation of bubbles by entrainment from impacting water drops and their subsequent radiation of sound are erratic processes and not easily predictable. However on comparing the half-octave energy spectra of noise of impact with the noise of subsequent bubble oscillation it is concluded that upon averaging over many droplets the two energies are about equal.

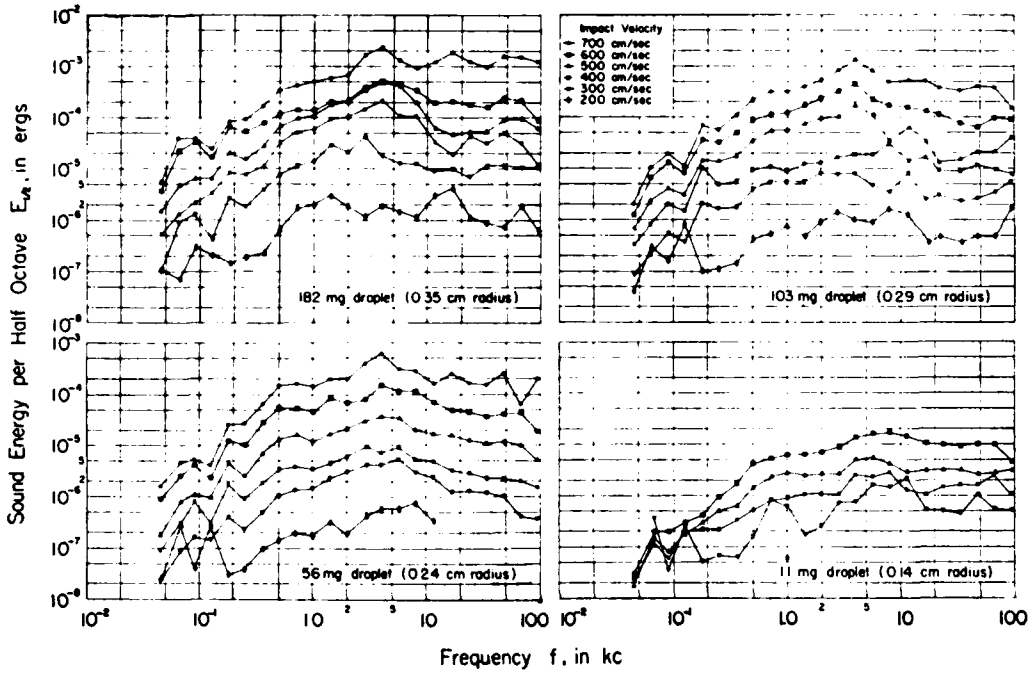

Fig. 7.9.2. The half-octave frequency spectra of the impact part of the sound energy radiated into the water by the splashes of single water droplets after [1].

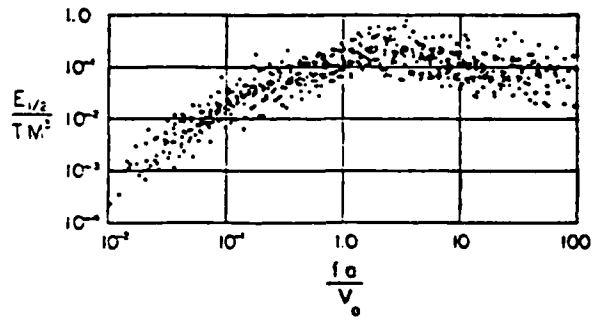

Fig. 7.9.3. The half-octave dimensionless frequency spectrum of the sound energy radiated into the water by the impact of single droplets of water after [1].

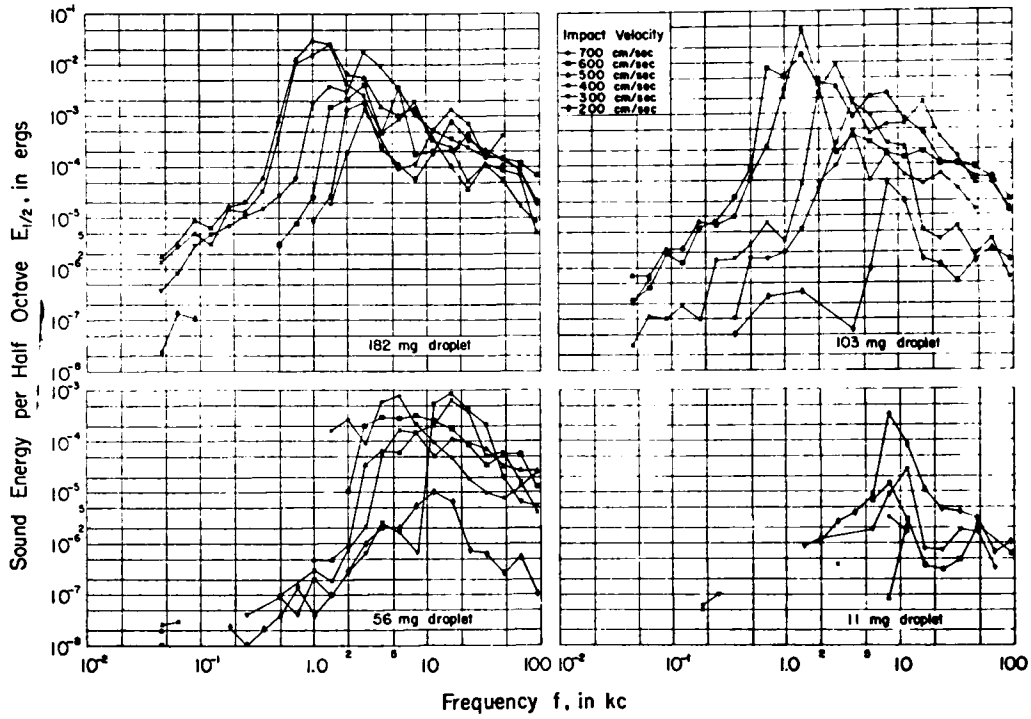

Fig. 7.9.4. The half-octave frequency spectra of the bubble part of the sound energy radiated into the water by the splashes of single water droplets [after [14]].

Figure 7.9.3 may be converted to a more useful form by conversion from energy in half-octave bands to spectral energy $E(\nu)d\nu$ in dimensionless band $d\nu \equiv (a/V)df$. This representation, Fig. 7.9.5, is a universal curve which can be used to estimate spectral energy density, $E(\nu)$, given the kinetic energy T of single droplets of water. The abscissa ν is the spectral frequency normalized by the ratio V_0/a. The maximum energy is near $f = V_0/a$. By use of such diagrams one can estimate the sound pressure spectrum level SPL in a 1 Hz band of the noise radiated underwater by a spray of waterdroplets. By definition,

$$\text{SPL} = 10 \log_{10} \frac{p_{AV}^2}{p_{\text{ref}}^2} \tag{7.9.9}$$

in which p_{AV}^2 is the time-average squared pressure level and p_{ref}^2 is the reference level. To calculate p_{AV}^2 one returns to 7.9.8 and chooses an integration time Δt units long over a unit area ΔS covered by the spray in the free surface,

$$\frac{p_{AV}^2}{\Delta S} = \frac{\int_{\Delta t} p^2(R, t)\,dt}{\Delta t \Delta S} = I \frac{3\rho c \cos^2\theta}{2\pi R^2}\left[1 + \left[\frac{c}{2\pi f R}\right]^2\right] \tag{7.9.10}$$

where

$$I = \frac{E}{\Delta t \Delta S} \quad \text{(units: Nms}^{-1}\text{m}^{-2}\text{)}.$$

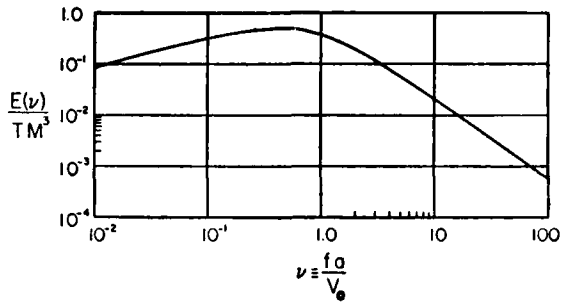

Fig. 7.9.5. The dimensionless spectral density of the sound energy radiated into the water by the impact of single droplets of water or by the splashes of a spray of water droplets after [1].

Assume now that the spray area is bounded by a circle which subtends an angle α from a point on the normal through the center h units below the surface. Then an elementary area of this spray on the free surface is given by,

$$dS = R^2 \sin\theta \cos\theta \, d\theta d\phi$$

in which

$$h = R \cos\theta.$$

Thus,

$$p_{AV}^2 = \frac{3\rho cI}{2\pi} \int_S \frac{1}{R^2} \cos^2\theta \left[1 + \left(\frac{c}{2\pi fR}\right)^2\right] R^2 \sin\theta \cos\theta \, d\theta d\phi$$

$$= \frac{3}{2} \rho cIG(\alpha) \tag{7.9.11}$$

$$G(\alpha) = (1 - \cos^2\alpha) + \frac{c^2(1 - \cos^4\alpha)}{2 \cdot 4\pi^2 f^2 h^2}.$$

Now one can define I in terms of Fig. 7.9.5 by introducing the kinetic energy (per unit time per unit area) of the spray, $(1/2)\rho V_0^2 \mathscr{V}$, where $\mathscr{V}$ is the volume of droplets impinging on the free surface per unit of time per unit of spary area,

$$I = \frac{1}{2} \rho V_0^2 \mathscr{V} \left(\frac{E}{TM^3}\right) M^3. \tag{7.9.12}$$

Since $M^3 = V_0^3/c^3$ and since the maximum sound energy is radiated at frequency f where $fa/V_0 \sim 1$ it is seen that per unit band of frequencies

$$\frac{P_{AV}^2}{f} \simeq \frac{3}{4c^2} \rho^2 V_0^4 a \mathscr{V} \left(\frac{E}{TM^3}\right) G(\alpha), \quad \text{(units: } N^2 sm^{-4}\text{)}. \tag{7.9.13}$$

Choosing MKS units throughout and a reference pressure of one micropascal (10^{-6} Nm^{-2}) per unit band, the sound-pressure-spectrum level underwater of a circular area spray of droplets, whose single droplet kinetic energy at impact velocity V_0 is T, is given in units of dB/re 1 μPa per unit band by

$$\text{SPL} = 120 + 10 \log_{10}\left\{\frac{3}{4c^2}\rho^2 V_0^4 a\, \mathcal{V}\left[\frac{E(\nu)}{TM^3}\right] G(\alpha)\right\} \tag{7.9.14}$$

in which $E(\nu)/TM^3$ is taken from Fig. 7.9.5 at $\nu \sim 1$.

When the spray area is other than circular in shape one can calculate p_{AV}^2 by 7.9.11, using however the appropriate expression for the elementary area dS as a function of spherical coordinates R, θ, ϕ.

7.9c SOUND RADIATED UNDERWATER BY IMPACT OF RAIN ON THE WATER SURFACE

To calculate the underwater sound caused by rain one can use 7.9.14. However it is necessary to know the impact velocity V_0, size of droplet a and the volume rate V. In the case of rain both a and V_0 are functions of rate of rainfall [16]. Using the data from this reference in 7.9.14 Franz [14] has calculated estimates of sound-pressure-spectrum level caused by rain. His results are reproduced here in Fig. 7.9.6. For comparison this figure displays the level of ambient noise at sea state 1 in the sea (excluding shipping noise) as a dotted line versus frequency. It is seen, for example, that a rainfall rate of 1 in. per hour is anticipated to raise the noise in the sea by about 10 dB re 2×10^{-4} dipole/cm^2 per 1 Hz band above sea-state 1 in the frequency range of approximately 400 Hz to 10 kHz. Such estimates are valid as long as the depth of measurement is greater than one wavelength from the surface. However, since attenuation accompanying propagation is not included in this figure it must be accounted for by application of propagation theory if measurements are made at points very deep in the sea.

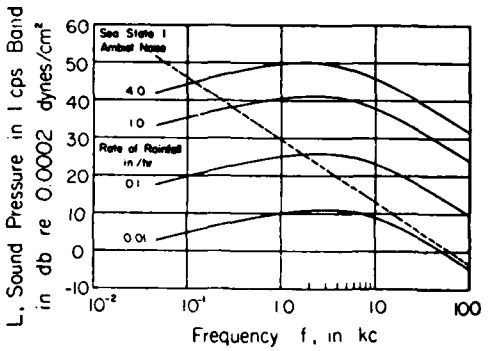

Fig. 7.9.6. The estimated sound pressure-spectrum levels of the underwater sound from the impact of rain on the surface, at depths greater than a wavelength from the surface.

When the band of frequencies is made very wide one can summarize Fig. 7.9.6 by two approximation formulas for the sound pressure level, SPL:

(1) for a band 0.1 to 10 kHz, $\text{SPL} \simeq 106 + 145 \log_{10} V$

(2) for a band 0.1 to 100 kHz, $\text{SPL} \simeq 109 + 14.5 \log_{10} V$ (7.9.15)

in which the units of SPL are dB re 1 μPa.

7.10 RADIATION OF SOUND FROM A POINT FORCE IN MOTION

A point force **f** per unit volume located at **y** undergoes accelerated motion $\mathbf{V}(t)$, radiating sound to observation point **x**. By use of the method of Lighthill, Curle (see Eq. 8.7.1), the acoustic pressure at **x** is found to be,

$$p = -\frac{1}{4\pi}\int \left[\frac{1}{r}\nabla\cdot\mathbf{f}\right]dV \tag{7.10.1}$$

in which the brackets indicate evaluation at retarded time $t' = t - r/c$, where $r = |\mathbf{r}|$, $\mathbf{r} = \mathbf{x} - \mathbf{y}$. Now **f** is a concentrated force and is represented by $\mathbf{f}(t)\ \delta\ (\mathbf{y} - \mathbf{y}_0)$. Thus one is required to find the divergence $\nabla \cdot (\mathbf{f}(t)\ \delta\ (\mathbf{y} - \mathbf{y}_0))$ in which $y_0 = y_0(t')$. By proper attention to the square brackets, it may be shown following Lowson [17] that the far field pressure p_1 is given by

$$p_1 = \left[\frac{c}{4\pi r(c - \boldsymbol{V}\cdot\boldsymbol{n})^2}\left(\boldsymbol{n}\cdot\frac{\partial \boldsymbol{f}}{\partial t} + \boldsymbol{n}\cdot\boldsymbol{f}\frac{\mathrm{d}\boldsymbol{V}}{\mathrm{d}t}\cdot\frac{}{c - \boldsymbol{V}\cdot\boldsymbol{n}}\right)\right] \tag{7.10.2}$$

in which $\hat{\mathbf{n}}$ is a unit vector in direction of **r**. Similarly, the near field is given by

$$p_2 = \left[\frac{c}{4\pi r^2(c - \boldsymbol{V}\cdot\boldsymbol{n})^2}\left(\boldsymbol{n}\cdot\boldsymbol{f}\frac{c^2 - V^2}{c - \boldsymbol{V}\cdot\boldsymbol{n}} - \boldsymbol{V}\cdot\boldsymbol{f}\right)\right] \tag{7.10.3}$$

REFERENCES

1. S. Poisson, Memories de l'Acad. Roy. des Sci. III (1819), 121.
2. B.B. Baker, E.T. Copson, "The Mathematical Theory of Huygens' Principle", Oxford, Clarendon Press 2 ED. 1953, page 12.
3. P.M. Morse, H. Feshbach, "Methods of Theoretical Physics", McGraw-Hill Book Co. 1953, Part I. page 847.

3a P.M. Morse, V. Ingard "Theoretical Acoustic," McGraw-Hill 1968, p. 312.

3b L.D. Landau, E.M. Lifshitz "Fluid Mechanics," Pergamon Press 1959, p. 28.

4. Ref. [3], p. 123, 837.
5. Ref. [3], p. 843.
6. V.R. Lauvstad, "Transient Scattering of a Monochromatic Acoustic Wave by a Scatter Fixed in Space", JASA *38*, 35: 1965.

6a Ref. [3], chap. 11.

6b W. Probst "Schallerzeugung Durch Expandierende Kugel" Acustica, *27*, p. 299-306, (1972).

7 Ref. [3], p. 888.

8 G.A. Campbell, R.M. Foster "Fourier Integrals for Practical Applications" Bell System Tech. Pub. Monograph B-584, 1942 p. 111. The symbols for impulse functions used in this reference differ from the text:

Campbell and Foster	Text
$S_0(t-g)$	$\delta_0(t-t_0)$, impulse
$S_1(t-g)$	$d/dt\ \delta_0(t-t_0)$, double impulse
$S_{-1}(t-g)$	$U(t-t_0)$, unit step.

9. J.N. Miles, "Transient Loading of a Baffled Piston" JASA *25*, p. 200 (1950).
10. L.D. Landau, E.M. Lifshitz "Fluid Mechanics," Addison-Wesley 1959, p. 286.
11. M.F. Gardner, J.L. Barnes "Transients in Linear Systems," J. Wiley, 1942, p. 342.
12. Ref [10] p. 286.
13. I.S. Gradshteyn, I.M. Ryzhik "Tables of Integrals," p. 195, Academic Press 1965, Formula 2.662.1.
14. G.J. Franz, J. Acous. Soc. Am., **31**, 1080-1096 (1959).
15. A.E.H. Love. "Mathematical Theory of Elasticity" Dover Pub. New York, 6th Ed. p. 286.
16. J.O. Laws, D.A. Parsons, Hydrology reports and papers, Am. Geophysics Union, 24th Annual Meeting, April 23,24, 1943.
17. M.V. Lowson, Proc. Roy. Soc.(A) **286** [1965], 559.

CHAPTER VIII
THEORY OF RANDOM RADIATION FROM A SURFACE

8.1 PARAMETRIC EQUATIONS AND DISPLACEMENTS OF A RADIATING ELASTIC SHELL

Let α_1, α_2 be the curvilinear coordinates of a surface S in a rectangular coordinate system x, y, z. A location vector $\vec{r}$ from the coordinate origin to point x_1, y_1, z_1 on the surface is,

$$\vec{r}(\alpha_1, \alpha_2) = x_1(\alpha_1, \alpha_2)\hat{e}_1 + y_1(\alpha_1, \alpha_2)\hat{e}_2 + z_1(\alpha_1, \alpha_2)\hat{e}_3 \tag{8.1.1}$$

in which $\hat{e}_i$ is a unit vector. A differential change $d\vec{r}$ in $\vec{r}$ lies in the surface and its magnitude squared is $d\vec{r} \cdot d\vec{r} = (ds)^2 = E(d\alpha_1)^2 + 2F\,d\alpha_1 d\alpha_2 + G(d\alpha_2)^2$. Assume α_1, α_2 are orthogonal so that curves $\alpha_1 = \text{const}$, $\alpha_2 = \text{const}$ form an orthogonal net. Then,

$$(ds)^2 = A_1^2(d\alpha_1)^2 + A_2^2(d\alpha_2)^2 \tag{8.1.2}$$

where $A_1 (= \sqrt{E})$, $A_2 = (\sqrt{G})$ are the scale factors, and $F = 0$.

At point x_1, y_1, z_1 let the displacement vector be,

$$\vec{d} = u_1\hat{a}_1 + u_2\hat{a}_2 + w\hat{a}_3 \qquad \text{(units: } m\text{)}$$

in which $\hat{a}_i$ are unit vectors in the direction of $\alpha_1 = \text{const}$, $\alpha_2 = \text{const}$ and the outward normal $\vec{n}$, defined as pointing from the concave to the convex side. In general $\vec{d}$ is a function of α_1, α_2 and time t. To describe it we assume an expansion in functions $\vec{Q}_m(\alpha_1, \alpha_2)$ which are orthogonal in coordinates α_1, α_2 over the surface,

$$\vec{d}(\alpha_1, \alpha_2, t) = \sum_n q_n(t)\vec{Q}_m(\alpha_1, \alpha_2) \tag{8.1.3}$$

The units of q_n are $m(=$ meters). The symbol $\vec{Q}_m$ is non-dimensional. The subscript n indicates a temporal mode. A natural choice of $\vec{Q}_m$ is the set of normal modes of free vibration whose n'th member is,

$$\vec{Q}_m \cos\omega_n t = u_{1_n}(\alpha_1, \alpha_2)\cos\omega_n t\,\hat{a}_1 + u_{2n}(\alpha_1, \alpha_2)\cos\omega_n t\,\hat{a}_2$$

$$+ w_n(\alpha_1, \alpha_2)\cos\omega_n t\,\hat{a}_3 \tag{8.1.4}$$

where ω_n is the radian frequency of a normal mode of free vibration. Since the normal modes are orthogonal to each other over the range of the coordinates α_1, α_2 one may express this orthogonality by an integral,

$$\text{(a)} \quad \int_S \int (\vec{Q}_m \cdot Q_n) A_1 A_2 \, d\alpha_1 d\alpha_2 = \delta_{mn} N_n$$

or

$$\text{(b)} \quad \int_S \int (u_{1m} u_{1n} + u_{2m} u_{2n} + w_m w_n) A_1 A_2 \, d\alpha_1 d\alpha_2 = \delta_{mn} N_n$$

in which

$$\delta_{mn} = 1, \; m = n$$

$$\delta_{mn} = 0, \; m \neq n$$

$$\text{(c)} \int_S \int (u_{1_n}^2 + u_{2_n}^2 + w^2) A_1 A_2 \, d\alpha_1 \, d\alpha_2 = N_n, \text{ (units: } m^2) \tag{8.1.5}$$

Eq. 8.1.3 is the *spectral representation* of the displacement and is fundamental in the spectral method of solving problems in the forced vibration of shells.

8.2. EQUATIONS OF MOTION OF A SHELL DRIVEN IN FORCED VIBRATION BY SURFACE LOADS

Let p_1, p_2, $-P$ be the forces per unit area exerted by external agencies on the surface in the $\alpha_1 =$ const, $\alpha_2 =$ const, and normal directions respectively. The negative sign indicates that the normal force acts into the surface. Upon substitution of 8.1.3 into the equations of motion of a thin materially homogeneous and elastically isotropic shell [1] it is found that the spectral method of solving them leads to a set of three ordinary differential equations,

$$\sum_{n=1}^{\infty} \left\{ \varrho h \frac{d^2 q_n}{dt^2} + \lambda \frac{dq_n}{dt} + (k + \varrho h \omega_n^2) q_n \right\} \begin{Bmatrix} u_{1m} \\ u_{2m} \\ w_m \end{Bmatrix} = \begin{Bmatrix} p_1(t) \\ p_1(t) \\ -P(t) \end{Bmatrix} \tag{8.2.1}$$

in which λ represents the damping coefficient (units: Nsm^{-3}), k the spring constant of the "foundation" supporting the shell (units: Nm^{-3}) h is the shell thickness (units: m) and ϱ is its mass density (units: Ns^2m^{-4}). Since this infinite set must obey 8.1.5, each equation is multiplied by U_{1m}, U_{2m}, W_m respectively, then added, then integrated over the orthogonality ranges of the surface. This procedure reduces 8.2.1 to one equation (as required) for determining q_n,

$$\text{(a)} \qquad \mathfrak{L}\{q_n(t)\} = \frac{1}{\varrho h} G_n(t)$$

in which

$$\text{(b)} \qquad \mathfrak{L} \equiv \left(\frac{d^2}{dt^2} + \frac{\lambda}{\varrho h} \frac{d}{dt} + \frac{(k + \varrho h \omega_n^2)}{\varrho h} \right) \tag{8.2.2}$$

$$\text{(c)} \qquad G_n = \frac{1}{N_n} \int_S \int (p_1 u_{1n} + p_2 u_{2n} - p w_n) A_1 A_2 \, d\alpha_1 d\alpha_2 \qquad \text{(units: } N/m^2)$$

It is to be understood that orthogonality of free modes is a valid assumption only if the shell is homogeneous and isotropic. The initial conditions of displacement $u_1(0)$, $u_2(0)$, $u_3(0)$, and of velocity $u_1(0)$, $u_2(0)$, $w(0)$, are also represented by spectral expansions,

$$\text{(a)} \quad u_i(0) = \sum_{n=1}^{\infty} q_n(0)\, u_{in},\ i = 1, 2, 3$$

$$\text{(b)} \quad \dot{u}_i(0) = \sum_{n=1}^{\infty} \dot{q}_n(0)\, u_{in},\ i = 1, 2, 3 \tag{8.2.3}$$

Application once more of the orthogonality of normal modes leads to explicit forms for $q_n(0)$, $\dot{q}_n(0)$:

$$\text{(a)} \quad q_n(0) = \frac{1}{N_n} \int_S\int (u_1(0)u_{1n} + u_2(0)\, u_{2n} + w(0)w_n)\, A_1A_2 d\alpha_1 d\alpha_2$$

$$\text{(b)} \quad \dot{q}_n(0) = \frac{1}{N_n} \int_S\int (\dot{u}_1(0)u_{1n} + \dot{u}_2(0)\, u_{2n} + \dot{w}_n(0)w_n)\, A_1A_2 d\alpha_1 d\alpha_2 \tag{8.2.4}$$

The solutions of 8.2.2 fall into these categories:

(1) *Complementary solution*

If there is an initial displacement $u_i(0)$ and/or an initial velocity, $\dot{u}_1(0)$ the shell responds in each mode with a decaying vibration (underdamped, critically damped, or overdamped).

(2) *Particular solution*

This is the part of the general solution caused by the forcing function $G_n(t)$. If $G_n(t)$ is a *unit* impulse (that is, a delta function) the response of the shell is the impulse response $h(t)$. If $G_n(t)$ is a steady state sinusoid at frequency ω the response of the shell is the complex frequency response $H(\omega)$. A basic result of Fourier analysis is that $h(t)$ and $H(\omega)$ are Fourier transform pairs,

$$H(\omega) = \int_{-\infty}^{\infty} h(t)e^{i\omega t}dt \tag{8.2.5}$$

We now omit from further consideration the effect of initial conditions. The amplitude $q_n(t)$ is then only the particular solution. It depends on the magnitude of damping. Three cases are obtained by applying the method of the Laplace transform to 8.2.2b.

(a) Case I. $\left(\frac{\lambda}{2\varrho h}\right)^2 < \left(\frac{k}{\varrho h} + \omega_m^2\right)$

Solution: $q_n(t) = \frac{1}{\varrho h \gamma_n} \int_0^t G_n(\tau)\, e^{-\lambda(t-\tau)/2\varrho h} \sin \gamma_n(t - \tau)\, d\tau$

$\gamma_n^2 = \frac{k}{\varrho h} + \omega_n^2 - \left(\frac{\lambda}{2\varrho h}\right)^2$ (units: s^{-2})

(b) Case II. $\left(\frac{\lambda}{2\varrho h}\right)^2 = \left(\frac{k}{\varrho h} + \omega_m^2\right)$

Solution: $q_n(t) = \frac{1}{\varrho h} \int_0^t G_n(\tau)\,(t - \tau) e^{-\lambda(t-\tau)/2\varrho h}\, d\tau$ (8.2.6)

(c) Case III. $\left(\frac{\lambda}{2\varrho h}\right)^2 > \left(\frac{k}{\varrho h} + \omega_m\right)^2$

Solution: $q_n(t) = \frac{1}{\varrho h \gamma_n} \int_0^t G_n(\tau)\, e^{-\lambda(t-\tau)/2\varrho h} \sinh \gamma_n(t - \tau)\, d\tau$

[2].

These equations allow one to calculate shell responses to forced drive.

8.3 TEMPORAL IMPULSE RESPONSE OF A HOMOGENEOUS ISOTROPIC SHELL

We consider now that the loading on the shell surface is due only to a normal force per unit area, $P(\alpha_1, \alpha_2, t)$. Assume the time variation is an impulse at $t = 0$,

$$P(\alpha_1, \alpha_2, t) = p_I(\alpha_1, \alpha_2)\, T_0\, \delta(t) \tag{8.3.1}$$

Here p_I is an impulse amplitude,

$$p_I(\alpha_1, \alpha_2)\, T_0 = \int P(\alpha_1, \alpha_2, t)\, dt, \qquad \text{(units: } Nsm^{-2}\text{)}$$

From 8.2.2c,

$$\text{(a)} \quad G_n(t) = \delta(t) p_{In}\, T_0 \qquad \text{(units:} Nm^{-2}\text{)} \tag{8.3.2}$$

where,

$$\text{(b)} \qquad P_{In} = \frac{1}{N_n} \iint_S p_I(\alpha_1, \alpha_2)\, w_n(\alpha_1, \alpha_2)\, A_1 A_2\, d\alpha_1 d\alpha_2 \qquad \text{(units: } Nm^{-2}\text{)}$$

Of the three cases given by Eq. 8.2.6 we take Case I (lightly damped) to be most representative of low frequency radiation problems. Substituting 8.3.2 into 8.2.6a gives the temporal impulse response in the n'th mode. Superposition of all modes then leads to the total impulse response 8.1.3:

$$w(\alpha_1, \alpha_2, t) = U(0)\, \frac{1}{\varrho h} \sum_{n=1}^{\infty} \frac{p_{In} T_0\, e^{-\lambda t/2\varrho h} \sin \gamma_n t}{\gamma_n}\, w_n(\alpha_1, \alpha_2), \text{(units: } m\text{)} \tag{8.3.3}$$

This equation states that under the influence of a spatially averaged force impulse the temporal response at surface coordinates α_1, α_2 is a sum of all modes in the form of lightly decaying sinusoids. The step function $U(0)$ indicates that the response begins at $t = 0$. To obtain the *unit* impulse $h(t)$ response in the n'th mode we regroup the symbols:

$$\text{(a)} \qquad w_n(\alpha_1, \alpha_2, t) = A_n[T_0 h_n(t)]$$

$$\text{(b)} \qquad A_n = \frac{p_{In} w_n(\alpha_1, \alpha_2)}{\varrho h \gamma_n^2} \qquad \text{(units: } m\text{)} \tag{8.3.4}$$

so that

$$\text{(c)} \qquad h_n(t) = \gamma_n \exp(-\lambda t/2\varrho h) \sin \gamma_n t \qquad \text{(units: } s^{-1}\text{)}$$

The essential step here is to make A_n have the dimensions of a displacement by multiplying and dividing by γ_n.

To obtain the steady state one may use 8.2.5:

$$H_n(\omega) = \int_{-\infty}^{\infty} U(0)\,\gamma_n\, e^{-\lambda t/2\varrho h} \sin \gamma_n t e^{i\omega t}\, dt$$

From a table of integrals [3], it is seen that,

$$H_n(\omega) = \frac{1}{1 - \left(\frac{\omega}{\gamma_n}\right)^2 - i\,\frac{\omega\lambda}{\varrho h \gamma_n^2} + \left(\frac{\lambda}{2\varrho h \gamma_n}\right)^2} \qquad \text{(units: none)} \quad (8.3.5)$$

The symbol $H(\omega)$ is the complex frequency response or complex transfer function of the vibrating shell. It's fundamental property is that it is nondimensional. The procedure for obtaining $H(\omega)$ is generalized in the following way: for time given by $\exp(-i\omega t)$ one replaces d/dt by $-i\omega$ in 8.2.2b. Then one defines a quantity γ_n^2 such that

$$\mathcal{L}(-i\omega) = \gamma_n^2\, H(\omega)^{-1}$$

so that

$$H(\omega) = \left[1 - \frac{\left(\omega + \frac{i\lambda}{2\varrho h}\right)^2}{\gamma_n^2}\right]^{-1}$$

In the time-domain we recast 8.2.2 in the form,

$$\text{(a)} \qquad \vartheta_n(t)\{q_n(t)\} = \left[1 + \frac{\left(\frac{d}{dt} + \frac{\lambda}{2\varrho h}\right)^2}{\gamma_n^2}\right] q_n(t) = F_n(t) \qquad (8.3.6)$$

$$\text{(b)} \qquad F_n(t) = \frac{G_n(t)}{\varrho h \gamma_n^2} \qquad \text{(units: } m\text{)}$$

Here $F_n(t)$ is the equivalent force in the n'th mode expressed in units of meters and $\vartheta_n(t)$ is a unit nondimensional operator. For a temporal loading $G_n(t)$ the temporal amplitude $q_n(t)$ is obtained by convolution:

$$\text{(a)} \qquad q_n(t) = \int_{\infty}^{t} F_n(\tau) h(t-\tau) d\tau$$

$$\text{(b)} \qquad q_n(t) = \int_0^{\infty} h_n(\tau)\, F_n(t-\tau) d\tau \qquad (8.3.7)$$

Thus, using 8.1.3 and 8.1.4, the normal component of displacement due to $F(t)$ is,

$$w(\alpha_1, \alpha_2, t) = \sum_{n=1}^{\infty} \left(\int_0^{\infty} h_n(\tau)\, F_n(t-\tau) d\tau\right) w_n(\alpha_1, \alpha_2) \qquad (8.3.8)$$

We next take the normal component of loading $P(\alpha_1, \alpha_2, t)$ to be a stationary random process of time. It follows then that $w(\alpha_1, \alpha_2, t)$ is also a random process whose autocorrelation is,

$$R_w(\alpha_1, \alpha_2, \tau) = \lim_{T\to\infty} \frac{1}{2T} \int_{-T}^{+T} \left\{ \sum_{n=1}^{\infty} \left[\int_0^{\infty} h_n(\tau_1) F_n(t - \tau_1)\, d\tau_1\, w_n(\alpha_1, \alpha_2) \right] \right. \tag{8.3.9}$$
$$\left. \times \sum_{m=1}^{\infty} \left[\int_0^{\infty} h_m(\tau_2) F_m(t - \tau - \tau_2)\, d\tau_2\, w_m(\alpha_1, \alpha_2) \right] \right\} dt$$

Two cases of 8.3.9 are possible: (1) the modes m, n are uncoupled, that is, are uncorrelated. Then all terms $m \neq n$ in the double series are zero. (2) the modes m, n are correlated. We considered here only the first case and sum only the terms $m = n$. For the n'th term then:

$$R_{wn} = w_n^2(\alpha_1, \alpha_2) \lim_{T\to\infty} \frac{1}{2T} \int_{-T}^{T} dt \int_0^{\infty} h_n(\tau_1) F_n(t - \tau_1) d\tau_1 \int_0^{\infty} h_m(\tau_2) F_n(t - \tau - \tau_2)\, d\tau_2$$

The total lag between the exciting forces is $t - \tau_1 - (t - \tau - \tau_2) = \tau + \tau_2 - \tau_1$. Interchanging the order of integration and noting that,

$$R_F = \lim_{T\to\infty} \frac{1}{2T} \int_{-T}^{T} F_n(t) F_n(\tau + \tau_2 - \tau_1)\, dt \qquad \text{(units: } m^2\text{)}$$

it is seen that

$$R_{wn}(\alpha_1, \alpha_2, \tau) = w_n^2(\alpha_1, \alpha_2) \int_0^{\infty} h(\tau_1) d\tau_1 \int_0^{\infty} h(\tau_2) R_F(\tau + \tau_2 - \tau_1) d\tau_2 \tag{8.3.10}$$

Now by definition the power spectral density $|S_{wn}(\alpha_1, \alpha_2, \omega)|^2$ is the Fourier transform of R_{w_n}:

$$|S_{wn}(\alpha_1, \alpha_2, \omega)|^2 = 2 \int_{-\infty}^{\infty} R_{wn}(\alpha_1, \alpha_2, \tau)\, e^{i\omega t}\, d\tau \tag{8.3.11}$$

The factor 2 is inserted for this reason: the spectral density contains real power for both positive and negative frequencies while the real power in R_{w_n} is only in the positive frequencies. Thus $|S_{w_n}(\omega)|^2$ contains twice the real power in the n'th mode. Since $h(t) = 0$ when $t < 0$ one can extend the integration limit from 0 to $-\infty$. Letting $\tau_3 = \tau + \tau_2 - \tau_1$ so that $\exp i\omega\tau = \exp + i\omega\tau_3 \exp(-i\omega\tau_2) \exp(i\omega\tau_1)$ and using 8.2.5 it is seen that,

$$|S_{wn}(\alpha_1, \alpha_2, \omega)|^2 = H_n(\omega)\, H_n(-\omega)\, |S_{F_n}(\omega)|^2\, w_n^2(\alpha_1, \alpha_2)$$

and

$$R_{wn}(\alpha_1, \alpha_2, \tau) = \left(\frac{1}{2} \int_{-\infty}^{\infty} |\mathrm{H}_n(\omega)|^2 |S_{F_n}(\omega)|^2\, e^{-i\omega\tau}\, \frac{d\omega}{2\pi} \right) w_n(\alpha_1, \alpha_2)$$

Noting that both $|H_n(\omega)|^2$ and $|S_{F_n}(\omega)|^2$ are even functions of ω one finds the temporal autocorrelation of displacement from 8.3.9 to be,

$$R_w(\alpha_1, \alpha_2, \tau) = \sum_{n=1}^{\infty} \left[\int_0^{\infty} |H_n(\omega)|^2 |S_{F_m}(\omega)|^2\, e^{-i\omega\tau}\, \frac{d\omega}{2\pi} \right] w_n^2(\alpha_1, \alpha_2) \tag{8.3.12}$$

When the modes are coupled temporally the temporal correlation becomes a complex number: the single series is replaced by a double series; $|H_n(\omega)|^2$ is replaced by $H_n(\omega)\, H_m(-\omega)$; $|S_{F_n}(\omega)|^2$ is replaced by the cross-spectral density $S_{F_n}(\omega)\, S_{F_m}(-\omega)$, and w_n^2 by $w_n\, w_m$.

8.4 THEORY OF RANDOM DISPLACEMENT DUE TO RANDOM FORCES ACTING ON A SHELL

Let the normal loading on the shell be a random function of position and time, $P(\vec{r}_0, t)$, (units: Nm^{-2}) where $\vec{r}_0 = (\alpha_1, \alpha_2)$. Assume it vanishes everywhere outside a time interval $(-T/2, T/2)$. The *average* power W_p over the interval will be proportional to P^2,

$$W_P(T) = \frac{1}{T} \int_{-T/2}^{T/2} P(\vec{r}_0, t)^2 \, dt = \frac{1}{T} \int_{-\infty}^{\infty} P(\vec{r}_0, t)^2 \, dt, \text{ (units: } N^2/m^4) \tag{8.4.1}$$

Let $P(\vec{r}_0, \omega)$ be the Fourier transform of $P(\vec{r}_0, t)$,

$$P(\vec{r}_0, \omega) = \int_{-\infty}^{\infty} P(\vec{r}_0, t) e^{i\omega t} dt \qquad \text{(units: } Nsm^{-2}) \tag{8.4.2}$$

then, according to Rayleigh's theorem for the Fourier pair ωt,

$$\text{total intensity of loading} = \int_{\infty}^{\infty} P(\vec{r}_0, t)^2 \, dt = \int_{-\infty}^{\infty} |P(\vec{r}_0, \omega)|^2 \, \frac{d\omega}{2\pi} \tag{8.4.3}$$

The average intensity (or power) of loading over duration T is then

$$\prod(T) = \frac{1}{T} \int_{-\infty}^{\infty} |P(\vec{r}_0, \omega)|^2 \, \frac{d\omega}{2\pi} \tag{8.4.4}$$

We next *define* an average intensity density $\mathscr{W}_p(\omega)$ of $P(\vec{r}_0, t)$ such that

$$\prod(T) = \frac{1}{2} \int_{-\infty}^{\infty} \mathscr{W}_P(\omega) \, \frac{d\omega}{2\pi} = \int_0^{\infty} \mathscr{W}_p(\omega) \, \frac{d\omega}{2\pi} \tag{8.4.5}$$

The factor ½ is inserted because we wish to calculate power in terms of positive frequencies only of $\mathscr{W}_p(\omega)$.

Comparing 8.4.4 with 8.4.5 shows that,

$$\mathscr{W}_P(\omega) \equiv \frac{2}{T} |P(\vec{r}_0, \omega)|^2 \qquad \text{(units: } N^2sm^{-4}) \tag{8.4.6}$$

Now in accordance with 8.1.3, the amplitude of normal displacement in the ω-domain is,

$$w(\vec{r}_0, \omega) = \sum_n q_n(\omega) \, w_n(\vec{r}_0) \tag{8.4.7}$$

where, from 8.3.6,

$$q_m(\omega) = H_n(\omega) \, F_n(\omega) = -H_n(\omega) \int_S \frac{P(\vec{r}_0, \omega) \, w_n(\vec{r}_0)}{N_n \varrho h \gamma_n^2} \, d\vec{r}_0$$

and where $w_m(\vec{r}_0)$ is a spatial mode. The time averaged power density of displacement 8.4.7 assumes the same form as 8.4.6:

$$\mathscr{W}_w(\vec{r}_0, \omega) = \frac{2}{T} w(\vec{r}_0, w) \, w^*(\vec{r}_0, \omega) \tag{8.4.8}$$

Substituting 8.4.7 into 8.4.8, one obtains,

$$\mathcal{W}_w(\vec{r}_0, \omega) = \sum_{n=1}^{\infty} \sum_{m=1}^{\infty} w_n(\vec{r}_0)\, w_m(\vec{r}_0)\, \frac{H_n(\omega)\, H_m^*(\omega)}{N_m N_n \varrho^2 h^2 \gamma_n^4} \times$$

$$\iint \frac{2}{T}\, P(\vec{r}_0, \omega)\, P^*(\vec{r}'_0, \omega)\, w_n(\vec{r}_0)\, w_m(\vec{r}'_0)\, d\vec{r}_0\, d\vec{r}'_0 \tag{8.4.9}$$

Suppose next that $H(\omega)$ is written in the form of magnitude and phase so that,

$$H_n(\omega)\, H_m^*(\omega) = |H_n(\omega)|\, |H_m(\omega)|\, e^{i\omega\tau}\, \tau$$
$$\equiv \frac{\theta_n - \theta_m}{\omega}$$

According to the Wiener-Khintchine theorem [4] the power density of random normal loading multiplied by phase $\exp(i\omega\tau)$ is equal to the correlation of loading at delay τ in a narrow frequency band $1/T$ units wide:

$$\mathcal{W}_p(\vec{r}_0, \vec{r}'_0, \omega) = \frac{2}{T}\, P(\vec{r}_0, \omega)\, P^*(r'_0, \omega)\, e^{i\omega\tau} = \int_{-T/2}^{T/2} P(\vec{r}_0, t)\, P(\vec{r}'_0, t + \tau)\, dt \quad \text{(units: } N^2 s m^{-4}\text{)}. \tag{8.4.10}$$

Thus, Eq. 8.4.7 reduces to,

$$\mathcal{W}_w(\vec{r}_0, \omega) = \sum_n \sum_m w_n(\vec{r}_0)\, w_m(\vec{r}_0)\, |H_n(\omega)|\, |H_m(\omega)|$$
$$\times \frac{1}{N_m N_n \varrho^2 h^2 \gamma_n^4} \iint \mathcal{W}_p(\vec{r}_0, \vec{r}'_0, \omega)\, w_n(\vec{r}_0)\, w_m(\vec{r}'_0)\, d\vec{r}_0\, d\vec{r}'_0 \quad \text{(units: } m^2 s\text{)} \tag{8.4.11}$$

We now assume that the correlation of loading forces is homogeneous in space, that is, it depends only on the vector difference $\vec{\xi} = \vec{r}_o - \vec{r}_o$. We introduce the space—time spectrum,

$$\text{(a)} \qquad \mathcal{W}_p(\vec{K}, \omega) = \int_{-\infty}^{\infty} \mathcal{W}_p(\vec{\xi}, \omega)\, e^{-i\vec{K}\cdot\vec{\xi}}\, d\vec{\xi} \qquad \text{(units: } N^2 s m^{-2}\text{)} \tag{8.4.12}$$

so that,

$$\text{(b)} \qquad \mathcal{W}_p(\vec{\xi}, \omega) = \int_{-\infty}^{\infty} \mathcal{W}_p(\vec{K}, \omega)\, e^{-\vec{K}\cdot\vec{\xi}}\, \frac{d\vec{K}}{(2\pi)^2}$$

Returning to 8.4.11 we extract the double integral and rewrite it with 8.4.12(b) in mind. Then we first let $n = m$ and recall that the correlation is homogeneous in space. The result is,

$$\text{(a)} \qquad \int\int\int \mathcal{W}_p(\vec{K}, \omega)\, w_n(r_0)\, e^{i\vec{K}\cdot\vec{r}_0}\, w_n(r'_0)\, e^{-i\vec{K}\cdot\vec{r}'_0} d\vec{r}_0\, d\vec{r}'_0\, d\vec{K}$$
$$= \int \mathcal{W}_p(\vec{K}, \omega)\, |S_{w_n}(\vec{K})|^2\, d\vec{K} \tag{8.4.13}$$

$$\text{(b)} \qquad S_{w_n}(\vec{K}) = \int w_n(\vec{r}_0)\, e^{i\vec{K}\cdot\vec{r}_0}\, d\vec{r}_0 \qquad \text{(units: } m^2\text{)}$$

The power spectral density of normal displacement at point $\vec{r}_0$ for uncoupled modes given by Eq. 8.4.11 becomes,

$$\mathcal{W}_w(\vec{r}_0, \omega) = \sum_n \frac{W_n^2(\vec{r}_0)|H_n(\omega)|^2}{N_n^2 \varrho^2 h^2 \gamma_n^4} \int \mathcal{W}_p(\vec{K}, \omega)|S_{w_n}(\vec{K})|^2 \frac{d\vec{K}}{(2\pi)^2} \quad \text{(units: } m^2 s\text{)} \tag{8.4.14}$$

A physical interpretation of this result states that the spectral power of the forcing load in both wavenumber and frequency ($= \mathcal{W}_p(K, \omega)$ is available to drive the shell structure. The structure selects out the energy in frequency bands described by $|H_n(\omega)|^2$, and in wavenumber bands described by $|S_{w_m}(K)|^2$. The structure therefore acts as a temporal and spatial filter of input energy, delivering this energy to the point $\vec{r}_0$. The spatially averaged displacement is obtained by averaging W_n^2 over the shell,

$$\langle w_n^2 \rangle = \frac{\int W_n^2(\vec{r}_0)\, d\vec{r}_0}{\int d\vec{r}_0}$$

A second application of the Wiener-Khintchine theorem shows that for ergodic processes (which are assumed in this analysis) the temporal autocorrelation of displacement at point $\vec{r}_0$ of the shell is related to the power spectral density,

$$R_w(\vec{r}_0, \tau) = \lim_{T\to\infty} \frac{1}{T} \int_{-T/2}^{T/2} w(\vec{r}_0, t)\, w(\vec{r}_0, t + \tau)\, dt \quad \text{(units: } m^2\text{)}$$

$$R_w(\vec{r}_0, \tau) = \frac{1}{2} \int_{-\infty}^{\infty} \mathcal{W}_w(\vec{r}_0, \omega)\, e^{-i\omega\tau}\, d\frac{\omega}{2\pi}$$

[4]. Now when $\tau = 0$ the correlation $R_w(\vec{r}_0, 0)$ is equal to the mean-square displacement at $\vec{r}_0$. Thus the time-averaged displacement ($=$ mean-square displacement) of the spatially averaged displacement is,

$$\langle w^2 \rangle = \sum_n \frac{\langle w_n^2 \rangle}{N_n^2 \varrho^2 h^2 \gamma_n^4} \int_0^\infty \frac{d\omega}{2\pi} |H_n(\omega)|^2 \int \mathcal{W}_p(\vec{K}, \omega)|S_{w_n}(\vec{K})|^2 \frac{d\vec{K}}{(2\pi)^2} \quad \text{(units: } m^2\text{)}$$

in which $\vec{K}$ is the 2-D space of wavenumbers.

8.5 THEORY OF RANDOM RADIATION

The total acoustic power (nearfield and farfield) developed in all space by a radiating surface S driven by random forces $P(\vec{r}_0, t)$ (units: Nm^{-2}), which generates a directivity pattern $D(\theta, \phi)$ is given by 6.6.17. This equation requires that the peak amplitude squared $|V_{AV}|^2$ of the normal component of surface velocity be known. The rms amplitude squared is just $|V_{AV}|^2/2$. To find it we use 8.4.15, with an adjustment to represent velocity rather than displacement. This adjustment is made by the replacement,

$$H(\omega) \to -i\omega H(\omega) = H_v(\omega) \tag{8.5.1}$$

with $H(\omega)$ again given by 8.3.5. Thus the total rms power radiated to the farfield is,

$$\text{(a)} \qquad W = \frac{k^2 \varrho c < \dot{w}^2 > S^2}{16\pi^2} \int_0^{2\pi} d\phi \int_0^{\pi + j\infty} |D(\theta, \phi)|^2 \sin\theta d\theta \tag{8.5.2}$$

in which

$$\text{(b)} \qquad <\dot{w}^2> = \sum_n \frac{<w_n^2>}{N_n \varrho^2 h^2 \gamma_n^4} \int_0^\infty \frac{d\omega}{2\pi} |H_v(\omega)|^2 \int \mathcal{W}_p(\vec{K}, \omega)| \, S_{w_n}(\vec{K})|^2 \frac{d\vec{K}}{(2\pi)^2}$$

in which,

$\mathcal{W}_p(\vec{K}, \omega)$ = power spectral density of $P(\vec{r}_0, t)$ Eq. 8.4.6, 8.4.12 (units: $N^2 s m^{-2}$)
$|S_{w_n}(\vec{K})|^2$ = wavenumber spectral density of the shell, Eq. 8.4.13 (units: m^4)
$|H_V(\omega)|^2$ = frequency spectral density of the shell excitation, Eqs. 8.5.1, 8.3.5 (units: s^{-2})
$< w_n^2 >$ = space-averaged orthogonal function squared, Eq. 8.1.4
N_n = normalization of w_n^2, Eq. 8.1.5c (units: m^2)
ϱ = mass density of shell material (units: $Ns^2 m^{-4}$)
h = shell thickness (units: m)
γ_n = generalized frequency (units: s^{-1}) Eq. 8.2.6(a).

It is important to note that 8.5.2b is a sum on uncoupled modes, meaning $n = m$ in 8.4.9. Energy to a surface point $\vec{r}_0$ is also delivered by coupled modes $n \neq m$. However, the displacements due to these modes tend to cancel when they are averaged over the surface because of the orthogonality of $w_n(\vec{r}_0)$.

A second method for computing the radiation from a surface driven by random loading makes use of the correlation function for the normal component of velocity. We outline this alternate method by first assuming a knowledge of the space-time power spectrum of loading $W_p(K, \omega)$ defined by 8.4.12(a)(b) whose units are $N^2 s m^{-2}$. Next we assume further that the radiating object is a shell which responds to the loading as a spatial and temporal filter with transfer function in the n'th mode given by,

$$\omega^2 |H_n(\omega)|^2 |S_{w_n}(\mathbf{K})|^2 \qquad \left[\text{units: } \frac{\text{m}^4}{\text{s}^2}\right]$$

The space-time power spectrum of the normal surface velocity (with appropriate constants) (see 8.4.9) is the product of W_p and this transfer function:

$$\mathcal{W}_{v_n}(\mathbf{K}, \omega) = \frac{\omega^2 |H_n(\omega)|^2 \mathcal{W}_p(\mathbf{K}, \omega) |S_{w_n}(\mathbf{K})|^2}{N_n^2 \rho^2 h^2 \gamma_n^4} \quad \text{(units: } m^4 s^{-1}) \tag{8.5.3}$$

According to the Wiener-Kintchine theorem the correlation function for normal velocity can be obtained from 8.5.3 by Fourier transformation:

$$R_{v_n}(\mathbf{l}, \tau) = \frac{1}{2} \int_{-\infty}^{\infty} \frac{d\omega}{2\pi} \iint_{-\infty}^{\infty} \mathcal{W}_{v_n}(\mathbf{K}, \omega) e^{-\omega\tau} e^{i\mathbf{K}\cdot\mathbf{l}} \frac{d^2\mathbf{K}}{(2\pi)^2} \qquad \left[\text{units: } \frac{m^2}{s^2}\right] \tag{8.5.4}$$

The factor of 1/2 appears here because the right-hand side contains *twice* the real energy when $\tau = 0 = |\mathbf{l}|$ (see Eq. 8.4.5).

To calculate the power radiated from a random surface we note these expressions:
(1) By definition, for a given random velocity $v(\mathbf{r}_0, t)$,

$$R_{v_n}(l,\tau) = \lim_{A,T\to\infty} \frac{1}{AT} \int v_n(\mathbf{r}_0,t)\, v_n(\mathbf{r}_0+\mathbf{l},\ t+\tau)\, d^2\mathbf{r}_0 dt \qquad \left[\text{units: } \frac{m^2}{s^2}\right]$$

(2) The velocity $v(r_0,t)$ has a spatial and temporal transform,

$$S_{v_n}(\mathbf{K},\omega) = \int\int_{-\infty}^{\infty}\int v_n(\mathbf{r}_0,t)\, e^{i\omega t}\, e^{-i\mathbf{K}\cdot\mathbf{r}_0}\, d^2\mathbf{r}_0 dt \qquad \text{(units: } m^3\text{)}$$

(3) By the Wiener-Kintchine Theorem, the inverse of 8.5.4 is,

$$\mathscr{W}_{v_n}(\mathbf{K},\omega) = 2\int\int\int R_v(\mathbf{l},\tau)\, e^{i\omega\tau} e^{-i\mathbf{K}\cdot\mathbf{l}}\, d\tau\, d\mathbf{l} \qquad \left[\text{units: } \frac{m^4}{s}\right]$$

(4) By an easy extension of 8.4.6 to spatial transformation,

$$|S_{v_n}(\mathbf{K},\omega)|^2 = \frac{AT}{2}\, \mathscr{W}_{v_n}(\mathbf{K},\omega) \qquad \text{(units: } m^6\text{)}$$

Thus,

$$|S_{v_n}(\mathbf{K},\omega)|^2 = AT \int\int\int R_v(\mathbf{l},\tau) e^{-i\mathbf{K}\cdot\mathbf{l}}\, d\tau\, d\mathbf{l}$$

(5) The farfield intensity, transformed to the frequency domain, is obtained from 6.6.17d

$$I_n(\omega) \simeq \frac{k^2\rho c}{32\pi^2 r^2} |S_{v_n}(\mathbf{K},\omega)|^2 \qquad \text{(units: } Nsm^{-1}\text{)}$$

(6) By the Rayleigh-Plancherel Theorem, for a time interval T seconds long,

$$\langle I_n(t)\rangle = \frac{1}{T}\int_{-\infty}^{\infty} I_n(\omega)\frac{d\omega}{2\pi} \qquad \textit{(units: } Ns^{-1}m^{-1}\text{)}$$

The acoustic power radiated to the *farfield* is therefore,

$$W_n = \frac{k^2\rho c}{32\pi^2 r^2}\int\int \langle I_n(t)\rangle\, dA$$

or

$$W_n = \frac{k^2\rho c}{32\pi^2}\int_{-\infty}^{\infty}\frac{d\omega}{2\pi}\int_0^{\pi}\frac{|S_{v_n}(\mathbf{K},\omega)|^2}{T}\sin\theta\, d\theta$$

Thus, the total radiated real power is:

$$W = \sum_n W_n = \sum_n \frac{k^2\rho cA}{32\pi^2}\int_{-\infty}^{\infty}\frac{d\omega}{2\pi}\int_0^{2\pi} d\phi \times \int_0^{\pi} d\theta\, \sin\theta \int\int\int R_{v_n}(\mathbf{l},\tau) e^{i\omega\tau} e^{-i\mathbf{K}\cdot\mathbf{l}}\, d\tau\, d\mathbf{l}^2 \qquad (8.5.5)$$

(units: Nms^{-1}).

Here, as before $v_n(\mathbf{r}_0)$ is *peak* amplitude. It is seen that the power radiated by n modes is the sum of n separate powers.

Summarizing: When an elastic shell is driven by a loading which is randomly distributed in space and time it vibrates in modes. If the assumptions are made (1) that the modes do not couple to each other (2) alternatively, that they are orthogonal in spite of the loading, (3) that the random loading is homogeneous in space and stationary in time, then the acoustic power radiated is a sum of the separate powers in each mode. To calculate these separate powers one

first formulates the space-time spectrum of the loading Eq. (8.4.6) and (8.4.12), then multiplies it by the shell transfer function of the n'th mode to obtain the space-time power spectrum of the normal velocity Eq. (8.5.3), which is then Fourier transformed to obtain the autocorrelation function Eq. (8.5.4) in the same n'th mode. From it the real acoustic power from all modes radiated to the farfield is obtained by Eq. 8.5.5.

The two methods of calculating the acoustic radiation from a randomly loaded shell, described by 8.5.2 and 8.5.5, are theoretically equivalent, but the calculation procedure is different. In 8.5.2 one is required to find a directivity function D which is a composite of all modes (see Eqs. (6.6.11) and (6.6.12)). In addition one must determine the mean displacement (hence mean velocity) over all modes. In 8.5.5 the procedure requires the determination of the correlation of normal velocity in each mode. Thus 8.5.5 is just as difficult to calculate as 8.5.2. In either case a substantial numerical effort is required. Often, however, only a few strategically selected modes are actually calculated to approximate the total radiation from all the modes.

A third method for computing radiation from randomly excited panels is to make use of the concept of radiating efficiency σ defined in 9.5.13. Then, by definition, the acoustic power density radiated by mode mn is $\frac{1}{2}\rho_0 C_0 A_p \sigma_{mn} < \dot{w}_{mn}^2 >$. Thus the total power density radiated in a band $\Delta\omega$ is the sum of powers radiated by all the modes which occur in this band:

$$W(\omega, \Delta\omega) = \frac{1}{2}\rho_0 C_0 A_p \sum_{\substack{m,n \\ \text{in } \Delta\omega}} \sigma_{mn} < \dot{w}_{mn}^2 > \qquad \text{(units: } Nm\text{)} \tag{8.5.6}$$

in which *peak* amplitudes of surface velocity are used and (again) the brackets $< >$ signify *spatial* averages in single modes. To find the total power one must integrate over the frequency content of the band.

8.6 RESPONSE OF FINITE SUPPORTED PLATES TO CONVECTING TURBULENT PRESSURE FIELDS

A turbulent pressure field convecting across an elastic panel with velocity U loads the panel with randomized pressures characterized by various spatial and temporal scales. Let $P(\mathbf{r}_0, t)$ be this random hydrodynamic pressure field. Its statistical properties can be represented by correlation models. Two currently used models have exponential and normal functional dependence. Using them one can represent the statistically averaged wall pressure between two points on the panel as,

$$\text{(a)} \quad < P(\mathbf{r}_0, t)\, P(\mathbf{r}'_0, t') > = < P^2 >_t \exp\left\{ -\frac{|\xi - vt|}{l_x} - \frac{|\eta|}{l_y} - \frac{|\tau|}{\theta} \right\} \tag{8.6.1}$$

$$\text{(b)} \quad < P(\mathbf{r}_0, t)\, P(\mathbf{r}'_0, t') > = < P^2 >_t \exp\left\{ -\frac{(\xi^2 + \eta^2)}{2w_c^2} - \frac{\tau^2}{2\omega_n^2} \right\}$$

in which l_x, l_y, w_a and θ, ω_n are mean statistical correlation distances and correlation times respectively measured from the origin of spatial and temporal coordinates, $< P^2 >_t$ is the mean square pressure averaged over time, and $\zeta = x - x'$, $\xi = y - y'$, $\tau = t - t'$. The exponential model is often used in the theory of random forcing of panels caused by turbulence. In a particular but useful, case, the spatial correlations can be neglected and emphasis focused on temporal events. The exponential model then becomes [5],

$$< P(\mathbf{r}_0, t) P(\mathbf{r}'_0, t') >_t = A_c < P^2 >_t \delta(\xi - U\tau)\delta(\eta) \exp\left\{ -\frac{|\tau|}{\theta} \right\} \tag{8.6.2}$$

in which $A_c (= 4 l_x l_y)$ is the correlation area of pressure fluctuations.

A plate excited by such pressures undergoes dynamic motion which can be described (at low enough frequency) by 4.2.8:

$$\left[D(1-i\eta)\,\nabla^4 + \rho h\frac{\partial^2}{\partial t^2} + \beta_0\frac{\partial}{\partial t}\right] w(x,y,t) = -P(x,y,t) \tag{8.6.3}$$

Here η represents hysteretic damping and β_0 represents viscous camping. The units of β_0 are Nsm^{-3}. For below-critical damping the complementary solution of 8.6.3 is a sum of transient modes:

$$w(x,y,t) = \sum_{m,n} w_{mn}(t)\, W_{m,n}(x,y) \tag{8.6.4}$$

in which amplitudes $w_{mn}(t)$ are decaying sinusoids with modal decay constant a_{mn}, (units: s^{-1}) and W_{mn} are nondimensional eigenfunctions (Sect. 8.3). The displacement in this model is then given by;

$$\text{(a)}\quad w(x,y,t) = \sum_{m,n} A_{mn}\exp(-a_{mn}t - i\omega_{mn}t)\; W_{mn}(x,y) \tag{8.6.5}$$

$$\text{(b)}\quad \int_S W_{mn}(x,y)\,W_{pq}(x,y)\,dS(x,y) = \delta_{mp}\delta_{nq}S$$

The constant A_{mn} (units: m) are may be found from 8.4.7. From 4.2.9 and 4.2.13 the eigenvalues of the operator ∇^4 in 8.6.3 obey the relation,

$$\nabla^4 W_{mn} = \Lambda_{mn}^4\; W_{mn},$$

$$\Lambda_{mn}^4 = \frac{\omega_{mn}^2\rho h}{D}$$

Substituting this relation together with 8.6.5 and 8.6.4 into 8.6.3 one finds the equation which governs W_{mn} for the choice $P = 0$:

$$D(1-i\eta)\,\Lambda_{mn}^4 + \rho h(-a_{mn} - i\omega_{mn})^2 + \beta_0(-a_{mn} - i\omega_{mn}) = 0 \tag{8.6.6}$$

For light damping, $a_{mn}^2 << \omega_{mn}^2$. Then the real and imaginary parts of 8.6.6 yield a pair of coupled equations,

$$\text{(a)}\quad \omega_{mn}^2 = \frac{D}{\rho h}\Lambda_{mn}^4 - \frac{\beta_0}{\rho h}A_{mn}\cdot \approx \frac{D}{\rho h}\Lambda_{mn}^4 \tag{8.6.7}$$

$$\text{(b)}\quad a_{mn} \simeq \frac{\beta_0}{2\rho h} + \frac{\eta\omega_{mn}}{2}.$$

With these values of resonant frequency and damping in mind we return to 8.4.15 and write the mean square displacement averaged over space, $< >_s$, in the mn'th mode on a plate of area A_p:

$$\text{(a)}\quad < W_{mn}^2(\omega) >_s = I_{mn}J_{mn} \qquad \text{(units: } m^2 s\text{)} \tag{8.6.8}$$

$$\text{(b)}\quad I_{mn} = \frac{< w_{mn}^2 >_s A_p^2}{N_m^2\rho^2h^2\gamma_m^4} \qquad \left[\text{units: } \frac{m^6}{N^2}\right]$$

$$\text{(c)}\quad J_{mn} = \frac{1}{A_p^2}\int \mathcal{W}_p(\mathbf{K},\omega)\,|S_{mn}(\mathbf{K})|^2\frac{d\mathbf{K}}{(2\pi)^2} \qquad \left[\text{units: } \frac{N^2 s}{m^4}\right]$$

$$\text{(d)} \quad \langle w_{mn}^2 \rangle_s = \frac{\int W_{mn}^2(\mathbf{r}_0)\, d\mathbf{r}_0}{\int d\mathbf{r}_0} \qquad \text{(units: nondimensional)}$$

The units of various quantities in this equation are listed in Sects. 8.3 and 8.4. This equation states that the mean square displacement in the mn'th mode depends on the coupling of the wall pressure power spectrum $\mathscr{W}_p$, 8.4.6 and 8.4.12, with the *panel acceptance* $|S_{mn}|^2$, 8.4.13b. Since this coupling is quite complicated it will be useful to first define its relevant parameters.

(1) the components of $\mathbf{K}$ are k_1 in the x-direction and k_3 in the y-direction. These are the general 2-D space of wavenumbers either of the plate or the pressure field.

(2) the specific modal components of $\mathbf{K}$ in the plate are k_m, k_n in the x,y directions respectively.

(3) U_c is the convection speed of the hydrodynamic flow in the medium; c_b is the speed of bending waves in the plate; c_l is the longitudinal bulk wave speed in the material of the plate. The wavenumbers associated with U_c, c_b and c_l are k_c, k_b, k_l respectively.

(4) for plates of thickness h,

$$c_b = \sqrt{\frac{\omega h c_l}{\sqrt{12}}}; \quad k_b = \sqrt{\frac{\omega\sqrt{12}}{h c_l}} \tag{8.6.9}$$

(5) hydrodynamic coincidence occurs when $k_c = k_m = k_1$; hydrodynamically slow flexural modes occur when $c_b < U_c$; hydrodynamically fast flexural modes occur when $c_b > U_c$

(6) k_0 is the acoustic wavenumber

(7) the wave number bandwidth Δk_c of the wall pressure power spectrum, calculated as if the spectrum is that of a single degree of freedom oscillatory process with exponential damping is

$$\Delta k_c = \frac{\Delta\omega}{U_c} = \frac{2\kappa}{U_c} = \frac{2}{\theta_\tau U_c} \tag{8.6.10}$$

in which κ is the "temporal damping" of the process and its reciprical θ_τ is the "time constant" of the process. In terms of logarithmic decrement $2\pi\gamma$, one may write $\kappa = 2\pi\gamma f$. Hence

$$\Delta k_c = 2\gamma_1 k_c, \quad k_c = \frac{\omega}{U_c} \tag{8.6.11}$$

(8) the bandwidth of *panel acceptance* $\Delta k_1 (= \Delta k_x)$, depends on the length L_x of the panel in the x-direction,

$$\Delta k_1 = 2\left(\frac{2\pi}{L_x}\right) \tag{8.6.12}$$

Essentially the characteristic length of the plate is taken as $L_x/2\pi$. Similarly in the y-direction,

$$\Delta k_3 = 2\left(\frac{2\pi}{L_y}\right). \tag{8.6.13}$$

With these definitions we return to 8.6.3.

The calculation of $J_{mn}(\omega)$, 8.6.8, in the general case is very difficult because $\mathscr{W}_p(\mathbf{K},\omega)$ and $|S_{mn}(\mathbf{K})|^2$ may peak at different values of $\mathbf{K}$. Fig. 8.6.1 is a sketch showing this peaking condition as a function of k_1 (ω = const, k_3 = const.). The hydrodynamic power spectrum always peaks at $k_c = \frac{\omega}{U_c}$, shown here to be greater than k_m (where the panel acceptance is greatest). Because $c_b > U_c$ this is the case of hydrodynamically fast modes. Fig. 8.6.2 is a superposition

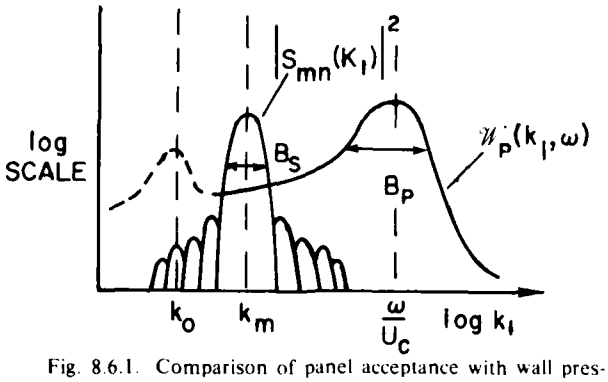

Fig. 8.6.1. Comparison of panel acceptance with wall pressure spectrum. $B_p = 2\frac{\kappa}{U_c}$; $B_s = 4\pi/L_x$; $k_z = \text{const}\ \omega = \text{const}$.

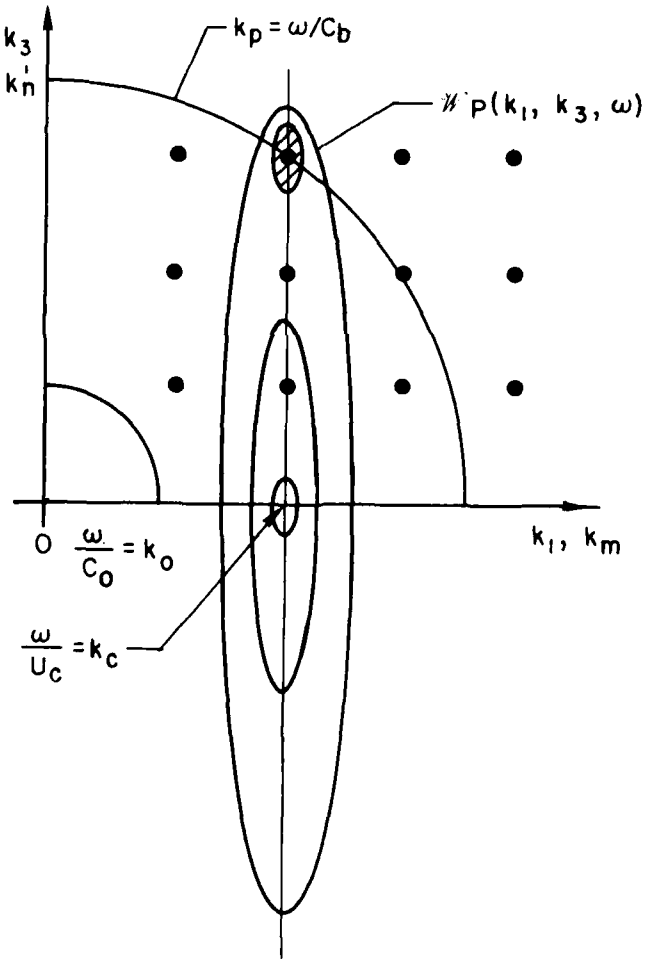

Fig. 8.6.2 Lattice of mn plate modes (where $|S_{mn}|^2$ is largest) with superimposed power spectrum of the wall pressure, H_p (where the forcing function is largest). Here $k_c < k_p$, signifying that the modes are hydrodynamically slow. The drive frequency is ω (after [9]).

on a two-dimensional wavenumber plane of the points representing a lattice of resonant frequencies (where the panel acceptance $|S_{mn}(k_m,k_n)|^2$ is the largest) and the hydrodynamic pressure spectrum (versus k_1, k_3) which are drawn as contours of equal amplitude coming out of the page. Here the convection wavenumber k_c is shown to be less than $k_p(=\omega/c_b)$. The mn modes that fall within the region of high panel acceptance are hydrodynamically slow because $c_b < U_c$. The region $k_c = k_m = k_1$ exhibits the case of hydrodynamic coincidence (where $c_b = U_c$). The shaded region on the curve k_p = const. surrounds a highly excited panel mode.

Figure 8.6.3 is a sketch of the response of a single (mn) mode under forced drive at frequency ω. Superimposed is a sketch of the power spectrum of hydrodynamic pressure plotted versus frequency. The effective "quality factor" of the plate mode vibrating under forced drive as a simple degree of freedom system is Q_{mn}. The amount of overlap between the spectrum and the mode determines the value of the integral J_{mn}, 8.6.8c.

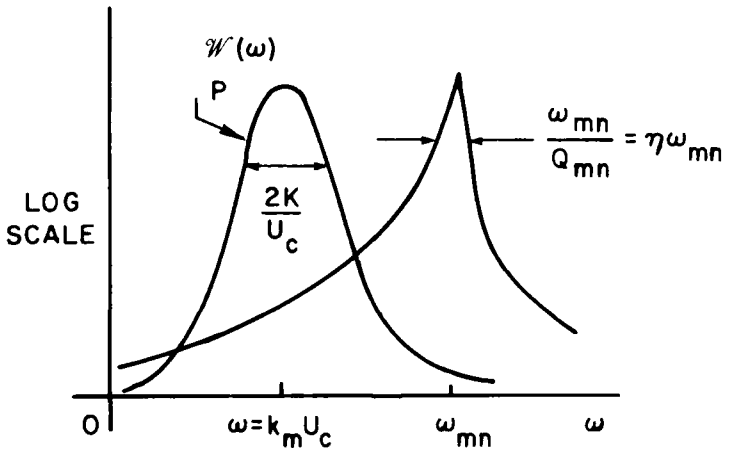

Fig. 8.6.3. Superposition of the amplitude spectrum of the mn'th mode and the power spectrum of the hydrodynamic wall pressure at fixed k_m, k_n

A convenient procedure for defining the ranges of slow and fast modes of the hydrodynamic type and the acoustic type is shown in Fig. 8.6.4. Here the dispersion relation $k_b = \sqrt{\omega\sqrt{12}/hc_l}$ is plotted as a function of frequency. The cross-over points ω_k, ω_a of the lines k_c and k_a define the limits of slow and fast modes as shown.

An alternative procedure is to plot regions of slow and fast hydrodynamic modes in the k_1, k_3 space. This is shown in Fig. 8.6.5. In this plot the direction of convection relative to the velocity $\mathbf{c}_b$ is $U_c\cos\phi$. At hydrodynamic coincidence $c_b = U_c$. Using 6.10.9 this becomes $k_1\frac{h}{\sqrt{12}}c_L = U_c$. Thus the locus of coincidence is,

$$k_1 = \frac{U_c\cos\phi}{(hc_L/\sqrt{12})}$$

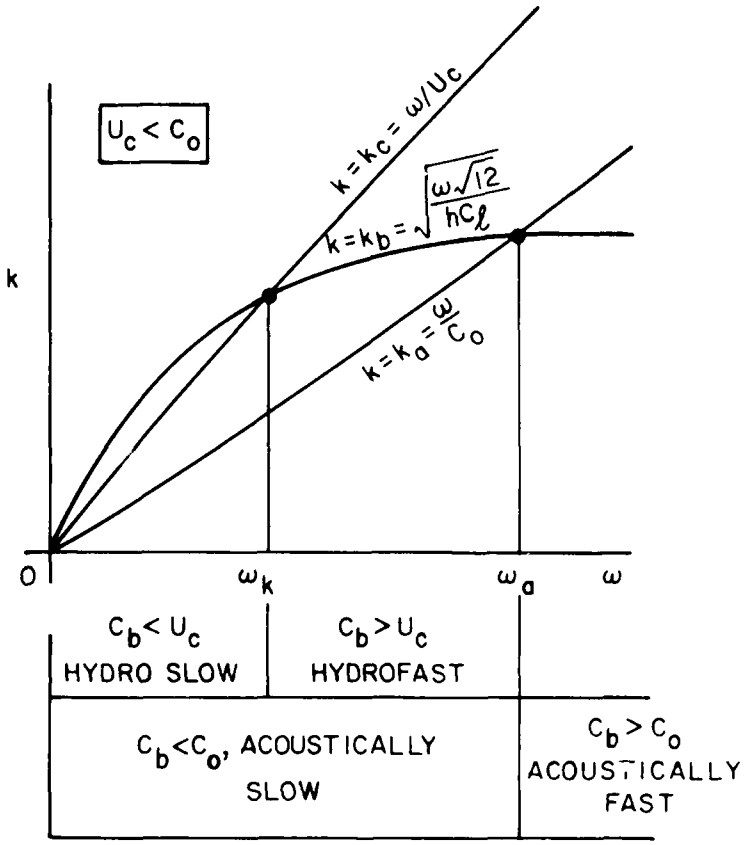

Fig. 8.6.4. Definition of slow and fast modes of hydrodynamic and acoustic vibration (after [9]).

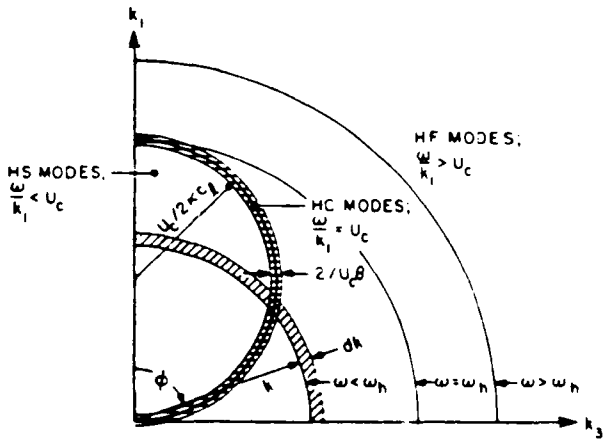

Fig. 8.6.5. Plot of wave numbers, pattern in k space (after [9]).

AD-A140 578 A TREATISE ON ACOUSTIC RADIATION(U) NAVAL RESEARCH LAB 5/7
WASHINGTON DC S HANISH 1981

UNCLASSIFIED F/G 20/1 NL

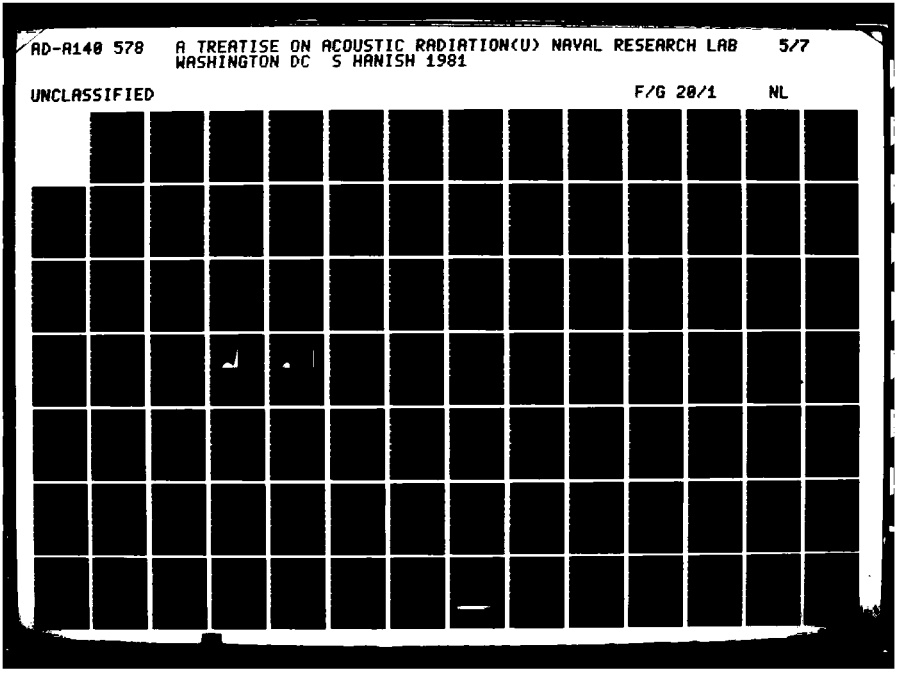

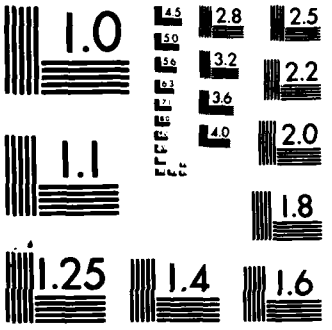

MICROCOPY RESOLUTION TEST CHART
NATIONAL BUREAU OF STANDARDS-1963-A

which is a circle of radius $U_c\sqrt{12}/2hc_L$. Inside this circle $c_b < U_c$ (that is, $\omega < k_1 U_c$). All combinations of k_1, k_3 which fall within the circle define hydrodynamically slow modes, and all that fall outside define fast modes. As noted in Sect. 9.5 a plot of $\omega =$ const. is a quarter cielce in k_1, k_3 space. The symbol ω_h is the hydrodynamic coincidence frequency. For the choice $k_1 = U_c\sqrt{12}/hc_L$ it has the value $k_1 c_b$.

The crucial point in the calculation of mean square modal displacement from 8.6.8 is the modeling of the power spectral density $\mathcal{W}_p(k_1,k_3,\omega)$ or, alternatively, the modeling of the spatial and temporal correlation function of the random wall pressure. A much used model of the latter is that of Dyer [5] which is identical with 8.6.2. From it one constructs. $\mathcal{W}_p$ by Fourier transformation:

$$\mathcal{W}_p(k_1,k_3,\omega) = A_c < P^2 >_t \int \delta(\xi - U_c\tau)\delta(\eta)\exp\left[-\frac{|\tau|}{\theta_\tau}\right] \exp(-ik_1\xi - ik_2\eta + i\omega\tau)\, d\xi\, d\eta\, d\tau$$

Using the Fourier transform pair,

$$-\frac{1}{2\beta}\, e^{-\beta|s|} <\!\!-\!\!\!-\!\!> \frac{1}{p^2 - \beta^2},\quad p = i\omega$$

[6]. One obtains,

$$\mathcal{W}_p(k_1,\omega) = A_c < P^2 >_t \frac{2\theta_\tau}{1 + \theta_\tau^2(k_1 U_c - \omega)^2} \tag{8.6.14}$$

Three forms of this power spectrum of hydrodynamic pressure are important:

$$\begin{aligned}
&\text{(a)}\ \ k_1 U_c << \omega\ \ \text{(fast modes)}: \quad \mathcal{W}_p = A_c < P^2 > \frac{2\theta_\tau}{1 + \theta_\tau^2\omega^2} \\
&\text{(b)}\ \ k_1 U_c = \omega\ \ \text{(coincidence)}: \quad \mathcal{W}_p = A_c < P^2 > 2\theta_\tau \\
&\text{(c)}\ \ k_1 U_c >> \omega\ \ \text{(slow modes)}: \quad \mathcal{W}_p = A_c < P^2 > \frac{2\theta_\tau}{1 + \theta_\tau^2 k_1^2 U_c^2}
\end{aligned} \tag{8.6.15}$$

The model given by 8.6.14 matches experiment only in a qualitative way. It over estimates the pressures at low wavenumbers as compared to those near $k_1 = k_c$. Also, the ω^{-2} dependence in 8.6.15a is not correct. An improvement to the model was made by Lyon [7] who replaced A_c by an "effective" correlation area $A_t(k_p)$ given by,

$$A_t(k_p) = \frac{2\pi}{< P^2 >} \int_0^{2\pi} d\phi \int_{-\infty}^{\infty} \mathcal{W}_p(k_1,k_2,\omega)\, d\omega \tag{8.6.16}$$

$$k_1 = k_p\cos\phi;\ k_3 = k_p\sin\phi,\ k_p = \omega/c_b$$

Actually k_3 was chosen to be nearly zero so that the integration of 8.6.1b was expectively restricted to the low wavenumber portion of the spectrum near $k_1 = k_p$. Evaluation of 8.6.16 leads to a graph of the type shown in Fig. 8.6.6. Here U_c is normalized to the free stream velocity U_1 in the x-direction, and the wavenumber k_p is nondimensionalized by multiplication with the boundary layer thickness δ_1.

The several models of $\mathcal{W}_p$ given by 8.6.15 serve to obtain estimates of the ω-power spectrum of the modal displacement 8.6.8. Multiplication by the frequency spectral density of the plate excitation $|H_v(\omega)|^2$ (see 8.5.1 and 8.3.5) then gives the ω-power spectrum of the modal velocity. By integrating radiation from modes in particular frequency bands one can calculate the acoustic power radiated to the far field through use of 8.5.2 or 8.5.6.

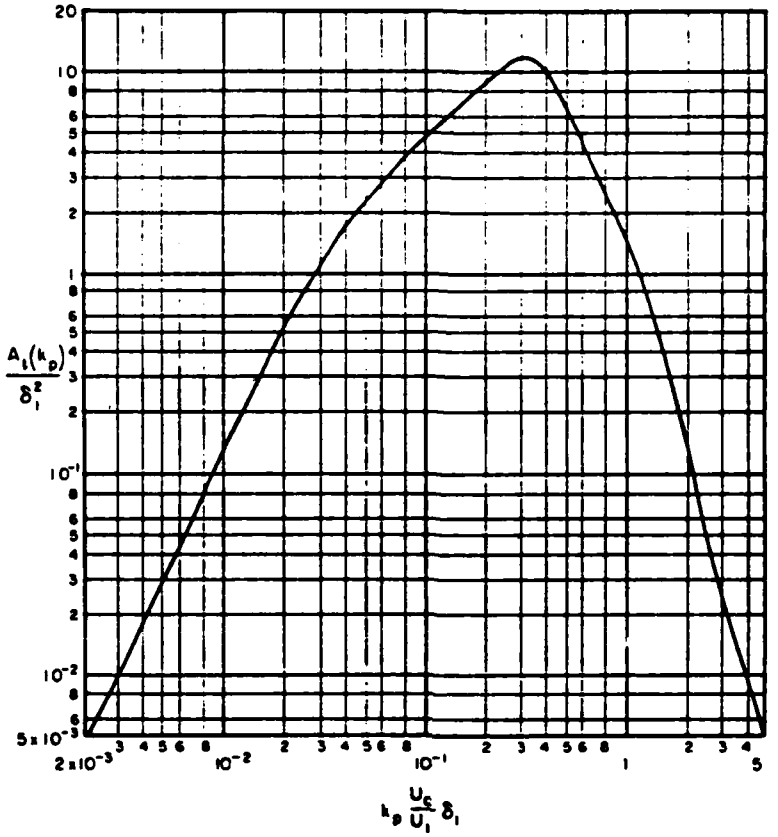

Fig. 8.6.6. Effective correlation area for turbulent excitation of HF waves (after [7]).

A case which occurs in typical hydroacoustic applications is one in which the hydrodynamic modes are fast, $c_b > U_c$, while the acoustic modes are slow $c_b < c_0$, see Fig. 8.6.4. The acoustic power (spectral density) radiated by a group of modes in a frequency band $\Delta\omega$ centered at frequency ω is,

$$W(\omega, \Delta\omega) = \frac{1}{2} \rho_0 c_0 A_p \sum_{m,n} \sigma_{mn} < \dot{w}_{mn}^2(\omega) >_s \quad \text{(units: } Nm\text{)} \tag{8.6.17}$$

where

$$< \dot{w}_{mn}^2(\omega) > = \omega^2 |H_{mn}(\omega)|^2 < w_{mn}^2(\omega) >_s$$

and peak amplitudes are implied. Total power is obtained by integration of $W(\omega, \Delta\omega)$ over ω in the band. The brackets $< >_s$ signify *spatial* average in one mode (see 8.6.8). The symbol $H_{mn}(\omega)$ is the frequency response of the shell in the mn mode as defined in 8.3.5. Some authors include this response in their definition of the power spectrum S_{mn} of the plate response, writing it as $S_{mn}(\mathbf{K}, \omega)$. However in this treatise the temporal response of the plate well be represented by its impulse response $h(t)$ or its complex transfer function $H(\omega)$ so that the plate transfer function for displacements becomes $H_{mn}(\omega)\, S_{mn}(\mathbf{K})$. Often the discrete sum in 6.10.17 is replaced by a simple average over all modes within the band. This average is

represented by an overbar. Thus if the quantity $<\dot{w}_{mn}^2>_s$ is to be averaged over all modes in $\Delta\omega$ one uses:

$$\overline{<\dot{w}_{mn}^2>_s} = \frac{1}{n_s(\omega)\Delta\omega} \sum_{m,n} <\dot{w}_{mn}^2(\omega_{mn})>_s \tag{8.6.18}$$

in which $n_s(\omega)$ is the density of modes per unit of bandwidth.

In applications to underwater acoustics the frequency band of interest usually centers at a frequency $\omega >> k_1 U_c$ where the hydrodynamic modes are fast. One can therefore use 8.6.15a for $\mathcal{W}_p$ with the observation that it is independent of wavenumber. Now it is customary to normalize $S_{mm}(\mathbf{K})$ such that,

$$\frac{1}{A_p} \iint |S_{mm}(\mathbf{K})|^2 \frac{d\mathbf{K}}{(2\pi)^2} = 1 \tag{8.6.19}$$

Thus, from 8.6.8,

$$\text{(a)}\quad A_p J_{mn} \simeq \mathcal{W}_p = A_c <P^2>_t \mathcal{P}_\tau(\omega) \qquad \text{(units: } N^2 s m^{-2}) \tag{8.6.20}$$

$$\text{(b)}\quad \mathcal{P}_\tau(\omega) = \frac{2\theta_\tau}{1+\omega^2\theta_\tau^2} \qquad \text{(units: } s)$$

From its dimensions one can interpret $\mathcal{W}_P$ is the mechanical energy per unit area per unit real mechanical admittance (G) of the plate. For an infinite plate excited by a point force, the admittance is,

$$G_\infty = \frac{\sqrt{12}}{8\rho_s h c_L} \qquad \text{(units: } m s^{-1} N^{-1}) \tag{8.6.21}$$

[8], in which ρ_s is the mass of the plate per unit area (units: Ns^2/m^3). Thus the mechanical energy per unit area due to *peak* turbulent wall pressures is,

$$G_{in} W_P = \frac{1}{2} \frac{\sqrt{12}}{8\rho_s h c_L} A_c <P^2>_t \mathcal{P}_\tau(\omega), \qquad \text{(units: } N m m^{-2}) \tag{8.6.22}$$

Corresponding to this energy there is the kinetic energy power spectrum in the mn'th mode,

$$\frac{1}{2}\rho_s <\dot{w}_{mn}^2>_s \tag{8.6.23}$$

whose units are $(Ns^2m^{-3})(m^2/s^2)s = \frac{Nm}{m^2}s$. This entity can be interpreted as energy per unit area per unit bandwidth. Assuming it is an *average* energy per unit band $\Delta\omega = \eta\omega$ one can find the total kinetic energy by simple multiplication with $\Delta\omega$. Equating total energies 8.6.22 and 8.6.23 leads to the convenient formula for mean-square velocity *density*,

$$<\dot{w}_{mn}^2(\omega)>_s = \frac{\sqrt{12}}{8\rho_s^2 h c_L} \frac{A_c <P^2> \mathcal{P}_\tau(\omega)}{\eta\omega_{mn}} \qquad \text{(units; } (m^2/s^2)s). \tag{8.6.24}$$

A formula closely allied to this has been derived by Lyon [7]. Equation (8.6.24) requires a model of the temporal power spectrum of the turbulent wall pressure ($\mathcal{P}_\tau(\omega)$). A universally accepted model valid over all temporal scales of turbulence is difficult to construct. Leibowitz [9], in a basic survey of the the problem of the response of turbulence-excited plates, recommends the following steps for calculation of mean-square plate displacements and acoustic radiation.

(1) The power spectral density of wall pressure fluctuations $\mathscr{W}_p(\xi,\omega)$ (units: N^2sm^{-4}), defined by 8.4.10, is calculated by use of the (air) model of Maestrello [10]. Using experimental data, Fig. 8.6.7, in turbulent channel flow in which semifrozen patterns of pressure turbulence are convected (velocity U_c) across a flexible panel, Maestrello plotted density of power spectrum $P(\omega)$ (units: N^2sm^{-4}) versus radian frequency ω. $P(\omega)$ is nondimensionalized by the factor $\tau_w^{-2}\, U\delta^{*-1}$ (τ_w is the wall shear stress (Nm^{-2}), U is the convection velocity and δ^* is the boundary layer thickness). The frequency ω is nondimensionalized by the factor $U\delta^{*-1}$. From this plot Maestrello constructed (by curve fitting) a normalized cross-correlation function of wall pressure fluctuation:

$$R(\xi,\eta,\tau) = e^{-k|U_c\tau|}\left\{\sum_{\gamma=1}^{3}\frac{A_\gamma K_\gamma}{K_\gamma^2+\left(\frac{1}{FU}\right)^2[(\xi-U_c\tau)^2+\eta^2]}\right\}\Bigg/\sum_{\gamma=1}^{3}\frac{A_\gamma}{K_\gamma}. \quad \text{(nondimensional)} \tag{8.6.25}$$

$K_1 = 0.470 \quad A_1 = 1.6 \qquad F = \delta^*/U$
$K_2 = 3.0 \quad A_2 = 7.2$
$K_3 = 14.0 \quad A_3 = 12.0$

The related power spectral density was found from this correlation function to be,

$$P(\omega) = \frac{\tau_w^2\delta^*}{U}\left[A_1\exp(-K_1\omega F) + A_2\exp(-K_2\omega F) + A_3\exp(-K_3\omega F)\right]$$

(units: N^2sm^{-4})

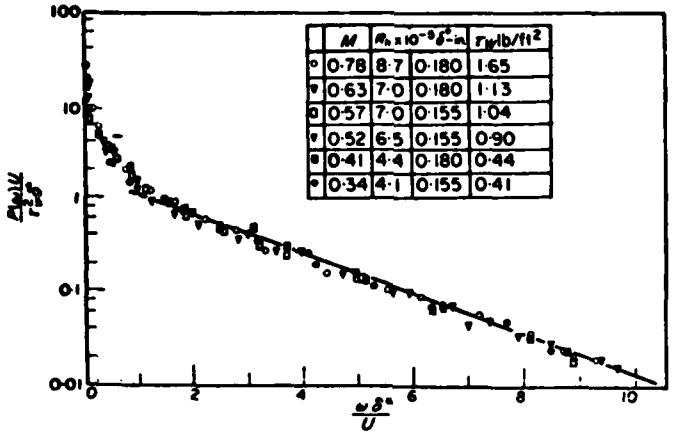

Fig. 8.6.7. Dimensionless power spectrum of the wall pressure fluctuations (after [10]).

2. Because of experimental errors introduced by finite sized wall pressure probes a correction factor is introduced into the above calculation of $P(\omega)$. The correction is provided by Lyamshev and Salosina [11] who replaced F by $\sqrt{r/\delta^*}$, where r is the size of the transducer. The corrections are shown in Fig. 8.6.8.

3. Under excitation 6.10.25 and 6.10.26 the vibration of the plate in air (= vacuo) is calculated by the procedures used by Warburton [12]. The dynamic input parameters of this method are: the mass M

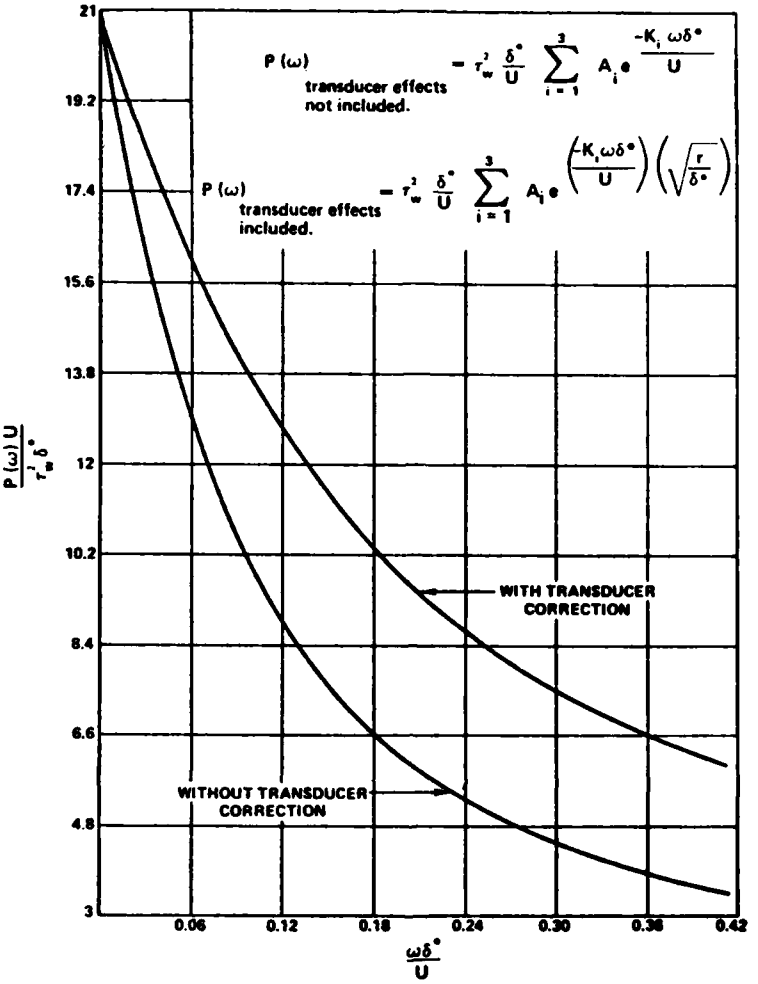

Fig. 8.6.8. Normalized turbulent pressure power spectral density with and without transducer effects (after [11]).

per unit area of the plate (units: Ns^2m^{-3}), the plate bending stiffness B (units: Nm), modal damping a_{mn} (units: s^{-1}) the plate modal resistence per unit area r_s (units: Nsm^{-3}), or the modal damping ratio δ_{mn} (units: nondimensional). The output parameters include the modal resonant frequency ω_{mn} and the displacement due to several cases of applied forces and boundary conditions.

4. The calculation of the displacement in water is made by correcting the air displacement for the effects of the water load. When the plate (in an infinite rigid baffle) is loaded with water, the reaction of the medium adds dynamic mass and radiation damping. The magnitude and frequency dependence of these reactions depend on the radiation classification of modes. A convenient classification can be made in k-space, Figs. 8.6.9a, 9b. Fig. 8.6.9a shows a frequency band Δk_f inside of which there are several modes k_{m1}, k_{m2}. In addition there are (1) a region $k \leqslant k_0$ of surface acoustic modes (2) hatched regions of x_1 edge (or strip) modes and x_2 edge modes and (3) a region (in between the latter) of corner modes. Figure 8.6.9b shows the relation of these radiating modes to hydrodynamic modes in k-space.

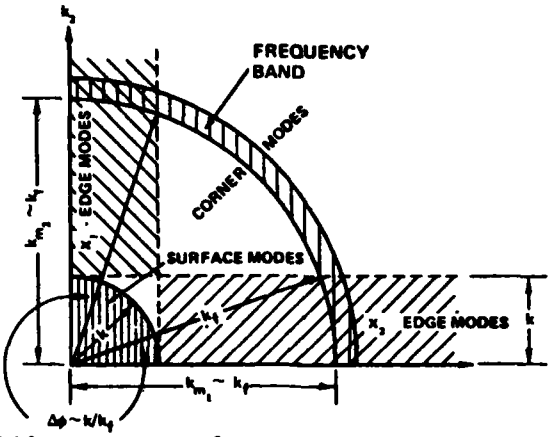

Fig. 8.6.9a. Radiation classification of modes in k space. The fraction of corner modes in the band = 1 − fraction of $x_1 + x_2$ edge modes in the band $1 = -(\Delta N/N)_{(x_1+x_2)\text{ edges in band}} = 1 - (4/\pi)\sin^{-1}(k/k_f)$. For k/k_f small, $\sin^{-1}(k/k_f) \rightarrow k/k_f$. The maximum corner mode radiation in the band, occurring when $k_{m_1} = k_f$ of $k_{m_2} = k_f$ is $< R_{\text{rad}}^{\text{corner}} >_{\Delta\omega} = \rho C A_p (8\lambda_c^2 \omega_c / \pi^3 A_p \omega)$ (after [9]).

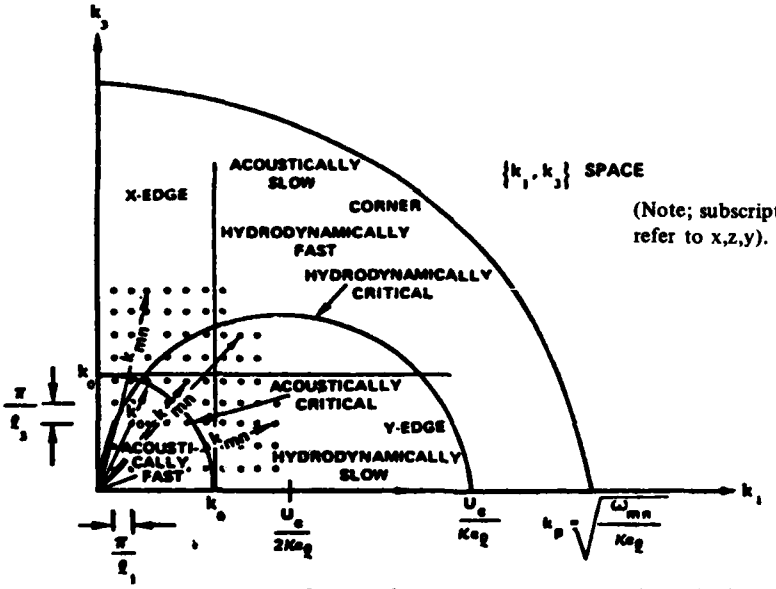

Fig. 8.6.9b. Classification of acoustic and hydrodynamic modes in k-space of a finite plate (after [9]).

The calculation of added mass on rectangular plates caused by random excitation has been performed by several independent authors. Leibowitz recommends the one worked out by Davies [13]. This is summarized in Fig. 8.10.10. Here *mn*, *qr* specify two distinct plate modes. The symbol m_{mn} is the added mass (units: Ns^2/m^3) in the *mn*'th mode while the symbol m_{mnqr} is the mass coupled from the *qr* mode into the *mn* mode. Although specialized, the cases considered are the ones most likely to be met in practice. When so calculated the masses m_{mn}, m_{mnqr} due to water load are added to the plate mass M to form the totalf mass M_p (units: Ns^2/m^3). This then becomes the mass parameter in Warburton's analysis procedure. From it and from the bending stiffness B the modal resonant frequency in water $\bar{\omega}_{mn}$) is calculated.

1. FOR ALL MODES IN K SPACE FOR WHICH $|k| > k_o$ (ACOUSTICALLY SLOW MODES)

$$m_{mn} = \frac{\rho_o}{(k_m^2 + k_n^2 - k^2)^{1/2}} = \frac{\rho_o}{(k_{mn}^2 - k_o^2)^{1/2}} \approx \frac{\rho_o}{k_{mn}} \; ; \; k_{mn}^2 > k_o^2$$

$$= 0 \; ; \; k_{mn} < k_o$$

Hence

$$M_p = m_p + m_{mn} = m_p\left(1 + \frac{\rho_o}{m_p k_{mn}}\right) \; ; \; k_{mn} > k_o$$

2. FOR (m,n) AN X-TYPE EDGE MODE AND (q,r) AN EDGE MODE

$$m_{mnqr} = \frac{4\rho_o \ell_1}{\pi A_p k_n k_r} \ln \frac{2k_{mn}}{k_o} \delta_{mq} + \frac{4\rho_o \ell_3 k_m k_q}{\pi A_p k_{mn}^2 k_{qn}^2} \delta_{nr}$$

3. FOR (m,n) AN X-TYPE EDGE MODE AND (q,r) A CORNER MODE

$$m_{mnqn} = \frac{4\rho_o \ell_3 k_m k_q}{\pi A_p k_{mn}^2 k_{qn}^2} \delta_{nr}$$

4. FOR (m,n) AN X-TYPE EDGE MODE AND (q,r) AN ACOUSTICALLY FAST MODE

$$m_{mnmr} = \frac{4\rho_o \ell_1 k_r}{A_p k_n k_o^2} \delta_{mq}$$

5. FOR (m,n) AND (q,r) CORNER MODES

$$m_{mnqr} = \frac{4\rho_o \ell_1 k_n k_r}{\pi A_p k_{mn}^2 k_{mr}^2} \delta_{mq} + \frac{4\rho_o \ell_3 k_m k_q}{\pi A_p k_{mn}^2 k_{qn}^2} \delta_{nr} + \frac{\rho_o}{k_{mn}} \delta_{mq} \delta_{nr}$$

A_p	plate area equal to $\ell_1 \ell_3$
c_o	velocity of sound in fluid
k_o	acoustic wavenumber equal to $\frac{\omega}{c_o}$
k_m, k_n	wavenumbers equal to $\frac{m\pi}{\ell_1}$ and $\frac{n\pi}{\ell_3}$ respectively; similarly for k_q, k_r
k_{mn}	surface wavenumber equal to $(k_m^2 + k_n^2)^{1/2}$; similarly for k_{mr} and k_{qn}
ℓ_1, ℓ_3	length and width of plate respectively
M_p	total mass per unit area
m_p	plate mass per unit area
m_{mn}	added mass per unit area for mn mode
m_{mnqr}	added mass per unit area associated with the coupled mn and qr modes; similarly for m_{mnqn} and m_{mnmr}
m, n, q, r	mode numbers
δ_{ij}	Kronecker delta equal to 1 for i = j, equal to 0 otherwise
ρ_o	mass density of fluid
ω	circular frequency
ω_c	acoustic critical frequency

Fig. 8.6.10. Formulas for calculating added mass caused by fluid loading on rectangular plates as derived by Davies [13].

5. The calculation of radiation damping due to fluid loading on a vibrating rectangular plate is a difficult task. Several important cases of modal damping and mode-coupled damping have been derived by Davies [13]. These are summarized in Fig. 8.6.11. The units of damping treated in this manner are those of characteristic impedance of the medium $\rho_0 c_0$, which are Nsm^{-3}. Again, the concepts of fast nodes, slow modes, corner modes, edge modes etc. noted in Fig. 8.6.10 are reviewed in earlier parts of this section. The radiation damping S_{mn} etc. so calculated is added to the modal resistance and the sum is used to calculate the modal damping $\bar{a}_{mn}$ in water,

$$\bar{a}_{mn} = \frac{(r_s + S_{mn})}{2M_p} = \frac{\bar{\delta}_{mn}\bar{\omega}_{mn}}{2} \qquad \text{(units: } s^{-1}\text{)}$$

(The over bar indicates water loaded).

6. The acoustic power radiated by turbulence driven panels is calculated from a knowledge of the (frequency dependent) panel radiation efficiency in the mn'th mode σ_{mn}, discussed in this treatise in Sect. 9.5. From 8.6.7 the total power in the frequency band $\Delta\omega$ for the case of uncoupled modes than becomes,

$$W(\Delta\omega) = \frac{1}{2}\rho_0 c_0 A_p \sum_{m,n}\int_{\Delta\omega} \sigma_{mn} < \dot{w}_{mn}^2(\omega) >_s d\omega \qquad 8.6.27$$

Alternatively, from the definition of radiation damping,

$$W(\Delta\omega) = \frac{1}{2}\sum_{m,n}\int_{\Delta\omega} S_{mnmn} < w_{mn}^2(\omega) >_s d\omega \qquad (8.6.28)$$

These radiated powers are statistical averages.

8.7 DIRECT RADIATION OF SOUND FROM COMPLIANT SURFACES EXCITED BY HYDRODYNAMIC PRESSURES CAUSED BY FLOW TURBULENCE. (Case of large plane surfaces with no edge effects.)

The radiation field at point $\vec{x}$, t caused by a turbulent boundary layer acting in a surface is governed by the equation of Curle [14]. It has the form of a sum of one volume integral and two surface integrals, resulting from the integration over source-time using the transient Green's function 1.8.18(a):

$$\begin{aligned}
&(a)\quad p(\vec{x}, t) = p_v + P_{SI} + P_{SII} \\
&(b)\quad p_V(\vec{x}, t) = \frac{1}{4\pi}\frac{\partial^2}{\partial x_i \partial x_j}\int [T_{ij}]\frac{dV}{r} \\
&(c)\quad p_{SI}(\vec{x}, t) = \frac{1}{4\pi}\frac{\partial}{\partial x_j}\int [\rho v_i v_n - P_i]\frac{dS}{r} \\
&(d)\quad p_{SII}(\vec{x}, t) = -\frac{1}{4\pi}\int \frac{\partial}{\partial t}[\rho v_n]\frac{dS}{r}
\end{aligned} \qquad (8.7.1)$$

in which T_{ij} are components of the stress tensor defined by Lighthill [15], v_i is the component of flow velocity in the $i = 1, 2, 3$ directions $v_n = v_2$ is the velocity normal to boundary surface S, and P_i is the force (units: Nm^2) exerted on the fluid by the surface in the x_i direction. The brackets [] denote retarded values in time wherein variable t is replaced by variable $t - r/a_0$, $r = |\vec{x} - \vec{x}_0|$. The corresponding spatial variable in these bracketed quantities is the source coordinate $\vec{x}_0$. Finally, repeated subscripts i, j signify summation over 1, 2 and 3.

I. For Entire Frequency Range

$$S_{mnqr} = \frac{8\rho_o c_o}{\pi A_p}\frac{k_o^2}{k_m k_q k_n k_r}\left[1-(-1)^m\frac{\sin k_o\ell_1}{k_o\ell_1}-(-1)^n\frac{\sin k_o\ell_3}{k_o\ell_3}+(-1)^{m+n}\frac{\sin k_o\sqrt{\ell_1^2+\ell_3^2}}{k_o\sqrt{\ell_1^2+\ell_3^2}}\right] \quad \text{for } k_m, k_n, k_q, k_r > k_o \text{ (corner modes)}$$

II. For High Frequency Range ($k_o\ell_1, k_o\ell_3 \gg \pi$)

$$S_{mnqr} = \frac{8\rho_o c_o}{\pi A_p}\frac{k_m k_q}{k_n k_r}k_o\left(\frac{\pi\ell_1}{4k_m^2}\delta_{mq}-\frac{1}{3k_o^2}\right); k_n, k_r > k_o; k_m, k_q < k_o$$

$$S_{mnqr} = \frac{8\rho_o c_o}{\pi A_p}\frac{k_m}{k_n k_r k_q}; k_n, k_r > k_o;\ k_m < k_o; k_q > k_o$$

$$S_{mnmn} = \frac{\rho_o c_o k_o}{(k_o^2-k_n^2)^{1/2}}; k_m = k_q < k_o; k_n = k_r < k_o; k_m^2 \ll k_o^2$$

$$S_{mnmn} = \rho_o c_o; k_m = k_q < k_o; k_n = k_r < k_o; k_m^2 + k_n^2 \ll k_o^2$$

$$S_{mnmr} = \frac{2\rho_o c_o}{A_p}\frac{k_o\ell_1}{k_n k_r}; k_m = k_q < k_o \text{ and } k_n, k_r > k_o$$

For (m, n) an X-Type Edge Mode and (q, r) an Edge Mode

$$S_{mnqr} = \frac{2\rho_o c_o}{A_p}\frac{k_o\ell_1}{k_n k_r}\delta_{mq}$$

For (m, n) an X-Type Edge Mode and (q, r) a Corner Mode

$$S_{mnqr} = \frac{2\rho_o c_o}{\pi A_p}\frac{k_m}{k_n k_r k_q}$$

For (m, n) an X-Type Edge Mode and (q, r) is an Acoustically Fast Mode

$$S_{mnqr} = (-1)^n\frac{4\rho_o c_o}{\pi A_p}\frac{k_r}{k_o k_o^2}k_o\ell_1\left(\frac{\pi}{2k_o\ell_3}\right)^{1/2}\cos\left(k_o\ell_3-\frac{\pi}{4}\right)\delta_{mq}$$

For (m, n) and (q, r) Acoustically Fast Modes

$$S_{mnqr} = \rho_o c_o\delta_{mq}\delta_{nr} + (-1)^n\frac{4\rho_o c_o}{\pi A_p}\frac{k_n k_r}{k_o^4}k_o\ell_1\left(\frac{\pi}{2k_o\ell_3}\right)^{1/2}\cdot\cos\left(k_o\ell_3-\frac{\pi}{4}\right)\delta_{mq} + (-1)^m\frac{4\rho_o c_o}{\pi A_p}\frac{k_m k_q}{k_o^4}k_o\ell_3\left(\frac{\pi}{2k_o\ell_1}\right)^{1/2}\cos\left(k_o\ell_1-\frac{\pi}{4}\right)\delta_{nr}$$

III. For Low Frequency Range ($k_o\ell_1, k_o\ell_3 < \pi$)

Same as S_{mnqr} given above for entire frequency range because all modes are of corner mode radiation character.

A_p	area of plate equal to $\ell_1\ell_3$
c_o	velocity of sound in fluid
k_o	acoustic wavenumber equal to $\frac{\omega}{c_o}$
k_m, k_o	wavenumbers equal to $\frac{m\pi}{\ell_1}$ and $\frac{n\pi}{\ell_3}$ respectively; similarly for k_q, k_r
ℓ_1, ℓ_3	plate length and width respectively
m, n, q, r	mode numbers
S_{mnqr}	modal radiation coupling term per unit area
δ_{ij}; δ_{mq} and δ_{nr}	Kronecker delta equal to 1 for $i = j$, equal to 0 otherwise
ρ_o	mass density of fluid
ω	circular frequency

Fig. 8.6.11. Formulas for calculating added damping on rectangular plates due to fluid loading as derived by Davis [13].

The role of the surface integrals in 8.7.1 in promoting (or amplifying) the direction sound from the volume integral is difficult to evaluate. Powell [16] invoked the concept that the boundary surface acts as a "mirror" which produces an *image* of the entire set of equations 8.7.1. He then superimposed the direct field and the image field and showed that when the boundary surface is pressure-release no amplification occurs: the surface plays a pure passive role and merely reflects (with opposite sign) the sound generated by the volume integral. The question then arises, is there amplification of radiated sound for other condition of surface impedance? Ffowce Williams [17] developed the following procedure for answering this question.

In 8.7.1 all terms that are nonlinear in v_n, and all viscous terms in T_{ij} are neglected. Decomposing the surface integrals into symmetric components (real field and image field equal with the same sign) and antisymmetric components (equality with opposite sign) relative to the boundary surface, and equating like components of the real and image systems, then applying Krichoff's theorem of volume sources and their equivalent surface source representation one finds the fields of the real (+) and image (−) systems to be:

$$\text{(a)} \quad \begin{cases} p(\vec{x}, t) = p_V^+ + p_{SI} + p_{SII} \\ 0 = p_V^- - p_{SI}^+ + p_{SII}^+ \end{cases}$$

$$\text{(b)} \quad p_{SI}^+(\vec{x}, t) = \frac{1}{4\pi} \frac{\partial}{\partial x_{n_+}} \int [p] \frac{dS}{r} = \mathcal{F}\left\{ \frac{1}{4\pi} \frac{\partial}{\partial x_{n_+}} \int [v_n] \frac{dS}{r} \right\} \tag{8.7.2}$$

$$\text{(c)} \quad p_{SI}^+(\vec{x}, t) = \frac{-1}{4\pi} \int \frac{\rho \partial [v_n]}{\partial t} \frac{dS}{r}$$

in which n_+ signifies the surface normal into volume V^+, and p is the surface pressure. The symbol $\mathcal{F}$ is a differential integral operator which relates surface pressure to surface velocity v_n. From (b) and (c) it is concluded that,

$$\rho \frac{\partial p_{SI}^+}{\partial t} = - \mathcal{F} \frac{\partial p_{SI}^+}{\partial x_{n_+}}. \tag{8.7.3}$$

Equation 8.7.3 immediately yields the radiated field when the boundary surface is rigid ($v_n = 0$), for then p_{SII}^+ vanishes and,

$$p(\vec{x}, t) = p_V^+ + p_V^-, \quad \text{(rigid surface)}. \tag{8.7.4}$$

This is expected doubling of the field. Similarly, for pressure-release boundary surfaces p_{SI}^+ vanishes and,

$$p(\vec{x}, t) = p_V^+ - p_V^- \quad \text{(pressure-release surface)}. \tag{8.7.5}$$

This means that the surface reflects a negative image of the field due to boundary layer turbulence.

Further progress in analyzing the effect of compliant boundaries in amplifying sound due to boundary layer turbulence can be made by considering various spatial and temporal scales of the turbulent source. To obtain these one first defines amplitudes of acoustic pressure, $p(\vec{K}, \omega)$, and stress tensor $T_{ij}(\vec{x}_0, \omega)$ in $\vec{K}, \omega$ space by means of Fourier transformation:

$$p(\vec{K}, \omega) = \int\int p(\vec{x}_{(s)}, t) \exp(i\omega t - i\vec{K} \cdot \vec{x}_s) d\vec{x}_s dt, \quad \text{(units: Ns)} \tag{8.7.6.}$$

$$T_{ij}(\vec{x}_0, \omega) = \int T_{ij}(\vec{x}_0, t) \exp(i\omega t) dt, \quad \text{(units: Nsm}^{-2}\text{)} \tag{8.7.7}$$

$$\vec{x}_0 = (x_{0(1)}, x_{0(2)}, x_{0(3)});\ \vec{x} = (x_1, x_2, x_3);\ \vec{K} = (k_1, k_3)$$
$$r = |\vec{x} - \vec{x}_0|;\ \vec{x}_s = (x_1, x_3);\ x_{0(s)} = (x_{0(1)}, x_{0(3)}).$$

The acoustic pressure on the boundary surface $p(\vec{x}_{(s)}, t)$ is then given by (8.7.1b) with full space factor 4π replaced by half-space 2π, and with the observation vector $\vec{x}_{(s)}$ being in the surface so that $k = |\vec{x}_{(s)} - x_0|$. Using the shift theorem in the theory of Fourier transformation one can write (8.7.6) from (8.7.1), in the form:

$$p_V(\vec{K}, \omega) = \int_t \int_{x_{0(s)}} \int_V \frac{1}{2\pi} \left[\int_{\omega^*} \frac{\partial^2}{\partial x_{(i)} \partial x_{0(j)}} T_{ij}(\vec{x}_0, \omega^*) e^{-i\frac{r}{a_0}\omega^*} e^{-i\omega^* t} \frac{d\omega^*}{2\pi} \right]$$

$$\times \frac{dV}{r} e^{i\omega t - i\vec{K}\cdot\vec{x}_{(s)}} d\vec{x}_{(s)} dt. \tag{8.7.8}$$

The integration over t yields the delta function $\delta(\omega - \omega^*)$ and the integration over ω^* merely replaces ω^* by ω. Hence,

$$p_V(\vec{K}, \omega) = \int_{x_{0(s)}} \left\{ \int_V \frac{1}{(2\pi)^2} \frac{\partial^2}{\partial x_{0(s)} \partial x_{0(j)}} T_{ij}(\vec{x}_0, \omega) e^{-i\frac{r}{a_0}\omega} \frac{dV(\vec{x}_0)}{r} \right\} e^{-i\vec{K}\cdot\vec{x}_{(s)}} d\vec{x}_{(s)}. \tag{8.7.9}$$

Now

$$\vec{K} \cdot \vec{x}_{(s)} = \vec{K} \cdot \vec{x}_0 - \vec{K} \cdot (\vec{x}_0 - \vec{x}_{(s)}) \tag{8.7.10}$$

and Weyl's formula is,

$$\frac{\exp\left[-\frac{i\omega r}{a_0}\right]}{r} = \frac{-i}{2\pi} \int_{-\infty}^{\infty} \int \exp -i\{k_1'(x_{0(1)} - x_1) + k_3'(x_{0(3)} - x_3) + k_2' x_{0(2)}\} \frac{dk_1' dk_3'}{k_2'}$$

$$k_2' = \sqrt{\left[\frac{\omega}{a_0}\right]^2 - (k_1'^2 + k_3'^3)}. \tag{8.7.11}$$

Upon insertion of 8.7.10 and (8.7.11) into (8.7.9) and integrating over $d\vec{x}_{(s)} = dx_1 dx_3$ one obtains

$$\exp[i(k_1 - k_1')x_{0(1)}] \exp[i(k_3 - k_3')x_{0(3)}] \delta(k_1 - k_1') \delta(k_3 - k_3').$$

Then integration over $dk_1'\, dk_3'$ merely replaces k_1', k_3' by k_1, k_3. Equation (8.7.9) then reduces to,

$$\text{(a)}\quad p_V(\vec{K}, \omega) = -\frac{i}{(2\pi)^3} \int_V \frac{\partial^2}{\partial x_i \partial x_j} T_{ij}(\vec{x}_0, \omega) \frac{\exp(-ik_2 x_{0(2)})}{k_2} e^{-i\vec{K}\cdot\vec{x}_0} dV(\vec{x}_0) \tag{8.7.12}$$

$$\text{(b)}\quad k_2 = \sqrt{\left[\frac{\omega}{a_0}\right]^2 - (k_1^2 + k_3^2)}. \tag{8.7.12}$$

[17]. Writing the volume integral in vector rotation and integrating by parts one has,

$$\int_V (\vec{\nabla}_0 \cdot \vec{\vec{T}} \cdot \vec{\nabla}_0) g dV_0 = \int_V \vec{\vec{T}} : (\vec{\nabla}_0 g \vec{\nabla}_0) dV$$

$$g = \frac{\exp\{-i[\vec{K} + \hat{j}k_2] \cdot \vec{x}\}}{k_2}$$

in which terms involving the divergence,

$$\int_V \nabla \cdot (g\vec{\vec{T}} \cdot \nabla_0) dV$$

vanish because $\vec{\vec{T}}$ vanishes outside the source region. Since

$$\vec{\nabla}_0 g \vec{\nabla}_0 = \frac{\partial^2}{\partial x_i \partial x_g} g = -[k_i + k_2\delta_{i2}][k_j + k_2\delta_{j2}]g$$

it is seen from (8.7.12) that

$$p_V(\vec{K}, \omega) = \frac{i}{(2\pi)^3} \int_V T_{ij}(\vec{x}_0, \omega)[k_i + k_2\delta_{i2}][k_j + k_2\delta_{j2}]$$
$$\times \frac{\exp(-ik_2 x_{0(2)} - i\vec{K} \cdot \vec{x}_0)}{k_2} dV(\vec{x}_0). \tag{8.7.13}$$

Now, $dV = dx_{0(2)} d\vec{x}_{0(s)}$. Integration over $dx_{0(s)}$ leads to a generalized three-dimensional (two spatial and one temporal) Fourier transform of the turbulence tensor:

$$T_{ij}(x_{0(2)}, \vec{K}, \omega) = \int_{\vec{x}_{0(s)}} T_{ij}(\vec{x}_0, \omega) \exp(-i\vec{K} \cdot \vec{x}_0) d\vec{x}_{0(s)}, \quad \text{(units: Ns)}. \tag{8.7.14}$$

In terms of this transform one can reformulate the pressure field on the surface (8.7.9) to, read:

$$p_V(\vec{K}, \omega) = \frac{i}{(2\pi)^3} \int_0^\infty T_{ij}(x_{0(2)}, \vec{K}, \omega)[k_i + k_2\delta_{i2}][k_j + k_2\delta_{j2}]$$
$$\frac{\exp(-ik_2 x_{0(2)})}{k_2} dx_{0(2)}, \quad \text{(units: } Ns\text{)}. \tag{8.7.15}$$

This is the K-ω space representation of the wall pressure generated by boundary layer turbulence. Except for the factor $(2\pi)^3$ due to differing definition of Fourier transformation it is identical with that of Fowcs-Williams [17].

Under excitation by these wall pressures the compliant wall vibrates with velocity $\dot{w}$. During vibration the compliant wall experiences additional forces due to the reaction of the medium. A simple procedure for calculating them is to assume the wavelength in the medium is small relative to any length scale of model vibration in the compliant surface. The reaction forces them correspond to those of an infinite surface under harmonic excitation forces. Choosing the surface to be an elastic plate excited by a sinusoidal acceleration in the x-direction ($= \ddot{w} \cos k_x x$) we infer that the acoustic field has the form,

$$p = P g_z(z, k_z) \cos k_x x$$

in which g_z is the 1-D Green's function given by (3.7.8) (multiplied by a factor of 2 to allow for half space rather than full space). At the surface $z = 0$ the boundary condition is,

$$\frac{\partial p}{\partial z} = -\rho_0 \ddot{w} \cos k_x x = ik_z P \left[\frac{\exp ik_z z}{k_z}\right]_{z=0} \cos k_x x$$

so that

$$P = i\rho_0 \ddot{w}.$$

Thus the reaction pressure due to the medium is,

$$p = \frac{i\rho_0 \ddot{w} \cos k_x x}{k_z}; \; k_z = \sqrt{(k_a^2 - k_x^2}; \; k_a = \frac{\omega}{c_0}. \tag{8.7.16}$$

At frequency ω, $\ddot{w} = -i\omega\dot{w}$. The specific acoustic impedance of the infinite plate is then,

$$z_a = \frac{p}{\dot{w}} = \frac{\rho_0\omega}{k_a\sqrt{1-\left[\frac{k_x}{k_a}\right]^2}} = \frac{\rho_0 c_0}{\sqrt{1-\left[\frac{k_x}{k_a}\right]^2}}. \tag{8.7.17}$$

Here k_x is treated as a continuous variable. When $k_a > k_x$ this reaction impedance is purely real: all the energy in the medium is radiated out to infinity. When, however, $k_a < k_x$ the medium load is purely imaginary corresponding to an inertial load, whose form is,

$$\begin{aligned} &(a)\ z_a = -i\omega m_a. \\ &(b)\ m_a = \frac{\rho_0}{\sqrt{k_x^2 - k_a^2}} \end{aligned} \tag{8.7.18}$$

Because of the absence of edges, and hence of long wavelength radiation, the specific acoustic resistance is infinite at $k_a = k_p$ and zero at $k_a < k_x$. Correspondingly, the inertial mass $m_a k_x/\rho_0$ rises from unity when $k_a \to 0$ to infinity when $k_a = k_x$. It vanishes when $k_a > k_x$.

With such a model of acoustic load we return to 4.2.8 and from it easily derive the relation of wall velocity amplitude $\dot{w}$ to the applied pressure $Q^{(A)}$ (which is p_v, 6.11.1b) by (1) assuming to plate the infinite in size (2) taking the space-time Fourier transform in the transform pairs $\vec{K},\vec{r}(x,y)$ and ω,t (3) noting that $\nabla^4 w(x,y,t)$ transforms to $k^4 w(\vec{K},\omega)$ where $k^2 = |\vec{K}|^2$. To account for plate damping loss the plate bending stiffness is made complex by writing $D(1 - i\eta)$. Thus,

$$\dot{w}(\mathbf{K},\omega) = \frac{Q^{(A)}(\mathbf{K},\omega)}{-i\omega m_p\left(1-\frac{Dk^4}{\rho h\omega^2}\right) + \eta\omega m_p\frac{Dk^4}{\rho h\omega^2} + \frac{\alpha\rho_0 c_0}{\sqrt{1-\frac{k^2}{k_a^2}}}},\quad k_a > k \tag{8.7.19}$$

The units of $\dot{W}(\mathbf{K},\omega)$ are m^3 and those of $Q^{(A)}(\mathbf{K},\omega)$ are Ns. $Q^{(A)}(\mathbf{K},\omega)$ in this context is identical with 8.7.15. The symbol α has a value of unity if only one side is loaded with the medium, and 2 if both sides are loaded. Multiplication of 8.11.19 by its conjugate gives an expression for the amplitude power spectrum of normal component of surface velocity $(=|\dot{w}(\mathbf{K},\omega)|^2)$ in terms of the amplitude power spectrum of the applied pressure $(=|Q^{(A)}(\mathbf{K},\omega)|^2)$:

$$|\dot{w}(\mathbf{K},\omega)|^2 = \frac{|Q^{(A)}(\mathbf{K},\omega)|^2}{\left[\eta\omega m_p\frac{Dk^4}{\rho h\omega^2} + \frac{\alpha\rho_0 c_0}{\sqrt{1-\frac{k^2c_0^2}{\omega_a^2}}}\right]^2 + \left[\omega m_p\left(1-\frac{Dk^4}{\rho h\omega^2}\right)\right]^2},\ \text{(units: } m^6\text{)} \tag{8.7.20}$$

Various regimes of wall surface velocity response can be defined from this relation by specifying the magnitude of $\omega/(\mathbf{K})c_0$ relative to unity. Evidently most intense vibration will occur at frequencies $\omega >> |\mathbf{K}|c_0$, together with wavenumbers in the vicinity of $k^4 = \rho h\omega^2/D$. The latter is the condition of free-wave response ($Q^{(A)} = 0$) of the infinite plate:

$$|\dot{w}(k_p,k_pc_b)|^2_{max} = \frac{|Q^{(A)}(k_p,k_pc_b)|^2}{k_p^2c_b^2m_p^2\left[\eta + \frac{\alpha\rho_0c_0}{m_pk_pc_b}\right]^2} \quad \text{(units: } m^6\text{)} \tag{8.7.21}$$

in which k_p is defined by 4.2.17 and c_b by 4.2.16.

Equation 8.7.19 may be used to deduce the form of the total spectral amplitude of wall pressure which is the sum of the applied pressure and the pressure corresponding to the medium reaction to the motion of the wall,

$$p_{tot}(\mathbf{K},\omega) = Q^{(A)}(\mathbf{K},\omega) + \frac{\alpha\rho_0c_0\dot{w}(\mathbf{K},\omega)}{\sqrt{1-\frac{k^2c_0^2}{\omega^2}}}, \quad \text{(units: } Ns\text{)} \tag{8.7.22}$$

It should be noted however that the surface velocity in the presence of medium loading is determined from the *applied* pressure $Q^{(A)}$. Also the radiated acoustics power is determined from the square of the surface velocity, hence ultimately by $|Q^{(A)}|^2$. Equation 8.7.19 suggests *defining* a specific acoustic impedance z_a and specific plate impedance z_p as follows:

$$(a)\ z_a(k) \equiv \frac{\alpha\rho_0c_0}{\sqrt{1-\frac{k^2c_0^2}{\omega^2}}} \quad \text{(units: } Nsm^{-3}\text{)} \tag{8.7.23}$$

$$(b)\ z_p \equiv \eta\omega m_p\frac{Dk^4}{\rho h\omega^2} - i\omega m_p\left[1-\frac{Dk^4}{\rho h\omega^2}\right] \quad \text{(units: } Nsm^{-3}\text{)}$$

Now

$$\frac{1}{k_z} = \frac{z_a}{\rho_0\omega} \text{ or } k_z = \rho_0\omega y_a,\ y_a = \frac{1}{z_a} \tag{8.7.24}$$

Thus in 8.7.15 the factor k_z is proportional to the specific acoustic admittance y_a of the medium. This suggests accounting for the compliance of the boundary surface by considering the plate and medium to be analogous in their response to circuit elements which are mechanically in series (that is, having the same applied force). The total admittance (including the plate) is then:

$$y_T = \frac{1}{z_a} + \frac{1}{z_p} = \frac{z_a + z_p}{z_az_p}$$

Thus k_z is replaced by,

$$\rho_0\omega\left[\frac{z_a + z_p}{z_az_b}\right]$$

and one *models* the wall pressure 8.7.15 to include wall compliance by writing:

$$p_v(\mathbf{K},\omega) = \frac{i}{(2\pi)^3}\int T_{ij}(x_{0(2)},\mathbf{K},\omega)[k_i + k_2\delta_{i2}][k_j + k_2\delta_{j2}]\frac{e^{-ik_2X_{0(2)}}}{\rho_0\omega}\frac{z_az_p}{z_a+z_p}\,dx_{0(2)} \tag{8.7.25}$$

Since the turbulent pressures on the wall are randomized quantities they will generate a randomized surface velocity. The autocorrelation of this velocity over time delay τ and distance l normalized to an A and duration T is found from 8.7.20;

$$R(\mathbf{l},\tau) = \frac{1}{2}\iint \frac{|\dot{w}(\mathbf{K},\omega)|^2}{AT}\, e^{i\mathbf{K}\cdot\mathbf{l}-i\omega\tau}\,\frac{d\mathbf{K}d\omega}{(2\pi)^3} \quad \text{(units: } m^2s^{-2}\text{)} \tag{8.7.26}$$

in which the power spectrum is calculated as peak values. Thus at zero delay τ and zero distance $\mathbf{l}$ the mean square surface velocity averaged over area A and direction T is

$$<\dot{w}(x,y,t)^2>_{\text{rms}} = R(0,0) = \frac{1}{2}\iint \frac{|\dot{w}(\mathbf{K},\omega)|^2}{AT}\,\frac{d\mathbf{K}d\omega}{(2\pi)^3} \quad \text{(units: } m^2s^{-2}\text{)} \tag{8.7.27}$$

Assuming the radiation efficiency σ (see 9.5.13) is known for vibrating area A one can find the rms radiated acoustic power from area A to be,

$$W_{\text{rms}} = \rho_0 c_0 A\sigma <\dot{w}(x,y,t)^2>_{\text{rms}} \quad \text{(units: } Nms^{-1}\text{)}$$

$$W_{\text{rms}} = \frac{1}{2}\rho_0 c_0 \sigma \iint \frac{|\dot{w}(\mathbf{K},\omega)|^2}{T}\,\frac{d\mathbf{K}d\omega}{(2\pi)^3} \tag{8.7.28}$$

For an infinite plate,

$$\sigma = \frac{A\mathfrak{Z}_a}{\rho_0 c_0 A} = \frac{1}{\sqrt{1-\dfrac{k^2c_0^2}{\omega_2}}}$$

It is to be noted that while $\sigma \to \infty$ when $\omega \to |\mathbf{K}|\, c_0$ the mean-square surface velocity approaches zero. Actually the maximum mean-square velocity is found at $k = k_p$ and $\omega >> |\mathbf{K}|c_0$, as indicated by 8.7.21. It is over this range of k and ω that the integral in 8.7.28 is a maximum and $\sigma \simeq 1$.

In practice the measurement of spectra is usually confined to one dimension at a time. A one-dimensional power spectrum in wave number k_1 is obtained by integration over k_3 and ω:

$$p(k_1) = \iint p(\mathbf{K},\omega)\, dk_3 d\omega \quad \text{(units: } Nm^{-1}\text{)} \tag{8.7.29}$$

The power spectrum $P(k_1)$ is then defined as

$$P(k_1) = |p(k_1)|^2 \quad \text{(units: } N^2m^{-2}\text{)} \tag{8.7.30}$$

The corresponding autocorrelation function over spatial lag l_1 is obtainable by use of the Wiener-Kintchine theorem,

$$R(l_1) = \frac{1}{2}\int \frac{P(k_1)c^{ik_1l_1}}{L}\,\frac{dk_1}{2\pi} \quad \text{(units: } N^2m^{-4}\text{)} \tag{8.7.31}$$

Here, L is the normalizing length. It is the largest scale of distance under consideration. Thus the mean square wall pressure field averaged along the 1-direction is,

$$<p^2>_{\text{1-direction}} = R(0) = \frac{1}{2}\int \frac{P(k_1)}{L}\,\frac{dk_1}{2\pi} \quad \text{(units: } N^2m^{-4}\text{)} \tag{8.7.32}$$

It is often asked, what is $P(k_1)$ as $k_1 \to 0$? The question may be answered by casting 8.7.29 in *dimensional form*. Let δ^* (the boundary thickness) be an appropriate scale of length for the hydrodynamic turbulent field and let U be the convection velocity. As for frequency, a scale can be adopted from the concept of the Strouhal number $S = \omega/(V/D)$ (V = hydrodynamic velocity, D = cylinder diameter) as it is used in the theory of votex streets. Thus let the frequency scale be $\omega \sim U/\delta^*$. Now assume k_i and k_j are much smaller than k_2, and that $k_2 \approx \omega/c_0$. Then 8.7.29, in conjunction with 8.7.15 becomes:

$$p(k_1) = \frac{i}{(2\pi)^3} \int_0^\infty \int_0^\infty dk_3 d\omega \; T_{ij}(x_{0(2)}, 0, \omega) \frac{\omega}{c_0} \exp\left[-i\frac{\omega}{c_0} x_{0(2)}\right] dx_{0(2)} \qquad (8.7.33)$$

The dimensionality of the various factors that appear inside the integral sign is:

$$\begin{aligned} &T_{ij}(\mathbf{x},t)\text{: } \rho U^2 \qquad (8.7.34)\\ &T_{ij}(\mathbf{x},\omega)\text{: } \rho U\delta^* \\ &T_{ij}(x_{0(2)},\mathbf{K},\omega)\text{: } \rho U\delta^{*3} \\ &k_3\text{: } \delta^{*-1} \\ &dx_{0(2)}\text{: } \delta^* \end{aligned}$$

Hence, the dimension form of 8.7.33 is:

$$p(k_1)\text{: } \rho \frac{U^2\delta^*}{c_0}$$

so that,

$$\lim_{k_1 \to 0} P(k_1)\text{: } \rho^2 M^2 U^4 \delta^{*2}, \text{ where } M = \frac{U}{c_0} \qquad (8.7.35)$$

[17]. The noteworthy feature of 8.7.35 is that in the low wave number regime the 1-dimensional power spectrum is asymptotically a non-zero constant. This is due to finite compressibility of the medium as $k_1 \to 0$.

A different dimensional form of 8.7.15 appears when the frequency ω approaches zero, rather than the wavenumber k_1. One then assumes $\omega << c_0|\mathbf{K}|$ so that $k_2 \to -ik$. (The negative sign is used to represent exponential decay in the factor $\exp(-ik_2 x_{0(2)})$). Thus,

$$p(k_1) = \frac{i}{2\pi)^3} \int dk_3 \int d\omega \int T_{ij}(x_{0(2)}, \mathbf{K}, \omega)$$

$$[k_i + (-ik)\delta_{i2}]\,[k_j + (-ik)\delta_{j2}]\,\frac{e^{-kx_{0(2)}}}{k}\,dx_{0(2)} \qquad (8.7.36)$$

The dimensional form of this equation is obtained from 8.7.34,

$$p(k_1)\text{: } \frac{1}{\delta^*}\frac{U}{\delta^*}\rho U\delta^{*3}\, k\delta^* = k\rho U^2\delta^{*2} \qquad (8.7.37)$$

in which k is explicitly returned in order to show power spectrum dependence on k in the incompressible regime ($\omega << c_0|\mathbf{K}|$). Thus,

$$\lim_{\omega \to 0} P(k_1)\text{: } k^2\rho^2 U^4 \delta^{*4}$$

The power spectrum of wall pressure therefore approaches zero as the square of the wavenumber. From 6.11.38 and 8.7.35 it is seen that the compressible and incompressible regimes yield power spectra which approach each other at a value of $k = k_0 = M/\delta^*$. Figure 8.7.1 is a generalized plot of the 1-dimensional power spectrum of wall pressure due to velocity turbulence which shows all these features. Because the energy of the turbulent flow is finite the spectrum effectively vanishes at high values of k.

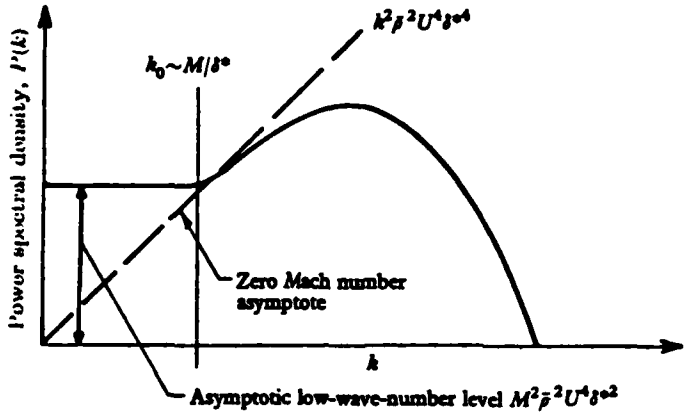

Fig. 8.7.1. General features of a 1-D wavenumber power spectrum of turbulence-generated wall pressure (after [17]).

Frequency power spectra $P(\omega)$ may be similarly characterized. For example, in 8.7.36 the integration over ω is replaced by an integration over k_1, resulting in

$$\lim_{\omega \to 0} P_1(\omega) : (\rho U \delta^*)^2 = \rho^2 \omega^2 \delta^{*4}$$

The spectrum therefore approaches zero as the square of the frequency. This conclusion is valid for the condition of incompressible flow. For compressible flow the power spectral density $P(\omega)$ is finite as $\omega \to 0$. These features are show in Fig. 8.7.2. Here is shown a region (to the right of the vertical line) where the frequency analysis of the fluid velocity at a point gives a spectrum which is approximately identical with the wave number analysis of the variation of velocity along a line in the direction of the stream (Taylor's hypothesis).

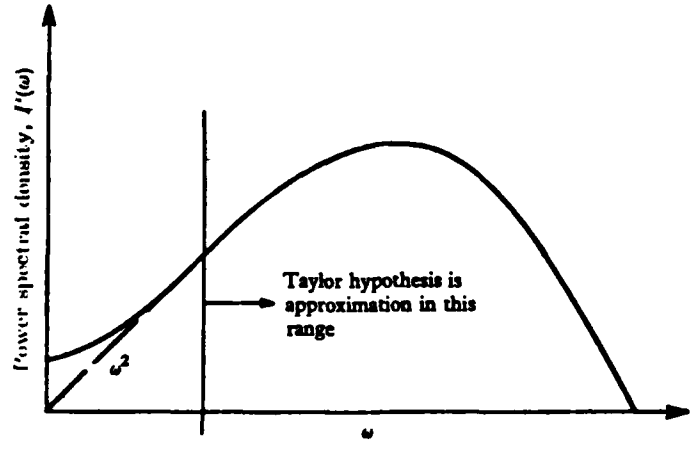

Fig. 8.7.2. General features of wave-number and frequency spectra of the surface-pressure field induced by a turbulent boundary layer at finite Mach numbers (after [17]).

8.8 SUMMARY CHART OF PRESSURE FIELDS GENERATED BY TRAVELING AND STANDING FLEXURAL WAVES OF AN ELASTIC PLATE

In Sections 8.6 and 8.7 the response of an elastic plate to random pressure fields in an adjacent medium was presented in detail. We summarize here the main results from another point of view.

Let a ribbed elastic plate, for whatever excitation, be carrying both flexural traveling waves and flexural standing waves. The pressure field in the medium, both acoustic and nonacoustic, can be described by a k, ω spectrum, here taken to be 1-dimensional. The component parts of this field and the acoustic spectrum are summarized in Fig. 8.8.1.

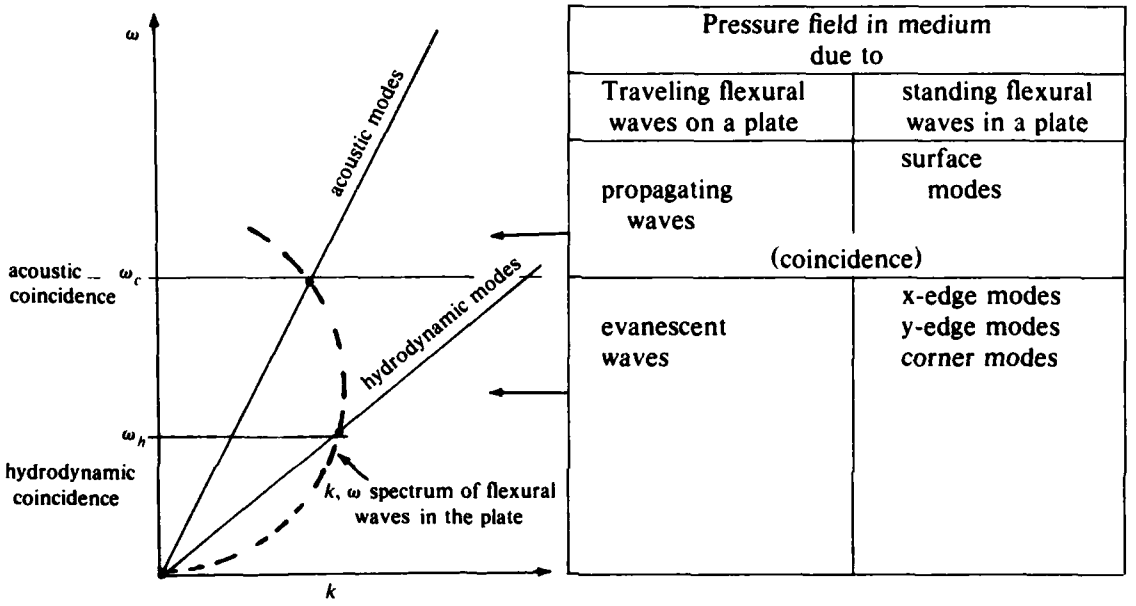

Pressure field in medium due to	
Traveling flexural waves on a plate	standing flexural waves in a plate
propagating waves	surface modes
(coincidence)	
evanescent waves	x-edge modes y-edge modes corner modes

Fig. 8.8.1. k, ω spectrum of flexural waves in a plate and associated pressure fields

The distinction between pressure fields due to traveling flexural waves and fields due to standing flexural waves is important to understanding acoustic radiation below acoustic coincidence. Traveling flexural waves generate only evanescent fields; standing flexural waves actually radiate to the farfield in the edge modes and corner modes described in Sections 8.6 and 8.7.

REFERENCES

1. H. Kraus "The Elastic Shells," J. Wiley and Sons, Inc. New York, chap. 9.

2. Ref. 1., p. 368.

3. I.S. Gradshteyn/I.M. Ryzhik "Table of Integrals, Series and Products" Academic Press 1965, p. 477.

4. D. Middleton "Introduction to Statistical Communication Theory" McGraw-Hill 1960, p. 144.

5. I. Dyer Jour. Acoust. Soc. Am. *31*, 922-928 (1959).

6. G.A. Campbell, R.M. Foster "Fourier Integrals for Practical Applications" D. VanNostrand, New York 1951, p. 44.

7. R.H. Lyon "Boundary layer noise response simulation with a sound field" Acoustical Fatigue in Aerospace Structures, Chap. 10, Syracuse U. Pross., 1965.

8. M.C. Junger, D. Feit "Sound, Structures and their Interactions" MIT Press, 1972 (p. 150).

9. R.C. Leibowitz, J. Sound and Vib. **40** (4), 441-495 (1975).

10. L. Maestrello, J. Sound and Vib. 5 (3), 407-448 (1967).

11. L.M. Lyamslev. S.A. Salosina, Sov. Phys. Acoust. **12**, 228-229 (1966).

12. G.B. Warburton, Proc. of Inst. of Mech. Eng. London **168**, 371-381.

13. H.G. Davies, J. Sound and Vib **15**, 107-126 (1971).

14. N. Curle, Proc. Roy. Soc. **A231**, 412 (1955).

15. M.J. Lighthill, Proc. Roy Soc. **A211**, 566 (1952), and **A222**, 1 (1954).

16. A. Powell, J. Acous. Soc. Am **32**, 8, 982 (1960).

17. J.E. Ffowce Williams J. Fluid Mech. **22**, 347 (1965) and **22**, 507 (1965).

CHAPTER IX
SELECTED EXAMPLES OF ACOUSTIC RADIATION FROM PLATES, FINITE CYLINDERS, FINITE RIBBED PLATES, ETC.

9.1 SOUND RADIATION BY A SEMIINFINITE PLATE [1]

A flexural plate, thickness h, occupies the x-axis ($0 \leqslant x \infty$) Fig. 9.1.1. It is submerged in a fluid of density ρ and excited by a transverse displacement (normal to the plate) of a *free* harmonic wave, $\zeta(x) = A \exp(\pm iK_{x0}x - i\omega t)$. The *free* wave number K_{x0} is the positive real root of the dispersion equation of the plate obtained when plane harmonic waves (parallel to the z-axis) are substitued into Eq. (4.2.8). This means K_{x0} is the root of:

$$K_x^4 - \kappa^4 = 2i\frac{\rho}{\rho_p}\frac{\kappa^4}{K_y h}, \quad \kappa^4 = \frac{\omega^2 \rho_p h}{D}. \tag{9.1.1}$$

The conditions underlying the derivation of this equation are (1) the pressure wave in the medium is planar, $p = A \exp(iK_x + iK_y - i\omega t)$ (2) the loading q on the plate is the difference between the acoustic pressure on the back side and the pressure on the front side, $p_- - p_+$. The right-hand side of this equation is itself derived as follows:

$$u_y = -\left.\frac{\partial \phi}{\partial y}\right|_{y=0} = -\frac{\partial}{\partial y}\left(\frac{p}{-i\omega\rho}\right) = \frac{1}{i\omega\rho}\left.\frac{\partial p}{\partial y}\right|_{y=0}.$$

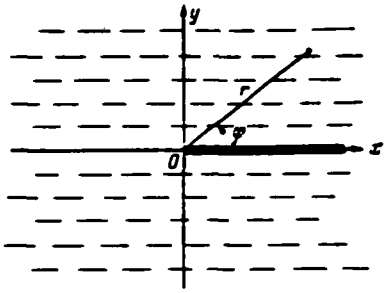

Fig. 9.1.1. Layout of the coordinate axes.

Since

$$\left.\frac{\partial p}{\partial y}\right|_{y=0} = iK_y p$$

then

$$U_y = \frac{1}{i\omega\rho} iK_y p = \frac{K_y p}{\omega\rho}.$$

But $u_y = -i\omega A$. Therefore,

$$p = \frac{\omega\rho(-i\omega)A}{K_y}. \tag{9.1.2}$$

The loading is thus seen to be,

$$q = p_- - p_+ = -2p_- = -2p = \frac{2i\omega^2\rho A}{K_y}$$

multiplying and dividing by $\rho_p h$ then leads to (9.1.1).

The pressure wave above and below the plate are obtained from (9.1.2):

$$p_+ = -\frac{i\omega^2\rho A}{K_y}\exp(iK_x x + iK_y y - i\omega t)$$

$$p_- = \frac{i\omega^2 \rho A}{K_y} \exp(iK_x x - iK_y y - i\omega t) \tag{9.1.3}$$

$$K_y = \sqrt{k^2 - K_x^2}.$$

In order to establish the boundary conditions at $x = 0$ unambiguously it is convenient to assume that the incident flexural wave comes from $+\infty$, that is, $\zeta(x) = A \exp - iK_{x0}x$. The acoustic field developed by this wave *before reflection* at $x = 0$ is a single harmonic plane wave [2]:

$$p_i(x,y) = -\frac{A\rho\omega^2}{\alpha} sgn(y) \exp(-ik_x x - \beta|y| - i\omega t) \tag{9.1.4}$$

$$sgn\ y = +, \text{ if } y > 0$$

$$sgn\ y = -, \text{ if } y < 0$$

$$\beta = \sqrt{K_x^2 - k^2} = -i\ K_y.$$

When $K_x > k$ the plate radiates only evanescent modes, but when $k > K_x$ the plate radiates real power to the far field. The power per unit length carried by the plate is,

$$W_1 = \frac{D\omega A^2 K_{x0}^2}{h} \quad \text{(units: } N\,\text{ms}^{-1}\,m^{-1}\text{)}. \tag{9.1.5}$$

The power per unit length carried by the medium is,

$$W_2 = \frac{D\omega}{4} \frac{A^2 K_{x0}(K_{x0}^4 - \kappa^4)}{K_{x0}^2 - k^2} \quad \text{(units: Ns}^{-1}\text{)} \tag{9.1.6}$$

The ratio,

$$W_1^0 = \frac{W_1}{W_1 + W_2} \tag{9.1.7}$$

versus kh is plotted in Fig. 9.1.2. Asymptotically as $kh \to 0$, the ratio $W_1^0 \to 0.8$. This figure shows that for $kh \approx 0.21$ about 90.2% of the energy is carried in the plate. Below this value of kh the plate carries about 80% of the total energy. Above the *critical region* $kh \sim 1$ an increasing fraction of the total energy to carried by the fluid.

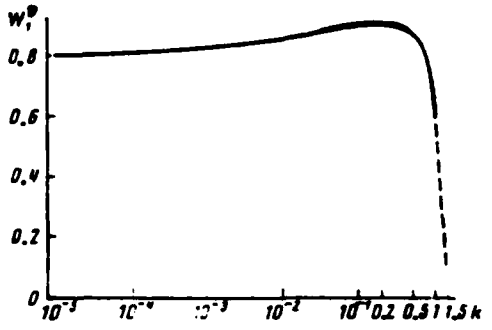

Fig. 9.1.2. Surface wave energy W_1^0 transported in the plate versus dimensionless wave number kh. (After [1]).

Upon reflection from the edge $x = 0$ an additional field p_r is developed in the medium. It is a *sum* of plane waves of all wavenumbers:

$$p_r(x,y) = A\frac{\omega^2\rho}{\sqrt{K_{x0}^2 - k^2}}\frac{sgn(y)}{2\pi i}\int_{-\infty}^{\infty} q(\lambda)\exp(i\lambda x - \sqrt{\lambda^2 - k^2}\,|y|)d\lambda \qquad (9.1.8)$$

in which $q(\lambda)$ is an amplitude (units: m). For arbitrary distance $|y|$ the calculation of the integral by contour integration is extremely difficult. However when $|y|$ is in the farfield of the radiator only a cylindrical wave survives,

$$P(x,y) = P(r\cos\phi,\ r\sin\phi) \approx \sqrt{\frac{2}{\pi kr}}\exp\left[i\left(kr - \frac{\pi}{4}\right)\right]\Phi(\phi) \qquad (9.1.9a)$$

$$\Phi(\phi) = \frac{A\rho\omega^2}{\sqrt{K_{x0}^2 - k^2}}\left(\frac{ikh}{2}\right)\sin\phi\ q(k\cos\phi). \qquad (9.1.9b)$$

Thus in direction ϕ the field is approximated by a single plane wave of amplitude $q(k\cos\phi)$. It is the amplitude of a cylindrical wave radiated from the edge. It is a function of angle ϕ because of interference in the medium of left and right travelling waves. Its value must be determined from the boundary conditions at the plate's edge ($x = 0$) [3]. When y is in the near field the acoustic pressure in the medium is the sum of contributions from one incident wave and one reflected wave (in the plate):

$$P(x,y) \approx -\frac{A\omega^2\rho}{\sqrt{K_{x0}^2 - k^2}}\,sgn(y)\{\exp(-iK_x x - \beta|y| - i\omega t) + \alpha(iK_x x - \beta|y| - i\omega t)\}. \qquad (9.1.10)$$

Here α is the reflection coefficient. It is a complex number depending on K_{x0}, k, κ^4, and on edge conditions (i.e., whether the plate is clamped or free). Figure 9.1.3 is a plot of modulus $|\alpha|$ and arg α versus kh for a steel-water system. It shows that when $kh > 1$ the *reflected* energy in the water drops very sharply because the incident plane wave suddenly begins to radiate very efficiently.

The acoustic power radiated by the edge of the plate into the far field per unit length of the plate is,

$$W = \int_0^{2\pi} w d\phi,\ w = \frac{|\Phi|^2}{\pi\rho\omega} \quad \text{(units: Ns}^{-1}\text{)}. \qquad (9.1.11)$$

The ratio of power radiated by the edge ($= w$) to total power in the medium ($= W_1 + W_2$) is w^0 a complicated function of angle ϕ [4]. A calculation of w^0 for a water-steel system is shown in Fig. 9.1.4. The solid lines are (1) $kh = 1$; (2) $kh = 0.5$; (3) $kh = 0.1$; (4) $kh = 0.01$. The dashed line is $kh = 2$. For angles $\phi > 180°$ use $w^0(\phi) = w^0(360° - \phi)$. As kh increases it is seen that more energy gets into the water (i.e., w^0 increases). For small kh the radiation is dipole; for large kh it is quadrupole. In the free-edge plate the quadrupole radiation appears earlier in values of kh, and is more pronounced.

9.2 SOUND RADIATION FROM AN INFINITE PLATE REINFORCED WITH A FINITE SET OF BEAMS AND DRIVEN BY A POINT FORCE [5]

An infinite plate, thickness h, density ρ_p, stiffness $D(=Eh^3/12(1-\nu^2))$, lies in the xz plane, Fig. 9.2.1. It is reinforced with a periodic (but finite) system of beams, and is driven by a point force $f_0\,e^{-i\omega t}$ at x_0, z_0. Under the action of this force the plate vibrates transversely

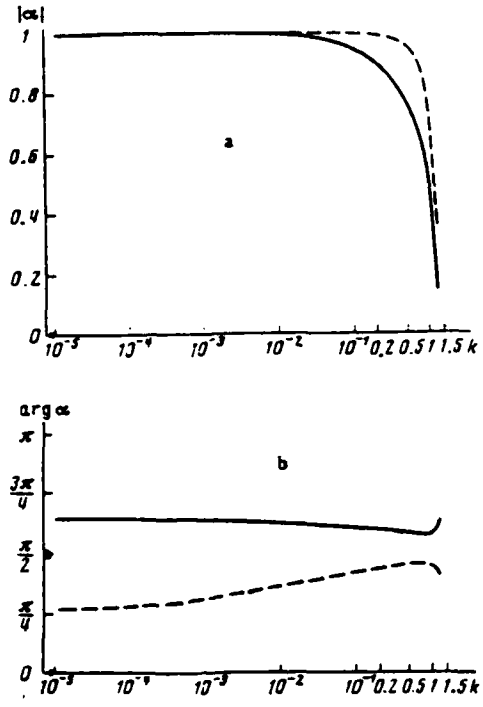

Fig. 9.1.3. Modulus (a) and argument (b) of the reflection coefficient α versus dimensionless wave number k. Dashed line, free edge; solid line, rigid edge. (After [1]).

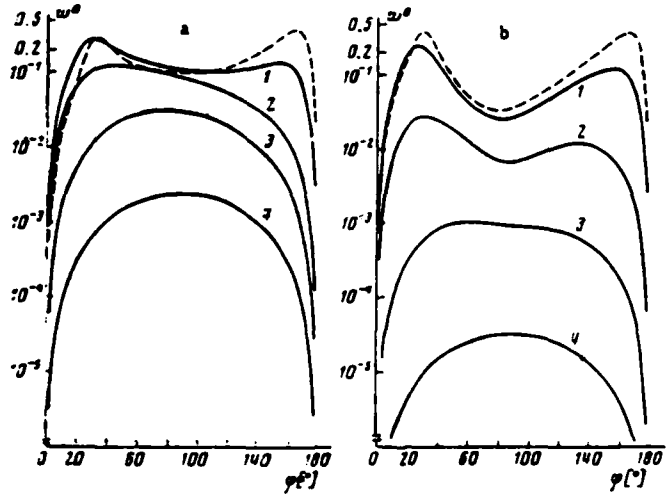

Fig. 9.1.4. Angular dependence of the radiation into the fluid for various values of the parameter kh, (a) Plate with clamped edge; (b) plate with free edge. (After [1]).

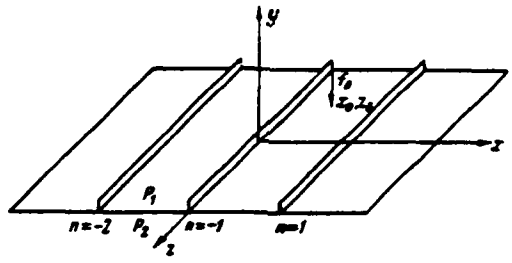

Fig. 9.2.1. Coordinate system. (After [5]).

with velocity $-i\omega w(x,z)e^{-i\omega t}$. Since the motion of the plate induces a reaction from the beams one can specify the forces and moments of this reaction as being proportional to the velocity:

$$F_j = -i\omega w(x_j, z)\,\delta(x - x_j)\,Z_F(\omega)$$

$$M_j = -i\omega\left[-\frac{\partial w}{\partial z}(x_j, z)\right]\delta(x - x_j)Z_M(\omega).$$

Here, Z_F, Z_M are the mechanical impedances per unit length of the force and moment respectively. The units of Z_F are $\mathrm{Nsm^{-2}}$, of Z_M are Ns, of F_j are $\mathrm{Nm^{-2}}$, and of M_j are $\mathrm{Nm^{-1}}$. The dynamic equation of force balance is,

$$(a)\quad D\left[\left(\frac{\partial^2}{\partial x^2}+\frac{\partial^2}{\partial z^2}\right)^2-\kappa^4\right]w(x,z) = -\sum_{-N_1}^{+N_2}F_i-\sum_{-N_1}^{+N_2}\frac{\partial M_j}{\partial x}-f_0\,\delta(x-x_0)\delta(z-z_0)$$

$$-P_1(x,z)+P_2(x,z) \qquad (9.2.1)$$

$$(b)\quad \kappa = \left[\frac{\omega^2\rho_p h}{D}\right]^{1/4} = \text{flexural wavenumber of the plate in a vacuum. (units: } \mathrm{m^{-1}})$$

P_1, P_2 = reactive loading of medium in upper (subscript 1) and lower (subscript 2) half space. (units: $\mathrm{Nm^{-2}}$).

N_1 = total number of beams in the region $x \leqslant 0$

N_2 = total number of beams in the region $x > 0$

The beams are labelled $n = \pm 1, \pm 2$, etc.

At the boundary of plate surface and medium the particle velocity must be continuous. Hence the forces acting on the medium must be in dynamic balance. For a medium of density ρ, the force balance is:

$$-\frac{\partial P_i}{\partial y} = \rho\ddot{w} \text{ or } \frac{\partial P_i}{\partial y} = \rho\omega^2 w, \quad i = 1, 2. \qquad (9.2.2)$$

Equations (9.2.1) and (9.2.2) form a system of differential equations. Because the plate is infinite one can write a solution in the form of an expansion of 2-dimensional plane waves:

$$w(x,z) = \int_{-\infty}^{\infty}\int \tilde{w}(K_x,K_z)\exp(iK_x x + iK_z z)\frac{dK_x dK_z}{(2\pi)^2} \tag{9.2.3}$$

in which $\tilde{w}$ (units: m^3) is the spatial Fourier transform, and K_x, K_z are the transform variables. Similarly, the acoustic pressure field is representable as an expansion in 3-D plane waves:

$$P_{1,2}(x,y,z) = \int_{-\infty}^{\infty}\int \tilde{P}_{1,2}(K_x,K_y)\exp(iK_x x + iK_z z \pm iK_y y)\frac{dK_x dK_z}{(2\pi)^2}$$

$$K_y = \sqrt{k^2 - K_x^2 - K_z^2} \tag{9.2.4}$$

Substitution of (9.2.4) and (9.2.3) into (9.2.2) and (9.2.1) leads to a system of $2(N_1 + N_2)$ algebraic equations in displacement $\tilde{w}$ and rotation $\partial\tilde{w}/\partial x$, expressed in the forms of 1—D z-transforms,

$$\tilde{w}(x_j,K_z) = \int_{-\infty}^{\infty}\tilde{w}(K_x,K_z)\exp(iKx_j)\frac{dK_x}{2\pi} \tag{9.2.5}$$

$$\frac{\partial\tilde{w}}{\partial x}(x_j,K_z) = \int_{-\infty}^{\infty} iK_x\tilde{w}(K_x,K_z)\exp(iK_x x_j)\frac{dK_x}{2\pi}$$

(see [5] for details). Because of the relation between acoustic pressure and plate displacement given by (9.2.2), the determination of (9.2.5) itself determines $P_{1,2}(K_x, K_z)$ as well:

$$\tilde{p}_1(K_x, K_z) = \frac{ik^2\rho c^2}{\sqrt{k^2 - K_x^2 - K_z^2}}\tilde{w}(K_x, K_z). \tag{9.2.6}$$

Application of (9.2.4) leads to explicit forms of radiated acoustic fields. These are expressed as a sum of three contributions,

$$P_1 = P_T + P_F + P_M$$

in which P_T is the contribution of an infinite plate without beam reinforcement, and P_F, P_M, are the contributions of the beams coupled by force F and bending moment M respectively. A plot of the equal-sound-pressure curves near the plate in the xy plane due to one beam on an infinite plate driven by a point-force is shown in Fig. 9.2.2. The calculation is based on taking $\kappa^2/k^2 = 32$, and the beam is assumed to be coupled to the plate by force only. It is a set of beam patterns of contributions $P_T + P_F$.

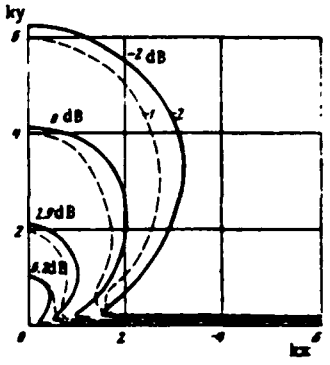

Fig. 9.2.2. Equal-sound-pressure curves for a force-coupled beam and plate. 1) Exact calculation; 2) approximate calculation. (After [5]).

Similarly, Fig. 9.23 shows the set of patterns near the plate for one beam coupled to an infinite plate by torque only and the plate driven by a point force. It is a set of patterns contributed by $P_T + P_M$. In both cases the dashed lines are an approximation for the condition that the driving point and observation point lie in a plane perpendicular to the reinforcing beams.

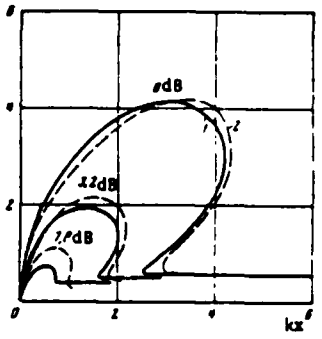

Fig. 9.2.3. Equal-sound-pressure curves for a torque-coupled beam and plate. 1) Exact calculation; 2) approximate calculation. (After [5]).

Figure 9.2.4 gives the spatial distribution of the sound pressure for a plate with four beams. Of the four, beams -1, $+1$, $+2$ are located at $x/l = 0$, 1, 2 respectively. The plate is driven by f_0 at midpoint between beams -1 and $+1$. Curve 1 characterizes the radiation of sound by the plate in the case where the mechanical impedance of the beams is large ($\alpha = \delta = 10^4$). By definition,

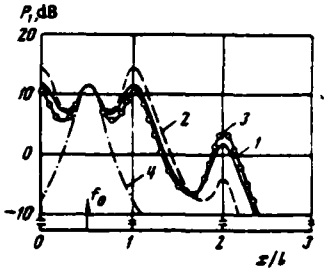

Fig. 9.2.4. Spatial distribution of the sound pressure for a plate with four beams. 1) Perfectly stiff beams; 2) perfectly stiff beams and an incompressible fluid; 3) freely supported beams; 4) plate without beams. (After [5]).

$$\alpha = \frac{iZ_F}{\left(\frac{D_0\kappa^3}{\omega}\right)}; \delta = \frac{iZ_M}{\left(\frac{D\kappa}{\omega}\right)}.$$

It is seen that even in this case sound is radiated at the junction of the second beam with the plate, i.e., vibrational energy caused by force f_0 is transmitted through the fluid and through the plate from the driven span to the next one. If the compressibility of the fluid is disregarded in the determination of the quantities $\tilde{w}(x_n)$ and $(\partial/\partial x)\tilde{w}(x_n)$ then energy is transmitted to the second beam only through the plate, and the sound pressure from the second beam is much

lower (curve 2). Correspondingly the energy that would have gone into the compressible medium reappears as an increase in the radiation at the junction of beam #1.

For the case in which the moment impedance of the beams is zero ($\alpha = 10^4$, $\delta = 0$) a large energy flux propagates through the plate, and the compressibility of the medium no longer has a significant influence on the sound pressure created by the second beam (curve 3).

Curve 4 in Fig. 9.2.4 describes the sound pressure for the plate without any reinforcing beams. It also follows from Fig. 9.2.4 that for the chosen beam and plate parameters the sound pressure in the driven span is determined in the vicinity of the beams bordering it by the radiation of sound from the beams, while opposite the driving point it is determined by the radiation of sound from the plate without beams. Outside the indicated span the radiation of sound is governed entirely by the presence of beams on the plate.

The curves in Fig. 9.2.5 describe the spatial distribution of the sound pressure for a plate with various numbers of beams and zero moment impedance ($\alpha = 10^4$, $\delta = 0$). Beams -1, $+1$, $+2$, $+3$, etc. are located at $x/l = 0$, 1, 2, 3, ... respectively. The plate is driven by a point-force f_0 at midpoint between beams -1 and $+1$.

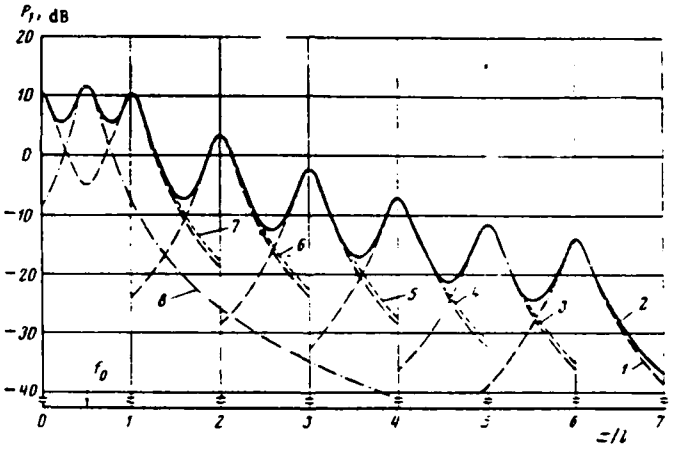

Fig. 9.2.5. Spatial distribution of the sound pressure for a plate with various numbers of freely supported beams, "Freely supported" signifies absence of moment coupling, i.e., $Z_M = 0$ 1). Radiation from individual beams; 2-7) total radiation from sets of 12, 10, 8, 6, 4, and 2 beams, respectively; 8 sound radiation from a plate without beams. (After [5]).

We see that increasing the number of beams on the plate does not alter the radiation from the previous beams, the directivity of the sound radiation is almost the same for all beams, and only the strength of the sources varies in the vicinity of the beams, depending on $\tilde{w}(x_n, 0)$.

It also follows from Fig. 9.2.5 that the absence of moment impedance of the beam causes the contribution of beams outside the driven span to the total radiation to become decisive. In

analyzing the problem for the case of excitation in a noise band the moment impedance of real beams can virtually always be neglected in the audible frequency range.

It is important to note that the foregoing conclusions refer to the case of a fairly large force impedance on the part of the beams ($\alpha = 10^4$); with a decrease in the force impedance the contribution of the beams to the total radiation will of course also diminish, until in the limit the situation goes over to a plate without reinforcing beams.

9.3 SOUND RADIATION BY AN INFINITE PERIODIC SLOTTED ARRAY [6]

An infinite periodic array of infinitely long rectangular parallelopipeds is located in an x,y,z coordinate system, Fig. 9.3.1. In each parallelepiped the surfaces $y = \pm h/2$ can undergo vibration and hence can radiate sound into half spaces $-\infty \leqslant y \leqslant +\infty$. The surfaces forming the slots (at $x = -d/2$, $x = +d/2$, etc.) are assumed rigid. A single radiating element is taken to be the array element (infinite rectangular surface) itself, of width $l - d$, plus the half slots $d/2$ on either side.

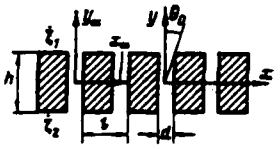

Fig. 9.3.1. Infinite periodic slotted array of rectangular elements.

Let $\dot{\xi}(x)$ be a particle velocity distribution forced across the upper half radiating face of one element and assume the radiation from the array is steered in direction θ_0. Then the normal component of surface velocity at the α element is taken to be,

$$\dot{\xi}_\alpha(x) = \dot{\xi}_0 \exp inl(k \sin\theta_0) e^{-i\omega t}, \quad n = 0, 1, 2, \ldots \tag{9.3.1}$$

in which $\dot{\xi}_0$ is the same for all elements. Each slot between element cross-sections is considered to be a waveguide with rigid walls. Its transverse eigenfunction is cosine $(m\pi x^*/d)$ (see Eq. (3.6.14)). Hence the slot's axial wavenumber is $k_m = \sqrt{k^2 - (m\pi/d)^2}$. The acoustic field inside one slot is then given by a sum of waveguide modes:

$$P_\alpha = \exp(i\alpha l(k \sin\theta_0)) \sum_{m=0}^{\infty} (A_m e^{ik_m y} + B_m e^{-ik_m y}) \cos\left[\frac{m\pi}{d}\left[x_\alpha - \frac{d}{2}\right]\right]. \tag{9.3.2}$$

Here $x^* = x_\alpha - \dfrac{d}{2}$. It is written in this way to insure that $\partial P_\alpha/\partial x = 0$ when $x_\alpha = \pm d/2$. The acoustic field in the medium can be obtained as the product of the field of one line source running along the z-coordinate direction and a second line source running along the x-direction. The field due to one parallelopiped (say $\alpha = 1$) depends on the excitation of volume velocity per unit of length, $\dot{\xi}(x)dx$ (units: $m^3s^{-1}m^{-1}$). For given velocity $\dot{\xi}$, at $y = h/2$ it is a cylindrical wave radiating into half space $y > 0$:

$$P = -2ik\rho c \int \dot{\xi}_1(x)\frac{i}{4} H_0^{(1)}(kR)dx\ ,\quad R = |\mathbf{r} - \mathbf{r}|. \tag{9.3.3a}$$

To determine R assume the ordinates of the source points and observation points have the simple form,

x - coordinate at the source point: $\alpha + x_\alpha$, $\alpha = 0, 1, 2\ldots$

x - coordinate at the observation point: $\alpha' l + x_\alpha$, $\alpha' = 0, 1, 2\ldots$ (9.3.3b)

These forms allow simple formulas for $\mathbf{r}_0$ and $\mathbf{r}$. The factor 2 appears here because all the radiation goes into half-space. The Hankel function $\frac{i}{4}H_0^{(1)}(kR)$ defines the Green's function for a line source in *full* space. Now the radiation in the *upper half-space* when each element has normal velocity $\dot{\xi}_1$ is the sum of the radiations from *all* the upper vibrating surfaces and 1/2 of the radiation from *all* the slots:

$$\begin{aligned} P_1(R) = \frac{k\rho c}{2} \sum_{\alpha=-\infty}^{\infty} e^{i\alpha l(k\sin\vartheta_0)} \int_{-d/2}^{l-d} \dot{\xi}_1(x_\alpha)\, H_0^{(1)}(kR)dx_\alpha \\ + \frac{1}{2} \sum_{\alpha=-\infty}^{\infty} e^{i\alpha l(k\sin\vartheta_0)} \sum_{m=0}^{\infty} k_m (A_m e^{ik_m h/2} - B_m e^{-ik_m h/2}) \\ \times \int_{-d/2}^{d/2} H_0^{(1)}(kR) \cos\left[\frac{\pi m}{2}\left(\frac{2x_\alpha}{d} - 1\right)\right] dx_\alpha. \end{aligned} \tag{9.3.4}$$

(Note that the subscript 1 refers quantities to the upper half space).

A similar set of equations can be formed for the acoustic pressure field P_2 in the lower half-space.

Since $\dot{\xi}_{1,2}$ are assumed known one can determine the modal coefficients A_m, B_m by invoking the boundary conditions:

$$\begin{aligned} &\text{at } y = h/2\text{: } P_\alpha = P_1 \\ &\text{at } y = -h/2\text{: } P_\alpha = P_2 \end{aligned} \tag{9.3.5}$$

in which $P_{1,2}$ are acoustic pressures due to *all* the radiating parallelopipeds and α is an integer designating the α th slot.

The first term in (9.3.4) contains a summation on α that is, a summation over the parallelopipeds and slots, while the second term has two summations, one on α and the second on the modal numbers m in one slot. If left and right side boundary conditions (9.3.5) are multiplied by $\cos\left[\frac{\pi m'}{2}\left(\frac{2x_{\alpha'}}{d} - 1\right)\right]$, and if $H_0'(kR)$ is expanded in plane waves containing variable $x_{\alpha'}$, and if the integration over x_α is performed, then one obtains an infinite system of algebraic equations in unknown A_m, B_m in terms of (1) integers m, m', α, α'. (2) geometric sizes, h, d, l, and (3) wave parameters λ, k, k_m (see [6]). Because the velocity $\dot{\xi}_{1,2}$ are finite the modal coefficients A_m, B_m, decrease in magnitude as m increases. Thus the infinite system can be solved for A_m, B_m by truncation.

Once A_m, B_m are determined for all m for a given value of $\dot{\xi}_{1,2}$ the far field may be obtained directly from (9.3.4) by use of the approximation,

$$H_0^{(1)}(R) \approx \frac{1}{\sqrt{2\pi kR}} \exp(ikR - i\pi/4) \exp(-ikx \sin\theta) \tag{9.3.6}$$

in which θ is the polar angle. Choosing a *unit cell* to consist of one vibrating surface plus a left and right half slot one evaluates (9.3.4) with the approximation (9.3.6) to obtain the far field pressure in the upper half-space due to a *unit cell*:

$$P_1(\theta)\Big|_{\alpha=0} = P_s(\theta) + P_{el}(\theta) \tag{9.3.7}$$

(see [6]). $P_s(\theta)$, $P_{el}(\theta)$ are the acoustic fields due to the slot and the elementary radiating surface respectively. The calculation is much simplified if $\dot{\xi}_{1,2}$ are assumed constant, and if the steering angle θ_0 is zero. A case of particular importance is $\dot{\xi}_2 = 0, \dot{\xi}_1 = 1$. Figure 9.3.2 shows a plot of far field pressure of a *unit cell* in the upper half plane at polar angle $\theta = 0$ versus slot height (normalized to wavelength) with parallelopiped width as a parameter. The entire array is assumed present. The field is seen to decrease drastically when the slot height is near an integral multiple of a half wavelength.

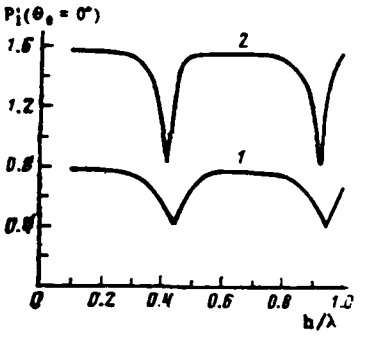

Fig. 9.3.2. Far-field pressure generated by one unit cell in the direction $\theta = \theta_0 = 0$ versus slot height. 1) $(l - d)/\lambda = 0.25$, $l/\lambda = 0.3$; 2) $(l - d)/\lambda = 0.5$, $l/\lambda = 0.55$. (After [6]).

The radiation field of a unit cell at the backside of the array in relative units of $P_2(180°)/P(0°)$ is plotted in Fig. 9.3.3 versus h/l with $(l - d)/\lambda = 0.1$. This is the radiation due to two half-slots because $\dot{\xi}_2$ is zero. An explicit formula for $P_2(\theta)$ is given by [6]. Again, when h/λ is near an integral number of half wavelengths the radiation to the rear of the array in direction $\theta = 180°$ is equal in magnitude to the radiation in direction $\theta = 0$. However, this conclusion is based on the choice $\left(\frac{l - d}{\lambda}\right) = 0.1$. For the choices $(l - d)/\lambda = 0.25, 0.50$ the peak of back radiation occurs at differing values of h/λ depending on l/λ. This is shown in Fig. 9.3.4.

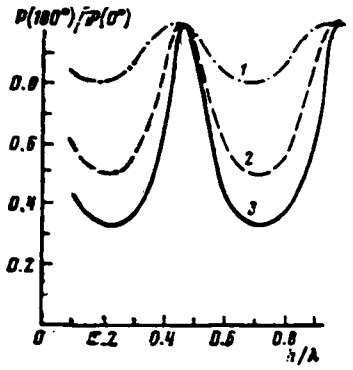

Fig. 9.3.3. Relative value of back-radiation level of element with $(l - d)/\lambda = 0.1$ versus slot height. 1) $l/\lambda = 0.5$; 2) $l/\lambda = 0.2$; 3) $l/\lambda = 0.15$. (After [6]).

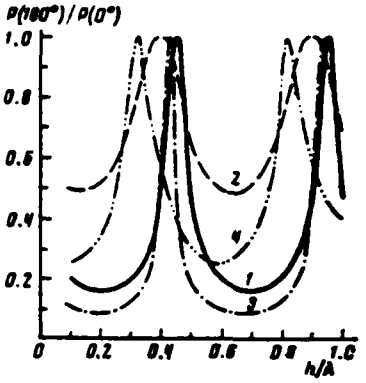

Fig. 9.3.4. Relative value of back-radiation level versus slot height for elements with $(l - \phi/\lambda = 0.25$ and: 1) $l/\lambda = 0.3$; 2) $l/\lambda = 0.5$, and with $c - d)/\lambda = 0.5$ and: 3) $l/\lambda = 0.55$; 4) $l/\lambda = 0.7$. (After [6]).

Besides the radiation field one is also interested in finding the radiation impedance of a unit cell in the presence of the entire array. To do this one returns to 9.3.4 and replaces the Hankel function by plane wave expansion,

$$H_0^{(1)}(kR) = \frac{1}{\pi}\int_{-\infty}^{\infty} e^{ik[l(\alpha'-\alpha)+x'_\alpha - x_\alpha]\beta}\,\frac{d\beta}{\sqrt{1-\beta^2}} \tag{9.3.8}$$

where

$$R = |\mathbf{r} - \mathbf{r}_0| = (l\alpha' + x'_0) - (l\alpha + x_\alpha)$$

multiplying both sides of 9.3.4 (thus modified) by

$$\exp - ik\alpha' l\beta_0,\ \beta_0 = \sin\theta_0$$

and using Poisson's Sum Formula (see 6.7.32)

$$\sum_{\alpha=-\infty}^{\infty} e^{ikl\beta_0(\alpha-\alpha')}e^{-ikl\beta(\alpha-\alpha')} = 2\pi\sum_{s=-\infty}^{\infty}\delta(kl(\beta-\beta_0) - 2\pi s) \tag{9.3.9}$$

one integrates term by term to find the total pressure on one parallelopiped surface:

$$\begin{aligned} p'(x_{\alpha'}) = {} & \frac{k\rho c}{2\pi}\xi_0\frac{\lambda}{l}\sum_{s=-\infty}^{\infty}\int_{d/2}^{l-d/2}\frac{e^{ik(x_{\alpha'}-x_\alpha)\beta}}{\sqrt{1-\beta_s^2}}\,dx_\alpha \\ & + \frac{1}{2\pi}\sum_{m=-0}^{\infty} k_m(A_m e^{ik_m h/2} - B_m e^{-ik_m h/2})\,\frac{\lambda}{l} \\ & \times\sum_{s=-\infty}^{\infty}\int_{-d/2}^{d/2}\frac{e^{ik(x_\alpha - x_\alpha)\beta_s}}{\sqrt{1-\beta_s^2}}\cos\left[\frac{\pi m}{2}\left[\frac{2x_\alpha}{d} - 1\right]\right]dx_\alpha. \end{aligned} \tag{9.3.10}$$

Here $\beta_s = \beta_0 + (2\pi s/kl) = \beta + s(\lambda/l)$.

A subsidiary integration of $P'(x_{\alpha'})$ over $x_{\alpha'}$ of one parallelopiped gives the real and imaginary parts of the complex radiation price per unit length in units of Nm^{-1} on it (see [6] for explicit forces). The radiation impedance of one parallelopiped per unit length (along x) normalized to $\rho c(l-d)$ is then,

$$Z_{\text{rad}} = \frac{F_{\alpha'}}{\dot{\xi}_0} = R_s - iX_s = \frac{rs}{\rho c(l-d)} - i\frac{x_s}{\rho c(l-d)} \quad \text{(units: } Nsm^{-2}\text{)} \qquad (9.3.11)$$

in which rs, x_s are specific acoustic impedances per unit length (along x).

Figure 9.3.5 shows a plot of R_s, X_s versus steering angle θ_0 for $(l-d)/\lambda = 0.3, 0.5$; $l/\lambda = 0.4, 0.7$. and various values of h/λ. Curves 1,2 shows sudden jumps at $\theta_0 = 25°$, attributable to the instability of the directivity pattern of an infinite array at that angle.

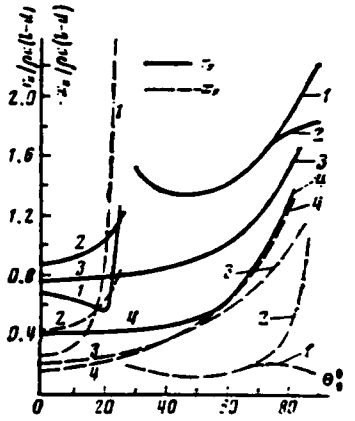

Fig. 9.3.5. Active component r_s and passive component x_s of the radiation impedance versus steering angle for element with $(l-d)/\lambda = 0.5$; $l/\lambda = 0.7$, and: 1) $h/\lambda = 0.2$; 2) $h/\lambda = 0.49$, and with $(l-d)/\lambda = 0.3$, $l/\lambda = 0.4$, and: 3) $h/\lambda = 0.1$; 4) $h/\lambda = 0.4$. (After [6]).

Figure 9.3.6 is a plot of normalized radiation impedance per unit of length along x vs slot height $(=h/r)$. Figure 9.3.7 is a plot of radiation impedance of one element versus spacing length $(=l/\lambda)$.

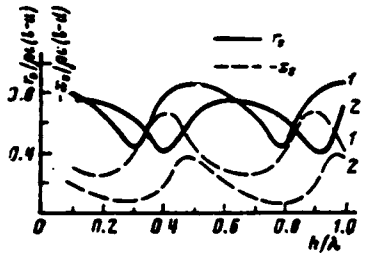

Fig. 9.3.6. Active component r_s and passive component x_s of the radiation impedance versus slot height. 1) $(l-d)/\lambda = 0.5$, $l/\lambda = 0.7$; 2) $(l-d)/\lambda = 0.3$, $l/\lambda = 0.4$. (After [6]).

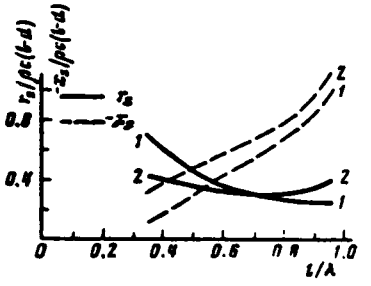

Fig. 9.3.7. Active component r_s and passive component x_s of the radiation impedance versus spacing l/λ of elements for element with $(l-d)/\lambda = 0.25$. 1) $h/l = 0.2$; 2) $h/l = 0.45$. (After [6]).

9.4 RADIATION IMPEDANCE OF A CYLINDER OF FINITE HEIGHT [7]

The acoustic potential field radiated by a cylinder of finite height does not conform to any system of coordinates in which the Helmholtz equation is separable. Thus the integral equation of linear acoustics, Eq. 1.10.1, must be solved numerically. Section 1.10 gives a discussion of this problem. An example of a structure on which such calculations can be made is shown in Fig. 9.4.1. Here the radiating surface is divided into N bands (6 of which are shown, consisting of $n_1 = 3$ on the ends, and $n_2 = 3$ on the sides) above the plane of symmetry defined by $z = 0$ and N bands below. The radiation is taken to be axisymmetric. The distribution of surface velocity in the direction z may be asymmetric.

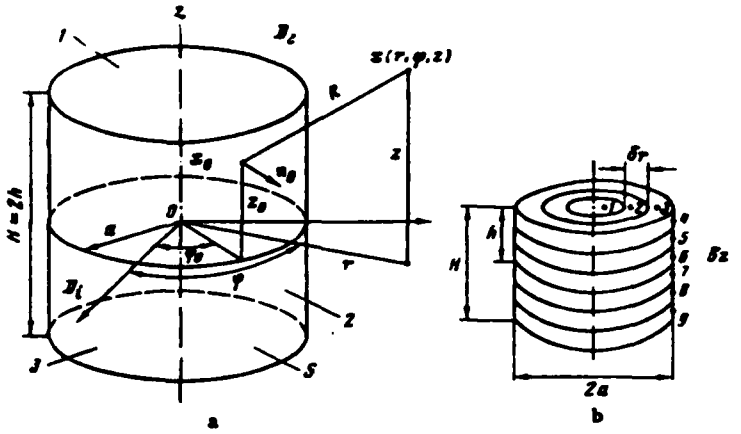

Fig. 9.4.1. a) Geometry of the radiator; b) method of partition of the cylinder surface into elementary rings and bands: total number of partition elements in the figure $2N = 12$; number of rings at each end $n_1 = 3$; number of bands on half the lateral surface $n_2 = 3$; $N = n_1 + n_2 = 6$. (After [7]).

Let the location vector of any point on the surface be $\mathbf{x}_0$ as measured from the origin. Then for a given (normal component) of surface velocity the velocity potential $\psi(\mathbf{x})$ anywhere on the surface $r = a$, ($\mathbf{r} = (x,y)$) is governed by the formula,

$$2\pi\psi(\mathbf{x}) - \mathscr{P}\int \psi(\mathbf{x}_0)\frac{\partial G}{\partial n_0}(\mathbf{x}|\mathbf{x}_0)dS(\mathbf{x}_0) = -\int G(\mathbf{x}|\mathbf{x}_0)v_n(\mathbf{x}_0)dS(\mathbf{x}_0) \qquad (9.4.1)$$

In this integral equation,

$$G(\mathbf{x}|\mathbf{x}_0) = \exp ikR/R, \quad R = |\mathbf{x} - x_0|$$

the positive normal points *into* the surface, and $\mathscr{P}$ means "principal part."

Label each band by a number (call it a node) assigned to its midband, and assume the velocity potential and velocity are constant over the area of each band, with freedom to differ from band to band. Equation (9.4.1) then reduces to a matrix equation in unknown $\psi_n(\mathbf{x})$, $n = 1, 2, \ldots N$:

$$\text{(a)}\quad [\mathcal{P}'_{nm} - H_{nm}]\,[\psi_m] = [f_n]$$

$$\text{(b)}\quad [f_n] = [V_{nm}]\,[v_m]. \tag{9.4.2}$$

The $N \times N$ matrices $[H_{nm}]$, $[V_{nm}]$ are easily deduced from 1.10.7c and 1.10.7d. In numerical calculation the diagonal elements of these matrices are seen to contain logarithmic singularity at nodal points $\mathbf{x} = \mathbf{x}_0$. To avoid these one employs the operation of taking "principal part" (= operation $\mathcal{P}$ of Eq. 9.4.1). One way of doing this is to enclose each nodal point with a 3-D ellipse and exclude the volume of this ellipse from the calculation.

Computation for each value of $ka \left(= \dfrac{2\pi a}{\lambda}\right)$ may be conducted as follows

1. the integration over area required by matrix elements in 9.4.1, 9.4.2 is accomplished by dividing each band into $l \times l_1$, cells, in which l_1 is the number ($\leqslant 6$) of divisions in circumference and l, is the number (2 to 6) of divisions in height. In one particular case for $N = n_1 + n_2 = 20$ bands the number of cells was $l \times l = 6 \times 6 = 36$ for each band.

2. In integrals requiring evaluation of principal parts an ellipse is chosen for avoidance of logarithmic singularities. Reference [7] chose ellipse with semiaxes $e_r = 0.005a$, $e_\phi = 0.005\pi$, $e_z = 0.0025$ to $0.0050h$.

3. The acoustic pressure on each band $p(x_0)$, mechanical radiation impedance, $Z_n(\omega)$ on each band, and the mutual mechanical impedance Z_{lm} between the l th and m'th band are determined from the solutions $\psi_n(\mathbf{x})$:

$$\text{(a)}\quad p_\omega(\mathbf{x}) = -\,i\omega\rho\,\psi_n(\mathbf{x})$$

$$\text{(b)}\quad Z_n(\omega) = \frac{1}{|V_0|^2}\iint_S p_n(\mathbf{x}_0,\omega)\,v_n^*(\mathbf{x}_0,\omega)\,dS(\mathbf{x}_0) \tag{9.4.3}$$

$$\text{(c)}\quad Z_{lm} = \frac{1}{V_l V_m^*}\iint p_l(\mathbf{x}_0,\omega)\,v_m^*(\mathbf{x}_0,\omega)\,dS(\mathbf{x}_0)$$

in which V_0 is a reference velocity, and V_m, V_l, p_m, V_n are rms magnitudes. For convenience the impedances are normalized by dividing Z by $\rho c S_{ra}$ where S_{ra} is the part of the band area included in the operation of taking principal parts. The radiation resistance α and reactance β are then,

$$\alpha_n - i\beta_n = \frac{Z_n}{\rho c S_{ra}}.$$

Several cases of theoretical and practical significance in which the radiation impedance of short cylinders has been numerically evaluated are now presented.

Case I. A short cylinder whose ratio of half-height h to radius a is 0.2588, is excited on its sides by a velocity $v = 1$ and on its ends by a velocity $v = 0$. Choosing N advantageously, to be $\leqslant 20$, and following the choices of l, l_1 and ellipse size noted in steps (2) and (3) above, ref. [7] calculated α, β for values of $ka\,(-2\pi a/\lambda = \omega/c)$, ranging from 0.2 t o 10.0. The result is shown in the full lines labelled 1,1 of Fig. 9.4.2. For $ka > 5.0$ the cylinder radiates very much like a flat piston. For comparison purposes these results are placed side by side with those of a

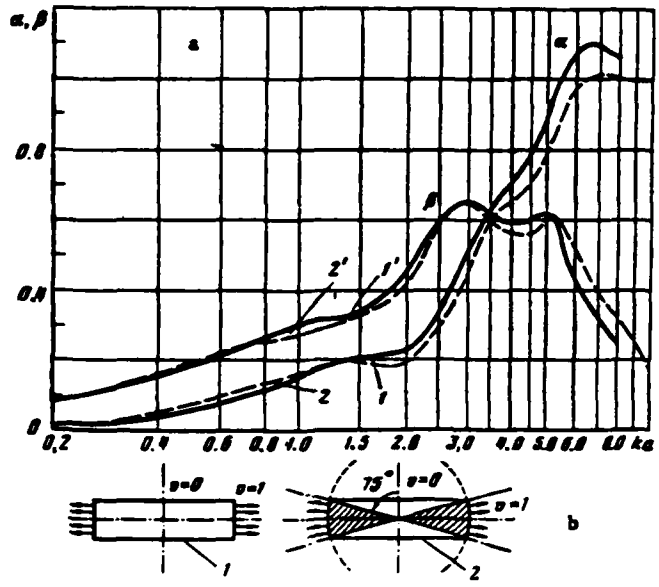

Fig. 9.4.2. a) Coefficients α and β of the radiation impedance of a cylinder with rigid ends, $h/a = 0.2588$ (curves 1 and 1') and of a spherical band with rigid funnel-shaped ends, $h/a = 0.2588$ (curves 1 and 2'); b) diagrams of the corresponding models. (After [7]).

different model, namely that of a spherical band of the same height and radius whose radiation is calculated by use of spherical harmonics. The two models agree well for $ka < 5.0$, but diverge beyond this value.

Case II. A cylinder with ratio of half height to radius (h/a) of 0.5 is excited by a velocity $v = 1$ on its sides Fig. 9.4.3. Three types of ends are modeled and the normalized mechanical radiation impedance is calculated versus ka as a parameter. In type 1 the cylinder is extended on either end by semi-infinite rigid baffles. The numerical values of α, β are plotted as line 1. In type 2 the cylinder is capped by rigid ends. The impedances are shown as line 2. In type 3 the cylinder is capped by compliant ends. Its radiation impedance are shown in line 3. From these results it is seen that types 1 and 2 are nearly identical for $ka < 1.0$ because the wavelengths are then very large and the baffles are acoustically small. In contrast, the introduction of compliant ends effectively cancels the volume velocity at low frequencies, hence effectively reduces the radiation resistance to low levels. However, above $ka = 2.0$ the radiation resistance becomes nearly independent of the existence of compliance at the ends while the radiation reactance still shows compliance effects up to values of $ka = 5.0$.

Case III. The radiation impedance of cylinders of various heights with rigid ends is shown in Fig. 9.4.4. Here it is seen that the radiation resistance is proportional to the relative height h/a of the cylinder in the intervals $kakh < 1$ and $0.2 \leqslant ka \leqslant 5$.

Case IV. Lateral and end surfaces of cylinders with various distributions of velocity exhibit mutual radiation impedance. Figure 9.4.5 shows values of mutual reactance α and mutual resistance β for relative heights h/a ranging from 0.2 to infinity.

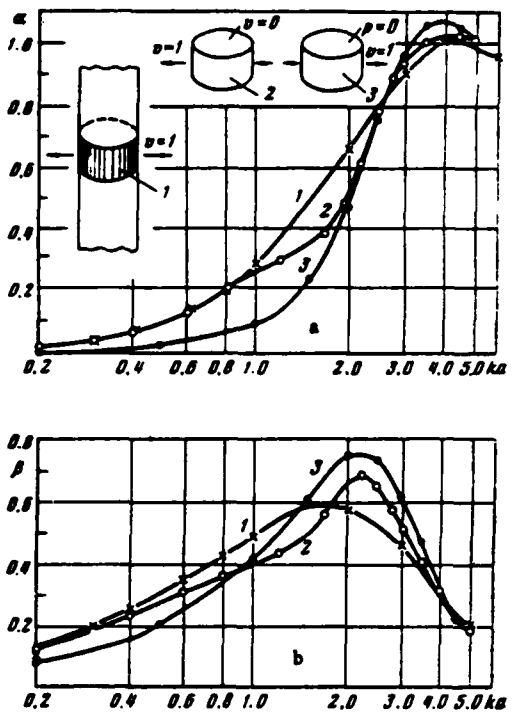

Fig. 9.4.3. Comparison of the radiation impedances for three models of a cylindrical radiator, $h/a = 0.5$. 1) Model of cylinder in semiinfinite baffles; 2) with rigid ends; 3) with compliant ends. (After [7]).

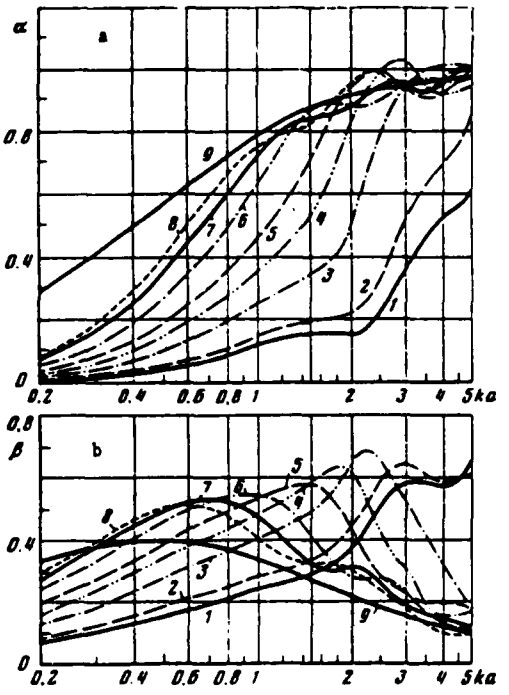

Fig. 9.4.4. Coefficients α (a) and β (b) of radiation impedance for cylinders of various heights with rigid ends. 1) $h/a = 0.2$; 2) 0.2588; 3) 0.5; 4) 0.75; 5) 1.0; 6) 1.5; 7) 2.0; 8) 2.5; 9) ∞. (After [7]).

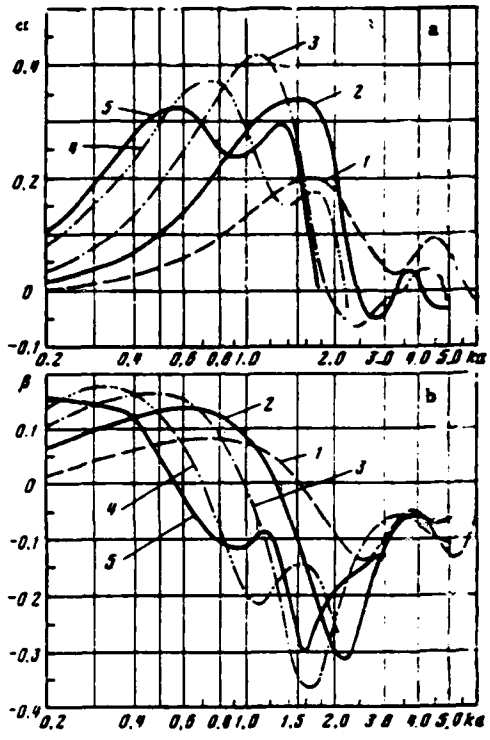

Fig. 9.4.5. Mutual radiation impedance between the lateral and end surfaces of a cylinder with a uniform velocity distribution on both surfaces. 1) $h/a = 0.2$; 2) 0.5; 3) 1.0; 4) 2.0; 5) 3.0. (After [7]).

9.5 RADIATION FIELD AND RADIATION RESISTANCE OF A FINITE CYLINDRICAL SHELL IN A RIGID BAFFLE

A thin elastic shell, radius a, length l is terminated at its ends by semi-infinite rigid baffles, Fig. 9.5.1. Let the shell be simply supported and write the radial displacements as an infinite sum of longitudinal and circumferential Fourier modes,

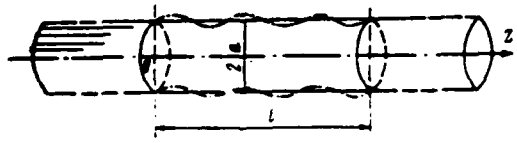

Fig. 9.5.1. Finite cylindrical shell in a baffle.

$$\xi(a, \phi, z, t) = \sum_{p=0}^{\infty} \sum_{q=1}^{\infty} \xi_{pq} \cos p\phi \sin \frac{q\pi z}{l} e^{-i\omega t}. \tag{9.5.1}$$

The pressure field radiated by such a distribution of displacement is the factored solution of the Helmholtz equation for $z = 0$ (=2-D solution) extended into the $z = 0$ domain (=3-D solution) (see Eq. 3.7.46),

$$P(r,\phi,z) = \sum_n A_n \cos n\phi \int_{-\infty}^{\infty} H_n^{(1)}[r\sqrt{k^2 - k_z^2}]\, e^{ik_z z}\, \frac{dk_z}{2\pi}. \tag{9.5.2}$$

At the surface $r = a$,

$$\text{(a)} \quad \left.\frac{\partial P}{\partial r}\right|_{r=a} = -i\omega\rho\dot{\xi} \tag{9.5.3a}$$

or,

$$\text{(b)} \quad \sum_{n=0}^{\infty} A_n \cos n\phi \int_{-\infty}^{\infty} f_n(a,k_z) e^{ik_z z} \frac{dk_z}{2\pi} = -\omega_\rho^2 \sum_{p=0}^{\infty}\sum_{q=1}^{\infty} \xi_{pq} \cos p\phi \sin\frac{q\pi z}{l} \tag{9.5.3b}$$

$$f_n(a, k_z) = H_n^{(1)'}(a\sqrt{k^2 - k_z^2})\sqrt{k^2 - k_z^2}$$

Here, $H_n^{(1)'}(ab) \equiv [dH_n^{(1)}(rb)/drb]_{r=a}$.

Because of the orthogonality of the cosines one sets $p = n$. Since the integral on the left-hand-side is a Fourier transformation one can recover the integrand by taking the inverse Fourier transformation. Multiplying both sides by $e^{-ik_z z}$ and integrating over the range $-\infty < z < \infty$ (= $0 < z < l$) it is seen that,

$$A_n f_n(a,k_z) = -\omega^2\rho \sum_{q=1}^{\infty} \xi_{nq}\, Z_q^*(k_z) \tag{9.5.4a}$$

$$Z_q^*(k_z) = \int_0^l \sin\left(\frac{q\pi z}{l}\right) e^{-ik_z z} dz. \tag{9.5.4b}$$

Solving (9.5.4) for A_n and substituting it into (9.5.2) lead to an explicit form of the field in terms of the surface displacements,

$$P(r,\phi,z) = \sum_n \cos n\phi \int_{-\infty}^{\infty} \frac{(-\omega^2\rho)\sum_{q=1}^{\infty} \xi_{nq} Z_q^*(k_{z)} H_n^{(1)}(r\sqrt{k^2 - k_z^2})\, e^{ik_z z}}{H_n^{(1)'}(a\sqrt{k^2 - k_z^2})\sqrt{k^2 - k_z^2}} \frac{dk_z}{2\pi}. \tag{9.5.5}$$

Now from the discussion in Section 4.2 we may describe the field at the surface $r = a$ as a sum of modes,

$$P(a,\phi,z) = \sum_s \sum_{s,m} P_{sm}(a,\phi,z)\, e^{-i\omega t}. \tag{9.5.6}$$

The symbol s refers to the ϕ-coordinate while m refers to the axial coordinate. Because of the symmetry and periodicity of the ϕ coordinate we identify s of 9.5.6 with the n of 9.5.5. However the q and m of these equations are different: each mode which describes P is coupled to *all* the modes which describe ξ,

$$P_{nm} = -i\omega \sum_{q=1}^{\infty} \xi_{nq}\, Z_{nm,nq} \tag{9.5.7}$$

The first set of subscripts (nm of $Z_{nm,nq}$ describes the pressure modes, while the second set (nq) describes the displacement modes. To find $Z_{nm,nq}$ one first expands (9.5.6) in the same eigenfunctions as were used in (9.5.1) and then uses their orthogonality to obtain,

$$P_{nm}(a,\phi,z) = \frac{\iint P(a,\phi,z) \cos n\phi \sin\left(\frac{m\pi z}{l}\right) a\,d\phi\,dz}{\frac{a\pi l}{2}}. \tag{9.5.8}$$

Multiplying both sides of (9.5.5) by $\cos n\phi \sin(m\pi z/l)$ and integrating over area $dS = a\,d\phi\,dz$ one obtains by use of orthogonality of the eigenfunctions, and (9.5.7), (9.5.8), the explicit formula,

$$Z_{nm,nq} = \frac{-i\omega\rho}{\pi l} \int_{-\infty}^{\infty} \frac{Z_m(k_z) Z_z^*(k_z) H_n^{(1)}(a\sqrt{k^2 - k_z^2})}{\sqrt{k^2 - k_z^2}\, H_n^{(1)'}(a\sqrt{k^2 - k_z^2})}\, dk_z \tag{9.5.9}$$

The units of $Z_{nm,nq}$ are those of specific acoustic impedance (Nsm^{-3}). In normalized form,

$$Z_{nm,nq} = \rho c \sigma_{nm,nq} - i\omega M \gamma_{nm,nq}$$

M = mass per unit area of the shell (units: Ns^2/m^3)

$\sigma_{nm,nq} \equiv$ modal efficiency

$\gamma_{nm,nq} \equiv$ additional—mass coefficient. (9.5.10)

The calculation of (9.5.9) is very troublesome when $m \neq q$ that is, when there is coupling between all acoustic modes in the water with each displacement mode in the cylindrical shell. It is useful therefore to find conditions which permit one to set $m = q$ and thus calculate only the "proper impedance", $Z_{nm,nm}$. These conditions can be best understood in terms of the following discussion of plate and shell theory. First we define key parameters.

(1) f_r is the ring frequency of the circular cylindrical shell, or the frequency at which the longitudinal wavelength λ_l in the shell material is equal to the shell circumference,

$$\lambda_l = 2\pi a, \text{ or } f_r = \frac{C_l}{2\pi a} \tag{9.5.11}$$

where C_l is the speed of longitudinal stress waves in the shell.

(2) f_c is the critical frequency, or the frequency at which the flexural speed in the equivalent plate is equal to the speed of sound in the surrounding material. The *equivalent plate* by definition is one which has the same size as the cylindrical shell "rolled out," same thickness and mass density, same Young's modulus and Poisson's ratio, but whose acoustical coupling between vibration "cells" is determined by cylindrical geometry, and whose circumferential modes are symmetrical.

(3) f_l is the frequency at which the sound wavelength in the medium is equal to the length l of the shell between supports, $f_l = c_0/l$.

(4) c_0 is the speed of sound in the medium.

c_b is the bending wave speed in the shell.

c_x, c_y are phase speeds in the equivalent flat plate along the plate edges.

With these definitions in mind one can classify and define the various modes of radiation:

Classification of Modes of the Equivalent Plate

Acoustically fast modes are defined by the condition $c_b \geqslant c_0$, $\sigma_{\text{fast}} \simeq 1$
Acoustically slow modes are defined by the condition $c_b < c_0$

(i) strip-modes:

x-strip, $c_y < c_0$ and $c_x > c_0$ $\sigma_s \ll 1$

y-strip, $c_x < c_0$ and $c_y > c_0$ $\sigma_s \ll 1$

(ii) piston modes

c_x and $c_y < c_0$ $\sigma_p \ll \sigma_s$

Here the symbol σ is the *radiation efficiency* of the entire panel. It is defined as the ratio of plate of radiation resistance to $\rho c A_p$:

$$\sigma = \frac{1}{\mathcal{Q}_{\text{RAD}}} \frac{\omega m_s}{\rho_0 c_0} = \frac{R_{\text{RAD}}}{\rho_0 c_0 A_p} \tag{9.5.12a}$$

$$\mathcal{Q}_{\text{RAD}} = \frac{\omega M}{R_{\text{RAD}}}; \quad m_s A_p = M$$

in which m_s is the mass per unit area of the panel, M is the total mass and $\rho_0 c_0$ is the characteristic impedance of the medium. In the equivalent flat plate which is excited to contain n_i, $i = 1, 2..$ resonant modes in a specified frequency band the efficiency σ is the simple average of the modal efficiencies,

$$\bar{\sigma} = \sum_i \frac{\sigma_i}{n_i}. \tag{9.5.12b}$$

Now an approximate formula for the resonance frequencies of a finite circular cylindrical shell having Poisson's ratio μ and longitudinal wave speed c_l has been derived by Heckl [8] for the case of simple support at its edges:

$$\text{(a)} \quad \nu^2 = \frac{(1-\mu^2)\left(\frac{m\pi a}{l}\right)^4}{\left[\left(\frac{m\pi a}{l}\right)^2 + n^2\right]^2} + \left\{\left[\left(\frac{m\pi a}{l}\right)^2 + n^2\right]^2 - A\right\} \frac{h^2}{12a^2}$$

$$\text{(b)} \quad \nu = \frac{\omega a}{c_l}; \quad c_l = \sqrt{\frac{E}{\rho h(1-\mu^2)}}; \quad A = \frac{1}{2}\left[n^2(4-\mu) - 2 - \mu\right]/(1-\mu^2) \tag{9.5.13}$$

$m = 1, 2, 3, \ldots$; $n = 0, 1, 2 \ldots$ = one half of the number of nodes in the complete circumference ($= 2\pi a$)

It is to be noted that in (9.5.13b the quantity ρh in this context is the mass per unit volume (units: Ns^2/m^4). The symbol m refers to axial modes and n refers to circumferential modes. In many cases of interest factor A can be neglected. The error involved is significant only when the second term in (9.5.13a) is nearly zero. But the frequencies for which this is true cover only a narrow range [8]. Neglecting A one can reduce (9.5.13a) to a form which makes use of the resonant frequencies of a thin, simply supported rectangular flat plate of sides a, b and thickness h:

$$f = \frac{1}{2\pi}\sqrt{\frac{D}{\rho h}}\left\{\left[\frac{m\pi}{a}\right]^2 + \left[\frac{n\pi}{b}\right]^2\right\}, \quad \mathrm{m} = 1, 2, 3 \ldots = n$$

$$D = \frac{Eh^3}{12(1-\mu^2)}. \tag{9.5.14}$$

Since

$$\nu = \frac{2\pi fa}{c_l} = \frac{f}{f_r}; \quad f_r = \text{ring frequency} = \frac{c_l}{2\pi a}$$

it is seen that the resonant frequencies (scaled to f_r) are given by

$$\nu^2 = \beta^2(ka)^4 + (1-\mu^2)\,(k_y/k_p)^4 \tag{9.5.15}$$

where

$$\beta^2 = h^2/12a^2$$

$$k_p^2 = (k_x^2 + k_y^2)$$

$$k_x^2 = \left[\frac{n}{a}\right]^2; \; k_y^2 = \left[\frac{m\pi}{l}\right]^2.$$

Here again (in the equivalent flat plate) $m = 1, 2, \ldots$. However n has a different meaning; it is one half of the nodes of displacement in the circumferential direction. The formula $\nu^2 = \beta^2(ka)^2$ lists the resonant frequencies of the equivalent flat plate while the total formula (9.5.15) describes (approximately) the resonant frequencies of a thin cylindrical shell. Evidently the second term shows the effects of shell curvature.

A first effect of shell curvature is to modify the loci of radiating modes in k-space, in comparison with the same modes in the equivalent flat plate. Flat plate loci are discussed in Section 4.2d. There it was seen that loci of constant k_p (that is, of constant frequency for a specific plate) are quarter circles. When applied to cylinders these equivalent plate loci correspond to the first term of (9.5.15). They are shown in Fig. 9.5.2 as two sets: one set for $\nu < 1$, that is $f < f_r$ (resonance frequency less than the ring frequency), and the second set for $\nu > 1$, that is $f > f_r$. The only modes that radiate when the cylinder is modeled as an equivalent plate are the circumferential-strip modes. These are the modes characterized by $m = 0, 1, 2 \ldots$ circumferential nodes of radial displacement. A discussion of strip-modes is made in Section 4.2d.

When cylinder radiation is modeled to include curvature effects both terms in (9.5.15) are used. The loci of radiating modes in k-space for this model are shown in Fig. 9.5.3. It is

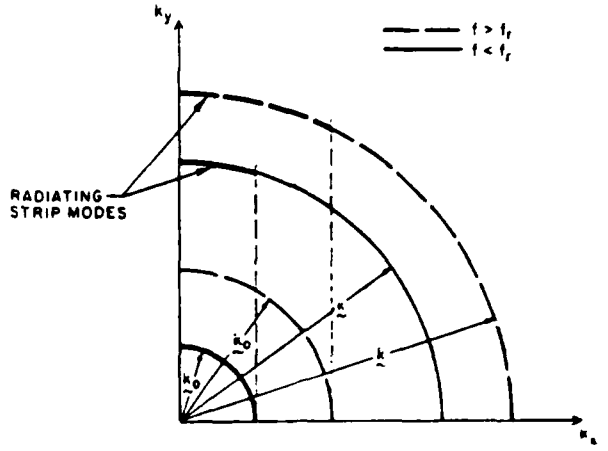

Fig. 9.5.2. Loci of radiating circumferential-strip modes of the "equivalent Plate" in k space for a given frequency. (After [9]).

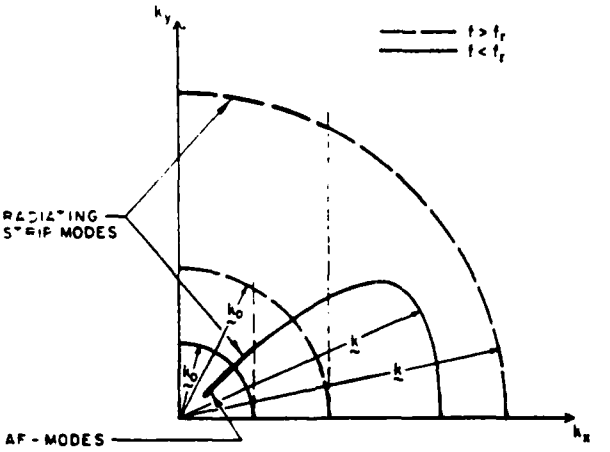

Fig. 9.5.3. Loci of radiating modes of a cylinder in k space for a given frequency. (After [9]).

immediately seen that when the resonance frequency is above the ring frequency only circumferential strip modes radiate. The flat plate model is then adequate. However, when the resonance frequency is below the ring frequency the curves of constant k_p bend inward rapidly toward the origin as the circumferential wavelength increase (that is as k_x decreases) [9]. Again one sees radiating strip modes for the condition $ak_x \leqslant (c_L/c_a)\nu$, (9.5.16). However,

when $k_x \leqslant k_0$ and $k_y < k_0$ a number of acoustically fast modes ($c_b \geqslant c_0$) appear. Qualitatively they satisfy the relation,

$$ak_x \leqslant \left(\frac{c_l}{c_a}\right) \nu \operatorname{Re}\left[\left\{(1-\mu^2)^{1/2} - \nu\left[1 - \left(\frac{\nu}{\nu_a}\right)^2\right]^{1/2}\right\}^{1/2}\right]. \tag{9.5.17}$$

The cylinder radiates efficiently in these modes even though the circumferential wavelengths are long.

The radiation efficiency of a cylinder vibrating in modes may be calculated by use of (9.5.12), that is by calculating the radiation resistance in each mode. A discussion of modal radiation resistance in the case of flat plates is found in Section 4.2d. When cylinder curvature effects are pronounced the k-space plots of Figs. 9.5.2, 9.5.3 must be used to find k_x, k_y for each mode at a fixed drive frequency. From these one may again calculate radiation resistance, hence calculate radiation efficency. Such calculations have been made by Manning and Maidanik [9]. Since a major interest centers on determining at which frequency a given mode becomes acoustically fast (that is, a good radiator) they introduced a parameter $\nu_g = f_g/f_r$ where f_g is the critical frequency (that is the frequency at which the phase speed of the bending wave in the cylinder shell equals the speed of sound in the medium). The larger ν_g is, the smaller is the effect of curvature near the critical frequency. Figures 9.5.4 and 9.5.5 show this effect. They are plots of $k_x a$ vs $\nu = (f/f_r)$ for various axial wavenumbers m. We discuss Fig. 9.5.4 first. It is read as follows. For a given cylinder radius ($=a$) and a given shell material (that is given c_l) the ring frequency fr is a fixed number. Hence the abscissa is essentially the (scaled) drive-frequency. Thus, for any choice of circumferential mode number $n = k_x a$ and any axial mode number $m = k_y l_2/\pi$ (l_2 is the length between axial nodes of bending) the shell resonant frequency f may be found. *The mode itself is labelled nm.* The full lines are loci of the resonant frequencies of the cylinder modes when curvature is included and the dashed lines are the same loci for the flat plate model. For example when $n = 4$ and $m = 3$, the (scaled) resonant frequency is $\nu \sim 0.7$ if curvature is included, and $\nu \sim 0.25$ if flat plate theory is used. The frequency spread over which given modes become acoustically fast is shown in the heavily shaded area. For example the $n = 4$ modes become acoustically fast if curvature theory is used in the frequency range $\nu \sim 0.3$ to $\nu \sim 1.1$ when $m = 1, 3, 5, 7$. However, the frequency labeled $n = 4$, $m = 9$ mode is acoustically slow. It is (in this case) a circumferential strip mode (lightly shaded area). The 4, 11 mode is fast again but all other $n = 4$, $m > 11$ modes do not radiate (that is, they lie outside the shaded areas). The frequency bounds within which circumferential strip modes occur are given by (9.5.16). On Fig. 9.5.4 this equation (with the equal sign) is plotted as the heavy dashed line. For fixed ν the magnitude $k_x a$, must fall below this line in order for the modes enclosed by the line to radiate as strip modes. Similarly the limit of occurrence of acoustically fast modes is (9.5.17) plotted (with the equal sign) as the heavy full line. Only modes enclosed by this line and the abscissa are acoustically fast, given the choice $\nu_g = 2.0$.

A similar chart, this time for $\nu_g = 4.0$ is shown in Fig. 9.5.5. It is read in the same way as Fig. 9.5.4.

We now return to the calculation of $Z_{nm,nm}$. Under what conditions one may ask is mode coupling (specified by $n \pm q$ in (9.5.7)) not significant? *It is seen in Figs. 9.5.4, 9.5.5 that* except for the lowest frequencies even relatively narrow frequency bands contain a substantial

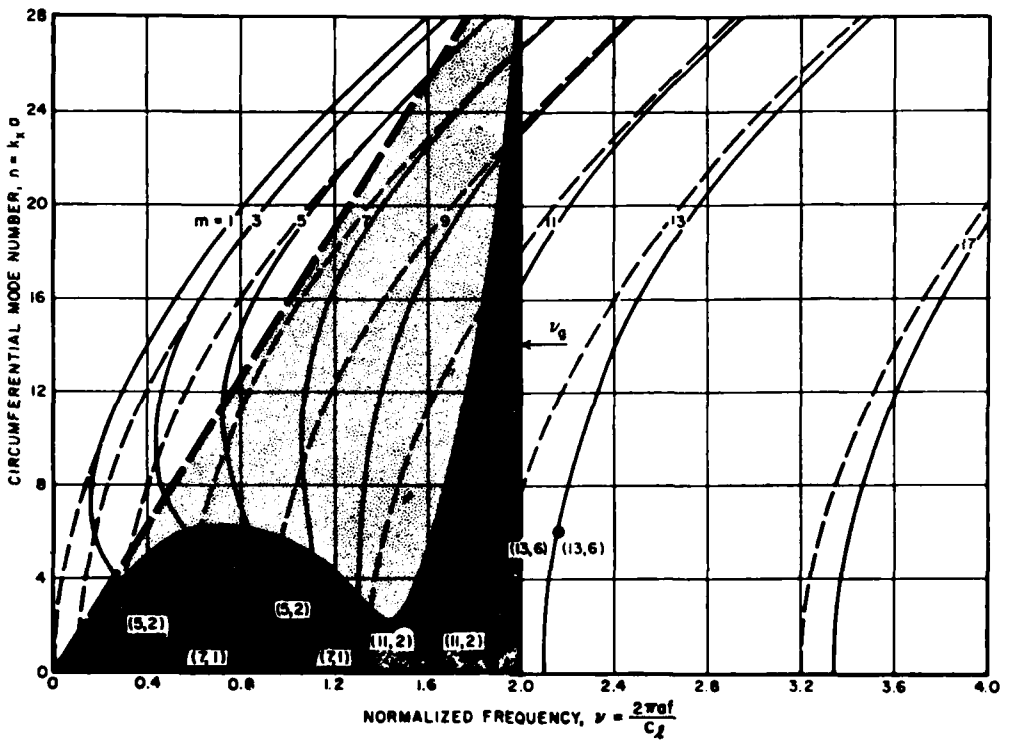

Fig. 9.5.4. Circumferential-mode numbers as a function of normalized frequency for various axial-mode numbers ($m = k_y l_2/\pi$) and for $\nu_g = 2$. ____ Loci of cylinder modes for a given axial-mode number. ---- Loci of "equivalent-plate" modes for a given axial-mode number. ○ Particular cylinder modes. Δ Corresponding "equivalent-plate" modes. *Heavily shaded area*: AF mode. *Lightly shaded area*: circumferential-strip mode. (After [9]).

number of shell resonant modes. The radiation efficiency as noted in (9.5.12b) is then an average of the efficiencies of these modes. When the number of modes is very large and contains (at random) groups that radiate and other groups non-radiating, the average radiation field becomes statistical. If each of the radiating modes is effectively a single degree of freedom oscillator not excessively damped (that with "high enough" mechanical Q), their mutual interaction is small. The average radiation efficiency is then a simple arithmetic average of noninteracting modes. The radiation impedance for each displacement mode is then "proper," meaning that it is coupled to only one acoustic pressure mode of the same subscripts. Setting $n = q$ in (9.5.9) we first evaluate $|Z_m(k_z)|^2$. Since $Z_m(k_z)$ is a standard integral [10], one arrives at the form,

$$|Z_m(k_z)|^2 = \frac{2k_m^2}{(k_m^2 - k_z^2)^2}\,[1 + (-1)^{m+1}\cos k_z l]$$

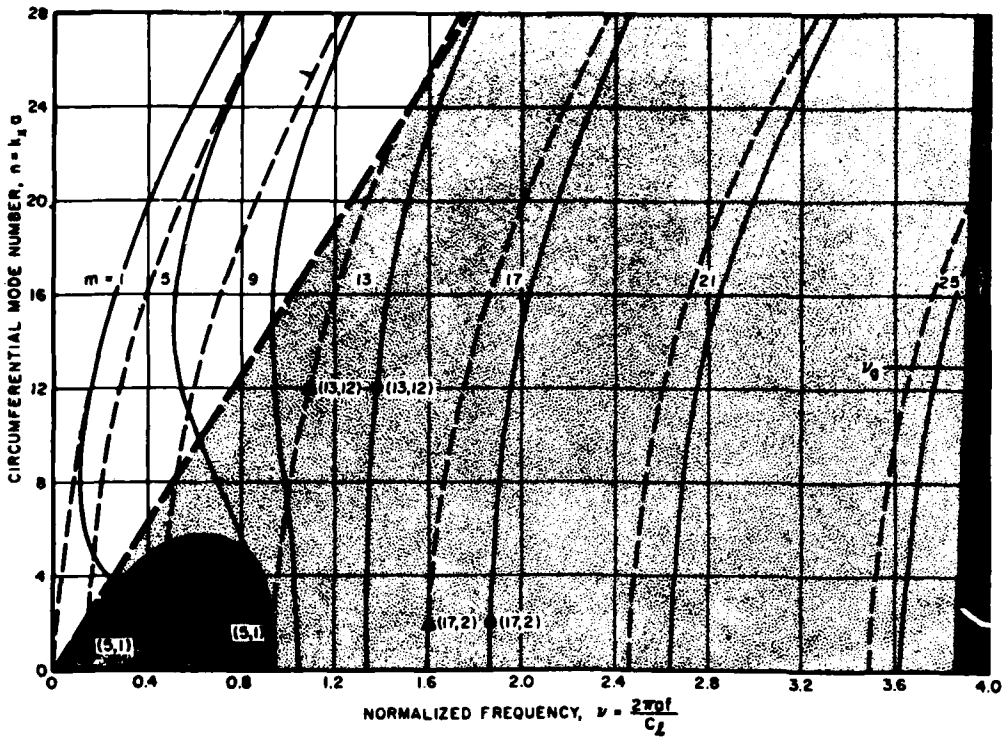

Fig. 9.5.5. Circumferential-mode numbers as a function of normalized frequency for various axial-mode numbers ($m = k_y l_2/\pi$) and for $\nu_g = 4$. ____ Loci of cylinder modes for a given axial-mode number. ---- Loci of "equivalent-plate" modes for a given axial-mode number. ○ Particular cylinder modes. △ Corresponding "equivalent-plate" modes. *Heavily shaded* area: AF mode. *Lightly shaded area:* circumferential-strip mode. (After [9]).

provided one assumes the shell is simply supported ($\sin k_m l = 0$, $k_m = m\pi/l$). Further simplification of (9.5.9) requires an asymptotic expression for the Hankel functions. Assume the drive frequency f is much greater than the shell resonant frequencies whose wavenumbers are given by $k_p^2 = k_x^2 + k_y^2$. Then n is a large number. Assume also $\sqrt{k^2 - k_z^2}\, a$ is also large. On these assumptions one can use the Debye Asymptotic form (for time given by exp $j\omega t$),

$$\left(\frac{\pi}{2}\right)^{1/2} H_n^{(2)}(x) \cong \frac{e^{\alpha}}{(n^2 - x^2)^{1/4}}$$

$$\alpha = (n^2 - x^2)^{1/2} - n \cosh^{-1}\frac{n}{x}$$

[11]. Let $\beta = \sqrt{k^2 - k_z^2}$. Then approximately, near and on the surface $r = a$,

$$\alpha \simeq (n^2 - \beta^2 r^2)^{1/2} = r\sqrt{\left(\frac{n}{r}\right)^2 - \beta^2} \simeq r\sqrt{\left(\frac{n}{a}\right)^2 - \beta^2}.$$

Now n/a is the circumferential wavenumber k_n. Thus the denominator inside the integration sign of (9.5.9), which is $[dH_m^{(1)}(\beta r)/dr]$ for $r = a$, is replaced by $\sqrt{k_n^2 - \beta^2}$, all other terms cancelling out. Hence,

$$Z_{nm,nm} = \frac{2k\rho c}{\pi l} \int_{-\infty}^{\infty} \frac{k_m^2[1 + (-1)^{m+1} \cos k_z l]}{(k_m^2 - k_z^2)^2 \sqrt{k^2 - k_z^2 - k_n^2}}\, dk_z \text{ (units: Nsm}^{-3}) \qquad (9.5.18)$$

in which

$$\sqrt{k_n^2 - \beta^2} = j\sqrt{\beta^2 - k_n^2} = -i\sqrt{k^2 - k_z^2 - k_n^2}.$$

The real part of $Z_{nm,nm}$ is the modal radiation resistance. It is determined by integration over the interval $|k_3| < \sqrt{k^2 - k_n^2}$. This suggests writing $k_z = \sqrt{k^2 - k_n^2}\cos\theta$ and integrating over $0 < \mathrm{Re}\,\theta < \pi$, $\mathrm{Im}\,\theta = 0$. The results of integration are found in [12],

$$\text{strip modes } \begin{pmatrix} k_n < k \\ k_m > k \end{pmatrix}: \quad R_{nm} = \frac{2k\rho c}{k_m^2 l} \frac{[1 - (k^2/2k_m^2) + (k_n^2/2k_m^2)]}{[1 - (k^2/k_m^2) + (k_n^2/k_m^2)]^{3/2}}, \quad f_l < f < f_c \qquad (9.5.19)$$

$$\text{acoustically fast modes } \begin{pmatrix} k_n < k \\ k_m < k \end{pmatrix}: \quad R_{nm} = \frac{\rho c}{\sqrt{1 - (k_p^2/k^2)}}, \quad k_p^2 = k_n^2 + k_m^2 \qquad (9.5.20)$$

$$\text{acoustic short-circuit modes } \begin{pmatrix} k_n > k \\ k_m > k \end{pmatrix}: \quad R_{nm} = 0 \qquad (9.5.21)$$

These modal radiation resistances are defined in terms of *rms* particle velocities and *rms* radiated power. Omitting the factor of 2 in 6.3.2, one has

$$R_{nm}(\omega) = \frac{W_{rms}}{S(V_{ref})^2} = \frac{W_{rms}}{S\langle \dot{\xi}_{nm}^2 \rangle}$$

$$\langle \dot{\xi}_{rms}^2 \rangle rms = \frac{1}{S}\int_S |\dot{\xi}_{nm}|^2 \cos^2 n\phi \sin^2 k_m z dS = \frac{|\dot{\xi}_{nm}|_{rms}^2}{4}. \qquad (9.5.22)$$

Once the radiation resistances are obtained one can calculate the modal radiation efficiency by use of (9.5.12). Such a calculation of $10 \log \sigma_{nm}$ vs k/k_p for a cylindrical steel shell, length 1.2 m, thickness 8 mm, radius 0.265 m in water is shown in Fig. 9.5.6 At the coincidence frequency ($k = k_p$) the radiation efficiency peaks at a value obtained from (9.5.18), namely,

$$\sigma = \frac{2}{3} k \sqrt{\frac{l}{\pi k_m}}$$

[12]. Below coincidence the efficiency decreases with increasing mode number. Above coincidence the efficiency tends toward unity.

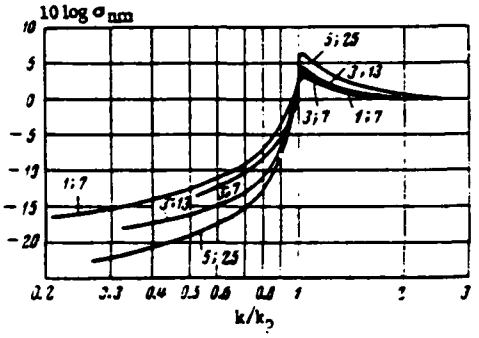

Fig. 9.5.6. Modal efficiency of sound radiation from a shell at high frequencies, $ka > 1$. (After [12]).

9.6 RADIATION FIELD OF RECTANGULAR PISTONS VIBRATING HARMONICALLY IN AN INFINITE RIGID BAFFLE

A rectangular piston, sides 2a and 2b, vibrates at frequency ω in an infinite rigid baffle. The acoustic velocity potential ψ at any field point $\mathbf{R} = (x, y, z)$ is a superposition of contributions of normal volume velocity $v_n(\mathbf{R})dS(\mathbf{R}_0)$ from each point $\mathbf{R}_0$ of the piston, Eq. (1.8.18). For the case when this velocity is spatially constant $v_n = \dot{W}_0$ one has,

$$\text{(a) } \psi(k, \mathbf{R}) = \frac{\dot{W}_0 e^{-i\omega t}}{2\pi} [\psi_1(k, \mathbf{R}) + i\psi_2(k, \mathbf{R})] \quad \text{(units: } m^2 s^{-1})$$

$$\text{(b) } \psi_1(k, \mathbf{R}) = \int_A \frac{\cos k|\mathbf{R}-\mathbf{R}_0|}{|\mathbf{R}-\mathbf{R}_0|} dx_0 dy_0; \quad \psi_2(k, \mathbf{R}) = \int_A \frac{\sin k|\mathbf{R}-\mathbf{R}_0|}{|\mathbf{R}-\mathbf{R}_0|} dx_0 dy_0 \quad (9.6.1)$$

$$\text{(c) } |\mathbf{R}-\mathbf{R}_0| = \sqrt{(x-x_0)^2 + (y-y_0)^2 + z^2}.$$

For convenience in writing let $x_0 - x = u_0$, $y_0 - y = v_0$. Since field coordinates x, y are constant during integration, the element of area $dA = du_0 dv_0$. In calculating 9.6.1 a great simplification occurs if one chooses the origin of source coordinates to be one corner of the rectangular piston. Then,

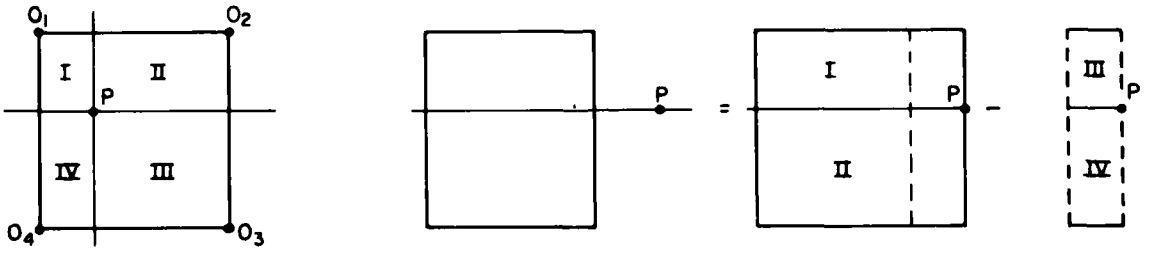

a. Field point projects on the radiating surface at P

b. Field point projects on the radiating surface at P

Fig. 9.6.1. Partitioning of the radiating area for calculation of the field of a rectangular piston

$$\text{(a) } \psi_1(x, y, z) = \int_{-x}^{2a-x} \int_{-y}^{2b-y} \frac{\cos\left[k\sqrt{u_0^2 + v_0^2 + z^2}\right]}{\sqrt{u_0^2 + v_0^2 + z^2}} du_0 dv_0;$$

$$\text{(b) } \psi_2(x, y, z) = \int_{-x}^{2a-x} \int_{-y}^{2b-y} \frac{\sin k\sqrt{u_0^2 + v_0^2 + z^2}}{\sqrt{u_0^2 + v_0^2 + z^2}} du_0 dy_0. \tag{9.6.2}$$

These integrals are difficult to evaluate for arbitrary x, y. A direct approach is to set $y = 0$ and calculate the potential field in the xz plane. Then

$$\text{(a) } \psi_2(x, z) = \int_{-x}^{2a-x} S[k\sqrt{u_0^2 + z^2},\ 2b]\, du_0$$

where (9.6.3)

$$\text{(b) } S[k\sqrt{u_0^2 + z^2},\ 2b] \equiv \int_0^{2b} \frac{\sin k\sqrt{u_0^2 + v_0^2 + z^2}}{\sqrt{u_0^2 + v_0^2 + z^2}} dv_0.$$

The function S, with change of variable $k^2u_0^2 \to u^2$, $k^2v_0^2 \to v^2$, $2b \to 2kb$, $2a \to 2ka$ $z \to kz$ is a tabulated quantity [13]. This same reference also tabulates a quantity C (with the same change of variables) which has the property that

$$\int_0^{2b} \frac{\cos k\sqrt{u_0^2 + v_0^2 + z^2}}{\sqrt{u_0^2 + v_0^2 + z^2}} dv_0 = \int_0^{2b} \frac{dv_0}{\sqrt{u_0^2 + v_0^2 + z^2}} - C[k\sqrt{v_0^2 + z^2},\ 2b]. \tag{9.6.4}$$

Substitution of this form in 9.6.2a and integration over v_o yields ψ_1:

$$\psi_1(x, z) = \int_{-x}^{2a-x} du_0 \left\{ \ln\left[\frac{2b + \sqrt{u_0^2 + z^2 + 4b^2}}{\sqrt{u_0^2 + z^2}} \right] - C[k\sqrt{u_0^2 + z^2},\ 2b]. \right. \tag{9.6.5}$$

From (9.6.3), (9.6.5) and (9.6.1) one obtains the pressure field $p(x, z)$ using the relation $p = \rho\partial\psi/\partial t$. A similar procedure allows the calculation of the potential field in the yz plane by exchanging x for y.

The burden of calculating ψ by (9.6.3) and (9.6.5) is much reduced by partitioning the integration area into four parts subscripted m = I, II, III, IV and superimposing four integrals of the type (9.6.2) [14]. The resultant formulas can be made explicit for two case of the location of the projection of the field point on to the xy plane. In the first case the field point **R** (x, y, z) projects on to the piston at $x = x_0 = 2a_m$, $y = y_0 = 2b_m$ where (as before) subscript m designates which partitioned rectangle is under consideration, Fig. 9.6.1a. The origins 0_1, 0_2, 0_3, and 0_4 are selected in sequence while the point $2a_m$, $2b_m$ remains the same. The quantities ψ_1 and ψ_2 then reduce to

$$\text{(a) } \psi_1(x, y, z) = \sum_{m=1}^{IV} F_m; \quad F_m = \int_0^{2a_m} \int_0^{2b_m} \frac{\cos k\sqrt{u_0^2 + v_0^2 + z^2}}{\sqrt{u_0^2 + v_0^2 + z^2}} du_0 dv_0 \tag{9.6.6}$$

$$\text{(b)}\ \psi_2(x, y, z) = \sum_{m=1}^{\text{IV}} G_m; \quad G_m = \int_0^{2a_m} \int_0^{2b_m} \frac{\sin k\sqrt{u_0^2 + v_0^2 + z^2}}{\sqrt{u_0^2 + v_0^2 + z^2}}\, du_0 dv_0.$$

In the second case the field point $\mathbf{R}(x, y, z)$ projects onto a point P outside of the radiating area, Fig. 9.6.1b. One then imagines fictitious pistons III, IV such that

$$\begin{aligned} &\text{(a)}\ \psi_1(x, y, z) = \sum_{\text{I,II}} F_m - \sum_{\text{III,IV}} F_m \\ &\text{(b)}\ \psi_2(x, y, z) = \sum_{\text{I,II}} G_m - \sum_{\text{III,IV}} G_m. \end{aligned} \tag{9.6.7}$$

In this alternative formulation (9.6.3) reduces to

$$\psi_{2(m)}(2a_m, 2b_m, z) = F_m = \int_0^{2a_m} S[\sqrt{u_0^2 + z^2},\ 2b_m]\, du_0. \tag{9.6.8}$$

Similarly upon performing the integrations called for in (9.6.5),

$$\begin{aligned} \psi_{1(m)}(2a_m, 2b_m, z) = G_m = {} & 2a_m \ln\left[\frac{2b_m + \sqrt{4a_m^2 + 4b_m^2 + z^2}}{\sqrt{4a_m^2 + z^2}}\right] \\ & + 2b_m \ln\left[\frac{2a_m + \sqrt{4a_m^2 + 4b_m^2 + z^2}}{\sqrt{4a_m^2 + z^2}}\right] \\ & - 2\pi z \text{ arc } tg \frac{2a_m b_m}{z\sqrt{4a_m^2 + 4b_m^2 + z^2}} \\ & - \int_0^{2a_m} C[k\sqrt{u_0^2 + z^2},\ 2b_m]. \end{aligned} \tag{9.6.9}$$

Examples of the numerical evaluation of the pressure field $p = -i\omega\rho\psi$ from (9.6.8), (9.6.9) and (9.6.1) for square pistons of side $2a$ for $ka = 4, 6, 8, 10$, and for 0 rectangular piston $ka = 10$, $kb = 5$ are given in [14]. The cases of the square piston $ka = 10$, and the rectangular piston are reproduced here as Figs. 9.6.2 and 9.6.3 respectively. Note that in this reference $p_a = k\psi_2/2\pi$, $p_m = \dfrac{k\psi_1}{2\pi}$ provided exp $i\omega t$ is changed to exp $-i\omega t$.

The radiation of a rectangular surface in the absence of a baffle can be described as a case of radiation from arbitrary surfaces, Section 1.10 or as a case of radiation from a spherical surface, Section 1.9c or spheroidal surface, Sections 1.9d and 9.9e.

Equations (9.6.6) and (9.6.1) may also serve to calculate the pressure amplitude (at frequency ω) at any point of the rectangular piston. It is only necessary to set $z = 0$ in these formulas and then evaluate the integrals by numerical means.

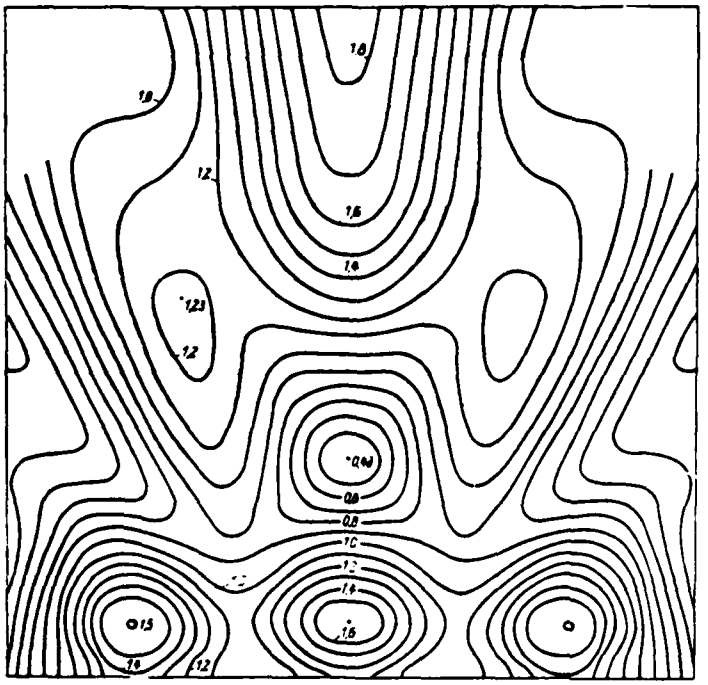

Fig. 9.6.2. Sound field in the *yz* plane in the immediate vicinity of a square piston (side 2a) of uniform velocity and acoustic size $ka = 10$. After [14].

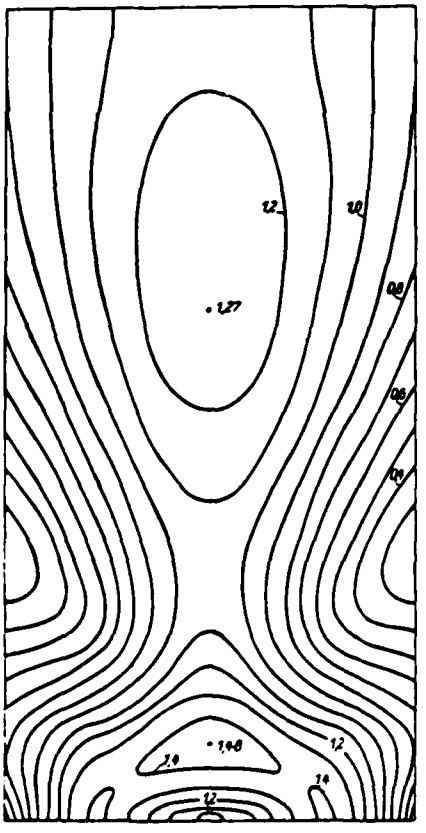

Fig. 9.6.3. Sound field in the *yz* plane in the immediate vicinity of a rectangular piston (sides 2a and 2b) and acoustic size $ka = 10$, $kb = 5$. After [14].

9.7 RADIATION OF SOUND BY FLUID FLOW OVER CONTOURED OBJECTS

The dynamic interaction of rigid bodies and fluctuating fluid flow leads to the generation of fluctuating volumes and forces in the medium. These are sources of acoustic phenomena which are discussed next.

9.7.a Radiation Caused by Linear Flow Over a Rigid Object

A finite object moving through a compressible medium can, under a variety of conditions, become a source of sound. Each such condition, or combination of conditions, generates its own (unique) type of acoustic radiation. Several cases are presented in the following discussion.

To begin with, the object moving at velocity $v(x)$ is assumed to present a smoothly varying cross-sectional area $A(x)$ is the x-direction of motion. Because the product of this area and its velocity is the normal volume velocity it is seen that as the finite object passes through a mathematical plane perpendicular to its motion it ejects (or sucks in) a variable volume $\delta\mathcal{Q}$ with each increment δx.

$$\delta\mathcal{Q}(x,t) = \frac{\partial}{\partial t}[\delta V] = \frac{\partial}{\partial t}[A(x)\delta x] \tag{9.7.1}$$

We now imagine the object fixed in the plane $x = 0$ and the fluid flowing past at with the same velocity $v(x)$. We further assume each increment δx to be a *point* source of strength $\delta\mathcal{Q}$. The increment of acoustic pressure radiated by segment δx to field point (x,y,z) is then found from 7.1.22 to be

$$\delta p(R,t) = \frac{\rho_0}{4\pi R}\frac{\partial}{\partial t^*}\delta\mathcal{Q}(x,t^*) \tag{9.7.2}$$

$$\delta p(R,t) = \frac{\rho_0 \delta x}{4\pi R}\frac{\partial}{\partial t^*}[A(x)\delta x)]$$

$$R = [x^2 + y^2 + z^2]^{1/2}$$

$$t^* = t - R/C$$

In reality the coordinate x is a function of time. Assume

$$x(t) = x_0 - X(t) \tag{9.7.3}$$

in which x_0 is the local spatial coordinate on the object, and $X(t)$ is the true velocity. Since

$$\frac{\partial A}{\partial t} = \frac{\partial A[x_0 - X(t)]}{\partial t} = -\frac{\partial X(t)}{\partial t}\frac{\partial Aa}{\partial x}(x) = -v\frac{\partial A}{\partial x} \tag{9.7.4}$$

this acoustic pressure becomes

$$\delta p(R(t^*)) = \frac{\rho_0 \delta_x}{4\pi_R}\left[v^2\frac{\partial^2 A(x)}{\partial x^2} - \frac{\partial v}{\partial t^*}\frac{\partial A}{(pdx}(x)\right] \tag{9.7.5}$$

$$x = x(tt^*)$$

Thus the pressure at distance R and time t is determined by the rate of change of the source strength a time R/C earlier which, in turn, depends on the first and second derivatives of the

object cross sectional area $A(x)$. For constant flow $\dot{v} = 0$, the pressure radiated is the proportional only to the second spatial derivative of $A(x)$. Thus if the object is an infinite cone one has $A''(x) = 0$ and the radiated pressure vanishes. A finite length cone in constant flow does radiate sound from its termination.

We next assume that the contour or the object is unsymmetrical relative to the flow and hence that the object experiences a lift force $L(x;v)$ per increment δx, which is an expicit function not only of position x but also the velocity v mass density δ_0. This is a net force exerted by the medium on the moving object applied in a direction normal to the flow. If the object is imagined free in the y-direction but fixed in the plane $x = 0$ this is the force $\delta F(t)$ in the y-direction exerted by the object in the medium resulting from the fluid motion:

$$\delta F(t) = \delta x \; L \; (x(t);v(t)) \quad (\text{units of } L\text{: } \mathrm{Nm}^{-1}) \tag{9.7.6}$$

This radiation corresponds to that of a transcent dipole whose formula is given by 7.1.13a. The derivative called for there is taken with respect to the total argument $t^* = t - R/C$. Using 9.7.3, 9.7.4 again and omitting nearfield components one obtains the radiated field p_D:

$$\delta p_L(R(t^*)) = \frac{\cos\theta}{4\pi RC}\delta t\left[-v\frac{\partial L}{\partial x} + \dot{v}\frac{\partial L}{\partial v}\right], \; x = x(t^*) = x_0 - X(t^*) \tag{9.7.7}$$

θ is the angle between the direction of the observation point from the incremental volume $A(x)\,\delta x$ and the flow direction.

An object experiencing a lift force will also experience a drag force D per increment δx. This is the force exerted by the fluid on the object in the direction of flow. The radiated field at long wavelengths is that of a transient dipole. Repeating the steps leading to 9.7.7 one obtains

$$\delta p_D(R(t^*)) = \frac{-\sin\theta\delta x}{4\pi RC}\left[-v\frac{\partial D}{\partial x} + \dot{v}\frac{\partial D}{\partial v}\right], \; x = x(t^*) = x_0 - X(t^*) \tag{9.7.8}$$

Here the direction $\cos\beta$ required by 7.1.13a is measured from the normal axis to the flow axis while the direction $\cos\theta$ is measured from the flow axis to the normal axis. Hence $\cos\beta = -\sin\theta$.

In each equation 9.7.5, 9.7.7 and 9.7.8 the sound field is generated by an increment δx of the object profile. To obtain the total sound field at R, t one must integrate over the entire profile.

9.7b Radiation Caused by Rotational Flow Over Rigid Objects

We consider next a collection of B contoured objects in a plane (say a propeller with its blades which sweep out an area S) rotating around a fixed axis. A (geometrically) simple case is one in which there is a force distribution $\mathscr{F}$ per unit area over the surface S rotating with angular velocity Ω. From 1.8.3 the source volume velocity for steady state is,

$$q(r_0,t_0) = -\int_{-\infty}^{t_0} \nabla\cdot\left[\frac{\mathscr{F}}{\rho_0}\right] dt_0 \rightarrow \frac{-1}{-i\omega\delta_0}\nabla\cdot\mathscr{F} \tag{9.7.9}$$

By redefining $\mathcal{F}$ to be the force per unit area, and integrating by parts one obtains 5.4.13,

$$\psi(\mathbf{r}) = -\int \nabla_0 g \cdot \left(\frac{\mathcal{F}}{i\omega\rho_0}\right) dS \tag{9.7.10}$$

We take the directional derivative $\nabla_0 g$ in direction of the field point $\hat{\mathbf{a}}$, and make the farfield approximation called for by 5.4.15b:

$$\nabla_0 g \simeq -\frac{ik}{4\pi}\left(\frac{e^{ikr}}{r}\right)\hat{a}_r \exp\{-ikr_0 \sin\theta \cos(\phi - \phi_0)\} \tag{9.7.11}$$

where θ, ϕ are spherical coordinates. The steady state radiated acoustic field $p = -i\omega\rho_0\psi$ depends on which component of $\mathcal{F}$ is selected. Assume first that $\mathcal{F}$ consists only of the normal component F_n: the pressure is then,

$$p_L(\mathbf{r},k) = -\frac{ik}{4\pi}\left(\frac{e^{ikr}}{r}\right)\cos\theta \int F_n(\mathbf{r}_0,t)\exp\{-ikr_0 \sin\theta \cos(\phi - \phi_0)\} r_0 dr_0 d\psi_0 \tag{9.7.12}$$

where $\hat{\mathbf{a}}_r \cdot \mathcal{F} = F_n \cos\theta, \mathcal{F} = F_n\hat{\mathbf{a}}_n$. Here $\hat{\mathbf{a}}_n$ is a unit magnitude vector pointing in the direction of the normal to the surface S.

The exponential in the integrand of 9.7.9 couples angles θ to angles ϕ. They can be uncoupled by use of the Fourier expansion,

$$\exp\{-ikr'_0 \sin\theta \cos(\phi - \phi_0) = \sum_{-\infty}^{+\infty} i^m J_m(kr'_0 \sin\theta)\, e^{im(\phi-\phi_0)}$$

Thus, 9.7.12 reduces to the steady state amplitude,

$$p_L(\mathbf{r},k) = -\frac{ik}{4\pi}\left(\frac{e^{ikr}}{r}\right)\cos\theta \sum_{m=-\infty}^{+\infty} \int F_n(\mathbf{r}_c,t)\, i^m J_m(kr_0 \sin\theta) e^{im(\phi - \phi_0)} r_0\, dr_0\, d\phi_0 \tag{9.7.13}$$

The force F_n at a fixed spatial point in the plane of the rotating object must be expressed as a Fourier series in the time t because it is temporally periodic. Also, because F_n is the lift force of the contoured object, whose magnitude depends on the square of the relative velocity between object and fluid flow, it is in general a spatially periodic function of angle ϕ_0 which is also in the plane of the rotating object. Thus F_n is a double Fourier series:

$$F_n(\mathbf{r}_0,t) = F_n^0(r_0) \sum_s \alpha_s(r_0) e^{-isB(\Omega t - \phi_0)} \sum_q \beta_q\,(r_0) e^{iq\phi_0} \tag{9.7.14}$$

In the farfield the acoustic pressure waves are nearly plane traveling waves whose phase must couple spatial and temporal dependence through the wavenumber k that is, it must be of the form,

$$\exp\, i\, s\frac{B\Omega}{c}(r - ct)$$

When 9.7.14 is used we must therefore set $k = \frac{sB\Omega}{c}$. The ϕ_0-dependence in the integrand is

$$exp[i\ (sB + q - m)\ \phi_0]$$

Now, if $p \neq 0$, $\oint = e^{ip\phi_0} d\phi_0 = 2\pi i \sum$ residues inside the circle of integration. Since there are no residues this integral vanishes. However, when $p = 0$ this integral equals 2π. Thus,

$$p_L(\mathbf{r}) = -\frac{iB\Omega}{4\pi cr} \exp\{i\frac{B\Omega}{c}\} \cos\theta \sum_s \sum_q i^{(sB+q)} e^{i(sBA+q)\phi} e^{-is\left|\frac{B\Omega}{c}\right|ct}$$

$$\times \int_0^a sF_n^0(r_0)\, \alpha_a(r_0)\beta_q(r_0)\, J_{sB+q}\left(s\frac{B\Omega}{c} r_0 \sin\theta\right) 2\pi r_0\, dr_0 \qquad (9.7.15)$$

in which the outermost radius of the contoured object is at distance a from the axis of rotation.

Equation 9.7.15 gives the time varying acoustic pressure p at a field point $\mathbf{r}$ caused by a propeller rotating in a nonuniform flow. The sum on s gives the Fourier components of periodic temporal discussion of the lift while the sum on q gives the Fourier components of periodic spatial fluctuation. If the flow is uniform one sets $q = 0$.

We assume next that $\mathcal{F}$ consists only of a tangential component $\mathbf{F} = \hat{\mathbf{a}}_\phi F_t$. The amplitude of directional derivative $\nabla_0 g$ in the direction $\hat{\mathbf{a}}_\phi$ in the farfield is

$$\nabla_0 g = \hat{\mathbf{a}}_\phi \frac{1}{r_0} \frac{e^{ikr}}{r\pi r} \sum_{m=-\infty}^{\infty} m\, i^m J_m(kr_0 \sin\theta) e^{im(\phi-\phi_0)} \qquad (9.7.16)$$

Using the same procedure that led to 9.7.15 one arrives at the expression for the acoustic pressure p_D due to this drag force F_t:

$$p_D(\mathbf{r}) = \frac{i \exp\{i\frac{B\Omega r}{c}\}}{4\pi r} \sum_s \sum_q (sB + q) i^{(sB+q)} e^{i(sB+q)\phi} e^{-i\left|\frac{B\Omega}{c}\right|ct}$$

$$\times \int_0^a \frac{s}{r_0} F_t^0(r_0)\, \alpha_s(r_0)\, \delta_q(r_0)\, J_{sB+q}\left(\frac{sB\Omega}{c} \sin\theta\right) 2\pi r,\, dr_0 \qquad (9.7.17)$$

Here the Fourier coefficient for the spatial expansion in ϕ is δ_q which is taken to be different from β_q.

Equations 9.7.17 and 9.7.15 are theoretical expressions. To evaluate them one is required to know the radial functional dependence of F_n, F_t, α_s, β_q, δ_q. Often, in the case of propellers, the only things known are the shaft horsepower p_h, the thrust T in units of pounds force, the radius of the propeller a_0 (units: feet) the tip mach number M_t and the distance of the field point r (units: feet). In these practical units the sum of 9.7.15 and 9.7.17 for the case of uniform flow ($q = 0$) and for each Fourier component s gives the total acoustical pressure in the far field

$$p_s = \frac{54sBM_t}{a_0 r}\left[\frac{0.76P_h}{M_t^2} - T\cos\theta\right] J_{sB}\, 0.8\, M_t,\, s\, B \sin\theta) \quad \text{(units:lb/ft}^2\text{)}. \qquad (9.7.18)$$

This is designated the "Gutin model" [15]. It gives reasonably good predictions of noise radiated by propellors [16].

9.7c Radiation From Moving Sound Sources

A sound source moving with arbitrary velocity V in a turbulent medium and radiating sound to an observer is difficult to model. A simple but useful case is one on which the velocity is uniform, the medium is homogeneous and quiescent and the observer is momentarily moving at the same speed as the source. The model can then be simplified to observer and source at rest with respect to each other and the medium is flowing past this at a speed V.

We begin first with $V = 0$. The two-dimensional wave equation in cylindrical coordinates r, q then gives

$$\mathscr{L}p = 0, \quad \mathscr{L} = \frac{1}{4}\frac{\partial}{\partial r}\left(r\frac{\partial}{\partial r}\right) + \frac{\partial^2}{\partial z^2} - \frac{1}{c^2}\frac{\partial^2}{\hat{c}t^2} \tag{9.7.19}$$

where $z \geqslant 0$ defines the location of the head and the coordinates for the body of the object and r i the radial distance to any field point. When the source u in motion we can implement the model by using a Galilean transformation modified for the case when $V/c(=M)$ is not negligible:

$$z' = \frac{z - Vt}{\sqrt{M^2 - 1}}$$

Since

$$dz' = \frac{\partial z'}{\partial z}\,dz + \frac{\partial z'}{\partial t}\,dt; \quad \frac{\partial z'}{\partial z} = \frac{1}{\sqrt{M^2 - 1}}, \quad \frac{\partial z'}{\partial t} = \frac{-V}{\sqrt{M^2 - 1}}$$

it is seen that

$$\frac{\partial}{\partial z} = \frac{1}{\sqrt{M^2 - 1}}\frac{\partial}{\partial z'}\,; \quad \frac{\partial}{\partial t} = -\frac{V}{\sqrt{M^2 - 1}}\frac{\partial}{\partial z'}.$$

Thus the explicit time coordinate vanishes and 9.7.19 reduces to the form,

$$\left[\frac{1}{r}\frac{\partial}{\partial r}\left(r\frac{\partial}{\partial r}\right) - \frac{\partial^2}{\partial z'^2}\right]p = 0$$

Substitution of $z(z',\ r)/\sqrt{r}$ for p in the equation simplifies the first term. The result is

$$\frac{\partial^2 g}{\partial r^2} - \frac{\partial^2 g}{\partial z'^2} - \frac{g}{4r^2} = 0 \tag{9.7.20}$$

At distances r very much greater than the largest dimension of the sound source the last term is negligible relative to the other two terms. The solution in that case is seen to be

$$g = g_1(r - z') - g_2\,(r + z')$$

In the first term g_1 the lines $r - z' =$ const. form the trace on the r, z' plane of a family of cones pointing toward the right (z' is positive toward the right). Similarly, in the second term the lines $r + z' =$ const. define traces of cones pointing toward the left. The solution g_2 is independent of the source and hence is rejected. Thus the radiated pressure is

$$p(r,z') = \frac{g(r - z')}{\sqrt{r}} \tag{9.7.21}$$

An explicit expression for g can be obtained only by solving 9.7.20 in connection with boundaries and source configurations. In this regard 9.7.5, 9.7.7 and 9.7.8 will give the monopole and dipole contributions due to volume and force fluctuations on the object. However the functional from of 9.7.21 is significant in its own right. Relative to the coordinate ζ of the object (where $V = 0$) one can set $z' = \zeta/\sqrt{M^2 - 1}$. Thus when z' is negative (as it is on the object) the lines,

$$r - z = r + \frac{\zeta}{\sqrt{M^2 - 1}} = \text{const.} \tag{9.7.22}$$

represent traces of a stationary family of many plane waves making an acute angle θ relative to the z' axis of travel, such that

$$\tan\theta = \left(\frac{dr}{dz'}\right) = \frac{1}{\sqrt{M^2 - 1}}; \quad \sin\theta = M^{-1} \tag{9.7.23}$$

Angle θ is real only when $M(=V/c) \geqslant 1$.

When $V/c \geqslant 1$ the lines represent the spatial radiation pattern of "sonic booms." Fig. 9.7.1 shows sonic booms for the case of two objects (a wing attached to a fuselage. The monopole boom originating at the head of one object is a compression wave, while that from a subscript discontinuity (or from the tail) of the object is an expansion (or rarefaction) wave. The dipole boom is a compression wave propagating in a direction opposite to the lift, and an expansion wave propagating on the same direction as the lift.

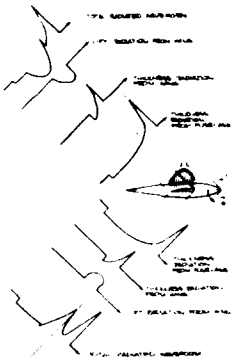

Fig. 9.7.1 — Near field disturbance from fuselage-wing combination (after [16]).

9.8 RADIATION OF SOUND INTO A LAYERED HALF-SPACE

Let the time variable be $\exp(j\omega t)$. Assume first that the medium consists of a liquid layer over a liquid half space, Fig. 9.8.1. A harmonic point source in 3-space expressed in cylindrical coordinates is given by 3.7.42 (where time is $\exp(-i\omega t)$). Noting from integral representation of Hankel function that $H_0^{(2)}(z) = -H_0^{(1)}(-z)$, and using the relation $J_0(z) = \frac{1}{2}[H_0^{(1)}(z) + H_0^{(2)}(z)]$ it is seen that for $j = -i$ the Green's function of a point source in full space is,

$$G = \frac{e^{-jkR}}{4\pi R} = \int_0^\infty A(\nu)\, J_0(\alpha\rho) e^{-\nu|z-z'|} d\alpha$$

where $\quad A = \alpha/4\pi\nu \qquad (9.8.1)$

$$\nu = \sqrt{d^2 - k^2}, \quad k = \frac{\omega}{c_1}$$

$$R = \sqrt{\rho^2 + (z - z')^2}$$

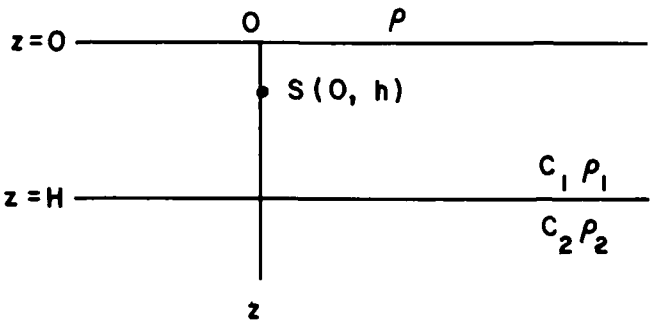

Fig. — 9.8.1. Point source in a layered medium.

For a point source of unit volume velocity the Green's function G is the same in magnitude as the velocity potential ψ.

The point source creates a system of spherical waves in the two layers. In layer 1 there are direct waves described by 9.8.1 plus a set of waves reflected at the interface $z = H$ in which $A(\nu)$ of 9.8.1 is replaced by an (unknown) amplitude $B(\nu)$, plus a set of waves reflected by the interface $z = 0$ in which $A(\nu)$ is replaced by an unknown amplitude $C(\nu)$. The total potential in layer 1 is then:

$$\psi_1 = \int_0^\infty A(\nu) J_0(\alpha_\rho) e^{-\nu_1|z-z'|}\, d\alpha + \int_0^\infty [B(\nu) + C(\nu)]\, J_0(\alpha\rho)\, e^{-\nu_1(z-z')}\, d\alpha \tag{9.8.2}$$

In medium 2 there are a set of transmitted waves described by replacing $A(\nu)$ by an (unknown) amplitude $D(\nu)$:

$$\psi_2 = \int_0^\infty D(\nu)\, J_0(\alpha\rho)\, e^{-\nu_2(z-z')}\, d\alpha \tag{9.8.3}$$

Thus the total system of wares of both layers features three unknown amplitudes B, C, D. To find them explicitly one uses three boundary conditions. Assume,

(1) at $z = 0$: $p = 0$, or $j\omega\rho, \psi_1, = 0$
(2) at $z = H$: $p_1 = p_2$, or $j\omega\rho\, \psi_1 = j\omega_{\rho_2} \psi_2$ (9.8.4)
(3) at $z = H$: $u_1 = u_2$, or $-\dfrac{\partial\psi_1}{\partial n} = -\dfrac{\partial\psi_2}{\partial n}$

Substitution of 9.8.2 and 9.8.3 into 9.8.4 gives three algebraic equations whose solution provides explicit expressions for B, C, D in terms of ρ_1, ρ_2, C_1, C_2, H and h. Thus the solution of the problem of radiation into two liquid layers is presented in the form of three integrals [17].

The evaluation of the integrals is difficult. In one procedure the integrands are rearranged to allow evaluation in terms of *rays*. In a second procedure the evaluation is done by contour integration using the method of steepest descent which leads to a description of the wave fields in terms of *normal modes* [18].

When the point source radiates into a multitude of layers, some solid, some liquid, the same approach to solution through satisfaction of the boundary conditions at each layer may be used. This results in a family of equations for unknown reflected and transmitted amplitudes in each layer. They are explicitly obtained by matrix inversion. The resultant integrals are again evaluated in terms of rays or normal modes. Because of the presence of elastic solids these solutions include shear waves as well as longitudinal waves.

CHAPTER IX
APPENDIX. CONVENTIONAL RADIATORS OF SOUND

9A.1 INTRODUCTION

Natural, or man-made, sources of sound consist in general of physical mechanisms which generate fluctuating volumes, or gradients of force, in a compressable medium. While these may be distributed in space it is the mechanism of *temporal fluctuation* which produces the sound. Section 1.7 discusses the point. Man-made sources of sound generally consist of an *exciter* coupled to a *resonator.* The exciter acts over one or more spatial points of resonator and may exhibit periodic, random, or impulsive contact with it. At any specific spatial point, area, or volume of the resonator the exciter imparts a temporal signal to it which also may be periodic, random, or impulsive. The combination of spatial and temporal excitation in man-made acoustic structures is unique to each structure. Several man-made and natural sources of sound are discussed in the following list.

9A.2 LIST OF CONVENTIONAL RADIATIONS OF SOUND AND THEIR MODELS

Tuning Fork (Fig. 9A.2.1)

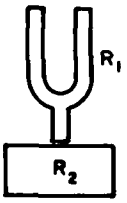

Fig. 9A.2.1

This is a resonator R_1 consisting of a bar bent into a *U*-shape. It can also be attached to a box resonator R_2. Both resonators acts as frequency selective filters. It is excited by an impulsive mechanical blow, or a periodic electric signal. It is modeled as a pair of interacting dipoles which generate a 4-clover leaf radiation pattern, each leaf of opposite phase to its immediate neighbors. Elements of a mathematical model can be constructed from Sections 5. and 7.

Supersonic Bullet (Fig. 9A.2.2)

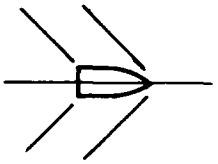

Fig. 9A.2.2

The bullet is a symmetrically contoured rigid object interacting with a flowing medium. At supersonic speed it radiates shock waves from its nose and tail. It is modeled as a monopole source of fluctuating volume (sonic booms) discussed in Section 9.7c.

Bell (Fig. 9A.2.3)

Fig. 9A.2.3

This is a single resonator in the form of a hollow cylinder closed at one end. The clapper delivers impulsive blows which cause the open rim to vibrate radially in elliptic modes. It is modeled as a double dipole (quadrupole) who features are discussed in Sections 5. and 7.

Musical Wind Instruments (Fig. 9A.2.4)

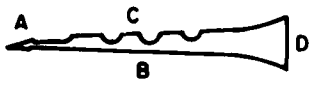

Fig. 9A.2.4

A reed *A* upon being blown generates periodic vortices. These excite a column of air *B* whose resonating length is controlled by holes *c* (or telescoping tubes). The bell (horn) *D* couples the sound to the medium. Its radiation is modeled as a monopole discussed in Section 1.7.

Musical Stringed Instruments (Fig. 9A2.5)

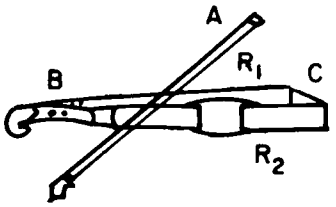

Fig. 9A.2.5

A bow *A* periodically or impulsively excites a resonator R_1 (string) whose resonant length is controlled by finger pressure and(or) tension *B*. The vibration is transmitted to resonator R_2 (wood box) via a bridge *C*. The radiation from the string is modeled as a dipole (Section 7) while that from the resonator R_2 as a vibrating plate (Section 1. A piano (or harpsicord) emits sound by impulsive excitation of a resonant string controlled by tension and thickness. The vibration is amplified by a second resonator (sounding board).

The human voice is a radiation generated by periodically or impulsively expelling breath across a resonator (vocal cords) whose resonant properties are controlled by tension and inter cord spacing. The sound is amplified and filtered by a sequence of auxiliary resonators (mouth cavity, sinuses, lips). The radiation itself is modeled as a monopole (Section 1.7).

Drum (Fig. 9A2.6)

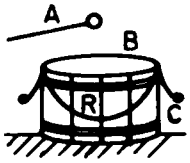

Fig. 9A.2.6

A drumstick *A* impulsively, or short burst periodically, strikes a resonator (drum membrane) whose resonant properties are controlled by tension screws and or finger pressure *C*. Membrane vibration is coupled directly to the volume resonator *R* which amplifies and filters the sound. The radiation from *B* is modeled as a vibrating membrane, Sect.

Gauze Tones (Fig. 9A2.7)

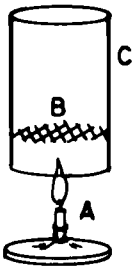

Fig. 9A.2.7

An exciting flame *A* heats a sheet of metal gauze *B* inside (at about 1/3 the length of) a long stiff tube *C*. When the flame is removed the heat gauze periodically excites the (air) column inside *C* which acts as a resonator. This generates the (Rijke) gauze tone of short duration. The maintenance of air column vibration is thought to be due to the in-phase interaction between the steady flow of air due to heat convection and the alternating flow of air due to air column vibration.

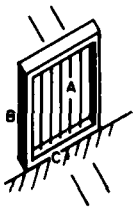

Fig. 9A.2.8

Aeolian Tones (Fig. 9A2.8)

Wind blowing across wires *A* under permanent tension in frame *B* breaks into periodic vortices. These drive the wires into resonant vibration which may be amplified by contact with a second resonator *C*. The radiation is modeled as dipole, Section 1.7.

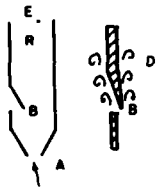

Fig. 9A.2.9

Edge Tones, Organ Pipes (Fig. 9A2.9)

A fluid *A* (air) in steady motion strikes an edge *B*. This creates a periodic train of vortices *D* which excite a resonant column of medium *R*. Radiation is modeled as a fluctuating volume (monopole) discussed in Sect. 1.7. The tone emitted depends on the length of the resonator. If the pipe is open it radiates from both *E* and *B*; if closed from *B* alone.

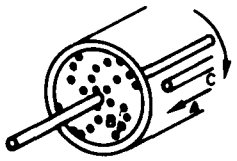

Fig. 9A.2.10

Sirene (Fig. 9A2.10) A disc *B* with radially spaced holes, placed at the end of a rigid pipe is rotated at a fixed angular speed. Air under pressure is conducted by a tube *C* located at a selected radius and is expelled into the succession of holes at the same radius in the disc. The resultant periodic sequence of a puffs of pressure constitute a fluctuation of volume which according to Section 1.7 radiates monopole sound.

Rockets (Fig. 9A2.11)

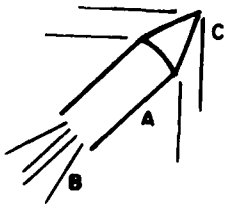

Fig. 9A.2.11

A rocket *A* is accelerated by emission of a gaseous mass, exhaust *B*. This exhaust, by creating time varying shear stresses in the medium, radiate sound through the mechanism of fluctuating gradients of force. This radiation, in the absence of rigid confining boundaries, is modeled as quadrupole, discussed in Sections 1.17, 5. and 7. If the rocket travels at supersonic speed it also radiates sonic booms discussed in Section 9.7c.

Propellers (Fig. 9A2.12)

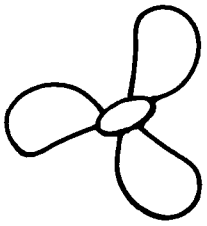

Fig. 9A.2.12

Propeller blades are smoothly contoured rigid objects rotating rapidly through uniform or non-uniforming flow of medium. Due to unsymmetrical shape of the blade the flow medium experiences local fluctuation of volume and of gradients of force. The resultant radiation is both monopole and dipole, and is discussed in Section 9.7b.

Moving Coil Loud Speaker (Fig. 9A2.13)

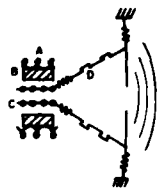

Fig. 9A.2.13

A periodic or impulsive electric current excites a magnetic field in coil *A* and iron-armature *B*. This field in turn drives the voice coil *C* which couples to a flexible cone *D* acting as a resonator, filter and acoustic amplifier. The radiation is modeled as that of fluctuating volumes (monopole), and is discussed in Section 1.7.

REFERENCES

1. V.A. Veshev, Sov. Phys. Acoust. **22**, 376-379 (1976).
2. P.M. Morse, U Ingard "Theoretical Acoustics," McGraw-Hill, 625 (1968).
3. Ref. 1, Eq. 16.
4. Ref. 1, Eq. 25.
5. V.N. Romanov, Sov. Phys. Acoust. **23**, 63-68 (1977).
6. O.A. Kudaskera, N.V. Sevryugora, Sov. Phys. Acoust., **22**, 216-219 (1976).
7. V.A. Kozyrev, E.L. Shenderov, Sov. Phys. Acoust. 26(3), p. 230 (1980).
8. JASA, **34**, 1553-1557 (1962).
9. J.E. Manning, G. Maidanik, JASA, **36**, 1691 (1964).
10. I.S. Gradshteyn, I.M. Ryzik "Tables of Integrals Series and Products," Academic Press, 1965, p. 196.
11. H. Bremmer, "Terrestrial Radio Waves," Elsevier, New York (1949).
12. M.V. Bernblit, Sov. Phys. Acoust. 23(4) July-Aug. 1977, page 301.
13. "The Annals of the Computation Laboratory of Harvard University," Vol. 18 (1949).
14. H. Stenzel, O. Broze "Leitfaden zur Berechrung von Schallvorgängen," Springer Verlag, 1958, p. 105.
15. L. Gutin, "On the Sound Field of a Rotating Air Screw" J. Tech. Phys. (USSR) **6**, 5 (1936).
16. R.H. Lyon, "Lectures on Transportation Noise."
17. W.M. Ewing, W.S. Jardetsky, F. Press, "Elastic Waves in Layered Media," McGraw-Hill, N.Y. 1957, p. 126.
18. C.L. Pekeris, "Theory of Propagation of Explosine Sound in Shallow Water," Goel. Soc. Amer. Mem. 17, 1948.

CHAPTER X
THERMAL GENERATION OF SOUND

10.1 THERMOOPTICAL SOURCES

In Sec. 1.8 the sound generated by injection of heat into a volume of fluid was modeled as a monopole whose source strength was,

$$q(\mathbf{r}_0,t) = \frac{\epsilon(\hat{\mathbf{r}}_0,t)\alpha\gamma\kappa}{c_p} = \frac{\epsilon(\mathbf{r}_0,t)\beta}{c_p} \qquad \text{(units: s}^{-1}\text{)}$$

in which $\epsilon(\mathbf{r}_0,t)$ (units: Nm m^{-3} s^{-1}) is the time rate of deposition of heat per unit volume, α (units: Nm^{-2} °K^{-1}) is the change in pressure per unit change in temperature at constant volume, γ is the ratio of specific heat at constant pressure c_p (units Nm m^{-3} °K^{-1}) to specific heat at constant volume, c_v, κ (units: m^2 N^{-1}) is the bulk compressibility of the medium, and β (units: °K^{-1}) is the coefficient of thermal expansion of the medium. When the source strength is very large, as in the case of powerful thermooptical converters, the parameter β is no longer taken to be the constant (measured at low amplitude) but becomes a function of ambient temperature and pressure, $\beta = \beta(T,p)$. At "high-enough" rates of heat injection the medium itself may exhibit nonlinear acoustic effects. We set these effects aside for the moment and consider the generation of sound at a local field point due to heat injection to be governed by the linear wave Eq. 1.7.3 in the velocity potential,

$$-\nabla^2\psi(\mathbf{r}_0,t) + \frac{1}{c_0^2}\frac{\partial^2\psi(\mathbf{r}_0,t)}{\partial t^2} = \frac{\epsilon(\mathbf{r}_0,t)\beta(T,p)}{c_p} \qquad \text{(units: s}^{-1}\text{).} \qquad (10.1.1)$$

Here we have chosen to omit the (arbitrary) factor 4π in the definition of source strength on the right hand side. Since acoustic pressure p (rather than velocity potential ψ) is the measurable field quantity one sets $p = \rho_0\partial\psi/\partial t$ and rewrites 10.1.1 in a second formulation,

$$-\nabla^2 p(\mathbf{r}_0,t) + \frac{1}{c_0^2}\frac{\partial^2 p}{\partial t^2}(\mathbf{r}_0,t) = \frac{\partial}{\partial t}\left[\beta\frac{\epsilon}{c_p^*}(\mathbf{r}_0,t)\right] \qquad \text{(units: Nm}^{-4}\text{)} \qquad (10.1.2)$$

c_p^* (units: m^2 °K^{-1} s^{-2}) is the specific heat per unit mass. There is a third formulation which has been preferred in those calculations which involve temperature rise ΔT due to the injection of heat. With the notice that at constant pressure and constant specific heat,

$$\epsilon = c_p\frac{\partial\Delta T}{\partial t} \qquad (10.1.3)$$

Eq. 10.1.2 can be reformulated as,

$$-\nabla^2 p(\mathbf{r}_0,t) + \frac{1}{c_0^2}\frac{\partial^2 p}{\partial t^2}(\mathbf{r}_0,t) = \rho_0\frac{\partial}{\partial t}\left[\beta\frac{\partial\Delta T}{\partial t}\right]. \qquad (10.1.4)$$

Equations 10.1.1 through 10.1.4 form the basis of modeling thermooptical generation of sound as a linear phenomonon.

The process of heat deposition caused by the interaction of high intensity light and a fluid medium is quite complex. An elementary, but useful, model of this deposition envisages a light beam of intensity $I(\mathbf{r}_0,t)$ (units: $\mathrm{Nms^{-1}\ m^{-2}}$) falling upon a medium whose absorption coefficient is α_0 (units: $\mathrm{m^{-1}}$) and penetrating a distance z_0. The space-time dependence of the intensity is assumed to be separable into a spatial component $I(x_0,y_0)e^{\alpha_0 z_0}$ and a temporal component $f(t/\tau_0)$,

$$I(\mathbf{r}_0,t) = I(x_0,y_0)e^{-\alpha_0 z_0} f(t/\tau_0) \tag{10.1.5}$$

in which τ_0 is the *characteristic time of energy-release*. If τ_0 is small relative to the diffusion time of the heat in the direction z then the deposition rate of heat h (units: $\mathrm{Nm\ m^{-3}}$) from 10.1.3 is modeled as,

$$\begin{aligned}
&\text{(a)}\quad \epsilon = \frac{\partial h}{\partial t} = \frac{\partial}{\partial t} c_p \Delta T \\
&\text{(b)}\quad h = \alpha_0 \tau_0 I(x_0,y_0) e^{-\alpha_0 z} \int_{-\infty}^{t/\tau_0} f(\xi)\, d\xi \qquad \text{(units: } \mathrm{Nm}m^{-3}\text{)} \\
&\text{(c)}\quad \Delta T = \frac{h}{c_p}.
\end{aligned} \tag{10.1.6}$$

In this model the temperature field is localized in a film thickness z_{eff} of the order α_0^{-1}. (Some authors use 3 to 5 times α_0^{-1}.)

Thus the linear acoustic equation governing the thermooptic generation of sound is modeled from 10.1.2 and 10.1.6 to be,

$$-\nabla^2 p(\mathbf{r}_0,t) + \frac{1}{c_0^2}\frac{\partial^2 p(\mathbf{r}_0,t)}{\partial t^2} = \frac{\partial}{\partial t}\left[\frac{\beta}{c_p^*}\frac{\partial}{\partial t}\alpha_0\tau_0 I(x_0y_0)e^{-\alpha_0 z}\int_{-\infty}^{t/\tau_0} f(\xi)\, d\xi\right] \tag{10.1.6}$$

Other, more complicated, models of thermooptic interaction will be noted later in this chapter.

10.2 SOLUTION OF EQ. 10.1.6 WHEN β IS CONSTANT

Assume, first, that in 10.1.6 the coefficient of thermal expansion (β) is a constant. Furthermore, to exemplify the time variation of heat deposition in a simple way let it be an elementary square wave,

$$\frac{\partial}{\partial t}\tau_0 \int_{-\infty}^{t/\tau_0} f(\xi)\, d\xi = U(t) - U(t+\tau_0) \tag{10.2.1}$$

in which $U(t)$ is the step function. Thus, 10.1.6 becomes,

$$-\nabla^2 p(\mathbf{r}_0,t) + \frac{1}{c_0^2}\frac{\partial^2 p}{\partial t^2}(\mathbf{r}_0,t) = \frac{\beta\alpha_0}{c_p^*} I(x_0,y_0)e^{-\alpha_0 z_0}[\delta(t) - \delta(t+\tau_0)]. \tag{10.2.2}$$

To solve 10.2.2 one begins by a Fourier transformation from t to ω:

$$\begin{aligned}
&\text{(a)}\quad (\nabla^2 + k^2)p(\mathbf{r}_0,\omega) = -Q(\mathbf{r}_0) \qquad \text{(units: } \mathrm{Nm^{-4}\ s}\text{)} \\
&\qquad\qquad p(\mathbf{r}_0,\omega) = \int_{-\infty}^{\infty} p(\mathbf{r}_0,t)e^{i\omega t}\, dt \qquad \text{(units: } \mathrm{Ns/m^2}\text{)} \\
&\text{(b)}\quad Q(x_0,y_0,z_0) = \frac{\beta\alpha_0\rho}{c_p} I(x_0,y_0)e^{-\alpha_0 z_0}[1 - e^{+\omega\tau_0}]
\end{aligned} \tag{10.2.3}$$

Since Q is a (temporal) density of true sources the acoustic field can be calculated from 1.7.9 by use of a suitable Green's function $G(\mathbf{r}/\mathbf{r}_0)$ constructed so that $\partial G/\partial n = 0$ at $z = 0$:

$$p(\mathbf{r},\omega) = \int_V Q(x_0,y_0,z_0)\, G(x,y,z\,|\,x_0,y_0,z_0)\, dV(x_0,y_0,z_0) \qquad \left[\text{units: } \frac{\text{Ns}}{\text{m}^2}\right] \tag{10.2.4}$$

In conformity with the theory of volume sources the negative sign of 10.2.3 disappears in 10.2.4. For the half-space Green's function, modified to be valid in the far field, we choose,

$$\begin{aligned} &G(\mathbf{r}/\mathbf{r}_0) \rightarrow \frac{e^{ikR}}{2\pi R} \exp\,(-ik_x x_0 - ik_y y_0 - ik_z z_0) \\ &R = (x^2 + y^2 + z^2)^{1/2} \\ &k_x = k\cos\phi\,\sin\theta;\;\; k_y = k\sin\phi\,\sin\theta;\;\; k_z = k\cos\theta \end{aligned} \tag{10.2.5}$$

(see Sec. 1.13). Substitution of 10.2.3 and 10.2.5 into 10.2.4, followed by a simple rearrangement, leads to the form,

$$\begin{aligned} &\text{(a)}\;\; p(\mathbf{r},\omega) = \alpha_0 \frac{\rho e^{ikR}}{2\pi R} \int_0^\infty e^{-\gamma z_0}\, dz_0 \iint_{-\infty}^{\infty} u(x_0,y_0) e^{-i[k_x x_0 + k_y y_0]}\, dx_0 dy_0 \\ &\text{(b)}\;\; \gamma = \alpha_0 + ik\cos\theta \qquad \text{(units: m}^{-1}\text{)} \\ &\text{(c)}\;\; u(x_0,y_0) = \frac{\beta I(x_0,y_0)}{c_p} \qquad \text{(units: ms}^{-1}\text{)}. \end{aligned} \tag{10.2.6}$$

In this formulation $u(x_0,y_0)$ is the *equivalent surface velocity* which is radiating sound from the plane $z = 0$ *into the half space* $0 \geqslant z < \infty$.

The integration of 10.2.6 over z_0 is standard:

$$\int_0^\infty e^{-\gamma z_0} dz_0 = \frac{\alpha_0 - ik\cos\theta}{\alpha_0^2 + k^2\cos^2\theta}. \tag{10.2.7}$$

In ordinary media (air, ocean) one can assume $\alpha_0 << |ik\alpha_0\cos\theta|$. Thus the α_0 term in the numerator of 10.2.7 can be neglected. To complete the integration it is necessary to select a model of the optical intensity $I(x_0,y_0)$ of the incident beam. A plausible model is a Gaussian distribution function,

$$I(x_0,y_0) = I_0 \exp\left[-\frac{x_0^2 + y_0^2}{a^2}\right]$$

in which a is the effective radius of the laser beam. Since

$$\int_{-\infty}^{\infty} dx_0 \exp\left[-\frac{x_0^2}{a^2}\right] \exp\,(-ikx_0\cos\phi\,\sin\phi) = a\sqrt{\pi}\,\exp\left[-\frac{k^2a^2\cos^2\phi\,\sin^2\theta}{4}\right]$$

[1] a subsequent integration over y_0 in conjunction with 10.2.7 then converts 10.2.6 to the form,

$$p(\mathbf{r},k) = -\frac{i\alpha_0\rho\beta I_0}{c_p}\,\frac{e^{ikR}}{2R}\left[\frac{ka^2\cos\theta}{\alpha_0^2 + k^2\cos^2\theta}\right]\exp\left[-\frac{k^2a^2\sin^2\theta}{4}\right](1 - e^{+ikcT_0}) \tag{10.2.8}$$

where, as before, $k = \omega/c$. To recover the time function one performs the inverse Fourier transform with respect to frequency,

$$p(\mathbf{r},t) = c\int_{-\infty}^{\infty} p(\mathbf{r},k)e^{ikct}\frac{dk}{2\pi} = cA\left[\int_{-\infty}^{\infty}\frac{e^{-\xi^2k^2}}{k^2+\zeta^2}\cos(ky)kdk + i\int_{-\infty}^{\infty}\frac{e^{-\xi^2k^2}}{k^2+\zeta^2}\sin(ky)kdk\right] \quad (10.2.9)$$

$$A = -\frac{i\alpha_0\rho\beta I_0}{c_p}\frac{a^2}{2R\cos\theta}\frac{1}{2\pi} \qquad \text{(units: Nsm}^{-3}\text{)}$$

$$\xi = \frac{a\sin\theta}{2}$$

$$\zeta = \frac{\alpha_0}{\cos\theta}$$

$$y_1 = R - ct, \quad y_2 = R - ct + c\tau_0.$$

In 10.2.9 the cosine term vanishes because it is an odd function of k. Since the sine term is an even function of k one can reduce 10.2.9 to the form,

$$p(\mathbf{r},t) = iA\,2c\int_0^{\infty}\frac{e^{-\xi^2k^2}}{k^2+\zeta^2}\sin(ky)kdk. \quad (10.2.10)$$

The integral is a sine transform of the argument. Its value is,

$$p(\mathbf{r},t) = iA\,2c\frac{\pi}{4}e^{\xi^2\zeta^2}\left[e^{-\zeta y_1}Erfc\left(\xi\zeta - \frac{y_1}{2\xi}\right) - e^{\zeta y_1}Erfc\left(\xi\zeta + \frac{y_1}{2\xi}\right)\right. \quad (10.2.11)$$

$$\left. - e^{-\zeta y_2}Erfc\left(\xi\zeta - \frac{y_2}{2\xi}\right) - e^{\zeta y_2}Erfc\left(\xi\zeta + \frac{y_2}{2\xi}\right)\right]$$

where

$$Erfc(x) = \frac{2}{\sqrt{\pi}}\int_x^{\infty}\exp(-t^2)dt.$$

[2]. If one writes

$$\text{(a)}\ \zeta y_1 = \frac{\alpha_0}{\cos\sigma}(R - ct) = \frac{R/c - t}{t_{\alpha_0}}, \quad \tau_{\alpha_0} = \frac{\cos\theta}{\alpha_0 c} \quad (10.2.12)$$

$$\text{(b)}\ \frac{y_1}{2\xi} = \frac{R - ct}{2\frac{a\sin\theta}{2}} = \frac{(R/c - t)}{\tau_a}, \quad \tau_a = \frac{a\sin\sigma}{c}$$

the symbols τ_{α_0} and τ_a can be interpreted as delay times associated with elementary thermal sources in a cylindrical volume πa^2 in horizontal area and α_0^{-1} in vertical depth: τ_{α_0} is the characteristic time (or delay time) accompanying the generation of the acoustic pressure from sources in a horizontal cross-section, and τ_μ is the characteristic time of sources in a vertical cross section [3].

To study the transient pulse shape at distance R as a function of time it is convenient to cite two extreme cases of 10.2.11.

Case I. $\xi\zeta >> 1$

In this case, since $\xi\zeta = \alpha_0 a \tan\theta/2$, one assumes that the thermal sources form a plane disk of large radius a or alternatively, one takes the observation angle θ to be large. In either case, the term $k^2 + \zeta^2$ in 10.2.10 is approximated by ζ^2 alone. The integral then becomes standard [4] and 10.2.10 reduces to,

$$p(\mathbf{r}_0,t) = \frac{iA\,2c}{\left(\frac{\alpha_0}{\cos\theta}\right)^2} \frac{\sqrt{\pi}}{4\left(\frac{a\sin\theta}{2}\right)^3} \tag{10.2.13}$$

$$\left\{(R - ct)\exp\left[-\frac{\left(\frac{R}{c} - t\right)^2}{\tau_a^2}\right] - (R - ct + c\tau_0)\exp\left[-\frac{\left(\frac{R}{c} - t + \tau_0\right)^2}{\tau_a^2}\right]\right\}.$$

The transient pressure at point R, θ, ϕ in the far field therefore consists of two pulses: the first is associated with the step function $U(t)$ of the laser illumination, and the second is associated with the step function $-U(t + \tau_0)$, Fig. 10.2.1,

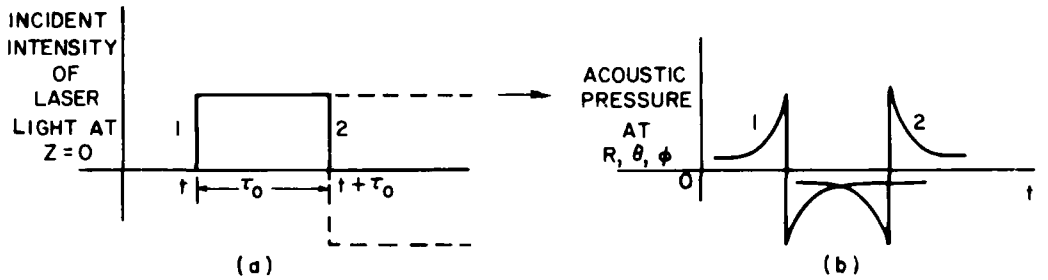

Fig. 10.2.1 — Sketch of the acoustic pressure pulses due to the incident light pulse

Kasoev and Lyamshev [3] have calculated 10.2.13 for both long and short laser pulses at different angles of observation which are large enough to satisfy the condition $\xi\zeta >> 1$. Their results are shown in Figs. 10.2.2 and 10.2.3. It is seen first that the transient fields are determined by τ_a and τ_0, and second, that as the laser pulse τ_0 becomes shorter in duration the acoustic pulses tend to run into each other.

Case II. $\xi\zeta << 1$

In this case the thermal sources constitute a narrow cylinder of small radius a, or alternatively the observation angle θ is small. The value of 10.2.10 is then determined primarily by values of $k \geqslant \zeta$ for which the exponential $\exp -\xi^2 k^2$ is negligible. Hence for $\xi\zeta << 1$,

$$p(\mathbf{r},t) = iA\,2c \int_0^\infty \frac{\sin(ky)\,kdk}{k^2 + \zeta^2} \tag{10.2.14}$$

$$p(\mathbf{r},t) = iA\,2c\,\frac{\pi}{2}\left\{e^{-y|\zeta|} - e^{-y\zeta}\right\}$$

[5].

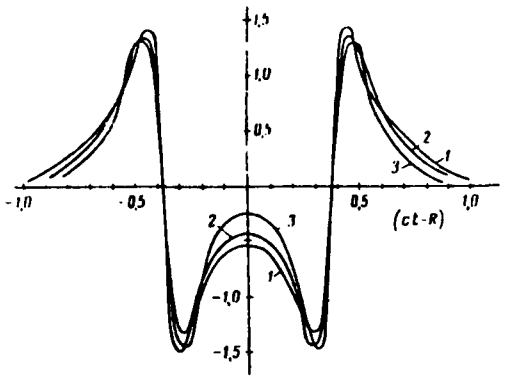

Fig. 10.2.2 — Relative acoustic pressure levels in water for a long laser pulse, $\tau = 5 \cdot 10^{-6}$ sec, $\mu = 5$ cm^{-1}, $a = 0.1$ cm, and three angles of observation. (1) $\theta = 30°$; (2) 45°; (3) 60°. Ref [3].

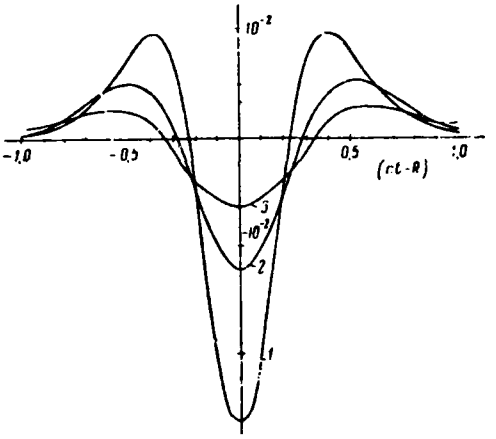

Fig. 10.2.3 — Relative acoustic pressure levels in water for a short laser pulse, $\tau = 5 \cdot 10^{-8}$ sec, $\mu = 5$ cm^{-1}, $a = 0.1$ cm, and the three angles of observation. (1) $\theta = 30°$; (2) 45°; (3) 60°. Ref. [3].

Because y_1 changes sign when $R = ct$, and y_2 changes sign when $R + c\tau = ct$ it will be useful to introduce the operator sgn $x = +$ when $x > 0$ and sgn $x = -$ when $x < 0$. Equation 10.2.14 may then be written

$$p(\mathbf{r},t) = i\,A2c\,\frac{\pi}{2}\left\{sgn(R-ct)\exp\left[sgn(R-ct)\frac{\left|\frac{R}{c}-t\right|}{\tau_\mu}\right]\right. \tag{10.2.15}$$

$$\left. - sgn(R-ct+c\tau_0)\exp\left[sgn(R-ct+c\tau_0)\frac{\left|\frac{R}{c}-t+\tau_0\right|}{\tau_\mu}\right]\right\}.$$

This expression is exact for observation angle $\theta = 0$ (along the axis of the laser beam). In the extreme case of very short laser pulse duration, $\tau_0/\tau_\mu << 1$, the acoustic response is primarily a negative excess pressure, Fig. 10.2.4.

The pulse shapes given by Figs. 10.2.2, 10.2.3, and 10.2.4 agree qualitatively with experimental measurements [6].

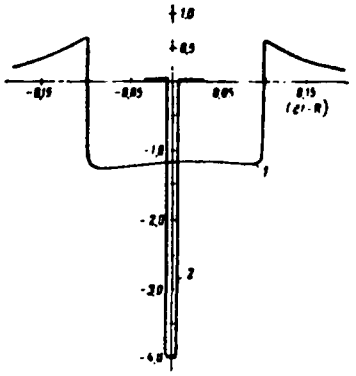

Fig. 10.2.4 — Relative acoustic pressure levels in water under the condition $\xi\zeta << 1$. (1) $\tau = 13 \cdot 10^{-6}$ sec, $\mu = 5$ cm^{-1}; (2) $\tau = 5 \cdot 10^{-6}$ sec, $\mu = 1$ cm^{-1}. Ref. [3].

10.3 SOUND GENERATION BY THERMAL SOURCES

Let $\epsilon(\mathbf{r}_0,t)$ (units: Nm m^{-3} s^{-1}) be the time rate of energy deposition in a small spherical volume (radius R_0). In a time interval τ_0 the energy deposited will be $dE = \epsilon\tau$ (units: Nm m^{-3}). Assume first that the ambient hydrostatic pressure is constant and that the deposited energy causes a rise in temperature ΔT (°K) in the volume. Before thermal diffusion occurs one has the thermodynamic relation,

$$dE = c_p \Delta T \tag{10.3.1}$$

in which c_p (units: °K^{-1} Nm m^{-3}) is the specific heat (per unit volume) at constant pressure. If the medium had time to expand under the influence of ΔT it would change volume (ΔV) by an amount determined by the coefficient of thermal expansion β:

$$\Delta V = \Delta T V \beta \qquad \text{(units: m}^3\text{)}. \tag{10.3.2}$$

Thus the energy injection into the volume would cause a potential volume increase,

$$dE = c_p \frac{\Delta V}{V\beta}. \tag{10.3.3}$$

However the time τ_0 is considered to be so short that the distance of wave propagation $c\tau_0$ at speed c is taken to be much smaller than the volume radius R_0. Then the volume expansion does not occur and the energy injection results in a rise in hydrodynamic pressure ΔP instead. The magnitude of ΔP is determined by the bulk compressibility k_s of the medium:

$$|\Delta P| = \frac{|\Delta V|}{V k_s} \qquad \text{(units: Nm}^{-2}\text{)}. \tag{10.3.4}$$

Using the value of ΔV from 10.3.3, and noting that the first (linear) approximation of the adiabatic compressibility $k_s = \rho c^2$ it is seen that the rise in pressure in the volume is,

$$\Delta P = \frac{\rho c^2 E \beta}{V c_p} \qquad \text{(units: Nm}^{-2}\text{)}. \tag{10.3.5}$$

Such a rise in pressure constitutes a sound source. The sound field generated by it can be calculated by means of methods described in Chap. I of this treatise, particularly Eq. (1.7.7).

10.4 RADIATION OF SOUND CAUSED BY TEMPERATURE OSCILLATIONS ON A PLANE SURFACE

On a surface $z = 0$ of a medium assume there is a temperature oscillation of value $\theta_0 \exp(-i\omega t)$. Let the medium have a thermal conductivity κ (units: Nm s^{-1} m^{-1} °K), a specific heat c_p (units: m^2 s^{-2} °K), and a density ρ_0 (units: Ns^2 m^{-4}). The ratio

$$\chi = \frac{\kappa}{\rho_0 c_p} \qquad \text{(units: m}^2\text{s}^{-1}\text{)} \tag{10.4.1}$$

is the *thermometric conductivity*. It is a quantity which can be used to establish a thermal length scale χ/c relative to the speed of sound and also a time χ/c^2. If the acoustic length scale at frequency ω is taken to be c/ω then the condition for effective radiation is given by the requirement that the acoustic length scale is much larger than the thermal length scale:

$$\frac{c_0}{\omega} >> \frac{\chi}{c_0}, \quad \text{or} \quad \frac{c_0^2}{c_0^2} >> \chi/\omega. \tag{10.4.2}$$

Hence it is assumed here that the period of one oscillation $(1/\omega)$ is much greater than the thermal time scale,

$$\frac{1}{\omega} >> \frac{\chi}{c_0^2}. \tag{10.4.3}$$

Now the equation of thermal conduction in one dimension is Fourier's equation,

$$\frac{\partial \theta}{\partial t} = \chi \frac{\partial^2 \theta}{\partial x^2}. \tag{10.4.4}$$

Since the surface is plane one can seek solutions in the form of thermal plane waves, $\theta = \theta_0 \exp(-i\omega t + ikx)$. Such solutions are possible when k has the special value

$$k = \left(\frac{i\omega}{\chi}\right)^{1/2} = 2i\sqrt{\frac{\omega}{2\chi}} = \pm (i+1)\sqrt{\frac{\omega}{2\chi}}. \tag{10.4.5}$$

[7].

The sign must be chosen to give physically decaying waves. Thus the thermal plane wave has the form

$$\theta(x,t) = \theta_0 \exp\left[-x\sqrt{\frac{\omega}{2\chi}}\right]\exp - i\omega\left[t - \frac{x}{c_\theta}\right] \tag{10.4.6}$$

$$c_\theta = \sqrt{2\chi\omega}$$

The thermal waves travel with the speed c_θ.

As the temperature oscillates on the surface the medium mass density also oscillates. The magnitude of oscillation above and below the ambient density is given by

$$\rho(t) = \left(\frac{\partial \rho}{\partial T}\right)_p \theta(t)$$

Since

$$-\frac{1}{\rho}\left(\frac{\partial \rho}{\partial T}\right)_p = \frac{1}{V}\left(\frac{\partial V}{\partial T}\right)_p = \beta$$

it is seen that in terms of the coefficient of thermal expansion β, the change in ρ is,

$$\rho(t) = -\rho_0 \beta \theta(t).$$

Now, in the Eulerian description of motion in which events in a fixed volume are described, any change of density with time must be due to the flow of mass across the boundary,

$$\rho_0 \frac{\partial v}{\partial x} = -\frac{\partial \rho}{\partial t} = i\omega\rho_0\beta\theta.$$

The velocity reached in distance x^* is,

$$v(x^*) = -i\omega\beta\theta_0 \int_0^{x^*} \exp\left[-x\sqrt{\frac{\omega}{2\chi}}\right]\exp - i\omega\left[t - \frac{x}{c_\theta}\right]dx. \tag{10.4.7}$$

Here, x^* is of the order of $(\chi/\omega)^{1/2}$, after which it is effectively zero. Thus the range of integration can be extended to infinity without error. The result of integration is,

$$v = \frac{1-i}{\sqrt{2}} \beta \sqrt{\omega\chi}\, \theta_0 e^{-i\omega t} \tag{10.4.8}$$

[8].

The power radiated per unit surface area due to oscillations of temperature of magnitude θ_0 varying sinusoidally in time on the surface is:

$$I = \frac{1}{2} \rho_0 c_0 \beta^2 \omega \chi \theta_0^2 \qquad \text{(units: Nmm}^{-2}\text{s}^{-1}\text{)} \tag{10.4.9}$$

When the medium is water the relevant constants to good approximation at 20°C, are,

$$\rho_0 = 10^3 \frac{\text{Ns}^2}{\text{m}^4};\ c_0 = 1.5 \times 10^3 \frac{\text{m}}{\text{s}};\ \beta = 1.4 \times 10^{-4}\ ^\circ\text{K}^{-1}$$

$$\chi = 1.48 \times 10^{-7} \frac{\text{m}^2}{\text{s}};\ \kappa = 0.619 \frac{\text{Nm}}{\text{sm}(^\circ\text{K})}.$$

A simple calculation reveals the thermal-acoustic conversion efficiency. Let the frequency $(\omega/2\pi)$ be 10^3 Hz, and the temperature fluctuation be 100°C: then

$$I = \frac{1}{2} \times 1.5 \times 10^6 \times (1.4 \times 10^4)^2 2\pi \times 10^3 \times 1.48 \times 10^{-7} \times (10^2)^2$$

$$I = 1.37 \times 10^{-1} \frac{\text{watts}}{\text{m}^2}.$$

For plane waves this acoustic intensity corresponds to an acoustic pressure $p = \sqrt{\rho_0 c_0 I} = \sqrt{1.5 \times 10^6 \times 1.37 \times 10^{-1}} = 4.53 \times 10^2\ \text{N/m}^2$ which is 53 dB re 1 Pa or 173 dB re 1 μ Pa.

10.5 SOUND RADIATED BY A COLLAPSING BUBBLE CONTAINING SUPERHEATED VAPOR

10.5a GROWTH RATES OF SUPERHEATED BUBBLES

A bubble forms in a fluid when, in a volume (called a nucleus), the hydrodynamic pressure inside is greater than outside. Such an unbalance of forces causes the bubble radius R to increase as a function of time.

The equation of radial motion of a bubble wall begins with an extended version of the early formulation of Rayleigh. To set this up we note that the rate of change of volume velocity of a bubble of radius R is

$$\frac{d}{dt}\left(\frac{d4}{dt3}\pi R^3\right) = 4\pi(2R\dot{R}^2 + R^2\ddot{R}). \tag{10.5.1}$$

If one assumes the liquid is incompressible and then applies Bernoulli's law of the flow of an incompressible fluid, one arrives at an equation of motion

$$\frac{R^2\ddot{R} + 2R\dot{R}^2}{r} - \frac{R^4\dot{R}^2}{2r^4} = \frac{p_{\text{int}} - p_{\text{ext}}}{\rho_f} \tag{10.5.2}$$

in which r is any radius $\geqslant R$ and the right-hand side is the difference between the internal pressure and the external pressure (divided by ρ_f). Setting $r = R$ and writing the internal pressure as the sum of the vapor pressure p_v and the permanent gas pressure p_g and the external pressure as the sum of the surface-tension pressure p_σ and the hydrostatic pressure p_∞, one can then write

$$\rho_f\left[R\ddot{R} + \frac{3}{2}\dot{R}^2\right] p_v + p_g - \left[p_\infty + \frac{2\sigma}{R}\right]. \tag{10.5.3}$$

We assume now that the dynamic force which causes the bubble to expand is provided by a temperature difference ΔT between the temperature T_{int} of saturated vapor in the interior of the bubble and temperature T_∞ of the fluid a great distance from the bubble. To simplify matters, one first neglects the internal gas pressure and then relates the quantity $\Delta p = p_v - p_\infty$ to the change in temperature ΔT by means of the Clausuis-Clapeyron equation

$$\Delta p = \frac{L}{T(v_v - v_f)}\Delta T \tag{10.5.4}$$

in which v_v and v_f denote the specific volume (units: m^3/Kg or m^4/Ns^2) of the vapor and fluid respectively, L is the latent heat of vaporization, (units: N-m/Kg or m^2/s^2) and ΔT is the rise in temperature above T. The temperature difference ΔT is determined by the solution of a problem involving heat conduction across a moving surface of evaporation (in spherical geometry). The solution for heat input of heat Q (units: Nm m^{-3} s^{-1}) is [9],

$$\text{(a)}\quad \Delta T(t) = \frac{-L\rho_v}{C_{p(f)}(\pi D)^{1/2}\rho_f} J(t) + \Delta\tau + \frac{Qt}{\rho_f C_{p(f)}}. \tag{10.5.5}$$

$$\text{(b)}\quad J(t) = \int_0^t \frac{R(t')\dot{R}(t')}{R(t)(t-t')^{1/2}}\left\{\exp\left[-\frac{(R-R')^2}{4D(t-t')}\right] - \exp\left[-\frac{(R+R')^2}{4D(t-t')}\right]\right\}dt'$$

Here ρ_v is the density of the vapor, $C_{p(f)}$ is the specific heat of the fluid (units: $m^2{}^\circ K^{-1}s^{-2}$), and D is the diffusivity (or thermometric conductivity) (units: m^2s^{-1})

The integral $J(t)$ is a functional of $R(t)$, that is, it is not a unique number but a range of numbers whose values are functions of time.

Substituting 10.5.4, 10.5.5 into the equation of motion, one obtains

$$R\ddot{R} + \frac{3}{2}\dot{R}^2 + \frac{\alpha}{R} - \beta + \gamma J(t) = Q^* t, \tag{10.5.6}$$

where

$$\alpha = \frac{2\sigma}{\rho_f},\ \beta = \frac{L\Delta\tau}{\rho_t T(v_v - v_f)},\ \gamma = \frac{L^2\rho_g}{\rho_f^2 T(v_v - v_f)(\pi D)^{1/2}C_{p(f)}},$$

$$Q^* = \frac{QL}{\rho_f^2 C_{p(f)} T(v_v - v_f)}.$$

This is an integral-differential equation in $R(t)$. A more revealing equation can be obtained by introducing the concept of *critical radius.* This is done by noting that for superheat $\Delta\tau$ there is a corresponding pressure rise

$$\Delta p_s = \frac{L\Delta\tau}{T(v_v - v_f)} = \beta\rho_f. \tag{10.5.7}$$

The bubble radius corresponding to a surface tension σ at pressure Δp_s is called the critical radius.

$$R_{crit} = \frac{2\sigma}{\Delta p_s} = \frac{2\sigma}{\beta\rho_f} = \frac{\alpha}{\beta}. \tag{10.5.8}$$

Dividing the equation of motion by R_{crit}^2, one has the more useful form,

$$r\ddot{r} + \frac{3}{2}\dot{r}^2 - \frac{A(r-1)}{r} + BJ = qt, \tag{10.5.9}$$

where

$$A = \frac{2\sigma}{\rho_f R_{crit}^3},\quad B = \frac{\gamma}{R_{crit}^2},\quad q = \frac{Q^*}{R_{crit}^2},\quad r = \frac{R}{R_{crit}}.$$

Because of the functional integral $J(t)$ the solution of this equation is intractable as it stands. Hence a general formula $r(t)$ for all time t is not available. Forster and Zuber [9] demonstrate that for very small bubbles one can neglect the water inertia during growth. They then reduce the problem to the solution of an integral equation of the Volterra type,

$$\frac{r-1}{r} + \frac{qt}{A} = \frac{1}{C^* r}\int_0^t \frac{r(t')\dot{r}(t')}{(t-t')^{1/2}}\,dt',\quad C^* = \frac{A}{BR_{crit}}, \tag{10.5.10}$$

in which $J(t)$ has been reduced by various arguments to the integral shown. Even this form is intractable. However an upper limit for $r(t)$ may be obtained by using the mean-value theorem to calculate the integral (which then becomes $2r\dot{r}t^{1/2}$). Using this approximation and assuming $\frac{qt}{A}$ is small relative to the other terms, one finally arrives at a solution for $r(t)$ implicitly given by

$$r + \ln\frac{r-1}{r_1 - 1} = C^* t^{1/2},\quad t > \left(\frac{r_1}{C^*}\right)^2. \tag{10.5.11}$$

The initial condition is $r = r_1$ for $t = r_1^2/C^{*2}$. To start the numerical calculation, one assumes r_1 is slightly greater than 1, say $r_1 = 1.01$. Since

$$C^* = \frac{A}{BR_{crit}} = \frac{2\sigma}{\rho_f R_{crit}^3}\,\frac{\rho_f^2 T(v_v - v_f)(\pi D)^{1/2} C_{p(f)} R_{crit}^2}{L^2 \rho_v R_{crit}}$$

$$= \frac{\rho_f \Delta T(\pi D)^{1/2} C_{p(f)}}{R_{crit} L \rho_v},$$

we can interpret ΔT to be the initial superheat. Hence

$$C^* = \frac{\Delta\tau\, C_{p(f)}(\pi D)^{1/2} v_v}{R_{crit} L v_f}. \tag{10.5.12}$$

This is a useful formula for estimating the numerical value of the right-hand side of the solution. To obtain a feeling for the magnitude of the terms and parameters involved we will calculate the following case.

The liquid (water) is superheated 5°C above boiling at atmospheric pressure. We desire to find R_{crit} and the time required to form a bubble of radius $R = 20\,\mu$m.

Solution: The thermodynamic chart for water shows that at $T = 373 + 5 = 378$°K, $v_v = 27$ ft^3/lb, $v_f = 0.02$ ft^3/lb, $L = 974$ Btu/lb, $C_j = 4.18$ J/g/°K, and $D = 1.43 \times 10^{-3}$ cm^2/s. Then

$$\beta = \frac{L\Delta\tau\, v_f}{T(v_v - v_f)} = \frac{(974\times 2.32)(\text{J/g}) \times 5\,\text{°K} \times 0.02 \times 62.4\ \text{cm}^3/\text{g}}{378\,\text{°K}[(27 - 0.02) \times 62.4]\ \text{cm}^3/\text{g}}$$

$$= 2.3 \times 10^5\ \text{cm}^2/\text{s}^2$$

and

$$\alpha = \frac{2\sigma}{\rho_f} = 2\sigma\, v_f = 2 \times 50 \times 0.02 \times 62.4 = 124.8\ \text{cm}^3/\text{s}^2.$$

Therefore

$$R_{crit} = \frac{\alpha}{\beta} = \frac{124.8\text{cm}^3/\text{s}^2}{2.3 \times 10^5\text{cm}^2/\text{s}^2} = 5.6 \times 10^{-4}\ \text{cm} = 5.6\,\mu\text{m}.$$

From this

$$C^* = \frac{\Delta\tau\,(\pi D)^{1/2} C_f v_v}{R_{crit} L v_f}$$

$$C = \frac{5\,\text{°K}(\pi \times 1.43 \times 10^{-3})^{1/2}\text{cm/s}^{1/2} \times 4.18(\text{J/g °K}) \times 27 \times 6.24\ \text{cm}^3/\text{g}}{5.6 \times 10^{-4}\ \text{cm} \times 974 \times 2.32(\text{J/g}) \times 0.02 \times 6.24\ \text{cm}^3/\text{g}}.$$

$$= 1494\ \text{s}^{-1/2}.$$

Since $r = R/R_{crit} = 20\,\mu\text{m}/5.6\,\mu\text{m} = 3.57$, we find

$$r + \ln\frac{r-1}{r_1 - 1} = C^* t^{1/2}$$

or

$$3.57 + \ln\frac{2.57}{0.01} = 1494 t^{1/2}$$

or

$$t = 37\,\mu\text{s}.$$

This is approximately the result that Forster and Zuber show in their Fig. 1 [9] where $R = 2 \times 10^{-3}$ cm corresponds to a formation time of about $30\,\mu$s. Note that t depends on C^* inversely; that is, the higher the superheat, the faster the time of formation of a bubble of specified size.

The difficulties associated with a general theory of bubble formation and collapse has led to simplifications which give ready (and fair) estimates of the underlying physical events.

10.5b SIMPLIFIED THEORY OF THE GROWTH AND COLLAPSES OF BUBBLES

A spherical expanding (or collapsing) surface of radius $R(t)$ in a incompressible medium has a velocity potential at any radius $r \geqslant R$ given by

$$\psi = \frac{R^2\dot{R}}{r}. \tag{10.5.13}$$

The surface velocity at r is then,

$$u(r) = -\frac{\partial\psi}{\partial r} = \frac{R^2\dot{R}}{r^2}. \tag{10.5.14}$$

Application of this form to the hydrodynamic law of *accelerative* flow leads to the equation of motion

$$R\ddot{R} + \frac{3}{2}\dot{R}^2 = \frac{-p_\infty}{\rho_f}, \quad \text{(collapse phase)}. \tag{10.5.15}$$

The left hand side can be integrated with respect to time by use of the integrating factor $2R^2\dot{R}$ to give $R^3\dot{R}^2$. The same integrating factor also permits the right hand side to be integrated over the limits $R(t)$ and $R(0)$. Thus,

$$\dot{R}^2 = \frac{2}{3}\frac{p_\infty}{\rho_f}\left[\frac{R^3(0) - R^3(t)}{R^3(t)}\right], \quad \text{collapse phase)}. \tag{10.5.16}$$

Taking the inverse of this equation, then changing variable $R = R(0)x^{1/3}$ and integrating with respect to x Rayleigh found the time of collapse to be,

$$T_c = 0.915\, R_{MAX}\sqrt{\frac{\rho_f}{p_\infty}} \tag{10.5.17}$$

[10]. Here $R_{MAX} = R(0)$.

The growth of a spherical cavity can similarly be described. In this case the driving pressure p_v (assumed constant during expansion) expands the bubble from a minimum radius $R_{MIN} = R(0)$. The equation of growth is,

$$R\ddot{R} + \frac{3}{2}\dot{R}^2 = \frac{p_v}{\rho_f}$$

Integration with respect to time leads to

$$\dot{R}^2 = \frac{2}{3}\frac{p_v}{\rho_f}\left[\frac{R^3(t) - R^{3}_{MIN}}{R^3(t)}\right], \quad \text{(growth phase)}. \tag{10.5.18}$$

In a more complicated but still useful model a spherical cavity expands from an initial radius R_{MIN} under the action of an initial internal pressure p_{max}. One can assume in first approximation that the expansion is *adiabatic* so that the internal pressure, for any radius R is

$$p_v = p_{max}\left[\frac{R^3_{min}}{R^3}\right]^\gamma \tag{10.5.19}$$

where γ is the ratio of specific heat of constant volume to the specific heat at constant pressure of the medium inside the cavity. The dynamic equation of motion of the expansion phase is given by 10.5.3 with the right hand side replaced by 10.5.19,

$$R\ddot{R} + \frac{3}{2}\dot{R}^2 = \frac{p_{max}}{\rho_f}\left[\frac{R_{min}^3}{R^3}\right]^{\gamma} \tag{10.5.20}$$

Here the positive direction of $\dot{R}^2(t)$ is chosen to be *outward*. Upon integration it is found that

$$\dot{R}^2 = \frac{2C_0^2}{3(\gamma-1)}\left\{\left[\frac{R_{min}}{R}\right]^3 - \left[\frac{R_{min}^3}{R^3}\right]^{\gamma}\right\}, \quad \text{(growth phase)} \tag{10.5.21}$$

$$C_0^2 = \frac{p_{max}}{\rho_f}.$$

From 10.5.20 and 10.5.19 one concludes that the initial acceleration is,

$$\ddot{R}(0) = \frac{C_0^2}{R_{min}} \tag{10.5.22}$$

and the maximum radial velocity is,

$$\dot{R}_{MAX} = \sqrt{\frac{2C_0^2}{3\gamma^{\gamma/(\gamma-1)}}} \tag{10.5.23}$$

which occurs when

$$\left[\frac{R^3}{R_{min}^3}\right]^{\gamma-1} = \gamma \tag{10.5.24}$$

[10].

The initial theory of bubble collapse, as analyzed by Rayleigh assumed the bubble cavity is a void. This assumption leads to difficulties in predicting events toward the end of the collapse process. A more refined analysis introduces the following corrections.

During the final stage of collapse the pressure p_g of *permanent* gases, initially neglected, must be inserted in the equation of motion in order to arrest the motion of collapse. Assuming isothermal contraction of these gases, Rayleigh [11] subtracted the potential energy of the permanent gases from the kinetic energy of the fluid and found the minimum radius of bubble R_{min} (at the point when the radial velocity R vanished) to be,

$$R_{min} \approx R_{max}\exp\left[-\frac{p_\infty}{3p_g(0)}\right] \tag{10.5.25}$$

in which $p_g(0)$ is the initial gas pressure. The maximum pressure reached in the cavity is then easily found (based on isothermal collapse) to be,

$$p_{max} = p_g(0)\left[\frac{R_{max}^3}{R_{min}^3}\right] = p_g(0)\exp\left[\frac{p_\infty}{p_g(0)}\right]. \tag{10.5.26}$$

When $p_g(0)/p_\infty = 0.01$ this formula predicts $p_{max} = 2.68 \times 10^{41}\, p_\infty$. In view of such predictions one can infer that on physical grounds it is more likely that the final stages of collapse are thermodynamically adiabatic rather than isothermal. A model of adiabatic collapse is obtained by inserting a term like 10.5.19 into the right hand side of 10.5.3,

$$R\ddot{R} + \frac{3}{2}\dot{R}^2 = -\frac{p_\infty}{\rho_f} + \frac{p_g(0)}{\rho_f}\left[\frac{R_{max}^3}{R^3}\right]^{\gamma} \quad \text{(collapse phase)}. \tag{10.5.26}$$

[12]. Upon solving this equation for $\dot{R}$ and setting it to zero it is found that the minimum bubble radius upon collapse is estimated to be,

$$R_{\min} \approx R_{\max} \left[\frac{p_g(0)}{p_\infty(\gamma - 1)} \right]^{\frac{1}{3(\gamma-1)}} \left[1 + \frac{p_g(0)}{p_\infty(\gamma - 1)} \right]^{-\frac{1}{3(\gamma-1)}} \tag{10.5.27}$$

provided $R_{\min} < 1/3\ R_{MAX}$. The gas pressure inside the bubble at this minimum radius is then,

$$p_{g(MAX)} \approx p_g(0) \left[\frac{p_\infty(\gamma - 1)}{p_g(0)} \right]^{\frac{\gamma}{\gamma-1}} \left[1 + \frac{p_g(0)}{p_\infty(\gamma - 1)} \right]^{\frac{\gamma}{\gamma-1}}. \tag{10.5.28}$$

When $p_\infty/p_g(0) = 100$, this formula predicts (for the choice $\gamma = 4/3$) a maximum pressure of about $1.2 \times 10^4\ p_\infty$, which is within reason. Also since the compression is adiabatic the maximum temperature at the termination of collapse is found from thermodynamic relations to be,

$$\theta_{\max} = \theta(0)\ \frac{p_{\max}}{p_g(0)} \left(\frac{R^3_{\min}}{R^3_{\max}} \right) = \theta(0) \left[\frac{p_\infty(\gamma - 1)}{p_g(0)} \right] \left[1 + \frac{p_g(0)}{p_\infty(\gamma - 1)} \right]. \tag{10.5.29}$$

In actual calculation the key Eq. (10.5.27) plays a major role in predicting the sound radiated by a collapsing bubble. However; its usefulness depends on a good estimate of the partial pressure of the initial gas pressure $p_g(0)$.

These results, and indeed all results based on 10.5.3, are based on the assumption that the fluid motion at any stage of growth or collapse shows no effect of fluid compressibility. One can say that as long as the radial velocity of bubble collapse is much less than the speed of sound no such effects of compressibility will modify these predictions. A reasonable limit of validity of incompressible theory is roughly estimated at a ratio M of fluid velocity to speed of sound of $M = 1/3$. Since the theory based on 10.5.26 predicts a maximum fluid velocity to be,

$$\dot{R}^2_{\max} \approx \frac{2}{3}\ \frac{p_\infty(\gamma - 1)}{\rho_f \gamma} \left[\frac{p_\infty(\gamma - 1)}{p_g(0)} \right]^{\frac{1}{\gamma-1}} \left[1 + \frac{p_g(0)}{p_\infty(\gamma - 1)} \right]^{\frac{\gamma}{\gamma-1}} \tag{10.5.30}$$

it is seen that this validity of Eq. 10.5.26 through 10.5.29 depends upon the ratio $p_g(0)/p_\infty$, and upon p_∞. For $M \approx 1/3$ and $\gamma = 4/3$ one calculates that at $p_\infty = 1$ atmos, $p_g(0)/p_\infty$ must be greater than 1%, at $p_\infty = 10$ atmos, $p_g(0)/p_\infty$ must be greater than 3%, etc. in order for incompressible theory to be valid.

10.5c ACOUSTIC RADIATION FROM A COLLAPSING BUBBLE

A spherical bubble collapsing in a fluid can be treated as a monopole radiator for which 7.1.9 is the governing formula:

$$p(r,t^*) = \frac{\rho_f \ddot{\mathcal{V}}(t^*)}{4\pi r}, \quad t^* = t - \frac{r}{c}. \tag{10.5.31}$$

The volume acceleration at any instant is,

$$\ddot{\mathcal{V}}(t) = \frac{d^2}{dt^2} \left(\frac{4\pi}{3} R^3 \right) = 4\pi R [R\ddot{R} + 2\dot{R}^2]. \tag{10.5.32}$$

The radial acceleration $\ddot{R}$ is obtainable from 10.5.3. In the present application of radiation of sound from a collapsing bubble we use the simplest model by neglecting p_v, p_g and surface tension:

$$R\ddot{R} = -\frac{p_\infty}{\rho_f} - \frac{3}{2}\dot{R}^2. \tag{10.5.33}$$

Substitution of this into 10.5.32 leads to,

$$\ddot{\mathscr{V}}(t) = 4\pi R\left[-\frac{p_\infty}{\rho_f} + \frac{1}{2}\dot{R}^2\right].$$

From 10.5.16 this becomes

$$\begin{aligned}
\ddot{\mathscr{V}}(t) &= 4\pi R\left\{\frac{-p_\infty}{\rho_f} + \frac{1}{2}\left[\frac{2}{3}\frac{p_\infty}{\rho_f}\left[\frac{R_{\max}^3}{R^3} - 1\right]\right]\right\} \\
\ddot{\mathscr{V}}(t) &= 4\pi\left\{\frac{1}{3}\frac{p_\infty R}{\rho_f}\left[\frac{R_{\max}^3}{R^3}\right] - \frac{4}{3}\frac{p_\infty R}{\rho_f}\right\} \\
\ddot{\mathscr{V}}(t) &= \frac{p_\infty}{\rho_f}\frac{V_{\mathrm{MAX}}}{R^2(t)}\left[1 - 4\frac{R^3(t)}{R_{\mathrm{MAX}}^3}\right]
\end{aligned} \tag{10.5.34}$$

where V_{MAX} is the volume of the bubble at the initiation of collapse. This formula, together with 10.5.31, allows one to predict the peak positive acoustic pressure at any observation radius r in terms of the minimum bubble radius R_{MIN} *which occurs at the termination of the collapse*,

$$p_{\mathrm{MAX}}^{+} = \frac{1}{3}p_\infty\frac{R_{\mathrm{MAX}}}{r}\left[\frac{R_{\mathrm{MAX}}^2}{R_{\mathrm{MIN}}^2}\right]\left[1 - 4\left[\frac{R_{\mathrm{MIN}}^3}{R_{\mathrm{MAX}}^3}\right]\right]. \tag{10.5.35}$$

An estimate of R_{MIN}, difficult to make in any case, can be inferred from 10.5.27 by estimating the initial pressure $p_g(0)$ of the permanent gases in the cavity.

The *total energy* $E_{c(\mathrm{RAD})}$ *radiated during the collapse phase* is obtained by noting that

$$E_{c(\mathrm{RAD})} = \int_0^\infty \frac{p^2}{\rho_f c_f} 4\pi r^2\, dt = \frac{\rho_f}{4\pi c_f}\int_0^t \ddot{\mathscr{V}}^2(t)\, dt. \tag{10.5.36}$$

Since $\dot{R}dt = dR$,

$$E_{c(\mathrm{RAD})} = \frac{\rho_f}{4\pi c_f}\int_{R_{\mathrm{MIN}}}^{R_{\mathrm{MAX}}} \frac{\ddot{\mathscr{V}}^2\, dR}{\dot{R}}. \tag{10.5.37}$$

Using 10.5.34 as a reasonable estimate of $\ddot{V}$, and calculating $R_{\min}$ from 10.5.27, the integration called for by this equation can be *approximated* on the assumption that $p_g(0)/p_\infty$ is of the order of 2% to 10%. In this case,

$$E_{c(\mathrm{RAD})} \approx p_\infty V_{\mathrm{MAX}} \times \frac{1}{3}\left[\frac{R_{\mathrm{MAX}}^3}{R_{\mathrm{Min}}^3}\right]^{1/2}\sqrt{\frac{2}{3}\frac{p_\infty}{\rho_f c_f^2}}. \tag{10.5.38}$$

This is the energy of a single collapse event. A rough estimate shows that near the value $p_g(0)/p_\infty \sim 2\%$ the radiated energy lies between 1/4 and 1/2 of the total potential energy in the bubble at its initial maximum radius, and that at $p_g(0)/p_\infty \sim 10\%$ the radiated energy lies between 1/20 and 1/10 of that value. When $p_g(0)/p_\infty$ is much less than $\sim 2\%$ Eq. 10.5.38 overestimates the radiated energy. A convenient rule of thumb that can be used in this case is that the energy radiated for *all* initial and subsequent collapses of the single bubble is about 2/3 of the potential energy $p_\infty V_{\mathrm{MAX}}$ at the start of the initial collapse. Thus as $p_g(0)/p_\infty$ becomes extremely small the total radiated energy for all cycles of collapse and rebound of a single bubble is approximately 2/3 of the initial potential energy of the bubble. These qualitative statements are pictured in Fig. 10.5.1 as calculated by Ref. [13]. This figure enables one to make rough estimates of radiation from single bubbles in the course of its life history.

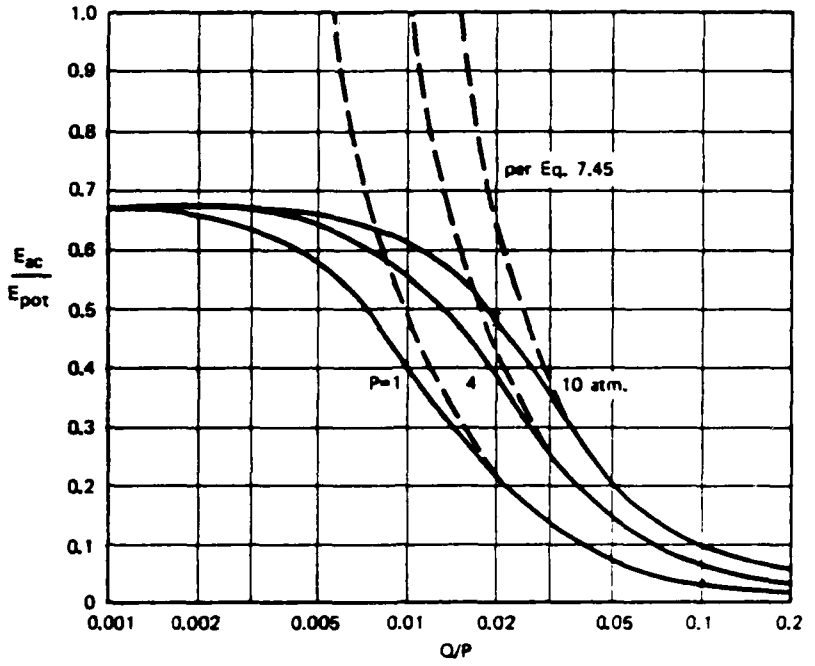

Fig. 10.5.1 — Fraction of energy radiated from a single collapsing bubble vs partial gas pressure (after Ross [13]).

10.6 RADIATION OF SOUND FROM CAVITATING VOLUMES

In Lighthill's theory of noise generated by fluid flow [14] the origin of the noise is attributed to net mechanical stresses T acting to change the temporal and spatial character of the mass density ρ of the fluid at a point. Thus sound generation is attributed to hydrodynamic (in this case turbulent) fluid motion over a volume of the fluid. Because the medium is compressible these changes in ρ are propagated away. A simple model of the propagation process can be formulated from the discussion in Section 1.8.

$$\frac{\partial^2 \rho}{\partial t^2} - c^2 \nabla^2 \rho = \frac{\partial^2 T_{ij}}{\partial x_i \partial x_j} \tag{10.6.1}$$

$$T_{ij} = \rho v_i v_j + p_{ij} - c^2 \delta_{ij} \rho'.$$

Here T_{ij} are components of the stress tensor T at point $x = (x,y,z)$. T_{ij} is the sum of (1) the Reynolds stress $\rho v_i v_j$ due to flow velocity v, (2) the static stress p_{ij} whose diagonal elements (on being averaged) make up the hydrodynamic pressure $(-p)$ in the fluid and whose off-diagonal elements constitute the viscous (or shear) stresses, and (3) the acoustic pressure proportional to the incremental change in mass density ρ'.

Suppose now there is a volume V_c of liquid of instantaneous mass density $\rho_c(t)$ which is driven into cavitation. Its mass density can then be written in terms of a parameter $b(t)$,

$$\rho(t) = \frac{\rho_c(t)}{1 + b(t)} \tag{10.6.2}$$

$$b(t) = \frac{4}{3} \pi n (R^3(t) - R_{MAX}^3) \quad \text{(units: } m^3 m^{-3}\text{)}$$

in which n is the number of bubbles per unit cavitating volume, each bubble having a time history of volume collapse described by the radius $R(t)$. There are two species of fluctuations described by this equation. The first are fluctuations $\rho_c(t)$ due to stress T_{ij} of 10.6.1. The second are additional fluctuations in mass density due to the cavitation effect $b(t)$. For many cases of interest we can assume that the fractional change in density (= $b(t)$) is small relative to unity so that $\rho(t)$ can be approximated by,

$$\rho(t) = \rho_c(t)(1 - b(t)).$$

In addition we further assume that only the Reynolds stress and terms involving $b(t)$ are significant in generating sound by collapsing bubbles in a fluid which has turbulent motion. Thus, the propagation of ρ_c in this case is governed by the relation [15],

$$\left[\frac{\partial^2}{\partial t^2} - c_0^2\nabla^2\right]\rho_c(\mathbf{x},t) \approx \rho_0 \frac{\partial^2 v_i v_j}{\partial x_i \partial x_j} - \rho_0 \frac{\partial^2 b(t) v_i v_j}{\partial x_i \partial x_j} + \rho_0 \frac{\partial^2 b(t)}{\partial t^2} \qquad (10.6.3)$$

in which ρ_0 is the background liquid density taken to be large compared to any density fluctuation caused by whatever agency, and c_0 is the background (homogeneous) sound speed. The source term due to $\nabla^2\rho_0 b$ is assumed negligible inside the cavitation volume V_c where the time t of bubble collapse is so short that ct is considerably smaller than the radius of V_c.

Equation 10.6.3 describes the changes in mass density everywhere, both inside and outside the cavitation volume, caused by sources (= right hand side) which derive energy from flow and cavitation. The change in mass density ρ_c' at great distances due solely to cavitation is obtained from the last term on the right hand side of 10.6.3 by use of an appropriate Green's function. For an infinite medium this is the free space Green's function,

$$G(\mathbf{r},t|\mathbf{r}_0,t_0) = \frac{1}{4\pi} \frac{\delta\left[\dfrac{|\mathbf{r} - \mathbf{r}_0|}{c_0} - (t - t_0)\right]}{|\mathbf{r} - \mathbf{r}_0|}.$$

Since at great distances $|\mathbf{r} - \mathbf{r}_0|$ is the denominator is approximately $r = |\mathbf{r}|$, one divides 10.6.3 with the acoustic source term only by c_0^2 to obtain the required canonical form and then integrates over space and time (see Eq. 7.1.7). The integration over time yields,

$$\rho_c'(\mathbf{r},t) = g\int_{V_c} \frac{\partial^2}{\partial t^2} b\left(t - \frac{|\mathbf{r} - \mathbf{r}_0|}{c_0}\right) dV_c(\mathbf{r}_0), \qquad (10.6.4)$$

$$g = \frac{\rho_0}{4\pi c_0^2 r}.$$

The integral is essentially the volume acceleration. Thus, 10.6.4 is closely analogous to the radiation equation of an acoustic monopole, 7.1.9. Since $b(t)$ is a random variable ρ_c' is also a random variable. Its autocorrelation at far field point $\mathbf{r}$ and time t is,

$$B_\rho(\mathbf{d},\tau) = \frac{1}{V_c T}\int\int\int\int \rho'(\mathbf{r},t)\rho'^*(\mathbf{r}+\mathbf{d},t+\tau)\,d\mathbf{r}\,dt, \quad \text{(units: } N^2s^4m^{-8}\text{)}. \qquad (10.6.5)$$

It is often convenient from the point of view of measurements to replace the integrand of 10.6.5 by a representation of the space-time Fourier power spectrum,

$$B_\rho(\mathbf{d},\tau) = \frac{1}{V_c T}\int_{\mathbf{k}}\int_{\omega} e^{i\omega\tau + i\mathbf{k}\cdot\mathbf{d}} |M(\mathbf{k},\omega)|^2 \frac{d\mathbf{k}\,d\omega}{(2\pi)^4} \qquad (10.6.6)$$

$$|M(\mathbf{k},\omega)|^2 = V_c T\int\int B_\rho(\mathbf{d},\tau)e^{+i\omega\tau - i\mathbf{k}\cdot\mathbf{d}}\,d\tau\,d\mathbf{d} \quad \text{(units: } N^2s^6m^{-2}\text{)}$$

in which $\mathbf{d}$ is the vector separation distance between two observation points, and τ their time difference. These relations are obtained by first writing a 3-D stochastic Fourier-Stieltjes integral

$$\rho(\mathbf{r},t) = \int_{\mathbf{k}}\int_{\omega} e^{-\omega t + i\mathbf{k}\cdot\mathbf{r}}\, Z(d\mathbf{k}d\omega)$$

for each ρ in 10.6.5. Then,

$$B_\rho(\mathbf{d},\tau) = \frac{1}{V_c T}\iint\Big[\int_{\mathbf{k}_1}\int_{\omega_1}\int_{\mathbf{k}_2}\int_{\omega_2} e^{-\omega_2\tau + i\mathbf{k}_2\cdot\mathbf{d}}\, e^{-i(\omega_1-\omega_2)t + i(\mathbf{k}_1-\mathbf{k}_2)\cdot\mathbf{r}}$$
$$\times\, Z(d\mathbf{k},d\omega)\,Z^*(d\mathbf{k}_2 d\omega_2)\Big]dt d\mathbf{r}.$$

Now

$$\int_{V_c}\int_t e^{-i(\omega_1-\omega_2)t + i(\mathbf{k}_1-\mathbf{k}_2)\cdot\mathbf{r}_c} Z(d\mathbf{k}_1 d\omega_1)\,Z^*(d\mathbf{k}_2 d\omega_2)\,dt d\mathbf{r}$$
$$= \delta(\mathbf{k}_1-\mathbf{k}_2)\delta(\omega_1-\omega_2)\,|M(\mathbf{k}_1,\omega)|^2 d\mathbf{k}_1 d\mathbf{k}_2 d\omega_1 d\omega_2.$$

Integration over $\mathbf{k}_2, \omega_2$ replaces them by $\mathbf{k}_1, \omega_1$. The result is 10.6.6.

When spectral expansion is applied to the function $b(\mathbf{r},t)$ one writes

$$b(\mathbf{r},t) = \int_{-\infty}^{\infty} \exp(-\omega t + i\mathbf{k}\cdot\mathbf{r})\,dC(\mathbf{k},\omega)$$

in which b and C have no dimensions. Following the procedure just completed for obtaining the autocorrelation of ρ we find that

$$B_\rho(\mathbf{d},\tau) = \frac{1}{V_c T}\Big[\int_{\mathbf{k}}\int_{\omega} g^2\omega^4 e^{-i\omega\tau} e^{i\mathbf{k}\cdot\mathbf{d}}\,|Q(\mathbf{k},\omega)|^2 \tag{10.6.8}$$
$$\times \int_{V_1}\int_{V_2} e^{i(\mathbf{k}-\frac{\omega}{c}\hat{\mathbf{a}})\cdot(\mathbf{r}_1-\mathbf{r}_2)}\,dV_c(r_1)\,dV_c(r_2)\,\frac{d\mathbf{k}d\omega}{(2\pi^4)}$$

Here $|Q(\mathbf{k},\omega)|$ (units: $m^6\ s^2$) is the space-time power spectrum of $b(r,t)$ and $\hat{\mathbf{a}}$ is the unit vector in the direction of observation. If V_c is finite all wavenumbers $\mathbf{k}$ are present. However, the calculation is simplified by extending V_c to infinity. Then,

$$\int_{-\infty}^{\infty}\int \exp\, i(\mathbf{k}-\frac{\omega}{c}\,\hat{\mathbf{a}})\cdot(\mathbf{r}_1-\mathbf{r}_2)\,dV_c(\mathbf{r}_1)\,dV_c(2) \tag{10.6.9}$$
$$= \delta\left(\mathbf{k}-\frac{\omega}{c}\,\hat{\mathbf{a}}\right)V_c \quad (\text{units: } m^6).$$

For very large V_c it is thus seen that only the wavenumber $\frac{\omega}{c}\hat{\mathbf{a}}$ in the direction of observation survives. Integrating the resultant 10.6.8 with respect to $\mathbf{k}$ we obtain

$$B_\rho(\mathbf{d},\tau) = \frac{g^2}{T}\, e^{i\mathbf{k}_s\cdot\mathbf{d}}\int \omega^4 |Q(\mathbf{k}_s,\omega)|^2 e^{-\omega\tau}\,d\omega, \quad \mathbf{k}_s = \frac{\omega}{c}\hat{\mathbf{a}} \tag{10.6.10}$$

A different form of this result is obtained by [15] in which a quantity ψ is defined,

$$\psi(\mathbf{k}_s,\omega) \equiv \frac{|Q(\mathbf{k}_s,\omega)|^2\rho_0}{V_c T} \quad (\text{units: } Ns^3m^{-1}) \tag{10.6.11}$$

Assuming $\mathbf{d} = 0$ these authors obtain,

$$B_p(\tau) = \frac{\rho_c V_c}{(4\pi)^2 c_0^4 r^2} \int_{-\infty}^{\infty} \omega^4 e^{-i\omega\tau} \psi(\omega, \mathbf{k}_s)\, d\omega. \tag{10.6.12}$$

It is to be noted that while the function ψ is called by them a "spectral power" its units have odd powers of dimensions.

When $\tau = 0$, $B(0,0)$ is the intensity of power radiated by the cavitating volume. The key problem in the numerical calculation of $B(0,0)$ from 10.6.10 is to form an estimate of $|Q(\mathbf{k}_s,\omega)|^2$. One approach is to assume each bubble is a linear oscillator in a random force field $F(\mathbf{x},t)$. To construct F we note that over a bubble of radius R_{MAX} at solid angle Ω the force exerted by pressure p_∞ is $\Omega R_{MAX}^2 p_\infty$. The force per unit of radius is $\Omega p_\infty R_{MAX}$. This gradient of force drives a mass of fluid $\rho_0 X$, $X = (4\pi/3)(R_{MAX}^3 - R^3(t))$, as the bubble collapses. Normalizing both force gradient and driven mass by the volume of cavitation V_c it is seen that over an angle of $\Omega = 4\pi$ the force field, normalized to ρ_0, is,

$$F(\mathbf{x},t) = \frac{4\pi R_{MAX} p_\infty(\mathbf{r},t)}{\rho_0 V_c} \quad \text{(units: } s^{-2}\text{)} \tag{10.6.13}$$

Thus the power spectrum of the force field is

$$|S(\mathbf{k}_s,\omega)|^2 = (4\pi)^2 \left(\frac{R_{MAX}}{V_c}\right)^2 \left|\frac{p_\infty(\mathbf{k}_s,\omega)}{\rho_0}\right|^2 \quad \left[\text{units: } \frac{m^6}{s^2}\right] \tag{10.6.14}$$

where

$$p_\infty(\mathbf{k}_s,\omega) = \iint_{V_t} p(\mathbf{r},t) e^{+i\omega t - i\mathbf{k}\cdot\mathbf{r}} dt d\mathbf{r}, \quad \text{(units: Nms)} \tag{10.6.15}$$

The bubble itself responds to this force field as a linear oscillator exhibiting acceleration, damping and stiffness (due to internal gases):

$$(\ddot{X} + \lambda \dot{X} + m^2 X) V_c^{-1} = f(t)$$

in which $f(t)$ is the normalized force. Here $\lambda = 2f_0\Lambda$, f_0 is the natural frequency of the bubble, Λ is the log decrement of damping and $m^2 = 3\gamma p_\infty/\rho_0 R_{MAX}^2$. The last term is the equivalent stiffness of the bubble due to internal gases.

Upon taking the Fourier transformation in time, and interpreting $X(\mathbf{k}_s,\omega)/V_c = b(\mathbf{k}_s,\omega)$ one arrives at the relation,

$$|Q(\mathbf{k}_s,\omega)|^2 = \frac{1}{(m^2-\omega^2)^2 + \omega^2\lambda^2} |S(\mathbf{k}_s,\omega)|^2 \quad \text{(units: } m^6 s^2\text{)} \tag{10.6.15}$$

Thus the power spectrum of cavitation volume fluctuation is related to the power spectrum of a forcing field given by 10.6.14. A similar formula, but with different arrangement of component factors is bound in [15].

Substitution of 10.6.15 into 10.6.10 gives the space-time correlation functionp in terms of incremental mass density for the random acoustic radiation at distance $|\mathbf{r}|$ well beyond the cavitating volume. A correlation function for acoustic pressure ($B_p(d,\tau)$) is obtained by multiplying it with C_0^4,

$$B_p(\mathbf{d},\tau) = \frac{\rho_0^2}{(4\pi)^2 r^2 T} e^{i\mathbf{k}_s\cdot\mathbf{d}} \int_\Omega \frac{\omega^4}{(m^2-\omega^2)^2 + \omega^2\lambda^2} |S(\mathbf{k}_s,\omega)|^2 e^{-i\omega\tau} d\omega, \quad \text{(units: } N^2 m^{-4}\text{)} \tag{10.6.6}$$

Hence the power spectrum of radiated noise pressure at far distance r (modeled on 10.6.7) is:

$$|P(\mathbf{k},\omega)|^2 = \frac{V_c \rho_0^2}{(4\pi)^2 r^2} \int_{V_c}\int_{\tau} e^{i\mathbf{k}_s \cdot \mathbf{d}}\, G(\Delta\Omega, m, \lambda, \tau)\, e^{+i\omega\tau - i\mathbf{k}\cdot\mathbf{d}}\, d\tau\, d\mathbf{d} \quad \text{(units: } N^2m^2s^2\text{)} \tag{10.6.17}$$

in which G is the integral of 10.6.16 and $\Delta\Omega$ is the bandwidth of the time signature of the temporal fluctuations of the cavitation volume.

10.7 CAVITATION NOISE AS A TRAIN OF SOUND PULSES GENERATED AT RANDOM TIMES [15]

A very simple model of the acoustic pulse developed by a collapsing bubble can be based on the assumption that the instantaneous radiated acoustic pressure everywhere is the maximum gas pressure in the bubble corrected for spherical spreading and exponential decay:

$$p(r,t) = p_{g\mathrm{MAX}} \left(\frac{R_{\min}}{r}\right) e^{-t/\theta} \tag{10.7.1}$$

in which θ is the (random) pulse width. By the use of 10.5.27 and 10.5.28 for the case $\gamma = 4/3$ Eq. 10.7.1 reduces to,

$$p = ae^{-t/\theta}, \quad a = \frac{R_{\max}}{r p_g^2(0)} \left(\frac{p_\infty}{3}\right)^3. \tag{10.7.2}$$

The time constant θ can be approximated as the time required for an acoustic wave in the medium to travel a distance equal to the minimum bubble radius ($R_{\min}$),

$$\theta \approx \frac{R_{\min}}{\sqrt{\dfrac{p_{g\max}}{\rho_0}}} \tag{10.7.3}$$

Using 10.5.27 and 10.5.28 again in this formula one can construct a scaled amplitude A such that,

$$A = a\theta = \frac{R_{\max}^2 \sqrt{p_g(0)\rho_0}}{r} \quad \text{(units: } Nsm^{-2}\text{)} \tag{10.7.4}$$

This entity can be interpreted as the radiated acoustic pressure amplitude per frequency band of the bubble time-signature expressed on a per bubble basis.

Actual radiation from a cavitating volume is a sum of pulses of the type given by 10.7.1. If the distance between bubbles is greater than the correlation distance of the acoustic radiation from them the individual pulses add incoherently,

$$p_{\mathrm{TOT}}(\mathbf{r},t) = \sum_i a_i F(t^*), \quad t^* = t - |\mathbf{r} - \mathbf{r}_i|/c_0 \tag{10.7.5}$$

in which $F(t^*)$ is the acoustic time signature of a train of acoustic pulses arriving at $\mathbf{r}$ in random time increments. The corresponding acoustic mass density is

$$\rho_c(\mathbf{r},t) = \sum_i a_i F\left(\frac{t^*}{\theta}\right) \tag{10.7.6}$$

Here two modifications of 10.7.5 have been made: the time t^* has been scaled by the time constant θ, and the entity F has been given the dimensions of reciprocal time (s^2m^{-2}). F may be thought of as a *sampling pulse*.

The amplitude spectrum of $F(t^*/\theta)$ is obtained from the similarity theorem [16], namely $\theta f(\omega\theta) = \mathscr{F}F(t/\theta)$ so that

$$f(\omega\theta) = \int_{-\infty}^{\infty} F(x) e^{i\omega\theta x}\, dx, \quad \text{(units: } s^2m^{-2}) \tag{10.7.7}$$

in which $x = t/\theta$ [15]. Since the pulsewidth θ is random one can assign a probability distribution $W(\theta)$ to it. Now the pulse F has a random arrival time, hence a random phase. Thus the complete transform of the n 'th pulse is $\theta_n f(\omega\theta_n)\exp - i\omega t_n$.

The power spectrum asociated with the train of pulses 10.7.6 is readily obtainable as a continuous spectrum if one assumes there are no periodic components in the samples. If the interval of observation is T seconds outside of which the train vanishes everywhere, then:

$$W_p(\omega) = \frac{2}{T}|\rho_c(\omega)|^2 \quad \text{(units: } N^2s^5m^{-8}) \tag{10.7.8}$$

$$|\rho_c(\omega)|^2 = \mathscr{E}\{|a_m\theta_m f(\omega\theta_m)\exp - i\omega t_m|^2\} \quad \left[\text{units: } \frac{Ns^6}{m^8}\right]$$

in which $\mathscr{E}$ is the expected value, and θ_m, t_m are random variables. The factor 2 signifies that only positive values of ω are to be used in defining the spectrum. This double sum can easily be reduced:

$$|\rho_c(\omega)|^2 = \left[\mathscr{E}\left\{\sum_m A_m^2 |f(\omega\theta_m)|^2\right\} + 2\mathscr{E}\right. \tag{10.7.9}$$

$$\left.\left\{\sum_{m-n=1}^{\infty} A_m A_n f(\omega\theta_m) f^*(\omega\theta_n)\exp - i\omega(t_m - t_n)\right\}\right.$$

Assume that the arrival times are uncorrelated with pulse widths so that the expected value of a product is the product of expected values. If the density of arrivals is very great per unit time and if the pulse amplitudes are nearly the same for all pulses one can rewrite 10.7.9 in the form of continuous integrals,

$$|\rho_c(\omega)|^2 = qA^2\left[K(\omega) + 2|H(\omega)|^2 \operatorname{Re}\frac{\phi(\omega)}{1-\phi(\omega)}\right] \quad \text{(units: } N^2s^6m^{-8}) \tag{10.7.10}$$

$$K(\omega) = \int_0^{\infty} |f(\omega\sigma)|^2 W(\theta)\, d\theta \quad \text{(units: } s^4m^{-4})$$

$$H(\omega) = \int_0^{\infty} = f(\omega\sigma)\, W(\theta)\, d\theta \quad \text{(units: } s^2m^{-2})$$

$$\phi_{\min}(\omega) = \mathscr{E}\{e^{-i\omega(t_m - t_n)}\} \text{ for all } m, n. \quad \text{(units: none)}$$

where q is the number of pulses and A is the average amplitude per pulse. Since the intervals $\mu = t_m - t_n$ between pulses are independent random variables then,

$$\phi_{mn}(\omega) = \phi_\mu^{m-n} \tag{10.7.11}$$

where ϕ_μ is the characteristic values,

$$\phi_\mu = \mathscr{E}\{e^{-i\omega\mu}\} \tag{10.7.12}$$

The sum over ϕ_μ constitutes an infinite geometric series. Upon performing the summation of this series one obtains 10.7.10.

The average number of pulses arriving at point r per unit time $n_1 = (q/T)$ is given by the total number of cavitation nuclei N in a volume V multiplied by the number of times n_c per unit time these nuclei generate a cavitation void. Since cavitation occurs when the hydrodynamic pressure falls below a specified level one car use the theory of *zero closings* to find n_c [17]. In this theory a random process $p(t)$ which obeys a normal distribution density,

$$W = \frac{\exp\left\{-\dfrac{p - <p>)^2}{2b_0}\right\}}{(2\pi b_0)^{1/2}} \tag{10.7.13}$$

will exhibit an average number of crossings at level p_c given by,

$$n_c = \frac{1}{\pi}\left[\frac{b_2}{b_0}\right] \exp\left[\frac{-(p_c - <p>)^2}{2b_0}\right] \quad \text{(units: } s^{-1}\text{)} \tag{10.7.14}$$

in which b_0, b_2 are the zeroth and second moments of the power spectrum of $W(\omega)$ of $p(t)$. Thus,

$$n_1 = Nn_c \quad \text{(units: } s^{-1}\text{)}$$

When the cavitation is associated with liquid flowing at (turbulent) velocity v it may be directly shown by scaling laws applied to 10.7.8 that the power spectrum of radiated noise is proportional to the fourth power of v [15].

REFERENCES

1. I.S. Gradshteyn, I.M. Ryzhik, "Tables of Integrals, Series and Products," Academic Press, 1965, p. 307.

2. H. Bateman, A. Erdelyi, "Tables of Integral Transforms," Vol. I., p. 74 (Eq. 26), McGraw-Hill, New York, 1954.

3. S.G. Kasoev, L.M. Lyamshev, Sov. Phys. Acoust. *23* (6), p. 510 (1977).

4. Ref. 1., p. 495.

5. Ref. 1., p. 406.

6. L. Hutcheson, O. Roth, F. Barnes, Record, 11th Symp. Electron, Ion and Lesser Beam Technology, Boulder, Co., (1971) p. 413.

7. L.D. Landau, E.M. Lifshitz, "Fluid Mechanics," Pergamon Press, Addison-Wesley Pub. Co., Mass., p. 304.

8. Ref. [7], p. 287.

9. H.K. Forster, N. Zuber, J. Appl. Phys. *25*, p. 474 (1958)

10. H. Lamb, "Hydrodynamics," Dover Pub., 6th Ed., New York, 1945, p. 122.

11. Lord Rayleigh, "On the pressure developed in a liquid during collapse of a spherical cavity," Phil. Mag. *34*, 94-98, (1917).

12. B.E. Noltingk, E.A. Neppiras, Proc. Phil. Soc. London, 63B, 674-685, (1950).

13. D. Ross, "Mechanics of Underwater Sound," Pergamon Press, N.Y., 1976, p. 219.

14. M.J. Lighthill, Proc. Roy. Soc. SerA *267*, 1329 (1962).

15. Yu. Boguslavskii, et al., Sov. Phys. Acoust. *16*, 17 (1960).

16. R. Bracewell, "The Fourier Transform and Its Applications," McGraw-Hill, 1965, p. 101.

17. D. Middleton, "Introduction to Statistical Communications Theory," McGraw-Hill, 1960, p. 428.

CHAPTER XI
GENERATION OF SOUND BY EXPLOSION

11.1a Experimental Curves of Shock Wave Formation and Propagation

An explosive chemical compound detonated underwater generates product gases at temperatures of some 3000°C and shock wave pressures in excess of 50,000 atmospheres. The detonation wave (stress wave, shock wave) travels outward with an initial radial speed well above five thousand feet per second, namely at a rate much higher than the propagation speed of small amplitude sound waves. As the wave propagates outward its speed drops. A typical curve of radial velocity of the shock wave versus distance from the source is shown in Fig. 11.1.1. In this illustrative graph the shock front begins at the initial radius a_0 (labeled point A for convenience) of the undetonated charge (assumed spherical). Here the weight of explosive (and its chemical nature) are assumed sufficient to generate an instantaneous shock wave pressure of 10^6 psi. The radial velocity of this wave is about 1.4×10^4 ft/sec. At the radial distance of approximately 1 foot (point B) the shock pressure has dropped to 1.8×10^5 psi with a corresponding velocity of 8.3×10^3 ft/sec. Points C and D show similar trends of diminishing radial velocity and diminishing pressure. When the wave advances an additional five feet beyond point D the wave velocity is nearly 4950 ft/sec, which is the speed of small amplitude

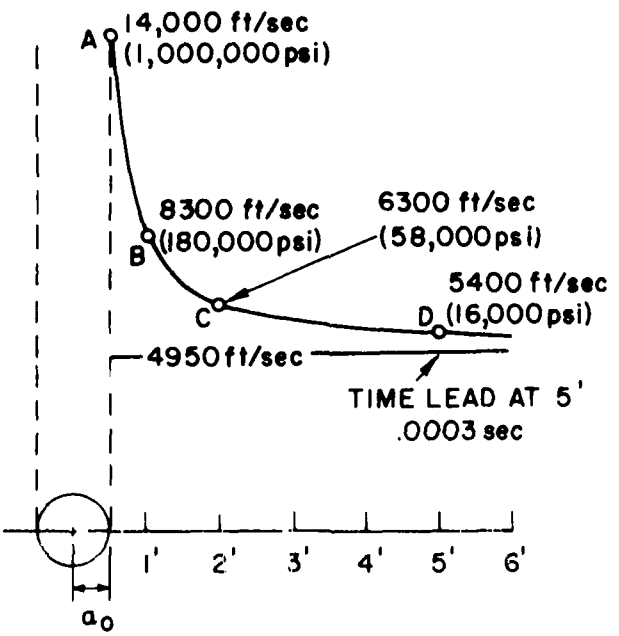

Fig. 11.1.1 Pressure and radial velocity of shock wave versus distance from source

acoustic signals in the ocean. An examination of the curve of pressure versus radial distance R shows that the space-rate of fall-off varies as R^{-M} where $M = M(R)$ i.e. the value of M depends on the radial distance selected. Roughly $M = 2.9$ at A, 1.3 at D, and 1.13 asymptotically beyond, until at very great distances $M \approx 1$, as in spherical spreading. From this one concludes: the inverse first power law of small amplitude acoustic waves in spherical expansion is not obeyed as long as the shock wave has "finite amplitude", or alternatively, as long as the particle velocity is an appreciable fraction of $C_0 = 4900$ ft/sec.

As the wave propagates beyond a distance of (roughly) 10 a_0 it exhibits marked unexpected phenomena. Fig. 11.1.2 shows a pressure distribution of 300 pounds TNT at three specific times. It is seen that the spatial profile of the shock wave changes from sharp peak (at 5 ft) to broad tail (at 500 ft) as the wave progresses outward from the origin. One notes again that the shock wave travels farther in a given time than a low amplitude acoustic wave (pictured as dotted profiles), and the reduction of pressure with distance is at a faster rate than R^{-1}.

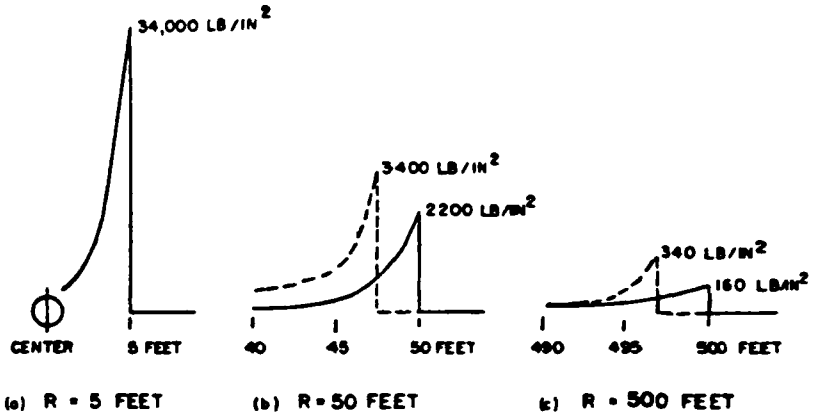

Fig. 11.1.2. The pressure distribution around a 300 pound TNT charge at 3 times after completion of detonation. [1].

A temporal history of a shock wave in a *bounded* (say ocean) medium also displays expected reflection. In Fig. 11.1.3a the pressure generated by 300 lbs of TNT is observed at a radial distance of 50 feet. The rise time of the shock wave is very nearly infinitesimal, while the decay time is roughly exponential. Fig. 11.1.3b shows the same wave observed at a distance of 500 ft. Here the effect of reflections from the boundaries of the water medium are clearly evident. The shock wave is initiated at time $t = 0$, following a pressure time curve A-B-C. At B however a negative reflection from an air-water interface D occurs which overrides the positive pressure, making the total pressure negative until a time of about 1.2 sec when a second reflection occurs, this time positive originating at a bottom-water interface. The addition of the positive reflection generates a second peak at F.

Additional peculiarities of shock wave propagation are illustrated in Fig. 11.1.4. This is a snapshot of the spatial distribution of shock wave pressure versus range r at a specified instant of time. At distance R from the origin the shock wave appears as a sharp rise in pressure, A. From R in toward the origin this pressure falls off initially as r^{-1}, then levels out to form a

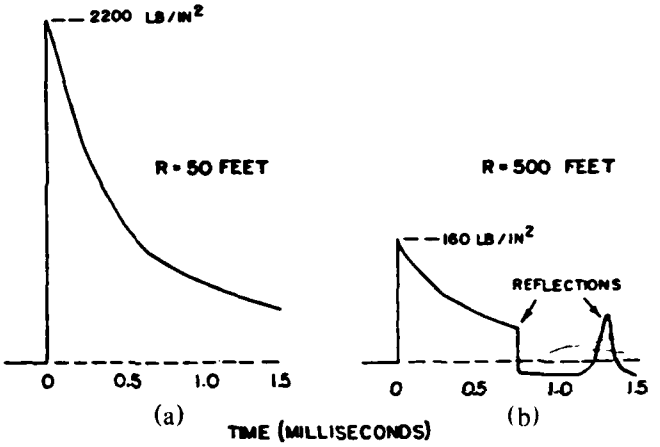

Fig. 11.1.3. Shock wave pressure-time curves at 2 distances from 300 pound TNT charges. [2].

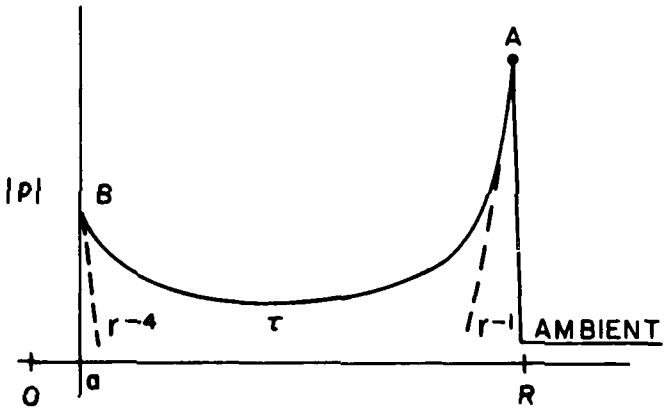

Fig. 11.1.4. Snapshot of shock wave amplitude versus range at given time instant.

trough T, the fall in pressure being caused by the inertial (i.e. Bernoulli) outward acceleration of incompressible fluid near the gas bubble (called the "afterflow effect"). Near the gas bubble this pressure rises again at a slope of r^{-4} until it reaches the instantaneous gas pressure, point B, at radius $a(t)$. As the bubble expansion proceeds the pressure at B falls, ultimately reaching a value below ambient. Finally the bubble stops expanding. The snapshot then shows a considerable length of trough below ambient.

Further discussion of the afterflow effect and the associated pressure-range plot of Fig. 11.1.4 will be undertaken in Sects. 11.1b and 11.1c below.

11.1b Bubble Oscillations

At a fraction of a millisec after detonation the shock wave is escaping from the scene at the rate of some 5500 ft/sec (Fig. 11.1.1) while the local mass of water surrounding the gas bubble is flowing outward at a speed of a few hundred feet per sec. The inertia of this water mass is so great that the bubble expansion continues even though the internal gas pressure falls below ambient. Ultimately the maximum radius (R_{max}) is reached when the outward expansion halts, reverses its direction, and the bubble collapses under the action of the differential pressure at the gas-water interface between ambient hydrostatic pressure and internal gas pressure with the associated surface tension. The radial motion of collapse accelerates inward with a wall speed from subsonic to supersonic depending on the pressure differential. A minimum radius (R_{min}) is soon reached, with internal gas pressure once again great exceeding ambient. At this point a second shock wave of smaller amplitude is radiated outward. The water flow then reverses as the bubble expands once more to repeat the cycle, but at considerable less energy.

Bubble oscillations can readily be observed in experiments. Cole [3] reports the detonation of 0.55 lb of tetryl at a depth of 300 ft. A history of bubble radius versus time is reproduced in Fig. 11.1.5. The gas sphere first expanded to the equilibrium radius (point B) of 12 inches in about 3 millisec, at which point the ambient pressure and internal gas pressure were equal. The expansion continued beyond this to a maximum radius of 1.48 ft in 0.014 sec, the internal gas pressure falling ultimately at point C to about 1/5 of the hydrostatic pressure. The gas sphere then collapsed, contracting to a minimum radius of 5 inches in 0.028 sec (point E). This completed the first cycle. Expansion resumed again to a second maximum of 13 inches in about 0.038 sec (point F), followed by a second contraction to a minimum of some 3 inches (point H) in about 0.050 sec to complete the second cycle. Several additional cycles were also recorded. It was also observed that the bubble moved vertically under the force of buoyancy during the cycling process. A theory of this migration is presented in Sect. 11.1e.

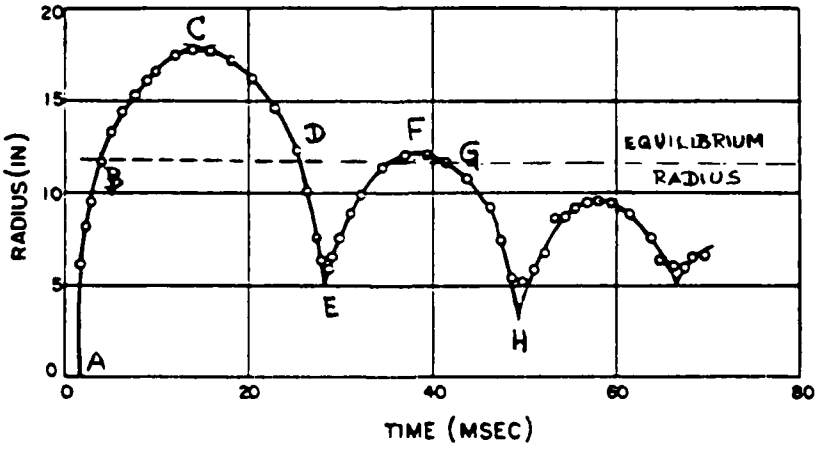

Fig. 11.1.5. Radius of the gas sphere as a function of time, for a 0.55 pound tetryl charge 300 feet below the surface [after [1]]

11.1c Pressure Pulses After Detonation

Each cycle of bubble oscillation generates a pressure pulse in the water at the point of minimum radius. A generalized pressure-time plot of these pulses taken at a specific radial distance near the source origin is shown in Fig. 11.1.6. The lettering corresponds to that of Fig. 11.1.5. At retarded time t_1 the shock wave passes the observation point. In the time between A and B the bubble expands, the pressure dropping at B to ambient, and in the time between BCD below ambient. The expansion halts at point C then the bubble collapses with ever increasing acceleration through time D, and a second pressure pulse arrives at the observation point in retarded time t_2, appearing there as a peak (point E). Additional peak pulses appear at H, etc, corresponding to minima of the bubble contractions. An experiment by Arons et al [4] reproduced in Fig. 11.1.7 in which 1/2 lb of TNT was exploded at 500 ft depth bears out the main features of Fig. 11.1.6 as shown by the corresponding letters.

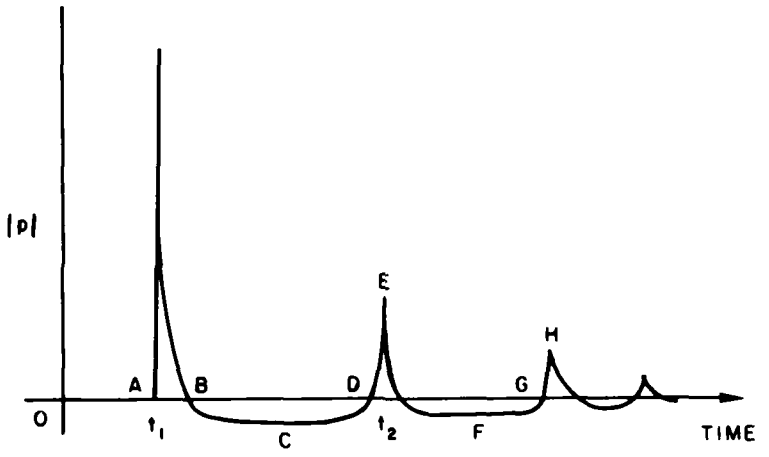

Fig. 11.1.6. Generalized pressure-time plot near explosive source.

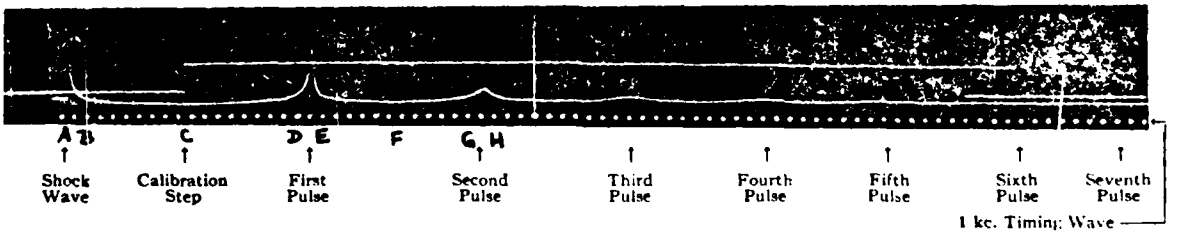

Fig. 11.1.7. Pressure-time record showing shock wave and bubble pulses. Charge: 0.505 lb. T.N.T.; Gauge dist.: 2.25 ft. Depth: 500 ft. [4]

11.1d Energy of Detonation and Its Dissipation

In the theory of acoustic effects of detonation it is useful to have an approximate estimate of the energy of a unit quantity of explosive. To obtain this one begins with a weight W of explosive, the detonation of which generates a bubble of volume $V(t)$. As noted above, V varies with time t during its history of expansion and contraction. A ready reference volume will be taken to be V_0 at the instant of pressure equilibrium with hydrostatic pressure p_0. It is then assumed that the pressure of the gas at any other time can be derived from p_0 by an adiabatic process, viz.

$$p = p_0 (V_0/V)^\gamma , \quad \gamma = C_p/C_v. \tag{11.1.1}$$

The potential energy $\mathscr{E}_b$ of the gas in the bubble at any time is then

$$\mathscr{E}_b = \int_{V_0}^{\infty} p\, dV = p_0 V_0^\gamma \int dV/V^\gamma = \frac{p_0 V_0}{\gamma - 1}. \tag{11.1.2}$$

The immediate problem is then to calculate V_0. To do this one can resort to an equation of state of simple form, assuming perfect gases,

$$p_0 V_0 = m \mathscr{R} \theta_0 \tag{11 1.3}$$

in which m is the mass of the gas in moles, $\mathscr{R}$ is the universal gas constant (units: energy per mole per degree) and θ_0 is the absolute temperature. Thus the gas energy is

$$E_b = m \mathscr{R} \theta_0/(\gamma - 1). \tag{11.1.4}$$

As an example of the use of this relation we take 1 gm of explosive of a specific type. From manufacturer's data (or chemical handbooks) it is known that under normal temperature and pressure (= NTP) the volume of detonation gas formed by this specific chemical compound is (say) 300 cc, and its initial temperature is 3273°K. By Avogadro's law,

$$m = \frac{300}{22,000} = 0.0136 \text{ moles.}$$

Taking $\gamma = 1.3$, $\mathscr{R} = 8.134 \times 10^7$ erg/mole°K, one obtains from 11.1.4,

$$\mathscr{E}_b = \frac{0.0136 \times 8.314 \times 10^9 \times 3272^\circ}{1.3 - 1} = 1.24 \times 10^{10} \text{ erg.}$$

In the absence of manufacturer's data one can use convenient estimates of energy released by explosion of chemical substances based on experience. For example, 1 gm TNT releases about 1060 calories, or $1.060 \times 10^3 \times 4.18 \times 10^7 = 4.44 \times 10^{10}$ erg; hence 1 lb of TNT releases about 2×10^{13} erg. Since 1 erg = 7.38×10^{-3} ft-lb, it is seen that 1 lb TNT releases 1.48×10^6 ft-lb of energy.

The dissipation of the energy of detonation has a time history of major importance in estimating the radiation output of the explosion. By resort to experiment [5] it has been found that the following (rough) estimates can be made: in the time duration of shock wave generation (say less han 10 millisec) about 32% of the available energy is lost as heat, and 25% as radiated shock wave. During the period of the first bubble pulse (Fig. 11.1.5 ABCDE), about 20% of the original energy is dissipated in velocity turbulence and 10% in acoustic radiation. Similarly, during the second bubble pulse (Fig. 11.1.5 EFGH) some 7% is lost in turbulence and 1% in acoustic radiation. Thus the energy dissipation over a time period from the instant

of explosion to the termination of the second bubble pulse is about 95% of that originally available. The radiation is 36% of the original total, some 25% going into the shock wave, and 11% going into acoustic radiation associated with the bubble pulses.

An important parameter in the use of underwater detonations as the source of sound for communication purposes is the energy available *after* the emission of the shock wave. Some estimate can be made from the above summary. Ramsauer [6] performed a set of experiments and found that after the shockwave was emitted there remained in the subsequent bubble oscillations about 41% of the original total energy, in close agreement with data presented above.

11.1e Rayleigh-Willis Curves for relating Collapse Time of a Bubble to Energy in the Bubble Caused by a Chemical Explosion

The uncertainties in explosion dynamics have led to empirical relations relating the energy radiated to the chemical energy in the explosive. The most satisfying procedure for obtaining this ratio is to measure the shock wave developed by the explosion directly. However, this always involves difficulties in measuring energy over all space.

To avoid the measurements difficulty use is made of the bubble oscillation period as a measure of energy. According to Rayleigh, the time τ for complete collapse of a bubble at hydrostatic pressure P and initial radius R_0 in a medium of density ρ with no boundaries is given by 10.5.17. The spherical void whose radius is R_0 corresponds to a storage of potential energy Q (units: Nm) which has a magnitude, according to Willis, of value given by the relation,

$$R_0 = \left\{\frac{3Q}{4\pi P}\right\}^{1/3} \tag{11.1.5}$$

Since the potential energy of the bubble and the chemical energy W of the source are related, one can write, in the first approximation, that $Q = KW$, where K is a constant. Upon combining 10.5.17 and 11.1 one obtains the Rayleigh-Willis formula for estimating the time T for one complete oscillation (2τ) of the initial volume of explosion,

$$T = 2 \times 0.914 \left\{\frac{3Q}{4\pi P}\right\}^{1/3} \left\{\frac{\rho}{P}\right\}^{1/2}$$

or

$$T = \frac{1.14\,\rho^{1/2}\,(KW)^{1/3}}{P^{5/6}}. \tag{11.1.6}$$

Thus a measurement of T and a knowledge of K lead directly to an estimate of the chemical energy W that was in the explosive. A theoretical Rayleigh-Willis curve is shown in Fig. 11.1.8 for a source at depth equivalent of 1 atmosphere. The value of K obtained by experiment is specifically that of "60% dynamite."

The simple Rayleigh-Willis curve must be corrected for the effects of surface boundaries and bubble buoyancy.

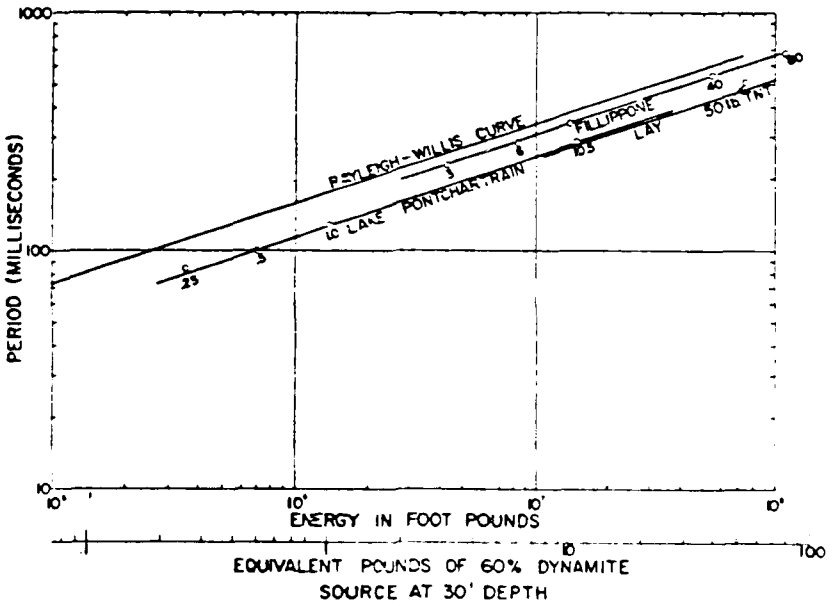

Fig. 11.1.8. Rayleigh-Willis diagram for 60% dynamite. (After Ref. [7]).

Effects of Surface Interface

The period of bubble pulsation predicted by the Rayleigh-Willis formula is modeled on the existence of an explosion bubble in an infinite medium. When the medium is bounded, say by air, the period of the bubble is strongly affected if the bubble is near the boundary. Fig. 11.1.9 illustrates this phenomenon. It shows the bubble period of 300 cubic inches of air at 2000 psi as a function of depth, starting at approximately 50-ft submergence and terminating at the surface. At first, as the bubble source approaches the surface, the period of the bubble pulse increases, as is required by the inverse 5/6 dependence of period on hydrostatic pressure as predicted by the Rayleigh-Willis curve. However, when the bubble is "near enough" to the air interface, the mass load on the bubble decreases. The period also decreases since it is proportional to the source root of the mass load. The decrease is significant, hence careful estimates of bubble period require correction for boundaries.

Buoyancy Effects

Fifty lb of TNT generate a maximum bubble diameter of some 20 ft (or ideally a spherical volume of 4200 feet), which corresponds to a buoyancy of 262,000 lb at a depth of 50 ft. The force of this buoyancy causes the bubble to migrate upward. A typical trajectory of bubble migration vs time is shown in Fig. 11.1.10a. Fig. 11.1.10b shows the corresponding variation of bubble radius with time. The pressure signature at a distance of 33 ft from the source versus time is shown in Fig. 11.1.10c. The radial component of particle velocity (Fig. 11.1.10d) on the surface of the spherical bubble is ideally computable if the pressure signature is known. For a *simple source* of source strength S (units: m^3/s), the acoustic pressure is,

$$p \sim \frac{\rho}{4\pi r} \frac{dS}{dt^*}, \quad t^* = t - \frac{r}{c} \tag{11.1.7}$$

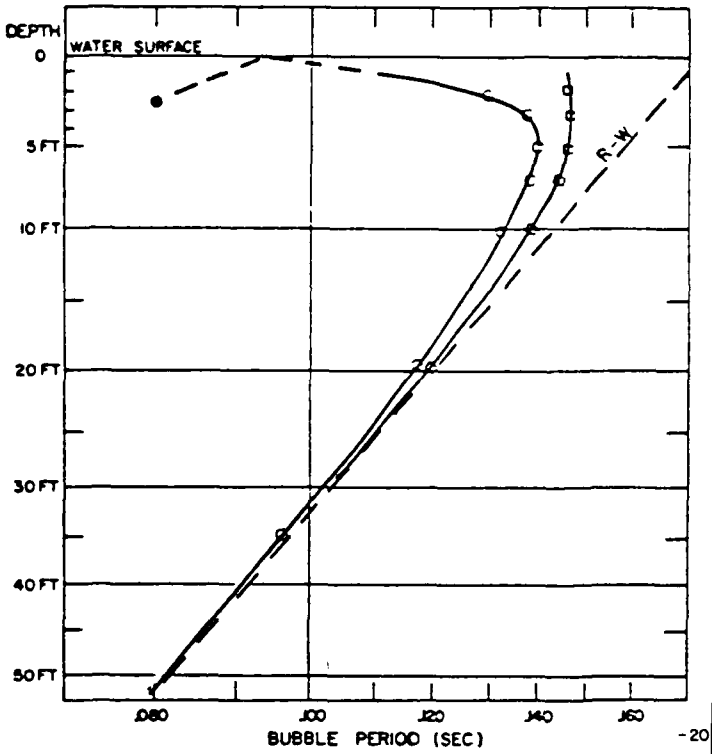

Fig. 11.1.9. Bubble oscillation period versus depth (300 in^3 of air at 2000 psi) showing effects of mass-unloading, and mass-loading. (After Ref. [7]).

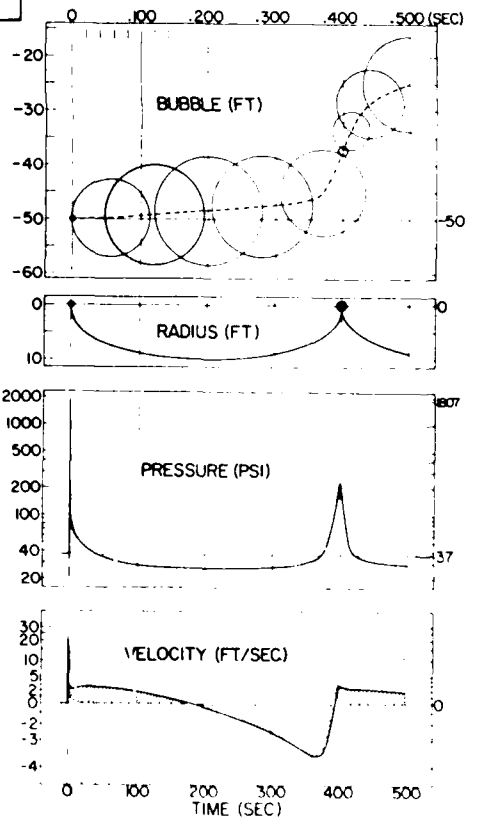

Fig. 11.1.10. Pressure and velocity signatures of 50 pound TNT explosion at 33′ distance. After [7].

Since $S = 4\pi r^2 u_r$, it is seen that at distance r from the (stationary) center of the bubble,

$$u_r(t) = \frac{1}{r\rho} \int_0^t p(t^*)\, dt^* \tag{11.1.8}$$

After the first collapse the radiation is effectively at single frequency ω. Then,

$$u_r = \frac{i\omega S}{4\pi rc} + \frac{S}{4\pi r^2}. \tag{11.1.9}$$

The first term on the right-hand side is the compressive flow, which accompanies the radiation real power, while the second term represents the velocity of incompressible flow, which corresponds to the generation of nearfield or wattless power. The solid line is the total radial component of velocity, while the dotted line represents compressive flow alone. The shaded portion is the incompressible flow, which predominates at all times except during the passage of the shock wave.

Spectral Content of the Pressure Signal Caused by an Explosion

Various forms of near-field pressure signal $F(t)$ of explosive sources are given by A, B, C, D, E in the left-hand side of Fig. 11.1.11. On the right-hand side are sketched the amplitude $A(\omega)$ and phase $\phi(\omega)$ spectra of the frequency asymptote content of these signals. To illuminate this chart, it will be convenient to examine the examples of Fig. 11.1.11. In A the impulse signal has zero rise time, a time width of 6 msec and the exponential fall shown. The amplitude spectrum shows unit value (i.e., zero dB) for frequencies approaching zero, a value of -3 dB at 26.5 Hz, -6 dB at 46 Hz, and an asymptotic slope of -6 dB octave at high frequencies. The low-frequency cutoff (here zero) is roughly determined as the inverse period (here *infinite) of the signal, while the high-frequency reflects the distribution in high frequencies* required to give zero rise time. The high-frequency cutoff is roughly the inverse time width of the signal. In B the pressure signature shows a finite rise time of 2 msec and a time width of 6 msec. Since the period is again infinite, the low-frequency cutoff zero. The time width of the signal is smaller than in A. Hence the high-frequency cutoff is higher (79.5 Hz). The high-frequency asymptote is now near 12 dB/octave, which reflects the few high frequencies needed to represent finite rise time. In C the pressure signature shows an overshoot, which corresponds roughly to introduction of periodicity. The appearance of a period is mirrored in the frequency domain by the appearance of a low-frequency cutoff. In D the pressure signature has a very pronounced sinusoidal tail. The overshoot is now damped oscillatory and dominates the signature. The smaller value of the period raises the low-frequency cutoff of the amplitude spectrum even more and simultaneously lowers the high-frequency cutoff. In E the period, time width and rise time change from cycle to cycle. The Fourier spectrum therefore displays numerous peaks, representing a superposition of modes. Successive peaks are seen to be harmonically related. E represents the time-signature $F(t)$ of a single 300 cubic inch air gun pressurized to 2000 psi discharged ("fired") into water.

RELATION BETWEEN BANDWIDTH, ENERGY, AND INITIAL PRESSURE OF SOURCE

The interrelation between the energy of the source and the subsequent time domain and frequency domain signatures developed in the medium can be established for any particular device by extensive experimentation and mathematical modeling. It is useful, however, to

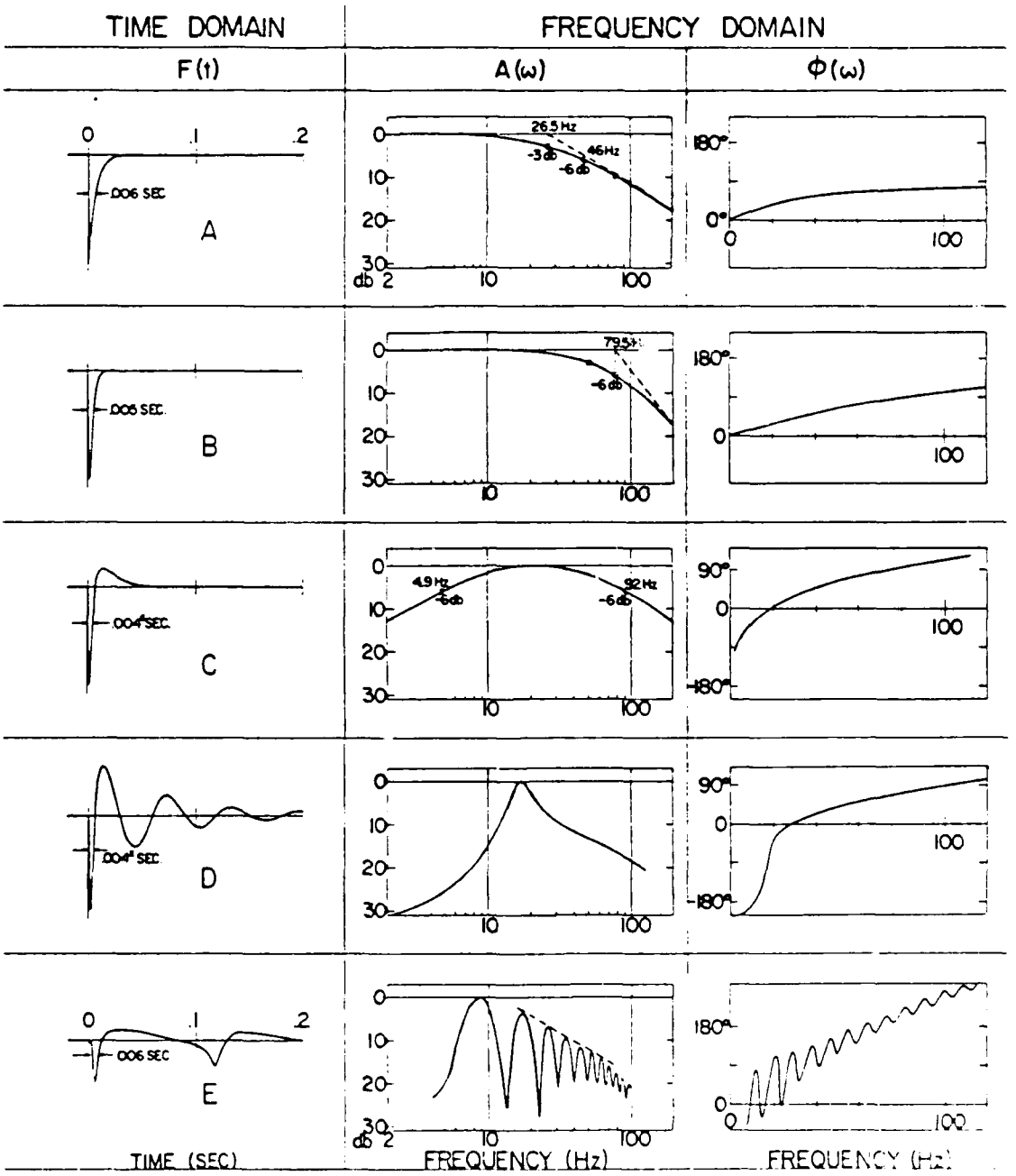

Fig. 11.1.11. Frequency spectra of familiar pulse types. (After [2])

AD-A140 578 A TREATISE ON ACOUSTIC RADIATION(U) NAVAL RESEARCH LAB 6/7
WASHINGTON DC S HANISH 1981

UNCLASSIFIED F/G 20/1 NL

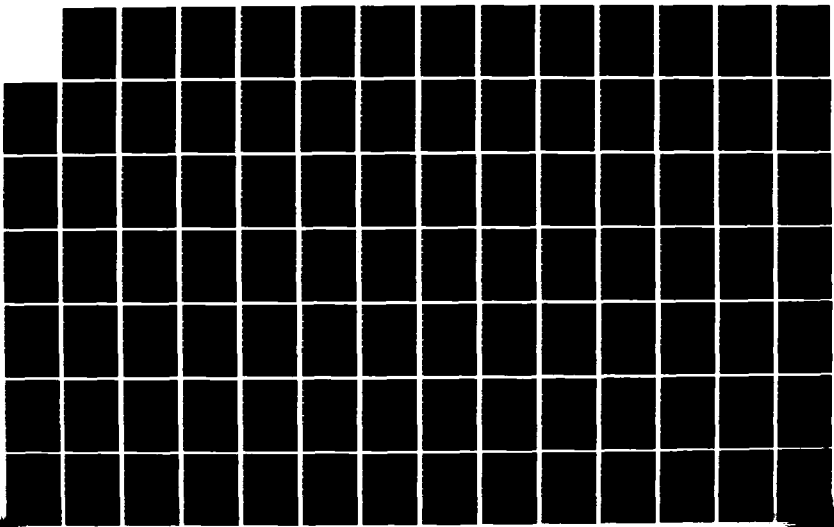

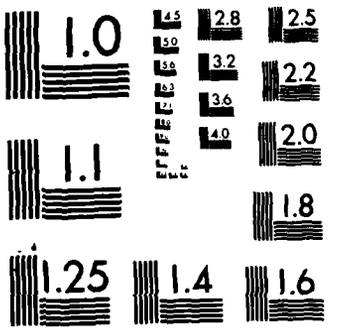

MICROCOPY RESOLUTION TEST CHART
NATIONAL BUREAU OF STANDARDS-1963-A

have available a convenient *example* to illuminate these interrelations. To this purpose one chooses the air gun pressurized at 2000 psi (initial pressure) operating at a depth of 30 ft with an intrinsic energy W selectable by varying the air chamber volume of the gun. Fig. 11.1.12a shows graphically the bandwidth and initial pressure of the gun as a function of energy and frequency. In it a volume of 540 in.^{3} at a pressure of 2000 psi it is seen that the low-frequency cutoff is 4.5 Hz and the high-frequency cutoff is 64 Hz. Based on this chart (and other experiments) one can use the following rules of thumb as preliminary estimates of acoustic and dynamic parameters of the explosion process. For a given energy W of the explosive sound:

The low-frequency cutoff varies as $W^{-1/2}$.
The high-frequency cutoff varies as $W^{-1/3}$.
The energy flux density per cycle per sec varies as $W^{4/3}$.
The energy flux density per octave varies as W.
The peak pressure in the initial pulse will vary as $W^{1/3}$.
The initial pulse width will vary as $W^{1/3}$.
To reduce the low-frequency cutoff by half requires an eightfold increase in system energy.

If the energy is held constant and if it is desired to increase the high-frequency cut-off, one must increase the initial pressure in the gun. A typical rule of thumb is that a doubling of the high-frequency cutoff requires an eightfold increase in initial system pressure. Fig. 11.1.12b shows this relation.

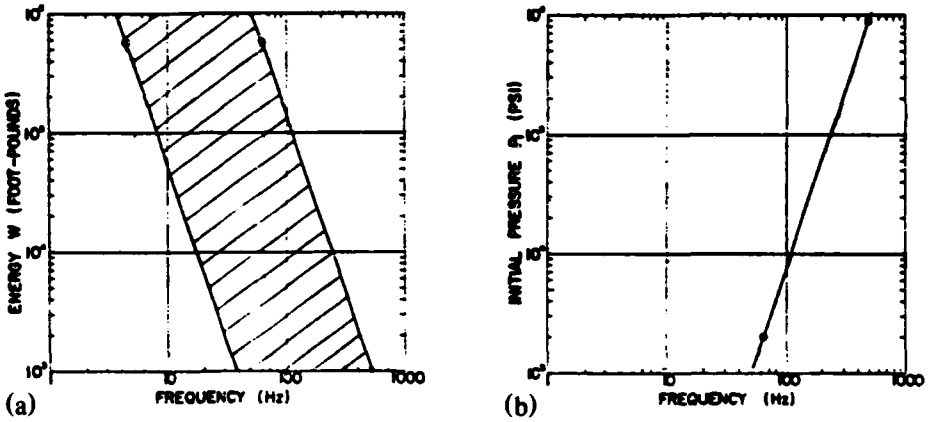

Fig. 11.1.12. Relation between bandwidth, cutoff frequencies, energy, and initial pressure of an air gun. (After [7]).

VALUES OF RATIO K = Q/W FOR THE POTENTIAL ENERGY OF THE BUBBLE

The potential energy Q of the bubble in the Rayleigh-Willis formula 11.1.6 is related to the intrinsic energy W of the source that generates the bubble. In a first approximation, the ratio Q/W is taken to be a constant (K), whose value must be determined for each particular pneumatic and seismic sound generator by experiment at a selected depth and under selected conditions. The low-frequency cutoff is similarly to be determined. A typical set of values of the ratio K and the low-frequency cutoff for some commercially available seismic sources is reproduced here from [7]. This is is shown Fig. 11.1.13. A comparison of the Rayleigh-Willis curve vs energy with a number of representative source systems is shown in Fig. 11.1.14.

Commercial Seismic Source and Energy Input (kilojoules)	K = QW	Low-Freq. Cutoff (Hz)
Sparkarray (1KJ)	.006	150
Boomer (1KJ)	.011	110
Sparkarray (5KJ)	.011	63
SSP (18KJ)	.016	39
WASSP (28KJ)	.060	21
2000 psi air gun (10 in.^{3})	.36	15
2000 psi air gun (300 in.^{3})		5
2000 psi air gun (2000 in.^{3})		2.5
Dinoseis (24" marine)	.092	15
WASSP (120KJ)		13
Aquapulse	.092	11
Seismojet		7
Dynamite (25 lb)	.20	6
Dynamite (80 lb)	.20	0.7

Fig. 11.1.13. Seismic sources. After [7].

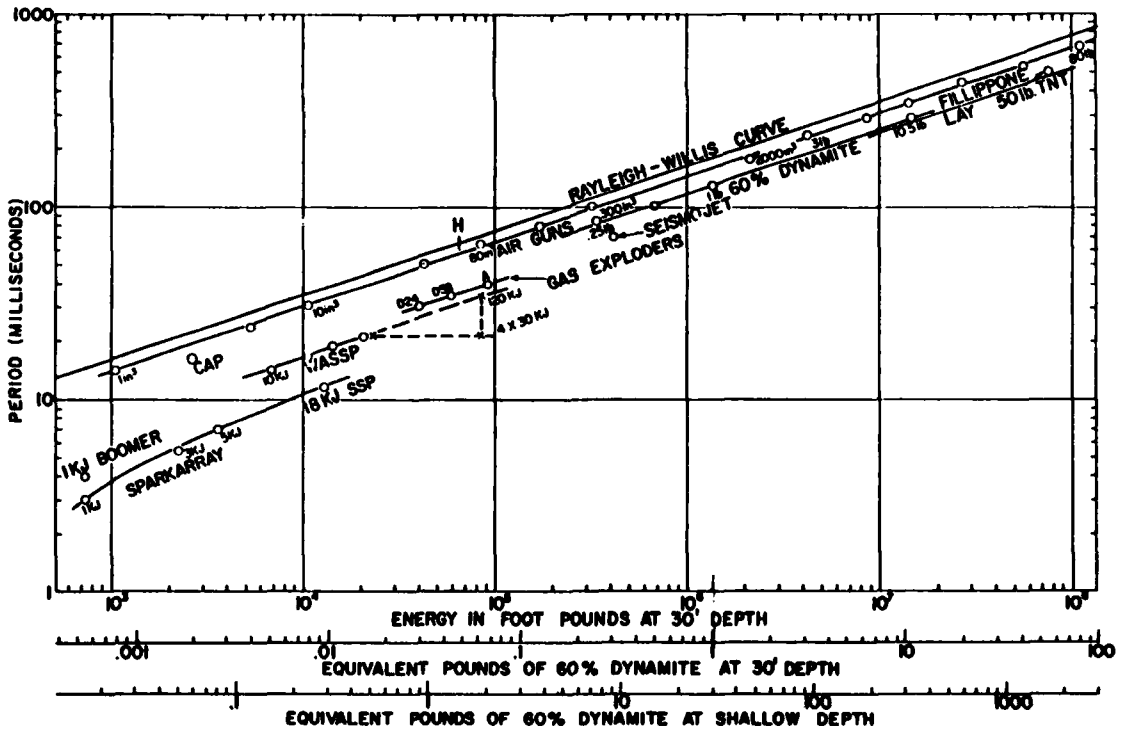

Fig. 11.1.14. Rayleigh-Willis diagram for representative energy source systems. Plotted for a source depth of 30'. *(From Ref. 7.)*

11.2 THEORETICAL MODEL OF PULSE PRESSURE RADIATION

11.2a Need for Approximations

The actual initial conditions of the detonation wavefront are not completely known. An adequate approximation can be made by assuming a model in which the explosion takes place adiabatically without change in volume, the gas pressure then being taken to be uniform throughout the gas sphere. Thus a spherical charge of radius a_0 is instantly replaced by an identical volume of hot gasses under very great pressure. Simultaneously, a sharp, steep compressional wave is assumed to radiate outward (and a rarefaction wave is assumed to radiate inward into the gas sphere).

Such a model can be handled mathematically in the following way: (1) the heat of thermochemical reaction at the initial temperature T_0 and P_0 is calculated, assuming no heat transfer to the medium during the explosion, (2) this heat is next applied to raise the temperature of the gas products to a final temperature at constant volume (taken to be very large), (3) the gas is next compressed at constant (final) temperature to the final volume.

While simple this model is clearly limited. The complexity of the detonation process is so great that all thermodynamic events which occur in a time duration equivalent to propagation of the shockfront out to approximately two charge radii ($= 2\ a_0$) cannot be modeled by such a simple theory. However, the propagation of the detonation wave beyond this limiting radius is modelable. Among several available models we choose that of Kirkwood-Bethe [8] to help establish the key features of shockwave formation and propagation. Additional models will be discussed in later sections.

We begin with a brief summary of the theory of shock waves in water.

11.2b Hydrodynamic and Thermodynamic Properties of Water at the Shock Front

We consider a shock wave propagating into an undisturbed region of water. At first we take the wave to be of negligible thickness and designate the region in front of the advancing wave to be region *f*, and the region just behind the wave to be region *b*. Across the surface of discontinuity constituting the wave the conservation of mass, momentum and energy must hold. In a *moving* (or Lagrangian) coordinate system, in which the surface of discontinuity is at rest, the conservation equations are:

$$\rho_f u_f = \rho_b u_b \equiv j \tag{11.2.1}$$

$$p_f + \rho_f u_f^2 = p_b + \rho_b u_b^2$$

$$h_f + \frac{1}{2}\, u_f^2 = h_b + \frac{1}{2}\, u_b^2.$$

This set, with change of symbols, is found in [9]. Here ρ is the mass density, u is the particle velocity, and h is the enthalpy of the fluid (i.e. $h = \epsilon + p\mathrm{v}$, ϵ is the internal energy and $\mathrm{v} = \rho^{-1}$).

To simplify actual measurement we switch to a *fixed* coordinate coordinate system in which the surface of discontinuity is in motion. Then $u_f = U$, where U is the speed of the

wavefront in this system. Just behind the wave front the particle velocity $u_b = U - u_2$, where u_2 is the particle velocity relative to the wave front. Hence, in a *fixed* coordinate system,

$$\rho_f U = \rho_b (U - u_2)$$

$$U = j\mathrm{v}_f = \mathrm{v}_f \sqrt{\frac{p_b - p_f}{\mathrm{v}_f - \mathrm{v}_b}} \tag{11.2.2}$$

$$p_b - p_f = \rho_f u_2 U$$

From this one deduces that,

$$u_2 = \sqrt{(p_b - p_f)(\mathrm{v}_f - \mathrm{v}_b)} \tag{11.2.3}$$

$$h_b = h_f = \frac{1}{2}(p_b - p_f)(\mathrm{v}_f + \mathrm{v}_b)$$

These sets of equations constitute the R-H or *Rankine-Hugoniot relations.* They can be visualized as follows: make the surface of discontinuity stationary. Then the water rushes to it at the speed U, and, in passing through it, undergoes a reduction in speed by amount u_2 as well as a change in pressure $p_b - p_f$, a change in enthalpy $h_b - h_f$, and a fall in specific volume $\mathrm{v}_f - \mathrm{v}_b$ (equivalently a rise in density $\rho_b - \rho_f$).

A plot of p vs v that obeys the R-H relations is called a shock adiabatic (or Hugoniot adiabatic). Each initial choice p_1, v_1 determines one adiabatic. Hence the collection such plots is a two-parameter family whose members depend on p_1, v_1 *separately.* If one member starts at p_1, v_1 and terminates in p_2, v_2, and a second member starts at p_2, v_2 and terminates in p_1, v_1, the two curves are not identical. Thus two members of a R-H family of shock adiabatics can share up to two points together, but no more. This is a consequence of the fact that the thermodynamic equation of state of shock adiabatics is of the form of $(p, \mathrm{v}) \neq$ constant.

In contrast an adiabatic which follows a course $s(p, \mathrm{v}) =$ constant is a Poisson adiabatic. Members of this family depend only on p_1 or v_1: they constitute a one parameter family. Two members of this family may coincide at all points.

If two points on a shock adiabatic are joined by a straight-line chord. The slope of this chord is $(p_2 - p_1)/(\mathrm{v}_2 - \mathrm{v}_1)$. By 11.2.2 this slope determines the velocity U of the surface of shock discontinuity. Thus the velocity of the shock front that began at state p_1, v_1 and is observed at p_2, v_2 depends on p_2, v_2.

The flow of fluid through a shock front is always accompanied by an increase in entropy. Hence, even though the flow approaching the front may be considered *potential flow*, the actual passage through the front is *rotational flow.*

TAIT Equation of State of Water

The R-H relations provide formulas which link values of p, v before and after the shock. They must be supplemented by an additional relation which displays the dependency of p and v at any spatial point. This relation is the thermodynamic *equation of state* for water, particularly under high pressure. Such a relation should agree with a shock adiabatic, i.e. be usable along

the R-H curve. However, it has been found that the use of a Poisson adiabatic in place of a R-H adiabatic introduces little error in practical work (Kirkwood, [10]). Thus a convenient choice is the Tait equation of state of the fluid (water) along p-v curves at constant entropy (Poisson adiabatic):

$$\frac{1}{\rho}\left(\frac{\partial \rho}{\partial P}\right)_s = \frac{1}{n(B+P)} \tag{11.2.4}$$

in which P is the pressure, ρ the density, and n, B are numerical factors dependent on temperature. Equivalently, the specific volume on this adiabatic is given by

$$\mathrm{v} = \mathrm{v}_1(T)\left\{1 - \frac{1}{n}\ln\left[1 + \frac{P}{B(T)}\right]\right\} \tag{11.2.5}$$

where $\mathrm{v}_1(T)$ is the specific volume at temperature T and zero pressure. Choosing the Poisson adiabatic through p = 1 atmosphere and T = 20°C leads to the approximation that $n = 7$ and $B = \rho_0 C_0^2/n$, where ρ_0, C_0 are equilibrium values of density and sound speed. With this approximation the pressure-density relation in region b is seen to reduce to the explicit form,

$$p_b = \frac{\rho_0 C_0^2}{n}\left[\left(\frac{\rho_b}{\rho_0}\right)^n - 1\right] \tag{11.2.6}$$

It will be useful in this formula and in the following set of formulas to give numerical estimates of parameters for a water medium. These will be enclosed in parentheses.

(Example: if p_b = 1 kilobar = $10^8 N/m^2$, then $\rho_b = 1.0390\ \rho_0$). Similarly, the speed of sound in region b where p_b = 1 kilobar is obtainable from the relation,

$$C_b = C_0\left(\frac{\rho_b}{\rho_0}\right)^{\frac{n-1}{\lambda}}, \quad \text{or } C = C_0 + \frac{n-1}{2}\sigma, \quad (\sigma \text{ defined below})$$

(Example: if $\rho_b = 1.0390\ \rho_0$ then $C_b = 1.1216 \times 4800 = 5384$ ft/sec). The Tait equation of state also permits calculation of two additional parameters that will be of considerable importance in numerical work. These are the Riemann function σ and the enthalpy function ω whose definitions are:

$$\sigma = \int_{\rho_0}^{\rho_b} C\,\frac{d\rho}{\rho}, \quad \omega = \int_{p_0}^{p_b}\frac{dp}{\rho} \tag{11.2.7}$$

from which it is seen that $C_b = C_0 + \frac{n-1}{2}\sigma$. Using the Tait equation of state one arrives at the explicit formulas,

$$\sigma = \frac{2\,C_0}{n-1}\left[\left(\frac{\rho_b}{\rho_0}\right)^{\frac{n-1}{2}} - 1\right], \quad \omega = C_0\sigma + \frac{n-1}{4}\sigma^2 \tag{11.2.8}$$

(Example: $\rho_b = 1.0390\ \rho_0$, C_0 = 1463 m/sec, σ = 59.3 m/sec, $\omega = 0.93 \times 10^5$ m^2/sec^2). From these results one can find u_2 from the R-H equation

$$u_2 = \sqrt{(p_b - p_0)\left[\frac{1}{\rho_0} - \frac{1}{\rho_b}\right]}$$

(Example: if $p_b = 10^8\ N/m^2$, $\rho_b = 1.0390\ \rho_0$, p_0 = negligible, $u_2 = 62.7$ m/sec). Similarly the velocity of the shock front is

$$U = \frac{p_b - p_0}{\rho_0 U_2}$$

(Example: $p_b = 10^2\ N/m^2$, $\rho_0 = 0.9982 \times 10^3$, $u_2 = 62.7$ m/sec, $U = 1.598 \times 10^3$ m/sec). The enthalpy increment at the shock front can also be deduced to be,

$$\Delta h = \frac{1}{2}\ (p_b - p_0) \left[\frac{1}{\rho_0} + \frac{1}{\rho_b}\right]$$

(Example: $p_b = 10^3\ N/m^2$, $\rho_0 = 0.9982 \times 10^3$, $h = 0.98 \times 10^5\ m^2/sec^2$, $\rho_b = 1.0390\ \rho_0$)

Another useful thermodynamic parameter is the temperature rise across the shock front. To calculate this we first note that the Tait equation of state has the functional form $v = f(p,T)$. Thus the change in specific volume across the shock front is

$$\Delta v = \Delta_p v + \Delta_T v, \tag{11.2.9}$$

where Δ_p, $\Delta_T \equiv$ change (or increment) at pressure or constant temperature respectively.

To find expressions for these quantities we let κ, the isothermal compressibility, and β, the thermal expansion coefficient, be given by,

$$\kappa = \frac{\kappa_1(T)}{1 + (p/B)}$$

$$\beta = \beta_1(T) \left\{1 - \frac{1}{n} \ln \left[1 + \frac{P}{B}\right]\right\} + \frac{\kappa T p}{B} \tag{11.2.10}$$

in which $\kappa_1(T)$ and $\beta(T)$ are the compressibilities and thermal expansion coefficients at zero pressure and temperature T. (Note: for values of $\kappa_1(T)$, $\beta_1(T)$, $C_p(T)$ and $v_1(T)$, (see International Critical Tables, Vol. III, V). Expressing the temperature rise across the shock front as ΔT, and the pressure rise as Δp, one can use average values $\bar{\kappa}$ of κ and $\bar{\beta}$ of β to find $\Delta_p v$ and $\Delta_T v$, i.e.

$$\Delta_p v = \bar{\beta}\ \Delta T;\ \ \Delta_T v = -\bar{\kappa}\ \Delta p \tag{11.2.11}$$

A second equation involving ΔT can be constructed from the definition of enthalpy change across the shock wave:

$$\Delta H = \Delta_p H + \Delta_T H \tag{11.2.12}$$

or

$$\Delta H = \bar{C}_p \Delta T + \int_{p_0}^{p} \left[v - T\left(\frac{\partial v}{\partial T}\right)_p\right] dp$$

Since the R-H relation requires

$$\Delta H = \frac{1}{2}\ (p - p_0)\ (v + v_0) = \Delta p \left[v_0 + \frac{\Delta_T v}{2} + \frac{\bar{\beta} \Delta T}{2}\right]$$

it is seen that

$$\Delta T = \frac{\left(v_0 + \frac{\Delta_T v}{2}\right)\Delta p - \Delta_T H}{\bar{C}_p - \frac{\bar{\beta}\,\Delta p}{2}} \tag{11.2.13}$$

The quantity $\Delta_T H$ is immediately calculatable as a function of T when the equation of state is known (i.e. $v(p,T)$ is known). By choosing Δp one calculates $\Delta_T v$ directly. Since the r.h.s. is a function of temperature the equation is solvable by successive approximation. Detailed calculations for the choice $\Delta p \approx 1$ kilobar $= 10^3\ N/m^2$, will not be given. However, it is found that for water,

$$\bar{\beta} = 3.17 \times 10^{-4}\ \text{cm}^3/\text{gm}\ ^\circ\text{C};\quad \bar{\kappa} = 0.0345\ \frac{\text{cm}^3}{\text{gm} \times \text{kilobar}}$$

$$\bar{T} = 21.97\,^\circ\text{C};\quad \Delta T = 1.97\,^\circ\text{C}$$

Several additional formulas that may be of use as aids in numerical work in calculating the thermodynamic properties of the shock wave are taken up in a later sections of this chapter.

11.2c Thermodynamic Properties of the Gas Sphere

The hydrodynamic and thermodynamic properties of the water just behind the shock wave must be complemented by the thermodynamic properties of the gaseous products of detonation in the expanding gas sphere. For this one requires another equation of state, this time of the gas. A convenient choice that is adapted for use at high temperature is the Wilson-Kistiakowsky equation,

$$p^* = \rho^* \mathcal{R}\, T^* \left(\frac{\nu}{M}\right)[1 + ye^{\beta y}] \tag{11.2.14}$$

$$y = \frac{\rho^*}{M}\,\frac{\mathcal{B}}{T^{*\alpha}};\quad \mathcal{B} = \sum_i \nu_i \mathcal{B}_i\ ;\quad \nu = \sum \nu_i$$

In which β, α are two empirical constants, taken here to be $\beta = 0.3$, $\alpha = 0.25$. Here γ is the number of moles of gas produced by one mole of solid explosive of molecular weight M, B_i is the covolume of the i^{th} gas mixture, defined below, and $\mathcal{R}$ is the universal gas constant.

The covolume is an empirical factor (with dimensions of volume per mole per $(\text{degree})^{1/4}$), calculated to obtain agreement of the equation of state with measurement. A table of B_i for explosion products is given here:

Covolumes $\mathcal{B}_i$ $(\text{cm}^2\ (\text{deg})^{1/4}/\text{mole})$:

$N_2 : 316\,;\ C_0 : 316\,;\ CO_2 : 549;\ H_2 : 54\,;\ H_2O : 241$

Since the detonation process is a function of time we will require initial conditions, i.e. the initial explosion temperature T_e, explosion pressure p_e, and density ρ_e. With good justification ρ_e can be taken to be the density of packing of the solid explosive. Methods of calculating T_e, p_e will be discussed next.

The thermal history of the explosion will require a knowledge of the mean molar heat capacity at constant volume $\bar{C}_v^*$ for the explosion products. A convenient algorithm for calculating this quantity for the i^{th} gas product is,

$$\bar{C}_v^* = A_{0i} + A_{1i}T$$

A table of the coefficients A_0, A_1 is given below:

Heat Capacity Coefficient A_0 (cal/deg mole)

CO : 5.61 ; CO_2 : 10.16 ; H_2 : 4.91 ; H_2O 7.86 ; N_2 : 5.54 ; C(solid) 3.94

Heat Capacity Coefficient A_1 (cal/deg^2 mole)

CO : 0.21 ; CO_2 : 0.46 ; H_2 : 0.30 ; H_20 : 0.55 ; N_2 0.21 ; C(solid) 0.27

The key unknown entity in the equation of state of the gas after detonation is the explosion temperature T_e. Several methods have been used to determine this quantity. Kirkwood and Montroll [11] have suggested the following. The energy balance of the explosion is to be carried out as a sum of three separate increments: (a) energy ΔE^* of isothermal reaction (at temperature $T_0 = 300°$ Abs) at zero pressure to give solid explosion products at zero pressure and gaseous products at zero density (b) energy $\int_{T_0}^{T_e} C_v^* dt$ of heating of products at zero density from T_0 to final temperature $T_e(c)$ energy $\Delta_{T_e} E$ of compression from zero density to ρ_g at constant temperature T_e. Since the energy conversion is assumed adiabatic one takes the sum of these energies to be zero,

$$\Delta E^* + \int_{T_0}^{T_e} C_v^* \, dt + \Delta_{T_e} E = 0 \tag{11.2.15}$$

The evaluation of each energy increment is straightforward. First, ΔE^*. This is the sum of the heat of explosion Q_e and the intrinsic energy $\nu \mathcal{R} T_0$ at $T_0 = 300°$Abs. Now Q_e is the negative of the heat of formation, $-H^*$, so that one can write,

$$\begin{aligned} Q_e = -\Delta H^* = \nu_1 Q_f(Y_1) + \nu_2 Q_f(Y_2) + \ldots \\ - [n_1 Q_F(X_1) + n_2 Q_F(X_2) + \ldots] \end{aligned} \tag{11.2.16}$$

in which ν_i is the number of moles of the i^{th} gaseous product, m_i the number of moles of the i^{th} solid constituent of the explosion; $Q_f(Y_i)$, $Q_F(\bar{X}_i)$ are the heats of formation of the gaseous products and the initial solid reactant respectively. Since all quantities are assumed known from the nature of the chemical reaction and from critical tables of chemical data, one calculates the sum

$$\Delta E^* = -(Q_e + \nu \mathcal{R} T_0) \tag{11.2.17}$$

The second increment is the heat capacity integral. This can be approximated in the form

$$\begin{aligned} \int_{300}^{T_e} C_v^* \, dT &= (A_0 + A_1 T_e)(T_e - 300) \\ A_0 &= \nu_1 A_0(Y_1) + \nu_2 A_0(Y_2) + \ldots \\ A_1 &= \nu_1 A_1(Y_1) + \nu_2 A_1(Y_2) + \ldots \end{aligned} \tag{11.2.18}$$

Tabulations of A_0, A_1 have been given above. The integral of course is a function of T_e, the unknown explosion temperature. The third energy increment is that of isothermal compression at T_e:

$$\Delta_{T_e} E = \alpha\ (\nu \mathscr{R} T_e)\ y_e C^{\beta y_e}\ ;\ \alpha = 0.25,\ \beta = 0.30$$

$$y_e = \rho_g \mathscr{B} T_e^{-1/4} / \nu \mathrm{M}_g \tag{11.2.19}$$

where M_g is the mean molecular weight of the gaseous products. The calculation of M_g is done in the following way:

$$\frac{\nu \mathrm{M}_g}{\rho_g} = \frac{M_e}{\rho_e} - \frac{M_{sp}}{\rho_{sp}} \tag{11.2.20}$$

Here M_e is the molecular weight of the solid explosive and M_{sp} is the molecular weight of the solid products of explosion, i.e.

$$\frac{M_e}{\rho_e} = \frac{m_1\ (X_1)}{\rho(X_1)} + \frac{m_2\ M(X_2)}{\rho(X_2)} + \cdots$$

$$\frac{M_{sp}}{\rho_{sp}} = \frac{\nu_{1s}\ M(Y_{1s})}{\rho(Y_{is})} + \frac{\nu_{2s}\ M(Y_{2s})}{\rho(Y_{2s})} + \cdots \tag{11.2.21}$$

As before, n_i is the number of moles of explosive solid X_i whose molecular weight is $M(X_i)$ and density (X_i); and ν_{is} is the number of moles of solid explosion product Y_{i_s} whose weight is $M(Y_{is})$ and density $\rho(Y_{is})$.

The explicit calculation of all the energy increments is now complete. To satisfy the adiabatic requirement all increments must sum to zero. This leads to an implicit quadratic equation in the unknown explosion temperature T_e, i.e.

$$T_e = \sqrt{a^2 + b^2} - a$$

$$a = \frac{1}{2}\left[\frac{A_0}{A_1} - 300\right] \tag{11.2.22}$$

$$b^2 = \frac{Q_e + 300\nu\mathscr{R} + 300 A_0 - \alpha \nu \mathscr{R} T_e y_e e^{\beta y_e}}{A_1}$$

This equation can be solved by iteration. Once T_e is found one can again use the equation of state for the gaseous products to find the explosion pressure p_e,

$$p_e = \frac{\nu T_e^{5/4}}{\mathscr{B}} I_2(y_e), \quad y_e = \mathscr{B} T_e^{-1/4} / \left[\frac{\nu\ \mathrm{M}_g}{\rho_g}\right] \tag{11.2.23}$$

$$I_2(y_e) = R\, y_e\ (1 + y_e\ C^{\beta y_e})$$

Note that $y_e = y_e(T_e)$, so that I_2 is directly calculatable. However its values are tied to specific explosive materials.

11.2d Thermodynamic Properties of the Gaseous Products

We revert again to the basic problem which is to calculate the temperature T along a selected Poisson adiabatic (along a curve, entropy = constant). Let us choose the adiabatic passing through the thermodynamic point T_0, y_0. Then the entropy is given by

$$S^*(T) = \nu \int_{T_0}^{T} \frac{C_v^-}{T}\, dT + S^*_{T_0} \tag{11.2.24}$$

Suppose C_v^* is taken to be adequately represented by its average $\tilde{C}_v^*$ over the temperature interval T_0, T. Then one must calculate the integral $\int_{T_0}^{T} dT/T$ where T is given by the equation of state. Allowing the change in entropy between T_0 and T to vanish one finally obtains the simple formula,

$$\frac{T}{T_0} = \left[\frac{I_0(y_0)}{I_0(y)}\right]^2$$

$$I_0(y) = \exp\left\{\frac{\alpha y\, e^{\beta y} + \dfrac{1 - e^{\beta y}}{\beta} - \log y}{2\left(\dfrac{\tilde{c}_v^*}{A} - \alpha\right)}\right\} \quad \text{(units: none)} \tag{11.2.25}$$

By choosing any temperature T, $y(T)$ becomes known, and hence $I_0(y)$ becomes known. The distinct advantage of these results is that T_0, y_0 on the adiabatic can be directly expressible in terms of the calculated explosion temperature T_e and parameter y_e. Thus

$$T_e = T_0\left[\frac{I_0(y_0)}{I_0(y_e)}\right]^2 \tag{11.2.26}$$

This will simplify the formulas of the thermodynamic properties of the gaseous products now to be derived.

A. *The Adiabatic Speed of Sound*

This is $C^* = \left(\dfrac{\partial p}{\partial \rho}\right)_s^{1/2}$. By use of the equation of state, one has,

$$C^{*2} = \frac{\nu \mathcal{R} T}{M} L;$$

$$L(y) = 1 + y(2 + \beta y)e^{\beta y} + \frac{[1 + y(1 - \alpha - \beta y)e^{\beta y}]^2}{\dfrac{C_v^*}{\mathcal{R}} + \alpha y(1 - \alpha - \alpha\beta y)e^{\beta y}} \tag{11.2.27}$$

Taking the adiabatic to pass through T_0, y_0 one obtains directly

$$C^*(y) = \left(\frac{\nu T_0}{M}\right)^{1/2} I_0(y_0)\, I_1(y)$$

$$I_1^2(y) = \frac{L\mathcal{R}}{I_0^2(y)} \qquad \left(\text{units of } I_1\text{: } \left[\frac{\text{Cal}}{\text{mole } ^\circ C}\right]^{1/2}\right) \tag{11.2.28}$$

However, since y_e and T_e are calculatable initial conditions, it is more convenient to write the sound speed as

$$C^* = \left[\frac{\nu T_e}{M}\right]^{1/2} I_0(y_e)\, I_1(y) \tag{11.2.29}$$

In numerical work one requires an average $\tilde{C}_v^*$. A rough value is obtainable by setting,

$$\nu\, \tilde{C}_v \approx (A_0 - 300\, A_1) + 2A_1\, \frac{(T_1 + T_0)}{2} \tag{11.2.30}$$

(The coefficient 300 appears here because the initial before-detonation temperature is taken at 300° abs).

B. The Adiabatic Gas Pressure p^*

By use of the equation of state of the gas, and the relation of T/T_0 given above it is easily seen that,

$$p^* = \frac{\nu\, T_0^{5/4}}{\mathscr{B}} \left[\frac{I_0(y_0)}{I_0(y)}\right]^{5/2} I_2(y)$$

$$I_2(y) = \mathscr{R}\, y\, (1 + y\, e^{\beta y}) \qquad \left(\text{units: } \frac{\text{Cal}}{\text{mole } ^\circ\text{C}}\right) \tag{11.2.31}$$

With greater convenience in calculation, one can write,

$$p^*(y) = \frac{\nu\, T_e^{*5/4}}{\mathscr{B}} \left[\frac{I_0(y_e)}{I_0(y)}\right]^{5/2} I_2(y) \tag{11.2.32}$$

We note again that $y = y(\rho, T)$ so that p^* is a function of several thermodynamic variables.

C. The Riemann Function σ^* and the Enthalpy Change ω^*

Along the initial adiabatic these parameters are defined by the relations,

$$\sigma^* = \int_{\rho_0}^{\rho} \frac{C^*\, d\rho}{\rho}\ ; \quad \omega^* = \int_{p_0}^{p} \frac{dp}{\rho} = \int_{\rho_0}^{\rho} \frac{C^2 d\rho}{\rho} \tag{11.2.33}$$

We may use the variable y to help obtain appropriate reformulation of these equations. Noting that

$$\rho^* = \frac{MT^\alpha}{\mathscr{B}}\, y\ ; \quad d\rho^* = \frac{MT^\alpha}{\mathscr{B}}\, dy + \frac{M}{\mathscr{B}}\, \frac{\partial T^\alpha}{\partial y}\, y\, dy$$

and using

$$T^* = T_0^* \left[\frac{I_0(y_0)}{I_0(y)}\right]^2\ ; \quad \frac{\partial T^*}{\partial y} = 2\, T_0 \left[\frac{I_0^2(y_2)}{I_0(y)}\right] \left[-\frac{1}{I_0^2(y)}\right]$$

one immediately obtains the forms

$$\sigma^* = \int_{y_0}^{y} \left[\frac{1}{y} + \frac{\alpha}{T}\left(\frac{\partial T^*}{\partial y}\right)_s\right] C(y)\, dy$$

$$\omega^* = \int_{y_0}^{y} \left[\frac{1}{y} + \frac{\alpha}{T}\left(\frac{\partial T^*}{\partial y}\right)_s\right] C^2(y)\, dy \tag{11.2.34}$$

The evaluation of these integrals must be done numerically. Since they involve $I_0(y)$ and $I_0(y_0)$ the results of numerical integration can be cast in the forms

$$\sigma^* = \left[\frac{\nu T_e}{M}\right]^{1/2} I_0(y_e)\,[I_s(y) - I_3(y_e)], \quad \left(\text{units of } I_3\text{: } \left[\frac{\text{Cal}}{\text{mole } ^\circ C}\right]^{1/2}\right) \tag{11.2.35}$$

$$\omega^* = \frac{\nu T_e}{M} I_0^2(y_e)\,[I_4(y) - I_4(y_e)]$$

The use of $I_3(y)$, $I_4(y)$ is purely a matter of convenience. Tabulations exist.

Summary: The formulas for C^*, σ^*, ω^*, p^*, ρ^* used by Kirkwood and Montroll have been presented above. They give the thermodynamic state of the gaseous products inside the expanding gas sphere after detonation. There are values to be found along the initial adiabatic expansion of the gases passing through T_0, y_0 (alternatively through T_e, y_e). For several reasons it will be very convenient to use p^* as a parameter and obtain $C^* = C^*(p^*)$, $\sigma^* = \sigma^*(p^*)$, $\omega^* = \omega^*(p^*)$, $\rho^* = \rho^*(p^*)$. The use of this parametric representation will be detailed below.

Range of Parameters y, $\tilde{C}_v^*$

In typical calculations y ranges from ≈ 0.5 to 3.00, and $\tilde{C}_v$ ranges from 5 to 8.

11.2e Sample Calculations of Thermodynamic Properties of Gas Products

Assume one mole of TNT of composition $C_7H_5(NO_2)_3$, density $\rho_e = 1.59$.

A. The decomposition equation

$$C_7H_5(NO_2)_3 = 3.5\ CO + 2.5\ H_2O + 1.5\ N_2 + 3.5C$$

All products are gaseous except the carbon. Thus, for the gases,

$$\nu = \nu_1 + \nu_2 + \nu_3 = 3.5 + 2.5 + 1.5 = 7.5$$

The molecular weight of TNT is:

$$M_e = 7 \times 12 + 5 \times 1 + 3 \times 14 + 6 \times 16 = 227.06 \text{ grams}$$

B. Heat of explosion

$$Q_e = 3.5\ Q_f(CO) + 2.5\ Q_f(H_2O) + 1.5\ Q_f(N_2)$$

In units of kilocalories,

$$Q_e = 3.5 \times 26.8 + 2.5 \times 57.8 + \text{neg.} -1(13)$$

or

$$Q_e = 225.3 \text{ kilocal.}$$

Choose units such that $\mathcal{R} = 1.98717 \times 10^{-3}$ kilocal/mole degree so that

$$\nu \mathcal{R} T_0 = 7.5 \times 1.98717 \times 10^{-3} \times 300^\circ = 4.5 \text{ kilocal}$$

Hence

$$\Delta E^* = -(Q_e + \nu \alpha T_0) = -229.8 \text{ kilocal.}$$

C. Heat Capacity and Associated Energy Increment

To calculate $\int_{t_0}^{T_e} C_v^* \, dT$, use the relation

$$\bar{C}_v^* = A_0 + A_1 T$$

in which

$$\begin{aligned} A_0 &= 3.5\, A_0(\text{CO}) + 2.5\, A_0(\text{H}_2\text{O}) + 1.5\, A_0(\text{N}_2) + 3.5\, A_0(C) \\ &= 3.5 \times 5.61 + 2.5 \times 7.86 + 1.5 \times 5.54 + 3.5 \times 3.94 \\ &= 61.38 \text{ cal/deg} = 6.138 \times 10^{-2} \text{ kcal/deg.} \\ A &= 3.5 \times 0.21 \times 10^{-3} + 2.5 \times 0.055 \times 10^{-3} + 1.5 \times 0.21 \times 10^{-3} + 3.5 \times .27 \times 10^{-3} \\ &= 3.37 \times 10^{-6} \text{ kcal/deg}^2. \end{aligned}$$

Hence,

$$\bar{C}^*_v = 6.138 \times 10^{-2} + 3.37 \times 10^{-6} T$$

and

$$\int_{300}^{T_e} C_v^* \, dT = (6.3138 \times 10^{-2} + 3.37 \times 10^{-6} T_e)\ (T_e - 300)$$

D. Calculation of Energy of Compression $\Delta_{T_e} E$

We must first calculate $y_e(T_e)$, where

$$y_e(T_e) = \frac{\dfrac{\mathscr{B} T_e^{1/4}}{\nu \text{M}_g}}{\rho_g}$$

Now, the covolume $\mathscr{B}$ is

$$\begin{aligned} \mathscr{B} &= \sum \nu_i \mathscr{B}_i = 3.5 \times 316 + 2.5 \times 241 + 1.5 \times 316 \\ &= 2182.5 \text{ cm}^3 \times (\text{deg})^{1/4} \end{aligned}$$

To calculate $\dfrac{\nu M_g}{\rho_g}$ use ρ carbon $= 2.25$:

$$\begin{aligned} \nu M_g/\rho_g &= \frac{M_e}{\rho_e} - \frac{\nu_{\text{carbon}} M_{\text{carbon}}}{\rho_{\text{carbon}}} = \frac{227.06}{1.59} - \frac{3.5 \times 12}{2.25} \\ &= 124.14 \text{ cm}^3 \end{aligned}$$

Thus,

$$\begin{aligned} y_e &= \frac{2182.5}{124.14} T_e^{-1/4} \\ &= 17.58\, T_e^{-1/4} \end{aligned}$$

and so,

$$\Delta_{T_0}E = \alpha\,(\nu \mathcal{R}\, T_e)\, y_e\, e^{\beta y_e}$$

$$= 0.25\,(7.5 \times 1.98717 \times 10^{-3}\, T_e)\,(17.58\, T_e^{-1/4})\, e^{0.3 \times 17.58\, T_e^{1/4}}$$

$$= 0.06550\, T_e^{3/4}\, e^{5.24/T_e^{1/4}} \text{ kcal.}$$

E. Calculation of T_e, y_e, p_e

The quadratic to be solved is

$$T_e = \sqrt{a^2 + b^2(T_e)} - a$$

where

$$a = \frac{1}{2}\left(\frac{A_0}{A_1} - 300\right) = \frac{1}{2}\left(\frac{6.138 \times 10^{-2}}{3.37 \times 10^{-6}} - 300\right) = 8957$$

$$b^2 = (Q_e + 300\,\nu R) + 300\,A_0 - \alpha \nu R\, T_e y_e\, e^{\beta y_e})/A_1$$

$$= \frac{229.8 + 300(6.138 \times 10^{-2}) - 0.0655\, T_e^{3/4}\, e^{5.27 + T_e^{-1/4}}}{3.37 \times 10^{-6}}$$

By successive trial solution, one finds,

$$T_e = 2809°$$

$$y_e = 2.415$$

To calculate p_e one requires,

$$I_2(y_e) = \mathcal{R} y_e\,(1 + y_e\, e^{\beta y_e})$$

$$= 1.99717 \times 10^{-3} \times 2.415\,(1 + 2.415\, e^{0.3 \times 2.415})$$

$$= 1.183\ \frac{\text{kcal}}{\text{deg. mole}} = 1.183 \times 10^9\ \frac{\text{erg}}{\text{deg. mole}}$$

Thus

$$p_e = 7.5(2809)^{5/4} \times 1.183 = 83.13 \text{ kilobar} = 83.13 \times 10^2 \text{N/m}^2.$$

F. Calculation of the Riemann Function σ^*, ω^*, and pressure p^*, velocity C^*.

To calculate σ^* one uses the relation,

$$\sigma^* = \left[\frac{\nu T_e}{M}\right]^{1/2} I_0(y_e)\,[I_3(y) - I_3(y_e)]$$

Since both I_0 and I_3 require a knowledge of $\bar{C}_v^*$, it will be convenient to use the approximation,

$$\nu\, \tilde{C}_v^* = (A_0 - 300\,A_1) + 2A_1\,\frac{(T + T_0)}{2}$$

For gas products alone, $A_0 = 47.95$ cal/deg, $A_1 = 2.425 \times 10^{-3}$ cal/deg^2, $\nu = 7.5$. We must next choose $(T + T_0)/2$ to be the temperature of the working range, T_{AV}. Some previous knowledge is required for estimating T_{AV}. Kirkwood and Montroll choose $(T + T_0)/2$ to be 0.8 T_e, thus making $\tilde{C}_v^* \approx 7.7$. Since this is an estimate it is rounded to $\tilde{C}_0^* = 7$.

The molecular weight M of the gas products is

$$M = M_e - \nu_{\text{carbon}} M_{\text{carbon}} = 227.06 - 42 = 185.1 \text{ gms}$$

Hence,

$$\left[\frac{\nu T_e}{M}\right]^{1/2} = \left[\frac{7.5 \times 2809}{185.1}\right] = 10.67$$

We next require a value for $I_0(y_e) = I_0(2.415) \approx I_0(2.4)$. From the formula for I_0 this is 0.6172. Similarly, $I_3(y_e) = I_3(2.4) = 540.8$. This latter number is tabulated in Kirkwood and Montroll [11], but is also obtainable from a numerical integration as, noted earlier. Finally we require $I_3(y)$. Arbitrarily choose $y = 1.8$, then $I_3(1.8) = 358.0$. All these values of course depend on the selected value of $\tilde{C}_v^* = 7$.

The Riemann parameter σ^* thus becomes,

$\sigma^*(1.8) = 10.67 \times 0.6172\,[358.0 - 540.8] = -1203$ m/sec. Note that in the tabulation of I_3 (units: $\left[\frac{\text{Cal}}{\text{mole } ^\circ\text{C}}\right]^{1/2}$) a multiplier has been used to make the units of σ^* to be meters per sec.

Again, using the arbitrary choice $y = 1.8$, and the tabulated values $I_4(1.8) = 31{,}950$, $I_4(2.4) = 128{,}350$, both at $\tilde{C}_v^* = 7$, one obtains

$$\omega^* = \frac{\nu T_e}{M} I_0^2(y_e)\,[I_4(y) - I_4(y_e)]$$

$$= \frac{7.5 \times 2809}{185.1} \times 0.6172^2\,[31{,}950 - 128{,}350]$$

$$= -4.18 \times 10^6 \text{ m}^2/\text{sec}^2$$

Again we note that I_4 (units: $\frac{\text{Cal}}{\text{mole } ^\circ\text{C}}$) has been scaled to give ω in units of meter^2 per sec^2.

The pressure p^* at $y = 1.8$ is

$$p^* = \frac{\nu T_e^{5/4}}{B}\left[\frac{I_0(y_e)}{I_0(y)}\right]^{5/2} I_2(y)$$

$$= \frac{7.5 \times 2809^{5/4}}{2182.5}\left[\frac{0.6172}{0.7142}\right]^{5/2} 0.6120 = 29.8 \text{ kilobars}$$

Here, I_2 (units: $\frac{\text{Cal}}{\text{mole } ^\circ\text{C}}$) has been scaled to give p^* in units of kilobar.

The calculation of the sound speed at arbitrary $y = 1.8$ is also straightforward:

$$C^* = \left(\frac{\nu T_e}{M}\right)^{1/2} I_0(y_e)\, I_1(1.8)$$

$$= \left(\frac{7.5 \times 2809}{185.1}\right)^{1/2} (0.6172)\ (422.2)$$

$$= 2780 \text{ m/sec}$$

(Here, I_1 (units: $\left(\frac{\text{Cal}}{\text{mole } ^\circ C}\right)^{1/2}$) is scaled to give C^* in units of meter per sec).

G. Calculation of the Temperature T^* and density ρ^*.

Along the initial adiabatic

$$T\,[I_0(y)]^2 = T_0\,[I_0(y_0)]^2 = T_e\,[I_0(y_e)]^2$$

Thus, at arbitrary $y = 1.8$

$$T = T_e \left[\frac{I_0(y_e)}{I_0(y)}\right]^2$$

$$= 2809 \left(\frac{0.6172}{0.7142}\right)^2 = 2097 \text{ deg abs.}$$

The gas density is then

$$\rho^* = M_y \cdot T^{1/4} / B$$

$$= 185.1 \times 1.8 \times 2097^{1/4}/2182.5 = 1.033 \ \frac{\text{gm}}{\text{cm}^3}$$

This completes the discussion on the thermodynamic and hydrodynamic properties of the gas sphere and water-propagating shock wave. We now summarize those portions of the Kirkwood-Bethe theory that are of interest here.

11.3 KIRKWOOD-BETHE THEORY OF SHOCK WAVE FORMATION

Let Ω be defined as the kinetic enthalpy per unit mass,

$$\Omega \equiv \omega + \frac{u^2}{2} \qquad \left(\text{units: } \frac{\text{Nm}}{\text{Kg}}\right) \tag{11.3.1}$$

where the thermodynamic equation for (internal energy per unit mass) ω is

$$d\omega = T\,dS + \frac{dp}{\rho} \tag{11.3.2}$$

or

$$\nabla\omega = T \nabla s + \frac{1}{\rho} \nabla p$$

The units of entropy are Nm/Kg/°K.

Under the adiabatic assumption,

$$\nabla\omega = \frac{1}{\rho}\nabla p \tag{11.3.3}$$

Using this in the Eulerian equation of motion leads to

$$\frac{\partial \mathbf{u}}{\partial t} + \mathbf{u}\cdot\nabla u = -\nabla\omega = -\nabla\Omega + \nabla\left[\frac{u^2}{2}\right] \tag{11.3.4}$$

Now

$$\mathbf{u}\cdot\nabla u = \nabla\frac{u^2}{2} + \mathbf{u}\times(\nabla\times\mathbf{u})$$

so that

$$\frac{\partial \mathbf{u}}{\partial t} + \mathbf{u}\times(\nabla\times\mathbf{u}) = -\nabla\Omega \tag{11.3.5}$$

The first major assumption is now made that the motion is irrotational, at least in the initial propagation of the shock wave. This cannot be exactly true, but is approximately valid. Thus

$$\frac{\partial \mathbf{u}}{\partial t} = -\nabla\Omega \tag{11.3.6}$$

Let $\mathbf{u}$ be expressed as a gradient of a potential ψ. Then

$$\frac{\partial\psi}{\partial t} = \Omega \tag{11.3.7}$$

A second equation is derived from the equation of continuity,

$$\frac{\partial\rho}{\partial t} + \nabla\cdot(\rho\mathbf{u}) = 0 \tag{11.3.8}$$

or, assuming $\nabla\rho\cdot\mathbf{u}$ is negligible,

$$\frac{1}{\rho}\frac{d\rho}{dt} = -\nabla\cdot\mathbf{u} \tag{11.3.8}$$

Using again the relation of adiabatic state,

$$d\omega = \frac{dp}{\rho} = C^2\frac{d\rho}{\rho}$$

one arrives at the equation

$$\nabla^2\psi = -\frac{1}{C^2}\frac{d\omega}{dt} \tag{11.3.9}$$

It is important to note that the time derivative is total, i.e. $d/dt = \partial/\partial t + \mathbf{u}\cdot\nabla$. Thus, from the definition of Ω,

$$\frac{d\omega}{dt} = \left[\frac{\partial}{\partial t} + \mathbf{u}\cdot\nabla\right]\left[\frac{\partial\psi}{\partial t} - \frac{u^2}{2}\right] = \frac{\partial^2\psi}{\partial t^2} + \mathbf{u}\cdot\nabla\left[\frac{u^2}{2}\right] - \frac{du^2}{dt} \tag{11.3.10}$$

The nonlinear equation of wave propagation is then

$$\nabla^2\psi - \frac{1}{C^2}\frac{\partial^2\psi}{\partial t^2} = \frac{1}{C^2}\left[\mathbf{u}\cdot\nabla\frac{u^2}{2} - \frac{du^2}{dt}\right] \tag{11.3.11}$$

$$\mathbf{u} = -\nabla\psi \;;\; \Omega = \frac{\partial\psi}{\partial t}$$

Choosing the case of spherical symmetry, setting a new potential $\phi = \psi\ r$, and defining a new parameter $G = r\Omega$ (so that $G = \frac{\partial \phi}{\partial t}$) one can find the equation of motion to be,

$$\frac{\partial^2 \phi}{\partial r^2} - \frac{1}{C^2}\frac{\partial^2 \phi}{\partial t^2} = \frac{r}{C^2}\left[\frac{u}{2}\frac{\partial u^2}{\partial r} - \frac{d\,u^2}{dt}\right] \tag{11.3.12}$$

where now there is only one component of motion, namely the radial velocity u.

The direct solution of this last equation is very difficult. A reasonable approach is to use the method of characteristics. Consider a solution in the form of a progressive wave of $r\Omega$ or G propagated *behind* the shock front with some velocity $\bar{C}$, defined by the equation,

$$\left[\frac{\partial r}{\partial t}\right]_G = \bar{C} \quad , \text{ on lines of constant } G. \tag{11.3.13}$$

Since G is constant there must be some time τ such that G at any r, t is related to G_a on radius $a(\tau)$ of the expanding sphere, i.e.

$$G_a(\tau) = G(r,t)$$

so that

$$\Omega(r,t) = \frac{a(\tau)}{r}\,\Omega_a(\tau) \tag{11.3.14}$$

It is readily seen that τ is the retarded time,

$$\tau = t - \int_{a(\tau)}^{r} \frac{dr'}{\bar{C}(r',\tau)} \tag{11.3.15}$$

Now assume the r is precisely on the shock front $r = R$ where the speed is $U(r\tau)$ so that

$$\tau_0(R) = \int_{a_0}^{R} \frac{dr'}{U(r',\tau_0)} - \int_{a(\tau_0)}^{R} \frac{dr'}{\bar{C}(r',\tau_0)} = \tau_U - \tau_{\bar{C}}. \tag{11.3.16}$$

Note that the first term is calculated from the charge radius a_0, while the second term from the variable radius $a(\tau_0)$. Since $\bar{C} > U$ for finite amplitude waves one must have $\tau(R = 0) = 0$, and $\tau_0(T)$ increasing with R (see Fig. 11.3.1). Thus at any shock front radius R the crest of the wave emitted in time $0 \leqslant t \leqslant \tau_0(R)$ overtakes the wavefront and is *destroyed in it*, that is, it is not realized. Only the waves emitted in time $t \geqslant \tau_0(R)$ appear at R. This effect is analogous to ocean waves running up a shore, the faster part of the wave overtaking the slower advancing front where it is destroyed causing thereby a steepening of the front.

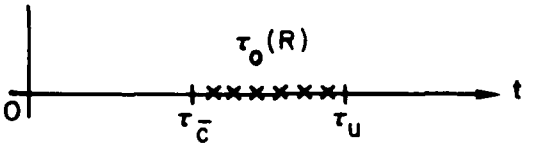

Fig. 11.3.1. Definition of $\tau_{\bar{C}}$, τ_u.

The estimation of $\bar{C}$ is difficult. As an approximation one can use the asymptotic result that to order O,

$$\bar{C} = C + u + O\left[\frac{\ln r}{r^2}\right] \tag{11.3.17}$$

in which $C = C_b$ is the local velocity of sound behind the shockfront, and u is the material radial velocity of the water.

The precise calculation of $G_a(t)$ is difficult. Experimental measurements of shock wave pressure-time curves lead to the very useful approximation that

$$G_a(t) = G_1 e^{-t/\theta_1} + G_2 \left[1 + \frac{t}{\theta_2}\right]^{-4/5} \tag{11.3.18}$$

in which θ_1, θ_2 are two empirical time constants, and G_1 G_2 are functions of initial conditions. However the further approximation that

$$G_a(t) \approx G_1 e^{-t/\theta_1};\ G_1 = a_0\left[\omega_1 + \frac{u_1^2}{2}\right] = A_0\Omega \tag{11.3.19}$$

gives very satisfactory results in most cases (Kirkwood-Bethe [8]).

Summarizing: the pressure-time curve at any radius r is based on the kinetic enthalpy $\Omega(a(t),t)$ of the water and the auxiliary function $G(a(t),t) = r\Omega(a(t),t)$, where $a(t)$ is the radius of the gas sphere at time t. The rapid fall in Ω from its initial value $\Omega_1(a_0,0)$ leads to the useful approximation that $G(a(t),t) = G_1 e^{-t/\theta_1}$ where $G_1(a_0,0) = a_0\Omega_1(a_0,0)$, and $\theta_1 = \dfrac{a_0}{C_\theta}$. The magnitude of C_θ will be given explicitly later in this section but is known to depend on the initial conditions ρ_1, C_1, ω_1 of the water, and initial conditions ρ_1^*, C_1^* and ω_1^* of the gas, all of which quantities can be thought of as functions of the initial pressure p_1 in the water. Methods of calculating p_1 are discussed below.

When $\Omega_1(a_0,0)$ is known it can be used to derive the magnitude of the kinetic enthalpy $\Omega(r,t)$ at any radius $r > a_0$:

$$\Omega(r,t') = x\,\frac{a_0}{r}\,\Omega_1(a_0,0)e^{-t'/\theta} \tag{11.3.20}$$

$$x(a,t') = \frac{G(a,t')}{G(a_0,0)}\ ;\ \theta = \gamma_t\theta_1;\ t' \geqslant t - r/c$$

Two new factors appear here: (1) the factor x, called the *dissipation parameter*, is a function of r/a_0, with magnitude $x \leqslant 1.0$. It shows that unlike spherical acoustic waves the product $r\Omega$ is not constant, but rather decreases with distance from the source, at first rapidly near the explosive gas sphere, then slowly farther out. (2) The *time spread factor* γ_t, also a function of r/a_0 which reduces the rate of fall-off of Ω with time at fixed r. Explicit formulas for x, γ_t are given later in this section. They too depend on initial values of ρ_1, C_1, ω and C_θ. Note that in the latter symbol, θ_1 is the value of θ at time $t = 0$.

The propagation of the shock pressure in the water as the shock wave radiates outward is governed by the approximation,

$$p = x\,\frac{a_0}{r}\,P_0\,e^{-t'/\theta} \tag{11.3.21}$$

$$P_0 = \rho\,\Omega_1\ ;\ \theta = \gamma_t\,\theta.$$

When r/a_0 is less than -25 the density ρ must be calculated as a thermodynamic function of the pressure so that the above formula is implicit. However when r/a_0 is greater than 25 one case use the acoustic approximation, $\rho \approx \rho_0$.

11.3a Calculation of the Dissipation Parameter X and the Time Spread Factor γ_t

We assume that at time $t = 0$ the hydrodynamic and thermodynamic properties of the adjacent water at radius a_0 are known, that is, p_1, U_1, σ, ω_1, θ_1 are known. Let us choose a field point precisely at the shock front $r = R$. From Eq. 11.3.16 the delay (or retarded) time is $\tau_0(R)$. By definition,

$$x(\tau_0) = \frac{G_a(\tau_0)}{G_a(0)} = \frac{G_a(\tau_0)}{G_1} \tag{11.3.22}$$

The problem is to find $\tau_0(R) = \tau_U - \tau_{\bar{C}}$. From Eq. 11.3.17 and Sect. 11.2

$$\bar{C} = C_0 + u = C_0[1 + 2\beta\sigma]; \; U = C_0[1 + \beta\sigma]$$

At the shock front the material velocity u equals the Riemann parameter σ. Hence by definition of Ω one has

$$\Omega_1 = \omega_1 + \frac{u_1^2}{2} = C_0\sigma + \frac{n-1}{4}\sigma^2 + \frac{u_1^2}{2} = C_0\sigma\left[1 + \frac{n+1}{4C_0}\sigma\right] \tag{11.3.23}$$

Since $\Omega(r,t) = G_2(\tau)/r$, then

$$C_0 r\sigma[1 + \beta\sigma] = G_a(\tau), \;\; \beta = \frac{n+1}{4C_0}, \;\; n \approx 7 \tag{11.3.24}$$

At time $t = 0$ one has $G_a(\tau) = a_0\Omega_1$. Thus

$$\frac{r}{a_0} = \frac{\Omega_1(z-1)^2\beta}{C_0 z}, \;\; z = 1 + \frac{1}{\beta\sigma} \tag{11.3.25}$$

With this definition, and with the definitions of Ω_1, $G_a(\tau)$, etc. given above, Kirkwood and Bethe [8] derived an *implicit* formula for τ_0 in the form $\tau_0 = f(G_a(\tau_0), G_1, \sigma_1, \beta_1 z(q))$, where the functional dependence f is an integral, and q *is a floating parameter.* By introducing the peak approximation $G_a(\tau) = G_1 e^{-\tau/\theta'}$, and neglecting negligible terms they arrived at the following approximations. It is convenient to define q such at $\frac{r}{a_0} = xq$:

$$x(q) = \frac{2K_1}{1 + [1 + 4\alpha K_1 K_0(q)]^{1/2}} \tag{11.3.27a}$$

$$K_1 = 1 + \frac{\alpha(z_1 - 1)}{2z}; \; K_0(q) = \frac{z_1 - 1}{2z_1} + \Gamma_1 y \tag{11.3.27b}$$

$$y = \ln\frac{z}{z_1} - 2\left(\frac{1}{z_1} - \frac{1}{z}\right) + \frac{1}{2}\left(\frac{1}{z_1^2} - \frac{1}{z^2}\right) \tag{11.3.27c}$$

$$z_1 = 1 + \frac{1}{\beta\sigma_1}; \; \Gamma_1 = \frac{\beta\Omega_1}{C_0}; \; \alpha = \frac{a_0}{C_0\theta_1} \tag{11.3.27d}$$

$$z = 1 + \frac{q}{2\Gamma_1} + \left[\frac{q}{\Gamma_1} + \left(\frac{q}{2\Gamma_1}\right)^2\right]^{1/2} \tag{11.3.27e}$$

All quantities subscripted 1 correspond to time $t = 0$ and are *presumed known*. Actually the calculation of θ_1 is complicated, but reasonable formulas are available to determine it. This is discussed below.

The method of calculation of $x(q)$ can be chosen according to one's goals. A convenient procedure is to select some particular value of r/a_0 then calculate $x(q)q$ to equal this value by successive approximation to q. Alternatively one can calculate $x(q)$ for arbitrary q, then determine r/a_0 corresponding to the product $x(q)q$. A sample calculation based on choosing q is presented below. We now turn to the question of θ_1.

Initial Time Constant θ_1

The physical picture of events at time $t = 0$ (i.e. detonation) is this: a shock wave advances outward into the water from an initial radius a_0, while simultaneously a rarefaction wave travels inward into the gas from radius $a(t)$. The shock wave is modeled as a wave of kinetic enthalpy $r\Omega$ (or G) propagating with velocity $\bar{C}$, while the rarefaction wave is also a wave of kinetic enthalpy propagating with velocity $\bar{C}^*$.

At the surface $a(t)$ of the gas sphere there must be continuity of pressure and material velocity (i.e. p, u). Thus for common p, u the initial and continuity conditions are

$$\begin{aligned} &\text{water:} \quad \frac{1}{\rho C^2}\frac{dp}{dt} = -\frac{\partial u}{\partial r} - \frac{2u}{a} \\ &\textit{gas:} \quad \frac{1}{\rho^* C^{*2}}\frac{dp}{dt} = -\left(\frac{\partial u}{\partial r}\right)^* - \frac{2u}{a} \end{aligned} \tag{11.3.28}$$

This comes from the relation $\frac{1}{\rho}\frac{\partial \rho}{\partial t} = -\nabla \cdot \mathbf{u}$. The problem then is to obtain formulas for dp/dt and u. Noting that

$$\frac{\partial G}{\partial t} + \bar{C}\frac{\partial G}{\partial r} = 0; \quad \frac{\partial p}{\partial r} = -\rho\frac{du}{dt}$$

and recalling that $\frac{d}{dt} = \partial/\partial t + \bar{u}\cdot\vec{\nabla}$, $dG = \Omega\, dr + rdp/\rho + rudu$ it is seen that

$$u(\bar{C} - u)\frac{\partial u}{\partial r} + \frac{1}{\rho}\frac{dp}{dt} - (\bar{C} - 2u)\frac{du}{dt} + \frac{\Omega\bar{C}}{r} = 0 \tag{11.3.29}$$

Eliminating $\partial u/\partial r$ from this equation and the above equation of continuity for water, then gas, leads to the following pair, valid at $r = a$ under the approximation $\bar{C} = C_b + u$, $\bar{C}^* = C_b^* - u$:

$$\frac{dp}{dt} = -\rho\rho^* CC^*\frac{jC + j^*C^*}{\rho C + \rho^* C^*}\frac{u}{a} \tag{11.3.29a}$$

$$\frac{du}{dt} = \frac{j\rho C^2 - j^*\rho^* C^{*2}}{\rho C + \rho^* C^*}\frac{u}{a} \tag{11.3.29b}$$

where

$$j = \frac{1}{uC}\left[\frac{C + u}{C - u}\omega - \frac{3u^2}{2} - \frac{u^3}{C - u}\right] \tag{11.3.29c}$$

$$j^* = \frac{1}{uC^*}\left[\frac{C^* - u}{C^* + u}\omega^* + \frac{3u^2}{2} - \frac{u^3}{C^* + u}\right] \tag{11.3.29d}$$

$$C = C_b,\ C^* = C_b^* \tag{11.3.29e}$$

Finally we seek to calculate θ_1. A convenient procedure is to approximate the enthalpy ω by a peak formula at radius $a(t)$:

$$\omega_a(t) = \int \frac{C d\rho}{\rho} = \int \frac{dp}{\rho} = \omega_1 e^{-t/\theta_1}$$

so that

$$\frac{1}{\theta_1} = -\frac{1}{\omega_1}\lim \frac{d\omega}{dt} = -\frac{1}{\omega_1 \rho_1}\lim_{t\to 0}\frac{dp}{dt}$$

When $a = a_0$ at time $t = 0$, one can write therefore

$$\theta_1 = a_0/C_{\theta_1} \tag{11.3.30}$$

where

$$C_{\theta_1} = \frac{\rho_1^* C_1^* u_1}{\omega_1}\,\frac{j_1 C_1 + j_1^* C_1^*}{\rho_1 C_1 + \rho_1^* C_1^*}\,C_1$$

in which (as before) subscript 1 denotes initial conditions on the surface of the gas sphere of radius a_0.

The required formulas for finding the initial time constant θ_1 have now been assembled. Before proceeding to a numerical example we will examine a formula for determining the time spread factor.

Time Spread Factor γ_t

A short time after the wave front has passed a point R the retarded time τ is equal to the retarded time τ_0 at the wavefront plus a small increment,

$$\tau = \tau_0 + \frac{1}{\gamma_t}(t - t_0),\ \frac{1}{\gamma_t} = \left(\frac{\partial \tau}{\partial t}\right)_R$$

Since

$$\tau = \tau_0 + \frac{1}{\gamma_t}(t - t_0),\quad \frac{1}{\gamma_t} = \left(\frac{\partial \tau}{\partial t}\right)_R$$

$$\tau = t - \int_{a(t)}^{r} dr'/\bar{c}\,(r', \tau)$$

it is seen that

$$\gamma_t = 1 - \frac{U_a(\tau)}{\bar{C}_a(\tau)} - \int_{a(\tau)}^{R}\frac{1}{\bar{C}^2}\left(\frac{\partial \bar{C}}{\partial \tau}\right)_R dr'$$

Using the same technique of expressing τ_0 as a function of $G_a(\tau_0)$, G_1, σ, etc. in order to calculate x, Kirkwood and Bethe [8] derive the following equation for γ_t,

$$\gamma_t = 1 - \frac{1}{\beta C_0}\,\frac{1}{z_a + 1} + 2\alpha x \Gamma_1 \left\{ \ln \frac{z}{z_a} - \frac{4(z - z_a)}{(z+1)(z_a + 1)} \right\} \tag{11.3.31}$$

$$z_a = 1 + \frac{x}{2\Gamma_1} + \left[\frac{x}{\Gamma_1} + \left(\frac{x}{2\Gamma_1} \right)^2 \right]^{1/2} \tag{11.3.32}$$

in which q_a, or the value of q on radius $a(t)$, has been approximated by setting $q_a = x$, the x being determined by the formulas appearing in Section 11.3a.

Summary: The principal features of the Kirkwood-Bethe theory of shock and detonation waves has been presented. While very complex it still allows a large number of stubborn physical events to be understood and numerically evaluated. The model is certainly approximate in so far as it does not account for bubble migration and medium surface effects. However, it does offer an opportunity to describe shock waves from first principles. Some numerical work has already been carried out. We continue below to present additional calculations involving the dissipation factor x and the timespread factor γ_t.

11.3b Continuation of Sample Calculation

As before we take one mole TNT (=227.06 grams), density 1.59 and assume its shape is spherical. We begin with determination of initial pressure p_1 and particle velocity u_1 at the moment of explosion.

A. *Particle velocity* u_1, *Initial Pressure* p_1

From the Rankine-Hugoniot equations we know that p, u just behind the shock front in the water obey the relation,

$$u = \sqrt{(p - p_0)(\mathrm{v}_0 - \mathrm{v})}, \qquad \mathrm{v} = \frac{1}{\rho}$$

in which the thermodynamic path is an adiabatic through the initial points p, v. Using the Tait equation of state for water we found that the pressure-density relation was given by Eq. 11.2.4. Thus choosing any arbitrary p we found v, hence we deduced the value of u. A list of corresponding entries is presented here:

ρ (kilobars)	u (m/sec)
25	841
30	960
35	1070
40	1170

To this point ρ is arbitrarily selected. There is however, a specific $\rho = \rho_1$ where the velocity u equals $-\sigma^*$ as required by the Riemann theory of the onset of a rarefaction wave in the gas sphere. Now the gas pressure $\rho^*(y)$ is given by Eq. 11.2.14, and the corresponding parameter $\sigma^*(\rho^*(y))$ is given by Eq. 11.2.25. Arbitrary selection of y then leads to the following table of σ^*:

y	ρ^* (kilobars)	$-\sigma^*$ (m/sec)
1.8	29.6	1231
1.9	35.4	1041
2.0	42.2	850.8

A superposition plot of u versus ρ, together with $-\sigma^*$ versus ρ^* shows that $u_1 + \sigma^*(\rho_1) = 0$ occurs at:

$$\rho_1 = 34.7 \text{ kilobars}$$

$$u_1 = 1065 \text{ m/sec}$$

$$y = 1.89$$

These are the conditions in the water at time $r = 0$ just after the shock point. Using the R-H relations again, plus the Tait equation of state gives the following parameters associated with ρ_1:

$$C_1 = C_0 + \frac{m-1}{2}\sigma = C_0 + 3\sigma = 1470 + 3(955.3) = 4336 \text{ m/sec}$$

$$\sigma_1 = 955.3 \text{ m/sec}$$

where σ is determined from Eq. 11.2.7, 11.2.8. This set of equations also defines ω:

$$\omega_1 = 26.6 \times 10^5 \text{ m}^2/\text{sec}^2$$

and by the Tait equation of state,

$$\rho_1 = 1.475 \text{ gm/cm}^3$$

B. *Initial Values of the Gas Parameters*

Let $y = 1.89$, then:

$C_1^* = 2.992 \times 10^2$ m/sec using Eq. 11.2.29

$-\omega_1^* = 3.8 \times 10^6$ m^2/sec^2 using Eq. 11.2.35

$-\sigma_1^2 = 10.65$ m/sec from $u_1 + \sigma_1^*(\rho_1^*) = 0$

$\rho_1^* = 1.17$ gm/cm^3 from Wilson-Kistikowsky eq. of state

C. *Calculation of* C_θ, θ_1

$j_1 = 0.500$ using Eq. 11.2.29c

$j_1^* = 1.01$ using Eq. 11.2.29d

Hence

$C_\theta = 3.187 \times 10^3$ m/sec using Eq. 11.3.30

and

$$\frac{\theta_1}{a_0} = \frac{1}{C_{\theta_1}} \approx 0.32 \times 10^{-3} \text{ sec/m}$$

D. *Calculation of* C_0, θ_1

The specific volume of the TNT is

$$v = \frac{M_e}{\rho_e} = \frac{227.06}{1.59} = 142.8 \text{ cm}^3/\text{gm}$$

Hence the initial radius is

$$a_0 = \left[\frac{3}{4\pi} \times 142.8\right]^{1/3} = 3.24 \text{ cm}$$

Thus the initial time constant is,

$$\theta_1 = \frac{3.24 \times 10^{-2} \text{ m}}{3.187 \times 10^3 \text{ m/sec}} = 1.017 \times 10^{-5} \text{ sec}$$

E. *Calculation of the Dissipation Factor*

Here we use the formulas presented in Sec. 11.3.

(a) $$\alpha = \frac{a_0}{C_0\theta_1} = \frac{3.24 \times 10^{-2} \text{ m}}{1.47 \times 10^3 \frac{\text{m}}{\text{sec}} \times 1.017 \times 10^{-5} \text{ sec}} = 2.16$$

(b) $$\beta = \frac{m+1}{4C_0} = \frac{8}{4 \times 1.47 \times 10^3} = 1.36 \times 10^{-3} \text{ sec/m}$$

(c) $$z_1 = 1 + \frac{1}{\beta\sigma_1} = 1 + (1.36 \times 10^{-3} \times 9.553 \times 10^2)^{-1} = 1.7696$$

(d) $$\Gamma_1 = \frac{\beta\Omega_1}{C_0} = \frac{1.36 \times 10^{-3}\left[26.6 \times 10^5 + \frac{1065^2}{2}\right]}{1.47 \times 10^3} = 2.985$$

(e) Choose $q = 25$ Then, using Eq. 11.3.27e

$$z = 1 + \frac{25}{2 \times 2.985} + \left[\frac{25}{2.985} + \left[\frac{25}{2 \times 2.985}\right]^2\right]^{1/2} = 9.848$$

(f) Using Eq. 11.3.27c

$$y = \ln\left[\frac{9.848}{1.7696}\right] - 2\left[\frac{1}{1.7696} - \frac{1}{9.848}\right] + \frac{1}{2}\left[\frac{1}{1.7696^2} - \frac{1}{9.848^2}\right] = 0.9438$$

(g) Using Eq. 11.3.21b

$$K_1 = 1 + \frac{2.16(1.7696 - 1)}{2(1.7696)} = 1.4696$$

(h) using Eq. 11.3.27b

$$K_0 = \frac{1.7696 - 1}{2 \times 1.7696} + 2.985(0.9438) = 3.034$$

(i) Finally, using Eq. 11.3.27a

$$x(\text{at } q = 25) = \frac{2 \times 1.4696}{1 + [1 + 4 \times 2.16 \times 1.4696 \times 3.034]^{1/2}} = 0.4.4$$

(j) Thus, the distance ratio is

$$\frac{r}{a_0} = x(q)q = 0.404 \times 25 \approx 10$$

F. *Calculation of the Spread Factor*

Using Eq. 11.3.3.2

$$z_a = 1 + \frac{0.40335}{2 \times 2.985} + \left[\frac{0.40335}{2.985} + \left[\frac{0.40335}{2 \times 2.985}\right]^2\right]^{1/2} = 1.459$$

Using Eq. 11.3.31

$$\gamma_t = 1 - (1.36 \times 10^{-3} \times 1.47 \times 10^3(1.459 + 1))^{-1}$$
$$+ (2 \times 2.16 \times 0.40335 \times 2.985)\left\{\ln \frac{9.848}{1.459} - \frac{4(9.898 - 1.459)}{(9.898 + 1)(1.459 + 1)}\right\}$$
$$= 4.2$$

Thus the time constant at $r/a_0 \approx 10$ is

$$\theta = \gamma_t \sigma_1 = 4.2 \times 1.017 \times 10^{-5} = 4.27 \times 10^{-5} \text{ sec}$$

G. *Calculation of Peak Pressure at* $R/a_0 = 10$

We use the formula

$$\Omega(R,t) = x\left(\frac{a_0}{R}\right)\Omega_1 e^{-t'/\theta}.$$

$$\Omega_1 = \omega_1 + \frac{u_1^2}{2} = 26.6 \times 10^5 + \frac{1065^2}{2} = 3.227 \times 10^6 \text{ m}^2/\text{sec}^2$$

$$\Omega = \frac{0.404}{10} \times 3.227 \times 10^6 \, e^{-t'/4.27 \times 10^{-5}}$$
$$= 1.3037 \times 10^5 \text{ m}^2/\text{sec}^2 \text{ at } t' = 0$$

Assume the acoustic approximation holds, i.e. $p = \rho_0$, so that,

$$p = \rho_0 \Omega = 10^3 \frac{N\text{sec}^2}{\text{m}^4} \times 1.303T \times 10^5 \frac{\text{m}^2}{\text{sec}^2} = 1.3037 \times 10^8 \text{ N/m}^2$$
$$= 1.8904 \times 10^4 \text{ psi}$$

Thus at a distance of 32.4 cm the peak pressure is 18,904 psi and it decays as $\exp(-t'/4.27 \times 10^{-5})$, where t' = time starting with arrival of pulse.

11.4 SECONDARY PRESSURE PULSES

Introduction

The radiation of sound from the pulsating gas bubble free to move in the ocean is difficult to calculate in the general case. After explosion the gas sphere migrates upward because it is buoyant, and continuously radiates energy but at an unequal rate. Also, near the ocean surface the spherical shape of the gas sphere becomes distorted. As a first approach it has been found satisfactory to calculate the secondary pressure pulses on the basis of the following assumptions: (1) the bubble is stationary, (2) the total energy of each cycle of pulsation is constant, (3) the dominant motion of the adjacent medium is adequately expressed as incompressible flow, (4) the gas in the gas sphere expands adiabatically according to the law $pv^{\gamma} = k_1 = \text{const.}$, (5) the bubble is not near any boundary of the medium, i.e. the medium is infinite in all directions, (6) the bubble is always spherical.

Several models have been constructed. The one used here is semiempirical, that is, the equations describing the motion of the gas sphere are derived from an energy balance, and are formulated in terms of three key parameters. Many experiments are then conducted in which a wide range of variation of charge weight, depth and distance of observation are recorded. A best fit is then made of theory to experimental data from which the best choices of the three parameters are deduced. The resultant formulas are then extrapolated to cover all other combinations of variables.

11.4a Formulation of the Theory of Secondary Pressure Pulses [12]

Assume the constant energy of the first cycle of pulsation is E_1 and let the mass of gas be M. The sum of potential and kinetic energies of bubble oscillation is then equal to E_1. In accord with the above theoretical approach it is first assumed that no radiation occurs. The energy balance then becomes:

$$T + U_H + U_g = E_1 \tag{11.4.1}$$

in which T is the kinetic energy, U_H is the potential energy stored in the hydrostatic pressure head P_0 and U_g is the potential energy stored in the gas. Both U_H and U_g are calculated as the work done in compressing the expanded bubble from an infinite radius to the instantaneous radius $A(t)$, the compression in the case of the gas being adiabatic. The energy balance is then reduced to,

$$2\pi\rho A^3\dot{A}^2 + \frac{4}{3}\pi A^3 P_0 + \frac{k_1 M^{\gamma}}{(\gamma - 1)A^{3(\gamma-1)}\left(\frac{4\pi}{3}\right)^{\gamma-1}} = E_1 \tag{11.4.2}$$

It is convenient to introduce scale factors L and C for length and time:

$$L = \left(\frac{3E_1}{4\pi P_0}\right)^{1/3}; \quad C = L\left(\frac{3\rho}{2P_0}\right)^{1/2} \tag{11.4.3a}$$

The reduced equation of energy then reads,

$$a^3\dot{a}^2 + a^3 + ka^{-3(\gamma-1)} = 1 \tag{11.4.3b}$$

$$k \equiv \frac{k_1 P_0^{\gamma-1}}{(\gamma-1)\epsilon^{\gamma}}; \quad a = A/L \tag{11.4.3c}$$

where ϵ is the bubble energy per unit mass of gas (or explosive charge).

This equation, though simple, contains much of the dynamics of the gas sphere. First one sets $\dot{a} = 0$. This results in a cubic equation in the (nondimensional) radius a defining the maximum bubble radius a_M or minimum bubble radius a_m,

$$a_M = [1 - ka_M^{-3(\gamma-1)}]^{1/3}; \quad a_m \simeq k^{[3(\gamma-1)]-1} \tag{11.4.4}$$

(Note that the true radii are $A_M = L_{a_M}$, $A_m = La_m$). Second, one solves for $\dot{a} = \frac{da}{dt}$, and proceeds to integrate with respect to a to obtain the nondimensional period of pulsation,

$$t = 2\int_{a_m}^{a_M} \frac{a^{3/2}}{[1 - a^3 - ka^{-3(\gamma-1)}]^{1/2}}\, da \tag{11.4.5}$$

the actual period being $T = Ct$. This equation can be solved by numerical methods or special techniques. Third, the excess pressure of incompressible flow at any point can be found from Bernoulli's equation in the velocity potential ϕ:

$$\Delta p = \rho\left[\partial\phi/\partial\tau - \frac{1}{2}(\nabla\phi)^2\right], \quad \tau = \text{dimensional time} \tag{11.4.6}$$

For spherical flow $\phi = A^2A^1/R$ [13]. Thus

$$\Delta p = \rho\left[\overline{\frac{\dot{A}^2\dot{A}}{R}} - \frac{1}{2}\nabla\left[\overline{\frac{\dot{A}^2\dot{A}}{R}}\right]\right] \tag{11.4.7}$$

The second term, or spatial gradient of $R^{-2}\, A^4\dot{A}^2$, is negligibly small (at any reasonable distance R) compared to the first term. Thus

$$\Delta p = 2P_0L(\overline{a^2\dot{a}})/3R \tag{11.4.8}$$

The problem is to find $\partial/\partial\tau[a^2\dot{a}]$. One procedure is to derive an equation of motion from the energy equation (by the method of Lagrange) and from it derive an expression for $\partial/\partial\tau(a^2\dot{a})$. It is

$$2\frac{\partial}{\partial\tau}(a^2\dot{a}) = a\dot{a}^2 - 3a + 3(\gamma-1)ka^{-3\gamma+1} \tag{11.4.9}$$

This leads to the following useful formula for the excess pressure,

$$\Delta p = \frac{P_0L}{R}\left[\frac{a^2\dot{a}}{3} - a + \frac{(\gamma-1)k}{a^{3\gamma-1}}\right] \tag{11.4.10}$$

The excess pressure at two distinct radii are of interest: (1) When bubble radius a is a maximum,

$$\Delta P_M = -\frac{P_0L}{R}\left[a_M - \frac{(\gamma-1)k}{a_M^{3\gamma-1}}\right] \tag{11.4.11}$$

Experimental data show that the second term on the r.h.s. is smaller than the first, and hence that ΔP_M is negative, i.e. below hydrostatic pressure. (2) When bubble radius a is a minimum,

$$\Delta P_m = \frac{P_0 L(\gamma - 1)}{Rk \dfrac{2}{3(\gamma - 1)}} \left[1 - \frac{k^{\frac{1}{\gamma - 1}}}{\gamma - 1}\right] \tag{11.4.12}$$

Again, experiment shows that the second term r.h.s. is smaller than the first, and hence that ΔP_m is always positive, i.e. above ambient hydrostatic pressure.

When $\partial/\partial\tau(a^2\dot{a})$ is available one can use it to determine the radius a_N where Δp is zero, or equivalently where $\partial/\partial\tau(a^2\dot{a}) = 0$: one has,

$$4a_N^3 = 1 - (4 - 3\gamma)ka_N^{-3(\gamma-1)} \tag{11.4.13}$$

together with the following formula in $(a^2\dot{a})_N$,

$$(a^2\dot{a})_N = 1.732a_N^2 \left[1 - \frac{(\gamma - 1)k}{a_N^{3\gamma}}\right]^{1/2} \tag{11.4.14}$$

These explicit quantities enable one to calculate the *positive* impulse I delivered by the pressure wave during each cycle's minimum-radius phase,

$$I = \int_{a_{N_1}}^{a_{N_2}} \Delta p d\tau \tag{11.4.15}$$

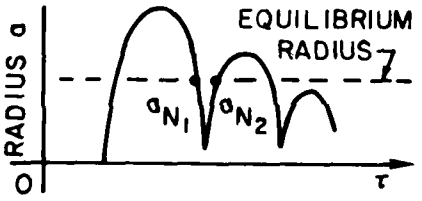

Fig. 11.4.1. Definition of a_{N_1}, a_{N_2}.

(see Fig. 11.4.1 for meaning of the range integration.)

$$\int_{a_{N_1}}^{a_{N_2}} = \int_{a_{N_1}}^{a_m} + \int_{a_m}^{a_{N_2}}$$

and noting that $\dot{a} = 0$ at $a = a_m$, it is seen that the impulse is,

$$I = \frac{2P_0}{3R}\left[L_1C_1(a^2\dot{a})_{N_1} + L_2C_2(a^2\dot{a})_{N_2}\right. \tag{11.4.16}$$

While the formulas for $(a^2\dot{a})N_1$ and $(a^2\dot{a})_{N_2}$ are the same, the energies in each cycle are different, with result that a_N and $\dot{a}_N$ are different.

The elementary model of bubble pulsation is now completed. It remains to assign experimental values to the parameters γ, R_1 and ϵ.

Choice of Parameters

The period of pulsation T is proportional to scale factor C, hence proportional to $P_0^{-1/2}P_0^{-1/3} = P_0^{-5/6}$, or equivalently to the inverse 5/6 power of the depth. Since this dependency on depth is experimentally verified, one is required to fix the value of γ to avoid significant deviation from it. A best fit occurs when γ is chosen to have the value 1.25.

To fix the remaining parameters one is required to agree on choice of units. In practical work it is convenient to take length in feet, energy E in calories, unit energy ϵ in calories per gram, explosive charge weight W in pounds, and time T,C in seconds. The scale factors then reduce to the following expressions in practical units:

$$L = 1.733\,\epsilon^{1/3}(W/Z_0)^{1/3};\quad C = 0.373\,\epsilon^{1/3}\left(\frac{W^{1/3}}{Z_0^{5/6}}\right) \tag{11.4.17}$$

where Z_0 is the absolute hydrostatic depth (i.e. $Z_0 = Z + 33$). Also one is required to choose some specific explosive. Let this be T.N.T. Actual experiments on determining the period of the first bubble pulse leads to the empirical formula,

$$T = 4.36\,W^{1/3}/Z_0^{5/6} \tag{11.4.18}$$

Since $T = Ct$, the relation between unit energy ϵ and non-dimensional time t is

$$\epsilon^{1/3}t = 11.7 \tag{11.4.19}$$

Now experimental evidence shows that k lies between 0.1 and 0.3 which, together with the choice $\gamma = 1.25$ gives $t \sim 1.483$. *Thus a best fit for* ϵ in the first cycle is

$$\epsilon_1 = 490 \text{ cal/gm.} \quad \text{(subscript is no. of cycle)} \tag{11.4.20}$$

Finally one must choose the value of k_1 in the theoretical formula

$$k = \frac{k_1 P_0^{\gamma-1}}{(\gamma - 1)\epsilon^{\gamma}} \tag{11.4.21}$$

The best fits for γ and ϵ have already been made. However k varies between 0.1 and 0.3 as noted. A best fit for k_1 has been obtained from experimental data on peak pressure difference ΔP_m in deep water under conditions of very small bubble migrations. It is found that,

$$k = 0.0552\,Z_0^{\gamma-1} \tag{11.4.22}$$

$$\Delta P_m = 3450\,\frac{W^{1/3}}{R}\,(1 - 4k^4)$$

The three parameters γ, k and ϵ_1 have now been fixed to make best fit with data. Calculations based on their use will now be compared with experiment.

A. *Maximum Bubble Radius,*

Many measurements show that

$$A_M = 12.6\,(W/Z_0)^{1/3} \tag{11.4.23}$$

Using scale factor L, and taking $\epsilon = 490$ cal/gm leads to the prediction that $a_M = 0.92$. The theoretical value $a_M = [1 - ka_M^{-3(\gamma-1)}]^{1/3}$ gives $0.90 < a_M < 0.94$ for the various depths used in the experiments. The agreement is satisfactory.

B. *Bubble radius* a_M at Excess Pressure = 0

High speed photography of bubble collapse shows that $a_N = 0.62$ at $\Delta p = 0$. The theoretical value $4a_N^3 = 1 - (4 - 3\gamma)ka_N^{-3(\gamma-1)}$ with $k = 0.0552\,Z_0^{\gamma-1}$ predicts $0.61 < a_N < 0.62$, in excellent agreement.

C. *Positive Impulse of First Bubble Pulse*

As noted earlier the calculation of the pulse I depends on a knowledge of L_2, C^2 or equivalently, on the knowledge of ϵ_2. In the first approximation

$$(\epsilon_2/\epsilon_1)^{1/3} = T_2/T_1 \tag{11.4.24}$$

Experimental measurements give $T_2/T_1 \simeq 0.72$. Thus,

$$\frac{I}{W^{1/3}} = 11.9\ Z_0^{-1/6} \left(\frac{W^{1/3}}{R}\right)(1 - 1.59\ k)^{1/2} \tag{11.4.25}$$

(assuming $a_{N_1} = a_{N_2}$). The units of the l.h.s are lb.sec/m^{2}lb$^{1/3}$. A comparison of predictions of this formula with experimental data for depths from 40 to 533 ft shows satisfactory agreement.

D. *Minimum Bubble Radius, A_m*

Using again $k = 0.0552\ Z_0^{\gamma-1}$, $\gamma = 1.25$, it is seen that $a_m k^{\frac{1}{3(\gamma-1)}}$ leads to,

$$a_m = 0.0210\ Z_0^{1/3} \tag{11.4.26}$$

$$A_m = 0.286\ W^{1/3} \qquad \text{(units: ft)}$$

Conclusion: The fixing of the parameters γ, ϵ and k helps establish a working model of the secondary pressure pulses in underwater explosions caused by the specific explosive TNT. Different choices of explosive substances may be similarly modeled. Some of these are discussed in Sect. 11.1. Only one cycle of bubble pulsation is fully explored above. We consider next a model of many cycles of bubble pulsation.

11.4b Several Periods of Pulsation

Formulas for the dynamic behavior of single cycles of pulsation have been derived and are valid whether they are the first, or the n th. The basic parameter that is required to calculate a given cycle is the unit energy ϵ_n. To obtain this quantity we resort to a major conclusion of the elementary theory used here, to the effect that unit energy and period of pulsation are related by the formula,

$$(\epsilon_n/\epsilon_{n-1})^{1/3} = T_n/T_{n-1} \tag{11.4.27}$$

Thus we are required to measure T_n. A large number of experiments by Arons et. al. [12] as well as theoretical arguments have shown that the period of the n th pulsation is given by, $T_n = K_n\ W^{1/3}/Z_0^{5/6}$. A summary table of period constants reported in this reference is reproduced below as Table I:

Table I. Summary of period constants for TNT $T_n = K_n W^{1/3}/Z_0^{5/6}$, T_n = period of nth oscillation (sec.). W = charge weight (lb.), Z = depth of charge below surface (ft), Z_0 = absolute

W	Z	Period constant, K_n							
(lb)	(ft)	K_1	K_2	K_3	K_4	K_5	K_6	K_7	K_8
0.505	250	4.36±.01	3.14±.03	2.56±.02	2.35±.03	2.16±.04	2.08±.04	1.96±0.1	–
0.505	300	4.36±.01	3.06±.01	2.51±.01	2.32±.02	2.15±.02	1.97±.02	1.90±.02	1.9±.1
2.507	250	4.27**	3.11	2.53	2.35	2.02	1.94	–	
2.507	500	4.26±.01	3.06±.01	2.48±.01	2.31±.01	2.17±.01	2.02±.01	–	–
12.01	500	4.29±.01	3.19±.01	2.56±.01	2.39±.01	2.16±.01	2.0±.01	1.94±.02	1.73±.05

*The stated error is the standard deviation of the mean.

**The error is not indicated since only two shots were made under these conditions. Results of the two shots agreed very closely.
(After [1]).

If we choose $\epsilon_1 = 490$ cal/gm, then for a 1/2 lb charge of TNT, $\epsilon_2 = \epsilon_1 (3.14/4.36)^3 = 183$ cal/gm., and $\epsilon_3 = 99$ cal/gm. Assuming 1 gram TNT releases 1060 cal we estimate that at the end of the second pulse only 9.3% of the original energy of the explosive remains in the gas bubble. This coincides with very similar estimates reported in Cole [5] noted in Sect. 11.1.

11.4c Similarity

In the Kirkwood-Bethe theory a key parameter is R/a_0, the ratio of distance R from the center of charge to the original charge radius a_0 (assuming charge is spherical). Since the linear dimension of the charge is proportional to the cube root of the volume, hence cube root of charge weight, it is seen that a_0 is proportional to $W^{1/3}$. Thus in all formulas R/a_0 can be replaced by $(R/W^{1/3}) \times$ const. One says that distance is scaled by $W^{1/3}$. This scaling is part of a more general "principle of similarity" which states that if the linear size of the charge be changed by a factor q the original pressure at distance R and time t will reappear at distance qR and time qt. Time itself is thus seen to scale as $t/W^{1/3}$. The practical significance of this principle is very great because it permits easy construction of universal pressure-time-space curves from single records.

Other parameters of shock waves besides peak pressure P_m obey similarity laws. Two of these are important in so far as physical damage due to the shock is concerned. The first is the impulse $I(t)$ in the water, defined as,

$$I(t) = \int_0^t p(t')dt' \quad \text{(units: } Nsm^{-2}\text{)} \tag{11.4.28}$$

On assumption that the charge is spherical the similarity laws lead to the proportionality

$$I \propto W^{1/3} f(W^{1/3}/R) \tag{11.4.29}$$

The second is the energy density of the shock wave in the water, defined by

$$E_f = \frac{1}{\rho_0 C_0}\int_0^t (P - P_0)^2 dt + \frac{1}{\rho_0 R}\int_0^t (P - P_0)\left[\int_0^{t'} (P - P_0)dt\right]dt' \tag{11.4.30}$$

(units: energy/area).

The similarity principle for E_f leads to the proportionality,

$$E_f \propto W^{1/3} f(W^{1/3}/R) \tag{11.4.31}$$

For actual numerical calculations one requires proportionality constants. These are not known from first principles; they must be determined by experiment. When the constants are inserted in the relevant formulas the similarity laws lead to the following set of empirical formulas,

$$\text{(a)} \quad P_m = f\left(\frac{W^{1/3}}{R}\right)^{\lambda}$$

$$\text{(b)} \quad I(t/W^{1/3}) = g\, W^{1/3}\left(\frac{W^{1/3}}{R}\right)^{\mu} \tag{11.4.32}$$

$$\text{(c)} \quad E_f(t/W^{1/3}) = h\, W^{1/3}\left(\frac{W^{1/3}}{R}\right)^{\nu}$$

Experiments with TNT, loose tetryl and pentolite have been conducted to fix f, g, h, and λ, μ, ν. The results appear in a compilation by Cole [14] and are reproduced below in Table II.

Table II — Value of Parameters in Eq. 11.4.32

Explosive	Peak pressure P_m		Impulse $I(t)$		Energy density $E(t)$		Time of integration
	$10^{-4}f$	λ	g	μ	$10^{-4}h$	ν	
TNT Density 1.52	2.16 (2.60)	1.13 (1.21)	1.46 (1.50)	0.89 (0.86)	2.41 (3.78)	2.05 (2.11)	6.7θ
Loose tetryl Density 0.93	2.14 (2.50)	1.15 (1.22)	1.73 (1.50)	0.98 (0.86)	3.00 (3.20)	2.10 (2.04)	5.0θ
Pentolite Density 1.60	2.25 (2.85)	1.13 (1.23)	2.18 (1.65)	1.05 (0.88)	3.27 (4.23)	2.12 (2.11)	6.7θ

It will be noted that the integration time in the formulas for impulse and energy is quite arbitrary. A best fit to the experimental data is obtained by making this time to be 5θ to 7θ, where θ is the decay constant appearing in the exponential model of the pressure-time curve of the shock wave, $P = P_m e^{-t/\theta}$.

By experiment and curve fitting it is found that similarity laws are reasonably valid in the range between 10 and 100 charge radii, and can be used without excessive error out to 900 charge radii, or pressures of the order of 100 psi. The pressure time history thereafter corresponds approximately to conventional acoustic laws. Arons [15] has extended previous experimental results to cover ranges of listening out to $R \simeq 2000\ W^{1/3}$ feet (W in lbs of charge). By plotting similarity curves he obtained best-fit data for TNT and pentolite. He finds that over the extended long range, the shock wave parameters can be represented in the form

$$\text{(a)}\quad P_{\max} = 2.16 \times 10^4 \left(\frac{W^{1/3}}{R}\right)^{1.13} \quad \text{(units: psi)}$$

$$\text{(b)}\quad \text{Impulse} = 1.78\ W^{1/3}\left(\frac{W^{1/3}}{R}\right)^{0.94} \quad \text{(units: lb sec/m}^2\text{)} \qquad (11.4.33)$$

$$\text{(c)}\quad \text{Time constant } \theta = 58\ W^{1/3}\left(\frac{W^{1/3}}{R}\right)^{-0.22} \quad \text{(units: sec)}$$

Weston [16] has found that a slightly better value of the time constant to represent the lower frequencies in the spectrum is

$$\theta = \frac{\text{Impulse } I}{P_{\max}} \qquad (11.4.34)$$

11.4d Empirical Model of the Pressure-Time Curve

Wakeley [17] has assembled an *empirical* pressure-time signature of both the detonation shock wave and the subsequent bubble pulses. His model is based on the work of Pritchett [18], Gaspin and Schuler [19] and Weston [16]. Briefly the pressure-signature representation appears as the continuous time function $P(t)$ given by

$$P(t) = P_0 \exp\left[-\frac{t}{t_0}\right] U(t) + \sum_{i=1}^{n}\left[P_i \exp\left|\frac{t - t_{Bi}}{t_i}\right| + P_{ii} \sin\pi\left[\frac{t - t_{Bi-1}}{t_{Bi} - t_{Bi-1}}\right](U(t - t_{Bi-1}) - U(t - t_{Bi})\right]$$

where $t_{Bi-1}\big|_{i=1} = 0$, $U(t - t_{BK}) = \begin{cases} 0 & t < t_{BK} \\ 1 & t \geq t_{BK} \end{cases}$,

$$P_{ii} = -\frac{\pi}{2}\left[\frac{p_{i-1}t_{i-1} + P_i t_i}{t_{Bi} - t_{Bi-1}}\right],$$

P_0 is the peak pressure and t_0 is the decay time constant of the shock wave, P_i is the peak pressure and t_i is the time constant of the ith bubble pulse, t_{Bi} is the time interval between the peak of the shock wave and the peak of the ith bubble pulse, and n represents the number of bubble pulses to be considered. It is assumed that the rise and decay time constants of the bubble pulses are equal. P_{ii} is the minimum pressure between the $(i-1)$th and the ith peak, where the 0th peak is the shock wave.

The meaning of the symbols and their units are shown in the following Table III:

Table III — Empirically Derived Functional Dependence of Various Parameters in the Pressure/Time Relationship of the Explosion

Parameter	Notation	Description[a]
Shock-wave pressure	P_0	$3.74 \times 10^{12}\left[\frac{W^{1/3}}{R}\right]^{1.13}$
Shock-wave-decay time constant	t_0	$1.75 \times 10^{-5} W^{1/3}\left[\frac{W^{1/3}}{R}\right]^{-0.26}$
First-bubble-pulse period	t_{B1}	$0.21\ \frac{W^{1/3}}{(D + 10.1)^{5/6}}$
Minimum pressure between ith and $(i-1)$th pulse	P_{ii}	$-\frac{\pi}{2(t_{Bi} - t_{Bi-1})}(P_{i-1}t_{i-1} + P_i t_i)$
First-bubble-pulse peak pressure	P_1	$9.02 \times 10^{11}\left[\frac{W^{1/3}}{R}\right]$
First-bubble-pulse rise-and-decay time constant[b]	t_1	$1.14 \times 10^{-3}\ \frac{1}{(D + [0.1)^{1/6}}$
Second-bubble-pulse period	t_{B2}	$1.71\ t_{B1}$
Second-bubble-pulse peak pressure	P_2	$0.22\ P_1$
Second-bubble-pulse rise-and-decay time constant[b]	t_2	$1.91\ t_1$
Third-bubble-pulse period	t_{B3}	$2.28\ t_{B1}$
Third-bubble-pulse peak	P_3	$0.10\ P_1$
Third-bubble-pulse rise-and-decay time constant[b]	t_3	$2.79\ t_1$
Fourth-bubble-pulse period	t_{B4}	$2.81\ t_{B1}$
Third-bubble-pulse peak	P_4	$0.03\ P_1$
Fourth-bubble-pulse rise-and-decay time constant[b] (estimated)	t_4	$2.79\ t_1$

[a] W = weight of explosive charge (g)
D = detonation depth of the charge below water surface (m)
R = range separation between explosive charge and the receiver at detonation (m)
All times in seconds
All pressure in μPa

[b] Rise and decay time may be unequal. More experimental data is needed for confirmation. (After [17]).

Calculations based on this model in the case of a Standard US Navy 816-g Mk 61 Signals Underwater Sound (SUS) charge detonated at a depth of 244 meters have been compared with experimental measurements. The agreement between model and measured pressure-time curves is good. However the predicted peak pressure was 2.9 dB higher than actually measured, a discrepancy which may be due to the limited bandwidth of the measuring system.

11.4e Experimental Measurements Procedure

The detonation of an explosive charge generates a transient pressure pulse $p(t)$ at a given field point. This pressure is detected by a wideband hydrophone. It is then processed in several ways:

A. *Wideband Energy Flux Density*

The pressure signature is squared ($=p^2(t)$) and is integrated over a selected time T, then divided by ρc. The result is the energy flux density, or energy that has flowed through a unit area,

$$E = \frac{\int_0^T p^2(t)\,dt}{\rho c} \quad \text{(units: Nmm}^{-2}\text{)}$$

B. *Energy Flux Spectrum Level*

The pressure signature is fed through a bandpass filter of specified bandwidth and central frequency f_0. The output of this filter is a time signal $p_{f_1}(t)$ which contains only those frequency components within the pass band,

$$p_{f_1}(t) = \int_{-\infty}^{\infty} p(t\,\tau)\,h_{f_1}(\tau)\,d\tau$$

in which h_{f_1} is the impulse response of the filter. For obtaining refined spectra the first filter must be high-Q (i.e. ultranarrowband). The signal p_{f_1} is then passed through a nonlinear device which performs a square-law transformation, so that the output becomes

$$p_{f_1^2}(t) = \alpha \int\int_{-\infty}^{\infty} p(t-\tau_1)p(t-\tau_2)\,h_{f_1}(\tau_1)\,h_{f_2}(\tau_2)\,d\tau_1 d\tau_2$$

If the filters are narrow enough their impulse responses are sinusoids. Thus approximately,

$$p_{f_1^2}(t) = 2\alpha \iint h_{0f_1}(\tau_1)\,h_{0f_2}(\tau_2)\,p(t-\tau_1)p(t-\tau_2) \times \cos[\omega_0(\tau_1-\tau_2) + \gamma_{0f_2}(\tau_2) - \gamma_{0f_1}(\tau_1)]\,d\tau_1 d\tau_2$$

where h_0's are slowly varying quantities, and γ_0's are phases. Finally, $p_{f_1^2}(t)$ a passed through an integrating filter which performs ar integration over a selected time duration T. The output of this last filter is recognized by the Wiener-Kinchine theorem to be proportional to the *power or intensity* spectrum of the original signal $p(t)$ centered on frequency f_0. Dividing this quantity by ρc times the bandwidth then yields the energy flux spectrum level in units of energy per unit area per hertz.

It is conventional to report the spectrum level of energy flux on a dB-scale by use of an appropriate reference energy. Weston [16] uses a reference of 1 erg per cm^2 per Hz; Urick [20] uses a reference of a plane wave having an amplitude of 1 dyne/cm^2 at 1 yd integrated over one sec. Thus, in general,

$$N = 10 \log_{10} \frac{E_{\text{measured}}}{E_{\text{reference}}} \quad \text{(units: dB re reference)} \tag{11.4.35}$$

A numerical example will serve to indicate magnitudes.

Example: (Urick, p. 77) a 1-lb charge of TNT delivers a peak pressure of some 2.3×10^6 dynes/cm^2 at 100 yds, which decays according to the constant $t_0 = 2 \times 10^{-4}$ sec. The energy flux over a time period of t_0 sec is

$$E_{\text{meas}} = \frac{p_0^2 t_0}{2\rho c} \tag{11.4.36}$$

so that,

$$N = 10 \log_{10} E_{\text{meas}} - 10 \log_{10} E_{\text{ref}} = 88 \text{ dB re } (1 \text{ dyne/cm}^2)^2 \cdot \text{sec} \tag{11.4.37}$$

This energy flux density is equivalent to a 1/2 sec. pulsed sinusoidal signal source level (referred to 1 yd) equal to $88 \div 40 + 3 = 131$ dB re 1 μbar. Here 40 dB accounts for change of distance from 100 yds to 1 yd, and 3 dB accounts for the change from 1/2 sec. pulse length to the reference 1 sec. dp

C. *Theoretical Energy Spectrum*

Let the shock wave be represented by $p(t) = P_0 e^{-t/t_0}$, and let $P(f)$ be the Fourier transform of $p(t)$. The total energy in the wave is then obtained by Parseval's theorem:

$$E \propto \int_{-\infty}^{\infty} |p(t)|^2 \, dt = \int_{-\infty}^{\infty} |P(f)|^2 \, df \tag{11.4.38}$$

Thus the quantity $|P(f)|^2$ is called the *energy spectrum.* Its units are pressure^2 $\times$ sec^2. One writes the symbol $E(f)$ for the spectrum:

$$\begin{aligned} E(f) = |P(f)|^2 &= \left| \int_{-\infty}^{\infty} p(t) e^{-i\omega t} dt \right|^2 \\ &= \int_{-\infty}^{\infty} p(t) e^{-i\omega t} dt \int_{-\infty}^{\infty} p(-t) e^{i\omega t} dt \\ &= \int_{0^+}^{\infty} P_0 e^{-t/t_0} e^{-i\omega t} dt \int_{-\infty}^{0^-} P_0 e^{t/t_0} e^{i\omega t} dt \\ &= \frac{P_0^2}{(1/t_0)^2 + 4\pi f^2} \qquad -\infty < f < \infty \end{aligned} \tag{11.4.39}$$

A sketch of this function is shown in Fig. 11.4.2. It is important to note that both positive and negative frequencies must be used. Since the spectrum is symmetrical one can easily define the spectrum only in terms of positive frequencies. Hence

$$E(f) = \frac{2P_0^2}{(1/t_0)^2 + 4\pi^2 f^2} \qquad f \geqslant 0 \tag{11.4.40}$$

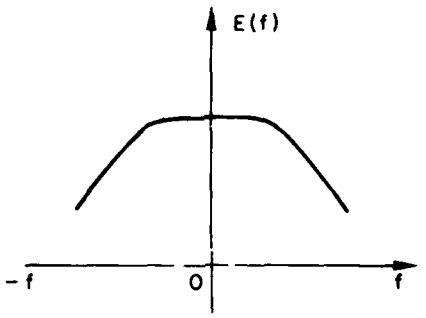

Fig. 11.4.2. Total energy spectrum.

The total energy flowing through a unit area averaged over the band $\Delta 3$ of frequencies is

$$\Pi = \frac{1}{\Delta B} \frac{\int |P(f)|^2 df}{\rho c} \quad \left[\text{units: } \frac{\text{energy}}{\text{area Hz}}\right] \tag{11.4.41}$$

REFERENCES

1. R. H. Cole "Underwater Explosions" Dover Publications p. 6.
2. Ref. 1 page 4
3. Ref. 1 page 271
4. A. B. Arons et. al. (JASA **20**, 271 (1948))
5. Ref. 1 page 283
6. Ramsauer Ann. de. Phys. **4**, 72 (1923)
7. Bendix United Geophysical Corp. "Seismic Energy Sources 1968 Handbook".
8. J. G. Kirkwood, H. A. Bethe OSRD 588 (1942)
9. L. D. Landau, E. M. Lifshitz "Fluid Mechanics" p. 319 (with change of symbols)
10. J. G. Kirkwood, "Collected Works"

11. J. G. Kirkwood, Montroll OSRD 761I, 1942

12. A. B. Arons, JASA 277 (1948)

13. H. Lamb "Hydrodynamics" Dover Publications 1945, p. 122

14. Ref. 1 p. 242

15. A. B. Arons, JASA 343 (1954)

16. D. Weston, Proc. Phy. Soc. 76 233 (1960)

17. Wakeley, US Jour. Underwater Acoustics 27, 445 (1977)

18. J.W. Pritchett, Info. Res. Assoc. IRA-TR-2-71 AD, 125 Univ. Ave. Berkeley, Ca. 94710, April.

19. J.B. Gaspin, V.K. Schuler, Tech. Rept. NOLTR 71-160 NOL, White Oak, Silver Spring, Md., Oct. 13, 1971.

20. R.J. Urick, "Fundamentals of Underwater Sound for Engineers," 1st Ed., McGraw-Hill, 1967.

CHAPTER XII

DISCRETE MODEL OF THE ELASTIC RADIATING SURFACE

12.1 INTRODUCTION

In many structures that are designed to radiate low frequency sound efficiently the surface of radiation is deliberately chosen to be elastic in order to give the designer an opportunity to mechanically resonate the equivalent spring and mass of the elastic surface to the operating frequency. In other cases the motion of the surface is designed to be rigid but becomes (accidentally or uncontrollably) elastic. Elasticity of radiating surfaces therefore plays an important role in the radiation of low frequency sound. The acoustic power radiated from these elastic surfaces is directly determined by the distribution of the normal component of surface velocity facing the medium. This velocity is written as $W(\mathbf{X},t)$ to emphasize that it is a *continuous* function of spatial coordinate $\mathbf{X}$ and time t, referred to an appropriate coordinate system. At the same space-time point the surface velocity vector $\dot{\mathbf{U}}(\mathbf{X},t)$ has other components $\dot{U}_1,\dot{U}_2$ which do not participate in radiation, but are required (in the general case) to be known in the dynamic analysis of the surface motion. Customarily in such analyses the surface velocity (and acceleration) are obtainable by time differentiation of the surface displacement vector $\mathbf{U}(\mathbf{X},t)$. Thus attention is focused on the determination of the displacement vector $\mathbf{U}$ under the action of applied external forces, applied initial conditions, and corresponding boundary conditions.

When the elastic radiating surface has a simple geometrical shape (circle, sphere, rod, cylinder, etc.), and displays symmetrical deformation during motion the integral-differential equations which couple this surface motion to the motion of the medium may be solved directly to yield a *continuum* discription of the surface displacement vector. Thus $\mathbf{U}$ is determined at every point $\mathbf{X},t$. However in cases where the shape of the radiating surface is arbitrary, or, if simple, undergoes unsymmetrical deformation caused by unsymmetrical forces (or unsymmetrical initial, or boundary, conditions) the solution of the equation of motion must be done numerically. It is then economic to replace the elastic continuum by an assembly of finite elements, and to perform on them a dynamic analysis in such a way as to closely approximate the actual motion of the real continuous surface. We discuss this technique of finite element analysis in the following sections.

12.2 CONSTRUCTION OF FINITE ELEMENTS OF AN ELASTIC CONTINUUM

We consider a radiating surface in the form of an elastic membrane, plate, or shell and locate it in a convenient coordinate system. Since the displacements of all surface points are to be analyzed these coordinates are called *global*. Upon this surface we draw (in imagination) a net (or lattice) of crossing lines, generally straight but can be curved. The cells of this lattice are prismatic surfaces, namely triangles, rectangles, pentagons, etc. The points of intersection are called *global nodes*. Because it is our intention to solve for the elastic behavior of the underlying continuum only at these global nodes we reserve the advantage of varying the number of cells of the lattice from area to area of the surface, making it more dense where the

elastic deformation is changing rapidly, and less dense where the deformation is uniform or changes slowly. Thus the distribution of global nodes is concentrated in some areas and sparse in others, as the designer sees fit. This is shown in Fig. 12.2.1

Let the location of the Nth global node be $\mathbf{X}^N$ (note that the superscripting is a matter of convenience), and write the displacement vector at these nodes as $\mathbf{U}^N(=\mathbf{U}(\mathbf{X}^N))$, $N = 1, 2 \ldots Q$. Thus, out of the infinite number of possible surface points with their associated displacements we select out a finite number $(=Q)$ to represent the displacement field of the surface. We say that the original information on the total displacement field will be solved for only at Q points of the surface. The displacement fields in between these global nodes (namely in the lattice cells) are not solved for directly: they will be derived by means of an *interpolation formula* from a knowledge of the displacements at the global nodes.

We now choose one lattice cell and its associated global nodes from the total lattice of the radiating surface and refer it to a second coordinate system, called the *local coordinate system*. This extracted cell is the finite element e, and a point in it is located at $\mathbf{x}$. Thus the *global nodes* which become the local nodes of the finite element e are located at $\mathbf{x}^n$, $n = 1, 2 \ldots q$, Fig. 12.2.2.

12.2a DEGREES OF FREEDOM OF A FINITE ELEMENT

Every local node of a finite element responds with motion under the action of applied external forces. From the theory of kinematics of point motion in Cartesean 3-space the node can have three possible translations along coordinates x, y, z respectively, and three possible rotations about these same axes. These possible motions are the *degrees of freedom* at the selected node. As a matter of convenience we assign the symbol u_j, $j = 1, 2 \ldots$ to represent these motions. For example at the first local node the degrees of freedom are subscripted $j = 1$ through 6. For the second local node a similar assignment can be made by writing $j = 7$ through 12 etc. In this way the degrees of freedom of the entire finite element are uniquely determined in consecutive order namely u_j, $j = 1, 2 \ldots N$ where the maximum value of N is $6K$, K being the number of local nodes in the finite element.

An alternative method of designating the degrees of freedom of a finite element is to consider the vector $\mathbf{u}_{(e)}^{(m)}$ to be a collection of all degrees of freedom at the selected $(=m\text{th})$ node. This is equivalent to writing u_j, $j = l, l+1, l+2 \ldots$ where l is a unique number for each finite element.

In numerical work the convenience of numbering the degrees of freedom of a finite element as consecutive integers $j = 1, 2 \ldots 6K$, where K is the number of local nodes, renders it the preferred method. We shall use both consecutive numbering and nodal vector symbols to designate the degrees of freedom.

Local forces can be generated not only at boundaries by boundary forces but also in the volume by volume forces. Among the latter are forces caused by piezoelectric coupling. This coupling provides additional degrees of freedom at the local nodes.

12.2b LOCAL NODES AND GLOBAL NODES

Let the displacement vector of the mth local node be $\mathbf{u}_{(e)}^{(m)}$. As we have noted above in the case of the global system, the displacement vector $\mathbf{u}_{(e)}(\mathbf{x})$ at any point on the finite element

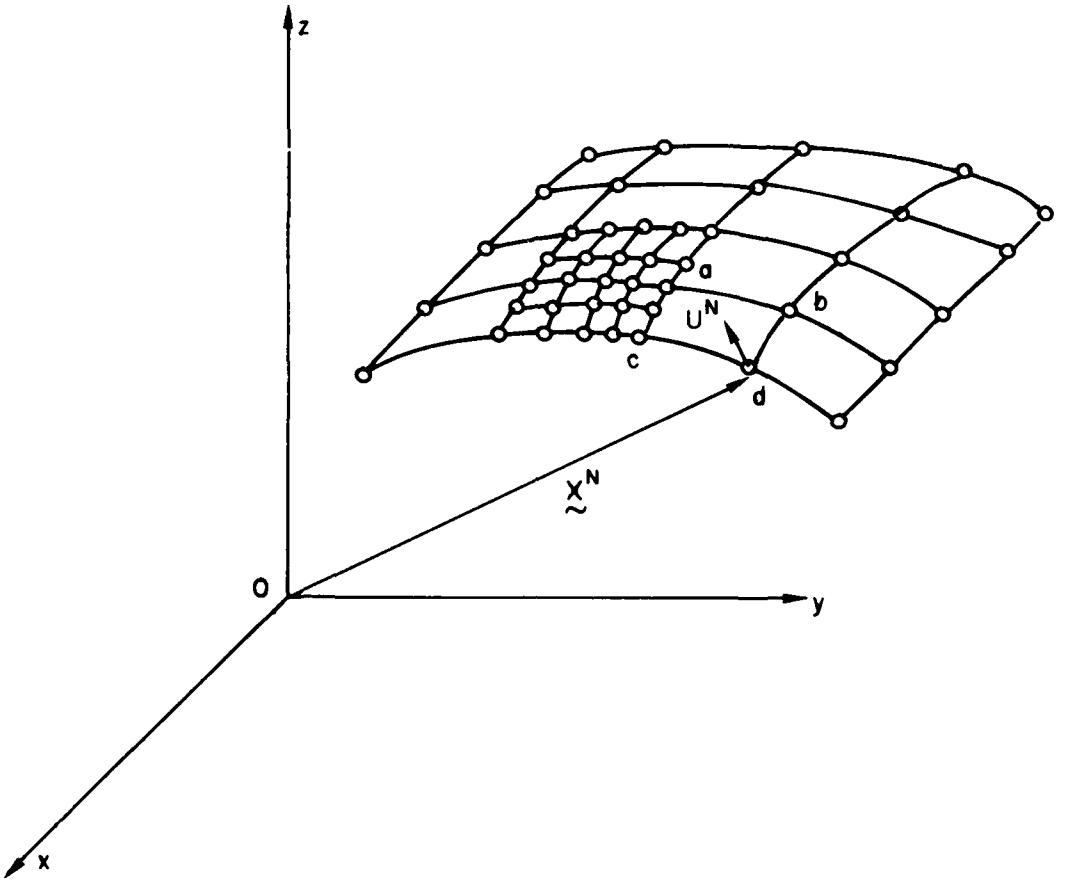

Fig. 12.2.1. Global nodes.

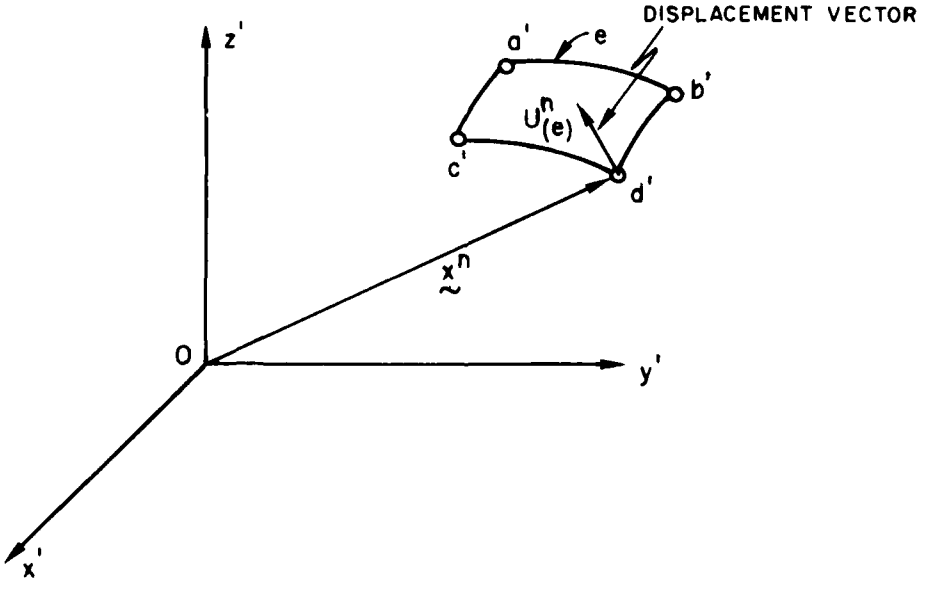

Fig. 12.2.2. Local nodes.

other than at the local nodes will not be obtained directly: it will be determined from a knowledge of the displacement field at the local nodes only. This transition from displacements at the local nodes to displacements anywhere on the finite element is effected by an interpolation function (or shape function, or basis function) $\psi_{(e)}(\mathbf{x})$ which is tailored by the analyst for the particular finite element e and local node n. The selected functional form of ψ must satisfy the element boundary connections and is most often such that the local field at any point is given as an expansion in basis functions,

$$\mathbf{u}_{(e)}(\mathbf{x}) = \sum_{n=1}^{q} \mathbf{u}_{(e)}^{n} \psi_{(e)n}(\mathbf{x}). \tag{12.2.1}$$

Although this equation is simple it is to be emphasized that $\mathbf{u}_{(e)}^{n}$ i.e., the value of the field at the local nodes, is at first unknown: it must be determined from a knowledge of the global displacements $\mathbf{U}^N$, which are the only displacements directly solved for. Thus we are required to show the connection between local nodes and global nodes. This is accomplished by use of a mapping function $\Omega_{(e)N}^{n}$ which shows how nodal points $\mathbf{X}^N$ in the global system are mapped into points $x_{(e)}^{n}$ in the local system. This mapping function is simple: it is given a value 1 if node n in the extracted element coincides with node N of the global model when the *finite element is restored to its correct position* in the global model. Otherwise it is given a value of zero. Thus the two classes of nodal points are related by the formula,

$$\mathbf{x}_{(e)}^{n} = \sum_{N=1}^{Q} \Omega_{(e)N}^{n} \mathbf{X}^N. \tag{12.2.2}$$

By construction, only one term in this sum differs from zero. Similarly the local nodal displacements and the global nodal displacements are related by the formula,

$$\mathbf{u}_{(e)}^{n} = \sum_{N=1}^{Q} \Omega_{(e)N}^{n} \mathbf{U}^N \tag{12.2.3}$$

Hence the local displacement anywhere in the element e is

$$\mathbf{U}_{(e)}(\mathbf{x}) = \sum_{n=1}^{q} \psi_{(e)n}(\mathbf{x}) \sum_{N=1}^{Q} \Omega_{(e)N}^{n} \mathbf{U}^N \tag{12.2.4}$$

These formulas will be used later to find the stresses and strains anywhere at *local points*.

We return next to the matter of global displacements $\mathbf{U}(\mathbf{X},t)$ anywhere on the elastic surface. These cannot be determined *directly* from the global nodal displacements $(=\mathbf{U}^N)$ since this determination would require a second interpolation formula in addition to $\psi_e(\mathbf{x})$. Instead we note that $u_{(e)}(\mathbf{x})$ has been expanded by 12.2.4 in global displacements U^N. Thus if $\mathbf{x}$ in a particular finite element coincides with $\mathbf{X}$ global then $\mathbf{U}(\mathbf{X},t)$ would be given by $u_{(e)}(\mathbf{x})$. As the global point $\mathbf{X}$ is varied over the surface it coincides successively with a point in each finite element. In this way the continuous function $\mathbf{U}(\mathbf{X},t)$ is approximated over the totality of elements E by the discrete model

$$\mathbf{U}(X,t) = \sum_{e=1}^{E} u_{(e)}(\mathbf{x})$$

$$\mathbf{U}(X,t) = \sum_{e=1}^{E} \sum_{n=1}^{q} u_{(e)n}(\mathbf{x}) \sum_{n=1}^{Q} \Omega_{(e)N}^{n} U^N(\mathbf{X}) \tag{12.2.5}$$

in which $\mathbf{x}$ in the local system coincides with $\mathbf{X}$ in the global system. In effect, moving the point $\mathbf{X}$ is equivalent to sampling points in each finite element, one element at a time. 12.2.5 serves to emphasize only one interpolation function $(\psi_{(e)n}(\mathbf{x}))$ is needed to interpolate fields in both local coordinates and global coordinates.

12.2c KINETIC AND POTENTIAL ENERGIES OF A FINITE ELEMENT IN DISCRETE FORM

As in all dynamic systems of mechanical nature it is very advantageous to derive the equations of motion from an energy principle. In the present application of forming discrete models we take this to be the principle of conservation of energy: namely, the time rate of change of the sum of the kinetic and potential energies of a system having time varying displacements **U** is equal to the rate of work done on the system by external forces acting through the same displacement **U**. Since the elastic system under consideration is an assemblage of finite elements we will first state the energy principle for a finite element and then derive from it an equation of motion in global form i.e., for all elements combined. We emphasize again that the technique of finite elements requires us to solve for the global displacements first, and then from them solve for the local displacements, local stresses and local strains.

Thus in the finite element e with q local nodes we let the displacement anywhere be $\mathbf{u}_{(e)}(\mathbf{x},t)$. As before we represent this local displacement as a sum of properly weighted displacements over the local nodes, $\mathbf{u}^n_{(e)}(t)$. In terms of the interpolation function $\psi_{(e)n}(\mathbf{x})$* we have,

$$\mathbf{u}_{(e)}(\mathbf{x},t) = \sum_{n=1}^{q} \mathbf{u}^n_{(e)}(t)\, \psi_{(e)n}(\mathbf{x}). \tag{12.2.6}$$

The kinetic energy of the element (of volume V_0) is then:

$$K_{(e)} = \frac{1}{2} \int_V \rho_0\, \dot{\mathbf{u}}_{(e)} \cdot \dot{\mathbf{u}}_{(e)}\, dV_0 \tag{12.2.7}$$

$$K_{(e)} = \frac{1}{2} \sum_n \sum_m m_{nn}\, \dot{\mathbf{u}}^n_{(e)(t)} \cdot \dot{\mathbf{u}}^m_{(e)(n)} \quad \text{(units: } Nm\text{)}$$

where

$$m_{nm} = \int_{V_0} \rho_0(\mathbf{x})\, \psi_{(e)n}(\mathbf{x}) \psi_{(e)m}(\mathbf{x})\, dV_0(\mathbf{x}), \quad \left[\text{units: } \left[\frac{Ns^2}{m}\right]\right. \tag{12.2.8}$$

The quantity m_{nm} is one coefficient of a $q \times q$ matrix of numbers. We note specifically that the formula for the kinetic energy is expressed in terms of the local *nodal* velocities $\dot{\mathbf{u}}^n_{(e)}(t)$: dependence on local $\mathbf{x}$ is averaged out by integration over the area of the element.

The potential energy $\prod$ of the finite element will be attributed only to the elastic deformation. Let $\sigma^{ij}_{(e)}(\mathbf{x})$ be the components of the stress tensor on element e, and ϵ_{ij} the components of the strain tensor. Then the local potential energy (in continuum form) is given by,

$$\prod_{(e)} = \sum_{i=1}^{s} \sum_{j=1}^{3} \int \sigma^{ij}_{(e)}(\mathbf{x})\, \epsilon_{ij}(\mathbf{x})\, dV_0(\mathbf{x}). \tag{12.2.9}$$

We require however the *discrete* form of $\prod_{(e)}$, meaning the discrete forms of its integrand. The discrete form of strain tensor can be directly written from the discrete form of the local displacements $\mathbf{u}_{(e)}(\mathbf{x},t)$ using 12.2.1:

$$\epsilon_{(e)ij} = \frac{1}{2}\left[\frac{\partial u_{(e)i}}{\partial x_j} + \frac{\partial u_{(e)i,j}}{\partial x_i} - \sum_{m,n} \delta_{mn} \frac{\partial u_{(e)m}}{\partial x_i} \frac{\partial u_{(e)n}}{\partial x_j}\right]$$

$$\epsilon_{(e)ij} = \frac{1}{2}\left[\sum_{n=1}^{q} u^n_{(e)} \frac{\partial \phi_{(e)n}}{\partial x_i}(\mathbf{x}) + \sum_{m=1}^{q} u^m_{(e)} \frac{\partial \phi_{(e)m}}{\partial x_j}(\mathbf{x})\right]$$

*(Note that $\psi_{(e)n}(\mathbf{x})$ is dimensionless.)

$$+ \sum_{n=1}^{q} \sum_{m=1}^{q} \sum_{k=1}^{3} u^{n}_{(e)k} u^{m}_{(e)k} \frac{\partial u_{(e)n}}{\partial x_i} \frac{\partial u_{(e)m}}{\partial x_j} \tag{12.2.10}$$

To find the discrete form of the stress tensor we might proceed as follows: first write out the continuum form of the constitutive equation relating stress to strain in the elastic material of the vibrating surface. This might conveniently be taken to be a linear version of Hookes Law:

$$\sigma^{ij} = C^{ijkl} \epsilon_{kl} \tag{12.2.11}$$

Next we could replace ϵ_{kl} by its discrete form as given by 12.2.10. However it is unnecessary at this stage of the derivation to specify in detail the explicit form of the stress-strain relation. A useful form of the discrete potential energy can be obtained by expanding the strain tensor $\epsilon_{(e)ij}$ alone in terms of displacement, as given by 12.2.10: this leads to,

$$\Pi = \sum_{m=1}^{q} \sum_{n=1}^{q} \sum_{k=1}^{3} \sum_{i=1}^{3} \sum_{j=1}^{3} \left[\int \sigma^{ij}_{(e)} \frac{\partial \psi^{n}_{(e)}}{\partial x_i} \left[\delta_{ik} + u^{m}_{(e)k} \frac{\partial \psi^{n}_{(e)}}{\partial x_j} \right] u^{n}_{(e)k} \right] dV_0. \tag{12.2.12}$$

We use this convenient form of the discretized potential energy in later discussions of this chapter.

The third quantity needed to implement the principle of conservation of energy is the rate of work done by the external forces on the elastic plate (or shell) system. The derivation of the appropriate formulas for this work done requires a careful consideration of the distinction between forces on a finite element and forces on all the elements in assembled (= global) form. We make this distinction in the next section.

12.2d GENERALIZED FORCES ON A FINITE ELEMENT

When an elastic surface under deformation is decomposed into an assembly of finite elements, and each element is withdrawn to be considered by itself, it carries with it the forces on its surfaces (and throughout its volumes if any) which keep it in mechanical (or dynamical) equilibrium. To describe these forces let $F^{V}_{(e)}(\mathbf{x},t)$ be the body force per unit undeformed volume of an element and $F^{S}_{(e)}(\mathbf{x},t)$ the system of surface forces in (deformed coordinates) per unit undeformed area of the element. Also let $\psi_{(e)}(\mathbf{x})$ be the interpolation formula (selectable at the discretion of th analyst), referred to the mode n of the element. The forces $\mathbf{F}^{V}_{(e)}$ and $F^{S}_{(e)}$ are in general distributed forces. We desire to concentrate an equivalent force system at the nodes. To do this we construct the generalized forces at the nodes by integration (i.e., by averaging). Thus, let $\mathbf{f}^{V}_{(e)n}(t)$ and $f^{S}_{(e)n}(t)$ be the generalized forces at the local node n, to which we give the definition,

$$\mathbf{f}^{V}_{(e)n}(t) = \int_{V_0} \hat{F}^{V}_{(e)}(\mathbf{x},t)\, \psi_{(e)n}(\mathbf{x})\, d\, V_0(\mathbf{x}) \tag{12.2.13}$$

$$f^{S}_{(e)}(t) = \oint_{A_0} \hat{F}^{S}_{(e)}(\mathbf{x},t)\, \psi_{(e)n}(\mathbf{x})\, d\, A_0(\mathbf{x}) \tag{12.2.14}$$

Here $\hat{F}^{V}, \hat{F}^{S}$ are global forms written as functions of local coordinates. These definitions are adopted to insure that the mechanical energy generated by the so-defined nodal forces acting on nodal displacements $u^{n}_{(e)}(t)$ is the same as the mechanical energy actually developed by $\hat{\mathbf{F}}^{V}(\mathbf{x},t)$, $\hat{\mathbf{F}}^{S}(\mathbf{x},t)$, and $\mathbf{u}(\mathbf{x},t)$ as distributed over the element. The total mechanical energy on element e is therefore found by summing over all its local nodes:

$$w_{(e)}(t) = \sum \mathbf{u}^{n}_{(e)} \cdot \mathbf{p}_{(e)n}(t), \quad \mathbf{p}_{(e)n}(t) = \mathbf{f}_{(e)n}(t) + \mathbf{s}_{(e)n}(t) \tag{12.2.15}$$

The total global energy equals the total nodal energy. Hence the global force at global node N is given by

$$P_N(t) = \sum_{e=1}^{E}\sum_{n=1}^{P} \overset{(e)\,n}{\Omega}_N \dot{p}_{(e)n}(t) = \sum_{e=1}^{E}\sum_{n=1}^{P} [\overset{(e)}{\Omega}{}^{n}_{N} f_{(e)n}(t) + \overset{(e)}{\Omega}{}^{n}_{N} s^{(t)}_{(e)n}] \tag{12.2.16}$$

Since these forces are averaged over element area they are called *generalized forces at the nodes.*

12.2e EQUATIONS OF MOTION IN DISCRETE FORM

Having derived expression for the kinetic and potential energies of a finite element, and of the work done by external forces, we now apply the principle of conservation of energy, which states that the power added to a finte elastic element by external forces is balanced by the rate of change of the element's kinetic and potential energies,

$$\frac{d}{dt}[K_{(e)} + \prod_{(e)}] = \dot{W}_{(e)}(t) \tag{12.2.17}$$

In discrete form this balance of powers reduces to the set of simultaneous equations,

$$\sum_{i=1}^{6}\sum_{n=1}^{q}\sum_{m=1}^{q}\left[m_{nm}\,\ddot{u}^{m}_{(e)i} + \sum_{j=1}^{6}\sum_{k=1}^{6}\int \sigma^{ij}\frac{\partial\psi_{(e)n}}{\partial x_j}\left(\delta_{ki} + \frac{\partial\psi_{(e)}}{\partial x_e}\,u_i^m\right)dV_0 \right. \tag{12.2.18}$$

$$\left. - p^{n}_{(e)i}\right]\dot{u}^{m}_{(e)i}(t) = 0. \tag{12.2.18}$$

Since $\dot{u}^{m}_{(e)i}$ is arbitrary the expression in the brackets must vanish for all choices of i and m. Thus the general equation of motion of a finite element is given by,

$$\sum_{m=1}^{q}\left[m_{nm}\,\ddot{u}^{m}_{(e)i}(t) + \sum_{j=1}^{6}\sum_{k=1}^{6}\int \sigma^{ij}(\mathbf{x},t)\,\frac{\partial\psi_{(e)n}}{\partial x_j}(\mathbf{x})\right.$$

$$\left.\times\left(\delta_{ki} + \frac{\partial\psi_{(e)n}}{\partial x_k}(\mathbf{x})\;u^{m}_{(e)i}(t)\right)dV_0\right] = p^{n}_{(e)i}(t),\quad i = 1, 2, \ldots 6 \tag{12.2.19}$$

This equation is not directly solvable because the local applied forces $p^{n}_{(e)}(t)$ are not given quantities. Thus the local displacements $u^{m}_{(e)i}(t)$ cannot be obtained with this equation. Instead we form the global equation of motion in which the global driving forces are specified quantities. Now local dynamic quantities (displacements, forces) are related to their global counterparts by the mapping function $\Omega^{n}_{(e)N}$. Hence,

$$\mathbf{u}^{n}_{(e)}(t) = \sum_{n=1}^{q}\Omega^{n}_{(e)N}\,\mathbf{U}^N(t)$$

$$\mathbf{P}_N(t) = \sum_{e=1}^{E}\sum_{n=1}^{q}\Omega^{n}_{(e)N}\,\mathbf{p}_{(e)n}(t). \tag{12.2.20}$$

Substitution of this expansion of $u^{n}_{(e)}(t)$ and its time derivatives (= local nodal velocities and accelerations) into the above 12.2.19 of motion of a finite element generates an equation of balance of resultant forces (l.h.s) and external forces (r.h.s) on a single local node of a single finite element. By summing force contributions from all local nodes of an element and then summing over all elements *as assembled in the system* (the latter statement being equivalent to multiplication by the mapping function $\Omega^{n}_{(e)N}$) one arrives at the global equation of motion for the global nodal displacements $\mathbf{U}^N$ induced in the elastic surface by an assigned generalized force $\mathbf{P}_\Gamma(t)$ at the global node Γ,

$$\sum_{N=1}^{Q} M_{\Gamma N}\,\ddot{\mathbf{U}}^N(t) + G_\Gamma(t) + \sum_N H_{\Gamma N}(t)\mathbf{U}^N(t) = \mathbf{P}_\Gamma(t) \tag{12.2.21}$$

where

$$M_{\Gamma N} = \sum_{e=1}^{E}\sum_{n=1}^{q}\sum_{m=1}^{q} \Omega^{n}_{(e)\Gamma}\, m_{(e)nm}\, \Omega^{m}_{(e)N} \tag{12.2.22}$$

$$G_{\Gamma i}(t) = \sum_{m=1}^{6}\sum_{j=1}^{6}\sum_{E=1}\sum_{En=1}^{q} \Omega^{n}_{\Gamma}\, \delta_{ji} \int \sigma^{mj}_{(e)}\, \frac{\partial \psi_{(e)n}}{\partial x_m}\, dV_0 \tag{12.2.23}$$

$$H_{\Gamma N}(t) = \sum_{e=1}^{E}\sum_{n=1}^{q}\sum_{m=1}^{q}\sum_{k=1}^{6}\sum_{j=1}^{6} \Omega^{n}_{(e)\Gamma}\Omega^{m}_{(e)N} \int \sigma^{kj}_{(e)}\, \frac{\partial \psi_{(e)n}}{\partial x_k}\, \frac{\partial \psi_{(e)m}}{\partial x_j}\, dV_0 \tag{12.2.24}$$

in which Q is the number of global nodes, E the number of finite elements in the model of the radiating surface, q the number of nodes in one element, and the number 6 is the (assumed) number of degrees of freedom per local node. This is the discrete model of the dynamic system of an elastic surface available to the designer for determining the vector displacement $\mathbf{U}^N(t)$ at the n'th node. By assigning global nodes to the elastic surface under analysis one has $6 \times K$ unknown components of translations and rotations to solve for and $6 \times K$ equations of the above type to make the solution.

A unique solution is however not obtainable until the (spatial) boundary conditions and (temporal) initial conditions are specified. These specifications must be made with care to avoid violation of basic assumptions of continuity and compatibility in describing the dynamical state of deformation of the surface. The following section reviews the methods available to solve the equations of motion, and discusses the proper choice of boundary conditions.

12.3 SOLUTION OF THE DISCRETE MODEL IN SPACE-TIME

The global equations of motion (12.2.21) is discrete in the space coordinates but continuous in time. To enjoy the advantages of machine computation we desire to make these equations discrete in time as well. To do this we return to the general equations of motion of a fingle finite element (namely 12.2.19) which is also continuous in time, and consider a small time interval $[t_1,t_2]$. In this interval we approximate both the nodal displacement function $\mathbf{u}^{n}_{(e)}(t)$ and the nodal forcing function $\mathbf{p}^{n}_{(e)}(t)$ by a finite time representation, which we choose to be the simple form given by,

$$\mathbf{u}^{n}_{e}(\tau) = \mathbf{A}_0 + \tau\mathbf{A}_1 + \frac{\tau^2}{2}\mathbf{A}_2 \tag{12.3.1}$$

$$\mathbf{p}^{n}_{(e)}(\tau) = \mathbf{B}_0 + \tau\mathbf{B}_1.$$

The coefficients $\mathbf{A}$, $\mathbf{B}$ are next explicity written in terms of *temporal nodal quantities*, viz.

$$\mathbf{u}^{n}_{(e)}(t_1),\ \mathbf{u}(e)^{m}(t_2),\ \dot{\mathbf{u}}^{m}_{(e)}(t_1)\mathbf{p}^{n}_{(e)}(t_1),\ \mathbf{p}^{n}_{(e)}(t_2)$$

by solving these representations as a set of simultaneous equations in $\mathbf{A}$ and in $\mathbf{B}$. The result is,

$$\mathbf{u}^{m}_{(e)}(t) = \frac{t_2^2 - t^2}{t_2^2}\,\mathbf{u}^{m}_{(e)}(t_1) + \frac{t^2}{t_2^2}\mathbf{u}^{n}_{(e)}(t_2) + \frac{t}{t_2}(t_2 - t)\,\dot{\mathbf{u}}^{m}_{(e)}(t_1) \tag{12.3.2}$$

$$\mathbf{p}^{n}_{(e)}(t) = \frac{t_2 - t}{t_2}\,\mathbf{p}^{n}_{(e)}(t_1) + \frac{t}{t_2}\,p^{n}_{(e)}(t_2) \tag{12.3.3}$$

Direct differentiation in time of $u^{m}_{(e)}(t)$ gives the velocity $\dot{\mathbf{u}}^{n}_{(e)}(t)$ and acceleration $\ddot{\mathbf{u}}^{m}_{(e)}(t)$ in terms of their values at the time nodes. Substitution of these approximate forms into the equations of motion of a single finite element finally makes it discrete in space but continuous in

time only in the interval $[t_1,t_2]$. However such a substitution transforms a differential equation (in time) into an algebraic equation, as can be seen by writing 12.2.19 out in full:

$$\sum_{m=1}^{q}\left\{m_{nm}\left[-\frac{2}{t_2^2}\,u^n_{(e)i}(t_1)+\frac{2}{t_2^2}\,u^n_{(e)i}(t_2)-\frac{2}{t_2}\,\dot{u}^n_{(e)i}(t_1)\right]\right.$$
$$+\sum_{j=1}^{3}\sum_{K-1}^{3}\int_{V_0}\sigma^{jk}(\mathbf{x},\,t)\,\frac{\partial\phi_{(e)n)}(\mathbf{x})}{\partial x_j}\left[\delta_{ji}+\frac{\partial\phi_{(e)m}(\mathbf{x})}{\partial x_k}\left[\frac{t_2-t^2}{t_2^2}u^m_{(e)i}(t_1)\right.\right.$$
$$\left.\left.+\frac{t^2}{t_2^2}\,u^m_{(e)i}\,(t_2)+\frac{t}{t_2}(t_2-t_1)\dot{u}^m_{(e)i}\;(t_1)\right]\right]dV_0$$
$$=\frac{t_2-t_1}{t_2}\,p^n_{(e)i}(t_1)+\frac{t}{t_2}\,p^n_{(e)i}\,(t_2). \tag{12.3.4}$$

Upon assuming that the interval $[t_1,t_2]$ is small enough we can average the time-varying displacement vector over this interval by direct integration in time. The result is,

$$\sum_{m=1}^{q}\left\{m_{nn}\left[\frac{2}{t_2^2}\,(u^n_{(e)i}(t_2)-u^n_{(e)i}\,(t_1))-\frac{2}{t_2}\,\dot{u}^n_{(e)i}(t_1)\right](t_2-t_1)\right.$$
$$+\sum_{j=1}^{3}\sum_{k=1}^{3}\int_{t_1}^{t_2}dt\int_{V_0}\sigma^{jk}(\mathbf{x},t)\,\frac{\partial\psi_{(e)n}(\mathbf{x})}{\partial x_j}\left[\delta_{ij}\right.$$
$$+\frac{\partial\psi^m_{(e)}}{\partial x_k}\left[\frac{t_2^2-t^2}{t_2^2}\,u^m_{(e)i}(t_1)+\frac{t^2}{t_2^2}\,u^m_{(e)i}\,(t_2)\right.$$
$$\left.\left.\left.+\frac{t}{t_2}\,(t_2-t_1)\,\dot{u}^n_{(e)i}(t_1)\right]\right]dV_0\Bigg\}$$
$$=-\frac{(t_2-t_1)^2}{2t_2}\,p^n_{(e)i}\,(t_1)+\frac{(t_2-t_1)^2}{t_2}\,p^n_{(e)i}(t_2). \tag{12.3.5}$$

We are now in a position to convert this equation into global form by use of the mapping function $\Omega^n_{(e)\Gamma}$. Using the previously defined quantities $M_{\Gamma N}$, G_{ni}, and $H_{\Gamma N}$ (see 12.2.21 to 12.2.23) we arrive at the discrete space time model in the following set of algebraic equations:

$$\sum_{N=1}^{Q}M_{\Gamma N}\left[\frac{2}{t_2^2}\left(\mathbf{U}^N(t_2)-\mathbf{U}^N(t_1)\right)-\frac{2}{t_2}\dot{\mathbf{U}}^N(t_1)\right](t_2-t_1)$$
$$+\mathbf{G}_\Gamma\,(t_1,t_2)+\mathbf{H}_\Gamma(t_1,t_2)=\mathbf{P}_\Gamma\,(t_2,t_1)$$

in which

$$\mathbf{G}_\Gamma\,(t_1,t_2,\mathbf{U}^\Gamma(t_1),\mathbf{U}^\Gamma(t_2),\,\dot{\mathbf{U}}^\Gamma(t_1))=\int_{t_1}^{t^2}\mathbf{G}_\Gamma\,(t)\,dt$$
$$\mathbf{H}_\Gamma\,(t_1,t_2,\mathbf{U}^\Gamma(t_1),\mathbf{U}^\Gamma(t_2),\,\dot{\mathbf{U}}^\Gamma(t_1))=\sum_N\int_{t_1}^{t^2}dt\;H_{\Gamma N}(t)$$

$$\times \left[\frac{t_2^2 - t^2}{t_2^2} \mathbf{U}^N(t_1) + \frac{t^2}{t_2^2} \mathbf{U}^N(t_2) + \frac{t}{t_2} (t_2 - t_1)\dot{\mathbf{U}}^N(t_1) \right]$$

$$\mathbf{P}_\Gamma (t_2,t_1) = - \frac{(t_2 - t_1)^2}{2t_2} \mathbf{P}_\Gamma (t_1) + \frac{(t_2 - t_1)^2}{t_2} \mathbf{P}_\Gamma(t_2) \tag{12.3.6}$$

The completion of this now allows us to pursue our original aim which was to reduce the equations of motion to an algebraic form so as to permit machine computation by numerical methods. Assuming we have constructed a total of K global nodes it is seen that the above equations form a set of 6K simultaneous equations in the unknown nodal displacements $\mathbf{U}^\Gamma(t_2)$ resulting from an application of *known* external forces $\mathbf{P}_\Gamma(t_1)$, $\mathbf{P}_\Gamma(t_2)$, and known initial $\mathbf{U}^\Gamma(t_1)$, $\dot{\mathbf{U}}^\Gamma(t_1)$. When $\mathbf{U}^\Gamma(t_2)$ is calculated, it can be considered, together with $\dot{\mathbf{U}}^\Gamma(t_2)$, $\mathbf{P}_\Gamma(t_2)$, $\mathbf{P}_\Gamma(t_3)$, as the group of initial conditions and applied forces that determine the displacement vector $\mathbf{U}^\Gamma(t)$ in the next interval $[t_2,t_3]$. Thus the result of the calculation of a particular interval becomes the input conditions for the interval following. In this way by iteration the entire time and space history of global displacement of the elastic surface is determined from stated global initial conditions (of displacement and velocity) and from a specified global temporal history of the loading.

Once the global displacements are determined one can immediately determine the local nodal displacements, local velocities and local acceleration by application of 12.2.20 and its time derivatives. Local displacements (and derivatives) anywhere in the element can be determined by 12.2.4, in which the designer-selected interpolation function $\psi_{(e)}(\mathbf{x})$ is known. The components of strain are similarly directly calculable from 12.2.10. Local stresses are then obtained by applying the constitutive equations to the known strains. Finally, local nodal forces are found by use of 12.2.20.

12.4 INTERPOLATION FORMULAS

The construction of interpolation formulas is the basic step in the application of the finite element technique of solving problems of the dynamic response of continua to applied forces. We begin with an example, and afterward generalize.

Let the finite element be a plane triangle with three (corner) local nodes. We place the triangle in a local coordinate system $X_{(1)}$, $X^{(2)}$ (that is, $X^{(1)} = x$, $x^{(2)} = y$), so that the nodes have the coordinates $(X^{(1)1}, X^{(2)1})$, $(X^{(1)2}, X^{(2)2})$, $(X^{(1)3}, X^{(2)3})$ respectively. Let $w(x)$ be the displacement field to be interpolated from the known values w^1, w^2, w^3 at the nodes. We desire to find an interpolation function that will satisfy the boundary conditions of the element. Choosing a linear relation between $w(\mathbf{x})$ for any $\mathbf{x}$ and the nodal values w^i, we first let $\mathbf{x}$ be the nodal points themselves. In terms of unknown quantities a_0, a_1, a_2 and we have,

$$w^1 = a_0 + a_1 x^{(1)1} + a_2 x^{(2)1}$$

$$w^2 = a_0 + a_1 x^{(1)2} + a_2 x^{(2)2}$$

$$w^3 = a_0 + a_1 x^{(1)3} + a_2 x^{(2)3}$$

i.e.,

$$\{w\} = [C]\{a\}. \tag{12.4.1}$$

We wish to find the relation between the a_i and the known nodal values w^i, and the matrix $[C]$ *evaluated at the nodal points.* Assuming $[C]$ has an inverse $[C]^{-1}$, we find the solution to be

$$\{a\} = [C]_n^{-1}\{w\}_n, \quad n \text{ indicates nodal form,}$$

or

$$\begin{aligned} a_0 &= C_{01}^{-1}w^1 + C_{02}^{-1}w^2 + C_{03}^{-1}w^3 \\ a_1 &= C_{11}^{-1}w^1 + C_{12}^{-1}w^2 + C_{13}^{-1}w^3 \\ a_2 &= C_{21}^{-1}w^1 + C_{22}^{-1}w^2 + C_{13}^{-1}w^3 \end{aligned} \tag{12.4.2}$$

in which C_{ij}^{-1} is the ij component of the matrix $[C]^{-1}$ and is written in terms of the nodal coordinates $x^{(i)n}$. In this way the interpolation factors a_i are found explicitly Next we suppose the point $\mathbf{x}$ on element e is not at the nodes. Then the displacement can be written in terms of explicit a's

$$\begin{aligned} w(\mathbf{x}) &= a_0 + a_1x^1 + a_xx^2 \\ w(\mathbf{x}) &= \sum_n [C_{0n}^{-1}w^n + C_{1n}w^n\hat{x^{(i)}} + C_{2n}^{-1}w^nx^{(2)}] \\ w(\mathbf{x}) &= \sum_{n=1}^{3} w_{(e)}^n\ \psi_{(e)n}(\mathbf{x}) \end{aligned} \tag{12.4.3}$$

in which

$$\begin{aligned} \psi_{(e)n}(\mathbf{x}) &= C_{0n}^{-1} + C_{1n}^{-1}x^{(1)} + C_{2n}^{-1}x^{(2)} \\ n &= a_n + b_{ni}x^i \end{aligned}$$

or

$$\{\psi_{(e)n} \cdot (\mathbf{x})\} = [C_n]^{-1}\begin{Bmatrix} 1 \\ x^{(1)} \\ x^{(2)} \\ \cdot \\ \cdot \\ \cdot \end{Bmatrix}_{(e)}$$

Thus the interpolation formula is a function of general local coordinates peculiar to the element in question and specific local coordinates associated with the matrix $[C]$.

As a second example we choose a one-dimensional finite element (namely a line) having two nodes. The coordinate system is $x^{(1)}$ and the nodes are $x^{(1)1}$, $x^{(1)2}$: thus,

$$\begin{bmatrix} w^1 \\ N^2 \end{bmatrix} = \begin{bmatrix} 1 & x^{(1)1} \\ 1 & x^{(1)2} \end{bmatrix}\begin{bmatrix} a_0 \\ a_1 \end{bmatrix}$$

or

$$\{\omega\}_n = [C]_n\{a\}.$$

Since the determinant of $[C]$ is $x^{(1)2} - x^{(1)1} = L =$ length of the line, the inverse of C is given by

$$[C]^{-1} = \frac{1}{L}\begin{bmatrix} x^{(1)2} & -1 \\ -x^{(1)1} & 1 \end{bmatrix}$$

The interpolation formulas then become:

$$\psi_{(e)1}(x) = \frac{x^{(1)2} - x^{(1)}}{L}; \psi_{(e)2}(x) = -\frac{x^{(1)1} + x^{(1)}}{L}.$$

Hence the displacement anywhere in the finite element is,

$$w(x) = \frac{w^1}{L}(x^{(1)2} - x^{(1)}) + \frac{w^2}{L}\left[x^{(1)} - x^{(1)1}\right] \tag{12.4.4}$$

12.4a GENERALIZATION OF INTERPOLATION FUNCTIONS

Let the finite element be imbedded in its lattice of K local nodes. The interpolation model is called *simplex* if we identify $k + 1$ local nodes and write

$$\psi_{(e)_n}(\mathbf{x}) = a_n + \sum_{i=1}^{k} b_{ni}\, x^i, \quad n = 1, 2 \ldots k + 1. \tag{12.4.5}$$

This is the model used in the above examples. On the other hand if we specify the number of nodes to be greater than $k + 1$, the model is called *complex*. In this case

$$\psi_{(e)_n}(\mathbf{x}) = a_n + \sum_{i=1}^{k} b_{n_i} x^i + \sum_{i}^{k}\sum_{j}^{k} C_{n_{ij}} x^i x^j \tag{12.4.6}$$

A third type of model of finite element is one in which element boundary must coincide with the coordinate lines (taken to be orthogonal) of the element coordinate system to achieve interelement continuity. These elements are called *multiplex models*, or *curvilinear finite element models*. A fourth type of model of finite element is called "isoparametric" and is designed to be suitable for use with continua which have very irregular boundaries. It has also a curvilinear-type element, but with this difference that the curvilinear coordinates ξ_i are arbitrary (that is, they do not belong to the orthogonal curvilinear coordinates widely used in physics). Let us suppose that a finite element with arbitrary boundaries is fixed in a cartesian coordinate system x^i, $i = 1, 2, 3$. The location of the local nodes is known to be at x^{ni}, $n = 1, 2 \ldots p$. We make the coordinate transformation

$$x^i = a^i + \sum_j a^i_j \xi^j + \sum_j \sum_k a^i_{jk}\, \xi^{jk} + \ldots . \tag{12.4.7}$$

In the new system ξ^i the local nodes are fixed at ξ^{ni} in such a way that,

$$x^{ni} = a^{ni} + \sum_j a^i_j \xi^{nj} + \sum_j \sum_k a^i_{jk}\, \xi^{njk} + \ldots . \tag{12.4.8}$$

This is a set of algebraic equations in the unknown coefficients a. Solving for a in the same manner that we used above to find $[C]$, we find its components in terms of the nodal values x^{ni}. It is easily seen that

$$x^i = \sum_n \psi_{(e)n}(\xi) x^{ni}$$

$$\psi_{(e)n}(\xi) = a^{-1}_{0n} + a^{-1}_{1n}\xi^{(1)} + a^{-1}_{2n}\, \xi^{(2)}. \tag{12.4.9}$$

Thus the local field w on element e can be approximated (in ξ coordinates) by writing

$$w(\xi) = \sum_{n=1}^{p} w^n_{(e)}\ \psi_{(e)n}(\xi). \tag{12.4.10}$$

In sum: a large variety of interpolation formulas can be constructed to satisfy the analyst's needs in analyzing different types of structures with different space-time boundary conditions.

Often to improve accuracy the analyst will devise more elaborate forms than are already available. On the other hand one may choose crude interpolation functions to expedite the numerical work. Thus there is great freedom in selecting $\psi_{(e)}(\mathbf{x})$.

12.5 ELEMENT-STIFFNESS MATRIX

After the construction of appropriate interpolation formulas to satisfy the boundary conditions (in space and time) it is necessary to return to the task of finding explicit formulas for the stiffness and mass terms in the kinetic and potential energies of the equations of motion of a finite element whose general formula appears in Eq. 12.2.19.

As noted in Sec. 12.1 and repeated here for convenience, at a local node there will be six possible motions (or motional degrees of freedom), namely three components of translation and three rotations. For a finite element having K local nodes there will thus be 6K motional degrees of freedom. We choose one of these degrees of freedom (call it the ith) and apply it to its node as a real motion with unit amplitude. The motions at all other nodes of the finite element are made zero. As a result of the real motion there is induced a strain field in the elastic body which is accompanied by a stress field (or force field). This (distributed) force field due to the ith degree of freedom at a particular node is then available for doing work at any point in the body.

We next choose from the number 6K a second (motional) degree of freedom (call it the jth) and assign it to a second node in the same finite element as a *virtual* motion. This virtual jth displacement allows the force field due to the *real* ith displacement to do work anywhere in the finite element through the motion of the virtual jth degree of freedom. If the stress field at a point in the finite element is $\sigma_i(\mathbf{x})$ due to the real motion of the ith degree of freedom of one node the related force field is $\sigma_j(\mathbf{x})\,dA_1$; and the virtual displacement (at the same point) of virtual strain ϵ_j due to a virtual displacement at a second node is $\epsilon_j\,dx_1$. Thus the virtual work done is given by the volume integral,

$$\Pi_{ij} = \int_{V_0} \sigma_i(\mathbf{x})\epsilon_j(\mathbf{x})\; dV_0(\mathbf{x}). \tag{12.5.1}$$

Note that because of the scheme of numbering the degrees of freedom of a finite element (Sec. 12.2a) the nodes at which forces and displacements occur here in themselves irrelevant in this discussion. Equation 12.5.1 is therefore the virtual work done by a real degree of freedom i acting on a second virtual degree of freedom j averaged over the volume of the finite element.

Because of the use of interpolation function $\psi(e)_i(x)$ the stress field due to a unit real motion of the ith degree of freedom at node n is expressed in terms of $\psi_{(e)i}(\mathbf{x})$ and is distributed over the finite element. The virtual strain at any point in the finite element is expressed as a nodal virtual displacement (call it δu_j in the jth degree of freedom) multiplied by the corresponding interpolation function $\psi_{(e)j}(\mathbf{x})$. Hence the volume integral of 12.5.1 is over $\psi_{(e)i}(\mathbf{x})$ and/or its derivatives multiplied by $\psi_{(e)j}(\mathbf{x})$ and/or its derivatives, multiplied by the virtual displacement δu_j. The ratio formed by dividing Π_{ij} by the virtual displacement δu_j is called the *element stiffness* coefficient $\rho_{(e)ij}$, i.e.,

$$\rho_{(e)ij} = \frac{\Pi_{ij}}{\delta u_j} \qquad \text{(no sum on indices)}. \tag{12.5.2}$$

When assembled these coefficients form a (maximum possible) 6K × 6K element-stiffness matrix for each finite element. Thus for a finite element in the form of a triangle (meaning 3

local nodes) the element stiffness matrix is a maximum 18 × 18. Generally, these matrices are symmetrical about the main diagonal. They thus have only $18 + \frac{(18 \times 18) - 18}{2} = 174$ independent components.

The degrees of freedom at a node can be thought of as the components of a vector. We write this vector $\mathbf{u}$ (or u_k, or $\{u\}$). Thus all terms containing $\mathbf{u}^n$ in previously derived formulas of this chapter refer to all the degrees of freedom in $\mathbf{u}$ at a node. In particular the expression for potential energy of deformation Π Eq. 12.2.12 equivalent to the work done Π_{ij}, and the integral in Eq. 12.5.1 is equivalent to the rate of work done in the virtual velocity $\dot{\mathbf{u}}_{(e)}$: this equivalence is written as,

$$\Pi_{ij} = \left(\int \sigma^{jk} \frac{\partial \psi_{(e)n}}{\partial_{x_j}} \delta_{ki} \, dV_0 \right) \dot{u}_{(e)i}$$

(no sum on i,j,k)

In dynamic analysis the local form of the stiffness matrix $\rho_{(e)ij}$ must be converted to global form. This is done by the mapping function $\Omega_{(e)}$. In most cases several local nodes contribute potential energy to one global point (center point f in Fig. 12.5.1) and so the (global) stiffness coefficient is the sum of the local stiffness coefficients incident on this point. Thus, using the figure, one has

$$\rho_{ii}^{(f)} = \sum_{m=1}^{5} \hat{\rho}_{ii}^{(m)}$$

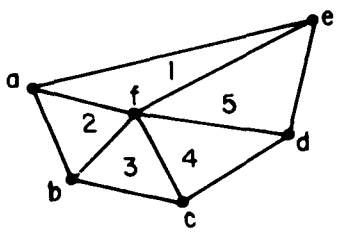

Figure 12.5.1. Local nodes a, b, c, d, e and global node f

in which the hat symbol indicates global forms.

12.5a ELEMENT-MASS MATRIX

The kinetic energy term of the equation of motion (12.2.8) requires the construction of the element-mass coefficient m_{ij}. A consistent procedure for doing this is outlined in this section.

We return to the vector $\mathbf{u}$ whose components u_i, $1 = 1, 2 \ldots 6K$, are the degrees of freedom of all the nodes and select the jth degree of freedom u_j. We form the second time derivative (or acceleration) $\ddot{u}_i$, and subject node n to a *unit* magnitude of $\ddot{u}_i$, restraining the motion of all other degrees of freedom to zero at all other nodes.

The acceleration developed anywhere in the finite element is $\ddot{u}_i \, \psi_{(e)i}(\mathbf{x})$ and the (interior) inertial force resisting this acceleration is $\rho_0(\mathbf{x}) \ddot{u}_i \psi_{(e)i}(\mathbf{x})$ in which $\ddot{u}_i = 1$. This force is available for doing work through the motion of any other degree of freedom. We choose the jth

degree of freedom of the finite element and give to its corresponding node a virtual unit displacement δu_i. The effect of this virtual displacement is distributed throughout the plate by means of the interpolation formula,

$$\delta u(\mathbf{x}) = \delta u_j \, \psi_{(e)j}(\mathbf{x}). \tag{12.5.4}$$

The work done by the force due to real acceleration in degree of freedom i acting through the virtual displacement δu_j is then seen to be

$$W_{ij} = \delta u_j m_{ij}, \; m_{ij} = \int \rho_0(\mathbf{x}) \, \psi_{(e)i}(\mathbf{x}) \psi_{(e)j}(\mathbf{x}) dV_0(\mathbf{x}). \tag{12.5.5}$$

The mass coefficient m_{ij} is the ith element of the element mass matrix. It is equivalent to 12.2.8 previously derived. It is emphasized however that this derivation is based on the principle of virtual work.

12.5b DAMPING MATRIX

The equation of motion (12.2.19) is a statement that internal mass and elastic forces (left hand side) balance the external applied forces (right hand side). When the vibrating structure is internally damped by viscous forces the equation of motion has an addition force $c_{ij} \dot{u}_j$ in which $\dot{u}_j$ the velocity of the jth degree of freedom, and c_{ij} is the damping coefficient. A brief derivation of c_{ij} is now undertaken.

We assume the finite element exhibits viscous clamping proportional to velocity, and let $c(\mathbf{x})$ represent the damping force per unit velocity. To calculate the *damping coefficient* we select the ith degree of freedom ($=u_i$) associated with a node and take its first derivative $\dot{u}_i$. All other velocities (namely of other degrees of freedom) are set to zero. The resultant (viscous) damping force distributed throughout the finite element is $c(\mathbf{x}) \dot{u}_i \, \psi_{(e)}(\mathbf{x})$. It is available for doing work through any virtual displacement (i.e., the same or any other degree of freedom). We select the jth degree of freedom in the vector $\mathbf{u}$ and make it virtual ($=\delta u_j$) at its corresponding node. The distributed virtual displacement corresponding to δu_j is $\delta u_j \, \psi_{(e)j}(\mathbf{x})$. We now define the damping coefficient c_{ij} to be the virtual work done when the real velocity $\dot{u}_i$ is given unit magnitude: i.e.,

$$c_{ij} = \frac{\Pi_{ij}}{\delta u_j} = \int_{V_0} c(\mathbf{x}) \psi_{(e)i}(\mathbf{x}) \, \psi_{(e)j}(\mathbf{x}) \, dV_0. \tag{12.5.6}$$

The damping matrix is $\mathbf{C}$ ($=[c_{ij}]$) is a $6K \times 6K$ matrix. Its explicit calculation allows one to add the viscous forces in the equation of motion 12.2.19 inserting the following term on the l.h.s., $\sum_{m=1} c_{nm} \, \dot{u}^m_{(e)i}(t)$. This insertion is very important in transient loading.

From this derivation it is evident that the damping coefficient serves the purpose of converting viscous forces distributed over the finite element into viscous forces concentrated at the nodes. The validity of the conversion is assured by making it satisfy the principle of virtual work.

Conclusion: The radiation of long-wavelength sound in low frequencies requires extensive active surfaces to overcome the highly reactive loads of the medium. Such surfaces often deform elastically during radiation, either by intension, or uncontrollably by extraneous forces in the mechanical drive, or in the medium. A theoretical analysis of the deformation of these surfaces is straightforward in cases where the surfaces have simple shapes (circles, cylinders,

etc.) and the exciting forces are symmetric in space and steady in time. For arbitrarily shaped surfaces, asymmetric forces and/or transient excitation the analysis of deformation is best accomplished by numerical means. Here the advantages of high speed computation on digital computers dictate the derivation of the equations of motion in *discrete form* so that the analysis reduces to the solution of a set of simultaneous algebraic equations in the unknown displacements. This requirement is well met by the use the theory of finite elements which enables the designer to calculate complicated structural vibration in a relatively rapid way by numerics in situations formerly regarded as impossible or uneconomical.

The construction of the discrete model of the equations of motion reduces to the calculation of local mass, stiffness and dissipation matrices, the components of which effectively concentrate these local distributed parameters into local nodal parameters. The local parameters are then transformed into global parameters, and from these the global equations of motion are constructed in discrete form. The solution of the latter is the essential step in the analysis, from which all other dynamic parameters (stress, strain, etc.) are derived.

The theory of finite elements has been applied to elasticity. It can also be applied in certain cases to radiation calculations in acoustics. The combination of finite element elasticity and finite element acoustics is a powerful tool of analysis. This combination is explored in the next chapter.

BIBLIOGRAPHY ON FINITE ELEMENT METHODS IN ACOUSTIC RADIATION

1. J.T. Oden, "Finite Elements of Nonlinear Continua," McGraw-Hill, 1972.

2. O.C. Zienkiewizc and Y.K. Cheung "The Finite Element Method in Structural and Continuum Mechanics," McGraw-Hill, New York, 1967.

3. G.M.L. Gladwell and V. Mason "Variational Finite Element Calculation of the Acoustic Response of a Rectangular Panel," J. Sound Vib. **14**, 115-135 (1971).

4. O.C. Zienkiewizc "The Finite Element Method in Engineering Science," McGraw Hill, New York, 1971.

5. O.C. Zienkiewizc and R.E. Newton "Coupled Vibrations of a Structure Submerged in a Compressible Fluid," Proc. Int. Symp. on Finite Element Techniques, Stuttgart, Germany, 10-12 June 1969.

CHAPTER XIII

FINITE ELEMENT RADIATION

13.1 INTRODUCTION

A chief feature of low frequency underwater sound sources is the large displacements needed to efficiently generate acoustic power. These displacements may be achieved by use of elastic structures operating in modes of vibration selected for low stiffness. Examples of low stiffness construction are rigid plates suspended by soft springs, flexing plates simply supported on bearings, flexing plates driven at single points, large diaphragms driven by hydraulic fluids, spherical rubberized bags with vibrating gas, and many others.

The design of these radiating structures is generally guided by two objectives: first, to radiate acoustic power effectively, and second, to account for the interface acoustic fluid load in a manner to optimize the performance of the electrical-mechanical-hydraulic components in the source. We consider below these two objectives simultaneously.

13.1a Symbolic Representation of Interacting Systems

An acoustic source can be represented as a cascade of three (or more) *interacting* power systems. For convenience the first or "driving system" is taken to be an $e\,i$ (volt-current) electrical system; the second, an $f\,\dot{u}$ (force-velocity) mechanical system (say an elastic structure); and the third a $p\,\dot{q}$ (pressure-volume velocity) acoustical system. We assume that i, $\dot{u}$, $\dot{q}$ are extensive or *flow* quantities and e, f, p are intensive or *across* quantities. This choice is arbitrary, but will prove useful in the discussion. Let applied quantities be represented by capital letters. The acoustic source is then described by three (or more) mutually coupled equation, viz.

$$\begin{aligned} &\text{(a)}\quad L_{i,i}\,\mathbf{i} + L_{i,u}\,\dot{\mathbf{u}} = \mathbf{E}\,(x,t) \\ &\text{(b)}\quad L_{u,u}\,\dot{\mathbf{u}} + L_{\dot{u},i}\,\mathbf{i} + \mathbf{L}_{\dot{u},p}p = \mathbf{F}\,(\mathbf{x},t) \\ &\text{(c)}\quad \mathbf{L}_{p,p}p + L_{p,\dot{u}}\dot{\mathbf{u}} = \dot{\mathbf{Q}}\,(x,t) \end{aligned} \tag{13.1.1}$$

$\mathbf{E}\,(x,t)$ $\mathbf{F}\,(x,t)$ $\dot{\mathbf{Q}}\,(x,t)$ are applied electric-field, applied mechanical force and applied volume velocity respectively in which the symbols L are differential operators, and their double subscripts indicate the coupling between one power system and another. For example, $L_{\dot{u},i}$, is an operator which couples the mechanical system with the electrical system through a $\dot{u}$, i or velocity-current coupling. The r.h.s. of each equation is an independently applied forcing function. In general, all system parameters $(e,i,p,\dot{q},f,\dot{u})$ are vectors and the operators L are dyadics.

This set of equations can be solved exactly, or approximately, by several well-known procedures. It is our purpose here, in conformity with the objectives of this chapter and Chapter XII to present techniques for solution that are ideally united to digital computers, and in particular, to emphasize the finite element technique.

Since the radiation properties of a source are functions of the interaction between the mechanical and acoustical systems we will for simplicity deal initially only with the systems of Eq. (13.1.1b) and (13.1.1c). Thus, the mechanical-acoustical interaction is represented by the pair,

$$\text{mechanical: } L_{\dot{u},\dot{u}}\dot{\mathbf{u}} + \mathbf{L}_{\dot{u},p}p = \mathbf{F}(\mathbf{T}) \tag{13.1.2a}$$

$$\text{acoustical: } \mathbf{L}_{p,p}p + L_{p,u}\dot{\mathbf{u}} = \dot{\mathbf{Q}}(t). \tag{13.1.2b}$$

Several subcases of these equation deserve discussion. In the first case we can restrict attention to the radiating surface by making the *applied* $\dot{\mathbf{Q}}(t)$ zero. This case is treated below in Section (13.2a). When the velocity $\dot{\mathbf{u}}$ and pressure p are calculated on the surface of the source the radiation field everywhere (including the far field) can be calculated by use of the Helmholtz integral, as explained in Sect. (13.3). A second case of importance occurs when the radiating surface together with a sphere of fluid of finite size surrounding it are both taken to be a generalized (*composite*) source. Then the interaction of the remaining medium upon the spherical surface constituting the source is visualized as a driving force identical with $\mathbf{F}(t)$. Application of (13.1.2a), (13.1.2b) then serve to determine the acoustic field. Other cases which can be treated by use of these equations will be mentioned below.

The principal objective in the following sections is to convert (13.1.2) into finite element form. This conversion is complicated by the different vibratory properties of fluids and solids and by the need to solve the set of equations simultaneously since they are coupled by the solid-fluid interaction. Complications also arise because structure vibration historically is treated as a force displacement *f,u* system rather than a force velocity system *f,u̇*. This point will be taken up in detail later in this chapter. At present we proceed to discuss fluid-solid interaction, and follow it with a discussion of the discretization of the acoustic field.

13.2 FLUID-SOLID INTERACTION OF RADIATING SURFACES

Chapter I has noted that the propagation of linear acoustic signals from volume distributed sources $Q(\mathbf{x},t)$ in a fluid of density ρ_w, and sound speed C_w is governed by the linear acoustic wave equation in three dimensions,

$$\nabla^2 p(\mathbf{x},t) - \frac{1}{C_w^2(\mathbf{x},t)} \frac{\partial^2 p}{\partial t^2}(\mathbf{x},t) = -\mathcal{Q}(\mathbf{x},t) \tag{13.2.1}$$

This equation states that at location $\mathbf{x}$, time t in the field the acoustic pressure is concentrating (denoted by $\nabla^2 p$) due to sources Q, but is simultaneously diminishing due to propagation (denoted by $\partial^2 p / C_w^2 \partial t^2$). At low frequencies the sources are advantageously represented as a collection of volume distributed multipoles:

$$\mathcal{Q}(\mathbf{x},t) = \rho_w \frac{dQ}{dt} - \nabla \cdot \mathbf{F} + \frac{1}{2} \nabla \cdot \bar{\mathbf{T}} \cdot \nabla - \ldots. \tag{13.2.2}$$

(see Chapter V). This first term r.h.s. describes all *monopole* sources (defined as those which radiate uniformly in all directions) in terms of a time rate of change of injection of mass Q (units: $m^3/s\ m^3$) into the medium. The second term describes all dipole sources in terms of a divergence of a fluid body force $\mathbf{F}$, the radiation from which varies with the cosine of the angle of observation relative to the direction of $\mathbf{F}$. The third term described all quadripole sources in terms of the double divergence of the stress tensor $\bar{\mathbf{T}}$ whose components are momentum flux stress and viscosity sheer stress. The radiation from these sources involves products of two

angles of direction. In conventional sound radiators the monopole source is associated with a contraction and expansion of a elastic volume, the dipole source with an alternating body force on a rigid volume, and the quadripole source with two differently directed body forces (or stresses) on one volume, equivalent to interacting gradients of momentum-flux (See Chapter I for discussion).

As noted in Sect. 13.1 most sources generate low frequency radiation by movement of solid (or gaseous) interfaces (e.g. elastic plates, diaphragms, rigid pistons, bubbles, etc). At low frequencies this acoustic radiation is often enhanced in efficiency by use of large size radiating surfaces that are chiefly elastic. The displacement motion $\mathbf{u}$ of these elastic radiating surfaces can generally be modeled by the wave equation of elastically isotropic and homogeneous solids, namely

$$(\lambda_e + \mu_e) \nabla (\nabla \cdot \mathbf{u}) + \mu_e \nabla \cdot \nabla \mathbf{u} - \rho \ddot{u} = -\rho_s \mathbf{f} \tag{13.2.3}$$

[1] where for simplicity the solid is taken to be elastically isotropic, of density ρ_s, with Lame' constants λ_e, μ_e, and driven by a body force $\mathbf{f}$. The displacement vector $\mathbf{u}$ has components U, V, W.

At the interface between fluid and solid the acoustic field p and the displacement field $\mathbf{u}$ are coupled. The problem in the theory of fluid-solid interaction is to formulate this coupling in mathematical terms and find ways to obtain p and $\mathbf{u}$ from solutions of the resultant equations.

A useful first step, is to solve (13.2.3) for the normal component of steady state velocity $\dot{W}(\mathbf{x}) \equiv -i\omega W$ under the action of a sinusoidal surface (normal) force $\mathbf{F} e^{-i\omega t}$. For ease in following the development we write the single (displacement W) component equation in the symbolic form, using $\mathscr{L}_w$ to represent a differential operator:

$$\mathscr{L}_w \{\dot{W}(\mathbf{x})\} = -F(\mathbf{x}) \tag{13.2.4}$$

We now make the assumptions that the operator $\mathscr{L}_w$ is linear, that it can be inverted and that a solution can be found in form of an integral,

$$\dot{W}(\mathbf{x}) = \oint F(\mathbf{x}_0)\ Y(\mathbf{x}|\mathbf{x}_0)\ dS(\mathbf{x}_0) \tag{13.2.5}$$

Here the symbol Y is an *influence function*, which gives the normal volume velocity at location $\mathbf{x}$ on the surface due to normal force F at location $\mathbf{x}_0$ (positive if pointing away from the medium where the acoustic field is generated). Now the forces F can be of two kinds: concentrated forces $F(\mathbf{x}_j)\ \delta(\mathbf{x} - x_j)$. $j = 1, 2, \ldots, N$, and distributed pressures $p(\mathbf{x}_j)$. Thus (13.2.5) has the form

$$\dot{W}(\mathbf{x}_\kappa) = -\int p(\mathbf{x}_j)\ Y(\mathbf{x}_\kappa|\mathbf{x}_j)\ dS(\mathbf{x}_j) + \sum_{j=1}^{N} F(\mathbf{x}_j)\ Y(\mathbf{x}_\kappa|x_j) \tag{13.2.6}$$

The term in pressure p is negative because it always points into the surface. To determine the form of p we turn to the case of acoustic radiation and consider a simple model of the radiator, taking it to be a collection of point sources, with $\mathscr{Q} = \rho \dot{Q}$ and volume velocity $\dot{Q} = \dot{W}(\mathbf{x}_0)\ dS(\mathbf{x}_0)$. The radiated pressure from such a collection of point sources can be obtained by solving (13.2.1),

$$p(\mathbf{x}) = \oint \dot{W}(\mathbf{x}_0)\ G(\mathbf{x}|\mathbf{x}_0)\ dS(\mathbf{x}_0) \tag{13.2.7}$$

in which G is the acoustic Green's function (defined as the pressure at $\mathbf{x}$ due to a delta function volume velocity at $\mathbf{x}_0$), whose form depends on the boundaries of the radiating system, and their associate boundary conditions of pressure and velocity. This interface pressure due to fluid coupling is identified in *form* with the applied pressure in (13.2.6). Thus the normal component of velocity $\dot{W}(\mathbf{x}_\kappa)$ is given by,

$$\dot{W}(\mathbf{x}_\kappa) = -\oint dS(\mathbf{x}_j) \oint dS(x_0)\ \dot{W}(\mathbf{x}_0)\ G(\mathbf{x}_j|\mathbf{x}_0)\ Y(\mathbf{x}_\kappa|x_j) + \sum_{j=1}^{N} F(\mathbf{x}_j)\ Y(\mathbf{x}_\kappa|\mathbf{x}_j). \tag{13.2.8}$$

This equation states that under the action of steady driving forces $F(x_j)$ the elastic structure will undergo a steady state vibration with a normal velocity amplitude distribution $\dot{W}(\mathbf{x}_\kappa)$ restrained by the loading of fluid-surface interaction given by the double surface integral. It is an *integral equation* in the unknown velocities $\dot{W}$. It may be solved under restricted conditions by being converted to a set of simultaneous algebraic equations which is then inverted. In favorable cases the influence Y is non-singular and has a nearly diagonal matrix representation. The solutions $\dot{W}(\mathbf{x}_\kappa)$ are then easily obtainable.

Thus the first approach in solving (13.2.1) and (13.2.3) has led to a single integral equation for obtaining normal velocities. Since the solution of integral equations tends to be tedious other procedures must be examined. A second approach is to retain the differential forms of (13.2.1) and 13.2.3) and formulate from them a pair of coupled differential equations in unknown velocities and unknown pressures, from which a deterministic solution can then be obtained. This approach is now described.

13.2a Continuum Equations of Plate-Fluid Interaction

When a vibrating elastic plate radiates sound into a fluid the plate motion and fluid motion are coupled. The acoustic field on the plate itself may be modelled on (13.2.1) using only the first (or monopole) term of (13.2.2) and 1.7.3:

$$\mathscr{L}_{p,p}p \equiv \nabla^2 p(\mathbf{x}_\perp,t) - \frac{1}{c^2}\frac{\partial^2 p}{\partial t^2}(\mathbf{x}_\perp,t) = -\rho_w \frac{\partial Q}{\partial t}(\mathbf{x}_\perp,t),\ \mathbf{x}_\perp = (x,y) \tag{13.2.9a}$$

Here $Q(\mathbf{x}_\perp,t)$ (units: $m^3s^{-1}m^{-3}$) is the local acoustic source strength of the plate, considered (as before) to be a collection of simple sources. If the normal velocity of the plate is $\dot{W}$, then $Q = \dot{W}\,\Delta S$ where ΔS is an area which is small relative to the acoustic wavelength being generated. The radiated field can also be written in terms of a velocity potential, ϕ, such that $p = \rho\dot{\phi}$; the result is,

$$\text{on surface } S: -\rho\nabla^2\dot{\phi} + \frac{1}{C^2}\rho\dddot{\phi} = \rho\,\Delta S\,\ddot{W} \tag{13.2.9b}$$

or

$$\nabla^2\phi - \frac{1}{C^2}\ddot{\phi} = -\Delta S\,\dot{W}$$

The displacement field of the plate is generated by the action of applied forces F_t. It is governed by a differential equation of the type,

$$\mathcal{L}_w \; W = F_E(\mathbf{x}_\perp, 0) - p(\mathbf{x}_\perp, 0) \tag{13.2.10}$$

in which p is the reaction force of the medium.

The coupling of (13.2.10) and (13.2.9) is made more visible by reducing them to operator form,

$$\begin{aligned} &\mathcal{L}_{p,p} p(\mathbf{x}_\perp, 0, t) = -\rho_n \Delta S \; \dot{W}(\mathbf{x}_\perp, 0) \\ &\mathcal{L}_w \; W(\mathbf{x}_\perp, 0, t) = F_E - \bar{p}(\mathbf{x}_\perp, 0, t). \end{aligned} \tag{13.2.11}$$

Our objective here is to discretize this pair of equations. To do this correctly requires a rigorous application of Hamilton's principle. This is discussed next.

13.2b The Discretized Acoustic Field

At a fluid field point where the acoustic pressure is $p(\mathbf{x})$ and the acoustic particle velocity is $\dot{\mathbf{u}}(\mathbf{x})$ the potential energy density ΔV and kinetic energy density ΔT are,

$$V = \frac{1}{2} \kappa p^2, \; \Delta T = \frac{1}{2} \rho_w \dot{u}^2 \tag{13.2.12}$$

in which κ is the compressibility and ρ_w the density of the medium. Since $p = \rho \dot{\phi}$ and $\dot{\mathbf{u}} = -\nabla \phi$, where ϕ is the velocity potential, it is seen that the global energy of the acoustic field over a finite volume $\mathcal{V}$ is,

$$E = T + V = \int \frac{1}{2} \left\{ \rho (\nabla \phi)^2 + \kappa \rho_w^2 \dot{\phi}^2 \right\} d\mathcal{V} \tag{13.2.13}$$

On the surface S of the volume $\mathcal{V}$ the work done per unit area by pressure p_s and displacement $\mathbf{u}$, is $p_s \mathbf{u}$. Since the pressure acts normal to the surface this work is done only by the normal component of displacement, W_s. Hence the global work done over surface S is

$$B = \int \rho \dot{\phi}_s \; W_s \, dS \tag{13.2.14}$$

Now according to Hamilton's principle the actual path followed by a dynamical process from time t_1 to time t_2 is given by the variation of an integral, namely,

$$\delta \int_{t_1}^{t_2} (V - T - B) \, dt = 0 \tag{13.2.15}$$

Hence

$$\delta J = \delta \int_{t_1}^{t_2} \left\{ \int \frac{1}{2} \left\{ \kappa \rho^2 \dot{\phi}^2 - \rho (\nabla \phi)^2 \right\} d\mathcal{V} - \oint \rho_w \dot{\phi}_s \, W_s \, dS \right\} dt = 0. \tag{13.2.16}$$

We desire to reformulate this principle in finite element form. The field $\phi(\mathbf{x}, t)$ will be discretized in finite elements by assuming that for each element a discrete representation in terms of shape functions ψ is possible for *acoustic* quantities.

$$\phi_{(e)}(\mathbf{x}, t) = \psi^{(e)^T}(\mathbf{x}) \cdot \phi_{(e)}(t) = \sum_N \psi_N^{(e)^T} \phi_{(e)}^N, \; N = 1, 2 \ldots . \tag{13.2.17}$$

(see Chapter 12 for discussion on finite elements) in which N is the number assigned to the nodal point in the fluid element, $\phi_{(e)}$ is a column matrix of nodal point values and $\psi^{(e)^T}$ is a transposed column matrix (=row matrix) of shape functions. The volume energy terms then appear as follows,

$$\text{potential energy: } V_e = \int \frac{1}{2} \kappa \rho_w^2 \dot{\phi}^T \dot{\phi}\, d\, \mathcal{V}_{(e)} = \frac{1}{2} \kappa \rho^2 \dot{\phi}_{(e)}^T \mathcal{U}\, \dot{\phi}_{(e)}$$

$$\mathcal{U} = \int \psi_{(e)}(\mathbf{x})\, \psi_{(e)}^T(\mathbf{x})\, d\, \mathcal{V}_{(e)} \tag{13.2.18}$$

$$\text{kinetic energy: } T_e = \frac{1}{2} \int \rho_w \nabla \phi^T \cdot \nabla \phi\, d\, \mathcal{V}_{(e)} = \frac{1}{2} \rho_w \phi_{(e)}^T \mathfrak{T}_e\, \phi_{(e)}$$

$$\mathfrak{T}_e = \int \nabla \psi_{(e)}(\mathbf{x}) \cdot \nabla \psi_{(e)}(\mathbf{x})^T\, d\mathcal{V}_{(e)}$$

Simularly the *elastic* displacement field $W(\mathbf{x},t)$ is also discretized in terms of shape functions $\eta(\mathbf{x}_\perp)$

$$w_{(e)}(\mathbf{x},t) = w_{(e)}(t)\quad \eta_{(e)}^T(\mathbf{x}_\perp) \tag{13.2.19}$$

where $\mathbf{x}_\perp$ is the location vector in the surface S of volume $\mathcal{V}$. (Note that η and ψ are generally different). Hence the work done by the surface pressure has the finite element representation,

$$B = \int \rho_w \dot{\phi}_{(e)}^T \psi_{(e)s}(\mathbf{x})\, \eta_{(e)}^T(x_\perp)\, w_{(e)}\, dS \tag{13.2.20}$$

$$= \dot{\phi}_{(e)}^T B_{(e)} w_{(e)} \rho_w$$

$$\mathbf{B}_{(e)} = \oint \psi_{(e)}(\mathbf{x})\, \eta_{(e)}^T(x_\perp)\, dS \tag{13.2.21}$$

in which

$$\psi_{(e)}(\mathbf{x}) = \psi_e(x_\perp, 0).$$

With these representations Hamilton's formulation in discretized form then may be reduced to the variational equation,

$$\delta \int_{t_i}^{t_2} \left\{ \frac{\kappa \rho^2}{2} \dot{\phi}_{(e)}^T \mathcal{U}_{(e)}\, \dot{\phi}_{(e)} - \frac{1}{2} \rho\, \phi_{(e)}^T \mathfrak{T}\, \phi_{(e)} - \rho\, \dot{\phi}_{(e)}^T \mathcal{B}_{(e)}\, w_{(e)} \right\} dt = 0 \tag{13.2.22}$$

[2] Now the variation in time is accomplished as follows,

$$\delta(\phi_{(e)}^T \phi_{(e)}) = 2\, \delta \phi^T \phi_e;\ \delta(\dot{\phi}_e^T w_{(e)}) = (\delta \dot{\phi}_{(2)}^T)\, w_{(e)} \tag{13.2.23}$$

Hence

$$\delta J = \int_{t_1}^{t_2} (\kappa \rho^2\, \delta \dot{\phi}^T \mathcal{U}_{(e)}\, \dot{\phi}_{(e)} - \rho\, \delta\, \phi_{(e)}^T \mathfrak{T}\, \phi_e - \rho\, \delta\, \dot{\phi}_{(e)}^T \mathcal{B}_{(e)}\, w_{(e)})\, dt = 0 \tag{13.2.24}$$

Integrating the first and third terms by parts, one obtains

$$\int_{t_1}^{t_2} \kappa \rho^2 \delta \dot{\phi}^T \mathcal{U}_{(e)}\, \dot{\phi}_{(e)}\, dt = \kappa \rho^2 \delta \phi^T \int_{t_1}^{t_2} \mathcal{U}\, \ddot{\phi}_{(2)}\, dt$$

$$\int \rho\, \delta\, \dot{\phi}_{(e)}^T \mathcal{B}_{(e)}\, w_e\, dt = \rho\, \delta \phi_{(e)}^T \int \mathcal{B}\, \dot{w}_{(e)}\, dt.$$

Thus (13.2.24) appears as,

$$\delta J = \int \delta \phi^T \left\{ \kappa \rho^2 \mathcal{U}_{(e)}\, \ddot{\phi}_{(e)} - \rho\, \mathfrak{T}_e\, \phi_{(e)} - \rho\, \mathcal{B}_{(e)}\, w_e \right\} dt = 0 \tag{13.2.25}$$

Since $\delta \phi^T$ vanishes at the end points t_1, t_2 and is other wise arbitrary the entity in the braces must vanish on each element. Differentiating (13.2.25) with respect to time yields

$$\kappa \rho_N^2 \mathcal{U}_{(e)}\, \ddot{\phi}_{(e)} - \rho_w \mathfrak{T}_{(e)}\, \dot{\phi}_{(e)} - \rho_w \mathcal{B}_{(e)}\, \dot{w}_{(e)} = 0 \tag{13.2.26}$$

Again, since $p = \rho_n \dfrac{\partial \phi}{\partial t}$, one has

$$\kappa \rho_w \mathscr{U}_{(e)} \ddot{\mathbf{p}}_{(e)} + \mathfrak{T} \mathbf{p}_{(e)} = \rho \mathscr{B}_{(e)} \ddot{\mathbf{w}}_{(e)} \tag{13.2.27}$$

in which $\mathbf{p}_{(e)}$ is the column matrix representing the set of nodal pressures on element e and $\ddot{\mathbf{w}}_{(e)}$ the set of nodal accelerations for elements on the surface S. Eq. (13.2.27) is the finite element form of the acoustic field on a single element. In subscript notation (repeated symbol j mean sum) the equation reads:

$$-\kappa \rho \, \mathscr{U}_{ij}^{(e)} \, \ddot{p}_{(e)}^{j} + \mathfrak{T}_{ij}^{(e)} \, p_{(e)}^{j} = \rho \, \mathscr{B}_{ij}^{(e)} \, \ddot{w}_{(e)}^{j} \quad \begin{matrix} i = 1, 2, \cdots N \\ j = 1, 2, \cdots N \end{matrix} \tag{13.2.28}$$

This is a set of i simultaneous differential equations, the first of which is seen to be,

$$-\kappa \rho \left\{ \mathscr{U}_{11}^{(e)} \, \ddot{p}_{(e)}^{(1)} + \mathscr{U}_{12} \, \ddot{p}_{(e)}^{(2)} + \cdots \right\} + \mathfrak{T}_{11}^{(e)} \, p_e^{(1)} + \mathfrak{T}_{12}^{(e)} \, p_e^{(2)} + \cdots$$

$$= \rho \, \mathscr{B}_{11}^{(e)} \, \dot{w}_{(e)}^{(1)} \, \rho \, \mathscr{B}_{12}^{(e)} \, \ddot{w}_{(e)}^{(2)} - \cdots \tag{13.2.29}$$

The remaining equations can be similarly constructed and have similar forms.

We require next the global form of these sets. According to (12.2.5) the global form is obtained by summing over all elements (i.e. sum over e). Now the global form of the pressure and acceleration at one local node j in terms of global nodes P^{Δ} and $\ddot{W}^{\Delta}$ are,

$$p_{(e)}^{j}(t) = \sum_{\Delta}^{D} \Omega_{\Delta}^{(e)j} \, P^{\Delta}(t), \quad \ddot{w}_{(e)}^{j}(t) = \sum_{\Delta}^{D} \Omega_{\Delta}^{(e)j} \, \ddot{W}^{\Delta}(t), \quad \Delta = 1, 2 \cdots D \tag{13.2.30}$$

Hence the global form of (13.2.27) is

$$-\sum_{e} \kappa \rho \, \mathscr{U}_{ij}^{(e)} \sum_{\Delta}^{D} \Omega_{\Delta_j}^{(e)} \, \ddot{P}^{\Delta}(t) + \sum_{e} \mathfrak{T}_{ij}^{(e)} \sum_{\Delta}^{D} \Omega_{\Delta}^{(e)j} \, P_{(t)}^{\Delta} = \rho \sum_{e} \mathscr{B}_{ij}^{(e)} \sum_{\Delta}^{D} \Omega_{\Delta}^{(e)j} \, \ddot{W}^{\Delta}(t) \tag{13.2.31}$$

[3] This is the ith equation of a set of Δ equations, $\Delta = 1, 2 \ldots D$. To elucidate the counting procedure we suppose there is a volume V that is discretized into 20 paralleopipeds with 8 nodes each, giving 160 local nodal points; and suppose further there are 50 global nodal points in the entire volume. There will then be 160 equations in the independent unknown $p_{(e)}^{j}$, $\ddot{w}_{(e)}^{j}$, of which only 50 will be independent in the unknown P^{Δ}, $\ddot{W}^{\Delta}$. To solve we must use the global set of $D = 50$ equations.

Clearly the number of equations, (counted either in terms of local field or global field) is only one half of the total required since both pressure and velocity are unknown. Hence (13.2.29) or (13.2.31) is one of a pair of sets of coupled equations which supply half of equations needed. The second set is provided by the discretization of the elastic equations of motion. This is discussed in the next section.

13.2c The Discretization of the Elastic System (Dynamic Bending of Plates).

We consider the radiating surface to be a thin isotropic elastic plate, thickness h, density ρ_s driven by an external force density F_E (units: Nm^{-2}) and restrained on one side by a water load which imposes a load pressure on its motion. The equation governing the normal component of displacement $w(\mathbf{x},t)$ in Cartesian coordinates is:

$$\mathscr{L}_w\, w = F_E - p \tag{13.2.32}$$

$$\mathscr{L}_w = \mathscr{M}_w + \mathscr{K}_w;\ \mathscr{M}_w = \rho_s\, h\, \partial^2/\partial t^2;\ \mathscr{K}_w = d\left(\frac{\partial^4}{\partial x^4} + \frac{\partial^4}{\partial x^2 y^2} + \frac{\partial^4}{\partial y^4}\right)$$

$$d = \frac{E\,h^3}{12\,(1-\nu^2)},\ E = \text{Young's Modulus},\ \nu = \text{Poisson's Ratio}$$

Following the procedures outlined above in the discretization of the acoustic equation we can discretize the above equation for each element of the plate:

$$\rho_s\, h\, \mathscr{M}_{(e)}\, \ddot{\mathbf{w}}_e + d\, \mathscr{K}_{(e)}\, \mathbf{w}_{(e)} = \mathbf{F}_{(e)} + \mathscr{B}^T_{(e)}\, \mathbf{p} \tag{13.2.33}$$

The structure of $\mathscr{M}, \mathscr{K}, \mathscr{B}^T$ is discussed in Sections 12.5, 12.5a, 12.5b. Here $\mathbf{F}_{(e)}(t)$ is discretized by use of the *elastic* shape function. Assuming a (normal) applied force $F_m(\mathbf{x},t)$ one has

$$\mathbf{F}_{(e)}(t) = \int F_m(\mathbf{x},t)\, \eta_{(e)}(\mathbf{x}_\perp)\, dS(\mathbf{x}).$$

In global terms,

$$F^{(j)}_{\{e\}} = \sum_{\Delta}^{D} \Omega^{(e)\,j}_{\Delta}\, F^{\Delta}$$

(See Sect. 12.4). In global form, the discretized equation appears as:

$$\sum_{e}^{E} \rho_s\, h\, \mathscr{M}^{(e)}_{ij} \sum_{\Delta}^{D} \Omega^{(e)\,j}_{\Delta}\, \ddot{W}^{\Delta} + \sum_{\Delta}^{D} d\, \mathscr{K}_{ij}\, \Omega^{(e)\,j}_{\Delta}\, W^{\Delta} = \sum_{e}^{E} \sum_{\Delta}^{D} \Omega^{(e)_i}_{\Delta}\, F^{\Delta}$$

$$+ \sum_{e}^{E} \mathscr{B}^{(e)^T}_{i_j} \sum_{\Delta}^{D} \Omega^{(e)_j}_{\Delta}\, P^{\Delta},\ i = 1, 2, \ldots N,\ j = 1, 2, \ldots N \tag{13.2.34}$$

This equation is a set of D independent equations in the unknown global nodal parameters (pressure P^{Δ} and displacement W^{Δ}). It will be used as a second set of a pair of coupled equations which describe the vibration of plates in the presence of a water load.

13.2d The Coupled Set of Discretized Equations of a Vibrating Plate in a Fluid

We now write (13.2.31) and (13.2.34) as a coupled pair, applicable to the surface S. We assume that on the surface the number of local nodes N and the global nodes D are the same for both plate and fluid. Thus, on the surface S, the discretized coupled pair of equations is:

$$(a)\ \rho_w \sum_{e=1}^{E} \sum_{j=1}^{N} \mathscr{B}^{(e)}_{ij} \sum_{\Delta}^{D} \Omega^{(e)\,j}_{\Delta}\, \ddot{W}^{\Delta}(t) + \sum_{e=1}^{E} \sum_{j=1}^{N} \mathfrak{T}_{ij} \sum_{\Delta}^{D} \Omega^{j}_{\Delta}\, P^{\Delta}(t)$$

$$- k\,\rho \sum_{e}^{E} \sum_{j=1}^{N} \mathscr{U}_{ij} \sum_{\Delta=1}^{D} \Omega^{j}_{\Delta}\, \ddot{P}^{\Delta}(t) = 0$$

$$(b)\ \rho_s\, h \sum_{e}^{E} \sum_{j=1}^{N} \mathscr{M}_{ij} \sum_{\Delta}^{D} \Omega^{(e)\,j}_{\Delta}\, \ddot{W}^{\Delta}(t) + \sum_{e}^{E} \sum_{j}^{N} \mathscr{B}^{T}_{ij} \sum_{\Delta}^{D} \Omega^{j}_{\Delta} P^{\Delta}(t) + d \sum_{e}^{E} \sum_{j=1}^{N} \mathscr{K}_{ij}\, \Omega^{j}_{\Delta}\, W^{\Delta}(t)$$

$$= \sum_{e}^{E} \sum_{\Delta}^{D} \Omega^{(e)\,i}_{\Delta}\, F^{\Delta}(t),\ i = 1, 2, \ldots N \tag{13.2.35}$$

Here the total number of local nodes is $E \times N$. The total number of global nodes is D. The pair of equations constitute a set of $2\,E \times N$ equations in the $2\,E \times N$ unknown local nodal pressures $p^{j}_{(e)}$, and nodal displacements $w^{j}_{(e)}$, and a set of $2D$ equations in the $2D$ unknown global nodal pressures P^{Δ} and nodal displacement W^{Δ}.

The latter must also satisfy the (surface) boundary condition

$$\frac{\partial P^{\Delta}}{\partial n} = -\rho \frac{\partial^2 W^{\Delta}}{\partial t^2}$$

while P^{Δ} itself must satisfy the Sommerfeld radiation condtion at infinity.

Clearly, to solve these sets of equations requires a complete calculation of matrix elements $\mathcal{B}_{ij}$, $\mathfrak{T}_{ij}$, $\mathcal{U}_{ij}$, $\mathcal{M}_{ij}$ and $\mathcal{K}_{ij}$. These are directly obtainable from the appropriate selection of the shape functions $\psi^{j}_{(e)}(\mathbf{x})$ and performance of the required integrations (13.2.18, 13.2.21). While the discretized set of equations appear complicated they can be reduced to a set of algorithms for easy calculations on a digital computer.

In applications to piezoelectricity the additional equation 13.1.1a is required. We first write the constitutive relation for the piezoelectric field. There are four sets of such relations [4]. We choose for illustrate purposes the set in which strain S and electric field E are the independent variables, and stress T and electric displacement flux D are the dependent variables,

$$(a)\ T_i = C^{E}_{ij}\, S_j - e_{mi}\, E_m$$
$$(b)\ D_m = e_{mi}\, S_i + E^{S}_{m\kappa}\, E_{\kappa}. \tag{13.2.36}$$

It is most convenient in particular cases to consider one component of each field at a time. Let this be the 3-component ($x = 1,\ y = 2,\ z = 3$). Thus the stress due to E_3 alone is

$$T_3 = -\, e_{33}\, E_3 \tag{13.2.37}$$

and the force (per unit volume) in the 3-direction is,

$$\frac{\partial T_3}{\partial z} = -\, e_{33} \frac{\partial E_3}{\partial z}. \tag{13.2.38}$$

Assume that we can construct an orthonormal (dimensionless) shape function $\zeta_{\lambda}(\mathbf{x})$ and let the applied electric field be $E_3(\mathbf{x},t)$ where $\mathbf{x} = (x,y,z)$. Then we can expand this function,

$$E_3(\mathbf{x},t) = \sum_{n} E^{N}_{3}(t)\, \zeta_n(\mathbf{x})$$
$$E^{N}_{3}(t) = \frac{1}{V} \int E_3(\mathbf{x},t)\, \zeta_n(\mathbf{x})\, d\mathbf{x} \tag{13.2.39}$$

The energy generated by the force 13.2.38 acting in the 3-direction on an element e of the surface is,

$$E_3 = \frac{-e_{33}}{2\,V} \frac{\partial E_3}{\partial \zeta}(\mathbf{x},t)\, w(x,t)$$
$$E_3 = \frac{-e_{33}}{2\,V} \sum_{M,N} \int E^{N}_{3_{(e)}}(t) \frac{\partial \zeta^{N}_{(e)}}{\partial z}(\mathbf{x})\, \eta^{M}_{(e)}(\mathbf{x})^{I}\, w^{M}_{(e)}(t)^{I}\, d\,V(\mathbf{x})$$

$$E_3 = \frac{-e_{33}}{2} \sum_{M,N} E_{3(e)}^{N(t)} \Lambda_{MN} w_{(e)}^{M}(t) \tag{13.2.40}$$

where

$$\Lambda_{NM} = \frac{1}{V} \int \frac{\partial \zeta_{(e)}^{N}}{\partial z}(\mathbf{x}) \eta_{(e)}^{M}(\mathbf{x})^{T} d\mathscr{V}(\mathbf{x}). \tag{13.2.41}$$

Thus the force per unit volume at the N'th node of element e due to the applied field E_3 is

$$F_{(e)}^{N}(t) = -e_{33} E_{3(e)}^{M}(t) \Lambda_{NM}. \tag{13.2.42}$$

Now the global force at the N'th node is

$$F_{(e)}^{N}(t) = \sum_{\Delta}^{D} \Omega_{\Delta}^{(e)N} F_{(e)}^{\Delta}(t) \tag{13.2.43}$$

These are the forces that appear on the right hand of 13.2.35.

13.3 HELMHOLTZ INTEGRAL REPRESENTATION OF THE ACOUSTIC INTERACTION PRESSURE

In (13.2.10) the acoustic interaction pressure is modeled by an equation that assumes the radiating source is acoustically a collection of simple sources. This representation is adequate for many cases where the radiation is into half space, a condition which allows a special choice of Green's function G. However, when the fluid medium surrounds the source completely it is more convenient to represent the interaction pressure by the Helmholtz integral formulation (Chapter I). For simplicity we take the steady state formulation of this integral for further discussion. Thus, in the absence of volume distributed sources, and considering only the steady state, 1.7.7 becomes:

$$p(\mathbf{x}_{\perp},0) = \oint [G_{\omega}(\mathbf{x}_{\perp}|\mathbf{x}_{\Omega}) \frac{\partial p}{\partial n}(\mathbf{x}_{\Omega,0}) - p(\mathbf{x}_{\Omega,0}) \frac{\partial G_{\omega}}{\partial n}(\mathbf{x}_{\perp}|\mathbf{x}_{\Omega})] d S_0 \tag{13.3.1}$$

in which G is no longer a special (i.e. a half space G) but is rather a general acoustic Green's function (see Chapter III).

This formula states that the pressure at any surface point on the source is due to a collection of existing *simple* sources (=first term) distributed over the surface plus a collection of existing dipole sources (=second term) also distributed over the surface. Actually the force driving the source-fluid system is the set of external forces F_E (see Eqs. (13.2.10a). Thus the interface pressures described by (13.3.1) are *reflections* from one surface location to another, of the sound field created by F_E. The representation of these pressures as originating from collections of simple sources and dipole sources distributed over the producting surface has the same physical meaning as that which appears in the propagation of light by summation of Huygens wavelets, in which an optical wavefront is treated as being generated from a previous wavefront through summation of elementary (source) wavelets. The Helmholtz formula (13.3.1) is now inserted into the equation of vibration (3.2.11), so that the balance of forces becomes,

$$L_w W(\mathbf{x}_{\perp,0}) + i\omega\rho \oint G_{\omega}(\mathbf{x}_{\perp}|\mathbf{x}_{\Omega}) \dot{W}(\mathbf{x}_{\Omega,0}) dS(\mathbf{x}_{\Omega}) + \oint p(\mathbf{x}_{\Omega}) \frac{\partial G_{\infty}}{\partial n}(\mathbf{x}_{\perp}|\mathbf{x}_{\Omega}) dS_0 = F_t. \tag{13.3.2}$$

If the general Green's function is used (meaning that $\partial G/\partial n \neq 0$) this equation is seen to couple pressure $p(\mathbf{x}_\Omega)$ and velocity $\dot{W}(\mathbf{x}_\Omega)$. Since both appear as unknowns an additional equation 13.2.1 is required, to obtain a solution for the displacement W. The more complicated expression for the pressure given by (13.3.1) has also a finite element representation. Choosing shape functions ψ to represent the spatial dependence of *both* unknowns, one has

$$p(\mathbf{x}_\perp) = \boldsymbol{\psi}^T_{(e)}(\mathbf{x}_\perp)\, \mathbf{p}_{(e)}(t) \tag{13.3.3a}$$

$$\dot{W}(\mathbf{x}_\perp) = \boldsymbol{\psi}^T_{(e)}(\mathbf{x}_\perp)\, \dot{\mathbf{w}}_{(e)}(t) \tag{13.3.3b}$$

in which $\mathbf{p}_{(e)}$ and $\dot{\mathbf{w}}_{(e)}$ are the pressure and velocity at the nodes of the elastic surface in its finite element representation. (13.3.1) can thus be written in the abbreviated form,

$$\mathbf{A}\, \mathbf{p}_{(e)}\, t = \mathbf{B}\, \dot{\mathbf{w}}_{(e)}(t) \tag{13.3.4a}$$

where the vectors **A**, **B** at point $\mathbf{x}_\perp$ have the matrix components,

$$A_j(\mathbf{x}_\perp) = \psi_j(\mathbf{x}_\perp) + \int \psi_j(\mathbf{y}_\perp)\, \frac{\partial G}{\partial n(\mathbf{y}_\perp)}(\mathbf{x}_\perp|\mathbf{y}_\perp)\, dS(y_\perp) \tag{13.3.4b}$$

$$B_j(\mathbf{x}_\perp) = -\, i\omega\rho \oint \psi_j(\mathbf{y}_\perp)\, G_\omega(\mathbf{x}_\perp|\mathbf{y}_\perp)\, dS(\mathbf{y}_\perp) \tag{13.3.4c}$$

By choosing the number of points $\mathbf{x}_\perp$ and the number of nodes j to be the same one can solve (13.3.4a) in the sense that

$$\mathbf{p}_{(e)}(t) = \mathbf{A}^{-1}\, \mathbf{B}\, \dot{w}_{(e)}(t) \tag{13.3.5}$$

The global form for the bending of a water-loaded plate can then be obtained from (13.2.34) by replacing the last term with (13.3.5) in global form. This is,

$$\sum_e^E \left\{ \rho_s h\, \mathcal{M}^{(e)}_{ij} \sum_\Delta^D \Omega^{(e)\,j}_\Delta\, \ddot{W}^\Delta_{(t)} + \sum_\Delta^D d\, \mathcal{K}_{ij}\, \Omega^{(e)\,2}_\Delta\, W^\Delta_{(t)} - \mathcal{B}_{ij}\, A_j^{-1} B_K \sum_{\Delta^D} \Omega^{(e)\,k}_\Delta\, \dot{W}^\Delta_{(t)} \right\}$$
$$= \sum_e^E \sum_\Delta^D \Omega^{(e)\,l}_\Delta\, F^\Delta(t) \tag{13.3.6}$$

(Note the inclusion of B_j which is required in a "consistent" formulation of the work done by the boundary pressures against the boundary motion). This is a set of D nodal equations in the global displacements W^Δ. Since the driving forces F are assumed known, and since the number of equations equals the number of unknowns this equation can be solved for W^Δ. From known W^Δ the calculation of the field pressure can be obtained by application of 13.3.1 through use of 13.3.5 choosing the field point **x** to be in the medium rather than on the surface.

Eq. 13.3.5 is modeled as one component (namely the normal W) of the three equations (U, V, W) of 13.1.2a. If the full vector equation given by 13.1.2a is to be used then the pressure p in the term $L_{u,p}\, p$ must be related only to the normal velocity $\dot{W}$. Now if the unit vector **n** is the normal to the surface, then

$$W = \mathbf{u} \cdot \mathbf{n} \tag{13.3.7}$$

From (13.2.19) the finite element representation of W is $w_{(e)}(t)\, \eta^I_{(e)}(x_\perp)$. If we assume that the shape functions for the solid are given by 13.2.17 then

$$\dot{w}_{(e)} \eta^T_{(e)}(\mathbf{x}_\perp) = \psi^{(e)\,I}(\mathbf{x}_\perp)\, \mathbf{n}(\mathbf{x}_\perp) \cdot \dot{\mathbf{u}}_{(e)}(\mathbf{x}_\perp)$$

or

$$\dot{w}_e(t) = j\omega(\eta_{(e)}^T)^{-1}(\mathbf{x}_\perp)\,\psi^{(e)T}(\mathbf{x}_\perp)\,[\mathbf{n}(x_\perp)\cdot\mathbf{u}_{(e)}(\mathbf{x}_\perp)]. \tag{13.3.8}$$

This form of surface displacement can now be used in the finite element representation of 13.1.2 which contemplates the calculation of three components of displacement at each nodal point of the surface.

Summary: The formulas derived an discussed in this last section complete the formulation of a finite element representation of radiating surfaces and acoustic solid-fluid interactions. The continuum analysis, upon which the finite element representation is based leads to either a single integral equation (13.2.8) in displacement, or a set of differential equations which couple cascaded power systems (13.1.1). In all cases the number of simultaneous finite element equations (3.2.35), (13.3.6) are quite large so that a premium must be placed on devising procedures and choosing surfaces such that the relevant matrices ($\mathcal{M}_{ij}$, $\mathcal{K}_{ij}$, etc.) are symmetric, banded, and non-singular. Other finite element representations are possible. One of these that has achieved some prominence is discussed next.

13.4 THE FLUID-SOLID AS ONE (COMPOSITE) CONTINUUM

An alternative method in formulating the mathematical description of the fluid-solid interaction is to consider the two power systems, structure and fluid, to act as a single composite elastic system in which the components differ from each other only in the specification of their material properties. When this composite system is decomposed into finite elements the fluid elements (parallelepipeds, tetrahedrons, etc.) are assigned three components of displacement to each node, plus their associated forces. The concept of a finite fluid element is then developed as an isotropic elastic substance which obeys the same equation of motion (13.2.3) as the solid with one significant change, viz. in the fluid element the shear modulus μ is taken to be negligibly small. Thus 13.2.3 of fluid vibration in the absence of applied forces reduces to the simple form,

$$C^2\nabla^2\mathbf{u} = \ddot{\mathbf{u}}, \quad C^2 = \lambda/\rho, \quad u = (u, v, w). \tag{13.4.1}$$

By comparison with the acoustic wave equation it is readily seen that the "Lamé constant λ" for the fluid is ρC^2. With these choices of the material constants λ, μ one proceeds to construct the mass and stiffness matrices of the solid-fluid composite in the conventional way and to formulate the finite-element equations of motion by methods of Chap. 12.

The use of finite elements of displacements requires special attention to the fluid-solid interface with respect to conditions at the nodes. Two options are available: in the first the nodes of the fluid element are identical with those of the solid element, as if welded together, making both normal and tangential motions the same across the interface. In the second the solid and fluid finite elements have different nodal structures. In this case one sets the (internal) requirement that normal components of motion are equal across the interface, but the tangential motions are independent (i.e. there is fluid slippage). Comparison calculations have been made between these two options[5]. They show that a model based on "welded" nodes differs little from a model based on tangential slippage of the fluid on the solid.

The fluid-solid composite model raises a difficulty peculiar to itself, namely the necessity of terminating the composite by an imaginary boundary to limit the number of fluid elements

that must be constructed. On this boundary one is then required to find the distribution of pressure and velocity which can be used subsequently to calculate the radiation anywhere in the medium beyond by use of the Helmholtz integral equation. Termination of the composite is discussed next.

13.4a Termination of the Solid-Fluid Composite

The problem of effectively terminating the solid-fluid composite in space is both geometrical and acoustical. The geometric problem is this: no matter what the shape of the sound source, it is required to choose a composite shape of source plus fluid medium such that its terminating surface permits calculation of radiation in a convenient way. The usual choices of composite shapes are rectangular parallelepipeds, cylinders, or spheres. The acoustic problem is twofold: first, the relation between pressure and velocity on the terminating surface must be such that the surface coordinates allow analytically simple relation to be established between them. A simple way of doing this is to arbitrarily fix the specific acoustic impedance of the terminating surface so that pressure and particle velocity are related by the specific acoustic impedance z, $p = z\,\dot{W}$, or alternately, to expand both pressure and velocity in orthogonal functions (say spherical wave functions) and relate them by acoustic formulas. A second acoustic problem is the proper selection of the size of finite element of fluid between the solid-fluid interface and the terminating boundary to avoid element resonance. These problems will now be taken up.

A simple procedure for establishing a convenient relation between pressure and velocity on the terminating surface is to place this surface at such a distance that one can assume a purely dissipative boundary on which the specific acoustic impedance is ρc. Here there is only one component of velocity, namely normal to the terminating surface, corresponding to which the associated acoustic pressure is $\rho\, c\, \hat{W}$. Thus upon solving for the pressure distribution throughout the interior of the fluid-solid composite one is simultaneously required to satisfy the boundary condition of a fixed impedance. Beyond the (imaginary) boundary the condition of dissipative impedance holds. The distance of the imaginary boundary where ρc begins from the solid-fluid interface is estimated at 1 to 1½ wavelengths of the radiating frequency.

An alternative procedure for terminating a solid-fluid interface is to surround the vibrating solid with an imaginary sphere of fluid just large enough to envelope the solid. Solution of the wave equation in the solid-fluid composite then leads to a list of pressures and particle velocities at the nodal points of the imaginary spherical boundary surface. Next one chooses a finite set of (orthogonal) spherical wavefunctions which interpolate between these nodal values transforming the pressure and velocity of the imaginary surface into continuous functions, at the price of a known error because of the finite number of the interpolation set. Following this transformation the radiation of the sound from the imaginary boundary to any field point is calculated by use of the Helmholtz integral formula 13.3.1 using a continuum representation in spherical wave functions.

The third problem of choosing element size is that of avoiding resonance effects in the composite volume. It is solvable if the shape of the finite element of fluid and its size relative to the radiating wave-length is known. Here one applies the classical theory of resonance vibration of solids to serve as a guide in the selection of size.

Experience has shown that the numerical problems posed in this section can be solved satisfactorily by use of sufficiently large computers. Thus in most cases the steady state radiation of a vibrating surface in the low frequency range can be calculated. There remains yet to make brief mention of unsteady, i.e. transient, radiation.

13.5 TRANSIENT RADIATION FROM A VIBRATING FLUID-SOLID INTERFACE

The solution of 13.2.35 yields a finite set of global nodal displacements W^Δ over the radiating surface. The field of normal displacement is effectively digitized by the finite element technique. This digitization is in the steady state so that one writes $W^\Delta = W^\Delta(\omega)$.

Similarly the global nodal pressures $P^\Delta(\omega)$ are also found by solution of 13.3.35. With W^Δ and P^Δ known on the surface of the radiator one can use several techniques to find the corresponding transient radiation. The simplest of these, at least in a conceptual sense, is the inverse Fourier transform. The transient displacement at each surface node, and the transient pressure, are given by the vector formulas,

$$\boldsymbol{W}(t) = \int_{-\infty}^{\infty} \boldsymbol{W}(\omega) e^{i\omega t} \frac{d\omega}{2\pi} \tag{13.4.2}$$

$$\boldsymbol{P}(t) = \int_{-\infty}^{\infty} \boldsymbol{P}(\omega) e^{i\omega t} \frac{d\omega}{2\pi} \tag{13.4.3}$$

in which

$$\mathbf{W}(\omega) = (W^1, W^2, \ldots W^\Delta \ldots W^D)$$

$$\mathbf{P}(\omega) = (P^1, P_2, \ldots P^\Delta \ldots P^D).$$

These integrals can be numerically evaluated by use of the computer programs based on the Fast Fourier Transform. The transient radiation due to these surface conditions is similarly found by first calculating the field pressure from 13.3.1, transforming it in the same manner as with surface pressures.

13.6 EXAMPLES OF CALCULATION OF RADIATON BY FINITE ELEMENTS

The method of calculations radiating fields, radiation loading and source transducer performance by use of finite elements, has been carried out by several authors. A brief bibliography is found at the conclusion of this chapter. We note in particular the work of Smith et al [6]. Using equations analogous to 13.2.35, 13.2.36 thru 13.2.42, these authors applied the method to piezoceramic sources of spherical and (finite) cylindrical shape. Figure 13.6.1 shows the finite element model of a piezoceramic sphere made of radially-poled leadzerconate-lead titanate ceramic. Here the sphere is sliced through the center to give a short axisymmetric cylinder (along the y-axis), on which each finite element is modeled as a curvilinearr prism of triangular cross-section and short length. Each element has 6 nodes and each node three degrees of freedom (r, z displacement, and electric potential). The dynamic resonance of the entire sphere is accounted for by judicious use of spherical symmetries. Under the forces created by the driving radial elastic field the radial displacement was calculated with use of equations analogous to 13.2.35. Then the electric current was found from 13.2.36b. From the applied voltage and calculated current one then predicted the electrical impedance. A comparison of predicted and measured in-water electrical impedance is shown in Fig. 13.6.2.

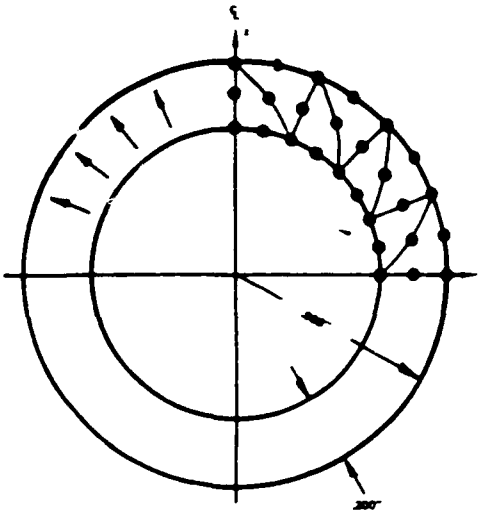

Fig. 13.6.1. Cross section of a hollow piezoelectric sphere showing finite element idealization (six-node triangles). (After [6])

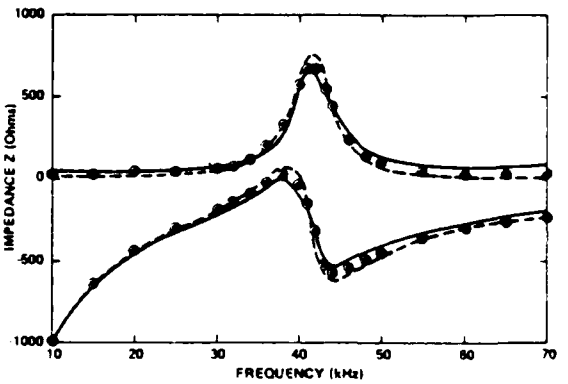

Fig. 13.6.2. In-water complex impedance plot of piezoelectric sphere. Solid line is experimental, dashed line is model not including material losses, and circles are from model which includes material losses via complex material parameters. Upper curves are Re(z), lower are Im(z). (After [6])

A second example calculated by [5] was that of a free-flooded piezoceramic cylinder 5.00 inches high, 15.25" in diameter and 1.15 inches thick, made up of material similar to ceramic B. It consisted of 32 staves tangentially poled in alternating directions, with the area between staves being silvered. The finite element is modeled as a "curved-face cube" (= isoparametric hexahedron) with eight nodes, each node having four degrees of freedom (displacement in x, y, z and electric potential). Figure 13.6.3 shows the radiating source. Upon being driven by a force due to the applied electrical potential the acoustic pressure field was determined by use of methods analogous to those of Sec. 13.3 at a point one meter from the cylinder on the plane of axial symmetry. This is the predicted transmitting voltage response. A comparison of measured and predicted response is shown in Fig. 13.6.4. In this figure the "fine model" had twice as many finite elements per unit volume as the "coarse model". In addition, using the far-field representation of the free-field Green's function (see Chap. I, of the treatise) and again applying the methods of Sec. 13.3, one obtains a directivity pattern of radiated sound. Figure 13.6.5 shows the vertical beam pattern of the free-flooded cylinder obtained by [5] using these finite element techniques.

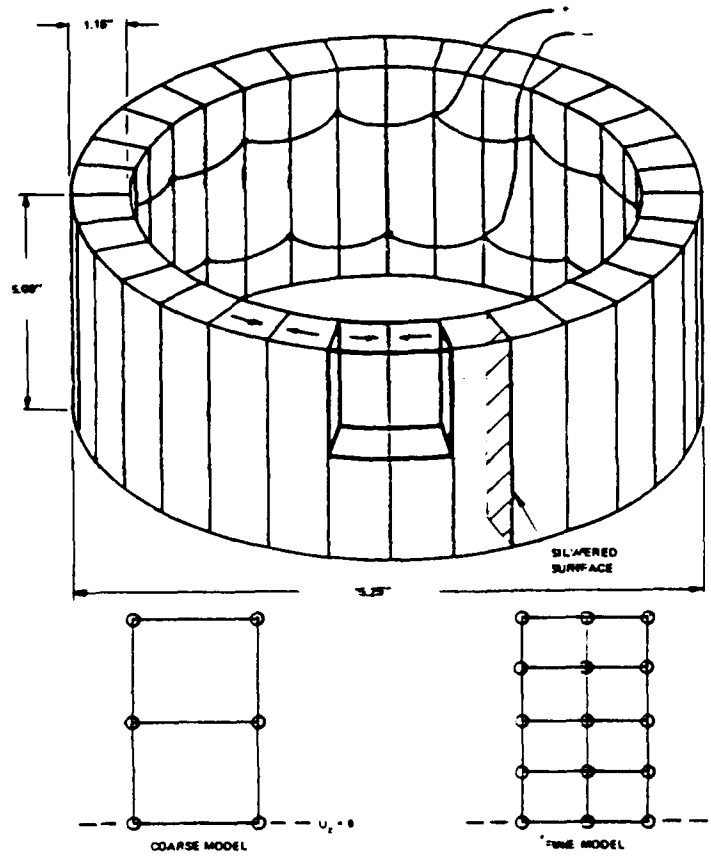

Fig. 13.6.3. Free-flooded cylinder showing direction of polarization (arrows) in each stave and silvered surfaces. Only volume in bold outline need be modeled. (After [6]).

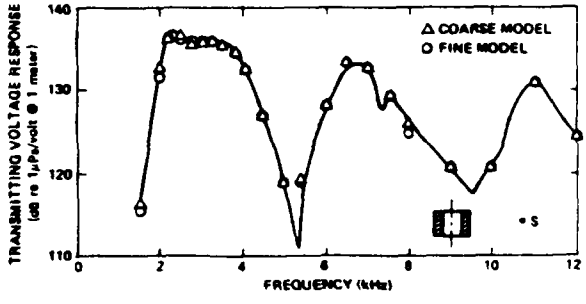

Fig. 13.6.4. Transmitting voltage response of free-flooded cylinder measured at point *S*. Solid line is experimental and points are from coarse or fine model as indicated. (After [6])

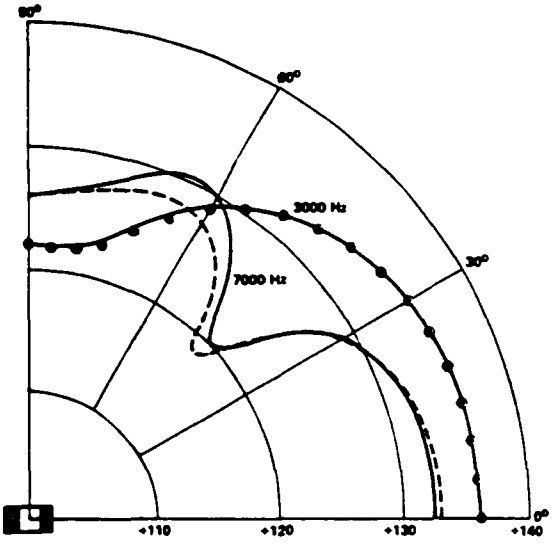

Fig. 13.6.5. Vertical beam pattern of free-flooded cylinder at 3000 Hz (primarily breathing and 7000 Hz (primarily bending). Solid lines are experimental, and dashed line and circles are from fine model. Scale is in decibels *re* 1 μPa/V @ 1 m. (After [6]).

The examples described above show good agreement between prediction and experiment. However, in application of the method of finite elements there are two sources of error: one is the finite element idealization of the geometry of the radiating surface and the second is the assumed interpolation (= shape) function for the acoustic pressure on the surface. A good measure of the error associated with these approximations is the magnitude of the off-diagonal matrix elements of the surface mass matrix. These elements vanish as the number of nodal points goes to infinity and the surface area of the finite element model facing the medium tends to zero. Other sources of error are the inaccuracy of pizoceramic material parameters (particularly the loss factors near resonance) and errors in measurement on physical models.

REFERENCES

1. P.M. Morse, H. Feshbach "Methods of Theoretical Physics," McGraw-Hill, 1953, p. 1776.

2. J.T. Oden "Finite Elements of Nonlinear Contenica," McGraw-Hill, New York, 1972, p. 153.

3. Ref. [1], p. 181.

4. "Ultrasonic Transducer Materials" Ed. O.E. Mattiat, Plenum Pres, N.Y.(1971) p. 64.

5. U.S.A. Dept. of Defense Document SVM-10 "Shock and Vibration Computer Programs," 1975, p. 405.

6. R.R. Smith, J.T. Hunt, D. Barach "Finite element analysis of acoustically radiating structures with application to sonar transducers," JASA **54**, 1277-1288 (1973).

BIBLIOGRAPHY

1. J.T. Hunt, M.R. Knittel, C.S. Nichols, and D. Barach "Finite Element Approach to Acoustic Scattering from Elastic Structures," JASA **57**, 287-299 (1973).

2. F.M. Henderson "Radiation Impedance Calculations with the X-Wave Computer Program," NRSDC Report No. 4033, 1973.

3. O.C. Zienkiewski and R.E. Newton, "Coupled Vibrations of a Structure Submerged in a Compressible Fluid," ISD-ISSC Proceedings on Finite Element Techniques," U. of Stuttgart, Germany, 1969.

4. J.L. Hunt, M.R. Knittel, and D. Barach "Finite Element Approach to Acoustic Radiation from Elastic Structures," JASA **55**, 269-280.

5. H. Allik and T.R. Hughes "Finite Element Method for Pizoelectric Vibration," Int. J. Num. Methods in Engineering **2**, 151-157 (1970).

CONCLUSIONS

The finite element technique for calculating *both* the surface deformation and the fluid interaction has been outlined in this chapter. This technique leads to a large number of simultaneous differential equations which are convertible to an equal number of algebraic equations by assignment of finite element shape functions and subsequent calculation of mass, stiffness and interaction matrices. The analysis thus directly leads to implementation of these solutions on large digital computers.

CHAPTER XIV
FINITE AMPLITUDE RADIATION BY USE OF PARAMETRIC ARRAYS

14.1 INTRODUCTION

The acoustic parametric transmitting array of active radiating sources transforms acoustic radiation at high frequency from a real plane or curved vibrating surface into equivalent end-fire radiation at low frequency from a fictitious end-fire array of virtual sources in the medium. This transformation is achieved by causing the actual radiating surface to radiate two spatially overlapping beams called primaries, one at frequency f_1, and the second at frequency f_2 (or one at a narrow band of frequencies centered on f_1 and the second at a narrow band of frequencies centered on f_2), at sufficiently high radiation intensity to force the medium to react elastically in a nonlinear way to the applied acoustic pressures. As a result of nonlinear mixing there appears in the region of overlap in the medium (called the zone of interaction) a new family of frequencies called intermodulation frequencies: the sum frequency $f_1 + f_2$, the difference frequency $f_1 - f_2$, and harmonics nf_1, nf_2 $n = 2, 3 \ldots$. Since the zone of interaction is usually long relative to the wavelengths of the intermodulation frequencies, the radiation generated by it is highly directional, even at the difference frequency, in spite of the fact that its wavelength may be quite large relative to the wavelength of the primaries that generated it. In application, the primaries and higher frequency intermodulations are absorbed in the medium long before the differency frequency component, leaving the latter the only survivor at great distances. In this way low frequency radiation is created directly from high frequency sound sources. When properly designed the radiation pattern of this low frequency sound exhibits no side lobes. This condition is caused by the exponential absorption of the primaries in the medium as they travel outward along the zone of inter-action creating a virtual end-fire array with an exponentially decreasing amplitude shading, correctly phased for constructive summation. The narrow beamwidth of this secondary wave field pattern is available not only at the single difference frequency of creation but is also available over a broadband of frequencies because, while the primaries may be generated by narrow band transducers with passband frequencies $f_1 \pm \Delta f_1$, and $f_2 \pm \Delta f_1$ corresponding to a mechanical $Q = (f_1 + f_2)/4\Delta f_1$, the secondary has a pass band $f_1 - f_2 \pm \Delta f_1$, corresponding to a mechanical Q of $(f_1 - f_2)/2\Delta f_1$. The ratio of secondary Q to primary Q is therefore approximately $2(f_1 - f_2)/(f_1 + f_2)$, which can be made quite small. This broadband feature together with narrow beam radiation are very advantageous in applications that demand these requirements to be available at low frequencies. However, the advantage is offset by the very low acoustic radiation efficiency which accompanies the conversion of the energies of the primaries into the energy in the secondary. This efficiency is generally less than one percent, although special designs have achieved efficiencies of some six percent. There is evidence that potentially higher efficiencies are possible.

14.1a ZONE OF INTERACTION IN VARIOUS MODELS

Analysis of parametric acoustic radiators has not to date yielded a unique model. Different experimental conditions lead to different models. The basic assumption in constructing a model is the location and extent of the zone of interaction. In the first (and best understood) Westervelt model [1] the zone of interaction is generated by two very narrow collinear pencil beams of relatively weak signals so that the vertical end-fire array in the medium is limited by absorption to the near field. This model does not apply to the sonar case where the acoustic radiation of the primaries is strong and the zone of interaction extends into the far field. A second model is that of Mellen and Moffett [2] in which the zone of interaction is again the nearfield, this time generated by strong primaries but limited to the Rayleigh distance R_0 by acoustic saturation of the medium. (See Sect. 1.13 of this treatise for a discussion on R_0). A third model is that in which the zone of interaction occurs in the farfield, limited by a combination of absorption saturation and wavefront divergence (i.e. amplitude fall-off due to expansion of spherical or cylindrical waves). This model has been analyzed by both Mellen and Moffett [2] and Berktay and Leahy [3]. A detailed presentation of these models is made below. The problem of the extent of the zone of interaction has been studied experimentally. An experiment designed by Hobaek [4] to measure the zone of interaction by plotting the axial pressure $|p|$ versus range r at the difference frequency of 1 MHz, the primaries being at 16.6 and 17.6 MHz, and the beam radius being $a = 6.8$ mm, shows the trend sketched in Fig. 14.1.1 (radiated acoustic pressure in arbitrary units). The Fresnel distance was $r = 27$ cm, and the attenuation of primaries was $\alpha_1 \approx \frac{1}{13}$ cm^{-1}. This experiment demonstrated that the zone of interation extends throughout the Fresnel zone into the farfield. The generated pressure reaches a maximum at distance D, then decreases with distance. The location of D from the radiating face varies with aperture size and beam intensity. The theoretical value of D for the case where the primaries are *infinite plane waves* is given by Naugol'nykh et al [5a] and Lauvstad et al [5b] to be

$$D = \frac{1}{\alpha_T} \ln\left(\frac{\alpha_1 + \alpha_2}{\alpha_-}\right)$$

in which α_1, α_2, α_- are the absorption coefficients of primaries 1, 2 and of the difference field respectively, and $\alpha_T = \alpha_1 + \alpha_2 - \alpha_-$. For the conditions of Hobaek's experiment measured D was 2 to 8 cm; the theoretical D is 45 cm. This discrepancy is attributed to finiteness of the actual beam, and to its divergence (nonplanarity).

14.1b PARAMETERS NEEDED FOR CALCULATING PARAMETRIC ACOUSTIC ARRAYS

In all models of parametric radiation several parameters peculiar to the acoustic nonlinear effect appear embedded in the formulas. Assignment of numerical values to these parameters will be required to permit prediction of performance. These parameters are:

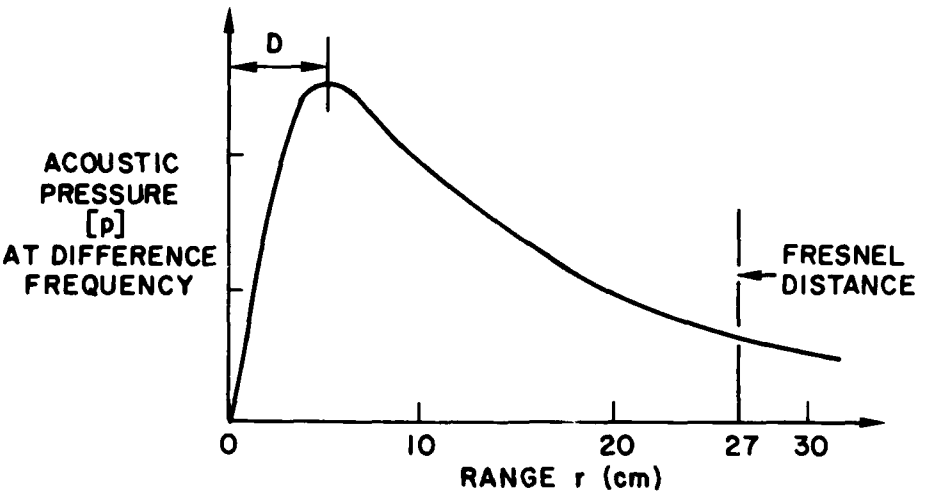

Fig. 14.1.1. Axial pressure versus range of a parametric source (ka = 27.5) at a difference frequency of 1 MHz after [4].

(1) β, the parameter of nonlinearity

β is a non-dimensional positive number whose magnitude is a measure of the elastic nonlinearity of the medium. It is specified in terms of two other parameters A, B defined by the constitutive relation between acoustic pressure increment Δp and acoustic density increment $\Delta\rho$ at constant entropy:

$$\Delta p = A\,(\Delta\rho/\rho_0) + \frac{B}{2}\left(\frac{\Delta\rho}{\rho_0}\right)^2 + \ldots$$

$$A = \rho_0 C_0^2;\; B = \rho_0^2 \left(\frac{\partial C^2}{\partial \rho}\right)_{s,\,\rho=\rho_0} \tag{14.1.1}$$

in which C_0 is the (linear) reference, or equilibrium, speed of sound in the medium; C the instantaneous speed of sound during passage of the acoustic wave, and ρ_0 is the equilibrium mass density of the medium. Values of A, B for a variety of liquids and solids are tabulated in various sources of materials data. A convenient reference is Beyer [6]. In that reference it is noted that the ratio B/A lies between 2 and 10 for most fluids and solids, and is less than unity for gases. Sea water at 20°C and 35 parts per thousand salinity has B/A = 5.25, a value which increases with temperature. The nonlinear parameter β appears in all models in the form,

$$\beta = 1 + \frac{B}{2A}. \tag{14.1.2}$$

Since the secondary (or difference) pressure is proportional to β one can increase the nonlinear conversion from primaries to secondary by preferring materials with larger values of β. For the standard sea water $\beta \approx 3.6$.

Occasionally the equation of state for fluids is written in the form,

$$p = A\left(\frac{\rho}{\rho_0}\right)^n - B. \tag{14.1.3}$$

The exponent n is tabulated in various handbooks under the symbol γ, the ratio of specific heats (C_p/C_γ). However in this application $\gamma = 1 + B/A$, hence $n = \gamma = 2\beta - 1$.

When the value of B/A is not listed it is convenient to *estimate* it by an empirical formula (Ballou's formula),

$$\frac{B}{A} = \frac{1.2 \times 10^4}{C_0} - 0.5 \tag{14.1.4}$$

in which C_0 is the equilibrium speed of sound (meters per second) in the material.

(2) α, the parameter of absorption

α is the absorption coefficient of the medium for acoustic waves. If the absorption is due to viscosity and heat conduction the acoustic intensity decreases with distance x in accordance with the law $e^{-2\alpha x}$ where α depends on frequency f and parameter a:

$$\frac{\alpha}{f^2} = 2\pi^2(2a)\,;\, 2a = \frac{1}{\rho_0 C_0^3}\left[\frac{4}{3}\eta + \zeta + \kappa\left(\frac{1}{C_v} - \frac{1}{C_p}\right)\right] \tag{14.1.5}$$

in which η is the shear viscosity, ζ is the dilatational viscosity, and κ is the thermal conductivity coefficient [7]. If the absorption is due to relaxation, the passage of sound transfers energy from the translational motion of the disturbed particles into rotational and oscillational motion, thereby reducing the acoustic pressure (which measures translational motion only). The relaxation absorption coefficient is given by

$$\alpha_R = \frac{C_\infty^2 - C_0^2}{2C_0^3}\,\frac{\omega^2\tau}{1 + \omega^2\tau} \tag{14.1.6}$$

in which τ is the relaxation time, C_∞ is the sound velocity for $\omega\tau >> 1$, and C_0 the sound velocity for low frequencies. Each medium has a speed C_∞ and a time τ, but relatively few have been tabulated [8]. Absorption in a monochromatic (single frequency) wave reduces the wave amplitude but does not change its shape. However waves having arbitrary time signatures, and therefore possessing many frequencies, are distorted in shape by absorption, which is frequency dependent (i.e. dispersive). An initial rectangular pulse undergoing absorption assumes the shape of a Gaussian normal distribution curve with distance x, exhibiting a width $(ax)^{1/2}$ where a is defined above.

The absorption of sound in sea water is particularly important in applications of nonlinear technology to the ocean. Liebermann [9] combines the effects of viscosity and relaxation and derives the frequency dependent absorption formula in terms of two constants a,b,

$$\alpha = a \frac{f_T f^2}{f_T^2 + f^2} + bf^2 \tag{14.1.7}$$

in which f_T is the relaxation frequency. Shulkin and Marsh [10] have used this formula and made a curve fit of ocean absorption measurements in the frequency range $2 - 25$ kHz. They find that

$$\alpha_{db} = \frac{1.86 \times 10^{-2} S f_T f^2}{f_T^2 + f^2} + \frac{2.68 \times 10^{-2} f^2}{f_T} \tag{14.1.8}$$

$$f_T = (21.9 \times 10^6)\ 10^{-\frac{1520}{T + 273}} \tag{14.1.9}$$

in which S is the salinity expressed in parts per thousand (35 ppt is the nominal standard ocean), f_T and f are expressed in kiloherz, α_{db} is in units of db per kiloyard and T is the temperature of the ocean in degrees centigrade. In design calculations it is often convenient to express α in nepers per meter,

$$\alpha = 1.0936 \times 10^{-4} \alpha_{db} \qquad \text{(nepers/meter)} \tag{14.1.10}$$

For frequencies outside the range of curve fit one can make an extrapolation using the available formulas, or can resort to experimental data. At very low frequencies the measured attenuation in the ocean is greater than that given by the formulas, a phenomenon for which an adequate theory is not currently available although it is believed to be due to absorption relaxation of boron. In this case one makes use of tabulated experimental data [11].

As an example, the calculation of α for sea water at $T = 5°C$ and $f = 100$ kHz leads to the result that the relaxation frequency is 74.6 kHz, and α is 32 dB/kiloyard or 3.4×10^{-3} nepers/meter.

The absorption coefficient for fresh water is variously quoted: Berktay [12] writes

$$\alpha = 3.8 \times 10^{-14} f^2 \qquad (f\text{:herz, } \alpha\text{:nepers/meter}) \tag{14.1.11}$$

while Shooter et al [13] estimate it to be,

$$\alpha = 2.38 \times 10^{-14} f^2 \qquad (f\text{:herz, } \alpha\text{:nepers/meter}) \tag{14.1.12}$$

It is evident that most values of the absorption coefficient obtained from formulas are only approximate. When accurate values are needed the only resort is experiment. However the above formulas can be used as guides in making estimates.

(3) R_0, nearfield-farfield separation distance

When the surface of a plane radiator is approached from infinity the intensity of the radiation field rises monotonically as R^{-2} until it reaches the nearfield-farfield separation distance R_0, after which, upon nearer approach, the intensity falls first to a zero, then rises again in a succession of closer and closer spaced maxima and minima. The location of R_0 depends on the shape and physical size of the radiator, the wavelength λ of the radiation and the baffle condi-

tions at the boundaries of the moving surface. Since the latter are difficult to apply it is convenient to idealize the baffle to be plane, rigid, and of infinite extent. The distance R_0 is then nominally taken to be S_A/λ, where S_A is the area of the radiator, and is called the "Rayleigh distance." More precise expressions for R_0 can be theoretically derived from available formulas for the radiation fields of differently shaped radiators. A few of the most important ones are listed here:

Type of radiator	Nearfield-farfield separation distance
(1) long strip, width d, length $l>>\lambda$	(1) $\frac{d^2}{4\lambda} - \frac{\lambda}{4}$
(2) circular piston, radius a	(2) $\frac{a^2}{\lambda} - \frac{\lambda}{4}$
(3) square piston, side $2b$	(3) b^2/λ
(4) square piston, side $2b$ [14]	(4) $1.5\ b^2/\lambda$
(5) circular piston radius a [15]	(5) $\frac{3}{4}\ a^2/\lambda$
(6) circular piston, diameter D [16]	(6) $\frac{\pi D^2}{4\lambda} \times \frac{1}{3} < R_0 < \frac{\pi D^2}{4\lambda} \times \frac{3}{4}$

The variety of expressions for R_0 illustrates the difficulty of accurate determination of this parameter, both in definition and magnitude. Zemanek [17] chooses R_0 as the range distance at which the farfield half power beamwidth is actually realized, a definition incorporated by Zemanek and Muir into entry 5 above using experimental data. Some authors use the Fresnel distance (approximately $\frac{S_A}{4\lambda}$) as a more appropriate R_0 (see entry 2 above). Others appeal to experiment, as in entry 6. Ultimately all choices of R_0 are approximate, but close estimates can be made in particular circumstances.

(4) C_0, the speed of sound

C_0 is the speed of sound in the medium under conditions of thermodynamic equilibrium, at frequencies considerably lower than the relaxation frequency (i.e. reciprocal of relaxation time). It is independent of amplitude, thus differing from the sound speed C of a finite amplitude sound wave which is a function of amplitude. C_0 is related to the adiabatic bulk modulus κ of the medium by the formula,

$$C_0^2 = \frac{\kappa}{\rho_0}, \qquad \kappa^{-1} = \frac{1}{\rho}\left(\frac{\partial \rho}{\partial P}\right)_s. \tag{14.1.13}$$

Tabulation of equilibrium sound speed (or adiabatic bulk modulus) of various fluids are found in treatises [18], and handbooks on thermodynamic properties of materials.

Summary: Numerical values of the parameters β, α, R_0 and C_0 that appear in all models of parametric sound sources are uncertain to within limited bounds. β and α are functions of the thermoviscous properties of the medium, R_0 is dependent on the baffle conditions of the radiation model, and C_0 is a function of the pressure and temperature at the point of measurement. Thus the performance of parametric transmitters predicted by various models can be estimated to within the knowledge of the parameters which can be good or poor according to circumstance.

14.2 PREDICTION MODELS OF PARAMETRIC ARRAYS

I. The Westervelt Model [1]

In this model the zone of interaction created by the superposition of two exactly collimated beams has a cross-section that is very small compared to the wavelength at the difference frequency, and is limited in range to the nearfield of the radiator by absorption. The assumed form of the primaries is then $P_{1,2} = P'_{1,2} \exp[-(\alpha_{1,2} + jk_{1,2})x]$, where $k = \frac{\omega}{C_0}$. For given acoustic powers W_1, W_2 radiated by area S of the primaries the difference (acoustic) pressure p_- radiated by the equivalent endfire array into the farfield is an axisymmetric directional spherical wave, amplitude $A_W(\alpha,R)$ and directionality $D_R(\theta)$,

$$
\begin{aligned}
&p_-(R,\theta) \rightarrow A_W(\alpha,R)\frac{e^{-jk_-R}}{R} D_R(\theta) \\
&A_W(\alpha,R) = \frac{\omega_-^2 (W_1 W_2)^{1/2}\beta\ e^{-\alpha_- R}}{2\pi C_0^3\ \alpha_T} \\
&D_R(\theta) = \left[1 + j\left[\frac{2k_-}{\alpha_T}\right]\sin^2\frac{\theta}{2}\right]^{-1} \\
&W_{1,2} = S(P_{1,2})^2/2\rho_0 C_0 \\
&\alpha_T = \alpha_1 + \alpha_2 - \alpha_-
\end{aligned}
\tag{14.2.1}
$$

Here the subscripts 1, 2 indicate primaries, and the subscript minus sign indicates properties at the difference frequency. It is convenient to group the quantities in the following way:

(a) magnitude of secondary pressure,

$$|p_-(R,\theta)| = \frac{A_w(\alpha,R)}{R} \tag{14.2.2a}$$

(b) directivity (in cylindrical coordinates),

$$|D_R(\theta)| = \frac{\alpha_T^2}{\alpha_T^2 + 4R_-^2 \sin^4\left[\frac{\theta}{2}\right]} \tag{14.2.2b}$$

(c) 3db beamwidth at the half-power points of the directivity pattern,

$$2\theta_{\frac{1}{2}} \approx 2\sqrt{\frac{2\alpha_T}{k_-}} \tag{14.2.2c}$$

Experiments by Hobaek [4] have shown that when the primary beams have a finite area (radius a) the directivity is even higher. Naze and Tjötta [19] have derived the formula for directivity for this case to be,

$$|D(\theta)| = |D_R(\theta)|\left|\frac{2J_1(ka\sin\theta)}{ka\sin\theta}\right| \tag{14.2.3}$$

which predicts a directivity closer to actual measurement. The generated pressure amplitude measured by [19] is lower than predicted by the Westervelt model, probably because of experimental disturbance of the Fresnel zone.

The Westervelt model is limited in applications to conditions where the zone of interaction is in the nearfield and the length of the equivalent endfire array is determined by absorption of the primaries. The primaries themselves are very narrow beams and are relatively weak.

II. The Mellen and Moffett Model

Mellen and Moffett [2] have modified the Westervelt model, replacing nearfield absorption by nearfield saturation as the limiting agency which determines the length of the equivalent endfire array. The primaries, centered at wavenumber k_0, are assumed collimated out to the Rayleigh distance R_0, but the secondary (or difference frequency) wave is collimated only to a shorter distance $R_1 = R_0(k_-/k_0)$ where k_- is the wavenumber at the difference frequency. Within R_1 the growth of the secondary wave is linear with distance, the secondary level is proportional to $(k_0/k_-)^2$ and is scaled by the parameter $e^{-2\alpha_- R_0}$. Beyond R_1, and generally less than R_0, the growth continues as the logarithm of the distance until saturation causes the theoretical growth to cease at the saturation distance L_{SAT} (see 14.2.9 below and Sect. 14.3b for a discussion of saturation). The effective length of the equivalent endfire array is approximately πL_{SAT}. The growth of the secondary level versus distance has been determined experimentally for primaries centered at 720 kHz, secondary at 50 kHz, with primary source level as parameter. The experimental curves are shown in Fig. 14.2.1. It is noted that, as the primary level increases, the effective length of the equivalent endfire array decreases, the variation being proportional to (input level)$^{-1}$. The directivity of shorter arrays is less, varying as (input level)$^{-1/2}$, and proportional to k_0/k_-. The result is a broadening of the beam as the input level rises, but a narrowing of the beam as the difference frequency increases (for fixed primary level).

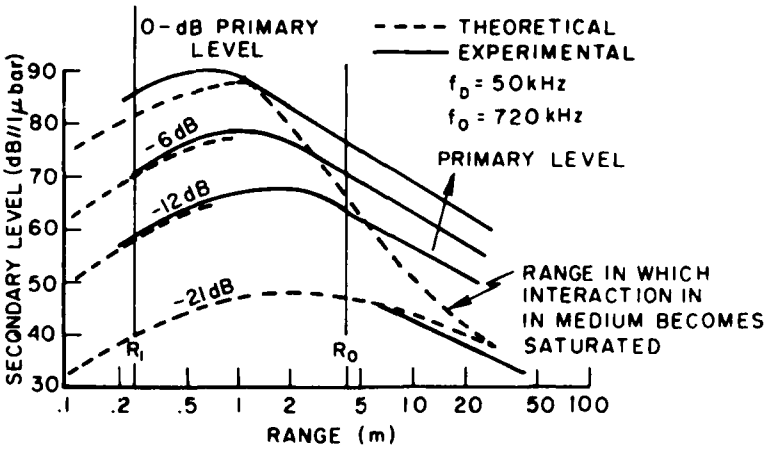

Fig. 14.2.1. Difference frequency level vs distance for several primary levels. (After [2])

A second modification by Mellen and Moffett of the Westervelt Model consisted in extending the zone of interaction to the farfield. They identified a distance $R_2 (= R_0 k_0 / k_-)$ beyond which both primary and secondary waves diverge and the secondary level increases as the logarithm of the distance, and is proportional to k_0/k_-. Growth continues in the farfield until terminated by absorption, saturation, divergence, etc. The scaling parameter for this farfield model is $2\alpha_- R_2$.

As a useful aid in application Mellen and Moffett prepared a general mathematical model based on appropriate modification of the Westervelt model. In the Westervelt modle the difference pressure can be written in the form

$$Rp_-(R,\theta) = -\frac{k_-^2 P_1' P_2' \beta}{2\rho_0 C_0^2} \left[\left(\frac{S}{2\pi\alpha_T} \right) \frac{e^{-(\alpha_- + jk_-)R}}{1 + j2\dfrac{k_-}{\alpha_T} \sin^2 \dfrac{\theta}{2}} \right] \tag{14.2.4}$$

in which the entity in brackets was originally derived (see Chap. I of this treatise) from a volume integral of the equivalent source strength over the assumed collimated beams (area S). Returning to the volume integral Mellen and Moffett inserted a more general source strength in the form of an amplitude taper T, and arrived at the form,

$$|Rp_-(R)| = \frac{\beta P_0^2 k_-^2}{2\rho_0 C_0^2} \left[\frac{1}{k_0} \int_0^\infty \frac{T^2(r')\,dr'}{\sqrt{1 + \left[\dfrac{k_-}{k_0} \dfrac{r'}{R_0} \right]^2}} \right]. \tag{14.2.5}$$

Two cases were treated: (1) for the absorption limited case, where α is the absorption

$$T_\alpha = e^{-\alpha r} \tag{14.2.6}$$

(2) for the amplitude case, where the amplitude of the primary is P_0,

$$T_\beta = \frac{1}{\sqrt{1 + (\frac{\phi}{2})^2}}\,; \phi = X \sinh^{-1} (\frac{r'}{R_0})\,; X = \frac{\beta P_0 k_0 R_0}{\rho_0 C_0^2} \tag{14.2.7}$$

In their general model they took the total loss in the primaries to be *approximated* by the product $T_\alpha T_\beta$. Thus the ratio of the secondary pressure $|rp_-|$ to the primary pressure amplitude $|R_0 P_0|$ is derived to be

$$\mathcal{P}_p = \left| \frac{rp_-}{R_0 P_0} \right| = \frac{X}{2} \left(\frac{k_-}{k_0} \right)^2 \int_0^\infty \frac{e^{-2\alpha r'} dr'/R_0}{\left[1 + \dfrac{X}{2} \sinh^{-1} \left[\dfrac{r'}{R_0} \right]^2 \right] \sqrt{1 + \left[\dfrac{k_- r'}{k_0 R_0} \right]^2}} \tag{14.2.8}$$

or

$$\mathcal{P}_p = \frac{X}{2} \left(\frac{k_-}{k_0} \right)^2 \int_0^\infty \left[\frac{1 + \sinh^2 u}{1 + \left[\dfrac{k}{k_0} \sinh u \right]^2} \right]^{1/2} \frac{e^{-2\alpha R_0 \sinh u}}{1 + \left[\dfrac{Xu}{2} \right]^2} du.$$

This ratio (when expressed in decibels) is designated the *parametric-source level efficiency*. It includes all previous models by appropriate choice of asymptotic forms:

$$\begin{aligned}
&\text{Westervelt case:} && X < 1,\ 2\alpha R_0 > 1 && \mathscr{E}_p \to X\left(\frac{k_-}{k_0}\right)^2 4\alpha R_0 \\
&\text{Saturation-limit case in near field:} && X > 1,\ 2\alpha R_0 < 1 && \mathscr{E}_p \to \frac{\pi}{2}\left(\frac{k_-}{k_0}\right)^2 \\
&\text{Spherical wave case (farfield limit):} && X < 1,\ 2\alpha R_0 < 1 && \mathscr{E}_p \to \frac{X}{2}\left(\frac{k_-}{k_0}\right) E_1(2\alpha R_2)
\end{aligned} \tag{14.2.9}$$

where

$$E_1(X) = \int_X^\infty \frac{\exp(-t)}{t}\, dt$$

Calculation of $\mathscr{E}_p$ for several choices of the parameters $2\alpha R_0$ and f_0/f_- allows the construction of a family of parametric efficiency curves (expressed in decibels) as a function of input source level (db re 1 μ bar). To make the curves move universal Mellen and Moffett have introduced a new parameter called "scaled mean input source level," $L_{sp}^{\cdot}$ defined as,

$$\begin{aligned}
L^{sp^{\cdot}} &= L_{sp} + 20 \log_{10} f_0 \\
L_{sp} &= \frac{1}{2}\left(L_{sp}^1 + L_{sp}^2\right)
\end{aligned} \tag{14.2.10}$$

in which $L_{sp}^{1,2}$ are the input source levels of the primaries (db re 1 μ bar) and f_0 is the average primary frequency in kiloherz. The secondary source level L_{ss} can then be determined from the formula,

$$L_{ss} = L_{sp} + 20 \log_{10} \mathscr{E}_p \tag{14.2.11}$$

in which $\mathscr{E}_p$ is a function of $L_{sp}^{\cdot}$ (as noted), and $20 \log_{10} \mathscr{E}_p$ is read from the curves in the form of a negative number of decibels.

Figure 14.2.2 reproduced from [2] shows those curves. It is based on a model consisting of a circular piston driven at frequencies $f_0 \pm f/2$, in which the *downshift ratio* (f/f) was taken as 10, the *absorption number* $2\alpha R_0$ was taken to lie between 0 and 1, and the scaled mean input source level ranged from 145 to 200 db re μ bar @ 1 m per kiloherz. The scaled levels above 180 db correspond to shock formation in the collimated zone.

A second performance parameter in applications of parametric projectors is the farfield directivity pattern $D_a(\theta)$. The primaries in all designs are the given quantities and have a normalized directivity $D_0(k_0,\theta)$ for the axisymmetric case. The integration over all the equivalent sources of the endfire array from 0 to ∞ that is called for in the Westervelt model (and all later modifications thereof) is conveniently divided into two ranges, the nearfield from 0 to R_2, and the farfield from R_2 to ∞. The contribution to the farfield directivity from an integration over a nearfield distribution of sources is obtained from the source level calculation,

$$\left|\frac{rp_-}{R_0 P_0}\right| \to D_0(k_0,\theta)\,\frac{X}{2}\left(\frac{k_-}{k_0}\right)^2 \int_0^{R_2} \frac{e^{-2\left(\alpha + ik_- \sin^2\frac{\theta}{2}\right)r'}}{\left(1 + \frac{X}{2}\sinh^{-1}\left(\frac{r'}{R_0}\right)^2\right)} \frac{dr'}{R_0} \tag{14.2.12}$$

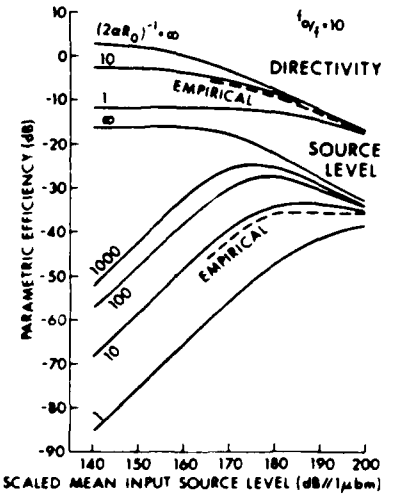

Fig. 14.2.2. Parametric gain E_p as a function of scaled input source level for various values of the absorption number $2\alpha R_0$. (From Mellen and Moffett [2]).

(see 14.2.7 for definition of symbols). From this integration one can derive the following asymptotic (i.e. θ small) forms of the farfield directivity, $D_a(\theta)$:

Limiting Case	Directivity $D_a(\theta)$	
(1) absorption limited nearfield		
$\alpha R_0 > 1,\ X < 1$	$\left[1+\left(\frac{k_-}{\alpha}\frac{\theta^2}{4}\right)^2\right]^{1/2}$	(14.2.13a)
(2) saturation limited nearfield		
$\alpha R_0 < 1,\ X > 1$	$\exp-\left(\frac{k_- R_0\theta^2}{X}\right)$	(14.2.13b)

(Note that $D_0\ (k_0,\theta)$ does not contribute directionality in the cases because $k_- < k_0$).

When the zone of interaction is in the farfield the source level contribution (including directivity) is,

$$\left|\frac{rp_-}{R_0 p_0}\right| \rightarrow D_0(k_0,\theta)^2\ \frac{X}{2}\ \frac{k}{k_0}\int_{R_2}^{\infty}\frac{e^{-2\alpha r'}\,dr'}{1+\left(\frac{X}{2}\sinh^{-1}\frac{r'}{R_0}\right)^2 r'}. \qquad (14.2.14)$$

These several expressions for directivity can be used to determine endfire gain by integrating them over space. The result of this integration is:

(1) gain due to nearfield sources,

$$G_a \to 2\frac{k_-}{\pi\alpha}, \quad \alpha R_0 > 1 \quad X < 1 \qquad \text{absorption limited case} \qquad (14.2.15a)$$

$$G_a \to \frac{4k_- R_0}{X}, \quad \alpha R_0 < 1, \quad X > 1 \qquad \text{saturation limited case} \qquad (14.2.15b)$$

(2) gain due to farfield sources:

$$G_b \to 2G_0 \approx 4k_0 R_0 \qquad G_0 = \text{gain of primaries} \qquad (14.2.15c)$$

The total gain of the secondary G_S when absorption, saturation and primary gain are all present is

$$G_S^{-1} = (G_a^{-1})_{\substack{\text{absorption} \\ \text{limit}}} + (G_a^{-1})_{\substack{\text{saturation} \\ \text{limit}}} + (G_b^{-1})_{\text{farfield}} \qquad (14.2.16)$$

Using the approximations noted above for these gains, and noting that the definition of directivity index is $N_{DI} = 10 \log_{10} G$, it is seen that

$$(N_{DI})_{\text{secondary}} = (N_{DI})_{\text{primary}} + 3 - 10 \log_{10}\left[1 + \frac{k_0}{k_-}(2\pi\alpha R_0 + X)\right]$$

where again X is defined by 14.2.7. Mellen and Moffett [2] have plotted a family of curves of $\Delta N_{DI} = N_{DI(S)} - N_{DI(p)}$ versus scaled mean input source level with $2\alpha R_0$ as a parameter. These appear here as Figs. 14.2.3, 14.2.4, and 14.2.5. Since directivity index is a positive number these curves indicate how the directivity of the secondary is increased or decreased in comparison with the directivity of the primary. From them it is noted that the directivity of the secondary has the following dependency: (1) it decreases as the scaled input source level increases (2) it increases as the absorption decreases (for fixed source level). (3) it decreases as the downshift ratio increases for fixed source level and fixed absorption. Sample theoretical beam patterns associated with the difference frequency are shown in Figs. 14.2.6, 14.2.7.

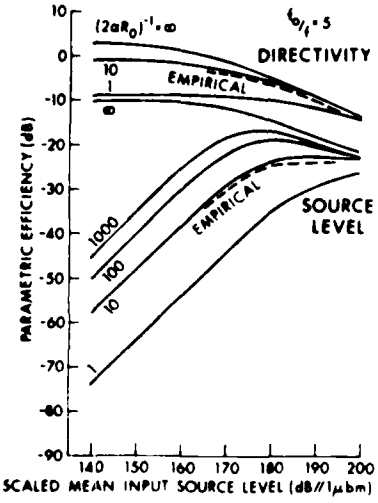

Fig. 14.2.3. Parametric efficiency vs primary level $f_0/f = 5$. After [2].

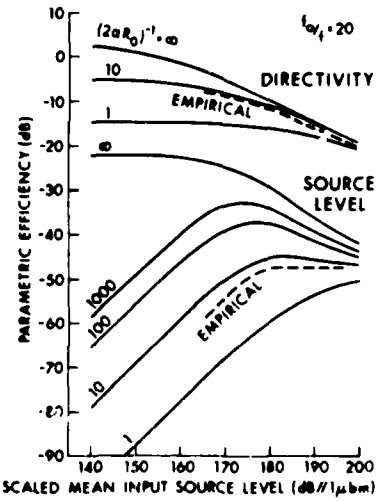

Fig. 14.2.4. Parametric efficiency vs primary level $f_0/f = 20$. After [2].

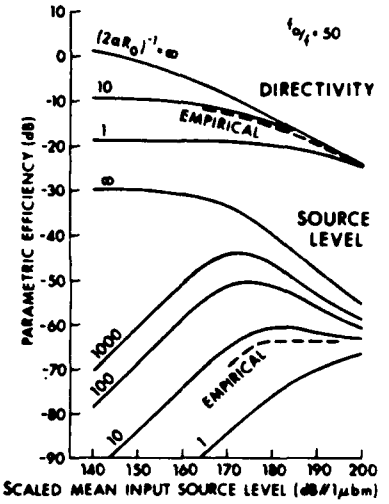

Fig. 14.2.5. Parametric efficiency vs primary level $f_0/f = 50$. After [2].

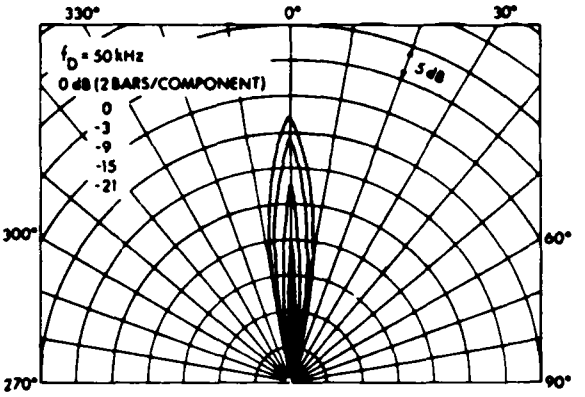

Fig. 14.2.6. Difference frequency (f_D) beam patterns for several primary levels. After [2].

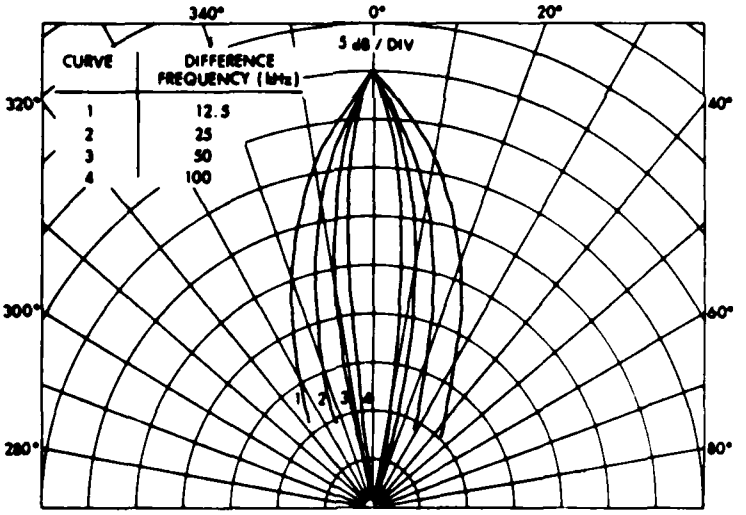

Fig. 14.2.7. Difference frequency beam patterns (normalized) for several downshift ratios. After [2].

Summarizing: the model proposed by Mellen and Moffett has been generalized from that of Westervelt to include nearfield saturation and divergent primary beams. It provides a convenient tool for calculation of the performance of parametric projector, namely source level, beam patterns and array gain of the secondary radiation for given source level (or power) and

directivity of the primaries. An advantageous feature of their approach is the family of performance curves from which rapid estimates can be made for a variety of conditions of operation.

III. Berktay and Leahy Model of a Parametric Projector

Berktay and Leahy [3] have constructed a detailed model of a parametric projector in which the zone of interaction of the primaries is assumed to take place in the *farfield* of the radiator. They begin by distributing the equivalent source points in this zone over the spherical coordinated r,γ,ϕ and assume a pair of primaries $p_{1,2}$ in the form of directional spherical waves,

$$p_{1,2} = P_{1,2} = D_{1,2}(\gamma,\phi)\exp[-(\alpha_{1,2} + jk_{1,2})r]/r \tag{14.2.17}$$

Following the Westervelt model, in which if p_i is the *total* primary acoustic pressure, the secondary p_- is given by

$$\begin{aligned} &\Box^2 p_- = -\rho_0 \frac{\partial q}{\partial t}, \qquad \Box^2 = \nabla^2 - \frac{1}{C_0^2}\frac{\partial^2}{\partial t^2} \\ &q = \frac{\beta}{\rho_0^2 C_0^4}\frac{\partial}{\partial t} p_i^2 \end{aligned} \tag{14.2.18}$$

they consider q to be a distribution of point sources over volume V, and use the freefield Green's function for a point radiator to construct the farfield difference pressure p_- at the point R,θ,η:

$$p_-(R,\theta,\eta) = \frac{\omega_-^2 P_1 P_2 \beta}{4\pi\rho_0 C_0^4}\iiint \frac{D_1(\gamma,\phi)D_2(\gamma,\phi)e^{-(\alpha_1+\alpha_2+jk_-)r}}{r^2|\mathbf{R}-\mathbf{r}|} \times e^{-(\alpha_- + jk_-)|\mathbf{R}-\mathbf{r}|}dV \tag{14.2.19}$$

In the far field approximation

$$|\mathbf{R}-\mathbf{r}| \cong R - ru, \qquad u = \cos\gamma\cos\theta\cos(\phi-\eta) + \sin\gamma\sin\theta$$

Fig. 14.2.8 shows the geometry of this approximation. Expanding all cosines and sine in infinite series, and retaining only terms to second order, it is seen that

$$u \cong 1 - \frac{1}{2}(\gamma-\theta)^2 - \frac{1}{2}(\phi-\eta)^2$$

$$\alpha_1 + \alpha_2 - \alpha_- u \cong \alpha_1 + \alpha_2 - \alpha_- \equiv \alpha_T, \quad \alpha_1 \ll \alpha_{1,2}$$

Inserting these farfield approximations into the volume integral one arrives at the farfield approximation to the difference pressure,

$$p_-(R,\theta,\tau) \cong -\frac{\omega_-^2 P_1 P_2 \beta}{4\pi\rho_0 C_0^4 R}\exp[-(\alpha_- + jk_-)R] \times \int_{-\pi/2}^{\pi/2}\frac{D_1(\gamma,\phi)D_2(\gamma,\phi)\cos\gamma}{\alpha_1 + jk(1-u)}\,d\gamma\,d\phi. \tag{14.2.20}$$

This formula is quite general and is suitable for any parametric projector for which the primaries have known directivity functions in their respective farfields.

Berktay and Leahy apply this formulation to the analysis of a rectangular piston located in Cartesian space, radiating into the x-direction, with side l parallel to y and side m parallel to z. The directivity function of this piston radiating sound at wavelength λ from an infinite rigid baffle is known to be,

$$D(\gamma,\phi) = \frac{\sin\left[\frac{kl\gamma}{2}\right]}{\left[\frac{kl\gamma}{2}\right]} \quad \frac{\sin\left[\frac{km\phi}{2}\right]}{\left[\frac{km\phi}{2}\right]} \tag{14.2.21}$$

At the half-power points of the primary beams, $|D(\gamma,\phi_1)| = 1/2$. This occurs at γ_1,ϕ, such that

$$\frac{kl}{2}\gamma_1 \cong \sqrt{2};\ \frac{kl}{2}\phi_1 \cong \sqrt{2}. \tag{14.2.22}$$

It is convenient to insert that $\sqrt{2}$ factor into the formula for $D(\gamma,\phi)$ in order to normalize all angles in an advantageous manner. The model chooses the Westervelt half-power angle $\theta_{\frac{1}{2}}$ (called here θ_d) to perform the normalization, and constructs two new parameters ψ_y,ψ_z such that

$$\psi_y \equiv \frac{\gamma_1}{\theta_2};\ \psi_z \equiv \frac{\phi_1}{\theta_d}$$

The source distribution anlges γ,ϕ and the field angles; θ,η are also normalized

$$\gamma' \equiv \frac{\gamma}{\theta_d};\ \phi' \equiv \frac{\phi}{\theta_d};\ \theta' \equiv \frac{\theta}{\theta_d};\ \eta' \equiv \frac{\eta}{\theta_d}$$

Inserting the normalized symbols, and the factor $\sqrt{2}$, into the formula for p_- it is seen that

$$p_-(R,\theta',\eta') \cong p_w(R,0)\,V(\psi_y,\psi_z,\theta',\eta')$$

$$p_w(R,0) \equiv -\frac{\omega^2\left[W_1W_2\right]^{\frac{1}{2}}\beta}{2\pi C_0^3 R\alpha_T}\exp\left[-(\alpha_- + jk_-)R\right]$$

$$V(\psi_y,\psi_z,\theta',\eta') \equiv \frac{lm}{\lambda^2}\theta_d^2\int_{-\frac{\pi}{2\theta_d}}^{\frac{\pi}{2\theta_d}} \frac{\sin^2\left[\frac{\sqrt{2}\gamma'}{\psi_y}\right]}{\left[\frac{\sqrt{2}\gamma'}{\psi_y}\right]^2} \frac{\sin^2\left[\frac{\sqrt{2}\phi'}{\psi_z}\right]}{\left[\frac{\sqrt{2}\phi'}{\psi_z}\right]^2}$$

$$\times \frac{d\gamma'd\phi}{\{1 + j[(\theta'-\gamma')^2 + (\eta'-\phi')^2]\}}. \tag{14.2.23}$$

Here $W_{1,2}$ are the radiated primary powers, and $V(0,0,0,0) = 1$. The function $V(\psi_y,\psi_z,\theta',\eta')$ (called the pressure reduction factor) is a complex number. Its magnitude $|V(\psi_y,\psi_z,0,0)|$ represents dependence of the difference pressure along the axis of propagation on the two

parameters ψ_y, ψ_z. The ratio $|V(\psi_y, \psi_z, \theta', \eta')| \div |V(\psi_y, \psi_z, 0, 0)|$ represents the normalized directivity pattern at normalized anlges θ', η'. Berktay and leahy have calculated the magnitude $|V(\psi_y, \psi_z, 0, 0)|$ for $0 \leqslant \psi_y \leqslant 12$ and $0 \leqslant \psi_z \leqslant 12$ by performing the integration called for at $\theta' = 0 = \phi'$. They have plotted $20 \log_{10}|V|$ versus ψ_y with ψ_z as parameter, reproduced here as Fig. 14.2.8. The figure states that along the axis of propagation (= axis of primaries) where $\theta' = 0 = \eta'$ the farfield pressure p_H at the difference frequency must be multiplied by the fraction V (given in db) which is dependent on the elevation angle (γ_1) and azimuthal angle (ϕ_1) of the primaries. Thus if $\psi_y = 10$, and $\psi_z = 10$, the fraction corresponds to -30 db, or 0.032. This plot also includes the case of square and circular transducers. Thus to calculate the secondary source level SL_S given the acoustic radiated power of the primaries one uses the formula

$$SL_S = 20 \log_{10} |p_H(R, 0)| + 20 \log_{10} |V(\psi_y, \psi_z, 0, 0)| \tag{14.2.24}$$

or

$$SL_s \cong 37 + 20 \log_{10} F_- - 40 \log_{10} \theta_d^0 + 10 \log_{10} W_1 + 10 \log_{10} W_2 + 20 \log_{10}|V|, \text{ dB re } 1\mu \text{ bar} \tag{14.2.25}$$

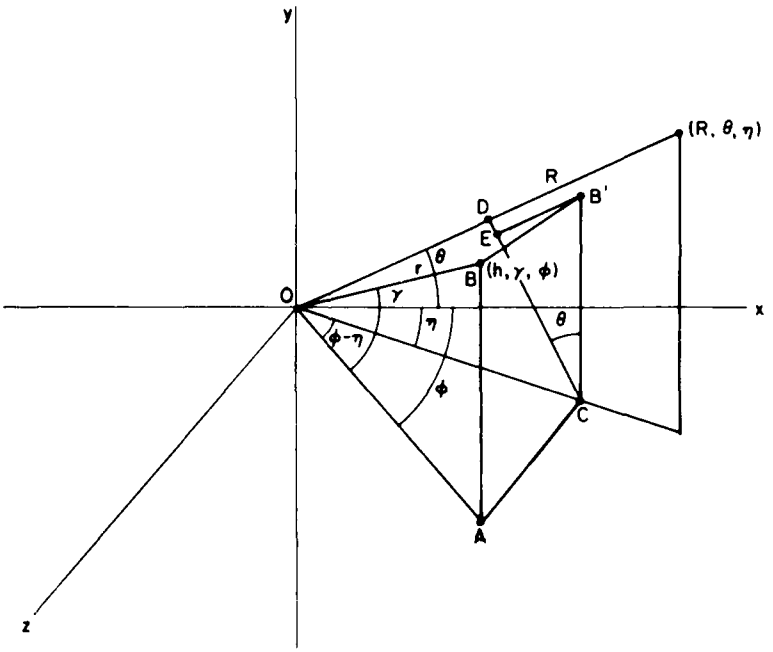

Fig. 14.2.8. Spherical geometry from which the farfield approximation of $|\mathbf{R} - \mathbf{r}|$ for the field at (R, θ, η) due to a source at r, γ, ϕ may be derived. The componetns of $\mathbf{r}$ ($r \cos\gamma, r \sin\gamma$) are each projected on to the direction $\mathbf{R}$ and their sum is subtracted from $|\mathbf{R}|$.

$$\begin{aligned} 0A &= r\cos\gamma \\ 0C &= 0A\cos(\phi - \eta) = r\cos\gamma\cos(\phi - \eta) \\ 0D &= 0C\cos\theta = r\cos\gamma\cos(\phi - \eta)\cos\theta \\ 0B &= r\sin\gamma \\ CB' &= r\sin\gamma \\ EB' &= CB'\sin\theta = r\sin\gamma\sin\theta \\ |\mathbf{R} - \mathbf{r}| &\simeq R - (0D + EB') \end{aligned}$$

in which F_- is the difference frequency in kiloherz, θ_d^0 is the Westervelt angle in degrees, $W_{1,2}$ are the primary radiated powers in watts, and the last term is obtainable from Fig. 14.2.9, or by performing the integration called for in the formula. A notable feature of this calculation is the fact that the source level decreases as ψ_y (or the half power angle of the primaries) increases.

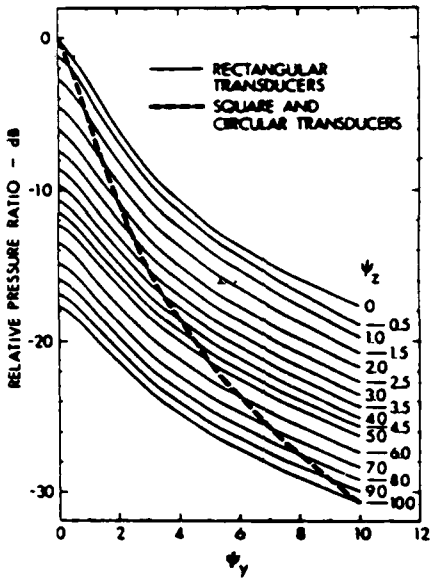

Fig. 14.2.9. Farfield behavior for given dimensions of transducer in the case of a parametric array (from Berktay and Leahy [3]).

A similar conclusion holds for ψ_z.

The model developed above also allows calculation of the total half-power beamwidth $2\theta_{1/2}$ in the xy plane, normalized relative to the total Westervelt half power angle $2\theta_d$. Berktay and Leahy have calculated these half power beamwidths as functions of ψ_z (with ψ_y as parameter) by finding those values of θ for which $|V(\psi_y,\psi_z,\theta,0)| = 0.707\,|V(\psi_y,\psi_z,0,0)|$. They plotted the results in the form $2\theta_{1/2}/2\theta_d$ versus ψ_z, $0 \leqslant \psi_z \leqslant 4.0$, with $0 \leqslant \psi_y \leqslant 4.0$, which appear here as Fig. 14.2.10. These plots show that near the origin (where $\psi_y \to 0$, $\psi_z \to 0$) the predicted half-power beamwidths are very nearly those of Westervelt's model. However, when $\psi_y \to 4.0$ and $\psi_z = 4.0$, the half-power beamwidths are approximately 3 times the Westervelt prediction (for the case of nearfield interaction). Thus the plots show the universal trend, namely the secondary beamwidth of the parametric array increases as ψ_y (i.e. the half power beamwidth of the primary) increases (for fixed ψ_z), or as ψ_z increases (for fixed ψ_y).

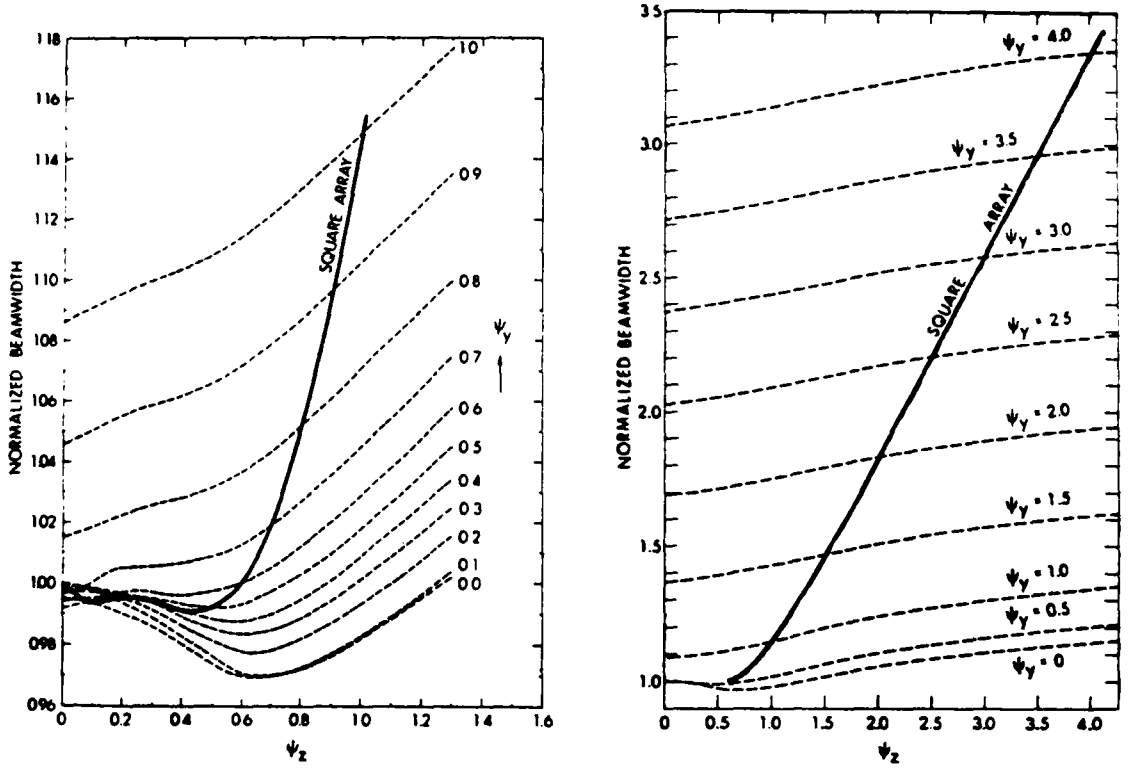

Fig. 14.2.10. Normalized half-power beamwidths, θ_{HP}/θ_d, for rectangular transducers. (The beamwidth in the x-y plane is shown.) (From Berktay and Leahy [3]).

Parametric projectors have been built with pistons of shapes other than rectangular. A popular one is the circular piston of radius a. The analysis of this radiator can be made in cylindrical coordinates R, γ, ϕ in which γ is the angle measured from the x-axis in the xy plane, and ϕ is the angle in the yz plane. Using the same approach as was used in the case of the rectangular piston Berktay and Leahy [3] arrive at the formula,

$$p_-(R,\theta) = p_w(R,0)\alpha_T\left[\frac{\pi a^2}{\lambda_1\lambda_2}\right]\int_0^{\frac{\pi}{2}} d\gamma \int_0^{2\pi} d\phi \; \frac{4J_1(k_1 a \sin\gamma)J_1(k_2 a \sin\gamma)}{k_1 k_2 a^2 \sin\gamma\,[\alpha_T + jk_-(1-u')]}$$

$$u' = \cos\theta\cos\gamma + \sin\theta\sin\gamma\cos\phi \qquad (14.2.26)$$

Fig. 14.2.11 shows the geometry of this approximation. A simplification of the integral can be made by considering all angles to be small, and by choosing the downshift ratio f_0/f_- to be much greater than unity. In this case one first performs the integration over ϕ, which then reduces to,

$$p_-(R,0) \cong p_w(R,0)\frac{k_0^2 a^2}{2}\int_0^{\frac{\pi}{2}} \left[\frac{2J_1(k_0 a\gamma)}{k_0 a\gamma}\right]^2 \frac{\gamma\, d\gamma}{\left[1 + j\left(\frac{\gamma}{\theta_d}\right)^2\right]}. \qquad (14.2.27)$$

The evaluation of this formula was further aided by a series approximation of the Bessel function, using five terms. Upon substitution of this simplification the actual calculation was based on the reduced formula,

$$\frac{p_-(R,0)}{p_W(R,0)} \simeq 2.25 \int_0^1 \frac{g(\mathrm{v})\,dV}{1 + jM_\mathrm{v}} \tag{14.2.28}$$

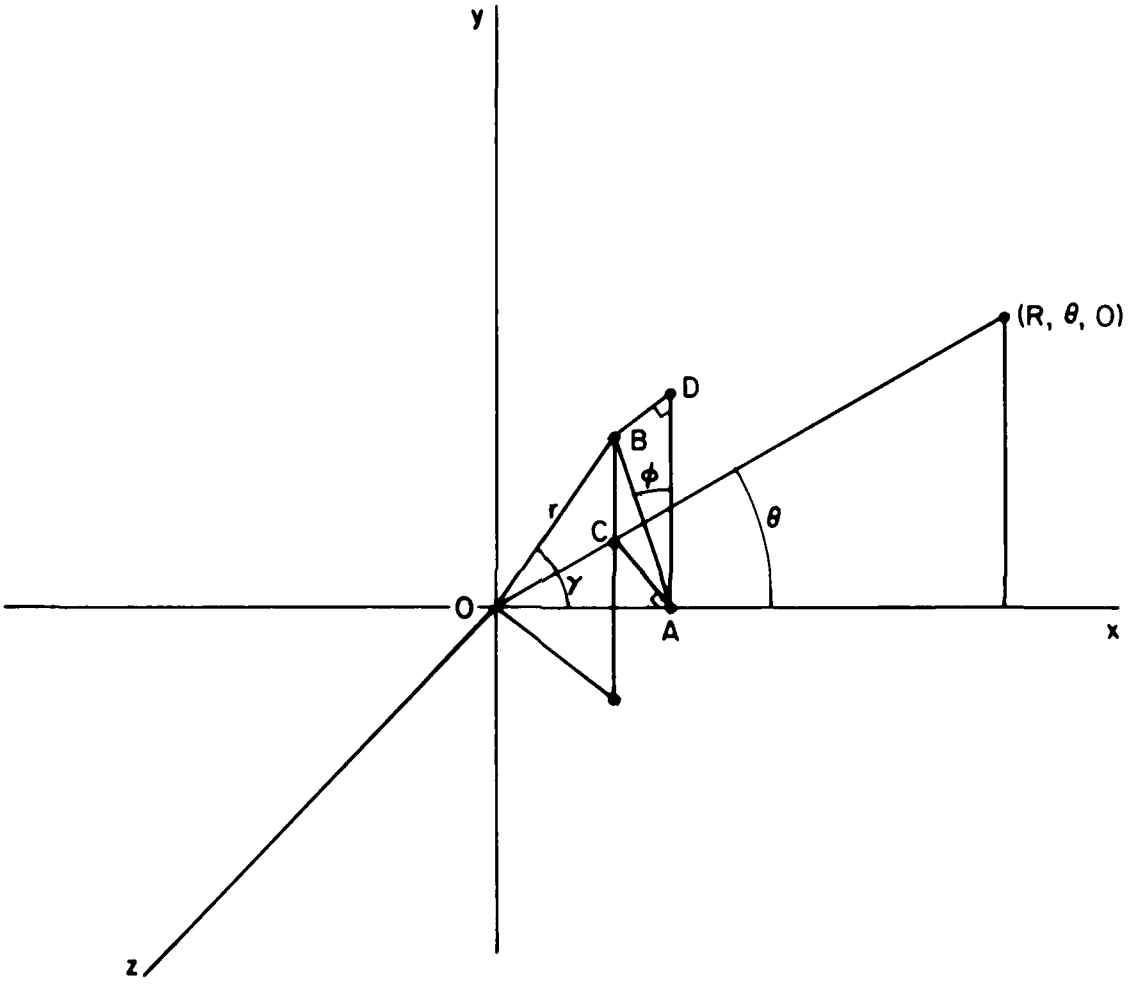

Fig. 14.2.11. Cylindrical geometry from which the farfield approximation of $|\mathbf{R} - \mathbf{r}|$ for the field at (R,θ,η) due to a source at r,γ,ϕ may be derived.

$$\begin{aligned}
0A &= r\cos\gamma \\
0C &= 0A\cos\theta = r\cos\gamma\cos\theta \\
AB &= r\sin\gamma \\
AD &= r\sin\gamma\cos\phi \\
BD &= AD\sin\theta = r\sin\gamma\cos\phi\sin\theta \\
|\mathbf{R}-\mathbf{r}| &\simeq R - (0C + BD)
\end{aligned}$$

in which

$$v = (\frac{1}{3}\ k_0 a\gamma)^2$$

$$g(v) = \left[\frac{2J_1(k_0 a\gamma)}{k_0 a\gamma}\right]^2$$

$$M_v = 3.48\,\psi_d;\ \psi_d = \frac{\gamma_1}{\theta_d};\ \gamma_1 = \frac{1.616}{k_0 a}$$

Here γ_1 is the half-power *point* in the primary directivity function. When calculations of the source level of the secondary were made for various values of ψ_d, and the results were compared to the performance parameters for square pistons having $\psi_y = \psi_d$ it was found they agreed so closely that one can model circular pistons of diameter $d = 2a$ as square pistons of side d.

Summarizing: A parmetric projector can be analyzed by use of the Berktay and Leahy model to give secondary source level and beamwidth. Estimates of performance can be made rapidly by the use of available plotted graphs. A comparison of this model with that of Mellen and Moffett is directly possible on the following basis:

for rectangular projectors: $2\alpha R_0$ of Mellen and Moffet approximates $(0.637/\psi_y\psi_z)$ of Berktay and Leahy.

for circular projectors: $2\alpha R_0$ of Mellen and Moffet approximates $0.650/\psi_d^2$ of Berktay and Leahy.

Actual comparison between models have been made. The two do not differ by more than 2.5 db for the case where the Berktay and Leahy analysis applies.

14.3 PARAMETRIC PROJECTORS WITH TRANSIENT PRIMARIES

The Westervelt model has been extended by Moffett et al [20] to include time-dependent primaries of the general form

$$p = P_1 g(t - \frac{x}{C_0}) e^{-\alpha_0 x} \cos(\omega_0 t - k_0 x) \tag{14.3.1}$$

in which $g(t)$ is assumed to have a narrow spectrum of frequencies. The equivalent source function in the nearfield zone of interaction is then

$$q = \frac{P_1^2 \beta}{2\rho_0^2 C_0^4} e^{-2\alpha_0 x} \frac{\partial}{\partial t} g^2(t - \frac{x}{C_0}). \tag{14.3.2}$$

Upon solution of the Westervelt equation for the secondary pressure,

$$\Box^2 p_S = -\rho_0 \frac{\partial q}{\partial t};\ \Box^2 = \nabla^2 - \frac{1}{C_0^2}\frac{\partial^2}{\partial t^2} \tag{14.3.3}$$

the authors found that in the farfield on the main axis ($\theta = 0$) at time t,

$$p_S(R,0,t) = \frac{W_0\beta}{8\pi C_0^3 R\alpha_0}\frac{\partial^2}{\partial t^2} g^2\left(t - \frac{R}{C_0}\right) \tag{14.3.4}$$

in which C_0, α_0 refer to the primaries, and W_0 is the value of acoustic power (the same for each primary) transmitted at the peak of the pulse envelope (of the primaries). In the case where the primaries (with amplitude $g(t)$) are pulsed at interval $T_0 = 2\pi/\omega_a$ the complex spectrum for the secondary pressure in the farfield on the main axis is derived to be,

$$p_S(R,0;\omega) = \frac{-\beta W_0}{8TC_0^3 R\alpha_0}\omega^2 G(\omega)\sum_{n=0}^{N-1}\exp(-jn\omega T_0) \tag{14.3.5}$$

Here $(G(\omega)$ is the spectrum of $g(t)$ and N is the number of pulses in the summation. When N is large this formula can be manipulated to show that the amplitude spectrum of this secondary pressure exhibits discrete frequency components at $\omega = m\omega_a$,

$$p_S(R,0;\omega) = \frac{-\beta W_0}{8\pi C_0^3 R\alpha_0}\sum_{m=1}^{M}(-1)^{mN}(m\omega_a)^2 NG_0(m\omega_a). \tag{14.3.6}$$

The two frequency case originally treted by Westervelt can be recovered from this analysis by writing $g(t) = g_1 + g_2$, $g_1 = \cos\omega_1 t$, $g_2 = \cos\omega_2 t$.

14.3a Bandwidth of Parametric Transmitters

The acoustic radiation of the primaries has a bandwidth defined by the mechanical Q of the radiating surface, namely the ratio of the reactive component of the mechanical impedance of the transducer to the acoustic resistance of the medium over the radiating surface. If the parametric array operates on a two-primary beam basis, each primary has its bandwidth, or mechanical Q, which can generally be designed to be equal in magnitude. Since the difference frequency of the secondary can be generated by taking differences of primaries over the *primary's* bandwidth it is seen that the bandwidth of the secondary can be made quite broad by small fractional changes in the primaries. This wideband property of the secondary can be used to transmit large time-bandwidth products, and hence achieve large signal processing gains.

The beam patterns of the parametric array at the difference frequency are controlled by the directivity functions of the primaries. If the Westervelt angle θ_d is much narrower than the primaries it has been shown above that the directivity function of the secondary is essentially the product of the directivity functions of the primaries. Since the latter do not vary much over the bandwidth of the primaries it is seen that the beamwidth of the secondary at the half-power points varies little over the bandwidth of the secondary. Experiments have shown less than 20% variation over two octaves [21].

14.3b Limit on the Performance of Parametric Projector by Acoustic Saturation

Acoustic saturation of the medium is a nonlinear phenomenon. In the simple case of a plane wave initiated at $x = 0$ with a particle velocity $u(0) = u_0 \sin\omega t$ the particle velocity $u(x)$ at any point x along the transmission path grows linearly with u_0 if the values of u_0 are infinitesimal, but breaks into a sum of the fundamental u_1, at ω, and harmonics $u_{2,3}\ldots$ at $2\omega, 3\omega$, etc. as u_0 becomes finite. According to theory, confirmed by experiment, the fundamental u_1 reaches a limiting magnitude as u_0 is increased—a value independent of u_0, but dependent on range x. Thus at every range where nonlinear saturation has appeared there is an assignable limiting magnitude. Two ranges are of particular importance: the "sawtooth region"

where the saturation waveform is sawtooth, and the "old age region" where the saturation waveform is quasi sinusoidal. Theoretical studies of these separate regions have been made. By the use of Fay's solution in the one dimensional wave equation Blackstock [23] has combined these regions into one formula for the fundamental of the particle velocity u_1,

$$u_1 = \frac{2\alpha C_0}{\beta k \sinh \alpha (x + \bar{x})}, \quad \bar{x} = \frac{C_0}{\beta k u_0}; \quad k = \frac{\omega}{C_0} \tag{14.3.7}$$

Here α is the small-signal attenuation coefficient, and $\bar{x}$ the shock formation distance. As the initial amplitude $u_0 \to \infty$, $\bar{x} \to 0$. The condition $\bar{x} = 0$ corresponds to acoustic saturation of the primary, which appears in the following forms for different values of αx,

$$(u_1)_{SAT} = \frac{2\alpha C_0}{\beta k \sinh \alpha x}; \quad (u_1)_{SAT}\Big|_{\alpha x << 1} = \frac{2C_0}{\beta k x}; \quad (u_1)_{SAT}\Big|_{\alpha x >> 1} = \frac{4\alpha C_0 e^{-\alpha x}}{\beta k}. \tag{14.3.8}$$

The condition $\alpha x << 1$ is the sawtooth region, while $\alpha x >> 1$ is the old-age region. In applications these formulas will be useful in making estimates.

A more common type of acoustic radiator is the one that radiates spherical waves. Shooter et al [13] have investigated acoustic saturation in this case. They begin by illustrating the case history of a high intensity spherical pressure wave $p(r,t)$ versus retarded time $t - r/C_0$ radiating from a sphere of radius a, where $p(a,t) = P_0 \sin \omega t$. at $r = a$ the wave is a sinusoid; at $r = r'$ the shock wave has formed (i.e. the maximum positive amplitude and maximum negative amplitude occur almost at the same value of retarded time); at $r = \hat{r}$ the full sawtooth waveform has appeared; and at $r = r_{MAX}$ the waveform is again almost sinusoidal. The locations of these distances from the origin depend on the parameters $\epsilon = P_0/\rho_0 C_0^2$, β, and $k = \omega/C_0$; they have the forms,

$$\begin{aligned} \bar{r} &= a \exp\left(\frac{1}{\beta \epsilon ka}\right) \\ \hat{r} &= a \exp\left(\frac{3}{\beta \epsilon ka}\right) \\ r_{MAX} &= \frac{\beta \epsilon ka/\alpha}{1 + \beta \epsilon ka \ln\left(\frac{r_{MAX}}{a}\right)}. \end{aligned} \tag{14.3.9}$$

Graphical plots of $\bar{r}, \hat{r}, r_{MAX}$ in yards versus peak source level P_0 (in dB re 1μb at 1 yd) with frequency $\omega = kC_0$ as parameter have been made by the use of these equations, for application to a source of effective radius $a = 1$ yd. in fresh water. These are reproduced from [13] as Figs. 14.3.1, 14.3.2, and 14.3.3. They can serve as guides to rapid estimation of the distances at which nonlinear effects become noticeable in spherical radiators for various choices of initial radiation amplitude. Inversely, by specificying a range over which nonlinear effects are to be negligible one can find in these charts the maximum allowable initial pressure P_{10}.

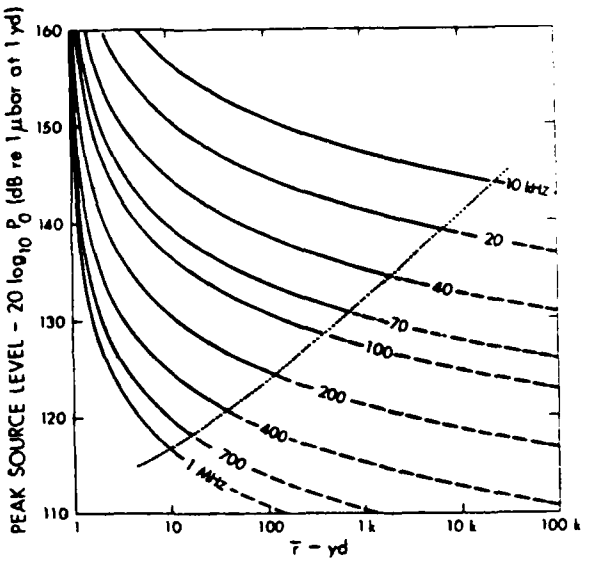

Fig. 14.3.1. Shock formation distance $\bar{r}$, as computed from Eq. 6, for a source of effective radius $r_0 = 1$ yd in fresh water. In the region to the right of the dotted locus line, absorption would prevent the formation of shocks. After [13].

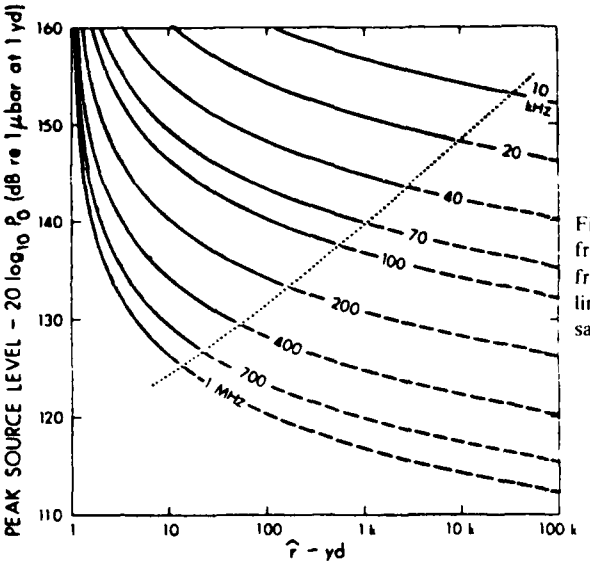

Fig. 14.3.2. Well-formed sawtooth distance $\hat{r}$, as computed from Eq. 7, for a source of effective radius $r_0 = 1$ yd in fresh water. In the region to the right of the dotted locus line, absorption would prevent the formation of true sawtooth. After [13].

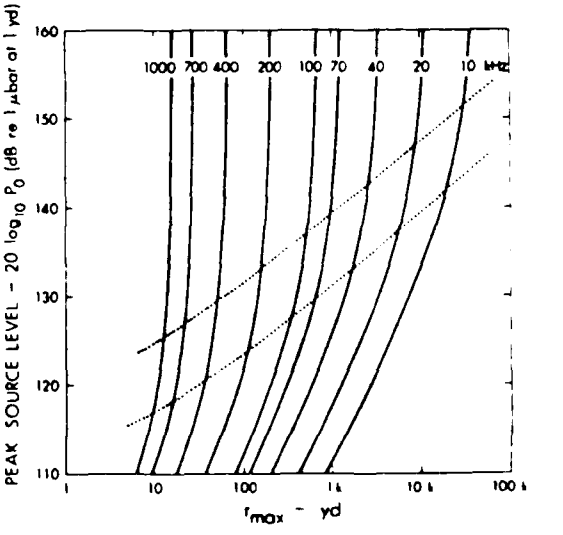

Fig. 14.3.3. Old age distance r_{max} (distance at which linear behavior is effectively restored), as computed from Eq. 8, for a source radius $r_0 = 1$ yd in fresh water. The upper dotted curve represents the locus $r_{max} = \hat{r}$ and the lower one the locus $r_{max} = \bar{r}$. After [13].

When shock formation has been initiated at distance $\bar{r}$ it becomes important to estimate the pressure levels at various distances thereafter. Blackstock [23] has shown that in the region between $\bar{r}$ and $\hat{r}$ the amplitude of the fundamental is given by,

$$p_1 = P_0 \frac{2(a/r)}{1+\sigma}; \quad p_{\text{SAT (SAWTOOTH)}} = \left. \frac{2\rho_0 C_0^2}{\beta k r \ln\left(\frac{r}{a}\right)} \right|_{\sigma >> 1}$$

$$\sigma = \beta \epsilon k a \ln (r/a) \tag{14.3.10}$$

This formula agrees with an earlier result of Laird [24] under the condition $\sigma >> 1$. The parameter σ appearing here is of special convenience in analysis because $\sigma = 1$ corresponds to the distance $\bar{r}$ and $\sigma = 3$ corresponds to the distance of the sawtooth, $\hat{r}$.

In this region of old age, $r \geqslant r_{MAX}$, Mair [25] obtained the following approximation for the fundamental component of the acoustic pressure,

$$p_1 = P_0 \frac{2(a/r)}{1+\sigma_{MAX}} \exp\left[-\alpha (r - r_{MAX})\right], \quad r \geqslant r_{MAX}$$

$$\sigma_{MAX} = \beta \epsilon k a \ln\left(\frac{r_{MAX}}{a}\right) \tag{14.3.11}$$

This model assumes that the amplitude p_1 is attenuated beyond r_{MAX} by absorption. As $P_0 \to \infty$ (i.e. as $\epsilon \to \infty$) it is seen that the influence of P_0 vanishes, and the true condition for old age saturation is established. Thus,

$$p_{SAT}\ (\text{old age}) = \frac{2\rho_0 C_0^2}{\beta k r \ln\left(\frac{r_{MAX}}{a}\right)} \exp\left[-\alpha (r - R_{MAX})\right]$$

$$R_{MAX} = \frac{1}{\alpha \ln\left(\frac{R_{MAX}}{a}\right)} \tag{14.3.12}$$

The formulas for the saturation presure p_{SAT} (sawtooth) and p_{SAT} (old age) calculated for $a = 1$ yd in fresh water and in sea water in units of db re 1 μ bar have been plotted versus range in yards. These appear as Figs. 14.3.4, 14.3.5. They show the maximum sound pressure level that can be attained at a given frequency at a given distance from the source. For example at 2.5 kHz the maximum attainable sound pressure level (as limited by acoustic saturation) at a distance of 10 kiloyards in sea water is 82 db re 1 μ bar no matter what the initial acoustic pressure is at the surface of the radiator is forced to be, assuming spherical wave propagation in a homogeneous medium.

Acoustic saturation naturally applies also to beamed spherical radiation. In this case one can make an estimate of the off-axis response of acoustic pressure in the farfield versus angle by weighting the amplitude parameter ϵ by the *small signal* directivity factor of the source and choosing the effective radius a of the source to be

$$\frac{S}{3\lambda} < a < \frac{3}{4}\frac{S}{\lambda} \tag{14.3.13}$$

where S is the area of the source.

AD-A140 578 A TREATISE ON ACOUSTIC RADIATION(U) NAVAL RESEARCH LAB 7/7
WASHINGTON DC S HANISH 1981

UNCLASSIFIED F/G 20/1 NL

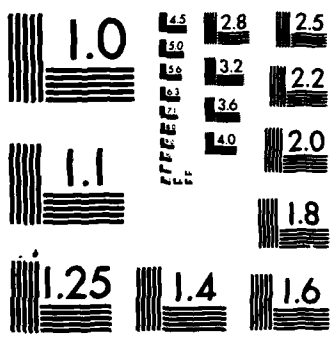

MICROCOPY RESOLUTION TEST CHART
NATIONAL BUREAU OF STANDARDS-1963-A

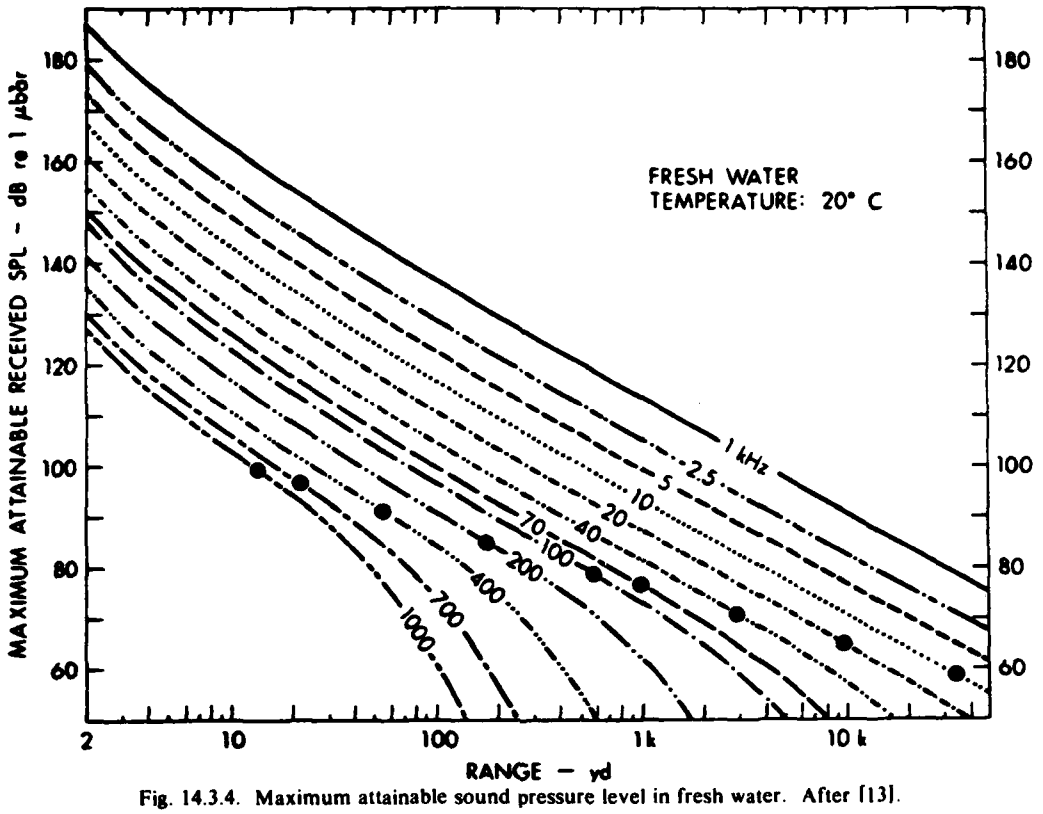

Fig. 14.3.4. Maximum attainable sound pressure level in fresh water. After [13].

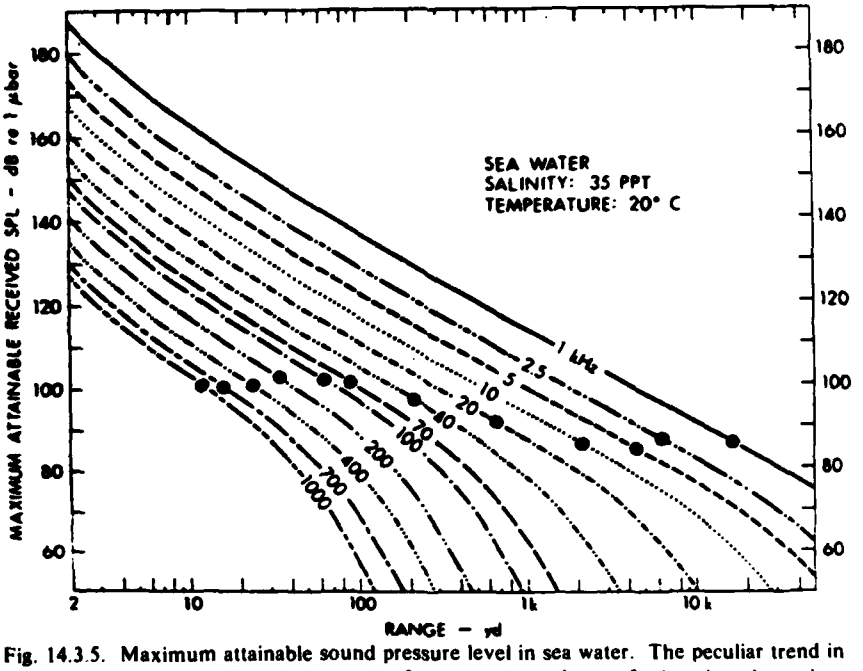

Fig. 14.3.5. Maximum attainable sound pressure level in sea water. The peculiar trend in the locus of points $r = R_{max}$ is due to the frequency dependence of relaxation absorption. After [13].

High amplitude excitation in acoustic radiators also exhibits important effects on beamwidth and side-lobe level. An experiment by Shooter et al [13] compared high amplitude (133 db re 1 μ bar @ 1 yd) patterns with low amplitude (115 db re 1 μ bar @ 1 yd) patterns at a frequency of 435 kHz, and found that at a maximum range of 111 yds the half-power beamwidths of the high amplitude patterns increased 80%, and the sidelobe suppression decreased by 7 db. The widening of the main lobe is due to high-amplitude-dependent attenuation which causes a rapid decay of intense waves on the beam axis. Loss of side-lobe suppression is due to this adverse shading of the central radiation of the original acoustic radiator relative to radiation delivered to the side lobes. The extra attenuation due to shock formation can be minimized by making the shock formation distance to be greater than the Rayleigh distance (= area/wavelength) of the projector. The ratio of these two distances is the *saturation parameter* χ,

$$\chi = \frac{\text{shock formation distance}}{\text{Rayleigh distance}} = \beta \epsilon k R_0$$

$$\epsilon = P_0/\rho_0 C_0^2 \tag{14.3.14}$$

Thus a design criterion to avoid excessive absorption loss due to shock formation is $\chi >> 1$.

14.3c Diffraction Effects in Parametric Arrays

Novikov et al [26] have analyzed the case of a parametric transmitter in which diffraction of the primaries plays a role. They base their work upon a nonlinear equation that is closely related to modern theories of diffraction. To understand the origin of the equation we begin with the article of Malyuzhinets [27]. A (nearly) plane wave $U = A(x,y,z)\, e^{ikx - i\omega t}$ is propagating in the x-direction in accordance with the linear wave equation in a homogeneous medium (viz. $\partial^2 U/\partial t^2 = c^2 \nabla^2 U$. By substitution of this plane wave solution one arrives an equation for the amplitude A,

$$\frac{\partial A}{\partial x} - \frac{D}{c}\frac{\partial^2 A}{\partial x^2} = \frac{D}{c}\left[\frac{\partial^2 A}{\partial y^2} + \frac{\partial^2 A}{\partial z^2}\right], \quad D = \frac{\lambda c}{4\pi i}. \tag{14.3.15}$$

It is first assumed that λ is small but finite, and that $\frac{D}{c}\frac{\partial^2 A}{\partial x^2}$ is negligible relative to $\partial A/\partial x$. Secondly one takes the x direction to be kinematic, namely, $x = ct$, which means, the coordinate system is placed on a moving wavefront such that $x = 0$ means $t = 0$. Then the equation of propagation can be written

$$\frac{\partial A}{\partial t} = D\nabla_\perp^2 A, \quad \nabla_\perp^2 = \frac{\partial^2}{\partial y^2} + \frac{\partial^2}{\partial z^2}. \tag{14.3.16}$$

This is a diffusion-type equation with a complex diffusion coefficient. An example is the diffraction of a wave propagating in the x direction through a hole in a screen which can be regarded as a diffusion of the diffracted wave transverse to x. For cases of circular symmetry it is convenient to use axisymmetric cylindricl coordinates (r,x), so that the diffraction limited propagation is governed by,

$$\frac{\partial A}{\partial x} = \frac{\lambda}{4\pi i}\left[\frac{\partial^2 A}{\partial r^2} + \frac{1}{r}\frac{\partial A}{\partial r}\right] \tag{14.3.17}$$

To account for losses due to thermoviscous dissipation and nonlinearity one includes them in the basic hydrodynamic equations, and derives the wave equation with a loss factor q. The result is a wave equation with a resistance term added. In terms of the velocity potential $\phi(\mathbf{u})$ where $\mathbf{u} = -\nabla\phi$), one has,

$$\frac{\partial^2\phi}{\partial t^2} - \frac{\partial q(\phi)}{\partial t} - \nabla^2\phi = 0 \tag{14.3.18}$$

Kuznetzov [28] has derived a form of q that is a nonlinear function of ϕ in which the nonlinear equation appears as,

$$\partial^2\phi/\partial t^2 - \frac{\partial}{\partial t}[b\nabla^2\phi + (\nabla\phi)^2 + a\left(\frac{\partial\phi}{\partial t}\right)^2 - \nabla^2\phi = 0$$

$$b = \rho_0^{-1}\left[\frac{4}{3}\eta + \zeta + \kappa\left(\frac{1}{C_v} - \frac{1}{C_p}\right)\right];$$

$$a = \frac{\gamma - 1}{2c^2}; \gamma = \frac{C_p}{C_v}.$$

Here b is the coefficient of thermoviscous dissipation, and a describes nonlinearity of the medium. Their presence in the equation gives rise to variations in the waveform in the direction of propagation. Several models of nonlinear propagation can be constructed from this equation. In the particular model of Zabolotskaya and Khokhlov [29] the variations in waveform are assumed to *weak* with time and distance. Hence one seeks a solution of the lossy wave equation in terms of "slow coordinates" by introducing new spatial coordinates $x^1 = \nu x$, $y^1 = (\nu y)^{1/2}$, $z^1 = (\nu z)^{1/2}$, $\nu < 1$. This means the rate of dissipation in y,z, is slower than in x. Secondly one seeks solutions in the form of plane waves whose phase dependence is $\exp - i\omega\tau$, where τ is the retarded time $t - x/C_0$. Since

$$\frac{d}{d\tau} = \frac{\partial}{\partial\tau} + \nu C_0\frac{\partial}{\partial x}$$

we may use ν to serve as a parameter of ordering. Retaining terms in the wave equation up to second order only in ν leads to the form

$$\frac{\partial}{\partial\tau}\left[\frac{\partial\phi}{\partial x} - \frac{\alpha}{2}\left[\frac{\partial\phi}{\partial\tau}\right]^2 - b'\frac{\partial^2\phi}{\partial\tau^2}\right] = \frac{C_0}{2}\nabla_\perp^2\phi \tag{14.3.19}$$

$$b' = b/2C_0^3,\ \alpha = (\gamma + 1)/2C_0^2$$

Letting $\partial\phi/\partial\tau = \Phi$ in this equation, then taking $\partial/\partial\tau$ of the result leads to the form,

$$\frac{\partial}{\partial\tau}\left[\frac{\partial\Phi}{\partial x} - \frac{\alpha}{2}\frac{\partial}{\partial\tau}\Phi^2 - b'\frac{\partial^2\Phi}{\partial\tau^2}\right] = \frac{C_0}{2}\nabla_\perp^2\Phi \tag{14.3.20}$$

In linear theory the wave equation in velocity potential is also obeyed by incremental density ρ due to the acoustic signals. Thus the entire development given above is valid when ρ replaces Φ. This replacement leads to the equation of Zabolotskaya and Kokhlov, for the propagation of a *confined* wave in a nonlinear thermoviscous medium, viz.

$$\frac{\partial}{\partial\tau}\left[\frac{\partial\rho}{\partial x} - \frac{\epsilon}{2C_0\rho_0}\frac{\partial\rho^2}{\partial\tau} - \frac{b}{2C_0^3\rho_0}\frac{\partial^2 p}{\partial\tau^2}\right] = \frac{C_0}{2}\left[\frac{\partial^2\rho}{\partial r^2} + \frac{1}{r}\frac{\partial\rho}{\partial r}\right] \tag{14.3.21}$$

$$\epsilon = (\gamma + 1)/2, \quad r = (y^2 + z^2)^{1/2}.$$

This is the equation used by Novikov et al [26] in their work on ultrasonic parametic sources. If dissipation (namely b), and nonlinearity (namely ϵ) are negligible, this equation becomes a linear parabolic equation in the amplitude of a *confined* harmonic wave,

$$\frac{\partial \rho}{\partial x} = \frac{C_0}{2i\omega}\left[\frac{\partial^2 \rho}{\partial r^2} + \frac{1}{r}\frac{\partial \rho}{\partial r}\right]$$

This is the same equation that is described by Malyuzhinets as the *diffusion approximation* for the diffraction of a planewave by an obstacle.

Novikov et al [26] consider a case where the parametic projector generates two monochromatic waves with frequencies ω_1, ω_2 at $x = 0$,

$$\rho(t, x = 0, r) = A_1(r) \sin \omega_1 t + A_2(r) \sin \omega_2 t \tag{14.3.22}$$

in which r is the transverse coordinate. Neglecting thermoviscous effects they consider only nonlinear alterations of the waveform, described by

$$\frac{\partial}{\partial \tau}\left[\frac{\partial \rho}{\partial x}\right] - \frac{C_0}{2}\left[\frac{\partial^2 \rho}{\partial_{,2}} + \frac{1}{r}\frac{\partial \rho}{\partial r} = \frac{\epsilon}{2\rho_0 C_0}\frac{\partial^2}{\partial \tau^2} A_1(r) A_2(r) \Phi(x) \cos \Omega \tau\right. \tag{14.3.23}$$

Here *the difference frequency* $\Omega = \omega_1 - \omega_2$, and $\Phi(x) = \Phi_1(x)\Phi_2(x)$. The functions $\Phi_1(x)$, $\Phi_2(x)$ describe the amplitude decay with distance of the two primaries. This is a linear equation, and is capable of solution of the form $\rho = B(x,r)e^{i\Omega\tau}$ in which $B(x,r)$ is the complex amplitude of the difference frequency wave. Upon substitution, one arrives at an equation for B,

$$\frac{\partial B}{\partial x} + \frac{ic}{2\Omega}\left[\frac{\partial^2 B}{\partial_{,2}} + \frac{1}{r}\frac{\partial B}{\partial r}\right] = \frac{i\epsilon\Omega}{2\rho_0 C_0} A_1(r) A_2(r) \Phi(x). \tag{14.3.24}$$

A convenient approach to the solution of this equation is the use of the integral (Bessel) transform $B(\lambda, x)$ where

$$B(r,x) = \int_0^\infty B(\lambda, x)\, J_0(\lambda r) \lambda\, d\lambda$$

and then transforming back to amplitude A, with the result that,

$$A = \frac{i\epsilon\Omega}{2C_0\rho_0}\int_0^x dx' \Phi(x') \int_0^\infty d\lambda \lambda f(\lambda) \exp\left[-\frac{iC_0}{2\Omega}\lambda^2 (x' - x)\right] J_0(\lambda r)$$

$$f(x) = \int_0^\infty r A_1(r) A_2(r) J_0(\lambda r)\, dr \tag{14.3.25}$$

The form of $A_{1,2}(r)$ (i.e. amplitude in the transverse direction) is not easily prescribed. For mathematical convenience it is taken to be Gaussian, i.e. $A_{1,2} = \exp(-r^2/a_{1,2}^2)$. Direct integration then leads to a simple (Gaussian) form for $f(\lambda)$. The amplitude then becomes

$$A(r,x) = \frac{i\epsilon\Omega}{2\rho_0 C_0} A_1 A_2 \int_0^x \frac{\Phi(x-y)}{1 - \frac{iy}{L_D}} \exp\left[-\frac{r^2/a^2}{1 - \frac{iy}{L_D}}\right] dy$$

$$\frac{1}{a^2} = \frac{1}{a_1^2} + \frac{1}{a_2^2}; \; y = x - x'. \tag{14.3.26}$$

The symbol L_D is $a^2\Omega/2C^0$, or $k_-a^2/2$, the diffraction length for the difference frequency wave.

The key issue then is the form of the attenuation function $\Phi(x-y)$. It is first assumed that nonlinearity does not affect the primaries (i.e. no shock wave formation). Then a plausible choice for Φ is,

$$\Phi(x-y) = \exp\left(\frac{y-x}{L_a}\right),\ L_a = \frac{2C_0^3\rho_0}{b(\omega_1^2+\omega_2^2)}. \tag{14.3.27}$$

Although the resultant integral for $A(r,x)$ is complicated, it can never the less be numerically evaluated. An important special case is the calculated amplitude along the beam axis ($r = 0$)

$$|A(0,x)| = \frac{\epsilon A_1 A_2 \Omega L_d}{2C_0\rho_0} e^{-\frac{x}{L_a}} \left| \mathscr{E}_i\left(\frac{x}{L_a} + i\frac{L_D}{L_a}\right) - \mathscr{E}_i\left(i\frac{L_D}{L_a}\right)\right| \tag{14.3.28}$$

in which $\mathscr{E}_i(\xi)$ is the integral exponential function. Two plots of this equation in the difference frequency amplitude have been made:

$$A_\Omega = \frac{2A\rho_0 C_2}{A_1 A_2 \epsilon\Omega L_a} \text{ vs } \frac{x}{L_a}, \text{ for fixed } L_a, \text{ with } \frac{L_D}{L_a} \text{ as parameter}$$

$$A_\Omega' = \frac{2A\rho_0 C_0}{A_1 A_2 \epsilon\Omega L_D} \text{ vs } \frac{x}{L_D}, \text{ for fixed } L_D, \text{ with } \frac{L_D}{L_a} \text{ as parameter.}$$

These are shown as Figs. 14.3.6, 14.3.7 from the article of Novikov et al.

The transverse distribution of signal amplitude at various distances x from the face of the radiator gives of width of the parametric beam. A conventional circular piston of radius a with aperture distribution (at $x = 0$) of $\Phi = A\exp(-r^2/a^2)e^{-i\Omega t}$ has a transverse distribution at the difference frequency given by,

$$A_\Omega = \frac{A\exp\left[-\dfrac{(r^2/a^2)}{1+\dfrac{x^2}{L^2}}\right]}{\sqrt{1+\dfrac{x^2}{L^2}}},\ /\ L = a^2\Omega/2C_0$$

In a parametric projector with the special form of $\Phi(x-y) = \exp\left(\frac{y-x}{L_a}\right)$ the magnitude $A(r,x)$ is

$$|A(r,x)| = \frac{\epsilon\Omega A_1 A_2}{2\rho_0 C_0}\left|\mathscr{E}_i\left(-\frac{r^2/a^2}{1-\dfrac{ix}{L_D}}\right) - \mathscr{E}_i\left(-\frac{r^2}{a^2}\right)\right|$$

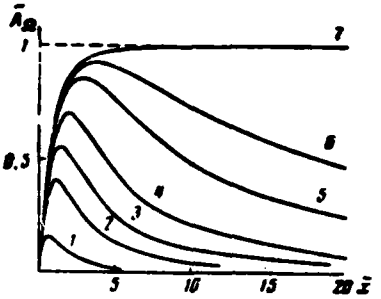

Fig. 14.3.6. Difference-frequency signal amplitude $\tilde{A}_\Omega = 2Ac_0\rho_0/A_1A_2\epsilon\Omega L_a$ on the beam axis vs distance $\tilde{x}_1 = x/L_a$ from the radiator for a fixed value of the attenuation length L_a and the following values of the ratio L_d/L_a: 1) 0; 2) 0.1; 3) 0.5; 4) 1; 5) 2. After [26].

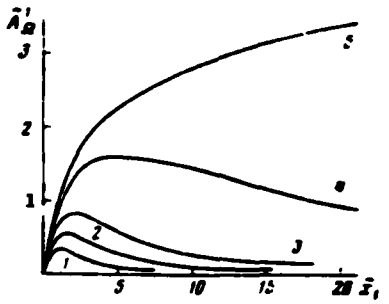

Fig. 14.3.7. Difference-frequency signal amplitude $\tilde{A}'_\Omega = 2Ac_0\rho/A_1A_2\epsilon\Omega L_d$ on the beam axis vs distance $\tilde{x}_1 = x/L_d$ and the following values of the ratio L_d/L_a: 1) 0; 2) 0.1; 3) 0.5; 4) 1; 5) 2. (After [26]).

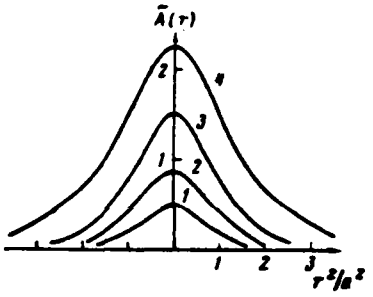

Fig. 14.3.8. Transverse distribution of signal amplitude $\tilde{A}(r) = 2Ac_0\rho_0/A_1A_2\epsilon\Omega L$ at various distances from the radiator, neglecting carrier attenuation. 1) $x/L_d = 0.5$; 2) 1; 3) 2; 4) 5. After [26].

A plot of $|A(r,x)|$ versus r^2/a^2 for various distances x/L_D is shown as Fig. 14.3.8 from the article of Novikov et al. This shows that at a distance of $x/L_D = 5$ the width of the conventional beam is $5a$ as compared to that of the parametric beam $1.4a$.

REFERENCES

[1] P.J. Westervelt, JASA 35, 538 (1963).
[2] R.H. Mellen, M. Moffett, U.S. Navy Jour. Underwater Acoustics 22, 105 (1972).
[3] H.O. Berktay, D.J. Leahy, JASA 55, 539 (1972).
[4] H. Hobaek, J. Sound Vib. 6 (3) 460.
[5a] K.A. Naugol'nykh et al., Sov. Phys. Acoust. 9, 155.
[5b] V. Lauvstad, J. Naze, S. Tjötta, Arbok V. Bergen, Mat. Nat. Ser. No. 12," Nonlinear Interaction of Two Sound Beams."
[6] R.R. Beyer, "Nonlinear Acoustics," Naval Sea Systems Command, 1974, p. 101.
[7] L.D. Landau, E.M. Lifshitz, "Fluid Mechanics," Addison Wesley, 1959, p. 300.
[8] Bhatia, "Ultrasonic Absorption," Oxfort Press, 1967.
[9] L.N. Liebermann, JASA 20, 868 (1948).
[10] M. Schulkin, W.H. Marsh, JASA 34, 864 (1962).

[11] R.J. Urick, "Principles of Underwater Sound for Engineers," 1st Ed., McGraw-Hill, Fig. 5.4.
[12] H.O. Berktay, J. Sound Vib. 2, 460 (1965).
[13] J.A. Shooter et al., JASA 55, 56 (1974).
[14] B. Friedman, JASA 32, 197.
[15] J. Zemanak, T. Muir, JASA 52, 1484.
[16] J.A. Shooter et al., JASA 55, 57.
[17] J. Zemanek, JASA 49, 181.
[18] K. Herzfeld, T. Litovitz, "Absorption and Dispersion of Sound of Ultrasonic Waves," Academic Press, 1959.
[19] J. Naze, S. Tjötta, JASA 37, 174.
[20] M. Moffett et al., JASA 49, 339.
[21] H.O. Berktay, Article in "Signal Processing," Ed. J.W.R. Griffiths, Academic Press, 1973, p. 311.
[22] D. Blackstock, JASA 36, 534.
[23] D. Blackstock, JASA 39, 1019.
[24] D.T. Laird, Ph.D. Thesis, Penn State U., 1955.
[25] T. Muir, Tech. Rept. ARL-TR-71-1, U. of Texas, Austin, Tex., 1971.
[26] B.K. Novikov et al., Sov. Phys. Acoust. 21, 365 (1976).
[27] G.D. Malyuzhinets, Sov. Phys. Uspi 67, 749 (1959).
[28] G.N. Kuznetzov, Sov. Phys. Acoust. 16, 467 (1971).
[29] E.A. Zablotskaya, R.V. Khokhlov, Sov. Phys. Acoust. 15, 35 (1969).

FILM